



FIBROSIS AND INFLAMMATION IN TISSUE PATHOPHYSIOLOGY

EDITED BY: Elvira Forte, Isotta Chimenti, Gonzalo del Monte-Nieto and
Susanne Sattler

PUBLISHED IN: *Frontiers in Physiology*, *Frontiers in Medicine* and
Frontiers in Cell and Developmental Biology



frontiers

Frontiers eBook Copyright Statement

The copyright in the text of individual articles in this eBook is the property of their respective authors or their respective institutions or funders. The copyright in graphics and images within each article may be subject to copyright of other parties. In both cases this is subject to a license granted to Frontiers.

The compilation of articles constituting this eBook is the property of Frontiers.

Each article within this eBook, and the eBook itself, are published under the most recent version of the Creative Commons CC-BY licence.

The version current at the date of publication of this eBook is CC-BY 4.0. If the CC-BY licence is updated, the licence granted by Frontiers is automatically updated to the new version.

When exercising any right under the CC-BY licence, Frontiers must be attributed as the original publisher of the article or eBook, as applicable.

Authors have the responsibility of ensuring that any graphics or other materials which are the property of others may be included in the CC-BY licence, but this should be checked before relying on the CC-BY licence to reproduce those materials. Any copyright notices relating to those materials must be complied with.

Copyright and source acknowledgement notices may not be removed and must be displayed in any copy, derivative work or partial copy which includes the elements in question.

All copyright, and all rights therein, are protected by national and international copyright laws. The above represents a summary only. For further information please read Frontiers' Conditions for Website Use and Copyright Statement, and the applicable CC-BY licence.

ISSN 1664-8714
ISBN 978-2-88974-497-8
DOI 10.3389/978-2-88974-497-8

About Frontiers

Frontiers is more than just an open-access publisher of scholarly articles: it is a pioneering approach to the world of academia, radically improving the way scholarly research is managed. The grand vision of Frontiers is a world where all people have an equal opportunity to seek, share and generate knowledge. Frontiers provides immediate and permanent online open access to all its publications, but this alone is not enough to realize our grand goals.

Frontiers Journal Series

The Frontiers Journal Series is a multi-tier and interdisciplinary set of open-access, online journals, promising a paradigm shift from the current review, selection and dissemination processes in academic publishing. All Frontiers journals are driven by researchers for researchers; therefore, they constitute a service to the scholarly community. At the same time, the Frontiers Journal Series operates on a revolutionary invention, the tiered publishing system, initially addressing specific communities of scholars, and gradually climbing up to broader public understanding, thus serving the interests of the lay society, too.

Dedication to Quality

Each Frontiers article is a landmark of the highest quality, thanks to genuinely collaborative interactions between authors and review editors, who include some of the world's best academicians. Research must be certified by peers before entering a stream of knowledge that may eventually reach the public - and shape society; therefore, Frontiers only applies the most rigorous and unbiased reviews. Frontiers revolutionizes research publishing by freely delivering the most outstanding research, evaluated with no bias from both the academic and social point of view. By applying the most advanced information technologies, Frontiers is catapulting scholarly publishing into a new generation.

What are Frontiers Research Topics?

Frontiers Research Topics are very popular trademarks of the Frontiers Journals Series: they are collections of at least ten articles, all centered on a particular subject. With their unique mix of varied contributions from Original Research to Review Articles, Frontiers Research Topics unify the most influential researchers, the latest key findings and historical advances in a hot research area! Find out more on how to host your own Frontiers Research Topic or contribute to one as an author by contacting the Frontiers Editorial Office: frontiersin.org/about/contact

FIBROSIS AND INFLAMMATION IN TISSUE PATHOPHYSIOLOGY

Topic Editors:

Elvira Forte, Jackson Laboratory, United States

Isotta Chimenti, Sapienza University of Rome, Italy

Gonzalo del Monte-Nieto, Monash University, Australia

Susanne Sattler, Imperial College London, United Kingdom

Citation: Forte, E., Chimenti, I., del Monte-Nieto, G., Sattler, S., eds. (2022).

Fibrosis and Inflammation in Tissue Pathophysiology. Lausanne: Frontiers Media SA. doi: 10.3389/978-2-88974-497-8

Table of Contents

- 06 Editorial: Fibrosis and Inflammation in Tissue Pathophysiology**
Isotta Chimenti, Susanne Sattler, Gonzalo del Monte-Nieto and Elvira Forte
- 11 BMPER Ameliorates Renal Fibrosis by Inhibiting Tubular Dedifferentiation and Fibroblast Activation**
Ting Xie, Zunen Xia, Wei Wang, Xiangjun Zhou and Changgeng Xu
- 26 Qishen Yiqi Dripping Pill Protects Against Diabetic Nephropathy by Inhibiting the Wnt/ β -Catenin and Transforming Growth Factor- β /Smad Signaling Pathways in Rats**
Qian Zhang, Xinhua Xiao, Jia Zheng, Ming Li, Miao Yu, Fan Ping, Tong Wang and Xiaojing Wang
- 40 Nicotinamide Mononucleotide Attenuates Renal Interstitial Fibrosis After AKI by Suppressing Tubular DNA Damage and Senescence**
Yan Jia, Xin Kang, Lishan Tan, Yifei Ren, Lei Qu, Jiawei Tang, Gang Liu, Suxia Wang, Zuying Xiong and Li Yang
- 51 Sos1 Modulates Extracellular Matrix Synthesis, Proliferation, and Migration in Fibroblasts**
Isabel Fuentes-Calvo and Carlos Martinez-Salgado
- 60 Role of Podoplanin-Positive Cells in Cardiac Fibrosis and Angiogenesis After Ischemia**
Maria Cimini and Raj Kishore
- 73 Evolving Roles of Muscle-Resident Fibro-Adipogenic Progenitors in Health, Regeneration, Neuromuscular Disorders, and Aging**
Marine Theret, Fabio M. V. Rossi and Osvaldo Contreras
- 96 EndMT Regulation by Small RNAs in Diabetes-Associated Fibrotic Conditions: Potential Link With Oxidative Stress**
Roberta Giordo, Yusra M. A. Ahmed, Hilda Allam, Salah Abusnana, Lucia Pappalardo, Gheyath K. Nasrallah, Arduino Aleksander Mangoni and Gianfranco Pintus
- 114 Animal and Organoid Models of Liver Fibrosis**
Yu-long Bao, Li Wang, Hai-ting Pan, Tai-ran Zhang, Ya-hong Chen, Shan-jing Xu, Xin-li Mao and Shao-wei Li
- 127 High Glucose Activates YAP Signaling to Promote Vascular Inflammation**
Jeremy Ortillon, Jean-Christophe Le Bail, Elise Villard, Bertrand Léger, Bruno Poirier, Christine Girardot, Sandra Beeske, Laetitia Ledein, Véronique Blanchard, Patrice Brieu, Souâd Naimi, Philip Janiak, Etienne Guillot and Marco Meloni
- 137 TMSB4 Overexpression Enhances the Potency of Marrow Mesenchymal Stromal Cells for Myocardial Repair**
Shiyuan Tang, Chengming Fan, Chukwuemeka Daniel Iroegbu, Wenwu Zhou, Zhigong Zhang, Ming Wu, Wangping Chen, Xiaoming Wu, Jun Peng, Zhihong Li and Jinfu Yang
- 150 Trimethylamine N-Oxide Exacerbates Renal Inflammation and Fibrosis in Rats With Diabetic Kidney Disease**
Qing Fang, Binjie Zheng, Na Liu, Jinfeng Liu, Wenhui Liu, Xinyi Huang, Xiangchang Zeng, Lulu Chen, Zhenyu Li and Dongsheng Ouyang

- 163** *In vitro Assays and Imaging Methods for Drug Discovery for Cardiac Fibrosis*
Giorgia Palano, Ariana Foinquinos and Erik Müllers
- 174** *Targeting Dermal Fibroblast Subtypes in Antifibrotic Therapy: Surface Marker as a Cellular Identity or a Functional Entity?*
Xin Huang, Yimin Khoong, Chengyao Han, Dai Su, Hao Ma, Shuchen Gu, Qingfeng Li and Tao Zan
- 190** *Expression and Pathogenic Analysis of Integrin Family Genes in Systemic Sclerosis*
Dan Xu, Ting Li, Ruikang Wang and Rong Mu
- 200** *Role of PDGF-A/B Ligands in Cardiac Repair After Myocardial Infarction*
Kunal Kalra, Joerg Eberhard, Nona Farbehi, James J. Chong and Munira Xaymardan
- 213** *High-Mobility Group A1 Promotes Cardiac Fibrosis by Upregulating FOXO1 in Fibroblasts*
Qingwen Xie, Qi Yao, Tongtong Hu, Zhulan Cai, Jinhua Zhao, Yuan Yuan, Qing Qing Wu and Qi-zhu Tang
- 224** *Distinct Metalloproteinase Expression and Functions in Systemic Sclerosis and Fibrosis: What We Know and the Potential for Intervention*
Edwin Leong, Michael Bezuhyly and Jean S. Marshall
- 233** *Lymphocytes: Versatile Participants in Acute Kidney Injury and Progression to Chronic Kidney Disease*
Chujin Cao, Ying Yao and Rui Zeng
- 251** *Amlexanox and Forskolin Prevents Isoproterenol-Induced Cardiomyopathy by Subduing Cardiomyocyte Hypertrophy and Maladaptive Inflammatory Responses*
Gabriel Komla Adzika, Hongjian Hou, Adebayo Oluwafemi Adekunte, Ruqayya Rizvi, Seyram Yao Adzraku, Kexue Li, Qi-Ming Deng, Richard Mprah, Marie Louise Ndzie Noah, Joseph Adu-Amankwaah, Jeremiah Ong'achwa Machuki, Wenkang Shang, Tongtong Ma, Stephane Koda, Xianluo Ma and Hong Sun
- 265** *Estrogen Attenuates Chronic Stress-Induced Cardiomyopathy by Adaptively Regulating Macrophage Polarizations via β_2 -Adrenergic Receptor Modulation*
Hongjian Hou, Gabriel Komla Adzika, Qi Wu, Tongtong Ma, Yanhong Ma, Juan Geng, Mingjin Shi, Lu Fu, Ruqayya Rizvi, Zheng Gong and Hong Sun
- 278** *The Potential Use of Cannabis in Tissue Fibrosis*
Nazar Pryimak, Mariia Zaiachuk, Olga Kovalchuk and Igor Kovalchuk
- 297** *Cardiomyocyte-Specific RIP2 Overexpression Exacerbated Pathologic Remodeling and Contributed to Spontaneous Cardiac Hypertrophy*
Jing-jing Yang, Nan Zhang, Zi-ying Zhou, Jian Ni, Hong Feng, Wen-jing Li, Shan-qi Mou, Hai-ming Wu, Wei Deng, Hai-han Liao and Qi-zhu Tang
- 313** *Augmented Liver Uptake of the Membrane Voltage Sensor Tetraphenylphosphonium Distinguishes Early Fibrosis in a Mouse Model*
Himanshi Pandita, Esteban Mezey and Shanmugasundaram Ganapathy-Kanniappan
- 324** *Erratum: Augmented Liver Uptake of the Membrane Voltage Sensor Tetraphenylphosphonium Distinguishes Early Fibrosis in a Mouse Model*
Frontiers Production Office

- 326 Targeting Mechanosensitive Piezo1 Alleviated Renal Fibrosis Through p38MAPK-YAP Pathway**
Yuanyuan Fu, Pengzhi Wan, Jie Zhang, Xue Li, Jia Xing, Yu Zou, Kaiyue Wang, Hui Peng, Qizhuo Zhu, Liu Cao and Xiaoyue Zhai
- 341 ADAM17, A Key Player of Cardiac Inflammation and Fibrosis in Heart Failure Development During Chronic Catecholamine Stress**
Joseph Adu-Amankwaah, Gabriel Komla Adzika, Adebayo Oluwafemi Adekunle, Marie Louise Ndzie Noah, Richard Mprah, Aisha Bushi, Nazma Akhter, Fei Huang, Yaxin Xu, Seyram Yao Adzraku, Iqra Nadeem and Hong Sun
- 356 circHIPK3 Exacerbates Folic Acid-Induced Renal Tubulointerstitial Fibrosis by Sponging miR-30a**
Yan Wu, Junjun Luan, Congcong Jiao, Shiwen Zhang, Cong Ma, Yixiao Zhang, Jingqi Fu, En Yin Lai, Jeffrey B. Kopp, Jingbo Pi and Hua Zhou



Editorial: Fibrosis and Inflammation in Tissue Pathophysiology

Isotta Chimenti^{1,2*}, *Susanne Sattler*³, *Gonzalo del Monte-Nieto*⁴ and *Elvira Forte*⁵

¹ Department of Medical Surgical Sciences and Biotechnologies, Sapienza University of Rome, Rome, Italy, ² Mediterranean Cardiocentro, Naples, Italy, ³ National Heart and Lung Institute, Imperial College London, London, United Kingdom, ⁴ Australian Regenerative Medicine Institute, Monash University, Clayton, VIC, Australia, ⁵ The Jackson Laboratory, Bar Harbor, ME, United States

Keywords: fibrosis, inflammation, tissue damage, tissue repair, fibroblasts, stromal cells, leucocytes

Editorial on the Research Topic

Fibrosis and Inflammation in Tissue Pathophysiology

Mammalian tissues react to damage by activating the highly specialized response of wound healing. Acute inflammation is the first and fastest mechanism activated in the damaged area, as a fundamental protective and transitional response with the purpose of progressive activation of endogenous tissue cells for reparative activities (Reinke and Sorg, 2012; Sattler, 2017). The balance between degree of damage, potency of the subsequent inflammatory wave, and the regenerative ability of resident cells determines the extent by which tissues can accomplish regeneration (for low-grade damage or in highly regenerative tissues, such as the liver) or fibrotic repair (for extensive damage or in poorly regenerative tissues, such as the myocardium). Persistent damage, complications, or repeated insults, can sustain the continuous or aberrant activation of repair pathways, leading to chronic inflammation and progressive tissue fibrosis (Sattler et al., 2017; Henderson et al., 2020). Despite the evolutionary advantage conferred to mammals by scarring as a rapid repair mechanism, biological and mechanical features of the original tissue architecture are disrupted in the scar area (Forbes and Rosenthal, 2014). Over time, chronic fibrosis thus leads to tissue adverse remodeling and impaired function. Persistent inflammation and fibrosis play a major role in a wide range of diseases, accounting for an increasingly large fraction of morbidity and mortality worldwide (Henderson et al., 2020).

While recent advances have unveiled many environmental and genetic causes of fibrotic disorders (Spagnolo et al., 2014; Cutting, 2015), a better understanding of both ubiquitous and tissue-specific regulatory pathways, and cellular dynamics could help to design new targeted therapies, and even to identify the etiology of idiopathic disease.

Within this Research Topic, we have gathered several contributions on the cellular and molecular mediators of fibrosis, and the intertwined pathophysiological role of fibrosis and inflammation in different tissues and diseases, with particular emphasis on renal and cardiac fibrosis.

CELLULAR AND MOLECULAR MEDIATORS OF FIBROSIS

Fibroblasts are increasingly regarded as a complex cell type. In fact, it has become clear that multiple phenotypes and functional states can be identified in the stroma of organs, with significantly different functions (Forte et al., 2018, 2020; Farbehi et al., 2019; Muhl et al., 2020; Mohenska et al., 2021; Plikus et al., 2021). Here, Huang et al. contributed a critical review on the association between specific fibroblast genes with biological and functional definitions, as this link seems to be subtle and blurred in many different tissues. The complex topic of fibroblast phenotypes is further complicated

OPEN ACCESS

Edited and reviewed by:

Geoffrey A. Head,
Baker Heart and Diabetes
Institute, Australia

*Correspondence:

Isotta Chimenti
isotta.chimenti@uniroma1.it

Specialty section:

This article was submitted to
Integrative Physiology,
a section of the journal
Frontiers in Physiology

Received: 07 December 2021

Accepted: 29 December 2021

Published: 21 January 2022

Citation:

Chimenti I, Sattler S, del
Monte-Nieto G and Forte E (2022)
Editorial: Fibrosis and Inflammation in
Tissue Pathophysiology.
Front. Physiol. 12:830683.
doi: 10.3389/fphys.2021.830683

under pro-fibrotic conditions by the trans-differentiation of endothelial cells into myofibroblasts by endothelial-to-mesenchymal transition—End-MT (Forte et al., 2017; Hulshoff et al., 2019). Giordo et al. contributed a review on the interesting relationship between non-coding RNAs, oxidative stress, and End-MT in fibrosis complications affecting the retina, kidneys, heart, and vessels during diabetes progression.

However, fibroblasts are not the only stromal cell type of interest for tissue fibrosis and repair (Forte et al., 2018; Farbehi et al., 2019). Tissue resident mesenchymal cells are described in multiple organs, where they are involved in homeostasis and disease (Lemos and Duffield, 2018). Theret et al. reviewed the literature about fibro-adipogenic progenitors in muscle integrity, extracellular matrix (ECM) deposition, and in response to injury, also analyzing their contribution to the pool of activated fibroblasts in muscle fibrosis and degenerative conditions. On a different perspective, cardiac cell therapy with mesenchymal cells holds promise for the treatment of myocardial infarction (Peruzzi et al., 2015; Pagano et al., 2019; Guo et al., 2020). Tang et al. described that thymosin- β 4 overexpression in bone-marrow mesenchymal cells significantly increases their therapeutic potential on cardiac function in a rat model. This effect is mediated, among others, by a reduction of the scar area and decrease in collagen deposition in the infarcted myocardium, and by increased activation of the Hypoxia-Inducible Factor 1-alpha (HIF-1 α) pathway.

One hallmark of fibrosis in multiple organs is excessive ECM deposition (Herrera et al., 2018). Leong et al. reviewed the literature about the key enzymes of ECM remodeling, matrix metalloproteinases (MMPs) and their tissue inhibitors, in systemic sclerosis, on the quest for novel therapeutic targets to treat tissue stiffening and loss of function. MMPs also regulate the bioavailability of humoral factors. Adu-Amankwaah et al. contributed a review on the multiple roles of A Disintegrin And Metalloproteinase 17 (ADAM17), which is emerging as a core regulatory factor in inflammation and fibrosis. In fact, ADAM17 can activate multiple cytokines and pro-fibrotic factors (e.g., Tumor Necrosis Factor alpha—TNF α , soluble Interleukin 6 Receptor—sIL-6R, Amphiregulin—AREG) in cardiac fibrosis and in catecholamine stress during heart failure progression, highlighting potential therapeutic targets. Moreover, cell–ECM interaction and crosstalk are responsible for the effects of tissue stiffening in fibrotic diseases on both parenchymal and stromal cells. Key transducers of ECM stiffening are integrins, and Xu et al. studied the integrin family expression in skin tissue of systemic sclerosis patients from the Gene Expression Omnibus-GEO database, describing the upregulation of several integrins involved in ECM turnover, leucocyte extravasation, Transforming Growth Factor beta 1 (TGF- β 1) signaling, and immune cell activation. These results highlight the strong relationship between ECM, resident cells, and immune cells in tissue remodeling and fibrosis.

Fuentes-Calvo et al. provided another contribution to the understanding of molecular mechanisms of fibroblast activation, by describing the role of Rat Sarcoma virus protein (RAS) activator Son Of Sevenless 1 (SOS1) in murine embryonic fibroblasts. Their results show that SOS1 mediates the response

to TGF- β 1 through AK strain Transforming (AKT) and Extracellular signal-Regulated Kinase (ERK), particularly by mediating proliferation and migration of activated fibroblasts.

Pandita et al. contributed a study on the relationship between mitochondrial voltage, as an indicator of oxidative phosphorylation levels, and the progression of fibrosis in the liver. They showed mechanistic association between the upregulation of mitochondrial electron transport chain enzymes, oxygen consumption, and the activation of the AMP-activated protein Kinase (AMPK) pathway, providing an interesting link between metabolism, hepatic insult responses, and early signs of fibrosis in the liver.

CARDIAC FIBROSIS

Myocardial fibrosis is involved in multiple cardiac diseases, and is fueled by continuous cardiomyocyte death, inflammatory cell recruitment, and direct activation of resident fibroblasts (Schirone et al., 2017; Forte et al., 2018, 2020; Panahi et al., 2018). Multiple signaling pathways are known to control fibroblast behavior (Plikus et al., 2021). Xie et al. investigated the role of High-Mobility Group A1 protein (HMGA1) in cardiac fibroblast activation, showing how it is overexpressed in an isoproterenol-treated mouse model, and that it mediates fibrosis via Forkhead box protein O1 (FOXO1). Conversely, its knockdown inhibits fibroblast responses to TGF- β 1, thus identifying a novel molecular target for possible anti-fibrotic treatments in the heart.

Platelet-derived growth factors (PDGFs) are important mediators of inflammation, angiogenesis, and fibroblasts activation, and represent possible therapeutic targets against myocardial remodeling. Kalra et al. reviewed the literature concerning PDGF signaling mechanisms and beneficial effects in cardiac injury, highlighting the potentials and pitfalls for translational research. Concerning the identification of specific markers for myocardial injury, Cimini et al. contributed a review on podoplanin, a novel marker upregulated in multiple cell types after infarction. During homeostasis, podoplanin is expressed by lymphatic endothelial cells, but after injury many cell types upregulate its expression, including fibroblasts and hematopoietic cells. The authors provide an overview of several studies evidencing a wide range of possible interactions mediated by podoplanin among different cell compartments.

Concerning novel synergistic therapeutic approaches for the heart, Hou et al. studied how estradiol supplementation in rats during isoproterenol-induced stress can prevent cardiac dysfunction and maladaptive myocardial hypertrophy. In particular, these effects were shown to be mediated by β 2-adrenoceptors and the resolution of inflammation due to an increased anti-inflammatory macrophage phenotype, evidencing an interesting endocrine/immune-modulatory circuit in the heart. Adzika et al. studied a possible combined therapy with forskolin (i.e., an adenylyl cyclase activator able to modulate cardiac and inflammatory responses) and amlexanox [i.e., a G protein-coupled Receptor Kinase 5 (GRK5) inhibitor of adaptive immune responses] to prevent pathological cardiac hypertrophy

in mice. This treatment was effective at preventing left ventricular systolic dysfunction during isoproterenol-induced chronic stress by attenuating maladaptive myocardial hypertrophy, fibrosis, and inflammatory responses. Finally, Yang et al. studied how Receptor Interacting Protein kinase 2 (RIP2) is upregulated in failing hearts, both in human patient samples and murine models of aortic banding, as well as in angiotensin II-treated neonatal rat cardiomyocytes. RIP2 overexpression indeed aggravates cardiac remodeling through phosphorylation of targets such as TGF β -Activated Kinase 1 (TAK1), p38 mitogen-activated protein kinase (p38MAPK), and Jun N-terminal Kinases (JNK1/2). Thus, inhibiting RIP2 or its targets may inhibit cardiac remodeling, representing another potential preventive strategy in cardiology.

RENAL FIBROSIS

Fibrosis and inflammation are also significantly involved in kidney pathophysiology and progressive functional impairment, particularly in chronic kidney disease (Panizo et al., 2021). Cao et al. reviewed the literature on the role of lymphocytes in kidney fibrosis and disease, discussing how different subsets play different and antagonistic roles: in fact, T-helper cells and innate-like lymphocytes exert mainly pathogenic roles, while CD4⁻/CD8⁻ double negative and T-reg cells are considered protective. Further elucidation of the different roles of lymphocytes in renal injury and fibrosis may guide the discovery of novel specific therapeutics. Instead, Fang et al. focused their attention on diabetic kidney disease and the gut microbiota: they show that the microbiota metabolite trimethylamine N-oxide accelerates kidney dysfunction by activating the inflammasome and releasing pro-inflammatory cytokines in a high-fat diet/low-dose streptozotocin-induced rat model of diabetes, providing new perspectives on the pathogenesis and potential treatment of diabetic kidney disease.

Zhang et al. reported a novel protective mechanism of the traditional Chinese medicine compound called Qishen Yiqi Dripping Pill on diabetic nephropathy. In a high-fat diet/streptozotocin rat model of diabetes this treatment yielded improved kidney function and reduced fibrosis; moreover, they evidenced inhibition of the Wingless-integration—Wnt/ β -catenin and the TGF- β /Smad2 signaling pathways, thus highlighting a potential direct effect on activation of tissue fibrosis. Regarding other related mechanisms of injury, Jia et al. described that attenuation of DNA damage and senescence in tubular cells by the NAD⁺ precursor nicotinamide mononucleotide (NMN) may exert a protective effect against acute kidney injury; they confirmed this therapeutic and preventive potential both *in vitro* and *in vivo*, in an ischemia-reperfusion injury mouse model showing cell protection and reduced inflammation.

Concerning direct interference with mechanisms of fibroblast activation and fibrosis, Xie et al. showed that exogenous transfection of the Bone Morphogenetic Protein binding Endothelial Regulator (BMPER) in a mouse model of renal fibrosis blocks fundamental mechanisms of fibroblast activation mediated by TGF- β 1, such as epithelial-to-mesenchymal

transition and tubular cells trans-differentiation, proposing another novel therapeutic strategy against renal fibrosis. In this regard, Wu et al. identified the circular RNA circHIPK3 as a possible novel therapeutic target for renal fibrosis. They found that circHIPK3 is upregulated in a mouse model of induced renal fibrosis. The study demonstrated that circHIPK3 reduces the activity of miRNA-30a, a known negative regulator of profibrotic genes, including TGF- β 1, fibronectin, and collagen 1. CircHIPK3 sequesters miRNA-30a in the cytoplasm of tubular epithelial cells by directly binding to it, and this promotes the expression of profibrotic genes and the progression of renal fibrosis.

Inflammation and fibrosis are closely connected to alterations in the composition and properties of the ECM (Pesce et al., 2017; Herrera et al., 2018). As for the heart, the mechanisms by which ECM stiffening may aggravate renal fibrosis are still under investigation. Fu et al. reported that enhanced substrate stiffness can activate mesangial cells toward fibrotic features through the Piezo1, p38MAPK, and Yes-Associated Protein (YAP) pathway. They showed both *in vitro* and *in vivo* in a unilateral ureteral occlusion model in mice, that Piezo1 knockdown can counteract this activation, as well as fibrosis progression, suggesting a novel mechanosensing-based strategy against renal fibrosis. Another contribution on mechanosensing is focused on diabetes and the vasculature. Diabetes represents the starting condition triggering multiple organ damage (Fрати et al., 2017; Cosentino et al., 2020). Orillon et al. reported that YAP signaling is activated *in vitro* in endothelial cells by exposure to high glucose, and *in vivo* in the vessels of db/db mice. Its activation is potentiated under flow stress, evidencing a novel role in enhancing diabetic inflammatory signals in the vasculature.

FIBROSIS MODELING AND DRUG TESTING

Research into novel treatments targeting fibrosis greatly benefits from advancements in relevant and reproducible animal models, as well as *in vitro* systems with increasing physiological relevance (Lagares and Hinz, 2021). As part of this article collection, Palano et al. summarized and discussed available assays to study cardiac fibrosis, with emphasis on the most recent innovations in multi-cellular 3D cultures and computational methods for scaling up and boosting preclinical and translational research. Bao et al., on the other hand, focused their review on the analysis and comparison of different animal models of liver fibrosis and their ability to mimic different etiologies and pathogenic mechanisms. They also presented the most recent advances in liver organoid cultures as relevant alternatives to *in vivo* testing.

Looking for novel anti-inflammatory and immunosuppressive therapeutic options, Pryimak et al. reviewed the growing body of literature suggesting that cannabinoids and *Cannabis sativa* extracts may exert anti-fibrotic effects at multiple levels and in multiple organs. In this review, the authors suggest the introduction of cannabinoids for the prevention and treatment of fibrosis as a versatile and widely applicable therapeutic strategy.

In conclusion, the present Research Topic has collected a significant amount of novel and interconnected contributions

on the multifaceted roles of inflammation and fibrosis in different tissues and diseases. The increasing knowledge in the field is paving the way towards multi-target therapeutic strategies against chronic diseases, as well as to novel treatments adaptable to various organs sharing similar pathogenetic pathways.

AUTHOR CONTRIBUTIONS

All authors listed have made a substantial, direct, and intellectual contribution to the work and approved it for publication.

REFERENCES

- Cosentino, F., Grant, P. J., Aboyans, V., Bailey, C. J., Ceriello, A., Delgado, V., et al. (2020). 2019 ESC guidelines on diabetes, pre-diabetes, and cardiovascular diseases developed in collaboration with the EASD. *Eur. Heart J.* 41, 255–323. doi: 10.1093/eurheartj/ehz486
- Cutting, G. R. (2015). Cystic fibrosis genetics: from molecular understanding to clinical application. *Nat. Rev. Genet.* 16, 45–56. doi: 10.1038/nrg3849
- Farbehi, N., Patrick, R., Dorison, A., Xaymardan, M., Janbandhu, V., Wystub-Lis, K., et al. (2019). Single-cell expression profiling reveals dynamic flux of cardiac stromal, vascular and immune cells in health and injury. *Elife* 8, e43882. doi: 10.7554/eLife.43882
- Forbes, S. J., and Rosenthal, N. (2014). Preparing the ground for tissue regeneration: from mechanism to therapy. *Nat. Med.* 20, 857–869. doi: 10.1038/nm.3653
- Forte, E., Chimenti, I., Rosa, P., Angelini, F., Pagano, F., Calogero, A., et al. (2017). EMT/MET at the crossroad of stemness, regeneration and oncogenesis: the ying-yang equilibrium recapitulated in cell spheroids. *Cancers (Basel)* 9, 98. doi: 10.3390/cancers9080098
- Forte, E., Furtado, M. B., and Rosenthal, N. (2018). The interstitium in cardiac repair: role of the immune-stromal cell interplay. *Nat. Rev. Cardiol.* 15, 601–616. doi: 10.1038/s41569-018-0077-x
- Forte, E., Skelly, D. A., Chen, M., Daigle, S., Morelli, K. A., Hon, O., et al. (2020). Dynamic interstitial cell response during myocardial infarction predicts resilience to rupture in genetically diverse mice. *Cell Rep.* 30, 3149.e6–3163.e6. doi: 10.1016/j.celrep.2020.02.008
- Fрати, G., Schirone, L., Chimenti, I., Yee, D., Biondi-Zoccai, G., Volpe, M., et al. (2017). An overview of the inflammatory signalling mechanisms in the myocardium underlying the development of diabetic cardiomyopathy. *Cardiovasc. Res.* 113, 378–388. doi: 10.1093/cvr/cvz011
- Guo, Y., Yu, Y., Hu, S., Chen, Y., and Shen, Z. (2020). The therapeutic potential of mesenchymal stem cells for cardiovascular diseases. *Cell Death Dis.* 11, 349. doi: 10.1038/s41419-020-2542-9
- Henderson, N. C., Rieder, F., and Wynn, T. A. (2020). Fibrosis: from mechanisms to medicines. *Nature* 587, 555–566. doi: 10.1038/s41586-020-2938-9
- Herrera, J., Henke, C. A., and Bitterman, P. B. (2018). Extracellular matrix as a driver of progressive fibrosis. *J. Clin. Invest.* 128, 45–53. doi: 10.1172/JCI93557
- Hulshoff, M. S., Del Monte-Nieto, G., Kovacic, J., and Krenning, G. (2019). Non-coding RNA in endothelial-to-mesenchymal transition. *Cardiovasc. Res.* 115, 1716–1731. doi: 10.1093/cvr/cvz211
- Lagares, D., and Hinz, B. (2021). Animal and human models of tissue repair and fibrosis: an introduction. *Methods*

FUNDING

IC was supported by grant # RG11916B85CDBF76 from Sapienza University of Rome. GM-N was supported by a Heart Foundation Future Leader Fellowship (102036) and Australian Research Council Discovery Project Grants (DP190101475, DP210102134). The Australian Regenerative Medicine Institute is supported by grants from the State Government of Victoria and the Australian Government. SS was generously supported by the British Heart Foundation (PG/16/93/32345).

- Mol. Biol.* 2299, 277–290. doi: 10.1007/978-1-0716-1382-5_20
- Lemos, D. R., and Duffield, J. S. (2018). Tissue-resident mesenchymal stromal cells: implications for tissue-specific antifibrotic therapies. *Sci. Transl. Med.* 10, ean5174. doi: 10.1126/scitranslmed.aan5174
- Mohenska, M., Tan, N. M., Tokolyi, A., Furtado, M. B., Costa, M. W., Perry, A. J., et al. (2021). 3D-cardiomics: a spatial transcriptional atlas of the mammalian heart. *J. Mol. Cell. Cardiol.* 163, 20–32. doi: 10.1016/j.yjmcc.2021.09.011
- Muhl, L., Genove, G., Leptidis, S., Liu, J., He, L., Mocci, G., et al. (2020). Single-cell analysis uncovers fibroblast heterogeneity and criteria for fibroblast and mural cell identification and discrimination. *Nat. Commun.* 11, 3953. doi: 10.1038/s41467-020-17740-1
- Pagano, F., Picchio, V., Chimenti, I., Sordano, A., De Falco, E., Peruzzi, M., et al. (2019). On the road to regeneration: “tools” and “routes” towards efficient cardiac cell therapy for ischemic cardiomyopathy. *Curr. Cardiol. Rep.* 21, 133. doi: 10.1007/s11886-019-1226-5
- Panahi, M., Vadgama, N., Kuganesan, M., Ng, F. S., and Sattler, S. (2018). Immunopharmacology of post-myocardial infarction and heart failure medications. *J. Clin. Med.* 7, 403. doi: 10.3390/jcm7110403
- Panizo, S., Martinez-Arias, L., Alonso-Montes, C., Cannata, P., Martin-Carro, B., Fernandez-Martin, J. L., et al. (2021). Fibrosis in chronic kidney disease: pathogenesis and consequences. *Int. J. Mol. Sci.* 22, 408. doi: 10.3390/ijms22010408
- Peruzzi, M., De Falco, E., Abbate, A., Biondi-Zoccai, G., Chimenti, I., Lotrionte, M., et al. (2015). State of the art on the evidence base in cardiac regenerative therapy: overview of 41 systematic reviews. *Biomed Res. Int.* 2015, 613782. doi: 10.1155/2015/613782
- Pesce, M., Messina, E., Chimenti, I., and Beltrami, A. P. (2017). Cardiac mechanoperception: a life-long story from early beats to aging and failure. *Stem Cells Dev.* 26, 77–90. doi: 10.1089/scd.2016.0206
- Plikus, M. V., Wang, X., Sinha, S., Forte, E., Thompson, S. M., Herzog, E. L., et al. (2021). Fibroblasts: Origins, definitions, and functions in health and disease. *Cell* 184, 3852–3872. doi: 10.1016/j.cell.2021.06.024
- Reinke, J. M., and Sorg, H. (2012). Wound repair and regeneration. *Eur. Surg. Res.* 49, 35–43. doi: 10.1159/000339613
- Sattler, S. (2017). The role of the immune system beyond the fight against infection. *Adv. Exp. Med. Biol.* 1003, 3–14. doi: 10.1007/978-3-319-57613-8_1
- Sattler, S., Fairchild, P., Watt, F. M., Rosenthal, N., and Harding, S. E. (2017). The adaptive immune response to cardiac injury—the true roadblock to effective regenerative therapies? *NPJ Regen Med.* 2, 19. doi: 10.1038/s41536-017-0022-3
- Schirone, L., Forte, M., Palmerio, S., Yee, D., Nocella, C., Angelini, F., et al. (2017). A review of the molecular mechanisms underlying the development and progression of cardiac remodeling. *Oxid. Med. Cell. Longev.* 2017, 3920195. doi: 10.1155/2017/3920195
- Spagnolo, P., Grunewald, J., and du Bois, R. M. (2014). Genetic determinants of pulmonary fibrosis: evolving concepts. *Lancet Respir. Med.* 2, 416–428. doi: 10.1016/S2213-2600(14)70047-5

Conflict of Interest: The authors declare that the research was conducted in the absence of any commercial or financial relationships that could be construed as a potential conflict of interest.

Publisher's Note: All claims expressed in this article are solely those of the authors and do not necessarily represent those of their affiliated organizations, or those of the publisher, the editors and the reviewers. Any product that may be evaluated in this article, or claim that may

be made by its manufacturer, is not guaranteed or endorsed by the publisher.

Copyright © 2022 Chimenti, Sattler, del Monte-Nieto and Forte. This is an open-access article distributed under the terms of the Creative Commons Attribution License (CC BY). The use, distribution or reproduction in other forums is permitted, provided the original author(s) and the copyright owner(s) are credited and that the original publication in this journal is cited, in accordance with accepted academic practice. No use, distribution or reproduction is permitted which does not comply with these terms.



BMPER Ameliorates Renal Fibrosis by Inhibiting Tubular Dedifferentiation and Fibroblast Activation

Ting Xie^{1†}, Zunen Xia^{2†}, Wei Wang^{3,4}, Xiangjun Zhou⁵ and Changgeng Xu^{6*}

¹ Department of Woman's Health Care, Maternal and Child Health Hospital of Hubei Province, Wuhan, China, ² Department of Clinical Laboratory, Renmin Hospital of Wuhan University, Wuhan, China, ³ Department of Urology, The First Affiliated Hospital of Anhui Medical University, Hefei, China, ⁴ Institute of Urology, Anhui Medical University, Hefei, China, ⁵ Department of Urology, Renmin Hospital of Wuhan University, Wuhan, China, ⁶ Department of Urology, The Central Hospital of Wuhan, Tongji Medical College, Huazhong University of Science and Technology, Wuhan, China

OPEN ACCESS

Edited by:

Susanne Sattler,
Imperial College London,
United Kingdom

Reviewed by:

George Bayliss,
Brown University, United States
Marie-Anne Mawhin,
Imperial College London,
United Kingdom

*Correspondence:

Changgeng Xu
smart_xcg2004@126.com

†These authors have contributed
equally to this work

Specialty section:

This article was submitted to
Molecular Medicine,
a section of the journal
Frontiers in Cell and Developmental
Biology

Received: 20 September 2020

Accepted: 08 January 2021

Published: 11 February 2021

Citation:

Xie T, Xia Z, Wang W, Zhou X and
Xu C (2021) BMPER Ameliorates
Renal Fibrosis by Inhibiting Tubular
Dedifferentiation and Fibroblast
Activation.
Front. Cell Dev. Biol. 9:608396.
doi: 10.3389/fcell.2021.608396

Tubulointerstitial fibrosis is both a pathological manifestation of chronic kidney disease and a driving force for the progression of kidney disease. A previous study has shown that bone morphogenetic protein-binding endothelial cell precursor-derived regulator (BMPER) is involved in lung fibrogenesis. However, the role of BMPER in renal fibrosis remains unknown. In the present study, the expression of BMPER was examined by real-time PCR, Western blot and immunohistochemical staining. The *in vitro* effects of BMPER on tubular dedifferentiation and fibroblast activation were analyzed in cultured HK-2 and NRK-49F cells. The *in vivo* effects of BMPER were dissected in unilateral ureteral obstruction (UUO) mice by delivery of BMPER gene via systemic administration of plasmid vector. We reported that the expression of BMPER decreased in the kidneys of UUO mice and HK-2 cells. TGF- β 1 increased inhibitor of differentiation-1 (Id-1) and induced epithelial mesenchymal transition in HK-2 cells, and knockdown of BMPER aggravated Id-1 up-regulation, E-cadherin loss, and tubular dedifferentiation. On the contrary, exogenous BMPER inhibited Id-1 up-regulation, prevented E-cadherin loss and tubular dedifferentiation after TGF- β 1 exposure. In addition, exogenous BMPER suppressed fibroblast activation by hindering Erk1/2 phosphorylation. Knockdown of low-density lipoprotein receptor-related protein 1 abolished the inhibitory effect of BMPER on Erk1/2 phosphorylation and fibroblast activation. Moreover, delivery of BMPER gene improved renal tubular damage and interstitial fibrosis in UUO mice. Therefore, BMPER inhibits TGF- β 1-induced tubular dedifferentiation and fibroblast activation and may hold therapeutic potential for tubulointerstitial fibrosis.

Keywords: tubulointerstitial fibrosis, BMPER, tubular dedifferentiation, fibroblast activation, signal transduction

BACKGROUND

Chronic kidney disease (CKD), unlike acute kidney injury, is manifested by a gradual decline in kidney function. The shared feature of CKD is tubulointerstitial fibrosis and glomerulosclerosis in tubular and glomerulus compartments (Ruiz-Ortega et al., 2020). Studies have shown that, compared with glomerulosclerosis, the degree of tubulointerstitial fibrosis can better reflect the impaired renal function (Boor and Floege, 2012). Tubulointerstitial fibrosis is not only a pathological appearance of CKD, but also

a driving force for the kidney disease progression (Herrera et al., 2018). Hence, strategies for ameliorating renal interstitial fibrosis could blunt kidney disease progression and improve kidney function. Although a variety of molecules have been found to regulate renal fibrosis in basic research, they have not been clinically used. Therefore, it is imperative to develop more effective treatment approaches for renal fibrosis.

Renal tubular cells are easily damaged and only have a certain ability to repair and regenerate. Persistent and repeated injury leads to maladaptive tubular repair and fibrosis, which destroy normal tissue structures (Qi and Yang, 2018). Incompletely epithelial cells repair lead to epithelial dedifferentiation, epithelial mesenchymal transition, and pro-fibrotic factors secretion, which induce fibroblast activation and proliferation (Gewin, 2018).

Renal fibroblasts are located in the renal interstitium and responsible for the production and degradation of extracellular matrix (ECM), maintaining physiological homeostasis and tubule repair after acute kidney injury. Under chronic kidney injury conditions, fibroblasts can be activated by pro-fibrotic cytokines and synthesize and secrete excessive ECM. Therefore, tubular maladaptive repair and fibroblast activation are two key processes in tubulointerstitial fibrosis, apart from tubulointerstitial inflammation. Simultaneous inhibition of tubular dedifferentiation and fibroblast activation may yield better anti-fibrosis effects. However, there is no such research yet.

In search for essential proteins for endothelial precursor cell differentiation, investigators discovered and identified bone morphogenetic protein-binding endothelial cell precursor-derived regulator (BMPER) (Moser et al., 2003). BMPER is recognized as a modulator for BMP signaling and its effect depends on BMP concentration (Kelley et al., 2009). Moreover, BMPER is a multifunctional molecule and implicated in blood vessel development, hematopoietic stem cells (HSC) maturation, endothelial barrier function and inflammation (Moser and Patterson, 2005; Helbing et al., 2017; Lockyer et al., 2017; McGarvey et al., 2017). Notably, BMPER promotes epithelial-mesenchymal transdifferentiation for heart cushions and participates in fibroblast activation and pulmonary fibrosis, indicating its function in fibrogenesis (Dyer et al., 2015; Huan et al., 2015). Our previous study has shown that BMPER expression decreased significantly in hydronephrotic kidneys (Yao et al., 2011). However, it is not clear whether BMPER is an active player in renal fibrosis.

In this study, by using *in vivo* unilateral ureteral obstruction (UUO) and *in vitro* TGF- β 1-induced renal fibrosis model, we found that BMPER regulated both tubular dedifferentiation and fibroblast activation, thereby affecting the process of renal fibrosis.

Abbreviations: BMPER, bone morphogenetic protein-binding endothelial cell precursor-derived regulator; UUO, unilateral ureteral obstruction; Id-1, inhibitor of differentiation-1; CKD, chronic kidney disease; ECM, extracellular matrix; HSC, hematopoietic stem cells; H&E, hematoxylin and eosin; PSR, picrosirius red; α -SMA, α -smooth muscle actin; LRP1, low-density lipoprotein receptor-related protein; EMT, epithelial mesenchymal transition; Erk1/2, extracellular regulated kinase 1/2.

MATERIALS AND METHODS

Materials and Reagents

Recombinant mouse BMPER (2299-CV-050) and recombinant human TGF- β 1 (240-B-010) were from R&D Systems (Minneapolis, MN, USA). The primary antibody sources were as follows: anti-collagen I (NB600-408) from NovusBio (CO, USA); anti-BMPER (ab75183), anti-Id-1 (ab230679), anti-fibronectin (ab2413) were from Abcam (Cambridge, UK); anti- α -smooth muscle actin (α -SMA) (ab124964) (BM0002), were from Abcam (Cambridge, UK) and Boshide (Wuhan, China), respectively; anti-E-cadherin (#3195) (20847-1-Ap), were from CST (Cell Signaling Technology, Beverly, MA) and Sanyin (Wuhan, China), respectively; anti-Erk1/2 (#4695), anti-p-Erk1/2 (#4370) from CST (Cell Signaling Technology, Beverly, MA); anti- β -actin (TDY051) from Tiandeyue (Beijing, China). HRP-goat anti-rabbit secondary antibody (AS-1107), CY3-labeled goat anti-mouse secondary antibody (AS-1111) and CY3-labeled goat anti-rabbit secondary antibody (AS-1109) were obtained from ASPEN (Wuhan, China). The BMPER expression plasmid was purchased from OriGene (MR210035) in which BMPER cDNA (NM_028472) was under control of a CMV6 promoter (pCMV6-BMPER). The empty expression plasmid vector pcDNA3 was from Invitrogen (San Diego, CA, USA).

Animals and Hydronephrotic Kidney Model

The Experimental Animal Center of Wuhan University provided Male C57BL/6 mice (body weight 18–20 g). Animals were group-housed in cages in the specific pathogen free animal room. The Institutional Animal Care and Use Committee at The Central Hospital of Wuhan approved and supervised the usage of mice. UUO and sham operation procedures were described previously (Chevalier et al., 2009). Briefly, mice were anesthetized with pentobarbital sodium (50 mg/kg) via intraperitoneal injection. The UUO model was constructed by ligating the left ureter, and the sham operation model was performed with the same surgical procedures without ureter ligation. To investigate the kidney localization and expression changes for BMPER, the mice were allocated into three groups with six mice in each group: (1) mice with sham-operation, (2) mice with 7-day UUO, (3) mice with 14-day UUO. To evaluate the therapeutic effect of exogenous BMPER on renal interstitial fibrosis, the mice were divided into three groups with six mice in each group: (1) mice with sham-operation, (2) seven-day UUO mice treated with empty expression plasmid pcDNA3, and (3) seven-day UUO mice treated with pCMV6-BMPER plasmid. A large number of plasmids were rapidly injected into the mouse circulation through the tail vein, as previously described (Yang et al., 2001a). In brief, 20 μ g of plasmid DNA was added to 1.6 ml of saline and injected into mice through the tail vein within 8–10 s. Mice were injected with pCMV6-BMPER plasmid 1 day before operation and 3 days after operation. Control UUO mice were injected with 20 μ g of empty vector pcDNA3 plasmid at the same time points in the same manner. All the mice were euthanized 7 or 14 days after UUO or sham operation. The cortex from half of the kidney was dissected and stored for mRNA and protein analysis, and the other half of the kidney

was fixed in 4% paraformaldehyde solution for histological and immunohistochemical examination.

Histological and Immunohistochemical Examination

Fixed kidney tissue was processed through a graded alcohol series, embedded in paraffin wax, and sectioned at 5 μ m. Picrosirius red (PSR) staining and hematoxylin and eosin (H&E) staining were operated based on described protocols (Sorensen et al., 2011). H&E staining was used to display tubular atrophy and interstitial expansion. The atrophic tubules were identified and appraised by a scoring system based on the percentage of atrophic tubules (0; 1, <25%; 2, 25–50%; 3, 50–75%; 4, >75%) (Zheng et al., 2019). PSR staining was used to evaluate collagen content. To assess the tubular atrophy and interstitial fibrosis, 20 microscopic fields under high power magnification (400 \times) were randomly selected. The ratio of the positive red area to the entire area was the percentage of fibrosis, which was calculated with Image J software (National Institute of Health, Bethesda, MD). IHC Tool Box plugin was used for PSR quantification. For immunohistochemistry, the kidney slides were incubated at 4 $^{\circ}$ C overnight with anti-collagen I antibody (1:100), anti-BMPER (1:100), anti-fibronectin antibody (1:100), anti- α -SMA antibody (1:200), and anti-E-cadherin antibody (1:100). The slides were then incubated with secondary antibody (1:5,000) and diaminobenzidine substrate. Finally, nuclei were counterstained with hematoxylin.

Real-Time Polymerase Chain Reaction (PCR)

Total RNA was extracted from frozen tissue or cultured cells using TRIzol (Invitrogen, Carlsbad, CA, USA). Reverse transcription was performed with FirstStrand cDNA synthesis kit (Thermo scientific, #K1621). Amplified cDNA was used as a template for PCR. Primers were synthesized from Sangon Biological Engineering Technology and Services (Shanghai, China), and specific primers were as follows: Forward 5'-AGGAC AGTGCTGCCCAATG-3' and Reverse 5'-TACTGACACGT CCCCTGAAAG-3' for human BMPER; Forward 5'-GGTGAA GGTGGTGTGAACG-3' and Reverse 5'-CTCGCTCCTG GAAGATGGTG-3' for human GAPDH. Forward 5'-GGTGC GCTGTGTTGTTTCATT-3' and Reverse 5'-TTCTCTCACG CACTGTGTCC-3' for mouse BMPER; Forward 5'-ATCAT CTCCGCCCTTCTG-3' and Reverse 5'-GGTCATGAGCC CTCCACAAC-3' for mouse GAPDH. Forward 5'-ACTGG GACGACATGGAAAAG-3' and Reverse 5'-CATCTCCAGA GTCCAGCACA-3' for rat α -SMA. Forward 5'-TGCTGAGTAT GTCGTGGAGTCTA-3' and Reverse 5'-AGTGGGAGTT GCTGTTGAAATC-3' for rat GAPDH. Specific primers were chosen from previous studies (Helbing et al., 2010; Zhang et al., 2010; Huan et al., 2015). A final reaction volume of 20 μ L sample was amplified according to the manufacturer's protocol (Takara Biotechnology, Japan). Real-time quantifications were carried out on the Prism 7500 SDS (Applied Biosystems, Thermo Fisher Scientific). The relative difference in mRNA expression between groups was calculated with the $\Delta\Delta$ Ct method.

Cell Culture and Treatment

HK-2 and NRK-49F cells were purchased from the American Type Culture Collection and were grown at 37 $^{\circ}$ C in Dulbecco's Modified Eagle's Medium (DMEM) with F12 (Gibco/Life Technologies, Grand Island, NY) supplemented with or without 10% fetal bovine serum (FBS) (Gibco/Life Technologies). When cells grew to about 60% confluence, they were used for *in vitro* experiments. To examine the effect of BMPER on epithelial cell dedifferentiation and fibroblast activation, cells were serum starved overnight and treated with designated amount of BMPER and recombinant TGF- β 1 (10 ng/mL for HK-2 or 2 ng/mL for NRK-49F) for the indicated time.

Cell Viability

Cell viability was measured using the 3-(4,5-dimethylthiazol-2-yl)-2,5-diphenyltetrazolium bromide (MTT) assay. HK-2 and NRK-49F cells were seeded at 1×10^4 cells/well in 96-well plates and exposed to BMPER at a final concentration of 5, 10, 20, 40, 80 nM. The cells were incubated with MTT solution (0.5 mg/ml) for 4 h at 37 $^{\circ}$ C. After MTT solution discarded, 100 μ L DMSO was added to each well. Complete dissolution of formazan by evenly shaking the 96-well plates and the optical density (OD) was measured at an absorbance wavelength of 570 nm.

Western Blot Analysis

Cells and kidney tissues were harvested and lysed with lysis buffer (Biyuntian, Wuhan, China). After the lysates were centrifuged at 12,000 \times g at 4 $^{\circ}$ C for 20 min, protein concentration was determined using a BCA kit (Biyuntian, Wuhan, China). A total of 20 μ g protein was detached on SDS-PAGE gel (Boshide, Wuhan, China) and transferred onto a nitrocellulose membrane (Merck-Millipore, Billerica, MA, USA). The blots were probed with the following primary antibodies overnight: anti-BMPER (1:500), anti-Id1 (1:1,000), anti-E-cadherin (1:1,000), anti- α -SMA (1:1,000), anti-fibronectin (1:500), anti-collagen I (1:500), anti-Erk1/2 (1:2,000), anti-p-Erk1/2 (1:1,000), and anti- β -actin (1:10,000). HRP-goat anti-rabbit secondary antibody (1:10,000) was used to conjugate primary antibodies. An enhanced chemiluminescence detection kit (GE Healthcare, Little Chalfont, UK) was used to visualize the bands.

Immunofluorescence Staining

HK-2 or NRK-49F cells were seeded on coverslips. Forty-eight hours after stimulated with TGF- β 1 and BMPER or TGF- β 1 and BMPER siRNA, the cells were fixed with 4% paraformaldehyde and stained with primary antibodies. For E-cadherin immunofluorescence staining, HK-2 cells were incubated with the anti-E-cadherin primary antibody (1:100). Subsequently, cells were incubated with CY3 labeled goat anti-rabbit secondary antibody (1:50). For α -SMA immunofluorescence staining, NRK-49F cells were incubated with anti- α -SMA primary antibody (1:200). Subsequently, cells were incubated with CY3 labeled goat anti-mouse secondary antibody (1:50). The fluorescent intensity of images was analyzed by Image J software in 10 randomly chosen, non-overlapping fields (magnification 400 \times) under a microscope. Mean = IntDen/Area.

Small RNA Interference

For silencing experiments, 25 pmol human BMPER siRNA (Cat. #AM16708, 127801, Thermo Fisher Scientific, Waltham, MA) and negative control siRNA (Cat. #1022076, Qiagen) were transfected into HK-2 cells using Lipofectamine 2000 (Invitrogen, Paisley, UK) in DMEM/F12 medium without serum and antibiotics. 20 pmol rat low-density lipoprotein receptor-related protein 1 (LRP1) siRNA (Cat. #4390771, s152487, Thermo Fisher Scientific, Waltham, MA) and negative control siRNA (Cat. #4390843 Thermo Fisher Scientific, Waltham, MA) were transfected into NRK-49F cells. After a 6-h transfection, the cells were supplemented with normal medium and cultured overnight, and then exposure to TGF- β 1 or BMPER for different times. In our pilot experiment, the treatment concentration used in this study has been optimized.

Statistical Analysis

All numerical results are presented as means \pm SEM. SPSS 18.0 software (SPSS Inc., Chicago, USA) was used for statistical analysis. Each group was compared by ANOVA and Tukey's *post-hoc* analysis. Statistical significance was defined as $P < 0.05$.

RESULTS

BMPER Is Down-regulated Under Stress Conditions

In our previous study, we have shown that BMPER is down-regulated in the hydronephrotic kidneys (Yao et al., 2011). In this study, we examined BMPER expression in UUO mice and HK-2 cells. First, we investigated the localization of BMPER protein in the sham-operated and obstructed kidney. Immunohistochemical staining indicated that BMPER was mainly located in renal tubular epithelial cells in the sham-operated kidneys. However, compared with sham controls, 7-day UUO resulted in decreased BMPER expression. Notably, BMPER was reduced in the dilated and degenerated tubules. Fourteen-day ureteral obstruction further reduced its expression (Figure 1A). This finding was verified by Western blot analysis and RT-qPCR (Figures 1B–D). These observations convincingly suggested that BMPER was related with the degeneration and dedifferentiation of the tubular cells. Then, to further evaluate the changes of BMPER expression *in vitro*, HK-2 cells were treated with TGF- β 1. After TGF- β 1 treatment, BMPER mRNA and protein expression was also decreased at various time points and different TGF- β 1 concentrations (Figures 1E–J). Therefore, BMPER levels by TGF- β 1 treatment were dosage- and time-dependent.

Endogenous BMPER Is Involved in Tubular Dedifferentiation

Epithelial mesenchymal transition (EMT) is an essential process in fibrosis and TGF- β 1 plays vital roles in EMT. A previous study has demonstrated that BMPER participates in EMT in heart cushions (Dyer et al., 2015). To assess whether BMPER is involved in EMT mediated by TGF- β 1, we examined the E-cadherin and α -SMA levels after BMPER down-regulation with siRNA knockdown in HK-2 cells. As shown in Figures 2A,B,D,E,

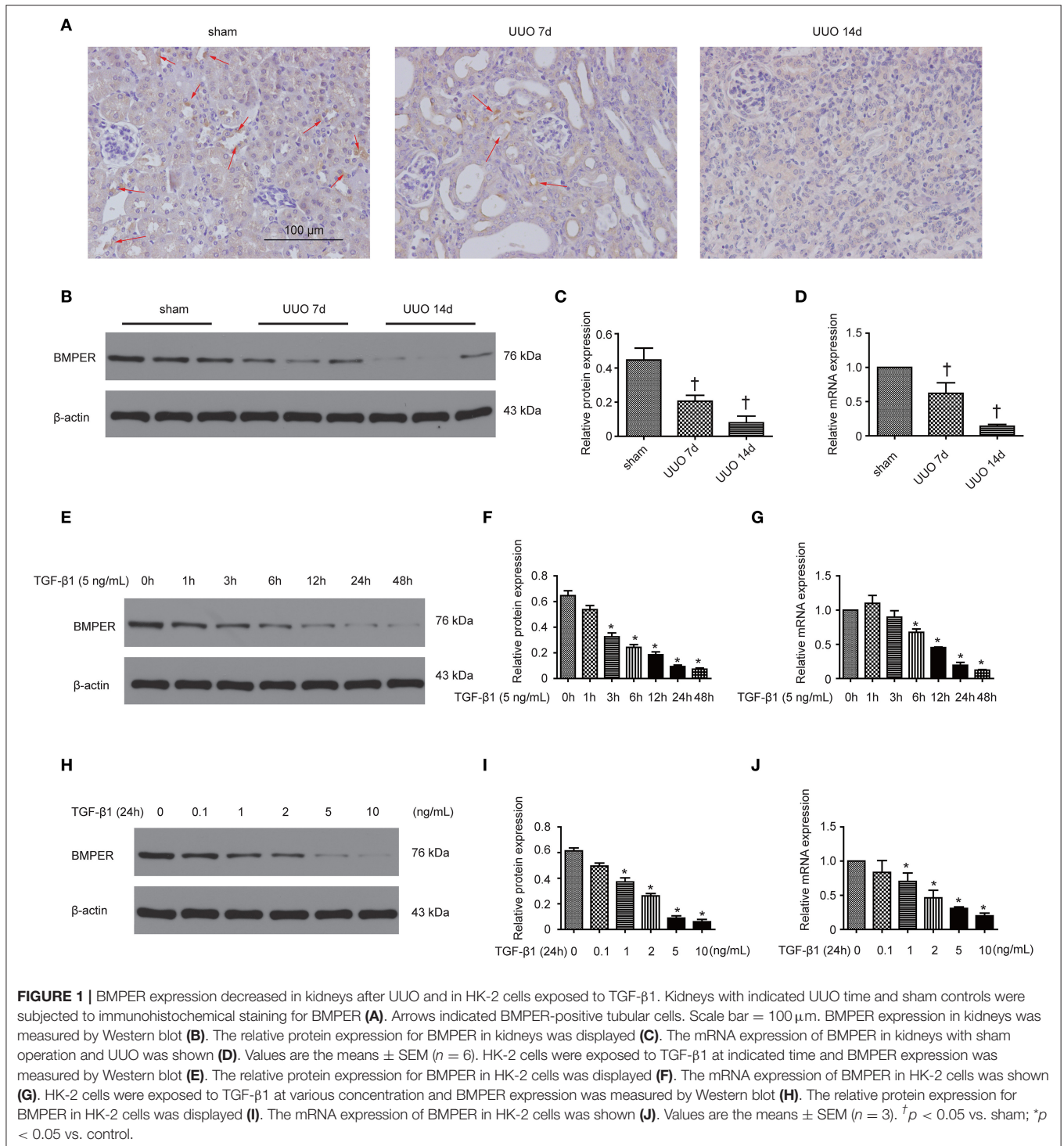
TGF- β 1 treatment led to EMT in HK-2 cells, as evidenced by decreased E-cadherin and increased α -SMA. BMPER knockdown led to decreased E-cadherin expression with TGF- β 1 exposure. However, α -SMA remained unchanged after BMPER knockdown and TGF- β 1 exposure compared with TGF- β 1 exposure alone. Meanwhile, TGF- β 1 treatment up-regulated Id1 in HK-2 cells and BMPER knockdown further increased Id1 (Figures 2A,C). Moreover, E-cadherin expression was examined in HK-2 cells by immunofluorescence study. Compared with the control group, tubular cells with BMPER knockdown showed trace E-cadherin staining after TGF- β 1 treatment (Figures 2E,G). Therefore, endogenous BMPER was involved in tubular dedifferentiation but not EMT, accompanied by increase in Id1.

Exogenous BMPER Inhibits Tubular Dedifferentiation

For investigating the function of BMPER in tubular cells, we studied the phenotypic change after BMPER treatment in HK-2 cells. HK-2 cells were treated with BMPER at various concentrations. Cell viability was examined by MTT assay. BMPER with 5 to 80 nM dose did not affect cell viability (Figure 3A). Therefore, 80 nM of BMPER was used *in vitro* experiments. As shown in Figures 3B–E, BMPER alone did not affect E-cadherin and α -SMA levels. TGF- β 1 treatment led to EMT in HK-2 cells. However, BMPER inhibited TGF- β 1-mediated E-cadherin loss in a dose-dependent style, without α -SMA change. BMPER alone resulted in a slight increase in Id1, but this change did not achieve statistical difference. BMPER prevented an increase in Id1 induced by TGF- β 1 (Figures 3B–E). Immunofluorescence staining for E-cadherin verified this finding (Figures 3E,G). Notably, the difference in E-cadherin expression was not due to the changed cell density after diverse treatments, because any kinds of treatment could not significantly alter HK-2 cell counts (Figure 3H). Therefore, exogenous BMPER inhibited tubular dedifferentiation but not EMT.

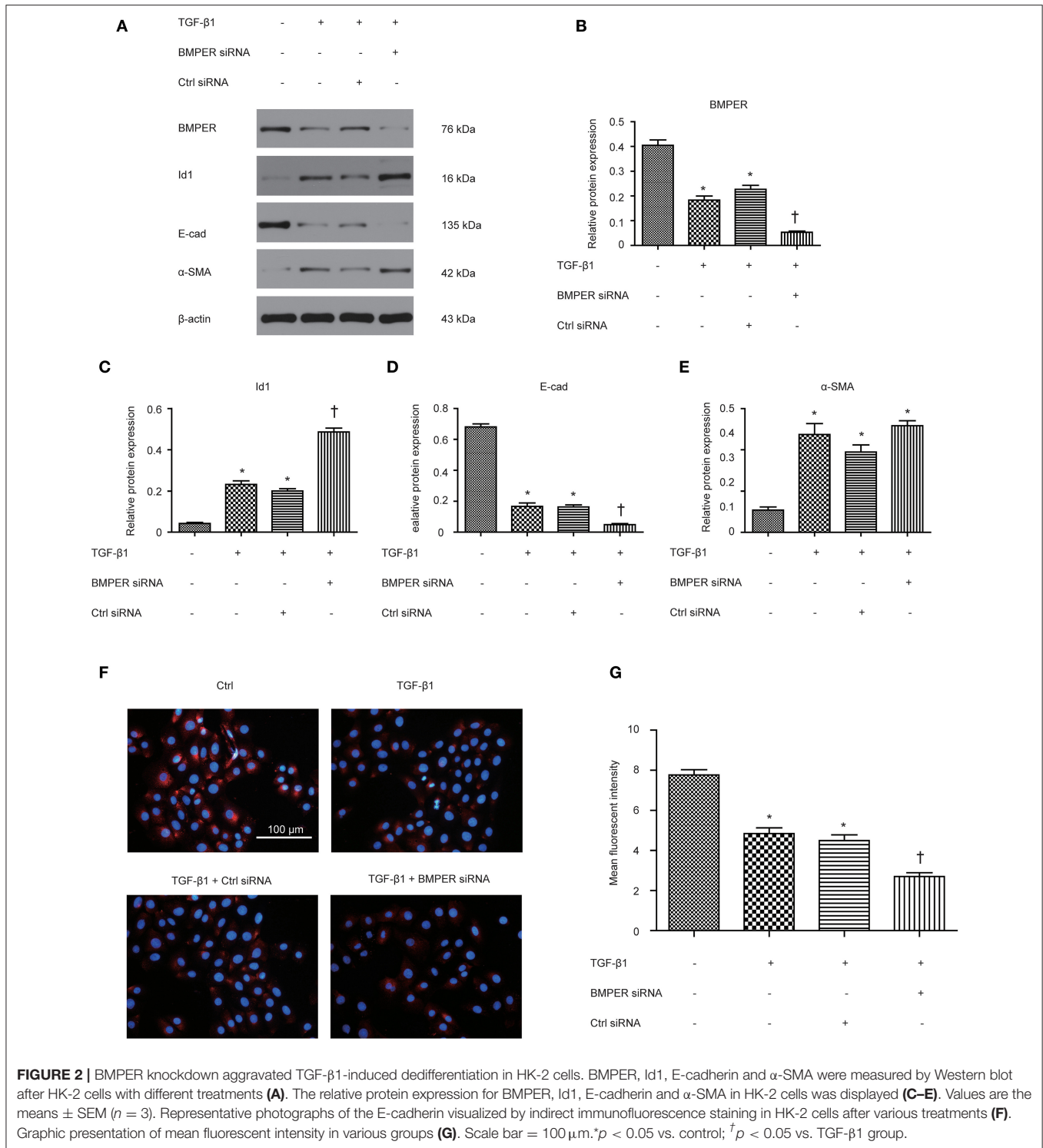
Exogenous BMPER Prevents Fibroblast Activation via Inhibiting Erk1/2 Phosphorylation

The transition of fibroblast into myofibroblast promotes the development of fibrosis, and various cytokines participate in this process. Blockage of fibroblast activation can attenuate or reverse fibrotic diseases. NRK-49F cells were exposure to BMPER of various concentrations. Cell viability was examined by MTT assay. BMPER with 5 to 80 nM dose did not affect cell viability (Figure 4A). As illustrated in Figure 4B, a dramatic increase in α -SMA in NRK-49F cells after 2 ng/mL TGF- β 1 treatment for 24 h. BMPER alone did not change α -SMA expression. However, BMPER could abolish the increase in α -SMA elicited by TGF- β 1 treatment (Figures 4B–D). The decreased α -SMA was accompanied by diminished collagen I production (Figures 4E,F). We further examined α -SMA expression in NRK-49F cells via immunofluorescence study. As shown in Figures 4G,H, compared with control groups, BMPER posed an inhibitory effect on up-regulation of α -SMA caused by TGF- β 1. Meanwhile, the difference in α -SMA expression



was not due to an altered cell number after diverse treatments, because neither treatment modalities significantly affected NRK-49F cell counts (Figure 4I). Therefore, exogenous BMPER could prevent fibroblast activation. Erk1/2 phosphorylation in fibroblast plays an important role in the process of fibrosis.

We determined if exogenous BMPER could affect Erk1/2 phosphorylation. As shown in Figures 5A,B, a notable increase in Erk1/2 phosphorylation after a 15 min-TGF- β 1 treatment. However, BMPER prevented the Erk1/2 phosphorylation elicited by TGF- β 1 in a dose-dependent manner. BMPER alone had



no effect on Erk1/2 phosphorylation 15 mins after treatment. BMPER also exhibited time-dependent inhibitory effect on Erk1/2 phosphorylation elicited by TGF-β1 (Figures 5C,D). Together, BMPER prevented fibroblast activation via inhibiting Erk1/2 phosphorylation in fibroblast.

The Inhibitory Effect of BMPER on Fibroblast Activation Is Dependent of LRP1
LRP1 is a cell surface receptor which controls tissue remodeling in several organs (Wujak et al., 2018). LRP1 is also located in fibroblast membrane and engaged in fibrogenesis. We

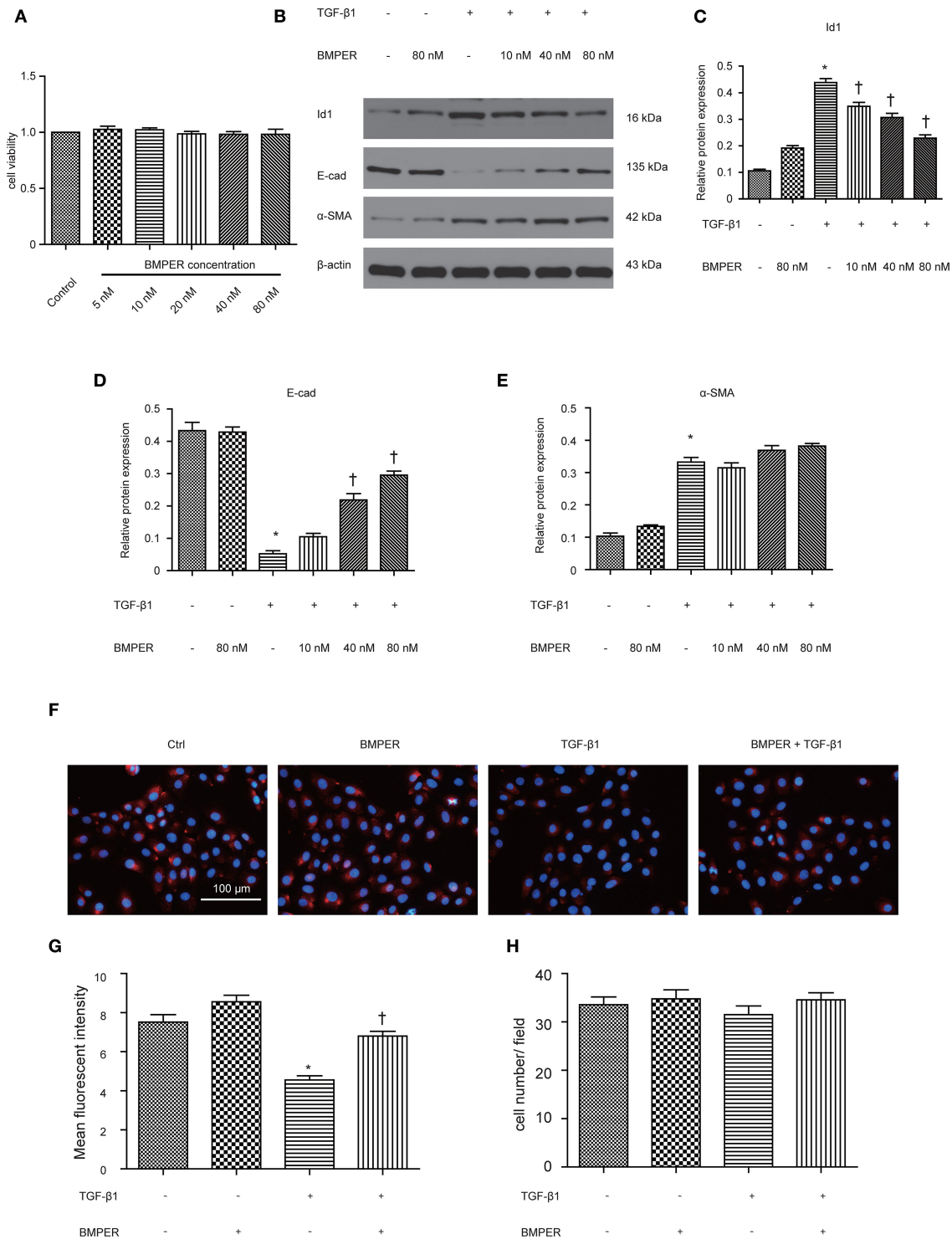


FIGURE 3 | Exogenous BMPER inhibited TGF-β1-induced dedifferentiation in HK-2 cells. HK-2 cells were incubated with increasing amounts of BMPER (5–80 nmol), and cell viability was detected by MTT (A). HK-2 cells were treated with 10 ng/ml TGF-β1 and increasing amounts of BMPER as indicated for 48 h, and the protein expression for Id1, E-cadherin and α-SMA was measured by Western blot (B). The relative protein expression for Id1, E-cadherin and α-SMA in HK-2 cells was displayed (C–E). Values are the means ± SEM (n = 3). Representative photographs for E-cadherin in HK-2 cells after various treatments were displayed by immunofluorescence staining (F). Graphic presentation of mean fluorescent intensity in various groups (G). Neither treatment modalities significantly affected HK-2 cell counts (H). Cell numbers were counted after various treatments for 48 h. Scale bar = 100 μm. *p < 0.05 vs. control; †p < 0.05 vs. TGF-β1 group.

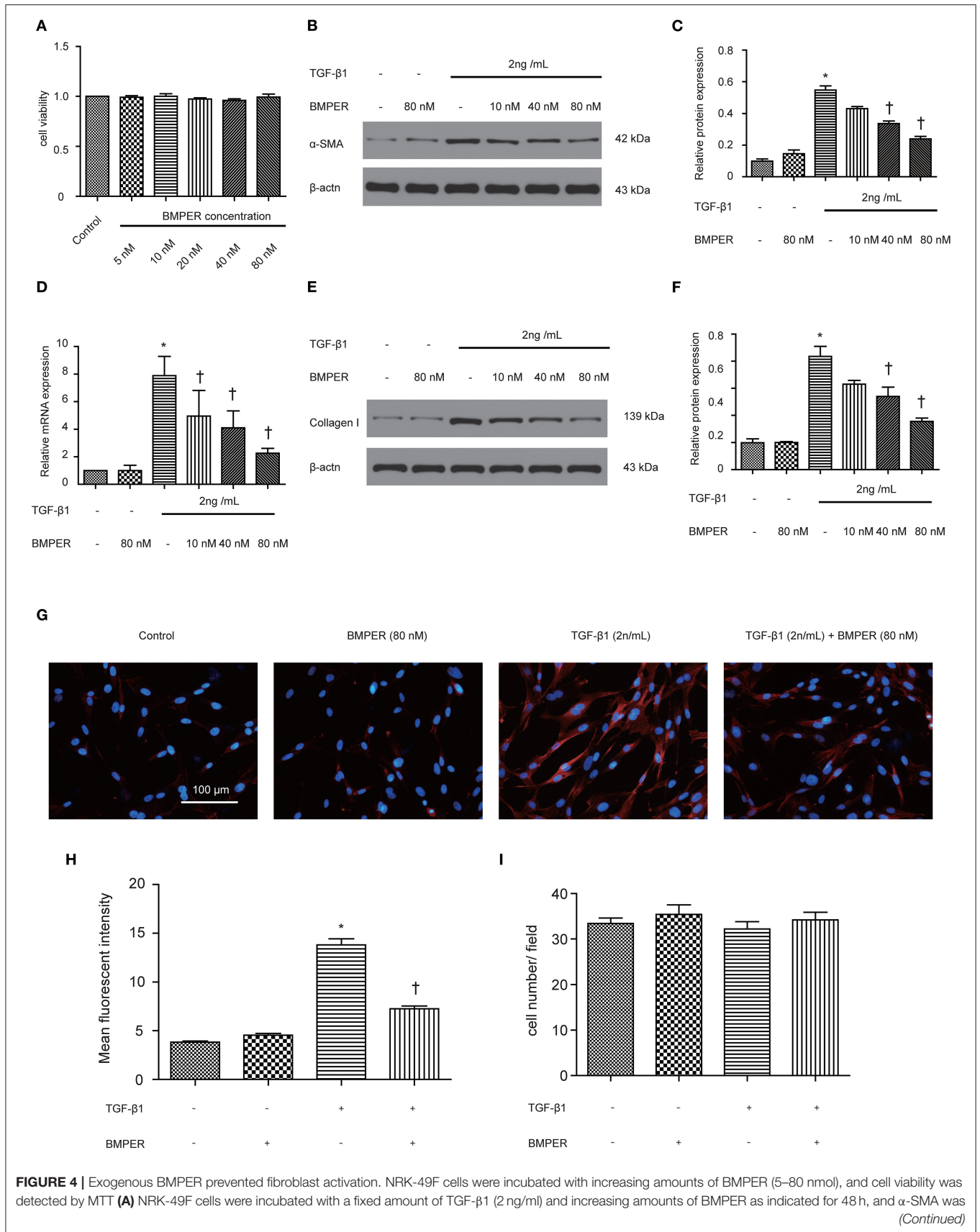
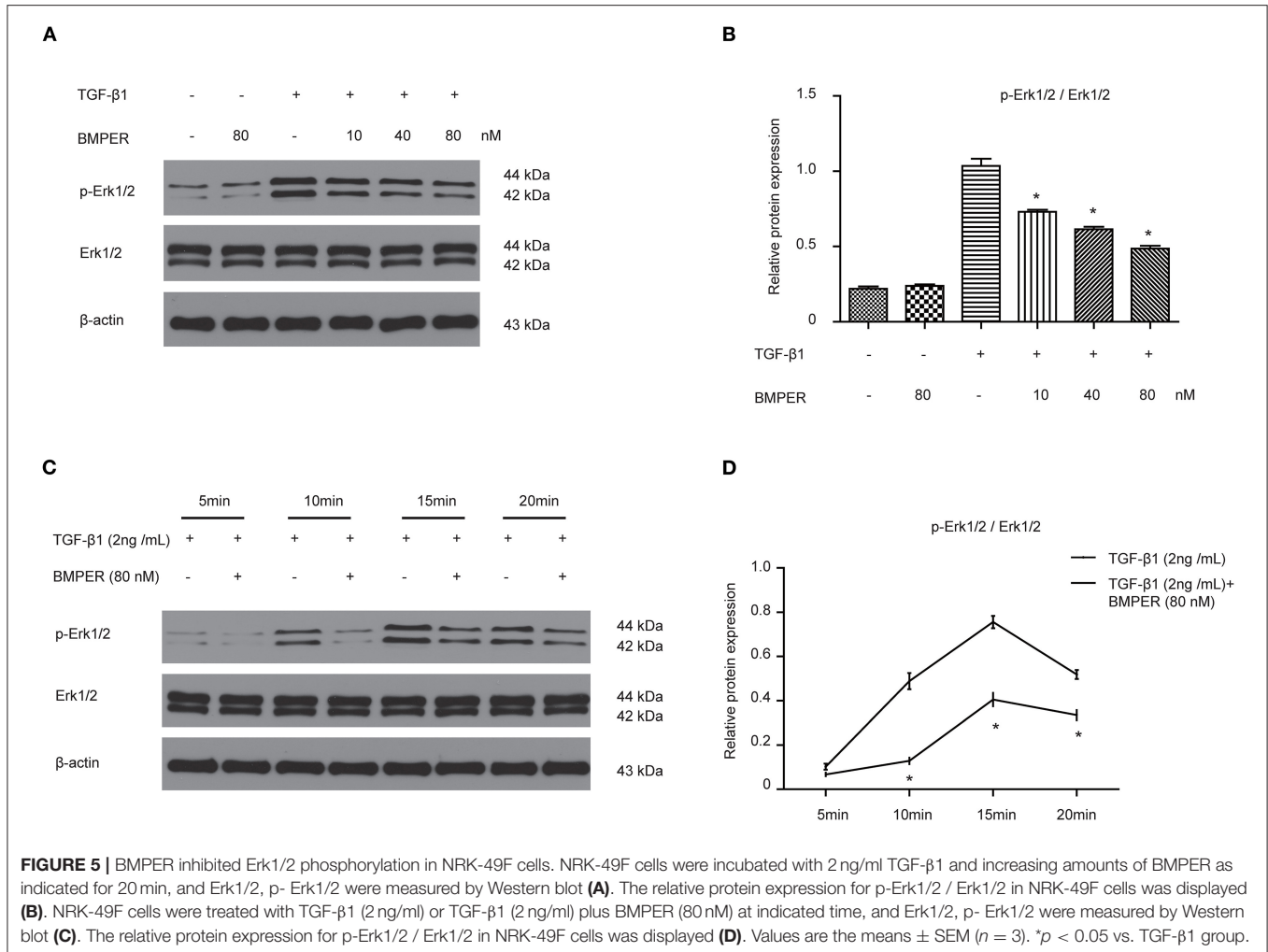


FIGURE 4 | measured by Western blot (**B**). The relative protein expression for α -SMA in NRK-49F cells was displayed (**C**). The relative mRNA expression for α -SMA in NRK-49F cells was shown (**D**). Collagen I was measured by Western blot (**E**) and the relative protein expression for collagen I (**F**). Values are the means \pm SEM ($n = 3$). Representative photographs for α -SMA in NRK-49F cells after various treatments were displayed by immunofluorescence staining (**G**). Graphic presentation of mean fluorescent intensity in various groups (**H**). Neither treatment modalities significantly affected NRK-49F counts. Cell numbers were counted after various treatments for 48 h (**I**). Scale bar = 100 μ m. * $p < 0.05$ vs. control; † $p < 0.05$ vs. TGF- β 1 group.

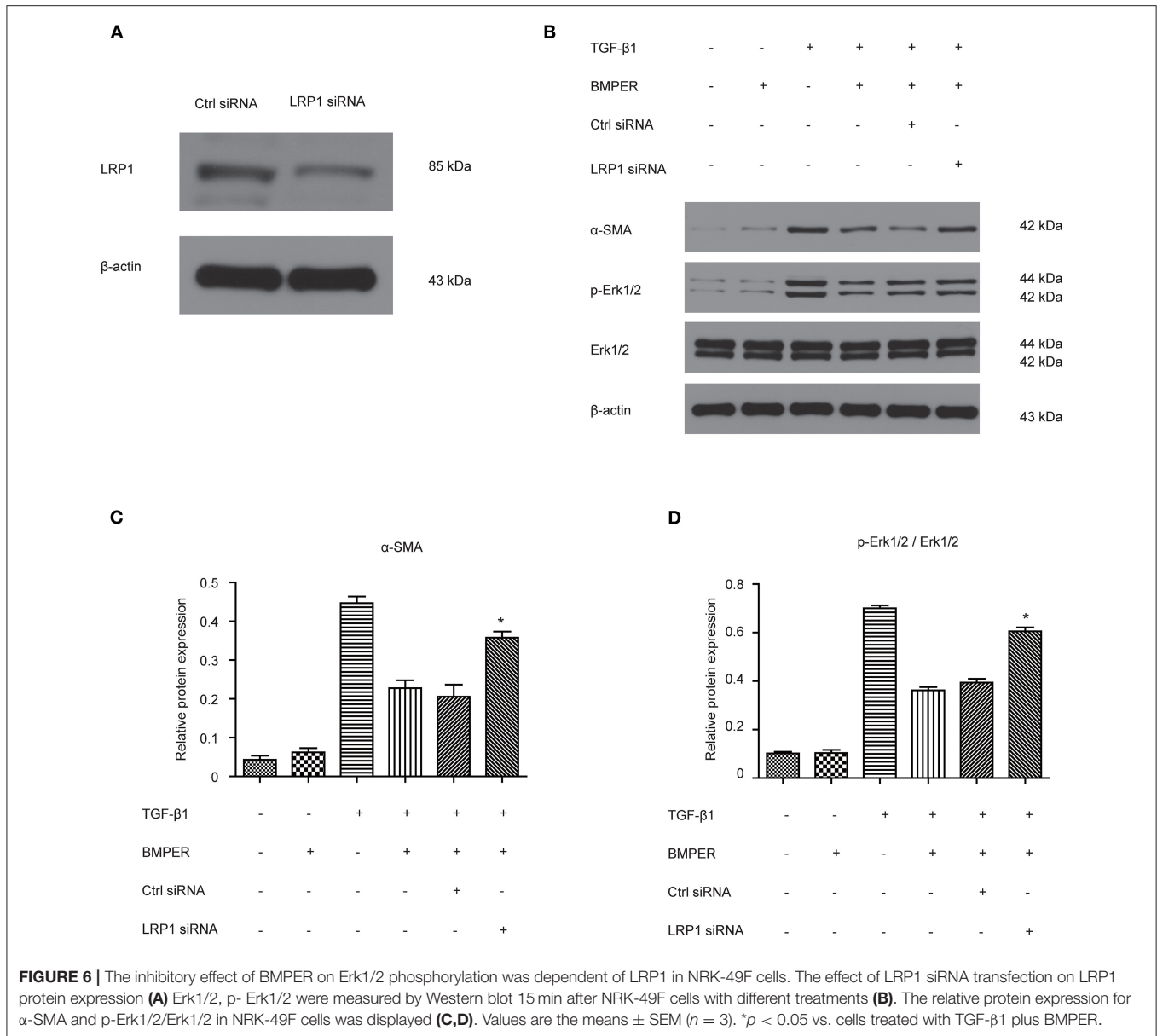


determined if LRP1 was responsible for inhibitory effect of BMPER on fibroblast activation. The result showed LRP1 siRNA transfection led to decreased LRP1 level (**Figure 6A**). As shown in **Figures 6B–D**, TGF- β 1 elicited an increase in Erk1/2 phosphorylation and α -SMA. However, LRP1 knockdown abrogated the inhibitory effect of BMPER on Erk1/2 phosphorylation and α -SMA. These findings suggested that the inhibitory effect of BMPER on fibroblast activation was dependent of LRP1.

Exogenous BMPER Attenuates Renal Fibrosis in UUO Mice

In view of the inhibitory effects of BMPER on tubular dedifferentiation and fibroblast activation, two essential processes in renal fibrosis, we determined if BMPER could attenuates

renal fibrosis *in vivo*. To deliver exogenous BMPER to the injured kidney, we injected plasmid encoding mouse BMPER cDNA by tail vein using a hydrodynamic gene transfer technique, as previously described (Yang et al., 2001b). Compared with sham-operated mice, UUO induced decrease in BMPER expression. However, BMPER gene transfer restored BMPER level (**Figures 7A,B**). Immunohistochemical staining showed increased expression of BMPER after hydrodynamic based gene transfer, especially in tubules (**Figure 7C**). BMPER ameliorated tubule atrophy and interstitial fibrosis, which were assessed by H&E and PSR staining, respectively (**Figure 8**). Furthermore, immunohistochemical staining displayed that UUO up-regulated the expression of fibronectin, collagen I, and α -SMA and decreased E-cadherin level. However, BMPER corrected these changes (**Figure 9A**). Western blot



analysis corroborated these findings (Figures 9B–F). Meanwhile, UUO promoted Erk1/2 phosphorylation, and BMPER inhibited this process (Figures 9G,H). Collectively, exogenous BMPER attenuated renal fibrosis in UUO mice.

DISCUSSION

BMPER, as a regulator of BMP signaling, is implicated in blood vessel development, vascular inflammation, HSC maturation and lung fibrosis (Huan et al., 2015; Lockyer et al., 2017; McGarvey et al., 2017; Esser et al., 2018). The findings in the present study demonstrated that BMPER was dramatically down-regulated in both UUO mice and HK-2 cells. BMPER could inhibit tubular dedifferentiation and fibroblast activation. In addition, up-regulation of BMPER could ameliorate tubulointerstitial fibrosis

in the kidneys of UUO mice. Therefore, BMPER holds the promise to be a new anti-fibrotic agent.

A previous study has shown that BMPER was decreased in hydronephrotic kidneys from human specimen with serious interstitial fibrosis (Yao et al., 2011). This finding promoted us to seek if BMPER is implicated in renal fibrogenesis and, if so, the underlying mechanism. Among kidney cells, tubular cell was one of the main cell types expressing BMPER. Immunohistochemistry staining showed that 7-day UUO resulted in diminished level of BMPER, especially in dilated and degenerative tubules, which indicated alteration in the kidney microenvironment induced by ureteral obstruction affected its level. Therefore, we examined if TGF-β1, a prominent pro-fibrotic cytokine in kidney after UUO, could suppressed the expression of BMPER. As expected, TGF-β1 could down-regulate

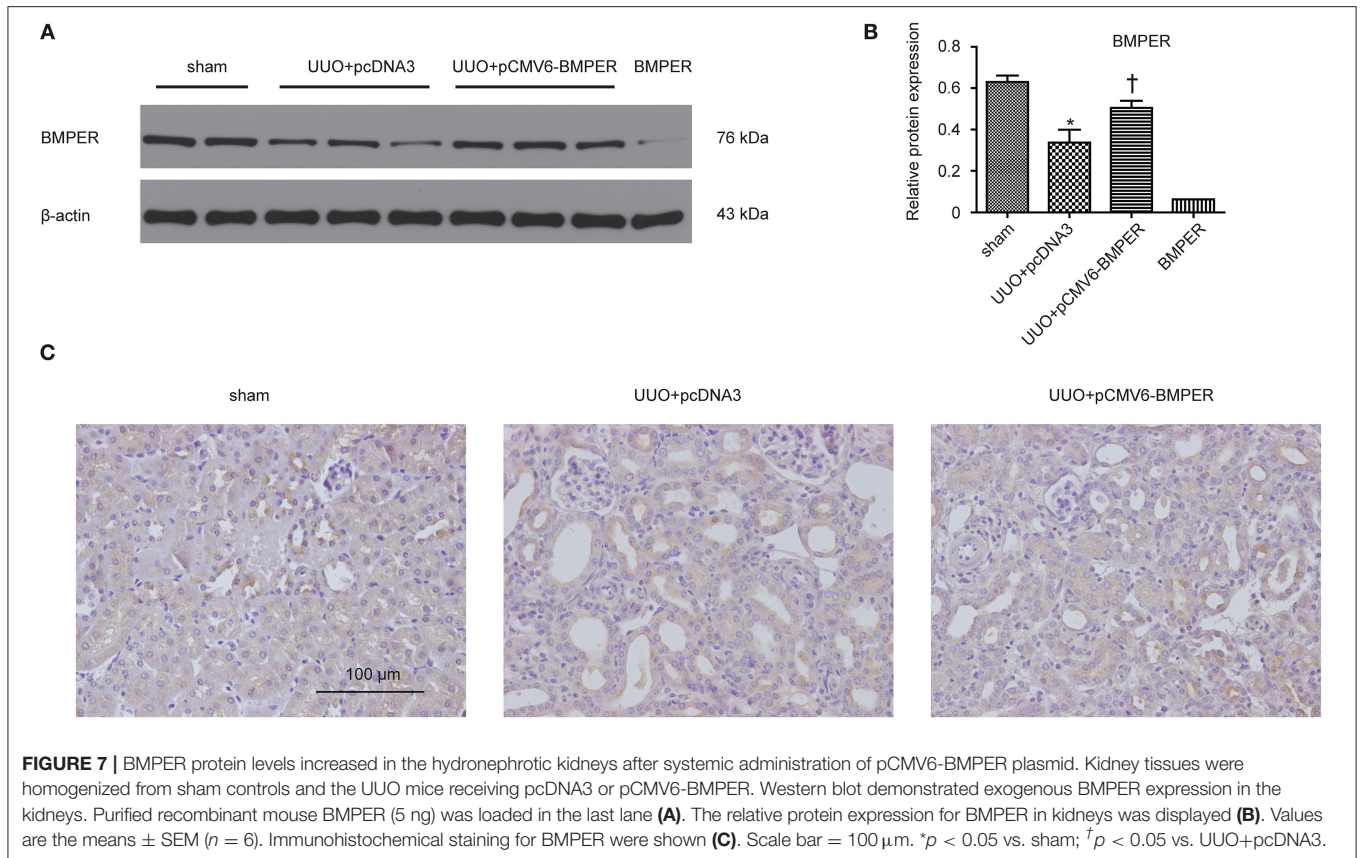


FIGURE 7 | BMPER protein levels increased in the hydronephrotic kidneys after systemic administration of pCMV6-BMPER plasmid. Kidney tissues were homogenized from sham controls and the UUO mice receiving pcDNA3 or pCMV6-BMPER. Western blot demonstrated exogenous BMPER expression in the kidneys. Purified recombinant mouse BMPER (5 ng) was loaded in the last lane (A). The relative protein expression for BMPER in kidneys was displayed (B). Values are the means \pm SEM ($n = 6$). Immunohistochemical staining for BMPER were shown (C). Scale bar = 100 μ m. * $p < 0.05$ vs. sham; † $p < 0.05$ vs. UUO+pcDNA3.

BMPER in a time- and dosage-dependent style. These findings suggest that BMPER may be a regulator for fibrogenesis caused by TGF- β 1.

BMPER, initially was identified as a regulator of vascular and blood cell development, could promote epithelial mesenchymal transition for developing heart cushions (Dyer et al., 2015). Epithelial mesenchymal transition poses an essential role in organ development, fibrosis, and tumor metastasis, and has a relatively conservative molecular mechanism in the three processes (Quaggin and Kapus, 2011). Hence, we assumed that BMPER could affect epithelial mesenchymal transition in renal fibrosis induced by UUO mice. TGF- β 1-stimulated HK-2 cells showed increased α -SMA and diminished E-cadherin, indicating EMT in HK-2 cells after TGF- β 1 exposure. Endogenous BMPER knockdown aggravated E-cadherin loss in TGF-treated HK-2 cells, and exogenous BMPER restored E-cadherin, without changes in α -SMA after TGF- β 1 treatment. These findings suggested BMPER could inhibit tubular dedifferentiation, not EMT. These results were verified by E-cadherin immunofluorescence staining. EMT can be divided into several stages (Liu, 2009). Epithelial cell dedifferentiation, a type of sublethal injury, manifested by loss of epithelial junction molecules, may be the basic event for renal tubular cells to undergo mesenchymal transition (Gwon et al., 2020). E-cadherin is an adhesion receptor between epithelium, which plays vital roles in maintaining epithelium differentiation. Loss

of E-cadherin will inevitably cause tubular epithelial cells to lose polarity. Matrix metalloproteinase could disrupt E-cadherin. Loss of E-cadherin promotes the mesenchymal gene expression, and the transcriptional repression of epithelial junction molecule in tubular epithelial cells (Zheng et al., 2009). The data in this study strengthen the significance of BMPER in maintenance of epithelial polarity.

Multiple signaling molecules and pathways regulate the dedifferentiation of epithelial cells. For example, Src families regulate dedifferentiation of tubular cell by activating EGFR/PI3K signaling (Zhuang et al., 2012). Epidermal growth factor receptor (EGFR) activation is necessary for cellular dedifferentiation after injury. Dedifferentiation process is characterized by increased expression of vimentin, decreased expression of E-cadherin, and loss of polarity (Hallman et al., 2008). Inhibitor of differentiation-1 (Id-1), a transcriptional inhibitor, drives tubular epithelial cell dedifferentiation (Li et al., 2007). BMPER impairs proliferation, migration, invasion in lung tumor cell by up-regulation of Id1 (Heinke et al., 2012). Therefore, we assumed that BMPER affected the dedifferentiation of epithelial cells through Id1. As expected, TGF- β 1 could induce increase in Id1, and endogenous BMPER knockdown further increased Id1 in TGF- β -treated HK-2 cells. Meanwhile, exogenous BMPER could decrease Id1, accompanied by E-cadherin changes in HK-2 cells after TGF- β 1 exposure. These findings indicate that BMPER inhibited dedifferentiation

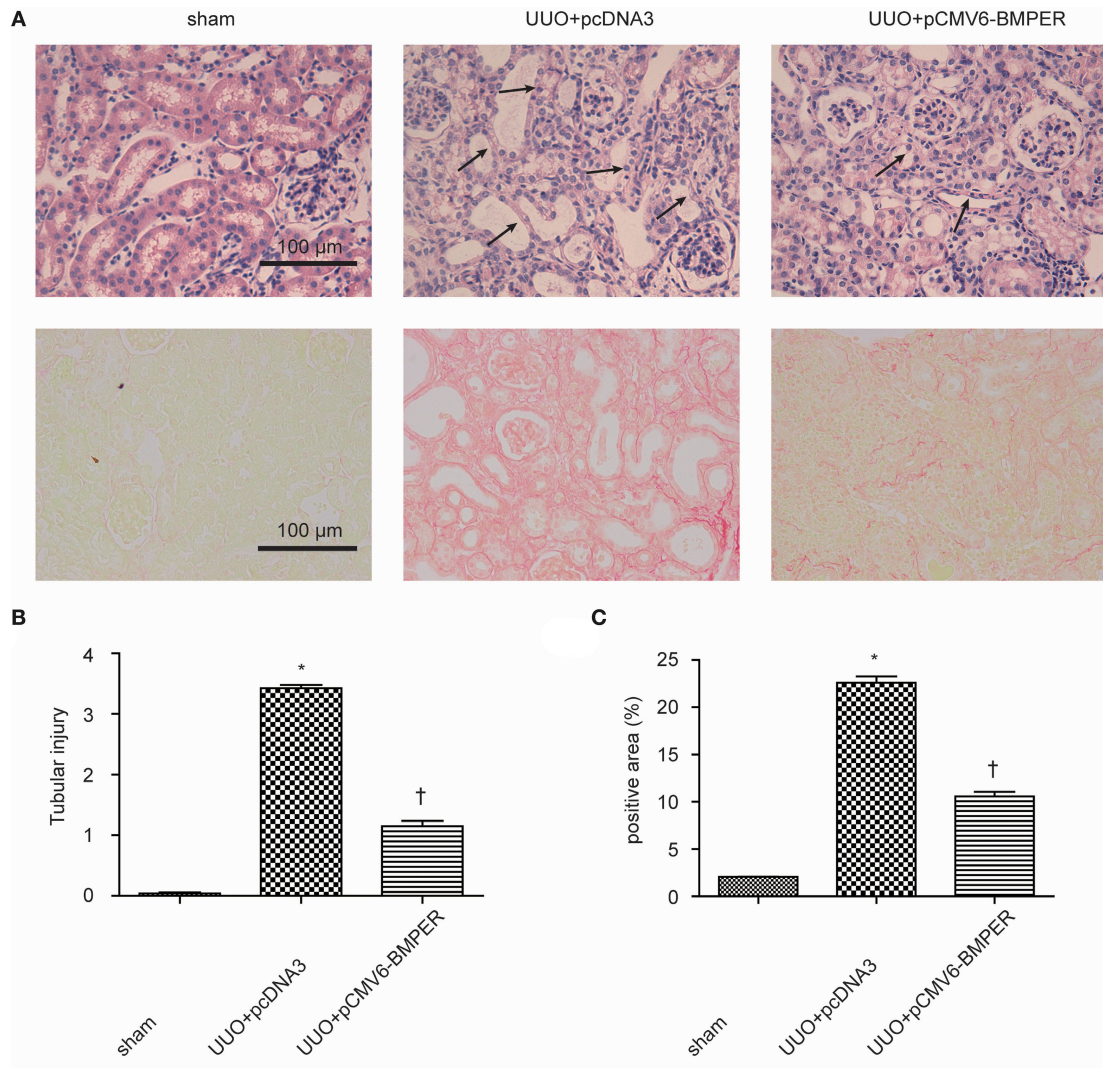


FIGURE 8 | BMPER ameliorated tubule atrophy and interstitial fibrosis. H&E staining showed BMPER ameliorated tubular injury [upper panel of (A)]. Arrows indicated tubular atrophy. PSR staining showed BMPER decreased interstitial fibrosis [lower panel of (A)]. Semi-quantitative analysis for tubule atrophy and interstitial fibrosis were shown in (B,C), respectively. Scale bar = 100 μm. Values are the means ± SEM ($n = 6$). * $p < 0.05$ vs. sham; † $p < 0.05$ vs. UUO+pcDNA3.

of epithelial cells induced by TGF- β 1 through Id1. Besides tumor cell and epithelium, Id1 is also a functional regulator in other cells. BMPER regulates endothelial barrier function by antagonizing BMP4-Smad5-Id1 signaling (Helbing et al., 2017). In lung epithelium, BMPER inhibits BMP activity by antagonizing BMP2-Id1 signaling and preventing decrease of E-cadherin mediated by BMP2, therefore, maintaining the integrity of the epithelium (Helbing et al., 2013). All the results indicate the universality of suppressive effect of BMPER on Id1 signals under various cellular environments.

In normal kidneys, a small number of fibroblasts are quiescent. Upon activation by profibrotic cytokines, fibroblasts acquire a myofibroblast phenotype, express α -SMA, and generate large amounts of ECM components. Activated fibroblasts may be derived from various sources through different mechanisms,

including fibroblasts and pericytes activation, tubular epithelial cells transdifferentiation, and circulating fibrocytes recruitment (Mack and Yanagita, 2015). Despite different sources, fibroblast activation is the basis for production of excessive extracellular matrix. BMPER mediates lung fibroblast activation *in vitro* and lung fibrosis in mice *in vivo* (Huan et al., 2015). Therefore, we asked if BMPER was involved in renal fibrosis by affecting fibroblast activation. As expected, BMPER could dose-dependently inhibit rat kidney fibroblast activation, which was displayed by immunofluorescence staining and Western blot for α -SMA.

The extracellular regulated kinase 1/2 (Erk1/2) pathway is activated in the process of renal fibrosis and is related to the differentiation and increased number of renal fibroblasts. For example, Erk1/2 activation was identified in α -SMA-positive

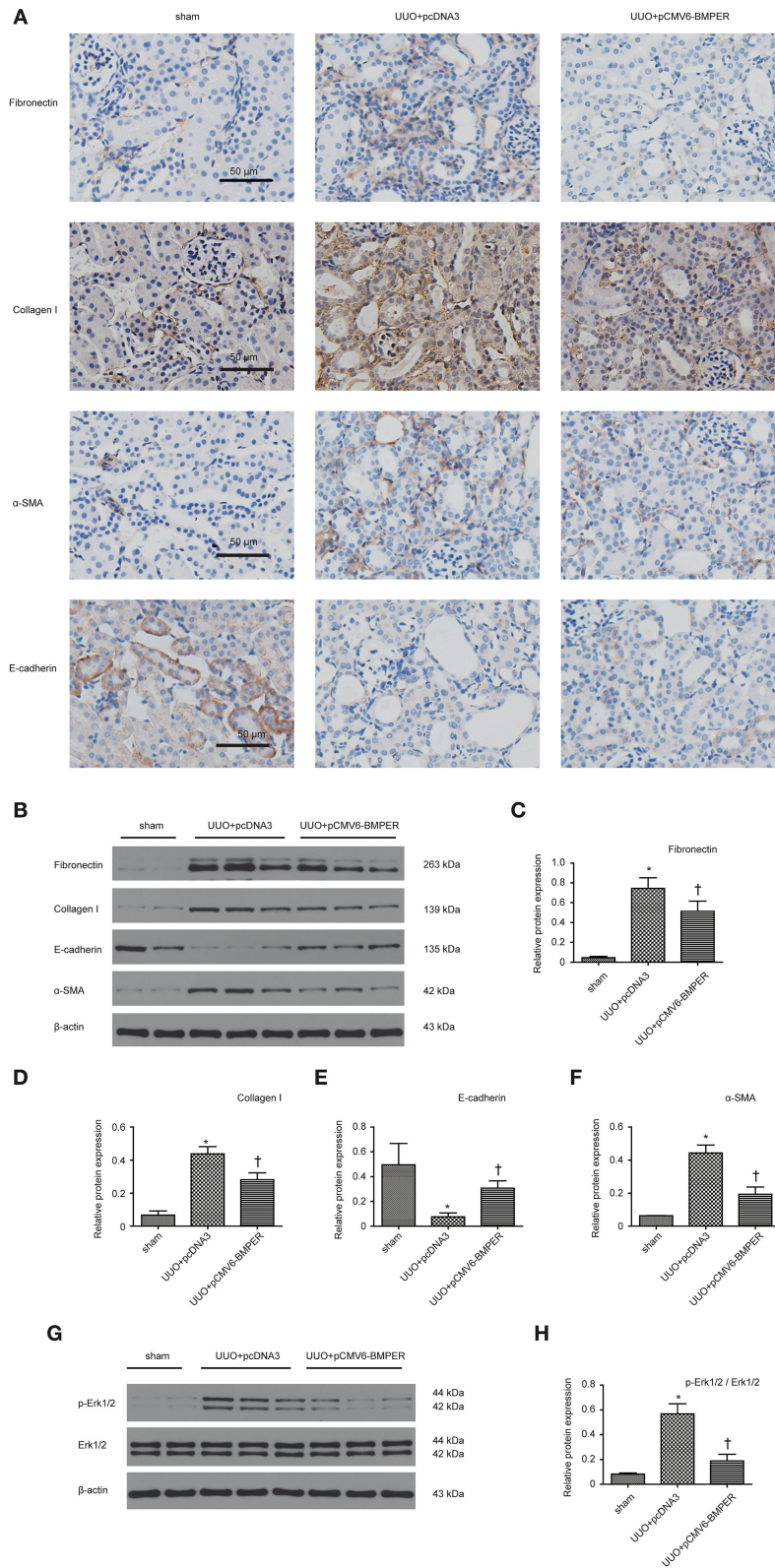


FIGURE 9 | BMPER changed levels of fibrosis-related indicators. Immunohistochemical staining for fibronectin, collagen I, E-cadherin and α -SMA in kidneys was displayed (A). Protein expression for fibronectin, collagen I, E-cadherin and α -SMA in kidneys was measured by Western blot (B). The relative protein expression for fibronectin, collagen I, E-cadherin and α -SMA in kidneys was displayed (C–F). Erk1/2 and p- Erk1/2 were measured by Western blot (G). The relative protein expression for p-Erk1/2 / Erk1/2 in kidneys was displayed (H). Scale bar = 50 μ m. Values are the means \pm SEM ($n = 6$). * $p < 0.05$ vs. sham; † $p < 0.05$ vs. UUO+pcDNA3.

fibroblasts in kidney biopsy specimen (Masaki et al., 2004). Erk1/2 activation has also been involved in IL-11 and TGF- β 1-induced activation of fibroblasts mediated by NADPH oxidase (Bondi et al., 2010; Schafer et al., 2017). Moreover, inhibition of Erk1/2 blunts the expansion of fibroblasts upon renal fibrosis (Andrikopoulos et al., 2019). Given the importance of Erk1/2 in renal fibrogenesis, we explored whether it mediated the inhibitory effect of BMPER on fibroblast activation. Our *in vitro* results demonstrated that BMPER could dose- and time-dependently suppress Erk1/2 activation in NRK-49F. Our *in vivo* findings revealed that BMPER could suppress Erk1/2 activation in the whole kidney lysis. In tubular cells, TGF- β 1-treatment resulted in an increased Erk1/2 activation, but BMPER failed to prevent this process (data not shown). Therefore, the inactivation of Erk1/2 was a fundamental signaling events of BMPER effects on renal interstitial cells. These findings are in agreement with previous results. Trametinib, by inhibiting the Erk1/2 pathway, not only hinders TGF- β 1-stimulated renal fibroblast activation, but also improves renal fibrosis in UUO mice (Andrikopoulos et al., 2019). Therefore, anti-fibrotic effect of BMPER may be explained, at least in part, via inhibiting Erk1/2 activation.

LRP1 is a ubiquitously expressed cell receptor protein that regulates the physiological and pathological inflammatory responses to control tissue remodeling in multiple organs (Wujak et al., 2018). High amounts of LRP1 are detected in various tissues and organs, such as in the liver, brain, kidney, and lung (Wujak et al., 2018). LRP1 can improve liver fibrosis by modulating hepatic stellate cells proliferation and migration (Kang et al., 2015). LRP1 also mediates anti-apoptotic effect of tissue-type plasminogen activator (tPA), a serine protease known for producing plasmin, in renal fibroblasts and myofibroblasts (Hu et al., 2008). These studies demonstrate diverse physiological functions, and document the involvement of LRP1 in tissue injury and repair. In our study, LRP1 knockdown abrogated the inhibitory effect of BMPER on Erk1/2 phosphorylation and fibroblast activation, which indicated Erk1/2 phosphorylation mediated the inhibitory effect of BMPER on fibroblast activation. LRP1 mediates different effects through multiple downstream molecules, such as HtrA1 and Erk1/2 (Muratoglu et al., 2013). In our study, LRP1 activated Erk1/2 and promoted fibrogenesis. In line with our result, LRP1 modulates hepatic stellate cells proliferation and migration also by activating Erk1/2 (Kang et al., 2015). In contrast, anti-apoptotic effect of tPA in renal myofibroblasts is mediated by deactivated Erk1/2 (Hu et al., 2008). These inconsistent studies suggest that extracellular cues determine the functional status of Erk1/2 downstream of LRP1.

REFERENCES

- Andrikopoulos, P., Kieswich, J., Pacheco, S., Nadarajah, L., Harwood, S. M., O'Riordan, C. E., et al. (2019). The MEK inhibitor trametinib ameliorates kidney fibrosis by suppressing ERK1/2 and mTORC1 signaling. *J. Am. Soc. Nephrol.* 30, 33–49. doi: 10.1681/ASN.2018020209
- Bondi, C. D., Manickam, N., Lee, D. Y., Block, K., Gorin, Y., Abboud, H. E., et al. (2010). NAD(P)H oxidase mediates TGF- β 1-induced activation of kidney myofibroblasts. *J. Am. Soc. Nephrol.* 21, 93–102. doi: 10.1681/ASN.2009020146

In this study, BMPER significantly inhibited the down-regulation of E-cadherin and fibroblast activation induced by TGF- β 1, and such effect was ignorable without TGF- β 1 treatment. Given that E-cadherin down-regulation and fibroblast activation only exist under pathological conditions, BMPER could ameliorate renal fibrosis without affecting constitutive TGF- β 1 signaling. In addition to improving tubulointerstitial fibrosis, BMPER can also improve tubular atrophy and preserve tubular epithelial morphology. Tubular atrophy can result from tubular EMT and apoptosis. However, BMPER did not directly improve renal tubular apoptosis and EMT caused by ureteral obstruction. Recent studies have shown that fibroblasts and excessively deposited extracellular matrix can cause tubule epithelial atrophy (Buhl et al., 2020), so we speculate that the preservation of tubule integrity by BMPER is due to its anti-fibrotic effect.

In summary, this study demonstrates that BMPER plays an important role in tubular dedifferentiation, fibroblast activation and tubulointerstitial fibrosis. BMPER holds a promise for inhibiting the progression of chronic kidney diseases.

DATA AVAILABILITY STATEMENT

The original contributions presented in the study are included in the article/supplementary materials, further inquiries can be directed to the corresponding author.

ETHICS STATEMENT

The animal study was reviewed and approved by Institutional Animal Care and Use Committee at The Central Hospital of Wuhan, Tongji Medical College, Huazhong University of Science and Technology.

AUTHOR CONTRIBUTIONS

CX and TX conceived the study. TX and ZX did experiments. TX, WW, and XZ analyzed the data. CX, TX, and ZX drafted the manuscript. The content was approved by all authors. All authors read and approved the final manuscript.

FUNDING

This study was supported by Hubei Provincial Natural Science Foundation of China (grant no. 2020CFB547) and the Hospital Research Foundation for Doctors (grant no. YB15B01).

- Boor, P., and Floege, J. (2012). The renal (myo-)fibroblast: a heterogeneous group of cells. *Nephrol. Dial. Transplant.* 27, 3027–3036. doi: 10.1093/ndt/gfs296
- Buhl, E. M., Djurdjaj, S., Klinkhammer, B. M., Ermert, K., Puelles, V. G., Lindenmeyer, M. T., et al. (2020). Dysregulated mesenchymal PDGFR-beta drives kidney fibrosis. *EMBO Mol. Med.* 12:e11021. doi: 10.15252/emmm.201911021
- Chevalier, R. L., Forbes, M. S., and Thornhill, B. A. (2009). Ureteral obstruction as a model of renal interstitial fibrosis and obstructive nephropathy. *Kidney Int.* 75, 1145–1152. doi: 10.1038/ki.2009.86

- Dyer, L., Lockyer, P., Wu, Y., Saha, A., Cyr, C., Moser, M., et al. (2015). BMPER promotes epithelial-mesenchymal transition in the developing cardiac cushions. *PLoS ONE* 10:e0139209. doi: 10.1371/journal.pone.0139209
- Esser, J. S., Steiner, R. E., Deckler, M., Schmitt, H., Engert, B., Link, S., et al. (2018). Extracellular bone morphogenetic protein modulator BMPER and twisted gastrulation homolog 1 preserve arterial-venous specification in zebrafish blood vessel development and regulate Notch signaling in endothelial cells. *FEBS J.* 285, 1419–1436. doi: 10.1111/febs.14414
- Gewin, L. S. (2018). Renal fibrosis: primacy of the proximal tubule. *Matrix Biol.* 68–69, 248–262. doi: 10.1016/j.matbio.2018.02.006
- Gwon, M. G., An, H. J., Kim, J. Y., Kim, W. H., Gu, H., Kim, H. J., et al. (2020). Anti-fibrotic effects of synthetic TGF-beta1 and Smad oligodeoxynucleotide on kidney fibrosis *in vivo* and *in vitro* through inhibition of both epithelial dedifferentiation and endothelial-mesenchymal transitions. *FASEB J.* 34, 333–349. doi: 10.1096/fj.201901307RR
- Hallman, M. A., Zhuang, S., and Schnellmann, R. G. (2008). Regulation of dedifferentiation and redifferentiation in renal proximal tubular cells by the epidermal growth factor receptor. *J. Pharmacol. Exp. Ther.* 325, 520–528. doi: 10.1124/jpet.107.134031
- Heinke, J., Kerber, M., Rahner, S., Mnich, L., Lassmann, S., Helbing, T., et al. (2012). Bone morphogenetic protein modulator BMPER is highly expressed in malignant tumors and controls invasive cell behavior. *Oncogene* 31, 2919–2930. doi: 10.1038/onc.2011.473
- Helbing, T., Herold, E. M., Hornstein, A., Wintrich, S., Heinke, J., Grundmann, S., et al. (2013). Inhibition of BMP activity protects epithelial barrier function in lung injury. *J. Pathol* 231, 105–116. doi: 10.1002/path.4215
- Helbing, T., Volkmar, F., Goebel, U., Heinke, J., Diehl, P., Pahl, H. L., et al. (2010). Kruppel-like factor 15 regulates BMPER in endothelial cells. *Cardiovasc. Res.* 85, 551–559. doi: 10.1093/cvr/cvp314
- Helbing, T., Wiltgen, G., Hornstein, A., Brauers, E. Z., Arnold, L., Bauer, A., et al. (2017). Bone morphogenetic protein-modulator BMPER regulates endothelial barrier function. *Inflammation* 40, 442–453. doi: 10.1007/s10753-016-0490-4
- Herrera, J., Henke, C. A., and Bitterman, P. B. (2018). Extracellular matrix as a driver of progressive fibrosis. *J. Clin. Invest.* 128, 45–53. doi: 10.1172/JCI93557
- Hu, K., Lin, L., Tan, X., Yang, J., Bu, G., Mars, W. M., et al. (2008). tPA protects renal interstitial fibroblasts and myofibroblasts from apoptosis. *J. Am. Soc. Nephrol.* 19, 503–514. doi: 10.1681/ASN.2007030300
- Huan, C., Yang, T., Liang, J., Xie, T., Cheng, L., Liu, N., et al. (2015). Methylation-mediated BMPER expression in fibroblast activation *in vitro* and lung fibrosis in mice *in vivo*. *Sci. Rep.* 5:14910. doi: 10.1038/srep14910
- Kang, L. I., Isse, K., Koral, K., Bowen, W. C., Muratoglu, S., Strickland, D. K., et al. (2015). Tissue-type plasminogen activator suppresses activated stellate cells through low-density lipoprotein receptor-related protein 1. *Lab. Invest.* 95, 1117–1129. doi: 10.1038/labinvest.2015.94
- Kelley, R., Ren, R., Pi, X., Wu, Y., Moreno, I., Willis, M., et al. (2009). A concentration-dependent endocytic trap and sink mechanism converts Bmp from an activator to an inhibitor of Bmp signaling. *J. Cell Biol.* 184, 597–609. doi: 10.1083/jcb.200808064
- Li, Y., Yang, J., Luo, J. H., Dedhar, S., and Liu, Y. (2007). Tubular epithelial cell dedifferentiation is driven by the helix-loop-helix transcriptional inhibitor Id1. *J. Am. Soc. Nephrol.* 18, 449–460. doi: 10.1681/ASN.2006030236
- Liu, Y. (2009). New insights into epithelial-mesenchymal transition in kidney fibrosis. *J. Am. Soc. Nephrol.* 21, 212–222. doi: 10.1681/ASN.2008121226
- Lockyer, P., Mao, H., Fan, Q., Li, L., Yu-Lee, L. Y., Eissa, N. T., et al. (2017). LRP1-dependent BMPER signaling regulates lipopolysaccharide-induced vascular inflammation. *Arterioscler. Thromb. Vasc. Biol.* 37, 1524–1535. doi: 10.1161/ATVBAHA.117.309521
- Mack, M., and Yanagita, M. (2015). Origin of myofibroblasts and cellular events triggering fibrosis. *Kidney Int.* 87, 297–307. doi: 10.1038/ki.2014.287
- Masaki, T., Stambe, C., Hill, P. A., Dowling, J., Atkins, R. C., and Nikolic-Paterson, D. J. (2004). Activation of the extracellular-signal regulated protein kinase pathway in human glomerulopathies. *J. Am. Soc. Nephrol.* 15, 1835–1843. doi: 10.1097/01.ASN.0000130623.66271.67
- McGarvey, A. C., Rytsov, S., Souilhol, C., Tamagno, S., Rice, R., Hills, D., et al. (2017). A molecular roadmap of the AGM region reveals BMPER as a novel regulator of HSC maturation. *J. Exp. Med.* 214, 3731–3751. doi: 10.1084/jem.20162012
- Moser, M., Binder, O., Wu, Y., Aitseaomo, J., Ren, R., Bode, C., et al. (2003). BMPER, a novel endothelial cell precursor-derived protein, antagonizes bone morphogenetic protein signaling and endothelial cell differentiation. *Mol. Cell Biol.* 23, 5664–5679. doi: 10.1128/MCB.23.16.5664-5679.2003
- Moser, M., and Patterson, C. (2005). Bone morphogenetic proteins and vascular differentiation: BMPing up vasculogenesis. *Thromb. Haemost.* 94, 713–718. doi: 10.1160/TH05-05-0312
- Muratoglu, S. C., Belgrave, S., Hampton, B., Migliorini, M., Coksaygan, T., Chen, L., et al. (2013). LRP1 protects the vasculature by regulating levels of connective tissue growth factor and HtrA1. *Arterioscler. Thromb. Vasc. Biol.* 33, 2137–2146. doi: 10.1161/ATVBAHA.113.301893
- Qi, R., and Yang, C. (2018). Renal tubular epithelial cells: the neglected mediator of tubulointerstitial fibrosis after injury. *Cell Death Dis.* 9:1126. doi: 10.1038/s41419-018-1157-x
- Quaggin, S. E., and Kapus, A. (2011). Scar wars: mapping the fate of epithelial-mesenchymal-myofibroblast transition. *Kidney Int.* 80, 41–50. doi: 10.1038/ki.2011.77
- Ruiz-Ortega, M., Rayego-Mateos, S., Lamas, S., Ortiz, A., and Rodrigues-Diez, R. R. (2020). Targeting the progression of chronic kidney disease. *Nat. Rev. Nephrol.* 16, 269–288. doi: 10.1038/s41581-019-0248-y
- Schafer, S., Viswanathan, S., Widjaja, A. A., Lim, W. W., Moreno-Moral, A., DeLaughter, D. M., et al. (2017). IL-11 is a crucial determinant of cardiovascular fibrosis. *Nature* 552, 110–115. doi: 10.1038/nature24676
- Sorensen, I., Susnik, N., Inhester, T., Degen, J. L., Melk, A., Haller, H., et al. (2011). Fibrinogen, acting as a mitogen for tubulointerstitial fibroblasts, promotes renal fibrosis. *Kidney Int.* 80, 1035–1044. doi: 10.1038/ki.2011.214
- Wujak, L., Schnieder, J., Schaefer, L., and Wygrecka, M. (2018). LRP1: A chameleon receptor of lung inflammation and repair. *Matrix Biol.* 68–69, 366–381. doi: 10.1016/j.matbio.2017.12.007
- Yang, J., Chen, S., Huang, L., Michalopoulos, G. K., and Liu, Y. (2001a). Sustained expression of naked plasmid DNA encoding hepatocyte growth factor in mice promotes liver and overall body growth. *Hepatology* 33, 848–859. doi: 10.1053/jhep.2001.23438
- Yang, J., Dai, C., and Liu, Y. (2001b). Systemic administration of naked plasmid encoding hepatocyte growth factor ameliorates chronic renal fibrosis in mice. *Gene Ther.* 8, 1470–1479. doi: 10.1038/sj.gt.3301545
- Yao, Y., Zhang, J., Ye, D. F., Tan, D. Q., Peng, J. P., Xie, M., et al. (2011). Left-right determination factor is down-regulated in fibrotic renal tissue of human hydronephrosis. *BJU Int.* 107, 1002–1008. doi: 10.1111/j.1464-410X.2010.09520.x
- Zhang, D., Sun, L., Xian, W., Liu, F., Ling, G., Xiao, L., et al. (2010). Low-dose paclitaxel ameliorates renal fibrosis in rat UUO model by inhibition of TGF-beta/Smad activity. *Lab. Invest.* 90, 436–447. doi: 10.1038/labinvest.2009.149
- Zheng, G., Lyons, J. G., Tan, T. K., Wang, Y., Hsu, T. T., Min, D., et al. (2009). Disruption of E-cadherin by matrix metalloproteinase directly mediates epithelial-mesenchymal transition downstream of transforming growth factor-beta1 in renal tubular epithelial cells. *Am. J. Pathol.* 175, 580–591. doi: 10.2353/ajpath.2009.080983
- Zheng, M., Cai, J., Liu, Z., Shu, S., Wang, Y., Tang, C., et al. (2019). Nicotinamide reduces renal interstitial fibrosis by suppressing tubular injury and inflammation. *J. Cell. Mol. Med.* 23, 3995–4004. doi: 10.1111/jcmm.14285
- Zhuang, S., Duan, M., and Yan, Y. (2012). Src family kinases regulate renal epithelial dedifferentiation through activation of EGFR/PI3K signaling. *J. Cell Physiol.* 227, 2138–2144. doi: 10.1002/jcp.22946

Conflict of Interest: The authors declare that the research was conducted in the absence of any commercial or financial relationships that could be construed as a potential conflict of interest.

Copyright © 2021 Xie, Xia, Wang, Zhou and Xu. This is an open-access article distributed under the terms of the Creative Commons Attribution License (CC BY). The use, distribution or reproduction in other forums is permitted, provided the original author(s) and the copyright owner(s) are credited and that the original publication in this journal is cited, in accordance with accepted academic practice. No use, distribution or reproduction is permitted which does not comply with these terms.



Qishen Yiqi Dripping Pill Protects Against Diabetic Nephropathy by Inhibiting the Wnt/ β -Catenin and Transforming Growth Factor- β /Smad Signaling Pathways in Rats

Qian Zhang, Xinhua Xiao*, Jia Zheng, Ming Li, Miao Yu, Fan Ping, Tong Wang and Xiaojing Wang

Key Laboratory of Endocrinology, Ministry of Health, Department of Endocrinology, Peking Union Medical College Hospital, Peking Union Medical College, Chinese Academy of Medical Sciences, Beijing, China

OPEN ACCESS

Edited by:

Isotta Chimenti,
Sapienza University of Rome, Italy

Reviewed by:

Xiao-ming Meng,
Anhui Medical University, China
Chunling Li,
Sun Yat-sen University, China

*Correspondence:

Xinhua Xiao
xiaoxh2014@vip.163.com

Specialty section:

This article was submitted to
Renal and Epithelial Physiology,
a section of the journal
Frontiers in Physiology

Received: 09 October 2020

Accepted: 31 December 2020

Published: 19 February 2021

Citation:

Zhang Q, Xiao X, Zheng J, Li M,
Yu M, Ping F, Wang T and Wang X
(2021) Qishen Yiqi Dripping Pill
Protects Against Diabetic
Nephropathy by Inhibiting
the Wnt/ β -Catenin and Transforming
Growth Factor- β /Smad Signaling
Pathways in Rats.
Front. Physiol. 11:613324.
doi: 10.3389/fphys.2020.613324

Diabetic nephropathy is a severe microvascular complication of diabetes. Qishen Yiqi dripping pill (QYDP) has been reported to be a renal protective drug. However, the mechanisms remain unclear. This study was performed to investigate the mechanisms. In this study, Sprague-Dawley rats were injected with streptozotocin to generate a diabetes model. Diabetic rats were administered 150 or 300 mg/kg/day QYDP. After 8 weeks of treatment, serum creatinine, serum blood urea nitrogen, and 24-h urinary albumin were measured. Kidney histological staining and immunostaining were analyzed. Then, the renal tissue was analyzed with a genome expression array. The results showed that QYDP treatment reduced serum creatinine, blood urea nitrogen, and 24-h urinary albumin and improved kidney histology and fibrosis. The gene array revealed that the expression of 189 genes was increased, and that of 127 genes was decreased in the high dosage QYDP group compared with the diabetic group. Pathway and gene ontology analyses showed that the differentially expressed genes were involved in the Wnt/ β -catenin and transforming growth factor- β (TGF- β)/Smad2 signaling pathways. QYDP reduced the renal Wnt1, catenin β 1, Tgfb1, and Smad2 gene expression and β -catenin, TGF- β , Smad2, collagen I, α -smooth muscle actin, and fibronectin protein expression in diabetic rats. Our results provide the first evidence that QYDP performs its renal-protective function by inhibiting the Wnt/ β -catenin and TGF- β /Smad2 signaling pathways in diabetic rats.

Keywords: TGF- β , Smad, β -catenin, diabetic nephropathy, Wnt

INTRODUCTION

In 2019, the International Diabetes Federation announced that diabetes affects approximately 463 million people worldwide. The number of affected individuals will reach 702 million by the year 2045 (Williams et al., 2020). Chronic tissue complications from diabetes worsen the health status of patients. Diabetic nephropathy (DN) is one of the most important microvascular complications. It

is estimated that more than 20% of diabetic patients will develop chronic kidney disease (CKD) (Nelson et al., 1996). Nephropathy contributes to the development of a cardiovascular disease, resulting in increased all-cause mortality (Go et al., 2004).

The pathological characteristics of DN include the accumulation of extracellular matrix (ECM) in the glomerulus and tubules of the kidney, which leads to proteinuria and renal failure. Several pathways have been implicated in the underlying mechanisms of DN progression, such as oxidative stress (Baynes, 1991), inflammation (Mariappan, 2012), accumulation of advanced glycation end products (AGEs) (Brownlee et al., 1988), activation of protein kinase C (Koya et al., 1997), reactive oxygen species (Ha et al., 2008), and endoplasmic reticulum (ER) stress (Cybulsky et al., 2011).

Qishen Yiqi dripping pill (QYDP) is a traditional Chinese medicine compound that comprises Radix Astragali (*Astragalus penduliflorus* Lam.), redroot sage (*Salvia miltiorrhiza* Bunge), pseudoginseng (*Panax pseudoginseng* Wall.), and fragrant rosewood (*Dalbergia odorifera* T.C. Chen). QYDP is approved by the State Food and Drug Administration of China (state medical license no. Z20030139). A clinical trial showed that QYDP treatment reduced the urinary album excretion rate in diabetic patients (Yongbin Chen, 2011). QYDP intervention attenuated renal interstitial fibrosis in CKD model rats induced by unilateral ureteral obstruction surgery (Zhou et al., 2016). However, little is known about the mechanism of QYDP in the diabetic model.

The systematic principle of Chinese medicine raises the theory that traditional Chinese medicines have the integrated functions of all their constituents. Thus, we hypothesized that QYDP has multiple targets in the kidney and moderates the kidney function in diabetic rats. To identify these pathways, we used a genome-wide array approach to analyze gene expression changes in the kidney and pathway analysis to gain deep insight into the gene expression alternations.

MATERIALS AND METHODS

Medicine

Qishen Yiqi dripping pill contains Radix Astragali (*A. penduliflorus* Lam., 62.24%), redroot sage (*S. miltiorrhiza* Bunge, 31.12%), pseudoginseng (*P. pseudoginseng* Wall., 6.22%), and fragrant rosewood (*D. odorifera* T.C. Chen, 0.42%). QYDP was provided by Tasly Pharmaceutical Group Co., Ltd. (Tianjin, China). All voucher specimens (no. QYDP19A-QYDP19D) were deposited at the Department of Endocrinology, Peking Union Medical College Hospital, Beijing, China. Detailed information about the four herbs is presented in **Supplementary Table 1**. The quality of the herbs and herbal extracts was consistent with the standards of Chinese Pharmacopoeia (2015). The four-component herbs, Radix Astragali (1,800 g), redroot sage (900 g), pseudoginseng (180 g), and fragrant rosewood (12 g), were soaked in 60% ethanol for 1 h and extracted twice by refluxing for 2 h. The condensed extracts were mixed with dextrin and sugar powder to produce QYDP.

Ultra-Performance Liquid Chromatography Analysis of Qishen Yiqi Dripping Pill

Qishen Yiqi dripping pill powder (0.3 g) was dissolved in methanol and then filtered through a 0.22- μ m filter membrane. QYDP was characterized using a Waters Acquity Ultra-Performance Liquid Chromatography (UPLC) (Waters Corp., Milford, MA, United States) with a symmetrical C18 column (100 \times 2.1 mm i.d., particle size 1.7 μ m, Waters Corp., Milford, MA, United States). The column was eluted at 30°C with a detection wavelength of 203 nm and an injection volume of 2 μ l. The flow rate of the mobile phase of acetonitrile (A) and water (B) was set at 0.2 ml/min. Gradient separation was based on the following: 0–2 min, 15% A; 2–3 min, 15–18% A; 3–10 min, 18–20% A; 10–12 min, 20–25% A; 12–13.5 min, 25–34% A; 13.5–19 min, 34% A; 19–19.1 min, 34–90% A; 22–22.1 min, 90–15% A, 22.1–25 min, 15% A.

Animal Treatments and Diet

A total of twenty four 5-week-old male Sprague-Dawley (SD) rats were purchased from the Institute of Laboratory Animal Sciences, Chinese Academy of Medical Sciences and Peking Union Medical College, Beijing, China and provided with a standard diet and water. The rats were kept under a 12-h light/12-h dark cycle and at 24°C. This study was conducted in strict accordance with the recommendations and with the approval of the Animal Care Committee of the Peking Union Medical Hospital Animal Ethics Committee (Project XHDW-2015-0051, 15 February 2015), and all efforts were made to minimize suffering. Diabetes was induced by injection of streptozotocin (Sigma-Aldrich, St. Louis, MO, United States) at a dose of 60 mg/kg body weight. The rats with fasted blood glucose levels > 11.1 mmol/L were considered diabetic. Diabetic rats were divided into three groups: a vehicle-treated group [diabetes mellitus (DM) group, $n = 6$], low dosage of Qishen Yiqi dripping pill group ($n = 6$), and high dosage of Qishen Yiqi dripping pill group (HQYDP group, $n = 6$). The typical human daily dose of QYDP is 1.5 g per 60 kg of body weight. Thus, according to the formula $d_{\text{rat}} = (37 \times d_{\text{human}})/6$, the corresponding dose of QYDP for rats is 154.2 mg/kg per day. Previous reports show that there is no toxic reaction in rats treated with 4,000 mg/kg QYDP for 26 weeks (Wang et al.,

TABLE 1 | Oligonucleotide sequences for qPCR analysis.

| Gene symbol | Gene bank ID | Forward primer | Reverse primer | Product size (bp) |
|-------------|--------------|--------------------------|--------------------------|-------------------|
| Wnt1 | NM_001105714 | TCTTCTCGGGA GACCCCTTT | ATACCACAGGG ACAGCAACG | 124 |
| Ctnnb1 | NM_053357 | ATCATTCTGGCC AGTGGTGG | GACAGCACCTTC AGCACTCT | 104 |
| Tgfb1 | NM_021578 | AGGGCTACCAT GCCAACTTC | CCACGTAGTAG ACGATGGGC | 168 |
| Smad2 | NM_001277450 | GCCGCCCGAA GGGTAGAT | TTCTGTTCTCC ACCACCTGC | 164 |

Wnt1, *Wnt* family member 1; *Ctnnb1*, catenin beta 1; *Tgfb1*, transforming growth factor beta 1.

2019). Therefore, the low dosage of Qishen Yiqi dripping pill and HQYDP groups were orally administered QYDP (Tasly Pharmaceutical Group Co., Ltd., Tianjin, China) at 150 and 300 mg/kg/day by gavage, respectively. The DM group and normal control (NC) group were given an equal volume of saline. All rats were anesthetized *via* intraperitoneal injection of sodium pentobarbital (150 mg/kg) and then killed at the eighth week after treatment. The kidneys were immediately collected.

Blood Sample Analysis and Sample Preparation

After 6 h of fasting, blood was collected through the intraorbital retrobulbar plexus. For 24-h urine collection, the rats were housed in individual metabolic cages at the end of the 8-week treatment. Urine was centrifuged at $3,000 \times g$ for 10 min at room temperature. Blood glucose, serum creatinine, blood urea nitrogen (BUN), and urine albumin levels were measured

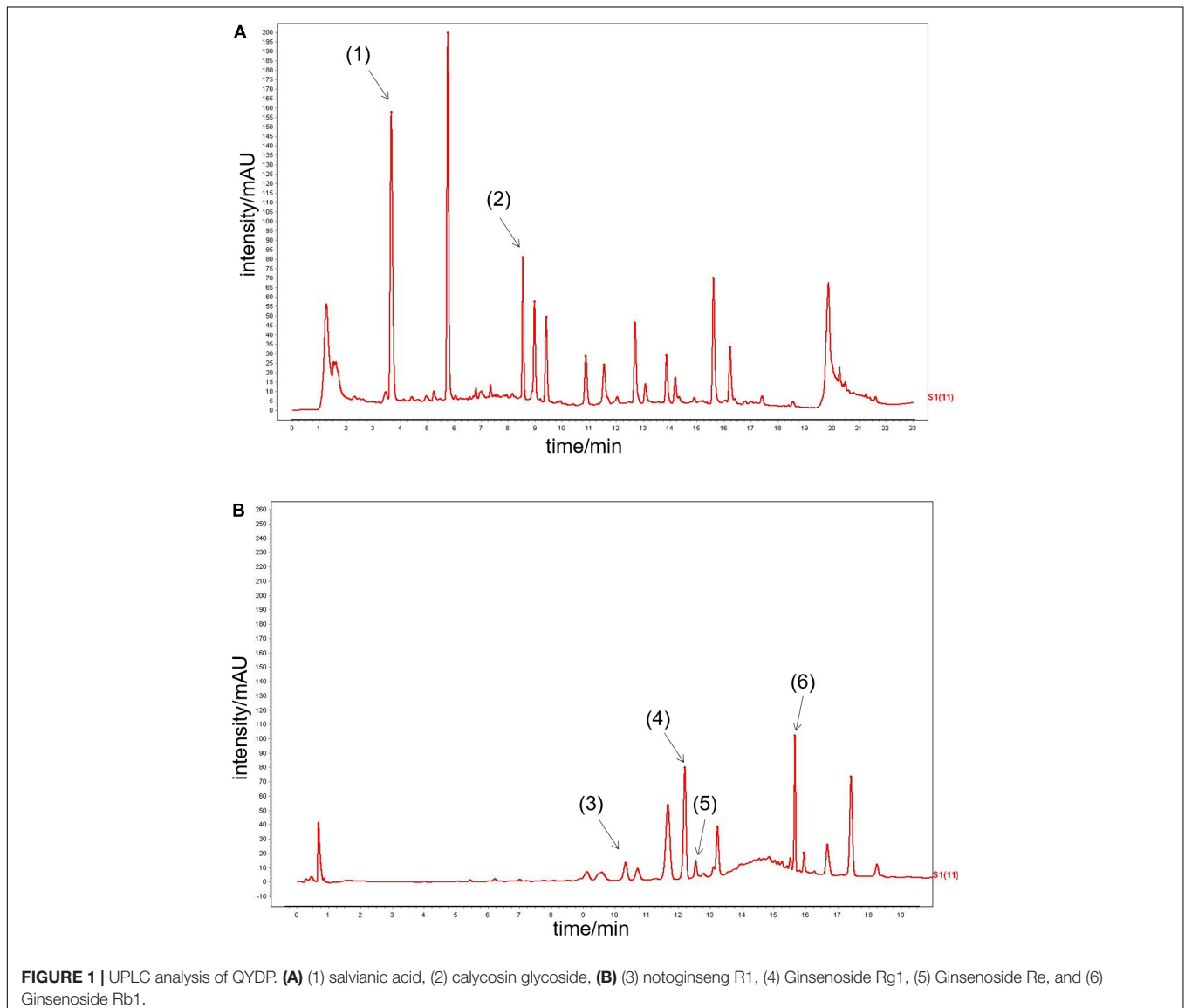
with a Beckman biochemical analyzer (Counter, AU5800, Germany).

Histological Examination of the Kidney

Kidneys were fixed in formalin and then embedded in paraffin. Five-micrometer-thick sections were stained with periodic-acid Schiff (PAS) and Masson's trichrome stain. Using PAS staining, the glomerular score of each rat was calculated as the arithmetic mean of 60 glomeruli ($400\times$ magnification) (el Nahas et al., 1987). The tubulointerstitial damage score (dilatation, atrophy, hyaline in the tubular lumen, visible detachment of tubular cells, interstitial infiltration of mononuclear cells, and interstitial fibrosis) was assessed as previously described (Piecha et al., 2008).

RNA Extraction and Gene Array Analysis

Total RNA was extracted from the kidney cortex using a mirVanaTM RNA isolation kit (Ambion, São Paulo, Brazil).



Double-stranded complementary DNA (cDNA) was synthesized from RNA. Then, biotinylated cDNA was hybridized to an Affymetrix GeneChip Rat Gene 2.0 ST whole transcript-based array (Affymetrix Technologies, Santa Clara, CA, United States). Genes that had a p -value < 0.05 and a fold change > 1.5 were selected. The data obtained have been deposited in the National Center for Biotechnology Information Gene Expression Omnibus database (accession number GSE134072).

The Database for Annotation, Visualization, and Integrated Discovery web-based software tool was used to perform gene ontology (GO) enrichment analysis. In addition, pathway enrichment analysis based on the Kyoto Encyclopedia of Genes and Genomes (KEGG) database was used to identify significant pathways.

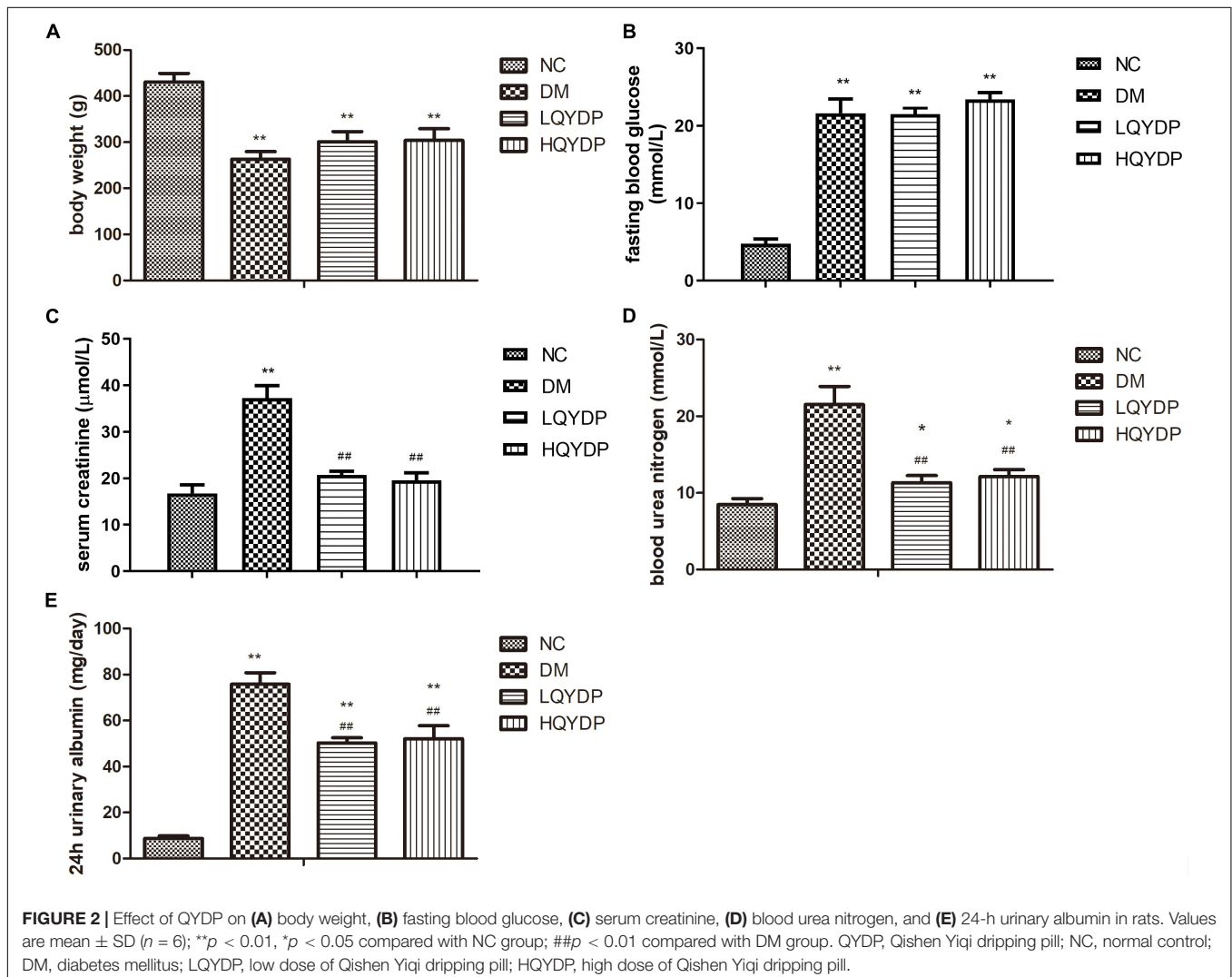
Real-Time PCR Analysis

cDNA was synthesized using SuperScript II reverse transcriptase (Life Technologies, Carlsbad, CA, United States). Real-time PCR was performed using a Real-time PCR Mater Mix Kit (Applied Biosystems, Foster City, CA, United States) and ABI SYBR Mix

(Applied Biosystems, Foster City, CA, United States). The specific primers are listed in **Table 1**. Data were analyzed using the $\Delta\Delta Ct$ method with glyceraldehyde 3-phosphate dehydrogenase as the constitutive marker.

Immunohistochemistry for Transforming Growth Factor- β , β -Catenin, and Smad2 in the Kidney

Five-micron-thick renal sections were deparaffinized, rehydrated, and immersed in phosphate-buffered saline. Then, the sections were stained with anti-TGF- β (1:100, Santa Cruz Biotechnology, Dallas, TX, United States), anti- β -catenin (1:100, Santa Cruz Biotechnology, Dallas, TX, United States), and anti-Smad2 (1:100, Santa Cruz Biotechnology, Dallas, TX, United States) antibodies at 4°C overnight. Tissue sections were then incubated with a horseradish peroxidase-conjugated secondary antibody (1:2,000, Santa Cruz Biotechnology, Dallas, TX, United States) for 1 h at room temperature. Immuno-labeling was visualized with 0.05% diaminobenzidine.



A digital microscope (Nikon, Tokyo, Japan) was used to analyze sections at 400 \times magnification to identify positive cells.

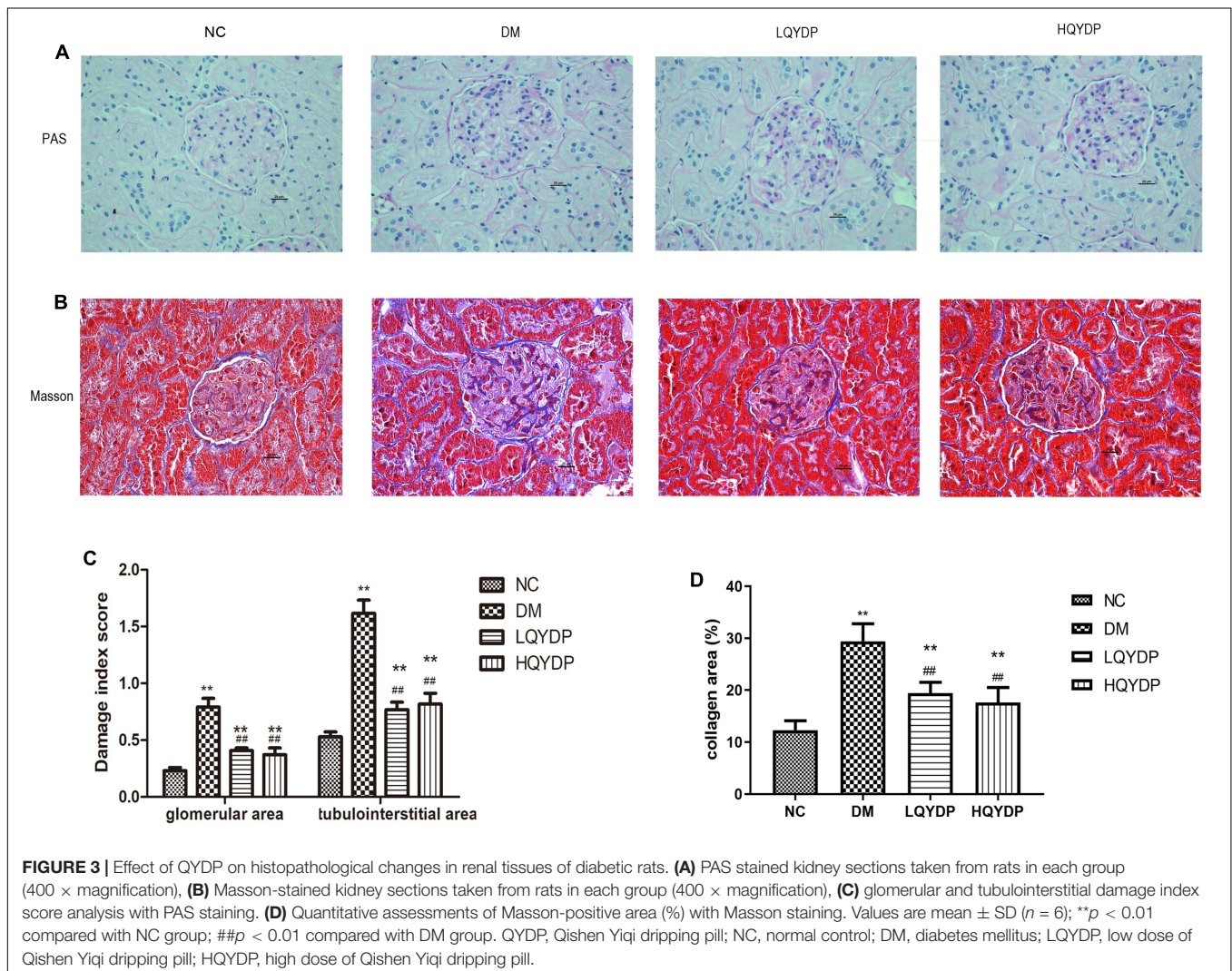
Western Blot Analysis

Kidneys were homogenized in radioimmunoprecipitation assay buffer (Millipore, Bedford, MA, United States) to obtain total proteins. Total protein (30 μ g) was loaded in 10% sodium dodecyl sulfate-polyacrylamide gels and transferred to polyvinylidene fluoride membranes (Bio-Rad, Hercules, CA, United States). Then, the membranes were blocked in Tris-buffered saline with skim milk for 1 h, followed by overnight incubation at 4°C with rabbit anti-TGF- β (1:1,000, Abcam, Cambridge, United Kingdom), rabbit anti- β -catenin (1:1,000, Abcam, Cambridge, United Kingdom), rabbit anti-Smad2 (1:1,000, Abcam, Cambridge, United Kingdom), rabbit anti-collagen I (1:1,000, Abcam, Cambridge, United Kingdom), rabbit anti- α -smooth muscle actin (α -SMA, 1:1,000, Abcam, Cambridge, United Kingdom), or rabbit anti-fibronectin (FN, 1:1,000, Abcam, Cambridge, United Kingdom) antibody. After washing, the membranes were incubated with horseradish

peroxidase-conjugated secondary antibody (1:3,000, Santa Cruz Biotechnology, Santa Cruz, CA, United States) for 2 h at room temperature. After another wash, membranes were developed using an enhanced chemiluminescence (Cell Signaling Technology, Danvers, MA, United States) assay. Bound proteins were scanned with an Epson V300 scanning system (Epson, Suwa, Japan). The density of protein bands was quantified with AlphaEaseFC software (Alpha Innotech, San Leandro, CA, United States). The housekeeping protein β -actin (1:3,000, Abcam, Cambridge, United Kingdom) was used for normalization.

Statistical Analysis

Data are shown as the mean \pm SD. Statistical analyses were calculated with two-way ANOVA followed by Tukey's *post hoc* test among the four groups. The Student's *t*-test was used to analyze differences between different groups. GraphPad Prism 6 (GraphPad Software Inc., CA, United States) was used for data analysis. $P < 0.05$ was considered to indicate significance.



RESULTS

Ultra-Performance Liquid Chromatography Analysis of Qishen Yiqi Dripping Pill

Six main QYDP components were confirmed by UPLC analysis. The UV detector for UPLC analysis was set to 203 nm according to the standard maximum absorption rate. The UPLC analysis of QYDP is presented in **Figures 1A,B**. The six main QYDP constituents are (1) salviatic acid (3.942 mg/g), (2) calycosin glycoside (0.2656 mg/g), (3) notoginseng R1 (0.618 mg/g), (4) Ginsenoside Rg1 (2.204 mg/g), (5) Ginsenoside Re (0.4484 mg/g), and (6) Ginsenoside Rb1 (1.9 mg/g).

Effect of Qishen Yiqi Dripping Pill on Body Weight and Fasting Blood Glucose

The DM group showed decreased body weight compared with that of the NC group ($p < 0.01$, **Figure 2A**). QYDP did not change the body weight of diabetic rats ($p > 0.05$, **Figure 2A**). The DM group had higher fasting blood glucose ($p < 0.01$, **Figure 2B**) than the control group. QYDP did not reduce fasting blood glucose in diabetic rats ($p > 0.05$, **Figure 2B**).

Effect of Qishen Yiqi Dripping Pill on Renal Function Parameters

Serum creatinine, BUN, and 24-h urinary albumin levels were significantly increased in the DM group ($p < 0.01$,

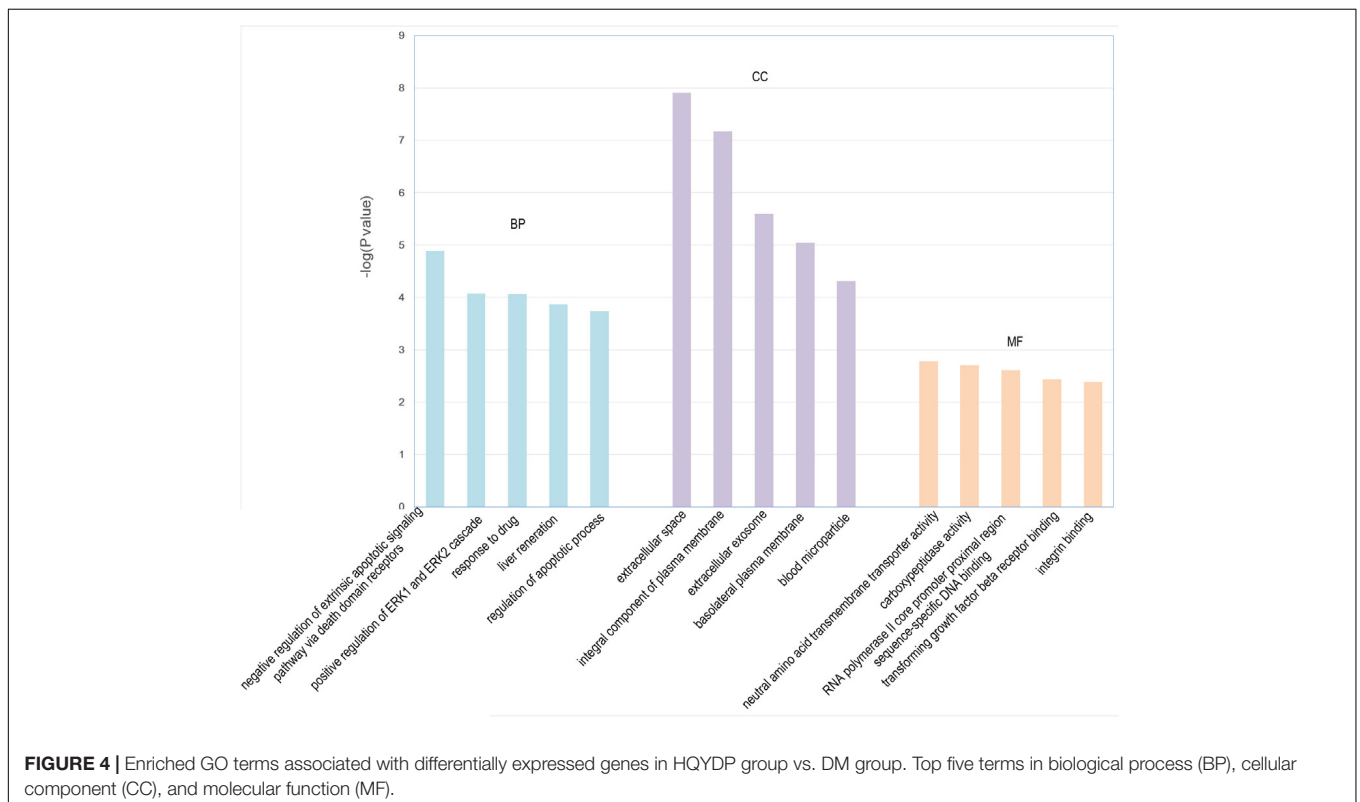
Figures 2C–E). QYDP treatment decreased serum creatinine, BUN, and 24-h urinary albumin levels ($p < 0.01$, **Figures 2C–E**). These results suggest that QYDP moderated renal function in diabetic rats.

Effect of Qishen Yiqi Dripping Pill Treatment on Histopathological Changes in Renal Tissue

With PAS staining, both a higher glomerular lesion score and higher tubulointerstitial lesion score were observed in diabetic rats compared with normal rats ($p < 0.01$, **Figures 3A,C**). Glomerular hypertrophy and tubulointerstitial changes were mostly prevented by QYDP treatment ($p < 0.01$, **Figures 3A,C**). Further examination of Masson's-stained renal tissue sections showed that the diabetic rats presented more collagen fibers in the glomerular mesangium and basement membrane ($p < 0.01$, **Figures 3B,D**). QYDP treatment significantly attenuated collagen deposition ($p < 0.01$, **Figures 3B,D**).

Gene Array, Pathway, Gene Ontology, and Network Analysis Results in the High Dosage of QishenYiqi Dripping Pill Group vs. the Diabetes Mellitus Group

We identified 316 significantly differentially expressed genes, including 189 upregulated genes and 127 downregulated genes in the HQYDP group, compared with the DM group (fold change > 1.5 , $p < 0.05$). To systematically identify biological connections among the differentially expressed genes and



to identify pathways associated with the effect of QYDP on the kidney, we performed GO and KEGG pathway analyses. **Figure 4** and **Table 2** show the top five terms in three categories, biological processes, cellular components, and molecular functions. Among the biological process ontology

results, the major GO terms affected by QYDP were negative regulation of extrinsic apoptotic signaling pathway *via* death domain receptors, positive regulation of ERK1 and ERK2 cascade, response to a drug, liver regeneration, and regulation of the apoptotic process. **Figure 5** and **Table 3** show the

TABLE 2 | Top 5 enriched GO terms in each catalog associated with differentially expressed genes in HQYDP group vs. DM group.

| term ID | term name | count | p value | fold enrichment | involved genes | catalog |
|------------|---|-------|-----------------------|-----------------|--|----------------------|
| GO:1902042 | negative regulation of extrinsic apoptotic signaling pathway via death domain receptors | 6 | 1.29×10^{-5} | 18.828 | ICAM1, FGG, FGA, SFRP2, FGB, HMOX1 | biological processes |
| GO:0070374 | positive regulation of ERK1 and ERK2 cascade | 12 | 8.42×10^{-5} | 4.454 | ICAM1, FGG, FGA, C1QTNF3, FGB, SEMA7A, P2RY1, PYCARD, TREM2, GPNMB, SLAMF1, TGFB1 | biological processes |
| GO:0042493 | response to drug | 21 | 8.64×10^{-5} | 2.746 | ICAM1, SLC8A1, MAT2A, LGALS1, IL1RN, GGH, CFTR, ABCA1, SLCO1A6, TGFB1, CTNNB1, CDKN1A, TNFRSF11B, ACE, HTR1B, PLIN2, SFRP2, ABCB1B, TGIF1, FAS, MYC | biological processes |
| GO:0097421 | liver regeneration | 7 | 1.36×10^{-4} | 8.786 | FGA, HMOX1, CLDN1, RGN, FAS, MYC, TGFB1 | biological processes |
| GO:0042981 | regulation of apoptotic process | 11 | 1.84×10^{-4} | 4.467 | TNFRSF1B, TNFRSF11B, BMP1, SFRP2, PYCARD, CIDEA, APAF1, FAS, GDF15, MYC, CTNNB1 | biological processes |
| GO:0005615 | extracellular space | 47 | 1.24×10^{-8} | 2.496 | GC, LTBP4, BTC, UMOD, TGFB1, LIF, WNT1, FGG, TNFRSF11B, WNT4, ACE, FGA, C1QTNF3, FGB, SEMA7A, PPP1R1A, VNN1, TFF3, SERPINB12, FAS, EGF, GCNT1, ANGPTL4, SPP1, SELP, ICAM1, BMP1, PLA2G15, LOC360919, C4B, LGALS1, IL1RN, KNG1L1, AXL, GGH, CPXM2, HILPDA, MFGE8, AFM, DKK1, SFRP2, LIPG, ACE2, ANXA13, IGFBP1, GDF15, PON3 | cellular components |
| GO:0005887 | integral component of plasma membrane | 37 | 6.76×10^{-8} | 2.745 | LOC361914, CLDN4, CADM2, SLC15A2, TSPAN4, KCNJ10, ABCA1, ATP12A, KCNJ13, INSR, TNFRSF1B, SLCO1A1, TNFRSF11B, HTR1B, SLC39A8, FAS, GPNMB, SLC22A2, ICAM1, SLC8A1, SLC6A13, SLC22A22, NPR2, SLC10A5, SLC7A13, SLCO1A6, SLC7A12, SLC26A4, SEMA6A, FOLH1, SLC16A4, SLC16A7, GRM8, SLC26A7, CLDN1, SLC13A1, STEAP1 | cellular components |
| GO:0070062 | extracellular exosome | 67 | 2.55×10^{-6} | 1.770 | PVR, GDA, SLC15A2, LTBP4, CTNNB1, SLC1A4, PRKAR2A, TUBB6, VNN1, RHOB, FAS, ATP6V0D2, SLC22A2, ICAM1, HIST1H1B, C4B, CFTR, MFGE8, BASP1, VAT1, SLC26A4, FOLH1, PSCA, PRPS2, MYO5A, GC, ACADSB, UMOD, ATP6V1B1, FGG, ACE, FGA, HNMT, C1QTNF3, FGB, TFF3, NDRG1, SERPINB12, EGF, SPP1, NAT8, DNM3, PLA2G15, CPNE4, HIST1H2BF, LGALS1, IL1RN, SLC6A13, KNG1L1, GGH, AXL, NID2, CRYZ, TPMT, CPVL, SLAMF1, AFM, PPIC, ACE2, MEP1A, ANXA13, HIST1H2AH, HIST1H2AK, PAPP2, APAF1, GDF15, PON3 | cellular components |
| GO:0016323 | basolateral plasma membrane | 14 | 9.07×10^{-6} | 4.727 | SLC8A1, CASR, NKD2, SLC22A22, UMOD, CFTR, KCNJ10, ATP6V1B1, ATP12A, CTNNB1, SLCO1A1, SLC26A7, P2RY1, SLC22A2 | cellular components |
| GO:0072562 | blood microparticle | 10 | 4.90×10^{-5} | 5.923 | GC, FGG, AFM, FGA, LOC691828, C4B, FGB, KNG1L1, TGFB1, ANGPTL4 | cellular components |
| GO:0015175 | neutral amino acid transmembrane transporter activity | 4 | 0.0017 | 16.453 | SLC1A4, LOC361914, SLC7A13, SLC7A12 | molecular function |
| GO:0004180 | carboxypeptidase activity | 4 | 0.0020 | 15.485 | FOLH1, ACE, ACE2, CPXM2 | molecular function |
| GO:0000978 | RNA polymerase II core promoter proximal region sequence-specific DNA binding | 14 | 0.0024 | 2.663 | AR, ELF3, SPI1, SMAD3, SMAD2, MYBL1, FOXP2, GCM1, NR1D1, OVOL1, TEF, TGIF1, POU3F1, MYC | molecular function |
| GO:0005160 | transforming growth factor beta receptor binding | 5 | 0.0037 | 7.835 | BMP1, SMAD3, SMAD2, GDF15, TGFB1 | molecular function |
| GO:0005178 | integrin binding | 7 | 0.0041 | 4.607 | ICAM1, CASR, SEMA7A, TSPAN4, MFGE8, GPNMB, SYK | molecular function |

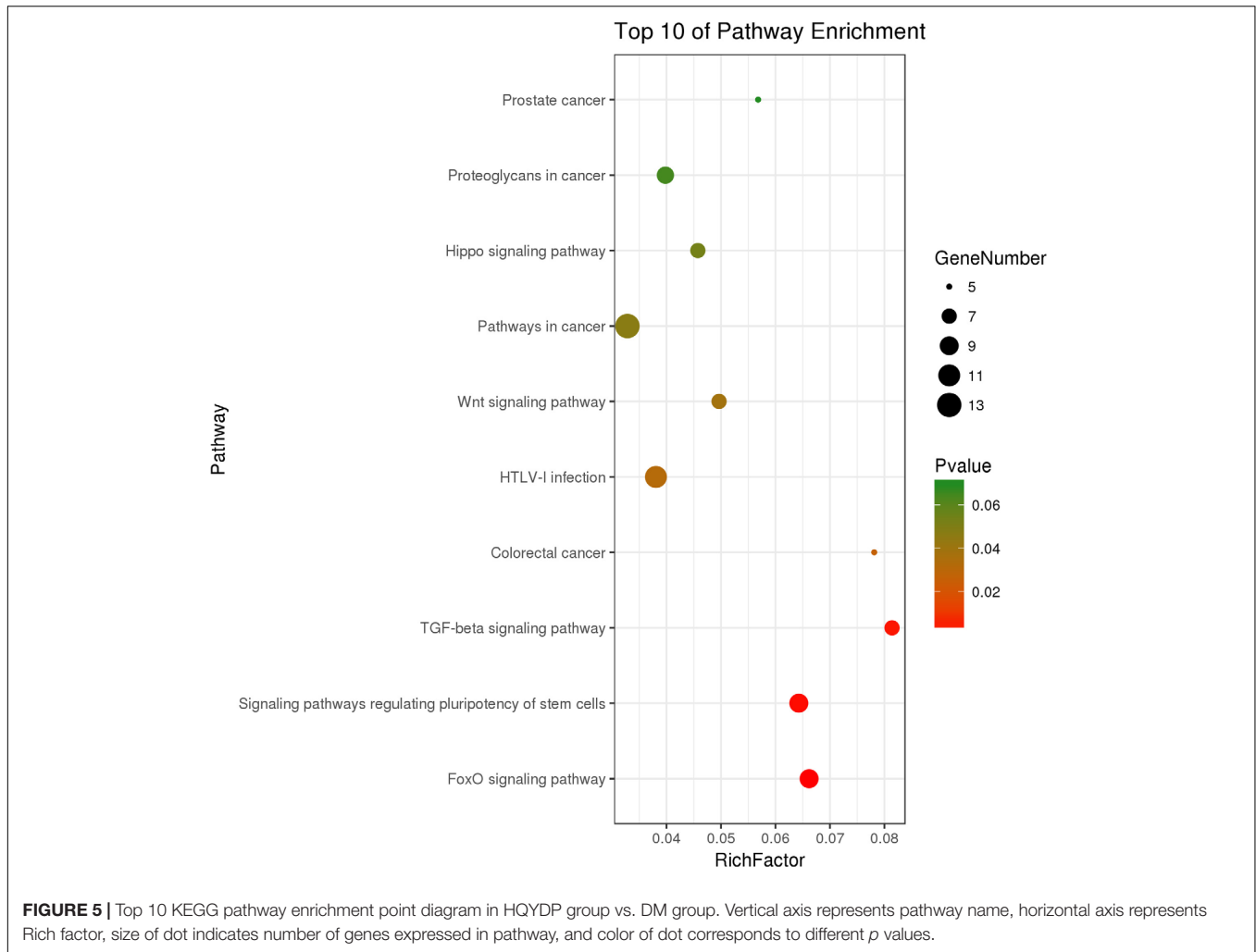


TABLE 3 | Top 10 enriched KEGG pathways associated with differentially expressed genes in HQYDP group vs. DM group.

| pathway ID | pathway term | count | fold enrichment | p value | involved genes |
|------------|--|-------|-----------------|-----------|---|
| rno04068 | FoxO signaling pathway | 9 | 3.716 | 0.003 | G6PC, SGK1, CDKN1A, S1PR1, PLK2, SMAD3, SMAD2, EGF, TGFB1 |
| rno04550 | Signaling pathways regulating pluripotency of stem cells | 9 | 3.610 | 0.003 | LIF, WNT1, WNT4, SMAD3, SMAD2, ID4, ID3, MYC, CTNNB1 |
| rno04350 | TGF-beta signaling pathway | 7 | 4.571 | 0.004 | TGIF1, SMAD3, SMAD2, ID4, ID3, MYC, TGFB1 |
| rno05210 | Colorectal cancer | 5 | 4.387 | 0.026 | SMAD3, SMAD2, MYC, TGFB1, CTNNB1 |
| rno05166 | HTLV-I infection | 11 | 2.137 | 0.032 | ICAM1, WNT1, CDKN1A, WNT4, SPI1, SMAD3, SMAD2, MYC, TGFB1, CTNNB1, TP53INP1 |
| rno04310 | Wnt signaling pathway | 7 | 2.788 | 0.039 | WNT1, WNT4, NKD2, DKK1, SFRP2, MYC, CTNNB1 |
| rno05200 | Pathways in cancer | 13 | 1.843 | 0.047 | WNT1, CDKN1A, AR, WNT4, SPI1, GNG13, SMAD3, SMAD2, FAS, EGF, MYC, TGFB1, CTNNB1 |
| rno04390 | Hippo signaling pathway | 7 | 2.569 | 0.054 | WNT1, WNT4, SMAD3, SMAD2, MYC, TGFB1, CTNNB1 |
| rno05205 | Proteoglycans in cancer | 8 | 2.235 | 0.065 | WNT1, CDKN1A, WNT4, HPSE2, FAS, MYC, TGFB1, CTNNB1 |
| rno05215 | Prostate cancer | 5 | 3.190 | 0.070 | CDKN1A, AR, EGF, CTNNB1, INSR |

top 10 pathways identified *via* KEGG pathway analysis affected by QYDP, including the FoxO signaling pathway, signaling pathways regulating pluripotency of stem cells, TGF- β signaling pathway, colorectal cancer, Human T- cell leukemia virus, type 1 infection, Wnt signaling pathway, pathways in

cancer, Hippo signaling pathway, proteoglycans in cancer, and prostate cancer.

By using String online software, the 316 differentially expressed genes were mapped in a network. Two hundred ninety-six nodes with 350 joint-edges were featured in this map

(Figure 6). Fifteen nodes with no less than 10 joint-edges were considered important functional molecules in QYDP-treated kidneys because they accounted for 66.8% of the function of all genes. Among these 15 nodes, glyceraldehyde-3-phosphate dehydrogenase, myelocytomatosis oncogene, catenin β 1 (Ctnnb1), transforming growth factor β 1 (Tgfb1), serum glucocorticoid regulated kinase 1, spleen tyrosine kinase, cyclin-dependent kinase inhibitor 1 A, mitogen-activated protein kinase 4, angiotensin I converting enzyme, and intercellular adhesion molecule 1 were ranked in the top 10.

Real-Time PCR Validation Results

Because the TGF- β signaling pathway and Wnt signaling pathway were among the top-ranked KEGG pathways associated with differentially expressed genes in the HQYDP group vs. the DM group, we selected several genes in these two pathways to assay expression among the four different groups using quantitative PCR. We found that diabetic rats had significantly increased Wnt family member 1 (Wnt1), Ctnnb1, Tgfb1, and Smad2 expression in the kidney ($p < 0.01$, Figure 7) compared with that in the control group. QYDP treatment reduced Wnt1, Ctnnb1, Tgfb1, and Smad2 expression in diabetic kidneys ($p < 0.01$, Figure 7). These results were consistent with the microarray results.

Effect of Qishen Yiqi Dripping Pill on Transforming Growth Factor- β , β -Catenin, and Smad2 Expression in the Kidney Determined by Immunohistochemistry Staining

Immunohistochemistry analyses showed that in the DM group, TGF- β , β -catenin, and Smad2 immunoreactivity was higher than in the NC group in the glomeruli, tubuli, and interstitial areas ($p < 0.01$, Figure 8). QYDP treatment inhibited TGF- β , β -catenin, and Smad2 levels in the glomerular and tubulointerstitial areas of diabetic kidneys ($p < 0.01$, Figure 8).

Effect of Qishen Yiqi Dripping Pill on the Protein Levels of Transforming Growth Factor- β , β -Catenin, Smad2 and Fibrotic Markers in the Kidney

Similar to the immunohistochemical analyses, an increase in TGF- β , β -catenin, and Smad2 was observed in diabetic rat kidneys ($p < 0.01$, Figure 9). Treatment with QYDP significantly decreased TGF- β , β -catenin, and Smad2 expression ($p < 0.01$, Figure 9). The expression levels of the fibrotic markers, collagen I, α -SMA, and FN were upregulated in diabetic rat kidneys

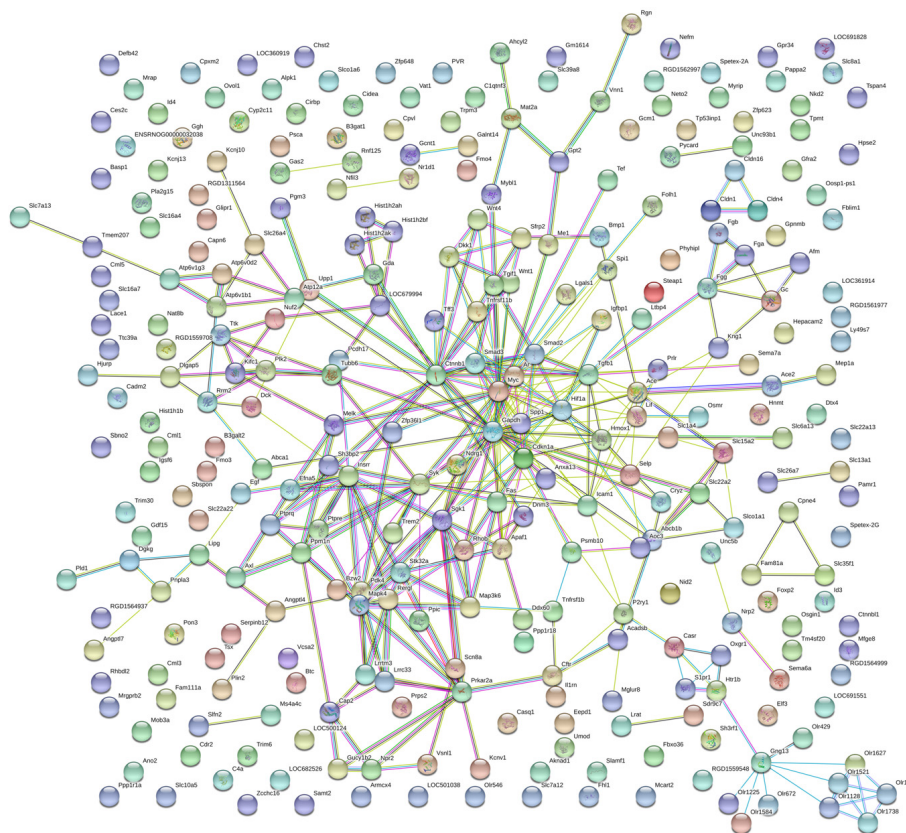
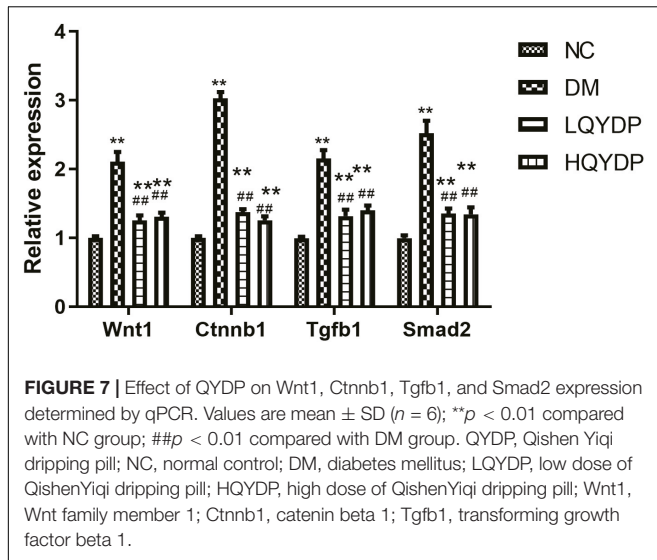


FIGURE 6 | Protein-protein interaction network in HQYDP group compared with DM group. Nodes stand for differentially expressed genes in HQYDP group compared with DM group. Lines represent interactions between two proteins.

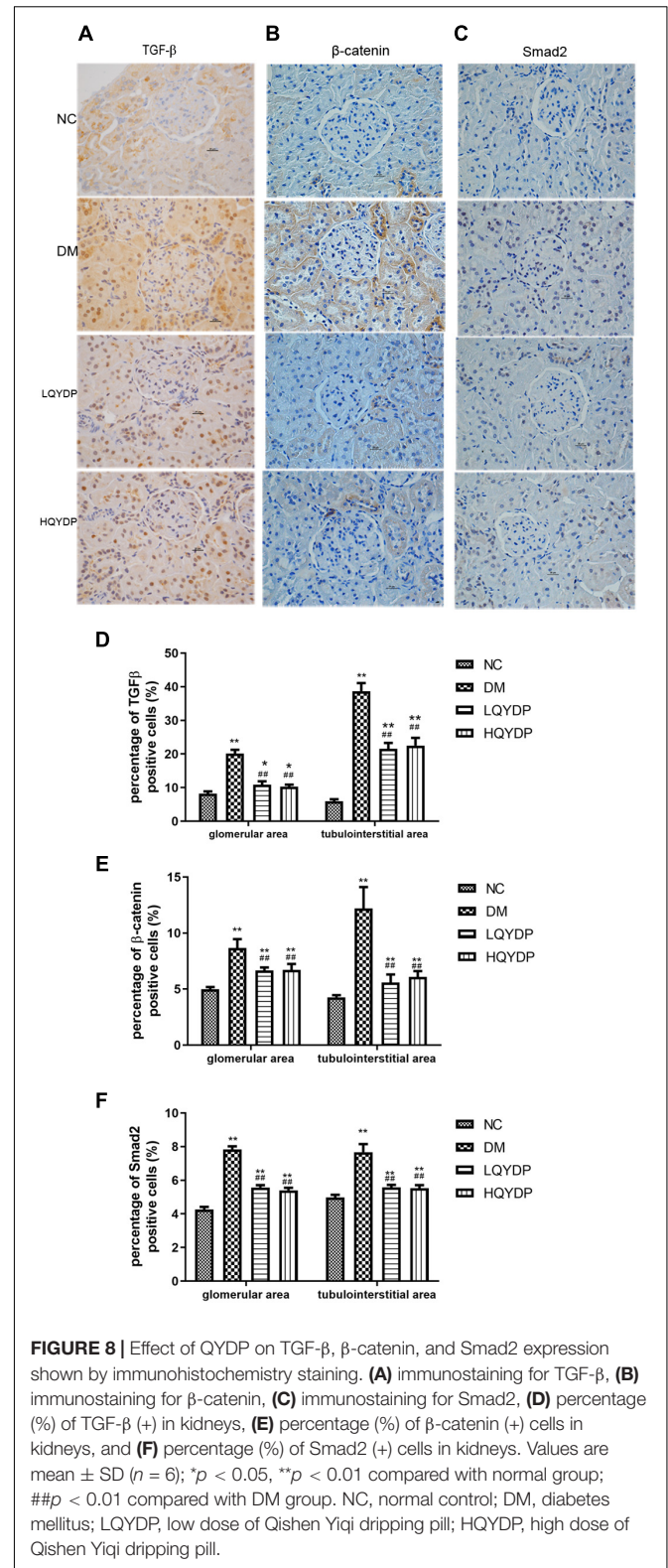


($p < 0.01$, **Figure 9**). QYDP treatment reversed the increases of these fibrotic markers ($p < 0.01$, **Figure 9**).

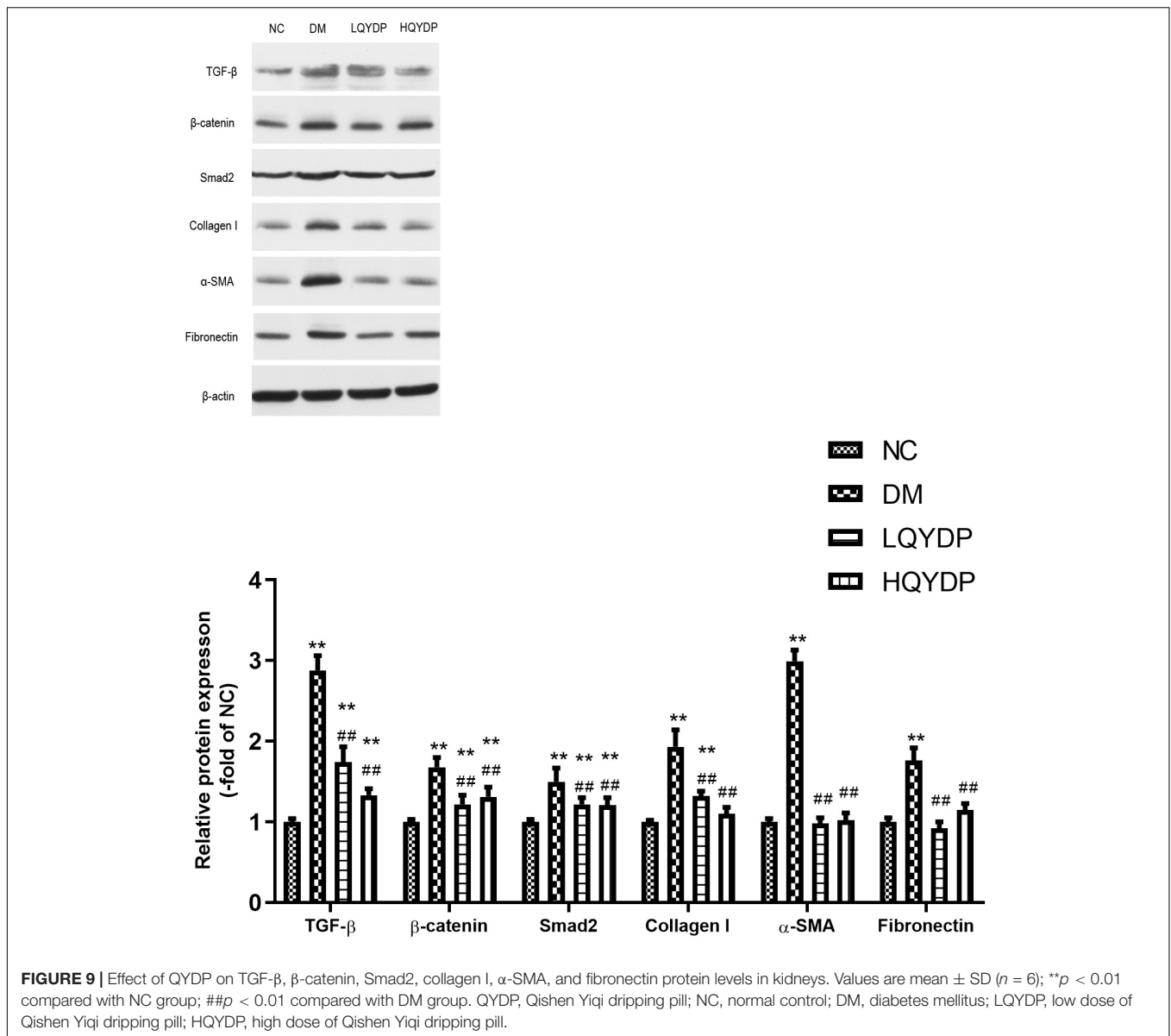
DISCUSSION

In this study, our data show that both the low and high QYDP dosage reduced serum creatinine, BUN, and 24-h urinary albumin and moderated kidney hypertrophy and renal histology in diabetic rats. No significant dosage-dependent effect was observed. The possible reason might be that the high dosage exceeds the maximum efficacy. Furthermore, we observed a significant downregulation of collagen I, α -SMA, and FN in QYDP-treated diabetic rats. Overall, QYDP moderated kidney function and renal fibrosis in diabetic rats. QYDP includes Radix Astragali (*A. penduliflorus* Lam.), redroot sage (*S. miltiorrhiza* Bunge), pseudoginseng (*P. pseudoginseng* Wall.), and fragrant rosewood (*D. odorifera* T.C. Chen). Astragalosides, which is an active ingredient of Radix Astragali, have a potent antioxidant effect and inhibit high glucose-induced mesangial cell proliferation *in vitro* (Sun et al., 2014; Chen et al., 2016). Radix Astragali significantly reduces oxidative activity in diabetic rat kidneys (Chen et al., 2016). Two major isoflavonoids in Radix Astragali have inhibitory effects on AGE-induced endothelial cell apoptosis (Tang et al., 2011). Redroot sage extracts have a renoprotection effect in streptozotocin-induced diabetic rats (Yin et al., 2014), ameliorated renal function, and reduced TGF- β 1 (Liu et al., 2005) and collagen IV (Lee et al., 2011).

Without reducing blood glucose, QYDP can moderate renal function in diabetic rats. This indicates that QYDP has direct beneficial effects on the kidney rather than indirect effects through moderating hyperglycemia. We further performed microarray gene expression profile analysis to determine the mechanism underlying the effect of QYDP on the kidneys of diabetic rats. Then, pathway analysis of the genes that were differentially expressed in the HQYDP-treated group compared with the DM group was performed. From this analysis, we



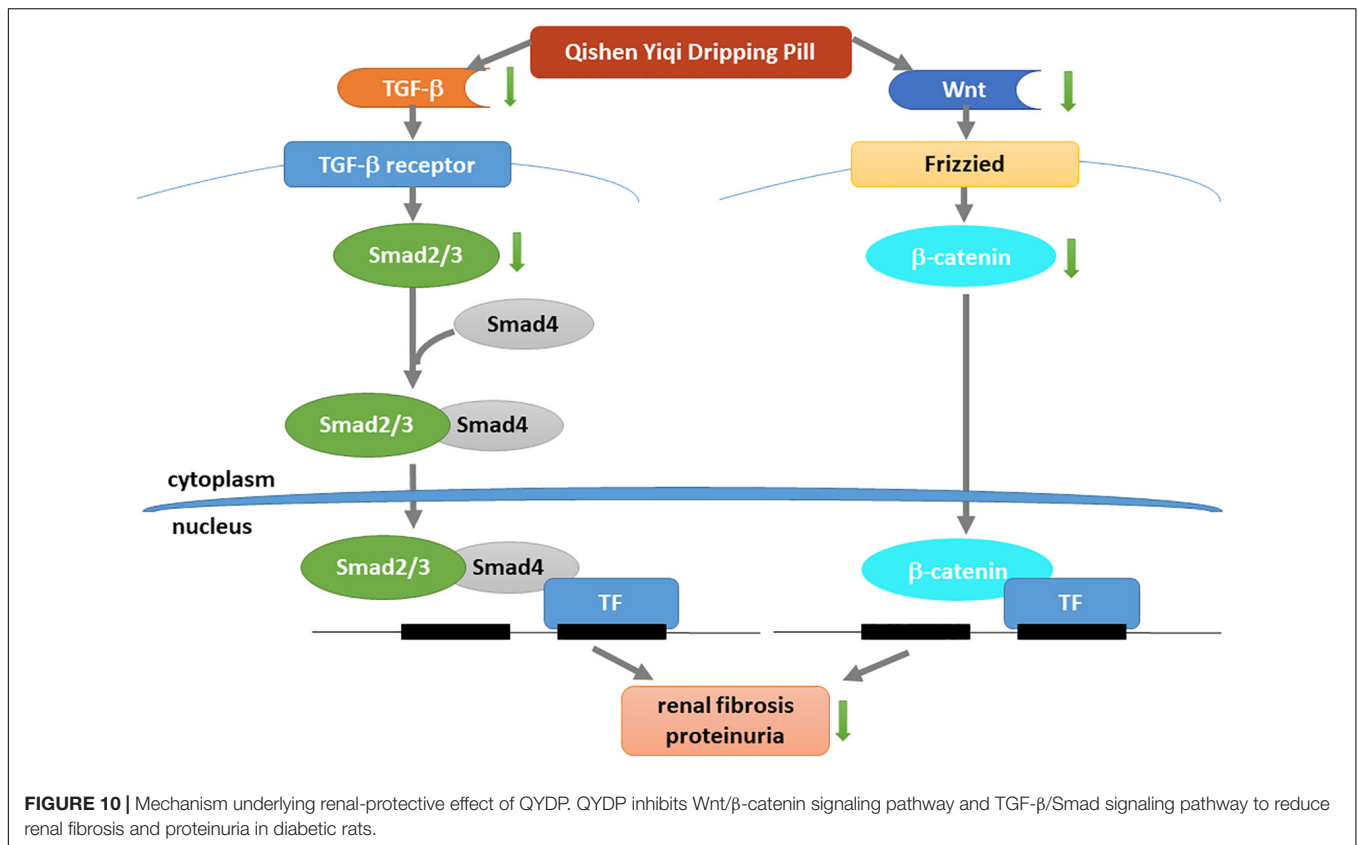
found that the Wnt signaling pathway was in the top 10 pathways. The Wnt signaling pathway diversifies into two branches: the canonical Wnt pathway (the β -catenin pathway) and the non-canonical Wnt pathway. In this study, we found



that QYDP reduced Wnt1 and Ctnnb1 expression in diabetic rats. Additionally, immunostaining analysis and western blotting showed that QYDP reduced β -catenin protein expression. In gene interaction analysis, Ctnnb1 was centrally located among all the differentially expressed genes in the HQYDP-treated group compared with those in the DM group. In CKD rats, QYDP also inhibited β -catenin expression (Zhou et al., 2016). The Wnt/ β -catenin pathway is involved in cellular growth and differentiation in DN (Xiao et al., 2013). In kidneys of both type 1 and 2 diabetic models, the Wnt pathway is activated abnormally (Zhou et al., 2012). This activation of Wnt/ β -catenin contributes to proteinuria (Kato et al., 2011), podocyte dysfunction (Dai et al., 2009), glomerulosclerosis, and renal interstitial fibrosis (He et al., 2009). *In vivo* and *in vitro*, overexpression of either Wnt1 or stabilized β -catenin leads to podocyte dysfunction (Dai et al., 2009). Blockade or knockout of Wnt/ β -catenin protects

against the development of podocyte lesions and albuminuria (Dai et al., 2009). Thus, QYDP treatment may alleviate kidney dysfunction by inhibiting the Wnt/ β -catenin pathway.

In addition, pathway analysis showed that the TGF- β signaling pathway ranked third among all pathways affected by QYDP in the kidneys. Immunostaining analysis and western blot analysis showed that QYDP reduced TGF- β expression. TGF- β is an essential mediator that stimulates glomerular ECM formation in DN (Yamamoto et al., 1994). Hyperglycemia leads to TGF- β activation. Chronic inhibition of TGF- β using neutralizing monoclonal antibody in db/db mice prevents glomerulosclerosis and renal dysfunction (Ziyadeh et al., 2000). Zhou et al. (2016) found that QYDP inhibits TGF- β 1-induced β -catenin upregulation in the cytoplasm but does not affect Smad2 and Smad3 phosphorylation and Smad4 or Smad7 expression in normal kidney proximal tubular (NRK52E) cells. However,



in our study, gene interaction analysis showed that Smad2, Smad3, and Tgfb1 were in the central position among all the differentially expressed genes in the HQYDP-treated group compared with the DM group. QYDP reduced Tgfb1 and Smad2 expression and inhibited TGF- β and Smad2 protein expression in diabetic kidneys. The reason for the different results in NRK52E cells and diabetic rats might be the different circumstances *in vivo* and *in vitro*. Unlike diabetic rats, NRK52E cells were used by Zhou et al. (2016). The Smad signaling pathway plays an important role in the TGF- β 1-stimulated accumulation of ECM. TGF- β 1/Smad signaling is a critical pathway for the development of renal fibrosis. TGF- β 1 activates Smad2 and Smad3 phosphorylation, and then, phospho-Smad2/3 binds to Smad4 to form hetero-oligomeric complexes (Meng et al., 2015). These complexes translocate to the nucleus to regulate the transcription factors of other genes related to kidney fibrosis (Massague and Chen, 2000). Hence, QYDP might inhibit TGF- β 1/Smad signaling to improve kidney function in diabetic rats.

CONCLUSION

In summary, this study reveals that QYDP significantly attenuates kidney function and renal fibrosis. Our study is the first to show that QYDP moderates kidney function by inhibiting the Wnt/ β -catenin pathway and TGF- β /Smad signaling in diabetic rats (Figure 10). These results provide a basis for the treatment

of DN patients in the future. Further *in vitro* research is still required to elucidate the mechanistic details of QYDP protection against DN.

DATA AVAILABILITY STATEMENT

The datasets presented in this study can be found in online repositories. The names of the repository/repositories and accession number(s) can be found in the article/Supplementary Material.

ETHICS STATEMENT

The animal study was reviewed and approved by this study was conducted in strict accordance with the recommendations and the approval of the Animal Care Committee of the Peking Union Medical Hospital Animal Ethics Committee (Project XHDW-2015-0051, 15 February 2015), and all efforts were made to minimize suffering.

AUTHOR CONTRIBUTIONS

XX designed the experiments and contributed reagents and materials. QZ, JZ, TW, and XW conducted the experiments. MY, ML, and FP analyzed the data. QZ wrote the manuscript. All authors have read and approved the article.

FUNDING

This work was supported by grants from National Key R&D Program of China (2017YFC1309603), National Natural Science Foundation of China (Nos. 81870579, 81870545, 81170736, and 81570715), Beijing Natural Science Foundation (7202163 and 7172169), Beijing Municipal Science & Technology Commission (Z201100005520011), Beijing Dongcheng District Outstanding Talent Funding Project (2019DCT-M-05), National Key Research and Development Program of China (2016YFA0101002 and 2018YFC2001100), Medical Epigenetics Research Centre, Chinese Academy of Medical Sciences (2017PT31036 and 2018PT31021), the Non-Profit Central Research Institute Fund of Chinese Academy of Medical Sciences (Nos. 2017PT32020 and 2018PT32001), National Natural Science Foundation for Young Scholars of China (No. 81300649), China Scholarship Council Foundation (201308110443), PUMC Youth Fund (33320140022) and Fundamental Research Funds for the Central Universities,

REFERENCES

- Baynes, J. W. (1991). Role of oxidative stress in development of complications in diabetes. *Diabetes Metab. Res. Rev.* 40, 405–412. doi: 10.2337/diab.40.4.405
- Brownlee, M., Cerami, A., and Vlassara, H. (1988). Advanced glycosylation end products in tissue and the biochemical basis of diabetic complications. *N. Engl. J. Med.* 318, 1315–1321. doi: 10.1056/nejm198805193182007
- Chen, X., Wang, D. D., Wei, T., He, S. M., Zhang, G. Y., and Wei, Q. L. (2016). Effects of astragalosides from Radix Astragali on high glucose-induced proliferation and extracellular matrix accumulation in glomerular mesangial cells. *Exp. Ther. Med.* 11, 2561–2566. doi: 10.3892/etm.2016.3194
- Cybulsky, A. V., Takano, T., Papillon, J., Kitzler, T. M., and Bijian, K. (2011). Endoplasmic reticulum stress in glomerular epithelial cell injury. *Am. J. Physiol. Renal Physiol.* 301, F496–F508. doi: 10.1152/ajprenal.00728.2010
- Dai, C., Stolz, D. B., Kiss, L. P., Monga, S. P., Holzman, L. B., and Liu, Y. (2009). Wnt/ β -catenin signaling promotes podocyte dysfunction and albuminuria. *J. Am. Soc. Nephrol.* 20, 1997–2008. doi: 10.1681/asn.2009010019
- el Nahas, A. M., Zoob, S. N., Evans, D. J., and Rees, A. J. (1987). Chronic renal failure after nephrotoxic nephritis in rats: contributions to progression. *Kidney Int.* 32, 173–180. doi: 10.1038/ki.1987.189
- Go, A. S., Chertow, G. M., Fan, D., McCulloch, C. E., and Hsu, C. Y. (2004). Chronic kidney disease and the risks of death, cardiovascular events, and hospitalization. *N. Engl. J. Med.* 351, 1296–1305. doi: 10.1056/NEJMoa041031
- Ha, H., Hwang, I. A., Park, J. H., and Lee, H. B. (2008). Role of reactive oxygen species in the pathogenesis of diabetic nephropathy. *Diabetes Res. Clin. Pract.* 82(Suppl. 1), S42–S45. doi: 10.1016/j.diabres.2008.09.017
- He, W., Dai, C., Li, Y., Zeng, G., Monga, S. P., and Liu, Y. (2009). Wnt/ β -catenin signaling promotes renal interstitial fibrosis. *J. Am. Soc. Nephrol.* 20, 765–776. doi: 10.1681/asn.2008060566
- Kato, H., Gruenewald, A., Suh, J. H., Miner, J. H., Barisoni-Thomas, L., Taketo, M. M., et al. (2011). Wnt/ β -catenin pathway in podocytes integrates cell adhesion, differentiation, and survival. *J. Biol. Chem.* 286, 26003–26015. doi: 10.1074/jbc.M111.223164
- Koya, D., Jirousek, M. R., Lin, Y. W., Ishii, H., Kuboki, K., and King, G. L. (1997). Characterization of protein kinase C β isoform activation on the gene expression of transforming growth factor- β , extracellular matrix components, and prostanoids in the glomeruli of diabetic rats. *J. Clin. Invest.* 100, 115–126. doi: 10.1172/jci119503
- Lee, S. H., Kim, Y. S., Lee, S. J., and Lee, B. C. (2011). The protective effect of *Salvia miltiorrhiza* in an animal model of early experimentally induced diabetic nephropathy. *J. Ethnopharmacol.* 137, 1409–1414. doi: 10.1016/j.jep.2011.08.007

and Scientific Activities Foundation for Selected Returned Overseas Professionals of Human Resources and Social Security Ministry, Chinese Academy of Medical Sciences Innovation Fund for Medical Sciences (CIFMS2017-I2M-1-008).

ACKNOWLEDGMENTS

We are very grateful to Beijing Compass Biotechnology Company for excellent technical assistance with the microarray experiments.

SUPPLEMENTARY MATERIAL

The Supplementary Material for this article can be found online at: <https://www.frontiersin.org/articles/10.3389/fphys.2020.613324/full#supplementary-material>

- Liu, G., Guan, G. J., Qi, T. G., Fu, Y. Q., Li, X. G., Sun, Y., et al. (2005). [Protective effects of *Salvia miltiorrhiza* on rats with streptozotocin diabetes and its mechanism]. *Zhong Xi Yi Jie He Xue Bao* 3, 459–462. doi: 10.3736/jcim20050610
- Mariappan, M. M. (2012). Signaling mechanisms in the regulation of renal matrix metabolism in diabetes. *Exp. Diabetes Res.* 2012:749812. doi: 10.1155/2012/749812
- Massague, J., and Chen, Y. G. (2000). Controlling TGF- β signaling. *Genes Dev.* 14, 627–644.
- Meng, X. M., Tang, P. M., Li, J., and Lan, H. Y. (2015). TGF- β /Smad signaling in renal fibrosis. *Front. Physiol.* 6:82. doi: 10.3389/fphys.2015.00082
- Nelson, R. G., Bennett, P. H., Beck, G. J., Tan, M., Knowler, W. C., Mitch, W. E., et al. (1996). Development and progression of renal disease in Pima Indians with non-insulin-dependent diabetes mellitus. Diabetic Renal Disease Study Group. *N. Engl. J. Med.* 335, 1636–1642. doi: 10.1056/nejm199611283352203
- Piecha, G., Kokeny, G., Nakagawa, K., Koleganova, N., Geldyyev, A., Berger, I., et al. (2008). Calcimimetic R-568 or calcitriol: equally beneficial on progression of renal damage in subtotaly nephrectomized rats. *Am. J. Physiol. Renal Physiol.* 294, F748–F757. doi: 10.1152/ajprenal.00220.2007
- Sun, L., Li, W., Li, W., Xiong, L., Li, G., and Ma, R. (2014). Astragaloside IV prevents damage to human mesangial cells through the inhibition of the NADPH oxidase/ROS/Akt/NF κ B pathway under high glucose conditions. *Int. J. Mol. Med.* 34, 167–176. doi: 10.3892/ijmm.2014.1741
- Tang, D., He, B., Zheng, Z. G., Wang, R. S., Gu, F., Duan, T. T., et al. (2011). Inhibitory effects of two major isoflavonoids in Radix Astragali on high glucose-induced mesangial cells proliferation and AGEs-induced endothelial cells apoptosis. *Planta Med.* 77, 729–732. doi: 10.1055/s-0030-1250628
- Wang, G., Zheng, C., Wang, Y., Hao, R., Xu, H., Pan, L., et al. (2019). “Study on the toxicity and toxicokinetics of Qishen Yiqi dropping pills after repeated intragastric administration for 26 weeks in rats,” in *Proceedings of the Annual Conference on Toxicology and safety evaluation of traditional Chinese medicine and natural drugs of Chinese society of Toxicology*, Berlin.
- Williams, R., Karuranga, S., Malanda, B., Saeedi, P., Basit, A., Besancon, S., et al. (2020). Global and regional estimates and projections of diabetes-related health expenditure: results from the international diabetes federation diabetes Atlas, 9(th) edition. *Diabetes Res. Clin. Pract.* 162:108072. doi: 10.1016/j.diabres.2020.108072
- Xiao, L., Wang, M., Yang, S., Liu, F., and Sun, L. (2013). A glimpse of the pathogenetic mechanisms of Wnt/ β -catenin signaling in diabetic nephropathy. *Biomed. Res. Int.* 2013:987064. doi: 10.1155/2013/987064
- Yamamoto, T., Noble, N. A., Miller, D. E., and Border, W. A. (1994). Sustained expression of TGF- β 1 underlies development of progressive kidney fibrosis. *Kidney Int.* 45, 916–927. doi: 10.1038/ki.1994.122

- Yin, D., Yin, J., Yang, Y., Chen, S., and Gao, X. (2014). Renoprotection of Danshen Injection on streptozotocin-induced diabetic rats, associated with tubular function and structure. *J. Ethnopharmacol.* 151, 667–674. doi: 10.1016/j.jep.2013.11.025
- Yongbin Chen, Y. W. (2011). Curative effect of Qishenyiqi Drop Pills on early diabetic nephropathy. *Chinese Gen. Practice* 14, 520–522.
- Zhou, T., He, X., Cheng, R., Zhang, B., Zhang, R. R., Chen, Y., et al. (2012). Implication of dysregulation of the canonical wntless-type MMTV integration site (WNT) pathway in diabetic nephropathy. *Diabetologia* 55, 255–266.
- Zhou, Z., Hu, Z., Li, M., Zhu, F., Zhang, H., Nie, J., et al. (2016). QiShenYiQi attenuates renal interstitial fibrosis by blocking the activation of beta-catenin. *PLoS One* 11:e0162873. doi: 10.1371/journal.pone.0162873
- Ziyadeh, F. N., Hoffman, B. B., Han, D. C., Iglesias-De La Cruz, M. C., Hong, S. W., Isono, M., et al. (2000). Long-term prevention of renal insufficiency, excess matrix gene expression, and glomerular mesangial matrix expansion by treatment with monoclonal antitransforming growth factor-beta antibody in db/db diabetic mice. *Proc. Natl. Acad. Sci. U.S.A.* 97, 8015–8020. doi: 10.1073/pnas.120055097
- Conflict of Interest:** The authors declare that the research was conducted in the absence of any commercial or financial relationships that could be construed as a potential conflict of interest.

Copyright © 2021 Zhang, Xiao, Zheng, Li, Yu, Ping, Wang and Wang. This is an open-access article distributed under the terms of the Creative Commons Attribution License (CC BY). The use, distribution or reproduction in other forums is permitted, provided the original author(s) and the copyright owner(s) are credited and that the original publication in this journal is cited, in accordance with accepted academic practice. No use, distribution or reproduction is permitted which does not comply with these terms.



Nicotinamide Mononucleotide Attenuates Renal Interstitial Fibrosis After AKI by Suppressing Tubular DNA Damage and Senescence

Yan Jia¹, Xin Kang², Lishan Tan¹, Yifei Ren², Lei Qu², Jiawei Tang², Gang Liu², Suxia Wang³, Zuying Xiong^{1*} and Li Yang^{2*}

¹ Department of Nephrology, Peking University Shenzhen Hospital, Shenzhen Peking University-The Hong Kong University of Science and Technology Medical Center, Shenzhen, China, ² Key Laboratory of Renal Disease, Renal Division, Department of Medicine, Peking University First Hospital, Peking University Institute of Nephrology, Ministry of Health of China, Beijing, China, ³ Laboratory of Electron Microscopy, Pathological Center, Peking University First Hospital, Beijing, China

OPEN ACCESS

Edited by:

Isotta Chimenti,
Sapienza University of Rome, Italy

Reviewed by:

Theodoros Eleftheriadis,
University of Thessaly, Greece

Chunling Li,
Sun Yat-sen University, China

Marie Migaud,
University of South Alabama,
United States

*Correspondence:

Zuying Xiong
xiongzy2005@163.com
Li Yang
li.yang@bjmu.edu.cn

Specialty section:

This article was submitted to
Renal and Epithelial Physiology,
a section of the journal
Frontiers in Physiology

Received: 05 January 2021

Accepted: 01 March 2021

Published: 23 March 2021

Citation:

Jia Y, Kang X, Tan L, Ren Y, Qu L,
Tang J, Liu G, Wang S, Xiong Z and
Yang L (2021) Nicotinamide
Mononucleotide Attenuates Renal
Interstitial Fibrosis After AKI by
Suppressing Tubular DNA Damage
and Senescence.
Front. Physiol. 12:649547.
doi: 10.3389/fphys.2021.649547

Acute kidney injury (AKI) is a worldwide health problem currently lacking therapeutics that directly promote renal repair or prevent the occurrence of chronic fibrosis. DNA damage is a feature of many forms of kidney injury, and targeting DNA damage and repair might be effective strategies for kidney protection in AKI. Boosting nicotinamide adenine dinucleotide (NAD⁺) levels is thought to have beneficial effects on DNA damage repair and fibrosis in other organs. However, no kidney-related studies of such effects have been performed to date. Here, we have shown that NMN (an NAD⁺ precursor) administration could significantly reduce tubular cell DNA damage and subsequent cellular senescence induced by hydrogen peroxide and hypoxia in human proximal tubular cells (HK-2 cells). The DNA damage inhibition, antiaging and anti-inflammatory effects of NMN were further confirmed in a unilateral ischemia-reperfusion injury (uIRI) mouse model. Most importantly, the antifibrosis activity of NMN was also shown in ischemic AKI mouse models, regardless of whether NMN was administered in advance or during the recovery phase. Collectively, these results suggest that NMN could significantly inhibit tubular cell DNA damage, senescence and inflammation. NMN administration might be an effective strategy for preventing or treating kidney fibrosis after AKI.

Keywords: AKI, NMN, DNA damage, senescence, renal fibrosis

INTRODUCTION

Acute kidney injury (AKI) is a worldwide health problem characterized by sudden impairment of kidney function as a result of a toxic or ischemic insult. It is very common in the clinic, affecting 25–45% of high-risk hospitalized patients, such as surgery, trauma and intensive care unit patients (Rewa and Bagshaw, 2014). The mortality rate of severe AKI patients reaches 50%, while approximately 20–50% of surviving patients develop chronic kidney disease (CKD), and approximately 3–15% progress to end stage renal disease (ESRD) (Ferenbach and Bonventre, 2015; Varrier et al., 2015; Yang et al., 2015). However, no approved therapeutics have been directly indicated to promote renal repair or to prevent the occurrence of chronic fibrosis yet, and studying the molecular mechanism of AKI progression to CKD and finding targets of intervention are urgently needed.

Renal proximal tubular epithelial cells (PTECs), the most prominent cell type in the renal cortical tubulointerstitium, are particularly sensitive to injury (Bonventre and Yang, 2011). While the pathogenesis of AKI is multifactorial, recent studies have shown that DNA damage in PTECs plays an important role in the progression of AKI to CKD (Yang et al., 2010; Ferenbach and Bonventre, 2015; Canaud et al., 2019; Kishi et al., 2019). Maintaining and guaranteeing the DNA integrity of renal tubular epithelial cells may protect their structure and function after AKI. Nicotinamide adenine dinucleotide (NAD⁺) is a cellular metabolite in all living cells that is critical for fundamental biological processes, namely, DNA repair and energy metabolism. Since renal tubular cells are highly metabolically active, they are very sensitive to NAD⁺ depletion and impairment of ATP production. Replenishment of NAD⁺ levels via administration of its precursors, such as nicotinamide riboside (NR), nicotinamide mononucleotide (NMN), and nicotinamide (NAM), has been demonstrated to display beneficial effects against fibrosis and age-related diseases (Mills et al., 2016; Pham et al., 2019; Zheng et al., 2019). Multiple lines of evidence suggest that NMN might have important roles in protecting against DNA damage and ameliorating the long-term profibrotic response following AKI. However, to our knowledge, no studies have yet demonstrated such effects.

In our study, we first demonstrated that hydrogen peroxide and hypoxia resulted in DNA damage and subsequent G2/M arrest and senescence in HK-2 cells. NMN could decrease these injury phenotypes. Furthermore, we confirmed the DNA damage inhibition and antiaging effects of NMN administration in ischemic AKI mouse models. The antifibrosis ability of NMN was also proven in ischemic AKI mouse models, regardless of whether it was administered in advance or during the recovery phase. These findings have high translational potential as a pharmacologic strategy for improving fibrosis after AKI.

MATERIALS AND METHODS

Cell Culture and Treatment

Human kidney-2 (HK-2) cells was cultured in Dulbecco's modified Eagle's medium (Gibco) with 10% fetal bovine serum (Gibco) at 37°C in a humidified 5% CO₂ atmosphere. To induce injury *in vitro*, HK-2 cells were seeded in 6-well plates at 1 × 10⁶ cells/well and then were stimulated with 1 mM hydrogen peroxide (H₂O₂, Beijing Chemical Works, A1029005) (Lee et al., 2006; Small et al., 2014) and 1% O₂ (Zhu et al., 2019) to generate a hypoxic environment using Whitley H35 hypoxystation (Don Whitley Scientific). Nicotinamide mononucleotide (β-NMN; Sigma-Aldrich; N3501) was dissolved in PBS and preserved at –20°C until use.

Animal Models

Male C57BL/6 mice were purchased from SPF (Beijing) Biotechnology Co., Ltd. They were maintained on a 12:12 h light-dark cycle in a temperature-controlled room and were allowed free access to standard rodent chow and water. All animal

studies were approved by the institutional Animal Care and Use Committee of Peking University First Hospital.

Warm ischemia was modeled by generating a unilateral ischemia-reperfusion injury (uIRI) in 8- to 10-week-old C57BL/6 mice. Briefly, mice were kept on a homeothermic unit and subjected to flank incisions. The left renal pedicle was exposed and clamped for 30 min. After removal of the clamp, the color of the kidneys turned from dark purple to pink. To examine the effect of NMN (β-NMN, Sigma-Aldrich, N3501) administration at the acute phase of uIRI, NMN (500 mg/kg body wt) (Guan et al., 2017; Li et al., 2017) or an equivalent amount of PBS was administered 20 min before the procedure by intraperitoneal injection and on days 1, 2, and 3 after surgery. Mice were euthanized at two time points: 4 h after the last injection (day 3) and day 21 after surgery (day 21), and then kidneys were collected from both sides. To examine the effect of NMN administration at the recovery phase of uIRI, NMN (500 mg/kg body wt) or an equivalent amount of PBS was administered intraperitoneally on days 3 and 14, and then mice were euthanized on day 21 after surgery, and kidneys were collected from both sides.

NAD⁺ Measurement

NAD⁺ levels of HK-2 cells and kidney tissues was measured with an NAD/NADH Quantification Kit (Beyotime, S0175) according to manufacture's instructions.

Flow Cytometry

For cell cycle analysis, HK-2 cells were trypsinized and then washed with PBS for two times. After fixed in 1 mL of ice-cold 75% ethanol at 4°C overnight, HK-2 cells were incubated with 500 μL of PI/RNase staining buffer (BD PharMingen, BD 550825) for 15 min at room temperature. Cell cycle analysis was performed by flow cytometry using a BD FACSCalibur and analyzed with ModFit LT software. For analysis of DNA damage, HK-2 cells were incubated with a γH2A.X (ser139) antibody (CST, #9719) according to the manufacturer's protocol.

Protein Extraction and Western Blot

Total protein from HK-2 cells was extracted with RIPA buffer (Sigma, R0278), and protein from the kidneys of mice was extracted with a Minute™ Total Protein Extraction Kit for Animal Cultured Cells/Tissues (Invent, SD-001) following standard protocols. Protein concentration was measured using a Pierce BCA Protein Assay kit (Thermo Fisher Scientific, 23227). Next, denatured proteins were separated in sodium dodecyl sulfate-polyacrylamide gels and then were electrically transferred onto polyvinylidene difluoride membranes (Millipore, IPVH00010). The membranes were blocked for 60 min in 5% fat-free milk dissolved in Tris-buffer saline with 0.1% Tween 20 (TBST). The blots were incubated with relevant primary antibodies overnight at 4°C as follows: γH2A.X (ser139) (Noves, NB100-74435, 1:1000), α-SMA (Abcam, ab32575, 1:2000), Collagen IV (Abcam, ab6586, 1:2000), Tubulin (ZSBio, TA-10, 1:5000) and GAPDH (Santa Cruz, sc-32233, 1:2000). After washing three times with TBST, the membranes were incubated with secondary HRP-conjugated secondary antibodies at a 1:1000 dilution for 1 h at room temperature. After five washes

with TBST, the membranes were incubated in chemiluminescent substance (Millipore, WBKLS0100) for 5 min, and images were captured by a ImageQuant LAS 4000 Mini system (GE Healthcare). The density of each band was quantified by ImageJ (Media Cybernetics, Silver Spring, MD, United States).

SA- β -gal Staining

Senescence-associated β -galactosidase (SA- β -gal) staining was performed using a senescence cell histochemical staining kit (Sigma-Aldrich, CS0030) according to the manufacturer's instructions. For *in vitro* experiments, cells were evaluated under a light microscope, and SA- β -gal-positive cells were counted in at least ten fields. For *in vivo* experiments, frozen sections (4 μ m thickness) of kidney tissues were used. At least fifteen fields were calculated under a light microscope, and the mean integrated optical density (IOD) of SA- β -gal expression was analyzed by Image-Pro Plus software (Media Cybernetics Co., Ltd).

EdU Incorporation

DNA replication activity was analyzed in cells with an EdU staining kit (Thermo Fisher Scientific, C10337). Briefly, HK-2 cells were seeded on coverslips in 12-well plates as previously described. EdU (10 μ M) was added to each well for 2 h until the cells were harvested 48 h after stimulation. Cells were collected and fixed with 4% paraformaldehyde for 10 min and then were permeabilized with 0.5% Triton X-100 for 10 min at room temperature. The cells were then stained with a Click-iT[®] Plus reaction cocktail kit for 30 min at room temperature. Finally, images were obtained with a microscope (Nikon, Tokyo, Japan) and then were analyzed with Image J (Media Cybernetics, Silver Spring).

Measurement of Cell Viability

HK-2 cells grown in 96-well plates were treated as previously described. Various concentrations of NMN (ranging from 0.03125 to 2 mM) were simultaneously added into the culture medium with H₂O₂ and while hypoxia stimuli was administered; treatment lasted 48 h. CellTiter-Fluor[™] Cell Viability Assay kit (Promega, Madison, WI, United States) was used to assess cell viability according to the manufacturer's instructions. Following incubation of the cells with the substrate for 60 min at 37°C, fluorescence was measured using a Synergy H1 reader (excitation: 400 nm/emission: 505 nm). Viability of the treated cells was normalized against the control cells.

Kidney Histopathological Analysis

To evaluate renal pathologic changes, kidney tissue samples were fixed overnight with 10% formalin in 0.01 mol/L phosphate buffer (pH 7.2) and then embedded in paraffin for histopathology analysis. The slide sections (3–4 μ m thickness) were stained with hematoxylin-eosin (HE) according to standard procedures and examined under a light microscope. The examination of renal pathology was performed in a blinded fashion, and the pathologic assessment was performed on the basis of the percentage of tubules with necrosis, detachment, cast formation, dilation, or cell swelling.

Sirius Red Staining

After deparaffinization and rehydration, paraffin sections were stained with Sirius red to evaluate collagen fibers according to manufacture's instruction (Solarbio, G1470), and were calculated as a percentage of the total area. The images of Sirius red-stained sections were obtained with a digital microscope camera (Nikon, Tokyo, Japan), and quantitative evaluation was performed using Image-Pro Plus software (Media Cybernetics Co., Ltd).

In situ TUNEL Assay

Apoptosis in the kidney tissues was detected in paraffin sections by *in situ* TUNEL assays that were performed according to a standard protocol (Beyotime Biotechnology, C1086). Ten to fifteen fields were selected randomly from each tissue section and the number of TUNEL-positive cells were determined per 400 \times field.

Immunofluorescence Staining

Immunofluorescence staining of the kidney was performed on paraffin sections. After fixation and antigen retrieval, non-specific binding was blocked with 3% BSA. Kidney sections were then incubated with the following primary antibodies: rabbit antibody to α -SMA (Abcam, ab32575, 1:200), rabbit antibody to Ki-67 (Abcam, ab66155, 1:500), and mouse antibody to p-H3 (ser10) (Abcam, ab14955, 1:1000). The slides were then exposed to FITC or Cy3-labeled secondary antibodies (Jackson ImmunoResearch) and were mounted with medium containing DAPI. The percentage of α -SMA-positive area to cortex and outer medulla section were calculated, respectively, using Image-Pro Plus software (Media Cybernetics Co., Ltd). For cell cycle analysis, results are expressed as the number of Ki-67 or p-H3 positive tubular cells per high-power field.

RNA Isolation and RT-PCR Analysis

Kidney tissues were collected in RNase-free tubes, and total RNA was extracted using TRIzol reagent (Invitrogen) according to the manufacturer's instructions. For cDNA synthesis, reverse transcription was performed from 2 μ g of total RNA using a FastKing RT Kit (Tiangen, KR116). The mRNA expression levels of IL-6, IL-8, TGF- β 1, and β -actin were determined using SuperReal PreMix Plus (SYBR Green) (FP205, Tiangen) based on the manufacturer's instructions. The sequences of the primers used are shown in **Table 1**. The PCR system consisted of SYBR Green Mix, forward and reverse primers, cDNA, and deionized RNase-free water. PCR was initially denatured at 95°C for 30 s followed by 95°C for 10 s and 65°C for 30 s for 40 cycles and then 81 cycles at 55–95°C for 10 s for melting curve analysis.

TABLE 1 | Primers used for real-time PCR.

| Genes | Forward primers (5'-3') | Reverse primers (5'-3') |
|----------------|-------------------------|-------------------------|
| IL-6 | CTGCAAGAGACTTCCATCCAG | AGTGGTATAGACAGGTCTGTTGG |
| IL-8 | TCGAGACCATTACTGCAACAG | CATTGCCGGTGGAATTCCTT |
| TGF- β 1 | CTCCCGTGGCTTCTAGTGC | GCCTTAGTTTGACAGGATCTG |
| β -actin | CAGCTGAGAGGGAAATCGTG | CGTTGCCAATAGTGATGACC |

PCR, polymerase chain reaction; IL-6, interleukin-6; IL-8, interleukin-8; TGF- β 1, transforming growth factor β 1.

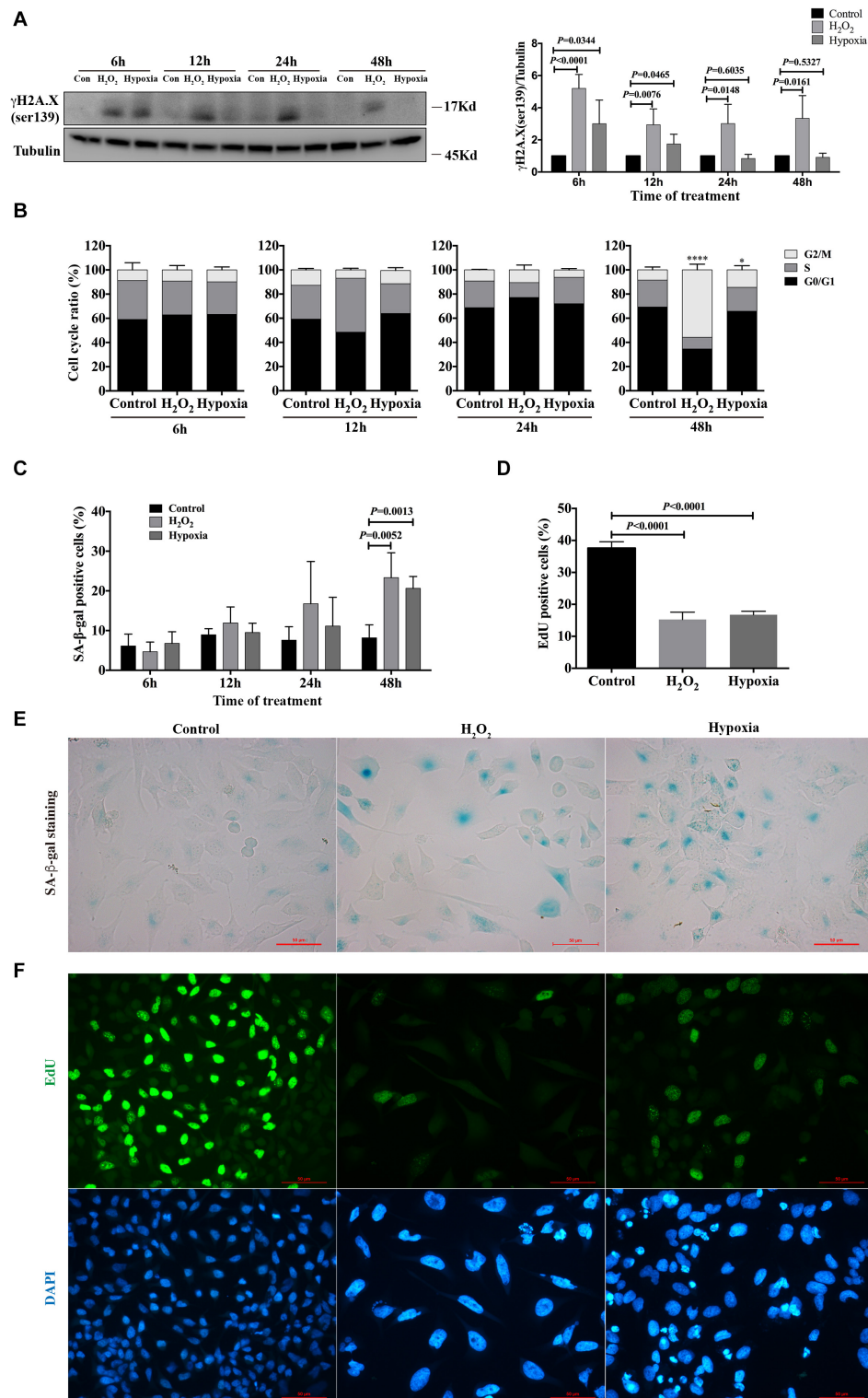


FIGURE 1 | Hydrogen peroxide and hypoxia resulted in DNA damage, G2/M arrest and senescence in HK-2 cells. **(A)** Representative western blots analysis of γH2A.X (ser139), and bar graphs showed the fold changes compared to control group at different time points. **(B)** Flow cytometry analysis of cell cycle. * $P < 0.05$, **** $P < 0.0001$, compared with control group. **(C)** SA-β-gal staining analysis at different time points. **(D)** EdU incorporation analysis at 48 h. **(E)** Representative SA-β-gal staining at 48 h, Scale bars, 50 μm. **(F)** Representative EdU incorporation images at 48 h showed decreased proliferation rate and larger cell size in H₂O₂ and hypoxia groups, Scale bars, 50 μm. $n = 3-5$ /group. Data are means ± SD. SA-β-gal, Senescence Associated β-Galactosidase; EdU, 5-Ethynyl-2'-deoxyuridine.

The comparative gene expression was calculated by the $2^{-\Delta\Delta Ct}$ method as described previously.

Statistical Analysis

GraphPad Prism 6.0 was used. Data from repeated experiments were analyzed and are shown as the mean \pm SD. A two-tailed unpaired *t*-test was applied for comparisons between two groups. Differences at the $P < 0.05$ level were considered statistically significant.

RESULTS

Hydrogen Peroxide and Hypoxia Stimulation Resulted in DNA Damage, G2/M Arrest, and Senescence in HK-2 Cells

To evaluate the phenotype of injury caused by stimuli in renal tubular cells *in vitro*, HK-2 cells were treated with hydrogen peroxide (H_2O_2) and subjected to hypoxia (1% O_2). After 6, 12, 24 and 48 h, the cells were harvested, and the degree of DNA damage, cell cycle distribution and senescence were examined. By western blot analysis, we found that the expression of $\gamma H2A.X$ (ser139), a DNA damage marker (Rogakou et al., 1998; Sharma et al., 2012), was significantly enhanced in both H_2O_2 - and hypoxia-treated groups at 6 h, and its expression were sustained for the duration of the study for the H_2O_2 -treated group (Figure 1A). For the hypoxia-treated group, the enhanced expression of $\gamma H2A.X$ (ser139) was rarely detected at 24 and 48 h (Figure 1A). Cell cycle analysis showed that H_2O_2 and hypoxia treatment did not cause significant changes in cell cycle distribution at 6, 12, and 24 h. However, the percentage of cells in G2/M increased significantly in the H_2O_2 - and hypoxia-treated groups at 48 h compared with the control group ($8.450\% \pm 2.350\%$), being $55.72\% \pm 4.682\%$ ($P < 0.0001$) and $14.42\% \pm 3.485\%$ ($P = 0.0131$), respectively (Figure 1B). Meanwhile, the percentages of senescent cells in both the H_2O_2 - and hypoxia-treated groups increased from $8.185\% \pm 1.629\%$ to $23.33\% \pm 3.140\%$ and $20.65\% \pm 1.491\%$, respectively (Figures 1C,E), as reflected by SA- β -gal staining. EdU incorporation analysis showed significantly decreased proliferation rates of HK-2 cells in the H_2O_2 and hypoxia groups at 48 h (Figures 1D,F). These results suggest that H_2O_2 and hypoxia stimuli could induce DNA damage in HK-2 cells and might thereby further result in G2/M arrest or senescence.

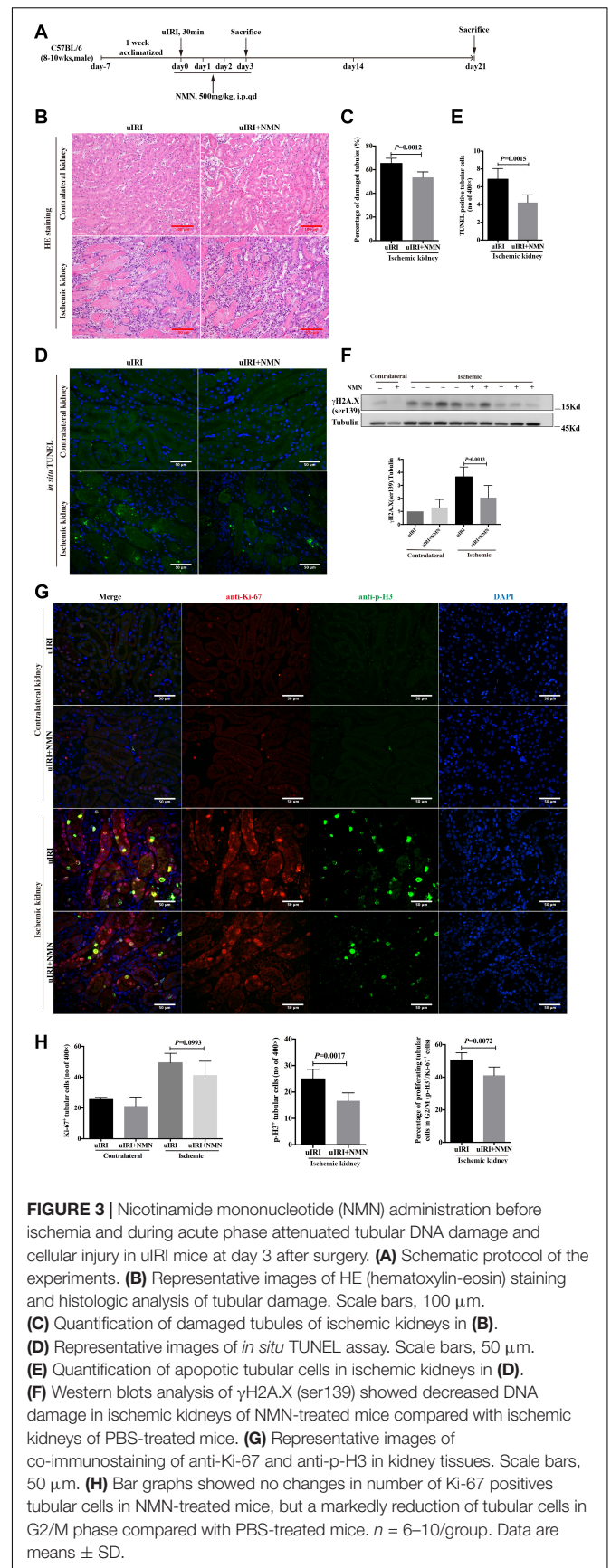
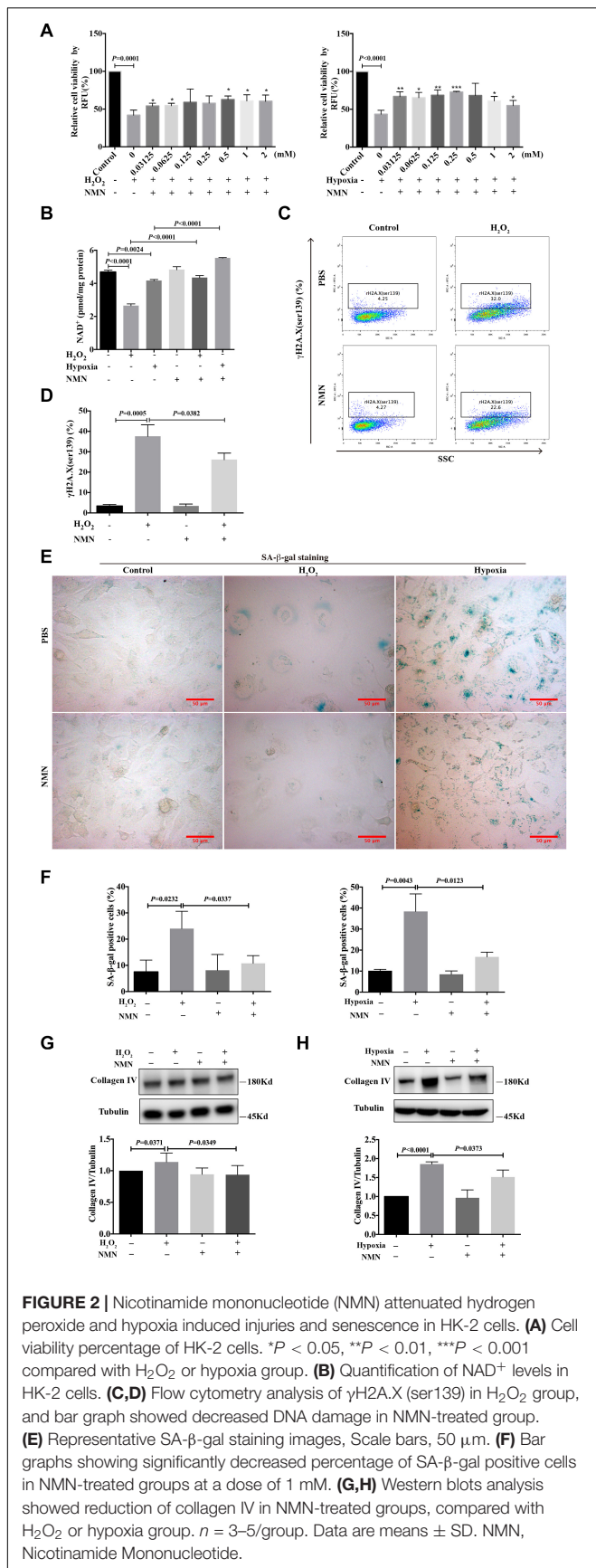
NMN Increased Cell Viability and Attenuated DNA Damage, Senescence and Collagen Production in HK-2 Cells After Hydrogen Peroxide and Hypoxia Stimulation

To investigate the effect of nicotinamide mononucleotide (NMN) on the injury phenotypes induced by H_2O_2 and hypoxia, HK-2 cells were simultaneously incubated for 48 h with various doses of NMN, during H_2O_2 and hypoxia exposure. CellTiter-Fluor™

cell viability assay was performed to examine cell viability. As shown in Figure 2A, NMN administration significantly enhanced the decreased cell viability caused by H_2O_2 and hypoxia stimulation in a dose-dependent manner starting at the lowest dose tested. Considering the improved cell viability and convenience of calculation, NMN at a dose of 1 mM was selected for the following *in vitro* studies. NMN could significantly restored decreased HK-2 cellular NAD^+ levels caused by H_2O_2 and hypoxia insult (Figure 2B). To explore the protective effect of NMN on DNA damage, the expression level of $\gamma H2A.X$ (ser139) was detected by flow cytometry. We found that the percentage of DNA-damaged cells was markedly decreased from 32.0% to 22.6% ($P = 0.0382$) by NMN administration in the H_2O_2 -treated group at 48 h (Figures 2C,D). In addition, NMN administration resulted in a decreased percentage of SA- β -gal-positive cells in the H_2O_2 and hypoxia groups (Figures 2E,F), indicating the effective antiaging activity of NMN *in vitro*. Furthermore, collagen IV protein production in H_2O_2 - and hypoxia-treated HK-2 cells was increased, but it could be suppressed by NMN administration, as determined by western blot analysis (Figures 2G,H). Similar protective effect of NMN was found in HK-2 cells subjected to hypoxia followed by oxygenation (Supplementary Figure 1). These *in vitro* data suggest the protective effect of NMN on tubular cell injury.

NMN Administration Before Ischemia and During the Acute Phase Attenuated Renal Tubular DNA Damage and Cellular Injury in uIRI Mice

To confirm the protective effects of NMN *in vivo*, we established an uIRI mouse model, and NMN or PBS was injected intraperitoneally 20 min before surgery as well as on days 1, 2, and 3 after surgery (totaling 4 consecutive days of injection) (Figure 3A). The mice were sacrificed 4 h after the last injection at day 3 after surgery, and both the ischemic left and healthy right kidneys were taken. Histological study showed intact structure in healthy right kidneys (Figure 3B). Significant renal tubular injury were seen in PBS-treated ischemic kidney, including severe dilation of the proximal tubules, cast formation, and massive detachment and necrosis of the tubular epithelium, while NMN-treated ischemic kidney showed significantly decreased tubular injury (Figures 3B,C). We further conducted an *in situ* TUNEL apoptosis assay and found an increase in tubular apoptosis after injury in PBS-treated mice, while NMN administration substantially reduced tubular apoptosis ($P = 0.0015$, Figures 3D,E). In addition, uIRI mice had elevated levels of DNA damage at day 3 after surgery, as determined by western blot analysis of $\gamma H2A.X$ (ser139), and NMN administration significantly decreased the upregulation of DNA damage (Figure 3F). This suggests that NMN has a protective effect against DNA damage *in vivo*, which is consistent with the *in vitro* results. To analyze the proliferation and cell cycle distribution of proximal tubular epithelial cells, immunohistochemistry co-staining of Ki-67 and phosphorylation of histone H3 at ser10 (p-H3) were performed. The uIRI mice had an increase in tubular cell



proliferation (Ki-67 positive) at day 3 after injury, and NMN administration did not cause obvious changes in the number of proliferating tubular cells. There was also an increase in the number of tubular cells in G2/M phase (p-H3 positive) after injury, and the percentage of tubular cells in G2/M phase (p-H3 positive) among all proliferating tubular cells decreased significantly in NMN-treated uIRI mice (from $50.53\% \pm 1.828\%$ to $41.19\% \pm 2.093\%$, $P = 0.0072$) (Figures 3G,H). This suggested that NMN administration before ischemia and during the acute phase could attenuate renal tubular DNA damage and cellular injury in uIRI mice.

NMN Administration Before Ischemia and During the Acute Phase Attenuated Renal Tubular Senescence, Chronic Inflammation and Fibrosis in uIRI Mice

To explore the effect of NMN on chronic kidney changes in uIRI mice, kidneys of uIRI mice were treated with PBS or NMN as described above, and then they were collected at day 21 after surgery. We found that tubular DNA damage was sustained at day 21 after surgery and could be significantly suppressed by NMN administration, as reflected by western blot analysis of γ H2A.X (ser139) (Figures 4A,B). Furthermore, the tubular cells of uIRI mice showed strong positive SA- β -gal staining, indicating that the cells were senescent, which could also be significantly reduced by NMN treatment (Figures 4C,D). Senescent tubular cells are thought to secrete cytokines and inflammatory factors, which are indicative of the senescence-associated secretory phenotype (SASP). SASP composition varies depending on cell and tissue of origin and the triggers involved, but IL-6 and IL-8 are a highly conserved part of the SASP and have an important role in propagating senescence and regulating its accompanying inflammatory phenotype. As shown by the qRT-PCR data (Figure 4E), the mRNA levels of *IL-6*, *IL-8*, and *TGF- β 1* were decreased in NMN-treated uIRI mice. These data indicated an inhibitory effect of NMN on uIRI-induced tubular premature senescence. Sirius red staining revealed a high level of collagen deposition in PBS-treated uIRI mice (Figure 5A), which was alleviated significantly in NMN-treated mice ($P = 0.0155$) (Figure 5B). Immunostaining of α -SMA together with western blot analysis of α -SMA and collagen IV confirmed the significantly decreased collagen deposition in NMN-treated uIRI mice (Figures 5C–F). These results indicate that fibrotic changes in the kidneys of uIRI mice could be alleviated by the administration of NMN before ischemia and during the acute phase.

NMN Administration During the Recovery Phase Attenuated the uIRI-Induced DNA Damage, Senescence and Fibrosis Phenotype

Considering that the use of prophylactic medication is not practical in clinical patients, we evaluated the renal fibrosis inhibitory effect of NMN administration during the recovery phase of IRI. Mice that underwent uIRI surgery were injected

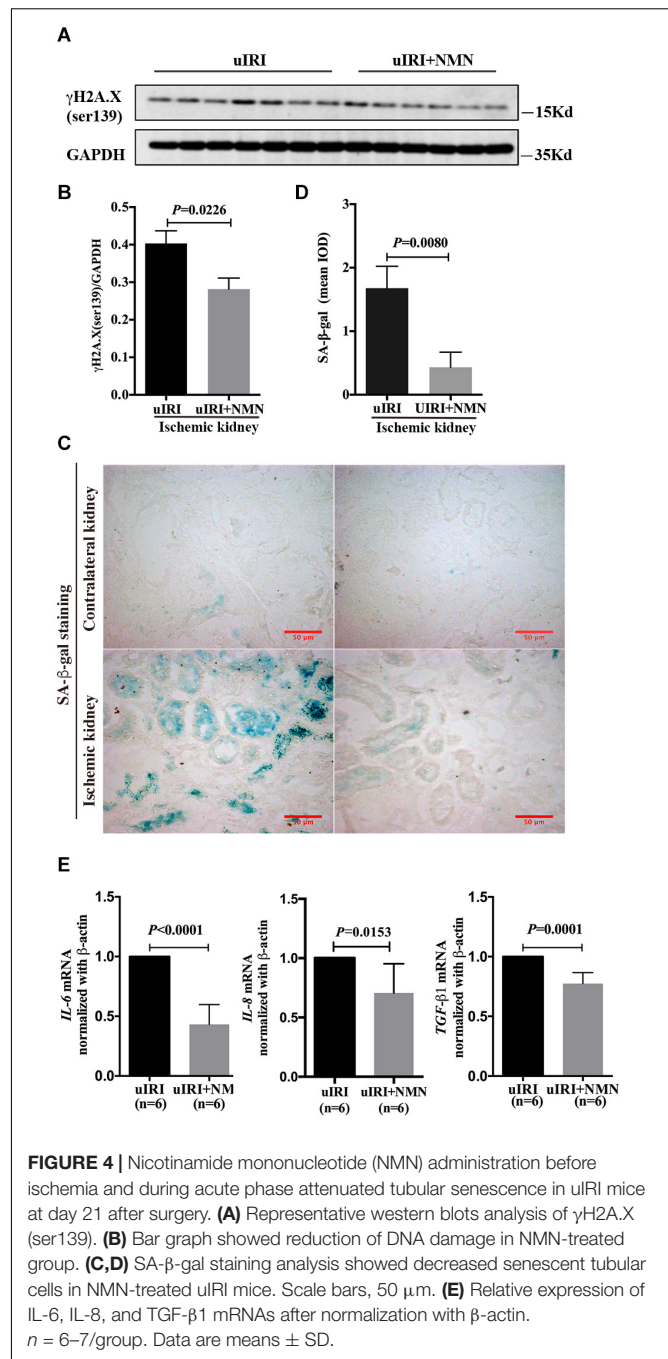
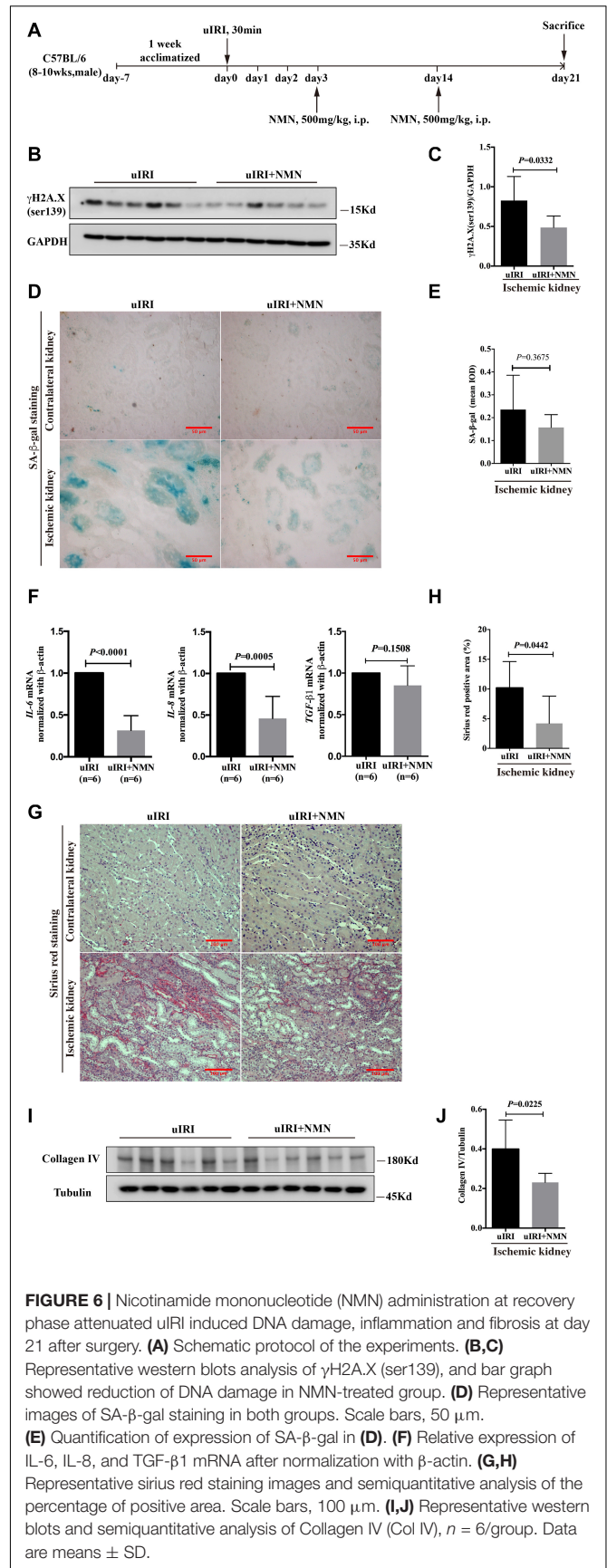
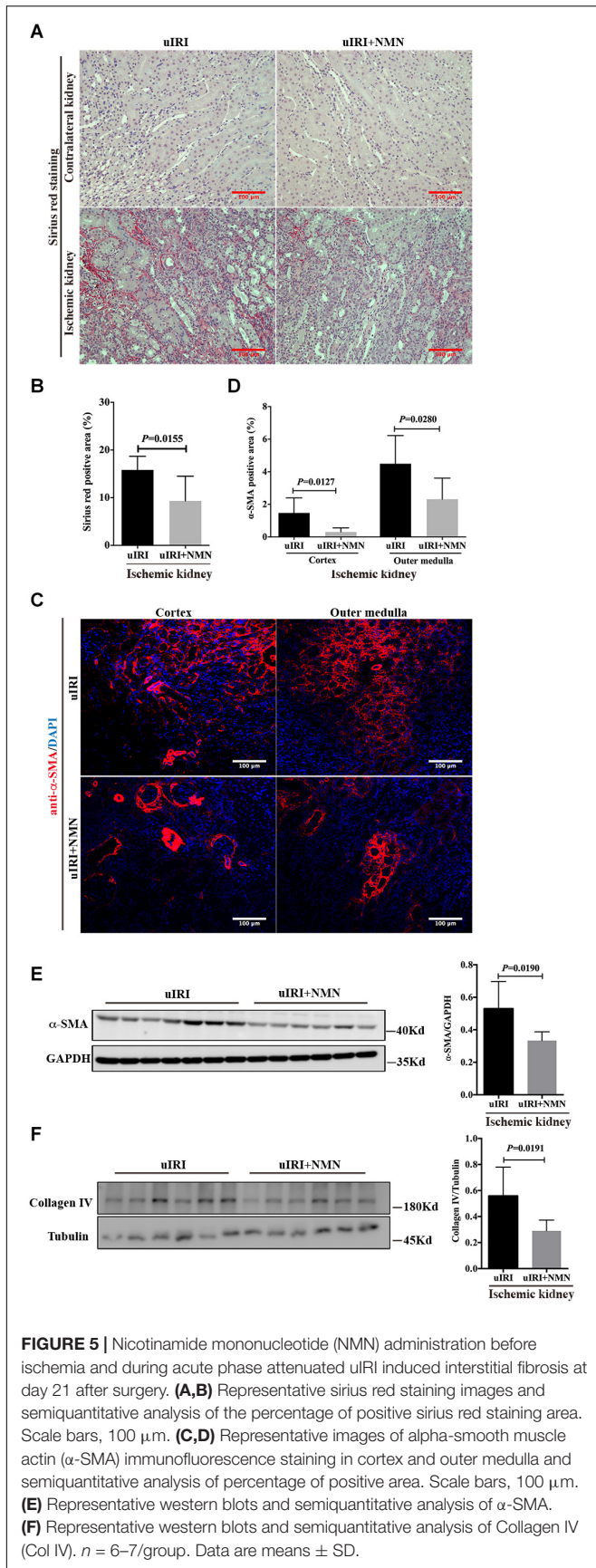


FIGURE 4 | Nicotinamide mononucleotide (NMN) administration before ischemia and during acute phase attenuated tubular senescence in uIRI mice at day 21 after surgery. (A) Representative western blots analysis of γ H2A.X (ser139). (B) Bar graph showed reduction of DNA damage in NMN-treated group. (C,D) SA- β -gal staining analysis showed decreased senescent tubular cells in NMN-treated uIRI mice. Scale bars, 50 μ m. (E) Relative expression of *IL-6*, *IL-8*, and *TGF- β 1* mRNAs after normalization with β -actin. $n = 6$ –7/group. Data are means \pm SD.

with NMN intraperitoneally on days 3 and 14 after surgery and were sacrificed on day 21 (Figure 6A). NMN administration significantly improved NAD^+ levels in the ischemic kidney (Supplementary Figure 2). And we found that the expression level of γ H2A.X (ser139) was significantly decreased in NMN-treated mice at day 21 (Figures 6B,C), which is consistent with the observations of NMN administration before ischemia and during the acute phase. NMN administration also alleviated SA- β -gal positive staining in renal tubular cells in NMN-treated uIRI mice but did not reach statistical significance (Figures 6D,E). The chronic interstitial inflammation reflected by the mRNA levels



of *IL-6* and *IL-8* was reduced significantly in NMN-treated uIRI mice (Figure 6F). *TGF- β 1* mRNA level also decreased, but didn't reach statistical significance. These observations suggest that NMN could inhibit DNA damage and might reduce senescence of renal tubular cells even during the recovery phase of uIRI. Sirius red staining revealed decreased collagen deposition in NMN-treated uIRI mice (Figures 6G,H). Additionally, the expression level of collagen IV was decreased significantly in the NMN-treated group compared with the PBS group (Figures 6I,J). These results indicate that fibrotic changes in the kidneys of uIRI mice could be alleviated by NMN administration even during the recovery phase.

DISCUSSION

Considering the high incidence of AKI and the high proportion of patients progressing to chronic kidney disease (CKD) and end stage renal disease (ESRD) (Yang, 2019), there is an urgent need to identify effective treatments for fibrosis after AKI. To our knowledge, this is the first report that NMN, an NAD⁺ precursor, could attenuate long-term fibrotic responses following experimental ischemic AKI, whether administered in advance or during the recovery phase. Our results also indicated that the anti-fibrotic effect of NMN might be achieved by reducing renal tubular DNA damage, and thus decreasing tubular senescence and senescence associated inflammation.

DNA damage is a feature of many forms of kidney injury, and it activates specific cell signaling cascades for DNA repair, cell cycle arrest, senescence, and cell death (Tsuruya et al., 2003; Yang et al., 2010; Zhu et al., 2015). Thus, targeting DNA damage and repair might be an effective strategy for protecting kidneys in AKI. NAD⁺ participates in DNA repair by serving as a substrate for poly-ADP-ribose polymerase (PARP) and sirtuins and by providing adenylate to DNA ligase IV, a key enzyme for DNA double-strand break (DSB) repair (de Murcia and Menissier de Murcia, 1994; de Murcia et al., 1994; Kim et al., 2004; De Vos et al., 2012; Fouquerel and Sobol, 2014; Fang et al., 2016; Chen and Yu, 2019). Thus, boosting NAD⁺ levels was predicted to have beneficial effects in DNA damage repair. Researchers have found that NMN could repair damaged DNA in the livers of old mice (Li et al., 2017) and that it could maintain telomere length, dampen the DNA damage response and rescue liver fibrosis in the livers of telomerase knockout mice (Amano et al., 2019). However, no kidney-related studies have been performed to date. In this study, we observed that stress-induced renal tubular DNA damage occurred upon acute insult and was sustained when subsequent chronic changes (senescence and fibrosis) occurred. And NMN administration both *in vivo* and *in vitro* showed reduced DNA damage phenotype. This gives evidence that boosting NAD⁺ might help to improve DNA repair capacity of the injured tissues, but direct correlation needs to be further studied. A recent encouraging study by Canto et al. showed that dihydronicotinamide riboside (NRH, a reduced form of NR) had unprecedented ability to increase NAD⁺ levels and could counteract cisplatin-induced kidney cellular damage and renal function decline (Giroud-Gerbetant et al., 2019). Therefore, it's

promising to evaluate the ability of NRH in preventing or treating renal fibrosis of various etiologies in the future.

Repeated or prolonged damage (ischemia or toxic injury) of tubular epithelial cells leads to senescence and maladaptive repair (Yang et al., 2010). Senescent cells often acquire a senescence-associated secretory phenotype (SASP), which is characterized by the expression and secretion of profibrotic and proinflammatory factors and are thought to be an important driver of fibrosis (Coppe et al., 2010; de Keizer, 2017). Recent evidence suggests that tubular senescence may play a key role in CKD progression (Valentijn et al., 2018). Senescent cell manipulation and depletion might represent novel therapies for treating AKI. In this study, we found that NMN markedly attenuated tubular senescence and blocked the accumulation of extracellular matrix (ECM) components both *in vitro* and *in vivo*. We also observed a reduction in the mRNA levels of *IL-6* and *IL-8* following NMN administration in the uIRI model, which might be due to the amelioration of senescence in tubular cells.

Another important finding of this study is that the protective effects of NMN on DNA damage inhibition, antisenescence and antifibrosis could be observed even when NMN was administered during the recovery phase of the ischemic AKI model. Although some studies have suggested the protective role of NAD⁺ precursors for renal function in various etiologies of experimental AKI models (Tran et al., 2016; Guan et al., 2017), in these studies, NMN was administered in advance. The use of prophylactic medication is not practical in many clinical conditions. Our study indicated a wide therapeutic time window of NMN in an ischemic AKI mouse model. Recently, several clinical trials have been carried out to determine the pharmacokinetics (US National Library of Medicine, 2014, 2015, 2016c) and bioavailability (US National Library of Medicine, 2017) of some NAD⁺ precursors, such as NMN, NR, and nicotinamide (NAM) (Tsubota, 2016). The efficacy of NR supplementation in obesity and insulin sensitivity is being tested (US National Library of Medicine, 2016a,b), and no adverse effects have been reported. Therefore, although preliminary, our results suggest that NMN administration might be an effective strategy for preventing or treating kidney fibrosis after AKI. For continued development and clinical translation, further elucidation of the mechanisms behind the therapeutic effects of NMN is needed. Preclinical studies in kidney and other organs suggested that augmentation of NAD⁺ not only enable efficient ATP production via fatty acid oxidation (FAO) but also broad cell-regulatory signaling networks that protect oxidative metabolism and mitochondrial health by acting as PARP1 and CD38 inhibitor (Li et al., 2017), sirtuins activator (Guan et al., 2017), mitochondrial fission inhibitor (Klimova et al., 2019; Lynch et al., 2019). Efficient FAO might also prevents toxic effect of accumulated lipids (Tran et al., 2016). Phosphorylation of NAD⁺ to NADP⁺ may potentiate defense against oxidant stress by promoting the reduction of glutathione and through the vasodilator nitric oxide (Ratliff et al., 2016). In order to understand the complex NMN-related network changes, high-throughput methods are indispensable, such as transcriptome, proteome, and metabolomics. The use of tracers to track the metabolic changes of NMN in circulation and different organs is

helpful to study the direct mechanism and the feasibility of its application in different diseases.

Collectively, our results suggest the DNA damage inhibition, antiaging and anti-inflammatory effects of NMN in kidneys, and NMN administration might be an effective strategy for preventing or treating kidney fibrosis after AKI.

DATA AVAILABILITY STATEMENT

The raw data supporting the conclusions of this article will be made available by the authors, without undue reservation.

ETHICS STATEMENT

The animal study was reviewed and approved by the Institutional Animal Care and Use Committee of Peking University First Hospital.

AUTHOR CONTRIBUTIONS

YJ collected the data, analyzed the data, interpreted the results, and drafted the article. LY conceived, designed, and organized

the study. LY and ZX interpreted the results and revised the manuscript. XK, LT, YR, LQ, and JT contributed to collecting samples. GL and SW contributed to pathologic analysis of kidney tissue. All authors contributed to the article and approved the submitted version.

FUNDING

This research was supported by grants from China Postdoctoral Science Foundation (No. 2018M640808), “San-ming” Project of Medicine in Shenzhen (No. SZSM201812097), National Natural Science Foundation of China (Nos. 91742205 and 81625004), Beijing Young Scientist Program (BJJWZYJH01201910001006), Peking University Clinical Scientists Program by the Fundamental Research Funds for the Central Universities, and Chinese Academy of Medical Sciences Research Unit (No. 2019RU023), Peking University.

SUPPLEMENTARY MATERIAL

The Supplementary Material for this article can be found online at: <https://www.frontiersin.org/articles/10.3389/fphys.2021.649547/full#supplementary-material>

REFERENCES

- Amano, H., Chaudhury, A., Rodriguez-Aguayo, C., Lu, L., Akhanov, V., Catic, A., et al. (2019). Telomere dysfunction induces sirtuin repression that drives telomere-dependent disease. *Cell. Metab.* 29, 1274–1290. doi: 10.1016/j.cmet.2019.03.001
- Bonventre, J. V., and Yang, L. (2011). Cellular pathophysiology of ischemic acute kidney injury. *J. Clin. Invest.* 121, 4210–4221. doi: 10.1172/JCI45161
- Canaud, G., Brooks, C. R., Kishi, S., Taguchi, K., Nishimura, K., Magassa, S., et al. (2019). Cyclin G1 and TASC regulate kidney epithelial cell G2-M arrest and fibrotic maladaptive repair. *Sci. Transl. Med.* 11:eaav4754. doi: 10.1126/scitranslmed.aav4754
- Chen, S. H., and Yu, X. (2019). Human DNA ligase IV is able to use NAD+ as an alternative adenylation donor for DNA ends ligation. *Nucleic Acids Res.* 47, 1321–1334. doi: 10.1093/nar/gky1202
- Coppe, J. P., Desprez, P. Y., Krtolica, A., and Campisi, J. (2010). The senescence-associated secretory phenotype: the dark side of tumor suppression. *Annu. Rev. Pathol.* 5, 99–118. doi: 10.1146/annurev-pathol-121808-102144
- de Keizer, P. L. (2017). The fountain of youth by targeting senescent cells? *Trends Mol. Med.* 23, 6–17. doi: 10.1016/j.molmed.2016.11.006
- de Murcia, G., and Menissier de Murcia, J. (1994). Poly(ADP-ribose) polymerase: a molecular nick-sensor. *Trends Biochem. Sci.* 19, 172–176. doi: 10.1016/0968-0004(94)90280-1
- de Murcia, G., Schreiber, V., Molinete, M., Saulier, B., Poch, O., Masson, M., et al. (1994). Structure and function of poly(ADP-ribose) polymerase. *Mol. Cell. Biochem.* 138, 15–24. doi: 10.1007/bf00928438
- De Vos, M., Schreiber, V., and Dantzer, F. (2012). The diverse roles and clinical relevance of PARPs in DNA damage repair: current state of the art. *Biochem. Pharmacol.* 84, 137–146. doi: 10.1016/j.bcp.2012.03.018
- Fang, E. F., Kassahun, H., Croteau, D. L., Scheibye-Knudsen, M., Marosi, K., Lu, H., et al. (2016). NAD(+) Replenishment improves lifespan and healthspan in ataxia telangiectasia models via mitophagy and DNA repair. *Cell. Metab.* 24, 566–581. doi: 10.1016/j.cmet.2016.09.004
- Ferenbach, D. A., and Bonventre, J. V. (2015). Mechanisms of maladaptive repair after AKI leading to accelerated kidney ageing and CKD. *Nat. Rev. Nephrol.* 11, 264–276. doi: 10.1038/nrneph.2015.3
- Fouquerel, E., and Sobol, R. W. (2014). ARTD1 (PARP1) activation and NAD(+) in DNA repair and cell death. *DNA Repair (Amst)* 23, 27–32. doi: 10.1016/j.dnarep.2014.09.004
- Giroud-Gerbetant, J., Joffraud, M., Giner, M. P., Cercillieux, A., Bartova, S., Makarov, M. V., et al. (2019). A reduced form of nicotinamide riboside defines a new path for NAD(+) biosynthesis and acts as an orally bioavailable NAD(+) precursor. *Mol. Metab.* 30, 192–202. doi: 10.1016/j.molmet.2019.09.013
- Guan, Y., Wang, S. R., Huang, X. Z., Xie, Q. H., Xu, Y. Y., Shang, D., et al. (2017). Nicotinamide mononucleotide, an NAD(+) precursor, rescues age-associated susceptibility to AKI in a sirtuin 1-dependent manner. *J. Am. Soc. Nephrol.* 28, 2337–2352. doi: 10.1681/ASN.2016040385
- Kim, M. Y., Mauro, S., Gevry, N., Lis, J. T., and Kraus, W. L. (2004). NAD+-dependent modulation of chromatin structure and transcription by nucleosome binding properties of PARP-1. *Cell* 119, 803–814. doi: 10.1016/j.cell.2004.11.002
- Kishi, S., Brooks, C. R., Taguchi, K., Ichimura, T., Mori, Y., Akinfolarin, A., et al. (2019). Proximal tubule ATR regulates DNA repair to prevent maladaptive renal injury responses. *J. Clin. Invest.* 129, 4797–4816. doi: 10.1172/JCI122313
- Klimova, N., Long, A., and Kristian, T. (2019). Nicotinamide mononucleotide alters mitochondrial dynamics by SIRT3-dependent mechanism in male mice. *J. Neurosci. Res.* 97, 975–990. doi: 10.1002/jnr.24397
- Lee, H. T., Kim, M., Jan, M., and Emala, C. W. (2006). Anti-inflammatory and antinecrotic effects of the volatile anesthetic sevoflurane in kidney proximal tubule cells. *Am. J. Physiol. Renal Physiol.* 291, 67–78. doi: 10.1152/ajprenal.00412.2005
- Li, J., Bonkowski, M. S., Moniot, S., Zhang, D., Hubbard, B. P., Ling, A. J., et al. (2017). A conserved NAD(+) binding pocket that regulates protein-protein interactions during aging. *Science* 355, 1312–1317. doi: 10.1126/science.aad8242
- Lynch, M. R., Tran, M. T., Ralto, K. M., Zsengeller, Z. K., Raman, V., Bhasin, S. S., et al. (2019). TFEB-driven lysosomal biogenesis is pivotal for PGC1alpha-dependent renal stress resistance. *JCI Insight* 5:e126749. doi: 10.1172/jci.insight.126749
- Mills, K. F., Yoshida, S., Stein, L. R., Grozio, A., Kubota, S., Sasaki, Y., et al. (2016). Long-term administration of nicotinamide mononucleotide mitigates age-associated physiological decline in mice. *Cell. Metab.* 24, 795–806. doi: 10.1016/j.cmet.2016.09.013

- Pham, T. X., Bae, M., Kim, M. B., Lee, Y., Hu, S., Kang, H., et al. (2019). Nicotinamide riboside, an NAD⁺ precursor, attenuates the development of liver fibrosis in a diet-induced mouse model of liver fibrosis. *Biochim. Biophys. Acta Mol. Basis Dis.* 1865, 2451–2463. doi: 10.1016/j.bbadis.2019.06.009
- Ratliff, B. B., Abdulmahdi, W., Pawar, R., and Wolin, M. S. (2016). Oxidant mechanisms in renal injury and disease. *Antioxid Redox Signal* 25, 119–146. doi: 10.1089/ars.2016.6665
- Rewa, O., and Bagshaw, S. M. (2014). Acute kidney injury-epidemiology, outcomes and economics. *Nat. Rev. Nephrol.* 10, 193–207. doi: 10.1038/nrneph.2013.282
- Rogakou, E. P., Pilch, D. R., Orr, A. H., Ivanova, V. S., and Bonner, W. M. (1998). DNA double-stranded breaks induce histone H2AX phosphorylation on serine 139. *J. Biol. Chem.* 273, 5858–5868. doi: 10.1074/jbc.273.10.5858
- Sharma, A., Singh, K., and Almasan, A. (2012). Histone H2AX phosphorylation: a marker for DNA damage. *Methods Mol. Biol.* 920, 613–626. doi: 10.1007/978-1-61779-998-3_40
- Small, D. M., Morais, C., Coombes, J. S., Bennett, N. C., Johnson, D. W., and Gobe, G. C. (2014). Oxidative stress-induced alterations in PPAR-gamma and associated mitochondrial destabilization contribute to kidney cell apoptosis. *Am. J. Physiol. Renal Physiol.* 307, 814–822. doi: 10.1152/ajprenal.00205.2014
- Tran, M. T., Zsengeller, Z. K., Berg, A. H., Khankin, E. V., Bhasin, M. K., Kim, W., et al. (2016). PGC1alpha drives NAD biosynthesis linking oxidative metabolism to renal protection. *Nature* 531, 528–532. doi: 10.1038/nature17184
- Tsubota, K. (2016). The first human clinical study for NMN has started in Japan. *NPJ Aging Mech. Dis.* 2:16021. doi: 10.1038/npjamd.2016.21
- Tsuruya, K., Furuichi, M., Tominaga, Y., Shinozaki, M., Tokumoto, M., Yoshimitsu, T., et al. (2003). Accumulation of 8-oxoguanine in the cellular DNA and the alteration of the OGG1 expression during ischemia-reperfusion injury in the rat kidney. *DNA Repair (Amst)* 2, 211–229. doi: 10.1016/s1568-7864(02)00214-8
- Us National Library of Medicine. (2014). *ClinicalTrials.gov*. Available Online at: <https://clinicaltrials.gov/ct2/show/NCT02191462>.
- Us National Library of Medicine. (2015). *ClinicalTrials.gov*. Available Online at: <https://clinicaltrials.gov/ct2/show/NCT02300740>.
- Us National Library of Medicine. (2016a). *ClinicalTrials.gov*. Available Online at: <https://clinicaltrials.gov/ct2/show/NCT02689882>.
- Us National Library of Medicine. (2016b). *ClinicalTrials.gov*. Available Online at: <https://clinicaltrials.gov/ct2/show/NCT02303483>.
- Us National Library of Medicine. (2016c). *ClinicalTrials.gov*. Available Online at: <https://clinicaltrials.gov/ct2/show/NCT02835664>.
- Us National Library of Medicine. (2017). *ClinicalTrials.gov*. Available Online at: <https://clinicaltrials.gov/ct2/show/NCT02712593>.
- Valentijn, F. A., Falke, L. L., Nguyen, T. Q., and Goldschmeding, R. (2018). Cellular senescence in the aging and diseased kidney. *J. Cell. Commun. Signal* 12, 69–82. doi: 10.1007/s12079-017-0434-2
- Varrier, M., Forni, L. G., and Ostermann, M. (2015). Long-term sequelae from acute kidney injury: potential mechanisms for the observed poor renal outcomes. *Crit. Care* 19:102. doi: 10.1186/s13054-015-0805-0
- Yang, L. (2019). How acute kidney injury contributes to renal fibrosis. *Adv. Exp. Med. Biol.* 1165, 117–142. doi: 10.1007/978-981-13-8871-2_7
- Yang, L., Besschetnova, T. Y., Brooks, C. R., Shah, J. V., and Bonventre, J. V. (2010). Epithelial cell cycle arrest in G2/M mediates kidney fibrosis after injury. *Nat. Med.* 16, 535–543. doi: 10.1038/nm.2144
- Yang, L., Xing, G., Wang, L., Wu, Y., Li, S., Xu, G., et al. (2015). Acute kidney injury in china: a cross-sectional survey. *Lancet* 386, 1465–1471. doi: 10.1016/S0140-6736(15)00344-X
- Zheng, M., Cai, J., Liu, Z., Shu, S., Wang, Y., Tang, C., et al. (2019). Nicotinamide reduces renal interstitial fibrosis by suppressing tubular injury and inflammation. *J. Cell. Mol. Med.* 23, 3995–4004. doi: 10.1111/jcmm.14285
- Zhu, R., Wang, W., and Yang, S. (2019). Cryptotanshinone inhibits hypoxia/reoxygenation-induced oxidative stress and apoptosis in renal tubular epithelial cells. *J. Cell. Biochem.* 120, 13354–13360. doi: 10.1002/jcb.28609
- Zhu, S., Pabla, N., Tang, C., He, L., and Dong, Z. (2015). DNA damage response in cisplatin-induced nephrotoxicity. *Arch. Toxicol.* 89, 2197–2205. doi: 10.1007/s00204-015-1633-3

Conflict of Interest: The authors declare that the research was conducted in the absence of any commercial or financial relationships that could be construed as a potential conflict of interest.

Copyright © 2021 Jia, Kang, Tan, Ren, Qu, Tang, Liu, Wang, Xiong and Yang. This is an open-access article distributed under the terms of the Creative Commons Attribution License (CC BY). The use, distribution or reproduction in other forums is permitted, provided the original author(s) and the copyright owner(s) are credited and that the original publication in this journal is cited, in accordance with accepted academic practice. No use, distribution or reproduction is permitted which does not comply with these terms.



Sos1 Modulates Extracellular Matrix Synthesis, Proliferation, and Migration in Fibroblasts

Isabel Fuentes-Calvo^{1,2} and Carlos Martinez-Salgado^{1,2*}

¹ Institute of Biomedical Research of Salamanca (IBSAL), Salamanca, Spain, ² Translational Research on Renal and Cardiovascular Diseases (TRECARD)-REDINREN (ISCIII), Department of Physiology and Pharmacology, University of Salamanca, Salamanca, Spain

OPEN ACCESS

Edited by:

Isotta Chimenti,
Sapienza University of Rome, Italy

Reviewed by:

Zhihong Yang,
Université de Fribourg, Switzerland
Yutang Wang,
Federation University Australia,
Australia

*Correspondence:

Carlos Martinez-Salgado
carlosms@usal.es

Specialty section:

This article was submitted to
Integrative Physiology,
a section of the journal
Frontiers in Physiology

Received: 23 December 2020

Accepted: 05 March 2021

Published: 06 April 2021

Citation:

Fuentes-Calvo I and
Martinez-Salgado C (2021) Sos1
Modulates Extracellular Matrix
Synthesis, Proliferation, and Migration
in Fibroblasts.
Front. Physiol. 12:645044.
doi: 10.3389/fphys.2021.645044

Non-reversible fibrosis is common in various diseases such as chronic renal failure, liver cirrhosis, chronic pancreatitis, pulmonary fibrosis, rheumatoid arthritis and atherosclerosis. Transforming growth factor beta 1 (TGF- β 1) is involved in virtually all types of fibrosis. We previously described the involvement of Ras GTPase isoforms in the regulation of TGF- β 1-induced fibrosis. The guanine nucleotide exchange factor Son of Sevenless (Sos) is the main Ras activator, but the role of the ubiquitously expressed Sos1 in the development of fibrosis has not been studied. For this purpose, we isolated and cultured Sos1 knock-out (KO) mouse embryonic fibroblasts, the main extracellular matrix proteins (ECM)-producing cells, and we analyzed ECM synthesis, cell proliferation and migration in the absence of Sos1, as well as the role of the main Sos1-Ras effectors, Erk1/2 and Akt, in these processes. The absence of Sos1 increases collagen I expression (through the PI3K-Akt signaling pathway), total collagen proteins, and slightly increases fibronectin expression; Sos1 regulates fibroblast proliferation through both PI3K-Akt and Raf-Erk pathways, and Sos1-PI3K-Akt signaling regulates fibroblast migration. This study shows that Sos1 regulates ECM synthesis and migration (through Ras-PI3K-Akt) and proliferation (through Ras-PI3K-Akt and Ras-Raf-Erk) in fibroblasts, and describe for the first time the role of the Sos1-Ras signaling axis in the regulation of cellular processes involved in the development of fibrosis.

Keywords: Sos1, fibrosis, proliferation, migration, fibroblasts, extracellular matrix synthesis (ECM), ERK, Akt

INTRODUCTION

In most cases, when organs suffer injuries motivated by different disorders or diseases, a complex cascade of cellular and molecular responses triggering fibrosis of the tissue begins. When this phenomenon occurs over a prolonged period of time, this ends up causing irreversible parenchymal damage, cellular dysfunction and functional failure of the organ (Rockey et al., 2015). This process is common in many diseases such as chronic renal failure, liver cirrhosis, chronic pancreatitis, pulmonary fibrosis, rheumatoid arthritis, and atherosclerosis. In almost all cases, fibrosis is not reversible, and therefore the only possible treatments in specific cases are substitution therapies (transplantation). On the other hand, the fact that so many different diseases cause fibrotic processes suggests that most of them share pathogenic pathways. One of the most relevant

intracellular pathways involved in virtually all types of fibrosis is that of transforming growth factor beta (TGF- β) (Rockey et al., 2015).

Previous studies of our research group have described the involvement of Ras GTPase isoforms in the regulation of TGF- β 1-induced fibrosis. Thus, both K-Ras, N-Ras and H-Ras regulate extracellular matrix (ECM) synthesis, proliferation and migration in fibroblasts (Martínez-Salgado et al., 2006; Fuentes-Calvo et al., 2012, 2013; Muñoz-Félix et al., 2016). We have also observed that deletion of H-Ras reduces renal fibrosis and myofibroblast activation in a fibrotic *in vivo* model induced by ureteral obstruction in mice (Grande et al., 2010). Activation of Ras and its effectors Erk and/or Akt mediates certain pathological effects of the molecules involved in renal fibrogenesis and chronic renal disease, as we reviewed in Martínez-Salgado et al. (2008). On the other hand, Ras participates in the regulation of fibrosis activated by other mediators. Thus, we have also found that TNF-related weak inducer of apoptosis (TWEAK) promotes kidney fibrosis and Ras-dependent proliferation of cultured renal fibroblasts (Ucero et al., 2013).

Son of Sevenless (Sos) proteins are the most widely expressed and functionally relevant family of Ras guanine nucleotide exchange factors (GEFs). There are 2 members in mammals, Sos1 (ubiquitously expressed) and Sos2 (Suire et al., 2019). Sos binds to Ras promoting the release of guanosine diphosphate (GDP) and the subsequent Ras activation after binding to guanosine triphosphate (GTP) (Quilliam et al., 2002). The location of Sos in the plasma membrane is necessary and sufficient for Ras activation (Innocenti et al., 2002). For that purpose, the Src homology 2 and 3 (SH2, SH3) domain-containing adaptor protein growth factor receptor-bound protein 2 (Grb2) recruits Sos to activated growth factor receptors after binding to its C-terminal region (Buday and Downward, 1993). Sos can also be activated by GTP-Ras in a positive feedback mechanism (Margarit et al., 2003). Sos1 and Ras mechanistically mediates kindling-2-induced fibrosis in human kidney tubular epithelial cells (Wei et al., 2014). Moreover, Grb2 and Sos downstream signaling pathways are essential for cardiac fibrosis regulation (Zhang et al., 2003).

Most of studies have been focused on identifying Sos1 functional roles, since the Sos2 isoform seems to be mostly dispensable (Esteban et al., 2000; Arai et al., 2009). However, the role of Sos1 in cellular processes involved in the development of fibrosis has not been studied in detail, nor is the implication of the Ras-mediated main intracellular pathways, Raf-Erk1/2 and PI3K-Akt known in these processes. For this purpose, we isolated and cultured Sos1 knock-out (KO) mouse embryonic fibroblasts (MEFs), the main ECM-producing cells, and we analyzed ECM synthesis and cell proliferation and migration in the absence of Sos1, as well as the role of Erk1/2 and Akt in these processes.

MATERIALS AND METHODS

Cell Culture and Stimulation

Mouse embryonic fibroblasts were subcultured and immortalized from Sos1-KO E13.5 embryos as previously reported

(Qian et al., 2000). Fibroblasts were grown at 37°C, 5% CO₂ in DMEM medium (Gibco-Invitrogen, Grand Island, NY, United States) supplemented with 10% fetal calf serum (FCS, Gibco-Invitrogen) and 100 U/ml penicillin/streptomycin. Cells were seeded in different plastic formats depending on the experiment to be carried out: 100 mm diameter Petri dishes for western blot and 24 well plates for proliferation studies and total collagen measurement. Fibroblasts, after achieving 10-20% (proliferation studies) or 70-80% confluence (studies on extracellular matrix proteins) and serum-starved for 24 h, were treated with human recombinant TGF- β 1 (1 ng/mL, R&D Systems Minneapolis, MN, United States) or control vehicle during 24-48 h in serum-free medium. Pharmacological inhibition was performed 30 min before TGF- β 1 stimulation with mitogen activated kinase/Erk kinase-1 (MEK-1) inhibitor U0126 (20 μ g/mL, Calbiochem-Merck, Madrid, Spain) or the PI3K inhibitor LY294002 (20 μ g/mL, Calbiochem-Merck). **Figure 1A** shows the absence of Sos1 expression in KO fibroblasts.

Crystal Violet Staining

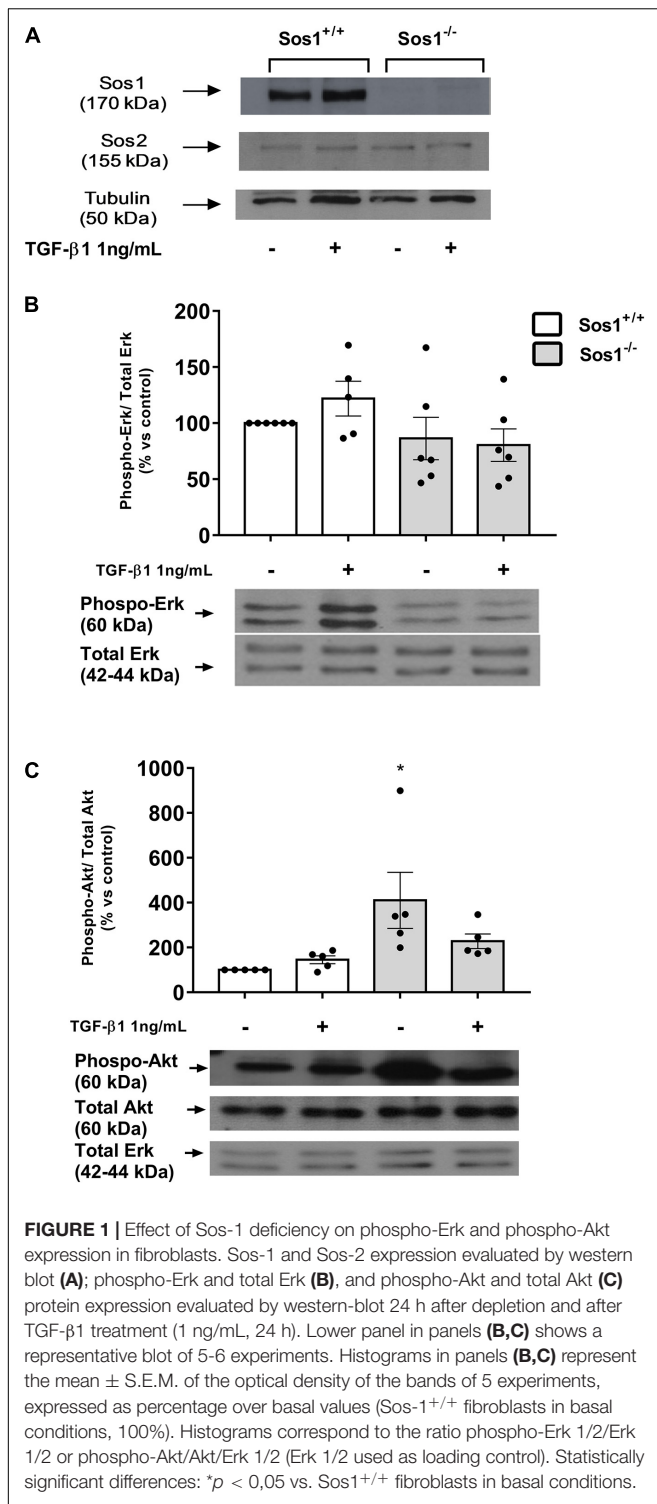
Total cell number was measured by crystal violet staining as previously described (Fuentes-Calvo et al., 2013). Fibroblasts in 24 well plates were fixed for 10 min with 10% glutaraldehyde, stained for 30 min in 1% crystal violet (Fluka, Buchs, Switzerland) solution and dried overnight. After dissolving with 10% acetic acid, optical absorbance, which was proportional to the number of viable cells in each well, was measured at 595 nm.

Western Blot Analysis

Protein expression was analyzed by western blot as previously described (Fuentes-Calvo et al., 2013), using the following antibodies: rabbit anti-human Sos1 and rabbit anti-mouse Sos2 (Santa Cruz Biotechnology, Santa Cruz, CA, United States, dilution: 1/1,000), rabbit anti-mouse Akt 1/2 (Santa Cruz Biotechnology, dilution: 1/1,000), rabbit anti-rat Erk1 (Santa Cruz Biotechnology, 1/10,000), mouse anti-human phospho-Erk (Santa Cruz Biotechnology, 1/2,000), rabbit anti-mouse phospho-Akt (Cell Signaling Technology, Danvers, MA, United States, 1/1,000), rabbit anti-mouse collagen type I (Chemicon international, Waltham, MA, United States, 1/20,000) and rabbit anti-mouse fibronectin (Chemicon international, 1/30,000), α -tubulin (Santa Cruz Biotechnology, dilution: 1/1,000). We used total Erk 1/2 levels as loading controls, as their expression does not change in fibroblasts after TGF- β 1 treatment, as we had previously found in H-Ras KO, N-Ras KO and H- and N-Ras double KO fibroblasts (Martínez-Salgado et al., 2006; Fuentes-Calvo et al., 2012, 2013; Muñoz-Félix et al., 2016), whereas expression of other frequently used loading controls (actin, tubulin) is modified after TGF- β 1 treatment.

Total Collagen Synthesis Measurement

The incorporation of [³H]-proline (American Radiolabelled Chemical, St. Louis, MO, United States) into collagen proteins was used to quantify collagen content in the culture medium, as previously described (Fuentes-Calvo et al., 2013). Radiolabelling was performed incubating 0.15 mM β -aminopropionitrile,



210 mM ascorbic acid, 183 mM proline and 1 μ Ci/well [³H]-Proline (specific activity: 40 Ci/mmol) for 24 h in fresh DMEM serum-free medium. Proteins were precipitated in ice-cold 10% trichloroacetic acid and the pellet was washed and resuspended in 0.1 N NaOH. [³H]-Proline incorporated into collagen proteins was measured in a Wallac 1409

DSA β liquid scintillation counter (Perkin Elmer, Waltham, MA, United States).

Wound-Healing Assay

In vitro scratched wounds were created with a straight incision on serum-starved confluent cell monolayers with a sterile disposable pipette tip, as previously described (Fuentes-Calvo et al., 2013). Cell migration into denuded area was monitored over a time course using digital microscopy and cell movement was calculated as the reduction of the wound area over time (in percentage, initial area of the wound: 100%).

Cell Migration Assay

Fibroblast migration was evaluated with a method based on the Boyden assay as previously described (Muñoz-Félix et al., 2016). Cells were resuspended in 10% FCS DMEM and stained with 2 μ M calcein-AM for 15 min in darkness. Cell suspension in 2% FCS medium was loaded into the chamber, and invading cells migrate through and attach to an 8 μ m pore size polycarbonate membrane (bottom chamber containing 10% FCS medium), while non-invading cells remain above. Cell migration was analyzed for 24 h after adding the cells in the upper chamber. The number of cells in the bottom of the chamber (migrating cells) was determined by cell fluorescence at $\lambda = 538$ each 2 h.

Statistical Methods

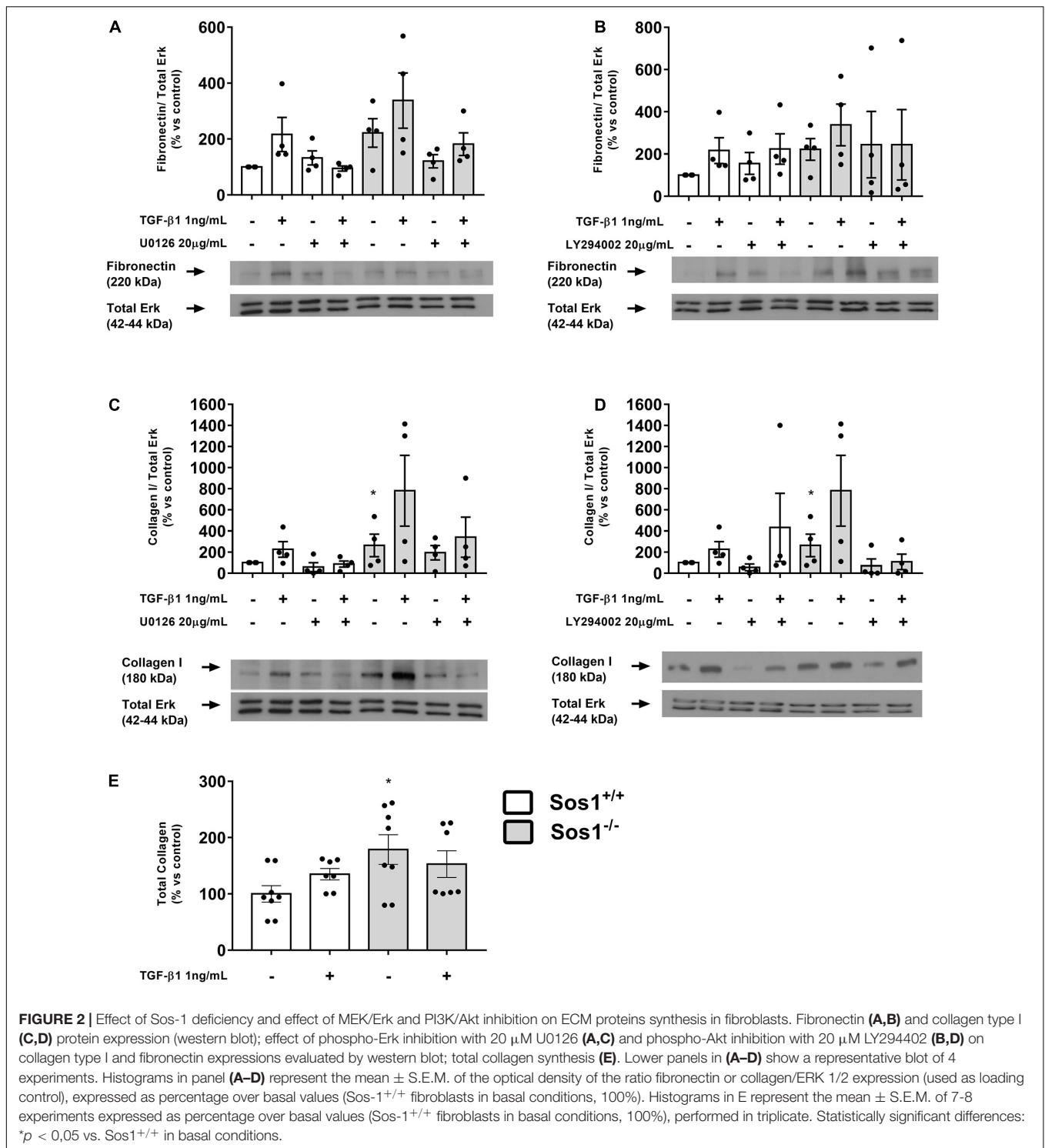
Data are expressed as mean \pm standard error of the mean (SEM). The Kolmogorov-Smirnov test was used to assess the normality of the data distribution. Comparison of means was performed by two way analysis of variance (ANOVA) and Bonferroni post-test. Statistical analysis was performed using Graph Pad Prism version 5.00 for Windows, Graph Pad Software, San Diego California United States, www.graphpad.com. A “ p ” value lower than 0.05 was considered statistically significant.

RESULTS

Increased Akt Expression in Sos1 KO Fibroblasts

We analyzed the changes induced by the absence of Sos1 in the activation of two of the main intracellular pathways stimulated by Ras: rapidly accelerated fibrosarcoma (Raf)-mitogen-activated protein kinase (MAPK) cascade, whose final effect is the phosphorylation (on Tyr204) of extracellular signal-regulated kinases (Erk), and the phosphatidylinositol 3-kinases pathway (PI3K) that leads to phosphorylation (on Ser473) of Akt (protein kinase B). The absence of Sos1 does not affect the expression of phospho-Erk in basal conditions (serum-depleted cells, Figure 1B) but induces a significant increase in the expression of phospho-Akt in these same conditions (Figure 1C).

We stimulated fibroblasts with transforming growth factor beta-1 (TGF- β 1), the main cytokine involved in fibrotic processes and in the synthesis of ECM (Leask and Abraham, 2004;



Rockey et al., 2015). TGF- β 1 (1 ng/mL, 24 h) induces slight increases in Erk and Akt phosphorylation, but those effects disappears completely in the absence of Sos1 (Figures 1B,C). These results indicate that Sos1 is involved in TGF- β 1-induced activation of the Raf-Erk and PI3K-Akt pathways, and its absence induces the activation of the PI3K-Akt pathway.

Increased ECM Proteins Synthesis in Sos1 KO Fibroblasts

We assessed the synthesis of ECM proteins by analyzing collagen I and fibronectin expression, as well as total collagen synthesis. The absence of Sos1 induces increases in fibronectin expression (Figures 2A,B), collagen I expression (Figures 2C,D) and in

the synthesis of total collagen proteins (Figure 2E). TGF- β 1 treatment (1 ng/mL, 24 h) stimulates the expression of fibronectin, collagen I and total collagen synthesis in wild type fibroblasts, but in the absence of Sos1, TGF- β 1 does not induce significant increases in fibronectin (Figure 2A,B) and collagen I (Figures 2C,D) expression, nor in the total synthesis of collagen (Figure 2E), because these KO fibroblasts already express high levels of these proteins, probably very close to the maximum synthesis capacity of fibroblasts in culture.

The inhibition of Erk phosphorylation with U0126 (20 μ g/mL, 30 min) does not affect the expression of fibronectin or collagen I either in the presence or absence of Sos1 (Figures 2A,C). The inhibition of Akt phosphorylation with LY294002 (20 μ g/mL, 30 min) did not induce any noticeable effect on fibronectin expression (Figure 2B) but reduces the expression of collagen I in Sos1 KO fibroblasts, both in basal conditions and after TGF- β 1 treatment (Figure 2D). These results show that the PI3K-Akt signaling pathway regulates collagen I expression only in the absence of Sos1.

Reduced Proliferation in Sos1 KO Fibroblasts

Cell proliferation is significantly lower in Sos1 KO fibroblasts compared to wild type fibroblasts in basal conditions (serum-depleted cells) as can be seen by a smaller increase in the number of viable cells (assessed by crystal violet nucleus staining) at 24 and 48 h (Figure 3A). In addition, TGF- β 1-induced fibroblast proliferation is reduced in the absence of Sos1 (Figure 3B).

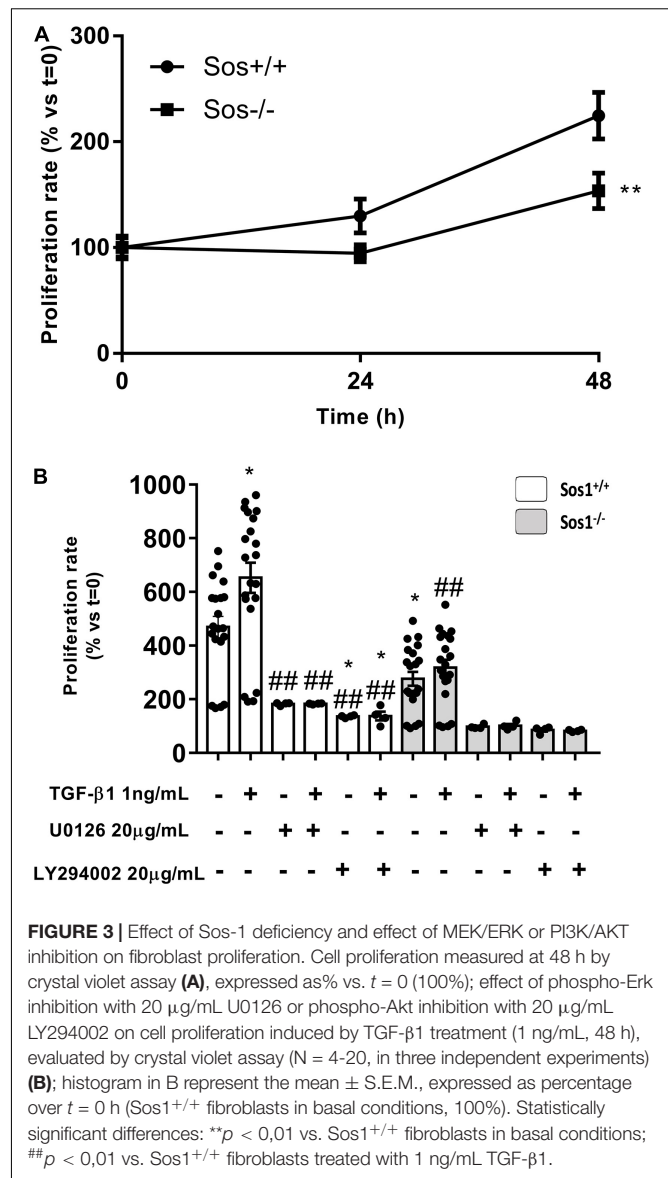
In the absence of Sos1, inhibition of Erk phosphorylation with U0126 significantly reduces cell proliferation, both at basal conditions and after TGF- β 1 treatment. In addition, pre-treatment with U0126 also inhibits TGF- β 1-induced proliferation in wild type fibroblasts. On the other hand, inhibition of Akt phosphorylation with LY294002 also significantly reduces cell proliferation, both at baseline conditions and after TGF- β 1 treatment, regardless of the presence of Sos1 (Figure 3B).

All these data suggest that the absence of Sos1 affects fibroblast proliferation, and this process is regulated both by the PI3K-Akt and by the Raf-Erk pathway, the latter signaling pathway being dependent on the presence of Sos1.

Reduced Migration in Sos1 KO Fibroblasts

To analyze the involvement of Sos1 in cell migration, we have performed two *in vitro* procedures: scratch time-course assay (Figures 4A-C) and migration chamber assay (Figures 4D,E). The absence of Sos1 impairs fibroblasts migration, as the reduction of the scratched area and the emitting fluorescence of migrated cells is always slower in *Sos1*^{-/-} than in wild type fibroblasts.

Inhibition of Erk phosphorylation with U0126 does not seem to have any effect on the reduction of the scratched area, regardless of the presence of Sos1 (Figures 4A,C). However, in the absence of Sos1, inhibition of Akt phosphorylation with LY294002 reduces the time of closure of the scratched area (Figures 4B,C). Both the inhibition of Erk phosphorylation and



Akt phosphorylation slightly reduces the number of migrated cells, both in the presence and absence of Sos1 (Figures 4D,E).

These data suggest that Sos1 is necessary for fibroblast migration, and that the Akt signaling pathway requires the presence of Sos1 to correctly regulate fibroblast migration.

DISCUSSION

In the last 14 years our research group has described the mediating role of the p21Ras family isoforms in fibroblast biology (Martínez-Salgado et al., 2006, 2008; Fuentes-Calvo et al., 2012, 2013; Uceró et al., 2013; Muñoz-Félix et al., 2016) and in renal fibrosis *in vivo* (Grande et al., 2010). Other research groups have described the involvement of different members and mediators of the p21Ras family in fibrotic processes. RAS p21 protein activator 1 (RASA1) is involved in miR-223 mediated

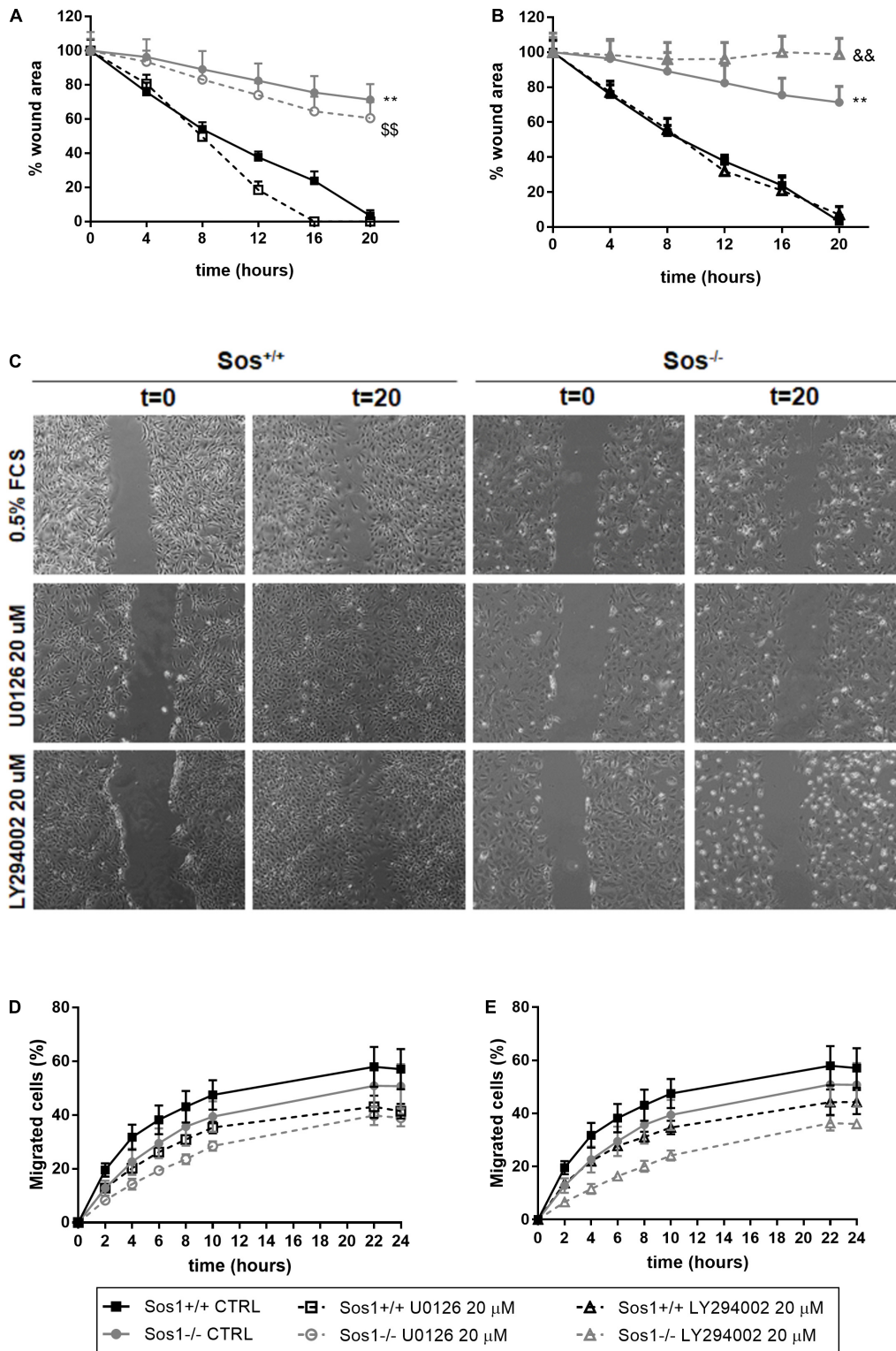


FIGURE 4 | Effect of Sos-1 deficiency on fibroblast migration. Analysis of cell mobility measuring wound closure area (**A–C**) and migration through transwells in a Boyden chamber (**D,E**), and effect of MEK/Erk inhibition with 20 μg/mL U0126 (**A,D**) or PI3K/Akt inhibition with 20 μg/mL LY294002 (**B,E**) in Sos-1 KO fibroblast migration; (**C**) shows representative images (50x) of wound closure at 0 and 20 h. Curve graphs in panels (**A,B**) represent the mean ± S.E.M. of 7 experiments of the time-course reduction of wound area (initial scratched area: 100%). Curve graphs in panels (**D,E**) represent mean ± S.E.M. of 6 experiments quantifying the migrated calcein-AM fluorescent cells expressed as percentage vs. total number of cells (t = 24 h, 100%). Statistically significant differences: **p < 0,01 vs. Sos1^{+/+} fibroblasts in basal conditions; \$\$p < 0,01 vs. Sos1^{+/+} fibroblasts treated with U0126; &&p < 0,01 vs. Sos1^{+/+} fibroblasts treated with LY294002.

cardiac fibrosis after myocardial infarction (Liu et al., 2018). The farnesyltransferase-Ras-Erk pathway participates in interstitial fibrosis in the aging heart (Trial et al., 2016). KrasG12D mutation contribute to pancreatic tumor development by promoting fibrosis through increased TGF- β signaling (Krantz et al., 2011; Shields et al., 2013). Silencing K-Ras expression inhibits renal fibrosis *in vivo* (Wang et al., 2012), and inhibition of fibroblast Ras/MEK/ERK signaling in fibroblasts might prevent fibrosis (Stratton et al., 2002).

Although the role of the different isoforms of the p21-Ras family on ECM production and fibrosis has been previously described by our group and others, the present study is the first to describe the role of Sos1, the main GEF of Ras, in the production of ECM proteins and associated proliferation and migration in fibroblasts. We show that the absence of Sos1 increases collagen I expression (through the PI3K-Akt signaling pathway), total collagen proteins, and slightly increases fibronectin expression; the absence of Sos1 influences fibroblast proliferation through both PI3K-Akt and Raf-Erk pathways, and Sos1-PI3K-Akt is necessary for fibroblast migration.

Sos1 and Sos2 isoforms show structural homology and similar expression patterns, but the specific functional properties of both isoforms are not fully known. The Sos2 isoform seems to be expendable, since adult Sos2-null mice are perfectly viable and fertile (Esteban et al., 2000). However, Sos1 null mice die during mid-embryonic development (Qian et al., 2000). Therefore, most functional studies have focused on the analysis of Sos1 functional role.

To date, there is only one study analyzing the role of Sos1 in MEFs with a 4-hydroxytamoxifen (4OHT)-inducible, conditional Sos1-null mutation (Liceras-Boillos et al., 2016). Our data are in agreement with this study which describes a mechanistic link between Sos1 and intracellular mitochondrial oxidative stress and shows the prevalence of Sos1 over Sos2 in the regulation of cellular proliferation, migration and viability. We observed that the absence of Sos1 affects fibroblast proliferation, and this process is regulated both by the PI3K-Akt and by the Raf-Erk pathways, the latter signaling pathway being dependent on the presence of Sos1. Our findings are consistent with previous studies of our research group, which show that TGF- β 1-induced fibroblast proliferation is reduced in *H-ras*^{-/-}/*N-ras*^{-/-} (Martínez-Salgado et al., 2006), *H-ras*^{-/-} (Fuentes-Calvo et al., 2012), *N-ras*^{-/-} (Fuentes-Calvo et al., 2013) and *K-ras*^{-/-} fibroblasts (Muñoz-Félix et al., 2016) with respect to wild type fibroblasts, and this decrease in proliferation is due to changes in Raf-MAPK and PI3K-Akt intracellular signaling. Our study shows that Sos1 is also necessary for fibroblast migration, and the Akt signaling pathway requires the presence of Sos1 to correctly regulate migration. We previously showed that Ras isoforms, as well as PI3K-Akt signaling, are also indispensable to maintain normal fibroblast motility, which was highly restricted in *H-ras*^{-/-} (Fuentes-Calvo et al., 2012), *N-ras*^{-/-} (Fuentes-Calvo et al., 2013) and in *K-ras*^{-/-} fibroblasts (Muñoz-Félix et al., 2016). The decrease in cell migration seems to be dependent on Sos1 and independent of Sos2, since it has also been described that Sos2-KO MEF cultures exhibited similar wound-closure kinetics than wild type fibroblasts (Liceras-Boillos et al., 2016).

Our results suggest that the absence of Sos1 affects cell proliferation and migration, possibly modifying the activity of the different Ras isoforms and two of their main signaling pathways, PI3K-Akt and Raf-Erk; in a similar way, Sos1-Ras might regulate cell migration, in this case mainly through the PI3K-Akt intracellular pathway. According to our hypothesis, it has been described that mir-155-containing macrophage exosomes inhibit cardiac fibroblasts proliferation by downregulating Sos1 (Wang et al., 2017). The role of Sos1 as a regulator of cell migration has been described in macrophages (Baruzzi et al., 2015), glioblastoma cells (Kapoor and O'Rourke, 2010) breast cancer cells (Lin et al., 2018), peripheral CD4(+) T cells (Guittard et al., 2015), etc.

The absence of Sos1 induces a significant increase in both collagen I expression and in the synthesis of total collagen proteins, as well as a slightly higher expression of fibronectin. This regulating role of Sos1 in ECM synthesis might be directly related with previous findings of our research group, which show that ECM synthesis is increased in basal conditions in *H-ras*^{-/-}/*N-ras*^{-/-} (Martínez-Salgado et al., 2006), *H-ras*^{-/-} (Fuentes-Calvo et al., 2012), *N-ras*^{-/-} (Fuentes-Calvo et al., 2013) and *K-ras*^{-/-} fibroblasts (Muñoz-Félix et al., 2016). To date, there are no studies in the scientific literature describing the involvement of Sos1 in the synthesis of ECM proteins. It is important to keep in mind that, as indicated above, TGF- β 1 does not modify ECM protein expression in *Sos1*^{-/-} fibroblasts, probably because the absence of Sos1 causes these fibroblasts to already express very high levels of these proteins, and therefore a profibrotic stimulus does not modify the ECM protein synthesis capacity of these cells, which may be close to their maximum level.

Sos1 is necessary for the regulation of collagen I expression through the PI3K-Akt signaling pathway. The absence of Sos1 induces a significant increase in the expression of phospho-Akt in basal conditions (serum-depleted cells). Moreover, the inhibition of Akt phosphorylation reduces the expression of collagen I in Sos1 KO fibroblasts, both in basal conditions and after TGF- β 1 treatment. The increase in Akt phosphorylation observed in the absence of Sos1 is consistent with previous studies showing a significant activation of the PI3K pathway in fibroblasts expressing dominant negative mSos1 constructs 53 (Park et al., 2000). This role of the Akt pathway has been previously described by our research group in the Akt-induced increase in ECM synthesis observed in the absence of H- and N-Ras, and for the fact that the inhibition of Akt activation also inhibits ECM synthesis in *H-ras*^{-/-}/*N-ras*^{-/-} fibroblasts (Martínez-Salgado et al., 2006). Similarly, *H-ras*^{-/-} (Fuentes-Calvo et al., 2012), *N-Ras*^{-/-} (Fuentes-Calvo et al., 2013) and *K-ras*^{-/-} fibroblasts (Muñoz-Félix et al., 2016) exhibited a higher basal PI3K/Akt activation than wild type fibroblasts, which was also directly related to the higher level of ECM expression presented by these KO fibroblasts. However, the absence of Sos1 does not influence the regulation of the expression of collagen I and fibronectin by the Raf-Erk signaling pathway. Based on these data and in our previous findings, we can affirm that the Sos1-Ras-PI3K-Akt pathway directly regulates collagen I expression.

The role of Sos1 in the regulation of the synthesis of collagen I, proliferation and cell migration that we describe in this study complements the previously cited studies of our research group that show similar effects in the absence of the H-, N- and K-Ras isoforms. All these data together suggest that the Sos1-Ras-PI3K-Akt and Sos1-Ras-Raf-Erk axes regulate the processes described above to a different extent. These data indicate that the absence of any of these mediators, Sos1 or any of the Ras isoforms, deregulates ECM production, proliferation and fibroblast migration. The presence of the three Ras isoforms seems to be necessary for the regulation of these processes, since the individual absence of each of them exerts quite similar effects, although in the case of H-Ras the regulation of these cellular processes seems to be more dependent on the Sos1-Ras-Raf-Erk pathway (Martínez-Salgado et al., 2006; Fuentes-Calvo et al., 2012). These studies confirm the role of the Sos1-Ras signaling axis in processes different of tumor oncogenesis, such as the regulation of cellular processes directly involved in the development of fibrosis. Although the physiological and pathophysiological regulation of fibrosis has an important pivotal axis in TGF- β 1 and its signaling pathways (mainly through Smads signaling), the interaction of TGF- β 1 and Ras [reviewed in Martínez-Salgado et al. (2008)] must be taken into account when it comes to understanding these processes.

REFERENCES

- Arai, J. A., Li, S., and Feig, L. A. (2009). Sos2 is dispensable for NMDA-induced Erk activation and LTP induction. *Neurosci. Lett.* 455, 22–25. doi: 10.1016/j.neulet.2009.03.047
- Baruzzi, A., Remelli, S., Lorenzetto, E., Sega, M., Chignola, R., and Berton, G. (2015). Sos1 regulates macrophage podosome assembly and macrophage invasive capacity. *J. Immunol.* 195, 4900–4912. doi: 10.4049/jimmunol.1500579
- Buday, L., and Downward, J. (1993). Epidermal growth factor regulates p21ras through the formation of a complex of receptor, Grb2 adapter protein, and Sos nucleotide exchange factor. *Cell* 73, 611–620. doi: 10.1016/0092-8674(93)90146-h
- Esteban, L. M., Fernandez-Medarde, A., Lopez, E., Yienger, K., Guerrero, C., Ward, J. M., et al. (2000). Ras-guanine nucleotide exchange factor Sos2 is dispensable for mouse growth and development. *Mol. Cell Biol.* 20, 6410–6413. doi: 10.1128/20.17.6410-6413.2000
- Fuentes-Calvo, I., Blázquez-Medela, A. M., Eleno, N., Santos, E., López-Novoa, J. M., and Martínez-Salgado, C. H. (2012). Ras isoform modulates extracellular matrix synthesis, proliferation, and migration in fibroblasts. *Am. J. Physiol. Cell Physiol.* 302, C686–C697. doi: 10.1152/ajpcell.00103.2011
- Fuentes-Calvo, I., Crespo, P., Santos, E., López-Novoa, J. M., and Martínez-Salgado, C. (2013). The small GTPase N-Ras regulates extracellular matrix synthesis, proliferation and migration in fibroblasts. *Biochim. Biophys. Acta Mol. Cell Res.* 1833, 2734–2744. doi: 10.1016/j.bbamcr.2013.07.008
- Grande, M. T., Fuentes-Calvo, I., Arévalo, M., Heredia, F., Santos, E., Martínez-Salgado, C., et al. (2010). Deletion of H-Ras decreases renal fibrosis and myofibroblast activation following ureteral obstruction in mice. *Kidney Int.* 77, 509–518. doi: 10.1038/ki.2009.498
- Guittard, G., Kortum, R. L., Balagopalan, L., Çuburu, N., Nguyen, P., Sommers, C. L., et al. (2015). Absence of both Sos-1 and Sos-2 in peripheral CD4+ T cells leads to PI3K pathway activation and defects in migration. *Eur. J. Immunol.* 45, 2389–2395. doi: 10.1002/eji.201445226
- Innocenti, M., Tenca, P., Frittoli, E., Faretta, M., Tocchetti, A., Di Fiore, P. P., et al. (2002). Mechanisms through which Sos-1 coordinates the activation of Ras and Rac. *J. Cell Biol.* 156:125. doi: 10.1083/jcb.200108035
- Kapoor, G. S., and O'Rourke, D. M. (2010). SIRP α 1 receptors interfere with the EGFRvIII signalosome to inhibit glioblastoma cell transformation and migration. *Oncogene* 29, 4130–4144. doi: 10.1038/nc.2010.164
- Krantz, S. B., Shields, M. A., Dangi-Garimella, S., Cheon, E. C., Barron, M. R., Hwang, R. F., et al. (2011). MT1-MMP cooperates with Kras G12D to promote pancreatic fibrosis through increased TGF- β signaling. *Mol. Cancer Res.* 9, 1294–1304. doi: 10.1158/1541-7786.MCR-11-0023
- Leask, A., and Abraham, D. J. (2004). TGF- β signaling and the fibrotic response. *FASEB J.* 18, 816–827. doi: 10.1096/fj.03-1273rev
- Liceras-Boillos, P., García-Navas, R., Ginel-Picardo, A., Anta, B., Pérez-Andrés, M., Lillo, C., et al. (2016). Sos1 disruption impairs cellular proliferation and viability through an increase in mitochondrial oxidative stress in primary MEFs. *Oncogene* 35, 6389–6402. doi: 10.1038/nc.2016.169
- Lin, C., Gao, B., Yan, X., Lei, Z., Chen, K., Li, Y., et al. (2018). MicroRNA 628 suppresses migration and invasion of breast cancer stem cells through targeting SOS1. *Onco. Targets Ther.* 11, 5419–5428. doi: 10.2147/OTT.S164575
- Liu, X., Xu, Y., Deng, Y., and Li, H. (2018). MicroRNA-223 regulates cardiac fibrosis after myocardial infarction by targeting RASA1. *Cell Physiol. Biochem.* 46, 1439–1454. doi: 10.1159/000489185
- Margarit, S. M., Sondermann, H., Hall, B. E., Nagar, B., Hoelz, A., Pirruccello, M., et al. (2003). Structural evidence for feedback activation by Ras.GTP of the Ras-specific nucleotide exchange factor SOS. *Cell* 112, 685–695. doi: 10.1016/s0092-8674(03)00149-1
- Martínez-Salgado, C., Fuentes-Calvo, I., García-Cenador, B., Santos, E., and López-Novoa, J. M. (2006). Involvement of H- and N-Ras isoforms in transforming growth factor- β -induced proliferation and in collagen and fibronectin synthesis. *Exp. Cell Res.* 312, 2093–2106. doi: 10.1016/j.yexcr.2006.03.008
- Martínez-Salgado, C., Rodríguez-Peña, A. B., and López-Novoa, J. M. (2008). Involvement of small Ras GTPases and their effectors in chronic renal disease. *Cell Mol. Life Sci.* 65, 477–492. doi: 10.1007/s00018-007-7260-2
- Muñoz-Félix, J. M., Fuentes-Calvo, I., Cuesta, C., Eleno, N., Crespo, P., López-Novoa, J. M., et al. (2016). Absence of K-Ras reduces proliferation and migration but increases extracellular matrix synthesis in fibroblasts. *J. Cell Physiol.* 231, 2224–2235. doi: 10.1002/jcp.25340

DATA AVAILABILITY STATEMENT

The raw data supporting the conclusions of this article will be made available by the authors, without undue reservation.

AUTHOR CONTRIBUTIONS

IF-C performed the experimental work and the statistical analysis. CM-S designed the study, conceived the experiments, analyzed the results, coordinated the study, and wrote the manuscript. Both authors reviewed the manuscript.

FUNDING

This work was supported by grants from Instituto de Salud Carlos III: Ministry of Economy and Competitiveness PI18/00996 and RETICS RD016/0009/0025 (REDINREN), co-funded by FEDER.

ACKNOWLEDGMENTS

We thank Prof. Eugenio Santos (Cancer Centre Research, Salamanca, Spain) for the kind gift of the mouse embryonic Sos1^{-/-} fibroblasts.

- Park, D., Pandey, S. K., Maksimova, E., Kole, S., and Bernier, M. (2000). Akt-dependent antiapoptotic action of insulin is sensitive to farnesyltransferase inhibitor. *Biochemistry* 39, 12513–12521. doi: 10.1021/bi000995y
- Qian, X., Esteban, L., Vass, W. C., Upadhyaya, C., Papageorge, A. G., Yienger, K., et al. (2000). The Sos1 and Sos2 Ras-specific exchange factors: Differences in placental expression and signaling properties. *EMBO J.* 19, 642–654. doi: 10.1093/emboj/19.4.642
- Quilliam, L. A., Rebhun, J. F., and Castro, A. F. (2002). A growing family of guanine nucleotide exchange factors is responsible for activation of Ras-family GTPases. *Prog. Nucleic Acid Res. Mol. Biol.* 71, 391–444. doi: 10.1016/s0079-6603(02)71047-7
- Rockey, D. C., Bell, P. D., and Hill, J. A. (2015). Fibrosis – a common pathway to organ injury and failure. *N. Engl. J. Med.* 373, 95–96. doi: 10.1056/NEJMc1504848
- Shields, M. A., Ebine, K., Sahai, V., Kumar, K., Siddiqui, K., Hwang, R. F., et al. (2013). Snail cooperates with KrasG12D to promote pancreatic fibrosis. *Mol. Cancer Res.* 11, 1078–1087. doi: 10.1158/1541-7786.MCR-12-0637
- Stratton, R., Rajkumar, V., Ponticos, M., Nichols, B., Shiwen, X., Black, C. M., et al. (2002). Prostacyclin derivatives prevent the fibrotic response to TGF-beta by inhibiting the Ras/MEK/ERK pathway. *FASEB J.* 16, 1949–1951. doi: 10.1096/fj.02-0204fje
- Suire, S., Baltanas, F. C., Segonds-Pichon, A., Davidson, K., Santos, E., Hawkins, P. T., et al. (2019). Frontline science: TNF- α and GM-CSF1 priming augments the role of SOS1/2 in driving activation of Ras, PI3K- γ , and neutrophil proinflammatory responses. *J. Leukoc Biol.* 106, 815–822. doi: 10.1002/JLB.2HI0918-359RR
- Trial, J. A., Entman, M. L., and Cieslik, K. A. (2016). Mesenchymal stem cell-derived inflammatory fibroblasts mediate interstitial fibrosis in the aging heart. *J. Mol. Cell Cardiol.* 91, 28–34. doi: 10.1016/j.yjmcc.2015.12.017
- Ucero, A. C., Benito-Martin, A., Fuentes-Calvo, I., Santamaria, B., Blanco, J., Lopez-Novoa, J. M., et al. (2013). TNF-related weak inducer of apoptosis (TWEAK) promotes kidney fibrosis and Ras-dependent proliferation of cultured renal fibroblast. *Biochim Biophys Acta Mol. Basis Dis.* 1832, 1744–1755. doi: 10.1016/j.bbadis.2013.05.032
- Wang, C., Zhang, C., Liu, L., Xi, A., Chen, B., Li, Y., et al. (2017). Macrophage-derived mir-155-containing exosomes suppress fibroblast proliferation and promote fibroblast inflammation during cardiac injury. *Mol. Ther.* 25, 192–204. doi: 10.1016/j.ymthe.2016.09.001
- Wang, J. H., Newbury, L. J., Knisely, A. S., Monia, B., Hendry, B. M., and Sharpe, C. C. (2012). Antisense knockdown of Kras inhibits fibrosis in a rat model of unilateral ureteric obstruction. *Am. J. Pathol.* 180, 82–90. doi: 10.1016/j.ajpath.2011.09.036
- Wei, X., Wang, X., Xia, Y., Tang, Y., Li, F., Fang, W., et al. (2014). Kindlin-2 regulates renal tubular cell plasticity by activation of Ras and its downstream signaling. *Am. J. Physiol. Physiol.* 306, F271–F278. doi: 10.1152/ajprenal.00499.2013
- Zhang, S., Weinheimer, C., Courtois, M., Kovacs, A., Zhang, C. E., Cheng, A. M., et al. (2003). The role of the Grb2-p38 MAPK signaling pathway in cardiac hypertrophy and fibrosis. *J. Clin. Invest.* 111, 833–841. doi: 10.1172/JCI16290

Conflict of Interest: The authors declare that the research was conducted in the absence of any commercial or financial relationships that could be construed as a potential conflict of interest.

Copyright © 2021 Fuentes-Calvo and Martinez-Salgado. This is an open-access article distributed under the terms of the Creative Commons Attribution License (CC BY). The use, distribution or reproduction in other forums is permitted, provided the original author(s) and the copyright owner(s) are credited and that the original publication in this journal is cited, in accordance with accepted academic practice. No use, distribution or reproduction is permitted which does not comply with these terms.



Role of Podoplanin-Positive Cells in Cardiac Fibrosis and Angiogenesis After Ischemia

Maria Cimini* and Raj Kishore*

Center for Translational Medicine, Lewis Katz School of Medicine, Temple University, Philadelphia, PA, United States

OPEN ACCESS

Edited by:

Gonzalo del Monte-Nieto,
Monash University, Australia

Reviewed by:

Steve P. Watson,
University of Birmingham,
United Kingdom
Yaoliang Tang,
Augusta University, United States

*Correspondence:

Maria Cimini
maria.cimini@temple.edu
Raj Kishore
raj.kishore@temple.edu

Specialty section:

This article was submitted to
Integrative Physiology,
a section of the journal
Frontiers in Physiology

Received: 12 February 2021

Accepted: 15 March 2021

Published: 12 April 2021

Citation:

Cimini M and Kishore R (2021)
Role of Podoplanin-Positive Cells
in Cardiac Fibrosis and Angiogenesis
After Ischemia.
Front. Physiol. 12:667278.
doi: 10.3389/fphys.2021.667278

New insights into the cellular and extra-cellular composition of scar tissue after myocardial infarction (MI) have been identified. Recently, a heterogeneous podoplanin-expressing cell population has been associated with fibrogenic and inflammatory responses and lymphatic vessel growth during scar formation. Podoplanin is a mucin-like transmembrane glycoprotein that plays an important role in heart development, cell motility, tumorigenesis, and metastasis. In the adult mouse heart, podoplanin is expressed only by cardiac lymphatic endothelial cells; after MI, it is acquired with an unexpected heterogeneity by PDGFR α -, PDGFR β -, and CD34-positive cells. Podoplanin may therefore represent a sign of activation of a cohort of progenitor cells during different phases of post-ischemic myocardial wound repair. Podoplanin binds to C-type lectin-like receptor 2 (CLEC-2) which is exclusively expressed by platelets and a variety of immune cells. CLEC-2 is upregulated in CD11b^{high} cells, including monocytes and macrophages, following inflammatory stimuli. We recently published that inhibition of the interaction between podoplanin-expressing cells and podoplanin-binding cells using podoplanin-neutralizing antibodies reduces but does not fully suppress inflammation post-MI while improving heart function and scar composition after ischemic injury. These data support an emerging and alternative mechanism of interaction in the heart that, when neutralized, leads to altered inflammatory response and preservation of cardiac function and structure. The overarching objective of this review is to assimilate and discuss the available evidence on the functional role of podoplanin-positive cells on cardiac fibrosis and remodeling. A detailed characterization of cell-to-cell interactions and paracrine signals between podoplanin-expressing cells and the other type of cells that compose the heart tissue is needed to open a new line of investigation extending beyond the known function of these cells. This review attempts to discuss the role and biology of podoplanin-positive cells in the context of cardiac injury, repair, and remodeling.

Keywords: podoplanin, fibrosis, pericyte, mesenchymal stem cells, telocyte

INTRODUCTION

New discoveries during the last decades have challenged the existing scientific dogmas and provided new conceptual developments in a number of scientific topics. We experienced intense effort in studying organ regeneration with stem and progenitor cells: an area that has evolved with the advent of new investigative tools like single-cell sequencing and cellular lineage tracing in intact

animals. In line with the growing knowledge on the post-MI cardiac responses, it is imperative to further detail the cellular composition and evolution of heart tissue after injury. In this regard, we (Cimini et al., 2017) characterized for the first time the presence of cells positive for a mucin-like transmembrane glycoprotein called podoplanin in the injured heart. These cells do not represent a new category of cells; on the contrary, podoplanin is co-expressed after injury by PDGFR α -, PDGFR β -, and CD34-positive cells and continue to be expressed by lymphatic endothelial cells. The importance of *de novo* podoplanin expression comes from the fact that this glycoprotein is the only known ligand of C-type lectin-like receptor 2 (CLEC-2), highly expressed in platelets, activated monocytes, macrophages, and lymphocytes, and CLEC-2 signaling cascade contributes to the pro-inflammatory lineage of the immune cells (Table 1). Within the four different types of podoplanin co-expressing cells in injured heart described above, each specific group can be analyzed separately, although PDGFR α -, PDGFR β -, CD34-positive cells and lymphatic endothelial cells have been collectively described to take part in regeneration, fibrosis, and inflammatory processes of the same pathologies. It is therefore meaningful to understand whether the already described activity of PDGFR α , PDGFR β , and CD34 cells is similar when they express podoplanin, whether podoplanin indicates a different phenotype of these cells, or whether these cells acquire podoplanin in response to injury-induced inflammation. Thus, the co-expression of podoplanin may suggest the different roles these cells may play in homeostasis versus pathological conditions. In this review, we will provide a description of all the cell categories that express podoplanin, their role in tissue homeostasis, and the evolution of pathologies.

PODOPLANIN-POSITIVE CELLS IN DISEASE AND HOMEOSTASIS: MULTIPLE ROLES OF ONE GLYCOPROTEIN

Podoplanin is a mucin-type, integral membrane glycoprotein also known as Aggrus, T1 α , D2-40, gp36, and RANDAM-2. It is composed of 162 amino acid residues (43 kDa), the N-terminus is directed outside the cell, and the sequence is preserved within species (Ugorski et al., 2016). The intracellular domain is characterized by three basic amino acids responsible for binding to the ezrin-radixin-moesin complex (ERM), which is essential for cell migration. Within the extracellular domain, three adjacent tandem repeats of amino acid sequences directly bind the only known podoplanin receptor: C-type lectin-like receptor 2 (CLEC-2) (Nagae et al., 2014; Ugorski et al., 2016). CLEC-2 is highly expressed in platelets, dendritic cells, and activated monocytes and lymphocytes (Ugorski et al., 2016). Physiologically, podoplanin is expressed primarily on lymphatic endothelial cells, stromal cells of lymph nodes, type-I pneumocytes, and glomerular podocytes (Astarita et al., 2012, 2015). In addition, podoplanin expression was found in the epithelial lining of the coelomic wall of the pericardio-peritoneal

canal, in the cell lining the pleural and pericardial cavity, and in the epicardium (Gittenberger-de Groot et al., 2007; Mahtab et al., 2008). Of late, podoplanin expression has been observed in a larger variety of cells but predominantly it determines the normal development of the lymphatic system, heart, and lung (Pan and Xia, 2015; Ugorski et al., 2016). During lymphangiogenesis, podoplanin-expressing cells from the cardinal vein bind CLEC-2 to platelets that aggregate to seal and separate the first lymphatic vessel from the cardinal vein (Pan and Xia, 2015). In heart development, podoplanin is fundamental for the epithelial-mesenchymal transition (EMT) of the pro-epicardial organ; it regulates the downregulation of E-cadherin, a process that allows epithelial cells to become mobile mesenchymal cells (Astarita et al., 2012). E-cadherin is downregulated by podoplanin in cancer cells and cancer-associated fibroblasts (CAFs), leading to invasive growth and metastasis (Mahtab et al., 2008; Ugorski et al., 2016).

C-Type Lectin Receptors and Podoplanin Signaling

Podoplanin binds to the non-canonical side face of CLEC-2, a receptor that belongs to a large family of innate immunity receptors that share a structurally homologous carbohydrate recognition domain (Lepenies et al., 2013; Nagae et al., 2014; Suzuki-Inoue et al., 2017). Specifically, CLEC-2 belongs to Dectin-1 subfamily of C-type lectin receptors, and it has been characterized by an extracellular C-Type lectin-like domain and a single intracellular hemITAM motif that recruits spleen tyrosine kinase (Syk). CLEC-2 is highly expressed on platelets (Rayes et al., 2017), and its expression has been reported on CD11b^{high} (monocytes) and Gr-1^{high} myeloid cells (a lower level than platelets), dendritic cells, as well on a variety of leukocytes and neutrophils following inflammatory stimuli (Kerrigan et al., 2009; Chang et al., 2010; Lowe et al., 2015b; Suzuki-Inoue et al., 2017). Physiologically, the CLEC-2/podoplanin interaction is essential for the formation of the lymphatic system, the pro-epicardial organ, cerebrovascular patterning, and lymph node development and maintenance (Schacht et al., 2003; Hess et al., 2014; Suzuki-Inoue et al., 2017). CLEC-2 and podoplanin highly interact for the preservation of high endothelial venules in the lymph node, vascular integrity under inflammatory conditions, and the wound healing process (Suzuki-Inoue et al., 2017). Furthermore, the CLEC-2/podoplanin axis contribute to the generation of optimal adaptive immune responses (Astarita et al., 2012, 2015; Acton et al., 2014; Benezech et al., 2014; Suzuki-Inoue et al., 2017). In myeloid cells, Syk-dependent signaling activation through podoplanin can variably lead to the production of reactive oxygen species (ROS) and/or induction of innate immune genes, including pro-inflammatory cytokines due to the final activation of NFAT through Syk cascade (Mourao-Sa et al., 2011). In platelets, CLEC-2 induces tyrosine phosphorylation of the hemITAM motif and downstream signaling, leading to calcium mobilization and platelet aggregation (Rayes et al., 2017). Recently, the binding between podoplanin and CLEC-2 following activation of CLEC-2

TABLE 1 | Podoplanin-positive cells markers.

| Type of cell | Markers | | | | | | | | |
|-----------------------------|---------|--------|--------|----------------|---------------|------|---------------|----------|------------|
| | LYVE-1 | Prox-1 | VEGFR3 | PDGFR α | PDGFR β | CD34 | α -SMA | Vimentin | Podoplanin |
| Podoplanin-positive cells | ✓ | ✓ | ✓ | ✓ | ✓ | ✓ | | | ✓ |
| Lymphatic endothelial cells | ✓ | ✓ | ✓ | | | | | | ✓ |
| Pericytes | | | | ✓ | ✓ | ✓ | ✓ | ✓ | ✓ |
| MSCs | | | | ✓ | ✓ | ✓ | | ✓ | ✓ |
| Mesenchymal stromal cells | | | | ✓ | ✓ | ✓ | | ✓ | ✓ |
| Telocytes | | | | ✓ | ✓ | ✓ | | ✓ | ✓ |

Podoplanin-positive cells positivity compared with lymphatic endothelial cells, pericytes, MSCs, mesenchymal stromal cells, and telocytes.

positive cells has been described in many pathologies; mostly, the acquisition of podoplanin by mesenchymal cells and the interaction with immune cells have been highlighted. The unique and versatile binding modes between podoplanin and CLEC-2 open a new area of investigation in order to understand the consequences of this interaction especially in pathological and inflammatory conditions.

Podoplanin in Tumor Biology

Podoplanin represents a marker of the major solid tumors, unfortunately with adverse prognosis and CAFs; it is also the master regulator of the cancer invasiveness due to the EMT-mediated cell migration and invasion. Podoplanin binding to ERM in cancer cells lead to RhoA-associated kinase-dependent ERM phosphorylation with a consequent mobilization of both cancer cells and CAFs (Fernandez-Munoz et al., 2011). On the other hand, podoplanin mediates the remodeling of the actin cytoskeleton in the absence of EMT by filopodia formation or invadopodia stability via the downregulation of the activities of small Rho family GTPases (Martin-Villar et al., 2015) or binding CLEC-2 on platelets and skipping the immune checkpoints. Podoplanin facilitates thrombus formation; in fact, tumor cells induce platelet aggregation, which protects cancer cells from shear stress and host immunological defense. This phenomenon results in increased tumor growth and enhanced metastatic potential of the tumors (Pula et al., 2013). Based on the importance and relevance of podoplanin in tumor biology, antibody-based immunotherapies, and antagonist that suppress podoplanin/CLEC-2 binding and following platelet aggregation and cancer metastasis have been developed (Kaneko et al., 2006, 2012; Kato et al., 2006; Ogasawara et al., 2008; Nakazawa et al., 2011; Fujita and Takagi, 2012; Takagi et al., 2013, 2014; Kato and Kaneko, 2014; Miyata et al., 2014; Chang Y. W. et al., 2015; Rayes et al., 2017; Krishnan et al., 2018). The efficacy of antibody-based immunotherapy is due to the activation of apoptosis, antibody-dependent and complement-dependent cellular cytotoxicity, or simply neutralizing the binding between ligand and receptor or a protein with a complement motif (Macor et al., 2015). Besides cell-to-cell or cell-to-ERM interaction, cancer cells and podoplanin-positive CAFs release extra-cellular vesicles and exosomes that contain podoplanin mRNA and protein (Carrasco-Ramirez et al., 2016). Exosomes containing podoplanin promoted lymphatic vessel formation,

EMT, upregulation of oncogenic protein, and diminished expression of tumor suppressors (Carrasco-Ramirez et al., 2016).

Podoplanin as a Key Facilitator of Stromal and Immune Cell Interaction

The podoplanin/CLEC-2 axis takes place not only *in utero* and cancer biology (Suzuki-Inoue et al., 2017); but they interact with each other under several pathological conditions since CLEC-2 expression has been reported on circulating CD11b positive cells, dendritic cells, and a variety of leukocytes and neutrophils in basal conditions and following inflammatory stimuli (Mourao-Sa et al., 2011; Lepenies et al., 2013; Yan et al., 2013; Lowe et al., 2015b). On the other hand, interstitial stromal cells acquire podoplanin after organ injury (Acton et al., 2012; Ugorski et al., 2016). Specifically, mesenchymal stromal cells upregulate podoplanin at sites of infection and chronic inflammation; functionally podoplanin enables the interaction with platelets, aggregation, and formation of microthrombi alongside the mesenchymal stromal cell migration capacity (Ward et al., 2019). It is known that mesenchymal stromal cells and interstitial stromal cells acquire podoplanin under interferon- γ , transforming growth factor- β and tumor necrosis factor- α stimuli, but the full mechanism behind the expression of this glycoprotein is still unknown (Kunita et al., 2018). The expression of podoplanin can be considered as involvement of mesenchymal cells in the inflammatory reaction since the receptor, CLEC-2, is highly expressed on activated immune cells.

Podoplanin in the Injured Heart

In the heart, the expression of podoplanin by interstitial cells was described for the first time by Cimini et al. (2017). They reported that podoplanin is expressed by a heterogeneous population of lymphangiogenic, fibrogenic, and mesenchymal progenitor cells (Cimini et al., 2017). In the adult heart, podoplanin-positive cells are rare, constituting less than 5% of the myocardial small cell population (Pinto et al., 2016). In fact, in homeostatic conditions, podoplanin is expressed only by cardiac lymphatic endothelial cells (Cimini et al., 2017). Cimini et al. (2017) analyzed the spatial and temporal distribution of the cells that acquire this glycoprotein after ischemic injury, and although podoplanin is a common lymphoendothelial marker, it is expressed with an unexpected heterogeneity and the appearance of podoplanin-positive cells increases over time from the acute

(2 days) to the chronic phase of the myocardial infarction (MI; 2 weeks and 1 month). The interstitial podoplanin-positive cells did not express LYVE-1, a specific lymphatic endothelial marker, Prox-1, a major transcription factor of the lymphatic endothelial fate, and VEGFR-3 unless organized in cardiac lymphatic vessels (Brakenhielm and Alitalo, 2019). This suggests that a large portion of podoplanin-positive cells do not possess a differentiated lymphatic endothelial phenotype. Additionally, podoplanin-positive cells do not express markers of mature endothelial cells like CD31 and VEGFR2 (Loukas et al., 2011). The immunohistochemistry and the flow cytometry analysis of the infarcted hearts at different time points after MI showed that the podoplanin-positive cells were distinctly PDGFR α positive. The co-localization of PDGFR β and CD34 with podoplanin was infrequent early after MI and strongly elevated at later stages of infarct healing in the mature scar. Since PDGFR α and CD34 are associated with the properties of immature mesenchymal cells and PDGFR β is a marker of pericytes the concordance of co-staining with podoplanin suggested that podoplanin-expressing cells contain also a population with progenitor capabilities. Podoplanin-positive cells are positive only for CD34 but negative for CD45, which exclude the hematopoietic origin. Of note, although PDGFR α and PDGFR β are also associated with fibrogenic behavior, podoplanin-positive cells do not express vimentin and α -Smooth muscle actin at any time point, suggesting that podoplanin-positive cells do not generate fully differentiated fibroblasts (Cimini et al., 2017). Therefore, podoplanin may represent a sign of activation of a cohort of cells during different phases of postischemic myocardial wound repair and it can be involved in mechanisms of inflammation and scar formation after MI. Cimini et al. (2019) investigated a neutralizing antibody treatment approach in a mouse MI model to inhibit cell-to-cell interaction of podoplanin-positive cells to inflammatory cells in the modulation of post-MI inflammation since an exacerbated and prolonged inflammatory response is the leading cause of adverse remodeling after myocardial injury (Prabhu and Frangogiannis, 2016; Frangogiannis, 2017) and reported improved cardiac function after MI with this approach. Targeted anti-inflammatory approaches were widely studied to reduce inflammation and improve cardiac repair (Frangogiannis, 2012, 2014); although, patients treated with highly selective strategies did not show a positive outcome after therapy (Saxena et al., 2016). The translational failure may be the result of exclusive inhibition of the recruitment of pro-inflammatory monocytes and decreased cytokine expression in the ischemic hearts (Saxena et al., 2016). The complete suppression of the inflammatory pathways interferes with the migration and activation of reparative and regenerative cells important for positive tissue remodeling (Saxena et al., 2016). Cimini et al. (2019) demonstrated that inhibition of the interaction between podoplanin-expressing cells and podoplanin-binding cells reduce but does not fully suppress the inflammation post MI and at the same time enhance an endogenous myocardial regeneration process after ischemic injury (Cimini et al., 2019). The histological data, vis-a-vis the functional one, demonstrated that the neutralizing activity of

podoplanin leads to the healthier tissue geometry organization in the treated animals compared to the scar formation in the control animals; enhanced cardiac performance, regeneration and angiogenesis post MI (Cimini et al., 2019). Modulating the interaction between podoplanin-positive cells and immune cells post MI positively affect the immune cells recruitment (Tugal et al., 2013; Frangogiannis, 2015; Roszer, 2015; Sica et al., 2015; Sager et al., 2017) and they did not observe any differences in podoplanin expression in acute and chronic phases after MI between the treated and untreated groups; the treatment with the neutralizing antibody does not affect the cell migration or the cell composition in the scar, thus, podoplanin-expressing cells resident in the heart displayed podoplanin under inflammatory condition and the neutralizing antibody could only interfere in the interaction of podoplanin with podoplanin-binding cells (Cimini et al., 2019).

Podoplanin in Vascular Pathophysiology

Similar observations were reported by other groups studying the biology of inflammation and possible selective targets in several pathologies. Specifically, in vascular biology, CLEC-2 is known to maintain the physiological state of blood vasculature under inflammatory conditions; mice with a deficiency in CLEC-2 as well as inhibition of podoplanin are protected against deep vein thrombosis with reduced platelet accumulation at the inferior vena cava (IVC) wall (Payne et al., 2017). Podoplanin was found in the IVC wall and was localized in the vicinity of the abluminal side of the endothelium in an animal model of deep vein thrombosis (Payne et al., 2017) or in aspirated coronary thrombi (lytic and organized) from a patient with ST-elevation myocardial infarction (Rakocevic et al., 2016). The level of podoplanin in the IVC increased after 48 h of stenosis to a substantially higher extent in mice with a thrombus versus those without a thrombus. Treatment of animals with an anti-podoplanin neutralizing antibody resulted in the development of smaller thrombi; thus, Payne et al. (2017) proposed a novel mechanism of deep vein thrombosis where CLEC-2 and the upregulation of podoplanin trigger the thrombus formation. Platelets form stable aggregates on mouse podoplanin at arterial shear through the CLEC-2 pathway, and podoplanin thus supports platelet capture and activation at arteriolar rates of shear (Lombard et al., 2018). Consistent with the expression of podoplanin in thrombi, this glycoprotein is highly relevant in the calcification of aortic valves (Napankangas et al., 2019) and atherosclerotic lesions (Hatakeyama et al., 2012). Podoplanin is critical in the early stages of osteoblast-to-osteocyte transition (Ikpegbu et al., 2018) and, as already mentioned is acquired by mesenchymal stromal cells (Kunita et al., 2018). During osteogenesis fibroblast growth factor-2 promotes osteocyte differentiation and podoplanin expression (Ikpegbu et al., 2018). The calcification of aortic valves origin from mesenchymal cells which have differentiated toward an osteoblastic phenotype; immunohistochemical analysis of human calcified valves showed podoplanin positivity in lymphatic vessels, osteoblast, osteocyte, chondrocytes, macrophages, and spindle cells with a myofibroblastic phenotype (Napankangas et al., 2019). As well as for the calcification of aortic

valves, podoplanin expression contributes to the thrombotic property of atherosclerotic lesions and might be a novel target for an anti-thrombus drug since it is highly co-localized with smooth muscle cells and macrophages in plaque with necrotic core compared with the early lesions composed by smooth muscle cells and small number of monocytes (Hatakeyama et al., 2012).

Podoplanin in Neuropathology

Podoplanin is also investigated in neurobiology. It is expressed on the developing neural tube and neuro epithelium and guides the maturation and integrity of developing vasculature in the brain (Lowe et al., 2015a). In the adult brain it is highly expressed in a subset of glial fibrillary acidic protein-positive astrocytes adjacent to gliomas (Kolar et al., 2015); is co-expressed with nestin, a marker of neural progenitor cells; and has been suggested to be a marker for reactive astrocytes (Kolar et al., 2015). In lipopolysaccharide-induced neuroinflammation, podoplanin is expressed in neurons but not in astrocytes with a concomitant upregulation of active caspase 3, cyclin D1, and CDK4, which decreased *in vivo* and *in vitro* after knocking down podoplanin by siRNA (Song et al., 2014). As is the case with MI, in a mouse model of ischemic stroke with a middle cerebral artery occlusion, the expression of CLEC-2 and podoplanin increased after ischemia/reperfusion injury, with a peak at 24 h post-injury (Meng et al., 2020). Podoplanin and CLEC-2 colocalized mainly in the ischemia/reperfusion cortex and were expressed in neurons and microglia. Anti-podoplanin antibody pretreatment drastically reduced the cerebral infarct and attenuated the neurological deficits during the acute stage of recovery; moreover, a significant decrease of IL-18 and IL-1 β was observed in mice pretreated with podoplanin neutralizing antibody (Meng et al., 2020). With this study, Meng et al. demonstrated that, like in the heart, the podoplanin/CLEC-2 axis plays an important role during inflammatory reactions (Cimini et al., 2019; Meng et al., 2020).

Podoplanin and Autoimmune Diseases

Podoplanin is also well studied in the biology of autoimmune diseases, specifically psoriasis and rheumatoid arthritis (Noack et al., 2016a,b). During psoriasis mainly T helper lymphocytes infiltrate the inflammatory site and interact with mesenchymal cells and fibroblast, enhancing the production of IL-8, IL-6, and IL-1 β ; but, within all the activated peripheral blood mononuclear cells, monocytes contribute to higher IL-17 secretion and podoplanin expressing mesenchymal cells, largely contributes to this massive secretion (Noack et al., 2016b). Using an anti podoplanin antibody, the interaction with activated monocytes and mesenchymal cells inhibited IL-17 secretion by 60% (Noack et al., 2016b). A similar mechanism has been investigated within synoviocytes and activated peripheral blood mononuclear cells during rheumatoid arthritis (Noack et al., 2016a). Co-culture of peripheral blood mononuclear cells and synoviocytes highly increased the production of IL-6, IL-1 β , and IL-17. Using podoplanin-neutralizing antibody during the co-culture reduced IL-17 secretion by 60%, inhibiting the binding between synoviocytes podoplanin positive and CLEC-2

positive activated monocytes (Noack et al., 2016a). These results lead to consider podoplanin as a potential target for chronic autoimmune diseases.

Podoplanin in Organ Injury

Recently, podoplanin has been investigated also in pancreatic injuries; a different type of insult from inflammation or cancer may change the equilibrium in the tissue. In fact, podoplanin and Prox-1 expression is highly increased in pancreatic islets after a hypercaloric diet (Taran et al., 2019). In a mouse model of 6 weeks of hypercaloric diet-induced hypertrophy of pancreatic islets with a focal expression of podoplanin and Prox-1, at 9 weeks on a hypercaloric diet, strong peri-insular inflammation was found around the hypertrophic islets, highly expressing podoplanin, suggesting that podoplanin may be involved in the early steps of pancreatic islet changes (Taran et al., 2019).

Podoplanin and New Insight Into Therapeutic Strategies

Taking together, neutralizing antibodies, antagonists, synthetic compounds, and CAR-T cells can inhibit podoplanin/CLEC-2 binding; and in all the pathologies where podoplanin is overexpressed any of these treatments may regulate the podoplanin function and improve the prognosis. Therefore, the contribution of podoplanin-positive cells in different pathologies must be fully investigated to generate information that goes beyond the cell-to-cell interaction and may involve also paracrine signals since the majority of podoplanin-positive cells have been described to release extracellular vesicles and exosomes (Krishnan et al., 2018).

LYMPHATIC ENDOTHELIAL CELLS AND PODOPLANIN

Based on the evidence from several research areas, podoplanin is acquired, specifically during inflammation, by a variety of cell types that do not express this glycoprotein at the baseline level, enhancing the inflammatory reaction mostly binding monocytes and platelets, and probably through paracrine factors. Which type of cells are resident podoplanin-positive cells in the heart? Looking overall at the markers of podoplanin-positive cells, few categories of well-known cells can be investigated. During physiological conditions podoplanin is expressed in the heart only by lymphatic endothelial cells (Pinto et al., 2016; Cimini et al., 2017); the cardiac lymphatic vasculature has been extensively investigated and studied (Brakenhielm and Alitalo, 2019) since an increase in lymphatics accompanied major cardiac pathological remodeling, such as acute and chronic ischemia, progressive atherosclerosis and hypertrophy, and myocarditis (Kholova et al., 2011). The lymphatic vasculature accompanies the blood vasculature, and it is essential for the maintenance of tissue fluid homeostasis and immune cell trafficking, specifically during and after a major injury (Brakenhielm and Alitalo, 2019). For this reason, many pharmacological treatments led to improved lymphangiogenesis (Yoon et al., 2003; Henri et al., 2016; Vieira et al., 2018) and thus the cardiac function

since new lymphatic vessel formation reduces secondary edema and facilitates pumping during the systole and diastole. Decreased hypertrophy leads to diminished remodeling and cardiomyocyte death due to stress with consequent reduced interstitial scarring (Yoon et al., 2003; Henri et al., 2016; Vieira et al., 2018).

Lymphangiogenesis and the Role of Lymphatic Endothelial Cells

New lymphatic vessels in any injury will enhance the removal of cell debris and contribute to the resolution of the inflammation recruiting the immune cells back to the circulation (Yoon et al., 2003; Henri et al., 2016; Vieira et al., 2018). This aspect is extremely important to enhance tissue repair, but what are the consequences to the oxygen distribution and the consequential vascularization? It is yet to be defined whether lymphangiogenesis enhances later vascular formation and if lymphatic endothelial cells themselves influence the physiology of the neighboring cells when they, like all the other cells in the tissue, are targeted by inflammatory signals. The improvement from the lymphangiogenesis comes from the capacity to create a more lymphatic vessel, but the lymphatic cells, as an entity, will receive stimuli and communicate their activation to other cells as well. The major lymphatic endothelial cell markers are as follows: Lyve-1, the receptor of hyaluronic acid, Prox-1, the major transcription factor for the lymphatic fate, VEGFR-3, vascular endothelial growth factor for the VEGF-C, and podoplanin (Yang et al., 2012). Mature lymphatic endothelial cells have a heterogeneous origin (Klotz et al., 2015; Norman and Riley, 2016) and derive from already resident lymphatic endothelial cell (Ratajska et al., 2014; Klotz et al., 2015), venous endothelial cells (Ratajska et al., 2014; Norman and Riley, 2016), angioblasts (Nicenboim et al., 2015), or pluripotent stem cells (Salven et al., 2003; Lee et al., 2015). Furthermore, it has been described that venous endothelial cells and pericytes can differentiate into lymphatic endothelial cells by upregulating expression of the major lymphatic transcription factor Prox-1 (Petrova et al., 2002; Hirakawa et al., 2003; Yee et al., 2017); it has been published that altering the level of Prox-1 expression during the embryonic, post-natal, or adult stages can reprogram the lymphatic endothelial cells phenotype to become blood endothelial cells (Petrova et al., 2002; Groger et al., 2004; Yang and Oliver, 2014). On the other hand, blood endothelial cells can be transcriptionally reprogrammed by overexpression of PROX1 *in vitro*, resulting in upregulation of lymphatic markers (Petrova et al., 2002; Hirakawa et al., 2003; Yang and Oliver, 2014; Yee et al., 2017). In the cardiac scar tissue after MI, perivascular PDGFR β -positive cells during the chronic phase of myocardial remodeling expressed both Prox-1 and podoplanin, which suggests that pericytes can differentiate into lymphatic endothelial cells and not only into fibroblast and contribute to the lymphatic vasculature (Cimini et al., 2017). Pericytes are another category of cells that have a lot in common with podoplanin-positive cells or are actually pericytes that acquire podoplanin during inflammatory conditions (Cimini et al., 2017).

PERICYTES: SENTINELS OF FEW, PRECURSORS OF MANY

Pericytes belong to the big family of adult mesenchymal progenitor cells and have potential to self-renew and differentiate into multiple mesenchymal cell types (Farini et al., 2014; Birbrair et al., 2015). Pericytes play a major role in the maintenance of blood vessel walls (Diaz-Flores et al., 2009), promote angiogenesis, vasculogenesis, tissue regeneration and repair, diapedesis of immune cells, and fibrogenic responses (Diaz-Flores et al., 2009; Wong et al., 2015). Pericytes have been studied mostly for their location and morphology; they can be spindle shaped, stellate, and with fingers-like projections surrounding vessels, and for these reasons reside in all the organs (Proebstl et al., 2012; Hall et al., 2014). They have been hypothesized to be precursors of mesenchymal stem cells (MSCs) since MSCs are anatomically found near the vasculature and perhaps can be isolated from most tissues around the body (Caplan, 2008; Feng et al., 2010; Crisan et al., 2012; Wong et al., 2015). Pericytes are recruited from endothelial cells through PDGF that binds PDGFR β , highly expressed on pericytes, and on the other side angiopoietin-1 released from pericytes, mediates the binding between the two types of cells via a Tie2 receptor (Sundberg et al., 2002; Bjarnegard et al., 2004; Cai et al., 2008; Birbrair et al., 2014). PDGFR β is probably the most well-known marker for pericytes found throughout, but there are others that are not uniquely found on pericytes and are often dynamically expressed (Armulik et al., 2005; Caplan, 2008; Crisan et al., 2008) or shared with endothelial cells, smooth muscle cells and MSCs (Crisan et al., 2012). Pericytes do not express hematopoietic and endothelial cells markers such as CD45, CD177, CD34, CD133, and CD31 (Crisan et al., 2008; Chen et al., 2015; Wong et al., 2015), but they are always positive for CD146, desmin, and 3G5 (Crisan et al., 2008). They irregularly express PDGFR α , NG2, and α SMA based on the vessel that they surround (Crisan et al., 2012; Chen et al., 2015). It has been described that, both *in vivo* and *in vitro*, pericytes express CD105, CD73, CD90, and Sca-1 as well as other well-known MSCs markers; on the other side also MSCs share with pericytes the expression of NG2, 3G5, CD146, PDGFR β , and α SMA (Chen et al., 2015). Due to the anatomical position, morphology, and markers it is very difficult to determine whether these cells represent counterparts of the same population unless MSCs are isolated from bone marrow (Bautch, 2011; Crisan et al., 2012; Lin and Lue, 2013; Bobryshev et al., 2015; Klein, 2016).

Pericytes and Podoplanin

Besides regenerative capacity, pericytes can contribute to perivascular and infiltrative fibrosis due to their plasticity (Thomas et al., 2017; Buhl et al., 2020); in fact, under hypoxia PDGFR β -positive cells undergo endothelial to mesenchymal transition. Furthermore, it is well known that perivascular tumors derive from activated pericytes and the cancer tissue is highly positive to PDGFR β (Palmieri et al., 2013). Recently it has been described that kidney fibrosis is characterized by the expansion of PDGFR β -positive cells, and the inhibition of

the PDGFR β reverses the fibrosis (Wakisaka et al., 2019; Buhl et al., 2020). Only a few tissues where pericytes-derived fibrosis is disadvantageous to organ function have been investigated for podoplanin-positive cells in the fibrotic area (Song et al., 2014; Kolar et al., 2015; Lowe et al., 2015a; Cimini et al., 2019; Meng et al., 2020). This connection leads to the fact that pericyte and podoplanin expression may be very connected (Cimini et al., 2017). In the central nervous system, in fact, pericytes accumulate after tissue injury and release collagen (Birbrair et al., 2014), reducing pericyte-derived scar promotes recovery after spinal cord injury (Dias et al., 2018). On the other hand, transplantation of allogenic pericytes improves myocardial vascularization after MI (Alvino et al., 2018) due to the regulation of the endothelium in angiogenesis (Caporali et al., 2017).

MESENCHYMAL STEM CELLS AND THEIR CONTRIBUTION TO TISSUE HOMEOSTASIS

A very thin line separates pericytes from MSCs, probably they derive from the same group of cells with a distinctive evolution in the tissue. Perivascular niche-derived MSCs must be CD105-, CD73-, and CD90-positive (Bautch, 2011; Crisan et al., 2012; Lin and Lue, 2013; Shammaa et al., 2020) and negative for CD45, CD34, CD14, CD11b, CD79a, CD19, and HLA-DR (Crisan et al., 2008; Shammaa et al., 2020). It is very important that MSCs adhere to plastic when cultured *in vitro* and undergo the tri-lineage differentiation into osteoblasts, chondrocytes, and adipocytes (Wong et al., 2015). Murine MSCs have been largely described to express also Sca-1, CD146, PDGFR α , and PDGFR β (Feng et al., 2010). In the bone marrow, a population of Sca-1-positive cells named sinusoidal endothelial cells express podoplanin and contribute to the maintenance of hematopoietic stem cell niche (Xu et al., 2018). Podoplanin-positive cells described in the heart share with MSCs the PDGFR α expression (Noseda et al., 2015; Cimini et al., 2017) since PDGFR α -positive MSCs as well as pericytes reside in the heart (Noseda et al., 2015; Beltrami and Madeddu, 2018), it could be that these two cell populations acquire podoplanin after injury in a time-dependent manner (Cimini et al., 2017). PDGFR α in the heart has been described to be associated with Sca-1 in cardiac progenitor/stem cells; these cells showed cardiomyocyte, endothelial and smooth muscle lineage potential after grafting and augmenting the cardiac function (Noseda et al., 2015). Specifically, PDGFR α demarcated the clonogenic/cardiogenic Sca-1 stem/progenitor cell (Noseda et al., 2015). As is the case with mesenchymal stem cells, mesenchymal stromal cells also express PDGFR α . The International Society for Cell and Gene Therapy (ISCT) has recently taken a position and made a statement to clarify the nomenclature because the two types of cells share most of the markers, especially when isolated from tissues different than bone marrow (Viswanathan et al., 2019). The ISCT continues to support the use of MSCs for both types of cells but supplemented with the tissue-source origin of the cells, intending to call them mesenchymal stromal cells, unless rigorous evidence for stemness can be supported by *in vivo* and *in vitro* data (Viswanathan et al.,

2019). Competent MSCs have multiple therapeutic utilities due to their properties, are immune privileged due to the low expression of MHC I/II, and are thus used in immune-based pathologies, produce an anti-neoplastic agent, induce anti-tumor immunity, and stimulate, through differentiation or paracrine factors, tissue regeneration (Shammaa et al., 2020). In the heart, MSCs stimulate cell-specific regenerative mechanisms after MI depending on the site of the niches; niches were detected intramyocardially in cell clusters and characterized by positive expression of vimentin, CD29, CD44, CD105, and PDGFR α (Klopsch et al., 2017). PDGFR α -positive cells only have been found in the heart in the epicardium, myocardium, and endocardium; *in vitro* differentiation of cardiac PDGFR α -positive cells generates a significant number of smooth muscle cells and endothelial cells only (Chong et al., 2013). These data suggest that cardiac MSCs PDGFR α -positive cells predominantly contribute to the vascular and mesenchymal compartments.

Mesenchymal Stromal Cells: A Heterogeneous Cell Population

Like MSCs, mesenchymal stromal cells have also been identified in the heart and specifically in both ventricles (Stadiotti et al., 2020). Histological analysis showed a greater percentage of stromal cells in the right ventricle versus the left one; cardiac mesenchymal stromal cells from the right ventricle show the same surface markers as the cells isolated from the left ventricle (Stadiotti et al., 2020). There is a very thin line that separates MSCs from mesenchymal stromal cells, and in the heart, a dynamic flux of cardiac stromal cells has been described, which is much that like when MSCs express PDGFR α (Farbehi et al., 2019). During MI, the population of PDGFR α -positive mesenchymal stromal cells is highly enriched in the ischemic area at 3 and 7 days post-surgery (Farbehi et al., 2019). The PDGFR α -positive stromal cells isolated after MI showed at the single-cell RNA sequencing either pro and anti-fibrotic characteristics, thus mesenchymal stromal cells follow a non-linear differentiation in myeloid or fibroblast lineage after injury (Farbehi et al., 2019). Based on these data, the mesenchymal stromal/stem cells belong to a heterogeneous population, which contributes to both regeneration and tissue homeostasis (repair) based on the stemness of the niches, and they share the expression of PDGFR α and can be pharmacologically targeted to manage fibrosis (Usunier et al., 2014; Klimczak and Kozłowska, 2016).

Podoplanin and Mesenchymal Cells

There is no evidence to support which type of PDGFR α -positive cell acquires podoplanin, be it MSCs or the mesenchymal stromal cells, at least in the heart. But it is very important to understand whether the activation of MSCs or mesenchymal stromal cells in fibrosis is marked by podoplanin. Recently, Forte et al. identified differences in epicardial- and endocardial-derived fibroblast of two different types of inbred mice based on the frequency of the left ventricle rupture after MI, and they found that the interstitial cell activation is crucial for the scar formation and organ survival after injury (Pinto et al., 2016; Forte et al., 2020). Based on these data, and the behavior of PDGFR α -positive

cells, it is possible to corroborate the idea that either MSCs or mesenchymal stromal cells acquire podoplanin after injury (Cimini et al., 2017). Ward et al. (2019), recently described the upregulation of podoplanin in mesenchymal stromal cells and showed the functional consequences of podoplanin expression on the migration of mesenchymal stromal cells and their interaction with platelets. In a co-culture system using porous *trans*-wells, podoplanin-expressing mesenchymal stromal cells were able to create microthrombi after capturing platelets, and treatment with recombinant soluble CLEC-2 inhibited the aggregation (Ward et al., 2019). Similar phenomena have been described in atherosclerotic lesions (Hatakeyama et al., 2012) and calcification of aortic valves (Napankangas et al., 2019), where mesenchymal cells have been described to enhance the podoplanin expression; specifically, MSCs have been the most mesenchymal cells isolated from calcified and inflamed aortas. Their origin has often been confirmed *in vitro* to show three lineage potentials (Ciavarella et al., 2017). Notably, MSCs like pericytes and podoplanin-positive CAFs showed an extracellular-vesicle mode of communication (Valente et al., 2015) that could participate in the mechanism of arterial calcification (Zazzeroni et al., 2018). MSCs can be histologically confused with another type of interstitial cells called telocytes, which share with MSCs the expression of PDGFR α but differ from MSCs by high expression of CD34 (Kucybala et al., 2017).

TELOCYTES AND PODOPLANIN

Telocytes are enigmatic interstitial cells with a very distinctive morphology and a small body with long extensions named telopodes; they have been characterized by specific markers, tissue localization/geometry, and physiological function (Kucybala et al., 2017). Projections are features that telocytes have in common with CAFs where they are called invadopodia (Martin-Villar et al., 2015), and MSCs and pericytes, named prolongations (Thomas et al., 2017), and lymphatic endothelial cells (Rusu and Hostiu, 2019). Telopodes from telocytes, except for neural axons, are the longest structures in the body: they branch and create a pattern (Popescu and Fausone-Pellegrini, 2010; Varga et al., 2016). Telocytes are located in almost all the organs, heart included, in the interstitium, extra epithelial space, between functional elements like arteries and nerves (Cretoiu et al., 2014; Rusu et al., 2014; Mirancea, 2016), and can be ultrastructurally confused with lymphatic endothelial cells due to the lack of basal lamina (Rusu and Hostiu, 2019). Telocytes are specifically positive for CD34, PDGFR α , PDGFR β , c-Kit, Sca-1, CD29, vimentin, and α -SMA (weak) (Chang Y. et al., 2015; Diaz-Flores et al., 2016; Fausone-Pellegrini and Gherghiceanu, 2016) and negative for CD45 (Bei et al., 2015a). In contrast, fibrocytes, bone-marrow-derived MSCs, doubly express CD34 and CD45 (Keeley et al., 2009; Piera-Velazquez et al., 2016). It is very difficult to differentiate telocytes from other types of cells, and the most appropriate marker to use to recognize them is the CD34 since MSCs, pericytes, fibroblasts, and neurons are negative for it (Bei et al., 2015b; Mirancea, 2016). These cells constitute a part of podoplanin-positive cells

after 15 days of MI (Cimini et al., 2017). Telocytes are well known to communicate with other cell types, specifically in the heart with cardiac stem cells, with stromal synapses, point contacts, nanocontacts (Manole et al., 2011; Fausone-Pellegrini and Gherghiceanu, 2016; Popescu et al., 2016) like MSCs, and pericytes via extra cellular vesicles and exosomes (Fertig et al., 2014; Fausone-Pellegrini and Gherghiceanu, 2016).

Telocytes and Cardiac Regeneration

The contacts built by telocytes have a mechanical function and allow intercellular communication as an exchange of information (Fausone-Pellegrini and Gherghiceanu, 2016) beyond the well-known paracrine communication (Manole et al., 2011; Edelstein et al., 2016). Physiologically, telocytes support cardiac growth, regeneration, renovation of connective tissue, and repair due to the unique communication with cardiac stem and progenitor cells (Popescu et al., 2015; Diaz-Flores et al., 2016; Li Y. et al., 2016). During the pathological condition, in the heart, the number of telocytes decreases; consequently cardiac stem cell niches are impaired with a consequent increase in fibrosis as a replacement for the loss of telocytes, cardiac stem cells, and signalization between telocytes and fibroblasts (Richter and Kostin, 2015; Kostin, 2016). The telocyte-associated diseases are named telocytopathies (Ibba-Manneschi et al., 2016; Varga et al., 2019). Telocytes are also found along the vascular system, are located in proximity of MSC perivascular niches, and are positive for CD34 and PDGFR β ; they connect cells within each other and support angiogenesis (Suciu et al., 2010; Cantarero et al., 2011; Zhang et al., 2015; Boos et al., 2016). Isolated rat telocytes for CD34/PDGFR α continue to express these two markers also *in vitro* together with vimentin (Li Y. Y. et al., 2016) as well as isolated murine telocytes (Chi et al., 2015) without losing their typical morphology. *In vitro* murine telocytes secretory profile has been investigated with and without the presence of cardiac stem cells; isolated telocytes express IL-2, IL-6, IL-10, IL-13, VEGF, MIP-1 α , and MIP-2 when cultured alone, and, in the presence of cardiac stem cells, MIP-1 α and MIP-2 increased (Albulescu et al., 2015). Like cytokines, they release extracellular vesicles were loaded with microRNAs to cardiac stem cells (Cismasiu and Popescu, 2015). In the heart, CD34-positive/CD45-negative cells co-stain with podoplanin during the chronic phase of MI (Cimini et al., 2017).

CONCLUSION

Podoplanin is not expressed physiologically in the heart except in lymphatic endothelial cells and pericardial area, which means that probably it can be acquired over time by pericytes, MSCs, and telocytes that reside in the heart and that are already positive for PDGFR β , PDGFR α , and CD34. Assimilating this information and interpreting the appearance of podoplanin over time after MI, we can speculate that at 2 days after MI, PDGFR α -positive cells acquire podoplanin, and then at 2 weeks, the PDGFR β - and then the CD34-positive cells become podoplanin positive. It could be that first MSCs, then pericytes and in the end telocytes, express this glycoprotein under inflammatory conditions from

the acute to the chronic phase of MI and thus orchestrate the cell-to-cell communication with monocyte, endothelial cell, and progenitor cell niches. In order to solve this mystery, lineage tracing is needed to understand if these determined categories of cells are the ones that acquire this glycoprotein, and, if they do, what the major signal that contributes to the podoplanin expression is. Furthermore, how this expression changes the biology of the cells after podoplanin acquisition and whether this acquisition results in loss of some specific markers are things that remain to be assessed. For example, podoplanin-positive cells do not express c-Kit, vimentin and α -SMA, CD34-positive telocytes probably lose the c-Kit after the expression of podoplanin (Zhou et al., 2015; Cimini et al., 2017; Hostiuc et al., 2018), or PDGFR β - and PDGFR α -positive cells activate their PDGFRs. The thin line between expression and activation is likely shown by the acquisition of podoplanin; functional studies of podoplanin-positive cells will help to understand the mechanism by which podoplanin-positive cells contribute to tissue homeostasis in health and disease (Frangogiannis, 2019). Podoplanin-positive cells do not have to be villains because each subpopulation actively contributes also to the regeneration of the necrotic area; telocytes are extremely important for the maintenance of cardiac stem cells niches, if they acquire podoplanin, it will be interesting to understand if one of the

consequences is a detrimental communication between telocytes and cardiac stem cells (Bei et al., 2015a, 2016). In conclusion, a lineage tracing (Pinto et al., 2016) and a single cell transcriptome profiling (Skelly et al., 2018) of all the subgroups of podoplanin-positive cells is needed to better understand where podoplanin cells come from. Understanding the origin of podoplanin-positive cells and their evolution can help to modulate the cell-to-cell and paracrine communication during inflammation, based on their role in physiological conditions, and may open a new line of investigation extending beyond known reparative properties.

AUTHOR CONTRIBUTIONS

All authors listed have made a substantial, direct and intellectual contribution to the work, and approved it for publication.

FUNDING

This work was supported in part by the NIH grants HL091983, HL143892, and HL134608 (RK) and American Heart Association Postdoctoral grant 265526-01 (MC).

REFERENCES

- Acton, S. E., Astarita, J. L., Malhotra, D., Lukacs-Kornek, V., Franz, B., Hess, P. R., et al. (2012). Podoplanin-rich stromal networks induce dendritic cell motility via activation of the C-type lectin receptor CLEC-2. *Immunity* 37, 276–289. doi: 10.1016/j.immuni.2012.05.022
- Acton, S. E., Farrugia, A. J., Astarita, J. L., Mourao-Sa, D., Jenkins, R. P., Nye, E., et al. (2014). Dendritic cells control fibroblastic reticular network tension and lymph node expansion. *Nature* 514, 498–502. doi: 10.1038/nature13814
- Albulescu, R., Tanase, C., Codrici, E., Popescu, D. I., Cretoiu, S. M., and Popescu, L. M. (2015). The secretome of myocardial telocytes modulates the activity of cardiac stem cells. *J. Cell Mol. Med.* 19, 1783–1794. doi: 10.1111/jcmm.12624
- Alvino, V. V., Fernandez-Jimenez, R., Rodriguez-Arabaolaza, I., Slater, S., Mangialardi, G., Avolio, E., et al. (2018). Transplantation of Allogeneic Pericytes Improves Myocardial Vascularization and Reduces Interstitial Fibrosis in a Swine Model of Reperused Acute Myocardial Infarction. *J. Am. Heart Assoc.* 7:6727. doi: 10.1161/JAHA.117.006727
- Armulik, A., Abramsson, A., and Betsholtz, C. (2005). Endothelial/pericyte interactions. *Circ. Res.* 97, 512–523. doi: 10.1161/01.RES.0000182903.16652.d7
- Astarita, J. L., Acton, S. E., and Turley, S. J. (2012). Podoplanin: emerging functions in development, the immune system, and cancer. *Front. Immunol.* 3:283. doi: 10.3389/fimmu.2012.00283
- Astarita, J. L., Cremasco, V., Fu, J., Darnell, M. C., Peck, J. R., Nieves-Bonilla, J. M., et al. (2015). The CLEC-2-podoplanin axis controls the contractility of fibroblastic reticular cells and lymph node microarchitecture. *Nat. Immunol.* 16, 75–84. doi: 10.1038/ni.3035
- Bautsch, V. L. (2011). Stem cells and the vasculature. *Nat. Med.* 17, 1437–1443. doi: 10.1038/nm.2539
- Bei, Y., Wang, F., Yang, C., and Xiao, J. (2015a). Telocytes in regenerative medicine. *J. Cell Mol. Med.* 19, 1441–1454. doi: 10.1111/jcmm.12594
- Bei, Y., Zhou, Q., Fu, S., Lv, D., Chen, P., Chen, Y., et al. (2015b). Cardiac telocytes and fibroblasts in primary culture: different morphologies and immunophenotypes. *PLoS One* 10:e0115991. doi: 10.1371/journal.pone.0115991
- Bei, Y., Zhou, Q., Sun, Q., and Xiao, J. (2016). Telocytes in cardiac regeneration and repair. *Semin. Cell Dev. Biol.* 55, 14–21. doi: 10.1016/j.semcdb.2016.01.037
- Beltrami, A. P., and Madeddu, P. (2018). Pericytes and cardiac stem cells: Common features and peculiarities. *Pharmacol. Res.* 127, 101–109. doi: 10.1016/j.phrs.2017.05.023
- Benezech, C., Nayar, S., Finney, B. A., Withers, D. R., Lowe, K., Desanti, G. E., et al. (2014). CLEC-2 is required for development and maintenance of lymph nodes. *Blood* 123, 3200–3207. doi: 10.1182/blood-2013-03-489286
- Birbrair, A., Zhang, T., Files, D. C., Mannava, S., Smith, T., Wang, Z. M., et al. (2014). Type-1 pericytes accumulate after tissue injury and produce collagen in an organ-dependent manner. *Stem Cell Res. Ther.* 5:122. doi: 10.1186/srct512
- Birbrair, A., Zhang, T., Wang, Z. M., Messi, M. L., Mintz, A., and Delbono, O. (2015). Pericytes at the intersection between tissue regeneration and pathology. *Clin. Sci.* 128, 81–93. doi: 10.1042/CS20140278
- Bjarnegard, M., Enge, M., Norlin, J., Gustafsdottir, S., Fredriksson, S., Abramsson, A., et al. (2004). Endothelium-specific ablation of PDGFB leads to pericyte loss and glomerular, cardiac and placental abnormalities. *Development* 131, 1847–1857. doi: 10.1242/dev.01080
- Bobryshev, Y. V., Orekhov, A. N., and Chistiakov, D. A. (2015). Vascular stem/progenitor cells: current status of the problem. *Cell Tissue Res.* 362, 1–7. doi: 10.1007/s00441-015-2231-7
- Boos, A. M., Weigand, A., Brodbeck, R., Beier, J. P., Arkudas, A., and Horch, R. E. (2016). The potential role of telocytes in Tissue Engineering and Regenerative Medicine. *Semin. Cell Dev. Biol.* 55, 70–78. doi: 10.1016/j.semcdb.2016.01.021
- Brakenhielm, E., and Alitalo, K. (2019). Cardiac lymphatics in health and disease. *Nat. Rev. Cardiol.* 16, 56–68. doi: 10.1038/s41569-018-0087-8
- Buhl, E. M., Djudjaj, S., Klinkhammer, B. M., Ermert, K., Puelles, V. G., Lindenmeyer, M. T., et al. (2020). Dysregulated mesenchymal PDGFR-beta drives kidney fibrosis. *EMBO Mol. Med.* 12:e11021. doi: 10.15252/emmm.201911021
- Cai, J., Kehoe, O., Smith, G. M., Hykin, P., and Boulton, M. E. (2008). The angiotensin/Tie-2 system regulates pericyte survival and recruitment in diabetic retinopathy. *Invest. Ophthalmol. Vis. Sci.* 49, 2163–2171. doi: 10.1167/iovs.07-1206
- Cantarero, I., Luesma, M. J., and Junquera, C. (2011). The primary cilium of telocytes in the vasculature: electron microscope imaging. *J. Cell Mol. Med.* 15, 2594–2600. doi: 10.1111/j.1582-4934.2011.01312.x
- Caplan, A. I. (2008). All MSCs are pericytes? *Cell Stem Cell* 3, 229–230. doi: 10.1016/j.stem.2008.08.008

- Caporali, A., Martello, A., Miscianinov, V., Maselli, D., Vono, R., and Spinetti, G. (2017). Contribution of pericyte paracrine regulation of the endothelium to angiogenesis. *Pharmacol. Ther.* 171, 56–64. doi: 10.1016/j.pharmthera.2016.10.001
- Carrasco-Ramirez, P., Greening, D. W., Andres, G., Gopal, S. K., Martin-Villar, E., Renart, J., et al. (2016). Podoplanin is a component of extracellular vesicles that reprograms cell-derived exosomal proteins and modulates lymphatic vessel formation. *Oncotarget* 7, 16070–16089. doi: 10.18632/oncotarget.7445
- Chang, C. H., Chung, C. H., Hsu, C. C., Huang, T. Y., and Huang, T. F. (2010). A novel mechanism of cytokine release in phagocytes induced by aggretin, a snake venom C-type lectin protein, through CLEC-2 ligation. *J. Thromb. Haemost.* 8, 2563–2570. doi: 10.1111/j.1538-7836.2010.04045.x
- Chang, Y. W., Hsieh, P. W., Chang, Y. T., Lu, M. H., Huang, T. F., Chong, K. Y., et al. (2015). Identification of a novel platelet antagonist that binds to CLEC-2 and suppresses podoplanin-induced platelet aggregation and cancer metastasis. *Oncotarget* 6, 42733–42748. doi: 10.18632/oncotarget.5811
- Chang, Y., Li, C., Lu, Z., Li, H., and Guo, Z. (2015). Multiple immunophenotypes of cardiac telocytes. *Exp. Cell Res.* 338, 239–244. doi: 10.1016/j.yexcr.2015.08.012
- Chen, W. C., Baily, J. E., Corselli, M., Diaz, M. E., Sun, B., Xiang, G., et al. (2015). Human myocardial pericytes: multipotent mesodermal precursors exhibiting cardiac specificity. *Stem Cells* 33, 557–573. doi: 10.1002/stem.1868
- Chi, C., Jiang, X. J., Su, L., Shen, Z. J., and Yang, X. J. (2015). In vitro morphology, viability and cytokine secretion of uterine telocyte-activated mouse peritoneal macrophages. *J. Cell Mol. Med.* 19, 2741–2750. doi: 10.1111/jcmm.12711
- Chong, J. J., Reinecke, H., Iwata, M., Torok-Storb, B., Stempien-Otero, A., and Murry, C. E. (2013). Progenitor cells identified by PDGFR- α expression in the developing and diseased human heart. *Stem Cells Dev.* 22, 1932–1943. doi: 10.1089/scd.2012.0542
- Ciavarella, C., Gallitto, E., Ricci, F., Buzzi, M., Stella, A., and Pasquinelli, G. (2017). The crosstalk between vascular MSCs and inflammatory mediators determines the pro-calcific remodelling of human atherosclerotic aneurysm. *Stem Cell Res. Ther.* 8:99. doi: 10.1186/s13287-017-0554-x
- Cimini, M., Cannata, A., Pasquinelli, G., Rota, M., and Goichberg, P. (2017). Phenotypically heterogeneous podoplanin-expressing cell populations are associated with the lymphatic vessel growth and fibrogenic responses in the acutely and chronically infarcted myocardium. *PLoS One* 12:e0173927. doi: 10.1371/journal.pone.0173927
- Cimini, M., Garikipati, V. N. S., de Lucia, C., Cheng, Z., Wang, C., Truongcao, M. M., et al. (2019). Podoplanin neutralization improves cardiac remodeling and function after acute myocardial infarction. *JCI Insight* 5:126967. doi: 10.1172/jci.insight.126967
- Cismasiu, V. B., and Popescu, L. M. (2015). Telocytes transfer extracellular vesicles loaded with microRNAs to stem cells. *J. Cell Mol. Med.* 19, 351–358. doi: 10.1111/jcmm.12529
- Cretoi, D., Hummel, E., Zimmermann, H., Gherghiceanu, M., and Popescu, L. M. (2014). Human cardiac telocytes: 3D imaging by FIB-SEM tomography. *J. Cell Mol. Med.* 18, 2157–2164. doi: 10.1111/jcmm.12468
- Crisan, M., Corselli, M., Chen, W. C., and Peault, B. (2012). Perivascular cells for regenerative medicine. *J. Cell Mol. Med.* 16, 2851–2860. doi: 10.1111/j.1582-4934.2012.01617.x
- Crisan, M., Yap, S., Castella, L., Chen, C. W., Corselli, M., Park, T. S., et al. (2008). A perivascular origin for mesenchymal stem cells in multiple human organs. *Cell Stem Cell* 3, 301–313. doi: 10.1016/j.stem.2008.07.003
- Dias, D. O., Kim, H., Holl, D., Werne Solnestam, B., Lundeberg, J., Carlen, M., et al. (2018). Reducing Pericyte-Derived Scarring Promotes Recovery after Spinal Cord Injury. *Cell* 173:e122. doi: 10.1016/j.cell.2018.02.004
- Diaz-Flores, L., Gutierrez, R., Diaz-Flores, L. Jr., Gomez, M. G., Saez, F. J., and Madrid, J. F. (2016). Behaviour of telocytes during physiopathological activation. *Semin. Cell Dev. Biol.* 55, 50–61. doi: 10.1016/j.semcdb.2016.01.035
- Diaz-Flores, L., Gutierrez, R., Madrid, J. F., Varela, H., Valladares, F., Acosta, E., et al. (2009). Pericytes. Morphofunction, interactions and pathology in a quiescent and activated mesenchymal cell niche. *Histol. Histopathol.* 24, 909–969. doi: 10.14670/HH-24.909
- Edelstein, L., Fuxe, K., Levin, M., Popescu, B. O., and Smythies, J. (2016). Telocytes in their context with other intercellular communication agents. *Semin. Cell Dev. Biol.* 55, 9–13. doi: 10.1016/j.semcdb.2016.03.010
- Farbehi, N., Patrick, R., Dorison, A., Xaymardan, M., Janbandhu, V., Wystub-Lis, K., et al. (2019). Single-cell expression profiling reveals dynamic flux of cardiac stromal, vascular and immune cells in health and injury. *Elife* 8:43882. doi: 10.7554/eLife.43882
- Farini, A., Sitzia, C., Erratico, S., Meregalli, M., and Torrente, Y. (2014). Clinical applications of mesenchymal stem cells in chronic diseases. *Stem Cells Int.* 2014:306573. doi: 10.1155/2014/306573
- Faussone-Pellegrini, M. S., and Gherghiceanu, M. (2016). Telocyte's contacts. *Semin. Cell Dev. Biol.* 55, 3–8. doi: 10.1016/j.semcdb.2016.01.036
- Feng, J., Mantesso, A., and Sharpe, P. T. (2010). Perivascular cells as mesenchymal stem cells. *Expert Opin. Biol. Ther.* 10, 1441–1451. doi: 10.1517/14712598.2010.517191
- Fernandez-Munoz, B., Yurrita, M. M., Martin-Villar, E., Carrasco-Ramirez, P., Megias, D., Renart, J., et al. (2011). The transmembrane domain of podoplanin is required for its association with lipid rafts and the induction of epithelial-mesenchymal transition. *Int. J. Biochem. Cell Biol.* 43, 886–896. doi: 10.1016/j.biocel.2011.02.010
- Fertig, E. T., Gherghiceanu, M., and Popescu, L. M. (2014). Extracellular vesicles release by cardiac telocytes: electron microscopy and electron tomography. *J. Cell Mol. Med.* 18, 1938–1943. doi: 10.1111/jcmm.12436
- Forte, E., Skelly, D. A., Chen, M., Daigle, S., Morelli, K. A., Hon, O., et al. (2020). Dynamic Interstitial Cell Response during Myocardial Infarction Predicts Resilience to Rupture in Genetically Diverse Mice. *Cell Rep.* 30, 3149–3163e3146. doi: 10.1016/j.celrep.2020.02.008
- Frangogiannis, N. G. (2012). Regulation of the inflammatory response in cardiac repair. *Circ. Res.* 110, 159–173. doi: 10.1161/CIRCRESAHA.111.243162
- Frangogiannis, N. G. (2014). The immune system and the remodeling infarcted heart: cell biological insights and therapeutic opportunities. *J. Cardiovasc. Pharmacol.* 63, 185–195. doi: 10.1097/FJC.0000000000000003
- Frangogiannis, N. G. (2015). Emerging roles for macrophages in cardiac injury: cytoprotection, repair, and regeneration. *J. Clin. Invest.* 125, 2927–2930. doi: 10.1172/JCI83191
- Frangogiannis, N. G. (2017). The extracellular matrix in myocardial injury, repair, and remodeling. *J. Clin. Invest.* 127, 1600–1612. doi: 10.1172/JCI87491
- Frangogiannis, N. G. (2019). Cardiac fibrosis: Cell biological mechanisms, molecular pathways and therapeutic opportunities. *Mol. Aspects Med.* 65, 70–99. doi: 10.1016/j.mam.2018.07.001
- Fujita, N., and Takagi, S. (2012). The impact of Aggrus/podoplanin on platelet aggregation and tumour metastasis. *J. Biochem.* 152, 407–413. doi: 10.1093/jb/mvs108
- Gittenberger-de Groot, A. C., Mahtab, E. A., Hahurij, N. D., Wisse, L. J., Deruiter, M. C., Wijffels, M. C., et al. (2007). Nkx2.5-negative myocardium of the posterior heart field and its correlation with podoplanin expression in cells from the developing cardiac pacemaking and conduction system. *Anat. Rec.* 290, 115–122. doi: 10.1002/ar.20406
- Groger, M., Loewe, R., Holthoner, W., Embacher, R., Pillinger, M., Herron, G. S., et al. (2004). IL-3 induces expression of lymphatic markers Prox-1 and podoplanin in human endothelial cells. *J. Immunol.* 173, 7161–7169. doi: 10.4049/jimmunol.173.12.7161
- Hall, C. N., Reynell, C., Gesslein, B., Hamilton, N. B., Mishra, A., Sutherland, B. A., et al. (2014). Capillary pericytes regulate cerebral blood flow in health and disease. *Nature* 508, 55–60. doi: 10.1038/nature13165
- Hatakeyama, K., Kaneko, M. K., Kato, Y., Ishikawa, T., Nishihira, K., Tsujimoto, Y., et al. (2012). Podoplanin expression in advanced atherosclerotic lesions of human aortas. *Thromb. Res.* 129, e70–e76. doi: 10.1016/j.thromres.2012.01.003
- Henri, O., Poueche, C., Houssari, M., Galas, L., Nicol, L., Edwards-Levy, F., et al. (2016). Selective Stimulation of Cardiac Lymphangiogenesis Reduces Myocardial Edema and Fibrosis Leading to Improved Cardiac Function Following Myocardial Infarction. *Circulation* 133, 1484–1497. doi: 10.1161/CIRCULATIONAHA.115.020143
- Hess, P. R., Rawnsley, D. R., Jakus, Z., Yang, Y., Sweet, D. T., Fu, J., et al. (2014). Platelets mediate lymphovenous hemostasis to maintain blood-lymphatic separation throughout life. *J. Clin. Invest.* 124, 273–284. doi: 10.1172/JCI70422
- Hirakawa, S., Hong, Y. K., Harvey, N., Schacht, V., Matsuda, K., Libermann, T., et al. (2003). Identification of vascular lineage-specific genes by transcriptional profiling of isolated blood vascular and lymphatic endothelial cells. *Am. J. Pathol.* 162, 575–586. doi: 10.1016/S0002-9440(10)63851-5
- Hostiuc, S., Marinescu, M., Costescu, M., Aluas, M., and Negoi, I. (2018). Cardiac telocytes. From basic science to cardiac diseases. II. Acute myocardial infarction. *Ann. Anat.* 218, 18–27. doi: 10.1016/j.aanat.2018.02.008

- Ibba-Manneschi, L., Rosa, I., and Manetti, M. (2016). Telocyte implications in human pathology: An overview. *Semin. Cell Dev. Biol.* 55, 62–69. doi: 10.1016/j.semcdb.2016.01.022
- Ikpegbu, E., Basta, L., Clements, D. N., Fleming, R., Vincent, T. L., Buttle, D. J., et al. (2018). FGF-2 promotes osteocyte differentiation through increased E11/podoplanin expression. *J. Cell Physiol.* 233, 5334–5347. doi: 10.1002/jcp.26345
- Kaneko, M. K., Kato, Y., Kitano, T., and Osawa, M. (2006). Conservation of a platelet activating domain of Aggrus/podoplanin as a platelet aggregation-inducing factor. *Gene* 378, 52–57. doi: 10.1016/j.gene.2006.04.023
- Kaneko, M. K., Kunita, A., Abe, S., Tsujimoto, Y., Fukayama, M., Goto, K., et al. (2012). Chimeric anti-podoplanin antibody suppresses tumor metastasis through neutralization and antibody-dependent cellular cytotoxicity. *Cancer Sci.* 103, 1913–1919. doi: 10.1111/j.1349-7066.2012.02385.x
- Kato, Y., and Kaneko, M. K. (2014). A cancer-specific monoclonal antibody recognizes the aberrantly glycosylated podoplanin. *Sci. Rep.* 4:5924. doi: 10.1038/srep05924
- Kato, Y., Kaneko, M. K., Kuno, A., Uchiyama, N., Amano, K., Chiba, Y., et al. (2006). Inhibition of tumor cell-induced platelet aggregation using a novel anti-podoplanin antibody reacting with its platelet-aggregation-stimulating domain. *Biochem. Biophys. Res. Commun.* 349, 1301–1307. doi: 10.1016/j.bbrc.2006.08.171
- Keeley, E. C., Mehrad, B., and Strieter, R. M. (2009). The role of circulating mesenchymal progenitor cells (fibrocytes) in the pathogenesis of fibrotic disorders. *Thromb. Haemost.* 101, 613–618. doi: 10.1160/th08-11-0726
- Kerrigan, A. M., Dennehy, K. M., Mourao-Sa, D., Faro-Trindade, I., Willment, J. A., Taylor, P. R., et al. (2009). CLEC-2 is a phagocytic activation receptor expressed on murine peripheral blood neutrophils. *J. Immunol.* 182, 4150–4157. doi: 10.4049/jimmunol.0802808
- Kholova, I., Dragneva, G., Cermakova, P., Laidinen, S., Kaskenpaa, N., Hazes, T., et al. (2011). Lymphatic vasculature is increased in heart valves, ischaemic and inflamed hearts and in cholesterol-rich and calcified atherosclerotic lesions. *Eur. J. Clin. Invest.* 41, 487–497. doi: 10.1111/j.1365-2362.2010.02431.x
- Klein, D. (2016). Vascular Wall-Resident Multipotent Stem Cells of Mesenchymal Nature within the Process of Vascular Remodeling: Cellular Basis, Clinical Relevance, and Implications for Stem Cell Therapy. *Stem Cells Int.* 2016:1905846. doi: 10.1155/2016/1905846
- Klimczak, A., and Kozłowska, U. (2016). Mesenchymal Stromal Cells and Tissue-Specific Progenitor Cells: Their Role in Tissue Homeostasis. *Stem Cells Int.* 2016:4285215. doi: 10.1155/2016/4285215
- Klopsch, C., Skorska, A., Ludwig, M., Gaebel, R., Lemcke, H., Kleiner, G., et al. (2017). Cardiac Mesenchymal Stem Cells Proliferate Early in the Ischemic Heart. *Eur. Surg. Res.* 58, 341–353. doi: 10.1159/000480730
- Klotz, L., Norman, S., Vieira, J. M., Masters, M., Rohling, M., Dube, K. N., et al. (2015). Cardiac lymphatics are heterogeneous in origin and respond to injury. *Nature* 522, 62–67. doi: 10.1038/nature14483
- Kolar, K., Freitas-Andrade, M., Bechberger, J. F., Krishnan, H., Goldberg, G. S., Naus, C. C., et al. (2015). Podoplanin: a marker for reactive gliosis in gliomas and brain injury. *J. Neuropathol. Exp. Neurol.* 74, 64–74. doi: 10.1097/NEN.0000000000000150
- Kostin, S. (2016). Cardiac telocytes in normal and diseased hearts. *Semin. Cell Dev. Biol.* 55, 22–30. doi: 10.1016/j.semcdb.2016.02.023
- Krishnan, H., Rayes, J., Miyashita, T., Ishii, G., Retzbach, E. P., Sheehan, S. A., et al. (2018). Podoplanin: An emerging cancer biomarker and therapeutic target. *Cancer Sci.* 109, 1292–1299. doi: 10.1111/cas.13580
- Kucybała, I., Janas, P., Ciuk, S., Cholopiak, W., Klimek-Piotrowska, W., and Holda, M. K. (2017). A comprehensive guide to telocytes and their great potential in cardiovascular system. *Bratislav Lek Listy* 118, 302–309. doi: 10.4149/BLL_2017_059
- Kunita, A., Baeriswyl, V., Meda, C., Cabuy, E., Takeshita, K., Giraudo, E., et al. (2018). Inflammatory Cytokines Induce Podoplanin Expression at the Tumor Invasive Front. *Am. J. Pathol.* 188, 1276–1288. doi: 10.1016/j.ajpath.2018.01.016
- Lee, S. J., Park, C., Lee, J. Y., Kim, S., Kwon, P. J., Kim, W., et al. (2015). Generation of pure lymphatic endothelial cells from human pluripotent stem cells and their therapeutic effects on wound repair. *Sci. Rep.* 5:11019. doi: 10.1038/srep11019
- Lepenies, B., Lee, J., and Sonkaria, S. (2013). Targeting C-type lectin receptors with multivalent carbohydrate ligands. *Adv. Drug Deliv. Rev.* 65, 1271–1281. doi: 10.1016/j.addr.2013.05.007
- Li, Y. Y., Zhang, S., Li, Y. G., and Wang, Y. (2016). Isolation, culture, purification and ultrastructural investigation of cardiac telocytes. *Mol. Med. Rep.* 14, 1194–1200. doi: 10.3892/mmr.2016.5386
- Li, Y., Zhang, X., Gao, J., Xiao, H., and Xu, M. (2016). Increased telocytes involved in the proliferation of vascular smooth muscle cells in rat carotid artery balloon injury. *Sci. China Life Sci.* 59, 678–685. doi: 10.1007/s11427-016-5075-9
- Lin, C. S., and Lue, T. F. (2013). Defining vascular stem cells. *Stem Cells Dev.* 22, 1018–1026. doi: 10.1089/scd.2012.0504
- Lombard, S. E., Pollitt, A. Y., Hughes, C. E., Di, Y., McKinnon, T., O'Callaghan, C. A., et al. (2018). Mouse podoplanin supports adhesion and aggregation of platelets under arterial shear: A novel mechanism of haemostasis. *Platelets* 29, 716–722. doi: 10.1080/09537104.2017.1356919
- Loukas, M., Abel, N., Tubbs, R. S., Grabska, J., Birungi, J., and Anderson, R. H. (2011). The cardiac lymphatic system. *Clin. Anat.* 24, 684–691. doi: 10.1002/ca.21104
- Lowe, K. L., Finney, B. A., Deppermann, C., Hagerling, R., Gazit, S. L., Frampton, J., et al. (2015a). Podoplanin and CLEC-2 drive cerebrovascular patterning and integrity during development. *Blood* 125, 3769–3777. doi: 10.1182/blood-2014-09-603803
- Lowe, K. L., Navarro-Nunez, L., Benezech, C., Nayar, S., Kingston, B. L., Nieswandt, B., et al. (2015b). The expression of mouse CLEC-2 on leucocyte subsets varies according to their anatomical location and inflammatory state. *Eur. J. Immunol.* 45, 2484–2493. doi: 10.1002/eji.201445314
- Macor, P., Secco, E., Mezzaroba, N., Zorzet, S., Durigutto, P., Gaiotto, T., et al. (2015). Bispecific antibodies targeting tumor-associated antigens and neutralizing complement regulators increase the efficacy of antibody-based immunotherapy in mice. *Leukemia* 29, 406–414. doi: 10.1038/leu.2014.185
- Mahtab, E. A., Wijffels, M. C., Van Den Akker, N. M., Hahuri, N. D., Lie-Venema, H., Wisse, L. J., et al. (2008). Cardiac malformations and myocardial abnormalities in podoplanin knockout mouse embryos: Correlation with abnormal epicardial development. *Dev. Dyn.* 237, 847–857. doi: 10.1002/dvdy.21463
- Manole, C. G., Cismasiu, V., Gherghiceanu, M., and Popescu, L. M. (2011). Experimental acute myocardial infarction: telocytes involvement in neo-angiogenesis. *J. Cell Mol. Med.* 15, 2284–2296. doi: 10.1111/j.1582-4934.2011.01449.x
- Martin-Villar, E., Borda-d'Agua, B., Carrasco-Ramirez, P., Renart, J., Parsons, M., Quintanilla, M., et al. (2015). Podoplanin mediates ECM degradation by squamous carcinoma cells through control of invadopodia stability. *Oncogene* 34, 4531–4544. doi: 10.1038/onc.2014.388
- Meng, D., Ma, X., Li, H., Wu, X., Cao, Y., Miao, Z., et al. (2020). A Role of the Podoplanin-CLEC-2 Axis in Promoting Inflammatory Response After Ischemic Stroke in Mice. *Neurotox Res.* 39, 477–488. doi: 10.1007/s12640-020-00295-w
- Mirancea, N. (2016). Telocyte - a particular cell phenotype. Infrastructure, relationships and putative functions. *Rom. J. Morphol. Embryol.* 57, 7–21.
- Miyata, K., Takagi, S., Sato, S., Morioka, H., Shiba, K., Minamisawa, T., et al. (2014). Suppression of Aggrus/podoplanin-induced platelet aggregation and pulmonary metastasis by a single-chain antibody variable region fragment. *Cancer Med.* 3, 1595–1604. doi: 10.1002/cam4.320
- Mourao-Sa, D., Robinson, M. J., Zelenay, S., Sancho, D., Chakravarty, P., Larsen, R., et al. (2011). CLEC-2 signaling via Syk in myeloid cells can regulate inflammatory responses. *Eur. J. Immunol.* 41, 3040–3053. doi: 10.1002/eji.201141641
- Nagai, M., Morita-Matsumoto, K., Kato, M., Kaneko, M. K., Kato, Y., and Yamaguchi, Y. (2014). A platform of C-type lectin-like receptor CLEC-2 for binding O-glycosylated podoplanin and nonglycosylated rhodocytin. *Structure* 22, 1711–1721. doi: 10.1016/j.str.2014.09.009
- Nakazawa, Y., Takagi, S., Sato, S., Oh-hara, T., Koike, S., Takami, M., et al. (2011). Prevention of hematogenous metastasis by neutralizing mice and its chimeric anti-Aggrus/podoplanin antibodies. *Cancer Sci.* 102, 2051–2057. doi: 10.1111/j.1349-7006.2011.02058.x
- Napankangas, J., Ohtonen, P., Ohukainen, P., Weisell, J., Vaisanen, T., Peltonen, T., et al. (2019). Increased mesenchymal podoplanin expression is associated with calcification in aortic valves. *Cardiovasc. Pathol.* 39, 30–37. doi: 10.1016/j.carpath.2018.11.006
- Nicenboim, J., Malkinson, G., Lupo, T., Asaf, L., Sela, Y., Maysel, O., et al. (2015). Lymphatic vessels arise from specialized angioblasts within a venous niche. *Nature* 522, 56–61. doi: 10.1038/nature14425

- Noack, M., Ndongo-Thiam, N., and Miossec, P. (2016a). Interaction among activated lymphocytes and mesenchymal cells through podoplanin is critical for a high IL-17 secretion. *Arthritis Res. Ther.* 18:148. doi: 10.1186/s13075-016-1046-6
- Noack, M., Ndongo-Thiam, N., and Miossec, P. (2016b). Role of podoplanin in the high interleukin-17A secretion resulting from interactions between activated lymphocytes and psoriatic skin-derived mesenchymal cells. *Clin. Exp. Immunol.* 186, 64–74. doi: 10.1111/cei.12830
- Norman, S., and Riley, P. R. (2016). Anatomy and development of the cardiac lymphatic vasculature: Its role in injury and disease. *Clin. Anat.* 29, 305–315. doi: 10.1002/ca.22638
- Noseda, M., Harada, M., McSweeney, S., Leja, T., Belian, E., Stuckey, D. J., et al. (2015). PDGFR α demarcates the cardiogenic clonogenic Sc α 1+ stem/progenitor cell in adult murine myocardium. *Nat. Commun.* 6:6930. doi: 10.1038/ncomms7930
- Ogasawara, S., Kaneko, M. K., Price, J. E., and Kato, Y. (2008). Characterization of anti-podoplanin monoclonal antibodies: critical epitopes for neutralizing the interaction between podoplanin and CLEC-2. *Hybridoma* 27, 259–267. doi: 10.1089/hyb.2008.0017
- Palmieri, C., Avallone, G., Cimini, M., Roccabianca, P., Stefanello, D., and Della Salda, L. (2013). Use of electron microscopy to classify canine perivascular wall tumors. *Vet. Pathol.* 50, 226–233. doi: 10.1177/0300985812456213
- Pan, Y., and Xia, L. (2015). Emerging roles of podoplanin in vascular development and homeostasis. *Front. Med.* 9:421–430. doi: 10.1007/s11684-015-0424-9
- Payne, H., Ponomaryov, T., Watson, S. P., and Brill, A. (2017). Mice with a deficiency in CLEC-2 are protected against deep vein thrombosis. *Blood* 129, 2013–2020. doi: 10.1182/blood-2016-09-742999
- Petrova, T. V., Mäkinen, T., Makela, T. P., Saarela, J., Virtanen, I., Ferrell, R. E., et al. (2002). Lymphatic endothelial reprogramming of vascular endothelial cells by the Prox-1 homeobox transcription factor. *EMBO J.* 21, 4593–4599. doi: 10.1093/emboj/cdf470
- Piera-Velazquez, S., Mendoza, F. A., and Jimenez, S. A. (2016). Endothelial to Mesenchymal Transition (EndoMT) in the Pathogenesis of Human Fibrotic Diseases. *J. Clin. Med.* 5:5040045. doi: 10.3390/jcm5040045
- Pinto, A. R., Ilinykh, A., Ivey, M. J., Kuwabara, J. T., D'Antoni, M. L., Debuque, R., et al. (2016). Revisiting Cardiac Cellular Composition. *Circ. Res.* 118, 400–409. doi: 10.1161/CIRCRESAHA.115.307778
- Popescu, L. M., and Faussone-Pellegrini, M. S. (2010). TELOCYTES - a case of serendipity: the winding way from Interstitial Cells of Cajal (ICC), via Interstitial Cajal-Like Cells (ICLC) to TELOCYTES. *J. Cell Mol. Med.* 14, 729–740. doi: 10.1111/j.1582-4934.2010.01059.x
- Popescu, L. M., Curici, A., Wang, E., Zhang, H., Hu, S., and Gherghiceanu, M. (2015). Telocytes and putative stem cells in ageing human heart. *J. Cell Mol. Med.* 19, 31–45. doi: 10.1111/jcmm.12509
- Popescu, L. M., Fertig, E. T., and Gherghiceanu, M. (2016). Reaching out: junctions between cardiac telocytes and cardiac stem cells in culture. *J. Cell Mol. Med.* 20, 370–380. doi: 10.1111/jcmm.12719
- Prabhu, S. D., and Frangogiannis, N. G. (2016). The Biological Basis for Cardiac Repair After Myocardial Infarction: From Inflammation to Fibrosis. *Circ. Res.* 119, 91–112. doi: 10.1161/CIRCRESAHA.116.303577
- Proebstl, D., Voisin, M. B., Woodfin, A., Whiteford, J., D'Acquisto, F., Jones, G. E., et al. (2012). Pericytes support neutrophil subendothelial cell crawling and breaching of venular walls in vivo. *J. Exp. Med.* 209, 1219–1234. doi: 10.1084/jem.20111622
- Pula, B., Witkiewicz, W., Dziegiel, P., and Podhorska-Okolow, M. (2013). Significance of podoplanin expression in cancer-associated fibroblasts: a comprehensive review. *Int. J. Oncol.* 42, 1849–1857. doi: 10.3892/ijo.2013.1887
- Rakocevic, J., Kojic, S., Orlic, D., Stankovic, G., Ostojic, M., Petrovic, O., et al. (2016). Co-expression of vascular and lymphatic endothelial cell markers on early endothelial cells present in aspirated coronary thrombi from patients with ST-elevation myocardial infarction. *Exp. Mol. Pathol.* 100, 31–38. doi: 10.1016/j.yemp.2015.11.028
- Ratajska, A., Gula, G., Flaht-Zabost, A., Czarnowska, E., Ciszek, B., Jankowska-Steifer, E., et al. (2014). Comparative and developmental anatomy of cardiac lymphatics. *Sci. World J.* 2014:183170. doi: 10.1155/2014/183170
- Rayes, J., Lax, S., Wichaiyo, S., Watson, S. K., Di, Y., Lombard, S., et al. (2017). The podoplanin-CLEC-2 axis inhibits inflammation in sepsis. *Nat. Commun.* 8:2239. doi: 10.1038/s41467-017-02402-6
- Richter, M., and Kostin, S. (2015). The failing human heart is characterized by decreased numbers of telocytes as result of apoptosis and altered extracellular matrix composition. *J. Cell Mol. Med.* 19, 2597–2606. doi: 10.1111/jcmm.12664
- Roszer, T. (2015). Understanding the Mysterious M2 Macrophage through Activation Markers and Effector Mechanisms. *Mediators Inflamm.* 2015:816460. doi: 10.1155/2015/816460
- Rusu, M. C., and Hostiu, S. (2019). Critical review: Cardiac telocytes vs cardiac lymphatic endothelial cells. *Ann. Anat.* 222, 40–54. doi: 10.1016/j.aanat.2018.10.011
- Rusu, M. C., Loreto, C., and Manoiu, V. S. (2014). Network of telocytes in the temporomandibular joint disc of rats. *Acta Histochem.* 116, 663–668. doi: 10.1016/j.acthis.2013.12.005
- Sager, H. B., Kessler, T., and Schunkert, H. (2017). Monocytes and macrophages in cardiac injury and repair. *J. Thorac. Dis.* 9(Suppl. 1), S30–S35. doi: 10.21037/jtd.2016.11.17
- Salven, P., Mustjoki, S., Alitalo, R., Alitalo, K., and Rafii, S. (2003). VEGFR-3 and CD133 identify a population of CD34+ lymphatic/vascular endothelial precursor cells. *Blood* 101, 168–172. doi: 10.1182/blood-2002-03-0755
- Saxena, A., Russo, I., and Frangogiannis, N. G. (2016). Inflammation as a therapeutic target in myocardial infarction: learning from past failures to meet future challenges. *Transl. Res.* 167, 152–166. doi: 10.1016/j.trsl.2015.07.002
- Schacht, V., Ramirez, M. I., Hong, Y. K., Hirakawa, S., Feng, D., Harvey, N., et al. (2003). T α 1/podoplanin deficiency disrupts normal lymphatic vasculature formation and causes lymphedema. *EMBO J.* 22, 3546–3556. doi: 10.1093/emboj/cdg342
- Shammaa, R., El-Kadiry, A. E., Abusarah, J., and Rafei, M. (2020). Mesenchymal Stem Cells Beyond Regenerative Medicine. *Front. Cell Dev. Biol.* 8:72. doi: 10.3389/fcell.2020.00072
- Sica, A., Erreni, M., Allavena, P., and Porta, C. (2015). Macrophage polarization in pathology. *Cell Mol. Life Sci.* 72, 4111–4126. doi: 10.1007/s00018-015-1995-y
- Skelly, D. A., Squiers, G. T., McLellan, M. A., Bolisetty, M. T., Robson, P., Rosenthal, N. A., et al. (2018). Single-Cell Transcriptomic Profiling Reveals Cellular Diversity and Intercommunication in the Mouse Heart. *Cell Rep.* 22, 600–610. doi: 10.1016/j.celrep.2017.12.072
- Song, Y., Shen, J., Lin, Y., Shen, J., Wu, X., Yan, Y., et al. (2014). Up-regulation of podoplanin involves in neuronal apoptosis in LPS-induced neuroinflammation. *Cell Mol. Neurobiol.* 34, 839–849. doi: 10.1007/s10571-014-0060-y
- Stadiotti, I., Piacentini, L., Vavassori, C., Chiesa, M., Scopece, A., Guarino, A., et al. (2020). Human Cardiac Mesenchymal Stromal Cells From Right and Left Ventricles Display Differences in Number, Function, and Transcriptomic Profile. *Front. Physiol.* 11:604. doi: 10.3389/fphys.2020.00604
- Suciu, L., Popescu, L. M., Gherghiceanu, M., Regalia, T., Nicolescu, M. I., Hinescu, M. E., et al. (2010). Telocytes in human term placenta: morphology and phenotype. *Cells Tissues Organs* 192, 325–339. doi: 10.1159/000319467
- Sundberg, C., Kowanetz, M., Brown, L. F., Detmar, M., and Dvorak, H. F. (2002). Stable expression of angiopoietin-1 and other markers by cultured pericytes: phenotypic similarities to a subpopulation of cells in maturing vessels during later stages of angiogenesis in vivo. *Lab. Invest.* 82, 387–401. doi: 10.1038/labinvest.3780433
- Suzuki-Inoue, K., Osada, M., and Ozaki, Y. (2017). Physiologic and pathophysiologic roles of interaction between C-type lectin-like receptor 2 and podoplanin: partners from in utero to adulthood. *J. Thromb. Haemost.* 15, 219–229. doi: 10.1111/jth.13590
- Takagi, S., Oh-hara, T., Sato, S., Gong, B., Takami, M., and Fujita, N. (2014). Expression of Aggrus/podoplanin in bladder cancer and its role in pulmonary metastasis. *Int. J. Cancer* 134, 2605–2614. doi: 10.1002/ijc.28602
- Takagi, S., Sato, S., Oh-hara, T., Takami, M., Koike, S., Mishima, Y., et al. (2013). Platelets promote tumor growth and metastasis via direct interaction between Aggrus/podoplanin and CLEC-2. *PLoS One* 8:e73609. doi: 10.1371/journal.pone.0073609
- Taran, D., Tarlui, V. N., Ceausu, R. A., Cimpean, A. M., Raica, M., and Sarb, S. (2019). Podoplanin and PROX1 Expression in Hypercaloric Diet-induced Pancreatic Injuries. *In Vivo* 33, 1157–1163. doi: 10.21873/invivo.11586
- Thomas, H., Cowin, A. J., and Mills, S. J. (2017). The Importance of Pericytes in Healing: Wounds and other Pathologies. *Int. J. Mol. Sci.* 18:18061129. doi: 10.3390/ijms18061129

- Tugal, D., Liao, X., and Jain, M. K. (2013). Transcriptional control of macrophage polarization. *Arterioscler. Thromb. Vasc. Biol.* 33, 1135–1144. doi: 10.1161/ATVBAHA.113.301453
- Ugorski, M., Dziegiel, P., and Suchanski, J. (2016). Podoplanin - a small glycoprotein with many faces. *Am. J. Cancer Res.* 6, 370–386.
- Usunier, B., Benderitter, M., Tamarat, R., and Chapel, A. (2014). Management of fibrosis: the mesenchymal stromal cells breakthrough. *Stem Cells Int.* 2014:340257. doi: 10.1155/2014/340257
- Valente, S., Rossi, R., Resta, L., and Pasquinelli, G. (2015). Exploring the human mesenchymal stem cell tubule communication network through electron microscopy. *Ultrastruct. Pathol.* 39, 88–94. doi: 10.3109/01913123.2014.960545
- Varga, I., Danisovic, L., Kyselovic, J., Gazova, A., Musil, P., Miko, M., et al. (2016). The functional morphology and role of cardiac telocytes in myocardium regeneration. *Can. J. Physiol. Pharmacol.* 94, 1117–1121. doi: 10.1139/cjpp-2016-0052
- Varga, I., Polak, S., Kyselovic, J., Kachlik, D., Danisovic, L., and Klein, M. (2019). Recently Discovered Interstitial Cell Population of Telocytes: Distinguishing Facts from Fiction Regarding Their Role in the Pathogenesis of Diverse Diseases Called “Telocytopathies”. *Medicina* 55:55020056. doi: 10.3390/medicina55020056
- Vieira, J. M., Norman, S., Villa Del, Campo, C., Cahill, T. J., Barnette, D. N., et al. (2018). The cardiac lymphatic system stimulates resolution of inflammation following myocardial infarction. *J. Clin. Invest.* 128, 3402–3412. doi: 10.1172/JCI97192
- Viswanathan, S., Shi, Y., Galipeau, J., Krampera, M., Leblanc, K., Martin, I., et al. (2019). Mesenchymal stem versus stromal cells: International Society for Cell & Gene Therapy (ISCT(R)) Mesenchymal Stromal Cell committee position statement on nomenclature. *Cytotherapy* 21, 1019–1024. doi: 10.1016/j.jcyt.2019.08.002
- Wakisaka, M., Kamouchi, M., and Kitazono, T. (2019). Lessons from the Trials for the Desirable Effects of Sodium Glucose Co-Transporter 2 Inhibitors on Diabetic Cardiovascular Events and Renal Dysfunction. *Int. J. Mol. Sci.* 20:20225668. doi: 10.3390/ijms20225668
- Ward, L. S. C., Sheriff, L., Marshall, J. L., Manning, J. E., Brill, A., Nash, G. B., et al. (2019). Podoplanin regulates the migration of mesenchymal stromal cells and their interaction with platelets. *J. Cell Sci.* 132, 222067. doi: 10.1242/jcs.222067
- Wong, S. P., Rowley, J. E., Redpath, A. N., Tilman, J. D., Fellous, T. G., and Johnson, J. R. (2015). Pericytes, mesenchymal stem cells and their contributions to tissue repair. *Pharmacol. Ther.* 151, 107–120. doi: 10.1016/j.pharmthera.2015.03.006
- Xu, C., Gao, X., Wei, Q., Nakahara, F., Zimmerman, S. E., Mar, J., et al. (2018). Stem cell factor is selectively secreted by arterial endothelial cells in bone marrow. *Nat. Commun.* 9:2449. doi: 10.1038/s41467-018-04726-3
- Yan, H., Ohno, N., and Tsuji, N. M. (2013). The role of C-type lectin receptors in immune homeostasis. *Int. Immunopharmacol.* 16, 353–357. doi: 10.1016/j.intimp.2013.04.013
- Yang, Y., and Oliver, G. (2014). Transcriptional control of lymphatic endothelial cell type specification. *Adv. Anat. Embryol. Cell Biol.* 214, 5–22. doi: 10.1007/978-3-7091-1646-3_2
- Yang, Y., Garcia-Verdugo, J. M., Soriano-Navarro, M., Srinivasan, R. S., Scallan, J. P., Singh, M. K., et al. (2012). Lymphatic endothelial progenitors bud from the cardinal vein and intersomitic vessels in mammalian embryos. *Blood* 120, 2340–2348. doi: 10.1182/blood-2012-05-428607
- Yee, D., Coles, M. C., and Lagos, D. (2017). microRNAs in the Lymphatic Endothelium: Master Regulators of Lineage Plasticity and Inflammation. *Front. Immunol.* 8:104. doi: 10.3389/fimmu.2017.00104
- Yoon, Y. S., Murayama, T., Gravereaux, E., Tkebuchava, T., Silver, M., Curry, C., et al. (2003). VEGF-C gene therapy augments postnatal lymphangiogenesis and ameliorates secondary lymphedema. *J. Clin. Invest.* 111, 717–725. doi: 10.1172/JCI15830
- Zazzeroni, L., Faggioli, G., and Pasquinelli, G. (2018). Mechanisms of Arterial Calcification: The Role of Matrix Vesicles. *Eur. J. Vasc. Endovasc. Surg.* 55, 425–432. doi: 10.1016/j.ejvs.2017.12.009
- Zhang, H. Q., Lu, S. S., Xu, T., Feng, Y. L., Li, H., and Ge, J. B. (2015). Morphological evidence of telocytes in mice aorta. *Chin. Med. J.* 128, 348–352. doi: 10.4103/0366-6999.150102
- Zhou, Q., Wei, L., Zhong, C., Fu, S., Bei, Y., Huica, R. I., et al. (2015). Cardiac telocytes are double positive for CD34/PDGFR-alpha. *J. Cell Mol. Med.* 19, 2036–2042. doi: 10.1111/jcmm.12615

Conflict of Interest: The authors declare that the research was conducted in the absence of any commercial or financial relationships that could be construed as a potential conflict of interest.

Copyright © 2021 Cimini and Kishore. This is an open-access article distributed under the terms of the Creative Commons Attribution License (CC BY). The use, distribution or reproduction in other forums is permitted, provided the original author(s) and the copyright owner(s) are credited and that the original publication in this journal is cited, in accordance with accepted academic practice. No use, distribution or reproduction is permitted which does not comply with these terms.



Evolving Roles of Muscle-Resident Fibro-Adipogenic Progenitors in Health, Regeneration, Neuromuscular Disorders, and Aging

Marine Theret^{1*}, Fabio M. V. Rossi¹ and Osvaldo Contreras^{2,3,4*}

¹ Biomedical Research Centre, Department of Medical Genetics, School of Biomedical Engineering, The University of British Columbia, Vancouver, BC, Canada, ² Departamento de Biología Celular y Molecular, Center for Aging and Regeneration (CARE-ChileUC), Facultad de Ciencias Biológicas, Pontificia Universidad Católica de Chile, Santiago, Chile, ³ St. Vincent's Clinical School, Faculty of Medicine, UNSW Sydney, Kensington, NSW, Australia, ⁴ Developmental and Stem Cell Biology Division, Victor Chang Cardiac Research Institute, Darlinghurst, NSW, Australia

Normal skeletal muscle functions are affected following trauma, chronic diseases, inherited neuromuscular disorders, aging, and cachexia, hampering the daily activities and quality of life of the affected patients. The maladaptive accumulation of fibrous intramuscular connective tissue and fat are hallmarks of multiple pathologies where chronic damage and inflammation are not resolved, leading to progressive muscle replacement and tissue degeneration. Muscle-resident fibro-adipogenic progenitors are adaptable stromal cells with multilineage potential. They are required for muscle homeostasis, neuromuscular integrity, and tissue regeneration. Fibro-adipogenic progenitors actively regulate and shape the extracellular matrix and exert immunomodulatory functions via cross-talk with multiple other residents and non-resident muscle cells. Remarkably, cumulative evidence shows that a significant proportion of activated fibroblasts, adipocytes, and bone-cartilage cells, found after muscle trauma and disease, descend from these enigmatic interstitial progenitors. Despite the profound impact of muscle disease on human health, the fibrous, fatty, and ectopic bone tissues' origins are poorly understood. Here, we review the current knowledge of fibro-adipogenic progenitor function on muscle homeostatic integrity, regeneration, repair, and aging. We also discuss how scar-forming pathologies and disorders lead to dysregulations in their behavior and plasticity and how these stromal cells can control the onset and severity of muscle loss in disease. We finally explore the rationale of improving muscle regeneration by understanding and modulating fibro-adipogenic progenitors' fate and behavior.

Keywords: skeletal muscle fibrosis, muscle FAPs, muscle regeneration, aging, muscle stem cells (MuSCs), macrophages, extracellular matrix (ECM), duchenne muscular dystrophy (DMD)

OPEN ACCESS

Edited by:

Elvira Forte,
The Jackson Laboratory,
United States

Reviewed by:

Luca Madaro,
Sapienza University of Rome, Italy
Lorenzo Giordani,
Sorbonne Université, France

*Correspondence:

Marine Theret
mtheret@brc.ubc.ca
Osvaldo Contreras
o.contreras@victorchang.edu.au

Specialty section:

This article was submitted to
Integrative Physiology,
a section of the journal
Frontiers in Physiology

Received: 27 February 2021

Accepted: 19 March 2021

Published: 20 April 2021

Citation:

Theret M, Rossi FMV and
Contreras O (2021) Evolving Roles of
Muscle-Resident Fibro-Adipogenic
Progenitors in Health, Regeneration,
Neuromuscular Disorders, and Aging.
Front. Physiol. 12:673404.
doi: 10.3389/fphys.2021.673404

Abbreviations: AMPK, AMP-activated kinase; BMP2, bone morphogenetic protein 2; BMP9, bone morphogenetic protein 9; CFU, colony-forming unit; CT, connective tissue; DAMP, damage-associated molecular pattern; DMD, duchenne muscular dystrophy; ECM, extracellular matrix; FSHD, facioscapulohumeral dystrophy; FAPs, fibro-adipogenic progenitors; FOP, fibrodysplasia ossificans progressive; HO, heterotopic ossification; HIF-1 α , hypoxia-inducible factor 1 α ; IL, interleukin; IMAT, intermuscular adipose tissue; LGMD, limb-girdle muscular dystrophy; Ly6C, lymphocyte antigen 6 complex; MPs, macrophages; MSCs, mesenchymal stem cells; MCT, muscle connective tissue; MuSCs, muscle stem cells; PDGFR α , platelet-derived growth factor receptor-alpha; PDGFR β , platelet-derived growth factor receptor-beta; PDGF, platelet-derived growth factor; PD-1, programmed death-1; PD-L1, programmed death-Ligand 1; SMA, spinal muscular atrophy; SCA-1, stem cell antigen-1; TGF- β , transforming growth factor type beta; TNF- α , tumor necrosis factor-alpha.

INTRODUCTION

Although reduced muscle function secondary to trauma, disease, neuromuscular disorders, and age-related sarcopenia affects millions of people each year, little is known about the origins of ectopic muscle scarring and the molecular pathways that underlie its development. Adult skeletal muscle is known not only for its ability to expand following hypertrophic stimuli or shrink when disused but also to restore its mass and function after injury. In this regenerative process, a key event is the presence of muscle-resident stem cells, a tightly coordinated immune response, and the transient deposition of a supportive matrix that eventually is reabsorbed when regeneration is successful. Thus, several precisely timed events need to take place for successful muscle regeneration requiring numerous cell types to engage in a complex network of cellular interactions through autocrine, paracrine, and juxtacrine signaling (Lemos et al., 2015; Malecova et al., 2018; Scott et al., 2019; Chazaud, 2020; Oprescu et al., 2020).

In the past decade, we have learned that efficient skeletal muscle regeneration does not rest only on muscle stem cells (MuSCs). Indeed, many different cell types -resident and non-resident- contribute to the cellular composition of muscles, including pericytes, endothelial cells, smooth muscle cells, fibro-adipogenic progenitors (FAPs), various immune cells, tenocytes, and nerve-associated cells such as glia and Schwann cells, all of which participate in this complex biological process (Blau et al., 2015; Mashinchian et al., 2018; Woszczyna and Rando, 2018). These diverse and heterogeneous cells act together to maintain muscle functions, tissue integrity, and regenerative properties.

Even though muscles are highly regenerative following acute damage, chronic pathologies often cause an increased and dysregulated accumulation of connective tissue (CT) and fat – also known as fibro-fatty infiltration- especially in muscle degenerative conditions associated with persistent or chronic inflammation (Grounds, 2008; Mann et al., 2011). Thus, fibro-fatty infiltration is commonly observed in several myopathies and neuromuscular disorders and correlates with the pathology's progression and extension. Muscle fibro-fatty scarring is also present after repeated cycles of damage, denervation, amyotrophic lateral sclerosis (ALS), rotator cuff tears, and during aging-related sarcopenia (discussed below in detail). Albeit to a different extent in every situation.

Continued deposition and increased stiffening of the matrix usually support a biochemical, biophysical, and biomechanical pro-fibrotic feedback loop sustaining stromal cell persistence in the tissue beyond their normal kinetics (Hinz and Lagares, 2020). This self-perpetuating mechanism is a well-known cellular and pathological hallmark of detrimental tissue degeneration and fibrosis. Therefore, changes in matrix quantity and quality, increased matrix complexity and tissue stiffness may help tip the affected tissue into a self-perpetuating pathological state. In this abnormal setting, the bioavailability of damage-induced cues is magnified and may lead to scarring in response to insults that would generally be below the threshold required (Klingberg et al., 2014; Karsdal et al., 2017; Murray et al., 2017; Pakshir et al., 2020). Although significant progress in understanding these phenomena has been made at the tissue level, a big question in the muscle field

has been identifying and characterizing the cell(s) that produce ectopic fibrous, fat, and bone in degenerated muscles.

Muscle-resident, PDGFR α -expressing FAPs have emerged as crucial players in tissue homeostasis, regeneration, and disease. These stromal cells expand clonally and have the ability to differentiate into stromal cell lineages, including fibroblast, adipocyte, chondrocyte, and osteocyte. In their multipotent state, FAPs modulate many signaling pathways. They produce crucial growth factors like IGF-1, TGF- β , Follistatin, CTGF/CCN2, WNTs, PDGFs, and multiple ILs (for a recent review, see Biferali et al., 2019). They also produce a plethora of matrix or matrisome proteins like collagens, proteoglycans (e.g., Decorin), integrins, laminins, and fibronectin, which impact the cellular physiology of many resident cells and non-resident cells in homeostasis, upon injury and disease.

Here, we outline the current knowledge of FAPs contributions to muscle homeostasis, neuromuscular integrity, regeneration, repair, and aging. We also discuss how their fate is regulated in a context-dependent manner and how the tissue microenvironment largely dictates FAP plasticity and behavior. Finally, we highlight therapeutic opportunities stemming from targeting these precursor cells and their activities to stimulate muscle regeneration in neuromuscular disorders, pathology, and aging.

MUSCLE GROWTH, LONG-TERM MAINTENANCE, AND REGENERATION REQUIRE UNIPOTENT MUSCLE STEM CELLS

Skeletal muscle has a particular capacity to regenerate fully (*restitutio ad integrum*) even after several rounds of injury (Günther et al., 2013; Tedesco et al., 2018). This remarkable ability is mainly attributable to a reservoir of quiescent adult MuSCs, called satellite cells (reviewed in Wang and Rudnicki, 2012; Almada and Wagers, 2016). In brief, these non-interstitial adult stem cells localize in between the muscle sarcolemma and the myofibers' basal lamina (Katz, 1961; Mauro, 1961; Church et al., 1966). Aiming to efficiently rebuild muscle following injury, MuSCs exit quiescence, activate, proliferate, differentiate, and fuse either with one another to form multinucleated muscle cells -myofibers- or with pre-existent damaged myofibers (Kuang et al., 2006; Robertson et al., 1990; Rudnicki et al., 2008; Sacco et al., 2008; Von Maltzahn et al., 2013). As functional adult unipotent muscle-resident stem cells, MuSCs can also self-renew to maintain the stem cell pool (reviewed in Relaix and Zammit, 2012). Genetic lineage-ablation of Pax7+ MuSCs demonstrated that muscle regeneration requires these adult stem cells (Lepper et al., 2011; Murphy et al., 2011; Sambasivan et al., 2011; Fry et al., 2015). Indeed, the absence of MuSCs leads to severe fibro-fatty deposition after myotrauma, resulting from the inability to rebuild the lost tissue (Lepper et al., 2011; Murphy et al., 2011; Sambasivan et al., 2011). Prepubertal skeletal muscle growth also requires MuSCs (Bachman et al., 2018), which once again demonstrates the essential functions of muscle stem cells in adult

muscle regeneration and growth. Remarkably, the expression of Pax7 itself is also crucial for muscle regeneration since its gene deletion impairs MuSC self-renewal and causes loss of regeneration following single or several rounds of injury (Oustanina et al., 2004; Günther et al., 2013; Von Maltzahn et al., 2013).

A growing body of work demonstrated that MuSCs are chronically activated during muscle pathology, which leads to their exhaustion and impaired skeletal muscle regeneration (Heslop et al., 2000; Sacco et al., 2010; Dadgar et al., 2014). This phenomenon also occurs in several neuromuscular disorders and contributes to disease progression and poor regenerative outcomes (Castets et al., 2011; Kudryashova et al., 2012; Ross et al., 2012). Hence, diseases marked by chronic muscle degeneration cause dysregulated MuSC fate and behavior. How pathology-driven satellite cell depletion could affect the pool of stromal cells (e.g., FAPs) is unknown, and therefore, further research is needed to address this question.

FIBRO-ADIPOGENIC PROGENITORS ARE ESSENTIAL FOR EFFICIENT AND SUFFICIENT SKELETAL MUSCLE REGENERATION AND REQUIRED FOR HOMEOSTATIC NEUROMUSCULAR INTEGRITY

Initial observations suggested that muscle-resident TCF7L2 (also known as T-cell factor 4, TCF4) expressing stromal cells regulate normal muscle development (Kardon et al., 2003; Mathew et al., 2011). Later, Vallecillo-García et al. (2017) showed that embryonic OSR1+ mesenchymal progenitor cells significantly contribute to adult fibro-adipogenic progenitors. The authors also reported that these muscle connective tissue cells regulate embryonic myogenesis. Remarkably, both cell lineages, TCF7L2 and OSR1 expressing cells, overlap during embryonic limb development (Vallecillo-García et al., 2017). In the adult, stromal TCF7L2+ cells and OSR1+ cells expand and accumulate after injury and disease (Contreras et al., 2016, 2020; Stumm et al., 2018). These include acute glycerol injury (Contreras et al., 2020), denervated muscles (Contreras et al., 2016), dystrophic muscles of the *mdx* mice (Acuña et al., 2014; Contreras et al., 2020), chronic chemical damage with BaCl₂ (Contreras et al., 2016), human skeletal muscle injury (Mackey et al., 2017), and in murine muscles of the symptomatic ALS transgenic mice hSOD1G93A (Gonzalez et al., 2017).

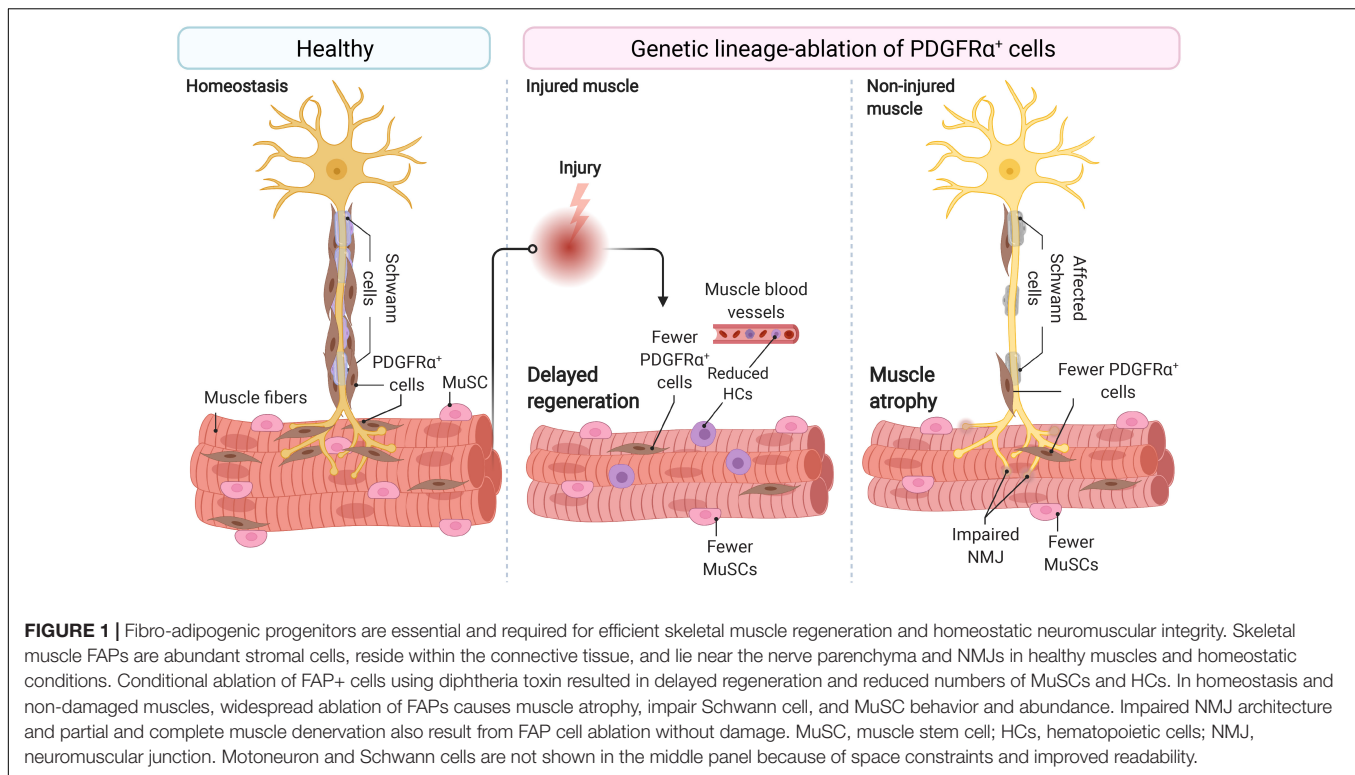
Aiming to understand the contribution of TCF7L2 expressing cells to muscle regeneration, Murphy et al. (2011) showed that the genetic lineage-ablation of about 40% of TCF7L2+ cells caused premature satellite cell differentiation and exhaustion of their regenerating pool, leading to a reduced size of the regenerated myofibers. The authors suggested that efficient muscle regeneration requires the interaction between TCF7L2+ stromal cells and satellite cells. In humans, interstitial TCF7L2 expressing cells also play a supportive role in myogenesis and skeletal muscle regeneration (Mackey et al., 2017). We recently

showed that the isolation through a pre-plating strategy of highly adherent muscle connective tissue fibroblasts allows the culture of a high proportion (~90%) of PDGFR α expressing FAPs (Contreras et al., 2019b). These isolated stromal cells also express the Wnt-responsive TCF7L2 transcription factor (Contreras et al., 2020). These findings strongly suggested a role for stromal cells in regulating skeletal muscle health and regeneration.

Roberts et al. (2013) reported that muscle-resident stromal cells expressing Fibroblast Activation Protein alpha (also known as FAP α) also express CD140a (PDGFR α), SCA-1, and CD90. The later three proteins are known markers of murine FAPs (Petrilli et al., 2020). The authors also showed that depletion of Fibroblast Activation Protein alpha expressing cells causes rapid weight loss, reduced skeletal muscle mass, and muscle atrophy (Roberts et al., 2013) (**Figure 1**). These changes are associated with increased expression of known atrophy-related genes, including *Atrogin-1* and *MuRF1* and decreased expression of *Follistatin* and the Laminin gene *Lama2*, explaining the muscle atrophy. In response to depletion of stromal cells that express Fibroblast Activation Protein alpha, this cachexic phenotype was also accompanied by altered hematopoiesis. Remarkably, cachectic mice bearing the C26 colon carcinoma showed a reduced number of Fibroblast Activation Protein alpha+ cells in hindlimb muscles, which again suggests the supportive role of these stromal cells in maintaining muscle mass and integrity (Roberts et al., 2013). Hence, this key and often forgotten study suggests that stromal cells (likely FAPs) are indispensable and necessary for skeletal muscle homeostasis and maintenance.

To better understand whether FAPs are necessary for normal skeletal muscle regeneration and homeostatic maintenance, Wosczyzna et al. (2019) ablated PDGFR α + cells using a diphtheria toxin mouse model. The lack of PDGFR α + cells and their lineage resulted in a decreased MuSC number during muscle regeneration and consequently, smaller myofibers. CD45+ cell number also declined in FAP-depleted muscles at day 3 post-injury. The authors utilizing regeneration assays, isotopic transplants, and FAP transplantation experiments elegantly demonstrated that FAPs are necessary for normal skeletal muscle regeneration. The authors also showed that FAP-ablated mice had about 30–40% less lean mass and generated significantly less force at 3, 6, and 9 months than non-ablated mice (Wosczyzna et al., 2019) (**Figure 1**). These results demonstrated that PDGFR α + FAPs are required for long-term homeostatic integrity and growth of skeletal muscle. Hence, the depletion of FAPs resulted in muscle regenerative deficits upon injury and atrophy in undamaged conditions.

These results were recently confirmed by the Tsuchida group, who demonstrated that the specific depletion of PDGFR α + expressing progenitors caused bodyweight reduction and decreased muscle strength and weight (Uezumi et al., 2021). Importantly, these changes were not attributable to decreased food intake in FAP-ablated mice. Although the number of myofibers was unchanged, the authors described reduced myofiber cross-sectional area and increased expression of the muscle-specific E3 ubiquitin ligase *MAFbx*, also known as *Atrogin-1*, in the ablated-muscles without overt signs of muscle injury or inflammation. Notably, PDGFR α + cell transplantation



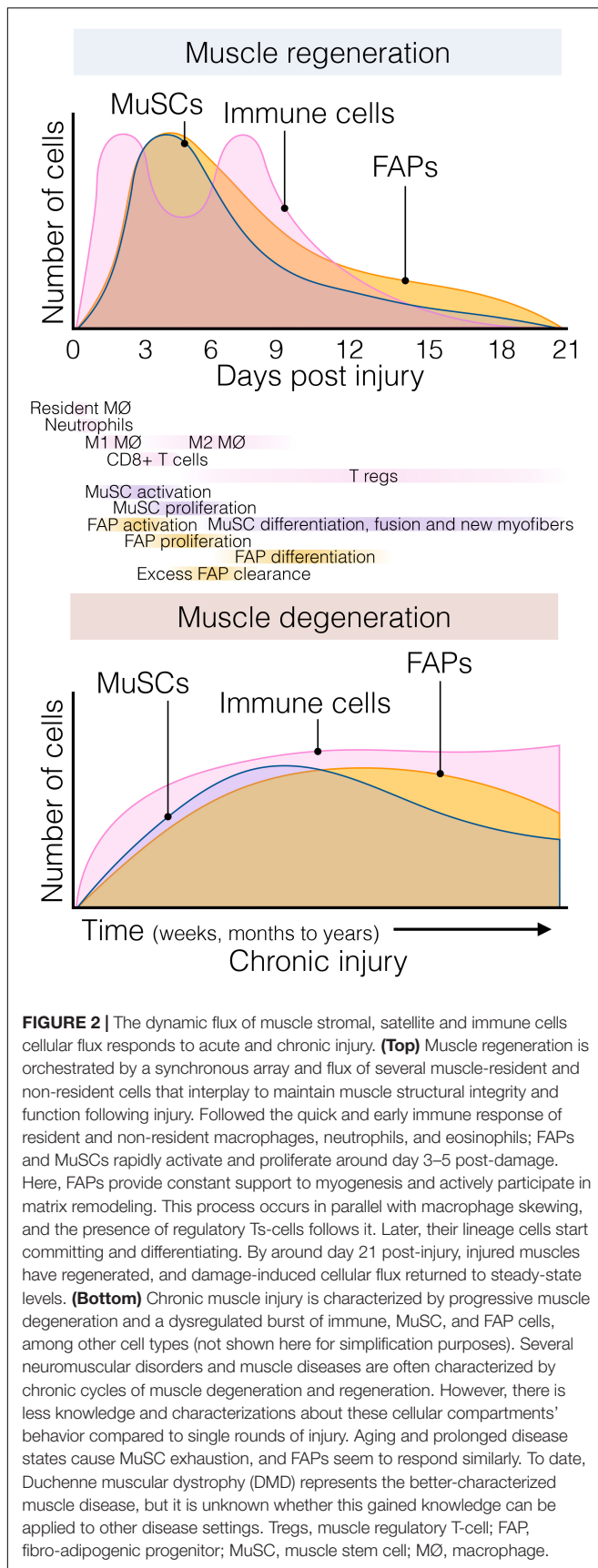
into the ablated mice's *tibialis anterior* muscle recovered muscle mass and fiber size (Uezumi et al., 2021). Hence, three groups independently have demonstrated that muscle-resident PDGFR α + FAPs are indispensable for steady-state muscle maintenance and integrity (Roberts et al., 2013; Wosczyzna et al., 2019; Uezumi et al., 2021) (**Figure 1**).

Muscle wasting associates with changes in myofiber type and muscle-nerve communication defects. Uezumi et al. (2021) also observed that PDGFR α + cells lie adjacent to motor nerve axons, Schwann cells, and cover the neuromuscular junction (NMJ) in undamaged muscles. In line with this, the genetic ablation, by Cre-mediated expression of diphtheria toxin, of PDGFR α + FAPs reduced the number of innervated NMJs and increased the proportion of partially denervated and denervated NMJs after 17 days of tamoxifen treatment (**Figure 1**). These effects increase at longer times (Uezumi et al., 2021). Remarkably, Schwann cell organization and gene expression were also disrupted by depletion of PDGFR α + FAPs. Mechanistically, the authors suggested that FAP-derived BMP3B is functionally relevant to maintaining muscle mass and integrity (Uezumi et al., 2021). These results collectively suggest that PDGFR α FAPs are required and sufficient for steady-state maintenance of the neuromuscular synapse and nerve-muscle communication and function.

The Supportive Role of Muscle-Resident Fibro-Adipogenic Progenitors on Myogenesis

In response to injury, skeletal muscle displays a dynamic multicellular response that involves several cell types and discrete

regenerative steps (**Figure 2**, top) (Bentzinger et al., 2013; Chazaud, 2020). The initial and rapid inflammatory response is followed by the concomitant activation of two quiescent muscle-resident cells, MuSCs, and interstitial PDGFR α + FAPs. Both populations reside close to each other but are separated by the myofiber-associated basal lamina. FAPs and MuSCs proliferate at enormous rates following injury, progressively increasing their numbers from days 2 to 5. From this time until 14–21 days after injury, when damage is resolved, they steadily return to their basal numbers (**Figure 2**, top) (Joe et al., 2010; Uezumi et al., 2010; Murphy et al., 2011; Lemos et al., 2015; Kopinke et al., 2017; Contreras et al., 2019a; Scott et al., 2019). Remarkably, although this crucial stromal-muscle stem cell interaction was suggested to participate in skeletal muscle regeneration a long time ago (Church, 1970), only recently cumulative evidence have demonstrated that FAPs regulate MuSC fate and behavior, and vice versa (Joe et al., 2010; Uezumi et al., 2010, 2021; Mathew et al., 2011; Murphy et al., 2011; Fiore et al., 2016; Moratal et al., 2019; Wosczyzna et al., 2019). In this context, FAPs are principally immunomodulatory cells secreting a large number of factors (discussed below) (Heredia et al., 2013; Scott et al., 2019; Uezumi et al., 2021). FAPs are also responsible for the muscle ECM remodeling after damage, producing a transient ECM (Scott et al., 2019) and supporting MuSC expansion, differentiation, and self-renewal (**Figure 2**, top) (Heredia et al., 2013; Mozzetta et al., 2013). In addition, it has been shown that the muscle ECM component Collagen VI, secreted from FAPs, specifically regulates MuSC quiescence (Urciuolo et al., 2013). Thus, the correct regulation of basal membrane and ECM composition by FAPs is critical for normal muscle regeneration. Indeed,



the biophysical and biomechanical properties of the ECM vary depending on its composition, and impact the fate of MuSCs (Lutolf and Blau, 2009). Gilbert et al. (2010), used bioengineered substrates of varying stiffness to recapitulate key biomechanical characteristics of the MuSCs niche. The authors showed that increased elastic modulus 10^6 kPa (rigid plastic dishes) stimulates MuSC motility, but 12 kPa (mimicking the elasticity of muscle) promotes MuSC proliferation and muscle engraftment (Gilbert et al., 2010). Besides FAPs' role in modulating ECM remodeling and stiffness, others and we have shown that $PDGFR\alpha+$ FAPs secrete various cytokines and growth factors, which directly induce myogenic cell proliferation and survival but may block their differentiation (Joe et al., 2010; Heredia et al., 2013; Biferali et al., 2019; Scott et al., 2019). These data strongly suggest that muscle-resident FAPs are critical to support MuSC trophic functions.

However, chronic injury makes this heterogenic, multi-step, and coordinated response persistent instead of transient, priming the muscle milieu into an aberrant state known as fibrofatty infiltration. In this context, exacerbated inflammation and accumulated scarring interferes with normal tissue function (Lieber and Ward, 2013; Dadgar et al., 2014; Ieronimakis et al., 2016; Buras et al., 2019). Indeed, we showed that after acute muscle injury, from day three onwards, macrophage-induced apoptosis clears the excess of $PDGFR\alpha+$ FAPs (Figure 2, top) and that this process can be pharmacologically stimulated by nilotinib (Lemos et al., 2015; Fiore et al., 2016). Hence, modifying propensity of FAPs to engage in apoptosis might be a protective way to avoid excessive accumulation of these cells and fibrosis deposition in pathology. However, in pathological and chronic conditions, $PDGFR\alpha+$ cells are over-activated and not efficiently cleared out, remaining in high numbers and differentiating toward multiple MSC lineages depending on the type and extension of the damage (Figure 2, bottom) (Lemos et al., 2015; Ieronimakis et al., 2016; Kopinke et al., 2017; Madaro et al., 2018; Malecova et al., 2018; Contreras et al., 2019a; Mázala et al., 2020).

Lastly, although most previous studies demonstrate that FAPs influence myogenic behavior and fate of MuSCs, the latter also exhibit trophic functions toward FAPs. Indeed, MuSCs and myotubes strongly reduce FAP adipogenic potential *in vitro* (Uezumi et al., 2010; Moratal et al., 2019). Co-culture experiments using primary myotubes suggest the presence of “unknown” factors in myogenic cells that inhibit the adipogenic differentiation of FAPs (Uezumi et al., 2010). Remarkably, the modulation of FAPs by myoblasts and myotubes is altered with aging and DMD as these myogenic cells lose their regulatory potential, which may explain the abundance of fat tissue in degenerated muscles (Moratal et al., 2019). Moratal et al. (2019) suggested that the myogenic progenitor secretome is crucial to regulate FAP lineages, and these “unknown” factors may influence PI3K-AKT, SMAD2, and GLI signaling pathways. These studies suggest that the myogenic lineage largely influences the plasticity of $PDGFR\alpha+$ FAPs, albeit the cellular and molecular mechanisms remain elusive.

In sum, non-cell-autonomous mechanisms (e.g., muscle microenvironmental factors such as cell-to-cell contact, growth

factors, cytokines/myokines, or matrix stiffness) also determine FAP dynamics. Hence, the destiny of FAP progeny, location, and abundance resolution within injured muscles can be modified extrinsically, aiming to boost skeletal muscle regeneration and enhanced tissue repair.

Fibro-Adipogenic Progenitors and Immune Cells: A Sentinel Relationship

It is now well known that muscle-resident and non-resident immune cells, in particular macrophages (MPs), play essential roles in tissue homeostasis, regeneration, repair, and disease (reviewed in Tidball and Villalta, 2010; Vannella and Wynn, 2017; Perandini et al., 2018; Theret et al., 2019; Chazaud, 2020). Indeed, MPs are responsible for modulating MuSC proliferation and differentiation, with their depletion inducing extensive alteration of muscle regeneration following injury (Arnold et al., 2007; Lemos et al., 2015; Juban et al., 2018). Nevertheless, the cellular and molecular interactions of PDGFR α + FAPs and macrophages at the resting state are unknown.

Surprisingly, genetic lineage-depletion of PDGFR α + cells does not affect muscle immune cell numbers at short (9–14 days) and long (9 months) periods post depletion in the absence of muscle injury (Wosczyzna et al., 2019). However, their cellular cross-talk is better described after a single round of damage, chronic damage and in disease. After acute injury, blood circulating Ly6C+ monocytes infiltrate the damaged area in the first 24 h after injury and differentiate into Ly6C+ MPs. This crucial infiltration is chemokine-dependent (e.g., CCL2, CCL3, or CX3CL1) and due to the release of DAMPs (Damage-associated Molecular Pattern) cues (**Figure 3**, top) (Martinez et al., 2009; Brigitte et al., 2010; Sun et al., 2011). While many cells are involved in MP attraction, damage-activated FAPs express a complex cocktail of chemokines and cytokines 24 h after injury, thus establishing an early niche rich in inflammatory cues (**Figure 3**, top) (Mashinchian et al., 2018; Scott et al., 2019). This intricate primary response of FAPs during the initiation and formation of granulation tissue supports the notion that they are important components and modulators of the early immune response. Eventually, Ly6C+ MPs skew into a pro-restorative phenotype, associated with the downregulation of Ly6C (**Figure 3**, top) (Arnold et al., 2007; Varga et al., 2013). Besides, others and we described that Ly6C+ MPs have an early pro-apoptotic effect on PDGFR α + FAPs through TNF- α production, keeping their number under control following injury resolution (Lemos et al., 2015; Juban et al., 2018). Therefore, posttraumatic inflammation stimulates local FAPs, leading to their activation, proliferation, accumulation, differentiation, and later resolution to steady-state conditions. These key concepts have been validated in the *Ccr2* knockout mice model (Lu et al., 2011a,b). The lack of infiltrating monocytes resulted in delayed PDGFR α + FAP clearance and impaired muscle regeneration but increased fibro-fatty deposition (Lemos et al., 2015). These results demonstrate that infiltrating monocytes are required for proper FAP clearance and avoid excessive ECM deposition during damage resolution.

On the other hand, Ly6C- MPs secrete TGF- β , which activates pro-survival signaling pathways in FAPs and promotes their

activation, ECM secretion, and myofibroblast differentiation (**Figure 3**, top) (Lemos et al., 2015; Juban et al., 2018; Contreras et al., 2019a,b, 2020; Stepien et al., 2020). Thus, the TNF- α /TGF- β balance needs to be carefully regulated since its disruption (lengthy exposure of TNF- α or increase of TGF- β levels) will induce drastic changes in FAP behavior, delaying skeletal muscle regeneration as often seen in degenerative myopathies (**Figure 3**, bottom) (Lemos et al., 2015; Muñoz-Cánoves and Serrano, 2015; Juban et al., 2018). The fact that intercellular communication within muscle is impaired during chronic damage might be one reason for tipping the system into dysregulated fibro-fatty remodeling and permanent scarring.

We postulate that chronic conditions and degenerative settings compromise the steady-state balance of FAPs. This latter hypothesis was recently corroborated by Saito et al. (2020). The authors, using an experimental autoimmune chronic inflammatory myopathy (CIM) model, showed that CIM-FAPs develop an anti-apoptotic phenotype compared to FAPs isolated from an acute injury model (intramuscular injection of BaCl₂) (**Figure 3**, bottom) (Saito et al., 2020). Mechanistically, FAPs undergo senescence -characterized by the upregulation of *Ckn2a* and *Trp53* expression and the histone variant γ H2A.X- upon acute muscle injury but not under CIM. Running exercise also induces rapid FAP senescence. Intriguingly, when subjecting the CIM mice to exercise combined with AICAR treatment, an AMP-activated kinase (AMPK) activator, both interventions restored muscle function, resulting in the induction of a pro-inflammatory and pro-apoptotic FAP phenotype that enhances muscle regeneration (Saito et al., 2020). AMPK has been previously shown to have a crucial role in macrophage polarization and MuSC self-renewal (Mounier et al., 2013; Theret et al., 2017; Juban et al., 2018). These results could explain the chronic accumulation of FAPs due to clearance deficiency as a consequence of senescence and apoptosis resistance in muscle pathologies, highlighting the potential of FAP-targeted therapeutic interventions employing exercise and AMPK activation for chronic muscle diseases.

Macrophages and FAPs lie near each other, especially after muscle trauma and pathology (Lemos et al., 2015; Contreras et al., 2016; Juban et al., 2018; Moratal et al., 2018). Aiming to decipher the interactions between MPs and FAPs, bone marrow-derived MPs can be treated *in vitro* with IL-4 to mimic an M2a/alternative activation (Murray et al., 2014), or IL-1 β to phenocopy mild inflammatory MPs (M1) as found in muscles (Arnold et al., 2007). Interestingly, treatment of human FAPs with conditioned media obtained from IL-1 β -polarized MPs reduced FAP adipogenesis via the TGF- β signaling pathway (Moratal et al., 2018). On the contrary, IL-4-polarized MPs enhanced FAP adipogenesis (Moratal et al., 2018). Recently, Stepien et al. (2020), using a combined fibrotic model of muscle damage, showed that decreasing the amount of infiltrating macrophage-derived TGF- β reduced fibrosis and proliferation of fibro-adipogenic progenitors and simultaneously enhanced muscle regeneration. To conclude, these studies performed in mouse and human muscles demonstrated that distinct subsets of macrophages could have opposite effects on FAP cellular states and fate, giving the possibility to explore regenerative outcomes by understanding their cellular cross-modulation.

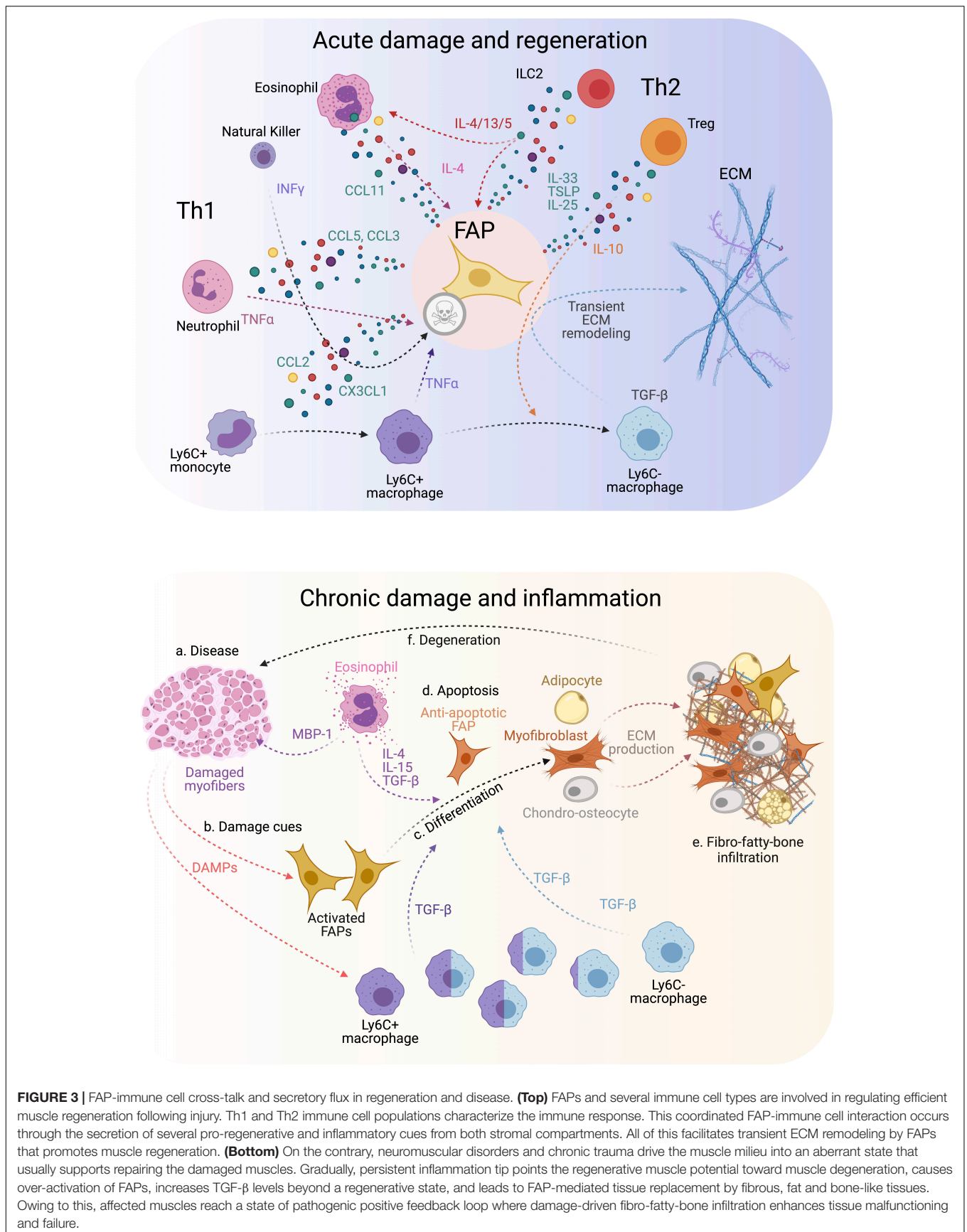


FIGURE 3 | FAP-immune cell cross-talk and secretory flux in regeneration and disease. **(Top)** FAPs and several immune cell types are involved in regulating efficient muscle regeneration following injury. Th1 and Th2 immune cell populations characterize the immune response. This coordinated FAP-immune cell interaction occurs through the secretion of several pro-regenerative and inflammatory cues from both stromal compartments. All of this facilitates transient ECM remodeling by FAPs that promotes muscle regeneration. **(Bottom)** On the contrary, neuromuscular disorders and chronic trauma drive the muscle milieu into an aberrant state that usually supports repairing the damaged muscles. Gradually, persistent inflammation tip points the regenerative muscle potential toward muscle degeneration, causes over-activation of FAPs, increases TGF- β levels beyond a regenerative state, and leads to FAP-mediated tissue replacement by fibrous, fat and bone-like tissues. Owing to this, affected muscles reach a state of pathogenic positive feedback loop where damage-driven fibro-fatty-bone infiltration enhances tissue malfunctioning and failure.

MPs are not the only inflammatory cell type that interact with FAPs in regeneration and repair. Usually, neutrophils are the first cells that infiltrate the damaged tissue (**Figure 2**, top). Coming from either the blood or the fascia (Brigitte et al., 2010; Bentzinger et al., 2013), neutrophils also produce TNF- α , which may help initiate FAP clearance and resolve their increased numbers after damage (Pizza et al., 2005). Later, NK cells infiltrate the injured muscle, secrete INF- γ and stimulate myogenic cell proliferation (Cheng et al., 2008). Notably, the potential regulatory function of NK cells toward PDGFR α + FAPs is unknown. In the same timeframe, eosinophils infiltrate the damaged muscle and secrete IL-4, which induces the proliferation of PDGFR α + FAPs, providing in return pro-myogenic trophic effect on MuSCs (**Figure 3**, top) (Heredia et al., 2013). Remarkably, IL-4 inhibits the adipogenic differentiation of muscle FAPs *in vitro* and *in vivo* (Heredia et al., 2013; Dong et al., 2014). Like IL-4, IL-15 also promotes FAP proliferation and expansion while inhibiting their adipogenic commitment and fatty muscle deposition following acute damage. The enhanced accumulation of PDGFR α + cells by intramuscular IL-15 triggers a transient increase of ECM, which seems to facilitate the regeneration of injured myofibers (Kang et al., 2018). Hence, the roles of ILs as therapeutic targets have opened new avenues in the search for effective muscle therapies to promote muscle regeneration and improve muscle atrophy associated with sarcopenia.

Type 2 immunity, due to the recent discovery of innate and type 2 lymphoid cells (ILC2), is a newly added component to our understanding of tissue homeostasis (Castiglioni et al., 2015; Tidball, 2017). ILC2 are tissue-resident cells and participate in the Th2 response by producing IL-4, IL-5, IL-13, and IL-9 (Licona-Limón et al., 2013). The release of IL-33, IL-25, and TSLP produced by MSCs after damage primarily recruits and activates ILC2 cells (**Figure 3**, top) (Yagi et al., 2014). Interestingly, muscle-resident MSCs (likely FAPs) from aged mice produced less IL-33 than their young counterparts, which delays ILC2 and Th2 inflammation (Kuswanto et al., 2016). Hence, FAP-derived IL-33 regulates the dynamics of muscle regulatory T-cells (Tregs) during muscle regeneration following acute injury (**Figure 3**, top). Owing to mammalian aging reduces the number of muscle-resident Tregs, it may explain the inefficiency of muscle regeneration and repair in the elderly population. Overall, ILC2s participates in tissue homeostasis, mostly in the lungs and the intestine (for ILC2 review, see Messing et al., 2020), but their function in muscle regeneration is underexplored. Muscle-resident Tregs (CD4+/FoxP3+ cells), however, limit the production of IFN- γ from NK cells, inhibiting local MP proliferation and pushing MP skewing during skeletal muscle regeneration (**Figure 3**, top) (Panduro et al., 2018). Indeed, Tregs-depleted muscle shows altered regeneration with increased inflammation and fibrosis, a typical phenotype of delayed Th1/Th2 skewing (Mounier et al., 2013; Panduro et al., 2018). Thus, disruption of the Th1/Th2 immunity impairs skeletal muscle homeostasis and regeneration.

Activated T cells express PD-1 (CD279) receptor, whereas MPs and dendritic cells present the ligands (PD-L1 and L2) at their cell surface (Zou, 2005). The PD-L1/PD-1 axis has been intensely investigated, mostly in cancer (Pardoll, 2012),

whereas almost no information exists for muscle. T cell activation requires the PD-1/PD-L1 interaction, and its inhibition induces T cell over-activation, leading to a Th2 inflammatory response (Pardoll, 2012). While those inhibitors have created significant opportunities for cancer therapies, their use often causes under-reported cardiac and skeletal myopathies, leading to lethal conditions in some cases (Johnson et al., 2016; Zimmer et al., 2016; Matas-García et al., 2020). Although T cells participate in skeletal muscle regeneration (Deyhle and Hyldahl, 2018), the mechanisms of how T cell over-activation can lead to muscle defects and myopathies are far from understood. Moreover, how NK cells, T cells, and ILC2s directly affect the fate and activities of muscle PDGFR α + FAPs is unclear. Previous studies have mostly focused on MuSC behavior in various immune-deficient mouse models without concentrating on the interstitial compartment. Accordingly, future work should address these questions and keep the muscle research field busy for the next few years.

FIBRO-ADIPOGENIC PROGENITORS AS PERIVASCULAR CELLS

Skeletal muscle is highly vascularized and adapted for enormous blood flow rate changes in response to exercise (Korthuis, 2011). Given the high amount of muscle mass that the human body encompasses, skeletal muscles' metabolic and endocrine functions are tightly linked to its vascular density (Olfert et al., 2016). Endothelial cells, pericytes, and smooth muscle cells form the vascular muscle milieu – capillaries, arterioles, arteries, and venules. Briefly, different populations of cells organized in concentric layers constitute the cellular wall of blood vessels: endothelial cells (known as tunica intima), mural cells of the tunica media (pericytes in capillaries or vascular smooth muscle in larger vessels), and adventitial or perivascular fibroblasts (tunica adventitia) (Cattaneo et al., 2020). As the role of skeletal muscle vasculature in homeostasis and disease has been reviewed elsewhere (Cooke and Losordo, 2015; Latroche et al., 2015a), here we focus on the participation of muscle-resident FAPs in modulating vascular remodeling.

Many PDGFR α + FAPs localize circumferentially around vessels in muscles but reside outside the basal membrane of vascular cells (Joe et al., 2010; Uezumi et al., 2010, 2021; Scott et al., 2019). Thus, PDGFR α + FAPs are a significant proportion of perivascular stromal cells residing in the vascular wall's tunica adventitia. Indeed, when muscle-resident mesenchymal cells are lineage traced based on the expression of *Hypermethylated in cancer 1* (*Hic1*, also known as HIC ZBTB Transcriptional Repressor 1), the vast majority of these cells are FAPs (Scott et al., 2019). HIC1 is an epigenetically-regulated zinc-finger transcription factor that acts as a transcriptional repressor, regulating cell growth, proliferation, and its dysregulated expression associates with several malignant disorders and cancer (Chen et al., 2003; Zheng et al., 2012; Scott et al., 2019; Contreras, 2020; Soliman et al., 2020). Only a small proportion (5%) of muscle-resident HIC1+ cells that are SCA-1 negative, identified as tenogenic cells and pericytes (Scott et al., 2019). Whether HIC1+ progenitors could give rise to vascular RGS5+ pericytes

is unknown, although the relative contribution of HIC1+ cells to vascular pericytes suggests a common hierarchy progenitor in adult muscles that may divide the perivascular cell ontogeny early during development (Contreras, 2020). However, the lineage relationship and ontology of HIC1+ cells with tenogenic cells and pericytes remains unclear.

In humans, resistance training is associated with increased proliferative PDGFR α + FAPs but a decreased abundance of pericytes (Farup et al., 2015). Hence, the active remodeling of the stromal compartment following exercise results in physiologically relevant cues for satellite cell expansion post-training, suggesting that physical activity may actively promote a healthy muscle niche to restrain age-related development IMAT and fibrosis during sarcopenia (Collao et al., 2020). Addressing these significant questions related to the possible roles of FAPs in skeletal muscle during exercise and sarcopenia will keep the field busy for the next few years.

While myogenesis and angiogenesis seem to be primarily affected by the MP inflammatory and secretory status during muscle regeneration (Latroche et al., 2017), the role of PDGFR α + FAPs in neo-angiogenesis are understudied. Indeed, co-culture of human umbilical vein endothelial cells (HUVECs) with human dermal fibroblasts does not affect capillaries' formation *in vitro* or *in vivo* angiogenesis (Latroche et al., 2017). However, dermal fibroblasts are significantly different from muscle FAPs. Santini et al. (2020) recently confirmed that PDGFR α + cells are found in a pericytic position in muscles, corroborating previous findings of FAPs being perivascular cells (Joe et al., 2010; Uezumi et al., 2010, 2021; Scott et al., 2019). The authors also showed that genetic ablation of PDGFR α + FAPs disrupts vessel organization and impairs revascularization, which leads to increased fibrosis and muscle damage after hind limb ischemia (HLI) (Santini et al., 2020). No ablation-dependent changes were seen in the absence of damage. Thus, this study established that muscle-resident FAPs are necessary for effective revascularization upon ischemia, although the regenerative cues or factor(s) they synthesized remain underexplored. An intriguing possibility is the participation of vascular growth factors, like angiopoietins or vascular endothelial growth factor (VEGF), known for regulating embryonic and postnatal angiogenesis. These secreted proteins are signaling hubs that promote blood vessels' growth and, within muscles, seem to be expressed by endothelial cells, MuSCs, and FAPs (Verma et al., 2018). The reason for the redundancy of expression is unknown, but we hypothesize that they could participate in autocrine signaling loops in a cell-type-specific fine-tuned manner. Utilizing a mouse model of heterotopic ossification (HO), Hwang et al. (2019) showed that mesenchymal progenitors, rather than endothelial cells, dynamically regulate the expression of *Vegfa* following trauma. The authors also showed that *Prx*-lineage derived VEGFA is necessary to induce ectopic bone formation (Hwang et al., 2019). These novel findings position muscle-resident mesenchymal progenitors (i.e., FAPs) as a critical source of vascular and angiogenesis factors in severe trauma and disease.

Although separated by their respective basal laminas, MuSCs and endothelial cells are in close contact (Christov et al., 2007; Verma et al., 2018), and neo-angiogenesis in response to

muscle trauma is essential to supply blood to the newly formed myofibers efficiently. While increased vascular density leads to augmented MuSC numbers and ameliorates DMD myopathology (Verma et al., 2010), mostly by increasing VEGF and FGF (Fibroblast Growth Factor) availability (Neuhaus et al., 2003; Deasy et al., 2009); altered muscle vasculature negatively impacts tissue maintenance, vascular tone, myofiber type density, and myogenic progenitor homeostasis (Matsakas et al., 2013). Indeed, blood vessel density and vascular integrity around myofibers are reduced in a number of mice models of neuromuscular disorders (Latroche et al., 2015b; Valle-Tenney et al., 2020). Hence, decreased blood perfusion of the skeletal muscle could contribute to its regeneration and revascularization defects. Interestingly, in dermatomyositis, loss of capillaries is associated with a decrease in the number of satellite cells in the affected area, in the absence of local muscle damage (Gitiaux et al., 2013). This interdependent relationship emphasizes the importance of the interaction between the two cell types. However, the exact interplay between MuSCs and endothelial cells *in vivo* needs further examination. Furthermore, the cellular interactions and the extension of the association between the vasculature and FAPs are practically unknown.

Muscle injury reduces the vascular network (Hardy et al., 2016; Morton et al., 2019) and leads to increased hypoxia and hypoxia-inducible factor 1 α (HIF-1 α), suggesting that injured muscles are in an hypoxic state (Drouin et al., 2019; Valle-Tenney et al., 2020). Recently, Drouin et al. (2019) showed that muscle damage-induced hypoxia promotes the activation and proliferation of SCA-1+ FAPs. Hypoxia reduces the adipogenic differentiation of FAPs, but it promotes their osteogenic differentiation. Accordingly, *in vitro* simulated hypoxia alters the fate of muscle-resident FAPs. Sustained activation of SMAD1/5/8 and induced expression of BMP9 appear to contribute to these hypoxia-mediated effects on FAP behavior (Drouin et al., 2019). Thus, loss of blood perfusion and reduced oxygen supply affect FAP fate. Remarkably, genetic loss of *Hif1a* in mesenchymal progenitors (*Prx* expressing lineage) prevents HO formation (Agarwal et al., 2016), which suggests that HIF-1 α could participate in regulating the chondrogenic and osteogenic fate of mesenchymal progenitor cells. Nevertheless, the specific role(s) of HIFs (e.g., HIF-1 α) in modulating the activities of PDGFR α + cells remain unrevealed to date.

FIBRO-ADIPOGENIC PROGENITORS AS PATHOLOGICAL DRIVERS OF MUSCLE FIBROSIS AND INTRAMUSCULAR FAT ACCUMULATION IN PATHOLOGY AND DISEASE

Fibrosis is the most common degenerative outcome of several diseases characterized by chronic damage and inflammatory response, can affect any organ, and accounts for about half of all deaths in the industrialized world (Henderson et al., 2020). Progressive and excessive ECM accumulation in connective tissue, also called CT hyperplasia, characterizes fibrosis (reviewed

in Serrano et al., 2011; Lieber and Ward, 2013; Henderson et al., 2020). The principal components of muscle CT are the ECM and its stromal cells that continuously reshape this complex structural and supportive microenvironment. Muscle pathological fibrosis is different from the transient physiological “fibrosis” or enhanced ECM deposition that follows a single round of injury (Smith and Barton, 2018). This physiological fibrosis is required to rebuild lost muscle architecture and facilitates muscle regeneration. However, under chronic damage, inflammatory-activated fibroblasts and myofibroblasts express large amounts of ECM proteins resulting in the replacement of myofibers with wound scar, thereby leading to muscle failure and even death (Fadic et al., 2006; Pakshir and Hinz, 2018). Hence, although active ECM remodeling is essential for tissue regeneration and repair, its exacerbated and disorganized accumulation during pathology often leads to tissue malfunctioning (Borthwick et al., 2013). Among the most affected tissues by fibrosis are the skin, liver, lungs, heart, kidney, eye, pancreas, intestine, brain, bone marrow, and skeletal muscles (Wynn and Ramalingam, 2012). Given the importance of scar formation in several tissues in pathology, disease, and aging (Brack and Rando, 2008; Grounds, 2008; Kharraz et al., 2014; Purslow, 2020), it is perhaps surprising that the biology of PDGFR α + FAPs is not well understood yet.

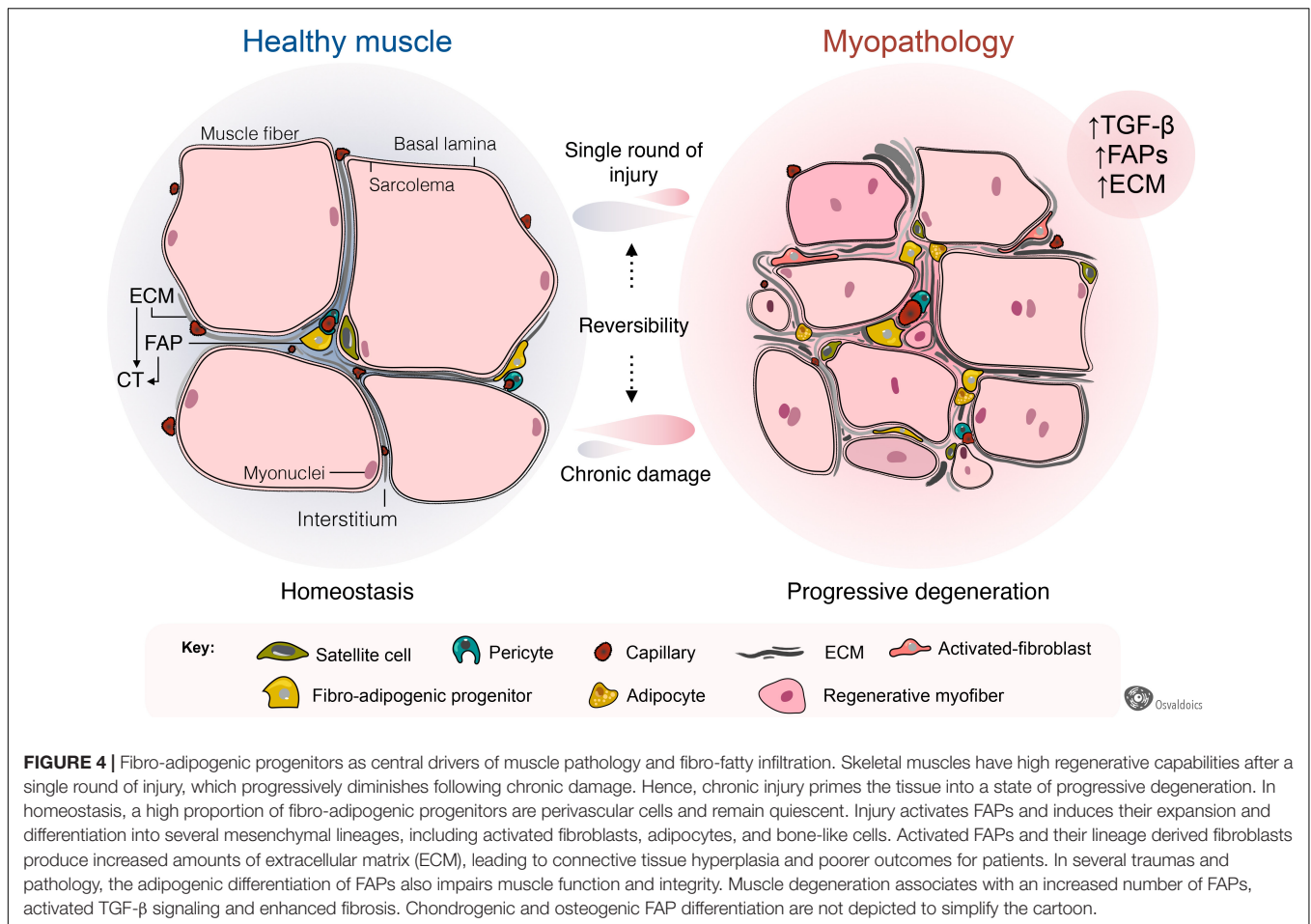
The *in vivo* fibrogenic potential of PDGFR α + cells was initially confirmed by PDGFR α ^{H2BEGFP}+ cell transplantation into irradiated skeletal muscle after toxin-induced muscle injury (Hamilton et al., 2003; Uezumi et al., 2011). Transplanted PDGFR α ^{H2BEGFP}+ cells did not form myofibers but accumulated in ECM-rich areas within the muscle interstitium. PDGFR α + progenitors also expand and gather in muscle fibrous-rich areas of Duchenne muscular dystrophy (DMD) patients and dystrophic mdx mice models (Uezumi et al., 2014; Ieronimakis et al., 2013; Lemos et al., 2015; El Agha et al., 2017; Kopinke et al., 2017; Contreras et al., 2019a; Mázala et al., 2020). Fibrogenic FAPs can also be identified by expression of *Collagen I* (Theret et al., 2021), although other muscle-resident cells like SCA-1 negative and MuSCs also express basal levels of this fibrillar Collagen gene (Chapman et al., 2016). Others and we have proposed that a significant proportion of activated fibroblasts and myofibroblasts are generated by PDGFR α + FAPs upon injury or *in vitro* through the stimulation of FAPs with profibrotic cytokines (e.g., TGF- β) combined with serial passaging in normoxic atmosphere (Contreras et al., 2019a,b, 2020; Santini et al., 2020; Stepien et al., 2020). Interestingly, MYOSTATIN, a secreted TGF- β family member that negatively regulates myofiber size, also induces FAP proliferation, myofibroblast differentiation, and muscle fibrosis (Zhao et al., 2008; Dong et al., 2017). Hence, these pro-fibrotic cues regulate how and when PDGFR α + progenitors expand and gather in muscle fibrous-rich areas.

Fibrosis is a common hallmark of several congenital muscular dystrophies, and notably, FAPs are pathologically dysregulated in most of them (Figure 4). These include mouse models of *Collagen VI*- (Noguchi et al., 2017; Mohassel et al., 2018), human DMD (Uezumi et al., 2014) and mouse models of DMD (Box 1) (Uezumi et al., 2011; Mozzetta et al., 2013; Lemos et al., 2015; Contreras et al., 2016, 2020; Ieronimakis et al., 2016; Kopinke et al., 2017; Mázala et al., 2020; Reggio et al., 2020; Giuliani et al., 2021), Facioscapulohumeral dystrophy (FSHD)

(Bosnakovski et al., 2017, 2020), Limb-girdle muscular dystrophy (LGMD) (Hogarth et al., 2019), and ALS neuromuscular disease (Gonzalez et al., 2017; Madaro et al., 2018). Increased muscle fibrosis and FAP expansion also occur after single and repeated cycles of intramuscular BaCl₂, notexin, cardiotoxin, or glycerol administrations (Uezumi et al., 2010; Dadgar et al., 2014; Pessina et al., 2014; Contreras et al., 2016, 2020; Theret et al., 2021), vastus medialis muscles of compromised knee osteoarthritis patients (Ikemoto-Uezumi et al., 2017), human anterior cruciate ligament injuries (Fry et al., 2017), induced hindlimb ischemia (Santini et al., 2020), degenerated muscles of type 2 diabetic patients (Farup et al., 2020), obesity-mediated diaphragm dysfunction of chronic high-fat diet-fed mice (Buras et al., 2019), and surgical muscle traumas including denervation and laceration (Brandan et al., 1992; Pessina et al., 2014; Contreras et al., 2016; Madaro et al., 2018; Rebolledo et al., 2019). Muscle-resident FAPs also increase and accumulate in a muscle fibrosis model of chronic kidney disease (Dong et al., 2017) and chronic kidney disease human patients (Abramowitz et al., 2018), and are accompanied by enhanced muscle atrophy and FAP-mediated adipogenesis (Hu et al., 2019). In each of these pathologies and models of muscle injury and scarring, the extension and degree of fibrosis largely depend on the type and extension of damage and myodegeneration. Consequently, we reason that muscle scarring originates from PDGFR α + FAPs (Figure 4).

Adult skeletal muscles fibrosis is also associated with adipose tissue accumulation following a single-round of injury (Pisani et al., 2010; Biltz and Meyer, 2017; Biltz et al., 2020; Xu et al., 2021) and in several myopathies, including DMD (Box 1) (Uezumi et al., 2011, 2014; Kopinke et al., 2017), LGMD (Hogarth et al., 2019), and after rotator cuff tears (Davies et al., 2016; Liu et al., 2016; Kang et al., 2018; Lee et al., 2020a). Remarkably, increased numbers of PDGFR α + FAPs are found in many of these myopathologies, being responsible, at least at some extent, for exacerbated fat deposition (Figure 4). Thus, growing evidence suggests that FAPs are, to some extent, drivers of the muscle loss and replacement by a non-contractile scar in disease and pathology (Box 1). Intriguingly, FAPs are the cells in charge of both physiological and pathological ECM and fat accumulation. However, the extrinsic or intrinsic mechanisms regulating FAP activation, plasticity, and fate during muscle loss progression and fibro-fatty replacement are still underexplored.

Remarkably, the passaging of PDGFR α + FAPs in plastic dishes and 20% oxygen is sufficient to induce their activation, acquisition of myofibroblast features, and loss of PDGFR α expression (Contreras et al., 2019b; Santini et al., 2020). Recently, Santini et al. (2020) injected PDGFR α -derived activated fibroblasts and myofibroblasts into nude mice after hindlimb ischemia to study whether differentiated myofibroblasts contribute to fibrosis and impair vessel maturation. Following HLI surgery, myofibroblast's transplantation differentiated from PDGFR α + FAPs increased vessel leakage, impaired regeneration, and increased fibrosis compared to PBS-injected nude mice. The injected cells survived for at least 3 weeks within the HLI damaged tissue and remained associated with ECM-rich foci near myofibers (Santini et al., 2020). Finally, by using a clonal Brainbow lineage tracing strategy, Santini et al. (2020) also demonstrated that most of the progeny of PDGFR α + FAPs



BOX 1 | Participation of muscle fibro-adipogenic progenitors in DMD pathology.

DMD is a severe human myopathy without cure to date. It is caused by mutations in the *DMD* gene encoding DYSTROPHIN and characterized by muscular degeneration in which progressive loss of muscle mass and weakness are expected consequences (Hoffman et al., 1987; Wallace and McNally, 2009). Myonecrosis, sarcolemmal disorganization, inflammation, and the accumulation of fibro-fatty scar tissue are observed early in DMD and increase with age (Cáceres et al., 2000; Porter et al., 2002; Reed and Bloch, 2005; Serrano et al., 2011; Grounds et al., 2020). Remarkably, FAPs generate activated fibroblasts, myofibroblasts, adipocytes, and bone-like cell progeny in muscular dystrophy, albeit to different extents depending on the degree of damage, inflammation and degeneration (Jezumi et al., 2011, 2014; Lemos et al., 2015; Contreras et al., 2016, 2019a; Ieronimakis et al., 2016; Kopinke et al., 2017; Eisner et al., 2020; Mázala et al., 2020). As known for other muscle-resident cells, the exit of FAPs from quiescence and their entry into proliferative and differentiation programs are not only finely tuned by microenvironmental cues (Jezumi et al., 2010; Heredia et al., 2013; Moratal et al., 2018, 2019) but also through intrinsic molecular mechanisms like epigenetic HDAC-dependent pathways (Mozzetta et al., 2013; Saccone et al., 2014; Sandonà et al., 2020) or Hic1-dependent quiescence maintenance (Scott et al., 2019; Contreras, 2020).

is associated with vessels and fibrotic tissues. Concurrently, a smaller proportion was identified in adipogenic regions following HLI, which indicates that ischemia primarily primes their fate toward a fibrogenic phenotype. In summary, PDGFR α + FAPs are required for muscle repair after HLI by actively remodeling ECM and supporting neovascularization.

Potentially, PDGFR α + lineage-derived myofibroblasts are not the only players in stromal fibroproliferative-disorders and scarring. The participation of other tissue-resident perivascular cells (e.g., pericytes) or immune cells (e.g., MPs) to matrix remodeling upon injury, and the establishment of permanent scars, cannot be excluded (Henderson et al., 2013; Mederacke et al., 2013; Lemos and Duffield, 2018; Van Caam et al., 2018;

Pakshir et al., 2020). For example, in tissues different from skeletal muscle (e.g., kidney), perivascular ADAM12+ progenitors that differentiate toward a myofibroblast-like phenotype when treated with TGF-β also contribute to tissue regeneration and fibrotic scarring following damage (Armulik et al., 2011; Lebleu et al., 2013; Birbrair et al., 2014). In skeletal muscles, Dulauroy et al. (2012) added a piece to the puzzle by characterizing both fetal and adult ADAM12+ progenitors. Postnatally, ADAM12+ cells represent two distinct populations of cells; NCC-derived Schwann cells (S100+) and perivascular PDGFRβ expressing pericytes (Dulauroy et al., 2012). Interestingly, even when tissue injury reactivates both subsets of ADAM12+ cells, and they expand accordingly within the muscle interstitium, only

ADAM12⁺-PDGFR β ⁺ perivascular cells -likely pericytes or a FAP subpopulation- but not NCC-derived cells generate myofibroblasts (Dulauroy et al., 2012). Thus, upon acute muscle injury, the ADAM12⁺-derived myofibroblasts are of the mesenchymal lineage but not of the Schwann cell lineage or NCCs-derived. Since ADAM12⁺ progenitors do not differentiate toward other MSC derivatives such as adipocytes, they may have lineage restrictions or represent a subset of pre-committed FAPs into a fibrogenic fate (Dulauroy et al., 2012). Likely, PDGFR α ⁺ and ADAM12⁺ cells merge their lineages to some extent, but PDGFR α ⁺ FAPs are a more broad-spectrum multipotent population.

Similarly, perivascular cells expressing the zinc finger protein Gli1 (also known as glioma-associated oncogene 1) undergo proliferative expansion and generate myofibroblasts after injuring kidney, lung, liver, and heart (Kramann et al., 2015). All the Gli1⁺ cells with CFU-F properties express PDGFR β , but only a tiny fraction of PDGFR β ⁺ cells in tissues and organs are Gli1 expressing cells (Kramann et al., 2015). There is also the possibility that muscle-resident Gli1⁺ cells are a subpopulation of muscle FAP cells. This idea was recently demonstrated by Yao et al. (2021). Lineage tracing of muscle-resident Gli1 expressing cells demonstrated that Gli1⁺ cells correspond to a small subpopulation -about 10 to 15%- of the total Sca1⁺/PDGFR α ⁺ cells in homeostasis (Yao et al., 2021). However, Gli1⁺ cells rapidly expand following notexin muscle injury, and their relative proportion increases to about 40% of the total FAPs 3 days post damage. Accordingly, Gli1⁺ FAPs possess higher clonogenicity (CFU-F frequency) and reduced adipogenesis than Gli1 negative FAPs. Remarkably, the authors also showed that the genetic ablation of Gli1⁺ FAPs delays muscle regeneration. Finally, utilizing single-cell profiling, the authors suggested that Gli1⁺ FAPs preferentially express pro-myogenic and anti-adipogenic genes than Gli1-FAPs. These results strongly suggest differential proliferative and fate capabilities within distinct muscle-resident FAP subpopulations.

CELLULAR ORIGINS OF MUSCLE HETEROTOPIC OSSIFICATION AND CALCIFICATION IN MYOPATHOLOGIES

In normal conditions, muscles do not accumulate ectopic bone or intramuscular calcium deposits. However, muscles of DMD patients and the *mdx* mouse model exhibit intramuscular calcium deposits and bone (Bozycki et al., 2018). When stimulated, PDGFR α ⁺ FAPs efficiently differentiate into the osteogenic lineage *in vitro* (Uezumi et al., 2010; Oishi et al., 2013). An increasing body of evidence suggests that murine and human stromal cells with osteogenic properties accumulate in muscles following injury, BMP2 intramuscular injections, and transplantation (Leblanc et al., 2011; Woszczyzna et al., 2012; Oishi et al., 2013; Eisner et al., 2020). These muscle-resident cells also contribute to bone fracture repair in mice (Glass et al., 2011). It has been previously suggested that these progenitors are the primary source of abnormal formation of ectopic bone in muscles (Dey et al., 2016; Lees-Shepard et al., 2018b). Remarkably, the cells responsible for the rapid expansion of

ectopic bone in fibrodysplasia ossificans progressiva (FOP), a genetic condition caused by mutations in ACTV1R1 that alter the intracellular signaling pathways triggered by ACTIVIN-A, have been identified as FAPs (Dey et al., 2016; Upadhyay et al., 2017; Lees-Shepard et al., 2018a,b). By utilizing lineage-tracing experiments and a BMP2-induced HO, we recently showed that muscle-resident PDGFR α ⁺ FAPs is the predominant cellular source of muscle ectopic ossification (Eisner et al., 2020). Using a parabiosis mice model, we also showed that muscle-resident PDGFR α ⁺ FAPs, and not bone-marrow-derived PDGFR α ⁺ cells, are the cellular source of heterotopic ossicles. Remarkably, DMD primes a osteogenic gene signature in these progenitor cells (Eisner et al., 2020). In addition, Mázala et al. (2020) showed that FAPs accumulate and deposit calcium-rich structures (bone) in higher proportions in a severe muscle disease DMD model D2-*mdx* mice (DBA/2J genetic background) than the mild dystrophic *mdx* mice (C57BL/10 genetic background). The authors also reported that the osteogenic differentiation of FAPs correlates with the level of muscle damage and TGF- β signaling (Mázala et al., 2020). Remarkably, intramuscular injections of a TGF- β signaling pathway inhibitor (ITD-1) blocked FAP accumulation and reduced fibro-calcification and muscle degeneration (Mázala et al., 2020). Others and we supported these findings, showing that FAPs expand and accumulate in relation to the type of muscle injury, TGF- β signaling, and wound scar (Uezumi et al., 2010, 2014; Lemos et al., 2015; Contreras et al., 2016, 2019a; Stepien et al., 2020). However, the reparative cues and signals that regulate bone differentiation of FAPs are unknown.

Collectively, these data strongly suggest three important conclusions: (1) The loss of regenerative muscle potential during myodegeneration leads to a chronic expansion of resident PDGFR α ⁺ FAPs, elevated pro-fibrotic signals, and increased scarring; (2) PDGFR α ⁺ precursor cells display MSC-like multipotency within the osteocyte, chondrocyte, activated fibroblast and myofibroblast, and adipocyte lineages; (3) The muscle microenvironment primarily dictates FAP developmental fate throughout damage-associated cues. In summary, FAP activity and responses are highly contextual, which suggests that signals emanating from the local niche determine their multi-lineage-fate.

Since most of the work related to FAPs biology used models of single or repeated rounds of injury, we propose that further studies should investigate the role of FAPs in atrophy-related pathologies such as aging-related sarcopenia, myasthenia gravis, polytrauma, and neuromuscular disorders.

EMERGING ROLES OF FIBRO-ADIPOGENIC PROGENITORS IN NEUROMUSCULAR DISORDERS AND NERVE TRAUMA

Altered FAP Activation, Fate, and Behavior in Neuromuscular Disorders

The behavior and plasticity of muscle-resident PDGFR α ⁺ FAPs in non-inflammatory or mild-inflammatory muscle perturbations such as mechanical denervation, neuropathies,

amyotrophic lateral sclerosis (ALS), spinal cord injury, and spinal muscular atrophy (SMA) have not been explored until very recently. A typical result of these degenerative neuromuscular disorders is muscle denervation, resulting in the loss of electrical nerve transmission and nerve-associated cues and supplies. Failure of muscle innervation can result from physical compression of nerves, toxins, trauma, diseases, aging, or surgical interventions (Slater and Schiaffino, 2008). The significant outcomes of sustained muscle denervation are the partial or complete loss of movement and control of the denervated muscle group, and lastly, increased muscle atrophy and loss of tissue homeostasis (Batt et al., 2006). Along with capillary density reduction, skeletal muscle also undergoes an inexorable course of myofiber replacement by fibro-fatty tissue in the absence of innervation (Gatchalian et al., 1989; Fadic et al., 1990; Dulor et al., 1998; Borisov et al., 2001; Carlson, 2014). Remarkably, complex tissue regeneration following digit tip amputation requires innervation (Johnston et al., 2016; Carr et al., 2019).

Denervation also hinders proper skeletal muscle regeneration upon toxin-induced injury, and transection of the sciatic nerve worsens the repair of dystrophic hind limb muscles in mice (Pessina et al., 2014). Interestingly, compared to models of acute or chronic muscle injuries, denervation does not activate a noticeable initial inflammatory response or abundant mononuclear infiltration of immune cells (Contreras et al., 2016; Madaro et al., 2018; Rebolledo et al., 2019). PDGFR α + FAPs proliferate and expand under these mild models of skeletal muscle damage, although to a lesser extent than in acute injuries (Contreras et al., 2016, 2019a; Malecova et al., 2018; Rebolledo et al., 2019). Sciatic nerve transection causes an early sustained activation and expansion of hind limb PDGFR α + FAPs, correlating with increased TGF- β levels and ECM production and deposition from day two after peripheral nerve injury (Gatchalian et al., 1989; Contreras et al., 2016, 2019a; Rebolledo et al., 2019).

Additionally, we showed that FAPs accumulate in ECM-rich areas of atrophied muscles of the post-symptomatic ALS mice model (hSOD1^{G93A}) (Gonzalez et al., 2017). Therefore, we can arguably speculate that PDGFR α + cells are responsive to weak damage stimuli and elicit early responses to maintain tissue homeostasis and regeneration upon nerve-related perturbations. Central to this idea, Madaro et al. (2018) demonstrated that PDGFR α + cells from denervated muscles have a different gene signature than cardiotoxin-derived cells, suggesting that FAP cellular and molecular responses differ from one model of injury to another. They also showed that *in vivo* treatment with a neutralizing IL-6 antibody or the inhibition of STAT3-dependent signaling using a pharmacological inhibitor prevented tissue atrophy and fibrosis in different mice models of muscle denervation. Thus, their work suggests that a FAP-driven cascade that involves IL-6-STAT3 activation can act as an initiator of muscle dysfunction by promoting fibrosis, and possibly myofiber atrophy, in denervated muscles, spinal cord injury, SMA, and ALS. These discoveries support the notion that PDGFR α + FAPs act as tissue-disturbance sensors and open new avenues for developing cellular specific targets for non-inflammatory or

mild-inflammatory neuromuscular disorders and for treating denervation-induced fibro-fatty deposition.

Although Madaro et al. (2018) observed no changes in the number of muscle infiltrating CD45+ cells after denervation, perhaps it would be interesting to evaluate the functional state of inflammatory cells such as neutrophils, eosinophils, natural killer cells, etc., which we know are required for proper skeletal muscle regeneration. Indeed, we think that regardless of whether there is or not an alteration in the number of these immune cells, changes in their activation status could be sufficient to induce an effect on the behavior and plasticity of FAPs. Moreover, we hypothesize that even a small level of immune activation in muscles after denervation (Hanwei and Zhao, 2010) or ALS (Gasco et al., 2017; Wang et al., 2017) could affect the quiescence of PDGFR α + FAPs. Future work should concentrate on studying the role of the immune compartment or inflammatory-related pathways on neuromuscular disorders' pathological features and their influence on FAP activation and fate.

We also raised the old-fashion hypothesis that a response of FAPs to denervation could be necessary to support efficient reinnervation. FAPs may assist and coordinate the attraction of axons toward specialized interstitial sites near to denervated myofibers -perisynaptic regions of neuromuscular junctions (NMJ)- by producing deposits of adhesive ECM molecules (e.g., n-cam, tenascin, fibronectin, and proteoglycans) (Covault and Sanes, 1985; Gatchalian et al., 1989; Court et al., 2008). The regenerative role of these nerve-associated cells is important since they are active contributors to the amputated digit tip (Johnston et al., 2016; Carr et al., 2019) and actively regulate muscle-nerve homeostasis, NMJ integrity, and Schwann cell behavior (Uezumi et al., 2021). Thus, upcoming research should also identify the cues involved in FAP activation after nerve trauma or neuromuscular disorders. We speculate that alterations of NMJ architecture, loss of nerve-associated factors, or even the absence of electrical stimulation could be playing a central role in determining the early activation of the stromal compartment in neuromuscular disorders.

FAP-Mediated Fibro-Fatty Degeneration in Rotator Cuff Tears

The rotator cuff is an array of different muscles and tendons surrounding the shoulder joint giving support to the upper arm and shoulder. Rotator cuff tear (RCT) injury is a common cause of pain and disability among adults and the elderly, leading to increased shoulder dysfunction prevalence (Yamamoto et al., 2010). Rotator cuff damage can result from either acute or chronic injury to the shoulder or progressive degeneration of the tendon and myotendinous tissue, the magnitude of which influences the extension and severity of rotator cuff disease (Laron et al., 2012). Functional impairment of the cuff muscles following RCTs is associated with the degree of muscular degeneration, atrophy, and fibro-fatty infiltration (Meyer et al., 2004). These myodegeneration hallmarks increase accordingly with the size of tears and aging (Laron et al., 2012). The functional and clinical outcomes of patients undergoing RCT surgical repair also correlates with fibrosis, fatty infiltration,

and atrophy of the *spinatus* muscles (Barry et al., 2013). Thus, poor functional outcomes result from massive tears in RCT patients who develop fibro-fatty deposition and muscle atrophy. No cure or effective treatments for these muscle pathologies are available to date.

Recent studies describe an increase of FAP number within RCT affected muscles. Indeed, FAPs and TIE2+ cells were initially proposed to be the cellular source of fibrosis and fat during this sustained muscle disease (Liu et al., 2016). Recently, the work led by Jensen et al. (2018) confirmed that the subpopulation of PDGFR β + cells that were PDGFR α + contribute to fibro-fatty deposition in a severe murine model of RCT. At the molecular level, increased TGF- β signaling and ECM expression are associated with muscle pathology in RCT murine models (Liu et al., 2014). As previously described, damage-induced TGF- β promotes fibrosis by modulating the behavior, fate, and plasticity of muscle-resident PDGFR α + FAPs. In this context, Davies et al. (2016) demonstrated that TGF- β signaling inhibition utilizing the SB431542 drug reduced fibro-fatty infiltration of RCT muscles. A significant reduction of PDGFR α + FAPs preceded the decreased fibro-fatty accumulation after *in vivo* treatment with SB431542, which again points to the pro-survival and mitogenic actions of the TGF- β pathway in FAPs (Davies et al., 2016).

Similarly, Shirasawa et al. (2017), by generating a new RCT mouse model of enhanced fibro-fatty infiltration, observed that denervation dramatically exacerbated RCT muscle pathology of the transected suprascapular muscle. The authors confirmed that FAPs expand in this novel RCT model and reported that the treatment with imatinib, a first-generation tyrosine kinase inhibitor, significantly diminishes muscle fatty infiltration (Shirasawa et al., 2017). These results agree with our previous studies showing that nilotinib ameliorates muscular dystrophy disease by inducing FAP death (Lemos et al., 2015; Fiore et al., 2016). TGF- β and PDGFR α pathways are two central transduction cascades governing connective tissue biology and fibrosis (Kim et al., 2018; Smith and Barton, 2018; Contreras et al., 2019a). Interestingly, both imatinib and nilotinib are potent inhibitors of PDGFR α and TGF- β signaling and the downstream mediator mitogen-activated protein kinase (MAPK) p38 (Lemos et al., 2015; Contreras et al., 2018; Theret et al., 2021). Besides, we recently reported a functional cross-talk between TGF- β and PDGFR α involved in regulating the biology of tissue-resident PDGFR α + cells (Contreras et al., 2019a). TGF- β negatively regulated the expression of PDGFR α in these cells, whereas PDGFR α signaling modulated TGF- β -mediated cellular and molecular effects (Contreras et al., 2019a). As for TGF- β , ILs are also known for being inflammatory mediators and appear to participate in RCT pathology. The expression of IL-15 positively correlates with the severity of ECM deposition, fibrosis, and FAP expansion in patients with chronic RCT (Kang et al., 2018). In conjunction, these data suggest active intercellular communication between immune cells and PDGFR α + lineage cells in RCT disease. However, how interactions between these two populations of cells regulate RCT disease and fibro-fatty development remains unknown and warrants further investigations.

Interestingly, the distribution of PDGFR α + FAPs is non-homogeneous between different muscle groups, and their anatomical locations seem to determine FAP expansion and behavior upon injury (Contreras et al., 2019a; Lee et al., 2020a). Interestingly, the RC *spinatus* muscle contains more FAPs per gram of tissue, and these cells show enhanced adipogenic and proliferative capacity compared to tibialis anterior- or gastrocnemius-derived FAPs, possibly explaining the increased propensity of *spinatus* muscles to form adipose tissue following RCT (Barry et al., 2013; Lee et al., 2020a). Hence, differences in the quantity and quality of PDGFR α + FAPs at steady-state levels may reflect their heterogeneity and plasticity following damage. These findings are also consistent with a model where the variation in FAP content between muscle groups is explained by the same intrinsic and extrinsic determining factors that influence FAP behavior following chronic and persistent injury. Remarkably, two recent similar studies suggested that intramuscular cell transplantation of UCP1+ FAPs into a denervated RC tendon tear model enhanced vascularization, myofiber size, and mitigated atrophy of the RCT affected muscle, whereas reducing fatty deposition and myodegeneration (Lee et al., 2020b,c). The amelioration of massive RCT pathology by PDGFR α + cell transplantation correlates with improved muscle quality and shoulder function after RC repair (Lee et al., 2020b,c). Thus, the first preclinical approaches using PDGFR α + FAP cultures for muscle repair in rotator cuff tears suggest safety and potential efficacy, although the action mechanisms are still unclear.

In summary, these studies further demonstrate that PDGFR α + FAPs are the primary cell source of the fibrous and fat tissues found in RCT disease. They also suggest the presence of PDGFR α + cell subpopulations that favor either permanent scar formation or successful regeneration. These studies also suggest that fibro-adipogenic progenitors are promising candidates for cellular therapy to increase vascularization and insufficient repair of patients with advanced RCT disease or muscle ischemia.

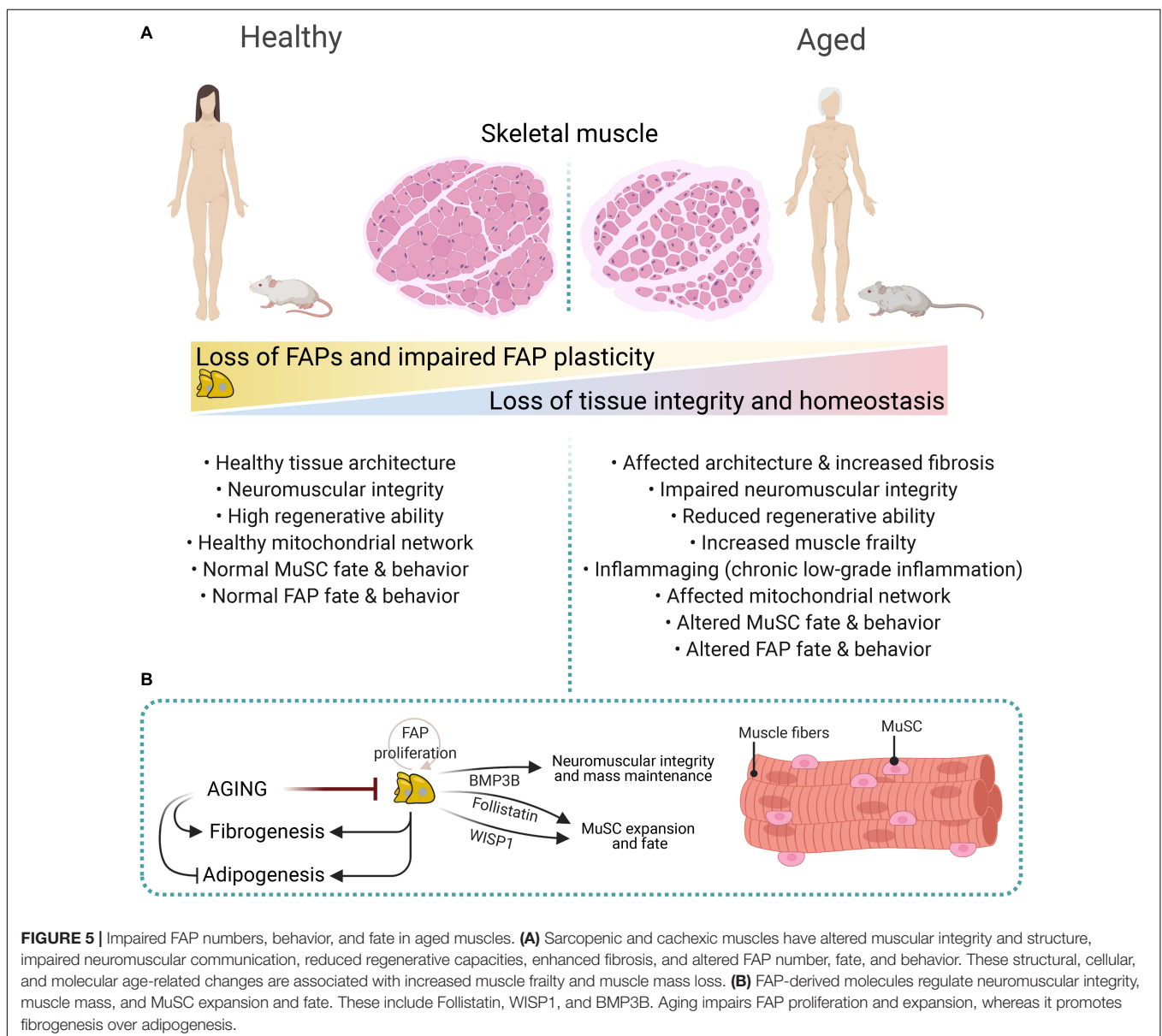
ALTERED FATE AND NUMBER OF MUSCLE FIBRO-ADIPOGENIC PROGENITORS IN AGING

The regenerative potential of muscles declines with age and associates with increased fibrosis and low-grade chronic inflammation (**Figure 5A**) (Brack et al., 2007; Brack and Rando, 2008; Etienne et al., 2020; Rahman et al., 2020). Impaired muscle stem cell fate and behavior, growth factors availability, altered stem cell niche, ECM composition and stiffness, loss of youthful systemic factors, and intrinsic molecular changes in muscle-resident cells are also associated with reduced muscle mass and increased atrophy, and tissue frailty with age (**Figure 5A**) (Etienne et al., 2020; Muñoz-Cánoves et al., 2020). Besides, aging primes FAPs to a fibrogenic state (Mueller et al., 2016; Lukjanenko et al., 2019). Recently, Lukjanenko et al. (2019) showed that aged FAPs have reduced proliferative capacity and adipogenic potential compared to young FAPs. Remarkably, the enhanced adipogenesis of cultured

young *mdx*-FAPs is also reduced in aged *mdx*-FAPs (Mozzetta et al., 2013). Lukjanenko et al. (2019) also showed that the aberrant secretion of ECM-related molecules from PDGFR α + cells during aging, particularly the reduced production of the matricellular protein CCN4/WISP1 (Cellular Communication Network Factor 4, WNT1-Inducible-Signaling Pathway Protein 1), disrupts MuSC behaviour and therefore, impairs muscle regeneration in old mice (Figure 5B). Notably, *in vivo* treatment of aged muscles subjected to acute injury with recombinant WISP1 increased the early proliferation of aged MuSCs and commitment of Pax7+/MyoD+ MuSCs, whereas it enhanced the proportion of newly formed myofibers and improved muscle architecture and myofiber cross-sectional area (Figure 5B) (Lukjanenko et al., 2019). Hence, systemic WISP1 administration ameliorates the impaired regenerative potential of

aged muscles suggesting that FAP-secreted molecules could serve as potential therapeutics to boost the endogenous regenerative potential of muscles.

Aged muscles have reduced numbers of muscle-resident FAPs, and individual aged FAPs show decreased expression of PDGFR α compared to young counterparts (Figure 5B) (Uezumi et al., 2021). Reduced expression of PDGFR α in muscle and heart FAPs is also seen after damage (Contreras et al., 2019a; Soliman et al., 2020). Notably, FAP-derived Bone Morphogenetic Protein 3B (BMP3B, also known as Growth/Differentiation Factor-10, GDF10) has pleiotropic effects on muscle myofibers and Schwann Cells by stimulating hypertrophic signaling pathways and Schwann cell characteristics, which positively influences NMJ stability and muscle integrity (Uezumi et al., 2021). These results strongly suggest that



aging-related changes influence FAPs' homeostatic supportive role (Figure 5). Hence, the modulation of FAP-derived cues offers excellent therapeutic potential for combating muscle cachexia and sarcopenia.

Mozzetta et al. (2013), utilizing co-culture experiments between MuSCs and FAPs, showed that aging impairs the *mdx*-FAP-stimulated formation of MuSC-derived multinucleated myotubes. The authors also corroborated *in vivo* that the co-transplantation of FAPs improved the engraftment potential of MuSC as well as muscle regeneration into old *mdx* mice. The authors suggested that FAP-derived Follistatin mediates their pro-myogenic effects on MuSCs, which is enhanced by treatment with HDACi (Figure 5B) (Mozzetta et al., 2013). Mechanistically, the HDACi-mediated pro-regenerative muscle effects seem to involve a FAP-mediated release and transfer of miRNA-containing extracellular vesicles to support MuSCs and other cell types (Mozzetta et al., 2013; Sandonà et al., 2020). Taken together, these results suggest that despite the central role of muscle stem cells in mediating the regenerative potential of muscles and its loss during aging (Cosgrove et al., 2014; Sousa-Victor et al., 2015), muscle-resident FAPs also exert a significant influence on regenerative failure with aging. The extrinsic cues or intrinsic molecular determinants that affect these stromal progenitor cells as the body and muscle tissue age are unknown to date.

DISCUSSION

Normal muscle regeneration occurs in a complex and tightly regulated sequence of overlapping phases involving loss of homeostasis, inflammation, proliferation, tissue remodeling, and damage resolution. The connective tissue performs central functions at all these stages through its structural role as well as the matrix-building, remodeling, and secretory activities of its cells. Nevertheless, muscle pathology, disease, fibrosis, and aging compromise these coordinated responses and leads to progressive and permanent scarring and tissue failure. Over the past decades, significant efforts have been made to identify and characterize the cells responsible for forming the wound scar or interstitial fibrosis within muscles. The significant outcome has been the molecular and functional characterization of a population of PDGFR α expressing cells known as fibro-adipogenic progenitors. However, several outstanding questions remain open within the field (Box 2). For example, how are FAP phenotype and function regulated spatiotemporally as skeletal muscle chronic damage, muscle degeneration, and aging-related sarcopenia and cachexia progress? What role(s) do FAPs play in regulating the onset and progression of neuromuscular disease? How does the interaction of FAPs and nerve cells affect muscle, nerve, and tissue integrity? In homeostatic settings, how is the cross-talk between immune cells and FAPs regulated? Can muscle-resident FAPs or subpopulations of them be therapeutically targeted to slow or prevent muscle degeneration and fibro-fatty-bone infiltration? Addressing these should enhance our knowledge about the biology behind

BOX 2 | Outstanding questions.

- (1) Do all FAPs originate from a common lineage during development? If not, which cell types can transition into FAPs?
- (2) How are FAP phenotype and function spatiotemporally regulated during the progression of skeletal muscle chronic damage, muscle degeneration, and aging-related sarcopenia and cachexia?
- (3) What is the role(s) of FAPs in regulating neuromuscular disease onset and progression? How does FAPs-nerve cell communication impact muscle, nerve, and tissue integrity?
- (4) How is the cross-talk between immune cells and FAPs regulated in homeostatic conditions?
- (5) Can the mapping of the molecular landscape of FAPs help us identify FAP-dependent pro-regenerative or pro-degenerative pathways?
- (6) Can muscle-resident FAPs or sub-populations of them be targeted therapeutically to delay or affect muscle degeneration and fibro-fatty-bone infiltration?
- (7) Can specific FAP sub-populations offer therapeutic windows in pathology and disease?

muscle FAPs and improve our current cell-based regenerative approaches and pharmacological treatments for debilitating muscle diseases and pathology.

PDGFR α + fibro-adipogenic progenitors are essential mediators of successful skeletal muscle regeneration and participate in tissue homeostasis and integrity. A growing body of evidence supports the hypothesis that the *in vivo* expansion and differentiation of FAPs mostly depends on the tissue environment, and thus, is extrinsically dictated by the surrounding niche. The notions of PDGFR α + FAP cells with intrinsic pro-regenerative, pro-inflammatory, and pro-fibrotic roles parallel their cell heterogeneity and fate. Nevertheless, their dysregulated activity directly leads to tissue scarring in muscle ischemia, pathology, neuromuscular disorders, and aging. Understanding FAP physiology will lead to significant advances in comprehending the pathogenesis of muscle fibrosis and exploring new therapeutic options for treating debilitating diseases in which permanent scars tip the balance to tissue malfunctioning and organ failure.

AUTHOR CONTRIBUTIONS

MT and OC conceived, designed, and drafted the manuscript and figures. FR edited and reviewed the manuscript. All authors read and approved the final version of the manuscript prior to submission.

FUNDING

This work was supported by Comisión Nacional de Ciencia y Tecnología CONICYT Beca Doctorado Nacional 2014 folio 21140378 "National Doctorate Fellowship," by Centro Basal de Excelencia en Envejecimiento y Regeneración (CONICYT-AFB 170005), and by the Victor Chang Cardiac Research Institute to OC; by Fondation pour la Recherche Médicale (FRM, 40248), by the European Molecular Biology Organization (EMBO, ALTF

115–2016), by the Association contre les Myopathies (AFM, 22576), and by Michael Smith Foundation for Health Research (MSFHR, 18351) to MT; and by the Canadian Institutes of Health Research (CIHR-FDN-159908) to FR. The funding agencies had no role in the review's design, data collection, and analysis, the decision to publish, or the preparation of the manuscript.

REFERENCES

Abramowitz, M. K., Paredes, W., Zhang, K., Brightwell, C. R., Newsom, J. N., Kwon, H. J., et al. (2018). Skeletal muscle fibrosis is associated with decreased muscle inflammation and weakness in patients with chronic kidney disease. *Am. J. Physiol. Ren. Physiol.* 315, F1658–F1669. doi: 10.1152/ajprenal.00314.2018

Acuña, M. J., Pessina, P., Olguin, H., Cabrera, D., Vio, C. P., Bader, M., et al. (2014). Restoration of muscle strength in dystrophic muscle by angiotensin-1-7 through inhibition of TGF- β signalling. *Hum. Mol. Genet.* 23, 1237–1249. doi: 10.1093/hmg/ddt514

Agarwal, S., Loder, S., Brownley, C., Cholok, D., Mangiavini, L., Li, J., et al. (2016). Inhibition of Hif1 α prevents both trauma-induced and genetic heterotopic ossification. *Proc. Natl. Acad. Sci. U.S.A.* 113, E338–E347. doi: 10.1073/pnas.1515397113

Almada, A. E., and Wagers, A. J. (2016). Molecular circuitry of stem cell fate in skeletal muscle regeneration, ageing and disease. *Nat. Rev. Mol. Cell Biol.* 17, 267–279. doi: 10.1038/nrm.2016.7

Armulik, A., Mäe, M., and Betsholtz, C. (2011). Pericytes and the blood-brain barrier: recent advances and implications for the delivery of CNS therapy. *Ther. Deliv.* 2, 419–422. doi: 10.4155/tde.11.23

Arnold, L., Henry, A., Poron, F., Baba-Amer, Y., Van Rooijen, N., Plonquet, A., et al. (2007). Inflammatory monocytes recruited after skeletal muscle injury switch into antiinflammatory macrophages to support myogenesis. *J. Exp. Med.* 204, 1057–1069. doi: 10.1084/jem.20070075

Bachman, J. F., Klose, A., Liu, W., Paris, N. D., Blanc, R. S., Schmalz, M., et al. (2018). Prepubertal skeletal muscle growth requires pax7-expressing satellite cell-derived myonuclear contribution. *Development* 145:dev167197. doi: 10.1242/dev.167197

Barry, J. J., Lansdown, D. A., Cheung, S., Feeley, B. T., and Ma, C. B. (2013). The relationship between tear severity, fatty infiltration, and muscle atrophy in the supraspinatus. *J. Shoulder Elb. Surg.* 22, 18–25. doi: 10.1016/j.jse.2011.12.014

Batt, J., Bain, J., Goncalves, J., Michalski, B., Plant, P., Fahnestock, M., et al. (2006). Differential gene expression profiling of short and long term denervated muscle. *FASEB J.* 20, 115–117. doi: 10.1096/fj.04-3640fje

Bentzinger, C. F., Wang, Y. X., Dumont, N. A., and Rudnicki, M. A. (2013). Cellular dynamics in the muscle satellite cell niche. *EMBO Rep.* 14, 1062–1072. doi: 10.1038/embor.2013.182

Biferali, B., Proietti, D., Mozzetta, C., and Madaro, L. (2019). Fibro-adipogenic progenitors cross-talk in skeletal muscle: the social network. *Front. Physiol.* 10:1074. doi: 10.3389/fphys.2019.01074

Biltz, N. K., Collins, K. H., Shen, K. C., Schwartz, K., Harris, C. A., and Meyer, G. A. (2020). Infiltration of intramuscular adipose tissue impairs skeletal muscle contraction. *J. Physiol.* 598, 2669–2683. doi: 10.1113/JP279595

Biltz, N. K., and Meyer, G. A. (2017). A novel method for the quantification of fatty infiltration in skeletal muscle. *Skelet. Muscle* 7:1. doi: 10.1186/s13395-016-0118-2

Birbrair, A., Zhang, T., Wang, Z. M., Messi, M. L., Mintz, A., and Delbono, O. (2014). Pericytes: multitasking cells in the regeneration of injured, diseased, and aged skeletal muscle. *Front. Aging Neurosci.* 6:245. doi: 10.3389/fnagi.2014.00245

Blau, H. M., Cosgrove, B. D., and Ho, A. T. V. (2015). The central role of muscle stem cells in regenerative failure with aging. *Nat. Med.* 21, 854–862. doi: 10.1038/nm.3918

Borisov, A. B., Dedkov, E. I., and Carlson, B. M. (2001). Interrelations of myogenic response, progressive atrophy of muscle fibers, and cell death in denervated skeletal muscle. *Anat. Rec.* 264, 203–218. doi: 10.1002/ar.1155

ACKNOWLEDGMENTS

OC acknowledges Matthew Maartensz for comments on the manuscript. **Figures 1, 2, 5** were created with BioRender.com. **Figures 3, 4** were created using Keynote (Apple Inc.) for macOS.

Borthwick, L. A., Wynn, T. A., and Fisher, A. J. (2013). Cytokine mediated tissue fibrosis. *Biochim. Biophys. Acta Mol. Basis Dis.* 1832, 1049–1060. doi: 10.1016/j.bbdis.2012.09.014

Bosnakovski, D., Chan, S. S. K., Recht, O. O., Hartweck, L. M., Gustafson, C. J., Athman, L. L., et al. (2017). Muscle pathology from stochastic low level DUX4 expression in an FSHD mouse model. *Nat. Commun.* 8:856. doi: 10.1038/s41467-017-00730-1

Bosnakovski, D., Shams, A. S., Yuan, C., da Silva, M. T., Ener, E. T., Baumann, C. W., et al. (2020). Transcriptional and cytopathological hallmarks of FSHD in chronic DUX4-expressing mice. *J. Clin. Invest.* 130, 2465–2477. doi: 10.1172/JCI133303

Bozycycki, L., Lukaszewicz, K., Matryba, P., and Pikula, S. (2018). Whole-body clearing, staining and screening of calcium deposits in the mdx mouse model of Duchenne muscular dystrophy. *Skelet. Muscle* 8:21. doi: 10.1186/s13395-018-0168-8

Brack, A. S., Conboy, M. J., Roy, S., Lee, M., Kuo, C. J., Keller, C., et al. (2007). Increased Wnt signaling during aging alters muscle stem cell fate and increases fibrosis. *Science* 317, 807–810. doi: 10.1126/science.1144090

Brack, A. S., and Rando, T. A. (2008). “Age-dependent changes in skeletal musculeregeneration,” in *Skeletal Muscle Repair and Regeneration*, eds S. Schiaffino and T. Partridge (Berlin: Springer), 359–374.

Brandan, E., Fuentes, M. E., and Andrade, W. (1992). Decorin, a chondroitin/dermatan sulfate proteoglycan is under neural control in rat skeletal muscle. *J. Neurosci. Res.* 32, 51–59. doi: 10.1002/jnr.490320107

Brigitte, M., Schilte, C., Plonquet, A., Baba-Amer, Y., Henri, A., Charlier, C., et al. (2010). Muscle resident macrophages control the immune cell reaction in a mouse model of notexin-induced myoinjury. *Arthrit. Rheum.* 62, 268–279. doi: 10.1002/art.27183

Buras, E. D., Converso-Baran, K., Davis, C. S., Akama, T., Hikage, F., Michele, D. E., et al. (2019). Fibro-adipogenic remodeling of the diaphragm in obesity-associated respiratory dysfunction. *Diabetes Metab. Res. Rev.* 68, 45–56. doi: 10.2337/db18-0209

Cáceres, S., Cuellar, C., Casar, J. C., Garrido, J., Schaefer, L., Kresse, H., et al. (2000). Synthesis of proteoglycans is augmented in dystrophic mdx mouse skeletal muscle. *Eur. J. Cell Biol.* 79, 173–181. doi: 10.1078/S0171-9335(04)70020-5

Carlson, B. M. (2014). The biology of long-term denervated skeletal muscle. *Eur. J. Transl. Myol.* 24:3293. doi: 10.4081/ejtm.2014.3293

Carr, M. J., Toma, J. S., Johnston, A. P. W., Steadman, P. E., Yuzwa, S. A., Mahmud, N., et al. (2019). Mesenchymal precursor cells in adult nerves contribute to mammalian tissue repair and regeneration. *Cell Stem Cell* 24, 240.e9–256.e9. doi: 10.1016/j.stem.2018.10.024

Castets, P., Bertrand, A. T., Beuvin, M., Ferry, A., Le Grand, F., Castets, M., et al. (2011). Satellite cell loss and impaired muscle regeneration in selenoprotein N deficiency. *Hum. Mol. Genet.* 20, 694–704. doi: 10.1093/hmg/ddq515

Castiglioni, A., Corna, G., Rigamonti, E., Basso, V., Vezzoli, M., Monno, A., et al. (2015). FOXP3+ T cells recruited to sites of sterile skeletal muscle injury regulate the fate of satellite cells and guide effective tissue regeneration. *PLoS One* 10:e0128094. doi: 10.1371/journal.pone.0128094

Cattaneo, P., Mukherjee, D., Spinozzi, S., Zhang, L., Larcher, V., Stallcup, W. B., et al. (2020). Parallel lineage-tracing studies establish fibroblasts as the prevailing in vivo adipocyte progenitor. *Cell Rep.* 30, 571.e2–582.e2. doi: 10.1016/j.celrep.2019.12.046

Chapman, M. A., Mukund, K., Subramaniam, S., Brenner, D., and Lieber, R. L. (2016). Three distinct cell populations express extracellular matrix proteins and increase in number during skeletal muscle fibrosis. *Am. J. Physiol. Cell Physiol.* 312, C131–C143. doi: 10.1152/ajpcell.00226.2016

Chazaud, B. (2020). Inflammation and skeletal muscle regeneration: leave it to the macrophages! *Trends Immunol.* 41, 481–492. doi: 10.1016/j.it.2020.04.006

- Chen, W. Y., Zeng, X., Carter, M. G., Morrell, C. N., Chiu Yen, R. W., Esteller, M., et al. (2003). Heterozygous disruption of *Hic1* predisposes mice to a gender-dependent spectrum of malignant tumors. *Nat. Genet.* 33, 197–202. doi: 10.1038/ng1077
- Cheng, M., Nguyen, M. H., Fantuzzi, G., and Koh, T. J. (2008). Endogenous interferon- γ is required for efficient skeletal muscle regeneration. *Am. J. Physiol. Cell Physiol.* 294, C1183–C1191. doi: 10.1152/ajpcell.00568.2007
- Christov, C., Chrétien, F., Abou-Khalil, R., Bassez, G., Vallet, G., Authier, F.-J., et al. (2007). Muscle satellite cells and endothelial cells: close neighbors and privileged partners. *Mol. Biol. Cell* 18, 1397–1409. doi: 10.1091/mbc.e06-08-0693
- Church, J. C. (1970). Cell populations in skeletal muscle after regeneration. *J. Embryol. Exp. Morphol.* 23, 531–537.
- Church, J. C. T., Noronha, R. F. X., and Allbrook, D. B. (1966). Satellite cells and skeletal muscle regeneration. *Br. J. Surg.* 53, 638–642. doi: 10.1002/bjs.1800530720
- Collao, N., Farup, J., and De Lisio, M. (2020). Role of metabolic stress and exercise in regulating fibro/adipogenic progenitors. *Front. Cell Dev. Biol.* 8:9. doi: 10.3389/fcell.2020.00009
- Contreras, O. (2020). *Hic1* deletion unleashes quiescent connective tissue stem cells and impairs skeletal muscle regeneration. *J. Cell Commun. Signal.* 14, 131–133. doi: 10.1007/s12079-019-00545-3
- Contreras, O., Cruz-Soca, M., Theret, M., Soliman, H., Tung, L. W., Groppa, E., et al. (2019a). Cross-talk between TGF- β and PDGFR α signaling pathways regulates the fate of stromal fibro-adipogenic progenitors. *J. Cell Sci.* 132:jcs232157. doi: 10.1242/jcs.232157
- Contreras, O., Rebolledo, D. L., Oyarzún, J. E., Olguín, H. C., and Brandan, E. (2016). Connective tissue cells expressing fibro/adipogenic progenitor markers increase under chronic damage: relevance in fibroblast-myofibroblast differentiation and skeletal muscle fibrosis. *Cell Tissue Res.* 364, 647–660. doi: 10.1007/s00441-015-2343-0
- Contreras, O., Rossi, F. M., and Brandan, E. (2019b). Adherent muscle connective tissue fibroblasts are phenotypically and biochemically equivalent to stromal fibro/adipogenic progenitors. *Matrix Biol. Plus* 2:100006. doi: 10.1016/j.mbplus.2019.04.003
- Contreras, O., Soliman, H., Theret, M., Rossi, F. M. V., and Brandan, E. (2020). TGF- β -driven downregulation of the transcription factor TCF7L2 affects Wnt/ β -catenin signaling in PDGFR α fibroblasts. *J. Cell Sci.* 133:jcs242297. doi: 10.1242/jcs.242297
- Contreras, O., Villarreal, M., and Brandan, E. (2018). Nilotinib impairs skeletal myogenesis by increasing myoblast proliferation. *Skelet. Muscle* 8:5. doi: 10.1186/s13395-018-0150-5
- Cooke, J. P., and Losordo, D. W. (2015). Modulating the vascular response to limb ischemia: angiogenic and cell therapies. *Circ. Res.* 116, 1561–1578. doi: 10.1161/CIRCRESAHA.115.303565
- Cosgrove, B. D., Gilbert, P. M., Porpiglia, E., Mourkioti, F., Lee, S. P., Corbel, S. Y., et al. (2014). Rejuvenation of the muscle stem cell population restores strength to injured aged muscles. *Nat. Med.* 20, 255–264. doi: 10.1038/nm.3464
- Court, F. A., Gillingwater, T. H., Melrose, S., Sherman, D. L., Greenshields, K. N., Morton, A. J., et al. (2008). Identity, developmental restriction and reactivity of extralaminar cells capping mammalian neuromuscular junctions. *J. Cell Sci.* 121, 3901–3911. doi: 10.1242/jcs.031047
- Covault, J., and Sanes, J. R. (1985). Neural cell adhesion molecule (N-CAM) accumulates in denervated and paralyzed skeletal muscles. *Proc. Natl. Acad. Sci. U.S.A.* 82, 4544–4548. doi: 10.1073/pnas.82.13.4544
- Dadgar, S., Wang, Z., Johnston, H., Kesari, A., Nagaraju, K., Chen, Y. W., et al. (2014). Asynchronous remodeling is a driver of failed regeneration in Duchenne muscular dystrophy. *J. Cell Biol.* 207, 139–158. doi: 10.1083/jcb.201402079
- Davies, M. R., Liu, X., Lee, L., Laron, D., Ning, A. Y., Kim, H. T., et al. (2016). TGF- β small molecule inhibitor sb431542 reduces rotator cuff muscle fibrosis and fatty infiltration by promoting fibro/adipogenic progenitor apoptosis. *PLoS One* 11:e0155486. doi: 10.1371/journal.pone.0155486
- Deasy, B. M., Feduska, J. M., Payne, T. R., Li, Y., Ambrosio, F., and Huard, J. (2009). Effect of VEGF on the regenerative capacity of muscle stem cells in dystrophic skeletal muscle. *Mol. Ther.* 17, 1788–1798. doi: 10.1038/mt.2009.136
- Dey, D., Bagarova, J., Hatsell, S. J., Armstrong, K. A., Huang, L., Ermann, J., et al. (2016). Two tissue-resident progenitor lineages drive distinct phenotypes of heterotopic ossification. *Sci. Transl. Med.* 8:366ra163. doi: 10.1126/scitranslmed.aaf1090
- Deyhle, M. R., and Hyldahl, R. D. (2018). The role of T lymphocytes in skeletal muscle repair from traumatic and contraction-induced injury. *Front. Physiol.* 9:768. doi: 10.3389/fphys.2018.00768
- Dong, J., Dong, Y., Chen, Z., Mitch, W. E., and Zhang, L. (2017). The pathway to muscle fibrosis depends on myostatin stimulating the differentiation of fibro/adipogenic progenitor cells in chronic kidney disease. *Kidney Int.* 91, 119–128. doi: 10.1016/j.kint.2016.07.029
- Dong, Y., Silva, K. A. S., Dong, Y., and Zhang, L. (2014). Glucocorticoids increase adipocytes in muscle by affecting IL-4 regulated FAP activity. *FASEB J.* 28, 4123–4132. doi: 10.1096/fj.14-254011
- Drouin, G., Couture, V., Lauzon, M. A., Balg, F., Faucheux, N., and Grenier, G. (2019). Muscle injury-induced hypoxia alters the proliferation and differentiation potentials of muscle resident stromal cells. *Skelet. Muscle* 9:18. doi: 10.1186/s13395-019-0202-5
- Dulauroy, S., Di Carlo, S. E., Langa, F., Eberl, G., and Peduto, L. (2012). Lineage tracing and genetic ablation of ADAM12 + perivascular cells identify a major source of profibrotic cells during acute tissue injury. *Nat. Med.* 18, 1262–1270. doi: 10.1038/nm.2848
- Dulor, J. P., Cambon, B., Vigneron, P., Reyne, Y., Nougues, J., Castella, L., et al. (1998). Expression of specific white adipose tissue genes in denervation-induced skeletal muscle fatty degeneration. *FEBS Lett.* 439, 89–92. doi: 10.1016/S0014-5793(98)01216-2
- Eisner, C., Cummings, M., Johnston, G., Tung, L. W., Groppa, E., Chang, C., et al. (2020). Murine tissue-resident PDGFR α fibro-adipogenic progenitors spontaneously acquire osteogenic phenotype in an altered inflammatory environment. *J. Bone Miner. Res.* 35, 1525–1534. doi: 10.1002/jbmr.4020
- El Agha, E., Kramann, R., Schneider, R. K., Li, X., Seeger, W., Humphreys, B. D., et al. (2017). Mesenchymal stem cells in fibrotic disease. *Cell Stem Cell* 21, 166–177. doi: 10.1016/j.stem.2017.07.011
- Etienne, J., Liu, C., Skinner, C. M., Conboy, M. J., and Conboy, I. M. (2020). Skeletal muscle as an experimental model of choice to study tissue aging and rejuvenation. *Skelet. Muscle* 10:4. doi: 10.1186/s13395-020-0222-1
- Fadic, R., Brandan, E., and Inestrosa, N. C. (1990). Motor nerve regulates muscle extracellular matrix proteoglycan expression. *J. Neurosci.* 10, 3516–3523. doi: 10.1523/jneurosci.10-11-03516.1990
- Fadic, R., Mezzano, V., Alvarez, K., Cabrera, D., Holmgren, J., and Brandan, E. (2006). Increase in decorin and biglycan in Duchenne muscular dystrophy: role of fibroblasts as cell source of these proteoglycans in the disease. *J. Cell. Mol. Med.* 10, 758–769. doi: 10.1111/j.1582-4934.2006.tb00435.x
- Farup, J., De Lisio, M., Rahbek, S. K., Bjerre, J., Vendelbo, M. H., Boppert, M. D., et al. (2015). Pericyte response to contraction mode-specific resistance exercise training in human skeletal muscle. *J. Appl. Physiol.* 119, 1053–1063. doi: 10.1152/jappphysiol.01108.2014
- Farup, J., Just, J., de Paoli, F., Lin, L., Jensen, J. B., Billeskov, T., et al. (2020). Human skeletal muscle CD90+ fibro-adipogenic progenitors are associated with muscle degeneration in type 2 diabetic patients. *bioRxiv* [Preprint]. doi: 10.1101/2020.08.25.243907
- Fiore, D., Judson, R. N., Low, M., Lee, S., Zhang, E., Hopkins, C., et al. (2016). Pharmacological blockage of fibro/adipogenic progenitor expansion and suppression of regenerative fibrogenesis is associated with impaired skeletal muscle regeneration. *Stem Cell Res.* 17, 161–169. doi: 10.1016/j.scr.2016.06.007
- Fry, C. S., Johnson, D. L., Ireland, M. L., and Noehren, B. (2017). ACL injury reduces satellite cell abundance and promotes fibrogenic cell expansion within skeletal muscle. *J. Orthop. Res.* 35, 1876–1885. doi: 10.1002/jor.23502
- Fry, C. S., Lee, J. D., Mula, J., Kirby, T. J., Jackson, J. R., Liu, F., et al. (2015). Inducible depletion of satellite cells in adult, sedentary mice impairs muscle regenerative capacity without affecting sarcopenia. *Nat. Med.* 21, 76–80. doi: 10.1038/nm.3710
- Gasco, S., Zaragoza, P., García-Redondo, A., Calvo, A. C., and Osta, R. (2017). Inflammatory and non-inflammatory monocytes as novel prognostic biomarkers of survival in SOD1G93A mouse model of amyotrophic lateral sclerosis. *PLoS One* 12:e0184626. doi: 10.1371/journal.pone.0184626
- Gatchalian, C. L., Schachner, M., and Sanes, J. R. (1989). Fibroblasts that proliferate near denervated synaptic sites in skeletal muscle synthesize the

- adhesive molecules tenascin(J1), N-CAM, fibronectin, and a heparan sulfate proteoglycan. *J. Cell Biol.* 108, 1873–1890. doi: 10.1083/jcb.108.5.1873
- Gilbert, P. M., Havenstrite, K. L., Magnusson, K. E. G., Sacco, A., Leonardi, N. A., Kraft, P., et al. (2010). Substrate elasticity regulates skeletal muscle stem cell self-renewal in culture. *Science* 329, 1078–1081. doi: 10.1126/science.1191035
- Gitiaux, C., Kostallari, E., Lafuste, P., Authier, F. J., Christov, C., and Gherardi, R. K. (2013). Whole microvascular unit deletions in dermatomyositis. *Ann. Rheum. Dis.* 72, 445–452. doi: 10.1136/annrheumdis-2012-201822
- Giuliani, G., Vumbaca, S., Fuoco, C., Gargioli, C., Giorda, E., Massacci, G., et al. (2021). SCA-1 micro-heterogeneity in the fate decision of dystrophic fibro/adipogenic progenitors. *Cell Death Dis.* 12:122. doi: 10.1038/s41419-021-03408-1
- Glass, G. E., Chan, J. K., Freidin, A., Feldmann, M., Horwood, N. J., and Nanchahal, J. (2011). TNF- α promotes fracture repair by augmenting the recruitment and differentiation of muscle-derived stromal cells. *Proc. Natl. Acad. Sci. U.S.A.* 108, 1585–1590. doi: 10.1073/pnas.1018501108
- Gonzalez, D., Contreras, O., Rebollo, D. L., Espinoza, J. P., Van Zundert, B., and Brandan, E. (2017). ALS skeletal muscle shows enhanced TGF- β signaling, fibrosis and induction of fibro/adipogenic progenitor markers. *PLoS One* 12:e0177649. doi: 10.1371/journal.pone.0177649
- Grounds, M. D. (2008). “Complexity of extracellular matrix and skeletal muscle regeneration,” in *Skeletal Muscle Repair and Regeneration*, eds S. Schiaffino and T. Partridge (Berlin: Springer), 269–302.
- Grounds, M. D., Terrill, J. R., Al-Mshhdani, B. A., Duong, M. N., Radley-Crabb, H. G., and Arthur, P. G. (2020). Biomarkers for Duchenne muscular dystrophy: myonecrosis, inflammation and oxidative stress. *DMM Dis. Model. Mech.* 13:dmm043638. doi: 10.1242/DMM.043638
- Günther, S., Kim, J., Kostin, S., Lepper, C., Fan, C.-M., and Braun, T. (2013). Myf5-positive satellite cells contribute to Pax7-dependent long-term maintenance of adult muscle stem cells. *Cell Stem Cell* 13, 590–601. doi: 10.1016/j.stem.2013.07.016
- Hamilton, T. G., Klinghoffer, R. A., Corrin, P. D., and Soriano, P. (2003). Evolutionary divergence of platelet-derived growth factor alpha receptor signaling mechanisms. *Mol. Cell. Biol.* 23, 4013–4025. doi: 10.1128/mcb.23.11.4013-4025.2003
- Hanwei, H., and Zhao, H. (2010). FYN-dependent muscle-immune interaction after sciatic nerve injury. *Muscle Nerve* 42, 70–77. doi: 10.1002/mus.21605
- Hardy, D., Besnard, A., Latil, M., Jouvion, G., Briand, D., Thépenier, C., et al. (2016). Comparative study of injury models for studying muscle regeneration in mice. *PLoS One* 11:e0147198. doi: 10.1371/journal.pone.0147198
- Henderson, N. C., Arnold, T. D., Katamura, Y., Giacomini, M. M., Rodriguez, J. D., McCarty, J. H., et al. (2013). Targeting of av integrin identifies a core molecular pathway that regulates fibrosis in several organs. *Nat. Med.* 19, 1617–1624. doi: 10.1038/nm.3282
- Henderson, N. C., Rieder, F., and Wynn, T. A. (2020). Fibrosis: from mechanisms to medicines. *Nature* 587, 555–566. doi: 10.1038/s41586-020-2938-9
- Heredia, J. E., Mukundan, L., Chen, F. M., Mueller, A. A., Deo, R. C., Locksley, R. M., et al. (2013). Type 2 innate signals stimulate fibro/adipogenic progenitors to facilitate muscle regeneration. *Cell* 153, 376–388. doi: 10.1016/j.cell.2013.02.053
- Heslop, L., Morgan, J. E., and Partridge, T. A. (2000). Evidence for a myogenic stem cell that is exhausted in dystrophic muscle. *J. Cell Sci.* 113, 2299–2308.
- Hinz, B., and Lagares, D. (2020). Evasion of apoptosis by myofibroblasts: a hallmark of fibrotic diseases. *Nat. Rev. Rheumatol.* 16, 11–31. doi: 10.1038/s41584-019-0324-5
- Hoffman, E. P., Brown, R. H., and Kunkel, L. M. (1987). Dystrophin: the protein product of the duchenne muscular dystrophy locus. *Cell* 51, 919–928. doi: 10.1016/0092-8674(87)90579-4
- Hogarth, M. W., Defour, A., Lazarski, C., Gallardo, E., Manera, J. D., Partridge, T. A., et al. (2019). Fibroadipogenic progenitors are responsible for muscle loss in limb girdle muscular dystrophy 2B. *Nat. Commun.* 10:2430. doi: 10.1038/s41467-019-10438-z
- Hu, F., Lin, Y., Zuo, Y., Chen, R., Luo, S., and Su, Z. (2019). CCN1 induces adipogenic differentiation of fibro/adipogenic progenitors in a chronic kidney disease model. *Biochem. Biophys. Res. Commun.* 520, 385–391. doi: 10.1016/j.bbrc.2019.10.047
- Hwang, C., Marini, S., Huber, A. K., Stepien, D. M., Sorkin, M., Loder, S., et al. (2019). Mesenchymal VEGFA induces aberrant differentiation in heterotopic ossification. *Bone Res.* 7:36. doi: 10.1038/s41413-019-0075-6
- Ieronimakis, N., Hays, A. L., Janebodin, K., Mahoney, W. M., Duffield, J. S., Majesky, M. W., et al. (2013). Coronary adventitial cells are linked to perivascular cardiac fibrosis via TGF β 1 signaling in the mdx mouse model of Duchenne muscular dystrophy. *J. Mol. Cell. Cardiol.* 63, 122–134. doi: 10.1016/j.jmcc.2013.07.014
- Ieronimakis, N., Hays, A., Prasad, A., Janebodin, K., Duffield, J. S., and Reyes, M. (2016). PDGFR α signalling promotes fibrogenic responses in collagen-producing cells in Duchenne muscular dystrophy. *J. Pathol.* 240, 410–424. doi: 10.1002/path.4801
- Ikemoto-Uezumi, M., Matsui, Y., Hasegawa, M., Fujita, R., Kanayama, Y., Uezumi, A., et al. (2017). Disuse atrophy accompanied by intramuscular ectopic adipogenesis in vastus medialis muscle of advanced osteoarthritis patients. *Am. J. Pathol.* 187, 2674–2685. doi: 10.1016/j.ajpath.2017.08.009
- Jensen, A. R., Kelley, B. V., Mosich, G. M., Ariniello, A., Eliasberg, C. D., Vu, B., et al. (2018). Neer Award 2018: platelet-derived growth factor receptor α co-expression typifies a subset of platelet-derived growth factor receptor β -positive progenitor cells that contribute to fatty degeneration and fibrosis of the murine rotator cuff. *J. Shoulder Elb. Surg.* 27, 1149–1161. doi: 10.1016/j.jse.2018.02.040
- Joe, A. W. B., Yi, L., Natarajan, A., Le Grand, F., So, L., Wang, J., et al. (2010). Muscle injury activates resident fibro/adipogenic progenitors that facilitate myogenesis. *Nat. Cell Biol.* 12, 153–163. doi: 10.1038/ncb2015
- Johnson, D. B., Balko, J. M., Compton, M. L., Chalkias, S., Gorham, J., Xu, Y., et al. (2016). Fulminant myocarditis with combination immune checkpoint blockade. *N. Engl. J. Med.* 375, 1749–1755. doi: 10.1056/nejmoa1609214
- Johnston, A. P. W., Yuzwa, S. A., Carr, M. J., Mahmud, N., Storer, M. A., Krause, M. P., et al. (2016). Dedifferentiated schwann cell precursors secreting paracrine factors are required for regeneration of the mammalian digit tip. *Cell Stem Cell* 19, 433–448. doi: 10.1016/j.stem.2016.06.002
- Juban, G., Saclier, M., Yacoub-Youssef, H., Kernou, A., Arnold, L., Boisson, C., et al. (2018). AMPK activation regulates LTBP4-dependent TGF- β 1 secretion by pro-inflammatory macrophages and controls fibrosis in duchenne muscular dystrophy. *Cell Rep.* 25, 2163.e6–2176.e6. doi: 10.1016/j.celrep.2018.10.077
- Kang, X., Yang, M. Y., Shi, Y. X., Xie, M. M., Zhu, M., Zheng, X. L., et al. (2018). Interleukin-15 facilitates muscle regeneration through modulation of fibro/adipogenic progenitors. *Cell Commun. Signal.* 16:42. doi: 10.1186/s12964-018-0251-0
- Kardon, G., Harfe, B. D., and Tabin, C. J. (2003). A Tcf4-positive mesodermal population provides a prepattern for vertebrate limb muscle patterning. *Dev. Cell* 5, 937–944. doi: 10.1016/S1534-5807(03)00360-5
- Karsdal, M. A., Nielsen, S. H., Leeming, D. J., Langholm, L. L., Nielsen, M. J., Manon-Jensen, T., et al. (2017). The good and the bad collagens of fibrosis – Their role in signaling and organ function. *Adv. Drug Deliv. Rev.* 121, 43–56. doi: 10.1016/j.addr.2017.07.014
- Katz, B. (1961). The termination of the afferent nerve fibre in the muscle spindle of the frog. *Philos. Trans. R. Soc. Lond. B. Biol. Sci.* 243, 221–240. doi: 10.1098/rstb.1961.0001
- Kharraz, Y., Guerra, J., Pessina, P., Serrano, A. L., and Muñoz-Cánoves, P. (2014). Understanding the process of fibrosis in duchenne muscular dystrophy. *Biomed. Res. Int.* 2014:965631. doi: 10.1155/2014/965631
- Kim, K. K., Sheppard, D., and Chapman, H. A. (2018). TGF- β 1 signaling and tissue fibrosis. *Cold Spring Harb. Perspect. Biol.* 10:a022293. doi: 10.1101/cshperspect.a022293
- Klingberg, F., Chow, M. L., Koehler, A., Boo, S., Buscemi, L., Quinn, T. M., et al. (2014). Prestress in the extracellular matrix sensitizes latent TGF- β 1 for activation. *J. Cell Biol.* 207, 283–297. doi: 10.1083/jcb.201402006
- Kopinke, D., Roberson, E. C., and Reiter, J. F. (2017). Ciliary hedgehog signaling restricts injury-induced adipogenesis. *Cell* 170, 340.e5–351.e5. doi: 10.1016/j.cell.2017.06.035
- Korthuis, R. J. (2011). Skeletal muscle circulation. *Colloq. Ser. Integr. Syst. Physiol. From Mol. to Funct.* 3, 1–144. doi: 10.4199/c00035ed1v01y201106isp023
- Kramann, R., Schneider, R. K., DiRocco, D. P., Machado, F., Fleig, S., Bondzie, P. A., et al. (2015). Perivascular Gli1+ progenitors are key contributors to injury-induced organ fibrosis. *Cell Stem Cell* 16, 51–66. doi: 10.1016/j.stem.2014.11.004

- Kuang, S., Chargé, S. B., Seale, P., Huh, M., and Rudnicki, M. A. (2006). Distinct roles for Pax7 and Pax3 in adult regenerative myogenesis. *J. Cell Biol.* 172, 103–113. doi: 10.1083/jcb.200508001
- Kudryashova, E., Kramerova, I., and Spencer, M. J. (2012). Satellite cell senescence underlies myopathy in a mouse model of limb-girdle muscular dystrophy 2H. *J. Clin. Invest.* 122, 1764–1776. doi: 10.1172/JCI59581
- Kuswanto, W., Burzyn, D., Panduro, M., Wang, K. K., Jang, Y. C., Wagers, A. J., et al. (2016). Poor repair of skeletal muscle in aging mice reflects a defect in local, interleukin-33-dependent accumulation of regulatory T cells. *Immunity* 44, 355–367. doi: 10.1016/j.immuni.2016.01.009
- Laron, D., Samagh, S. P., Liu, X., Kim, H. T., and Feeley, B. T. (2012). Muscle degeneration in rotator cuff tears. *J. Shoulder Elb. Surg.* 21, 164–174. doi: 10.1016/j.jse.2011.09.027
- Latroche, C., Gitiaux, C., Chrétien, F., Desguerre, I., Mounie, R., and Chazaud, B. (2015a). Skeletal muscle microvasculature: a highly dynamic lifeline. *Physiology* 30, 417–427. doi: 10.1152/physiol.00026.2015
- Latroche, C., Matot, B., Martins-Bach, A., Briand, D., Chazaud, B., Wary, C., et al. (2015b). Structural and functional alterations of skeletal muscle microvasculature in dystrophin-deficient mdx mice. *Am. J. Pathol.* 185, 2482–2494. doi: 10.1016/j.ajpath.2015.05.009
- Latroche, C., Weiss-Gayet, M., Muller, L., Gitiaux, C., Leblanc, P., Liot, S., et al. (2017). Coupling between myogenesis and angiogenesis during skeletal muscle regeneration is stimulated by restorative macrophages. *Stem Cell Rep.* 9, 2018–2033. doi: 10.1016/j.stemcr.2017.10.027
- Leblanc, E., Trens, F., Haroun, S., Drouin, G., Bergeron, É., Penton, C. M., et al. (2011). BMP-9-induced muscle heterotopic ossification requires changes to the skeletal muscle microenvironment. *J. Bone Miner. Res.* 26, 1166–1177. doi: 10.1002/jbmr.311
- Lebleu, V. S., Taduri, G., O'Connell, J., Teng, Y., Cooke, V. G., Woda, C., et al. (2013). Origin and function of myofibroblasts in kidney fibrosis. *Nat. Med.* 19, 1047–1053. doi: 10.1038/nm.3218
- Lee, C., Agha, O., Liu, M., Davies, M., Bertoy, L., Kim, H. T., et al. (2020a). Rotator cuff fibro-adipogenic progenitors demonstrate highest concentration, proliferative capacity, and adipogenic potential across muscle groups. *J. Orthop. Res.* 38, 1113–1121. doi: 10.1002/jor.24550
- Lee, C., Liu, M., Agha, O., Kim, H. T., Feeley, B. T., and Liu, X. (2020b). Beige FAPs transplantation improves muscle quality and shoulder function after massive rotator cuff tears. *J. Orthop. Res.* 38, 1159–1166. doi: 10.1002/jor.24558
- Lee, C., Liu, M., Agha, O., Kim, H. T., Liu, X., and Feeley, B. T. (2020c). Beige fibro-adipogenic progenitor transplantation reduces muscle degeneration and improves function in a mouse model of delayed repair of rotator cuff tears. *J. Shoulder Elb. Surg.* 29, 719–727. doi: 10.1016/j.jse.2019.09.021
- Lees-Shepard, J. B., Nicholas, S. A. E., Stoessel, S. J., Devarakonda, P. M., Schneider, M. J., Yamamoto, M., et al. (2018a). Palovarotene reduces heterotopic ossification in juvenile fop mice but exhibits pronounced skeletal toxicity. *eLife* 7:e40814. doi: 10.7554/eLife.40814
- Lees-Shepard, J. B., Yamamoto, M., Biswas, A. A., Stoessel, S. J., Nicholas, S. A. E., Cogswell, C. A., et al. (2018b). Activin-dependent signaling in fibro/adipogenic progenitors causes fibrodysplasia ossificans progressiva. *Nat. Commun.* 9:471. doi: 10.1038/s41467-018-02872-2
- Lemos, D. R., Babaeijandaghi, F., Low, M., Chang, C. K., Lee, S. T., Fiore, D., et al. (2015). Nilotinib reduces muscle fibrosis in chronic muscle injury by promoting TNF-mediated apoptosis of fibro/adipogenic progenitors. *Nat. Med.* 21, 786–794. doi: 10.1038/nm.3869
- Lemos, D. R., and Duffield, J. S. (2018). Tissue-resident mesenchymal stromal cells: implications for tissue-specific antifibrotic therapies. *Sci. Transl. Med.* 10:eaan5174. doi: 10.1126/scitranslmed.aan5174
- Lepper, C., Partridge, T. A., and Fan, C. M. (2011). An absolute requirement for pax7-positive satellite cells in acute injury-induced skeletal muscle regeneration. *Development* 138, 3639–3646. doi: 10.1242/dev.067595
- Licona-Limón, P., Kim, L. K., Palm, N. W., and Flavell, R. A. (2013). TH2, allergy and group 2 innate lymphoid cells. *Nat. Immunol.* 14, 536–542. doi: 10.1038/ni.2617
- Lieber, R. L., and Ward, S. R. (2013). Cellular mechanisms of tissue fibrosis. 4. structural and functional consequences of skeletal muscle fibrosis. *Am. J. Physiol. Cell Physiol.* 305, C241–C252. doi: 10.1152/ajpcell.00173.2013
- Liu, X., Joshi, S. K., Ravishankar, B., Laron, D., Kim, H. T., and Feeley, B. T. (2014). Upregulation of transforming growth factor- β signaling in a rat model of rotator cuff tears. *J. Shoulder Elb. Surg.* 23, 1709–1716. doi: 10.1016/j.jse.2014.02.029
- Liu, X., Ning, A. Y., Chang, N. C., Kim, H., Nissenson, R., Wang, L., et al. (2016). Investigating the cellular origin of rotator cuff muscle fatty infiltration and fibrosis after injury. *Muscles Ligaments Tendons J.* 6, 6–15. doi: 10.11138/mltj/2016.6.1.006
- Lu, H., Huang, D., Ransohoff, R. M., and Zhou, L. (2011a). Acute skeletal muscle injury: CCL2 expression by both monocytes and injured muscle is required for repair. *FASEB J.* 25, 3344–3355. doi: 10.1096/fj.10-178939
- Lu, H., Huang, D., Saederup, N., Charo, I. F., Ransohoff, R. M., and Zhou, L. (2011b). Macrophages recruited via CCR2 produce insulin-like growth factor-1 to repair acute skeletal muscle injury. *FASEB J.* 25, 358–369. doi: 10.1096/fj.10-171579
- Lukjanenko, L., Karaz, S., Stuelsatz, P., Gurriaran-Rodriguez, U., Michaud, J., Dammone, G., et al. (2019). Aging disrupts muscle stem cell function by impairing matricellular WISP1 secretion from fibro-adipogenic progenitors. *Cell Stem Cell* 24, 433.e7–446.e7. doi: 10.1016/j.stem.2018.12.014
- Lutolf, M. P., and Blau, H. M. (2009). Artificial stem cell niches. *Adv. Mater.* 21, 3255–3268. doi: 10.1002/adma.200802582
- Mackey, A. L., Magnan, M., Chazaud, B., and Kjaer, M. (2017). Human skeletal muscle fibroblasts stimulate in vitro myogenesis and in vivo muscle regeneration. *J. Physiol.* 595, 5115–5127. doi: 10.1113/JP273997
- Madaro, L., Passafaro, M., Sala, D., Etxaniz, U., Lugarini, F., Proietti, D., et al. (2018). Denervation-activated STAT3–IL-6 signalling in fibro-adipogenic progenitors promotes myofibres atrophy and fibrosis. *Nat. Cell Biol.* 20, 917–927. doi: 10.1038/s41556-018-0151-y
- Malecova, B., Gatto, S., Etxaniz, U., Passafaro, M., Cortez, A., Nicoletti, C., et al. (2018). Dynamics of cellular states of fibro-adipogenic progenitors during myogenesis and muscular dystrophy. *Nat. Commun.* 9:3670. doi: 10.1038/s41467-018-06068-6
- Mann, C. J., Perdiguer, E., Kharraz, Y., Aguilar, S., Pessina, P., Serrano, A. L., et al. (2011). Aberrant repair and fibrosis development in skeletal muscle. *Skelet. Muscle* 1:21. doi: 10.1186/2044-5040-1-21
- Martinez, F. O., Helming, L., and Gordon, S. (2009). Alternative activation of macrophages: an immunologic functional perspective. *Annu. Rev. Immunol.* 27, 451–483. doi: 10.1146/annurev.immunol.021908.132532
- Mashinchian, O., Piscanti, A., Le Moal, E., and Bentzinger, C. F. (2018). The muscle stem cell niche in health and disease. *Curr. Top. Dev. Biol.* 126, 23–65. doi: 10.1016/bs.ctdb.2017.08.003
- Matas-García, A., Milisenda, J. C., Selva-O'Callaghan, A., Prieto-González, S., Padrosa, J., Cabrera, C., et al. (2020). Emerging PD-1 and PD-1L inhibitors-associated myopathy with a characteristic histopathological pattern. *Autoimmun. Rev.* 19:102455. doi: 10.1016/j.autrev.2019.102455
- Mathew, S. J., Hansen, J. M., Merrell, A. J., Murphy, M. M., Lawton, J. A., Hutcheson, D. A., et al. (2011). Connective tissue fibroblasts and Tcf4 regulate myogenesis. *Development* 138, 371–384. doi: 10.1242/dev.057463
- Matsakas, A., Yadav, V., Lorca, S., and Narkar, V. (2013). Muscle ER γ mitigates Duchenne muscular dystrophy via metabolic and angiogenic reprogramming. *FASEB J.* 27, 4004–4016. doi: 10.1096/fj.13-228296
- Mauro, A. (1961). Satellite cell of skeletal muscle fibers. *J. Biophys. Biochem. Cytol.* 9, 493–495. doi: 10.1083/jcb.9.2.493
- Mázala, D. A. G., Novak, J. S., Hogarth, M. W., Nearing, M., Adusumalli, P., Tully, C. B., et al. (2020). TGF- β -driven muscle degeneration and failed regeneration underlie disease onset in a DMD mouse model. *JCI Insight* 5:e135703. doi: 10.1172/jci.insight.135703
- Mederacke, I., Hsu, C. C., Troeger, J. S., Huebener, P., Mu, X., Dapito, D. H., et al. (2013). Fate tracing reveals hepatic stellate cells as dominant contributors to liver fibrosis independent of its aetiology. *Nat. Commun.* 4:2823. doi: 10.1038/ncomms3823
- Messing, M., Jan-Abu, S. C., and McNagny, K. (2020). Group 2 innate lymphoid cells: central players in a recurring theme of repair and regeneration. *Int. J. Mol. Sci.* 21:1350. doi: 10.3390/ijms21041350
- Meyer, D. C., Hoppeler, H., von Rechenberg, B., and Gerber, C. (2004). A pathomechanical concept explains muscle loss and fatty muscular changes following surgical tendon release. *J. Orthop. Res.* 22, 1004–1007. doi: 10.1016/j.orthres.2004.02.009

- Mohassel, P., Reghan Foley, A., and Bönnemann, C. G. (2018). Extracellular matrix-driven congenital muscular dystrophies. *Matrix Biol.* 71–72, 188–204. doi: 10.1016/j.matbio.2018.06.005
- Moratal, C., Arrighi, N., Dechesne, C. A., and Dani, C. (2019). Control of muscle fibro-adipogenic progenitors by myogenic lineage is altered in aging and Duchenne muscular dystrophy. *Cell. Physiol. Biochem.* 53, 1029–1045. doi: 10.33594/00000196
- Moratal, C., Raffort, J., Arrighi, N., Rekima, S., Schaub, S., Dechesne, C. A., et al. (2018). IL-1 β - and IL-4-polarized macrophages have opposite effects on adipogenesis of intramuscular fibro-adipogenic progenitors in humans. *Sci. Rep.* 8:17005. doi: 10.1038/s41598-018-35429-w
- Morton, A. B., Norton, C. E., Jacobsen, N. L., Fernando, C. A., Cornelison, D. D. W., and Segal, S. S. (2019). Barium chloride injures myofibers through calcium-induced proteolysis with fragmentation of motor nerves and microvessels. *Skelet. Muscle* 9:27. doi: 10.1186/s13395-019-0213-2
- Mounier, R., Théret, M., Arnold, L., Cuvellier, S., Bultot, L., Göransson, O., et al. (2013). AMPK α 1 regulates macrophage skewing at the time of resolution of inflammation during skeletal muscle regeneration. *Cell Metab.* 18, 251–264. doi: 10.1016/j.cmet.2013.06.017
- Mozzetta, C., Consalvi, S., Saccone, V., Tierney, M., Diamantini, A., Mitchell, K. J., et al. (2013). Fibroadipogenic progenitors mediate the ability of HDAC inhibitors to promote regeneration in dystrophic muscles of young, but not old Mdx mice. *EMBO Mol. Med.* 5, 626–639. doi: 10.1002/emmm.201202096
- Mueller, A. A., Van Velthoven, C. T., Fukumoto, K. D., Cheung, T. H., and Rando, T. A. (2016). Intronic polyadenylation of PDGFR α in resident stem cells attenuates muscle fibrosis. *Nature* 540, 276–279. doi: 10.1038/nature20160
- Muñoz-Cánoves, P., Neves, J., and Sousa-Victor, P. (2020). Understanding muscle regenerative decline with aging: new approaches to bring back youthfulness to aged stem cells. *FEBS J.* 287, 406–416. doi: 10.1111/febs.15182
- Muñoz-Cánoves, P., and Serrano, A. L. (2015). Macrophages decide between regeneration and fibrosis in muscle. *Trends Endocrinol. Metab.* 26, 449–450. doi: 10.1016/j.tem.2015.07.005
- Murphy, M. M., Lawson, J. A., Mathew, S. J., Hutcheson, D. A., and Kardon, G. (2011). Satellite cells, connective tissue fibroblasts and their interactions are crucial for muscle regeneration. *Development* 138, 3625–3637. doi: 10.1242/dev.064162
- Murray, I. R., Gonzalez, Z. N., Baily, J., Dobie, R., Wallace, R. J., Mackinnon, A. C., et al. (2017). α v integrins on mesenchymal cells regulate skeletal and cardiac muscle fibrosis. *Nat. Commun.* 8:1118. doi: 10.1038/s41467-017-01097-z
- Murray, P. J., Allen, J. E., Biswas, S. K., Fisher, E. A., Gilroy, D. W., Goerdt, S., et al. (2014). Macrophage activation and polarization: nomenclature and experimental guidelines. *Immunity* 41, 14–20. doi: 10.1016/j.immuni.2014.06.008
- Neuhaus, P., Oustanina, S., Loch, T., Krüger, M., Bober, E., Dono, R., et al. (2003). Reduced mobility of fibroblast growth factor (FGF)-deficient myoblasts might contribute to dystrophic changes in the musculature of FGF2/FGF6/mdx triple-mutant mice. *Mol. Cell. Biol.* 23, 6037–6048. doi: 10.1128/mcb.23.17.6037-6048.2003
- Noguchi, S., Ogawa, M., Malicdan, M. C., Nonaka, I., and Nishino, I. (2017). Muscle weakness and fibrosis due to cell autonomous and non-cell autonomous events in collagen VI deficient congenital muscular dystrophy. *EBioMedicine* 15, 193–202. doi: 10.1016/j.ebiom.2016.12.011
- Oishi, T., Uezumi, A., Kanaji, A., Yamamoto, N., Yamaguchi, A., Yamada, H., et al. (2013). Osteogenic differentiation capacity of human skeletal muscle-derived progenitor cells. *PLoS One* 8:e0056641. doi: 10.1371/journal.pone.0056641
- Olfert, I. M., Baum, O., Hellsten, Y., and Egginton, S. (2016). Advances and challenges in skeletal muscle angiogenesis. *Am. J. Physiol. Heart Circ. Physiol.* 310, H326–H336. doi: 10.1152/ajpheart.00635.2015
- Opreacu, S. N., Yue, F., Qiu, J., Brito, L. F., and Kuang, S. (2020). Temporal dynamics and heterogeneity of cell populations during skeletal muscle regeneration. *iScience* 23:100993. doi: 10.1016/j.isci.2020.100993
- Oustanina, S., Hause, G., and Braun, T. (2004). Pax7 directs postnatal renewal and propagation of myogenic satellite cells but not their specification. *EMBO J.* 23, 3430–3439. doi: 10.1038/sj.emboj.7600346
- Pakshir, P., and Hinz, B. (2018). The big five in fibrosis: macrophages, myofibroblasts, matrix, mechanics, and miscommunication. *Matrix Biol.* 68–69, 81–93. doi: 10.1016/j.matbio.2018.01.019
- Pakshir, P., Noskovicova, N., Lodyga, M., Son, D. O., Schuster, R., Goodwin, A., et al. (2020). The myofibroblast at a glance. *J. Cell Sci.* 133:jcs227900. doi: 10.1242/jcs.227900
- Panduro, M., Benoist, C., and Mathis, D. (2018). Treg cells limit IFN- γ production to control macrophage accrual and phenotype during skeletal muscle regeneration. *Proc. Natl. Acad. Sci. U.S.A.* 115, E2585–E2593. doi: 10.1073/pnas.1800618115
- Pardoll, D. M. (2012). The blockade of immune checkpoints in cancer immunotherapy. *Nat. Rev. Cancer* 12, 252–264. doi: 10.1038/nrc3239
- Perandini, L. A., Chimin, P., Lutkemeyer, D., da, S., and Câmara, N. O. S. (2018). Chronic inflammation in skeletal muscle impairs satellite cells function during regeneration: can physical exercise restore the satellite cell niche? *FEBS J.* 285, 1973–1984. doi: 10.1111/febs.14417
- Pessina, P., Cabrera, D., Morales, M. G., Riquelme, C. A., Gutiérrez, J., Serrano, A. L., et al. (2014). Novel and optimized strategies for inducing fibrosis in vivo: focus on duchenne muscular dystrophy. *Skelet. Muscle* 4:7. doi: 10.1186/2044-5040-4-7
- Petrilli, L. L., Spada, F., Palma, A., Reggio, A., Rosina, M., Gargioli, C., et al. (2020). High-dimensional single-cell quantitative profiling of skeletal muscle cell population dynamics during regeneration. *Cells* 9:1723. doi: 10.3390/cells9071723
- Pisani, D. F., Bottema, C. D. K., Butori, C., Dani, C., and Dechesne, C. A. (2010). Mouse model of skeletal muscle adiposity: a glycerol treatment approach. *Biochem. Biophys. Res. Commun.* 396, 767–773. doi: 10.1016/j.bbrc.2010.05.021
- Pizza, F. X., Peterson, J. M., Baas, J. H., and Koh, T. J. (2005). Neutrophils contribute to muscle injury and impair its resolution after lengthening contractions in mice. *J. Physiol.* 562, 899–913. doi: 10.1113/jphysiol.2004.073965
- Porter, J. D., Khanna, S., Kaminski, H. J., Sunil Rao, J., Merriam, A. P., Richmonds, C. R., et al. (2002). A chronic inflammatory response dominates the skeletal muscle molecular signature in dystrophin-deficient mdx mice. *Hum. Mol. Genet.* 11, 263–272. doi: 10.1093/hmg/11.3.263
- Purslow, P. P. (2020). The structure and role of intramuscular connective tissue in muscle function. *Front. Physiol.* 11:495. doi: 10.3389/fphys.2020.00495
- Rahman, F. A., Angus, S. A., Stokes, K., Karpowicz, P., and Krause, M. P. (2020). Impaired ECM remodeling and macrophage activity define necrosis and regeneration following damage in aged skeletal muscle. *Int. J. Mol. Sci.* 21, 1–23. doi: 10.3390/ijms21134575
- Rebolledo, D. L., González, D., Faundez-Contreras, J., Contreras, O., Vio, C. P., Murphy-Ullrich, J. E., et al. (2019). Denervation-induced skeletal muscle fibrosis is mediated by CTGF/CCN2 independently of TGF- β . *Matrix Biol.* 82, 20–37. doi: 10.1016/j.matbio.2019.01.002
- Reed, P., and Bloch, R. J. (2005). Postnatal changes in sarcolemmal organization in the mdx mouse. *Neuromuscul. Disord.* 15, 552–561. doi: 10.1016/j.nmd.2005.03.007
- Reggio, A., Rosina, M., Kraemer, N., Palma, A., Petrilli, L. L., Maiolatesi, G., et al. (2020). Metabolic reprogramming of fibro/adipogenic progenitors facilitates muscle regeneration. *Life Sci. Alliance* 3:e202000646. doi: 10.26508/lsa.202000660
- Relaix, F., and Zammit, P. S. (2012). Satellite cells are essential for skeletal muscle regeneration: the cell on the edge returns centre stage. *Dev.* 139, 2845–2856. doi: 10.1242/dev.069088
- Roberts, E. W., Deonaraine, A., Jones, J. O., Denton, A. E., Feig, C., Lyons, S. K., et al. (2013). Depletion of stromal cells expressing fibroblast activation protein- α from skeletal muscle and bone marrow results in cachexia and anemia. *J. Exp. Med.* 210, 1137–1151. doi: 10.1084/jem.20122344
- Robertson, T. A., Grounds, M. D., Mitchell, C. A., and Papadimitriou, J. M. (1990). Fusion between myogenic cells in Vivo: an ultrastructural study in regenerating murine skeletal muscle. *J. Struct. Biol.* 105, 170–182. doi: 10.1016/1047-8477(90)90111-O
- Ross, J., Benn, A., Jonuschies, J., Boldrin, L., Muntoni, F., Hewitt, J. E., et al. (2012). Defects in glycosylation impair satellite stem cell function and niche composition in the muscles of the dystrophic largemyd mouse. *Stem Cells* 30, 2330–2341. doi: 10.1002/stem.1197

- Rudnicki, M. A., Le Grand, F., McKinnell, I., and Kuang, S. (2008). "The molecular regulation of muscle stem cell function," in *Cold Spring Harbor Symposia on Quantitative Biology*, 323–331. doi: 10.1101/sqb.2008.73.064
- Sacco, A., Doyonnas, R., Kraft, P., Vitorovic, S., and Blau, H. M. (2008). Self-renewal and expansion of single transplanted muscle stem cells. *Nature* 456, 502–506. doi: 10.1038/nature07384
- Sacco, A., Mourkioti, F., Tran, R., Choi, J., Llewellyn, M., Kraft, P., et al. (2010). Short telomeres and stem cell exhaustion model duchenne muscular dystrophy in mdx/mTR mice. *Cell* 143, 1059–1071. doi: 10.1016/j.cell.2010.11.039
- Saccone, V., Consalvi, S., Giordani, L., Mozzetta, C., Barozzi, I., Sandomá, M., et al. (2014). HDAC-regulated myomiRs control BAF60 variant exchange and direct the functional phenotype of fibro-adipogenic progenitors in dystrophic muscles. *Genes Dev.* 28, 841–857. doi: 10.1101/gad.234468.113
- Saito, Y., Chikenji, T. S., Matsumura, T., Nakano, M., and Fujimiya, M. (2020). Exercise enhances skeletal muscle regeneration by promoting senescence in fibro-adipogenic progenitors. *Nat. Commun.* 11:889. doi: 10.1038/s41467-020-14734-x
- Sambasivan, R., Yao, R., Kissenfennig, A., van Wittenberghe, L., Paldi, A., Gayraud-Morel, B., et al. (2011). Pax7-expressing satellite cells are indispensable for adult skeletal muscle regeneration. *Development* 138, 3647–3656. doi: 10.1242/dev.067587
- Sandomá, M., Consalvi, S., Tucciarone, L., De Bardi, M., Scimeca, M., Angelini, D. F., et al. (2020). HDAC inhibitors tune miRNAs in extracellular vesicles of dystrophic muscle-resident mesenchymal cells. *EMBO Rep.* 21:e50863. doi: 10.15252/embr.202050863
- Santini, M. P., Malide, D., Hoffman, G., Pandey, G., D'Escamard, V., Nomura-Kitabayashi, A., et al. (2020). Tissue-Resident PDGFR α progenitor cells contribute to fibrosis versus healing in a context- and spatiotemporally dependent manner. *Cell Rep.* 30, 555.e7–570.e7. doi: 10.1016/j.celrep.2019.12.045
- Scott, R. W., Arostegui, M., Schweitzer, R., Rossi, F. M. V., and Underhill, T. M. (2019). Hic1 defines quiescent mesenchymal progenitor subpopulations with distinct functions and fates in skeletal muscle regeneration. *Cell Stem Cell* 25, 797.e9–813.e9. doi: 10.1016/j.stem.2019.11.004
- Serrano, A. L., Mann, C. J., Vidal, B., Ardite, E., Perdiguero, E., and Muñoz-Cánoves, P. (2011). Cellular and molecular mechanisms regulating fibrosis in skeletal muscle repair and disease. *Curr. Top. Dev. Biol.* 96, 167–201. doi: 10.1016/B978-0-12-385940-2.00007-3
- Shirasawa, H., Matsumura, N., Shimoda, M., Oki, S., Yoda, M., Tohmonda, T., et al. (2017). Inhibition of PDGFR signaling prevents muscular fatty infiltration after rotator cuff tear in mice. *Sci. Rep.* 7:41552. doi: 10.1038/srep41552
- Slater, C. R., and Schiaffino, S. (2008). "Innervation of regenerating muscle," in *Skeletal Muscle Repair and Regeneration*, eds S. Schiaffino and T. Partridge (Berlin: Springer), 303–334.
- Smith, L. R., and Barton, E. R. (2018). Regulation of fibrosis in muscular dystrophy. *Matrix Biol.* 68–69, 602–615. doi: 10.1016/j.matbio.2018.01.014
- Soliman, H., Paylor, B., Scott, R. W., Lemos, D. R., Chang, C. K., Arostegui, M., et al. (2020). Pathogenic Potential of Hic1-expressing cardiac stromal progenitors. *Cell Stem Cell* 26, 205.e8–220.e8. doi: 10.1016/j.stem.2019.12.008
- Sousa-Victor, P., García-Prat, L., Serrano, A. L., Perdiguero, E., and Muñoz-Cánoves, P. (2015). Muscle stem cell aging: regulation and rejuvenation. *Trends Endocrinol. Metab.* 26, 287–296. doi: 10.1016/j.tem.2015.03.006
- Stepien, D. M., Hwang, C., Marini, S., Pagani, C. A., Sorkin, M., Visser, N. D., et al. (2020). Tuning macrophage phenotype to mitigate skeletal muscle fibrosis. *J. Immunol.* 204, 2203–2215. doi: 10.4049/jimmunol.1900814
- Stumm, J., Vallecillo-García, P., Vom Hofe-Schneider, S., Ollitrault, D., Schrewe, H., Economides, A. N., et al. (2018). Odd skipped-related 1 (Osr1) identifies muscle-interstitial fibro-adipogenic progenitors (FAPs) activated by acute injury. *Stem Cell Res.* 32, 8–16. doi: 10.1016/j.scr.2018.08.010
- Sun, L., Louie, M. C., Vannella, K. M., Wilke, C. A., Levine, A. M., Moore, B. B., et al. (2011). New concepts of IL-10-induced lung fibrosis: fibrocyte recruitment and M2 activation in a CCL2/CCR2 axis. *Am. J. Physiol. Lung Cell. Mol. Physiol.* 300, L341–L353. doi: 10.1152/ajplung.00122.2010
- Tedesco, S., De Majo, F., Kim, J., Trenti, A., Trevisi, L., Fadini, G. P., et al. (2018). Convenience versus biological significance: are PMA-differentiated THP-1 cells a reliable substitute for blood-derived macrophages when studying in vitro polarization? *Front. Pharmacol.* 9:71. doi: 10.3389/fphar.2018.00071
- Theret, M., Gsaier, L., Schaffer, B., Juban, G., Ben Larbi, S., Weiss-Gayet, M., et al. (2017). AMPK α 1-LDH pathway regulates muscle stem cell self-renewal by controlling metabolic homeostasis. *EMBO J.* 36, 1946–1962. doi: 10.15252/embr.201695273
- Theret, M., Low, M., Rempel, L., Li, F., Tung, L. W., Contreras, O., et al. (2021). Targeting fibrosis in the duchenne muscular dystrophy mice model: an uphill battle. *bioRxiv* [Preprint]. doi: 10.1101/2021.01.20.427485v1
- Theret, M., Mounier, R., and Rossi, F. (2019). The origins and non-canonical functions of macrophages in development and regeneration. *Development* 146:dev156000. doi: 10.1242/dev.156000
- Tidball, J. G. (2017). Regulation of muscle growth and regeneration by the immune system. *Nat. Rev. Immunol.* 17, 165–178. doi: 10.1038/nri.2016.150
- Tidball, J. G., and Villalta, S. A. (2010). Regulatory interactions between muscle and the immune system during muscle regeneration. *Am. J. Physiol. Regul. Integr. Comp. Physiol.* 298, R1173–R1187. doi: 10.1152/ajpregu.00735.2009
- Uezumi, A., Fukada, S., Yamamoto, N., Ikemoto-Uezumi, M., Nakatani, M., Morita, M., et al. (2014). Identification and characterization of PDGFR + mesenchymal progenitors in human skeletal muscle. *Cell Death Dis.* 5:e1186. doi: 10.1038/cddis.2014.161
- Uezumi, A., Fukada, S. I., Yamamoto, N., Takeda, S., and Tsuchida, K. (2010). Mesenchymal progenitors distinct from satellite cells contribute to ectopic fat cell formation in skeletal muscle. *Nat. Cell Biol.* 12, 143–152. doi: 10.1038/ncb2014
- Uezumi, A., Ikemoto-Uezumi, M., Zhou, H., Kurosawa, T., Yoshimoto, Y., Nakatani, M., et al. (2021). Mesenchymal Bmp3b expression maintains skeletal muscle integrity and decreases in age-related sarcopenia. *J. Clin. Invest.* 131:e139617. doi: 10.1172/JCI139617
- Uezumi, A., Ito, T., Morikawa, D., Shimizu, N., Yoneda, T., Segawa, M., et al. (2011). Fibrosis and adipogenesis originate from a common mesenchymal progenitor in skeletal muscle. *J. Cell Sci.* 124, 3654–3664. doi: 10.1242/jcs.086629
- Upadhyay, J., Xie, L. Q., Huang, L., Das, N., Stewart, R. C., Lyon, M. C., et al. (2017). The expansion of heterotopic bone in fibrodysplasia ossificans progressiva is activin a-dependent. *J. Bone Miner. Res.* 32, 2489–2499. doi: 10.1002/jbmr.3235
- Urciuolo, A., Quarta, M., Morbidoni, V., Gattazzo, F., Molon, S., Grumati, P., et al. (2013). Collagen VI regulates satellite cell self-renewal and muscle regeneration. *Nat. Commun.* 4:1964. doi: 10.1038/ncomms2964
- Vallecillo-García, P., Orgeur, M., Vom Hofe-Schneider, S., Stumm, J., Kappert, V., Ibrahim, D. M., et al. (2017). Odd skipped-related 1 identifies a population of embryonic fibro-adipogenic progenitors regulating myogenesis during limb development. *Nat. Commun.* 8:1218. doi: 10.1038/s41467-017-0120-3
- Valle-Tenney, R., Rebolledo, D. L., Lipson, K. E., and Brandan, E. (2020). Role of hypoxia in skeletal muscle fibrosis: Synergism between hypoxia and TGF- β signaling upregulates CCN2/CTGF expression specifically in muscle fibers. *Matrix Biol.* 87, 48–65. doi: 10.1016/j.matbio.2019.09.003
- Van Caam, A., Vonk, M., Van Den Hoogen, F., Van Lent, P., and Van Der Kraan, P. (2018). Unraveling SSc pathophysiology; The myofibroblast. *Front. Immunol.* 9:2452. doi: 10.3389/fimmu.2018.02452
- Vannella, K. M., and Wynn, T. A. (2017). Mechanisms of organ injury and repair by macrophages*. *Annu. Rev. Physiol.* 79, 593–617. doi: 10.1146/annurev-physiol-022516-034356
- Varga, T., Mounier, R., Gogolak, P., Poliska, S., Chazaud, B., and Nagy, L. (2013). Tissue LyC6 - macrophages are generated in the absence of circulating LyC6 - monocytes and Nur77 in a model of muscle regeneration. *J. Immunol.* 191, 5695–5701. doi: 10.4049/jimmunol.1301445
- Verma, M., Asakura, Y., Hirai, H., Watanabe, S., Tastad, C., Fong, G. H., et al. (2010). Flt-1 haploinsufficiency ameliorates muscular dystrophy phenotype by developmentally increased vasculature in mdx mice. *Hum. Mol. Genet.* 19, 4145–4159. doi: 10.1093/hmg/ddq334
- Verma, M., Asakura, Y., Murakonda, B. S. R., Pengo, T., Latroche, C., Chazaud, B., et al. (2018). Muscle satellite cell cross-talk with a vascular niche maintains quiescence via VEGF and notch signaling. *Cell Stem Cell* 23, 530.e9–543.e9. doi: 10.1016/j.stem.2018.09.007
- Von Maltzahn, J., Jones, A. E., Parks, R. J., and Rudnicki, M. A. (2013). Pax7 is critical for the normal function of satellite cells in adult skeletal muscle.

- Proc. Natl. Acad. Sci. U.S.A.* 110, 16474–16479. doi: 10.1073/pnas.1307680110
- Wallace, G. Q., and McNally, E. M. (2009). Mechanisms of muscle degeneration, regeneration, and repair in the muscular dystrophies. *Annu. Rev. Physiol.* 71, 37–57. doi: 10.1146/annurev.physiol.010908.163216
- Wang, H. A., Lee, J. D., Lee, K. M., Woodruff, T. M., and Noakes, P. G. (2017). Complement C5a-C5aR1 signalling drives skeletal muscle macrophage recruitment in the hSOD1G93A mouse model of amyotrophic lateral sclerosis. *Skelet. Muscle* 7:10. doi: 10.1186/s13395-017-0128-8
- Wang, Y. X., and Rudnicki, M. A. (2012). Satellite cells, the engines of muscle repair. *Nat. Rev. Mol. Cell Biol.* 13, 127–133. doi: 10.1038/nrm3265
- Wosczyzna, M. N., Biswas, A. A., Cogswell, C. A., and Goldhamer, D. J. (2012). Multipotent progenitors resident in the skeletal muscle interstitium exhibit robust BMP-dependent osteogenic activity and mediate heterotopic ossification. *J. Bone Miner. Res.* 27, 1004–1017. doi: 10.1002/jbmr.1562
- Wosczyzna, M. N., Konishi, C. T., Perez Carbajal, E. E., Wang, T. T., Walsh, R. A., Gan, Q., et al. (2019). Mesenchymal stromal cells are required for regeneration and homeostatic maintenance of skeletal muscle. *Cell Rep.* 27, 2029.e5–2035.e5. doi: 10.1016/j.celrep.2019.04.074
- Wosczyzna, M. N., and Rando, T. A. (2018). A muscle stem cell support group: coordinated cellular responses in muscle regeneration. *Dev. Cell.* 46, 135–143. doi: 10.1016/j.devcel.2018.06.018
- Wynn, T. A., and Ramalingam, T. R. (2012). Mechanisms of fibrosis: therapeutic translation for fibrotic disease. *Nat. Med.* 18, 1028–1040. doi: 10.1038/nm.2807
- Xu, Z., You, W., Chen, W., Zhou, Y., Nong, Q., Valencak, T. G., et al. (2021). Single-cell RNA sequencing and lipidomics reveal cell and lipid dynamics of fat infiltration in skeletal muscle. *J. Cachexia. Sarcopenia Muscle* 12, 109–129. doi: 10.1002/jcsm.12643
- Yagi, R., Zhong, C., Northrup, D. L., Yu, F., Bouladoux, N., Spencer, S., et al. (2014). The transcription factor GATA3 is critical for the development of all IL-7R α -expressing innate lymphoid cells. *Immunity* 40, 378–388. doi: 10.1016/j.immuni.2014.01.012
- Yamamoto, A., Takagishi, K., Osawa, T., Yanagawa, T., Nakajima, D., Shitara, H., et al. (2010). Prevalence and risk factors of a rotator cuff tear in the general population. *J. Shoulder Elb. Surg.* 19, 116–120. doi: 10.1016/j.jse.2009.04.006
- Yao, L., Tichy, E. D., Zhong, L., Mohanty, S., Wang, L., Ai, E., et al. (2021). Gli1 defines a subset of fibroadipogenic progenitors that promote skeletal muscle regeneration with less fat accumulation. *J. Bone Miner. Res.* [Epub ahead of print]. doi: 10.1002/jbmr.4265
- Zhao, B. L., Kollias, H. D., and Wagner, K. R. (2008). Myostatin directly regulates skeletal muscle fibrosis. *J. Biol. Chem.* 283, 19371–19378. doi: 10.1074/jbc.M802585200
- Zheng, J., Xiong, D., Sun, X., Wang, J., Hao, M., Ding, T., et al. (2012). Significance of hypermethylated in cancer 1 (HIC1) as tumor suppressor gene in tumor progression. *Cancer Microenviron.* 5, 285–293. doi: 10.1007/s12307-012-0103-1
- Zimmer, L., Goldinger, S. M., Hofmann, L., Loquai, C., Ugurel, S., Thomas, L., et al. (2016). Neurological, respiratory, musculoskeletal, cardiac and ocular side-effects of anti-PD-1 therapy. *Eur. J. Cancer* 60, 210–225. doi: 10.1016/j.ejca.2016.02.024
- Zou, W. (2005). Immunosuppressive networks in the tumour environment and their therapeutic relevance. *Nat. Rev. Cancer* 5, 263–274. doi: 10.1038/nrc1586

Conflict of Interest: The authors declare that the research was conducted in the absence of any commercial or financial relationships that could be construed as a potential conflict of interest.

Copyright © 2021 Theret, Rossi and Contreras. This is an open-access article distributed under the terms of the Creative Commons Attribution License (CC BY). The use, distribution or reproduction in other forums is permitted, provided the original author(s) and the copyright owner(s) are credited and that the original publication in this journal is cited, in accordance with accepted academic practice. No use, distribution or reproduction is permitted which does not comply with these terms.



EndMT Regulation by Small RNAs in Diabetes-Associated Fibrotic Conditions: Potential Link With Oxidative Stress

Roberta Giordo¹, Yusra M. A. Ahmed¹, Hilda Allam¹, Salah Abusnana^{2,3}, Lucia Pappalardo⁴, Gheyath K. Nasrallah^{5,6*}, Arduino Aleksander Mangoni^{7,8*} and Gianfranco Pintus^{1,9*}

OPEN ACCESS

Edited by:

Isotta Chimenti,
Sapienza University of Rome, Italy

Reviewed by:

Subrata Chakrabarti,
Western University, Canada
Swayam Prakash Srivastava,
Yale University, United States

*Correspondence:

Gheyath K. Nasrallah
gheyath.nasrallah@qu.edu.qa
Arduino Aleksander Mangoni
arduino.mangoni@flinders.edu.au
Gianfranco Pintus
gpintus@sharjah.ac.ae

Specialty section:

This article was submitted to
Molecular Medicine,
a section of the journal
*Frontiers in Cell and Developmental
Biology*

Received: 21 March 2021

Accepted: 26 April 2021

Published: 19 May 2021

Citation:

Giordo R, Ahmed YMA, Allam H, Abusnana S, Pappalardo L, Nasrallah GK, Mangoni AA and Pintus G (2021) EndMT Regulation by Small RNAs in Diabetes-Associated Fibrotic Conditions: Potential Link With Oxidative Stress. *Front. Cell Dev. Biol.* 9:683594. doi: 10.3389/fcell.2021.683594

¹ Department of Medical Laboratory Sciences, College of Health Sciences and Sharjah Institute for Medical Research, University of Sharjah, Sharjah, United Arab Emirates, ² Department of Diabetes and Endocrinology, University Hospital Sharjah, Sharjah, United Arab Emirates, ³ Department of Clinical Sciences, College of Medicine, University of Sharjah, Sharjah, United Arab Emirates, ⁴ Department of Biology, Chemistry and Environmental Studies, American University of Sharjah, Sharjah, United Arab Emirates, ⁵ Department of Biomedical Sciences, College of Health Sciences Member of QU Health, Qatar University, Doha, Qatar, ⁶ Biomedical Research Center, Qatar University, Doha, Qatar, ⁷ Discipline of Clinical Pharmacology, College of Medicine and Public Health, Flinders University, Adelaide, SA, Australia, ⁸ Flinders Medical Centre, Adelaide, SA, Australia, ⁹ Department of Biomedical Sciences, University of Sassari, Sassari, Italy

Diabetes-associated complications, such as retinopathy, nephropathy, cardiomyopathy, and atherosclerosis, the main consequences of long-term hyperglycemia, often lead to organ dysfunction, disability, and increased mortality. A common denominator of these complications is the myofibroblast-driven excessive deposition of extracellular matrix proteins. Although fibroblast appears to be the primary source of myofibroblasts, other cells, including endothelial cells, can generate myofibroblasts through a process known as endothelial to mesenchymal transition (EndMT). During EndMT, endothelial cells lose their typical phenotype to acquire mesenchymal features, characterized by the development of invasive and migratory abilities as well as the expression of typical mesenchymal products such as α -smooth muscle actin and type I collagen. EndMT is involved in many chronic and fibrotic diseases and appears to be regulated by complex molecular mechanisms and different signaling pathways. Recent evidence suggests that small RNAs, in particular microRNAs (miRNAs) and long non-coding RNAs (lncRNAs), are crucial mediators of EndMT. Furthermore, EndMT and miRNAs are both affected by oxidative stress, another key player in the pathophysiology of diabetic fibrotic complications. In this review, we provide an overview of the primary redox signals underpinning the diabetic-associated fibrotic process. Then, we discuss the current knowledge on the role of small RNAs in the regulation of EndMT in diabetic retinopathy, nephropathy, cardiomyopathy, and atherosclerosis and highlight potential links between oxidative stress and the dyad small RNAs-EndMT in driving these pathological states.

Keywords: EndMT, miRNAs, diabetes, fibrosis, oxidative stress

INTRODUCTION

Diabetes mellitus (DM) is one of the most common chronic diseases worldwide (Lin X. et al., 2020). A prediction study estimated a significant further increase in the number of people suffering from diabetes, especially in developing countries, with a global prevalence of 7.7% (439 million adults) by 2030 (Shaw et al., 2010; Lin X. et al., 2020). Long-term hyperglycemia is the main driver of the onset and the progression of common diabetic complications, particularly those affecting the eye, kidney, nervous system, and cardiovascular system (Deshpande et al., 2008). Such complications are secondary to structural and functional alterations of organs and tissues that are caused by an increased cellular glucose uptake (Wellen and Hotamisligil, 2005). This activates inflammatory pathways which ultimately leads to excessive deposition of extra cellular matrix (ECM) proteins and consequent thickening of the vessel wall (Wellen and Hotamisligil, 2005; Wynn, 2008). Tissue fibrosis is therefore the common denominator of most diabetic complications, including atherosclerosis, cardiomyopathy, nephropathy and retinopathy (Ban and Twigg, 2008). Myofibroblasts are the key mediators of pathological ECM accumulation (Kendall and Feghali-Bostwick, 2014). These cells are normally involved in tissue repair and are subsequently removed by apoptosis at the end of the repair process. However, under pathological situations, their unrestrained activation leads to excessive ECM deposition (Micallef et al., 2012). Myofibroblasts originate from different precursor cells, depending on the organ and the type of initial injury (Bochaton-Piallat et al., 2016). Although fibroblasts represent the primary source of myofibroblasts, the latter can also originate from the inresident or bone marrow-derived mesenchymal cells as well as epithelial and endothelial cells (ECs), through a process known as epithelial/endothelial to mesenchymal transition (Micallef et al., 2012; Kendall and Feghali-Bostwick, 2014). In particular, endothelial to mesenchymal transition (EndMT), the process involving ECs, is emerging as an important player in the pathogenesis of diabetic fibrosis (Srivastava et al., 2013; Cao et al., 2014; Souilhol et al., 2018). ECs, constituting the inner layer of blood vessels, are responsible for maintaining vascular homeostasis in response to endogenous and exogenous perturbations (Sandoo et al., 2010; Khaddaj Mallat et al., 2017). There is good evidence that ECs, when exposed to hyperglycemia, undergo significant alterations that result in an imbalance between vasodilation and vasoconstriction as well as the development of inflammatory and vascular complications (Bakker et al., 2009; Meza et al., 2019). Moreover, high glucose concentrations have been shown to trigger the shift of the endothelium toward the mesenchymal phenotype (Yu et al., 2017; Giordo et al., 2021). Overall, EndMT appears to represent the key link in the interaction between inflammation and endothelial dysfunction in diabetic complications (Cho et al., 2018; Man et al., 2019). In the setting of EndMT, ECs lose their typical cobblestone morphology and tight junctions and acquire increased motility and the ability to secrete ECM proteins (Dejana et al., 2017). In addition, concurrently with the loss of typical endothelial markers, such as vascular endothelial cadherin (VE-cadherin), platelet endothelial

cell adhesion molecule (PECAM-1), also known as CD31, and von Willebrand Factor (vWF), they acquire the ability to express several mesenchymal markers, such as alpha-smooth muscle actin (α -SMA), smooth muscle protein 22 alpha (SM22 α), fibronectin, vimentin, and fibroblast specific protein-1 (FSP-1) (Dejana et al., 2017; Hong et al., 2018). EndMT is involved in many chronic and fibrotic disease states and appears to be regulated by several factors (Evard et al., 2016; Thuan et al., 2018; Phan et al., 2020). In diabetes, oxidative stress is emerging as an important trigger of the ECs transformation into myofibroblasts and vascular remodeling (Montorfano et al., 2014; Thuan et al., 2018). Indeed, hyperglycemia can increase the production of reactive oxygen species (ROS), which in turn activate signaling pathways leading to the disruption of ECs hemostasis (Russell et al., 2002; Peng et al., 2013; Li et al., 2017; Volpe et al., 2018). Several signaling pathways have been demonstrated to be involved in EndMT regulation, e.g., transforming growth factor-beta (TGF- β) signaling, Notch signaling, fibroblast growth factor/fibroblast growth factor receptor 1 (FGF/FGFR1) signaling pathway, Smad2/3-mediated pathways (Piera-Velazquez and Jimenez, 2019) and pro-inflammatory signaling cascades (Lin et al., 2018; Ferreira et al., 2019). An important role in the regulation of EndMT is also played by micro RNAs (miRNAs), a class of short endogenous non-coding RNAs that regulate gene expression at post-transcriptional level by binding to the 3'-untranslated region of messenger RNA (mRNA) (Kim et al., 2015; Michlewski and Cáceres, 2019). A single miRNA can target multiple mRNAs, thus influencing several processes such as cell differentiation, proliferation, and apoptosis (Vidigal and Ventura, 2015). miRNAs can also target significant parts of pathways since miRNAs with similar (seed) sequence target similar sets of genes and thus similar sets of pathways (Kehl et al., 2017). Moreover miRNAs can, either positively or negatively, regulate gene expression (Catalanotto et al., 2016). As a result, they represent promising markers and druggable targets for many diseases, including diabetes (Regazzi, 2018; Cao et al., 2019; Fan et al., 2020). An increasing amount of evidence also suggests that diabetes progression is linked to the alteration of miRNAs expression profiles; indeed, profibrotic miRNAs, such as miR-125b, let-7c, let-7g, miR-21, miR-30b, and miR-195 have been shown to be upregulated in EndMT. By contrast, antifibrotic miRNAs, such as miR-122a, miR-127, miR-196, and miR-375, with inhibitory action toward genes responsible for EndMT, have been shown to be downregulated (Ghosh et al., 2012; Kim, 2018; Srivastava et al., 2019). In addition to miRNAs, recent studies have also demonstrated the involvement of another class of small RNAs, known as long non-coding RNAs (lncRNAs), in diabetes-associated EndMT (Feng et al., 2017; Leung and Natarajan, 2018). Compared to miRNAs, the concentrations of lncRNAs are almost tenfold lower, with the latter exhibiting significant tissue and cell specificity (Cabali et al., 2011). However, the knowledge of the function and the regulation of lncRNAs are still limited. This review aims to summarize and discuss the available knowledge on the role of small RNAs in the regulation of EndMT in diabetes-associated fibrotic complications such as retinopathy, nephropathy, cardiomyopathy, atherosclerosis, and its potential link with oxidative.

DIABETIC NEPHROPATHY

Diabetic nephropathy (DN) is the leading cause of chronic kidney disease in about 40% of patients with type 1 and type 2 diabetes (Gross et al., 2005). Poorly controlled blood glucose concentrations can damage the filtering functionality of the kidneys, which become unable to remove waste products and extra fluids from the body (Rheinberger and Böger, 2014; Ruiz-Ortega et al., 2020). The symptoms of DN do not generally manifest in the early stages, but rather when kidney function has significantly deteriorated (Lim, 2014). Therefore, a tight blood glucose control is key to prevent the onset and progression of DN (Lewis and Maxwell, 2014; Ruiz-Ortega et al., 2020). The progression of DN is defined by various clinical stages which reflect the gradual involvement of tissue damage to different kidney compartments: glomerulus, tubules, vasculature and interstitium (Mogensen et al., 1983). The final stage of DN is characterized by renal fibrosis and organ failure, which are the result of the excessive accumulation of ECM (Calle and Hotter, 2020). Renal fibrosis is driven by multiple mechanisms, including glucose metabolism abnormalities associated with oxidative stress, inflammatory processes, and hemodynamic changes (Brosius, 2008). Consequently, many signaling pathways and cell types (mesangial cells, endothelial cells and podocytes) are involved in the fibrotic process (Badal and Danesh, 2014; Aghadavoud et al., 2017). As mentioned above, alterations of glucose metabolism not only activate various signaling pathways (Badal and Danesh, 2014; Aghadavoud et al., 2017) but also induce oxidative stress, a key pathophysiological step in the onset and progression of diabetes-associated vascular complications (Kashihara et al., 2010; Mima, 2013; Oguntibeju, 2019). Indeed, high glucose concentrations activate the diacylglycerol-protein kinase C (DAG-PKC) pathway, which is associated with endothelial dysfunction, increased production of extracellular matrix and activation of cytokines and transforming growth factor- β (TGF- β) (Koya and King, 1998; Evcimen and King, 2007). In addition, protein kinase C (PKC) induces oxidative stress by activating mitochondrial NADPH oxidase (Chen et al., 2014; Giordo et al., 2021). Increased glucose can also activate aldose reductase and the polyol pathway, leading to the depletion of Nicotinamide Adenine Dinucleotide Phosphate (NADPH), which is also required for the generation of the cellular antioxidant nitric oxide (NO) (Teschfariam, 1994; Hummel et al., 2006; Ying, 2008; Zhao et al., 2008). The reduced NO availability compromises the balance between ROS generation and antioxidant defense, one of the leading causes of endothelial dysfunction (Schiffirin, 2008). Furthermore, hyperglycemia enhances the formation of advanced glycation end products (AGEs), proteins or lipids that become glycated as a result of exposure to sugars (Goldin et al., 2006). AGEs increase ROS production and promote inflammation and fibrosis through the activation of PKC, the nuclear factor kappa light chain enhancer of activated B cells (NF- κ B) and TGF- β (Aghadavoud et al., 2017; Rhee and Kim, 2018). Within the hemodynamic factors driving renal fibrosis, an important role is played by the over-activation of the renin-angiotensin-aldosterone system (RAAS), a crucial hormone system in blood pressure regulation

and fluid balance (Benigni et al., 2010; Patel et al., 2017). Hyperglycemia and insulin resistance increases the release of angiotensin II (Ang II) a potent vasoconstrictor belonging to the RAAS system (Giacchetti et al., 2005; Benigni et al., 2010; Williams and Scholey, 2018). Angiotensin II plays an important role in renal fibrosis by activating a number of factors responsible for ECM production such as TGF- β , PKC and NF- κ B (Badal and Danesh, 2014; Aghadavoud et al., 2017). On the other hand, Angiotensin-converting enzyme2 (ACE2), the main modulator of the RAAS system (Benigni et al., 2010), prevents the accumulation of Ang II by catalyzing the conversion of Ang II into the vasodilator Angiotensin I (Ang I) (Batlle et al., 2010; Williams and Scholey, 2018). Although no cure is available for DN, the control of blood sugar levels and blood pressure, together with a healthy lifestyle, can slow or stop its progression. The most common DN treatments are based on the RAAS system inactivation; precisely with the use of either the ACE inhibitors (ACEis) or angiotensin receptor blockers (ARBs) or their combination (Anand and Tamura, 2012; Pathak and Dass, 2015). This type of treatments allows the lowering of proteinuria and the blood pressure within the glomerular capillaries. In addition, ACEis can also ameliorates kidney fibrosis in combination with other drugs. Is this the case of *N*-acetyl-seryl-aspartyl-lysyl-proline (AcSDKP) an antifibrotic peptide that, in combination with the ACEi, imidapril, improves kidney fibrosis restoring antifibrotic miRNAs, such as miR-29 and miR-let-7 and increasing the inhibition of the profibrotic dipeptidyl peptidase-4 (DPP-4) (Nitta et al., 2016; Srivastava et al., 2020a). DPP-4 inhibitors are another class of medicines used for DN's treatment. In this context, due to the highest affinity for DPP-4, the drug Linagliptin is one of the most widely used (Kanasaki, 2018). In addition, promising data also come from treatments aiming at restoring Sirtuin 3 (SIRT3), which appear to ameliorate renal damage, via inhibition of aberrant glycolysis and preserving mitochondrial homeostasis (Srivastava et al., 2018; Locatelli et al., 2020).

miRNAs REGULATION OF DN-ASSOCIATED EndMT

The ECM is a three-dimensional network of macromolecules (proteoglycans and fibrous proteins), present in all tissues and organs, that contributes to tissue morphogenesis, differentiation and homeostasis. Collagens, elastins, fibronectins, and laminins are the main proteins constituting the ECM (Frantz et al., 2010; Yue, 2014). The excessive deposition of ECM components is the hallmark of fibrosis, which represents a key pathophysiological step in many chronic inflammatory diseases, including diabetes (Herrera et al., 2018). Myofibroblasts are the main cellular mediators of fibrosis as they have the ability to invade the interstitial space and produce excessive amounts of ECM proteins (Zent and Guo, 2018). Although resident mesenchymal cells are the main source of myofibroblasts, the latter can also derive from other type of cells including pericytes, fibrocytes, epithelial and endothelial cells (ECs). The process involving ECs, known as EndMT, has been shown to actively contribute to

the progression of renal fibrosis (Zeisberg et al., 2008; Curci et al., 2014; Sun et al., 2016). Besides, the mesenchymal shift contribution to kidney fibrosis can also be accelerated by the crosstalk between endothelium and epithelium, since EndMT can influence and induce EMT in tubular cells (Li et al., 2020b). In this context, *N*-acetyl-seryl-aspartyl-lysyl-proline (AcSDKP) plays a crucial role in inhibiting both EndMT and EndMT-mediated EMT. Its inhibitory action is exerted by targeting the fibroblast growth factor receptor 1 (FGFR1), an antifibrotic endothelial receptor (Li et al., 2020b), and by controlling the metabolic switch between glucose and fatty acid metabolism. Indeed, defects in normal kidney metabolism can accelerate EndMT and EndMT-mediated EMT contributing to kidney fibrosis (Srivastava et al., 2018, 2020b). An increasing body of evidence suggests that miRNAs are key regulators of EndMT as they appear differentially expressed under fibrotic stimuli such as high glucose, TGF β , and hypoxia (Glover et al., 2019). This differential expression also reflects the specific role, profibrotic or antifibrotic, played by miRNAs (Hulshoff et al., 2019; Srivastava et al., 2019). The most potent inducer of kidney fibrosis is TGF- β (Wang J. et al., 2016; Wang Z. et al., 2017), which can trigger EndMT either by activation of specific signaling pathways, such as Akt and Smad (Wang J. et al., 2016; Wang Z. et al., 2017), or by increasing the expression of pro-fibrotic miRNAs (Srivastava et al., 2019). In this context, TGF- β mediates EndMT through the up-regulation of miR-21, a key modulator of fibrosis (Srivastava et al., 2013; Huang et al., 2015). Specifically, TGF- β elicits miR-21 increase through the activation of Smad3 which regulates miR-21 expression both at a transcriptional and a post-transcriptional level (Zhong et al., 2011). In addition, Smad3 modulates the expression of other miRNAs and activates the expression of various fibrotic genes (Loboda et al., 2016). Another mechanism used by miR-21 to stimulate renal fibrosis is the inhibition of Smad7 protein, a negative regulator of TGF- β 1/Smad3 signaling. In this context, Smad7 has been shown to suppress renal fibrosis by down-regulating pro-fibrotic miRNAs such as miR-21 and miR-192 while up-regulating the anti-fibrotic miR-29b (Chung et al., 2013; Loboda et al., 2016). Additionally, miR-21 also regulates TGF- β -mediated EndMT through the PTEN/Akt pathway (Kumarswamy et al., 2012). Specifically, TGF- β increases the endothelial expression of miR-21, which in turn decreases the expression of PTEN, ultimately promoting EndMT by Akt activation (Meadows et al., 2009; Medici et al., 2011; Kumarswamy et al., 2012). Another molecule linked to TGF- β signaling in kidney fibrosis is the dipeptidyl peptidase-4 (DPP-4), a multi-functional protein expressed on the surface of most cell types, including ECs (Deacon, 2019). DPP-4 overexpression induces TGF- β -mediated EndMT in diabetic nephropathy (Shi et al., 2015; Kanasaki, 2016). Furthermore, recent studies have reported a relationship between DPP-4 and miR-29 in diabetic kidney fibrosis, where the overexpression of DPP-4 results associated with the suppression of miR-29s family anti-fibrotic activity (Kriegel et al., 2012; Harmanici et al., 2017). In line with these observations, the use of the DPP-4 inhibitor, linagliptin, ameliorates kidney fibrosis by restoring miR-29s and consequentially inhibiting EndMT in diabetic mice (Kanasaki et al., 2014). The anti-fibrotic peptide, AcSDKP which suppresses

the TGF- β -induced EndMT in diabetic kidney (Nagai et al., 2014; Hrenak et al., 2015) can also, alone or in combination with angiotensin-converting enzyme inhibitor (ACEi), ameliorates renal fibrosis by suppressing DPP-4 and restoring the anti-fibrotic miR-29s and miR-let-7s expression in TGF- β -induced EndMT (Srivastava et al., 2020a). The crosstalk between miR-29s and miR-let-7s is crucial for maintaining endothelial cell homeostasis and AcSDKP potentiates this crosstalk regulation (Srivastava et al., 2019). Indeed, the presence of AcSDKP upregulates the antifibrotic miR-let-7 families, especially miR-let-7b, which suppress TGF β 1 and TGF β signaling (Srivastava et al., 2016). Suppression of TGF β signaling results in the up-regulation of the miR-29 family expression, which in turn induce FGFR1 phosphorylation, a critical step for miR-let-7 production (Srivastava et al., 2016, 2019). The associated expression of miR-29 and miR-let-7 is also regulated by an alternative mechanism involving interferon-gamma (IFN γ) (Srivastava et al., 2019). Precisely, miR-29 target the profibrotic IFN γ (Ma et al., 2011) blocking its inhibitory action toward FGFR1 which in turn induces the expression of miR-let-7 (Chen et al., 2012; Srivastava et al., 2019). Although not strictly related to DN, an additional anti-fibrotic mechanism, occurring by the suppression of DPP-4, involves miR-448-3p. EndMT inhibition and amelioration of vascular dysfunction has been indeed observed in both diabetic mice and cell models overexpressing miR-448-3p (Guan et al., 2020). A further regulatory mechanism of EndMT in diabetic nephropathy involves miR-497 and its two targets, ROCK1 and ROCK2, which belong to the rho-associated kinases (ROCKs) family and are activated in diabetes (Kolavennu et al., 2008; Liu et al., 2018; Matoba et al., 2020). A recent study showed that ROCKs inhibition, following treatment with melatonin (*N*-acetyl-5-methoxytryptamine), suppressed TGF- β 2-induced EndMT. Specifically, the negative modulation of ROCK1 and ROCK2 is associated with the melatonin-induced up-regulation of miR-497, both in glomerular cells and diabetic rats (Liu et al., 2018). See figures and associated tables to overview of the signaling pathways involving both anti-fibrotic (**Figure 1** and **Table 1**) and pro-fibrotic (**Figure 2** and **Table 2**) miRNAs.

DIABETIC CARDIOMYOPATHY

Diabetic cardiomyopathy (DCM), another common complication in diabetes, refers to myocardial dysfunction in the absence of conventional cardiovascular complications (coronary artery disease, valvular disease) and risk factors (hypertension, dyslipidemia) (Boudina and Abel, 2010; Jia et al., 2018). In the early stages, DCM is usually asymptomatic and characterized by left ventricular (LV) hypertrophy, LV diastolic dysfunction with diastolic filling abnormalities, myocardial fibrosis and cell signaling abnormalities. Disease progression leads to systolic dysfunction (left ventricular low ejection fraction) accompanied by heart failure, which is characterized by marked hypertrophy and fibrosis in the advanced stages (Boudina and Abel, 2010; Jia et al., 2018; Tan et al., 2020). Hyperglycemia, insulin resistance, lipid metabolism defects and oxidative stress up-regulate the production of advanced

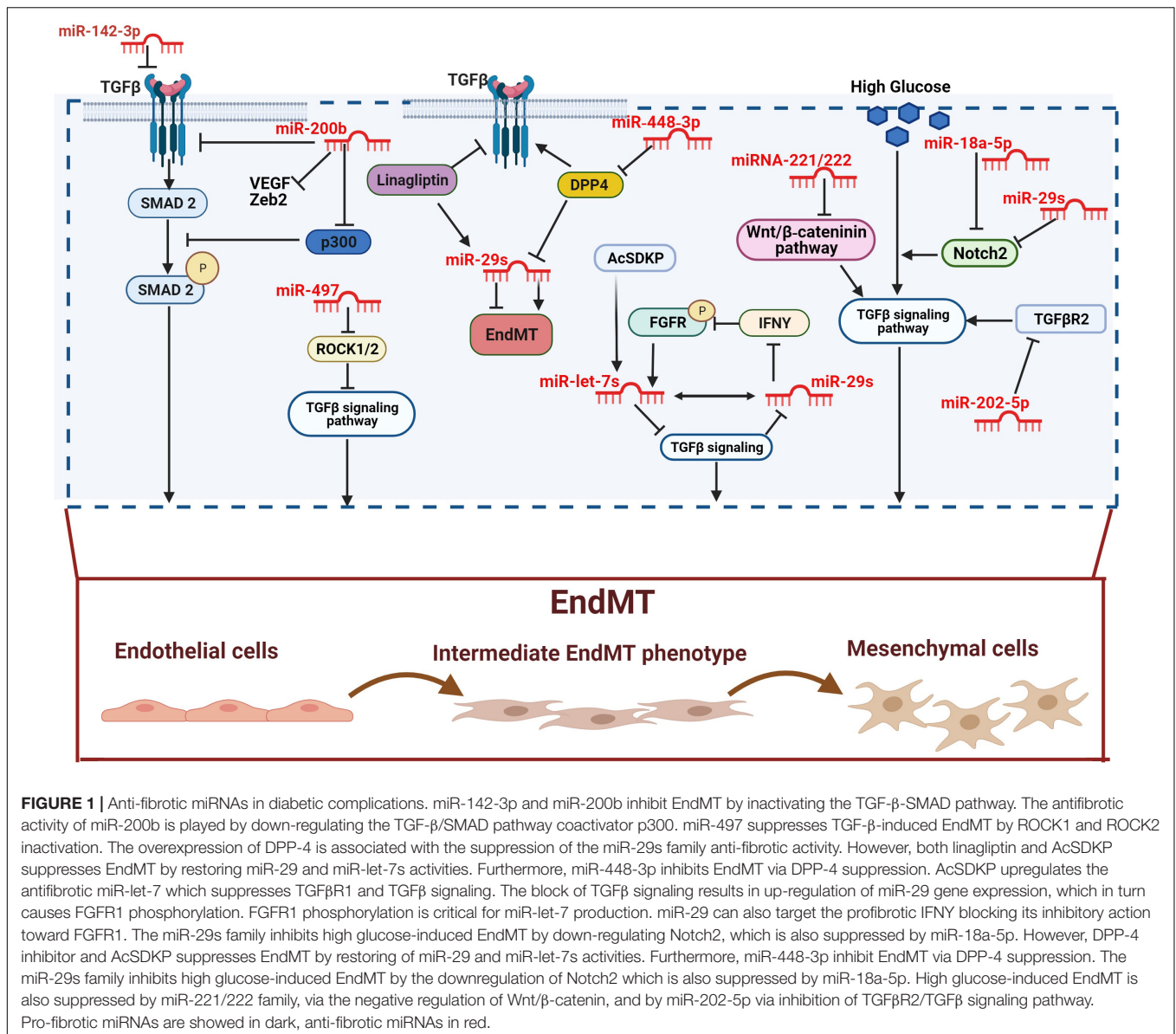


FIGURE 1 | Anti-fibrotic miRNAs in diabetic complications. miR-142-3p and miR-200b inhibit EndMT by inactivating the TGF-β-SMAD pathway. The antifibrotic activity of miR-200b is played by down-regulating the TGF-β/SMAD pathway coactivator p300. miR-497 suppresses TGF-β-induced EndMT by ROCK1 and ROCK2 inactivation. The overexpression of DPP-4 is associated with the suppression of the miR-29s family anti-fibrotic activity. However, both linagliptin and AcSDKP suppresses EndMT by restoring miR-29 and miR-let-7s activities. Furthermore, miR-448-3p inhibits EndMT via DPP-4 suppression. AcSDKP upregulates the antifibrotic miR-let-7 which suppresses TGFβR1 and TGFβ signaling. The block of TGFβ signaling results in up-regulation of miR-29 gene expression, which in turn causes FGFR1 phosphorylation. FGFR1 phosphorylation is critical for miR-let-7 production. miR-29 can also target the profibrotic IFNγ blocking its inhibitory action toward FGFR1. The miR-29s family inhibits high glucose-induced EndMT by down-regulating Notch2, which is also suppressed by miR-18a-5p. However, DPP-4 inhibitor and AcSDKP suppresses EndMT by restoring of miR-29 and miR-let-7s activities. Furthermore, miR-448-3p inhibit EndMT via DPP-4 suppression. The miR-29s family inhibits high glucose-induced EndMT by the downregulation of Notch2 which is also suppressed by miR-18a-5p. High glucose-induced EndMT is also suppressed by miR-221/222 family, via the negative regulation of Wnt/β-catenin, and by miR-202-5p via inhibition of TGFβR2/TGFβ signaling pathway. Pro-fibrotic miRNAs are showed in dark, anti-fibrotic miRNAs in red.

TABLE 1 | Anti-fibrotic miRNAs in diabetic complications.

Anti-fibrotic miRNAs in diabetic complications

| miRNAs | DN | DR | Other | DCM | References |
|-------------------------|----------------|------------|----------------|---------------|--|
| miR-142-3p | | | | TGFβ-SMAD | Zhu et al., 2018 |
| miR-200b miR-200b | | TGFβ1-p300 | | TGFβ-p300 | Cao et al., 2014; Feng et al., 2016 |
| miR-202-5p | | TGFβR2 | | | Gu et al., 2020 |
| miR-497b | ROCK1/2 | | | | Liu et al., 2018 |
| miR-221/222 miR-221/222 | | | | Wnt-β/Catenin | Verjans et al., 2018; Wang et al., 2020 |
| miR-29s miR-29s | TGFβ signaling | Notch2 | | | Srivastava et al., 2016, 2019, 2020a; Zhang et al., 2019 |
| miR-Let7 | TGFβ signaling | | | | Srivastava et al., 2016, 2019, 2020a |
| miR-448-3p | | | TGFβ signaling | | Guan et al., 2020 |
| miR-18a-5p | | | | Notch2 | Geng and Guan, 2017 |

Summarizes the references describing the anti-fibrotic miRNAs in diabetic complication. DN, diabetic nephropathy; DR, diabetic retinopathy; DCM, diabetic cardiomyopathy.

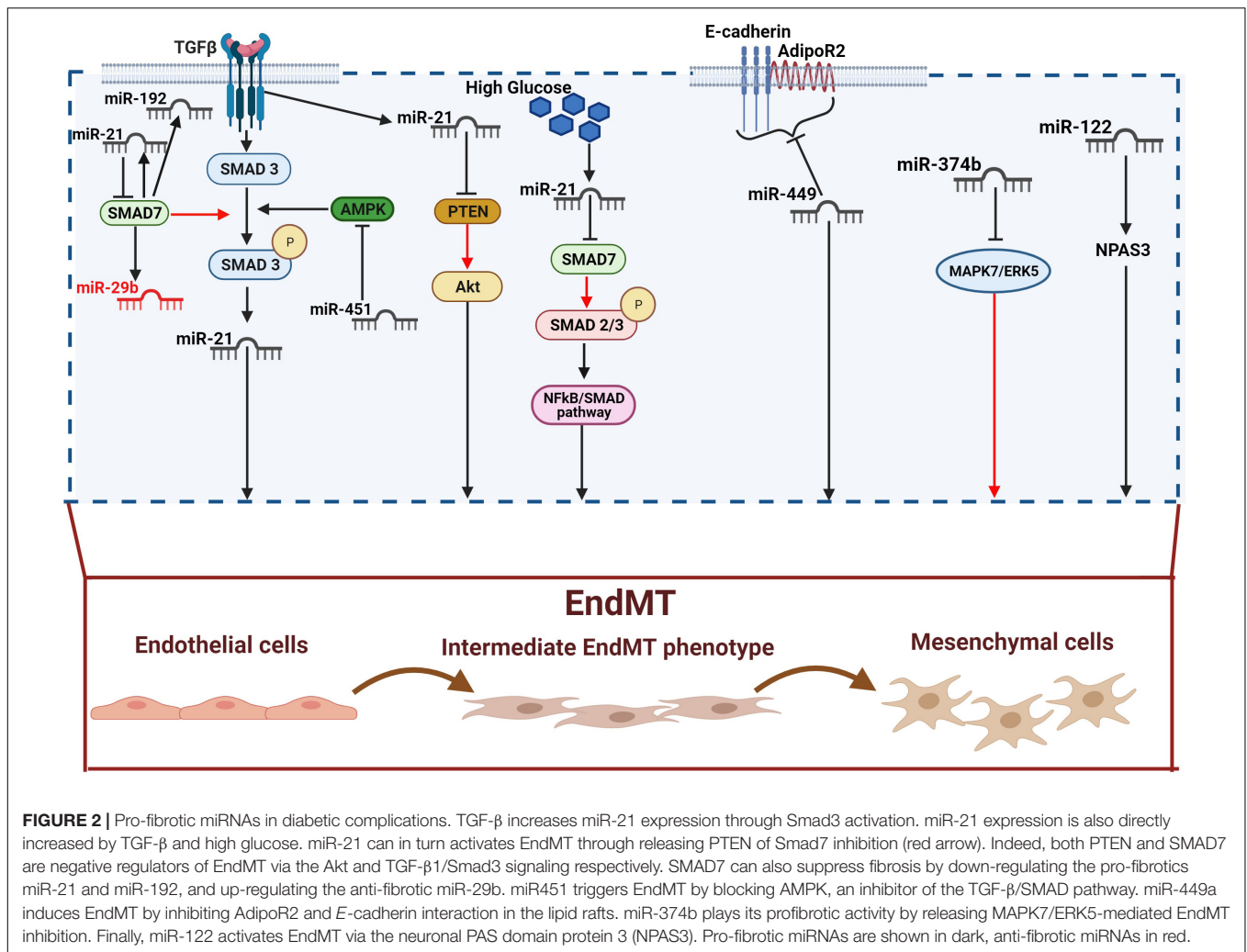


TABLE 2 | Pro-fibrotic miRNAs in diabetic complications.

Pro-fibrotic miRNAs in diabetic complications

| miRNAs | DN | DR | AS | DCM | References |
|----------|-------------------|----|--------------------|--------------------|-------------------------|
| miR-21 | TGF β -SMAD | | | | Srivastava et al., 2013 |
| miR-21 | PTEN/Akt | | | | Kumarswamy et al., 2012 |
| miR-21 | | | | NF κ B/SMAD | Li Q. et al., 2020 |
| miR-451 | | | | TGF β -SMAD | Liang et al., 2019 |
| miR-449 | | | E-cadherin/AdipoR2 | | Jiang et al., 2019 |
| miR-374b | | | MAPK7/ERK | | Vanchin et al., 2019 |
| miR-122 | | | NPAS3 | | Wu et al., 2021 |

Summarizes the references describing the pro-fibrotic miRNAs in diabetic complications. DN, diabetic nephropathy; DR, diabetic retinopathy; DCM, diabetic cardiomyopathy; AS, atherosclerosis.

glycation end-products (AGEs) and Ang II, which in turn induce mitochondrial dysfunction in cardiomyocytes and ECs (Tan et al., 2002; Dikalov and Nazarewicz, 2013; Yan et al., 2014; Brunvand et al., 2017). Mitochondrial dysfunction, as well as the Ang II-induced NADPH oxidases stimulation, increases ROS production and oxidative stress (Dikalov and Nazarewicz, 2013; Siasos et al., 2018). Additionally, oxidative stress is also increased

by lipid accumulation caused by an insulin resistance-induced cardiomyocytes metabolic shift. Indeed, the increased intake of fatty acid is not adequately metabolized by β -oxidation resulting in lipotoxicity (Boudina and Abel, 2010; Tan et al., 2020). Oxidative stress can in turn trigger endoplasmic reticulum (ER) stress, impairment of mitochondrial Ca^{2+} uptake, cardiomyocyte hypertrophy, ECs damage, microvascular dysfunction and the

profibrotic responses by fibroblasts and inflammatory cells (Boudina and Abel, 2010; Tan et al., 2020). All these effects contribute to the accumulation of ECM, especially collagen type I and III, leading to myocardial fibrosis (Jia et al., 2018; Gollmer et al., 2019). The main signaling pathways underlying these pathophysiological events include TGF β /SMAD, NF κ B/SMAD, PKC, MAPK, Wnt/ β -catenin, Notch2 and AcSDKP-FGFR1 signaling pathway (Nemir et al., 2014; Hu et al., 2018; Ma et al., 2018; Hortells et al., 2019; Li et al., 2020b; Yousefi et al., 2020). Most of these pathways lead to the development of cardiac fibrosis through the differentiation of fibroblasts into myofibroblasts as well as the endothelial-to-mesenchymal or epithelial-to-mesenchymal transition (Kovacic et al., 2012). Furthermore, increasing evidence suggests that miRNAs are the main players in the regulation of multiple pathways and cellular processes leading to cardiac fibrosis (Guo and Nair, 2017; Nandi and Mishra, 2018; Yousefi et al., 2020).

miRNAs REGULATION OF DCM-ASSOCIATED EndMT

The hyperglycemia-induced ECs damage and activation, resulting in vascular remodeling and EndMT, has been confirmed in myocardial fibrosis (Sharma et al., 2017). As suggested by experimental evidence, cardiac fibrogenesis involves the presence of a subset of EndMT-derived activated cardiac fibroblasts (Widyantoro et al., 2010; Sharma et al., 2017; Sánchez-Duffhues et al., 2018). Similarly, miRNAs are an important regulatory mechanism in cardiac fibrosis and heart failure (Wang Z. et al., 2016; Wang and Cai, 2017). In this context, miR-21, which has been widely described in pulmonary and renal fibrosis (Liu et al., 2016), plays an important role also in the pathogenesis of cardiac fibrosis and DCM (Adam et al., 2012; Guo and Nair, 2017; Yuan et al., 2017; Dai et al., 2018). A recent *in vivo* study confirmed the involvement of miR-21 in EndMT activation and myocardial fibrosis, showing that the hyperglycemia-induced up-regulation of miR-21 in diabetic mice is associated with the down-regulation of endothelial markers and the up-regulation of fibroblast markers (Li Q. et al., 2020). Moreover, similarly to the mechanism described in diabetic nephropathy (Zhong et al., 2011), miR-21 regulates EndMT through the NF- κ B-SMAD signaling pathway by targeting SMAD7. The consequent SMAD7 inhibition increases SMAD2 and SMAD3 phosphorylation, resulting in EndMT activation (Li Q. et al., 2020). An additional mechanism, requiring the TGF- β /SMAD pathway, involves miR-142-3p, which has been shown to attenuate the hyperglycemia-induced EndMT in human aortic endothelial cells (HAECs) (Zhu et al., 2018). Indeed, miR-142-3p overexpression inhibits EndMT by inactivating both TGF- β 1 and the downstream target gene SMAD2. By contrast, TGF- β 1 overexpression significantly abolishes the inhibitory effects of miR-142-3p (Zhu et al., 2018). A negative regulation of glucose-induced EndMT in the heart is also played by miR-200b (Feng et al., 2016). In a recent study, the expression of specific fibrotic markers, such as vascular endothelial growth factor (VEGF) (Yang et al., 2014), zinc finger E-box-binding homeobox (Zeb2)

(Jahan et al., 2018), and TGF- β 1 (Biernacka et al., 2011) was prevented in diabetic mice overexpressing miR-200b (Feng et al., 2016). Moreover, miR-200b overexpression also induces the down-regulation of p300, a transcription coactivator known to contribute to cardiac fibrosis and hypertrophy via TGF- β /SMAD (Bugyei-Twum et al., 2014; Feng et al., 2016). Although the inhibitory role of the whole miR-200 family is well established, both in EMT (Korpál and Kang, 2008; Korpál et al., 2008) and EndMT (Feng et al., 2016; Zhang et al., 2017), unexpectedly a recent study shown that miR-200c-3p exerted the opposite effect, being able to promote EndMT and aortic graft remodeling both *in vivo* and *in vitro* (Chen et al., 2021). Finally, a further TGF- β /SMAD pathway-mediated regulatory mechanism involves miR-451 whose effects on EndMT are AMPK-dependent. Indeed, miR451 knockdown in diabetic mouse hearts suppresses EndMT through the activation of AMPK, which in turn inhibits the TGF- β /SMAD pathway (Liang et al., 2019). As previously mentioned, in addition to TGF- β /SMAD, other pathways underlie the pathophysiological events leading to cardiac fibrosis. One of them is the Wnt signaling pathway, known to promote fibroblast activation and proliferation (Tao et al., 2016). On the other hand, the anti-fibrotic role of miRNA-221/222 family has been confirmed, as their down-regulation was associated with heart failure (Verjans et al., 2018). The interplay between Wnt and miR-222 in EndMT regulation has been recently suggested (Wang et al., 2020); specifically, miR-222 is able to suppress the hyperglycemia-induced EndMT and inhibit cardiac fibrosis by negatively regulating the Wnt/ β -catenin pathway in diabetic mice (Wang et al., 2020). Lastly, a further protective effect versus EndMT is exerted through the notch pathway and involves miR-18a-5p (Geng and Guan, 2017). The role of the notch pathway in heart development and control of the balance between fibrotic and regenerative repair in the adult heart has been widely confirmed (Nemir et al., 2014). Moreover, Notch2 activation results essential for driving ECs differentiation (Nosedá et al., 2004; Kovacic et al., 2019) in cardiovascular disease and for promoting EndMT independently or in association with TGF- β /SMAD3 signaling (Fu et al., 2009; Chang et al., 2011). Notch2 is a target of miR-18a-5p which recently confirmed its antifibrotic role via the suppression of Notch2 and consequent inhibition of hyperglycemia-induced EndMT in human aortic valvular endothelial cells (HAVECs) (Geng and Guan, 2017). See figures and associated tables to overview of the signaling pathways involving both anti-fibrotic (**Figure 1** and **Table 1**) and pro-fibrotic (**Figure 2** and **Table 2**) miRNAs.

DIABETIC RETINOPATHY

Diabetic retinopathy (DR) is a common and severe microvascular complication of the eye that represents the leading cause of blindness in diabetes (Sabanayagam et al., 2016). The prevalence increases with disease progression and consequently with the exposure to the major risk factors, hyperglycemia and hypertension (Ding and Wong, 2012; Lee et al., 2015). Generally, a tight blood glucose control is cornerstone to reduce

the risk of DR progression (Cheung and Wong, 2008). The condition is initially characterized by an asymptomatic stage, non-proliferative diabetic retinopathy (NPDR), that involves increased vascular permeability and capillary occlusion. Retinal neovascularization, by contrast, predominates in a later stage, proliferative diabetic retinopathy (PDR) (Lechner et al., 2017; Kusuhara et al., 2018), as consequence of hypoxia. However, as new vessels are relatively fragile, they tend to bleed into the macular region causing vision difficulties and, in the worst-case scenario, diabetic macular edema (DME), the main cause of blindness in DR (Wang and Lo, 2018). DME is described as a swelling of the macula due to fluid accumulation following breakdown of the blood-retinal barrier (BRB). This event can occur both in the PDR and in the NPDR stage (Das et al., 2015; Romero-Aroca et al., 2016). The BRB is composed of two distinct barriers: the outer BRB, consisting of retinal pigment epithelium and the inner BRB, composed of endothelial cells regulating the transport across retinal capillaries. Besides, the BRB is established by tight cellular junctions, both in the inner and outer barrier, as well as by the scarcity of endocytic vesicles within cells, which further ensure the integrity of the BRB (Klaassen et al., 2013; Díaz-Coránguez et al., 2017). In addition, pericytes, specialized mural cells with a central role in angiogenesis, regulate and stabilize this tight structure through the Angiopoietin-1/Tie-2, platelet-derived growth factor (PDGF) and TGF- β signaling pathways (Caporarello et al., 2019; Trost et al., 2019). BRB breakdown is a complex process involving different mechanisms; it can occur either in the inner BRB, the outer BRB, or both sites. The loss of integrity of the endothelial cell-cell junctions, the loss of pericytes and the thickening of the basement membrane are the major alterations observed in the inner BRB (Hammes et al., 2011; Das et al., 2015). Several studies have shown that hyperglycemia represents the main risk factor contributing to the pathogenesis of diabetic retinopathy (Engerman and Kern, 1986; Das et al., 2015; Eshaq et al., 2017). Furthermore, using a BRB model formed by retinal pericytes, astrocytes and endothelial cells, it has been recently reported that high glucose exposure elicits BRB breakdown, enhances BRB permeability and reduces the levels of junction proteins such as ZO-1 and VE-cadherin (Fresta et al., 2020). Besides, elevated ROS as well as pro-inflammatory mediators (IL-1 β , IL-6) and oxidative stress-related enzymes (iNOS, Nox2) have also been shown to be increased (Fresta et al., 2020). The major biochemical pathways involved in the BRB breakdown are the polyol pathway, the AGEs pathway, the PKC pathway and the hexosamine pathway. Oxidative stress and inflammation are responsible for the upregulation of growth factors and cytokines, such as VEGF, tumor necrosis factor (TNF), interleukins (ILs), and matrix metalloproteinases (MMPs), which contribute to the BRB breakdown and to the development of DME (Aiello et al., 1994; Brownlee, 2005; Gupta et al., 2013; Das et al., 2015). Studies have confirmed the role of the pro-angiogenic factor VEGF as main modulator of PDR and DME. VEGF is secreted by retinal pigmented epithelial cells, pericytes, and endothelial cells in response to hypoxia conditions caused by the obstruction and loss of retinal capillaries (Gupta et al., 2013; Romero-Aroca et al., 2016). VEGF,

in addition to promoting neovascularization in PDR, participates in the breakdown of the BRB via increasing permeability of retinal vessels (Ray et al., 2004). Indeed, high levels of VEGF increase the expression of the inflammatory intercellular adhesion molecule-1 (ICAM-1) which in turn facilitates the adhesion of leukocytes to the diabetic retinal vasculature, promoting capillary occlusion (Aiello et al., 1994; Jousseaume et al., 2002; Romero-Aroca et al., 2016).

miRNAs REGULATION OF DR-ASSOCIATED EndMT

Hyperglycemia-induced increased production of ECM and thickening of the vascular basement membrane is the hallmark of diabetic retinopathy (Roy et al., 2015). As previously mentioned, hyperglycemia promotes fibrosis progression through the generation of ECs-derived myofibroblasts, EndMT. This process has been shown to play an important role also in the pathogenesis of DR (Cao et al., 2014). Similar to other diabetic complications, TGF- β is an important EndMT mediator, mainly through the activation of the SMAD signaling pathways (Van Geest et al., 2010; Cao et al., 2014; Pardali et al., 2017). Moreover, the transcriptional activator p300, already known for increasing the expression of ECM proteins (Kaur et al., 2006), and miR-200b have been described as key regulators of the TGF- β -mediated EndMT in diabetic mice (Cao et al., 2014). Although the specific mechanism played by miR-200b and p300 remains partially unknown, the anti-fibrotic activity of miR-200b, already described in other diabetic complications (McArthur et al., 2011; Feng et al., 2016), has also been confirmed in DR. Specifically, the EndMT observed in the retinas of wild-type diabetic mice was suppressed by the overexpression of miR-200b (Cao et al., 2014). As mentioned before, the outer BRB is composed of tight junctions of retina pigment epithelial cells (RPECs) which secrete various factors, nutrients and signaling molecules that influence the surrounding tissues (Campbell and Humphries, 2013; Liu and Liu, 2019). Chronic hyperglycemia alters RPECs functions contributing to the fluid accumulation in DME and the development of DR (Desjardins et al., 2016). Under stress conditions RPECs cells can release large amounts of exosomes, nanoscale vesicles that mediate many intercellular activities such as cell-to-cell communication, immune regulation, inflammatory response, extracellular matrix turnover and neovascularization (Klingeborn et al., 2017; Liu et al., 2020). A recent study confirmed the importance of the crosstalk between ECs and RPECs cells in the progression of fibrosis in patients with DR (Gu et al., 2020). Specifically, it was observed that hyperglycemia increased the ability of RPECs to release miR-202-5p-enriched exosomes. On the other hand, hyperglycemia induced EndMT through the TGF β signaling pathway activation in ECs. However, when ECs were treated with RPECs-derived exosomes, the hyperglycemia-induced TGF β signaling pathway activation was significantly counteracted as well as the increased proliferation and migration (Gu et al., 2020). In addition, miR-202-5p, by targeting specifically TGF β R2, was responsible for the TGF β signaling pathway inactivation and EndMT suppression

(Gu et al., 2020). This study, in addition to providing additional evidence that hyperglycemia-induced EndMT involves the activation of TGF β signaling, also showed that the release of miR-202-5p-enriched exosomes from RPE cells leads to the suppression of EndMT. The RPE cells-derived exosomes are therefore important mediators of the ECs-RPE cells crosstalk in the development of DR (Gu et al., 2020). Additional miRNAs involved in EndMT regulation in DR include two members of the mi-RNA29 family, miR-29a and miR-29b, already described in fibrosis development associated with diabetic complications (He et al., 2013; Kanasaki et al., 2014; Zhang Y. et al., 2014; Srivastava et al., 2020a). The anti-fibrotic activity of miR-29a/b has been recently confirmed also in DR where their overexpression suppressed the hyperglycemia-induced EndMT in human retinal microvascular endothelial cells (HRMECs) (Zhang et al., 2019). The inhibitory effect of miR-29a/b was exerted through the down-regulation of the transmembrane protein Notch2, known to activate morphological and functional changes of ECs as well as promote EndMT (Tian et al., 2017; Zhang et al., 2019). See figures and associated tables to overview of the signaling pathways involving both anti-fibrotic (**Figure 1** and **Table 1**) and pro-fibrotic (**Figure 2** and **Table 2**) miRNAs.

ATHEROSCLEROSIS

Atherosclerosis (AS) is characterized by plaque formation, secondary to the deposition of fats, cholesterol, and calcium, which lead to ischemia and its clinical manifestations, such as myocardial infarction and stroke (Lnsis, 2000). Although AS is classically associated with alterations of lipid metabolism and hypercholesterolemia (Wang H.H. et al., 2017), its pathogenesis is more complex and involves various factors. Endothelial dysfunction and inflammation are key steps in the sequence of events leading to AS (Davignon and Ganz, 2004; Hansson, 2009). The presence of mechanical stress, such as blood flow turbulence, can activate the endothelium, which responds by recruiting monocytes, adhesion molecules and pro-inflammatory cytokines. Monocytes, facilitated by adhesion molecules and cytokines, infiltrate the intima and can differentiate in macrophages which actively participate in lipid uptake through phagocytosis (Ilhan and Kalkanli, 2015). Diabetes and AS share several pathological mechanisms (La Sala et al., 2019b); indeed, the metabolic alterations that drive the development of diabetes are also involved in the pathogenesis of atherosclerosis (Federici and Lauro, 2005; Poznyak et al., 2020). In addition, both type 1 and type 2 diabetes can either induce atherosclerosis and accelerate its progression (Poznyak et al., 2020). In this context, a crucial role is played by the prolonged exposure to hyperglycemia and insulin resistance which are responsible for the increased atherosclerosis-related inflammation of the arterial wall (Reddy et al., 2010; Katakami, 2017). In addition to triggering the onset and progression of diabetes, insulin resistance also promotes dyslipidemia, hypertension and other metabolic abnormalities, important components of the pro-atherogenic milieu (Semenkovich, 2006;

Katakami, 2017). At the same time, an insufficient insulin signaling elicits an abnormal lipid metabolism and glucose transport and increase the production of glucose in the liver. Pancreatic β cells respond to hyperglycemia by increasing insulin secretion; however, the continued stimulation of β cells leads to their progressive functional failure and diabetes development (Cavaghan et al., 2000; Mangiafico et al., 2011). Prolonged exposure to hyperglycemia increases oxidative stress (Yu et al., 2011; Volpe et al., 2018), the primary activator of signaling pathways driving AS and diabetes progression (Vanessa Fiorentino et al., 2013; Yuan et al., 2019). Overproduction of ROS increases the formation of AGEs, modifications of proteins or lipids that become non-enzymatically glycated (Moreno-Viedma et al., 2016; Katakami, 2017). AGEs are involved in each step of atherosclerosis, being responsible for monocyte migration into the sub-endothelial space, release of cytokines by macrophages and stimulation of vasoconstriction (Katakami, 2017). Moreover, the binding of AGEs to the receptor RAGE activates TGF- β , ERK, JNK, p38, NF- κ B, PKC and the polyol pathways as well as maintaining the chronic pro-inflammatory state of the arterial wall (Katakami, 2017; Yamagishi and Matsui, 2018).

miRNAs REGULATION OF AS-ASSOCIATED EndMT

As previously mentioned, endothelial dysfunction driven by oxidative stress plays a critical role in the development of AS. Persistent activation of ECs induces EndMT, which contributes to both the initiation and the progression of atherosclerosis (Chen et al., 2015; Evrard et al., 2017). Moreover, the extent of EndMT in the human plaque appears to be strongly correlated with the severity of the disease (Souilhol et al., 2018). A recent study showed the up-regulation of 17 miRNAs in atherosclerotic plaques; among them, miR-449a, already known for its role in lipid and cholesterol anabolism as well as inflammation (Zhang H. et al., 2014), was significantly higher compared with normal arteries (Jiang et al., 2019). The authors reported that miR-449a induces EndMT and promotes the development of AS by targeting the interaction between adiponectin receptor 2 (AdipoR2) and *E*-cadherin in lipid rafts (Jiang et al., 2019). In this context, miR-449a has displayed a multilevel and complex regulatory mechanism by promoting proliferation and enhancing the migrating ability of ECs as well as their expression of atherosclerotic markers (Jiang et al., 2019). The ability to induce EndMT was confirmed by the reduced *E*-cadherin expression concurrently with the increased expression of α -SMA and SMAD3 (Jiang et al., 2019). miR-449a pro-atherosclerotic properties are exerted by inhibition AdipoR2 and *E*-cadherin migration into the lipid raft fractions of ECs and consequent suppression *E*-cadherin-AdipoR2 of interaction. Additionally, the authors reported that blocking miR-449a protects diabetic mice from developing AS (Jiang et al., 2019). Similarly to miR-449a, miR-374b was reported to be up-regulated both in atheroprone regions from mice and pigs and in TGF- β 1-treated ECs (Vanchin et al., 2019). Additionally, the overexpression

of miR-374b was associated with a reduction in endothelial markers (VE-Cadherin and eNOS), and a concomitant increase of mesenchymal markers (TAGLN and Calponin). Besides, miR-374b was able to induce EndMT through the silencing of the Mitogen-Activated Protein Kinase 7 (MAPK7) also known as ERK5 (Vanchin et al., 2019). MAPK7 is an antagonist of EndMT and its signaling activity is generally lost in vessel areas that are undergoing pathological remodeling (Nithianandarajah-Jones et al., 2014; Krenning et al., 2016). Similarly, MAPK7 signaling activity was lost in the sites of vascular remodeling, providing an additional confirmation of the inhibitory action of miR-374b. By contrast, the recovery of MAPK7 signaling abrogated the pathological effect of miR-374b (Vanchin et al., 2019). miR-122, another miRNA recently reported as EndMT mediator in AS, has been shown to be up-regulated both in the aortic intima of diabetic mice and in the cellular EndMT model (Wu et al., 2021). The regulatory action of miR-122 is mediated by the neuronal PAS domain protein 3 (NPAS3). Indeed, inhibition of miR-122 prevented atherosclerosis and regulated NPAS3-mediated EndMT (Wu et al., 2021). miR-122 might therefore represent a druggable target in preventing EndMT-associated atherosclerosis. See figures and associated tables to overview of the signaling pathways involving both anti-fibrotic (Figure 1 and Table 1) and pro-fibrotic (Figure 2 and Table 2) miRNAs.

LONG NON-CODING RNAs REGULATION IN DIABETES-ASSOCIATED EndMT

Besides miRNAs, small RNAs also include long non-coding RNAs (lncRNAs) and circular RNAs (circRNAs) which are emerging as key regulators implicated in a significant number of biological processes (Qu et al., 2017; Statello et al., 2020). Unlike linear RNAs, circRNAs form a covalently closed continuous loop, without 5' or 3' ends (Qu et al., 2015). lncRNAs are instead linear RNAs, with a nucleotide length > 200, that can affect gene transcription both at the epigenetic, transcriptional and post-transcriptional level (Dykes and Emanueli, 2017; Wang C. et al., 2017). Thus, lncRNAs can differently interact with mRNAs, proteins, and DNA elements; moreover, the binding of transcriptional factors to the lncRNA promoter's target sites can regulate their expression (Taft et al., 2010). lncRNAs are also precursors of many types of miRNAs, although more frequently they overlap both physically and functionally with the latter. Moreover, lncRNAs compete with miRNAs for the binding to the same target genes and can trigger miRNAs degradation (Taft et al., 2010; Chen et al., 2018). Hence, lncRNAs are involved in a variety of human diseases where they appear differentially expressed or genetically perturbed (Harries, 2012; Shi et al., 2013). In this context, most of the knowledge pertaining to lncRNAs is derived from cancer however there is increasing evidence of their involvement in other conditions, such as Alzheimer's disease, diabetes, cardiac complications (DiStefano, 2018; Greco et al., 2018; Leung and Natarajan, 2018) and fibrosis (He Z. et al., 2020; Li et al., 2020a; Lin J. et al., 2020). One important function of lncRNAs is

their role as a molecular sponge to certain miRNAs, hindering their expression (Biswas et al., 2018). This mechanism has been confirmed in diabetic kidney fibrosis, where the down-regulation of the anti-fibrotic miR-29 was associated with lncRNA H19 up-regulation, whereas its knockdown restored miR-29 activity and significantly inhibited TGF- β 2-induced EndMT in diabetic mice (Shi et al., 2020). However, the role of H19 in diabetes-associated EndMT remains unclear; indeed, H19 overexpression prevented glucose-induced EndMT by reducing the TGF- β 1 levels in DR (Thomas et al., 2019). Further studies are required to clarify the role of H19 in regulating EndMT in diabetic conditions. Another lncRNA involved in DR is the maternally expressed gene 3 (MEG3) which showed an inhibitory effect on hyperglycemia-induced EndMT. MEG3 resulted indeed able to suppress EndMT both *in vivo* and *in vitro* by inhibiting the PI3K/AKT/mTOR signaling pathway (He Y. et al., 2020). On the other hand, MEG3 methylation mediated by DNA methyltransferase 1 (DNMT1) attenuated MEG3 expression and consequently accelerated EndMT (He Y. et al., 2020). This finding clarifies the role of MEG3 in EndMT and provide additional confirmation that increased levels of DNA methylation represent a potential risk factor for the development of DR (Maghbooli et al., 2015). As previously reported, oxidized low density lipoproteins (ox-LDL), being able to trigger plaque formation and EndMT, are key players in AS development (Su et al., 2018). A recent study reported that miR-30c-5p and LINC00657, also known as non-coding RNA activated by DNA damage (NORAD), are both involved in ox-LDL-induced EndMT but with opposite effects (Wu et al., 2020). miR-30c-5p inhibited ox-LDL-induced EndMT via activation of the Wnt7b/ β -catenin pathway whereas LINC00657, acting as sponge of miR-30c-5p, suppressed the EndMT inhibition (Wu et al., 2020). Indeed, the expression level of LINC00657 resulted elevated both in sera from AS patients and in ox-LDL-stimulated ECs (Wu et al., 2020).

POTENTIAL ROS-EndMT-SMALL RNAs INTERPLAY IN DIABETES-ASSOCIATED FIBROTIC CONDITIONS

Oxidative stress is a key player in the diabetic complications' pathophysiology described in this review. Hyperglycemia is not only the main factor responsible for the increase in ROS but also favors the increase of inflammatory mediators, which ultimately leads to vascular dysfunction (Luc et al., 2019). Both genetic and epigenetic factors can regulate the development and exacerbation of oxidative stress; in this context, different studies have highlighted the key role played by miRNAs (Grieco et al., 2019). Indeed, hyperglycemia can alter miRNAs expression, which in turn contributes to the development of endothelium dysfunction and diabetic vascular disease (Luc et al., 2019). Besides, in diabetic complications the molecular mechanisms and signaling pathways triggered by oxidative stress appear similar to those involved in miRNAs regulation (Grieco et al., 2019; Qadir et al., 2019). Finally, hyperglycemia-induced oxidative stress can affect the expression

of specific miRNAs, which in turn can exacerbate oxidative stress, in addition to regulating the fibrotic process through the mechanisms summarized in this review (Grieco et al., 2019; Qadir et al., 2019). On the other hand, oxidative stress is emerging as a key trigger of EndMT (Montorfano et al., 2014; Thuan et al., 2018). Therefore, although a direct oxidative stress-small RNAs-EndMT link has not been demonstrated in diabetes yet, a substantial body of evidence supports this interplay. For example, an indirect proof of a ROS-miR-21-EndMT link has been reported with kallistatin, an endogenous protein with beneficial effects on EndMT-associated fibrosis (Guo et al., 2015). Kallistatin treatment blocked TGF- β -induced EndMT, NADPH oxidase-dependent ROS formation and the expression of the pro-fibrotic miR-21, confirming the role of both miR-21 and ROS as major mediators of EndMT (Guo et al., 2015). Many studies indicated a direct link between mi-R21 and oxidative stress in diabetic subjects, where ROS generation has been suggested as a downstream effect of miR-21 overexpression (La Sala et al., 2019a). The pro-oxidant effect of miR-21 is exerted through the suppression of genes which usually limit oxidative damage such as KRIT1 (Krev/Rap1 Interaction Trapped-1), Nuclear Factor erythroid Related Factor 2 (NRF2), and MnSOD2 (Manganese-dependent Superoxide Dismutase2). By contrast, inhibition of miR-21 decreases ROS levels (La Sala et al., 2018; Grieco et al., 2019). A relationship between up-regulation of miR-21 and increased ROS levels has also been shown during the development of diabetic cardiac dysfunctions (Yildirim et al., 2013). The miR-200 family, the anti-fibrotic activity of which has been described both in diabetic nephropathy and retinopathy, has also been shown to be associated with a decrease in oxidative stress in diabetes; specifically, the antioxidant effect of miR-200 is exerted by silencing the O-GlcNAc transferase, also known as OGT, whose enzymatic activity is associated with diabetic complications and endothelial inflammation (Qadir et al., 2019). Another proof of the oxidative stress-small RNAs-EndMT interconnection comes from a study investigating the activity of miR-451 (Ruknarong et al., 2021). The latter, previously described for its ability to induce EndMT in diabetic mouse heart (Liang et al., 2019), has been recently reported to be up-regulated in diabetic subjects with high oxidative stress. The association between miR-451 and oxidative stress has been further confirmed with the use of the antioxidant Vitamin C; indeed, Vitamin C administration in diabetic subjects decreased both the expression of miR-451 and ROS levels (Ruknarong et al., 2021). Finally, an interplay being the basis of mitochondrial functions in kidney ECs involves the miR-let-7 family, (FGF)/FGFR1 signaling pathway and SIRT3 (Srivastava et al., 2020c). The integrity of the FGFR1-miR-let-7 axis, on which depends the modulation of SIRT3, is crucial for maintaining the mitochondrial functionality (Srivastava et al., 2020c). SIRT3, for its part, controls mitochondrial redox homeostasis by modulation of ROS levels (Jing et al., 2011; Bause and Haigis, 2013) mainly via activation of the antioxidant enzyme superoxide-dismutase 2 (Qiu et al., 2010). On the contrary, the loss of the FGFR1-miR-let-7axis impairs SIRT3 and miR-29 levels with consequent disruption of mitochondrial

integrity and activation of pro-mesenchymal signaling (Wnt signaling, BMP, Notch, TGF- β signaling) promoting EndMT (Srivastava et al., 2020c).

CONCLUSION AND FUTURE DIRECTIONS

This review has highlighted the key role of EndMT in the fibrotic process occurring in the development of the major diabetic complications. Environmental factors (high glucose, hypoxia, oxidative stress, pro-inflammatory cytokines) are important determinants of EndMT induction through the activation of specific signaling pathways, such as TGF- β , Notch, Wnt, and the modulation of the expression of microRNAs. The evidence reviewed in this article indicates that some microRNAs, e.g., miR-29, miR-200, and miR-Let7, have anti-fibrotic effects and inhibit EndMT whereas others, e.g., miR-21 and miR-122, possess pro-fibrotic properties and promote EndMT. The anti-fibrotic activity of some microRNAs appears univocal not only within diabetic complications but also in other pathological conditions. For instance, miR-29a/b and miR-200b have been shown to inhibit fibrosis in pulmonary fibrosis (Yang et al., 2012; Cushing et al., 2015), systemic sclerosis (Harmanci et al., 2017) as well as in DCM, DN, and DR (Cao et al., 2014; Kanasaki et al., 2014; Feng et al., 2016; Zhang et al., 2019). Similarly, miR-21 is generally up-regulated in different fibrotic diseases (Huang et al., 2015; Liu et al., 2016) as well as in diabetic complications such as DN, DR, and DCM (Srivastava et al., 2013; Chen et al., 2017; Li Q. et al., 2020). Moreover, since the expression levels of miR-21 in the plasma of diabetic patients were correlated with disease progression, miR-21 might be used as a marker of diabetes severity (Jiang et al., 2017). On the other hand, the function of other microRNAs is only partially established in *in vitro* models or in specific pathological conditions. Further, for some miRNAs the evidence is still controversial, such as the case of the lncRNA H19 which showed pro-fibrotic activity in DN (Shi et al., 2020) and an opposite effect in DR (Thomas et al., 2019). Additionally, since the markers for EndMT used in individual studies are often different, a complete understanding of the regulatory mechanisms played by miRNAs, or an exact comparison between them, is currently challenging. In this regard, future directions in the study of diabetic complications should involve (a) a thorough characterization of the mechanisms involved in the ROS-EndMT-small RNAs interplay and its relationship with the onset and severity of specific complications, (b) the conduct of epidemiological studies investigating the association between specific miRNAs and lncRNAs and metabolic control, surrogate markers of organ damage, and morbidity and mortality in patients with diabetes, and (c) the effects of specific pharmacological and non-pharmacological interventions targeting EndMT on the risk and progression of diabetic complications. Such studies might contribute to the identification of new diagnostic and therapeutic strategies to prevent or limit the structural and functional damage that leads to organ and system failure in diabetes.

AUTHOR CONTRIBUTIONS

RG, YMAA, and GP: conceptualization. GKN, AAM, and GP: resources. RG and YMAA: writing the original manuscript draft. RG, YMAA, HA, SA, LP, GKN, AAM, and GP: review and editing the different manuscript versions. AAM and GP: final editing and supervision. GP: submission. All authors: read and agreed to the published version of the manuscript.

REFERENCES

- Adam, O., Löhlfel, B., Thum, T., Gupta, S. K., Puhl, S.-L., Schäfers, H.-J., et al. (2012). Role of miR-21 in the pathogenesis of atrial fibrosis. *Basic Res. Cardiol.* 107:278.
- Aghadavoud, E., Nasri, H., and Amiri, M. (2017). Molecular signaling pathways of diabetic kidney disease; new concepts. *J. Prevent. Epidemiol.* 2, e09–e.
- Aiello, L. P., Avery, R. L., Arrigg, P. G., Keyt, B. A., Jampel, H. D., Shah, S. T., et al. (1994). Vascular endothelial growth factor in ocular fluid of patients with diabetic retinopathy and other retinal disorders. *N. Engl. J. Med.* 331, 1480–1487. doi: 10.1056/nejm199412013312203
- Anand, S., and Tamura, M. K. (2012). Combining angiotensin receptor blockers with ACE inhibitors in elderly patients. *Am. J. Kidney Dis. Offic. J. Natl. Kidney Foundat.* 59:11. doi: 10.1053/j.ajkd.2011.09.002
- Badal, S. S., and Danesh, F. R. (2014). New insights into molecular mechanisms of diabetic kidney disease. *Am. J. Kidney Dis.* 63, S63–S83.
- Bakker, W., Eringa, E. C., Sipkema, P., and van Hinsbergh, V. W. (2009). Endothelial dysfunction and diabetes: roles of hyperglycemia, impaired insulin signaling and obesity. *Cell Tissue Res.* 335, 165–189. doi: 10.1007/s00441-008-0685-6
- Ban, C. R., and Twigg, S. M. (2008). Fibrosis in diabetes complications: pathogenic mechanisms and circulating and urinary markers. *Vascul. Health Risk Manage.* 4:575. doi: 10.2147/vhrm.s1991
- Battle, D., Soler, M. J., and Ye, M. (2010). ACE2 and diabetes: ACE of ACEs? *Diabetes* 59, 2994–2996. doi: 10.2337/db10-1205
- Bause, A. S., and Haigis, M. C. (2013). SIRT3 regulation of mitochondrial oxidative stress. *Exp. Gerontol.* 48, 634–639. doi: 10.1016/j.exger.2012.08.007
- Benigni, A., Cassis, P., and Remuzzi, G. (2010). Angiotensin II revisited: new roles in inflammation, immunology and aging. *EMBO Mol. Med.* 2, 247–257. doi: 10.1002/emmm.201000080
- Biernacka, A., Dobaczewski, M., and Frangogiannis, N. G. (2011). TGF- β signaling in fibrosis. *Growth Fact.* 29, 196–202.
- Biswas, S., Thomas, A. A., and Chakrabarti, S. (2018). LncRNAs: proverbial genomic “junk” or key epigenetic regulators during cardiac fibrosis in diabetes? *Front. Cardiovasc. Med.* 5:28. doi: 10.3389/fcvm.2018.00028
- Bochaton-Piallat, M.-L., Gabbiani, G., and Hinz, B. (2016). The myofibroblast in wound healing and fibrosis: answered and unanswered questions. *F1000Research* 5, F1000FacultyRev–752.
- Boudina, S., and Abel, E. D. (2010). Diabetic cardiomyopathy, causes and effects. *Rev. Endocr. Metab. Disord.* 11, 31–39. doi: 10.1007/s11154-010-9131-7
- Brosius, F. C. (2008). New insights into the mechanisms of fibrosis and sclerosis in diabetic nephropathy. *Rev. Endocr. Metab. Disord.* 9, 245–254.
- Brownlee, M. (2005). The pathobiology of diabetic complications: a unifying mechanism. *Diabetes* 54, 1615–1625. doi: 10.2337/diabetes.54.6.1615
- Brunvand, L., Heier, M., Brunborg, C., Hanssen, K. F., Fugelsest, D., Stensaeth, K. H., et al. (2017). Advanced glycation end products in children with type 1 diabetes and early reduced diastolic heart function. *BMC Cardiovasc. Disord.* 17:1–6. doi: 10.1186/s12872-017-0551-0
- Bugyei-Twum, A., Advani, A., Advani, S. L., Zhang, Y., Thai, K., Kelly, D. J., et al. (2014). High glucose induces Smad activation via the transcriptional coregulator p300 and contributes to cardiac fibrosis and hypertrophy. *Cardiovasc. Diabetol.* 13, 1–12.
- Cabili, M. N., Trapnell, C., Goff, L., Koziol, M., Tazon-Vega, B., Regev, A., et al. (2011). Integrative annotation of human large intergenic noncoding RNAs reveals global properties and specific subclasses. *Genes Dev.* 25, 1915–1927. doi: 10.1101/gad.17446611
- Calle, P., and Hotter, G. (2020). Macrophage phenotype and fibrosis in diabetic nephropathy. *Int. J. Mol. Sci.* 21:2806. doi: 10.3390/ijms21082806
- Campbell, M., and Humphries, P. (2013). *The blood-retina barrier. Biology and Regulation of Blood-Tissue Barriers.* Berlin: Springer, 70–84.
- Cao, Q., Chen, X. M., Huang, C., and Pollock, C. A. (2019). MicroRNA as novel biomarkers and therapeutic targets in diabetic kidney disease: an update. *FASEB BioAdv.* 1, 375–388. doi: 10.1096/fba.2018-00064
- Cao, Y., Feng, B., Chen, S., Chu, Y., and Chakrabarti, S. (2014). Mechanisms of endothelial to mesenchymal transition in the retina in diabetes. *Investigat. Ophthalmol. Vis. Sci.* 55, 7321–7331. doi: 10.1167/iovs.14-15167
- Caporarello, N., D’Angeli, F., Cambria, M. T., Candido, S., Giallongo, C., Salmeri, M., et al. (2019). Pericytes in microvessels: from “mural” function to brain and retina regeneration. *Int. J. Mol. Sci.* 20:6351. doi: 10.3390/ijms20246351
- Catalanotto, C., Cogoni, C., and Zardo, G. (2016). MicroRNA in control of gene expression: an overview of nuclear functions. *Int. J. Mol. Sci.* 17:1712. doi: 10.3390/ijms17101712
- Cavaghan, M. K., Ehrmann, D. A., and Polonsky, K. S. (2000). Interactions between insulin resistance and insulin secretion in the development of glucose intolerance. *J. Clin. Investig.* 106, 329–333. doi: 10.1172/jci10761
- Chang, A. C., Fu, Y., Garside, V. C., Niessen, K., Chang, L., Fuller, M., et al. (2011). Notch initiates the endothelial-to-mesenchymal transition in the atrioventricular canal through autocrine activation of soluble guanylyl cyclase. *Dev. Cell* 21, 288–300. doi: 10.1016/j.devcel.2011.06.022
- Chen, D., Zhang, C., Chen, J., Yang, M., Afzal, T. A., An, W., et al. (2021). miRNA-200c-3p promotes endothelial to mesenchymal transition and neointimal hyperplasia in artery bypass grafts. *J. Pathol.* 253, 209–224. doi: 10.1002/path.5574
- Chen, F., Yu, Y., Haigh, S., Johnson, J., Lucas, R., Stepp, D. W., et al. (2014). Regulation of NADPH oxidase 5 by protein kinase C isoforms. *PLoS One* 9:e88405. doi: 10.1371/journal.pone.0088405
- Chen, P.-Y., Qin, L., Baeyens, N., Li, G., Afolabi, T., Budatha, M., et al. (2015). Endothelial-to-mesenchymal transition drives atherosclerosis progression. *J. Clin. Investig.* 125, 4514–4528. doi: 10.1172/jci82719
- Chen, P.-Y., Qin, L., Barnes, C., Charisse, K., Yi, T., Zhang, X., et al. (2012). FGF regulates TGF- β signaling and endothelial-to-mesenchymal transition via control of let-7 miRNA expression. *Cell Rep.* 2, 1684–1696. doi: 10.1016/j.celrep.2012.10.021
- Chen, Q., Qiu, F., Zhou, K., Matlock, H. G., Takahashi, Y., Rajala, R. V., et al. (2017). Pathogenic role of microRNA-21 in diabetic retinopathy through downregulation of PPAR α . *Diabetes* 66, 1671–1682. doi: 10.2337/db16-1246
- Chen, X., Sun, Y., Cai, R., Wang, G., Shu, X., and Pang, W. (2018). Long noncoding RNA: multiple players in gene expression. *BMB Rep.* 51:280. doi: 10.5483/bmbrep.2018.51.6.025
- Cheung, N., and Wong, T. Y. (2008). Diabetic retinopathy and systemic vascular complications. *Prog. Retinal Eye Res.* 27, 161–176. doi: 10.1016/j.preteyeres.2007.12.001
- Cho, J. G., Lee, A., Chang, W., Lee, M.-S., and Kim, J. (2018). Endothelial to mesenchymal transition represents a key link in the interaction between inflammation and endothelial dysfunction. *Front. Immunol.* 9:294. doi: 10.3389/fimmu.2018.00294
- Chung, A. C., Dong, Y., Yang, W., Zhong, X., Li, R., and Lan, H. Y. (2013). Smad7 suppresses renal fibrosis via altering expression of TGF- β /Smad3-regulated microRNAs. *Mol. Therap.* 21, 388–398. doi: 10.1038/mt.2012.251
- Curci, C., Castellano, G., Stasi, A., Divella, C., Loverre, A., Gigante, M., et al. (2014). Endothelial-to-mesenchymal transition and renal fibrosis in

FUNDING

This work has been made possible thanks to grants from the University of Sharjah (Seed 2001050151) to GP; (collaborative 2101050160) to GP and AAM; Qatar University (IRCC-2019-007) to GKN and GP; and (fondo UNISS di Ateneo per la Ricerca 2020) to GP.

- ischaemia/reperfusion injury are mediated by complement anaphylatoxins and Akt pathway. *Nephrol. Dial. Transplant.* 29, 799–808. doi: 10.1093/ndt/gft516
- Cushing, L., Kuang, P., and Lü, J. (2015). The role of miR-29 in pulmonary fibrosis. *Biochem. Cell Biol.* 93, 109–118. doi: 10.1139/bcb-2014-0095
- Dai, B., Li, H., Fan, J., Zhao, Y., Yin, Z., Nie, X., et al. (2018). MiR-21 protected against diabetic cardiomyopathy induced diastolic dysfunction by targeting gelsolin. *Cardiovasc. Diabetol.* 17, 1–17.
- Das, A., McGuire, P. G., and Rangasamy, S. (2015). Diabetic macular edema: pathophysiology and novel therapeutic targets. *Ophthalmology* 122, 1375–1394. doi: 10.1016/j.ophtha.2015.03.024
- Davignon, J., and Ganz, P. (2004). Role of endothelial dysfunction in atherosclerosis. *Circulation* 109, III–27–III–32.
- Deacon, C. F. (2019). Physiology and pharmacology of DPP-4 in glucose homeostasis and the treatment of type 2 diabetes. *Front. Endocrinol.* 10:80. doi: 10.3389/fendo.2019.00080
- Dejana, E., Hirschi, K. K., and Simons, M. (2017). The molecular basis of endothelial cell plasticity. *Nat. Commun.* 8, 1–11. doi: 10.1007/978-1-59259-253-1_1
- Deshpande, A. D., Harris-Hayes, M., and Schootman, M. (2008). Epidemiology of diabetes and diabetes-related complications. *Phys. Therap.* 88, 1254–1264. doi: 10.2522/ptj.20080020
- Desjardins, D. M., Yates, P. W., Dahrouj, M., Liu, Y., Crosson, C. E., and Ablonczy, Z. (2016). Progressive early breakdown of retinal pigment epithelium function in hyperglycemic rats. *Investig. Ophthalmol. Vis. Sci.* 57, 2706–2713. doi: 10.1167/iovs.15-18397
- Díaz-Coránguez, M., Ramos, C., and Antonetti, D. A. (2017). The inner blood-retinal barrier: Cellular basis and development. *Vis. Res.* 139, 123–137. doi: 10.1016/j.visres.2017.05.009
- Dikalov, S. I., and Nazarewicz, R. R. (2013). Angiotensin II-induced production of mitochondrial reactive oxygen species: potential mechanisms and relevance for cardiovascular disease. *Antioxid. Redox Signal.* 19, 1085–1094. doi: 10.1089/ars.2012.4604
- Ding, J., and Wong, T. Y. (2012). Current epidemiology of diabetic retinopathy and diabetic macular edema. *Curr. Diab. Rep.* 12, 346–354. doi: 10.1007/s11892-012-0283-6
- DiStefano, J. K. (2018). The emerging role of long noncoding RNAs in human disease. *Dis. Gene Identificat.* 1706, 91–110. doi: 10.1007/978-1-4939-7471-9_6
- Dykes, I. M., and Emanuelli, C. (2017). Transcriptional and post-transcriptional gene regulation by long non-coding RNA. *Genomics Proteom. Bioinform.* 15, 177–186. doi: 10.1016/j.gpb.2016.12.005
- Engerman, R. L., and Kern, T. S. (1986). Hyperglycemia as a cause of diabetic retinopathy. *Metabolism* 35, 20–23. doi: 10.1016/0026-0495(86)90182-4
- Eshaq, R. S., Aldalati, A. M., Alexander, J. S., and Harris, N. R. (2017). Diabetic retinopathy: breaking the barrier. *Pathophysiology* 24, 229–241. doi: 10.1016/j.pathophys.2017.07.001
- Evcimen, N. D., and King, G. L. (2007). The role of protein kinase C activation and the vascular complications of diabetes. *Pharmacol. Res.* 55, 498–510. doi: 10.1016/j.phrs.2007.04.016
- Evrard, S. M., Lecce, L., Michelis, K. C., Nomura-Kitabayashi, A., Pandey, G., Purushothaman, K.-R., et al. (2016). Endothelial to mesenchymal transition is common in atherosclerotic lesions and is associated with plaque instability. *Nat. Commun.* 7, 1–16.
- Evrard, S. M., Lecce, L., Michelis, K. C., Nomura-Kitabayashi, A., Pandey, G., Purushothaman, K.-R., et al. (2017). Corrigendum: endothelial to mesenchymal transition is common in atherosclerotic lesions and is associated with plaque instability. *Nat. Commun.* 8:14710.
- Fan, B., Chopp, M., Zhang, Z. G., and Liu, X. S. (2020). Emerging roles of microRNAs as biomarkers and therapeutic targets for diabetic neuropathy. *Front. Neurol.* 11:558758. doi: 10.3389/fneur.2020.558758
- Federici, M., and Lauro, R. (2005). Diabetes and atherosclerosis—running on a common Road. *Aliment. Pharmacol. Therapeut.* 22, 11–15. doi: 10.1111/j.1365-2036.2005.02617.x
- Feng, B., Cao, Y., Chen, S., Chu, X., Chu, Y., and Chakrabarti, S. (2016). miR-200b mediates endothelial-to-mesenchymal transition in diabetic cardiomyopathy. *Diabetes* 65, 768–779. doi: 10.2337/db15-1033
- Feng, S.-D., Yang, J.-H., Yao, C. H., Yang, S.-S., Zhu, Z.-M., Wu, D., et al. (2017). Potential regulatory mechanisms of lncRNA in diabetes and its complications. *Biochem. Cell Biol.* 95, 361–367. doi: 10.1139/bcb-2016-0110
- Ferreira, F. U., Souza, L. E. B., Thomé, C. H., Pinto, M. T., Origassa, C., Salustiano, S., et al. (2019). Endothelial cells tissue-specific origins affects their responsiveness to TGF- β 2 during endothelial-to-mesenchymal transition. *Int. J. Mol. Sci.* 20:458. doi: 10.3390/ijms20030458
- Frantz, C., Stewart, K. M., and Weaver, V. M. (2010). The extracellular matrix at a glance. *J. Cell Sci.* 123, 4195–4200. doi: 10.1242/jcs.023820
- Fresta, C. G., Fidio, A., Caruso, G., Caraci, F., Giblin, F. J., Leggio, G. M., et al. (2020). A new human blood–retinal barrier model based on endothelial cells, pericytes, and astrocytes. *Int. J. Mol. Sci.* 21:1636. doi: 10.3390/ijms21051636
- Fu, Y., Chang, A., Chang, L., Niessen, K., Eapen, S., Setiadi, A., et al. (2009). Differential regulation of transforming growth factor β signaling pathways by Notch in human endothelial cells. *J. Biol. Chem.* 284, 19452–19462. doi: 10.1074/jbc.m109.011833
- Geng, H., and Guan, J. (2017). MiR-18a-5p inhibits endothelial–mesenchymal transition and cardiac fibrosis through the Notch2 pathway. *Biochem. Biophys. Res. Commun.* 491, 329–336. doi: 10.1016/j.bbrc.2017.07.101
- Ghosh, A. K., Nagpal, V., Covington, J. W., Michaels, M. A., and Vaughan, D. E. (2012). Molecular basis of cardiac endothelial-to-mesenchymal transition (EndMT): differential expression of microRNAs during EndMT. *Cell. Signal.* 24, 1031–1036. doi: 10.1016/j.cellsig.2011.12.024
- Giacchetti, G., Sechi, L. A., Rilli, S., and Carey, R. M. (2005). The renin–angiotensin–aldosterone system, glucose metabolism and diabetes. *Trends Endocrinol. Metabol.* 16, 120–126. doi: 10.1016/j.tem.2005.02.003
- Giordo, R., Nasrallah, G. K., Posadino, A. M., Galimi, F., Capobianco, G., Eid, A. H., et al. (2021). Resveratrol-Elicited PKC Inhibition Counteracts NOX-Mediated Endothelial to Mesenchymal Transition in Human Retinal Endothelial Cells Exposed to High Glucose. *Antioxidants* 10:224. doi: 10.3390/antiox10020224
- Glover, E. K., Jordan, N., Sheerin, N. S., and Ali, S. (2019). Regulation of endothelial-to-mesenchymal transition by microRNAs in chronic allograft dysfunction. *Transplantation* 103:e64. doi: 10.1097/tp.0000000000002589
- Goldin, A., Beckman, J. A., Schmidt, A. M., and Creager, M. A. (2006). Advanced glycation end products: sparking the development of diabetic vascular injury. *Circulation* 114, 597–605. doi: 10.1161/circulationaha.106.621854
- Gollmer, J., Zirlik, A., and Bugger, H. (2019). Established and emerging mechanisms of diabetic cardiomyopathy. *J. Lipid Atheroscler.* 8:26. doi: 10.12997/jla.2019.8.1.26
- Greco, S., Salgado Somoza, A., Devaux, Y., and Martelli, F. (2018). Long noncoding RNAs and cardiac disease. *Antioxid. Redox Signal.* 29, 880–901.
- Grieco, G. E., Brusco, N., Licata, G., Nigi, L., Formichi, C., Dotta, F., et al. (2019). Targeting microRNAs as a therapeutic strategy to reduce oxidative stress in diabetes. *Int. J. Mol. Sci.* 20:6358. doi: 10.3390/ijms20246358
- Gross, J. L., De Azevedo, M. J., Silveiro, S. P., Canani, L. H., Caramori, M. L., and Zelmanovitz, T. (2005). Diabetic nephropathy: diagnosis, prevention, and treatment. *Diab. Care* 28, 164–176.
- Gu, S., Liu, Y., Zou, J., Wang, W., Wei, T., Wang, X., et al. (2020). Retinal pigment epithelial cells secrete miR-202-5p-containing exosomes to protect against proliferative diabetic retinopathy. *Exp. Eye Res.* 201:108271. doi: 10.1016/j.exer.2020.108271
- Guan, G. Y., Wei, N., Song, T., Zhao, C., Sun, Y., Pan, R. X., et al. (2020). miR-448-3p alleviates diabetic vascular dysfunction by inhibiting endothelial–mesenchymal transition through DPP-4 dysregulation. *J. Cell. Physiol.* 235, 10024–10036. doi: 10.1002/jcp.29817
- Guo, R., and Nair, S. (2017). Role of microRNA in diabetic cardiomyopathy: from mechanism to intervention. *Biochim. Biophys. Acta Mol. Basis Dis.* 1863, 2070–2077. doi: 10.1016/j.bbdis.2017.03.013
- Guo, Y., Li, P., Bledsoe, G., Yang, Z.-R., Chao, L., and Chao, J. (2015). Kallistatin inhibits TGF- β -induced endothelial–mesenchymal transition by differential regulation of microRNA-21 and eNOS expression. *Exp. Cell Res.* 337, 103–110. doi: 10.1016/j.yexcr.2015.06.021
- Gupta, N., Mansoor, S., Sharma, A., Sapkal, A., Sheth, J., Falatoonzadeh, P., et al. (2013). Diabetic retinopathy and VEGF. *Open Ophthalmol. J.* 7:4.
- Hammes, H.-P., Feng, Y., Pfister, F., and Brownlee, M. (2011). Diabetic retinopathy: targeting vasoregression. *Diabetes* 60, 9–16. doi: 10.2337/db10-0454

- Hansson, G. (2009). Inflammatory mechanisms in atherosclerosis. *J. Thromb. Haemostas.* 7, 328–331.
- Harmanci, D., Erkan, E. P., Kocak, A., and Akdogan, G. G. (2017). Role of the microRNA-29 family in fibrotic skin diseases. *Biomed. Rep.* 6, 599–604. doi: 10.3892/br.2017.900
- Harries, L. W. (2012). Long non-coding RNAs and human disease. *Biochem. Soc. Transact.* 40, 902–906.
- He, Y., Dan, Y., Gao, X., Huang, L., Lv, H., and Chen, J. (2020). DNMT1-mediated lncRNA MEG3 methylation accelerates endothelial-mesenchymal transition in diabetic retinopathy through the PI3K/AKT/mTOR signaling pathway. *Am. J. Physiol. Endocrinol. Metabol.* 320, E598–E608.
- He, Y., Huang, C., Lin, X., and Li, J. (2013). MicroRNA-29 family, a crucial therapeutic target for fibrosis diseases. *Biochimie* 95, 1355–1359. doi: 10.1016/j.biochi.2013.03.010
- He, Z., Yang, D., Fan, X., Zhang, M., Li, Y., Gu, X., et al. (2020). The roles and mechanisms of lncRNAs in liver fibrosis. *Int. J. Mol. Sci.* 21:1482. doi: 10.3390/ijms21041482
- Herrera, J., Henke, C. A., and Bitterman, P. B. (2018). Extracellular matrix as a driver of progressive fibrosis. *J. Clin. Investig.* 128, 45–53. doi: 10.1172/jci.93557
- Hong, L., Du, X., Li, W., Mao, Y., Sun, L., and Li, X. (2018). EndMT: a promising and controversial field. *Eur. J. Cell Biol.* 97, 493–500. doi: 10.1016/j.ejcb.2018.07.005
- Hortells, L., Johansen, A. K. Z., and Yutzey, K. E. (2019). Cardiac fibroblasts and the extracellular matrix in regenerative and nonregenerative hearts. *J. Cardiovasc. Dev. Dis.* 6:29. doi: 10.3390/jcdd6030029
- Hrenak, J., Paulis, L., and Simko, F. (2015). N-acetyl-seryl-aspartyl-lysyl-proline (Ac-SDKP): potential target molecule in research of heart, kidney and brain. *Curr. Pharmaceut. Design* 21, 5135–5143. doi: 10.2174/1381612821666150909093927
- Hu, Q., Li, J., Nitta, K., Kitada, M., Nagai, T., Kanasaki, K., et al. (2018). FGFR1 is essential for N-acetyl-seryl-aspartyl-lysyl-proline regulation of mitochondrial dynamics by upregulating microRNA let-7b-5p. *Biochem. Biophys. Res. Commun.* 495, 2214–2220. doi: 10.1016/j.bbrc.2017.12.089
- Huang, Y., He, Y., and Li, J. (2015). MicroRNA-21: a central regulator of fibrotic diseases via various targets. *Curr. Pharmaceut. Design* 21, 2236–2242. doi: 10.2174/1381612820666141226095701
- Hulshoff, M. S., del Monte-Nieto, G., Kovacic, J., and Krenning, G. (2019). Non-coding RNA in endothelial-to-mesenchymal transition. *Cardiovasc. Res.* 115, 1716–1731. doi: 10.1093/cvr/cvz211
- Hummel, S. G., Fischer, A. J., Martin, S. M., Schafer, F. Q., and Buettner, G. R. (2006). Nitric oxide as a cellular antioxidant: a little goes a long way. *Free Radic. Biol. Med.* 40, 501–506. doi: 10.1016/j.freeradbiomed.2005.08.047
- Ilhan, F., and Kalkanli, S. T. (2015). Atherosclerosis and the role of immune cells. *World J. Clin. Cases WJCC* 3:345. doi: 10.12998/wjcc.v3.i4.345
- Jahan, F., Landry, N. M., Rattan, S. G., Dixon, I., and Wigle, J. T. (2018). The functional role of zinc finger E box-binding homeobox 2 (Zeb2) in promoting cardiac fibroblast activation. *Int. J. Mol. Sci.* 19:3207. doi: 10.3390/ijms19103207
- Jia, G., Hill, M. A., and Sowers, J. R. (2018). Diabetic cardiomyopathy: an update of mechanisms contributing to this clinical entity. *Circulat. Res.* 122, 624–638. doi: 10.1161/circresaha.117.311586
- Jiang, L., Hao, C., Li, Z., Zhang, P., Wang, S., Yang, S., et al. (2019). miR-449a induces EndMT, promotes the development of atherosclerosis by targeting the interaction between AdipoR2 and E-cadherin in Lipid Rafts. *Biomed. Pharmacother.* 109, 2293–2304. doi: 10.1016/j.biopha.2018.11.114
- Jiang, Q., Lyu, X.-M., Yuan, Y., and Wang, L. (2017). Plasma miR-21 expression: an indicator for the severity of Type 2 diabetes with diabetic retinopathy. *Biosci. Rep.* 37:BSR20160589.
- Jing, E., Emanuelli, B., Hirschey, M. D., Boucher, J., Lee, K. Y., Lombard, D., et al. (2011). Sirtuin-3 (Sirt3) regulates skeletal muscle metabolism and insulin signaling via altered mitochondrial oxidation and reactive oxygen species production. *Proc. Natl. Acad. Sci.* 108, 14608–14613. doi: 10.1073/pnas.1111308108
- Joussen, A. M., Poulaki, V., Qin, W., Kirchhof, B., Mitsiades, N., Wiegand, S. J., et al. (2002). Retinal vascular endothelial growth factor induces intercellular adhesion molecule-1 and endothelial nitric oxide synthase expression and initiates early diabetic retinal leukocyte adhesion in vivo. *Am. J. Pathol.* 160, 501–509. doi: 10.1016/s0002-9440(10)64869-9
- Kanasaki, K. (2016). The pathological significance of dipeptidyl peptidase-4 in endothelial cell homeostasis and kidney fibrosis. *Diabetol. Int.* 7, 212–220. doi: 10.1007/s13340-016-0281-z
- Kanasaki, K. (2018). The role of renal dipeptidyl peptidase-4 in kidney disease: renal effects of dipeptidyl peptidase-4 inhibitors with a focus on linagliptin. *Clin. Sci.* 132, 489–507. doi: 10.1042/cs20180031
- Kanasaki, K., Shi, S., Kanasaki, M., He, J., Nagai, T., Nakamura, Y., et al. (2014). Linagliptin-mediated DPP-4 inhibition ameliorates kidney fibrosis in streptozotocin-induced diabetic mice by inhibiting endothelial-to-mesenchymal transition in a therapeutic regimen. *Diabetes* 63, 2120–2131. doi: 10.2337/db13-1029
- Kashihara, N., Haruna, Y., Kondeti, V. K., and Kanwar, Y. S. (2010). Oxidative stress in diabetic nephropathy. *Curr. Med. Chem.* 17, 4256–4269.
- Katakami, N. (2017). Mechanism of development of atherosclerosis and cardiovascular disease in diabetes mellitus. *J. Atheroscler. Thromb.* 2017:RV17014.
- Kaur, H., Chen, S., Xin, X., Chiu, J., Khan, Z. A., and Chakrabarti, S. (2006). Diabetes-induced extracellular matrix protein expression is mediated by transcription coactivator p300. *Diabetes* 55, 3104–3111. doi: 10.2337/db06-0519
- Kehl, T., Backes, C., Kern, F., Fehlmann, T., Ludwig, N., Meese, E., et al. (2017). About miRNAs, miRNA seeds, target genes and target pathways. *Oncotarget* 8:107167. doi: 10.18632/oncotarget.22363
- Kendall, R. T., and Feghali-Bostwick, C. A. (2014). Fibroblasts in fibrosis: novel roles and mediators. *Front. Pharmacol.* 5:123. doi: 10.3389/fphar.2014.00123
- Khaddaj Mallat, R., Mathew John, C., Kendrick, D. J., and Braun, A. P. (2017). The vascular endothelium: A regulator of arterial tone and interface for the immune system. *Crit. Rev. Clin. Lab. Sci.* 54, 458–470. doi: 10.1080/10408363.2017.1394267
- Kim, J. (2018). MicroRNAs as critical regulators of the endothelial to mesenchymal transition in vascular biology. *BMB Rep.* 51:65. doi: 10.5483/bmbrep.2018.51.2.011
- Kim, J.-D., Lee, A., Choi, J., Park, Y., Kang, H., Chang, W., et al. (2015). Epigenetic modulation as a therapeutic approach for pulmonary arterial hypertension. *Exp. Mol. Med.* 47:e175. doi: 10.1038/emmm.2015.45
- Klaassen, I., Van Noorden, C. J., and Schlingemann, R. O. (2013). Molecular basis of the inner blood-retinal barrier and its breakdown in diabetic macular edema and other pathological conditions. *Prog. Retinal Eye Res.* 34, 19–48. doi: 10.1016/j.preteyeres.2013.02.001
- Klingeborn, M., Dismuke, W. M., Rickman, C. B., and Stamer, W. D. (2017). Roles of exosomes in the normal and diseased eye. *Prog. Retinal Eye Res.* 59, 158–177. doi: 10.1016/j.preteyeres.2017.04.004
- Kolavennu, V., Zeng, L., Peng, H., Wang, Y., and Danesh, F. R. (2008). Targeting of RhoA/ROCK signaling ameliorates progression of diabetic nephropathy independent of glucose control. *Diabetes* 57, 714–723. doi: 10.2337/db07-1241
- Korpai, M., and Kang, Y. (2008). The emerging role of miR-200 family of microRNAs in epithelial-mesenchymal transition and cancer metastasis. *RNA Biol.* 5, 115–119. doi: 10.4161/rna.5.3.6558
- Korpai, M., Lee, E. S., Hu, G., and Kang, Y. (2008). The miR-200 family inhibits epithelial-mesenchymal transition and cancer cell migration by direct targeting of E-cadherin transcriptional repressors ZEB1 and ZEB2. *J. Biol. Chem.* 283, 14910–14914. doi: 10.1074/jbc.c800074200
- Kovacic, J. C., Dimmeler, S., Harvey, R. P., Finkel, T., Aikawa, E., Krenning, G., et al. (2019). Endothelial to mesenchymal transition in cardiovascular disease: JACC state-of-the-art review. *J. Am. College Cardiol.* 73, 190–209.
- Kovacic, J. C., Mercader, N., Torres, M., Boehm, M., and Fuster, V. (2012). Epithelial-to-mesenchymal and endothelial-to-mesenchymal transition: from cardiovascular development to disease. *Circulation* 125, 1795–1808. doi: 10.1161/circulationaha.111.040352
- Koya, D., and King, G. L. (1998). Protein kinase C activation and the development of diabetic complications. *Diabetes* 47, 859–866. doi: 10.2337/diabetes.47.6.859
- Krenning, G., Barauna, V. G., Krieger, J. E., Harmsen, M. C., and Moonen, J.-R. A. (2016). Endothelial plasticity: shifting phenotypes through force feedback. *Stem Cells Int.* 2016:9762959.
- Kriegel, A. J., Liu, Y., Fang, Y., Ding, X., and Liang, M. (2012). The miR-29 family: genomics, cell biology, and relevance to renal and cardiovascular injury. *Physiol. Genomics* 44, 237–244. doi: 10.1152/physiolgenomics.00141.2011
- Kumarswamy, R., Volkmann, I., Jazbutyte, V., Dangwal, S., Park, D.-H., and Thum, T. (2012). Transforming growth factor- β -induced endothelial-to-mesenchymal

- transition is partly mediated by microRNA-21. *Arterioscler. Thromb. Vasc. Biol.* 32, 361–369. doi: 10.1161/atvbaha.111.234286
- Kusuhara, S., Fukushima, Y., Ogura, S., Inoue, N., and Uemura, A. (2018). Pathophysiology of diabetic retinopathy: the old and the new. *Diab. Metabol. J.* 42:364. doi: 10.4093/dmj.2018.0182
- La Sala, L., Mrakic-Sposta, S., Micheloni, S., Prattichizzo, F., and Ceriello, A. (2018). Glucose-sensing microRNA-21 disrupts ROS homeostasis and impairs antioxidant responses in cellular glucose variability. *Cardiovasc. Diabetol.* 17, 1–14. doi: 10.2174/978160805189211101010001
- La Sala, L., Mrakic-Sposta, S., Tagliabue, E., Prattichizzo, F., Micheloni, S., Sangalli, E., et al. (2019a). Circulating microRNA-21 is an early predictor of ROS-mediated damage in subjects with high risk of developing diabetes and in drug-naïve T2D. *Cardiovasc. Diabetol.* 18, 1–12. doi: 10.2165/11533370-000000000-00000
- La Sala, L., Prattichizzo, F., and Ceriello, A. (2019b). The link between diabetes and atherosclerosis. *Eur. J. Prevent. Cardiol.* 26, 15–24.
- Lechner, J., O'Leary, O. E., and Stitt, A. W. (2017). The pathology associated with diabetic retinopathy. *Vis. Res.* 139, 7–14. doi: 10.1016/j.visres.2017.04.003
- Lee, R., Wong, T. Y., and Sabanayagam, C. (2015). Epidemiology of diabetic retinopathy, diabetic macular edema and related vision loss. *Eye Vis.* 2, 1–25.
- Leung, A., and Natarajan, R. (2018). Long noncoding RNAs in diabetes and diabetic complications. *Antioxid. Redox Signal.* 29, 1064–1073. doi: 10.1089/ars.2017.7315
- Lewis, G., and Maxwell, A. P. (2014). Risk factor control is key in diabetic nephropathy. *Practitioner* 258, 13–17.
- Li, J., Cao, L.-T., Liu, H.-H., Yin, X.-D., and Wang, J. (2020a). Long non coding RNA H19: An emerging therapeutic target in fibrosing diseases. *Autoimmunity* 53, 1–7. doi: 10.1080/08916934.2019.1681983
- Li, J., Liu, H., Srivastava, S. P., Hu, Q., Gao, R., Li, S., et al. (2020b). Endothelial FGFR1 (fibroblast growth factor receptor 1) deficiency contributes differential fibrogenic effects in kidney and heart of diabetic mice. *Hypertension* 76, 1935–1944. doi: 10.1161/hypertensionaha.120.15587
- Li, Q., Lin, Y., Wang, S., Zhang, L., and Guo, L. (2017). GLP-1 inhibits high-glucose-induced oxidative injury of vascular endothelial cells. *Sci. Rep.* 7, 1–9.
- Li, Q., Yao, Y., Shi, S., Zhou, M., Zhou, Y., Wang, M., et al. (2020). Inhibition of miR-21 alleviated cardiac perivascular fibrosis via repressing EndMT in T1DM. *J. Cell. Mol. Med.* 24, 910–920. doi: 10.1111/jcmm.14800
- Liang, C., Gao, L., Liu, Y., Liu, Y., Yao, R., Li, Y., et al. (2019). MiR-451 antagonist protects against cardiac fibrosis in streptozotocin-induced diabetic mouse heart. *Life Sci.* 224, 12–22. doi: 10.1016/j.lfs.2019.02.059
- Lim, A. K. (2014). Diabetic nephropathy—complications and treatment. *Int. J. Nephrol. Renovasc. Dis.* 7:361. doi: 10.2147/ijnrd.s40172
- Lin, J., Jiang, Z., Liu, C., Zhou, D., Song, J., Liao, Y., et al. (2020). Emerging Roles of Long Non-Coding RNAs in Renal Fibrosis. *Life* 10:131. doi: 10.3390/life10080131
- Lin, Q., Zhao, J., Zheng, C., and Chun, J. (2018). Roles of notch signaling pathway and endothelial-mesenchymal transition in vascular endothelial dysfunction and atherosclerosis. *Eur. Rev. Med. Pharmacol. Sci.* 22, 6485–6491.
- Lin, X., Xu, Y., Pan, X., Xu, J., Ding, Y., Sun, X., et al. (2020). Global, regional, and national burden and trend of diabetes in 195 countries and territories: an analysis from 1990 to 2025. *Sci. Rep.* 10, 1–11.
- Liu, F., Zhang, S., Xu, R., Gao, S., and Yin, J. (2018). Melatonin attenuates endothelial-to-mesenchymal transition of glomerular endothelial cells via regulating miR-497/ROCK in diabetic nephropathy. *Kidney Blood Pressure Res.* 43, 1425–1436. doi: 10.1159/000493380
- Liu, J., Jiang, F., Jiang, Y., Wang, Y., Li, Z., Shi, X., et al. (2020). Roles of Exosomes in Ocular Diseases. *Int. J. Nanomed.* 15:10519. doi: 10.2147/ijn.s277190
- Liu, L., and Liu, X. (2019). Roles of drug transporters in blood-retinal barrier. *Drug Transporters in Drug Disposition. Effects Toxicity* 2019, 467–504. doi: 10.1007/978-981-13-7647-4_10
- Liu, R. H., Ning, B., Ma, X. E., Gong, W. M., and Jia, T. H. (2016). Regulatory roles of microRNA-21 in fibrosis through interaction with diverse pathways. *Mol. Med. Rep.* 13, 2359–2366. doi: 10.3892/mmr.2016.4834
- Lnsis, A. (2000). Atherosclerosis. *Nature* 407, 233–241.
- Loboda, A., Sobczak, M., Jozkowicz, A., and Dulak, J. (2016). TGF- β 1/Smads and miR-21 in renal fibrosis and inflammation. *Mediat. Inflamm.* 2016:8319283.
- Locatelli, M., Zoja, C., Zanchi, C., Corna, D., Villa, S., Bolognini, S., et al. (2020). Manipulating Sirtuin 3 pathway ameliorates renal damage in experimental diabetes. *Sci. Rep.* 10, 1–12. doi: 10.1155/2015/780903
- Luc, K., Schramm-Luc, A., Guzik, T., and Mikolajczyk, T. (2019). Oxidative stress and inflammatory markers in prediabetes and diabetes. *J. Physiol. Pharmacol.* 70, 809–824.
- Ma, F., Xu, S., Liu, X., Zhang, Q., Xu, X., Liu, M., et al. (2011). The microRNA miR-29 controls innate and adaptive immune responses to intracellular bacterial infection by targeting interferon- γ . *Nat. Immunol.* 12, 861–869. doi: 10.1038/ni.2073
- Ma, Z.-G., Yuan, Y.-P., Wu, H.-M., Zhang, X., and Tang, Q.-Z. (2018). Cardiac fibrosis: new insights into the pathogenesis. *Int. J. Biol. Sci.* 14:1645. doi: 10.7150/ijbs.28103
- Maghbooli, Z., Hossein-nezhad, A., Larijani, B., Amini, M., and Keshtkar, A. (2015). Global DNA methylation as a possible biomarker for diabetic retinopathy. *Diab. Metabol. Res. Rev.* 31, 183–189. doi: 10.1002/dmrr.2584
- Man, S., Duffhues, G. S., Ten Dijke, P., and Baker, D. (2019). The therapeutic potential of targeting the endothelial-to-mesenchymal transition. *Angiogenesis* 22, 3–13. doi: 10.1007/s10456-018-9639-0
- Mangiafico, S. P., Lim, S. H., Neoh, S., Massinet, H., Joannides, C. N., Proietto, J., et al. (2011). A primary defect in glucose production alone cannot induce glucose intolerance without defects in insulin secretion. *J. Endocrinol.* 210:335. doi: 10.1530/joe-11-0126
- Matoba, K., Takeda, Y., Nagai, Y., Kanazawa, Y., Kawanami, D., Yokota, T., et al. (2020). ROCK Inhibition May Stop Diabetic Kidney Disease. *JMA J.* 3, 154–163. doi: 10.31662/jmaj.2020-0014
- McArthur, K., Feng, B., Wu, Y., Chen, S., and Chakrabarti, S. (2011). MicroRNA-200b regulates vascular endothelial growth factor-mediated alterations in diabetic retinopathy. *Diabetes* 60, 1314–1323. doi: 10.2337/db10-1557
- Meadows, K. N., Iyer, S., Stevens, M. V., Wang, D., Shechter, S., Perruzzi, C., et al. (2009). Akt promotes endocardial-mesenchyme transition. *J. Angiogene. Res.* 1, 1–9.
- Medici, D., Potenta, S., and Kalluri, R. (2011). Transforming growth factor- β 2 promotes Snail-mediated endothelial-mesenchymal transition through convergence of Smad-dependent and Smad-independent signalling. *Biochem. J.* 437, 515–520. doi: 10.1042/bj20101500
- Meza, C. A., La Favor, J. D., Kim, D.-H., and Hickner, R. C. (2019). Endothelial dysfunction: is there a hyperglycemia-induced imbalance of NOX and NOS? *Int. J. Mol. Sci.* 20:3775. doi: 10.3390/ijms20153775
- Micallef, L., Vedrenne, N., Billet, F., Coulomb, B., Darby, I. A., and Desmoulière, A. (2012). The myofibroblast, multiple origins for major roles in normal and pathological tissue repair. *Fibrogene. Tissue Repair* 5(Suppl. 1):S5.
- Michlewski, G., and Cáceres, J. F. (2019). Post-transcriptional control of miRNA biogenesis. *RNA* 25, 1–16. doi: 10.1261/rna.068692.118
- Mima, A. (2013). Inflammation and oxidative stress in diabetic nephropathy: new insights on its inhibition as new therapeutic targets. *J. Diab. Res.* 2013:248563.
- Mogensen, C., Christensen, C., and Vittinghus, E. (1983). The stages in diabetic renal disease: with emphasis on the stage of incipient diabetic nephropathy. *Diabetes* 32(Suppl. 2), 64–78. doi: 10.2337/diab.32.2.s64
- Montorfano, I., Becerra, A., Cerro, R., Echeverría, C., Sáez, E., Morales, M. G., et al. (2014). Oxidative stress mediates the conversion of endothelial cells into myofibroblasts via a TGF- β 1 and TGF- β 2-dependent pathway. *Lab. Investig.* 94, 1068–1082. doi: 10.1038/labinvest.2014.100
- Moreno-Viedma, V., Amor, M., Sarabi, A., Bilban, M., Staffler, G., Zeyda, M., et al. (2016). Common dysregulated pathways in obese adipose tissue and atherosclerosis. *Cardiovasc. Diabetol.* 15, 1–12.
- Nagai, T., Kanasaki, M., Srivastava, S. P., Nakamura, Y., Ishigaki, Y., Kitada, M., et al. (2014). N-acetyl-seryl-aspartyl-lysyl-proline inhibits diabetes-associated kidney fibrosis and endothelial-mesenchymal transition. *BioMed Res. Int.* 2014:696475.
- Nandi, S. S., and Mishra, P. K. (2018). *Targeting miRNA for therapy of juvenile and adult diabetic cardiomyopathy. Exosomes, Stem Cells and MicroRNA*. Berlin: Springer, 47–59.
- Nemir, M., Metrich, M., Plaisance, I., Lepore, M., Cruchet, S., Berthonneche, C., et al. (2014). The Notch pathway controls fibrotic and regenerative repair in the adult heart. *Eur. Heart J.* 35, 2174–2185. doi: 10.1093/eurheartj/ehs269

- Nithianandarajah-Jones, G. N., Wilm, B., Goldring, C. E., Müller, J., and Cross, M. J. (2014). The role of ERK5 in endothelial cell function. *Biochem. Soc. Transact.* 42, 1584–1589. doi: 10.1042/bst20140276
- Nitta, K., Shi, S., Nagai, T., Kanasaki, M., Kitada, M., Srivastava, S. P., et al. (2016). Oral administration of N-acetyl-seryl-aspartyl-lysyl-proline ameliorates kidney disease in both type 1 and type 2 diabetic mice via a therapeutic regimen. *BioMed Res. Int.* 2016:9172157.
- Nosedá, M., McLean, G., Niessen, K., Chang, L., Pollet, I., Montpetit, R., et al. (2004). Notch activation results in phenotypic and functional changes consistent with endothelial-to-mesenchymal transformation. *Circulat. Res.* 94, 910–917. doi: 10.1161/01.res.0000124300.76171.c9
- Oguntibeju, O. O. (2019). Type 2 diabetes mellitus, oxidative stress and inflammation: examining the links. *Int. J. Physiol. Pathophysiol. Pharmacol.* 11:45.
- Pardali, E., Sanchez-Duffhues, G., Gomez-Puerto, M. C., and Ten Dijke, P. (2017). TGF- β -induced endothelial-mesenchymal transition in fibrotic diseases. *Int. J. Mol. Sci.* 18:2157. doi: 10.3390/ijms18102157
- Patel, S., Rauf, A., Khan, H., and Abu-Izneid, T. (2017). Renin-angiotensin-aldosterone (RAAS): The ubiquitous system for homeostasis and pathologies. *Biomed. Pharmacother.* 94, 317–325. doi: 10.1016/j.biopha.2017.07.091
- Pathak, J. V., and Dass, E. E. (2015). A retrospective study of the effects of angiotensin receptor blockers and angiotensin converting enzyme inhibitors in diabetic nephropathy. *Ind. J. Pharmacol.* 47:148. doi: 10.4103/0253-7613.153420
- Peng, C., Ma, J., Gao, X., Tian, P., Li, W., and Zhang, L. (2013). High glucose induced oxidative stress and apoptosis in cardiac microvascular endothelial cells are regulated by FoxO3a. *PLoS One* 8:e79739. doi: 10.1371/journal.pone.0079739
- Phan, T. H. G., Paliogiannis, P., Nasrallah, G. K., Giordo, R., Eid, A. H., Fois, A. G., et al. (2020). Emerging cellular and molecular determinants of idiopathic pulmonary fibrosis. *Cell. Mol. Life Sci.* 2020, 1–27.
- Piera-Velazquez, S., and Jimenez, S. A. (2019). Endothelial to mesenchymal transition: role in physiology and in the pathogenesis of human diseases. *Physiol. Rev.* 99, 1281–1324. doi: 10.1152/physrev.00021.2018
- Poznyak, A., Grechko, A. V., Poggio, P., Myasoedova, V. A., Alfieri, V., and Orekhov, A. N. (2020). The diabetes mellitus–atherosclerosis connection: The role of lipid and glucose metabolism and chronic inflammation. *Int. J. Mol. Sci.* 21:1835. doi: 10.3390/ijms21051835
- Qadir, M. M. F., Klein, D., Álvarez-Cubela, S., Domínguez-Bendala, J., and Pastori, R. L. (2019). The role of microRNAs in diabetes-related oxidative stress. *Int. J. Mol. Sci.* 20:5423. doi: 10.3390/ijms20215423
- Qiu, X., Brown, K., Hirschev, M. D., Verdin, E., and Chen, D. (2010). Calorie restriction reduces oxidative stress by SIRT3-mediated SOD2 activation. *Cell Metabol.* 12, 662–667. doi: 10.1016/j.cmet.2010.11.015
- Qu, S., Yang, X., Li, X., Wang, J., Gao, Y., Shang, R., et al. (2015). Circular RNA: a new star of noncoding RNAs. *Cancer Lett.* 365, 141–148. doi: 10.1016/j.canlet.2015.06.003
- Qu, S., Zhong, Y., Shang, R., Zhang, X., Song, W., Kjems, J., et al. (2017). The emerging landscape of circular RNA in life processes. *RNA Biol.* 14, 992–999. doi: 10.1080/15476286.2016.1220473
- Ray, D., Mishra, M., Ralph, S., Read, I., Davies, R., and Brenchley, P. (2004). Association of the VEGF gene with proliferative diabetic retinopathy but not proteinuria in diabetes. *Diabetes* 53, 861–864. doi: 10.2337/diabetes.53.3.861
- Reddy, K. J., Singh, M., Bangit, J. R., and Batsell, R. R. (2010). The role of insulin resistance in the pathogenesis of atherosclerotic cardiovascular disease: an updated review. *J. Cardiovasc. Med.* 11, 633–647. doi: 10.2459/jcm.0b013e328333645a
- Regazzi, R. (2018). MicroRNAs as therapeutic targets for the treatment of diabetes mellitus and its complications. *Expert Opin. Therapeut. Targets* 22, 153–160. doi: 10.1080/14728222.2018.1420168
- Rhee, S. Y., and Kim, Y. S. (2018). The role of advanced glycation end products in diabetic vascular complications. *Diab. Metabol. J.* 42:188. doi: 10.4093/dmj.2017.0105
- Rheinberger, M., and Böger, C. (2014). Diabetic nephropathy: new insights into diagnosis, prevention and treatment. *Deutsche Medizinische Wochenschrift* 139, 704–706.
- Romero-Aroca, P., Baget-Bernaldiz, M., Pareja-Rios, A., Lopez-Galvez, M., Navarro-Gil, R., and Verges, R. (2016). Diabetic macular edema pathophysiology: vasogenic versus inflammatory. *J. Diab. Res.* 2016: 2156273.
- Roy, S., Bae, E., Amin, S., and Kim, D. (2015). Extracellular matrix, gap junctions, and retinal vascular homeostasis in diabetic retinopathy. *Exp. Eye Res.* 133, 58–68. doi: 10.1016/j.exer.2014.08.011
- Ruiz-Ortega, M., Rodriguez-Diez, R. R., Lavozy, C., and Rayego-Mateos, S. (2020). Special issue “diabetic nephropathy: Diagnosis, prevention and treatment”. Basel: Multidisciplinary Digital Publishing Institute.
- Ruknarong, L., Boonthongkaew, C., Chuangchot, N., Jumnainsong, A., Leelayuwat, N., Jusakul, A., et al. (2021). Vitamin C supplementation reduces expression of circulating miR-451a in subjects with poorly controlled type 2 diabetes mellitus and high oxidative stress. *PeerJ* 9:e10776. doi: 10.7717/peerj.10776
- Russell, J. W., Golovoy, D., Vincent, A. M., Mahendru, P., Olzmann, J. A., Mentzer, A., et al. (2002). High glucose-induced oxidative stress and mitochondrial dysfunction in neurons. *FASEB J.* 16, 1738–1748. doi: 10.1096/fj.01-1027com
- Sabanayagam, C., Yip, W., Ting, D. S., Tan, G., and Wong, T. Y. (2016). Ten emerging trends in the epidemiology of diabetic retinopathy. *Ophthalmol.* 23, 209–222. doi: 10.1080/09286586.2016.1193618
- Sánchez-Duffhues, G., García de Vinuesa, A., and Ten Dijke, P. (2018). Endothelial-to-mesenchymal transition in cardiovascular diseases: developmental signaling pathways gone awry. *Dev. Dynam.* 247, 492–508. doi: 10.1002/dvdy.24589
- Sandoo, A., van Zanten, J. J. V., Metsios, G. S., Carroll, D., and Kitas, G. D. (2010). The endothelium and its role in regulating vascular tone. *Open Cardiovasc. Med. J.* 4:302. doi: 10.2174/1874192401004010302
- Schiffirin, E. L. (2008). Oxidative stress, nitric oxide synthase, and superoxide dismutase: a matter of imbalance underlies endothelial dysfunction in the human coronary circulation. *Hypertension* 51, 31–32. doi: 10.1161/hypertensionaha.107.103226
- Semenkovich, C. F. (2006). Insulin resistance and atherosclerosis. *J. Clin. Investig.* 116, 1813–1822.
- Sharma, V., Dogra, N., Saikia, U. N., and Khullar, M. (2017). Transcriptional regulation of endothelial-to-mesenchymal transition in cardiac fibrosis: role of myocardin-related transcription factor A and activating transcription factor 3. *Canad. J. Physiol. Pharmacol.* 95, 1263–1270. doi: 10.1139/cjpp-2016-0634
- Shaw, J. E., Sicree, R. A., and Zimmet, P. Z. (2010). Global estimates of the prevalence of diabetes for 2010 and 2030. *Diab. Res. Clin. Pract.* 87, 4–14. doi: 10.1016/j.diabres.2009.10.007
- Shi, S., Song, L., Yu, H., Feng, S., He, J., Liu, Y., et al. (2020). Knockdown of LncRNA-H19 Ameliorates Kidney Fibrosis in Diabetic Mice by Suppressing miR-29a-Mediated EndMT. *Front. Pharmacol.* 11:1936. doi: 10.3389/fphar.2020.586895
- Shi, S., Srivastava, S. P., Kanasaki, M., He, J., Kitada, M., Nagai, T., et al. (2015). Interactions of DPP-4 and integrin β 1 influences endothelial-to-mesenchymal transition. *Kidney Int.* 88, 479–489. doi: 10.1038/ki.2015.103
- Shi, X., Sun, M., Liu, H., Yao, Y., and Song, Y. (2013). Long non-coding RNAs: a new frontier in the study of human diseases. *Cancer Lett.* 339, 159–166. doi: 10.1016/j.canlet.2013.06.013
- Siasos, G., Tsigkou, V., Kosmopoulos, M., Theodosiadis, D., Simantiris, S., Tagkopoulos, N. M., et al. (2018). Mitochondria and cardiovascular diseases—from pathophysiology to treatment. *Ann. Translat. Med.* 6:256.
- Souilhol, C., Harmsen, M. C., Evans, P. C., and Krenning, G. (2018). Endothelial-mesenchymal transition in atherosclerosis. *Cardiovasc. Res.* 114, 565–577. doi: 10.1093/cvr/cvx253
- Srivastava, S. P., Goodwin, J. E., Kanasaki, K., and Koya, D. (2020a). Inhibition of angiotensin-converting enzyme ameliorates renal fibrosis by mitigating dpp-4 level and restoring antifibrotic micrornas. *Genes* 11:211. doi: 10.3390/genes11020211
- Srivastava, S. P., Goodwin, J. E., Kanasaki, K., and Koya, D. (2020b). Metabolic reprogramming by N-acetyl-seryl-aspartyl-lysyl-proline protects against diabetic kidney disease. *Br. J. Pharmacol.* 177, 3691–3711. doi: 10.1111/bph.15087
- Srivastava, S. P., Hedayat, A. F., Kanasaki, K., and Goodwin, J. E. (2019). MicroRNA crosstalk influences epithelial-to-mesenchymal, endothelial-to-mesenchymal, and macrophage-to-mesenchymal transitions in the kidney. *Front. Pharmacol.* 10:904. doi: 10.3389/fphar.2019.00904

- Srivastava, S. P., Kanasaki, K., and Goodwin, J. E. (2020c). Loss of Mitochondrial Control Impacts Renal Health. *Front. Pharmacol.* 11:2133. doi: 10.3389/fphar.2020.543973
- Srivastava, S. P., Koya, D., and Kanasaki, K. (2013). MicroRNAs in kidney fibrosis and diabetic nephropathy: roles on EMT and EndMT. *BioMed Res. Int.* 2013:125469.
- Srivastava, S. P., Li, J., Kitada, M., Fujita, H., Yamada, Y., Goodwin, J. E., et al. (2018). SIRT3 deficiency leads to induction of abnormal glycolysis in diabetic kidney with fibrosis. *Cell Death Dis.* 9, 1–14.
- Srivastava, S. P., Shi, S., Kanasaki, M., Nagai, T., Kitada, M., He, J., et al. (2016). Effect of antifibrotic microRNAs crosstalk on the action of N-acetyl-seryl-aspartyl-lysyl-proline in diabetes-related kidney fibrosis. *Sci. Rep.* 6, 1–12. doi: 10.1155/2014/696475
- Statello, L., Guo, C.-J., Chen, L.-L., and Huarte, M. (2020). Gene regulation by long non-coding RNAs and its biological functions. *Nat. Rev. Mol. Cell Biol.* 2020, 1–23. doi: 10.1007/978-3-030-17086-8_1
- Su, Q., Sun, Y., Ye, Z., Yang, H., and Li, L. (2018). Oxidized low density lipoprotein induces endothelial-to-mesenchymal transition by stabilizing snail in human aortic endothelial cells. *Biomed. Pharmacother.* 106, 1720–1726. doi: 10.1016/j.biopha.2018.07.122
- Sun, Y. B. Y., Qu, X., Caruana, G., and Li, J. (2016). The origin of renal fibroblasts/myofibroblasts and the signals that trigger fibrosis. *Differentiation* 92, 102–107. doi: 10.1016/j.diff.2016.05.008
- Taft, R. J., Pang, K. C., Mercer, T. R., Dinger, M., and Mattick, J. S. (2010). Non-coding RNAs: regulators of disease. *J. Pathol. J. Pathol. Soc. Great Br. Irel.* 220, 126–139. doi: 10.1002/path.2638
- Tan, K. C., Chow, W.-S., Ai, V. H., Metz, C., Bucala, R., and Lam, K. S. (2002). Advanced glycation end products and endothelial dysfunction in type 2 diabetes. *Diab. Care* 25, 1055–1059. doi: 10.2337/diacare.25.6.1055
- Tan, Y., Zhang, Z., Zheng, C., Wintergerst, K. A., Keller, B. B., and Cai, L. (2020). Mechanisms of diabetic cardiomyopathy and potential therapeutic strategies: preclinical and clinical evidence. *Nat. Rev. Cardiol.* 17, 585–607. doi: 10.1038/s41569-020-0339-2
- Tao, H., Yang, J.-J., Shi, K.-H., and Li, J. (2016). Wnt signaling pathway in cardiac fibrosis: new insights and directions. *Metabolism* 65, 30–40. doi: 10.1016/j.metabol.2015.10.013
- Tesfamariam, B. (1994). Free radicals in diabetic endothelial cell dysfunction. *Free Radic. Biol. Med.* 16, 383–391. doi: 10.1016/0891-5849(94)90040-x
- Thomas, A. A., Biswas, S., Feng, B., Chen, S., Gonder, J., and Chakrabarti, S. (2019). lncRNA H19 prevents endothelial-mesenchymal transition in diabetic retinopathy. *Diabetologia* 62, 517–530. doi: 10.1007/s00125-018-4797-6
- Thuan, D. T. B., Zayed, H., Eid, A. H., Abou-Saleh, H., Nasrallah, G. K., Mangoni, A. A., et al. (2018). A potential link between oxidative stress and endothelial-to-mesenchymal transition in systemic sclerosis. *Front. Immunol.* 9:1985. doi: 10.3389/fimmu.2018.01985
- Tian, D.-Y., Jin, X.-R., Zeng, X., and Wang, Y. (2017). Notch signaling in endothelial cells: is it the therapeutic target for vascular neointimal hyperplasia? *Int. J. Mol. Sci.* 18:1615. doi: 10.3390/ijms18081615
- Trost, A., Bruckner, D., Rivera, F. J., and Reitsamer, H. A. (2019). Pericytes in the Retina. *Pericyte Biol. Differ. Organs* 1122, 1–26.
- Van Geest, R. J., Klaassen, I., Vogels, I. M., Van Noorden, C. J., and Schlingemann, R. O. (2010). Differential TGF- β signaling in retinal vascular cells: a role in diabetic retinopathy? *Investigat. Ophthalmol. Vis. Sci.* 51, 1857–1865. doi: 10.1167/iovs.09-4181
- Vanchin, B., Offringa, E., Friedrich, J., Brinker, M. G., Kiers, B., Pereira, A. C., et al. (2019). MicroRNA-374b induces endothelial-to-mesenchymal transition and early lesion formation through the inhibition of MAPK7 signaling. *J. Pathol.* 247, 456–470. doi: 10.1002/path.5204
- Vanessa Fiorentino, T., Priolella, A., Zuo, P., and Folli, F. (2013). Hyperglycemia-induced oxidative stress and its role in diabetes mellitus related cardiovascular diseases. *Curr. Pharmaceut. Design* 19, 5695–5703. doi: 10.2174/1381612811319320005
- Verjans, R., Peters, T., Beaumont, F. J., van Leeuwen, R., van Herwaarden, T., Verhesen, W., et al. (2018). MicroRNA-221/222 family counteracts myocardial fibrosis in pressure overload-induced heart failure. *Hypertension* 71, 280–288. doi: 10.1161/hypertensionaha.117.10094
- Vidigal, J. A., and Ventura, A. (2015). The biological functions of miRNAs: lessons from in vivo studies. *Trends Cell Biol.* 25, 137–147. doi: 10.1016/j.tcb.2014.11.004
- Volpe, C. M. O., Villar-Delfino, P. H., Dos Anjos, P. M. F., and Nogueira-Machado, J. A. (2018). Cellular death, reactive oxygen species (ROS) and diabetic complications. *Cell Death Dis.* 9, 1–9.
- Wang, C., Wang, L., Ding, Y., Lu, X., Zhang, G., Yang, J., et al. (2017). lncRNA structural characteristics in epigenetic regulation. *Int. J. Mol. Sci.* 18:2659. doi: 10.3390/ijms18122659
- Wang, H. H., Garruti, G., Liu, M., Portincasa, P., and Wang, D. Q.-H. (2017). Cholesterol and lipoprotein metabolism and atherosclerosis: recent advances in reverse cholesterol transport. *Ann. Hepatol.* 16, S27–S42.
- Wang, H., and Cai, J. (2017). The role of microRNAs in heart failure. *Biochim. Biophys. Acta Mol. Basis Dis.* 1863, 2019–2030.
- Wang, J., Liew, O. W., Richards, A. M., and Chen, Y.-T. (2016). Overview of microRNAs in cardiac hypertrophy, fibrosis, and apoptosis. *Int. J. Mol. Sci.* 17:749. doi: 10.3390/ijms17050749
- Wang, W., and Lo, A. C. (2018). Diabetic retinopathy: pathophysiology and treatments. *Int. J. Mol. Sci.* 19:1816. doi: 10.3390/ijms19061816
- Wang, Z., Han, Z., Tao, J., Wang, J., Liu, X., Zhou, W., et al. (2017). Role of endothelial-to-mesenchymal transition induced by TGF- β 1 in transplant kidney interstitial fibrosis. *J. Cell. Mol. Med.* 21, 2359–2369. doi: 10.1111/jcmm.13157
- Wang, Z., Han, Z., Tao, J., Wang, J., Liu, X., Zhou, W., et al. (2016). Transforming growth factor- β 1 induces endothelial-to-mesenchymal transition via Akt signaling pathway in renal transplant recipients with chronic allograft dysfunction. *Medical Sci. Monit.* 21, 775–783. doi: 10.12659/aot.899931
- Wang, Z., Wang, Z., Gao, L., Xiao, L., Yao, R., Du, B., et al. (2020). miR-222 inhibits cardiac fibrosis in diabetic mice heart via regulating Wnt/ β -catenin-mediated endothelium to mesenchymal transition. *J. Cell. Physiol.* 235, 2149–2160. doi: 10.1002/jcp.29119
- Wellen, K. E., and Hotamisligil, G. S. (2005). Inflammation, stress, and diabetes. *J. Clin. Investig.* 115, 1111–1119.
- Widyantoro, B., Emoto, N., Nakayama, K., Anggrahini, D. W., Adiarto, S., Iwasa, N., et al. (2010). Endothelial cell-derived endothelin-1 promotes cardiac fibrosis in diabetic heart through endothelial-to-mesenchymal transition. *Circulation* 121, 2407–2418. doi: 10.1161/circulationaha.110.938217
- Williams, V. R., and Scholey, J. W. (2018). Angiotensin-converting enzyme 2 and renal disease. *Curr. Opin. Nephrol. Hypertens.* 27, 35–41.
- Wu, H., Liu, T., and Hou, H. (2020). Knockdown of LINC00657 inhibits ox-LDL-induced endothelial cell injury by regulating miR-30c-5p/Wnt7b/ β -catenin. *Mol. Cell. Biochem.* 472, 145–155. doi: 10.1007/s11010-020-03793-9
- Wu, X., Du, X., Yang, Y., Liu, X., Liu, X., Zhang, N., et al. (2021). Inhibition of miR-122 reduced atherosclerotic lesion formation by regulating NPAS3-mediated endothelial to mesenchymal transition. *Life Sci.* 265:118816. doi: 10.1016/j.lfs.2020.118816
- Wynn, T. A. (2008). Cellular and molecular mechanisms of fibrosis. *J. Pathol. J. Pathol. Soc. Great Br. Irel.* 214, 199–210.
- Yamagishi, S.-I., and Matsui, T. (2018). Role of hyperglycemia-induced advanced glycation end product (AGE) accumulation in atherosclerosis. *Ann. Vasc. Dis.* 11, 253–258. doi: 10.3400/avd.ra.18-00070
- Yan, D., Luo, X., Li, Y., Liu, W., Deng, J., Zheng, N., et al. (2014). Effects of advanced glycation end products on calcium handling in cardiomyocytes. *Cardiology* 129, 75–83. doi: 10.1159/000364779
- Yang, L., Kwon, J., Popov, Y., Gajdos, G. B., Ordog, T., Brekken, R. A., et al. (2014). Vascular endothelial growth factor promotes fibrosis resolution and repair in mice. *Gastroenterology* 146, 1339–1350.
- Yang, S., Banerjee, S., de Freitas, A., Sanders, Y. Y., Ding, Q., Matalon, S., et al. (2012). Participation of miR-200 in pulmonary fibrosis. *Am. J. Pathol.* 180, 484–493. doi: 10.1016/j.ajpath.2011.10.005
- Yildirim, S. S., Akman, D., Catalucci, D., and Turan, B. (2013). Relationship between downregulation of miRNAs and increase of oxidative stress in the development of diabetic cardiac dysfunction: junctin as a target protein of miR-1. *Cell Biochem. Biophys.* 67, 1397–1408. doi: 10.1007/s12013-013-9672-y
- Ying, W. (2008). NAD⁺/NADH and NADP⁺/NADPH in cellular functions and cell death: regulation and biological consequences. *Antioxid. Redox Signal.* 10, 179–206. doi: 10.1089/ars.2007.1672

- Yousefi, F., Shabaninejad, Z., Vakili, S., Derakhshan, M., Movahedpour, A., Dabiri, H., et al. (2020). TGF- β and WNT signaling pathways in cardiac fibrosis: non-coding RNAs come into focus. *Cell Commun. Signal.* 18, 1–16.
- Yu, C.-H., Gong, M., Liu, W.-J., Cui, N.-X., Wang, Y., Du, X., et al. (2017). High glucose induced endothelial to mesenchymal transition in human umbilical vein endothelial cell. *Exp. Mol. Pathol.* 102, 377–383. doi: 10.1016/j.yexmp.2017.03.007
- Yu, T., Jhun, B. S., and Yoon, Y. (2011). High-glucose stimulation increases reactive oxygen species production through the calcium and mitogen-activated protein kinase-mediated activation of mitochondrial fission. *Antioxid. Redox Signal.* 14, 425–437. doi: 10.1089/ars.2010.3284
- Yuan, J., Chen, H., Ge, D., Xu, Y., Xu, H., Yang, Y., et al. (2017). Mir-21 promotes cardiac fibrosis after myocardial infarction via targeting Smad7. *Cell. Physiol. Biochem.* 42, 2207–2219. doi: 10.1159/000479995
- Yuan, T., Yang, T., Chen, H., Fu, D., Hu, Y., Wang, J., et al. (2019). New insights into oxidative stress and inflammation during diabetes mellitus-accelerated atherosclerosis. *Redox Biol.* 20, 247–260. doi: 10.1016/j.redox.2018.09.025
- Yue, B. (2014). Biology of the extracellular matrix: an overview. *J. Glaucoma* 23(8 Suppl. 1), S20–S23.
- Zeisberg, E. M., Potenta, S. E., Sugimoto, H., Zeisberg, M., and Kalluri, R. (2008). Fibroblasts in kidney fibrosis emerge via endothelial-to-mesenchymal transition. *J. Am. Soc. Nephrol.* 19, 2282–2287. doi: 10.1681/asn.2008050513
- Zent, J., and Guo, L.-W. (2018). Signaling mechanisms of myofibroblastic activation: outside-in and inside-out. *Cell. Physiol. Biochem.* 49, 848–868. doi: 10.1159/000493217
- Zhang, H., Feng, Z., Huang, R., Xia, Z., Xiang, G., and Zhang, J. (2014). MicroRNA-449 suppresses proliferation of hepatoma cell lines through blockade lipid metabolic pathway related to SIRT1. *Int. J. Oncol.* 45, 2143–2152. doi: 10.3892/ijo.2014.2596
- Zhang, H., Hu, J., and Liu, L. (2017). MiR-200a modulates TGF- β 1-induced endothelial-to-mesenchymal shift via suppression of GRB2 in HAECs. *Biomed. Pharmacother.* 95, 215–222. doi: 10.1016/j.biopha.2017.07.104
- Zhang, J., Zeng, Y., Chen, J., Cai, D., Chen, C., Zhang, S., et al. (2019). miR-29a/b cluster suppresses high glucose-induced endothelial-mesenchymal transition in human retinal microvascular endothelial cells by targeting Notch2. *Exp. Therapeut. Med.* 17, 3108–3116.
- Zhang, Y., Huang, X.-R., Wei, L.-H., Chung, A. C., Yu, C.-M., and Lan, H.-Y. (2014). miR-29b as a therapeutic agent for angiotensin II-induced cardiac fibrosis by targeting TGF- β /Smad3 signaling. *Mol. Therap.* 22, 974–985. doi: 10.1038/mt.2014.25
- Zhao, Y., Zhang, J., Li, H., Li, Y., Ren, J., Luo, M., et al. (2008). An NADPH sensor protein (HSCARG) down-regulates nitric oxide synthesis by association with argininosuccinate synthetase and is essential for epithelial cell viability. *J. Biol. Chem.* 283, 11004–11013. doi: 10.1074/jbc.m708697200
- Zhong, X., Chung, A. C., Chen, H.-Y., Meng, X.-M., and Lan, H. Y. (2011). Smad3-mediated upregulation of miR-21 promotes renal fibrosis. *J. Am. Soc. Nephrol.* 22, 1668–1681. doi: 10.1681/asn.2010111168
- Zhu, G.-H., Li, R., Zeng, Y., Zhou, T., Xiong, F., and Zhu, M. (2018). MicroRNA-142-3p inhibits high-glucose-induced endothelial-to-mesenchymal transition through targeting TGF- β 1/Smad pathway in primary human aortic endothelial cells. *Int. J. Clin. Exp. Pathol.* 11:1208.

Conflict of Interest: The authors declare that the research was conducted in the absence of any commercial or financial relationships that could be construed as a potential conflict of interest.

Copyright © 2021 Giordo, Ahmed, Allam, Abusnana, Pappalardo, Nasrallah, Mangoni and Pintus. This is an open-access article distributed under the terms of the Creative Commons Attribution License (CC BY). The use, distribution or reproduction in other forums is permitted, provided the original author(s) and the copyright owner(s) are credited and that the original publication in this journal is cited, in accordance with accepted academic practice. No use, distribution or reproduction is permitted which does not comply with these terms.



Animal and Organoid Models of Liver Fibrosis

Yu-long Bao^{1†}, Li Wang^{1†}, Hai-ting Pan¹, Tai-ran Zhang¹, Ya-hong Chen², Shan-jing Xu³, Xin-li Mao^{3,4,5*} and Shao-wei Li^{4,5*}

¹ College of Basic Medicine, Inner Mongolia Medical University, Hohhot, China, ² Health Management Center, Taizhou Hospital of Zhejiang Province Affiliated to Wenzhou Medical University, Linhai, China, ³ School of Medicine, Shaoxing University, Shaoxing, China, ⁴ Key Laboratory of Minimally Invasive Techniques & Rapid Rehabilitation of Digestive System Tumor, Taizhou Hospital of Zhejiang Province Affiliated to Wenzhou Medical University, Linhai, China, ⁵ Department of Gastroenterology, Taizhou Hospital of Zhejiang Province Affiliated to Wenzhou Medical University, Linhai, China

OPEN ACCESS

Edited by:

Elvira Forte,

Jackson Laboratory, United States

Reviewed by:

Soraia K. P. Costa,

University of São Paulo, Brazil

Louis Charles Penning,

Utrecht University, Netherlands

*Correspondence:

Shao-wei Li

li_shaowei81@hotmail.com

Xin-li Mao

maoxl@enzemed.com

† These authors have contributed equally to this work

Specialty section:

This article was submitted to

Integrative Physiology,

a section of the journal

Frontiers in Physiology

Received: 09 February 2021

Accepted: 03 May 2021

Published: 26 May 2021

Citation:

Bao Y-l, Wang L, Pan H-t, Zhang T-r, Chen Y-h, Xu S-j, Mao X-l and Li S-w (2021) Animal and Organoid Models of Liver Fibrosis. *Front. Physiol.* 12:666138. doi: 10.3389/fphys.2021.666138

Liver fibrosis refers to the process underlying the development of chronic liver diseases, wherein liver cells are repeatedly destroyed and regenerated, which leads to an excessive deposition and abnormal distribution of the extracellular matrix such as collagen, glycoprotein and proteoglycan in the liver. Liver fibrosis thus constitutes the pathological repair response of the liver to chronic injury. Hepatic fibrosis is a key step in the progression of chronic liver disease to cirrhosis and an important factor affecting the prognosis of chronic liver disease. Further development of liver fibrosis may lead to structural disorders of the liver, nodular regeneration of hepatocytes and the formation of cirrhosis. Hepatic fibrosis is histologically reversible if treated aggressively during this period, but when fibrosis progresses to the stage of cirrhosis, reversal is very difficult, resulting in a poor prognosis. There are many causes of liver fibrosis, including liver injury caused by drugs, viral hepatitis, alcoholic liver, fatty liver and autoimmune disease. The mechanism underlying hepatic fibrosis differs among etiologies. The establishment of an appropriate animal model of liver fibrosis is not only an important basis for the in-depth study of the pathogenesis of liver fibrosis but also an important means for clinical experts to select drugs for the prevention and treatment of liver fibrosis. The present study focused on the modeling methods and fibrosis characteristics of different animal models of liver fibrosis, such as a chemical-induced liver fibrosis model, autoimmune liver fibrosis model, cholestatic liver fibrosis model, alcoholic liver fibrosis model and non-alcoholic liver fibrosis model. In addition, we also summarize the research and application prospects concerning new organoids in liver fibrosis models proposed in recent years. A suitable animal model of liver fibrosis and organoid fibrosis model that closely resemble the physiological state of the human body will provide bases for the in-depth study of the pathogenesis of liver fibrosis and the development of therapeutic drugs.

Keywords: liver, fibrosis, animal, organoid, model

INTRODUCTION

Liver fibrosis is a pathophysiological process caused by a variety of pathogenic factors that induce the abnormal proliferation of connective tissue in the liver. The repair and healing processes of liver injury can be accompanied by the development of liver fibrosis, and if the factors underlying such injury are not addressed, the process of fibrosis continues, eventually leading to cirrhosis (Hernandez-Gea and Friedman, 2011; Parola and Pinzani, 2019). Viruses, toxins, drugs, alcohol, hereditary factors, metabolism, cholestasis and parasites, among other factors, can damage liver cells, destroying the dynamic balance between collagen fiber synthesis, deposition, degradation and absorption, thus leading to the development of liver fibrosis. Therefore, liver fibrosis is not a unique disease; instead, different factors can lead to it, and regardless of the factors causing the relevant liver injury, the fibrosis process is similar (Mehal et al., 2011; Sebastiani et al., 2014; Kamdem et al., 2018; Testino et al., 2018).

The stimulation of different factors can lead to liver cell damage, which in turn causes inflammation. A continuous inflammatory response often leads to the formation of fibrosis. This is because inflammation causes cell damage, which further enhances the release of inflammatory mediators, such as cytokines and chemokines. These mediators recruit a large number of inflammatory cells to the site of inflammation, such as lymphocytes, neutrophils, eosinophils, basophils, mast cells and macrophages. The collected inflammatory cells further activate effector cells, which promote fibrosis (Hernandez-Gea and Friedman, 2011; Koyama and Brenner, 2017; Parola and Pinzani, 2019). The activation of hepatic stellate cells (HSCs) is the core event of liver fibrosis. HSCs are activated and differentiated into myofibroblasts (MFs), which secrete and deposit a large amount of extracellular matrix (ECM). When liver injury persists for a long time, chronic inflammatory stimulation and the continuous deposition of ECM together lead to the gradual replacement of normal liver tissue by fibrous tissue (Higashi et al., 2017; Zhangdi et al., 2019; **Figure 1**). As a common pathological stage of chronic liver disease, liver fibrosis is necessary for the development of liver cirrhosis and even liver cancer. Indeed, persistent liver inflammation and fibrosis are known to eventually induce cirrhosis and liver cancer (Uehara et al., 2013).

Studies in rodent models and humans have shown that liver fibrosis is reversible if the damage is ameliorated in a timely manner (Campana and Iredale, 2017). Matrix Metalloproteinase 13 (MMP13) is involved in the degradation of newly formed matrix during the recovery of liver fibrosis in rats. Although not all HSCs express MMP13, the production of MMP13 by HSCs plays a critical role in the process of fibrosis recovery (Watanabe et al., 2000). MMP9 secreted by Kupffer plays a key role in reversing hepatic fibrosis induced by thioacetamide (TAA) in mice (Feng et al., 2018). Dendritic cells can promote fibrosis regression by producing MMP9 (Jiao et al., 2012).

At present, the mechanism underlying liver fibrosis is unclear, and recent research has mostly focused on the etiology and mechanism of the disease. Although there has been some progress in the diagnosis and treatment of fibrosis, effective drugs and treatment are still lacking. The prevention, treatment and

even reversal of liver fibrosis have always been the key to the successful treatment of chronic liver injury. The pathogenesis of liver fibrosis is of great clinical significance for the development of therapeutic drugs and overall improvement of therapeutic approaches. It is therefore important to study the pathogenesis of liver fibrosis and develop therapeutic drugs to construct the animal model of liver fibrosis with similar pathogeneses.

We herein report various liver fibrosis models, which are classified according to the modeling method used, to facilitate their utility as a reference for liver fibrosis researchers.

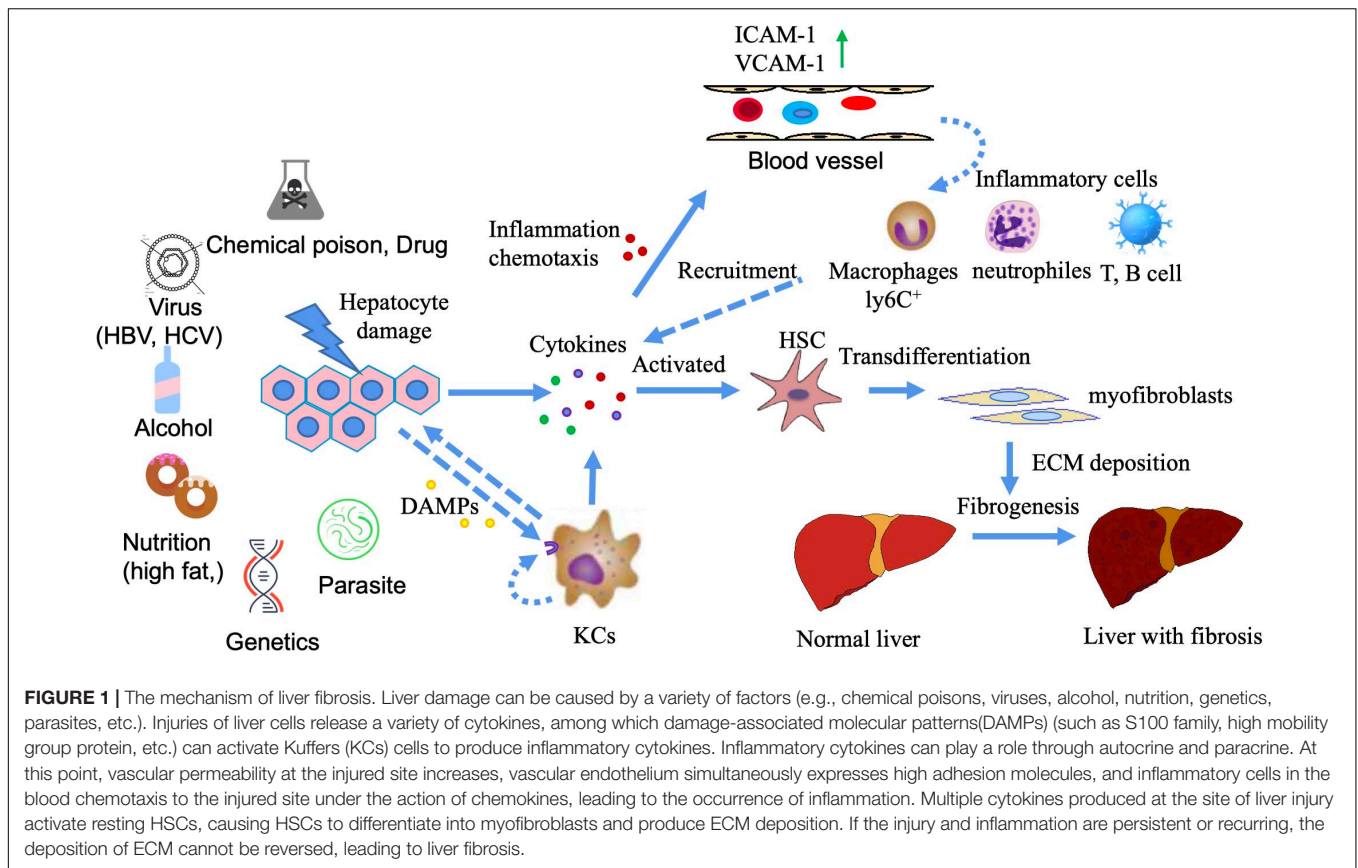
CHEMICAL DRUG-INDUCED LIVER FIBROSIS MODEL

Chemical liver fibrosis is induced by chemicals that can cause hepatotoxicity. The liver cells are damaged and consequently repaired, resulting in the abnormal growth of connective tissue in the liver. Models of chemical-induced liver injury are usually injected intraperitoneally, which is relatively easy to perform and results in stable development for use in studies concerning clinical liver fibrosis.

Carbon Tetrachloride (CCl₄)

Carbon tetrachloride is a colorless non-polar organic compound, highly toxic, that can dissolve many substances such as fat and paint. It is a typical liver poison, but the concentration and frequency of exposure can affect its action site and toxicity. CCl₄ directly damages liver cells (mainly endothelial cells and hepatic parenchyma cells in the hepatic portal vein region) by altering the permeability of lysosomes and mitochondrial membranes (Weber et al., 2003). The oxidase system in liver cells can also form highly active free radical metabolites through CYP2E1, leading to severe central lobular necrosis (Zangar et al., 2000). The damage mechanism of CCl₄ is mainly oxidative damage caused by lipid peroxidation. Cytochrome P450 enzyme, especially CYP2E1, converts CCl₄ into highly toxic trichloromethyl radical ($\cdot\text{CCl}_3$) and trichloromethyl peroxide ($\cdot\text{CCl}_3\text{O}_2$) (Slater et al., 1985; Unsal et al., 2020). This model has been widely used to study the pathogenesis of liver fibrosis and cirrhosis.

More standardized procedures are needed for experimental liver fibrosis studies due to dramatic changes in animal welfare regulations in Europe. Scholten proposed standard operating procedure (SOPs) for the CCl₄ mouse model and summarized the widely accepted experimental model for inducing liver injury leading to liver fibrosis (Scholten et al., 2015). The toxicological mechanism of liver fibrosis induced by CCl₄ may be related to multiple biological processes, pathways and targets (Dong et al., 2016). After 15 weeks of CCl₄ induction, multiple well-differentiated hepatocellular carcinoma (HCC) cells were found in the livers of all mice. CD133 was significantly up-regulated after CCl₄ treatment, and the levels of desmin and glial fibrillary acidic protein, the representative markers of HSC, were also significantly increased. The EGF expression was significantly reduced, contrary to what has been observed in humans. In A/J mice, chronic liver injury induced by CCl₄ differs from HCC



induced by human cirrhosis (Fujii et al., 2010). The collagen expression was found to be significantly increased after CCl₄ injury, and the number of cells expressing cytoglobin was also increased. Cytoglobin may be an early biomarker of liver fibrosis (Man et al., 2008). In addition to intraperitoneal injection, CCl₄ can also be inhaled to establish a liver fibrosis model. Rats were exposed to CCl₄ vapor twice a week for 30 s each time, while phenobarbital (0.3 g/L) was added to drinking water. The duration of inhalation was increased by 30 s after the first three sessions and by 1 min after every three sessions until a steady state was reached for 5 min. After 9 weeks, it can lead to liver fibrosis (Leeming et al., 2013; Marfà et al., 2016). Compared with intraperitoneal injection, inhalation route is a complex process, with great individual differences, and can cause multiple organ damage. An intraperitoneal injection can reach the liver directly from the hepatic portal vein. The animal model of liver fibrosis induced by CCl₄ is relatively low-cost to develop, and the implementation method is relatively simple. Furthermore, it is a classic model and one of the earliest, most widely used and most frequently selected by researchers.

TAA

Thioacetamide is an organic compound with the molecular formula CH₃CSNH₂, found as a colorless or white crystal. TAA is widely used as a model for inducing experimental liver fibrosis, and can also be used to induce acute liver failure and liver tumors by controlling the dose and duration of administration.

The TAA model is suitable for the study of connective tissue metabolism in fibrotic and cirrhotic models (Müller et al., 1988). TAA itself is not hepatotoxic, and its active metabolites covalently bind to proteins and lipids, causing oxidative stress leading to central lobular necrosis of the liver. Compared with CCl₄, TAA resulted in more periportal inflammatory cell infiltration and more pronounced ductal hyperplasia. The intraperitoneal administration of 150 mg/kg of TAA 3 times per week for 11 weeks in rats and TAA administration in drinking water at 300 mg/L for 2-4 months in mice can successfully and repetitively cause chronic liver injury and fibrosis (Wallace et al., 2015). The continued administration of TAA (after the continuous TAA injection for more than 11 weeks) induced sustained liver fibrosis in common marmosets, and this primate-like model of liver fibrosis was thus able to be used to evaluate the therapeutic effect of liver fibrosis (Inoue et al., 2018). In *Macaca fascicularis* fibrosis models induced by TAA and CCl₄, TAA induced significant fibrosis, but CCl₄ did not. Both TAA and CCl₄ increased the Child-Pugh score, but only the TAA model showed an increased retention of indocyanine green. TAA-induced *M. fascicularis* fibrosis was similar to Child-Pugh grade B fibrosis in humans. This model is evaluable by clinical indicators and can be used in preclinical studies (Matsuo et al., 2020). Although both CCl₄ and TAA-induced liver injury and fibrosis are dependent on CYP2E1, in some cases, CYP2A5 may have a protective effect against TAA-induced liver injury and fibrosis but has no effect on the hepatotoxicity of CCl₄ (Hong et al., 2016). The serum

amino acid pattern in the TAA-induced chronic cirrhosis model is partially similar to the corresponding human disease (Fontana et al., 1996). The hepatic fibrosis model of rats was established by injecting TAA solution for 7 weeks. Serum and urine samples were collected weekly for a nuclear magnetic resonance metabolomics analysis to search for differential metabolites associated with TAA-induced injury. That study helped clarify the role of metabolic dynamics in the course of hepatic fibrosis disease (Wei et al., 2014). The levels of fibrogenic cytokines, such as transforming growth factor- β (TGF- β), platelet derived growth factor (PDGF) and connective tissue growth factor (CTGF), also increased in the liver tissue of all three models, but the levels of CTGF in the liver tissue and serum were the highest in the CCl₄ group (Park et al., 2016). After 12-week oral administration of TAA in rats, bile duct fibrosis was induced, characterized by tubular hyperplasia surrounded by fibrous tissue (Hata et al., 2013). Both CCl₄ and TAA can cause lipid oxidative damage in liver cells. The model of liver fibrosis induced by CCl₄ is more suitable for studying the mechanism of spontaneous reversal of liver fibrosis. The hepatic fibrosis model induced by TAA is more suitable for the study of the mechanism of hepatic fibrosis, the screening of therapeutic drugs and the reliability evaluation of hepatic fibrosis serological markers.

DMN and Diethylnitrosamine (DEN)

The toxicity of various nitrosamines in animals and humans is well established, and trace amounts of DEN or DMN can cause severe liver injury in either the enteric or oral form. The most prominent manifestations are extensive neutrophilic infiltration, extensive central lobular hemorrhaging and necrosis, bile duct hyperplasia, fibrosis, bridging necrosis and ultimately HCC. Due to the stability of DMN- and DEN-induced liver changes, the administration of these agents to rodents has become a commonly used experimental model (Tolba et al., 2015).

Iron deposition and fat accumulation were shown to play an important role in the pathological changes of DMN-induced liver fibrosis in rats (He et al., 2007). Rats were intraperitoneally injected with DMN 3 days a week for 3 weeks. Severe central lobular congestion and hemorrhaging and necrosis were observed on day 7. On day 14, central lobular necrosis and numerous neutrophils infiltration were observed. Collagenous fibrous deposition was seen on day 21, along with severe central lobular necrosis, focal fatty changes, bile duct hyperplasia and bridging necrosis and fibrosis around the central vein. DMN-induced liver injury in rats seems to be an animal model similar to early human cirrhosis (George et al., 2001). The model shows significantly increased liver collagen fibraldehyde content due to DMN administration, and the cross-linking of liver fibrosis collagen induced by DMN is greater than that in normal liver. Furthermore, the deposition of type III collagen is more obvious than that of type I collagen in early fibrosis (George and Chandrakasan, 1996). The percentage of collagen fibrosis in rat liver fibrosis induced by DMN has been shown to be closely correlated with the serum levels of hyaluronic acid (HA), laminin (LN) and type IV collagen (Li et al., 2005). After 4 weeks of DEN treatment, 30% of zebrafish showed hyperplasia of reticular fibers. After 6 weeks, reticular and collagen fibers showed active

hyperplasia, and the proliferation rate of reticular fibers increased to 80%, successfully generating a stable liver fibrosis model in zebrafish (Wang et al., 2014).

In the comparative study of dimethylnitrosamine (DMN), CCl₄ and TAA rat liver fibrosis models, lipid peroxidation was highest in the CCl₄ model, and the serum liver enzyme levels increased with severity. The DMN and TAA models showed significant changes in liver fibrosis. The Alpha-SAM levels significantly increased in the DMN model. In summary, while the modeling time with this method is short, its development is simple, and the fibrosis degree is stable. However, because of the toxicity of nitrosamines, researchers should ensure proper safety measures are taken.

Acetaminophen (APAP)

Acetaminophen overdose is a major cause of drug-induced acute liver failure in many developed countries. Mitochondrial oxidative stress is considered the core event of APAP-induced liver injury (Yoon et al., 2016; Yan et al., 2018). N-acetyl-p-phenylquinone imine (NAPQI), a metabolite of APAP, is hepatotoxic and can increase the mRNA expression of α -SMA, COL1A1, COL3A1 and TGF- β , inducing the phosphorylation of ERK1/2 and SMAD2/3 and nuclear translocation of EGR-1 in hepatic stellate LX2 cells. The long-term administration of APAP can induce liver fibrosis in mice (Bai et al., 2017). When the liver is first exposed to APAP, a necrotizing inflammatory process is kicked off, followed by liver regeneration. However, the liver begins to form fibrosis after the second exposure to APAP (AlWahsh et al., 2019). Of note, a new model of cirrhosis in which rats were gavaged with corn oil daily and APAP 500 mg/day for 3 weeks resulted in the development of focal biliary cirrhosis (Tropskaya et al., 2020).

IMMUNE DAMAGE-INDUCED LIVER FIBROSIS MODEL

Immune liver injury liver fibrosis mainly refers to liver fibrosis caused by clinical autoimmune hepatitis (AIH) and virus infection, but such animal models of immune liver injury lack the sustained replication stage of human virus infection and the pathological process of sustained damage of human liver immunity.

Concanavalin A (ConA), a lectin purified from Brazilian kidney bean (Soares et al., 2011), is widely used in the mouse model of immune-mediated hepatitis. Unlike other models of liver injury, ConA-induced injury is mainly caused by the activation and recruitment of T cells to the liver (Heymann et al., 2015). Therefore, the pathogenesis of the ConA model has something in common with human immune-mediated hepatitis, such as AIH (Wang et al., 2012) and viral hepatitis. The mouse hepatitis model induced by ConA (20 mg/kg, 12 h) reflects most of the pathogenicity of human type I AIH. This provides a reliable animal model for the study of the immune pathogenesis of AIH and the rapid evaluation of new therapeutic methods (Ye et al., 2018). In acute autoimmune liver injury induced by ConA, HSCs are activated early, and the expression of TGF- β 1 and TGF- β 3

is unbalanced, which may be related to liver dysfunction and fibrosis development (Wang et al., 2017). Repeated injections of Con A resulted in liver fibrosis in mice (Louis et al., 2000). The model of immune fibrosis in mice was established by injecting saffra protein A (0.3 mg/body) once a week for 4 weeks. IFN- β can inhibit liver cell damage caused by repeated injections of ConA but has no effect on the development of fibrosis (Tanabe et al., 2007).

ALCOHOL-INDUCED LIVER FIBROSIS MODEL

Alcoholic liver disease (ALD) is a chronic liver disease caused by long-term heavy drinking. Fatty liver is usually present in the initial stage, which can develop into alcoholic hepatitis, alcoholic liver fibrosis and alcoholic cirrhosis. Almost all heavy drinkers develop fatty liver, but only 20-40% develop more severe ALD, and the underlying mechanism leading to disease progression is still unclear (Tsukamoto and Lu, 2001; Seitz et al., 2018). Although rodents differ from humans with regard to their alcohol metabolism (Holmes et al., 1986) and immune system, experimental animal models of ALD, especially rodent models, have been widely used in the study of human ALD (Mathews et al., 2014; Lamas-Paz et al., 2018).

After the daily administration of alcohol to rats for 16 weeks, the rates of liver steatosis, necrosis, inflammation and fibrosis were increased (Zhou et al., 2013). Chronic ethanol feeding (10 days free oral Lieber-decarli ethanol liquid diet) plus single alcoholic ethanol feeding induced liver injury, inflammation and fatty liver, simulating acute and chronic alcoholic liver injury in humans. This simple model is very useful for the study of ALD and other organs damaged by alcohol consumption (Bertola et al., 2013). Mice treated with CCl₄ combined with ethanol (up to 16%) showed extremely high rates of fibrotic alcoholic fatty liver disease 7 weeks later. The pattern of steatosis, inflammation and fibrosis involved in ALD in this mouse model is similar to that in humans and is suitable as a preclinical model for drug development (Brol et al., 2019). The same CCl₄ vapor exposure combined with chronic alcohol feeding resulted in extensive liver fibrosis in rats at week 5 and micronodular cirrhosis at week 10. This animal model simulates how some chronic liver damage in humans may be due to the presence of other hepatotoxins in the environment that play a role in enhancing the effects of alcohol (Hall et al., 1991). A new experimental model of porcine hepatosclerosis was established by CCl₄ and ethanol. Cirrhosis was induced by the intraperitoneal injection of CCl₄ twice a week for 9 weeks. Corn flour was the only food consumed during the period, and a 5% alcohol-water mixture was consumed. After 9 weeks, 83.3% of the pigs had cirrhosis, and 33.3% had died (Zhang et al., 2009). In combination with chronic alcohol administration and a non-alcoholic steatohepatitis (NASH)-induced high-fat diet, this new model enables the study of the combined effects of alcohol and a high-fat diet on liver injury, which may contribute to the development of liver fibrosis by enhancing TLR₄ signaling (Gäbele et al., 2011). To cause progressive alcoholic liver injury, the animal must be given too

much alcohol and maintain a persistently high blood alcohol level. Because of the rats' natural aversion to alcohol, the method of feeding them alcoholic liquid food was greatly restricted. In addition, the experiment cycle is long, the cost is high and the success rate is low, so it has been rarely used. At present, the more commonly used method is alcohol combined with chemical poison gavage, during the control of diet to replicate the model of alcoholic liver fibrosis. The model has the advantages of simple operation, short cycle and high molding rate.

DIET METABOLISM-INDUCED LIVER FIBROSIS MODEL

Non-alcoholic fatty liver disease (NAFLD) is a clinicopathological syndrome characterized by excessive fat deposition in hepatocytes except for alcohol and other clear liver damage factors, which is closely related to insulin resistance and genetic susceptibility of acquired metabolic stress liver injury (Cobbina and Akhlaghi, 2017). NAFLD is becoming a common chronic liver injury due to lifestyle changes. NAFLD can cause inflammation, ballooning degeneration of hepatocytes, and varying degrees of fibrosis, known as non-alcoholic steatohepatitis (NASH). Patients with advanced liver fibrosis or cirrhosis are at risk of developing complications, such as HCC and esophageal varices (Stål, 2015).

A choline-deficient high-fat (CDHF) diet induces NASH in mice. Hepatic histopathology has shown that a CDHF diet causes severe steatosis, inflammation and pericellular fibrosis (Honda et al., 2017). A modified choline-deficient, L-amino acid-defined, high-fat diet (CDAHFD) rapidly induces liver fibrosis in mice. This model will contribute to a better understanding of human NASH disease and may be useful for the development of effective treatments (Matsumoto et al., 2013). AIM^{-/-} mice fed the D09100301 diet showed similar phenotypes to non-obese patients with NAFLD, indicating their utility as a pathophysiological model for studying obesity-induced HCC (Komatsu et al., 2019). Dietary control combined with chemical toxicants may be an effective means of reducing the modeling time of diet-induced NAFLD models. A fast food diet (FFD) combined with a trace dose of CCl₄ (0.5 mL/kg body weight) for 8 weeks resulted in histological features of NAFLD, including steatosis, inflammation and fibrosis, in Wistar rat models within 8 weeks, suggesting that the model has potential utility in developing NAFLD and anti-fibrosis therapy (Chheda et al., 2014). Furthermore, using a high-fat, high-fructose and high-cholesterol diet combined with a weekly low dose of CCl₄ as an accelerant shortened the cycle of a mouse NASH model of fibrosis and HCC (Tsuchida et al., 2018). The mechanism of fatty liver fibrosis is still unclear, among which oxidative stress/lipid peroxidation is an important cause of fatty liver fibrosis. Unlike alcoholic fatty liver, which leads directly to liver fibrosis, non-alcoholic fatty liver must pass through an intermediate stage of steatohepatitis before it can develop into liver fibrosis. In other words, inflammation itself is a prerequisite for fatty liver fibrosis. The diet-induced NASH mouse model is characterized by good simulation of obesity, type

2 diabetes mellitus, dyslipidemia, and metabolic syndrome, but with less liver fibrosis.

SURGERY-INDUCED LIVER FIBROSIS MODEL

Cholestasis is an obstruction of both bile flow formation and excretion. Continuous cholestasis leads to chronic inflammation, which damages bile duct cells and liver cells, activates MFBs through a number of regulatory factors and causes the excessive deposition of ECM, leading to liver fibrosis (Li and Apte, 2015).

Surgical bile duct ligation (BDL) is one of the most widely used experimental models of cholestatic liver injury in mice and rats. The BDL model is a classic model of liver fibrosis. BDL was first achieved by the double ligation of bile ducts in rats. In brief, at 7–10 days after surgery, bile duct stenosis, increased bile duct pressure, upstream dilatation of bile ducts, increased liver volume composed of portal vein and bile duct hyperplasia are observed (Rodríguez-Garay et al., 1996). BDL protocols have been improved over time, but basically, animals are anesthetized and then undergo laparotomy. The bile duct is exposed from the abdominal cavity and ligated twice using a surgical cord. Mice and rats that undergo the procedure develop a strong fibrotic response (Kirkland et al., 2010). During the procedure, the animal can be placed on a heated plate at 37°C and permanently connected to the anesthesia system. At the time of the operation, the bile ducts are double-ligated but not dissected. This procedure induces highly repeatable morphological phenotypic changes in the liver and allows for the study of fiber formation at specific points in time (Tag et al., 2015). The standard model for cholestasis studies is total BDL (tBDL), but this model can cause severe liver damage in mice, so a new cholestasis model using partial BDL (pBDL) has been established (Heinrich et al., 2011). A mouse model of recanalization of biliary tract obstruction was previously established by performing anastomosis between the gallbladder and jejunum (G-J anastomosis), which has some value for studying the recovery from cholestasis liver fibrosis (Yoshino et al., 2021).

TRANSGENIC ANIMAL LIVER FIBROSIS MODEL

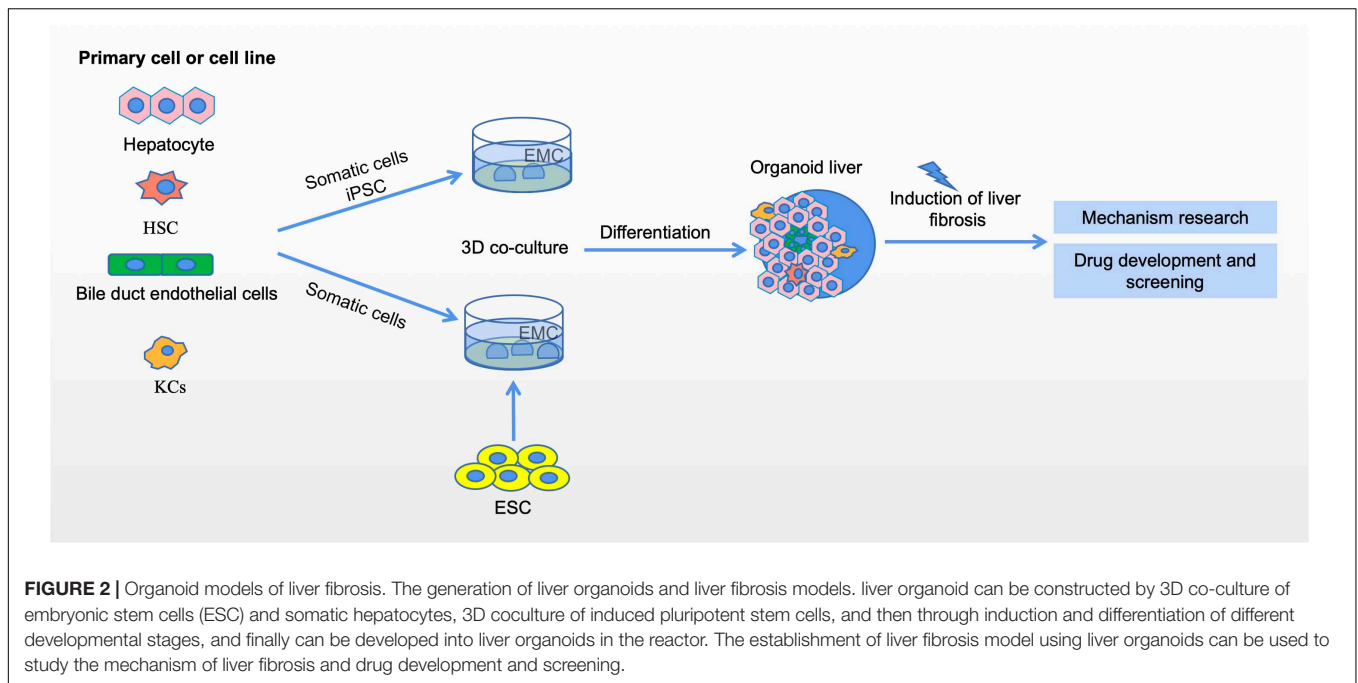
A chronic hepatitis C virus infection leads to liver fibrosis and cirrhosis. For a long time, chimpanzees were the only available non-human model of HCV infection (Pellicoro et al., 2014). Since the host range of HBV is relatively narrow and it only infects humans, it is very difficult to establish an animal model of HBV infection. Only chimpanzees and tupaia have previously been used for infection experiments (Walter et al., 1996; Dandri et al., 2005). The construction of humanized liver chimeric transgenic mice enables the stable regrowth of human liver cells in mice, and even the normal function and morphology of human liver, which has become an important bridge between mouse and

human preclinical studies (Kato et al., 2008). Hepatitis virus infects human TK-NOG mice and UPA-SCID mice with severe combined immunodeficiency (UPA-SCID). All human TK-NOG and UPA-SCID mice injected with hepatitis B virus infected serum developed viremia. The occurrence of HCV viremia in TK-NOG mice was significantly higher than that in UPA-SCID mice. TK-NOG mice are more beneficial for the study of hepatitis virus virology and the evaluation of antiviral drugs (Kosaka et al., 2013).

In addition to humanized mice, many transgenic mice were constructed for the study of liver fibrosis according to the different pathogenesis of liver fibrosis and the key functional genes of liver fibrosis regulation (Hayashi and Sakai, 2011). Immunodeficiency NOD induced natural killer T cell (NKT) transgenic population mediated spontaneous multi-organ chronic inflammation and fibrosis, non-obese diabetic inflammation and fibrosis (N-IF) mice. Due to fibrosis components, early onset, spontaneity, and reproducibility, this novel mouse model provides further insight into the underlying mechanisms that mediate the transformation of chronic inflammation into fibrosis (Fransén-Pettersson et al., 2016). Although the pathology of BDL is similar to chronic cholestasis in humans, the severity of surgical stress and cholestasis injury limits the application of the BDL model. MDR2 (ABCB4) is a mouse homologous gene MDR3 (ABCB4) that encodes a tubule phospholipid transporter. MDR2^{-/-} mice, also known as ABCB4^{-/-} mice, are another mature model of chronic cholestatic liver injury (Ikenaga et al., 2015). MDR2 knockout (MDR2^{-/-}) mice are a genetic model similar to patients with primary sclerosing cholangitis (Nishio et al., 2019). Transgenic mice that overexpress the transforming growth factor-β1 (TGF-β1) fusion gene [C-reactive protein (CRP)/TGF-β1] are able to control the expression level of TGF-β1. This model can be used to study the regulation of collagen synthesis, fibrinolysis and the degree of reversibility of liver fibrosis. CRP/TGF-β1 transgenic mouse model can be used as an anti-fibrotic test model (Kanzler et al., 1999). Similarly, TGF-β1 overexpression transgenic mice were established based on the tetracycline regulation gene expression system. This model will help to analyze the role of TGF-β1 in fibrogenesis (Ueberham et al., 2003). The role of platelet-derived growth factor A (PDGF-A) in the formation of liver fibrosis *in vivo* can be evaluated in transgenic mice with hepatocellular specific overexpression of PDGF-A by the C-reactive protein (CRP) gene promoter (Thieringer et al., 2008). Metalloproteinase-1 tissue inhibitor (TIMP-1) is upregulated during liver fibrogenesis, but its role in liver fibrosis and carcinogenesis in mice is not necessarily direct (Thiele et al., 2017). Transgenic mice overexpressing human TIMP-1 (HTIMP-1) in the liver under the control of albumin promoter/enhancer can be used to investigate the role of TIMP-1 in promoting liver fibrosis (Yoshiji et al., 2000). Mouse models carrying human apolipoprotein E*3-leiden and cholesterol ester transfer protein, fed a “Western” diet, lead to liver inflammation and fibrosis that are highly dependent on genetic background and have a large overlap of pathways between human diseases (Hui et al., 2018).

TABLE 1 | Advantages and disadvantages of different methods in hepatic fibrosis models.

| Model type | Model | species | Method | Advantages | Disadvantages | References |
|--|---|--------------------------|--|---|--|---|
| Chemical drug-induced liver fibrosis model | Carbon tetrachloride | Mouse/Rat | Intraperitoneal injection/inhalation | Simplicity of operator, commonly used, high reproducibility | Highly toxic and volatile, different from human liver fibrosis | Slater et al., 1985; Weber et al., 2003; Leeming et al., 2013; Scholten et al., 2015; Marfà et al., 2016; Unsal et al., 2020 |
| | Thioacetamide | Mouse/Rat/ Monkey | Intraperitoneal injection | Simplicity of operator, commonly used, high reproducibility | Highly toxic | Müller et al., 1988; Fontana et al., 1996; Wei et al., 2014; Wallace et al., 2015; Inoue et al., 2018 |
| | Dimethylnitrosamine or diethylnitrosamine | Mouse/Rat/ Zebra fish | Intraperitoneal injection | Simplicity of operator, commonly used, high reproducibility | Highly toxic and volatile | George et al., 2001; Wang et al., 2014; Tolba et al., 2015 |
| | Acetaminophen | Mouse/Rat | Intraperitoneal injection, gavage | Simplicity of operator, similar to the drug liver fibrosis | — | Yoon et al., 2016; Yan et al., 2018; Tropkaya et al., 2020 |
| Immune damage-induced liver fibrosis model | Concanavalin A | Mouse/Rat | tail vein injection | High success rate, low animal mortality and simple operation | Similar to liver fibrosis caused by chronic virus or autoimmunity in humans | Tanabe et al., 2007; Wang et al., 2012; Heymann et al., 2015; Ye et al., 2018 |
| Alcohol-induced liver fibrosis model | Alcohol | Mouse/Rat | Gavage | Suitable for the study of alcoholic liver disease | Alcohol tolerance in rodents | Bertola et al., 2013; Zhou et al., 2013 |
| | Alcohol combined with chemical poisons | Mouse/Rat/Pig | Gavage | Suitable for the study of alcoholic liver disease, short model cycle | Alcohol tolerance in rodents | Hall et al., 1991; Zhang et al., 2009; Brol et al., 2019 |
| Diet metabolism-induced liver fibrosis model | Dietary deficiencies | Mouse/Rat | Feeding | Close to human NASH | Long time to develop mild fibrosis | Matsumoto et al., 2013; Honda et al., 2017 |
| | Dietary deficiencies combined with chemical poisons | Mouse/Rat | Feeding | Close to human NASH | — | Chheda et al., 2014; Tsuchida et al., 2018 |
| Surgery-induced liver fibrosis model | Surgical bile duct ligation | Mouse/Rat | Surgery | Fast molding and high repeatability Close to human cholestatic injury | Surgical operation required, high mortality rate | Rodríguez-Garay et al., 1996; Kirkland et al., 2010; Heinrich et al., 2011; Tag et al., 2015 |
| Transgenic animal liver fibrosis model | Humanized liver chimeric transgenic mice | Mouse | Transgenic mice combined with human hepatocyte transplantation | Simulate the process of human infection with hepatitis virus | Transplant surgery is complicated. The source of primary human hepatocytes was deficient | Katoh et al., 2008; Kosaka et al., 2013 |
| | Transgenic/knockout mice | Mouse | Transgenic mice | Identify the role of a gene in liver fibrosis | Long time to develop Expensive price | Kanzler et al., 1999; Ueberham et al., 2003; Thieringer et al., 2008; Fransén-Pettersson et al., 2016; Nishio et al., 2019; Yoshiji et al., 2000 |
| Organoid liver fibrosis modes | Liver organoids | Human/Mouse | 3D <i>in vitro</i> culture technology | Homology with target organs Functionally similar with target organs | High model cost Difficulty of model Uncontrollable factors | Leite et al., 2016; Artegiani and Clevers, 2018; Coll et al., 2018; Ouchi et al., 2019; Pingitore et al., 2019; Prior et al., 2019; Brovold et al., 2020; Chusilp et al., 2020; Elbadawy et al., 2020 |

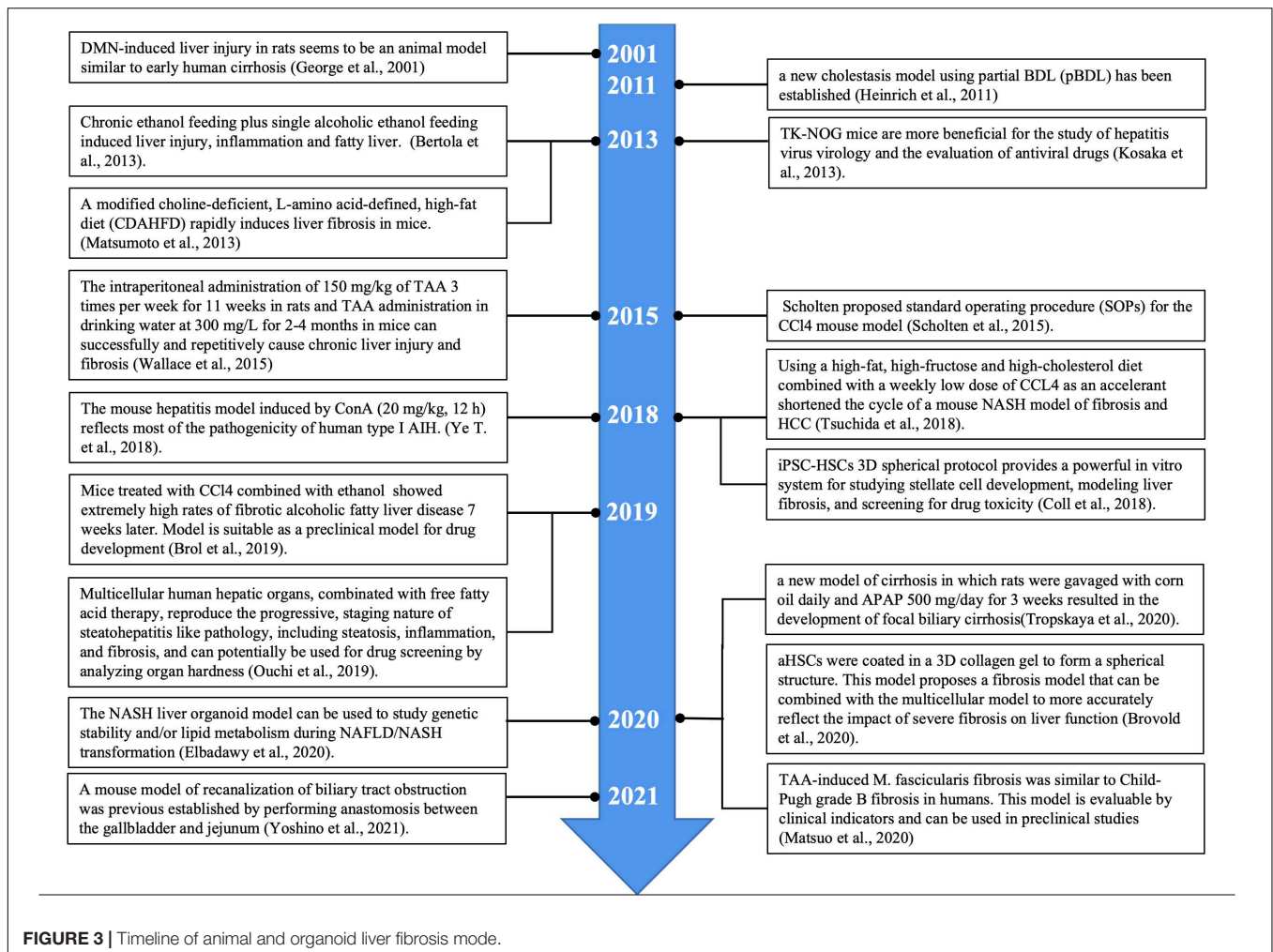


ORGANOID LIVER FIBROSIS MODES

Studying tissue and organ biology in mammals is challenging, and progress may be hampered by the availability of samples and ethical issues, especially in humans (Rossi et al., 2018). Although traditional 2D cell culture systems have many advantages, these models lack the ability to maintain *in situ* cellular characteristics and reflect cell-to-cell and cell-to-matrix interactions. The primary cells obtained by purification and isolation will also lose their original functions and characteristics after 2D culture *in vitro*. Organoids are 3D organ-like cells that are derived from embryonic or adult stem cells that are cultured *in vitro* and have a definite structure and function. Although these cellular structures are not human organs in the true sense, they can mimic real organs in structure and function, so they are playing an increasingly important role in scientific research. Organoids *in vitro* culture systems are characterized by self-renewing stem cell populations that include cells capable of differentiating into organs with similar spatial tissue functions (Artegiani and Clevers, 2018). Organoids can be used to simulate organ development and disease, and have a wide range of applications in basic research, drug development, and regenerative medicine (Lancaster and Knoblich, 2014; Huch et al., 2017; Xia et al., 2019). While mouse models and cell lines have advanced our understanding of liver biology and related diseases, they have significant drawbacks in simulating human liver tissue, particularly its complex structure and metabolic function. Currently, a variety of liver organoids have been established from induced pluripotent stem cells, embryonic stem cells, hepatoblasts and adult tissue-derived cells (Prior et al., 2019).

HepaRG (Hep) and primary human HSCs were cultured into 3D spheres in 96-well plates. The metabolic capacity of the organoid exceeds 21 days. This novel liver organ culture model

is the first capable of detecting hepatocellular dependence and compound-induced HSC activation and represents an important advance in the *in vitro* compound assessment of drug-induced liver fibrosis (Leite et al., 2016). Induced pluripotent stem cell-hepatic stellate cells (iPSC-HSCs) are very similar to primary human HSCs at the transcriptional, cellular, and functional levels. iPSC-HSCs exhibit a static phenotype when they remain 3D spherical with HepaRG hepatocytes, but are activated in response to wound-healing mediator stimulation and hepatocytotoxicity, resulting in fibrotic responses and secretion of procollagen, and accumulation of retinol in lipid droplets, similar to their *in vivo* counterparts. Thus, this protocol provides a powerful *in vitro* system for studying stellate cell development, modeling liver fibrosis, and screening for drug toxicity (Coll et al., 2018). Activated hepatic stellate cells (aHSCs) produced by 2D culture were coated in a 3D collagen gel to form a spherical structure, which created a stiffer environment and expressed higher levels of TIMP1 and LOXL2 compared to LX-2 cells cultured in 2D culture. This model proposes a fibrosis model that can be combined with the multicellular model to more accurately reflect the impact of severe fibrosis on liver function (Brovd et al., 2020). Using organoids from intrahepatic bile ducts, APAP was used to induce organoid injury in culture medium. The injury model suggested that bile duct cell apoptosis and its fibrotic response played a role in the initiation of the fibrotic process of bile duct diseases, such as biliary atresia (BA) (Chusilp et al., 2020). Genetically susceptible NAFLD organoid systems composed of hepatocytes (HepG2) and HSCs (LX-2) can be used to clarify the molecular mechanisms underlying the accumulation of lipids that induces the early stage of fibrogenesis. In addition, these systems can be used to identify new compounds for treating NASH through high-throughput drug screening (Pingitore et al., 2019). It is difficult to select



media and extracellular matrix that can co-maintain multiple cell lineages. A novel organ-like culture method was developed for co-differentiation of epithelial and mesenchymal lineages from PSCs. Using 11 different health and disease pluripotent cell lines, a repeatable method was developed to obtain multicellular human liver-like organs composed of hepatocytes, stellate cells, and Kupffer like cells that exhibit transcriptome similarity to tissue of *in vivo* origin. These multicellular human hepatic organs (HLOs), in combination with free fatty acid therapy, reproduce the progressive, staging nature of steatohepatitis like pathology, including steatosis, inflammation, and fibrosis, and can potentially be used for drug screening by analyzing organ hardness (Ouchi et al., 2019). Liver organoids were generated from mice with mild (NASH A), moderate (NASH B), and severe (NASH C) methionine and choline deficiency diets-induced NASH models that reproduce the characteristics of NASH disease liver tissue. The NASH liver organoid model can be used to study genetic stability and/or lipid metabolism during NAFLD/NASH transformation (Elbadawy et al., 2020).

In conclusion, organoid technology is one of the most important advances in stem cell research. Organoids are three-dimensional cell cultures that reproduce some of the key cell

types and structural characteristics of the organs they represent. Organoids remove the confounding variables that might be introduced by animal models and are more complex than homogenized cell cultures. Organoid culture has a high degree of gene stability, maintaining the genotype and phenotype of the source tissue. Thus, organoids can be used to model diseases, to study the mechanisms and progression of diseases, and to predict patients' individual responses to drug therapy (Figure 2).

CONCLUSION AND PERSPECTIVES

A reasonable model of liver fibrosis should resemble the characteristics and pathogenesis of human disease. It is universally recognized that "animal welfare" includes five freedoms: freedom from hunger and thirst; comfort; freedom from pain, injury and disease; freedom from fear and sadness and expression of nature. In laboratory animals, it is difficult to achieve all five freedoms at the same time. In particular, damage to these creatures' health is often a byproduct of the natural course of research. Due to such factors as animal suffering and scientific exploration, the three R principles are widely

recognized: including replacement, reduction and refinement (Lindsjö et al., 2016). This requires animal experiments to have stable experimental methods, a high mold-forming rate and good reproducibility. Thus far, researchers have successfully developed a number of hepatic fibrosis models using different experimental animals and different methods. However, due to the complexity of the pathogenesis of human liver fibrosis and differences in the genetic background between human and other animal species, there is no modeling method that can perfectly replicate the process of human liver fibrosis. Researchers can only use different models of liver fibrosis to mimic, as much as possible, the different pathologies that cause liver fibrosis in humans. **Table 1** briefly compares the advantages and disadvantages of different liver fibrosis models (**Table 1**). Although the liver fibrosis model induced by chemical poisons is different from the pathogenesis of human liver fibrosis, it is often used to study the mechanism of liver fibrosis due to its simple operation and good reproducibility. The immune-induced liver injury fibrosis model most closely replicates the clinical situation, which is similar to the liver fibrosis caused by human AIH and virus infection. Due to the complex pathogenesis of ALD and NAFLD, and the great differences between animal genetics, metabolism and immunity and human beings, it is relatively difficult to construct a model similar to human diseases through liver fibrosis induced by alcohol and the diet metabolism. BDL can simulate liver fibrosis induced by cholestasis, requiring only a short time with good reproducibility for model construction. However, it has drawbacks of substantial operational requirements, the need for an aseptic surgical setting and high animal mortality. Humanized transgenic chimeric mice and transgenic/knockout mice are emerging modeling methods that have been established in recent decades. Humanized liver chimeric transgenic mice constitute a good animal model of hepatitis virus infection, and transgenic/knockout mice are a good animal model for studying

the role of the functional genes involved in liver fibrosis. The latest organoid model makes up for the great difference between the traditional *in vitro* cell culture and human organs. Liver organoids are expected to be a useful new model for *in vitro* experiments that closely resembles the actual situation in human liver diseases. Although the techniques are becoming more advanced, liver fibrosis models are becoming more complex. Researchers continue to make various models of liver fibrosis in order to bring them closer to the true pathogenesis of human liver fibrosis (**Figure 3**). Each model has its advantages and disadvantages, and it remains a challenge to identify the most reasonable and stable hepatic fibrosis model.

AUTHOR CONTRIBUTIONS

All authors contributed to the writing and editing of the manuscript and contributed to the article and approved the submitted version.

FUNDING

This work was supported in part by the Program of Inner Mongolia Autonomous Region Tumor Biotherapy Collaborative Innovation Center, Medical Science and Technology Project of Zhejiang Province (2021PY083), Program of Taizhou Science and Technology Grant (20ywb29), Major Research Program of Taizhou Enze Medical Center Grant (19EZZDA2), Key Technology Research and Development Program of Zhejiang Province (2019C03040), and Open Fund of Key Laboratory of Minimally Invasive Techniques & Rapid Rehabilitation of Digestive System Tumor of Zhejiang Provinces (21SZDSYS01 and 21SZDSYS09).

REFERENCES

- AlWahsh, M., Othman, A., Hamadneh, L., Telfah, A., Lambert, J., Hikmat, S., et al. (2019). Second exposure to acetaminophen overdose is associated with liver fibrosis in mice. *EXCLI J.* 18, 51–62.
- Artegiani, B., and Clevers, H. (2018). Use and application of 3D-organoid technology. *Hum. Mol. Genet.* 27:ddy187. doi: 10.1093/hmg/ddy187
- Bai, Q., Yan, H., Sheng, Y., Jin, Y., Shi, L., Ji, L., et al. (2017). Long-term acetaminophen treatment induced liver fibrosis in mice and the involvement of Egr-1. *Toxicology* 382, 47–58. doi: 10.1016/j.tox.2017.03.008
- Bertola, A., Mathews, S., Ki, S. H., Wang, H., and Gao, B. (2013). Mouse model of chronic and binge ethanol feeding (the NIAAA model). *Nat. Protoc.* 8, 627–637. doi: 10.1038/nprot.2013.032
- Brol, M. J., Rösch, F., Schierwagen, R., Magdaleno, F., Uschner, F. E., Manekeller, S., et al. (2019). Combination of CCl₄ with alcoholic and metabolic injuries mimics human liver fibrosis. *Am. J. Physiol. Gastroint. Liver Physiol.* 317, G182–G194. doi: 10.1152/ajpgi.00361.2018
- Brovold, M., Keller, D., and Soker, S. (2020). Differential fibrotic phenotypes of hepatic stellate cells within 3D liver organoids. *Biotechnol. Bioeng.* 117, 2516–2526. doi: 10.1002/bit.27379
- Campana, L., and Iredale, J. P. (2017). Regression of Liver Fibrosis. *Semin. Liver Dis.* 37:1597816. doi: 10.1055/s-0036-1597816
- Chheda, T. K., Shivakumar, P., Sadasivan, S. K., Chandrasekharan, H., Moollemath, Y., Oommen, A. M., et al. (2014). Fast food diet with CCl₄ micro-dose induced hepatic-fibrosis—a novel animal model. *BMC Gastroenterol.* 14:89. doi: 10.1186/1471-230X-14-89
- Chusilp, S., Lee, C., Li, B., Lee, D., Yamoto, M., Ganji, N., et al. (2020). A novel model of injured liver ductal organoids to investigate cholangiocyte apoptosis with relevance to biliary atresia. *Pediatr. Surg. Int.* 36, 1471–1479. doi: 10.1007/s00383-020-04765-2
- Cobbina, E., and Akhlaghi, F. (2017). Non-alcoholic fatty liver disease (NAFLD) - pathogenesis, classification, and effect on drug metabolizing enzymes and transporters. *Drug Metab. Rev.* 49, 197–211. doi: 10.1080/03602532.2017.1293683
- Coll, M., Perea, L., Boon, R., Leite, S. B., Vallverdú, J., Mannaerts, I., et al. (2018). Generation of Hepatic Stellate Cells from Human Pluripotent Stem Cells Enables In Vitro Modeling of Liver Fibrosis. *Cell Stem Cell* 23, 101.e–113.e. doi: 10.1016/j.stem.2018.05.027
- Dandri, M., Volz, T. K., Lütgehetmann, M., and Petersen, J. (2005). Animal models for the study of HBV replication and its variants. *J. Clin. Virol.* 34(Suppl. 1), S54–S62.
- Dong, S., Chen, Q.-L., Song, Y.-N., Sun, Y., Wei, B., Li, X.-Y., et al. (2016). Mechanisms of CCl₄-induced liver fibrosis with combined transcriptomic and proteomic analysis. *J. Toxicol. Sci.* 41, 561–572. doi: 10.2131/jts.41.561

Elbadawy, M., Yamanaka, M., Goto, Y., Hayashi, K., Tsunedomi, R., Hazama, S., et al. (2020). Efficacy of primary liver organoid culture from different stages of non-alcoholic steatohepatitis (NASH) mouse model. *Biomaterials* 237:119823. doi: 10.1016/j.biomaterials.2020.119823

Feng, M., Ding, J., Wang, M., Zhang, J., Zhu, X., and Guan, W. (2018). Kupffer-derived matrix metalloproteinase-9 contributes to liver fibrosis resolution. *Int. J. Biol. Sci.* 14, 1033–1040. doi: 10.7150/ijbs.25589

Fontana, L., Moreira, E., Torres, M. I., Fernández, M. I., Ríos, A., Sánchez de Medina, F., et al. (1996). Serum amino acid changes in rats with thioacetamide-induced liver cirrhosis. *Toxicology* 106, 197–206. doi: 10.1016/0300-483x(95)03177-h

Fransén-Petersson, N., Duarte, N., Nilsson, J., Lundholm, M., Mayans, S., Larefalk, Å, et al. (2016). A New Mouse Model That Spontaneously Develops Chronic Liver Inflammation and Fibrosis. *PLoS One* 11:e0159850. doi: 10.1371/journal.pone.0159850

Fujii, T., Fuchs, B. C., Yamada, S., Lauwers, G. Y., Kulu, Y., Goodwin, J. M., et al. (2010). Mouse model of carbon tetrachloride induced liver fibrosis: Histopathological changes and expression of CD133 and epidermal growth factor. *BMC Gastroenterol.* 10:79. doi: 10.1186/1471-230X-10-79

Gäbele, E., Dostert, K., Dorn, C., Patsenker, E., Stickel, F., and Hellerbrand, C. (2011). A new model of interactive effects of alcohol and high-fat diet on hepatic fibrosis. *Alcohol Clin. Exp. Res.* 35, 1361–1367. doi: 10.1111/j.1530-0277.2011.01472.x

George, J., and Chandrakasan, G. (1996). Molecular characteristics of dimethylnitrosamine induced fibrotic liver collagen. *Biochim. Biophys. Acta* 1292, 215–222. doi: 10.1016/0167-4838(95)00202-2

George, J., Rao, K. R., Stern, R., and Chandrakasan, G. (2001). Dimethylnitrosamine-induced liver injury in rats: the early deposition of collagen. *Toxicology* 156, 129–138. doi: 10.1016/s0300-483x(00)00352-8

Hall, P. D., Plummer, J. L., Ilsley, A. H., and Cousins, M. J. (1991). Hepatic fibrosis and cirrhosis after chronic administration of alcohol and "low-dose" carbon tetrachloride vapor in the rat. *Hepatology* 13, 815–819. doi: 10.1016/0270-9139(91)90246-r

Hata, M., Iida, H., Yamanegi, K., Yamada, N., Ohyama, H., Hirano, H., et al. (2013). Phenotypic characteristics and proliferative activity of hyperplastic ductule cells in cholangiofibrosis induced by thioacetamide in rats. *Exp. Toxicol. Pathol.* 65, 351–356. doi: 10.1016/j.etp.2011.11.004

Hayashi, H., and Sakai, T. (2011). Animal models for the study of liver fibrosis: new insights from knockout mouse models. *Am. J. Physiol. Gastrointest Liver Physiol.* 300, G729–G738. doi: 10.1152/ajpgi.00013.2011

He, J.-Y., Ge, W.-H., and Chen, Y. (2007). Iron deposition and fat accumulation in dimethylnitrosamine-induced liver fibrosis in rat. *World J. Gastroenterol.* 13, 2061–2065. doi: 10.3748/wjg.v13.i14.2061

Heinrich, S., Georgiev, P., Weber, A., Vergopoulos, A., Graf, R., and Clavien, P.-A. (2011). Partial bile duct ligation in mice: a novel model of acute cholestasis. *Surgery* 149, 445–451. doi: 10.1016/j.surg.2010.07.046

Hernandez-Gea, V., and Friedman, S. L. (2011). Pathogenesis of liver fibrosis. *Annu. Rev. Pathol.* 6, 425–456. doi: 10.1146/annurev-pathol-011110-130246

Heymann, F., Hamesch, K., Weiskirchen, R., and Tacke, F. (2015). The concanavalin A model of acute hepatitis in mice. *Lab. Anim.* 49(1 Suppl.), 12–20. doi: 10.1177/0023677215572841

Higashi, T., Friedman, S. L., and Hoshida, Y. (2017). Hepatic stellate cells as key target in liver fibrosis. *Adv. Drug Deliv. Rev.* 121, 27–42. doi: 10.1016/j.addr.2017.05.007

Holmes, R. S., Duley, J. A., Algar, E. M., Mather, P. B., and Rout, U. K. (1986). Biochemical and genetic studies on enzymes of alcohol metabolism: the mouse as a model organism for human studies. *Alcohol Alcohol.* 21, 41–56.

Honda, T., Ishigami, M., Luo, F., Lingyun, M., Ishizu, Y., Kuzuya, T., et al. (2017). Branched-chain amino acids alleviate hepatic steatosis and liver injury in choline-deficient high-fat diet induced NASH mice. *Metabolism* 69, 177–187. doi: 10.1016/j.metabol.2016.12.013

Hong, F., Si, C., Gao, P., Cederbaum, A. I., Xiong, H., and Lu, Y. (2016). The role of CYP2A5 in liver injury and fibrosis: chemical-specific difference. *Naunyn Schmiedeberg's Arch. Pharmacol.* 389, 33–43. doi: 10.1007/s00210-015-1172-8

Huch, M., Knoblich, J. A., Lutolf, M. P., and Martinez-Arias, A. (2017). The hope and the hype of organoid research. *Development* 144, 938–941. doi: 10.1242/dev.150201

Hui, S. T., Kurt, Z., Tuominen, I., Norheim, F., Davis, R. C., Pan, C., et al. (2018). The Genetic Architecture of Diet-Induced Hepatic Fibrosis in Mice. *Hepatology* 68, 2182–2196. doi: 10.1002/hep.30113

Ikenaga, N., Liu, S. B., Sverdlov, D. Y., Yoshida, S., Nasser, I., Ke, Q., et al. (2015). A new Mdr2(-/-) mouse model of sclerosing cholangitis with rapid fibrosis progression, early-onset portal hypertension, and liver cancer. *Am. J. Pathol.* 185, 325–334. doi: 10.1016/j.ajpath.2014.10.013

Inoue, T., Ishizaka, Y., Sasaki, E., Lu, J., Mineshige, T., Yanase, M., et al. (2018). Thioacetamide-induced hepatic fibrosis in the common marmoset. *Exp. Anim.* 67, 321–327. doi: 10.1538/expanim.17-0156

Jiao, J., Sastre, D., Fiel, M. I., Lee, U. E., Ghiassi-Nejad, Z., Ginhoux, F., et al. (2012). Dendritic cell regulation of carbon tetrachloride-induced murine liver fibrosis regression. *Hepatology* 55, 244–255. doi: 10.1002/hep.24621

Kamdern, S. D., Moyou-Somo, R., Brombacher, F., and Nono, J. K. (2018). Host Regulators of Liver Fibrosis During Human Schistosomiasis. *Front. Immunol.* 9:2781. doi: 10.3389/fimmu.2018.02781

Kanzler, S., Lohse, A. W., Keil, A., Henninger, J., Dienes, H. P., Schirmacher, P., et al. (1999). TGF-beta1 in liver fibrosis: an inducible transgenic mouse model to study liver fibrogenesis. *Am. J. Physiol.* 276, G1059–G1068. doi: 10.1152/ajpgi.1999.276.4.G1059

Katoh, M., Tateno, C., Yoshizato, K., and Yokoi, T. (2008). Chimeric mice with humanized liver. *Toxicology* 246:12. doi: 10.1016/j.tox.2007.11.012

Kirkland, J. G., Godfrey, C. B., Garrett, R., Kakar, S., Yeh, B. M., and Corvera, C. U. (2010). Reversible surgical model of biliary inflammation and obstructive jaundice in mice. *J. Surg. Res.* 164, 221–227. doi: 10.1016/j.jss.2009.08.010

Komatsu, G., Nonomura, T., Sasaki, M., Ishida, Y., Arai, S., and Miyazaki, T. (2019). AIM-deficient mouse fed a high-trans fat, high-cholesterol diet: a new animal model for nonalcoholic fatty liver disease. *Exp. Anim.* 68, 147–158. doi: 10.1538/expanim.18-0108

Kosaka, K., Hiraga, N., Imamura, M., Yoshimi, S., Murakami, E., Nakahara, T., et al. (2013). A novel TK-NOG based humanized mouse model for the study of HBV and HCV infections. *Biochem. Biophys. Res. Commun.* 441, 230–235. doi: 10.1016/j.bbrc.2013.10.040

Koyama, Y., and Brenner, D. A. (2017). Liver inflammation and fibrosis. *J. Clin. Invest.* 127, 55–64. doi: 10.1172/JCI88881

Lamas-Paz, A., Hao, F., Nelson, L. J., Vázquez, M. T., Canals, S., Gómez Del Moral, M., et al. (2018). Alcoholic liver disease: Utility of animal models. *World J. Gastroenterol.* 24, 5063–5075. doi: 10.3748/wjg.v24.i45.5063

Lancaster, M. A., and Knoblich, J. A. (2014). Organogenesis in a dish: modeling development and disease using organoid technologies. *Science* 345:1247125. doi: 10.1126/science.1247125

Leeming, D. J., Byrjalsen, I., Jiménez, W., Christiansen, C., and Karsdal, M. A. (2013). Protein fingerprinting of the extracellular matrix remodelling in a rat model of liver fibrosis—a serological evaluation. *Liver Int.* 33, 439–447. doi: 10.1111/liv.12044

Leite, S. B., Roosens, T., El Taghdouini, A., Mannaerts, I., Smout, A. J., Najimi, M., et al. (2016). Novel human hepatic organoid model enables testing of drug-induced liver fibrosis in vitro. *Biomaterials* 78:026. doi: 10.1016/j.biomaterials.2015.11.026

Li, C.-H., Piao, D.-M., Xu, W.-X., Yin, Z.-R., Jin, J.-S., and Shen, Z.-S. (2005). Morphological and serum hyaluronic acid, laminin and type IV collagen changes in dimethylnitrosamine-induced hepatic fibrosis of rats. *World J. Gastroenterol.* 11, 7620–7624. doi: 10.3748/wjg.v11.i48.7620

Li, T., and Apte, U. (2015). Bile Acid Metabolism and Signaling in Cholestasis, Inflammation, and Cancer. *Adv. Pharmacol.* 74, 263–302. doi: 10.1016/bs.apha.2015.04.003

Lindsjö, J., Fahlman, Å, and Törnqvist, E. (2016). ANIMAL WELFARE FROM MOUSE TO MOOSE—IMPLEMENTING THE PRINCIPLES OF THE 3RS IN WILDLIFE RESEARCH. *J. Wildl. Dis.* 52(2 Suppl.), S65–S77. doi: 10.7558/52.2S.S65

Louis, H., Le Moine, A., Quertinmont, E., Peny, M. O., Geerts, A., Goldman, M., et al. (2000). Repeated concanavalin A challenge in mice induces an interleukin 10-producing phenotype and liver fibrosis. *Hepatology* 31, 381–390. doi: 10.1002/hep.510310218

Man, K.-N. M., Philipsen, S., and Tan-Un, K. C. (2008). Localization and expression pattern of cytoglobin in carbon tetrachloride-induced liver fibrosis. *Toxicol. Lett.* 183, 36–44. doi: 10.1016/j.toxlet.2008.09.015

- Marfà, S., Morales-Ruiz, M., Oró, D., Ribera, J., Fernández-Varo, G., and Jiménez, W. (2016). Sipal11 is an early biomarker of liver fibrosis in CCl4-treated rats. *Biol. Open* 5, 858–865. doi: 10.1242/bio.018887
- Mathews, S., Xu, M., Wang, H., Bertola, A., and Gao, B. (2014). Animals models of gastrointestinal and liver diseases. Animal models of alcohol-induced liver disease: pathophysiology, translational relevance, and challenges. *Am. J. Physiol. Gastrointest Liver Physiol.* 306, G819–G823. doi: 10.1152/ajpgi.00041.2014
- Matsumoto, M., Hada, N., Sakamaki, Y., Uno, A., Shiga, T., Tanaka, C., et al. (2013). An improved mouse model that rapidly develops fibrosis in non-alcoholic steatohepatitis. *Int. J. Exp. Pathol.* 94:12008. doi: 10.1111/iep.12008
- Matsuo, M., Murata, S., Hasegawa, S., Hatada, Y., Ohtsuka, M., and Taniguchi, H. (2020). Novel liver fibrosis model in Macaca fascicularis induced by thioacetamide. *Sci. Rep.* 10:2450. doi: 10.1038/s41598-020-58739-4
- Mehal, W. Z., Iredale, J., and Friedman, S. L. (2011). Scraping fibrosis: expressway to the core of fibrosis. *Nat. Med.* 17, 552–553. doi: 10.1038/nm0511-552
- Müller, A., Machnik, F., Zimmermann, T., and Schubert, H. (1988). Thioacetamide-induced cirrhosis-like liver lesions in rats—usefulness and reliability of this animal model. *Exp. Pathol.* 34, 229–236. doi: 10.1016/s0232-1513(88)80155-5
- Nishio, T., Hu, R., Koyama, Y., Liang, S., Rosenthal, S. B., Yamamoto, G., et al. (2019). Activated hepatic stellate cells and portal fibroblasts contribute to cholestatic liver fibrosis in MDR2 knockout mice. *J. Hepatol.* 71, 573–585. doi: 10.1016/j.jhep.2019.04.012
- Ouchi, R., Togo, S., Kimura, M., Shinozawa, T., Koido, M., and Koike, H. (2019). Modeling Steatohepatitis in Humans with Pluripotent Stem Cell-Derived Organoids. *Cell Metab.* 30, 374.e–384.e. doi: 10.1016/j.cmet.2019.05.007
- Park, H.-J., Kim, H.-G., Wang, J.-H., Choi, M.-K., Han, J.-M., Lee, J.-S., et al. (2016). Comparison of TGF- β , PDGF, and CTGF in hepatic fibrosis models using DMN, CCl4, and TAA. *Drug Chem. Toxicol.* 39, 111–118. doi: 10.3109/01480545.2015.1052143
- Parola, M., and Pinzani, M. (2019). Liver fibrosis: Pathophysiology, pathogenetic targets and clinical issues. *Mol. Aspects Med.* 65, 37–55. doi: 10.1016/j.mam.2018.09.002
- Pellicoro, A., Ramachandran, P., Iredale, J. P., and Fallowfield, J. A. (2014). Liver fibrosis and repair: immune regulation of wound healing in a solid organ. *Nat. Rev. Immunol.* 14, 181–194. doi: 10.1038/nri3623
- Pingitore, P., Sasidharan, K., Ekstrand, M., Prill, S., Lindén, D., and Romeo, S. (2019). Human Multilineage 3D Spheroids as a Model of Liver Steatosis and Fibrosis. *Int. J. Mol. Sci.* 20:20071629. doi: 10.3390/ijms20071629
- Prior, N., Inacio, P., and Huch, M. (2019). Liver organoids: from basic research to therapeutic applications. *Gut* 68, 2228–2237. doi: 10.1136/gutjnl-2019-319256
- Rodríguez-Garay, E. A., Agüero, R. M., Pisani, G., Trbojevič, R. A., Farroni, A., and Viglianco, R. A. (1996). Rat model of mild stenosis of the common bile duct. *Res. Exp. Med.* 196, 105–116. doi: 10.1007/s004330050017
- Rossi, G., Manfrin, A., and Lutolf, M. P. (2018). Progress and potential in organoid research. *Nat. Rev. Genet.* 19, 671–687. doi: 10.1038/s41576-018-0051-9
- Scholten, D., Trebicka, J., Liedtke, C., and Weiskirchen, R. (2015). The carbon tetrachloride model in mice. *Lab. Anim.* 49(1 Suppl.):23677215571192. doi: 10.1177/0023677215571192
- Sebastiani, G., Gkouvatso, K., and Pantopoulos, K. (2014). Chronic hepatitis C and liver fibrosis. *World J. Gastroenterol.* 20, 11033–11053. doi: 10.3748/wjg.v20.i32.11033
- Seitz, H. K., Bataller, R., Cortez-Pinto, H., Gao, B., Gual, A., Lackner, C., et al. (2018). Alcoholic liver disease. *Nat. Rev. Dis. Primers* 4:16. doi: 10.1038/s41572-018-0014-7
- Slater, T. F., Cheeseman, K. H., and Ingold, K. U. (1985). Carbon tetrachloride toxicity as a model for studying free-radical mediated liver injury. *Philos. Trans. R. Soc. Lond. B Biol. Sci.* 311, 633–645. doi: 10.1098/rstb.1985.0169
- Soares, P. A. G., Nascimento, C. O., Porto, T. S., Correia, M. T. S., Porto, A. L. F., and Carneiro-da-Cunha, M. G. (2011). Purification of a lectin from *Canavalia ensiformis* using PEG-citrate aqueous two-phase system. *J. Chromatogr. B Analyt. Technol. Biomed. Life Sci.* 879, 457–460. doi: 10.1016/j.jchromb.2010.12.030
- Stål, P. (2015). Liver fibrosis in non-alcoholic fatty liver disease - diagnostic challenge with prognostic significance. *World J. Gastroenterol.* 21, 11077–11087. doi: 10.3748/wjg.v21.i39.11077
- Tag, C. G., Sauer-Lehnen, S., Weiskirchen, S., Borkham-Kamphorst, E., Tolba, R. H., Tacke, F., et al. (2015). Bile duct ligation in mice: induction of inflammatory liver injury and fibrosis by obstructive cholestasis. *J. Vis. Exp.* 2015:52438. doi: 10.3791/52438
- Tanabe, J., Izawa, A., Takemi, N., Miyachi, Y., Torii, Y., Tsuchiyama, H., et al. (2007). Interferon-beta reduces the mouse liver fibrosis induced by repeated administration of concanavalin A via the direct and indirect effects. *Immunology* 122, 562–570. doi: 10.1111/j.1365-2567.2007.02672.x
- Testino, G., Leone, S., Fagoonee, S., and Pellicano, R. (2018). Alcoholic liver fibrosis: detection and treatment. *Minerva Med.* 109, 457–471. doi: 10.23736/50026-4806.18.05844-5
- Thiele, N. D., Wirth, J. W., Steins, D., Koop, A. C., Ittrich, H., Lohse, A. W., et al. (2017). TIMP-1 is upregulated, but not essential in hepatic fibrogenesis and carcinogenesis in mice. *Sci. Rep.* 7:714. doi: 10.1038/s41598-017-00671-1
- Thieringer, F., Maass, T., Czochra, P., Klopke, B., Conrad, I., Friebe, D., et al. (2008). Spontaneous hepatic fibrosis in transgenic mice overexpressing PDGF-A. *Gene* 423, 23–28. doi: 10.1016/j.gene.2008.05.022
- Tolba, R., Kraus, T., Liedtke, C., Schwarz, M., and Weiskirchen, R. (2015). Diethylnitrosamine (DEN)-induced carcinogenic liver injury in mice. *Lab. Anim.* 49(1 Suppl.), 59–69. doi: 10.1177/0023677215570086
- Tropskaya, N. S., Kislyakova, E. A., Vilko, I. G., Kislytsyna, O. S., Gurman, Y. V., Popova, T. S., et al. (2020). Experimental Model of Cirrhosis of the Liver. *Bull. Exp. Biol. Med.* 169, 416–420. doi: 10.1007/s10517-020-04899-2
- Tsuchida, T., Lee, Y. A., Fujiwara, N., Ybanez, M., Allen, B., Martins, S., et al. (2018). A simple diet- and chemical-induced murine NASH model with rapid progression of steatohepatitis, fibrosis and liver cancer. *J. Hepatol.* 69, 385–395. doi: 10.1016/j.jhep.2018.03.011
- Tsukamoto, H., and Lu, S. C. (2001). Current concepts in the pathogenesis of alcoholic liver injury. *FASEB J.* 15, 1335–1349. doi: 10.1096/fj.00-0650rev
- Ueberham, E., Löw, R., Ueberham, U., Schöning, K., Bujard, H., and Gebhardt, R. (2003). Conditional tetracycline-regulated expression of TGF-beta1 in liver of transgenic mice leads to reversible intermediary fibrosis. *Hepatology* 37, 1067–1078. doi: 10.1053/jhep.2003.50196
- Uehara, T., Ainslie, G. R., Kutanzi, K., Pogribny, I. P., Muskhelishvili, L., Izawa, T., et al. (2013). Molecular mechanisms of fibrosis-associated promotion of liver carcinogenesis. *Toxicol. Sci.* 132, 53–63. doi: 10.1093/toxsci/kfs342
- Unsal, V., Cicek, M., and Sabancilar, I. (2020). Toxicity of carbon tetrachloride, free radicals and role of antioxidants. *Rev. Environ. Health* 2020:48. doi: 10.1515/revh-2020-0048
- Wallace, M. C., Hamesch, K., Lunova, M., Kim, Y., Weiskirchen, R., Strnad, P., et al. (2015). Standard operating procedures in experimental liver research: thioacetamide model in mice and rats. *Lab. Anim.* 49(1 Suppl.), 21–29. doi: 10.1177/0023677215573040
- Walter, E., Keist, R., Niederöst, B., Pult, I., and Blum, H. E. (1996). Hepatitis B virus infection of tupaia hepatocytes in vitro and in vivo. *Hepatology* 24, 1–5. doi: 10.1053/jhep.1996.v24.pm0008707245
- Wang, H.-X., Liu, M., Weng, S.-Y., Li, J.-J., Xie, C., He, H.-L., et al. (2012). Immune mechanisms of Concanavalin A model of autoimmune hepatitis. *World J. Gastroenterol.* 18, 119–125. doi: 10.3748/wjg.v18.i2.119
- Wang, K., Liu, L., Dai, W., Chen, X., Zheng, X., and Hou, J. (2014). Establishment of a hepatic fibrosis model induced by diethylnitrosamine in zebrafish. *Nan Fang Yi Ke Da Xue Xue Bao* 34, 777–782.
- Wang, L., Tu, L., Zhang, J., Xu, K., and Qian, W. (2017). Stellate Cell Activation and Imbalanced Expression of TGF-1/TGF-3 in Acute Autoimmune Liver Lesions Induced by ConA in Mice. *Biomed. Res. Int.* 2017:2540540. doi: 10.1155/2017/2540540
- Watanabe, T., Nioka, M., Hozawa, S., Kameyama, K., Hayashi, T., Arai, M., et al. (2000). Gene expression of interstitial collagenase in both progressive and recovery phase of rat liver fibrosis induced by carbon tetrachloride. *J. Hepatol.* 33, 224–235. doi: 10.1016/s0168-8278(00)80363-3
- Weber, L. W. D., Boll, M., and Stampfl, A. (2003). Hepatotoxicity and mechanism of action of haloalkanes: carbon tetrachloride as a toxicological model. *Crit. Rev. Toxicol.* 33, 105–136. doi: 10.1080/713611034
- Wei, D.-D., Wang, J.-S., Wang, P.-R., Li, M.-H., Yang, M.-H., and Kong, L.-Y. (2014). Toxic effects of chronic low-dose exposure of thioacetamide on rats based on NMR metabolic profiling. *J. Pharm. Biomed. Anal.* 98, 334–338. doi: 10.1016/j.jpba.2014.05.035
- Xia, X., Li, F., He, J., Aji, R., and Gao, D. (2019). Organoid technology in cancer precision medicine. *Cancer Lett.* 457, 20–27. doi: 10.1016/j.canlet.2019.04.039

- Yan, M., Huo, Y., Yin, S., and Hu, H. (2018). Mechanisms of acetaminophen-induced liver injury and its implications for therapeutic interventions. *Redox Biol.* 17, 274–283. doi: 10.1016/j.redox.2018.04.019
- Ye, T., Wang, T., Yang, X., Fan, X., Wen, M., Shen, Y., et al. (2018). Comparison of Concanavalin a-Induced Murine Autoimmune Hepatitis Models. *Cell Physiol. Biochem.* 46, 1241–1251. doi: 10.1159/000489074
- Yoon, E., Babar, A., Choudhary, M., Kutner, M., and Pysopoulos, N. (2016). Acetaminophen-Induced Hepatotoxicity: a Comprehensive Update. *J. Clin. Transl. Hepatol.* 4, 131–142. doi: 10.14218/JCTH.2015.00052
- Yoshiji, H., Kuriyama, S., Miyamoto, Y., Thorgeirsson, U. P., Gomez, D. E., Kawata, M., et al. (2000). Tissue inhibitor of metalloproteinases-1 promotes liver fibrosis development in a transgenic mouse model. *Hepatology* 32, 1248–1254. doi: 10.1053/jhep.2000.20521
- Yoshino, K., Taura, K., Iwaisako, K., Masano, Y., Uemoto, Y., Kimura, Y., et al. (2021). Novel mouse model for cholestasis-induced liver fibrosis resolution by cholecystojejunostomy. *J. Gastroenterol. Hepatol.* 2021:15406. doi: 10.1111/jgh.15406
- Zangar, R. C., Benson, J. M., Burnett, V. L., and Springer, D. L. (2000). Cytochrome P450 2E1 is the primary enzyme responsible for low-dose carbon tetrachloride metabolism in human liver microsomes. *Chem. Biol. Interact.* 125, 233–243. doi: 10.1016/s0009-2797(00)00149-6
- Zhang, J. J., Meng, X. K., Dong, C., Qiao, J. L., Zhang, R. F., Yue, G. Q., et al. (2009). Development of a new animal model of liver cirrhosis in swine. *Eur. Surg. Res.* 42, 35–39. doi: 10.1159/000167855
- Zhangdi, H.-J., Su, S.-B., Wang, F., Liang, Z.-Y., Yan, Y.-D., Qin, S.-Y., et al. (2019). Crosstalk network among multiple inflammatory mediators in liver fibrosis. *World J. Gastroenterol.* 25, 4835–4849. doi: 10.3748/wjg.v25.i33.4835
- Zhou, J.-Y., Jiang, Z.-A., Zhao, C.-Y., Zhen, Z., Wang, W., and Nanji, A. A. (2013). Long-term binge and escalating ethanol exposure causes necroinflammation and fibrosis in rat liver. *Alcohol Clin. Exp. Res.* 37, 213–222. doi: 10.1111/j.1530-0277.2012.01936.x

Conflict of Interest: The authors declare that the research was conducted in the absence of any commercial or financial relationships that could be construed as a potential conflict of interest.

Copyright © 2021 Bao, Wang, Pan, Zhang, Chen, Xu, Mao and Li. This is an open-access article distributed under the terms of the Creative Commons Attribution License (CC BY). The use, distribution or reproduction in other forums is permitted, provided the original author(s) and the copyright owner(s) are credited and that the original publication in this journal is cited, in accordance with accepted academic practice. No use, distribution or reproduction is permitted which does not comply with these terms.



High Glucose Activates YAP Signaling to Promote Vascular Inflammation

Jeremy Ortilon¹, Jean-Christophe Le Bail¹, Elise Villard¹, Bertrand Léger¹, Bruno Poirier¹, Christine Girardot¹, Sandra Beeske¹, Laetitia Ledein¹, Véronique Blanchard², Patrice Brieu², Souâd Naimi², Philip Janiak¹, Etienne Guillot¹ and Marco Meloni^{1*}

¹ Cardiovascular Research Unit, Sanofi R&D, Chilly-Mazarin, France, ² Molecular Histopathology and Bio-Imaging Translational Sciences, Sanofi R&D, Chilly-Mazarin, France

OPEN ACCESS

Edited by:

Isotta Chimenti,
Sapienza University of Rome, Italy

Reviewed by:

Julian Albarran Juarez,
Aarhus University, Denmark
Irena Levitan,
University of Illinois at Chicago,
United States

*Correspondence:

Marco Meloni
marco.meloni@sanofi.com

Specialty section:

This article was submitted to
Vascular Physiology,
a section of the journal
Frontiers in Physiology

Received: 09 February 2021

Accepted: 11 May 2021

Published: 04 June 2021

Citation:

Ortilon J, Le Bail J-C, Villard E, Léger B, Poirier B, Girardot C, Beeske S, Ledein L, Blanchard V, Brieu P, Naimi S, Janiak P, Guillot E and Meloni M (2021) High Glucose Activates YAP Signaling to Promote Vascular Inflammation. *Front. Physiol.* 12:665994. doi: 10.3389/fphys.2021.665994

Background and Aims: The YAP/TAZ signaling is known to regulate endothelial activation and vascular inflammation in response to shear stress. Moreover, YAP/TAZ signaling plays a role in the progression of cancers and renal damage associated with diabetes. However, whether YAP/TAZ signaling is also implicated in diabetes-associated vascular complications is not known.

Methods: The effect of high glucose on YAP/TAZ signaling was firstly evaluated *in vitro* on endothelial cells cultured under static conditions or subjected to shear stress (either laminar or oscillatory flow). The impact of diabetes on YAP/TAZ signaling was additionally assessed *in vivo* in *db/db* mice.

Results: *In vitro*, we found that YAP was dephosphorylated/activated by high glucose in endothelial cells, thus leading to increased endothelial inflammation and monocyte attachment. Moreover, YAP was further activated when high glucose was combined to laminar flow conditions. YAP was also activated by oscillatory flow conditions but, in contrast, high glucose did not exert any additional effect. Interestingly, inhibition of YAP reduced endothelial inflammation and monocyte attachment. Finally, we found that YAP is also activated in the vascular wall of diabetic mice, where inflammatory markers are also increased.

Conclusion: With the current study we demonstrated that YAP signaling is activated by high glucose in endothelial cells *in vitro* and in the vasculature of diabetic mice, and we pinpointed YAP as a regulator of high glucose-mediated endothelial inflammation and monocyte attachment. YAP inhibition may represent a potential therapeutic opportunity to improve diabetes-associated vascular complications.

Keywords: YAP/TAZ, diabetes, inflammation, endothelial cells, vascular complications

INTRODUCTION

High glucose-induced endothelial dysfunction is a crucial initiating factor in the development of diabetes-associated vascular complications which, in turn, are responsible for shortened life expectancy, high rate of hospitalization, and high morbidity and mortality in patients with diabetes (Grundny et al., 2002; Schalkwijk and Stehouwer, 2005; Beckman and Creager, 2016).

The diabetic endothelium is characterized by increased expression of adhesion molecules and proinflammatory cytokines, resulting in a prothrombotic and proinflammatory state that favors the development of atherosclerosis (Anderson et al., 1995; Plutzky, 2003). Recent studies based on gene deletion have demonstrated the implication of YAP (Yes-Associated Protein) and TAZ (Transcriptional coactivator with PDZ-binding motif) in regulating endothelial activation and vascular inflammation (Lv et al., 2018). YAP and TAZ are transcriptional regulators and the main downstream mediators of the Hippo pathway, which regulates cell proliferation, survival and differentiation, thus controlling organ development and tissue regeneration (Pan, 2010; Yu and Guan, 2013; Piccolo et al., 2014). When the Hippo pathway is active, YAP and TAZ are phosphorylated/inactivated resulting in cytoplasmic localization and subsequent ubiquitin-mediated degradation (Zhao et al., 2010). Inhibition of the Hippo pathway promotes YAP and TAZ dephosphorylation and activation, followed by their translocation into the nucleus where they interact with the transcriptional enhancer associated domain (TEAD) leading to the activation of target genes associated with cell proliferation and differentiation (Piccolo et al., 2014).

The YAP/TAZ signaling is implicated in the regulation of vascular mechanotransduction and homeostasis (Dupont et al., 2011), and participates in the early structural and inflammatory events that occur in response to shear stress variation in large arteries (Wang et al., 2012; Choi et al., 2018; He et al., 2018). Wang et al. (2012) have demonstrated that YAP expression increases after carotid artery injury, and that YAP/TAZ mediates vascular remodeling during the progression of carotid stenosis. Moreover, Xu and colleagues have shown that YAP/TAZ inactivation protects against endothelial inflammation in the setting of laminar flow (Xu et al., 2016). Furthermore, turbulent flow has been demonstrated to activate YAP/TAZ and promote an atheroprone phenotype characterized by increased endothelial cell dysfunction and inflammation in the mouse carotid artery (Wang K. C. et al., 2016). Conversely, laminar flow was shown to inhibit RhoA (which is known to regulate YAP signaling), thus leading to YAP phosphorylation/inactivation (Wang K. C. et al., 2016). In addition, a role for YAP/TAZ signaling has also been unveiled in the context of diabetes: in fact, it has been indicated that YAP favors cancer incidence and progression in patients with diabetes, and that it plays an important role in diabetes-associated renal damage (Chen and Harris, 2016; Wang C. et al., 2016; Zhang et al., 2018; Ma et al., 2019). It is not known, however, whether YAP/TAZ signaling is also implicated in diabetes-associated vascular complications.

With the current study we investigated the importance of YAP/TAZ signaling on endothelial cell activation and vascular inflammation in the settings of diabetes. Using *in vitro* and *in vivo* approaches, we demonstrated that YAP signaling is activated in the diabetic vasculature and plays a role in the regulation of endothelial inflammation and monocyte attachment induced by high glucose.

MATERIALS AND METHODS

Cell Culture

Human umbilical vein endothelial cells (HUVECs, PromoCell) were cultured in endothelial cell medium (PromoCell) added with Growth Medium Supplement Pack (PromoCell) in a humidified atmosphere at 37°C and 5% CO₂. Human aortic endothelial cells (TeloHAEC) were immortalized by stably expressing human telomerase catalytic subunit hTERT (ATCC). In addition, TeloHAECs were also stably transduced with the IncuCyte™ NucLight™ red Fluorescent Protein Lentivirus Reagents (Essen BioScience) and with Tead Luciferase lentiviral construct (Vectalys) containing wild type or 7× mutated (inactive form) TEAD-responsive synthetic element/region (8×GTTC region followed by a minimal chicken TNNT2 promoter, before the luciferase gene, called TEADwt-Luc and TEADmut-Luc, respectively) driving luciferase expression (Kim and Gumbiner, 2015). To mimic the diabetes environment, HUVECs or TeloHAECs were cultured with high glucose (15 or 25 mM) for 24 h under static conditions. In order to replicate the *in vivo*-like flow conditions of an artery, HUVECs were additionally exposed to fluidic conditions. Briefly, HUVECs (2.5 × 10⁵ cells) were seeded onto glasses 0.4 mm Luer μ-slides I (Ibidi; channel length, 50 mm; channel width, 5 mm; and channel height, 0.4 mm) coated with rat tail collagen I (Gibco; 100 μg/ml in PBS) and grown until confluence. The slides were assembled into flow chambers and connected to an Ibidi Pump System (Ibidi). HUVECs were cultured with high glucose (25 mM) and exposed to steady laminar shear stress (12 dyn/cm²) or oscillatory shear stress (0.5 ± 6 dyn/cm²; 1 Hz) for 72 h without renewal of the culture medium. Glucose concentration at baseline (0 h) or after 72 h was not assessed: given the volume of medium used in the Ibidi Pump System (12 ml) and based on previous reports (Barcelos et al., 2009; Mangialardi et al., 2013; Zhang J. et al., 2019), glucose concentration is not expected to change in these experimental settings. The flow system was maintained at 37°C, and the circulating medium was equilibrated with a humidified atmosphere of 5% CO₂. For all experiments, HUVECs were used between P2 and P5. Human monocytic cell line THP-1 (Leibniz Institute DSMZ-German Collection, GmbH) were transfected with the IncuCyte™ NucLight™ Green Fluorescent Protein (GFP) Lentivirus Reagents (Essen BioScience). THP-1-GFP were cultured in RPMI 1640 medium (Gibco) and 10% FBS (Gibco).

In vitro YAP/TAZ Inhibition

Inhibition of the YAP/TAZ signaling pathway was obtained by using either siRNAs against YAP and TAZ or the small molecule

TEAD inhibitor K-975 (Kaneda et al., 2020). For siRNA-mediated inhibition of YAP/TAZ, HUVECs were transfected with siRNAs using LipofectamineTM RNAiMAX reagent (Thermo Fischer) in Opti-MEM and L-Glutamine (Gibco) according to the manufacturer's instruction. Endogenous YAP/TAZ expression was knocked down by transfecting cells with 100 nM of siRNA against YAP (Silencer-select siRNA s20366, Ambion) and TAZ (ON-TargetPlus siRNA, Horizon discovery). Control cells were transfected with negative control siRNA (Ambion). Cells were incubated with transfection complexes at 37°C in 5% CO₂ for 4 h and media was replaced with complete endothelial growth medium for 20 h. Then, HUVEC were cultured for additional 24 h on either normal (5 mM) or high glucose (25 mM) condition in endothelial cell medium added with Growth Medium Supplement Pack (PromoCell). For the purpose of TEAD inhibition, K-975 was synthesized internally based on Kaneda et al. (2020). K-975 at 200 nM was added to HUVECs cultured on either normal (5 mM) or high glucose (25 mM) for 24 h, and under either static conditions or subjected to fluidic conditions. DMSO (0.01%, v/v) was used as control.

Luciferase Assay

TeloHAECs were seeded at the density of 15×10^3 cells/well in a 96-well plate format and maintained in a complete medium (CM) composed of Vascular Cell basal medium (BM), 5.5 mM glucose supplemented with Vascular Endothelial Cell Growth Kit-VEGF with 2% FBS and cytokines (ATCC), and incubated at 37°C in 5% CO₂ for 24 h. Then, the medium was removed, and cells were kept in BM supplemented with 0.1% BSA with or without K-975, or under high glucose conditions (25 mM). After 24 h of incubation, the fluorescence intensity was detected by a fluorescence plate reader (Clariostar, BMG Labtech). Then, cells were lysed and the Luc-ScreenTM Extended-Glow Luciferase Reporter Gene Assay System (Invitrogen) was used to detect luciferase activity (according to the manufacturer's instruction). This reporter assay allows a direct investigation of the interaction between YAP/TAZ and TEAD: if TEAD interacts with YAP/TAZ the luciferase activity increases; if their interaction is prevented (i.e., by a TEAD inhibitor like K-975) the luciferase activity decreases.

Monocyte Adhesion Assay

The adhesion assay was performed by perfusing the THP-1-GFP positive cells on HUVECs cultured under either normal or high glucose conditions (with or without K-975, 200 nM), and already subjected to laminar flow (12 dyn/cm²) for 72 h. THP-1-GFP were resuspended at the concentration of 5×10^5 cells per mL in RPMI 1640 (supplemented with 10% serum), then perfused on the HUVECs monolayer for 60 min at 37°C. To allow THP-1 cells attachment to HUVECs, the laminar flow conditions were set at 5 dyn/cm². After removing the non-attached THP-1 cells (by washing with RPMI), fluorescent images were taken using an IN Cell Analyser 2200 (GE Healthcare). To distinguish THP-1-GFP cells from HUVECs, HUVECs were prelabelled with Hoechst (Invitrogen). IN Cell Analyser software was used to quantify the number of adherent THP-1 cells.

Western Blot

Human umbilical vein endothelial cells were lysed in ice-cold cell extraction Buffer (Invitrogen) supplemented with protease/phosphatase inhibitor mixture (Sigma). Protein concentration was determined with the Pierce BCA Protein Assay Kit (Thermo Fischer). Equal amounts of protein (10 µg) were loaded and resolved by SDS/PAGE. After electrophoresis, proteins were transferred to PVDF membranes, followed by blocking with 10% blotting-Grade Blocker (Bio-Rad). The membranes were incubated with primary antibodies against phospho-YAP (Ser-127) (1:1,000), YAP (1:1,000), phospho-TAZ (Ser-89) (1:1,000), TAZ (1:2,500), VCAM-1 (1:1,000), ICAM-1 (1:1,000), cytokines connective tissue growth factor (CTGF; 1:1,000), cysteine-rich angiogenic inducer 61 (CYR61; 1:1,000) (all from Cell Signaling), GAPDH (Santa Cruz Biotechnologies, 1:10,000), β-actin (Sigma, 1:10,000) with gentle agitation overnight at 4°C. The membranes were washed three times for 10 min each with TBS-T (containing 0.1% Tween-20) and incubated with horseradish-peroxidase (HRP)-conjugated anti-mouse-IgG (Jackson ImmunoResearch, 1:10,000) or HRP-conjugated anti-rabbit-IgG (Jackson ImmunoResearch, 1:10,000) followed by chemiluminescence detection using GE Healthcare ECL western blotting substrate according to the manufacturer's protocol. The blot image was acquired using G:BOX Chemi XL 1.4 (Syngene) imaging system and the band density was quantified by using GENETOOLS V4.03 (Syngene) software.

qPCR

Total RNA was isolated from HUVECs by using the Maxwell RSC simply RNA Tissue kit (Promega). The concentration of RNA was determined by using a NanoDrop spectrophotometer (Thermo Fischer). One microgram of total RNA was reversely transcribed into cDNA by using SuperScript VILO cDNA Synthesis Kit (Invitrogen). The real-time PCR was carried out with TaqMan Universal PCR Master Mix (Applied Biosystems) on Stratagene Mx3000P (Agilent Technologies) detection system. Primer sets used in our study (predesigned by Thermo Fischer) were as follows: CTGF (Hs00170014_m1); CYR61 (Hs00155479_m1). The relative gene expression was determined by $2^{-\Delta\Delta Ct}$ method.

Flow Cytometry Analysis

Human umbilical vein endothelial cells were briefly washed with sterile HBSS (Gibco), detached from the plate using versene with 5% of trypsin-EDTA (0.025%, v/v), then washed with staining buffer (BD Pharmingen). Cells were then transferred to a FACS plate, washed and resuspended in 10% PE-conjugated mouse anti-human ICAM-1 and FITC-conjugated mouse anti-human VCAM-1 (both from BD Pharmingen) in staining buffer for 30 min on ice and in the dark. Then cells were washed, resuspended in HBSS and analyzed using a Guava EasyCyte flow cytometer (Merck-Millipore). Data analysis was performed using the Guava software (Merck-Millipore). Mouse IgG1κ-FITC and PE were used as isotype controls.

Animals and Ethics Statement

Diabetic male *db/db* mice and sex- and age-matched non-diabetic *db/+* control mice (on the C57BL/6J background; Jackson Laboratories) were used to conduct animal studies. Mice were housed with free access to standard chow diet (Harlan) and water. Blood glucose levels were measured before tissue collection with Accu-Chek® glucose meter (Roche). All procedures involving animals were performed in agreement with the European Community standard on the care and use of laboratory animals (2010/63/UE) and were approved by the IACUC of Sanofi R&D. All procedures were performed in AAALAC-accredited facilities in full compliance with the recommendations of the French Ministry of Research.

In vivo Alteration of Shear Stress

To induce changes in shear stress, a perivascular shear stress modifying cast was tied around the right common carotid artery of 18-week-old mice for 4 weeks. The cast consists of 2 longitudinal halves which, when put together, form a cylinder with an inner diameter of 500 μm (non-constrictive) that gradually declines to 250 μm , thus producing a gradual stenosis and gradual increase in shear stress (Cheng et al., 2005) (Sepran; Sepra, Delft, Netherlands). Briefly, mice were anesthetized with isoflurane, and the right anterior cervical triangle was accessed by incision. The right common carotid artery was dissected from connective tissue and both halves were placed and tied with a suture. Wounds were closed and animals were allowed to recover. The left carotid artery was left untouched and served as control.

Immunohistochemical Analyses

Twenty-two-week-old mice were euthanized by exsanguination under profound anesthesia and immediately perfusion-fixed with heparinized PBS followed by 4% formalin. Both left (control) and right carotid arteries were removed and embedded in paraffin. All samples were cut into transverse sections (5 μm in thickness) and prepared for subsequent immunohistochemical analyses. For cast-instrumented arteries, sections were cut approximately 250 μm downstream of the cast, in the region of low and oscillatory shear stress (Cheng et al., 2005). Immunostaining were performed using the Ventana Discovery XT or BenschMark Ultra automated Systems (Ventana Medical System, Inc., Roche) with standard DabMab or UltraMab detection systems. Paraffin-embedded sections were incubated with primary antibodies against phospho-YAP (Ser127) (D9W2I, Cell Signaling, 1:1,000), YAP (D8H1X, Cell Signaling, 1:50) and VCAM-1 (ab134047, Abcam, 1:500). Optimal concentrations for each antibody were determined by individual pilot studies. Samples were counterstained with hematoxylin II and bluing reagent (Ventana) and coverslipped with Pertex. For all immunostaining, images of the entire slides were acquired on an Olympus Virtual Slide scanner (VS120) and quantitatively analyzed on whole tissue sections using Area Quantification Brightfield v1.0 module of Indica Labs HALO software (based on the intensity of the immunolabeling). Briefly, the intima-media area of the analyzed sections was manually delimited on images and positive stained

area including weak (in yellow), moderate (in orange) and strong (in red) positive pixels was automatically quantified for each animal (as illustrated in **Supplementary Figure 1**).

Statistical Analysis

Values are presented as mean \pm standard error of mean (SEM). Non-parametric two-tailed Mann-Whitney test or parametric two-tailed Student's *t* test was used for comparisons between two groups, and non-parametric Kruskal-Wallis test was used to compare more groups, respectively. Statistical analysis was performed using GraphPad Prism software 8.0.2. A *p* value < 0.05 was interpreted to denote statistical significance.

RESULTS

High Glucose Induces YAP Activation in Endothelial Cells

A series of *in vitro* experiments using two endothelial cell models, HUVECs and TeloHAECs, were carried out to investigate the consequence of high glucose culture conditions on YAP signaling. As shown in **Figure 1A**, phospho-YAP was decreased in HUVECs exposed to high glucose, as compared to normal glucose. By contrast, no differences were observed on total YAP, phospho-TAZ and total TAZ (**Figures 1A,B**). In addition, Western blot and qRT-PCR analysis showed that the expression of both CTGF and CYR61 (two transcriptional target genes of YAP/TAZ/TEAD) (Zhao et al., 2008; Shome et al., 2020) were increased by high glucose conditions (**Figure 1C** and **Supplementary Figure 2**, respectively). Accordingly, the signal response was increased by high glucose in TeloHAECs transduced with TEAD-luciferase reporter (**Figure 2A**). The specificity of the model was previously validated by using inactive TEAD-mutant or inhibition with TEAD inhibitor K-975 (**Supplementary Figure 3**). Taken together, these results suggest that high glucose activates YAP but not TAZ in endothelial cells.

YAP Is Involved in High Glucose-Induced Endothelial Activation

The consequences of YAP activation in endothelial cells in response to high glucose were characterized in HUVECs by hampering YAP activity by using either siRNA-mediated YAP/TAZ deletion or the TEAD inhibitor K-975. VCAM-1 expression was monitored as a marker of endothelial activation known to be highly sensitive to YAP/TAZ deletion (Choi et al., 2018) and CTGF was chosen as a downstream signal of TEAD activity (Zhao et al., 2008). The expression of VCAM-1 and ICAM-1 was induced by high glucose as assessed by Western blot (**Figures 2B,C,E** for VCAM-1 and **Figure 2E** for ICAM-1) and flow cytometry (**Figure 2F**). siRNA-mediated deletion of YAP/TAZ prevented the increase in VCAM-1 (**Figures 2B,C**) and CTGF expression (**Figures 2B,D**) as observed under high glucose exposure. Accordingly, K-975, as a blocker of the YAP/TEAD activation cascade, blunted glucose-mediated alteration of VCAM-1 and ICAM-1 expression and cell surface expression (**Figures 2E,F**). These findings suggest

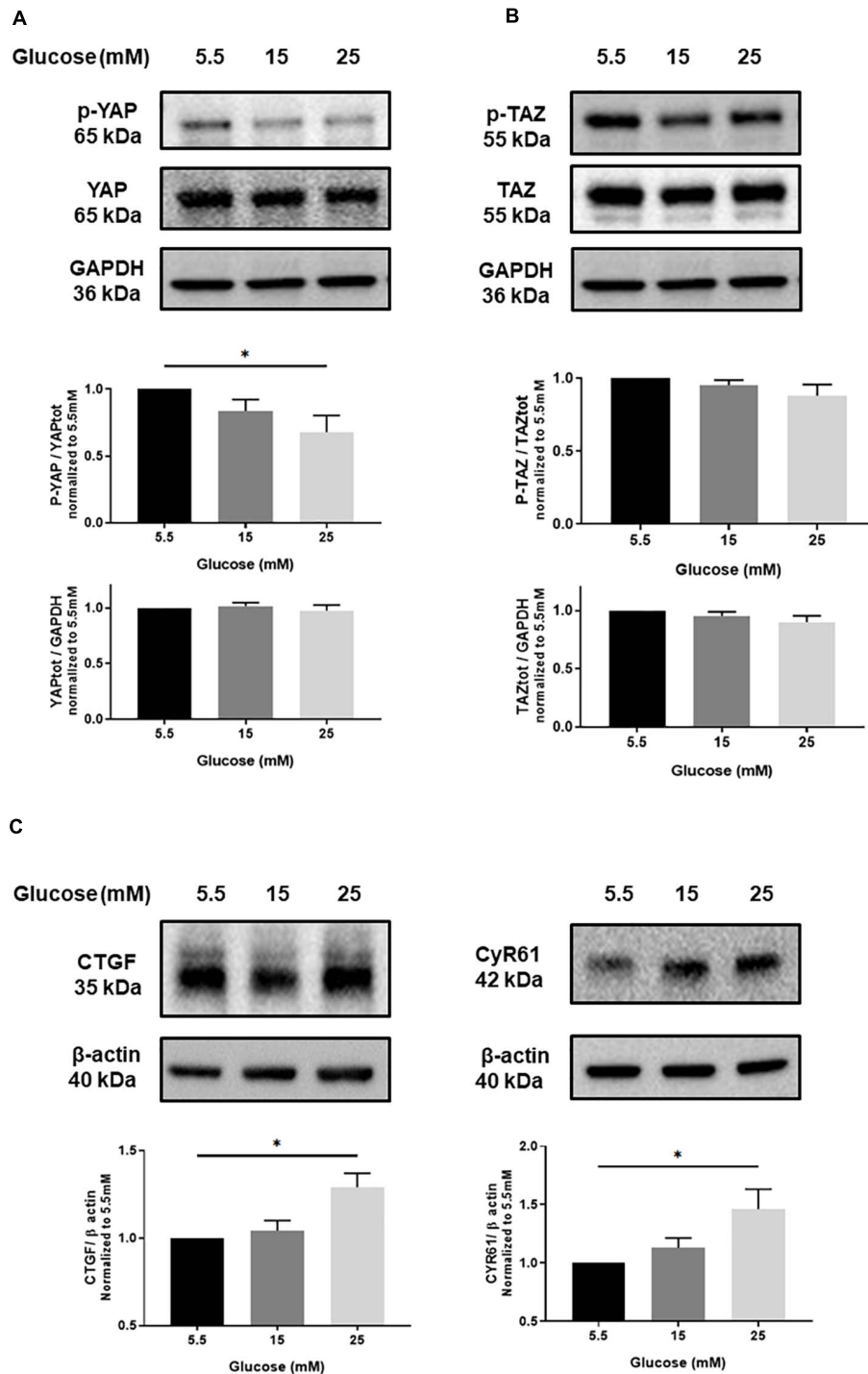
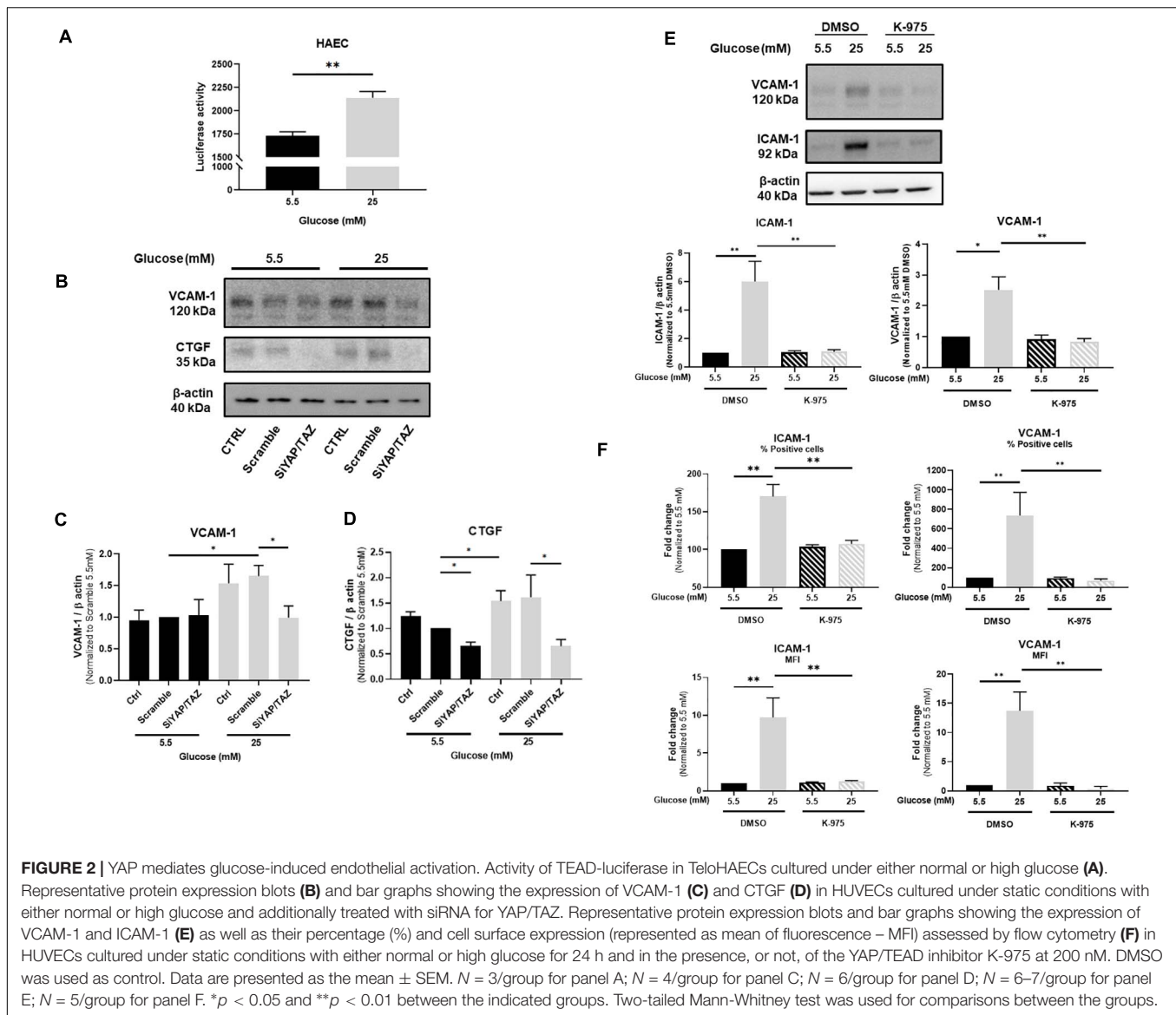


FIGURE 1 | Effect of high glucose on YAP activation in endothelial cells. Representative protein expression blots and bar graphs of phospho-YAP (p-YAP; S127) and total YAP (**A**), phospho-TAZ (p-TAZ; S89) and total TAZ (**B**), CTGF and CYR61 (**C**) in HUVECs cultured under static conditions with different concentrations of glucose for 24 h. The control images of GAPDH are re-used for illustrative purposes. Data are presented as the mean \pm SEM. $N = 5$ /group for panels A and B; $N = 7$ /group for panel C. * $p < 0.05$ between the indicated groups. Two-tailed Student's t test was used for comparisons between the groups.

that YAP/TAZ signaling plays a critical role in high glucose-induced endothelial activation. Confirmation of siRNA-mediated deletion of YAP/TAZ is shown in **Supplementary Figure 4**. The

residual expression of TAZ observed after the siRNA approach is in line with what has been already published by others (Yu et al., 2012; Rausch et al., 2019). Importantly, combination of YAP

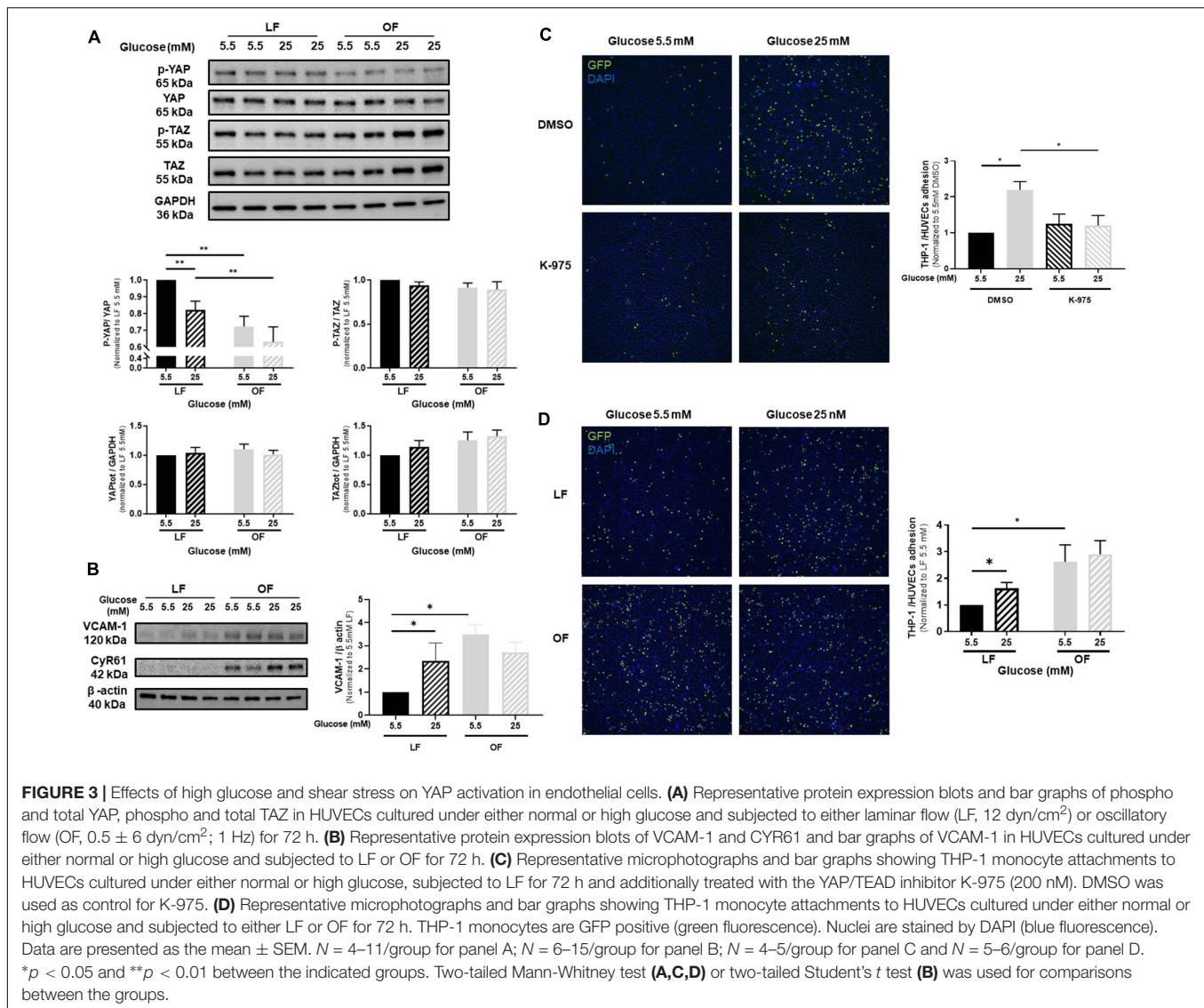


and TAZ siRNAs was preferred to siRNA YAP alone to efficiently block the pathway and avoid any possible compensation due to the residual expression of TAZ, as already shown (Nallet-Staub et al., 2014; Choi et al., 2018). **Supplementary Figure 5** shows that K-975-mediated inhibition of YAP/TEAD prevented the increased expression of the YAP/TEAD downstream effectors CTGF and CYR61 otherwise observed in HUVECs under high glucose, thus confirming the inhibitory effect of K-975 on YAP/TEAD signaling.

Effects of High Glucose and Shear Stress on YAP Activation in Endothelial Cells

Since vascular mechanotransduction was shown to activate YAP/TAZ signaling, we next evaluated the effects of high glucose on YAP phosphorylation in HUVECs exposed to oscillatory flow, compared to laminar flow conditions. Whereas the expression

of total YAP, phospho-TAZ and total TAZ was not altered by high glucose under either laminar or oscillatory flow, phospho-YAP significantly declined under laminar flow and high glucose exposure (**Figure 3A**). YAP phosphorylation was reduced by oscillatory flow conditions, but high glucose additional effect was not significant (**Figure 3A**). The expression of VCAM-1 (**Figure 3B**) was increased by high glucose under laminar flow, as compared to normal glucose conditions. Similarly, VCAM-1 expression increased under oscillatory flow conditions, but high glucose in combination with oscillatory flow conditions did not exert any additional effects on VCAM-1 expression (**Figure 3B**). Interestingly, a similar response was also observed for the expression of CYR61 (**Figure 3B** and **Supplementary Figure 6**). Subsequently, the rate of monocyte-endothelial cells attachment was increased by high glucose under laminar flow, as compared to normal glucose conditions (**Figure 3C**). Conversely K-975 blunted the glucose-induced THP1 monocyte attachments



to HUVECs (Figure 3C). The rate of monocyte attachment to HUVECs subjected to oscillatory flow was significantly increased compared to laminar flow exposure (Figure 3D). However, no additional effects were observed when cells were cultured in high glucose conditions (Figure 3D).

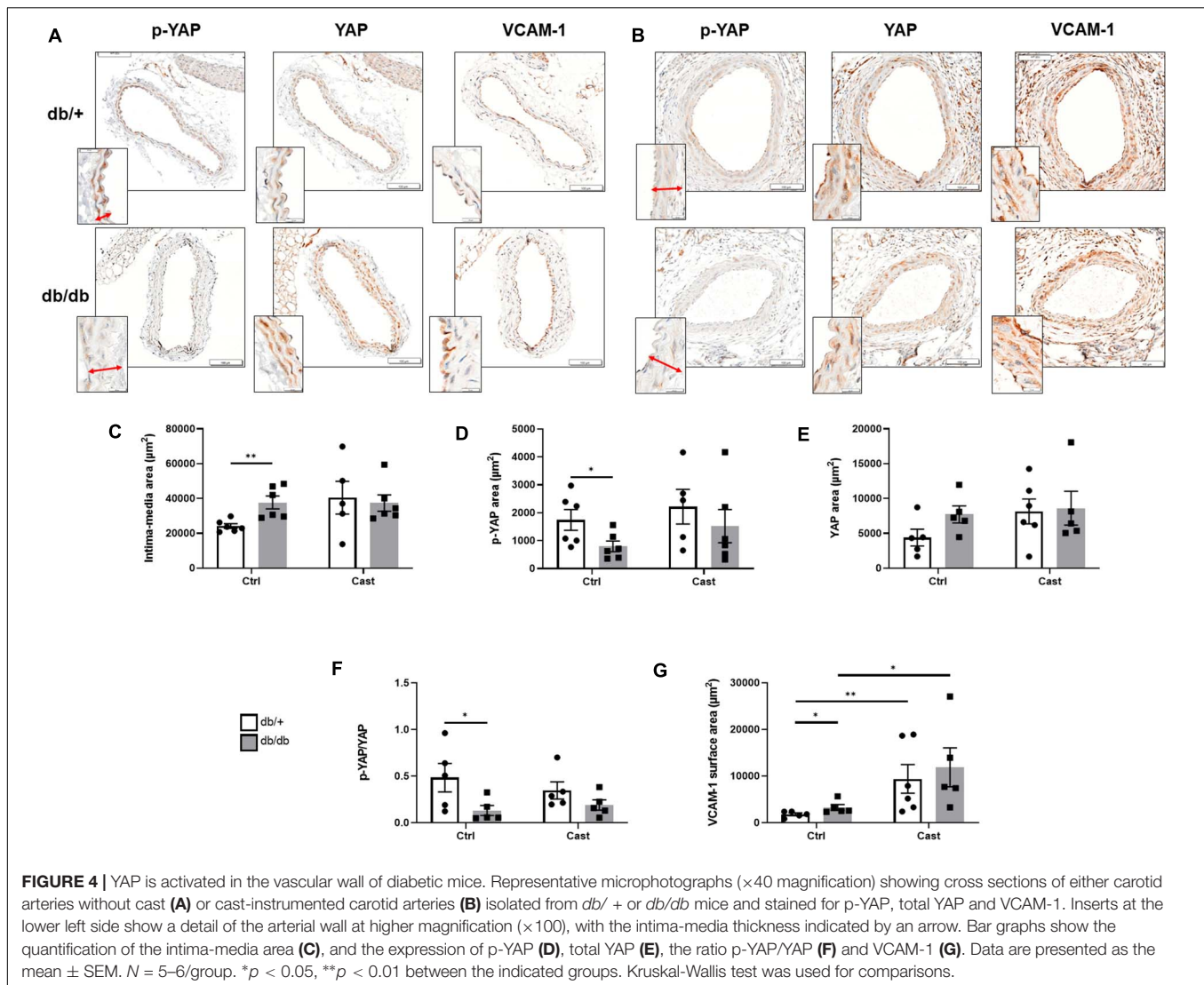
Diabetes Induces YAP Activation in the Vascular Wall of Mice

Next, we aimed to evaluate the effects of high glucose and shear stress on YAP in the vasculature of type 2 diabetic mice. First, high blood glucose levels in *db/db* mice (658 ± 115 mg/dL) compared to *db/+* mice (255 ± 22 mg/dL) were confirmed before tissue collection. Then, we analyzed the vascular wall of carotid arteries without casts in *db/db* and *db/+* mice. As shown in Figures 4A,C, compared to *db/+* mice, an enlargement of the intima-media thickness was observed in control carotid arteries of *db/db* mice. Phospho-YAP was detected in the vascular wall of *db/+* mice and significantly decreased

in *db/db* mice (Figures 4A,D). No difference in the expression of total YAP was observed (Figures 4A,E), thus resulting in a decrease in phospho/total YAP ratio and YAP activation in the vascular wall of diabetic mice (Figure 4F). Additional immunohistochemical analysis showed that the expression of VCAM-1 increased in the carotid artery vascular wall of diabetic mice (Figures 4A,G). Finally, with the exception of VCAM-1 expression, no differences were observed for all other parameters in cast-instrumented carotid arteries compared to carotid arteries without cast (Figures 4B–G), and no differences were observed in cast-instrumented carotid arteries between diabetic and non-diabetic mice (Figures 4A–G).

DISCUSSION

Previous reports have shown that YAP/TAZ plays a role in initiating and potentiating early steps of atherosclerosis



(Wang et al., 2012). Understanding the mechanisms that regulate the early steps of atherosclerosis in the settings of diabetes is essential to identify biomarkers and/or therapeutic targets for the treatment of diabetes-associated vascular complications.

First, we observed that only YAP is activated by high glucose and this likely participates in the described diabetes-induced endothelial activation and inflammation (Chen and Harris, 2016). Using two different inhibitory approaches we demonstrated that YAP inhibition reduces the expression of VCAM-1 and prevents monocyte attachment to endothelial cells under high glucose and either static condition or laminar shear stress, thus attenuating high glucose-mediated impairment of endothelial inflammation. However, we do not know whether YAP inhibition could also improve endothelial inflammation in our animal model of type 2 diabetes. Importantly, the effect of high glucose on YAP phosphorylation and VCAM-1 expression observed under laminar flow *in vitro* is consistent with that observed in the vasculature of *db/db* mice without cast. Nonetheless, although a trend was observed between *db/+* mice

with or without cast, the response induced by *in vitro* oscillatory flow on YAP phosphorylation was not observed in the vasculature of mice subjected to carotid cast-induced turbulent flow for 4 weeks. However, we cannot exclude that turbulent flow induced by the cast for shorter or longer time could produce similar effects as those observed *in vitro*. In addition, oscillatory flow imposed *in vitro* on endothelial cells might not fully be translatable in nature and magnitude with the turbulent flow generated downstream of the cast. Vascular regions exposed to disturbed flow are known to be more prone to atherogenesis (Cunningham and Gotlieb, 2005; Wang Y. et al., 2016). On the other side, vascular regions exposed to laminar flow are protected against endothelial inflammation and atherogenesis (Chen et al., 2003; Xu et al., 2016). Interestingly, our *in vitro* and *in vivo* observations suggest that high glucose exerts a detrimental effect (increased inflammation) on vascular regions exposed to laminar flow, which is likely due to YAP activation and that may confer these vascular regions an atheroprone phenotype similar to that observed in vascular regions exposed to oscillatory flow. In our

study, we found that the combination of high glucose with oscillatory flow does not further decrease YAP phosphorylation (although a trend was observed both *in vitro* and *in vivo*), and this could be due to the fact that YAP is already maximally activated (dephosphorylated) by either high glucose or oscillatory flow alone. Indeed, although from different origin, high glucose on vascular regions exposed to laminar flow and oscillatory flow seems to exert similar effects by converging to the YAP signaling pathway. Importantly, our study focused on the effect of high glucose and shear stress on YAP activation in endothelial cells. However, we cannot exclude that high glucose and/or shear stress may also affect YAP activation in other vascular cells (like vascular smooth muscle cells), and further studies are needed to clarify these aspects.

To date, the involvement of YAP/TAZ signaling in the context of diabetes has only been shown in pathologies that are not directly associated with vascular diseases. The expression of YAP and CTGF increase *in vitro* and *in vivo* in renal proximal tubule epithelial cells under high glucose and in the kidney of type 2 diabetic patients, indicating that YAP may play a critical role in renal damage associated with diabetes (Chen and Harris, 2016; Ma et al., 2019). Several studies have also shown the crosstalk between YAP activation and high glucose in different types of cancers. In particular, it has been shown that high glucose increases O-GlcNAcylation, which is an important post-translational protein modification that plays pro-oncogenic roles (Teo et al., 2010; Peng et al., 2017; Zhang et al., 2017). More precisely, in breast cancer cells, O-GlcNAcylation of YAP was shown to precede its dephosphorylation (Peng et al., 2017). O-GlcNAcylation could also be the main driver of YAP activation in the diabetic vasculature. Moreover, it has also been demonstrated that mechanical stimuli modulate YAP/TAZ activities through RhoA in the vasculature (Dupont et al., 2011; Wang K. C. et al., 2016). A limitation of our study is that we didn't evaluate whether glucose induces O-GlcNAcylation which, in turn, may promote YAP activation in endothelial cells or in the diabetic vasculature, and whether this mechanism converges (or not) to the RhoA-mediated mechanism that may induce YAP activation by oscillatory flow. However, to understand the exact mechanisms additional studies using specific knockout animal models should be performed. Additionally, antidiabetic drugs such as metformin and liraglutide, also known to attenuate the development of atherosclerosis, were recently suspected to activate the hippo pathway independently of glucose lowering effect (Li et al., 2018; Wu et al., 2019; Zhang J. J. et al., 2019). Therefore, blocking YAP activation may elicit their beneficial

effects observed in the setting of atherosclerosis and vascular dysfunction (Li et al., 2017; Wang et al., 2017).

In conclusion, we demonstrate for the first time that YAP is activated by high glucose and perturbed shear stress in endothelial cells, and that inhibition of YAP attenuates cell activation and monocyte attachment which is otherwise promoted by high glucose. Although translation *in vivo* of YAP inhibition remains to be tested, these findings bring the first evidences that in vascular regions exposed to laminar flow, hyperglycemia may promote an atheroprone phenotype like that occurring in vascular regions exposed to oscillatory flow, and that YAP inhibition may be a potential therapeutic opportunity to improve vascular complications associated with diabetes.

DATA AVAILABILITY STATEMENT

The raw data supporting the conclusions of this article will be made available by the authors, without undue reservation.

ETHICS STATEMENT

The animal study was reviewed and approved by the IACUC of Sanofi R&D.

AUTHOR CONTRIBUTIONS

JO, J-CL, EV, BL, CG, and LL performed the *in vitro* experiments. JO, BP, and SB performed the *in vivo* experiments. JO, VB, and PB performed the immunohistochemical staining and analyses. JO, J-CL, EV, SN, PJ, EG, and MM wrote and edited the manuscript. All authors contributed to the article and approved the submitted version.

FUNDING

This study was sponsored by Sanofi.

SUPPLEMENTARY MATERIAL

The Supplementary Material for this article can be found online at: <https://www.frontiersin.org/articles/10.3389/fphys.2021.665994/full#supplementary-material>

REFERENCES

- Anderson, T. J., Gerhard, M. D., Meredith, I. T., Charbonneau, F., Delagrè, D., Creager, M. A., et al. (1995). Systemic nature of endothelial dysfunction in atherosclerosis. *Am. J. Cardiol.* 75, 71B–74B.
- Barcelos, L. S., Duplaa, C., Krankel, N., Graiani, G., Invernici, G., Katare, R., et al. (2009). Human CD133+ progenitor cells promote the healing of diabetic ischemic ulcers by paracrine stimulation of angiogenesis and activation of Wnt signaling. *Circ. Res.* 104, 1095–1102. doi: 10.1161/circresaha.108.192138
- Beckman, J. A., and Creager, M. A. (2016). Vascular complications of diabetes. *Circ. Res.* 118, 1771–1785.
- Chen, J., and Harris, R. C. (2016). Interaction of the EGF receptor and the hippo pathway in the diabetic kidney. *J. Am. Soc. Nephrol.* 27, 1689–1700. doi: 10.1681/asn.2015040415
- Chen, X. L., Varner, S. E., Rao, A. S., Grey, J. Y., Thomas, S., Cook, C. K., et al. (2003). Laminar flow induction of antioxidant response element-mediated genes in endothelial cells. A novel anti-inflammatory mechanism. *J. Biol. Chem.* 278, 703–711. doi: 10.1074/jbc.m203161200

- Cheng, C., van Haperen, R., de Waard, M., van Damme, L. C., Tempel, D., Hanemaaijer, L., et al. (2005). Shear stress affects the intracellular distribution of eNOS: direct demonstration by a novel in vivo technique. *Blood* 106, 3691–3698. doi: 10.1182/blood-2005-06-2326
- Choi, H. J., Kim, N. E., Kim, B. M., Seo, M., and Heo, J. H. (2018). TNF- α -induced YAP/TAZ activity mediates leukocyte-endothelial adhesion by regulating VCAM1 expression in endothelial cells. *Int. J. Mol. Sci.* 19:3428. doi: 10.3390/ijms19113428
- Cunningham, K. S., and Gotlieb, A. I. (2005). The role of shear stress in the pathogenesis of atherosclerosis. *Lab. Invest.* 85, 9–23. doi: 10.1038/labinvest.3700215
- Dupont, S., Morsut, L., Aragona, M., Enzo, E., Giulitti, S., Cordenonsi, M., et al. (2011). Role of YAP/TAZ in mechanotransduction. *Nature* 474, 179–183.
- Grundy, S. M., Howard, B., Smith, S. Jr., Eckel, R., Redberg, R., and Bonow, R. O. (2002). Prevention conference VI: diabetes and cardiovascular disease: executive summary: conference proceeding for healthcare professionals from a special writing group of the American heart association. *Circulation* 105, 2231–2239. doi: 10.1161/01.cir.0000013952.86046.dd
- He, J., Bao, Q., Yan, M., Liang, J., Zhu, Y., Wang, C., et al. (2018). The role of Hippo/yes-associated protein signalling in vascular remodelling associated with cardiovascular disease. *Br. J. Pharmacol.* 175, 1354–1361. doi: 10.1111/bph.13806
- Kaneda, A., Seike, T., Danjo, T., Nakajima, T., Otsubo, N., Yamaguchi, D., et al. (2020). The novel potent TEAD inhibitor, K-975, inhibits YAP1/TAZ-TEAD protein-protein interactions and exerts an anti-tumor effect on malignant pleural mesothelioma. *Am. J. Cancer Res.* 10, 4399–4415.
- Kim, N. G., and Gumbiner, B. M. (2015). Adhesion to fibronectin regulates Hippo signaling via the FAK-Src-PI3K pathway. *J. Cell. Biol.* 210, 503–515. doi: 10.1083/jcb.201501025
- Li, J., Liu, X., Fang, Q., Ding, M., and Li, C. (2017). Liraglutide attenuates atherosclerosis via inhibiting ER-induced macrophage derived microvesicles production in T2DM rats. *Diabetol. Metab. Syndr.* 9:94.
- Li, Y., Du, J., Zhu, E., Zhang, J., Han, J., Zhao, W., et al. (2018). Liraglutide suppresses proliferation and induces adipogenic differentiation of 3T3-L1 cells via the Hippo-YAP signaling pathway. *Mol. Med. Rep.* 17, 4499–4507.
- Lv, Y., Kim, K., Sheng, Y., Cho, J., Qian, Z., Zhao, Y. Y., et al. (2018). YAP controls endothelial activation and vascular inflammation through TRAF6. *Circ. Res.* 123, 43–56. doi: 10.1161/circresaha.118.313143
- Ma, R., Ren, J. M., Li, P., Zhou, Y. J., Zhou, M. K., Hu, Z., et al. (2019). Activated YAP causes renal damage of type 2 diabetic nephropathy. *Eur. Rev. Med. Pharmacol. Sci.* 23, 755–763.
- Mangialardi, G., Katare, R., Oikawa, A., Meloni, M., Reni, C., Emanuelli, C., et al. (2013). Diabetes causes bone marrow endothelial barrier dysfunction by activation of the RhoA-Rho-associated kinase signaling pathway. *Arterioscler. Thromb. Vasc. Biol.* 33, 555–564. doi: 10.1161/ATVBAHA.112.300424
- Nallet-Staub, F., Marsaud, V., Li, L., Gilbert, C., Dodier, S., Bataille, V., et al. (2014). Pro-invasive activity of the Hippo pathway effectors YAP and TAZ in cutaneous melanoma. *J. Invest. Dermatol.* 134, 123–132. doi: 10.1038/jid.2013.319
- Pan, D. (2010). The hippo signaling pathway in development and cancer. *Dev. Cell* 19, 491–505.
- Peng, C., Zhu, Y., Zhang, W., Liao, Q., Chen, Y., Zhao, X., et al. (2017). Regulation of the Hippo-YAP pathway by glucose sensor O-GlcNAcylation. *Mol. Cell* 68, 591–604.e5.
- Piccolo, S., Dupont, S., and Cordenonsi, M. (2014). The biology of YAP/TAZ: hippo signaling and beyond. *Physiol. Rev.* 94, 1287–1312. doi: 10.1152/physrev.00005.2014
- Plutzky, J. (2003). The vascular biology of atherosclerosis. *Am. J. Med.* 115(Suppl. 8A), 55S–61S.
- Rausch, V., Bostrom, J. R., Park, J., Bravo, I. R., Feng, Y., Hay, D. C., et al. (2019). The Hippo pathway regulates caveolae expression and mediates flow response via caveolae. *Curr. Biol.* 29, 242–255.e6.
- Schalkwijk, C. G., and Stehouwer, C. D. (2005). Vascular complications in diabetes mellitus: the role of endothelial dysfunction. *Clin. Sci. (Lond.)* 109, 143–159. doi: 10.1042/cs20050025
- Shome, D., von Woedtke, T., Riedel, K., and Masur, K. (2020). The HIPPO transducer YAP and Its Targets CTGF and Cyr61 Drive a paracrine signalling in cold atmospheric plasma-mediated wound healing. *Oxid. Med. Cell. Longev.* 2020:4910280.
- Teo, C. F., Wollaston-Hayden, E. E., and Wells, L. (2010). Hexosamine flux, the O-GlcNAc modification, and the development of insulin resistance in adipocytes. *Mol. Cell. Endocrinol.* 318, 44–53. doi: 10.1016/j.mce.2009.09.022
- Wang, C., Jeong, K., Jiang, H., Guo, W., Gu, C., Lu, Y., et al. (2016). YAP/TAZ regulates the insulin signaling via IRS1/2 in endometrial cancer. *Am. J. Cancer Res.* 6, 996–1010.
- Wang, K. C., Yeh, Y. T., Nguyen, P., Limquenco, E., Lopez, J., Thorossian, S., et al. (2016). Flow-dependent YAP/TAZ activities regulate endothelial phenotypes and atherosclerosis. *Proc. Natl. Acad. Sci. U.S.A.* 113, 11525–11530. doi: 10.1073/pnas.1613121113
- Wang, Q., Zhang, M., Torres, G., Wu, S., Ouyang, C., Xie, Z., et al. (2017). Metformin suppresses diabetes-accelerated atherosclerosis via the inhibition of Drp1-mediated mitochondrial fission. *Diabetes* 66, 193–205. doi: 10.2337/db16-0915
- Wang, X., Hu, G., Gao, X., Wang, Y., Zhang, W., Harmon, E. Y., et al. (2012). The induction of yes-associated protein expression after arterial injury is crucial for smooth muscle phenotypic modulation and neointima formation. *Arterioscler. Thromb. Vasc. Biol.* 32, 2662–2669. doi: 10.1161/atvbaha.112.254730
- Wang, Y., Qiu, J., Luo, S., Xie, X., Zheng, Y., Zhang, K., et al. (2016). High shear stress induces atherosclerotic vulnerable plaque formation through angiogenesis. *Regen. Biomater.* 3, 257–267. doi: 10.1093/rb/rbw021
- Wu, Y., Zheng, Q., Li, Y., Wang, G., Gao, S., Zhang, X., et al. (2019). Metformin targets a YAP1-TEAD4 complex via AMPK α to regulate CCNE1/2 in bladder cancer cells. *J. Exp. Clin. Cancer Res.* 38:376.
- Xu, S., Koroleva, M., Yin, M., and Jin, Z. G. (2016). Atheroprotective laminar flow inhibits Hippo pathway effector YAP in endothelial cells. *Transl. Res.* 176, 18–28.e2.
- Yu, F. X., and Guan, K. L. (2013). The Hippo pathway: regulators and regulations. *Genes Dev.* 27, 355–371. doi: 10.1101/gad.210773.112
- Yu, F. X., Zhao, B., Panupinthu, N., Jewell, J. L., Lian, I., Wang, L. H., et al. (2012). Regulation of the Hippo-YAP pathway by G-protein-coupled receptor signaling. *Cell* 150, 780–791. doi: 10.1016/j.cell.2012.06.037
- Zhang, J., Guo, Y., Ge, W., Zhou, X., and Pan, M. (2019). High glucose induces apoptosis of HUVECs in a mitochondria-dependent manner by suppressing hexokinase 2 expression. *Exp. Ther. Med.* 18, 621–629.
- Zhang, J. J., Zhang, Q. S., Li, Z. Q., Zhou, J. W., and Du, J. (2019). Metformin attenuates PD-L1 expression through activating Hippo signaling pathway in colorectal cancer cells. *Am. J. Transl. Res.* 11, 6965–6976.
- Zhang, X., Qiao, Y., Wu, Q., Chen, Y., Zou, S., Liu, X., et al. (2017). The essential role of YAP O-GlcNAcylation in high-glucose-stimulated liver tumorigenesis. *Nat. Commun.* 8:15280.
- Zhang, X., Zhao, H., Li, Y., Xia, D., Yang, L., Ma, Y., et al. (2018). The role of YAP/TAZ activity in cancer metabolic reprogramming. *Mol. Cancer* 17:134.
- Zhao, B., Li, L., Tumaneng, K., Wang, C. Y., and Guan, K. L. (2010). A coordinated phosphorylation by Lats and CK1 regulates YAP stability through SCF(beta-TRCP). *Genes Dev.* 24, 72–85. doi: 10.1101/gad.1843810
- Zhao, B., Ye, X., Yu, J., Li, L., Li, W., Li, S., et al. (2008). TEAD mediates YAP-dependent gene induction and growth control. *Genes Dev.* 22, 1962–1971. doi: 10.1101/gad.1664408

Conflict of Interest: All authors are Sanofi employees.

The authors declare that the research was conducted in the absence of any commercial or financial relationships that could be construed as a potential conflict of interest.

Copyright © 2021 Ortillon, Le Bail, Villard, Léger, Poirier, Girardot, Beeske, Ledein, Blanchard, Brieu, Naimi, Janiak, Guillot and Meloni. This is an open-access article distributed under the terms of the Creative Commons Attribution License (CC BY). The use, distribution or reproduction in other forums is permitted, provided the original author(s) and the copyright owner(s) are credited and that the original publication in this journal is cited, in accordance with accepted academic practice. No use, distribution or reproduction is permitted which does not comply with these terms.



TMSB4 Overexpression Enhances the Potency of Marrow Mesenchymal Stromal Cells for Myocardial Repair

Shiyuan Tang¹, Chengming Fan^{1*}, Chukwuemeka Daniel Iroegbu¹, Wenwu Zhou², Zhigong Zhang², Ming Wu², Wangping Chen¹, Xiaoming Wu¹, Jun Peng³, Zhihong Li^{4*} and Jinfu Yang^{1,3*}

¹ Department of the Cardiovascular Surgery, The Second Xiangya Hospital, Central South University, Changsha, China, ² Department of the Cardiovascular Surgery of the Hunan Provincial People's Hospital, Changsha, China, ³ Hunan Provincial Key Laboratory of Cardiovascular Research, Changsha, China, ⁴ Institute of Senile and Aging Diseases, The Second Xiangya Hospital of Central South University, Changsha, China

OPEN ACCESS

Edited by:

Susanne Sattler,
Imperial College London,
United Kingdom

Reviewed by:

Nazareth Rocha,
Fluminense Federal University, Brazil
Yu Zhao,
Capital Medical University, China

*Correspondence:

Chengming Fan
fanchengming@csu.edu.cn
Zhihong Li
lizhihong@csu.edu.cn
Jinfu Yang
yjf19682005@sina.com

Specialty section:

This article was submitted to
Molecular Medicine,
a section of the journal
Frontiers in Cell and Developmental
Biology

Received: 22 February 2021

Accepted: 06 May 2021

Published: 09 June 2021

Citation:

Tang S, Fan C, Iroegbu CD,
Zhou W, Zhang Z, Wu M, Chen W,
Wu X, Peng J, Li Z and Yang J (2021)
TMSB4 Overexpression Enhances
the Potency of Marrow Mesenchymal
Stromal Cells for Myocardial Repair.
Front. Cell Dev. Biol. 9:670913.
doi: 10.3389/fcell.2021.670913

Objective: The actin-sequestering proteins, thymosin beta-4 (T β 4) and hypoxia-inducible factor (HIF)-1 α , are known to be associated with angiogenesis after myocardial infarction (MI). Herein, we aimed to identify the mechanism of HIF-1 α induction by T β 4 and investigate the effects of bone marrow mesenchymal stromal cells (BMMSCs) transfected with the T β 4 gene (*TMSB4*) in a rat model of MI.

Methods: Rat BMMSCs were isolated, cultured, and transfected with the *TMSB4* gene by using the lentivirus-mediated method. Rats with surgically induced MI were randomly divided into three groups ($n = 9$ /group); after 1 week, the rats were injected at the heart infarcted border zone with TMSB4-overexpressed BMMSCs (BMMSC-TMSB4^{OE}), wild-type BMMSCs that expressed normal levels of TMSB4 (BMMSC-TMSB4^{WT}), or medium (MI). The fourth group of animals ($n = 9$) underwent all surgical procedures necessary for MI induction except for the ligation step (Sham). Four weeks after the injection, heart function was measured using transthoracic echocardiography. Infarct size was calculated by TTC staining, and collagen volume was measured by Masson staining. Angiogenesis in the infarcted heart area was evaluated by CD31 immunofluorescence histochemistry. *In vitro* experiments were carried out to observe the effect of exogenous T β 4 on HIF-1 α and explore the various possible mechanism(s).

Results: *In vivo* experiments showed that vascular density 4 weeks after treatment was about twofold higher in BMMSC-TMSB4^{OE}-treated animals than in BMMSC-TMSB4^{WT}-treated animals ($p < 0.05$). The cardiac function and infarct size significantly improved in both cell-treatment groups compared to controls. Notably, the cardiac function and infarct size were most prominent in BMMSC-TMSB4^{OE}-treated animals (both $p < 0.05$). HIF-1 α and phosphorylated HIF-1 α (p-HIF-1 α) *in vitro* were significantly enhanced by exogenous T β 4, which was nonetheless blocked by the factor-inhibiting HIF (FIH) promoter (YC-1). The expression of prolyl hydroxylase domain proteins (PHD)

was decreased upon treatment with T β 4 and further decreased with the combined treatment of T β 4 and FG-4497 (a specific PHD inhibitor).

Conclusion: TMSB4-transfected BMMSCs might significantly improve recovery from myocardial ischemia and promote the generation of HIF-1 α and p-HIF-1 α via the AKT pathway, and inhibit the degradation of HIF-1 α via the PHD and FIH pathways.

Keywords: thymosin beta-4, hypoxia-inducible factor-1 α , mesenchymal stromal cell, angiogenesis, heart failure, AKT, YC-1

INTRODUCTION

The mortality rate of myocardial infarction (MI) is positively associated with the infarct size. As the functionality of cardiomyocytes proliferation is limited in an adult mammal heart, promotion of angiogenesis remains the most crucial strategy in salvaging myocytes at the infarcted border zone. Thus, discovering practical or appropriate clinical interventions, sparing less severely damaged myocytes at border zones, could effectively reduce infarct size and save lives (Fan et al., 2020a). Mesenchymal stromal cells (MSCs) represent a promising tool for cell therapy, particularly for heart-related diseases. The essential mechanisms include preserving myocardial contractility, modulating fibrosis, and promoting angiogenesis (White and Chong, 2020).

Cell-based therapies for MI using MSC-derived exosomes are well studied owing to their strong pro-angiogenic effect. Genetic modification is one of the most common methods used to enhance exosome therapy (Sun et al., 2020), and vascular endothelial growth factor (VEGF), fibroblast growth factor (FGF), hypoxia-inducible factor (HIF)-1 α , and thymosin beta-4 (T β 4) have been identified as the most promising candidates (Fan et al., 2020a,b; Sun et al., 2020; Ye et al., 2013). The transcription factor HIF-1 plays an important role in cellular response to systemic oxygen levels in mammals, and its activity is age dependent. Mouse studies suggest that aging impairs ischemia-induced vascular remodeling by inhibiting the induction of HIF-1 and its downstream target genes, thereby blocking both the production of angiogenic signals and the ability of bone marrow-derived angiogenic cells (BMDACs) to respond to them (Rey et al., 2009). Combined HIF-1 α -based gene and cell therapy reduced tissue necrosis even when BMDAC donors and ischemic recipient mice were 17 months old, suggesting that this approach may have therapeutic utility in elderly patients with critical limb ischemia. T β 4 is known to be involved in angiogenesis as a pro-angiogenic and fibroblast-activating peptide (Qian et al., 2012). Significantly, T β 4 was identified as

essential for all aspects of coronary vessel development in mice (Smart et al., 2007a).

It is believed that T β 4 induces angiogenesis by increasing the expression of growth factors such as HIF-1 α and stabilizing HIF-1 α protein levels in an oxygen-independent manner (Jo et al., 2010; Ock et al., 2012). However, the mechanism of HIF-1 α expression and T β 4-induced degradation largely remains unknown. Herein, we aimed to identify the mechanism of HIF-1 α induction by T β 4 and investigate the effects of bone marrow mesenchymal stromal cells (BMMSCs) transfected with the T β 4 gene (*TMSB4*) in a rat model of MI.

MATERIALS AND METHODS

Isolation and Cultivation of MSCs From Bone Marrow of Sprague–Dawley Rats

Sprague–Dawley rats were purchased from the Department of Experimental Animal Center, Second Xiangya Hospital, Central South University, Changsha, China. All animals received humane care in compliance with the “Guide for the Care and Use of Laboratory Animals” prepared by the Institute of Laboratory Animal Resources, National Research Council, and published by the “Guide to the Care and Use of Experimental Animals” by the Chinese Council on Animal Care. BMMSCs were isolated in a lymphocyte separation medium and by density gradient centrifugation as previously described (Yang et al., 2009; Tang et al., 2013).

Four-week-old Sprague–Dawley female rats (weight, ~100 g) were selected. The cells were isolated from the bone marrow of upper and lower limb bones and separated by gradient centrifugation with 1.073 g/ml Percoll solution (Promega, United States). The cells were cultured in Dulbecco’s Modified Eagle’s medium (DMEM, Gibco, United States) containing 15% fetal bovine serum, 1 ng/ml basic fibroblast growth factor, and 200 mmol/L glutamine at 37°C in a humidified atmosphere containing 5% carbon dioxide (Forma, United States).

Renew half of the culture medium for the first 8 h and then replace whole medium with fresh DMEM every 3 days. Purified BMMSCs were observed after four times of medium exchange. For morphological observations, the cells were inoculated in a 60-mm culture dish at a density of $1 \times 10^7/\text{cm}^2$. The first, third, fifth, and seventh passage of cells were selected and counted. The cell numbers from days 1 to 14 and each passage’s growth curves were generated and analyzed. Cells from passages 3 to 8 were used for the study.

Abbreviations: T β 4, thymosin beta-4; HIF, hypoxia-inducible factor; p-HIF-1 α , phosphorylated HIF-1 α ; FIH, factor-inhibiting HIF; CHX, cycloheximide; WM, wortmannin; PHD, prolyl hydroxylase domain proteins; YC1, 3-(5'-hydroxymethyl-2'-furyl)-1-benzyl indazole; BMMSC, bone marrow mesenchymal stromal cell; BMMSC-TMSB4^{OE}, TMSB4-overexpressed BMMSCs; BMMSC-TMSB4^{WT}, wild-type BMMSCs which express normal levels of TMSB4; MI, myocardial infarction; TTC, 2,3,5-triphenyltetrazolium chloride; LAD, left anterior descending branch of coronary artery; β -actin, beta-actin; EF, ejection fraction (left ventricular); FS, fractional shortening.

TMSB4 Transfection Into MSCs

Lentivirus plasmids and TMSB4-pLent-GFP-Puro-CMV were purchased from ViGene Biosciences (Shandong, China). Extraction and identification of plasmids were performed according to the manufacturer's recommendations. In brief, TMSB4 (NM_031136: ATGTCTGACAAACCCGATATGGCTGAGATCGAGAAATTCGATAAGTTCGAAGTTGAAGAAGACAGAAACACAAGAGAAATCCTCTGCCTTCAAAAAGAAACAATTGAACAAGAGAGCAAGCTGGCGAATCGTAA) was amplified by polymerase chain reaction (PCR) and then recombined into the target vector—pLent-GFP-Puro-CMV (AsiI-MluI enzyme digestion vector)—to obtain the full-length construction of *TMSB4* gene. First, 24 h before transfection, the fifth generation of MSCs (~70–80% confluent) was digested by 0.05% Trypsin and 0.02% EDTA. Second, the MSCs were then vaccinated onto 12-pore plates using an opioid sterilized round cover glass (~1 × 10⁵ MSCs/pore, each pore containing 1 ml L-DMEM culture solution with 15% fetal bovine serum). Finally, the MSCs were cultured in the traditional incubator with 5% carbon dioxide at 37°C in a saturated humidified atmosphere.

The MSCs were transfected with lentiviral supernatants of 0, 1, 2.5, and 5 μl. The culture medium was completely replaced after 24 h. The expression of fluorescent protein in the transfected cells was observed under a fluorescence microscope after 72 h.

The transfection efficiency of BMMSCs was observed under a confocal microscope after 7 days of co-culture. Puromycin (5 μg/ml) was used for the selection and maintenance of cell lines.

The TMSB4-overexpressing BMMSCs (BMMSC-TMSB4^{OE}) were used for flow cytometric (FACSort, B-D Co., United States) analysis to detect the cellular markers including CD90, CD29, CD45, CD34, CD11B, CD105, CD73, HLA-DR, and CD19. MSCs were gathered and diluted using PBS at a concentration of 10⁶ cells/ml. After incubating with fluorescence-labeled antibodies for 15 min at room temperature, cells were then washed twice with PBS and dispersed to make a single-cell suspension. The tripotent differentiation, including osteogenesis, chondrogenesis, and adipogenesis, were induced according to previously described methods (Yang et al., 2007, 2009; Tang et al., 2013).

Detection of TMSB4 Expression in the Target Cells

GFP, a marker gene, would be expressed automatically along with the target gene. Thus, the expression of fluorescent-labeled *GFP* was considered representative for the expression of *TMSB4*. The transfected cells were observed and detected at different time points. The expression of *GFP* was observed using an inverted microscope with an excitation wavelength of 490 nm. Western blot assay was used to explore the expression of *Tβ4*, *HIF-1α*, *p-HIF-1α*, *p-AKT*, and *VEGF* in transfected MSCs.

Experimental Animals

Surgical induction of MI was performed on female Sprague-Dawley rats. In brief, rats were intubated and breathing *via* a ventilator with 2% isoflurane USP (FlurisoTM, VetOne) to

maintain anesthesiaTM. After a thoracotomy was performed *via* the left fourth intercostal space, the anterior descending branch of the left coronary artery (LAD) was surgically ligated using a 6–0 suture. Thirty animals were used to establish the MI model. However, 3/30 rats died due to peri-/post-operative complications.

The surviving animals were randomly divided into three groups ($n = 9/\text{group}$). After the first week of MI, the rats were injected with the fifth passage of TMSB4-overexpressing BMMSCs (BMMSC-TMSB4^{OE}), the same passage of wild-type BMMSCs that expressed normal levels of TMSB4 (BMMSC-TMSB4^{WT}), or the same volume (150 μl) of medium (MI) at three different sites (1 × 10⁶ cells/50 μl/site) in the border zone of the anterior wall of the left ventricle (LV) (3 × 10⁶ cells/150 μl/animal). The fourth group of animals ($n = 9$) underwent all surgical procedures necessary for MI induction except for the ligation step (Sham).

Western Blot Assay

Protein concentration was detected by the BCA protein assay kit (Solarbio life sciences, Beijing, China) according to the manufacturer's protocols. A 2 × sample buffer was added to an equivalent sample according to the protein concentration denatured at 100°C for 5 min. SDS-PAGE electrophoresis (25 μg/pore) was then performed at a constant voltage of 120 V. After that, the protein was transferred to polyvinylidene difluoride (PVDF) membranes (Trans-Blot[®] TurboTM Mini PVDF Transfer Packs, Bio-Rad) at 120 V for about 2 h. Subsequently, the membrane was blocked by a blocking buffer [5% dried skim milk, 25-mm Tris-buffer saline (TBS)] for 2 h, followed by incubation with primary antibodies at 4°C overnight.

Next, the membrane was washed thrice with TBST (for approximately 10–15 min each time), incubated with horseradish peroxidase [(HRP)-conjugated secondary antibody (diluted 1:1,000)] at room temperature for 1 h, and washed again. Finally, an ECL reagent was added, and the membrane was exposed. Western blot signals were measured by densitometry and analyzed using software (AlphaView SA software 3.4, ProteinSimple). The housekeeping protein β-actin was used for Western blot normalization.

Immunostaining and Fluorescence Microscopy

Following the different treatment methods used, the rat hearts were harvested on the 28th day and processed according to previously described methods (Fan et al., 2020a). Briefly, hearts were fixed with 4% paraformaldehyde at 4°C for 4 h, followed by immersion in 30% sucrose at 4°C overnight. Then, 10-μm-thick serial cryosections were obtained, and every 30th section was selected and permeabilized with 0.2% Triton X-100 for 10 min at room temperature. The sections were blocked in 5% donkey serum in DPBS at a pH of 7.4 for 30 min at room temperature before different antibodies were used.

Primary antibodies were diluted 1:100–1:1,000 with the blocking buffer (1.5% BSA, 100 mM glycine in PBS) and incubated at 4°C overnight. Secondary antibodies (Jackson

ImmunoResearch Laboratory) were diluted 1:200 with the blocking buffer and incubated in the dark for 2 h at room temperature. Nuclei were stained or co-stained with 4,6-diamidino-2-phenyl-indole (DAPI, 100 ng/ml, Sigma-Aldrich). Negative controls were stained with only secondary antibodies. The stained sections were analyzed using a fluorescence microscope.

Echocardiography

Heart function from pre- and post-MI rats (1 and 4 weeks after intervention) were detected by transthoracic echocardiography as previously described (Tang et al., 2013; Fan et al., 2020a). In short, rats were maintained under 1.5–2% isoflurane USP (Fluriso, VetOne) anesthesia until the heart rate was stabilized at 500–700 beats per minute. The two-dimensional M-mode and B-mode images were acquired from both parasternal short- and long-axis views with a high-resolution ultrasound system (Vevo 2100, VisualSonics, Inc.). Finally, the heart beats were recorded and the functional parameters including left ventricular ejection fraction (EF) and fractional shortening (FS) were calculated from several short-axis views using a modified Simpson's rule and the Vevo analysis software. The operator was blinded to the experimental groups.

TTC Staining and Determination of Infarct Size

Following the different treatment methods used, on the 28th day, the hearts were excised under deep anesthesia and the infarct sizes were evaluated. Briefly, the freshly harvested heart tissue was cut into five slices using a rodent heart section mold. To maximize saving the heart tissue, each slice was cut down to a thinner slice (1 mm per slice) and used for TTC staining. The remnants were used for IHC and IF (**Supplementary Figure 1**). Tissues were then placed in 1% TTC solution (Solarbio, Cat: G3005) and incubated at room temperature in the dark for 15 min. The stained tissues were then photographed under a light microscope (Olympus).

Digital images of the stained sections were captured to assess the changes of infarct size at post-treatment day 28. Morphometric analyses were carried out using NIH Image J software. The infarcted size was calculated according to the formula: infarct size (%) = [sum of (scar circumferential length × thickness of each of the short axis)/sum of (short axis left ventricle length × thickness of the short axis)] × 100%.

Masson and DAB Staining

The explanted hearts were collected on day 28 post-treatment. The tissue was fixed with 4% paraformaldehyde at 4°C for 4 h and then immersed in 30% sucrose at 4°C overnight. Ten-micrometer-thick serial cryosections were obtained, and every 30th section was selected and permeabilized with 0.2% Triton X-100 for 10 min at room temperature. Masson Trichrome Kit and Tunel Cell Apoptosis Detection Kit were purchased from Thermo Fisher Scientific (Cat: 87019) and Servicebio (G1507-20T), respectively. The staining was performed according to the manufacturer's recommendations. The volume fraction of

interstitial collagen was calculated as the ratio of the fibrotic area to the total surface area of the left ventricle. Intramural vessels, perivascular collagen, endocardium, and trabeculae were excluded from this particular analysis. The apoptotic cells were quantified as the number of TUNEL-positive cells divided by the total number of cells and expressed as a percentage (six views per slice and five slices per heart were analyzed).

Antibodies and Reagents

| Primary antibodies | Cat. No. | Source | Dilutions |
|--------------------------------|------------|-------------|----------------------------------|
| Thymosin β4 | ab14334 | Abcam | 1:1,000 |
| HIF | 20960-1-AP | Proteintech | 1:200 |
| P-HIF | 3434S | CST | 1:1,000 |
| VEGF | ab1316 | Abcam | 1:1,000 |
| p-AKT | 9275s | CST | 1:1,000 |
| PHD | ab108980 | Abcam | 1:1,000 |
| FIH | 4426s | CST | 1:1,000 |
| Sarcomeric Alpha Actinin (αSA) | ab9465 | Abcam | 1:100 |
| CD31 | ab182981 | Abcam | 1:100 |
| CD34-Alexa Fluor® 647 | a187283 | Abcam | 10 μl for 10 ⁶ cells |
| Isotype Control | ab176103 | Abcam | 20 μl for 10 ⁶ cells |
| CD11B-PE | 201807 | Biologend | 0.2 μg for 10 ⁶ cells |
| Isotype Control | 400211 | Biologend | 0.2 μg for 10 ⁶ cells |
| CD29-PE | 102207 | Biologend | 0.2 μg for 10 ⁶ cells |
| Isotype Control | 400907 | Biologend | 0.2 μg for 10 ⁶ cells |
| CD45-FITC | 202205 | Biologend | 0.2 μg for 10 ⁶ cells |
| Isotype Control | 400107 | Biologend | 0.2 μg for 10 ⁶ cells |
| CD90-PE | 205903 | Biologend | 0.2 μg for 10 ⁶ cells |
| Isotype Control | 400311 | Biologend | 0.2 μg for 10 ⁶ cells |
| β-actin | 60008-1-Ig | Proteintech | 1:5,000 |

| Reagents | Cat. No. | Source |
|---|---|--------|
| Osteogenesis differentiation medium | RASMX-90021 | Cyagen |
| Chondrogenesis differentiation medium | RASMX-90041 | Cyagen |
| Adipogenesis differentiation medium | RASMX-90031 | Cyagen |
| Cycloheximide (CHX) | 2112S | CST |
| Wortmannin | 9951 | CST |
| YC-1 | ab120915 | Abcam |
| Thymosin β4 | Kindly provided by RegeneRx Biopharmaceuticals Inc. Rockville, MD, United States. | |
| FG-4497 | Synthesized at Fibro Gen, Inc. (San Francisco, CA United States) | |
| Forward oligonucleotide sequences of TMSB4 primers (Tmsb4x-F) | TGCCCGCGGATGCGATGTCTGACAAACCCG | |
| Reverse oligonucleotide sequences of TMSB4 primers (Tmsb4x-R) | CGGCCGCGTACGCGTTTACGATTGCCCAGC | |

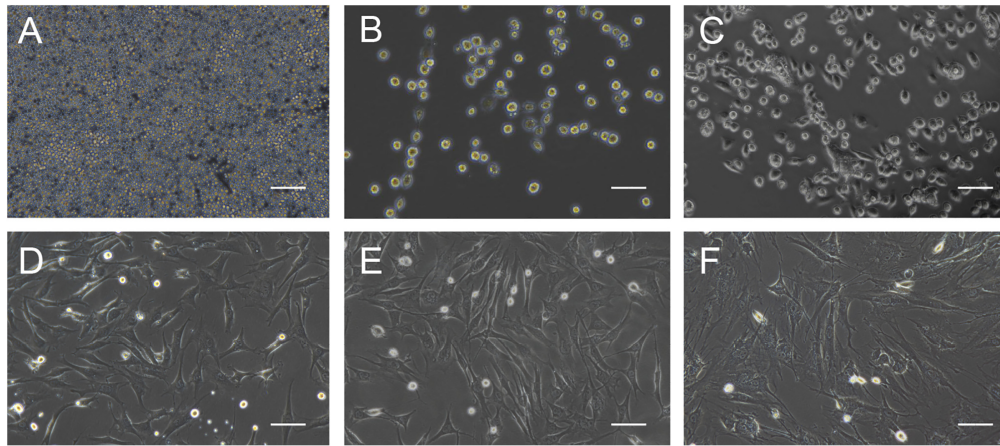


FIGURE 1 | Cell morphology during BMMSCs culture. **(A)** Round mononuclear cells were observed after seeding of 4 h. **(B)** The adherent cells in the shape of short rods were seen 24 h after the first half-volume medium exchange. **(C)** The cells that showed spindle shape and clonal growth were detected after primary culture for 3 days. **(D)** The typical fusiform cells cloned in a fish-like manner were observed on the 7th day of primary culture. **(E)** The third generation of the cultured cells. **(F)** Most of the cells become wide and flat, and granular substances were detected in the cytoplasm after passing through seven times. Scale bar = 200 μm .

Statistical Analysis

Data are expressed as mean \pm SE and median. All statistical calculations were performed using the SPSS software (version 14.0; IBM Corporation, Armonk, NY, United States). An independent-sample *t*-test was used to determine differences between the two groups. One-way ANOVA with Dunn's multiple comparisons test was used to compare the variables between multiple groups. For all analyses, $p < 0.05$ was considered to indicate statistically significant differences.

RESULTS

Characterization of Rat BMMSCs

The morphology of the cultured BMMSCs was measured by optical microscopy from the beginning of seeding to the seventh passage (**Figures 1A–F**). The BMMSCs from the SD rats were firmly attached (**Figure 1A**), and the typical spindle shape was observed 24 h after seeding (**Figure 1B**). Radial colony tendency (**Figure 1C**) was shown with continued culture. Fish-like distribution (**Figure 1D**) was observed when the cells expanded between 70 and 80%. Cells grew vigorously and rapidly at the third passage (**Figure 1E**) and could be passaged and stabilized over seven passages. After that, the morphology of BMMSCs changed to a flat and enlarged shape (**Figure 1F**).

The growth curve (**Supplementary Figure 2**) showed that BMMSCs strictly followed the S growth model, while cells in passages 3–5 expanded faster than the rest. BMMSCs in the third passage were negative for CD34 (**Supplementary Figure 3A**), CD11B (**Supplementary Figure 3B**), and CD45 (**Supplementary Figure 3C**), but positive for CD90 (**Supplementary Figure 3D**) and CD29 (**Supplementary Figure 3E**), which was detected by flow cytometry. Furthermore, the cells were positive for CD105 and CD73, and negative for HLA-DR and CD19 (**Supplementary Figures 3F–I**).

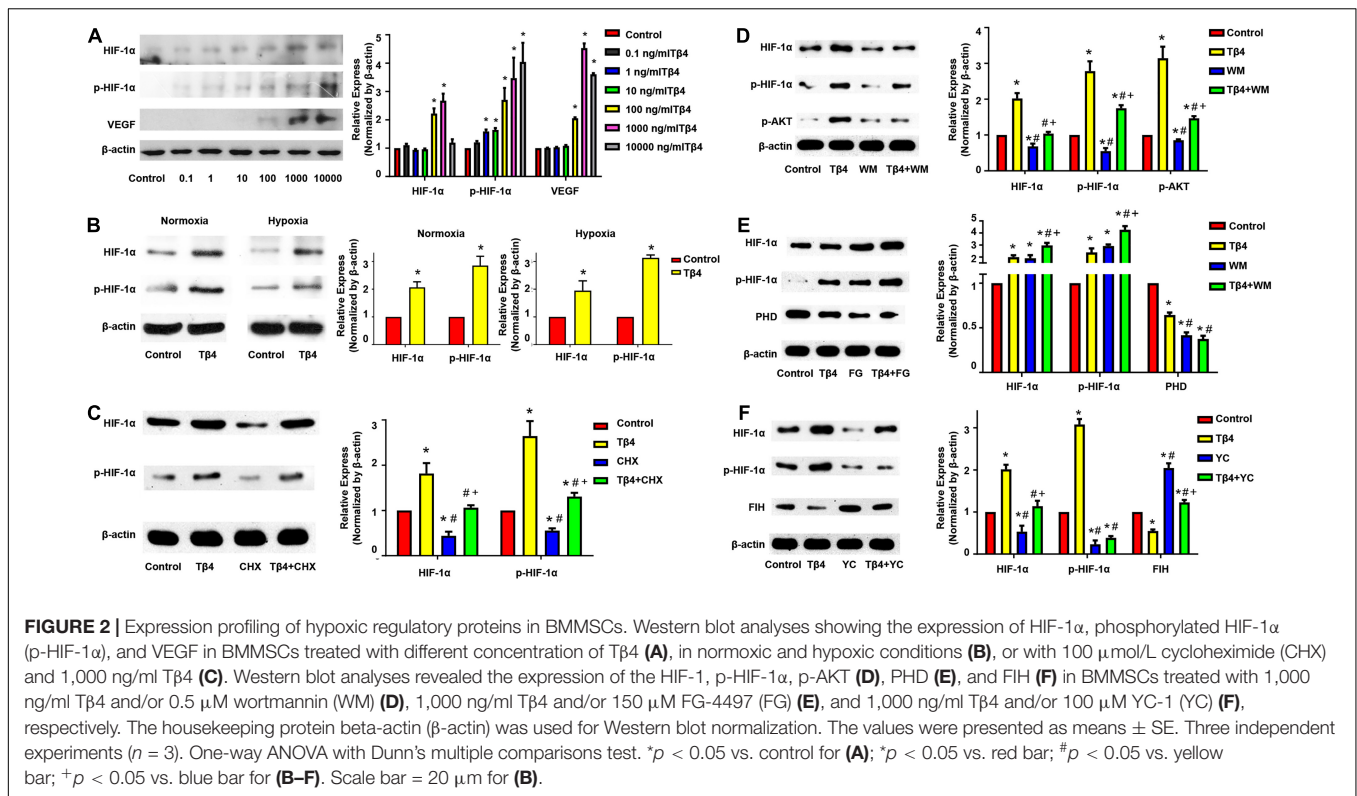
T β 4 Promoted Phosphorylation of HIF-1 α and Inhibited Degradation

The BMMSCs were treated with various concentrations of T β 4 (0.1, 1, 10, 100, 1,000, or 10,000 ng/ml) under normoxia (21% O₂) for 24 h and then the total cellular protein was isolated and subjected to Western blot analyses. The semi-quantitative Western blot analyses showed that the expression levels of both HIF-1 α , phosphorylated HIF-1 α (p-HIF-1 α), and VEGF were significantly upregulated when the dose increased (**Figure 2A**).

The BMMSCs were treated with 1,000 ng/ml T β 4 under normoxia or hypoxia (1% O₂, 5% CO₂) for 24 h. Western blot analyses revealed that the expression levels of HIF-1 α and p-HIF-1 α were significantly upregulated in both normoxic and hypoxic conditions (**Figure 2B**). The results suggest that T β 4 promoted HIF-1 α and p-HIF-1 α protein expressions in an oxygen-independent manner.

To confirm the effect of T β 4 on HIF-1 α protein synthesis, we performed Western blotting after treatment of the BMMSCs with cyclohexamide (CHX), an inhibitor of protein synthesis. The expression of both HIF-1 α and p-HIF-1 α was decreased after treatment with CHX for 24 h. However, when treated with T β 4 after 2 h of CHX pretreatment, the level of HIF-1 α and p-HIF-1 α was not decreased but rather slightly increased (**Figure 2C**). A previous report showed that BMMSCs protect the myocardium from I/R injury through the PI3K pathway (Angoulvant et al., 2011).

As shown in **Figure 2D**, AKT phosphorylation was increased when incubated with T β 4, while the increases of HIF-1 α and p-HIF-1 α were partly blocked by wortmannin (WM, an inhibitor of PI3K) (**Figure 2D**). HIF-1 α was normoxic degraded by prolyl hydroxylase domain proteins (PHD), and factor-inhibiting HIF (FIH) mediated proteasome system (Brahimi-Horn and Pouyssegur, 2009). We treated the BMMSCs with FG-4497 (a specific PHD inhibitor) and YC1 [3-(5'-hydroxymethyl-2'-furyl)-1-benzyl indazole], an activator of HIF-1 α degradation *via* the



stimulation of FIH as shown in **Figures 2E,F**. The expression of PHD was decreased upon T β 4 treatment and further decreased with the combined treatment of T β 4 and FG-4497. HIF-1 α and p-HIF-1 α were significantly increased in the treatment of T β 4, FG-4497, and T β 4 + FG compared to the control. It was notably prominent in the treatment of the T β 4 + FG group (**Figure 2E**). Similarly, the expression of FIH was decreased with the treatment of T β 4. In addition, the enhancement of HIF-1 α and p-HIF-1 α was significantly reduced only in the YC1-treated group and not the T β 4 + YC1 group (**Figure 2F**). These results indicate that the increase in HIF-1 α and p-HIF-1 α was because of increased protein synthesis, reduction of degradation, and partly through the PI3K-AKT pathway.

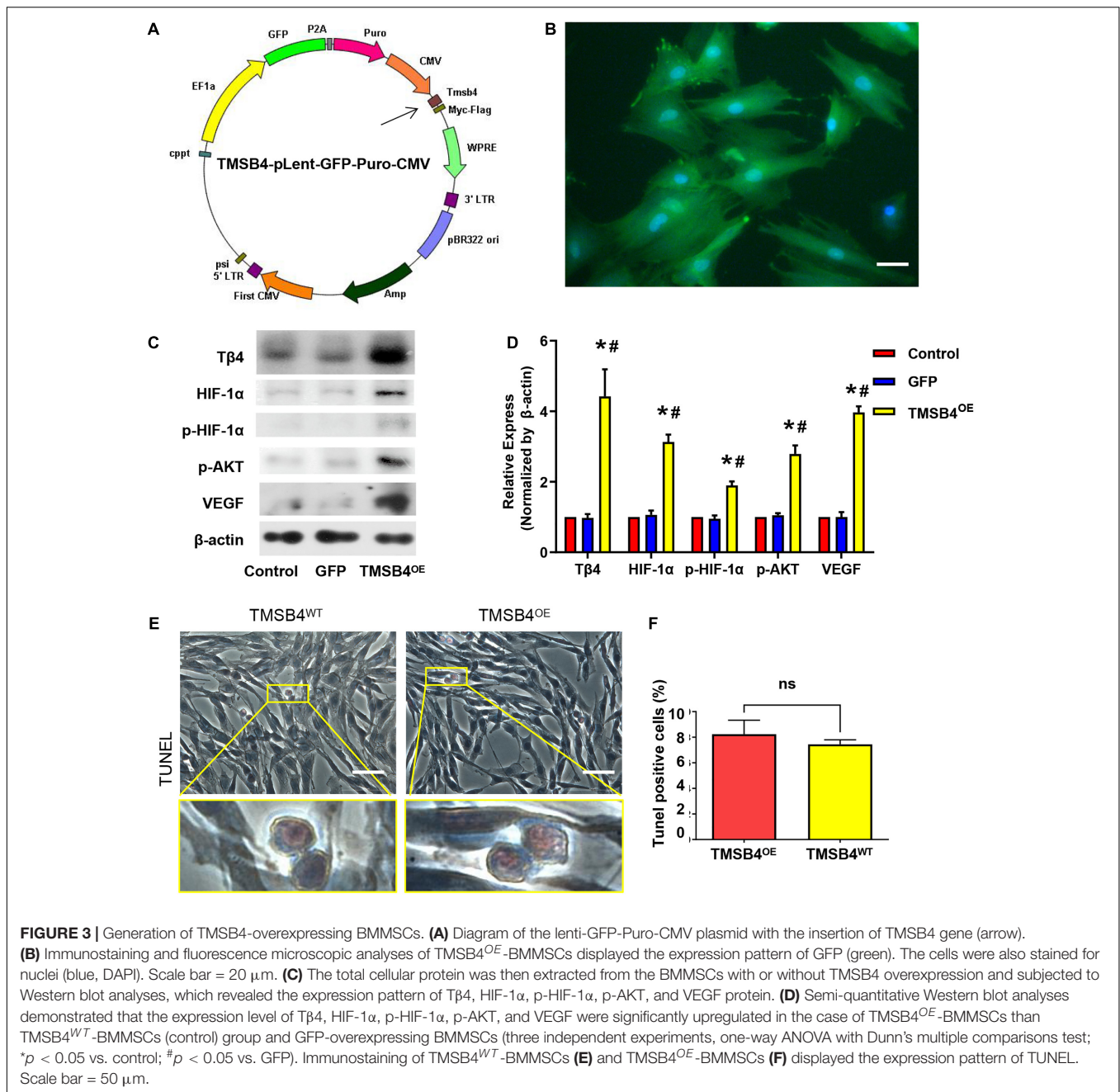
TMSB4^{OE}-BMSCs Enhance Cardiac Function of the MI Rat

TMSB4-overexpressing (TMSB4^{OE}) BMSCs were successfully established (**Figures 3A-D**). The expression of T β 4, HIF-1 α , p-HIF-1 α , p-AKT, and VEGF were significantly upregulated in TMSB4^{OE} cells (**Figures 3C,D**). To explore if the high-level intracellular HIF-1 α would lead to cytotoxicity, TUNEL staining of TMSB4^{OE}-BMSCs and TMSB4^{WT}-BMSCs was carried out, which showed no significant intergroup differences (**Figures 3E,F**). The biological identification of BMSC-TMSB4^{OE} based on surface markers was carried out along with tripotent differentiation; no significant intergroup differences were detected (**Supplementary Figures 3, 4**). The left ventricle functional parameters were evaluated in rats intramyocardially injected with TMSB4^{OE}-BMSCs or TMSB4^{WT}-BMSCs after

surgically induced MI to determine the effect of TMSB4-overexpressed BMSCs on heart function. MI was induced by permanently ligating the anterior descending coronary artery. After 1 week, cells (3×10^6 cells/animal) were intramyocardially injected into three sites (1×10^6 cells/site) in the border zone of the anterior wall of the LV. The third group of animals (the MI group) was treated with equivalent injections of cell-free PBS after MI injury, while the animals in the Sham group underwent all surgical procedures for MI induction except for the ligation step. Echocardiographic measurements (**Figures 4A-D**) of LVEF (**Figure 4E**) and FS (**Figure 4F**) 4 weeks after treatments showed that LV function was significantly greater in both cell-treatment groups than in the MI group. It was also more prominent in the TMSB4^{OE}-BMSC-treated than TMSB4^{WT}-BMSCs-treated animals. The other parameters detected in echocardiography included the heart rate, end-diastolic diameter, and anterior and posterior wall thickness (**Supplementary Figure 5**).

TMSB4^{OE}-BMSCs Smaller Infarct Size, Apoptosis, and Hypertrophy After MI Than TMSB4^{WT}-BMSCs

The infarct size from each group was assessed by TTC staining (**Figures 5A-D**) and showed that the TMSB4^{OE}-BMSCs-treated animals exhibited more significant reductions in infarct size (**Figure 5E**) and had greater LV wall thickness (**Figure 5F**) than TMSB4^{WT}-BMSCs-treated and untreated controls subjected to MI. This cardiac recovery effect was



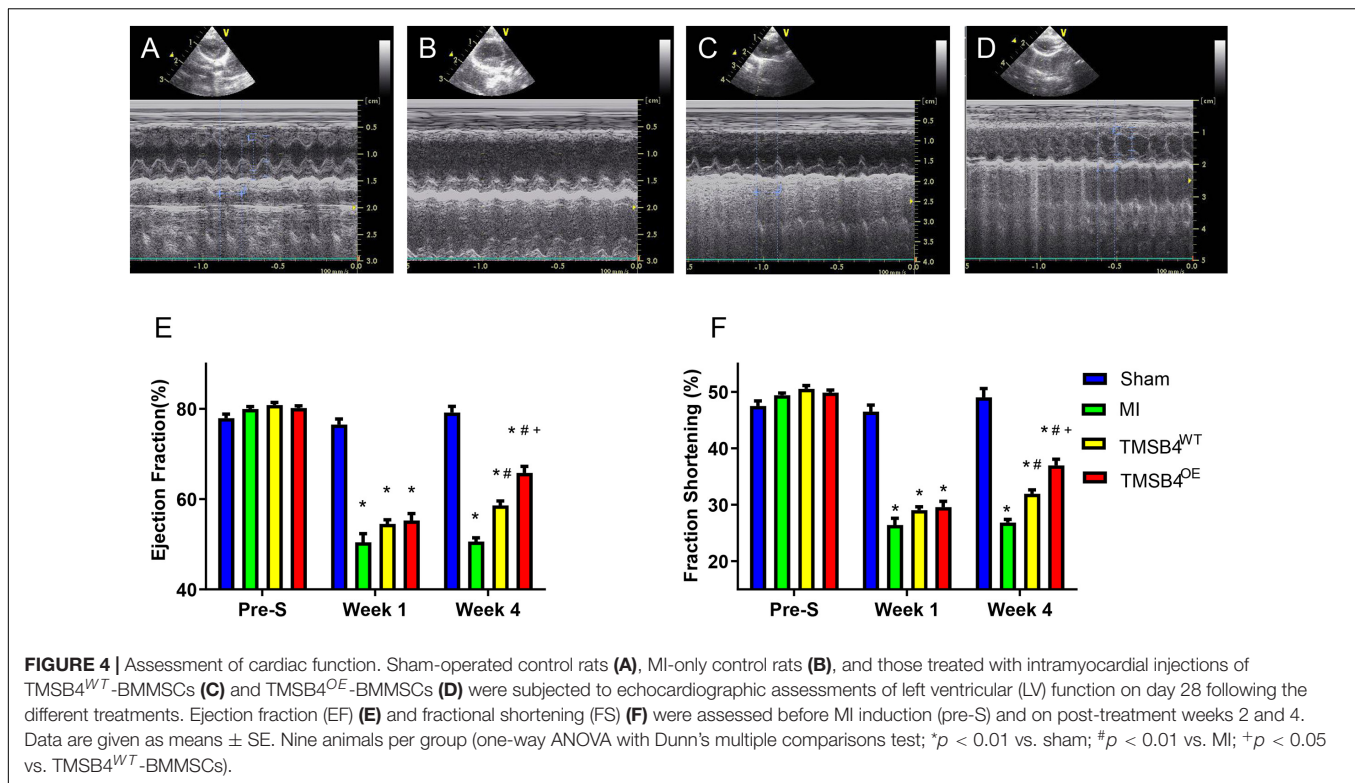
corroborated by a significant reduction in collagen volume fraction with Masson staining (Figures 6A–E).

TMSB4^{OE}-BMSCs were detected in the heart's border zone 4 weeks after transplantation (Figure 7). Next, the neo-angiogenic response assessment in MI rats was evaluated by immunostaining, using endothelial phenotypic markers, i.e., CD31 (Figure 8A) and VEGF expression (Figure 8B). The TMSB4^{OE}-BMSCs-treated animals showed significantly elevated vessel density and VEGF expression compared to the TMSB4^{WT}-BMSCs-treated and untreated MI groups (Figures 8A,B). Finally, the cardiomyocyte apoptosis assessment in MI rats was evaluated by TUNEL immunostaining. The

number of TUNEL-positive cardiomyocytes was significantly smaller in both cell-treatment groups than in MI rats, which was most prominent in BMSC-TMSB4^{OE}-treated animals (Figure 8C).

DISCUSSION

In the present study, we found for the first time that BMSCs transfected with pro-angiogenic gene (*TMSB4*) significantly improved the cardiac function and infarct size in rat post-MI heart (Figures 4, 5). Improvement in the heart function



was accompanied by a significant enhancement of angiogenesis. Intracoronary infusion of autologous bone marrow cells (BMCs) has been proposed as a therapeutic strategy to enhance tissue perfusion, reduce scar formation, and improve heart function after MI (Wollert and Drexler, 2010). The identification of paracrine-acting proteins, including well-known cytokines, chemokines, and growth factors, acts as a central mechanism where cell-based therapies improve tissue perfusion and contractile functions (Jay and Lee, 2013). Angiogenesis or neovascularization, the first step of tissue repair, plays a critical role in promoting myocardial regeneration in patients with cardiac disease (Mathison and Rosengart, 2018). Inducing angiogenesis is a novel approach for the functional recovery of ischemic tissues (Bonauer et al., 2009; Korf-Klingebiel et al., 2015). Tβ4 is a potent stimulator of coronary vasculogenesis and angiogenesis. Thus, pre-treating hearts using Tβ4 might further improve cardiac function and scar area (Smart et al., 2007a; Qian et al., 2012). In the process of ischemic heart disease treatment, the strategy of using donor cells with target genes to structurally rebuild the ventricular wall likely has favorable prospects in forthcoming biotherapies (Tang et al., 2013).

We have previously shown that transplantation of VEGF or SHH gene-transfected MSCs can better improve myocardial perfusion and restore heart function than either cellular or gene therapy alone (Yang et al., 2007, 2009). Therapeutic neovascularization can be achieved in the adult organism through either protein application, gene overexpression, or cell therapy. Preclinical and clinical data suggest that therapeutic neovascularization is achievable but requires

novel factors that induce both capillary growth and vessel maturation to induce functional neovascularization. Thymosin β4 (Tβ4) improves wound healing *via* a variety of different mechanisms, namely, enhanced angiogenesis, improved keratinocyte migration, collagen deposition, as well as wound contracture. In addition, Tβ4 has anti-inflammatory properties. Thymosin β4 is essential not only for vascular development but also for cardiomyocyte differentiation and maturation. The combination of Tβ4 and adeno-associated viruses (AAV) was tested in translational large animals of chronic myocardial ischemia with or without cardiovascular risk factors. Thymosin β4 could induce therapeutic neovascularization in wild-type pigs as well as in pigs suffering from diabetes mellitus (Hinkel et al., 2018). To study whether prolonged release is necessary for observed cardioprotection, we tried intramyocardial injection of Tβ4 peptide (400 μg in 150 μl PBS) immediately after the LAD ligation procedure. All animals were assessed 4 weeks after treatment. Interestingly, we did not observe a similar cardioprotection following the direct intramyocardial injection of Tβ4 (data not shown). It is reasonable to believe that the cardioprotective effect could hardly be achieved by a single shot of the peptide, which would likely be squeezed and rapidly washed away. This finding was in accordance with the report by Bock-Marquette et al., which suggested that a prolonged release of these chemicals is important for the chemicals to exert their cardioprotective effects. In the present study, we found that TMSB4^{OE}-BMMSCs enhance angiogenesis and reduce the cardiac infarct size, which results in a significant induction of cardiac recovery in the post-MI rat. Notably,

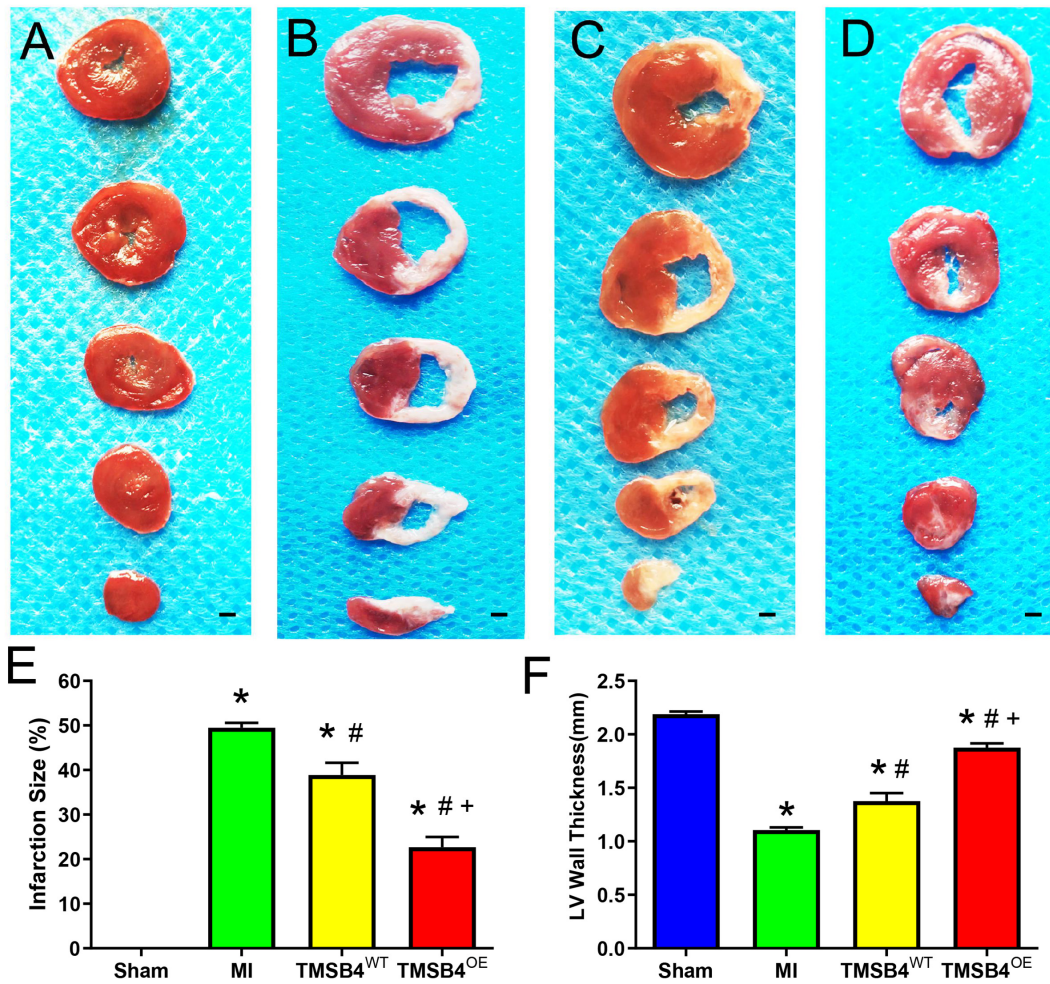


FIGURE 5 | Assessment of infarct size and left ventricular morphology. TTC staining showed the areas of infarcted (white, non-viable) and non-infarcted (red, viable) zones in post-treatment day 28 ventricular tissue sections in Sham-operated control rats (A), MI-only control rats (B), and those treated with TMSB4^{WT}-BMSCs (C) and TMSB4^{OE}-BMSCs (D). The infarct size was quantified as the ratio of the scar area to the total surface area of the left ventricle and expressed as a percentage (E) and quantified as left anterior wall thickness (F). Data are presented as means \pm SE. Nine animals per group (one-way ANOVA with Dunn's multiple comparisons test; * p < 0.01 vs. sham; # p < 0.05 vs. MI; + p < 0.05 vs. TMSB4^{WT}-BMSCs. Scale bar = 1 mm for panels (A–D).

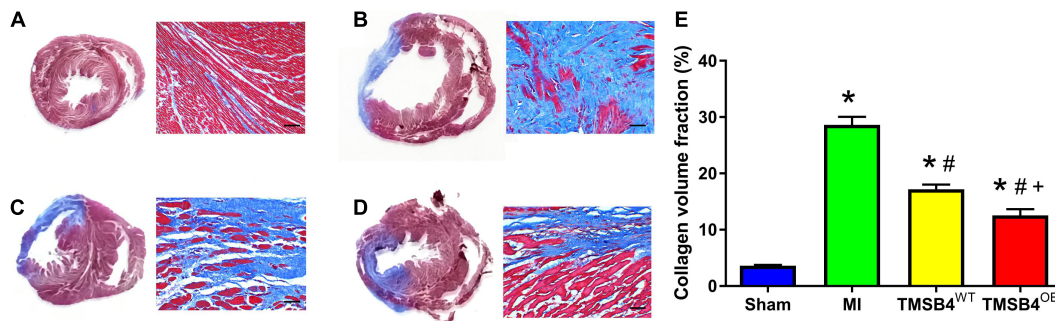


FIGURE 6 | Assessment of collagen volume. Masson staining showed the areas of fibrotic (blue, non-viable) and non-fibrotic (red, viable) zones in post-treatment day 28 ventricular tissue sections in Sham (A), MI (B), TMSB4^{WT}-BMSCs (C), and TMSB4^{OE}-BMSCs (D) treated groups. The collagen volume was quantified as the area occupied by connective tissue divided by the sum of the areas and expressed as a percentage (E). Data are presented as means \pm SE. Nine animals per group. One-way ANOVA with Dunn's multiple comparisons test. * p < 0.01 vs. sham; # p < 0.05 vs. MI; + p < 0.05 vs. TMSB4^{WT}-BMSCs. Scale bar = 100 μ m.

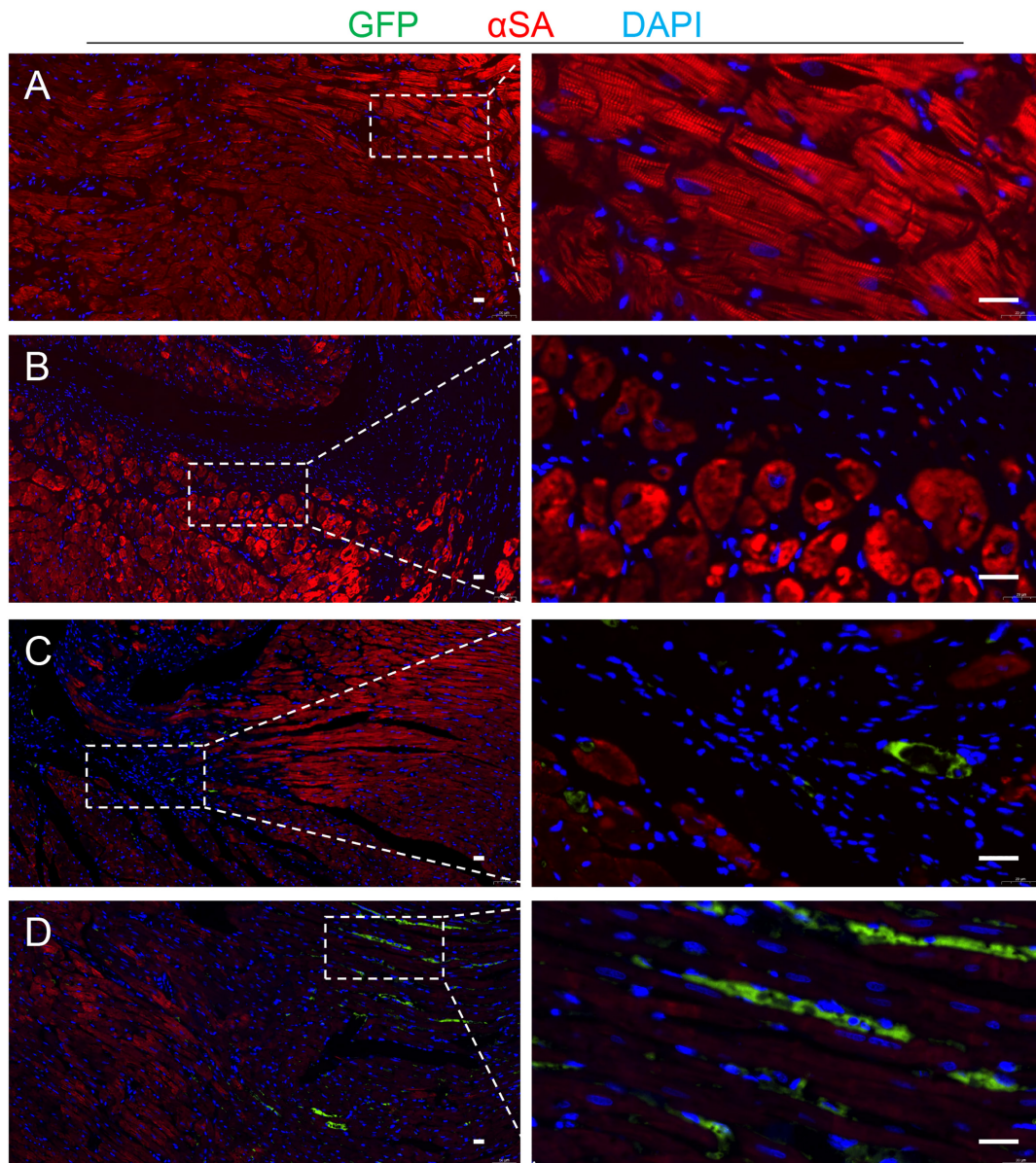
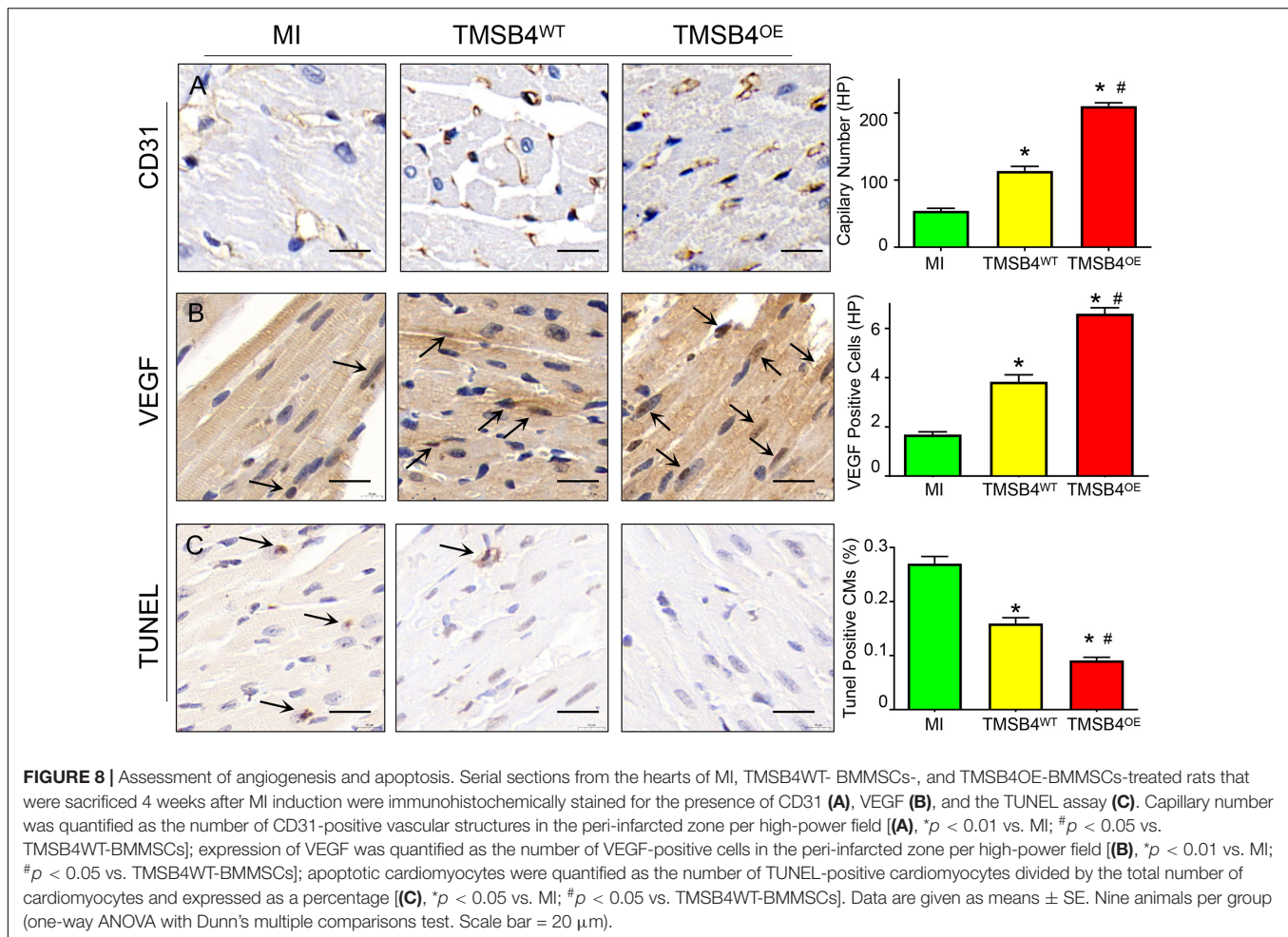


FIGURE 7 | Detection of the transplanted cells. Serial sections from the hearts of TMSB4^{OE}-BMMSCs-treated rats that were sacrificed 4 weeks after MI induction were stained for the presence of GFP and α -sarcomeric actin (α SA), and the nuclei were counterstained with DAPI in Sham **(A)**, TMSB4^{WT}-BMMSCs **(B)** and TMSB4^{OE}-BMMSCs **(C,D)** treated groups. Then, the transplanted cells were defined as the cells that expressed GFP and DAPI. GFP was undetected in the TMSB4^{WT}-BMMSCs-treated hearts. Five randomly selected viewing fields were evaluated per section, and 20 sections were evaluated per animal. Scale bar = 20 μ m.

lower collagen deposits were partly because of angiogenesis and possibly reduced inflammation and oxidative stress. The defects in the molecular pathways responsible for suppression and resolution of the post-infarction inflammatory reaction may be involved in the pathogenesis of adverse remodeling and heart failure following MI. *In vitro* studies have suggested that TGF- β 1-induced myofibroblast conversion may be mediated through both canonical Smad-dependent and Smad-independent signaling pathways. Moreover, neutralization experiments using gene therapy with the extracellular domain of the type II TGF- β

receptor in a model of MI suggested that early inhibition may worsen dysfunction, accentuating the inflammatory response, while late disruption of TGF- β signaling may protect from interstitial fibrosis and hypertrophic remodeling (Prabhu and Frangogiannis, 2016). Over the past 15 years, several studies have contributed toward our understanding of the mechanism of T β 4 function; it is now recognized that T β 4 is involved in a wide range of cellular processes aside from regulating cytoskeletal assembly. The most notable of genes from an angiogenic perspective is probably *VEGF*. An upregulation



of VEGF was first described following overexpression of Tβ4 in B16-F10 lung tumor cells; conversely, a downregulation of VEGF *in situ* was observed in Tβ4 knockdown hearts, suggesting that appropriate VEGF expression may require Tβ4 (Smart et al., 2007b). In the present study, VEGF was detected significantly enhanced by exogenous Tβ4 (Figure 2A) as well as the Tβ4-overexpressed BMMSCs (Figure 3C). Furthermore, we found that Tβ4 induces angiogenesis by stabilizing HIF-1α protein in an oxygen-independent manner, which is consistent with existing literature (Jo et al., 2010; Ock et al., 2012).

HIF-1α was normoxic degraded by prolyl hydroxylase domain proteins (PHD), and FIH mediated proteasome system. Thus, we detected the degradation effects of Tβ4 treatment and found that enhancement of HIF-1α and p-HIF-1α proteins was blocked by FIH promoter (YC-1). Moreover, the expression of PHD was decreased with the treatment of Tβ4 and further decreased when combined with Tβ4 and FG-4497 (Figure 2). These results show that the increase in HIF-1α and p-HIF-1α was due to increased protein synthesis and reduced degradation and partly through the PI3K-AKT pathway.

Our study has some limitations. Apart from the anti-fibrotic and pro-angiogenic potential, intramyocardial transplantation

of MSCs improves cardiac repair by promoting the polarization of macrophages and increasing the induction of Tregs, thereby regulating immune response as well. In this study, we did not detect the expression of HIF-1α and p-HIF-1α *in vivo* and the other cardioprotective effects of TMSB4^{OE}-BMMSCs such as inflammation, immunity, myocardial hypertrophy, cell migration, and proliferation. Future studies should consider investigating the therapeutic role of the Tβ4 gene in the PI3K-AKT pathway.

CONCLUSION

Our data suggest that 4 weeks after MI treatment, significant repair of an injured LV can be achieved by a novel BMMSC line showing TMSB4 overexpression. The small infarct size observed in TMSB4^{OE}-BMMSCs-treated animals can also lead to a corresponding increase in the activation of paracrine mechanisms such as the increase in angiogenesis at the border zone, 4 weeks after transplantation. This increase in paracrine activity may also contribute to improvements in LV remodeling and LV chamber function. Furthermore, the increase in HIF-1α and p-HIF-1α induced by Tβ4 was

partly because of an increase in protein synthesis *via* the AKT pathway and the reduction of degradation *via* the PHD and FIH pathways, which may serve as potential therapeutic targets for the treatment of MI.

DATA AVAILABILITY STATEMENT

The raw data supporting the conclusions of this article will be made available by the authors, without undue reservation.

ETHICS STATEMENT

The animal study was reviewed and approved by the Research Ethics Committee of Second Xiangya Hospital.

AUTHOR CONTRIBUTIONS

ST carried out data collection and/or assembly of data, data analysis, and wrote the manuscript. ST, WZ, ZZ, MW, WC, and XW carried out data collection. ZL, JP, and JY carried out data analysis and interpretation and manuscript revision.

REFERENCES

- Angoulvant, D., Ivanov, F., Ferrera, R., Matthews, P. G., Nataf, S., and Ovize, M. (2011). Mesenchymal stem cell conditioned media attenuates in vitro and ex vivo myocardial reperfusion injury. *J. Heart Lung Transplant.* 30, 95–102. doi: 10.1016/j.healun.2010.08.023
- Bonaer, A., Carmona, G., Iwasaki, M., Mione, M., Koyanagi, M., Fischer, A., et al. (2009). MicroRNA-92a controls angiogenesis and functional recovery of ischemic tissues in mice. *Science* 324, 1710–1713. doi: 10.1126/science.1174381
- Brahimi-Horn, M. C., and Pouyssegur, J. (2009). HIF at a glance. *J. Cell Sci.* 122, 1055–1057. doi: 10.1242/jcs.035022
- Fan, C., Oduk, Y., Zhao, M., Lou, X., Tang, Y., Pretorius, D., et al. (2020a). Myocardial protection by nanomaterials formulated with CHIR99021 and FGF1. *JCI Insight* 5:e132796. doi: 10.1172/jci.insight.132796
- Fan, C., Tang, Y., Zhao, M., Lou, X., Pretorius, D., Menasche, P., et al. (2020b). CHIR99021 and fibroblast growth factor 1 enhance the regenerative potency of human cardiac muscle patch after myocardial infarction in mice. *J. Mol. Cell. Cardiol.* 141, 1–10. doi: 10.1016/j.yjmcc.2020.03.003
- Hinkel, R., Klett, K., Bahr, A., and Kupatt, C. (2018). Thymosin beta4-mediated protective effects in the heart. *Expert Opin. Biol. Ther.* 18, 121–129. doi: 10.1080/14712598.2018.1490409
- Jay, S. M., and Lee, R. T. (2013). Protein engineering for cardiovascular therapeutics: untapped potential for cardiac repair. *Circ. Res.* 113, 933–943. doi: 10.1161/CIRCRESAHA.113.300215
- Jo, J. O., Kim, S. R., Bae, M. K., Kang, Y. J., Ock, M. S., Kleinman, H. K., et al. (2010). Thymosin beta4 induces the expression of vascular endothelial growth factor (VEGF) in a hypoxia-inducible factor (HIF)-1alpha-dependent manner. *Biochim. Biophys. Acta* 1803, 1244–1251. doi: 10.1016/j.bbamcr.2010.07.005
- Korf-Klingebiel, M., Rebold, M. R., Klede, S., Brod, T., Pich, A., Polten, F., et al. (2015). Myeloid-derived growth factor (C19orf10) mediates cardiac repair following myocardial infarction. *Nat. Med.* 21, 140–149. doi: 10.1038/nm.3778
- Mathison, M., and Rosengart, T. K. (2018). Heart regeneration: the endothelial cell comes first. *J. Thorac. Cardiovasc. Surg.* 155, 1128–1129. doi: 10.1016/j.jtcvs.2017.09.106

CF and JY designed and conceptualized the study and carried out manuscript revision. All authors read and approved the final manuscript.

FUNDING

This work was supported by the Major Research Plan of the National Natural Science Foundation of China (No. 91539111 to JY) and the Key project of science and technology of Hunan Province (No. 2020SK53420 to JY).

ACKNOWLEDGMENTS

We thank Dr. Qin Wu for her excellent technical assistance.

SUPPLEMENTARY MATERIAL

The Supplementary Material for this article can be found online at: <https://www.frontiersin.org/articles/10.3389/fcell.2021.670913/full#supplementary-material>

- Ock, M. S., Song, K. S., Kleinman, H., and Cha, H. J. (2012). Thymosin beta4 stabilizes hypoxia-inducible factor-1alpha protein in an oxygen-independent manner. *Ann. N. Y. Acad. Sci.* 1269, 79–83. doi: 10.1111/j.1749-6632.2012.06657.x
- Prabhu, S. D., and Frangogiannis, N. G. (2016). The biological basis for cardiac repair after myocardial infarction: from inflammation to fibrosis. *Circ. Res.* 119, 91–112. doi: 10.1161/CIRCRESAHA.116.303577
- Qian, L., Huang, Y., Spencer, C. I., Foley, A., Vedantham, V., Liu, L., et al. (2012). In vivo reprogramming of murine cardiac fibroblasts into induced cardiomyocytes. *Nature* 485, 593–598. doi: 10.1038/nature11044
- Rey, S., Lee, K., Wang, C. J., Gupta, K., Chen, S., McMillan, A., et al. (2009). Synergistic effect of HIF-1alpha gene therapy and HIF-1-activated bone marrow-derived angiogenic cells in a mouse model of limb ischemia. *Proc. Natl. Acad. Sci. U.S.A.* 106, 20399–20404. doi: 10.1073/pnas.0919211106
- Smart, N., Risebro, C. A., Melville, A. A., Moses, K., Schwartz, R. J., Chien, K. R., et al. (2007a). Thymosin beta4 induces adult epicardial progenitor mobilization and neovascularization. *Nature* 445, 177–182. doi: 10.1038/nature05383
- Smart, N., Rossdeutsch, A., and Riley, P. R. (2007b). Thymosin beta4 and angiogenesis: modes of action and therapeutic potential. *Angiogenesis* 10, 229–241. doi: 10.1007/s10456-007-9077-x
- Sun, J., Shen, H., Shao, L., Teng, X., Chen, Y., Liu, X., et al. (2020). HIF-1alpha overexpression in mesenchymal stem cell-derived exosomes mediates cardioprotection in myocardial infarction by enhanced angiogenesis. *Stem Cell. Res. Ther.* 11:373. doi: 10.1186/s13287-020-01881-7
- Tang, T., Wu, M., and Yang, J. (2013). Transplantation of MSCs transfected with SHH gene ameliorates cardiac dysfunction after chronic myocardial infarction. *Int. J. Cardiol.* 168, 4997–4999. doi: 10.1016/j.ijcard.2013.07.126
- White, S. J., and Chong, J. J. H. (2020). Mesenchymal stem cells in cardiac repair: effects on myocytes, vasculature, and fibroblasts. *Clin. Ther.* 42, 1880–1891. doi: 10.1016/j.clinthera.2020.08.010
- Wollert, K. C., and Drexler, H. (2010). Cell therapy for the treatment of coronary heart disease: a critical appraisal. *Nat. Rev. Cardiol.* 7, 204–215. doi: 10.1038/nrcardio.2010.1

- Yang, J., Tang, T., Li, F., Zhou, W., Liu, J., Tan, Z., et al. (2009). Experimental study of the effects of marrow mesenchymal stem cells transfected with hypoxia-inducible factor-1alpha gene. *J. Biomed. Biotechnol.* 2009:128627. doi: 10.1155/2009/128627
- Yang, J., Zhou, W., Zheng, W., Ma, Y., Lin, L., Tang, T., et al. (2007). Effects of myocardial transplantation of marrow mesenchymal stem cells transfected with vascular endothelial growth factor for the improvement of heart function and angiogenesis after myocardial infarction. *Cardiology* 107, 17–29.
- Ye, L., Zhang, P., Duval, S., Su, L., Xiong, Q., and Zhang, J. (2013). Thymosin beta4 increases the potency of transplanted mesenchymal stem cells for myocardial repair. *Circulation* 128, S32–S41.

Conflict of Interest: The authors declare that the research was conducted in the absence of any commercial or financial relationships that could be construed as a potential conflict of interest.

Copyright © 2021 Tang, Fan, Iroegbu, Zhou, Zhang, Wu, Chen, Wu, Peng, Li and Yang. This is an open-access article distributed under the terms of the Creative Commons Attribution License (CC BY). The use, distribution or reproduction in other forums is permitted, provided the original author(s) and the copyright owner(s) are credited and that the original publication in this journal is cited, in accordance with accepted academic practice. No use, distribution or reproduction is permitted which does not comply with these terms.



Trimethylamine N-Oxide Exacerbates Renal Inflammation and Fibrosis in Rats With Diabetic Kidney Disease

Qing Fang^{1,2,3,4,5}, Binjie Zheng^{1,2,3,4,5}, Na Liu^{1,2,3,4,5}, Jinfeng Liu^{1,2,3,4,5}, Wenhui Liu^{1,2,3,4,5}, Xinyi Huang^{1,2,3,4,5}, Xiangchang Zeng^{1,2,3,4,5}, Lulu Chen⁵, Zhenyu Li^{6*†} and Dongsheng Ouyang^{1,2,3,4,5*†}

¹ Department of Clinical Pharmacology, Xiangya Hospital, Central South University, Changsha, China, ² Hunan Key Laboratory of Pharmacogenetics, Institute of Clinical Pharmacology, Central South University, Changsha, China, ³ Engineering Research Center of Applied Technology of Pharmacogenomics, Ministry of Education, Changsha, China, ⁴ National Clinical Research Center for Geriatric Disorders, Changsha, China, ⁵ Hunan Key Laboratory for Bioanalysis of Complex Matrix Samples, Changsha Duxact Biotech Co., Ltd., Changsha, China, ⁶ Department of Geriatric Medicine, Xiangya Hospital, Central South University, Changsha, China

OPEN ACCESS

Edited by:

Gonzalo del Monte-Nieto,
Monash University, Australia

Reviewed by:

Ana María Puyó,
University of Buenos Aires, Argentina
Ashish K. Solanki,
Medical University of South Carolina,
United States

*Correspondence:

Zhenyu Li
liy1552@csu.edu.cn
Dongsheng Ouyang
801940@csu.edu.cn

†ORCID:

Zhenyu Li
orcid.org/0000-0002-1743-8610
Dongsheng Ouyang
orcid.org/0000-0002-1743-8610

Specialty section:

This article was submitted to
Renal and Epithelial Physiology,
a section of the journal
Frontiers in Physiology

Received: 18 March 2021

Accepted: 24 May 2021

Published: 16 June 2021

Citation:

Fang Q, Zheng B, Liu N, Liu J,
Liu W, Huang X, Zeng X, Chen L, Li Z
and Ouyang D (2021) Trimethylamine
N-Oxide Exacerbates Renal
Inflammation and Fibrosis in Rats With
Diabetic Kidney Disease.
Front. Physiol. 12:682482.
doi: 10.3389/fphys.2021.682482

The gut microbiota plays a pivotal role in the onset and development of diabetes and its complications. Trimethylamine N-oxide (TMAO), a gut microbiota-dependent metabolite of certain nutrients, is associated with type 2 diabetes and its complications. Diabetic kidney disease (DKD) is one of the most serious microvascular complications. However, whether TMAO accelerates the development of DKD remains unclear. We tested the hypothesis that TMAO accelerates the development of DKD. A high-fat diet/low-dose streptozotocin-induced diabetes rat model was established, with or without TMAO in the rats' drinking water. Compared to the normal rats, the DKD rats showed significantly higher plasma TMAO levels at the end of the study. TMAO treatment not only exacerbated the kidney dysfunction of the DKD rats, but also renal fibrosis. Furthermore, TMAO treatment activated the nucleotide-binding domain, leucine-rich-containing family, pyrin domain-containing-3 (NLRP3) inflammasome and resulted in the release of interleukin (IL)-1 β and IL-18 to accelerate renal inflammation. These results suggested that TMAO aggravated renal inflammation and fibrosis in the DKD rats, which provides a new perspective to understand the pathogenesis of DKD and a potential novel target for preventing the progression of DKD.

Keywords: trimethylamine N-oxide, diabetic kidney disease, inflammation, NLRP3, fibrosis

INTRODUCTION

Diabetic kidney disease (DKD), or diabetic nephropathy, is one of the most fatal complications of diabetes mellitus, and it is the most prevailing element of end-stage renal disease (Cansby et al., 2020). Metabolic changes caused by diabetes lead to proteinuria, progressive mesangial expansion, glomerular basement membrane thickening, tubulointerstitial fibrosis, and impaired renal function (Alicic et al., 2017). The underlying pathogenesis of DKD is complex and involves many different pathways. Studies have shown that several factors are major contributors in the pathophysiology of DKD, including oxidative stress, inflammation, overexpression of transforming growth factor- β 1 (TGF- β 1), and other metabolic alterations (Liu Y. et al., 2020;

Pourheydar et al., 2020). Despite improved prognosis over the years, the pathogenesis of DKD has not been fully elucidated. Understanding the mechanism of DKD will enable prevention and early intervention, which will result in better outcomes.

The gut microbiota plays an important role in many diseases. Trimethylamine N-oxide (TMAO), which is a gut microbiota-dependent metabolite of L-carnitine, choline, and phosphatidylcholine (Wang et al., 2011), has been implicated in the pathogenesis of various human diseases, including metabolic disorders (Chen S. et al., 2019), cardiovascular disorders, and neurological disorders (Vogt et al., 2018). Many studies have revealed that TMAO levels are higher in people with diabetes than in healthy people (Winther et al., 2019). A number of clinical studies have also demonstrated a strong association between TMAO levels and diabetes mellitus (Dambrova et al., 2016; Shan et al., 2017; Dong et al., 2018). Moreover, TMAO levels are strongly associated with the degree of renal function (Missailidis et al., 2016; Stubbs et al., 2016), and increased TMAO levels can directly contribute to progressive renal fibrosis and dysfunction in animal models (Tang et al., 2015; Sun et al., 2017; Li et al., 2018). However, the roles and mechanisms of TMAO in DKD have not been elucidated.

The nucleotide-binding domain, leucine-rich-containing family, pyrin domain-containing-3 (NLRP3) inflammasome is an important factor in aggravating kidney inflammation and fibrosis by the processing and secretion of the pro-inflammatory cytokines interleukin (IL)-1 β and IL-18 in DKD. Upon activation, the NLRP3 inflammasome promotes the secretion of IL-1 β and IL-18, thereby contributing to the development of DKD (Li L. H. et al., 2019). Accumulating evidence from recent studies have suggested that renal NLRP3 is activated in DKD animal models, while the inhibition of its activity could reduce the inflammation of renal tissues and improve renal functions (Wang et al., 2017; Chen K. et al., 2019; Han et al., 2019). Furthermore, TMAO promotes the release of inflammatory factors by activating the NLRP3 inflammasome, thereby promoting vascular calcification, myocardial fibrosis, and vascular inflammation aggravating cardiovascular disease (Chen et al., 2017; Liu et al., 2019; Zhang et al., 2020). However, NLRP3 inflammasome in TMAO-mediated DKD remains unknown.

Here, we examined the effects of elevated TMAO levels on the development of DKD in diabetic rats. Investigating the effects and potential mechanisms of TMAO in DKD could provide a new perspective in the understanding of DKD.

MATERIALS AND METHODS

Materials

TMAO was purchased from Aladdin Industrial Corporation (Shanghai, China). The purity of the TMAO, which was measured by high-performance liquid chromatography, was > 98%. Streptozotocin (STZ) was purchased from Beijing Solarbio Science & Technology Co., Ltd. (Beijing, China). Sodium citrate buffer (0.1 mol/L, pH 4.5, sterile) was also purchased from Beijing Solarbio Science & Technology Co., Ltd. (Beijing, China).

Animals and Treatment

Adult male Sprague Dawley rats ($n = 32$) weighing 180–200 g were obtained from Hunan SJA Laboratory Animal Co., Ltd. (Hunan, China). All rats were maintained under specific pathogen-free conditions with a constant temperature of $23 \pm 1^\circ\text{C}$ and a dark-light cycle of 12:12 h. The study followed the National Guidelines for Laboratory Animal Welfare and was approved by the Experimental Animal Ethics Committee of Central South University (2019 sydw0208). All rats adapted to the laboratory environment for 7 days. They were then fed a normal diet or high-fat diet (HFD) and given drinking water with or without TMAO 0.2% (w/v) for 12 weeks, resulting in 4 experimental groups ($n = 8$ per group): CON, CON + TMAO, DKD, DKD + TMAO. For 4 weeks, the DKD groups were fed a HFD (Medicience, Ltd., Jiangsu, China) with the following composition: common breeding material, 63.5%; lard oil, 10%; sucrose, 20%; cholesterol, 2.5%; and sodium cholate, 0.5%. The DKD groups were then injected intraperitoneally with STZ at a low dose of 35 mg/kg diluted in citrate buffer. The control group was injected with citrate buffer. Diabetes was confirmed by measuring glucose levels after 72 h of the STZ injection. Rats with glucose levels ≥ 16.7 mmol/L were considered to be diabetic. The DKD groups continued to be fed the HFD for 8 weeks. All rats were put in metabolic cages for 24-h urine collection at the end of the 12 weeks. Blood samples were obtained by cardiac puncture at the time of euthanasia. Serum and plasma were then separated by centrifugation and stored at -80°C for subsequent experiments. In addition, the kidney was excised, weighed, and kept in liquid nitrogen or fixed in 4% paraformaldehyde.

Biochemical Parameters Detection

The blood glucose levels of the rats were measured every 2 weeks after the STZ injection with glucose test strips (ACCU-CHEK, Shanghai, China). Total cholesterol (TC), triglyceride (TG), serum creatinine (Scr), and blood urea nitrogen (BUN) levels were detected by an automatic biochemical analyzer (Chemray 800, Shenzhen, China). Total 24-h urinary protein concentrations were detected with corresponding kits (Nanjing Jiancheng Bioengineering Institute, Nanjing, China).

Circulating TMAO Measurements

TMAO levels were determined by measured by ultra-high-performance liquid chromatography-tandem mass spectrometry (UHPLC-MS) using d $_9$ -(trimethyl)-labeled internal standards as described previously (Jaworska et al., 2017).

Histological Analysis

The renal tissues were fixed in 4% paraformaldehyde, embedded in paraffin, sectioned to a 5- μm thickness, and then stained with hematoxylin-eosin (H&E) and Masson stains for histological examination under a light microscope. Renal fibrosis was calculated based on the percentage of the collagen-positive area in the total tissue area (Tang et al., 2015). Tubular injury was graded from 0–4 based

on the area of inflammatory cell infiltration, tubular epithelial cell atrophy, tubular vacuolization, and dilation region, as follows: 0%, 0; < 25%, 1; 25–50%, 2; 50–75%, 3; and > 75%, 4.

Immunohistochemical Analysis

The expression of NLRP3 and caspase-1 in the renal tissue was detected by immunohistochemistry. All samples were fixed in 4% paraformaldehyde and embedded in paraffin. Then, the paraffin-embedded specimens were cut into 4-mm sections, deparaffinized, and rehydrated. Subsequently, the sections were placed in 3% H₂O₂ to eliminate endogenous peroxidase activity for 25 min. Next, the sections were blocked with normal goat serum, followed by incubation with 3% BSA for 30 min, followed by incubation with anti-NLRP3 (Affinity, DF7438, 1:100) and anti-caspase-1 (Abways, 1:100, CY5429) antibodies overnight at 4°C. After rinsing with phosphate-buffered saline, the sections were stained with a polymer horseradish peroxidase detection system (Servicebio, Beijing, China) and counterstained with hematoxylin. A total of 10 fields from each sample were randomly selected, and the positive-staining percentage was analyzed by Image-Pro Plus 6.0 software (Media Cybernetics).

Enzyme Linked Immunosorbent Assay

The IL-1 β in the renal tissue, IL-18 in the serum, and microalbumin in the urine (UAlb) were measured by enzyme-linked immunosorbent assay (ELISA). The kidney was cut into pieces, and the cut kidney tissue was prepared into its homogenate with 9 times the volume of normal saline. The homogenate was centrifuged at 3,500 r/min for 10 min to separate the supernatant, and the supernatant was preserved at 4°C for later use. The serum was centrifuged at 1,000 g for 15 min, and the supernatant was separated for later use. The IL-1 β content in the renal tissue, the IL-18 content in the serum, and the microalbumin content in the urine were detected by ELISA according to kit instructions [MultiSciences (Lianke) Biotech Co., Ltd., Hangzhou, China; Cusabio Biotech Co., Ltd., Wuhan, China, CSB-E04610r; Cusabio Biotech Co., Ltd., Wuhan, China, CSB-E12991r].

Western Blot Analysis

The kidney tissue was homogenized in mammalian protein extraction reagent lysis buffer (Merck Millipore, 92590) with protease inhibitor (NCM Biotech, P001). The supernatant was removed by centrifugation at 12,000 g for 15 min at 4°C. The total protein concentration was determined using the Micro BCA Protein Kit Assay (Pierce, Rockford, IL, United States). Protein from each sample (100 μ g) was resolved by sodium dodecyl sulphate-polyacrylamide gel electrophoresis under reducing conditions, transferred to polyvinylidene fluoride membranes, and then blocked with 5% non-fat dry milk and 0.1% Tween-20 in Tris-buffered saline at room temperature for 2 h. Membranes were incubated overnight at 4°C with primary antibodies against GAPDH (Affinity, AF7021, 1:5,000), TGF- β 1 (Affinity, AF1027, 1:1,000), α -SMA (Affinity, AF1032, 1:1,000), IL-1 β (Affinity, AF5103, 1:1,000),

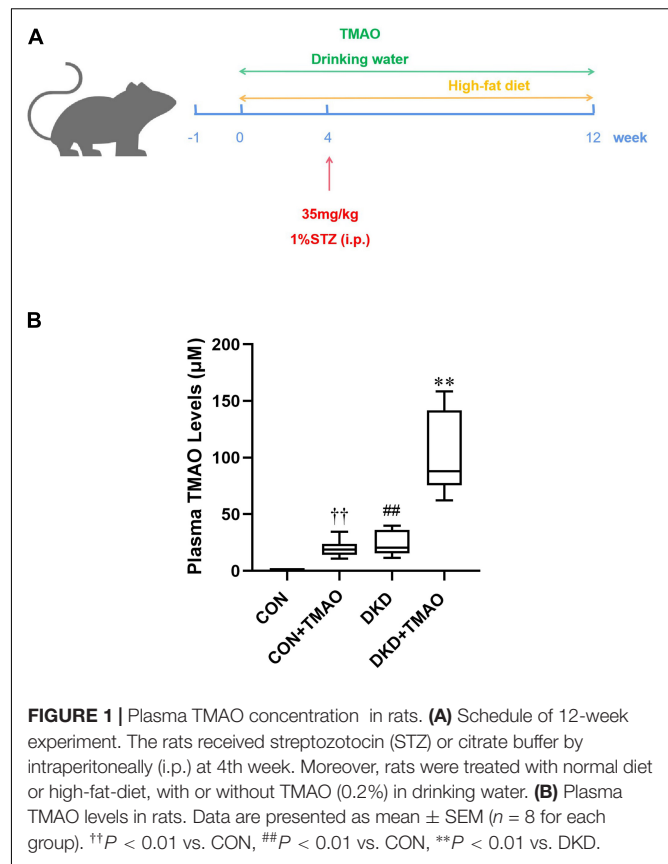


FIGURE 1 | Plasma TMAO concentration in rats. **(A)** Schedule of 12-week experiment. The rats received streptozotocin (STZ) or citrate buffer by intraperitoneally (i.p.) at 4th week. Moreover, rats were treated with normal diet or high-fat-diet, with or without TMAO (0.2%) in drinking water. **(B)** Plasma TMAO levels in rats. Data are presented as mean \pm SEM ($n = 8$ for each group). †† $P < 0.01$ vs. CON, ## $P < 0.01$ vs. CON, ** $P < 0.01$ vs. DKD.

and IL-18 (Affinity, DF6252, 1:1,000). After washing with Tris-buffered saline with Tween-20, membranes were incubated with a secondary goat anti-rabbit IgG horseradish peroxidase conjugate (1:5,000 dilution in secondary antibody dilution buffer) antibody (Affinity, S0001) or a secondary goat anti-rabbit IgG horseradish peroxidase conjugate (1:5,000 dilution in secondary antibody dilution buffer) antibody (Affinity, S0002) at room temperature for 1 h. Membranes were detected with a western blot detection system (WEST-ZOLR Plus, Intron Biotechnology, Shanghai, China) according to the manufacturer's instructions and then exposed to X-ray film (Thermo Scientific, Shanghai, China). All experiments were repeated 3 times.

Statistical Analyses

All statistical analyses were performed using the SPSS Statistics 22 software. GraphPad PRISM 8.0 (Vienna, Austria, 2018) was used to generate graphs. Data were expressed in terms of the mean \pm SEM. Weights and blood glucose levels were analyzed using repeated measures analysis of variance (ANOVA). One-way ANOVA was used for comparisons between groups, and the least significant difference method was used to compare the variance among groups. The Spearman correlation was used to determine the associations between the circulating TMAO levels and other measured parameters. A $P < 0.05$ was considered statistically significant.

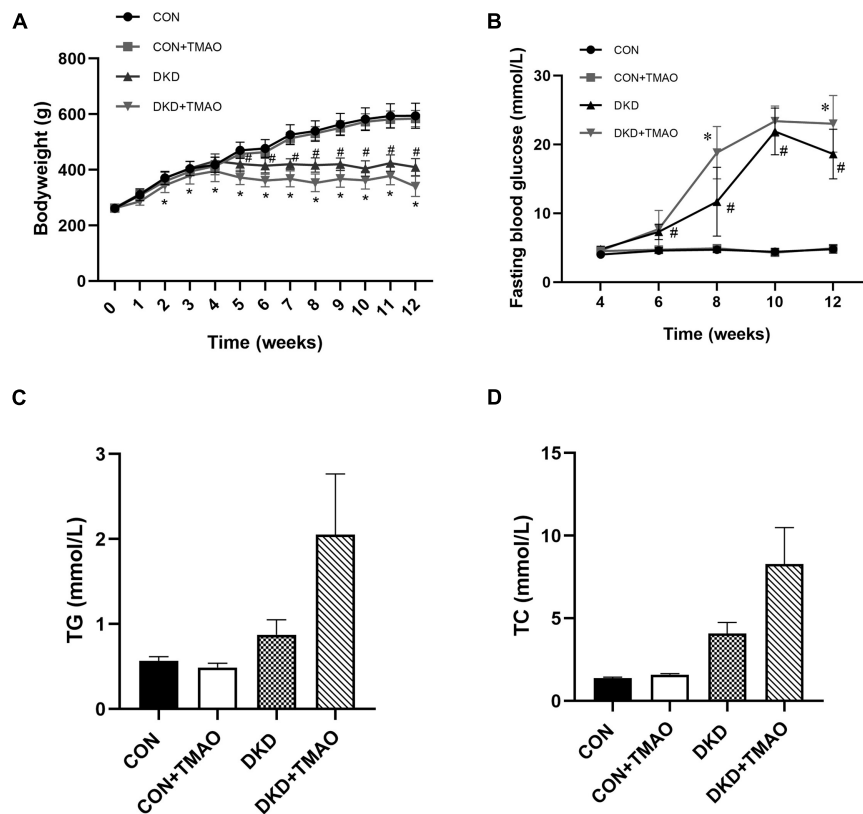


FIGURE 2 | Body weight and metabolic parameters in rats. **(A)** Body weight, **(B)** Fasting blood glucose, **(C)** Cholesterol, **(D)** Triglyceride. Data are presented as mean \pm SEM ($n = 8$ for each group). # $P < 0.05$ vs. CON, * $P < 0.05$ vs. DKD.

RESULTS

Elevated Plasma TMAO Levels in DKD Rats

To analyze the effects of TMAO on DKD, we administered a HFD and intraperitoneal STZ injections to establish a diabetic rat model. The rats were given drinking water with or without TMAO for 12 weeks (Figure 1A). After 12 weeks of TMAO treatment, the plasma TMAO levels in the TMAO water-treated groups were elevated compared to those in the plain water-treated groups (CON, $0.91 \pm 0.37 \mu\text{M}$ vs. CON + TMAO, $20.00 \pm 7.03 \mu\text{M}$; DKD, $24.01 \pm 10.03 \mu\text{M}$ vs. DKD + TMAO $100.48 \pm 34.36 \mu\text{M}$). The TMAO levels in the DKD rats were significantly higher than those in the normal rats (Figure 1B).

Effects of TMAO on Body Weight and Metabolic Parameters

The body weights were similar at baseline (Figure 2A). Compared to the rats in the CON group, the body weights of the rats in the DKD group were decreased from the fifth week and the fasting blood glucose levels of the rats in the DKD group were higher from the sixth week. There were no body weight or fasting blood glucose differences between the CON and CON + TMAO groups. The body weights of the rats in the DKD + TMAO group

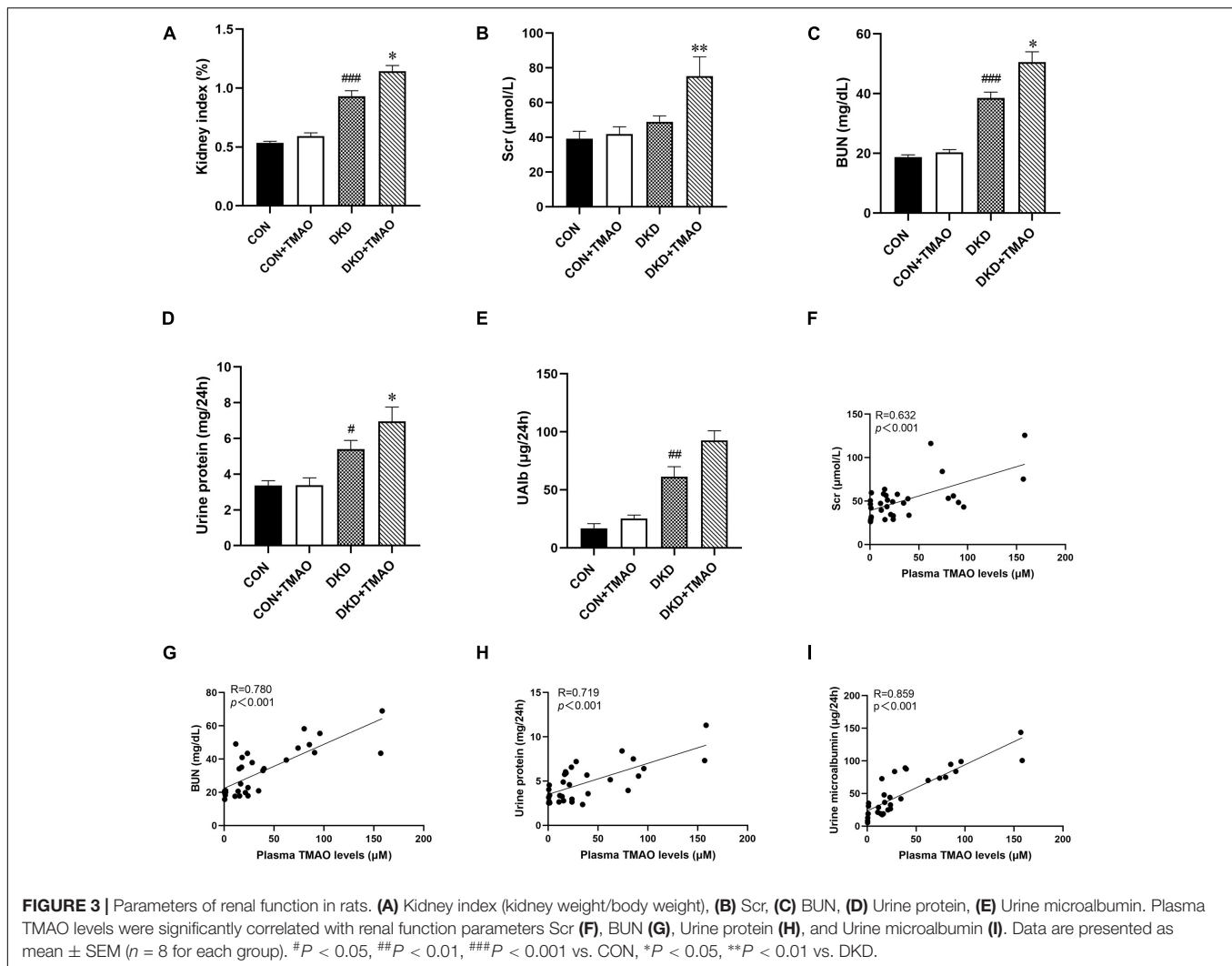
were decreased compared to those of the rats in the DKD group from the third week (Figure 2A). The fasting blood glucose levels of the rats in the DKD + TMAO group were higher than those of the rats in the DKD group at the eighth and twelfth weeks (Figure 2B). Compared to the CON group, the serum TC and TG levels were not significantly higher in the DKD group. Further, there were no differences in the serum TC and TG levels between the DKD and DKD + TMAO groups (Figures 2C,D).

Effects of TMAO on Renal Function

Compared to the CON group, the kidney index, BUN, urine protein, and UAlb levels were significantly higher in the DKD group. There were no differences in these parameters between the CON and CON + TMAO groups. The kidney index, Scr, BUN, and urine protein levels were significantly higher in the DKD + TMAO group compared to those in the DKD group (Figures 3A–E). Importantly, the plasma TMAO levels were positively correlated with the renal function parameters of Scr, BUN, urine protein, and UAlb levels (Figures 3F–I).

Effects of TMAO on Renal Histopathological Changes

The H&E staining results showed that inflammatory cell infiltration, tubular dilatation, cavitation of distal convoluted tubules, and tubular atrophy were present in the DKD group



compared to the CON group. In contrast to the CON group, a small amount of inflammatory cell infiltration in the tubular interstitium and slight tubular dilation were present in the rats in the CON + TMAO group. The DKD + TMAO group experienced more serious renal pathological alterations compared to the DKD group (Figures 4A,B). The Masson staining results showed that a larger fibrosis area was present in the rats in the DKD group compared to the rats in the CON group. In contrast to the rats in the CON group, the fibrosis area in the rats in the CON + TMAO group was significantly increased. Meanwhile, the fibrosis area in the DKD rats was significantly increased after the TMAO intervention (Figures 4A,C). Furthermore, the plasma TMAO levels were positively correlated with renal fibrosis area (Figure 4D).

Effects of TMAO on the Expression of TGF- β_1 and α -SMA

To further examine whether elevated plasma TMAO levels contributed to renal fibrosis, we measured the expression of TGF- β_1 and α -SMA in the kidney tissue by western blot analysis

(Figure 5). The results showed that the expression of TGF- β_1 was significantly increased in the kidney tissue of the rats in the DKD group compared to that of the rats in the CON group (Figure 5A). There was no significant difference in the expression of TGF- β_1 or α -SMA between the CON and CON + TMAO groups (Figures 5A,B). The expression of α -SMA was significantly increased in the kidney tissue of the rats in the DKD + TMAO group compared to that of the rats in the DKD group (Figure 5B). However, the expression of TGF- β_1 was not significantly increased in the kidney tissue of the rats in the DKD + TMAO group (Figure 5A).

Effects of TMAO on Renal Inflammation

The NLRP3 inflammasome signaling pathway, including NLRP3, caspase-1, IL-1 β , and IL-18, was evaluated using immunohistochemistry, western blot analysis, and ELISA in order to explore the presumed mechanism of the pro-inflammatory activity of TMAO (Figure 6). The results showed that the levels of NLRP3 and IL-18 were significantly increased in the DKD group compared to the CON group (Figures 6B,G). Compared to the DKD group, the levels of

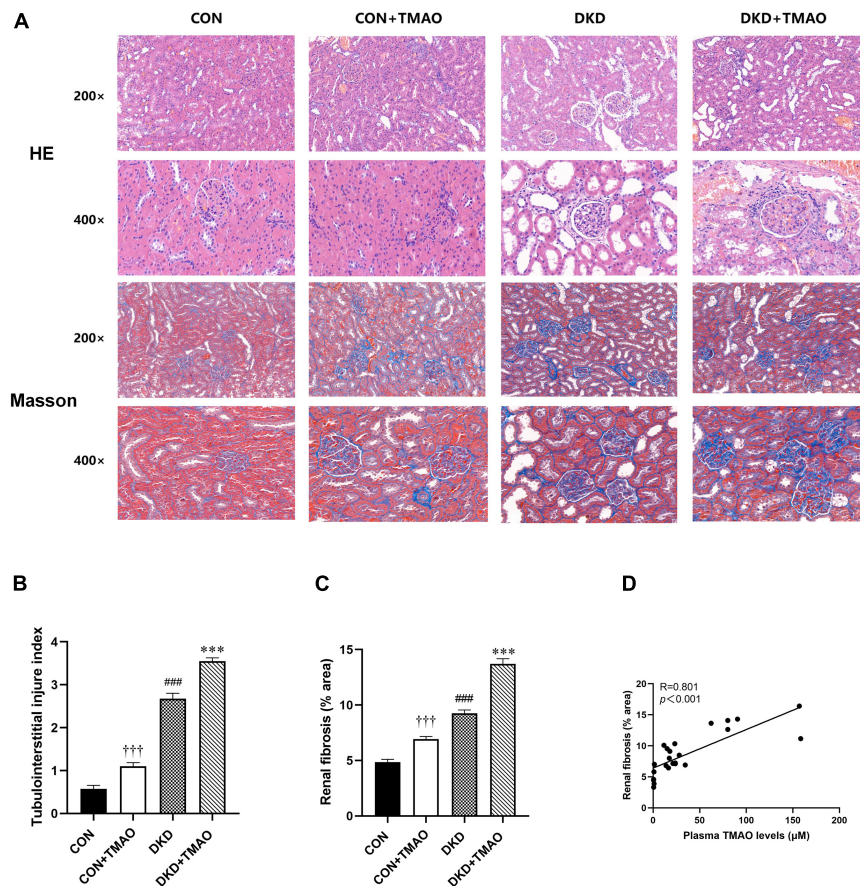


FIGURE 4 | Pathology results in kidney of rats. **(A)** The results of HE staining and Masson staining in all rat groups (enlargement factor: 200 \times , 400 \times). **(B)** Tubulointerstitial injure index. **(C)** Fibrosis area of Masson staining. **(D)** The relationship between plasma TMAO levels and renal fibrosis area. Data are presented as mean \pm SEM ($n > 6$ for each group). ††† $P < 0.001$ vs. CON, ### $P < 0.001$ vs. CON, *** $P < 0.001$ vs. DKD.

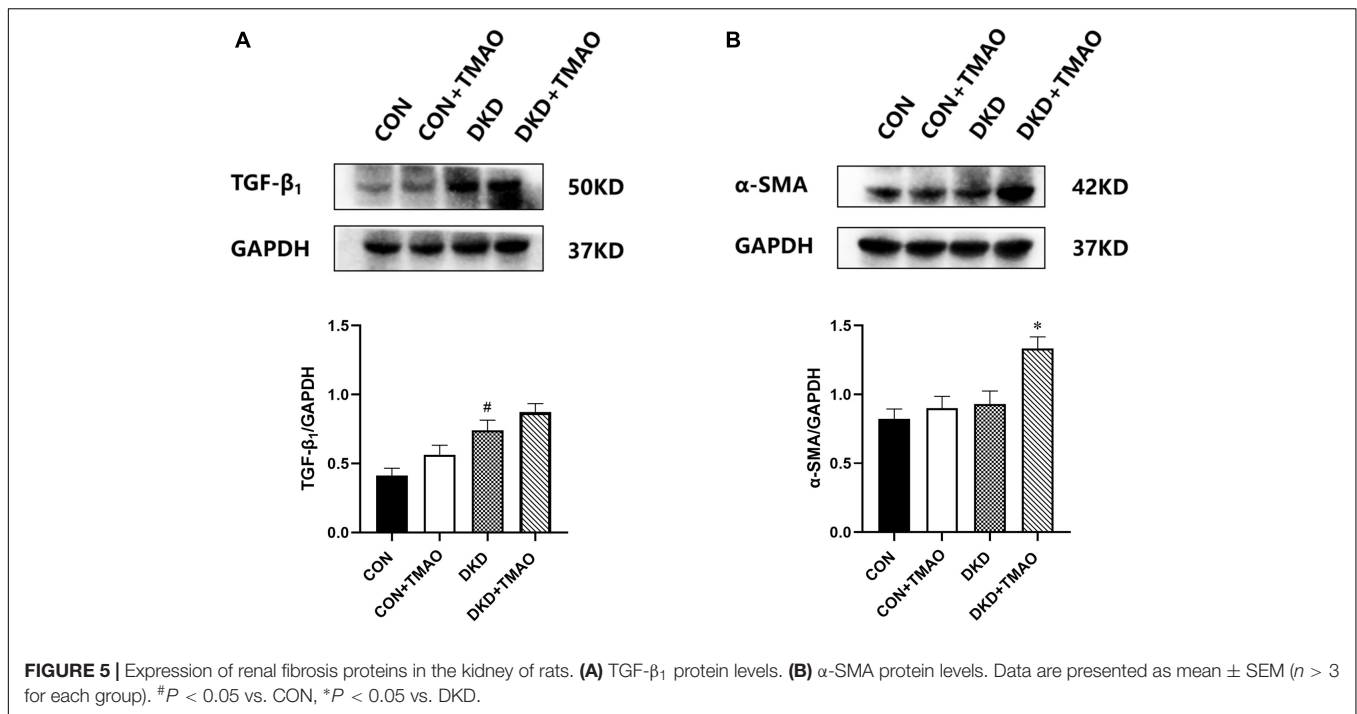
NLRP3, caspase-1, IL-1 β , and IL-18 were all significantly increased in the DKD + TMAO group (Figures 6B–G). Further, the levels of NLRP3 and caspase-1 in the CON + TMAO group were significantly increased compared to those in the CON group (Figures 6B,C).

DISCUSSION

The major findings of this study were: (1) the rats with DKD had increased circulating TMAO levels; (2) the circulating TMAO levels of the CON + TMAO rats administered TMAO for 12 weeks were almost the same as those of the DKD rats; (3) TMAO administration in the DKD group decreased the body weights and increased the fasting blood glucose levels of the rats, while it had no effect on TG and TC levels; and (4) TMAO facilitated tubulointerstitial injury and renal fibrosis, and it activated the NLRP3 inflammasome to exacerbate renal inflammation. Collectively, these findings suggest that elevated TMAO levels exacerbate renal fibrosis and renal inflammation to accelerate the development of DKD (Figure 7).

More and more clinical evidence supports the close relationship between elevated plasma TMAO levels and

increased risk of cardiovascular disease risk (Kanitsoraphan et al., 2018; Yang S. et al., 2019). Elevated TMAO levels also appear in many other diseases, including diabetes, chronic kidney disease, non-alcoholic fatty liver disease, and neurodegenerative diseases (Pelletier et al., 2019; Tan et al., 2019; Zhao L. et al., 2019; Zhuang et al., 2019). We previously found that people with DKD had higher TMAO levels than healthy people. In this study, we found that the plasma TMAO levels of the DKD rats were significantly higher than those of the normal rats. Most previous animal experiments have increased the levels of TMAO in the animals by adding 1% choline or 0.12% TMAO to their diets (Tang et al., 2015; Zhu et al., 2016). Adding TMAO at a concentration of 333 mg/L to the animals' drinking water or administering TMAO by gavage at a dose of 120 mg/kg/day can also increase the levels of TMAO in the animals (Huc et al., 2018; Zhao Z. H. et al., 2019). In this study, we dissolved TMAO in the rats' drinking water for 12 weeks. The plasma TMAO levels in the CON + TMAO group ($20.00 \pm 7.03 \mu\text{M}$) increased to about 22 times those in the normal control group ($0.91 \pm 0.37 \mu\text{M}$). The plasma TMAO levels of the rats with diabetic nephropathy were similar ($24.01 \pm 10.03 \mu\text{M}$). Thus, administering male Sprague Dawley rats a 0.2% TMAO solution for 12 weeks can effectively



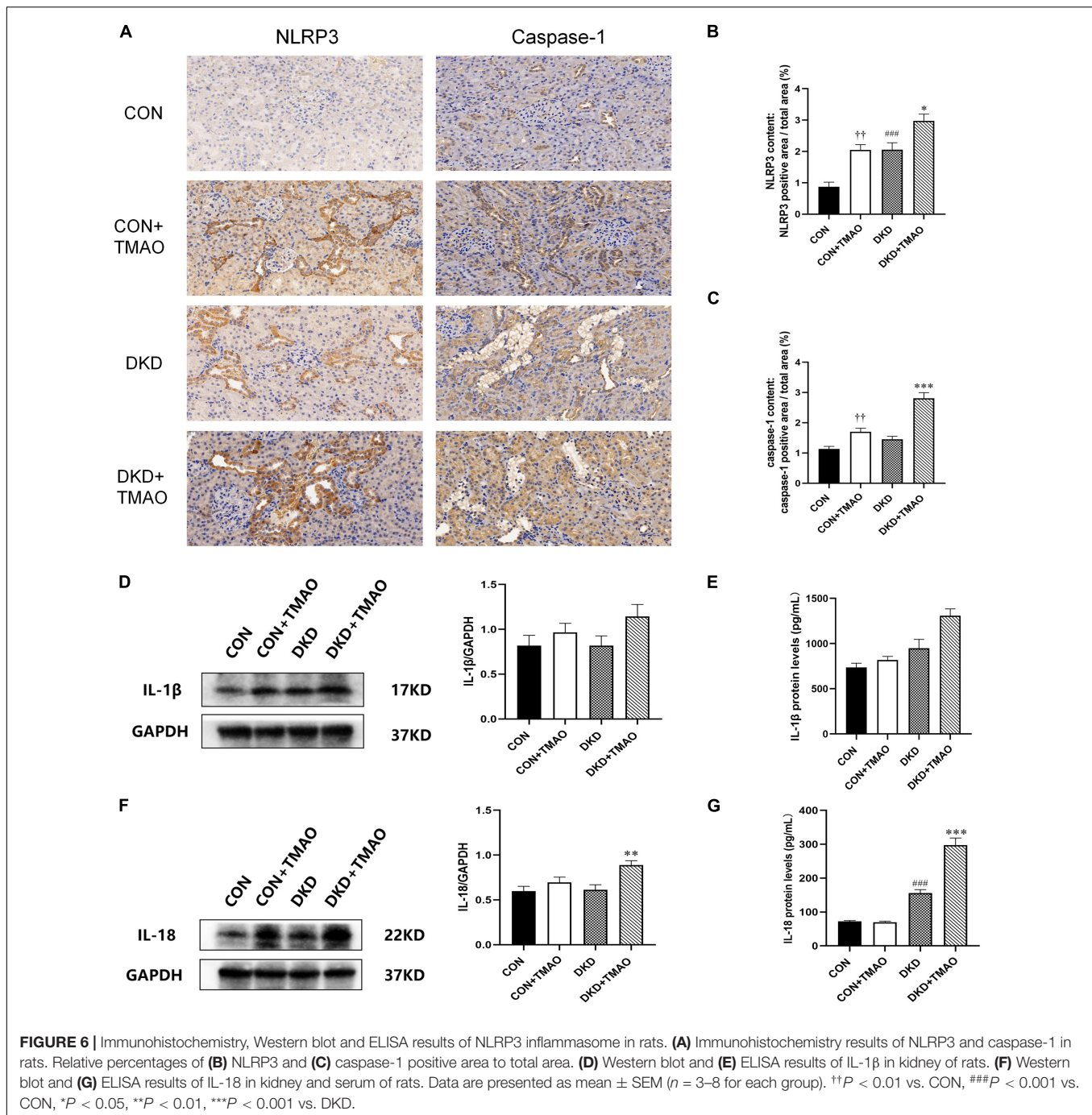
increase their plasma TMAO levels to a level equivalent to the pathological state of DKD. This result can provide a reference for TMAO dose selection in the study of TMAO and diabetes or its complications.

In recent years, a growing body of evidence has demonstrated that the gut microbiota plays a pivotal role in the onset and development of diabetes and its complications. TMAO, a gut microbiota-dependent metabolite from foods such as red meat, eggs, and fish (Cho et al., 2017), is associated with type 2 diabetes and its complications (Dambrova et al., 2016; Shan et al., 2017; Liu W. et al., 2020). Furthermore, diet-induced changes in TMAO and its precursors are significantly associated with improvements in glycemia and insulin sensitivity (Heianza et al., 2019). Higher TMAO concentrations can impair glucose tolerance in HFD-fed mice (Gao et al., 2014, 2015). In the present study, we found that TMAO significantly increased the fasting blood glucose levels of the diabetic rats, but it did not affect the normal rats, while other studies have found that TMAO had no significant effect on fasting glucose levels in HFD-fed mice (Gao et al., 2014, 2015). The discrepancy may result from many factors, such as the administration of TMAO with STZ and the long-term treatment with TMAO in our study. Lipid metabolism disturbance is a pathogenic factor associated with DKD, with increased TC and TG levels in people and animals with DKD (Alaofi, 2020; Liu L. et al., 2020). The lipid metabolism disorder caused by TMAO has been proven in a number of animal experiments. A high-cholinergic diet can significantly increase the serum total TC and TG levels in mice fed a HFD (Yang C. et al., 2020). Furthermore, serum TG and TC levels have been shown to increase after intraperitoneal injection of TMAO in rats (Liu et al., 2021). In this study, we detected the serum TC and TG concentrations in the rats. The results showed that the serum TC and TG

concentrations of the DKD + TMAO group were higher than those of the DKD group, but the difference was not statistically significant, which may be due to the large difference within the group. In our follow-up study, we may further expand the sample size to verify the effect of TMAO on lipid metabolism.

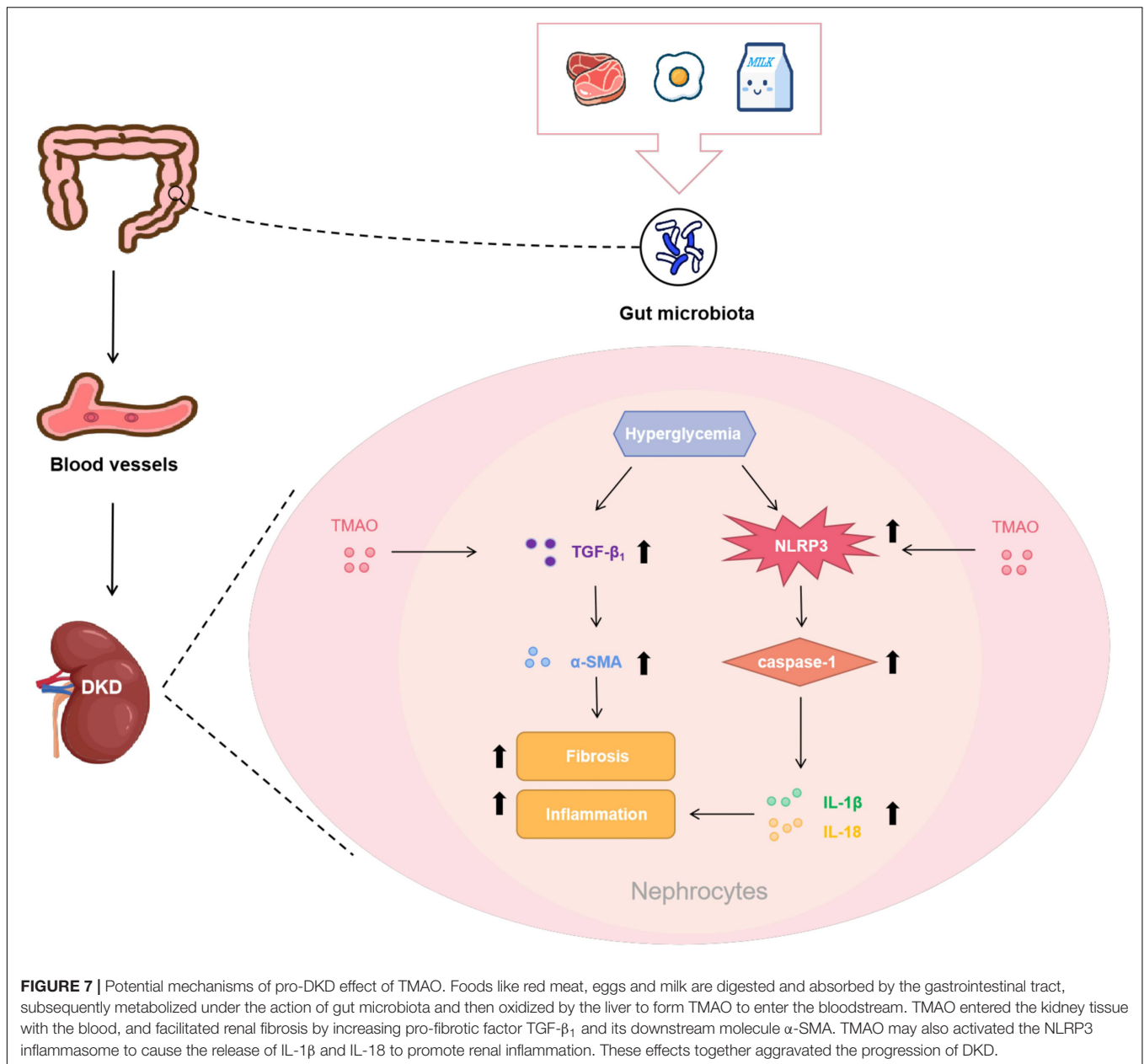
Accumulating evidence has also shown that increased TMAO levels are associated with a risk for all-cause mortality, and increased TMAO levels have been identified as an independent predictor of mortality in patients with chronic kidney disease (CKD) (Tang et al., 2015; Burdmann et al., 2016). We previously demonstrated in Chinese patients with CKD that combinations of TMAO and its precursors were related to glomerular filtration rate, which is an indicator of kidney function (Guo et al., 2020). Some animal studies suggest that elevated TMAO levels may directly impair renal function by contributing to oxidative stress, endothelial dysfunction, renal fibrosis, and other mechanisms (Sun et al., 2017; Li et al., 2018). In this study, we found that in the process of DKD, the renal function parameters of renal index, Scr, BUN, urine protein, and UAlb concentrations were increased after TMAO administration, although there was no significant difference in UAlb between the two groups. Pearson correlation analysis results showed that the plasma TMAO levels were positively correlated with Scr, BUN, 24-h urinary total protein, and UAlb levels, and the H&E staining results showed that TMAO further aggravated the degree of renal tubular damage. Taken together, we can infer that TMAO can promote reduced renal function, which may be a risk factor for DKD.

Renal fibrosis plays an important role in the development of DKD. It is an irreversible pathological change and the final and only common pathway for DKD to progress to end-stage renal disease (Zeng et al., 2019). Epithelial-to-mesenchymal transition is the main pathological process of renal interstitial fibrosis, and



it is the initial step of renal fibrosis. It refers to the transformation of renal tubular epithelial cells into mesenchymal cells, and it can increase the expression of α -SMA, the marker protein of mesenchymal cells (Zhang et al., 2017). Renal interstitial fibrosis is also regulated by a variety of pro-fibrotic factors, among which TGF- β_1 , which plays an important role in renal interstitial fibrosis, is a very important regulatory factor. The expression of TGF- β_1 mRNA and the TGF- β_1 protein in the kidney tissue of people with diabetes is increased (Zhang et al., 2017). TGF- β_1 is directly involved in the epithelial-to-mesenchymal

transition process of DKD, leading to renal interstitial fibrosis (Zheng et al., 2016; Yang Y. et al., 2020), and it can activate the downstream Smad signaling pathway, thereby mediating fibrogenesis (Hathaway et al., 2015). The role of TMAO in promoting fibrosis has also been demonstrated in many studies. TMAO can activate the TGF- β receptor type I/Smad2 pathway, increase the expression of α -SMA and type I collagen, and promote the induction of cardiac fibrosis (Yang W. et al., 2019). In addition, TMAO can promote cardiac fibrosis by activating the Smad3 pathway in Sprague Dawley rats (Huang et al., 2018).



TMAO can also aggravate Adriamycin-induced cardiac fibrosis in mice by activating the TGF- β /Smad3 pathway (Liu et al., 2019). Moreover, the TMAO inhibitor 3,3-dimethyl-1-butanol (DMB) can inhibit the TGF- β_1 /Smad3 pathway by reducing TMAO levels, thereby alleviating cardiac fibrosis in mice (Wang et al., 2020). Iodomethylcholine can inhibit the progression of adenine-induced CKD in mice by inhibiting TMAO levels and reducing collagen deposition (Zhang et al., 2021), and it can also inhibit the expression of pro-fibrotic genes, such as those encoding for TGF- β , type I collagen, tissue inhibitor of metalloproteinase 1, and α -SMA, to alleviate renal tubular interstitial fibrosis and dysfunction in CKD mice (Gupta et al., 2020). In this study, the Masson staining results directly showed renal interstitial fibrosis in the rats with DKD, and the degree of renal interstitial

fibrosis in the DKD + TMAO group was further aggravated. More interestingly, we observed slight renal interstitial fibrosis in the normal rats administered TMAO. Through the detection of renal interstitial fibrosis-related proteins, we found that the expression of α -SMA increased significantly in the DKD rats after TMAO treatment, and the expression of TGF- β_1 also increased, but there was no statistically significant difference. These results suggested that TMAO could promote renal interstitial fibrosis in the rats with DKD and that TMAO could slightly adversely affect the kidneys of the normal rats, but the specific mechanism of TMAO in promoting fibrosis needs to be further explored.

Emerging evidence suggests that inflammation plays a key role in the DKD progression (Moreno et al., 2018). Numerous preclinical studies have shown that several anti-inflammatory

molecules can effectively improve DKD (Al Hroob et al., 2018; Olatunji et al., 2018; Feng et al., 2019). Interestingly, accumulating studies have shown that TMAO accelerates the progression of many inflammatory diseases, including cardiovascular disease, CKD, and central nervous system disease, by activating inflammatory pathways, such as the MAPK, NF- κ B, and NLRP3 signaling pathways, and then increasing pro-inflammatory molecules, including tumor necrosis factor alpha, IL-6, IL-1 β , and IL-18 (Seldin et al., 2016; Sun et al., 2017; Geng et al., 2018; Zhang et al., 2019, 2020). The NLRP3 inflammasome, which comprises different domains, such as NLRP3, ASC, caspase-1, IL-1 β , and IL-18, has been shown to have a crucial role in DKD (Ram et al., 2020), and to be related to renal inflammation and fibrosis (Alzahrani et al., 2020; An et al., 2020). One study has shown that NLRP3 knockout in diabetic mice protects against diabetic nephropathy, improves the urine albumin/creatinine ratio, and attenuates glomerular hypertrophy, mesangial expansion, interstitial fibrosis, inflammation, and TGF- β ₁ expression (Wu et al., 2018). Recently, several studies have shown that TMAO exacerbates cardiac fibrosis, vascular calcification, and endothelial dysfunction by activating the NLRP3 inflammasome (Boini et al., 2017; Li X. et al., 2019; Zhang et al., 2020). In the present study, we demonstrated that TMAO could increase the expression of NLRP3, caspase-1, IL-1 β , and IL-18 in the kidney of DKD rats, while TMAO could also significantly increase the protein levels of NLRP3 and caspase-1 in the kidney of normal rats. Thus, we speculate that TMAO may activate the NLRP3 inflammasome to aggravate renal inflammation to facilitate the development of DKD.

This study has some limitations. First, this study used the method of adding TMAO to increase the TMAO levels in the animals in order to explore the effects of TMAO on the disease, which was also the method used in many similar studies (Wang et al., 2011; Tang et al., 2015; Zhu et al., 2016). In the future, we intend to use TMAO inhibitors, such as DMB and iodomethylcholine, to further explore whether TMAO can be a therapeutic target for DKD. Finding new compounds that can inhibit TMAO levels is also an important research goal. Second, many studies have suggested that inflammation is an important mechanism for TMAO to promote the occurrence and development of diseases (Yang G. et al., 2019). In addition to the NLRP3 inflammasome in this study, it is also necessary to further explore whether TMAO promotes the progression of DKD through other inflammatory pathways, such as the NF- κ B, MAPK, etc. pathways. Finally, several recent studies have reported that TMAO can directly increase the production of reactive oxygen species (Govindarajulu et al., 2020; Wu et al., 2020; Chang et al., 2021). The excessive production of reactive oxygen species caused by oxidative stress plays an important role in the pathogenesis of DKD (Jha et al., 2016). At the same

time, reactive oxygen species are also a risk factor to activate the NLRP3 inflammasome (Han et al., 2018). Whether TMAO can directly activate oxidative stress to promote the progression of DKD remains to be further explored.

In conclusion, the results of our study can help improve our understanding of DKD by providing a novel mechanistic link between TMAO and DKD. We demonstrated that TMAO promotes renal inflammation and fibrosis in DKD rats. In addition, we found that NLRP3 inflammasome-mediated renal inflammation may be an important mechanism for TMAO to facilitate DKD. These findings may provide new insights into the mechanisms underlying DKD. Targeting TMAO may be a novel strategy for the prevention and treatment of DKD.

DATA AVAILABILITY STATEMENT

The raw data supporting the conclusions of this article will be made available by the authors, without undue reservation.

ETHICS STATEMENT

The animal study was reviewed and approved by the Experimental Animal Ethics Committee of the central south University.

AUTHOR CONTRIBUTIONS

QF, BZ, and NL conceived and designed the experiments. QF, BZ, NL, WL, and JL performed the experiments. QF, XH, and XZ analyzed the data. QF, LC, ZL, and DO wrote the manuscript. All authors contributed to the article and approved the submitted version.

FUNDING

This work was supported by the National Development of Key Novel Drugs for Special Projects of China (grant no. 2017ZX09304014), the Hunan Key Laboratory for Bioanalysis of Complex Matrix Samples (grant no. 2017TP1037), the Key R&D Programs of Hunan Province (grant no. 2019SK2241), the Innovation and Entrepreneurship Investment Project in Hunan Province (grant no. 2019GK5020), the International Scientific and Technological Innovation Cooperation Base for Bioanalysis of Complex Matrix Samples in Hunan Province (grant no. 2019CB1014), the Science and Technology Project of Changsha (grant no. kh1902002), and the Hunan Science and Technology Innovation Plan project (grant no. 2018SK52008).

REFERENCES

- Al Hroob, A., Abukhalil, M., Alghonmeen, R., and Mahmoud, A. (2018). Ginger alleviates hyperglycemia-induced oxidative stress, inflammation and apoptosis and protects rats against diabetic nephropathy. *Biomed. Pharmacother.* 106, 381–389. doi: 10.1016/j.biopha.2018.06.148
- Alaofi, A. (2020). viaSinaptic Acid Ameliorates the Progression of Streptozotocin (STZ)-Induced Diabetic Nephropathy in Rats NRF2/HO-1

- Mediated Pathways. *Front. Pharmacol.* 11:1119. doi: 10.3389/fphar.2020.01119
- Alicic, R., Rooney, M., and Tuttle, K. (2017). Diabetic Kidney Disease: Challenges, Progress, and Possibilities. *Clin. J. Am. Soc. Nephrol.* 12, 2032–2045. doi: 10.2215/cjn.11491116
- Alzahrani, S., Zaitone, S., Said, E., El-Sherbiny, M., Ajwah, S., Alsharif, S., et al. (2020). Protective effect of isoliquiritigenin on experimental diabetic nephropathy in rats: Impact on Sirt-1/NFκB balance and NLRP3 expression. *Int. Immunopharmacol.* 87:106813. doi: 10.1016/j.intimp.2020.106813
- An, X., Zhang, Y., Cao, Y., Chen, J., Qin, H., and Yang, L. (2020). Puncalagin protects diabetic nephropathy by inhibiting pyroptosis based on TXNIP/NLRP3 pathway. *Nutrients* 12:nu12051516. doi: 10.3390/nu12051516
- Boini, K. M., Hussain, T., Li, P.-L., and Koka, S. S. (2017). Trimethylamine-N-oxide instigates NLRP3 inflammasome activation and endothelial dysfunction. *Cell Physiol. Biochem.* 44, 152–162. doi: 10.1159/000484623
- Burdmann, E. A., Missailidis, C., Hällqvist, J., Qureshi, A. R., Barany, P., Heimbürger, O., et al. (2016). Serum Trimethylamine-N-Oxide Is Strongly Related to Renal Function and Predicts Outcome in Chronic Kidney Disease. *PLoS One* 11:0141738.
- Cansby, E., Caputo, M., Gao, L., Kulkarni, N., Nerstedt, A., Ståhlman, M., et al. (2020). Depletion of protein kinase STK25 ameliorates renal lipotoxicity and protects against diabetic kidney disease. *JCI Insight* 2020:140483. doi: 10.1172/jci.insight.140483
- Chang, Q.-X., Chen, X., Yang, M.-X., Zang, N.-I., Li, L.-Q., Zhong, N., et al. (2021). Trimethylamine N-Oxide increases soluble fms-like tyrosine Kinase-1 in human placenta via NADPH oxidase dependent ROS accumulation. *Placenta* 103, 134–140. doi: 10.1016/j.placenta.2020.10.021
- Chen, K., Feng, L., Hu, W., Chen, J., Wang, X., Wang, L., et al. (2019). Optineurin inhibits NLRP3 inflammasome activation by enhancing mitophagy of renal tubular cells in diabetic nephropathy. *FASEB J.* 33, 4571–4585. doi: 10.1096/fj.201801749RRR
- Chen, M. L., Zhu, X. H., Ran, L., Lang, H. D., Yi, L., and Mi, M. T. (2017). Trimethylamine-N-Oxide Induces Vascular Inflammation by Activating the NLRP3 Inflammasome Through the SIRT3-SOD2-mtROS Signaling Pathway. *J. Am. Heart. Assoc.* 6:006347. doi: 10.1161/JAHA.117.006347
- Chen, S., Henderson, A., Petriello, M. C., Romano, K. A., Gearing, M., Miao, J., et al. (2019). Trimethylamine N-oxide binds and activates PERK to promote metabolic dysfunction. *Cell Metab.* 2019:021. doi: 10.1016/j.cmet.2019.08.021
- Cho, C. E., Taesuwan, S., Malysheva, O. V., Bender, E., Tulchinsky, N. F., Yan, J., et al. (2017). Trimethylamine-N-oxide (TMAO) response to animal source foods varies among healthy young men and is influenced by their gut microbiota composition: a randomized controlled trial. *Mol. Nutr. Food Res.* 61:1600324. doi: 10.1002/mnfr.201600324
- Dambrova, M., Latkovskis, G., Kuka, J., Strele, I., Konrade, I., Grinberga, S., et al. (2016). Diabetes is associated with higher trimethylamine N-oxide plasma levels. *Exp. Clin. Endocrinol. Diabetes* 124, 251–256. doi: 10.1055/s-0035-1569330
- Dong, Z., Liang, Z., Guo, M., Hu, S., Shen, Z., and Hai, X. (2018). The Association between Plasma Levels of Trimethylamine N-Oxide and the Risk of Coronary Heart Disease in Chinese Patients with or without Type 2 Diabetes Mellitus. *Dis. Markers* 2018:1578320. doi: 10.1155/2018/1578320
- Feng, Y., Weng, H., Ling, L., Zeng, T., Zhang, Y., Chen, D., et al. (2019). Modulating the gut microbiota and inflammation is involved in the effect of Bupleurum polysaccharides against diabetic nephropathy in mice. *Int. J. Biol. Macromol.* 132, 1001–1011. doi: 10.1016/j.jbiomac.2019.03.242
- Gao, X., Liu, X., Xu, J., Xue, C., Xue, Y., and Wang, Y. (2014). Dietary trimethylamine N-oxide exacerbates impaired glucose tolerance in mice fed a high fat diet. *J. Biosci. Bioeng.* 118, 476–481. doi: 10.1016/j.jbiosc.2014.03.001
- Gao, X., Xu, J., Jiang, C., Zhang, Y., Xue, Y., Li, Z., et al. (2015). Fish oil ameliorates trimethylamine N-oxide-exacerbated glucose intolerance in high-fat diet-fed mice. *Food Funct.* 6, 1117–1125. doi: 10.1039/c5fo00007f
- Geng, J., Yang, C., Wang, B., Zhang, X., Hu, T., Gu, Y., et al. (2018). Trimethylamine N-oxide promotes atherosclerosis via CD36-dependent MAPK/JNK pathway. *Biomed. Pharmacother.* 97, 941–947. doi: 10.1016/j.biopha.2017.11.016
- Govindarajulu, M., Pinky, P. D., Steinke, I., Bloemer, J., Ramesh, S., Kariharan, T., et al. (2020). Gut Metabolite TMAO Induces Synaptic Plasticity Deficits by Promoting Endoplasmic Reticulum Stress. *Front. Mol. Neurosci.* 13:138. doi: 10.3389/fnmol.2020.00138
- Guo, F., Dai, Q., Zeng, X., Liu, Y., Tan, Z., Zhang, H., et al. (2020). Renal function is associated with plasma trimethylamine-N-oxide, choline, L-carnitine and betaine: a pilot study. *Int. Urol. Nephrol.* 53, 539–551. doi: 10.1007/s11255-020-02632-6
- Gupta, N., Buffa, J., Roberts, A., Sangwan, N., Skye, S., Li, L., et al. (2020). Targeted inhibition of gut microbial trimethylamine N-oxide production reduces renal tubulointerstitial fibrosis and functional impairment in a murine model of chronic kidney disease. *Am. Heart. Assoc.* 40, 1239–1255. doi: 10.1161/atvbaha.120.314139
- Han, W., Ma, Q., Liu, Y., Wu, W., Tu, Y., Huang, L., et al. (2019). Huangkui capsule alleviates renal tubular epithelial-mesenchymal transition in diabetic nephropathy via inhibiting NLRP3 inflammasome activation and TLR4/NF-κB signaling. *Phytomedicine* 57, 203–214. doi: 10.1016/j.phymed.2018.12.021
- Han, Y., Xu, X., Tang, C., Gao, P., Chen, X., Xiong, X., et al. (2018). Reactive oxygen species promote tubular injury in diabetic nephropathy: The role of the mitochondrial ros-txnip-nlrp3 biological axis. *Redox Biol.* 16, 32–46. doi: 10.1016/j.redox.2018.02.013
- Hathaway, C., Gasim, A., Grant, R., Chang, A., Kim, H., Madden, V., et al. (2015). Low TGFβ1 expression prevents and high expression exacerbates diabetic nephropathy in mice. *Proc. Natl. Acad. Sci. U.S.A.* 112, 5815–5820. doi: 10.1073/pnas.1504777112
- Heianza, Y., Sun, D., Li, X., DiDonato, J. A., Bray, G. A., Sacks, F. M., et al. (2019). Gut microbiota metabolites, amino acid metabolites and improvements in insulin sensitivity and glucose metabolism: the POUNDS Lost trial. *Gut* 68, 263–270. doi: 10.1136/gutjnl-2018-316155
- Huang, W., Xu, Y., Xu, Y., Zhou, L., and Gao, C. (2018). Short-chain fatty acids prevent diabetic nephropathy in vivo and in vitro. *Am. Diabetes Assoc.* 67(Suppl. 1):92–OR.
- Huc, T., Drapala, A., Gawrys, M., Konop, M., Bielinska, K., Zaorska, E., et al. (2018). Chronic, low-dose TMAO treatment reduces diastolic dysfunction and heart fibrosis in hypertensive rats. *Am. J. Physiol. Heart. Circ. Physiol.* 315, H1805–H1820. doi: 10.1152/ajpheart.00536.2018
- Jaworska, K., Huc, T., Samborowska, E., Dobrowolski, L., Bielinska, K., Gawlak, M., et al. (2017). Hypertension in rats is associated with an increased permeability of the colon to TMA, a gut bacteria metabolite. *PLoS One* 12:e0189310. doi: 10.1371/journal.pone.0189310
- Jha, J. C., Banal, C., Chow, B. S. M., Cooper, M. E., and Jandeleit-Dahm, K. (2016). Diabetes and kidney disease: Role of oxidative stress. *Antioxidants Redox Signal.* 25, 657–684. doi: 10.1089/ars.2016.6664
- Kanitsoraphan, C., Rattanawong, P., Charoensri, S., and Senthong, V. (2018). Trimethylamine N-Oxide and Risk of Cardiovascular Disease and Mortality. *Curr. Nutr. Rep.* 7, 207–213. doi: 10.1007/s13668-018-0252-z
- Li, L.-H., Lin, J.-S., Chiu, H.-W., Lin, W.-Y., Ju, T.-C., Chen, F.-H., et al. (2019). Mechanistic insight into the activation of the NLRP3 inflammasome by *Nisseria gonorrhoeae* in macrophages. *Front. Immunol.* 10:1815. doi: 10.3389/fimmu.2019.01815
- Li, T., Gua, C., Wu, B., and Chen, Y. (2018). Increased circulating trimethylamine N-oxide contributes to endothelial dysfunction in a rat model of chronic kidney disease. *Biochem. Biophys. Res. Commun.* 495, 2071–2077. doi: 10.1016/j.bbrc.2017.12.069
- Li, X., Geng, J., Zhao, J., Ni, Q., Zhao, C., Zheng, Y., et al. (2019). Trimethylamine N-Oxide Exacerbates Cardiac Fibrosis via Activating the NLRP3 Inflammasome. *Front. Physiol.* 10:866. doi: 10.3389/fphys.2019.00866
- Liu, L., Xia, R., Song, X., Zhang, B., He, W., Zhou, X., et al. (2020). Association between the triglyceride-glucose index and diabetic nephropathy in patients with type 2 diabetes: A cross-sectional study. *J. Diabetes Investig.* 2020:13371. doi: 10.1111/jdi.13371
- Liu, M., Han, Q., and Yang, J. (2019). Trimethylamine-N-oxide (TMAO) increased aquaporin-2 expression in spontaneously hypertensive rats. *Clin. Exp. Hypertens* 41, 312–322. doi: 10.1080/10641963.2018.1481420

- Liu, W., Wang, C., Xia, Y., Xia, W., Liu, G., Ren, C., et al. (2020). Elevated plasma trimethylamine-N-oxide levels are associated with diabetic retinopathy. *Acta Diabetol.* 58, 221–229. doi: 10.1007/s00592-020-01610-9
- Liu, Y., Kou, D., Chu, N., and Ding, G. (2020). Cathelicidin-BF attenuate kidney injury through inhibiting oxidative stress, inflammation and fibrosis in streptozotocin-induced diabetic rats. *Life Sci.* 257:117918. doi: 10.1016/j.lfs.2020.117918
- Liu, Y., Lai, G., Guo, Y., Tang, X., Shuai, O., Xie, Y., et al. (2021). Protective effect of *Ganoderma lucidum* spore extract in trimethylamine-N-oxide-induced cardiac dysfunction in rats. *J. Food Sci.* 86, 546–562. doi: 10.1111/1750-3841.15575
- Missailidis, C., Hallqvist, J., Qureshi, A. R., Barany, P., Heimbürger, O., Lindholm, B., et al. (2016). Serum Trimethylamine-N-Oxide Is Strongly Related to Renal Function and Predicts Outcome in Chronic Kidney Disease. *PLoS One* 11:e0141738. doi: 10.1371/journal.pone.0141738
- Moreno, J., Gomez-Guerrero, C., Mas, S., Sanz, A., Lorenzo, O., Ruiz-Ortega, M., et al. (2018). Targeting inflammation in diabetic nephropathy: a tale of hope. *Expert Opin. Investig. Drugs* 27, 917–930. doi: 10.1080/13543784.2018.1538352
- Vogt, N. M., Romano, K. A., Darst, B. F., Engelman, C. D., Johnson, S. C., and Carlsson, C. M. et al. (2018). The gut microbiota-derived metabolite trimethylamine N-oxide is elevated in Alzheimer's disease. *Alzheimers Res. Ther.* 10:124. doi: 10.1186/s13195-018-0451-2
- Olatunji, O., Chen, H., and Zhou, Y. (2018). Lycium chinense leaves extract ameliorates diabetic nephropathy by suppressing hyperglycemia mediated renal oxidative stress and inflammation. *Biomed. Pharmacother.* 102, 1145–1151. doi: 10.1016/j.biopha.2018.03.037
- Pelletier, C. C., Croyal, M., Ene, L., Aguesse, A., Billon-Crossouard, S., Krempf, M., et al. (2019). Elevation of Trimethylamine-N-Oxide in Chronic Kidney Disease: Contribution of Decreased Glomerular Filtration Rate. *Toxins* 11:1110635. doi: 10.3390/toxins11110635
- Pourheydar, B., Samadi, M., Habibi, P., Nikibakhsh, A., and Naderi, R. (2020). Renoprotective effects of tropisetron through regulation of the TGF- β 1, p53 and matrix metalloproteinases in streptozotocin-induced diabetic rats. *Chem. Biol. Interact.* 335:109332. doi: 10.1016/j.cbi.2020.109332
- Ram, C., Jha, A., Ghosh, A., Gairola, S., Syed, A., Murty, U., et al. (2020). Targeting NLRP3 inflammasome as a promising approach for treatment of diabetic nephropathy: Preclinical evidences with therapeutic approaches. *Eur. J. Pharmacol.* 885:173503. doi: 10.1016/j.ejphar.2020.173503
- Seldin, M., Meng, Y., Qi, H., Zhu, W., Wang, Z., Hazen, S., et al. (2016). Trimethylamine N-Oxide Promotes Vascular Inflammation Through Signaling of Mitogen-Activated Protein Kinase and Nuclear Factor- κ B. *J. Am. Heart Assoc.* 5:2767. doi: 10.1161/jaha.115.002767
- Shan, Z., Sun, T., Huang, H., Chen, S., Chen, L., Luo, C., et al. (2017). Association between microbiota-dependent metabolite trimethylamine-oxide and type 2 diabetes. *Am. J. Clin. Nutr.* 106, 888–894. doi: 10.3945/ajcn.117.157107
- Stubbs, J. R., House, J. A., Ocque, A. J., Zhang, S., Johnson, C., Kimber, C., et al. (2016). Serum Trimethylamine-N-Oxide is Elevated in CKD and Correlates with Coronary Atherosclerosis Burden. *J. Am. Soc. Nephrol.* 27, 305–313. doi: 10.1681/ASN.2014111063
- Sun, G., Yin, Z., Liu, N., Bian, X., Yu, R., Su, X., et al. (2017). Gut microbial metabolite TMAO contributes to renal dysfunction in a mouse model of diet-induced obesity. *Biochem. Biophys. Res. Commun.* 493, 964–970. doi: 10.1016/j.bbrc.2017.09.108
- Tan, X., Liu, Y., Long, J., Chen, S., Liao, G., Wu, S., et al. (2019). Trimethylamine N-Oxide Aggravates Liver Steatosis through Modulation of Bile Acid Metabolism and Inhibition of Farnesoid X Receptor Signaling in Nonalcoholic Fatty Liver Disease. *Mol. Nutr. Food Res.* 63:e1900257. doi: 10.1002/mnfr.201900257
- Tang, W. H., Wang, Z., Kennedy, D. J., Wu, Y., Buffa, J. A., Agatista-Boyle, B., et al. (2015). Gut microbiota-dependent trimethylamine N-oxide (TMAO) pathway contributes to both development of renal insufficiency and mortality risk in chronic kidney disease. *Circ. Res.* 116, 448–455. doi: 10.1161/CIRCRESAHA.116.305360
- Wang, G., Kong, B., Shuai, W., Fu, H., Jiang, X., and Huang, H. (2020). 3,3-Dimethyl-1-butanol attenuates cardiac remodeling in pressure-overload-induced heart failure mice. *J. Nutr. Biochem.* 78:108341. doi: 10.1016/j.jnutbio.2020.108341
- Wang, S., Li, Y., Fan, J., Zhang, X., Luan, J., Bian, Q., et al. (2017). Interleukin-22 ameliorated renal injury and fibrosis in diabetic nephropathy through inhibition of NLRP3 inflammasome activation. *Cell Death Dis.* 8:e2937. doi: 10.1038/cddis.2017.292
- Wang, Z., Klipfell, E., Bennett, B. J., Koeth, R., Levison, B. S., Dugar, B., et al. (2011). Gut flora metabolism of phosphatidylcholine promotes cardiovascular disease. *Nature* 472, 57–63. doi: 10.1038/nature09922
- Winther, S. A., Øllgaard, J. C., Tofte, N., Tarnow, L., Wang, Z., Ahluwalia, T. S., et al. (2019). Utility of plasma concentration of trimethylamine N-oxide in predicting cardiovascular and renal complications in individuals with type 1 diabetes. *Diabetes Care* 42, 1512–1520. doi: 10.2337/dc19-0048
- Wu, M., Han, W., Song, S., Du, Y., Liu, C., Chen, N., et al. (2018). NLRP3 deficiency ameliorates renal inflammation and fibrosis in diabetic mice. *Mol. Cell Endocrinol.* 478, 115–125. doi: 10.1016/j.mce.2018.08.002
- Wu, P., Chen, J., Chen, J., Tao, J., Wu, S., Xu, G., et al. (2020). Trimethylamine N-oxide promotes apoE^{-/-} mice atherosclerosis by inducing vascular endothelial cell pyroptosis via the SDHB/ROS pathway. *Cell. Physiol. Biochem.* 235, 6582–6591. doi: 10.1002/jcp.29518
- Yang, C., Zhao, Y., Ren, D., and Yang, X. (2020). Protective Effect of Saponins-Enriched Fraction of *Gynostemma pentaphyllum* against High Choline-Induced Vascular Endothelial Dysfunction and Hepatic Damage in Mice. *Biol. Pharm. Bull.* 43, 463–473. doi: 10.1248/bpb.b19-00805
- Yang, G., Lin, C. C., Yang, Y., Yuan, L., Wang, P., Wen, X., et al. (2019). Nobiletin Prevents Trimethylamine Oxide-Induced Vascular Inflammation via Inhibition of the NF- κ B/MAPK Pathways. *J. Agric. Food Chem.* 67, 6169–6176. doi: 10.1021/acs.jafc.9b01270
- Yang, S., Li, X., Yang, F., Zhao, R., Pan, X., Liang, J., et al. (2019). Gut Microbiota-Dependent Marker TMAO in Promoting Cardiovascular Disease: Inflammation Mechanism, Clinical Prognostic, and Potential as a Therapeutic Target. *Front. Pharmacol.* 10:1360. doi: 10.3389/fphar.2019.01360
- Yang, W., Zhang, S., Zhu, J., Jiang, H., Jia, D., Ou, T., et al. (2019). Gut microbe-derived metabolite trimethylamine N-oxide accelerates fibroblast-myofibroblast differentiation and induces cardiac fibrosis. *J. Mol. Cell Cardiol.* 134, 119–130. doi: 10.1016/j.yjmcc.2019.07.004
- Yang, Y., Wang, Y., He, Z., Liu, Y., Chen, C., Wang, Y., et al. (2020). via Trimetazidine Inhibits Renal Tubular Epithelial Cells to Mesenchymal Transition in Diabetic Rats Upregulation of Sirt1. *Front. Pharmacol.* 11:1136. doi: 10.3389/fphar.2020.01136
- Zeng, L., Xiao, Y., and Sun, L. (2019). A Glimpse of the Mechanisms Related to Renal Fibrosis in Diabetic Nephropathy. *Adv. Exp. Med. Biol.* 1165, 49–79. doi: 10.1007/978-981-13-8871-2_4
- Zhang, C., Li, Q., Lai, S., Yang, L., Shi, G., Wang, Q., et al. (2017). Attenuation of diabetic nephropathy by Sanziguben Granule inhibiting EMT through Nrf2-mediated anti-oxidative effects in streptozotocin (STZ)-induced diabetic rats. *J. Ethnopharmacol.* 205, 207–216. doi: 10.1016/j.jep.2017.05.009
- Zhang, W., Miikeda, A., Zuckerman, J., Jia, X., Charugundla, S., Zhou, Z., et al. (2021). Inhibition of microbiota-dependent TMAO production attenuates chronic kidney disease in mice. *Sci. Rep.* 11:518. doi: 10.1038/s41598-020-80063-0
- Zhang, X., Li, Y., Yang, P., Liu, X., Lu, L., Chen, Y., et al. (2020). Trimethylamine-N-Oxide Promotes Vascular Calcification Through Activation of NLRP3 (Nucleotide-Binding Domain, Leucine-Rich-Containing Family, Pyrin Domain-Containing-3) Inflammasome and NF- κ B (Nuclear Factor κ B) Signals. *Arterioscler. Thromb. Vasc. Biol.* 40, 751–765. doi: 10.1161/ATVBAHA.119.313414
- Zhang, Y., Zhang, C., Li, H., and Hou, J. (2019). The Presence of High Levels of Circulating Trimethylamine N-Oxide Exacerbates Central and Peripheral Inflammation and Inflammatory Hyperalgesia in Rats Following Carrageenan Injection. *Inflammation* 42, 2257–2266. doi: 10.1007/s10753-019-01090-2
- Zhao, L., Zhang, C., Cao, G., Dong, X., Li, D., and Jiang, L. (2019). Higher Circulating Trimethylamine N-oxide Sensitizes Sevoflurane-Induced Cognitive Dysfunction in Aged Rats Probably by Downregulating Hippocampal Methionine Sulfoxide Reductase A. *Neurochem. Res.* 44, 2506–2516. doi: 10.1007/s11064-019-02868-4
- Zhao, Z.-H., Xin, F.-Z., Da Zhou, Y.-Q. X., Liu, X.-L., Yang, R.-X., Pan, Q., et al. (2019). Trimethylamine N-oxide attenuates high-fat high-cholesterol diet-induced steatohepatitis by reducing hepatic cholesterol

- overload in rats. *World J. Gastroenterol.* 25:2450. doi: 10.3748/wjg.v25.i20.2450
- Zheng, Z., Guan, M., Jia, Y., Wang, D., Pang, R., Lv, F., et al. (2016). The coordinated roles of miR-26a and miR-30c in regulating TGF β 1-induced epithelial-to-mesenchymal transition in diabetic nephropathy. *Sci. Rep.* 6:37492. doi: 10.1038/srep37492
- Zhu, W., Gregory, J. C., Org, E., Buffa, J. A., Gupta, N., Wang, Z., et al. (2016). Gut Microbial Metabolite TMAO Enhances Platelet Hyperreactivity and Thrombosis Risk. *Cell* 165, 111–124. doi: 10.1016/j.cell.2016.02.011
- Zhuang, R., Ge, X., Han, L., Yu, P., Gong, X., Meng, Q., et al. (2019). Gut microbe-generated metabolite trimethylamine N-oxide and the risk of diabetes: A systematic review and dose-response meta-analysis. *Obes. Rev.* 20, 883–894. doi: 10.1111/obr.12843
- Conflict of Interest:** QF, BZ, NL, JL, WL, XH, XZ, LC, and DO were employed by the company Changsha Duxact Biotech Co., Ltd.
- The remaining author declares that the research was conducted in the absence of any commercial or financial relationships that could be construed as a potential conflict of interest.
- Copyright © 2021 Fang, Zheng, Liu, Liu, Liu, Huang, Zeng, Chen, Li and Ouyang. This is an open-access article distributed under the terms of the Creative Commons Attribution License (CC BY). The use, distribution or reproduction in other forums is permitted, provided the original author(s) and the copyright owner(s) are credited and that the original publication in this journal is cited, in accordance with accepted academic practice. No use, distribution or reproduction is permitted which does not comply with these terms.



In vitro Assays and Imaging Methods for Drug Discovery for Cardiac Fibrosis

Giorgia Palano¹, Ariana Foinquinos² and Erik Müllers^{2*}

¹ Division of Physiological Chemistry I, Department of Medical Biochemistry and Biophysics, Karolinska Institutet, Stockholm, Sweden, ² Bioscience Cardiovascular, Research and Early Development, Cardiovascular, Renal and Metabolism, BioPharmaceuticals R&D, AstraZeneca, Gothenburg, Sweden

OPEN ACCESS

Edited by:

Isotta Chimenti,
Sapienza University of Rome, Italy

Reviewed by:

Chiara Borrelli,
University of Pisa, Italy
Janos Palocz,
National Institutes of Health (NIH),
United States

*Correspondence:

Erik Müllers
erik.muellers@astrazeneca.com

Specialty section:

This article was submitted to
Clinical and Translational Physiology,
a section of the journal
Frontiers in Physiology

Received: 21 April 2021

Accepted: 07 June 2021

Published: 08 July 2021

Citation:

Palano G, Foinquinos A and
Müllers E (2021) *In vitro* Assays
and Imaging Methods for Drug
Discovery for Cardiac Fibrosis.
Front. Physiol. 12:697270.
doi: 10.3389/fphys.2021.697270

As a result of stress, injury, or aging, cardiac fibrosis is characterized by excessive deposition of extracellular matrix (ECM) components resulting in pathological remodeling, tissue stiffening, ventricular dilatation, and cardiac dysfunction that contribute to heart failure (HF) and eventually death. Currently, there are no effective therapies specifically targeting cardiac fibrosis, partially due to limited understanding of the pathological mechanisms and the lack of predictive *in vitro* models for high-throughput screening of antifibrotic compounds. The use of more relevant cell models, three-dimensional (3D) models, and coculture systems, together with high-content imaging (HCI) and machine learning (ML)-based image analysis, is expected to improve predictivity and throughput of *in vitro* models for cardiac fibrosis. In this review, we present an overview of available *in vitro* assays for cardiac fibrosis. We highlight the potential of more physiological 3D cardiac organoids and coculture systems and discuss HCI and automated artificial intelligence (AI)-based image analysis as key methods able to capture the complexity of cardiac fibrosis *in vitro*. As 3D and coculture models will soon be sufficiently mature for application in large-scale preclinical drug discovery, we expect the combination of more relevant models and high-content analysis to greatly increase translation from *in vitro* to *in vivo* models and facilitate the discovery of novel targets and drugs against cardiac fibrosis.

Keywords: cardiac fibrosis, *in vitro* assays, 3D models, co-culture systems, high-content imaging, drug discovery

INTRODUCTION

Cardiac fibrosis is a common feature in the pathology of many forms of cardiovascular diseases. It is characterized by excessive production and deposition of extracellular matrix (ECM) components in the connective tissue of the heart, mainly collagens, that confer stiffness and loss of contractility, thereby reducing cardiac function (reviewed in Kong et al., 2014; Liu et al., 2017).

Abbreviations: 3D, three-dimensional; AI, artificial intelligence; ECM, extracellular matrix; TGF- β , transforming growth factor-beta; PDGF, platelet-derived growth factor; TNF α , tumor necrosis factor-alpha; HF, heart failure; IL-1 β , interleukin-1 beta; TAK1, transforming growth factor- β -activated kinase 1; JNK, c-Jun N-terminal kinase; PI3K, phosphoinositide 3-kinase; RhoA, Ras homolog family member A; α -SMA, alpha-smooth muscle actin; MMPs, matrix metalloproteinases; CCN2, connective tissue growth factor; RT-qPCR, real-time quantitative polymerase chain reaction; IF, immunofluorescence; ELISA, enzyme-linked immunosorbent assay; WB, Western blot; PICP, procollagen type I carboxy-terminal propeptide; SEM, scanning electron microscopy; HPCL, high-performance liquid chromatography; LC-MS, liquid chromatography-mass spectrometry; MS, mass spectrometry; iPSCs, induced pluripotent stem cells; HCI, high-content imaging; RAAS, renin-angiotensin-aldosterone system; ML, machine learning.

At the cellular level, the main cells responsible for cardiac fibrosis are cardiac fibroblasts (CFs), which are producing collagen and other ECM proteins. Following cardiac injury, CFs become activated and can differentiate into myofibroblasts (myoFBs), a cell type exhibiting stress fibers and characterized by the expression of alpha-smooth muscle actin (α -SMA) and other contractile proteins (Gabbiani et al., 1971; Skalli et al., 1989). It is well known that one of the molecular mechanisms driving cardiac fibrosis is the transforming growth factor-beta (TGF- β) signaling pathway. TGF- β is a potent inducer of collagen synthesis that can induce phenotypic changes in CFs and their differentiation into myoFBs (Desmouliere et al., 1993). MyoFBs secrete high levels of ECM proteins, such as collagens, including collagen type I, which is the most abundant protein of the cardiac ECM and the main component of fibrotic tissue. It is synthesized as a collagen precursor (procollagen) that is processed to form mature collagen, which is released into the extracellular space (reviewed in Canty and Kadler, 2005). The excessive accumulation of mature collagen and deposition of ECM can lead to either reparative fibrosis or reactive fibrosis. Reparative fibrosis is mainly seen after an acute myocardial infarction (MI) to replace dead cardiomyocytes with fibrotic scar tissue or in end-stage heart failure (HF). Also, reactive fibrosis is seen after MI and HF, but it mainly occurs as a pathological condition related to age and HF with preserved ejection fraction (HFpEF) (Heymans et al., 2015).

Preclinical studies indicate that cardiac fibrosis can be attenuated, reduced, and even reversed by the pharmaceutical intervention (Nagaraju et al., 2019). Thus, there is an enormous interest to find new treatments for cardiac fibrosis and to better understand its pathogenesis. New promising pathways involving several noncoding RNAs, such as microRNA 21 (miRNA-21), miR-208a, nuclear enriched abundant transcript 1 (Neat1), and maternally expressed 3 (Meg 3), have emerged in preclinical studies. Also, candidates like galectin-3 (Gal-3), neutrophil gelatinase-associated lipocalin (NGAL), cardiotrophin-1 (CT-1), and NADPH oxidase 2 (NOX2) have been associated clinically and preclinically with collagen dysregulation (Sharma et al., 2004; Yndestad et al., 2009; Murdoch et al., 2014; Heymans et al., 2015; Piccoli et al., 2017; Kenneweg et al., 2019).

Physiologically relevant, predictive, and reliable *in vitro* assays are required to study the underlying molecular mechanisms and to find drugs against cardiac fibrosis. In this study, we review different assays and imaging methods to detect cardiac fibrosis *in vitro*, and we discuss the challenges and future directions of the development of novel assays.

IN VITRO ASSAYS FOR CARDIAC FIBROSIS

Challenges Assessing Cardiac Fibrosis *in vitro*

Cardiac fibrosis is a complex, multistep cellular and molecular process that takes weeks to months *in vivo* and has, thus, proven difficult to recapitulate *in vitro*. Progress to develop

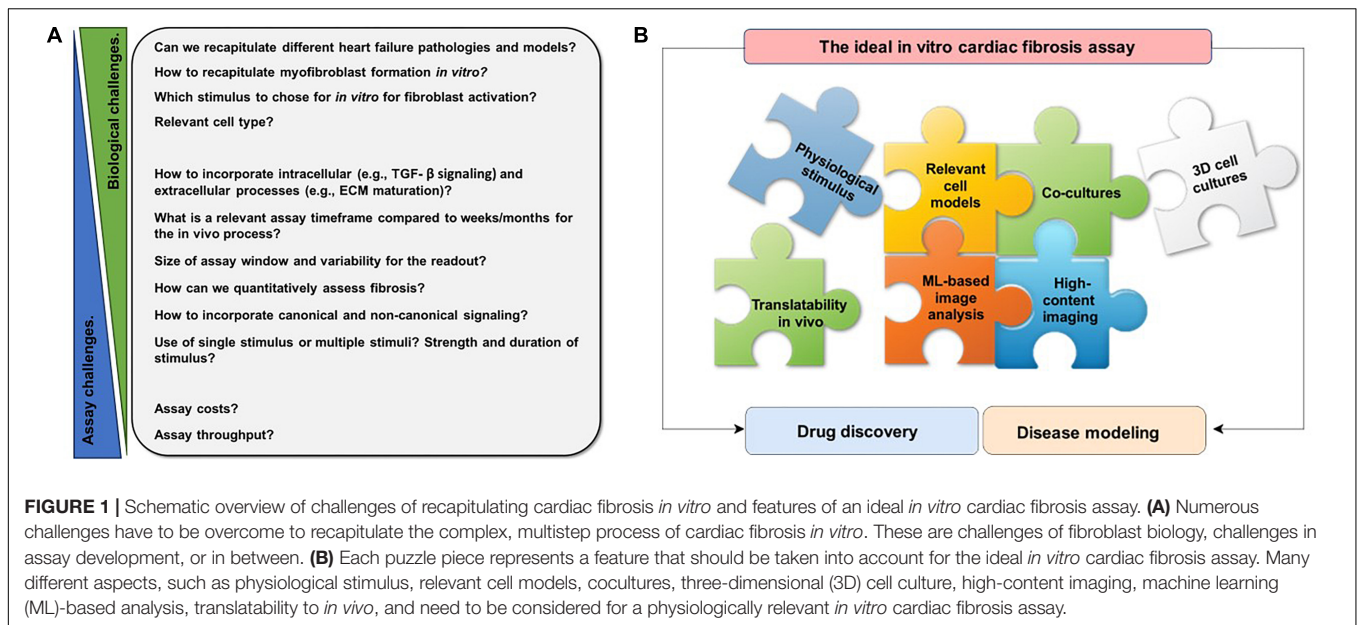
physiologically relevant cardiac cell culture models has been slower compared to other organ tissues, for example, kidney, liver, or tumors. The discovery of treatments for cardiac fibrosis has, therefore, been hampered by the lack of reliable and predictive *in vitro* assays with sufficient throughput for drug discovery. An ideal cardiac fibrosis assay needs to recapitulate multiple, highly complex processes, such as:

- (a) Formation of myoFBs, which differentiate from fibroblasts or epithelial to mesenchymal trans-differentiation upon induction of cytokine, and differentiation to CFs (Bryant et al., 2009; Li et al., 2016).
- (b) Activation/differentiation of fibroblasts, driven by multiple cytokine stimuli such as TGF- β , angiotensin II, platelet-derived growth factor (PDGF), endothelin-1, tumor necrosis factor-alpha (TNF α), interleukin-1 beta (IL-1 β), and others, inflammation-mediated or triggered by mechanical stress (reviewed in Aujla and Kassiri, 2021).
- (c) Activation of multiple canonical (e.g., Smad3/4) and noncanonical [e.g., transforming growth factor- β -activated kinase 1 (TAK1), c-Jun N-terminal kinase (JNK), phosphoinositide 3-kinase (PI3K), and Ras homolog family member A (RhoA) (reviewed in Zhang, 2017) signaling pathways, resulting in the induction of fibrogenic gene transcription] encoding proteins such as α -SMA, collagen, matrix metalloproteinases (MMPs), and connective tissue growth factor (CCN2), which increase deposition of collagen and other ECM proteins.
- (d) Production, secretion, processing, and maturation of ECM proteins such as collagens (Canty and Kadler, 2005).

Thus, there are multiple challenges to recapitulating cardiac fibrosis in a dish (**Figure 1A**). The ideal cardiac fibrosis assay should build on physiologically relevant cells and needs to incorporate relevant readouts. In order to be applicable for drug screening, it needs to be robust, cost- and time-effective, and high-throughput. If possible, it should recapitulate the effects of three-dimensional (3D) structure and incorporate multiple relevant cell types involved. Finding the ideal *in vitro* assay is a complex puzzle of many pieces (**Figure 1B**).

Readouts of Cardiac Fibrosis Assays

Naturally, *in vitro* assays can only recapitulate parts of the *in vivo* situation. MyoFB is central to cardiac fibrosis and, thus, to any cardiac fibrosis *in vitro* assay. Formation of myoFB and activation of fibroblast can result from different cell types and integrating several major biochemical pathways (**Figure 2A**). In principle, any of these pathways and their downstream signaling can provide the basis for an assay readout. Notably, an *in vitro* assay is often limited to a single or few cell types (see sections “Cell Models” and “Three-Dimensional Models and Coculture Systems”), therefore, limiting the possibility of paracrine fibroblast activation. In fibroblast-only cell culture, TGF- β is the major pathway for activation of fibroblast and the stimulus of choice for the majority of cardiac fibrosis assays (**Figure 2B**).



Current cardiac fibrosis assays can broadly be divided into four groups based on their main readout: (a) TGF- β pathway activation/TGF- β -dependent gene expression; (b) α -SMA expression; (c) (mature) collagen detection; and (d) fibroblast proliferation or migration (**Figure 2B** and **Table 1**).

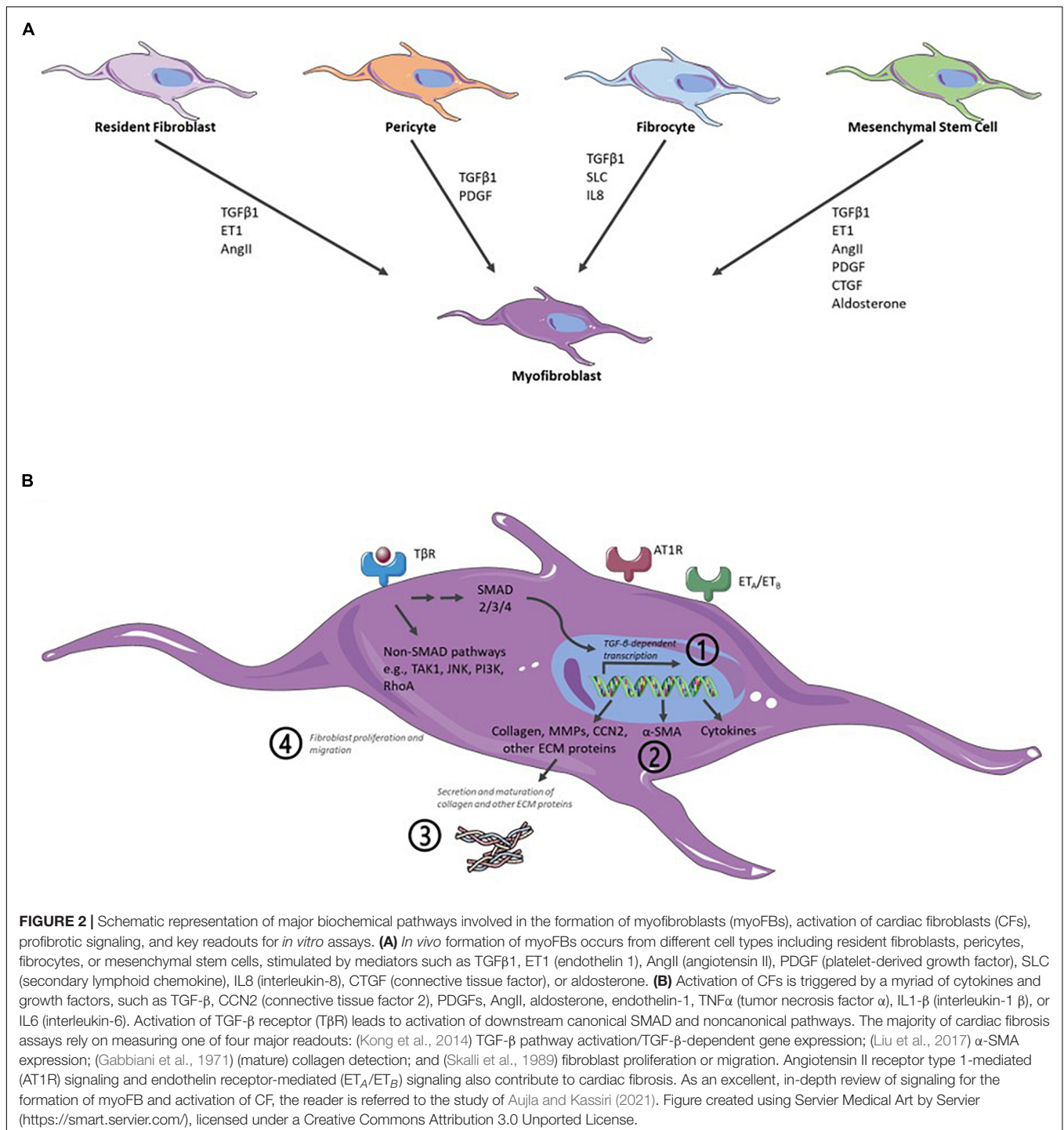
Due to the complexity of fibrosis *in vivo*, it is very difficult to mimic with a single *in vitro* assay. Typically, each assay aims to model a key event in the fibrotic pathway, such as myoFB differentiation, TGF- β pathway activation, or collagen production. These assays are well suited to capture the respective parts of the fibrotic process and to evaluate specific effects of compounds *in vitro*; nonetheless, the current assays have a poor history of finding hits that translate to clinical applications. The reasons for this are manifold. Target- or biomarker-specific assays capture a single process very well but do not capture cardiac fibrosis as a whole. Reporter cell lines for TGF- β -dependent gene expression allow for robust, cell-based, and high-throughput screening (Tesseur et al., 2006). However, the engineered cells do not fully reflect the physiology of CFs. Hits are likely limited to the TGF- β -receptor \rightarrow SMAD3/4 \rightarrow TGF- β -dependent gene expression signaling axis and, thus, limited to early signaling nodes and TGF- β as a stimulus. Such assays can provide valuable information for target deconvolution, i.e., they can indicate or exclude specific target/pathway activity if the target or mechanism of action for a hit compound is not known. As such, they should be integral parts of a drug-screening cascade for cardiac fibrosis.

Similarly, assays that measure biomarkers, such as quantification of PICP (propeptide of procollagen type I) or hydroxyproline, can provide valuable information in a drug-screening cascade. Assessing these biomarkers *in vitro* increases the understanding of the mechanism of action of a compound and, thus, improves the chances for *in vivo* translation. As such, these types of assays are best suited for not only initial

high-throughput screening (HTS) but also downstream profiling of hits.

Alpha-smooth muscle actin protein expression is an early hallmark in cardiac fibrosis. Many high-quality immunoreagents are available, and thus, especially immunofluorescence of α -SMA has emerged as an attractive readout to screen for compounds with antifibrotic activity in the heart (Rehman et al., 2019) or other tissues (Sieber et al., 2018; Weigle et al., 2019). Formation and secretion of mature collagen follow further downstream of TGF- β and α -SMA (**Figure 2B**). Quantification of mature collagen integrates upstream signaling, and, as a major component of excessive production of ECM, collagen contributes to the *in vivo* pathomechanism. However, there are many different forms of collagen and assays and reagents to specifically and quantitatively assess whether mature collagen is sparse. Interestingly, several recent screening approaches utilize immunofluorescence of both α -SMA and collagen, which could be seen as the first step to a multiparametric approach (Weigle et al., 2019; Turner et al., 2020).

Schimmel et al. (2020) analyzed three readouts, namely, the proliferation of human CFs, modulation of apoptosis, and expression of ECM, when screening a natural compound library for molecules for the treatment of cardiac fibrosis. Sieber et al. (2018) combined high-content imaging (HCI) with an impedance-based assay and multiplexed quantification of α -SMA and collagen 1 α . The incorporation of multiple readouts adds additional information and reduces the intrinsic bias in any screening assay (Abraham et al., 2014). Omics-type approaches, such as transcriptomics, proteomics, and phenomics (i.e., HCI), are phenotypic drug discovery approaches and as such provide the opportunity to discover novel targets or compounds with novel mechanisms of action. Although less biased and very rich in information, they require special infrastructure, expertise, and



resources to deconvolute the hits from a screen (also see section “High-Content Imaging”).

Cell Models

The *in vitro* cell model is of high importance for antifibrotic effects to translate to *in vivo*. More physiologically relevant cell models often come with higher complexity and, thus, lower throughput for drug screening (Horvath et al., 2016; Table 2).

The NIH 3T3 murine fibroblast cell line is a widely used cell line for proof-of-concept studies due to their high cell proliferation rate and easy handling in cell culture. TGF-β1 treatment of NIH 3T3 fibroblasts results in transformation into activated myoFBs with characteristics of α-SMA (Desmouliere et al., 1993) and collagen expression (Grande et al., 1997). Primary fibroblasts isolated from rat or murine hearts are an alternative model that many researchers chose for their translational advantages

TABLE 1 | Examples of assays to assess features of cardiac fibrosis *in vitro*.

| Assay readout | Method (example references) | Advantages | Limitations |
|--|---|--|---|
| TGF- β -dependent gene expression | RT-qPCR (Ranganathan et al., 2007) | <ul style="list-style-type: none"> • High sensitivity • Quantitative analysis | <ul style="list-style-type: none"> • Often measurement of a single/a few gene(s) only |
| TGF- β dependent gene expression | Reporter cell lines (Tesseur et al., 2006) | <ul style="list-style-type: none"> • High-throughput^a • Quantitative analysis | <ul style="list-style-type: none"> • Bias to a single promoter readout • Requires cell line engineering |
| α -SMA protein expression | IF staining (Shinde et al., 2017; Baranyi et al., 2019) | <ul style="list-style-type: none"> • Allows assessment of intracellular localization and single-cell analysis • Quantitative analysis • Can be set up in high-throughput • Sensitive to changes in cell number and density | <ul style="list-style-type: none"> • Requires quantitative fluorescence microscopy instruments • Dependent on good, specific immunoreagents • Requires only low cell number |
| Collagen protein expression | Western blot | <ul style="list-style-type: none"> • Detection of different forms and type • Semi-quantitative analysis | <ul style="list-style-type: none"> • Antibodies exist only in specific forms and types of collagen • Highly dependent on immunoreagents • Requires larger amounts of cells |
| Collagen protein expression | ELISA (Baranyi et al., 2019) | <ul style="list-style-type: none"> • High sensitivity and specificity • Quantitative analysis • Can be set up in high-throughput • Requires less material than WB | <ul style="list-style-type: none"> • Dependent on immunoreagents |
| Visualization of collagen fibers | Sirius Red dye (Junqueira et al., 1979; Whittaker et al., 1994) | <ul style="list-style-type: none"> • Mature collagen fiber formation is a late hallmark of cardiac fibrosis • Semi-quantitative analysis | <ul style="list-style-type: none"> • <i>In vivo</i> method that is difficult to adapt to <i>in vitro</i> |
| Visualization of collagen fibers | Masson's trichrome staining | <ul style="list-style-type: none"> • Mature collagen fiber formation is a late hallmark of cardiac fibrosis • Semi-quantitative analysis | <ul style="list-style-type: none"> • <i>In vivo</i> method that is difficult to adapt to <i>in vitro</i> |
| Collagen peptide detection | PIP (Querejeta et al., 2000, 2004) | <ul style="list-style-type: none"> • <i>In vivo</i> biomarker that can be adapted to <i>in vitro</i> • Quantitative analysis • Potentially high-throughput | <ul style="list-style-type: none"> • Bias to a single-marker readout that is not fully specific for cardiac fibrosis |
| Direct visualization of collagen fibers | Electron microscopy | <ul style="list-style-type: none"> • Mature collagen fiber formation is a late hallmark of cardiac fibrosis | <ul style="list-style-type: none"> • No quantitative analysis • Requires electron microscopy equipment and expertise, usually only available in highly specialized laboratories • Low throughput • Does not distinguish different types and forms |
| Hydroxyproline quantification | HPCL/LC-MS (Qiu et al., 2014) | <ul style="list-style-type: none"> • <i>In vivo</i> biomarker that can be adapted to <i>in vitro</i> • Quantitative analysis | <ul style="list-style-type: none"> • Requires HPLC capabilities, mass spectrometry equipment, and high-level of technology-specific expertise • Bias to a single-marker readout that is not specific for cardiac fibrosis |
| Collagen detection | MS (van Huizen et al., 2020) | <ul style="list-style-type: none"> • Possible to detect different forms and types of collagen • Semi-quantitative analysis | <ul style="list-style-type: none"> • Low throughput • Requires mass spectrometry instrument and high-level of technology-specific expertise |
| Cardiac fibroblast migration | Cell migration assay (scratch assay) (Liang et al., 2007) | <ul style="list-style-type: none"> • Semi-quantitative analysis • Medium throughput | <ul style="list-style-type: none"> • Can be adapted for 3D and coculture models |
| Cardiac fibroblast proliferation | Cell count or proliferation markers | <ul style="list-style-type: none"> • Quantitative analysis • Low cost and high-throughput • Adaptable for IF staining and imaging • Can be combined with ELISA and/or flow cytometry • Can be adapted for 3D and coculture models | <ul style="list-style-type: none"> • Counter-screening required to identify fibroblast-specific proliferators • Fibroblast proliferation is not predictive for cardiac fibrosis |
| Multiparametric readout, i.e., phenotypic fingerprints | Transcriptomics or proteomics (Barallobre-Barreiro et al., 2012; Abonnenc et al., 2013; Jonsson et al., 2016) | <ul style="list-style-type: none"> • Multiple parameters integrated to score fibrosis phenotype • Allows for unbiased detection of also unknown phenotypes | <ul style="list-style-type: none"> • Necessary instrumentation is usually only available in highly specialized laboratories • Requires infrastructure for data handling and specific expertise for data analysis • High cost and low throughput • Little precedence for <i>in vitro</i> application • Readouts can be difficult to interpret |

(Continued)

TABLE 1 | Continued

| Assay readout | Method (example references) | Advantages | Limitations |
|--|---|--|---|
| Multiparametric readout, i.e., phenotypic fingerprints | High-content imaging (Pantazis et al., 2010; Palano et al., 2020) | <ul style="list-style-type: none"> • Multiple parameters integrated to score fibrosis phenotype • Allows for unbiased detection of also unknown phenotypes • Low cost and high-throughput • Single-cell analysis | <ul style="list-style-type: none"> • Requires quantitative fluorescence microscopy instruments • Requires infrastructure for data handling and specific expertise for data analysis |

^aAn assay is considered high-throughput if it can generally be run in 96-well format at reagent costs > 1\$ per data point.

(Sahadevan and Allen, 2021). Using primary cells requires specific techniques of cell isolation and culture to maintain them for a limited amount of passages. Special care is to be taken as cultured primary fibroblasts differentiate into myoFBs *in vitro* upon prolonged culture and repeated passaging (Santiago et al., 2010). From a translational point of view, human primary fibroblasts derived from cardiac tissue are the leading choice. They are commercially available and allow us to study the remodeling of both physiological and pathological cardiac matrix. However, primary fibroblasts can be transformed after prolonged culture (Baranyi et al., 2019). Other important factors to consider when using primary fibroblasts in drug screening campaigns are the need for supply of large amounts of cells and donor-to-donor variations, i.e., the risk that findings might be specific to a certain donor. The use of immortalized primary CFs can mitigate some of these issues and thus reduce assay variability.

Three-Dimensional Models and Coculture Systems

Two-dimensional (2D) monocultures are inherently unable to represent the complexity of *in vivo* cardiac structure, dynamics, and microenvironment. The development of 3D models and coculture systems could help to better mimic antifibrotic effects *in vitro*.

Multiple 3D cardiac organoid systems have been described (reviewed in Zuppinger, 2019). Organoids can be generated from induced pluripotent stem cells (iPSCs) that can be differentiated into different cardiac cell types, such as cardiomyocytes, endothelial cells, and fibroblasts (Filippo Buono et al., 2020). Alternatively, organoids can be generated from patient-derived primary cells, which of one or several cell types. Combinations of iPSCs, primary cells, and/or cell lines also exist. As 3D cardiac organoids can better recapitulate structure, cell composition, and function of heart tissue, they improve upon current multi-scaled drug screening platforms including *in vitro* assays and modeling diseases like cardiac fibrosis (Nugraha et al., 2018). The 3D models are currently being developed to fully recapitulate the composition of ECM, spatial distributions of cells, architectural organization of ECM, and cell crosstalk. Thus, 3D cardiac organoids are an attractive alternative *in vitro* model for cardiac diseases and HF. They are a promising tool for drug screening and assessing cardiotoxic effects, proliferation, and cell viability (Polonchuk et al., 2017) and can potentially contribute to the development of more physiologically relevant preclinical

TABLE 2 | Cell models used in *in vitro* cardiac fibrosis assays.

| Cell model | Advantages | Limitations |
|---|--|---|
| NIH 3T3 murine fibroblasts | <ul style="list-style-type: none"> • High cell proliferation rate • Easy handling • Unlimited cell supply | <ul style="list-style-type: none"> • Limited translation to <i>in vivo</i> studies |
| Primary rat or murine cardiac fibroblasts | <ul style="list-style-type: none"> • Higher physiological relevance • Better translation to <i>in vivo</i> as mouse or rat is often the first <i>in vivo</i> model | <ul style="list-style-type: none"> • Requires specific techniques of isolation and culture • Cells differentiate to myofibroblasts upon prolonged culture • Limited amount of passages |
| Primary human cardiac fibroblasts | <ul style="list-style-type: none"> • Higher likelihood for translation to clinical studies • Allow to study physiological and pathological matrix remodeling | <ul style="list-style-type: none"> • Can be transformed after prolonged culture • Limited cell supply • High costs • Donor-to-donor variations |
| Immortalized human cardiac fibroblasts | <ul style="list-style-type: none"> • Higher likelihood for translation to clinical studies • Larger amount of passages • Reduces assay variability | <ul style="list-style-type: none"> • High costs |

platforms to better predict *in vivo* drug efficacy. They can also be used for drug discovery for personalized medicine (Nugraha et al., 2019).

Coculture systems of different cardiac cell types have been developed both in 2D and 3D. Coculture of multiple cardiac cell types can better model disease features such as cardiac fibrosis (Baudino et al., 2008). However, finding physiologically relevant coculture models to develop cardiac fibrosis assays is challenging. Among others, it needs to identify optimal cell types (Pinto et al., 2016; Litvinukova et al., 2020), culture conditions (Zuppinger, 2019), and coculture cell ratios (Pinto et al., 2016), so that the coculture better mimics the *in vivo* situation.

From the perspective of an assay, it is important to understand whether a 3D and/or coculture model has greater physiological relevance, i.e., predictivity, for cardiac fibrosis. To adequately compare models, it is essential to use holistic, integrative readouts, i.e., a better model might show more *in vivo*-like (Kong et al., 2014) gene expression (Chothani et al., 2019), (Liu et al., 2017) protein expression, (Gabbiani et al., 1971) organoid structure and cellular composition (Lee et al., 2019),

or (Skalli et al., 1989) more *in vivo*-like functional response, that is, higher predictivity for known modulators of cardiac fibrosis (Palano et al., 2020).

We are currently on the brink, where not only 2D but also 3D and coculture models are constantly improved and display their greater relevance. They will soon reach sufficient throughput, cost-effectiveness, and robustness for applications in large-scale drug screening.

HIGH-CONTENT IMAGING

High-Content Imaging to Measure Cardiac Fibrosis *in vitro*

High-content imaging is a particularly attractive method to assay complex phenotypes such as cardiac fibrosis. Traditionally, HCI has been used as a cost-effective way to assess one or a few readouts that are thought to be most relevant for the process, e.g., antibody staining for α -SMA levels or certain forms of collagen as a proxy for cardiac fibrosis (see section “Readouts of Cardiac Fibrosis Assays”). Nowadays, staining, imaging, and image analysis can be automated in multi-well format, which allows to minimize the number of precious cells, reduces the number of reagents needed, and, thus, reduces costs, while at the same time increasing throughput and robustness. Modern image analysis methods allow us to integrate hundreds of parameters from microscopy images, i.e., creating a phenotypic profile instead of a single-marker readout [reviewed in Warchal et al. (2016); Scheeder et al. (2018)].

A Phenotypic High-Throughput *in vitro* Cardiac Fibrosis Assay

We recently established cell culture conditions that promote deposition of mature collagen from primary human CFs *in vitro* (Palano et al., 2020). Based on these conditions, we set up a high-content immunofluorescence assay allowing for high-throughput, phenotypic identification of compounds with antifibrotic activity (Palano et al., 2020). Features extracted from the microscopy images, such as fluorescence intensity, cellular morphology, and staining texture, served as a basis for a linear classifier to classify cells into fibrotic or non-fibrotic phenotype. The assay can be run at low costs in 96-well or 384-well format, allowing to robustly assess the values of dose dependency and half-maximal effective concentration (EC50) potency for potential antifibrosis *in vitro*. Our *in vitro* assay correctly identified compounds with reported antifibrotic effects *in vivo*, targeting diverse cellular pathways (Palano et al., 2020), thus, highlighting its utility for high-throughput screening to discover novel compounds and targets for the treatment of cardiac fibrosis. The HCI assay has several advantages, i.e., (1) screening in high-throughput; (2) analyses in microwell format requiring fewer cells and minimizing the amounts of reagents; and (3) quantification of multiparametric readouts on a single-cell basis. In comparison with other traditional approaches, the *in vitro* cardiac fibrosis assay coupled with HCI analysis is ideal for large-scale screening and machine learning (ML)-based drug

discovery. However, the *in vitro* phenotypic assay might not be able to fully reflect *in vivo* conditions of cardiac fibrosis. From the perspective of drug discovery, the hit compounds identified in our *in vitro* cardiac fibrosis assay need to be validated in more complex systems, such as 3D models, that could better mimic antifibrotic effects *in vivo*. In this way, the most promising candidates can be identified and selected for further characterization in animal models of cardiac fibrosis.

Perspective and Outlook

The incorporation of multiple complex features instead of a single-marker readout reduces the intrinsic bias of any screening assay toward its readout (Abraham et al., 2014). These profiles can be analyzed by ML-based classification of the fibrotic phenotype on a well or single-cell level. HCI-based phenotypic classification also biases an assay toward the desired phenotype that the experimenter used to train the classification algorithm. While unsupervised ML approaches can partly mitigate this bias (Grys et al., 2017), robust validation of the control conditions (e.g., fibrotic and non-fibrotic) by orthogonal methods is essential to ensure that the phenotype, thus, hit compounds, and targets will be biologically relevant (Scannell and Bosley, 2016; Moffat et al., 2017).

Phenotypic drug discovery approaches are especially well suited to discover novel targets or novel compound mechanisms of action. Often, however, it is very resource intensive to deconvolute the hits from a screen. A combination of phenotypic and multiparametric assays, with clustered regularly interspaced short palindromic repeats (CRISPR)-based library screening, provides an attractive alternative. Turner et al. (2020) recently described an image-based CRISPR screening to identify regulators of kidney fibrosis. The authors used α -SMA as their main readout, combined with fibroblast proliferation and collagen expression, to identify genetic hits and novel targets in kidney fibrosis (Turner et al., 2020).

Major advantages of HCI compared with, for example, transcriptomics or proteomics are its lower cost and single-cell resolution. As such, HCI is well suited also for the analysis of 3D models and coculture systems. The increased complexity of these models requires single-cell resolution and analysis of diverse morphological characteristics to leverage their higher physiological relevance. In the long run, incorporation of multiplex staining mass cytometry could further increase the number of cellular markers and analyzed parameters while providing subcellular resolution, further reducing the number of precious cells needed (Giesen et al., 2014). However, 3D models still present major challenges for whole-mount imaging, data storage, image analysis, and data interpretation, warranting investment and further research studies to demonstrate their value to improve drug discovery (reviewed in Booij et al., 2019). The 2D and 3D models need to be carefully compared for their predictive value of *in vivo* efficacy.

Application of HCI and image analysis using ML-based classifiers, as in our phenotypic cardiac fibrosis assay (see section “A Phenotypic High-Throughput *in vitro* Cardiac Fibrosis Assay”; Palano et al., 2020), provides a way forward to develop such an assay toward a coculture and/or 3D model. Having set up

a robust biochemical validation and a toolbox of known *in vivo* modulators of cardiac fibrosis allows for direct comparison and assay optimization toward increased predictivity of *in vivo* outcomes and, thus, increased physiological relevance.

It is attractive to envision a multiparametric assay, such as our HCI assay, as the basis of a screening cascade for novel treatments of cardiac fibrosis. The combination of HCI and ML provides a low-cost high-throughput assay for either screening chemical libraries for new equity or screening CRISPR libraries to identify new targets. Counterscreening for TGF- β pathway modulation could be a second level to provide an initial indication of the mechanism of action. Hits could then be profiled further downstream the cascade in coculture and/or 3D model that builds on similar HCI/ML principles before going *in vivo*.

Another interesting direction would be to develop multiparametric assays for different pathological models. Fibrosis is a hallmark of different pathologies of HF. Tool compounds that modulate specific phenotypes of fibrosis *in vivo* could be used to train ML models to recognize and predict specific mechanisms of actions in *in vitro* assays. Also, here continued assay development will lead the way, such as to choose physiologically relevant stimuli, cell composition, i.e., coculture, and/or pathology-specific patient cells, and to choose the best readouts to capture different pathologies of HF.

FUTURE DIRECTIONS

What We Still Need to Know About Fibroblasts

To better characterize *in vitro* models of cardiac fibrosis and to get more reliable and translational results, it is important to have a better understanding of the biology of CFs. Cardiac fibrosis is an extremely complex process, and, on one hand, blocking it to restore cardiac function and prevent disease progression into HF is the ultimate aim. On the other hand, once cardiac fibrosis is established, the question is to what extent it can be reversed. A recent study, examining the possibility of phenotypic reversion of fibrosis, found that by inhibiting TGF- β 1 receptor kinase in CFs isolated from cardiac tissue collected from patients, they could promote dedifferentiation of myoFBs and reduce the expression profile of certain profibrotic genes (Nagaraju et al., 2019).

But the question remains whether these findings would translate to an *in vivo* scenario. Due to their phenotypic plasticity, fibroblasts can be reverted to a quiescent phenotype. Recent studies have shown that CFs can be maintained in a resting state *in vitro* using elastic silicone substrate (Landry et al., 2019) or can be reversed by culturing them on soft hydrogels or blocking them with inhibitors (Gilles et al., 2020). Using small molecule inhibitors, cardiac fibrosis can be attenuated in mouse models (Wang et al., 2018).

However, the challenges of reversing fibrosis go beyond the properties of fibroblast itself, but they extend to the reabsorption of the ECM by reducing expression of α -SMA and production of collagen (Shinde et al., 2017) and to the restoration of the cardiac

structure. For this to work, cooperation between all cardiac cell types is needed.

Current *in vitro* Assays Driving Drug Development

Currently available *in vitro* assays have contributed to drug candidates targeting cardiac fibrosis, such as TGF- β inhibitors, renin-angiotensin-aldosterone system (RAAS) inhibitors, endothelin inhibitors, MMP inhibitors, relaxin, and others (reviewed in Fang et al., 2017). Their failure in clinical trials highlights the need for more physiologically relevant assays to discover new antifibrotic drugs.

In a recent study, a novel antifibrotic therapeutic based on a naturally derived substance was developed using two different hypertension-dependent rodent models (Schimmel et al., 2020). These antifibrotic drug candidates were identified by functional screening of 480 chemically diverse natural compounds in primary human CFs, subsequent validation, and mechanistic *in vitro* and *in vivo* studies. High-throughput natural compound library screening identified 15 substances with antiproliferative effects. Hits were analyzed for dose-dependent inhibition of proliferation, modulation of apoptosis, and expression of ECM. Using multiple *in vitro* fibrosis assays and stringent selection algorithms, the authors identified the steroid bufalin and the alkaloid lycorine to be effective antifibrotic molecules both *in vitro* and *in vivo*. These *in vitro* findings were confirmed *in vivo* with an angiotensin II-mediated murine model of cardiac fibrosis in both preventive and therapeutic settings and in the Dahl salt-sensitive rat model (Schimmel et al., 2020). Another study, using NIH 3T3 mouse fibroblasts, demonstrated that long noncoding RNA (lncRNA) Neat1 has important functions for fibroblast survival, migration, and proliferation. These findings were confirmed in a MI model using the genetic loss of Neat1 mice (Kenneweg et al., 2019). Likewise, noncoding RNAs, such as miRNA-21, miR-208a, and Meg 3, have recently emerged as promising targets (Piccoli et al., 2017; Kenneweg et al., 2019). Studies like these promote new angles for therapeutic approaches with regard to antifibrotic agents and highlight the translational importance of well-established *in vitro* assays for the discovery of novel targets and development of drugs against cardiac fibrosis.

CONCLUSIONS: WHERE ARE WE HEADING?

The switch from immortalized cell lines to primary cells, cocultures, and 3D models is a step forward in filling the translational gap. The use of more physiologically relevant *in vitro* models in preclinical development will lead to drugs having better efficacy and safety parameters *in vivo* and in the clinic. For *in vitro* effects to translate to *in vivo*, it is essential that the *in vitro* assay readout is predictive for *in vivo* effects. For cardiac fibrosis, assays with single, well-defined readouts have shown only limited translatability toward *in vivo*. Multiparametric readouts, such as omics or high-content techniques, provide a way forward, integrating a holistic, phenotypic fibrotic response. HCI provides a multiparametric

readout at low costs, suitable for high-throughput screening, and it allows analysis on a single-cell level thus supporting analysis of cocultures and 3D models. These advantages make HCI and ML-based data analysis our method of choice for multiparametric assessment of cardiac fibrosis. As these new approaches come not without challenges and the need for investments, there remains a strong need for these technologies and each *in vitro* assay setup to clearly demonstrate improved predictivity toward *in vivo* and ultimately translation to the clinics. Ideally, *in vitro* assay setups are cross validated with collections of molecules that have confirmed the benefits of treating cardiac fibrosis *in vivo*. In addition, Booij et al. (2019) suggested that multiparametric phenotypic approaches allow us to determine a footprint of successful medicines and optimize new drugs toward this.

Multiple different pieces are coming together toward developing a physiologically relevant, predictive, and high-throughput *in vitro* assay for novel treatments against cardiac

fibrosis. While the ideal will likely never be reached, the substantial improvements made in recent years will lead to a better and earlier prediction of drug efficacy and identification of novel antifibrotic drug mechanisms and, thereby, will reduce failures, cost, and time in clinical trials.

AUTHOR CONTRIBUTIONS

All authors were involved in the design and writing of this manuscript.

ACKNOWLEDGMENTS

The authors thank Katharina Schimmel and Bramasta Nugraha for critical proofreading and valuable input for the manuscript.

REFERENCES

- Abonnenc, M., Nabeebaccus, A. A., Mayr, U., Barallobre-Barreiro, J., Dong, X., Cuello, F., et al. (2013). Extracellular matrix secretion by cardiac fibroblasts: role of microRNA-29b and microRNA-30c. *Circ. Res.* 113, 1138–1147. doi: 10.1161/circresaha.113.302400
- Abraham, Y., Zhang, X., and Parker, C. N. (2014). Multiparametric analysis of screening data: growing beyond the single dimension to infinity and beyond. *J. Biomol. Screen* 19, 628–639. doi: 10.1177/1087057114524987
- Aujla, P. K., and Kassiri, Z. (2021). Diverse origins and activation of fibroblasts in cardiac fibrosis. *Cell Signal.* 78:109869. doi: 10.1016/j.celsig.2020.109869
- Barallobre-Barreiro, J., Didangelos, A., Schoendube, F. A., Drozdov, I., Yin, X., Fernandez-Caggiano, M., et al. (2012). Proteomics analysis of cardiac extracellular matrix remodeling in a porcine model of ischemia/reperfusion injury. *Circulation* 125, 789–802. doi: 10.1161/circulationaha.111.056952
- Baranyi, U., Winter, B., Gugerell, A., Hegedus, B., Brostjan, C., Laufer, G., et al. (2019). Primary human fibroblasts in culture switch to a myofibroblast-like phenotype independently of TGF Beta. *Cells* 8:721. doi: 10.3390/cells8070721
- Baudino, T. A., McFadden, A., Fix, C., Hastings, J., Price, R., and Borg, T. K. (2008). Cell patterning: interaction of cardiac myocytes and fibroblasts in three-dimensional culture. *Microsc. Microanal.* 14, 117–125. doi: 10.1017/s1431927608080021
- Booij, T. H., Price, L. S., and Danen, E. H. J. (2019). 3D cell-based assays for drug screens: challenges in imaging, image analysis, and high-content analysis. *SLAS Discov.* 24, 615–627. doi: 10.1177/2472555219830087
- Bryant, J. E., Shamhart, P. E., Luther, D. J., Olson, E. R., Koshy, J. C., Costic, D. J., et al. (2009). Cardiac myofibroblast differentiation is attenuated by alpha(3) integrin blockade: potential role in post-MI remodeling. *J. Mol. Cell Cardiol.* 46, 186–192. doi: 10.1016/j.yjmcc.2008.10.022
- Canty, E. G., and Kadler, K. E. (2005). Procollagen trafficking, processing and fibrillogenesis. *J. Cell Sci.* 118(Pt 7), 1341–1353. doi: 10.1242/jcs.01731
- Chothani, S., Schafer, S., Adami, E., Viswanathan, S., Widjaja, A. A., Langley, S. R., et al. (2019). Widespread translational control of fibrosis in the human heart by RNA-binding proteins. *Circulation* 140, 937–951.
- Desmouliere, A., Geinoz, A., Gabbiani, F., and Gabbiani, G. (1993). Transforming growth factor-beta 1 induces alpha-smooth muscle actin expression in granulation tissue myofibroblasts and in quiescent and growing cultured fibroblasts. *J. Cell Biol.* 122, 103–111. doi: 10.1083/jcb.122.1.103
- Fang, L., Murphy, A. J., and Dart, A. M. A. (2017). Clinical perspective of anti-fibrotic therapies for cardiovascular disease. *Front. Pharmacol.* 8:186.
- Filippo Buono, M., von Boehmer, L., Strang, J., Hoerstrup, S. P., Emmert, M. Y., and Nugraha, B. (2020). Human cardiac organoids for modeling genetic cardiomyopathy. *Cells* 9:1733. doi: 10.3390/cells9071733
- Gabbiani, G., Ryan, G. B., and Majne, G. (1971). Presence of modified fibroblasts in granulation tissue and their possible role in wound contraction. *Experientia* 27, 549–550. doi: 10.1007/bf02147594
- Giesen, C., Wang, H. A., Schapiro, D., Zivanovic, N., Jacobs, A., Hattendorf, B., et al. (2014). Highly multiplexed imaging of tumor tissues with subcellular resolution by mass cytometry. *Nat. Methods* 11, 417–422. doi: 10.1038/nmeth.2869
- Gilles, G., McCulloch, A. D., Brakebusch, C. H., and Herum, K. M. (2020). Maintaining resting cardiac fibroblasts in vitro by disrupting mechanotransduction. *PLoS One* 15:e0241390. doi: 10.1371/journal.pone.0241390
- Grande, J. P., Melder, D. C., and Zinsmeister, A. R. (1997). Modulation of collagen gene expression by cytokines: stimulatory effect of transforming growth factor-beta1, with divergent effects of epidermal growth factor and tumor necrosis factor-alpha on collagen type I and collagen type IV. *J. Lab. Clin. Med.* 130, 476–486. doi: 10.1016/s0022-2143(97)90124-4
- Grys, B. T., Lo, D. S., Sahin, N., Kraus, O. Z., Morris, Q., Boone, C., et al. (2017). Machine learning and computer vision approaches for phenotypic profiling. *J. Cell Biol.* 216, 65–71. doi: 10.1083/jcb.201610026
- Heymans, S., Gonzalez, A., Pizard, A., Papageorgiou, A. P., Lopez-Andres, N., Jaisser, F., et al. (2015). Searching for new mechanisms of myocardial fibrosis with diagnostic and/or therapeutic potential. *Eur. J. Heart Fail.* 17, 764–771. doi: 10.1002/ejhf.312
- Horvath, P., Aulner, N., Bickle, M., Davies, A. M., Nery, E. D., Ebner, D., et al. (2016). Screening out irrelevant cell-based models of disease. *Nat. Rev. Drug Discov.* 15, 751–769. doi: 10.1038/nrd.2016.175
- Jonsson, M. K. B., Hartman, R. J. G., Ackers-Johnson, M., Tan, W. L. W., Lim, B., van Veen, T. A. B., et al. (2016). A transcriptomic and epigenomic comparison of fetal and adult human cardiac fibroblasts reveals novel key transcription factors in adult cardiac fibroblasts. *JACC Basic Transl. Sci.* 1, 590–602. doi: 10.1016/j.jacbs.2016.07.007
- Junqueira, L. C., Bignolas, G., and Brentani, R. R. (1979). Picrosirius staining plus polarization microscopy, a specific method for collagen detection in tissue sections. *Histochem J.* 11, 447–455. doi: 10.1007/bf01002772
- Kenneweg, F., Bang, C., Xiao, K., Boulanger, C. M., Loyer, X., Mazlan, S., et al. (2019). Long Noncoding RNA-enriched vesicles secreted by hypoxic

- cardiomyocytes drive cardiac fibrosis. *Mol. Ther. Nucleic Acids* 18, 363–374. doi: 10.1016/j.omtn.2019.09.003
- Kong, P., Christia, P., and Frangogiannis, N. G. (2014). The pathogenesis of cardiac fibrosis. *Cell Mol. Life Sci.* 71, 549–574.
- Landry, N. M., Rattan, S. G., and Dixon, I. M. C. (2019). An improved method of maintaining primary murine cardiac fibroblasts in two-dimensional cell culture. *Sci. Rep.* 9:12889.
- Lee, M. O., Jung, K. B., Jo, S. J., Hyun, S. A., Moon, K. S., Seo, J. W., et al. (2019). Modelling cardiac fibrosis using three-dimensional cardiac microtissues derived from human embryonic stem cells. *J. Biol. Eng.* 13:15.
- Li, M., Luan, F., Zhao, Y., Hao, H., Zhou, Y., Han, W., et al. (2016). Epithelial-mesenchymal transition: an emerging target in tissue fibrosis. *Exp. Biol. Med. (Maywood)* 241, 1–13. doi: 10.1177/1535370215597194
- Liang, C. C., Park, A. Y., and Guan, J. L. (2007). In vitro scratch assay: a convenient and inexpensive method for analysis of cell migration in vitro. *Nat. Protoc.* 2, 329–333. doi: 10.1038/nprot.2007.30
- Litvinukova, M., Talavera-Lopez, C., Maatz, H., Reichart, D., Worth, C. L., Lindberg, E. L., et al. (2020). Cells of the adult human heart. *Nature* 588, 466–472.
- Liu, T., Song, D., Dong, J., Zhu, P., Liu, J., Liu, W., et al. (2017). Current understanding of the pathophysiology of myocardial fibrosis and its quantitative assessment in heart failure. *Front. Physiol.* 8:238.
- Moffat, J. G., Vincent, F., Lee, J. A., Eder, J., and Prunotto, M. (2017). Opportunities and challenges in phenotypic drug discovery: an industry perspective. *Nat. Rev. Drug Discov.* 16, 531–543. doi: 10.1038/nrd.2017.111
- Murdoch, C. E., Chaubey, S., Zeng, L., Yu, B., Ivetic, A., Walker, S. J., et al. (2014). Endothelial NADPH oxidase-2 promotes interstitial cardiac fibrosis and diastolic dysfunction through proinflammatory effects and endothelial-mesenchymal transition. *J. Am. Coll. Cardiol.* 63, 2734–2741. doi: 10.1016/j.jacc.2014.02.572
- Nagaraju, C. K., Robinson, E. L., Abdeselem, M., Trenson, S., Dries, E., Gilbert, G., et al. (2019). Myofibroblast phenotype and reversibility of fibrosis in patients with end-stage heart failure. *J. Am. Coll. Cardiol.* 73, 2267–2282. doi: 10.1016/j.jacc.2019.02.049
- Nugraha, B., Buono, M. F., and Emmert, M. Y. (2018). Modelling human cardiac diseases with 3D organoid. *Eur. Heart J.* 39, 4234–4237. doi: 10.1093/eurheartj/ehy765
- Nugraha, B., Buono, M. F., von Boehmer, L., Hoerstrup, S. P., and Emmert, M. Y. (2019). Human cardiac organoids for disease modeling. *Clin. Pharmacol. Ther.* 105, 79–85. doi: 10.1002/cpt.1286
- Palano, G., Jansson, M., Backmark, A., Martinsson, S., Sabirsh, A., Hulthenby, K., et al. (2020). A high-content, in vitro cardiac fibrosis assay for high-throughput, phenotypic identification of compounds with anti-fibrotic activity. *J. Mol. Cell Cardiol.* 142, 105–117. doi: 10.1016/j.jmcc.2020.04.002
- Pantazis, P., Maloney, J., Wu, D., and Fraser, S. E. (2010). Second harmonic generating (SHG) nanoprobe for in vivo imaging. *Proc. Natl. Acad. Sci. U.S.A.* 107, 14535–14540. doi: 10.1073/pnas.1004748107
- Piccoli, M. T., Gupta, S. K., Viereck, J., Foinquinos, A., Samolovac, S., Kramer, F. L., et al. (2017). Inhibition of the cardiac fibroblast-enriched lncRNA Meg3 prevents cardiac fibrosis and diastolic dysfunction. *Circ. Res.* 121, 575–583. doi: 10.1161/circresaha.117.310624
- Pinto, A. R., Ilinykh, A., Ivey, M. J., Kuwabara, J. T., D'Antoni, M. L., Debuque, R., et al. (2016). Revisiting cardiac cellular composition. *Circ. Res.* 118, 400–409. doi: 10.1161/circresaha.115.307778
- Polonchuk, L., Chabria, M., Badi, L., Hoflack, J. C., Figtree, G., Davies, M. J., et al. (2017). Cardiac spheroids as promising in vitro models to study the human heart microenvironment. *Sci Rep.* 7, 7005.
- Qiu, W., Wei, F., Sun, X., Wang, X., Duan, B., Shi, C., et al. (2014). Measurement of hydroxyproline in collagen with three different methods. *Mol. Med. Rep.* 10, 1157–1163. doi: 10.3892/mmr.2014.2267
- Querejeta, R., Lopez, B., Gonzalez, A., Sanchez, E., Larman, M., Martinez Ubago, J. L., et al. (2004). Increased collagen type I synthesis in patients with heart failure of hypertensive origin: relation to myocardial fibrosis. *Circulation* 110, 1263–1268. doi: 10.1161/01.cir.0000140973.60992.9a
- Querejeta, R., Varo, N., Lopez, B., Larman, M., Artinano, E., Etayo, J. C., et al. (2000). Serum carboxy-terminal propeptide of procollagen type I is a marker of myocardial fibrosis in hypertensive heart disease. *Circulation* 101, 1729–1735. doi: 10.1161/01.cir.101.14.1729
- Ranganathan, P., Agrawal, A., Bhushan, R., Chavalmane, A. K., Kalathur, R. K., Takahashi, T., et al. (2007). Expression profiling of genes regulated by TGF-beta: differential regulation in normal and tumour cells. *BMC Genomics* 8:98. doi: 10.1186/1471-2164-8-98
- Rehman, M., Vodret, S., Braga, L., Guarnaccia, C., Celsi, F., Rossetti, G., et al. (2019). High-throughput screening discovers antifibrotic properties of haloperidol by hindering myofibroblast activation. *JCI Insight* 4: e123987.
- Sahadevan, P., and Allen, B. G. (2021). Isolation and culture of adult murine cardiac atrial and ventricular fibroblasts and myofibroblasts. *Methods* (in press).
- Santiago, J. J., Dangerfield, A. L., Rattan, S. G., Bathe, K. L., Cunnington, R. H., Raizman, J. E., et al. (2010). Cardiac fibroblast to myofibroblast differentiation in vivo and in vitro: expression of focal adhesion components in neonatal and adult rat ventricular myofibroblasts. *Dev. Dyn.* 239, 1573–1584. doi: 10.1002/dvdy.22280
- Scannell, J. W., and Bosley, J. (2016). When quality beats quantity: decision theory, drug discovery, and the reproducibility crisis. *PLoS One* 11:e0147215. doi: 10.1371/journal.pone.0147215
- Scheeder, C., Heigwer, F., and Boutros, M. (2018). Machine learning and image-based profiling in drug discovery. *Curr. Opin. Syst. Biol.* 10, 43–52. doi: 10.1016/j.coisb.2018.05.004
- Schimmel, K., Jung, M., Foinquinos, A., Jose, G. S., Beaumont, J., Bock, K., et al. (2020). Natural compound library screening identifies new molecules for the treatment of cardiac fibrosis and diastolic dysfunction. *Circulation* 141, 751–767.
- Sharma, U. C., Pokharel, S., van Brakel, T. J., van Berlo, J. H., Cleutjens, J. P., Schroen, B., et al. (2004). Galectin-3 marks activated macrophages in failure-prone hypertrophied hearts and contributes to cardiac dysfunction. *Circulation* 110, 3121–3128. doi: 10.1161/01.cir.0000147181.65298.4d
- Shinde, A. V., Humeres, C., and Frangogiannis, N. G. (2017). The role of alpha-smooth muscle actin in fibroblast-mediated matrix contraction and remodeling. *Biochim. Biophys. Acta Mol. Basis Dis.* 1863, 298–309. doi: 10.1016/j.bbdis.2016.11.006
- Sieber, P., Schafer, A., Lieberherr, R., Le Goff, F., Stritt, M., Welford, R. W. D., et al. (2018). Novel high-throughput myofibroblast assays identify agonists with therapeutic potential in pulmonary fibrosis that act via EP2 and EP4 receptors. *PLoS One* 13:e0207872. doi: 10.1371/journal.pone.0207872
- Skalli, O., Pelte, M. F., Pelet, M. C., Gabbiani, G., Gugliotta, P., Bussolati, G., et al. (1989). Alpha-smooth muscle actin, a differentiation marker of smooth muscle cells, is present in microfilamentous bundles of pericytes. *J. Histochem. Cytochem.* 37, 315–321. doi: 10.1177/37.3.2918221
- Tesseur, I., Zou, K., Berber, E., Zhang, H., and Wyss-Coray, T. (2006). Highly sensitive and specific bioassay for measuring bioactive TGF-beta. *BMC Cell Biol.* 7:15.
- Turner, R. J., Golz, S., Wollnik, C., Burkhardt, N., Sternberger, I., Andag, U., et al. (2020). A Whole genome-wide arrayed CRISPR screen in primary organ fibroblasts to identify regulators of kidney fibrosis. *SLAS Discov.* 25, 591–604. doi: 10.1177/2472555220915851
- van Huizen, N. A., Ijzermans, J. N. M., Burgers, P. C., and Luider, T. M. (2020). Collagen analysis with mass spectrometry. *Mass Spectrom. Rev.* 39, 309–335. doi: 10.1002/mas.21600
- Wang, Z., Stuckey, D. J., Murdoch, C. E., Camelliti, P., Lip, G. Y. H., and Griffin, M. (2018). Cardiac fibrosis can be attenuated by blocking the activity of transglutaminase 2 using a selective small-molecule inhibitor. *Cell Death Dis.* 9:613.
- Warchal, S. J., Unciti-Broceta, A., and Carragher, N. O. (2016). Next-generation phenotypic screening. *Future Med. Chem.* 8, 1331–1347. doi: 10.4155/fmc-2016-0025
- Weigle, S., Martin, E., Voegtle, A., Wahl, B., and Schuler, M. (2019). Primary cell-based phenotypic assays to pharmacologically and genetically study fibrotic diseases in vitro. *J. Biol. Methods* 6:e115. doi: 10.14440/jbm.2019.285
- Whittaker, P., Kloner, R. A., Boughner, D. R., and Pickering, J. G. (1994). Quantitative assessment of myocardial collagen with picrosirius red staining

- and circularly polarized light. *Basic Res. Cardiol.* 89, 397–410. doi: 10.1007/bf00788278
- Yndestad, A., Landro, L., Ueland, T., Dahl, C. P., Flo, T. H., Vinge, L. E., et al. (2009). Increased systemic and myocardial expression of neutrophil gelatinase-associated lipocalin in clinical and experimental heart failure. *Eur. Heart J.* 30, 1229–1236. doi: 10.1093/eurheartj/ehp088
- Zhang, Y. E. (2017). Non-smad signaling pathways of the TGF-beta Family. *Cold Spring Harb. Perspect. Biol.* 9:a022129. doi: 10.1101/cshperspect.a022129
- Zuppinger, C. (2019). 3D cardiac cell culture: a critical review of current technologies and applications. *Front. Cardiovasc. Med.* 6:87.
- Conflict of Interest:** AF and EM are employees of AstraZeneca.
- The remaining author declares that the research was conducted in the absence of any commercial or financial relationships that could be construed as a potential conflict of interest.
- Copyright © 2021 Palano, Foinquinos and Müllers. This is an open-access article distributed under the terms of the Creative Commons Attribution License (CC BY). The use, distribution or reproduction in other forums is permitted, provided the original author(s) and the copyright owner(s) are credited and that the original publication in this journal is cited, in accordance with accepted academic practice. No use, distribution or reproduction is permitted which does not comply with these terms.



Targeting Dermal Fibroblast Subtypes in Antifibrotic Therapy: Surface Marker as a Cellular Identity or a Functional Entity?

Xin Huang[†], Yimin Khoong[†], Chengyao Han, Dai Su, Hao Ma, Shuchen Gu, Qingfeng Li* and Tao Zan*

Department of Plastic and Reconstructive Surgery, Shanghai Ninth People's Hospital, School of Medicine, Shanghai Jiao Tong University, Shanghai, China

OPEN ACCESS

Edited by:

Elvira Forte,
Jackson Laboratory, United States

Reviewed by:

Radhika P. Atit,
Case Western Reserve University,
United States
Edward Tredget,
University of Alberta Hospital, Canada

*Correspondence:

Qingfeng Li
dr.liqingfeng@yahoo.com
Tao Zan
zantaodoctor@yahoo.com

[†]These authors have contributed
equally to this work

Specialty section:

This article was submitted to
Integrative Physiology,
a section of the journal
Frontiers in Physiology

Received: 14 April 2021

Accepted: 16 June 2021

Published: 15 July 2021

Citation:

Huang X, Khoong Y, Han C, Su D,
Ma H, Gu S, Li Q and Zan T (2021)
Targeting Dermal Fibroblast Subtypes
in Antifibrotic Therapy: Surface Marker
as a Cellular Identity or a Functional
Entity? *Front. Physiol.* 12:694605.
doi: 10.3389/fphys.2021.694605

Fibroblasts are the chief effector cells in fibrotic diseases and have been discovered to be highly heterogeneous. Recently, fibroblast heterogeneity in human skin has been studied extensively and several surface markers for dermal fibroblast subtypes have been identified, holding promise for future antifibrotic therapies. However, it has yet to be confirmed whether surface markers should be looked upon as merely lineage landmarks or as functional entities of fibroblast subtypes, which may further complicate the interpretation of cellular function of these fibroblast subtypes. This review aims to provide an update on current evidence on fibroblast surface markers in fibrotic disorders of skin as well as of other organ systems. Specifically, studies where surface markers were treated as lineage markers and manipulated as functional membrane proteins are both evaluated in parallel, hoping to reveal the underlying mechanism behind the pathogenesis of tissue fibrosis contributed by various fibroblast subtypes from multiple angles, shedding lights on future translational researches.

Keywords: fibroblast subtypes, fibroblast heterogeneity, fibrosis, surface marker, antifibrotic therapy

INTRODUCTION

Fibroblast (Fb), as a vital interstitial cell, is involved in a wide variety of biological functions such as conferring structural support to tissues, secreting extracellular matrix (ECM), participating in tissue damage repair and immune responses (Lynch and Watt, 2018). Besides, Fb is also the chief effector cell in fibrotic diseases. Abnormal Fb function, such as cellular hyperproliferation and excessive extracellular matrix deposition, can directly mediate tissue fibrosis (Jiang and Rinkevich, 2020). Fb has always been thought to be stable and unitary in terms of its composition and function. In the past, based on the histological characteristics of the skin, Fb was mainly classified into three types, namely papillary layer, deep reticular layer, hair shaft and papillary region of the hair follicle (Lynch and Watt, 2018). Unfortunately, due to the lack of surface markers that can effectively distinguish different fibroblast subtypes, accurate separation of different fibroblast subtypes has always been an obstacle, and has greatly restricted the further in-depth study of the functional characteristics of this complex cell population.

In recent years, development of omic sequencing technology, especially in single-cell omics, has enabled people to understand the phenotype and functional characteristics of cells on the single-cell level, thereby increased the depth and accuracy in our understanding of the complex cell populations (Prakadan et al., 2017). With the help of omics technology, fibroblast subpopulations

were studied in detail and were found to be highly heterogeneous in their compositions. Previously characterized papillary and reticular Fb were demonstrated to contain a complex population of cells that do not share a specific marker (Ascensión et al., 2020; Vorstandlechner et al., 2020). At present, several studies have been performed to uncover the Fb heterogeneity in normal human skin tissues. Tabib et al. (2018) discovered that dermal Fb can be divided into two main subpopulations characterized by SFRP2 and FMO1; and into several subpopulations according to their expression of CRABP1, COL11A1, FMO2, PRG4, and C2ORF40. Philippeos et al. (2018) performed transcriptome sequencing on the papillary and reticular dermal tissues, and revealed several pan-Fb markers, including CD90, platelet-derived growth factor receptor (PDGFR, including PDGFR α and PDGFR β). Besides, CD39, COL6A5, COL23A1, APCDD1, HSPB3, and WIF1 were found highly expressed in papillary Fb, while CD36 was specifically highly expressed in reticular Fb (Philippeos et al., 2018). Using flow cytometry, Korosec et al. (2019) found that Fbs characterized by fibroblast activation protein (FAP) positive and CD90 negative phenotype are enriched in the papillary dermis and expressed both PDPN and NTN1, displayed active proliferation, and are relatively resistant to adipogenic differentiation. On the other hand, FAP-CD90+ Fbs expressed high levels of ACTA2, MGP, PPAR γ , and CD36 and possessed a higher adipogenic potential, contributing to features of reticular Fbs.

The research on Fb heterogeneity in healthy skin is still very much in its infancy. Based on currently available evidence, it is acknowledged that pan-Fb surface markers of human skin Fb are CD90, PDGFR α and PDGFR β , while the surface markers of Fb subtypes are FAP, CD26, CD36, and CD39. These surface markers hold the promise of future antifibrotic therapies by targeting Fb subtypes with small molecule inhibitors or inhibitory antibodies. However, evidence regarding the functional characteristics and dynamic alteration of Fb subtypes in both healthy or fibrotic skin is still scarce. More importantly, there is a discrepancy between Fb surface markers as lineage markers or as functional entities in the previous studies, which further complicates the interpretation of cellular functions, hampering future development of targeted therapy (Jacob et al., 2012). In this review, we aim to summarize the current evidence of Fb surface markers in fibrotic disorders of skin as well as of other organ systems. Specifically, we would like to compare the role of these surface markers in fibrotic diseases as lineage markers or as functional membrane proteins. Besides, antifibrotic therapies targeting certain Fb subtypes or particular surface marker proteins would be evaluated, hoping to shed light on the significance of these Fb subtypes during the fibrotic process, and to provide some valuable insights for future translational research.

PAN FIBROBLAST SURFACE MARKERS

CD90

CD90, also known as Thy1, is a glycosylphosphatidylinositol-anchored glycoprotein that is expressed on the surfaces of T cells, neuronal cells, endothelial cells, mesenchymal stem cells

and fibroblasts (Jiang and Rinkevich, 2018). CD90 regulates cell adhesion and migration, and plays an important role in the processes of axon growth, T cell activation, cell proliferation and apoptosis regulation, and tumor cell migration (Shaikh et al., 2016). In human dermis, it was shown that CD90 is widely expressed in all skin layers, including papillary dermis, reticular dermis and hypodermis, thus it is also known as a pan-Fb surface marker (Driskell et al., 2013; Philippeos et al., 2018). However, Korosec et al. (2019) stated that the uppermost papillary Fbs possessed a CD90 negative phenotype. Besides, CD90 cannot clearly distinguish between dermal mesenchymal stem cells and dermal Fbs, suggesting that CD90 alone is not an accurate marker to define Fbs in general or its subtypes (Jiang and Rinkevich, 2018).

CD90+ Fbs were found to be accumulated in the collagen packed loci of several fibrotic diseases, including systemic sclerosis (Nazari et al., 2016), cholestatic liver injury (Katsumata et al., 2017), pathological scarring (Ho et al., 2019) and contracted capsule induced by tissue expander implantation (Hansen et al., 2017). Moreover, the expression level of CD90 in Fbs was positively correlated with the severity of tissue fibrosis (Nazari et al., 2016; Katsumata et al., 2017), suggesting the positive role of CD90+ Fbs in the pathogenesis of these diseases. CD90+ Fbs were also regarded to be functionally activated as myofibroblast marker α -smooth muscle actin (α SMA) and ECM related genes were both highly expressed (Hansen et al., 2017; Ho et al., 2019). Besides, CD90+ Fbs inhibited ECM degradation through the upregulation of Tissue Inhibitors of Metalloproteinases-1 (TIMP-1) (Katsumata et al., 2017).

However, CD90 exerted contradictory functions in different disease models. For instance, the depletion of CD90 would halt fibrosis in prosthesis-induced scar formation (Hansen et al., 2017) and idiopathic pulmonary fibrosis (IPF) (Fiore et al., 2015). These antifibrotic effects may be attributed to the inhibition of the association between CD90 and the α v β 3 integrins upon CD90 depletion, further blocking Src family kinase recruitment and Rho signaling activation (Gerber et al., 2013; Fiore et al., 2015). In contrast, in IPF, CD90 was found to be lowly expressed in the fibroblastic foci (Sanders et al., 2008). Also, Lung Fbs from CD90 knockout mice showed increased cell proliferation and collagen deposition, revealing antifibrotic properties of CD90 (Nicola et al., 2009). The inconsistencies across studies suggested that: (1) CD90+ Fb may act differently during fibrosis formation depending on the organ system involved; (2) CD90 is widely expressed in multiple mesenchymal cells, thus global depletion of CD90 cells may not be limited to just CD90+ Fbs, but also other CD90+ cells, thereby significantly complicating the interpretation of results (Rege and Hagood, 2006).

Small molecular compounds such as OSU-CG5 and monoclonal antibodies targeting CD90 have already been used to inhibit CD90+ tumor cells in solid or hematological malignancy (Ishiyama et al., 2010; Chen et al., 2015). However, to date none has been tested for treatment of fibrotic diseases. Apart from directly targeting CD90 *per se* or CD90+ cells, other treatment options which inhibits the differentiation of endothelial cells into CD90+ Fb (Wei et al., 2020) or disrupts the interaction between CD90 and integrin α v (Tan et al., 2019),

might also achieve desirable therapeutic effects on tissue fibrosis (Figure 1).

Platelet-Derived Growth Factor Receptor (PDGFR)

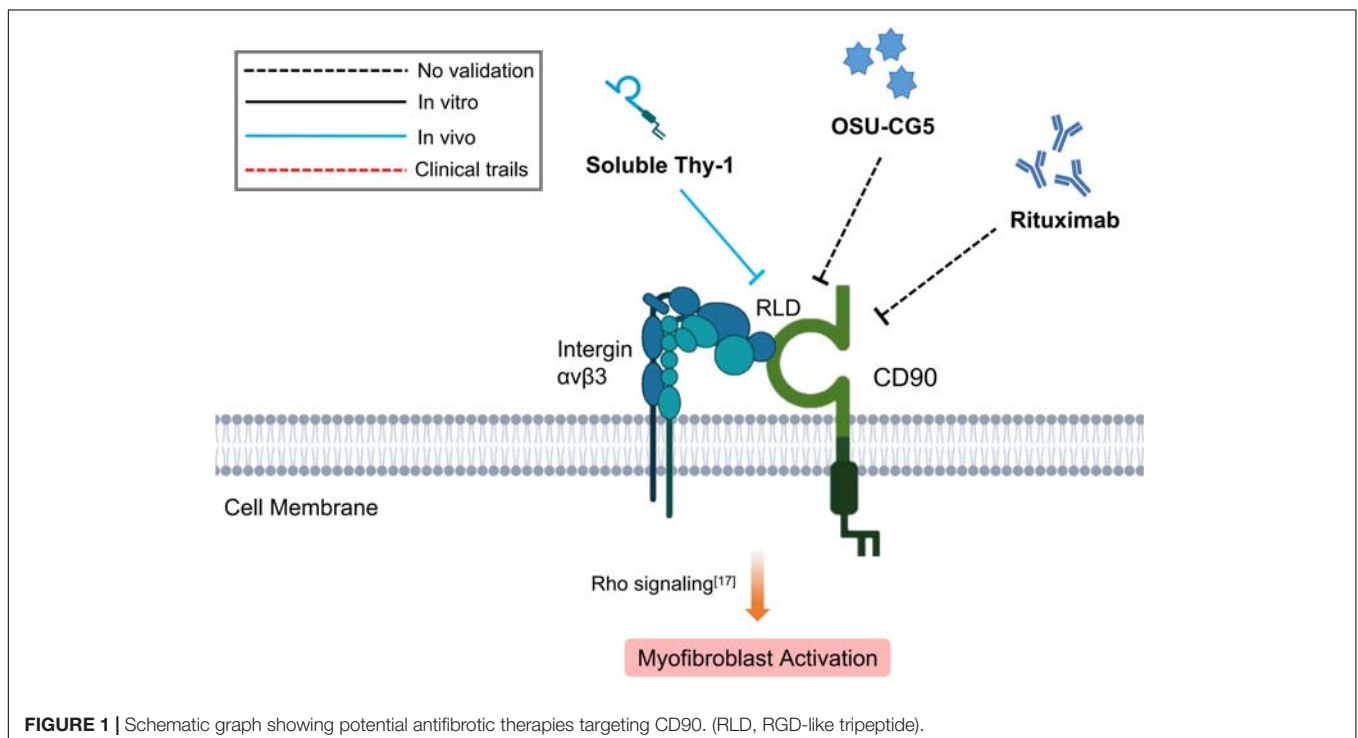
Platelet-derived growth factor receptor belongs to the receptor tyrosine-specific protein kinase family. It possesses intrinsic kinase activity and is widely expressed in Fbs, endothelial cells and myoepithelial cells (Lynch and Watt, 2018). The binding of PDGF isoforms to PDGFR dimers $\alpha\alpha$, $\alpha\beta$, $\beta\beta$ would trigger autophosphorylation of PDGFRs on different tyrosine residues and subsequent activation of downstream signaling pathways, regulating cell proliferation, apoptosis, differentiation, migration, and angiogenesis (Östman, 2017; Klinkhammer et al., 2018). It plays important roles in physiological processes including growth and development, and wound repair; as well as in pathological processes such as tumorigenesis (Pietras et al., 2003).

In normal human skin, PDGFR α and PDGFR β are indiscriminately expressed in the papillary and reticular dermis (Philippeos et al., 2018). It has been reported that upon muscle and skin injury, a lineage of ADAM12+ cells would be induced into a distinct subset of PDGFR α + cells, namely the ADAM12+ PDGFR α + Fbs which mediates scarring repair by producing collagen (Dulauroy et al., 2012). Similar fibrogenic potential of PDGFR α + cells has also been observed in other organs. It has been reported that PDGFR α + progenitor cells give rise to major matrix-producing Fbs in tendon repair (Harvey et al., 2019), liver fibrosis (Ramachandran et al., 2019), and kidney and heart ischemic injury (Santini et al., 2020). PDGF-enriched microenvironment would also contribute to tissue

fibrosis as seen in Duchenne muscular dystrophy (DMD), where PDGFR α + Sca1 + CD45- mesenchymal progenitor cells would be activated into tissue remodeling cells after receiving PDGF-AA ligands from the surrounding muscle cells (Ieronimakis et al., 2016). Besides, PDGFR α , which is also expressed in the adipose precursor cells (Driskell and Watt, 2015; Marcelin et al., 2017), would be activated, resulting in the transformation of cells into PDGFR α + CD9^{high} Fbs that act as the pivotal cells in tissue metabolism and white adipose tissue (WAT) fibrosis (Marcelin et al., 2017).

Profibrotic effect of PDGF signaling pathway has been evaluated in multiple organs including liver (Hayes et al., 2014; Ramachandran et al., 2019), skin (Olson and Soriano, 2009), kidney (Ostendorf et al., 2003) and heart (Pontén et al., 2003). Other than activating the classic fibrogenic ERK, AKT, and NF- κ B pathways which ultimately resulting in excessive tissue fibrosis (Kocabayoglu et al., 2015; Higashi et al., 2017), PDGFR signaling, specifically PDGF β signaling is also accountable for functional activation of Fbs as shown by upregulation of α SMA and profibrotic cytokines such as matrix metalloproteinases (MMPs) and TIMPs (Czochra et al., 2006). In addition, PDGF-BB is involved in promoting the secretion of extracellular vesicles containing PDGFR α , which in turn facilitates the activation of cellular function of hepatic stellate cells, promoting liver fibrosis (Kostallari et al., 2018).

As the critical role of PDGF/PDGFR signaling in promoting tissue fibrosis has been well documented, numerous antifibrotic approaches targeting this pathway have been developed (Papadopoulos et al., 2018). Basically, these treatment strategies are mainly divided into three categories (Papadopoulos et al., 2018): (1) sequestering PDGF ligands or inhibiting their binding



to their respective receptors using neutralizing antibodies or aptamers, which are single-stranded DNA or RNA molecules that possess selective binding affinity to the PDGF ligands, consequently blocking the activation of PDGFRs; (2) inhibiting ligand-receptor interactions by blocking the extracellular domain of PDGFR with antibodies or small molecular drugs; (3) blocking the activation of intracellular tyrosine kinase or downstream pathways of PDGFR signaling with low molecular weight inhibitors.

Hao et al. (2012) demonstrated that PDGF-B kinoid immunogen, a kind of PDGF-B-derived epitope-carrier protein heterocomplexes, would elicit the production of neutralizing anti-PDGF-B autoantibodies responsible for the suppression of proliferation and activation of the hepatic stellate cells (HSCs), which would ultimately inhibit liver fibrosis. Similar antifibrotic effects can also be achieved through direct administration of PDGF-BB specific neutralizing antibody (MOR8457) (Yoshida et al., 2014; Kuai et al., 2015) or soluble dominant negative PDGFR β (Borkham-Kamphorst et al., 2004), as demonstrated in mice model of hepatic fibrosis. For small molecular drugs, tyrosine kinase inhibitors (TKIs) have been proven to be one of the most promising antifibrotic therapies that target the enzymatic activity of PDGFR (Papadopoulos et al., 2018), such as in hepatic (Liu et al., 2011; Shaker et al., 2011) and pulmonary (Vuorinen et al., 2007; Fleetwood et al., 2017) fibrosis. With respect to skin fibrosis, Imatinib inhibited the proliferation and production of ECM, including collagen 1 and fibronectin *in vitro* in dermal Fbs obtained from systemic sclerosis patients (Distler et al., 2007; Soria et al., 2008). *In vivo*, Imatinib administration reduced dermal thickening and prevented the differentiation of resting Fbs into myofibroblasts in TSK-1 mice and bleomycin-induced dermal fibrosis (Akhmetshina et al., 2009). Similar protective effects on dermal fibrotic diseases would also be observed with Sunitinib, Dasatinib, and Nilotinib *in vivo* (Akhmetshina et al., 2008; Kavian et al., 2012). However, clinical trials evaluating the therapeutic efficacy of Imatinib on systemic sclerosis gave multifarious results (Khanna et al., 2011; Spiera et al., 2011; Prey et al., 2012; Fraticelli et al., 2014; Gordon et al., 2014). Kay and High (2008) first reported progressive improvement of skin thickening and tethering following initiation of Imatinib in two patients with nephrogenic systemic fibrosis. However, recurrence of skin lesions were observed shortly after therapy withdrawal (Kay and High, 2008). In 26 systemic sclerosis interstitial lung disease, the use of low dose Imatinib (200 mg/day) for 6 months was associated with good drug tolerance and stabilized lung function, however, without significant effects on skin lesions (Fraticelli et al., 2014). Another phase 2 trial showed that the use of Imatinib 400 mg/day would improve both forced vital capacity and skin thickening (Spiera et al., 2011; Gordon et al., 2014). Yet, using similar dose of Imatinib (400 mg/day), Prey et al. (2012) failed to demonstrate therapeutic efficacy of Imatinib in regards to impact on dermal thickness, pulmonary function and quality of life. By further increasing the dose to 600 mg/day, Khanna et al. (2011) only reported a trend toward improved lung function and skin thickness, but were associated with significant adverse effects. The reasons for the inconsistencies between these studies are

unclear, but may be due to drug dosage, treatment duration, and patient groups and thus requires further investigation (Khanna et al., 2011). In conclusion, the curative effect of TKIs in the treatment of fibrotic disease requires further studies to confirm its effectiveness (Figure 2).

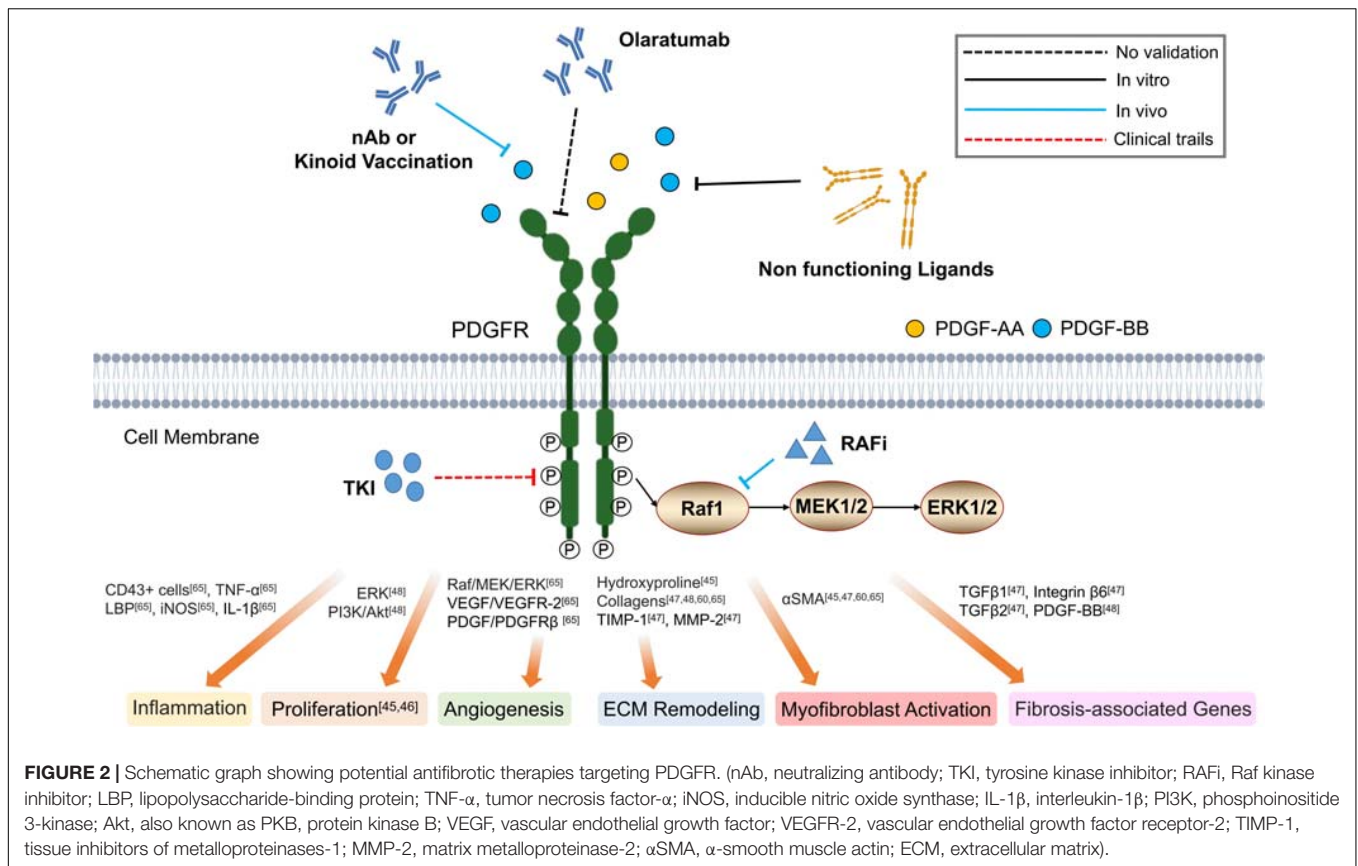
It has been reported that the auto-phosphorylated PDGFR and downstream activation of Ras, RAF pro-oncogene serine/threonine protein kinase (RAF-1), mitogen-activated protein kinase (MEK) and extracellular signal-regulated protein kinase (ERK) signaling pathways facilitate the progression of hepatic fibrosis (Ying et al., 2017). Sorafenib, a potent inhibitor of PDGFR β and RAF kinase, has been demonstrated to effectively reduce the portal pressure and portosystemic collaterals in a rat model of portal hypertension, thereby reducing the level of intrahepatic fibrosis (Figure 2) (Mejias et al., 2009).

SURFACE MARKERS FOR FIBROBLAST SUBTYPES

Fibroblast Activation Protein (FAP)

Fibroblast activation protein is an integral membrane glycoprotein of the serine proteases family, possessing dual collagenase and dipeptidase activities, which aids in the degradation of gelatin, type I collagen and a variety of dipeptides (Kelly, 2005). Although FAP and CD26 both belong to the same S9B prolyl oligopeptidase subfamily and are highly homologous, they are not interchangeable (Kelly, 2005). Previous studies reported that FAP was highly expressed in the cancer associated fibroblasts (CAFs), which in turn mediated cancer invasion and metastasis through the degradation of extracellular matrix (Kalluri and Zeisberg, 2006).

In normal human skin, FAP + CD90- Fbs are commonly regarded as the papillary Fbs, which showed increased proliferation potential and lower adipogenic differentiation as compared to the reticular Fbs (Korosec et al., 2019). FAP is also found to be highly expressed in the collagen-accumulated loci of several fibrotic diseases including keloid (Dienus et al., 2010), liver fibrosis (Levy et al., 2002), myocardial infarction (Tillmanns et al., 2015), lung fibrosis (Acharya et al., 2006), Crohn's disease (Truffi et al., 2018), and arthritis (Croft et al., 2019). FAP+ Fbs generally highly express α SMA as observed in infarcted heart tissues of human and mice model, suggesting these Fbs express an activated contractive phenotype (Tillmanns et al., 2015). Further, Avery et al. found that the expression of FAP and α SMA is regulated by ECM composition, elasticity and transforming growth factor- β (TGF- β) signaling (Avery et al., 2018). In fibronectin-enriched matrix, TGF- β preferentially upregulates the expression of FAP; whereas in Collagen 1-enriched matrix, α SMA is induced instead (Avery et al., 2018). FAP^{Hi} α SMA^{low} and FAP^{low} α SMA^{Hi} Fbs displayed distinct functional differences in that the former has a higher capacity of ECM deposition, while the latter showed a more contractive potential (Avery et al., 2018). In addition, FAP has been reported to be vital for various cellular functions like cell proliferation (Croft et al., 2019), migration (Wang et al., 2005; Dienus et al., 2010), invasion (Wang et al., 2005; Dienus et al., 2010), apoptosis



(Wang et al., 2005) and production of profibrotic proteins (such as TIMPs) (Truffi et al., 2018). The therapeutic effects of FAP targeted approaches are partly attributed to the regulation of cellular functions of the culprit FAP expressing cells. However, it has been noted that the choice of animal model or intervention approach would influence the final interpretation of therapeutic effect by targeting the FAP+ Fbs (Kimura et al., 2019). For instance, FAP+ cell depletion by T cells expressing FAP chimeric antigen receptors or global FAP knockout showed increased level of pulmonary fibrosis in bleomycin-induced lung fibrosis, but had only minimal effects on the Ad-TGF β induced model (Kimura et al., 2019). These phenomena highlight the fact that different fibrosis models may have distinct mechanisms of action upon initiating insults and that FAP+ Fbs may have adapted to different functions throughout the fibrotic processes.

Although various FAP targeting strategies have been established, including inhibition of enzymatic activity of FAP, depletion of FAP expressing cells and targeted delivery of cytotoxic compounds, their applications in fibrotic diseases have been limited so far (Figure 3) (Busek et al., 2018).

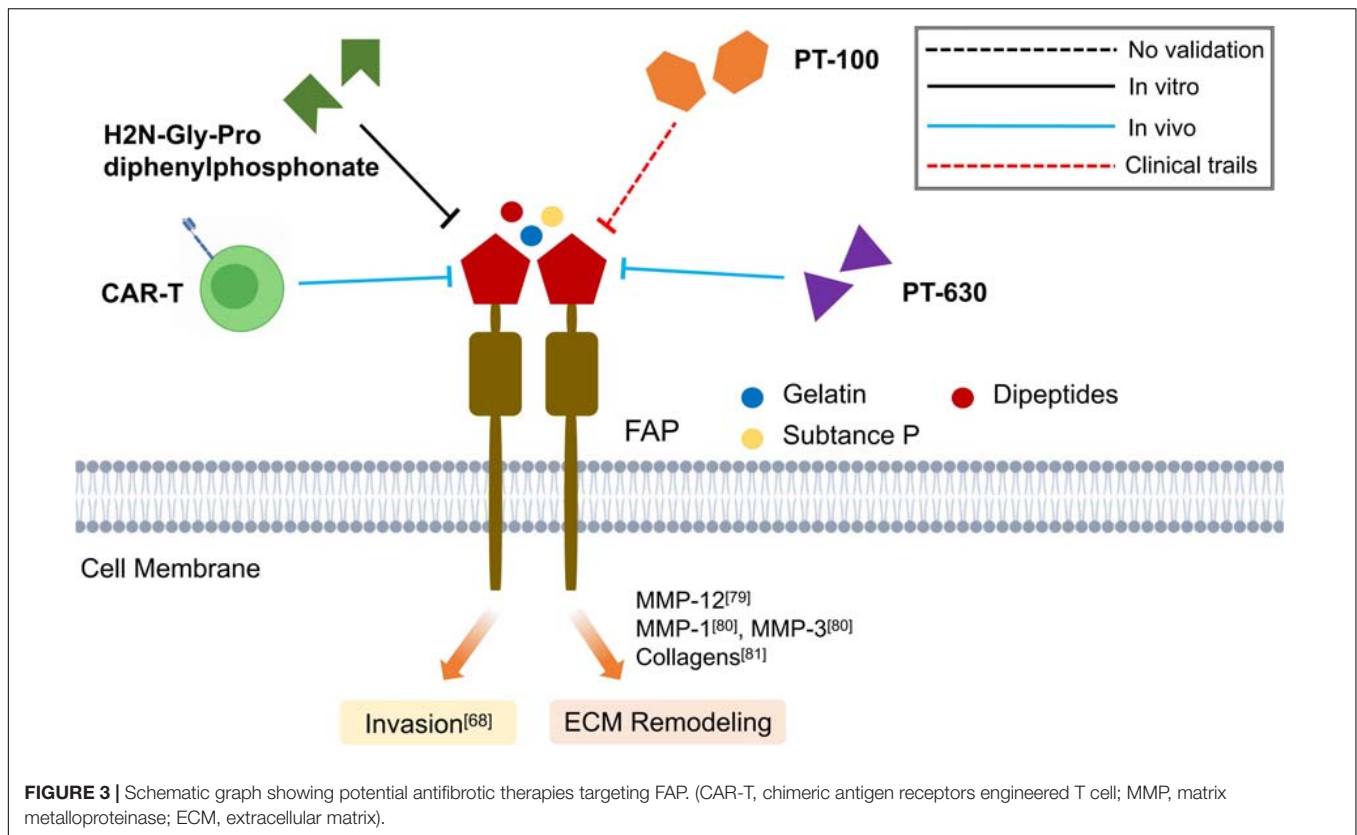
Targeted inhibition of FAP using H2N-Gly-Pro diphenylphosphonate, an irreversible inhibitor of FAP (Gilmore et al., 2006), has been shown to impair the invasiveness of keloid Fbs *in vitro* (Dienus et al., 2010). Similarly, Talabostat mesylate (PT-100), an extracellular dipeptidylpeptidases inhibitor, would reduce bleomycin-induced lung injury by downregulating FAP and MMP-12 expression and increasing macrophage activation

(Egger et al., 2017). Moreover, oral administration of L-glutamyl L-boroproline (PT-630), a more specific FAP inhibitor, in murine model of rheumatoid arthritis has found to exert inhibitory effects on the invasiveness of synovial Fbs (Ospelt et al., 2010). However, PT-630 which is relatively non-selective often inhibits both CD26 and FAP activities, thus the development of more selective FAP inhibitors is warranted, as well as the assessment of their antifibrotic activity in preclinical and clinical trials (Jacob et al., 2012). Recently, chimeric antigen receptors (CARs) engineered T cells that specifically target the FAP have been demonstrated to prevent cardiac fibrosis and improve cardiac function *in vivo*, suggesting a novel direction to develop anti-FAP therapies (Aghajanian et al., 2019) (Figure 3).

CD26

CD26 (also known as dipeptidyl peptidase IV, DPP IV) is a highly conserved type II transmembrane serine exopeptidase that hydrolyzes proline or alanine from the N-terminus of a broad range of polypeptides (Hu and Longaker, 2016). CD26 is widely expressed in a variety of cells and tissues, and participates in the regulation of nutrient absorption, tumor invasion and metastasis, and many other physiological and pathological processes (Ibegbu et al., 2009).

The role of CD26 in renal fibrosis (Takagaki et al., 2017), cardiac fibrosis (Bando and Murohara, 2016), hepatic fibrosis (Itou et al., 2013), wound healing and cutaneous diseases (Hu and Longaker, 2016; Patel et al., 2020) has been extensively discussed



by recent reviews. Here, we would like to mainly address the advances of CD26 in skin fibrosis. The profibrotic nature of CD26 can be inspected from two intriguing observations: Dipeptidyl Peptidase-4 inhibitors (DPP4-Is) are novel oral hypoglycemics drugs used in clinical practice that work by blocking the enzymatic function of DPP-4 (Panchapakesan and Pollock, 2015). In a retrospective study, the occurrence rate of pathological scars (keloids and hypertrophic scars) after median sternotomy was significantly reduced in patients who have received DPP4-I treatment (Suwanai et al., 2020). Furthermore, CD26+ Fb population appeared more abundant in the human skin than in the gingiva, which may be associated with a better regeneration and less scarring property of gingiva (Mah et al., 2017). During the scarring process, fewer CD26+ Fbs was found in the regenerated gingival wounds as compared to the hypertrophic-like scars (Mah et al., 2017). Through rigorous lineage tracing experiments, Rinkevich et al. (2015) demonstrated that Engrailed-1 lineage-positive Fbs are the major cells responsible for matrix deposition in wound healing in mice skin. Moreover, cytometric screening identified CD26 as a surface marker for 94% of Engrailed-1 lineage-positive Fbs, and inhibition of CD26 with Diprotin A has resulted in mitigation of skin scarring (Rinkevich et al., 2015).

In contrast to the mice skin, studies of CD26 in human skin are relatively inconsistent (Philippeos et al., 2018; Tabib et al., 2018; Korosec et al., 2019; Vorstandlechner et al., 2020). Tabib et al. (2018) and Vorstandlechner et al. (2020) proposed that CD26+ Fbs that accumulate in both papillary and reticular layers have

been demonstrated to be the major Fb subpopulation responsible for ECM assembly in normal skin and healing wounds in humans (Vorstandlechner et al., 2020; Worthen et al., 2020). In contrast, Philippeos et al. (2018) showed that CD26+ Fbs are enriched in the reticular dermis; while Korosec et al. (2019) believed that CD26+ Fbs are located in the papillary dermis but are also detectable in other dermal layers. Although consensus on the localization of CD26+ Fbs in human skin has yet to be reached, CD26+ Fbs derived from keloid, a typical fibrotic skin disorder after injury, demonstrated markedly elevated ability of cell proliferation and migration; greater expression of inflammatory and fibrotic factors such as TGF- β 1, insulin growth factor-1 (IGF-1), and interleukin-6 (IL-6); and increased production of ECM components such as collagen 1, collagen 3 and fibronectin (Xin et al., 2017). In systemic sclerosis, CD26+ Fbs expressed high level of myofibroblast marker α SMA and collagen (Soare et al., 2020). The functional status of CD26 decides on the regulation of a series of cellular functions like cell proliferation, migration and collagen production. CD26 inhibition by genetic knockout or DPP4-I exerted potent antifibrotic effects in bleomycin-induced skin fibrosis (Soare et al., 2020).

It has been reported that the inhibition of CD26 exerted hypoglycaemic, anti-inflammatory, and antifibrotic effects (Panchapakesan and Pollock, 2015). The mechanism behind the antifibrotic role of CD26 is complex and has been investigated in several aspects. Primarily, it has been reported that CD26 blockage using established small molecular drugs would abrogate the classic TGF- β 1 signaling pathways in hepatic

(Kaji et al., 2014; Zhang et al., 2019; Khalil et al., 2020), pulmonary (Xu et al., 2018), renal (Seo et al., 2019; Kim et al., 2020), and adipose tissue (Marques et al., 2018) fibrosis. In high glucose culture environment, DPP4-I would decrease the expression of phosphorylated protein of the IGF/Akt/mTOR signaling pathway in hypertrophic scar-derived Fbs, inhibiting their *trans*-differentiation into myofibroblasts (Li et al., 2019). In addition, DPP4-I would reduce the level of inflammatory signals including NLR Family Pyrin Domain Containing 3 (NLRP3) inflammasome, endoplasmic reticulum (ER) stress and proinflammatory cytokine including IL-1 β , IL-6, and tumor necrosis factor α (TNF- α) in the mice model of renal (Seo et al., 2019) and hepatic fibrosis (Jung et al., 2014). Apart from mediating the fibrotic and inflammatory pathways, DPP4-I also attenuated fibrogenesis by modulating the cellular status and phenotype including lipotoxicity-induced apoptosis (Lee et al., 2020) and endothelial-mesenchymal transition (EndMT) (Kanasaki et al., 2014; Suzuki et al., 2017; Xu et al., 2018). Aroor et al. (2015) reported the use of DPP4-I as a therapeutic rescue in patients with hepatic steatosis through the enhancement of mitochondrial glucose utilization and triacylglycerol secretion/export, thereby suppressing the accumulation of hepatic triacylglycerol and diacylglycerol. Taken together, these suggest that the metabolic regulation property of DPP4-I would be one of the main factors accounting for its antifibrotic effect.

Until now, DPP4-I has been proven to exhibit prominent anti-fibrotic effects on liver (Jung et al., 2014; Kaji et al., 2014; Aroor et al., 2015; Zhang et al., 2019; Khalil et al., 2020; Lee et al., 2020), lung (Suzuki et al., 2017; Xu et al., 2018), kidney (Kanasaki et al., 2014; Gangadharan Komala et al., 2016; Uchii et al., 2016; Seo et al., 2019; Kim et al., 2020), adipose tissue (Marques et al., 2018) and skin (Long et al., 2018; Li et al., 2019; Soare et al., 2020). These studies signify the potential use of DPP4-I in combating fibrotic diseases (Figure 4). However, further clinical trials are still required to verify its effect. What's more, the comparison of different types of DPP4-I regarding their antifibrotic effectiveness on various organ system is scarce in current researches. In addition, a more detailed knowledge concerning the dosage and adverse effects of a particular type of DPP4-I may be beneficial for future clinical application.

CD36

CD36 (also known as scavenger receptor B2), is identified as a single chain transmembrane glycoprotein with two transmembrane domains and an extracellular region (Yang et al., 2017). The versatile function of CD36 is attributed to its wide range of ligands, which mainly includes the long-chain fatty acids, oxidized lipids and phospholipids, advanced oxidation protein products (AOPPs), thrombospondin and advanced glycation end products (AGEPs) (Yang et al., 2017). This ligand-receptor complex on the response element suggested the important role of CD36 in lipid metabolism, immunological response, inflammatory stress response, fibrosis and angiogenesis and atherosclerosis (Febbraio et al., 2001; Sweetwyne and Murphy-Ullrich, 2012).

CD36 is expressed in multiple cells including renal tubule epithelial cells, podocytes, macrophages, microvascular

endothelial cells and dermal Fbs (Febbraio et al., 2001; Philippeos et al., 2018). It has been reported that Lin-CD90 + CD36+ Fbs, which mainly located in the reticular dermis, possessed an inflammatory phenotype that included higher expression of α SMA, MGP, PPAR γ ; greater secretion of ECM and inflammatory factors; increased sensitivity upon interferon- γ (IFN- γ) stimulation; and stronger adipogenic differentiation (Philippeos et al., 2018; Korosec et al., 2019). In IPF, a group of CD36 + CD97+ Fbs has been identified in the remodeled areas of IPF tissue but with low expression of α SMA and ECM, suggesting that these Fbs are quiescent and are non-ECM producers in pulmonary fibrosis (Heinzelmann et al., 2018).

Although CD36 + Fbs have not shown fibrogenic phenotype, CD36 receptor would, however, associate with thrombospondin-1 (TSP-1)/latent TGF β 1 (L-TGF β 1) and facilitate the release of mature TGF- β 1, initiating tissue fibrotic response (Yehualaeshet et al., 2000). The inhibition of this CD36/TSP-1/L-TGF β 1 regulatory pathway has been demonstrated to exert antifibrotic effects in lung (Yehualaeshet et al., 2000; Wang et al., 2009) and kidney (Yang et al., 2007; Pennathur et al., 2015) fibrotic diseases. On the other hand, the lipid transportation function of CD36 also contributed to tissue fibrogenesis. In tubular epithelial cell-specific CD36 overexpressed transgenic mice model, Kang et al. (2015) discovered the association of the increased long-chain fatty acid transportation with increasing α SMA and collagen 1 expression, which then facilitates the development of renal fibrosis. On the contrary, Rabinowitz and Mutlu (2019) and Zhao et al. (2019) found that the transplantation of CD36-overexpressed fibroblasts into the mouse skin would effectively reduce the radiation-induced skin fibrosis by activating fatty acid utilization while inhibiting glycolysis pathway. Therefore, there remains controversies concerning the relationship between fatty acid transportation function of CD36 and fibrosis as the choice of animal models and interventions would lead to completely distinct outcomes. On the other hand, the inflammation regulatory role of CD36 has also been reported in the CD36 expressing macrophages that have been reported to promote chronic kidney fibrogenesis by facilitating the activation of nuclear factor- κ B (NF- κ B) signaling and increasing oxidative stress (Okamura et al., 2009). The binding of lipoproteins, a biological ligand, to CD36 allows the activation of Toll-like receptors (TLRs), Sodium-Potassium Adenosine Triphosphatase (Na⁺/K⁺ ATPase), the NLRP3 inflammasome, protein kinase C-nicotinamide adenine dinucleotide phosphate oxidase (NAPDH) oxidase, Src-family kinases (Scr/Lyn/Fyn), mitogen-activated protein kinases, and TGF- β signaling pathways (Yang et al., 2017). As such, synthetic amphipathic helical peptides (SAHPs) can mimic the domain of lipoprotein and bind to the CD36 without exerting activation effects (Souza et al., 2016). In mice models of nephrectomy and angiotensin II-induced chronic renal fibrosis, SAHP 5A decreased the expression of inflammation-associated genes and attenuated the progression of glomerular sclerosis and interstitial fibrosis, thereby providing renal protection. However, due to the relatively low selectivity of SAHP 5A which also targets other scavenger receptors (SR BI/II), a

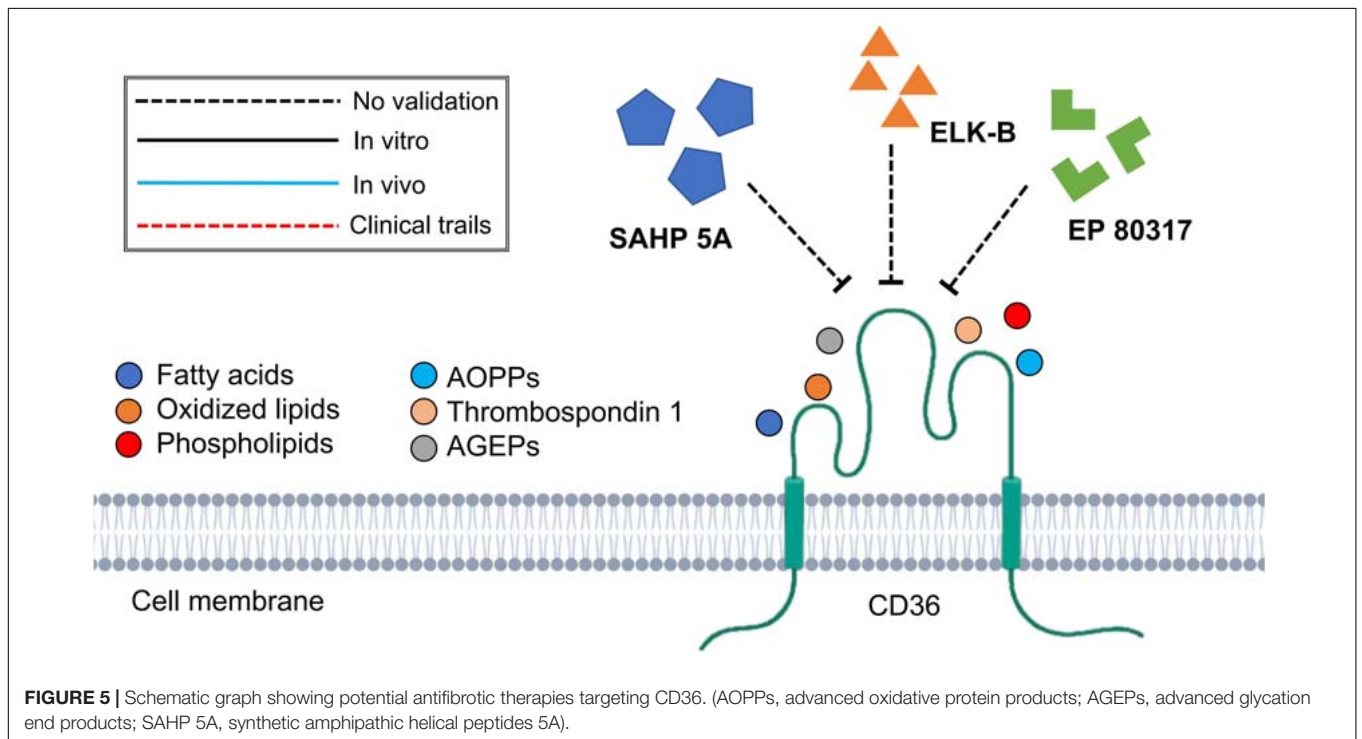
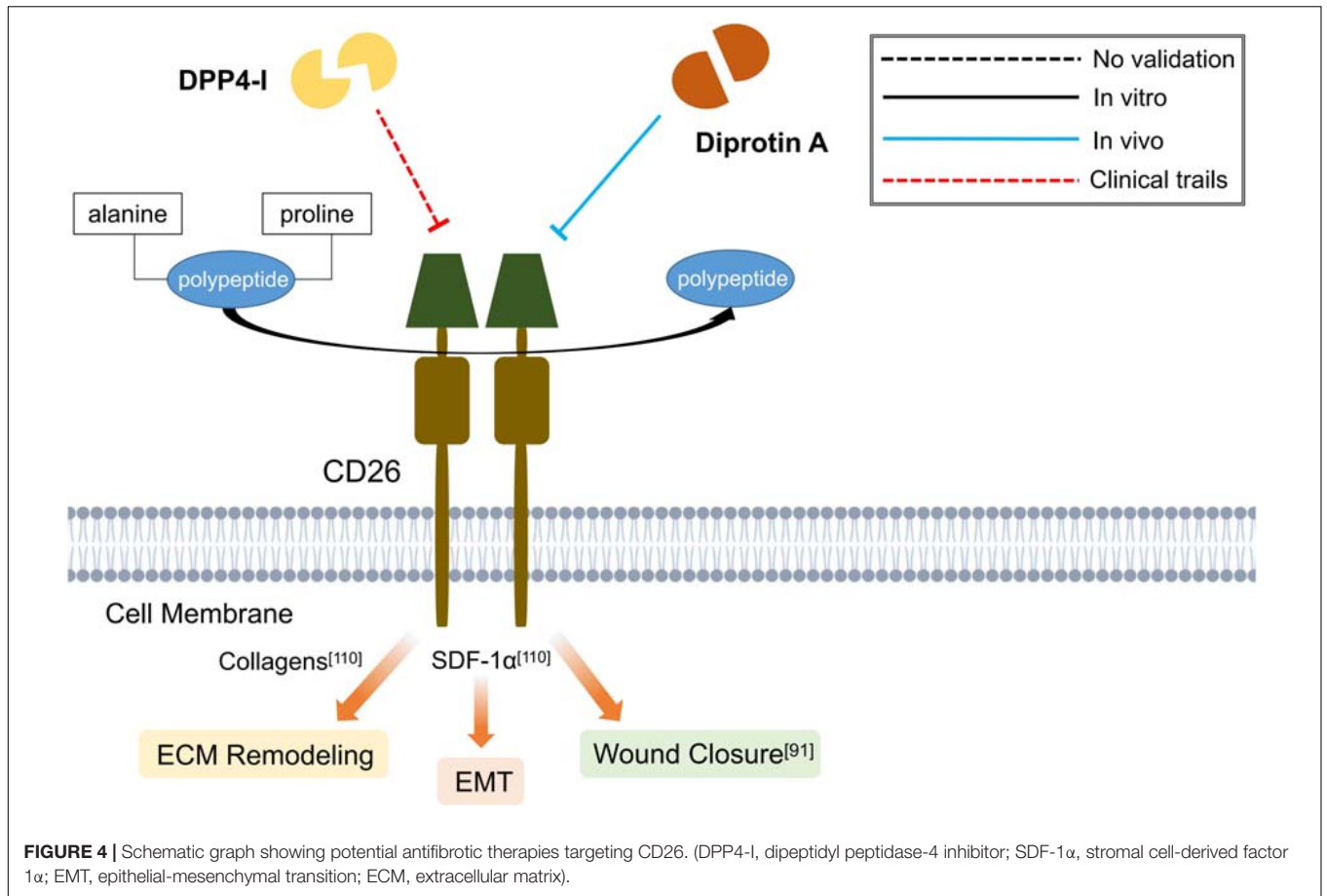


TABLE 1 | The function of Fb subtypes in tissue fibrosis.

| Fb subtypes | Models and diseases | description | Effect |
|--------------------------------------|--|---|----------------|
| CD90 + CD34– | Human scars (Ho et al., 2019) | Colocalize with α SMA and procollagen-1 | Fibrogenic |
| CD90 + podoplanin + CD34– | Human SSC (Nazari et al., 2016) | Expanded cell population | Fibrogenic |
| CD90 + CD45– | Murine cholestatic liver injury (Katsumata et al., 2017) | High level of expression of α SMA, collagen-1 and TIMP-1 | Fibrogenic |
| PDGFR α + CD9 ^{high} | Murine obesity-induced WAT fibrosis (Marcelin et al., 2017) | Give rise to profibrotic cells; modulate omental WAT fibrogenesis | Fibrogenic |
| PDGFR α + TPPP3+ | Murine tendon injury (Harvey et al., 2019) | Fibrotic scars formation in healing tendons | Fibrogenic |
| PDGFR α + | Human cirrhotic liver; murine CCl4-induced liver fibrosis (Ramachandran et al., 2019) | Expanded cell population in fibrotic niche | Fibrogenic |
| PDGFR α + | Murine ischemic injury (Santini et al., 2020) | Promotion of skeletal muscle fibrosis upon ischemic injury. | Fibrogenic |
| PDGFR α + Sca1 + CD45– | Murine DMD (Ieronimakis et al., 2016) | Expanded cell population; major matrix-forming Fbs | Fibrogenic |
| PDGFR α + ADAM12+ | Murine muscle and skin injury (Dulauroy et al., 2012) | Major fraction of collagen-overproducing cells | Fibrogenic |
| FAP + CD90– | Human skin (Korosec et al., 2019) | High proliferative potential; low adipogenic potential; enriched in the papillary dermis | Non-fibrogenic |
| FAP+ | Human and rat myocardial infarction (Tillmanns et al., 2015) | Located in peri-infarct area with co-expression of prolyl-4-hydroxylase β , α SMA, and vimentin | Fibrogenic |
| CD26 + Sca1– | Murine skin (Driskell et al., 2013; Philippeos et al., 2018) | Papillary Fbs with upregulation of Wnt pathway related genes (Philippeos et al., 2018); large fraction of dermal Fbs in adult mice (Driskell et al., 2013) | Non-fibrogenic |
| CD26+ | Murine (Rinkevich et al., 2015) and human wound (Vorstandlechner et al., 2020; Worthen et al., 2020) | Major scar-forming Engrailed1+ Fbs (Rinkevich et al., 2015); main ECM-producing Fbs during the remodeling phase of wound healing (Vorstandlechner et al., 2020; Worthen et al., 2020) | Fibrogenic |
| CD26+ | Human keloid (Xin et al., 2017) | Expanded cell population; upregulated proliferation, invasion and expression of profibrotic genes | Fibrogenic |
| Lin-CD90 + CD36+ | Human skin (Philippeos et al., 2018; Korosec et al., 2019) | Localize in lower reticular dermis and hypodermis; high adipogenic potential; high expression of ECM and inflammatory related genes | Inflammatory |
| CD36 + CD97+ | Human IPF (Heinzelmann et al., 2018) | Low cell proliferation rate; low expression of α SMA and ECM | Non-fibrogenic |
| Lin-CD90 + CD39+ | Human and mice skin (Philippeos et al., 2018; Korosec et al., 2019) | Enriched in papillary dermis; low adipogenic potential; low expression of ECM and inflammatory related genes | Non-fibrogenic |

SSC, systemic sclerosis; WAT, white adipose tissue; DMD, duchenne muscular dystrophy; IPF, idiopathic pulmonary fibrosis.

more specific CD36 binding SAHP, namely ELK-SAHPs, has been synthesized (Yang et al., 2017). Among them, ELK-B has been shown to improve lung function in the mice model of sepsis by effectively reducing pulmonary infiltration (Bocharov et al., 2016). Another strategy to inhibit the function of CD36 is by using hexapeptide growth hormone-releasing peptides (GHRPs) analog, namely EP 80317. EP 80317 has been found to protect against atherosclerosis progression (Marleau et al., 2005) and myocardial ischemia/reperfusion injury (Bessi et al., 2012). Nevertheless, the above therapies targeting the CD36 are currently under preclinical animal studies and have only been validated in inflammatory and fibrotic diseases of the kidney, lung and heart. Further studies are warranted to verify the anti-fibrosis effect of targeting CD36 in fibrotic diseases of other organ systems (**Figure 5**). Considering the pleiotropic effects of CD36, a deeper knowledge regarding the cellular specificity of CD36 function would be

necessary for a better development of pharmaceutical strategy (Yang et al., 2017).

CD39

CD39 (also known as ectonucleoside triphosphate diphosphohydrolase-1, ENTPD1) is an integral cell membrane glycoprotein that exhibit extracellular nucleotide hydrolase activity (Faas et al., 2017). CD39 converts extracellular adenosine triphosphate (ATP) to the adenosine monophosphate (AMP), which is then converted to adenosine (ADO) by CD73 (Faas et al., 2017). The phosphohydrolysis of ATP to AMP is a rate-limiting step in ADO generation (Faas et al., 2017). Philippeos et al. (2018) first uncovered the use of CD39 as a marker for papillary Fb subtype and demonstrated that CD39+ Fbs exhibited higher proliferation rate and can better support epidermal growth in comparison with CD36+ reticular Fbs. On the contrary, papillary CD39+ Fbs showed lower expression level of ECM and

TABLE 2 | The function of surface markers *per se* in tissue fibrosis.

| Markers | Diseases | Intervention and models | Mechanism | Effect |
|--------------------------|---|--|---|---------------|
| CD90 | Periprosthetic capsular (Hansen et al., 2017) | Lentiviral depletion; scar-derived Fbs | Collagen production; myofibroblast activation | Profibrotic |
| | IPF (Fiore et al., 2015) | Plasmid overexpression and lentiviral knockdown; human and mice lung Fbs | CD90 and $\alpha\beta3$ integrins interaction; mechanosensitive Rho signaling pathway | Profibrotic |
| | Lung development (Nicola et al., 2009) | Thy-1 ^{-/-} transgenic mice | Cell proliferation; production of collagen and elastin; TGF- β signaling pathway | Antifibrotic |
| | IPF (Sanders et al., 2008) | DNA methyltransferase Inhibitors; rat and human lung Fbs | Methylation-regulated expression of CD90; myofibroblast activation | Antifibrotic |
| PDGFR α / β | Systemic fibrosis (Olson and Soriano, 2009) | PDGFR α knockin mice in Ink4a/Arf-deficient background | Growth of connective tissue; collagen production | Profibrotic |
| | Liver fibrosis (Hayes et al., 2014) | PDGFR α GFP reporter mice; PDGFR α heterozygous mice | Expression of PDGFR α and fibrogenic genes; collagen deposition | Profibrotic |
| | Liver fibrosis (Kocabayoglu et al., 2015) | PDGFR β ^{fl/fl} ; GFAP ^{Cre} ; PDGFR β ^{beta/+} ; GFAP ^{Cre} | Expression of collagen and α SMA; ERK, AKT, and NF- κ B signaling pathways | Profibrotic |
| | Liver fibrosis (Czochra et al., 2006) | Transgenic mice overexpressing PDGF-B in the liver | Myofibroblast activation; collagen deposition; production of MMP-2, MMP-9, and TIMP-1 | Profibrotic |
| FAP | Lung fibrosis (Kimura et al., 2019) | FAP targeting CAR-T cells; FAP knockout mice | Collagen production; myofibroblast activation; leukocyte infiltration | Contradictory |
| | Crohn's disease (Truffi et al., 2018) | FAP targeting antibody; primary mucosal myofibroblasts | Collagen and TIMP-1 production; myofibroblast migration | Profibrotic |
| | Liver injury (Wang et al., 2005) | Plasmid overexpression; HSC cell line | Cell adhesion, migration, invasion and apoptosis | Profibrotic |
| CD26 | Systemic sclerosis (Soare et al., 2020) | DPP4-knockout and DPP4-I; murine model of bleomycin-induced fibrosis | Cell proliferation and migration; expression of collagen and contractile proteins; TGF- β /ERK signaling pathway | Profibrotic |
| | Hypertrophic scar (Li et al., 2019) | DPP4-I; HSF | Myofibroblast differentiation; IGF/Akt/mTOR signaling pathway | Profibrotic |
| | Keloid (Thielitz et al., 2008) | Lys[Z(NO ₂)]-thiazolidide and Lys[Z(NO ₂)]-pyrrolidide; keloid-derived Fbs | Cell proliferation; expression of TGF- β and procollagen type I; mitogen-activated protein kinases pp38 and pERK1/2 signaling pathway | Profibrotic |
| | Diabetic Wound Healing (Long et al., 2018) | DPP4-I; human fibroblast cell line; murine model of diabetic wounds; patients with refractory ulcers | Collagen deposition; SDF-1 α production; keratinocyte EMT | Profibrotic |
| CD36 | Pulmonary fibrosis (Yehualaeshet et al., 2000) | CD36 inhibitory peptide; rt model of bleomycin-induced fibrosis | Production of TGF- β 1, inflammatory factors, and ECM | profibrotic |
| | Skin fibrosis (Rabinowitz and Mutlu, 2019; Zhao et al., 2019) | Transplantation of CD36 ^{high} Fb or CD36 ^{KO} Fb; murine model of radiation-induced skin fibrosis | Fatty acid oxidation; degradation of collagen-1; ECM accumulation | Antifibrotic |
| | Renal fibrosis (Kang et al., 2015) | Pax8rtTA/TRE-CD36 double-transgenic mice | Intracellular lipid accumulation; expression of collagen-1 and α SMA | Profibrotic |
| | Renal fibrosis (Souza et al., 2016) | CD36 antagonist (apolipoprotein AI-mimetic peptide 5A); murine model of unilateral ureteral obstruction | Macrophage infiltration; expression of inflammasome genes; interstitial fibrosis | Profibrotic |
| | Renal fibrosis (Okamura et al., 2009) | CD36 ^{-/-} transgenic mice | Regulation of oxidative stress; myofibroblast activation; NF- κ B signaling pathway | Profibrotic |
| | Chronic kidney injury (Pennathur et al., 2015) | CD36-deficient mice | Production of intracellular bioactive oxidized lipids, TNF- α and TGF- β 1 | Profibrotic |
| | Renal tubule fibrosis (Yang et al., 2007) | siRNA knockdown; LLCOPK1 cell line | Albumin production; expression of TGF- β 1 and fibronectin | Profibrotic |
| | Lung fibrosis (Wang et al., 2009) | Lentiviral depletion; rat silicosis model | Activation of L-TGF- β 1; production of hydroxyproline and ECM | Profibrotic |
| CD39 | Chronic renal Fibrosis (Roberts et al., 2017) | CD39 over-expressing transgenic mice | Adenosine generation | Profibrotic |
| | Skin fibrosis (Fernández et al., 2013) | CD39 knockout mice | Adenosine generation; production of collagen and profibrotic cytokines; myofibroblast activation | Profibrotic |
| | Pancreatitis (Künzli et al., 2008) | CD39-null mice; PSC with CD39 depletion | Cell proliferation; expression of procollagen- α 1 and IFN- γ | Profibrotic |
| | Chronic renal injury (Wang et al., 2012) | CD39 over-expressing transgenic mice | CD25+ Treg cells; production of urinary protein and serum creatinine level | Antifibrotic |
| | Chronic kidney injury (Roberts et al., 2016) | CD39 over-expressing transgenic mice | No protective effects on renal fibrosis | Non-effective |
| | Sclerosing cholangitis (Rothweiler et al., 2019) | Global or myeloid-specific CD39-deficient mice | Collagen production; expression of profibrotic genes <i>Tgf-β1</i> , <i>Tnf-α</i> , and <i>α-Sma</i> | Antifibrotic |

IPF, idiopathic pulmonary fibrosis; HSC, hepatic stellate cells; PSC, pancreatic stellate cells; HSF, hypertrophic scar-derived fibroblasts; EMT, epithelial-mesenchymal transition.

inflammatory cytokine, lower adipogenic capacity and are less responsive to inflammatory signals such as IFN- γ , as compared to CD36+ reticular Fbs (Philippeos et al., 2018).

At present, such studies investigating the cellular function of CD39+ Fbs are scarce, especially regarding their role in the process of tissue fibrosis. However, the role of CD39 protein *per se* in fibrotic diseases have been studied and showed competing results. On one hand, CD39 hyperfunction caused the accumulation of extracellular ADO and facilitated the activation of ADO signaling pathway, resulting in tissue fibrosis (Roberts et al., 2017). In renal ischemia-reperfusion injury models, overexpression of CD39 in the transgenic mice showed significantly more severe renal fibrosis via upregulating ADO and stimulating profibrotic downstream pathways through interaction with adenosine A2B receptors (Roberts et al., 2017). Consistently, antifibrogenic effects of CD39 depletion have been observed in bleomycin-induced skin fibrosis (Fernández et al., 2013) and cyclosporin-induced pancreatitis (Künzli et al., 2008) models, probably through modulating the accumulation of ADO (Fernández et al., 2013) and the expression of profibrotic factors (Fernández et al., 2013) and pro-collagen proteins (Künzli et al., 2008). However, other studies argued that the fibrogenic nature of CD39 appeared to be quite inconsistent between organ systems and fibrosis induction methods (Wang et al., 2012; Roberts et al., 2016; Rothweiler et al., 2019). For instance, in the Adriamycin-induced nephropathy model, transplantation of CD39 overexpressing CD25+ regulatory T cells showed renal protective effects by attenuating ATP-induced cell apoptosis and inflammation (Wang et al., 2012). Moreover, global CD39 overexpression showed no difference in fibrotic parameters in the unilateral ureteric obstructive mice model, which is inconsistent with that reported in the renal ischemia-reperfusion injury mice models (Roberts et al., 2016; Roberts et al., 2017). Similar discordance has also been observed in hepatic and biliary system where global CD39 depletion attenuated pancreatitis

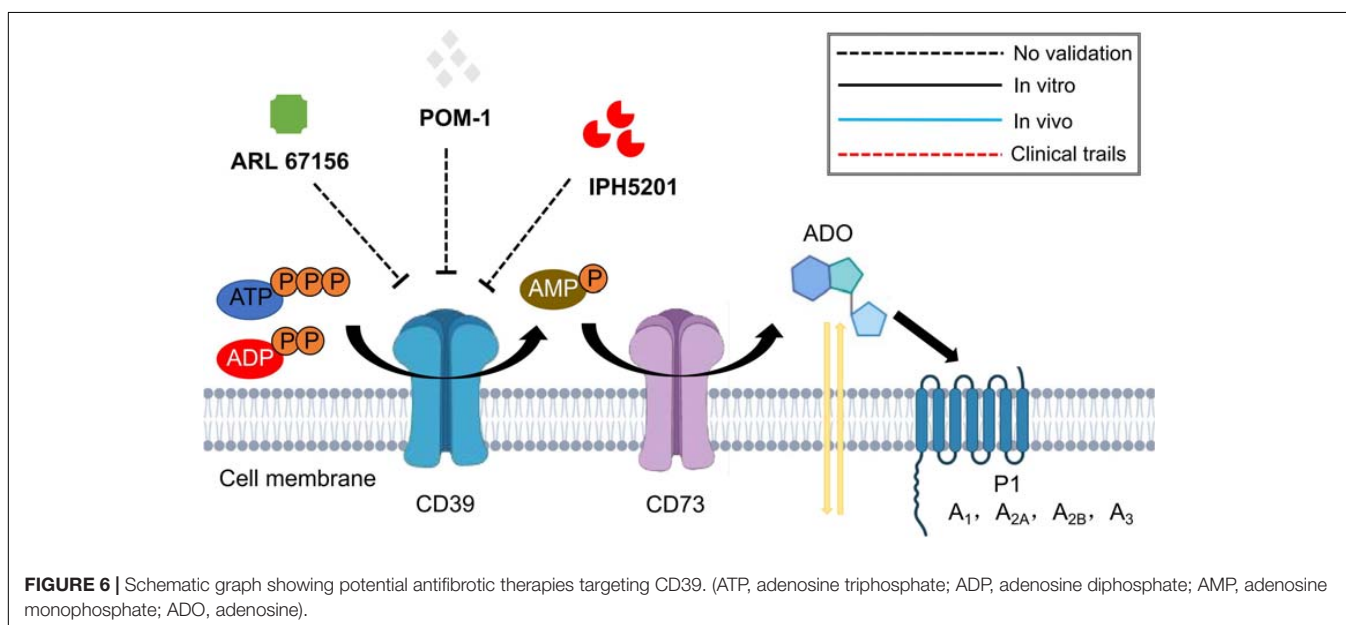
related fibrosis (Künzli et al., 2008) yet exacerbated 3,5-diethoxycarbonyl-1,4-dihydrocollidine (DDC) induced biliary fibrosis (Rothweiler et al., 2019).

The reason for the inconsistency between these studies may be various: (1) Firstly, CD39-mediated purinergic signaling pathway is relatively intricate. Both P1 receptor sensing ADO and P2 receptor sensing ATP have been reported for their profibrotic role (Burnstock et al., 2012; Ferrari et al., 2016). The hyperfunction of CD39 would result in decreased ATP signaling and enhanced ADO signaling, so the outcome in different tissues or cells is reliant on the superposition of the activation states of the two kinds of receptors (Roberts et al., 2016); (2) Secondly, due to the diverse distribution patterns of P1 and P2 receptors and their subtypes in different tissues, the functional changes of CD39 would serve different outcomes in different tissues (Ferrari et al., 2016); (3) Finally, the underlying pathogenesis of fibrotic diseases in different organ systems are distinct, and CD39 may not necessarily be crucial for every type of tissue fibrosis.

To date, several components are available for CD39 targeting, which include the small molecular drugs ARL 67156 trisodium salt and POM-1 (Fang et al., 2016; Yang et al., 2020), and the monoclonal antibody IPH5201 (Perrot et al., 2019). These targeted treatments have shown promising safety profile and therapeutic potential in the regulation of inflammatory response and tumor microenvironment (Fang et al., 2016; Perrot et al., 2019; Yang et al., 2020). However, there is still a lack of studies evaluating their application in fibrotic process, and is definitely worthy of further exploration (Figure 6).

SUMMARY AND PERSPECTIVES

The advances of high-throughput sequencing technologies have greatly facilitated the investigation on tissue fibrosis, a multiplexed process involving different cell types and factors.



In this review, we focused on several surface markers of human dermal Fbs identified in recent years and discussed their respective roles as lineage markers or functional entity in fibrotic diseases. Since the initial discovery, more references are available concerning the role of Fbs defined by CD90, FAP, PDGFR α /PDGFR β and CD26 solely, or in combination with other markers. However, only Fbs defined by PDGFR α /PDGFR β or CD26 showed consistent fibrogenic potential between studies and appeared in accordance with the molecular function of surface markers *per se* (see **Tables 1, 2**). As there are limited literatures on the more recently identified Fb markers like CD36 and CD39, this demands further researches to investigate their respective roles in fibrotic diseases. Moreover, the function of both of these membrane bound proteins showed comprehensive regulatory network in tissue fibrosis and distinct results across different organs, complicating the interpretation of their biological functions. Surface membrane proteins are considered as the ideal therapeutic targets as they own extracellular domains for ligand binding (Bansal et al., 2016). However, the surface marker does not necessarily account for all of the functional dysregulation of certain Fb subtype. Therefore, an in depth profiling to investigate the key functional targets that characterize Fb subtypes is still required to provide a better and more effective targeting strategy.

At the same time, there are also some methodological and technical difficulties at this stage: (1) Most Fb subtype surface markers are co-expressed, thus it is challenging to manipulate and to perform research on a specific group of Fbs (Ascensión et al., 2020). (2) It has been suggested that the phenotype of Fb subtypes requires a specific *in vivo* microenvironment (Korosec et al., 2019), which is, however, hard to maintain after *in vitro* culture, indicating that functional profiling directly after cell isolation might provide more reliable information than *in vitro* experiments. (3) Many newly discovered Fb subtypes still lack verification on their selective tissue localization. Emerging techniques like imaging mass cytometry and spatial transcriptomics (Giesen et al., 2014; Vickovic et al., 2019) can provide the possibility for combined analysis of functional sequencing and spatial profiling data. (4) Since most of mechanistic studies of Fb subtypes so far are based on animal models, in view of the limited conservation of Fb subtypes between human and mice skin (Philippeos et al., 2018), verification of the function of Fb subtypes or related therapies using human samples, cells or humanized animals is undoubtedly essential and should be the main focus

in upcoming studies. (5) The investigation on Fb subtypes in human subjects would definitely be a challenge due to the multifactorial causation of the disease development and tremendous heterogeneity that exists among patients. Thus, it is suggested to pay particular attention on strict selection of homogeneous clinical samples. Besides, analyzing samples from different points in the disease course to reduce bias caused by focusing only on the healthy and diseased states, might provide additional hints on disease progression (Shaw and Rognoni, 2020). (6) The current understanding of the origin of different Fb subtypes remains incomplete. Recent studies demonstrated the conversion of circulating myeloid cells to Fbs during wound healing, indicating a dedicate regulation of Fb fate switching (Sinha et al., 2018; Guerrero-Juarez et al., 2019). Further investigation into the evolution of Fb subtypes and factors influencing the Fbs plasticity could facilitate the development of potential therapeutic approaches in treating fibrotic diseases.

In the future, a more comprehensive transcriptomic, proteomic or genome-wide epigenetic profiling of Fb subtypes defined by different surface markers would be instrumental for a more in-depth understanding of the evolution and functional characteristics of each Fb subtype in tissue fibrosis. Hopefully, a more precise dissection of phenotype features and functional regulation of Fb subtypes would bring greater clinical insights for targeted treatment strategies for fibrotic diseases.

AUTHOR CONTRIBUTIONS

XH, QL, and TZ: conception and design. XH, YK, SG, CH, DS, and HM: collection and assembly of data. XH and YK: data analysis and interpretation and manuscript revision. XH, CH, DS, HM, and SG: graphic illustration. All authors wrote and approved the final manuscript.

FUNDING

This work was supported by grants from National Natural Science Foundation of China (81772086 and 82072177), “Two Hundred Talent” program, “Outstanding Youth Medical Talents” Shanghai “Rising Stars of Medical Talent” Youth Development Program, and Shanghai Jiao Tong University “Chenxing” Youth Development Program (Associate Professor Type A).

REFERENCES

- Acharya, P. S., Zukas, A., Chandan, V., Katzenstein, A. L., and Puré, E. (2006). Fibroblast activation protein: a serine protease expressed at the remodeling interface in idiopathic pulmonary fibrosis. *Hum. Pathol.* 37, 352–360. doi: 10.1016/j.humpath.2005.11.020
- Aghajanian, H., Kimura, T., Rurik, J. G., Hancock, A. S., Leibowitz, M. S., Li, L., et al. (2019). Targeting cardiac fibrosis with engineered T cells. *Nature* 573, 430–433.
- Akhmetshina, A., Dees, C., Pileckyte, M., Maurer, B., Axmann, R., Jüngel, A., et al. (2008). Dual inhibition of c-abl and PDGF receptor signaling by dasatinib and nilotinib for the treatment of dermal fibrosis. *FASEB J.* 22, 2214–2222. doi: 10.1096/fj.07-105627
- Akhmetshina, A., Venalis, P., Dees, C., Busch, N., Zwerina, J., Schett, G., et al. (2009). Treatment with imatinib prevents fibrosis in different preclinical models of systemic sclerosis and induces regression of established fibrosis. *Arthritis Rheumat.* 60, 219–224. doi: 10.1002/art.24186
- Aroor, A. R., Habibi, J., Ford, D. A., Nistala, R., Lastra, G., Manrique, C., et al. (2015). Dipeptidyl peptidase-4 inhibition ameliorates Western diet-induced hepatic steatosis and insulin resistance through hepatic lipid remodeling and modulation of hepatic mitochondrial function. *Diabetes* 64, 1988–2001. doi: 10.2337/db14-0804

- Ascensión, A. M., Fuertes-Álvarez, S., Ibañez-Solé, O., Izeta, A., and Araúzo-Bravo, M. J. (2020). Human dermal fibroblast subpopulations are conserved across single-Cell RNA sequencing studies. *J. Invest. Dermatol.* [Epub ahead of print]. doi: 10.1016/j.jid.2020.11.028
- Avery, D., Govindaraju, P., Jacob, M., Todd, L., Monslow, J., and Puré, E. (2018). Extracellular matrix directs phenotypic heterogeneity of activated fibroblasts. *Matrix Biol.* 67, 90–106. doi: 10.1016/j.matbio.2017.12.003
- Bando, Y. K., and Murohara, T. (2016). Heart failure as a comorbidity of diabetes: role of dipeptidyl peptidase 4. *J. Atheroscl. Thromb.* 23, 147–154. doi: 10.5551/jat.33225
- Bansal, R., Nagórniwicz, B., and Prakash, J. (2016). Clinical advancements in the targeted therapies against liver fibrosis. *Mediat. Inflamm.* 2016:7629724.
- Bessi, V. L., Labbé, S. M., Huynh, D. N., Ménard, L., Jossart, C., Febbraio, M., et al. (2012). EP 80317, a selective CD36 ligand, shows cardioprotective effects against post-ischaemic myocardial damage in mice. *Cardiovasc. Res.* 96, 99–108. doi: 10.1093/cvr/cvs225
- Bocharov, A. V., Wu, T., Baranova, I. N., Birukova, A. A., Sviridov, D., Vishnyakova, T. G., et al. (2016). Synthetic amphipathic helical peptides targeting CD36 attenuate lipopolysaccharide-induced inflammation and acute lung injury. *J. Immunol.* 197, 611–619.
- Borkham-Kamphorst, E., Stoll, D., Gressner, A. M., and Weiskirchen, R. (2004). Inhibitory effect of soluble PDGF-beta receptor in culture-activated hepatic stellate cells. *Biochem. Biophys. Res. Commun.* 317, 451–462. doi: 10.1016/j.bbrc.2004.03.064
- Burnstock, G., Knight, G. E., and Greig, A. V. (2012). Purinergic signaling in healthy and diseased skin. *J. Invest. Dermatol.* 132(3 Pt 1), 526–546. doi: 10.1038/jid.2011.344
- Busek, P., Mateu, R., Zupal, M., Kotackova, L., and Sedo, A. (2018). Targeting fibroblast activation protein in cancer - prospects and caveats. *Front. Biosci.* 23:1933–1968. doi: 10.2741/4682
- Chen, W. C., Chang, Y. S., Hsu, H. P., Yen, M. C., Huang, H. L., Cho, C. Y., et al. (2015). Therapeutics targeting CD90-integrin-AMPK-CD133 signal axis in liver cancer. *Oncotarget* 6, 42923–42937. doi: 10.18632/oncotarget.5976
- Croft, A. P., Campos, J., Jansen, K., Turner, J. D., Marshall, J., Attar, M., et al. (2019). Distinct fibroblast subsets drive inflammation and damage in arthritis. *Nature* 570, 246–251. doi: 10.1038/s41586-019-1263-7
- Czochra, P., Klopčič, B., Meyer, E., Herkel, J., Garcia-Lazaro, J. F., Thieringer, F., et al. (2006). Liver fibrosis induced by hepatic overexpression of PDGF-B in transgenic mice. *J. Hepatol.* 45, 419–428. doi: 10.1016/j.jhep.2006.04.010
- Dienus, K., Bayat, A., Gilmore, B. F., and Seifert, O. (2010). Increased expression of fibroblast activation protein-alpha in keloid fibroblasts: implications for development of a novel treatment option. *Arch. Dermatol. Res.* 302, 725–731. doi: 10.1007/s00403-010-1084-x
- Distler, J. H., Jüngel, A., Huber, L. C., Schulze-Horsel, U., Zwerina, J., Gay, R. E., et al. (2007). Imatinib mesylate reduces production of extracellular matrix and prevents development of experimental dermal fibrosis. *Arthritis Rheumat.* 56, 311–322. doi: 10.1002/art.22314
- Driskell, R. R., Lichtenberger, B. M., Hoste, E., Kretzschmar, K., Simons, B. D., Charalambous, M., et al. (2013). Distinct fibroblast lineages determine dermal architecture in skin development and repair. *Nature* 504, 277–281. doi: 10.1038/nature12783
- Driskell, R. R., and Watt, F. M. (2015). Understanding fibroblast heterogeneity in the skin. *Trends Cell Biol.* 25, 92–99. doi: 10.1016/j.tcb.2014.10.001
- Dulauroy, S., Di Carlo, S. E., Langa, F., Eberl, G., and Peduto, L. (2012). Lineage tracing and genetic ablation of ADAM12(+) perivascular cells identify a major source of profibrotic cells during acute tissue injury. *Nat. Med.* 18, 1262–1270. doi: 10.1038/nm.2848
- egger, C., Cannet, C., Gérard, C., Suply, T., Ksiazek, I., Jarman, E., et al. (2017). Effects of the fibroblast activation protein inhibitor, PT100, in a murine model of pulmonary fibrosis. *Eur. J. Pharmacol.* 809, 64–72. doi: 10.1016/j.ejphar.2017.05.022
- Faas, M. M., Sáez, T., de Vos, P., and Extracellular, A. T. P. (2017). and adenosine: the Yin and Yang in immune responses? *Mol. Aspects Med.* 55, 9–19. doi: 10.1016/j.mam.2017.01.002
- Fang, F., Yu, M., Cavanagh, M. M., Hutter Saunders, J., Qi, Q., Ye, Z., et al. (2016). Expression of CD39 on activated T cells impairs their survival in older individuals. *Cell Rep.* 14, 1218–1231. doi: 10.1016/j.celrep.2016.01.002
- Febbraio, M., Hajjar, D. P., and Silverstein, R. L. (2001). CD36: a class B scavenger receptor involved in angiogenesis, atherosclerosis, inflammation, and lipid metabolism. *J. Clin. Invest.* 108, 785–791. doi: 10.1172/jci14006
- Fernández, P., Perez-Aso, M., Smith, G., Wilder, T., Trzaska, S., Chiriboga, L., et al. (2013). Extracellular generation of adenosine by the ectonucleotidases CD39 and CD73 promotes dermal fibrosis. *Am. J. Pathol.* 183, 1740–1746. doi: 10.1016/j.ajpath.2013.08.024
- Ferrari, D., Gambari, R., Idzko, M., Müller, T., Albanesi, C., Pastore, S., et al. (2016). Purinergic signaling in scarring. *FASEB J.* 30, 3–12. doi: 10.1096/fj.15-274563
- Fiore, V. F., Strane, P. W., Bryksin, A. V., White, E. S., Hagoood, J. S., and Barker, T. H. (2015). Conformational coupling of integrin and Thy-1 regulates Fyn priming and fibroblast mechanotransduction. *J. Cell Biol.* 211, 173–190. doi: 10.1083/jcb.201505007
- Fleetwood, K., McCool, R., Glanville, J., Edwards, S. C., Gsteiger, S., Daigl, M., et al. (2017). Systematic review and network meta-analysis of idiopathic pulmonary fibrosis treatments. *J. Manag. Care Special. Pharm.* 23(3–b Suppl.), S5–S16.
- Fraticelli, P., Gabrielli, B., Pomponio, G., Valentini, G., Bosello, S., Riboldi, P., et al. (2014). Low-dose oral imatinib in the treatment of systemic sclerosis interstitial lung disease unresponsive to cyclophosphamide: a phase II pilot study. *Arthritis Res. Ther.* 16:R144.
- Gangadharan Komala, M., Gross, S., Zaky, A., Pollock, C., and Panchapakesan, U. (2016). Saxagliptin reduces renal tubulointerstitial inflammation, hypertrophy and fibrosis in diabetes. *Nephrology* 21, 423–431. doi: 10.1111/nep.12618
- Gerber, E. E., Gallo, E. M., Fontana, S. C., Davis, E. C., Wigley, F. M., Huso, D. L., et al. (2013). Integrin-modulating therapy prevents fibrosis and autoimmunity in mouse models of scleroderma. *Nature* 503, 126–130. doi: 10.1038/nature12614
- Giesen, C., Wang, H. A., Schapiro, D., Zivanovic, N., Jacobs, A., Hattendorf, B., et al. (2014). Highly multiplexed imaging of tumor tissues with subcellular resolution by mass cytometry. *Nat. Methods* 11, 417–422. doi: 10.1038/nmeth.2869
- Gilmore, B. F., Lynas, J. F., Scott, C. J., McGoohan, C., Martin, L., and Walker, B. (2006). Dipeptide proline diphenyl phosphonates are potent, irreversible inhibitors of seprase (FAPalpha). *Biochem. Biophys. Res. Commun.* 346, 436–446. doi: 10.1016/j.bbrc.2006.05.175
- Gordon, J., Udeh, U., Doobay, K., Magro, C., Wildman, H., Davids, M., et al. (2014). Imatinib mesylate (Gleevec™) in the treatment of diffuse cutaneous systemic sclerosis: results of a 24-month open label, extension phase, single-centre trial. *Clin. Exp. Rheumatol.* 32(6 Suppl. 86), 189–193.
- Guerrero-Juarez, C. F., Dedhia, P. H., Jin, S., Ruiz-Vega, R., Ma, D., Liu, Y., et al. (2019). Single-cell analysis reveals fibroblast heterogeneity and myeloid-derived adipocyte progenitors in murine skin wounds. *Nat. Commun.* 10:650.
- Hansen, T. C., Woeller, C. F., Lacy, S. H., Koltz, P. F., Langstein, H. N., and Phipps, R. P. (2017). Thy1 (CD90) expression is elevated in radiation-induced periprosthetic capsular contracture: implication for novel therapeutics. *Plast. Reconstruct. Surg.* 140, 316–326. doi: 10.1097/prs.0000000000003542
- Hao, Z. M., Fan, X. B., Li, S., Lv, Y. F., Su, H. Q., Jiang, H. P., et al. (2012). Vaccination with platelet-derived growth factor B kinoids inhibits CCl4-induced hepatic fibrosis in mice. *J. Pharmacol. Exp. Therap.* 342, 835–842. doi: 10.1124/jpet.112.194357
- Harvey, T., Flamenco, S., and Fan, C. M. (2019). A Tppp3(+)/Pdgfra(+) tendon stem cell population contributes to regeneration and reveals a shared role for PDGF signalling in regeneration and fibrosis. *Nat. Cell Biol.* 21, 1490–1503. doi: 10.1038/s41556-019-0417-z
- Hayes, B. J., Riehle, K. J., Shimizu-Albergine, M., Bauer, R. L., Hudkins, K. L., Johansson, F., et al. (2014). Activation of platelet-derived growth factor receptor alpha contributes to liver fibrosis. *PLoS One* 9:e92925. doi: 10.1371/journal.pone.0092925
- Heinzelmann, K., Lehmann, M., Gerckens, M., Noskovičová, N., Frankenberger, M., Lindner, M., et al. (2018). Cell-surface phenotyping identifies CD36 and CD97 as novel markers of fibroblast quiescence in lung fibrosis. *Am. J. Physiol. Lung Cell. Mol. Physiol.* 315, L682–L696.
- Higashi, T., Friedman, S. L., and Hoshida, Y. (2017). Hepatic stellate cells as key target in liver fibrosis. *Adv. Drug Deliv. Rev.* 121, 27–42. doi: 10.1016/j.addr.2017.05.007
- Ho, J. D., Chung, H. J., Ms Barron, A., Ho, D. A., Sahni, D., Browning, J. L., et al. (2019). Extensive CD34-to-CD90 fibroblast transition defines

- regions of cutaneous reparative, hypertrophic, and keloidal scarring. *Am. J. Dermatopathol.* 41, 16–28. doi: 10.1097/dad.0000000000001254
- Hu, M. S., and Longaker, M. T. (2016). Dipeptidyl peptidase-4, wound healing, scarring, and fibrosis. *Plast. Reconstruct. Surg.* 138, 1026–1031. doi: 10.1097/prs.00000000000002634
- Ibegbu, C. C., Xu, Y. X., Fillos, D., Radziewicz, H., Grakoui, A., and Kouritis, A. P. (2009). Differential expression of CD26 on virus-specific CD8(+) T cells during active, latent and resolved infection. *Immunology* 126, 346–353. doi: 10.1111/j.1365-2567.2008.02899.x
- Ieronimakis, N., Hays, A., Prasad, A., Janebodin, K., Duffield, J. S., and Reyes, M. (2016). PDGFR α signalling promotes fibrogenic responses in collagen-producing cells in Duchenne muscular dystrophy. *J. Pathol.* 240, 410–424. doi: 10.1002/path.4801
- Ishiura, Y., Kotani, N., Yamashita, R., Yamamoto, H., Kozutsumi, Y., and Honke, K. (2010). Anomalous expression of Thy1 (CD90) in B-cell lymphoma cells and proliferation inhibition by anti-Thy1 antibody treatment. *Biochem. Biophys. Res. Commun.* 396, 329–334. doi: 10.1016/j.bbrc.2010.04.092
- Itou, M., Kawaguchi, T., Taniguchi, E., and Sata, M. (2013). Dipeptidyl peptidase-4: a key player in chronic liver disease. *World J. Gastroenterol.* 19, 2298–2306.
- Jacob, M., Chang, L., and Puré, E. (2012). Fibroblast activation protein in remodeling tissues. *Curr. Mol. Med.* 12, 1220–1243. doi: 10.2174/156652412803833607
- Jiang, D., and Rinkevich, Y. (2018). Defining skin fibroblastic cell types beyond CD90. *Front. Cell Dev. Biol.* 6:133. doi: 10.3389/fcell.2018.00133
- Jiang, D., and Rinkevich, Y. (2020). Scars or regeneration?—Dermal fibroblasts as drivers of diverse skin wound responses. *Int. J. Mol. Sci.* 21:617. doi: 10.3390/ijms21020617
- Jung, Y. A., Choi, Y. K., Jung, G. S., Seo, H. Y., Kim, H. S., Jang, B. K., et al. (2014). Sitagliptin attenuates methionine/choline-deficient diet-induced steatohepatitis. *Diabetes Res. Clin. Pract.* 105, 47–57. doi: 10.1016/j.diabres.2014.04.028
- Kaji, K., Yoshiji, H., Ikenaka, Y., Noguchi, R., Aihara, Y., Douhara, A., et al. (2014). Dipeptidyl peptidase-4 inhibitor attenuates hepatic fibrosis via suppression of activated hepatic stellate cell in rats. *J. Gastroenterol.* 49, 481–491. doi: 10.1007/s00535-013-0783-4
- Kalluri, R., and Zeisberg, M. (2006). Fibroblasts in cancer. *Nat. Rev. Cancer* 6, 392–401.
- Kanasaki, K., Shi, S., Kanasaki, M., He, J., Nagai, T., Nakamura, Y., et al. (2014). 4 inhibition ameliorates kidney fibrosis in streptozotocin-induced diabetic mice by inhibiting endothelial-to-mesenchymal transition in a therapeutic regimen. *Diabetes* 63, 2120–2131. doi: 10.2337/db13-1029
- Kang, H. M., Ahn, S. H., Choi, P., Ko, Y. A., Han, S. H., Chinga, F., et al. (2015). Defective fatty acid oxidation in renal tubular epithelial cells has a key role in kidney fibrosis development. *Nat. Med.* 21, 37–46. doi: 10.1038/nm.3762
- Katsumata, L. W., Miyajima, A., and Itoh, T. (2017). Portal fibroblasts marked by the surface antigen Thy1 contribute to fibrosis in mouse models of cholestatic liver injury. *Hepatol. Commun.* 1, 198–214. doi: 10.1002/hep4.1023
- Kavian, N., Servettaz, A., Marut, W., Nicco, C., Chéreau, C., Weill, B., et al. (2012). Sunitinib inhibits the phosphorylation of platelet-derived growth factor receptor β in the skin of mice with scleroderma-like features and prevents the development of the disease. *Arthrit. Rheum.* 64, 1990–2000. doi: 10.1002/art.34354
- Kay, J., and High, W. A. (2008). Imatinib mesylate treatment of nephrogenic systemic fibrosis. *Arthrit. Rheum.* 58, 2543–2548. doi: 10.1002/art.23696
- Kelly, T. (2005). Fibroblast activation protein-alpha and dipeptidyl peptidase IV (CD26): cell-surface proteases that activate cell signaling and are potential targets for cancer therapy. *Drug Resist. Updates* 8, 51–58. doi: 10.1016/j.drug.2005.03.002
- Khalil, R., Shata, A., Abd El-Kader, E. M., Sharaf, H., Abdo, W. S., Amin, N. A., et al. (2020). Vildagliptin, a DPP-4 inhibitor, attenuates carbon tetrachloride-induced liver fibrosis by targeting ERK1/2, p38 α , and NF- κ B signaling. *Toxicol. Appl. Pharmacol.* 407, 115246. doi: 10.1016/j.taap.2020.115246
- Khanna, D., Saggar, R., Mayes, M. D., Abtin, F., Clements, P. J., Maranian, P., et al. (2011). A one-year, phase I/IIa, open-label pilot trial of imatinib mesylate in the treatment of systemic sclerosis-associated active interstitial lung disease. *Arthrit. Rheum.* 63, 3540–3546. doi: 10.1002/art.30548
- Kim, M. J., Kim, N. Y., Jung, Y. A., Lee, S., Jung, G. S., Kim, J. G., et al. (2020). Evogliptin, a Dipeptidyl Peptidase-4 inhibitor, attenuates renal fibrosis caused by unilateral ureteral obstruction in mice. *Diabetes Metab. J.* 44, 186–192. doi: 10.4093/dmj.2018.0271
- Kimura, T., Monslow, J., Klampatsa, A., Leibowitz, M., Sun, J., Liouisa, M., et al. (2019). Loss of cells expressing fibroblast activation protein has variable effects in models of TGF- β and chronic bleomycin-induced fibrosis. *Am. J. Physiol. Lung Cell. Mol. Physiol.* 317, L271–L282.
- Klinkhammer, B. M., Floege, J., and Boor, P. (2018). PDGF in organ fibrosis. *Mol. Aspects Med.* 62, 44–62. doi: 10.1016/j.mam.2017.11.008
- Kocabayoglu, P., Lade, A., Lee, Y. A., Dragomir, A. C., Sun, X., Fiel, M. I., et al. (2015). β -PDGF receptor expressed by hepatic stellate cells regulates fibrosis in murine liver injury, but not carcinogenesis. *J. Hepatol.* 63, 141–147. doi: 10.1016/j.jhep.2015.01.036
- Korosec, A., Frech, S., Gesslbauer, B., Vierhapper, M., Radtke, C., Petzelbauer, P., et al. (2019). Lineage identity and location within the dermis determine the function of papillary and reticular fibroblasts in human skin. *J. Invest. Dermatol.* 139, 342–351. doi: 10.1016/j.jid.2018.07.033
- Kostallari, E., Hirsova, P., Prasnicka, A., Verma, V. K., Yaqoob, U., Wongjarupong, N., et al. (2018). Hepatic stellate cell-derived platelet-derived growth factor receptor-alpha-enriched extracellular vesicles promote liver fibrosis in mice through SHP2. *Hepatology* 68, 333–348. doi: 10.1002/hep.29803
- Kuai, J., Mosyak, L., Brooks, J., Cain, M., Carven, G. J., Ogawa, S., et al. (2015). Characterization of binding mode of action of a blocking anti-platelet-derived growth factor (PDGF)-B monoclonal antibody, MOR8457, reveals conformational flexibility and avidity needed for PDGF-BB to bind PDGF receptor- β . *Biochemistry* 54, 1918–1929. doi: 10.1021/bi5015425
- Künzli, B. M., Nuhn, P., Enjyoji, K., Banz, Y., Smith, R. N., Csizmadia, E., et al. (2008). Disordered pancreatic inflammatory responses and inhibition of fibrosis in CD39-null mice. *Gastroenterology* 134, 292–305. doi: 10.1053/j.gastro.2007.10.030
- Lee, M., Shin, E., Bae, J., Cho, Y., Lee, J. Y., Lee, Y. H., et al. (2020). Dipeptidyl peptidase-4 inhibitor protects against non-alcoholic steatohepatitis in mice by targeting TRAIL receptor-mediated lipooptosis via modulating hepatic dipeptidyl peptidase-4 expression. *Sci. Rep.* 10:19429.
- Levy, M. T., McCaughan, G. W., Marinos, G., and Gorrell, M. D. (2002). Intrahepatic expression of the hepatic stellate cell marker fibroblast activation protein correlates with the degree of fibrosis in hepatitis C virus infection. *Liver* 22, 93–101. doi: 10.1034/j.1600-0676.2002.01503.x
- Li, Y., Zhang, J., Zhou, Q., Wang, H., Xie, S., Yang, X., et al. (2019). Linagliptin inhibits high glucose-induced transdifferentiation of hypertrophic scar-derived fibroblasts to myofibroblasts via IGF/Akt/mTOR signalling pathway. *Exp. Dermatol.* 28, 19–27. doi: 10.1111/exd.13800
- Liu, Y., Wang, Z., Kwong, S. Q., Lui, E. L. H., Friedman, S. L., Li, F. R., et al. (2011). Inhibition of PDGF, TGF- β , and Abl signaling and reduction of liver fibrosis by the small molecule Bcr-Abl tyrosine kinase antagonist Nilotinib. *J. Hepatol.* 55, 612–625. doi: 10.1016/j.jhep.2010.11.035
- Long, M., Cai, L., Li, W., Zhang, L., Guo, S., Zhang, R., et al. (2018). DPP-4 inhibitors improve diabetic wound healing via direct and indirect promotion of epithelial-mesenchymal transition and reduction of scarring. *Diabetes* 67, 518–531.
- Lynch, M. D., and Watt, F. M. (2018). Fibroblast heterogeneity: implications for human disease. *J. Clin. Invest.* 128, 26–35. doi: 10.1172/jci93555
- Mah, W., Jiang, G., Olver, D., Gallant-Behm, C., Wiebe, C., Hart, D. A., et al. (2017). Elevated CD26 expression by skin fibroblasts distinguishes a profibrotic phenotype involved in scar formation compared to gingival fibroblasts. *Am. J. Pathol.* 187, 1717–1735. doi: 10.1016/j.ajpath.2017.04.017
- Marcelin, G., Ferreira, A., Liu, Y., Atlan, M., Aron-Wisniewsky, J., Pelloux, V., et al. (2017). A PDGFR α -mediated switch toward CD9(high) adipocyte progenitors controls obesity-induced adipose tissue fibrosis. *Cell Metab.* 25, 673–685. doi: 10.1016/j.cmet.2017.01.010
- Marleau, S., Harb, D., Bujold, K., Avallone, R., Iken, K., Wang, Y., et al. (2005). EP 80317, a ligand of the CD36 scavenger receptor, protects apolipoprotein E-deficient mice from developing atherosclerotic lesions. *FASEB J.* 19, 1869–1871. doi: 10.1096/fj.04-3253fj
- Marques, A. P., Cunha-Santos, J., Leal, H., Sousa-Ferreira, L., Pereira de Almeida, L., Cavadas, C., et al. (2018). Dipeptidyl peptidase IV (DPP-IV) inhibition prevents fibrosis in adipose tissue of obese mice. *Biochim. Biophys. Acta Gen. Subj.* 1862, 403–413. doi: 10.1016/j.bbagen.2017.11.012

- Mejias, M., Garcia-Pras, E., Tiani, C., Miquel, R., Bosch, J., and Fernandez, M. (2009). Beneficial effects of sorafenib on splanchnic, intrahepatic, and portocollateral circulations in portal hypertensive and cirrhotic rats. *Hepatology* 49, 1245–1256. doi: 10.1002/hep.22758
- Nazari, B., Rice, L. M., Stifano, G., Barron, A. M., Wang, Y. M., Korndorf, T., et al. (2016). Altered dermal fibroblasts in systemic sclerosis display podoplanin and CD90. *Am. J. Pathol.* 186, 2650–2664. doi: 10.1016/j.ajpath.2016.06.020
- Nicola, T., Hagood, J. S., James, M. L., Macewen, M. W., Williams, T. A., Hewitt, M. M., et al. (2009). Loss of Thy-1 inhibits alveolar development in the newborn mouse lung. *Am. J. Physiol. Lung Cell. Mol. Physiol.* 296, L738–L750.
- Okamura, D. M., Pennathur, S., Pasichnyk, K., López-Guisa, J. M., Collins, S., Febbraio, M., et al. (2009). CD36 regulates oxidative stress and inflammation in hypercholesterolemic CKD. *J. Am. Soc. Nephrol.* 20, 495–505. doi: 10.1681/asn.2008010009
- Olson, L. E., and Soriano, P. (2009). Increased PDGFR α activation disrupts connective tissue development and drives systemic fibrosis. *Dev. Cell* 16, 303–313. doi: 10.1016/j.devcel.2008.12.003
- Opstel, C., Mertens, J. C., Jüngel, A., Brentano, F., Maciejewska-Rodriguez, H., Huber, L. C., et al. (2010). Inhibition of fibroblast activation protein and dipeptidylpeptidase 4 increases cartilage invasion by rheumatoid arthritis synovial fibroblasts. *Arthritis Rheum.* 62, 1224–1235. doi: 10.1002/art.27395
- Ostendorf, T., van Roeyen, C. R., Peterson, J. D., Kunter, U., Eitner, F., Hamad, A. J., et al. (2003). A fully human monoclonal antibody (CR002) identifies PDGF-D as a novel mediator of mesangioproliferative glomerulonephritis. *J. Am. Soc. Nephrol.* 14, 2237–2247. doi: 10.1097/01.asn.0000083393.00959.02
- Östman, A. (2017). PDGF receptors in tumor stroma: biological effects and associations with prognosis and response to treatment. *Adv. Drug Deliv. Rev.* 121, 117–123. doi: 10.1016/j.addr.2017.09.022
- Panchapakesan, U., and Pollock, C. (2015). The role of dipeptidyl peptidase - 4 inhibitors in diabetic kidney disease. *Front. Immunol.* 6:443. doi: 10.1042/CS20180031
- Papadopoulos, N., Lennartsson, J., and The, P. D. G. F. (2018). /PDGFR pathway as a drug target. *Mol. Aspects Med.* 62, 75–88. doi: 10.1016/j.mam.2017.11.007
- Patel, P. M., Jones, V. A., Kridin, K., and Amber, K. T. (2020). The role of Dipeptidyl Peptidase-4 in cutaneous disease. *Exp. Dermatol.* 30, 304–318. doi: 10.1111/exd.14228
- Pennathur, S., Pasichnyk, K., Bahrami, N. M., Zeng, L., Febbraio, M., Yamaguchi, I., et al. (2015). The macrophage phagocytic receptor CD36 promotes fibrogenic pathways on removal of apoptotic cells during chronic kidney injury. *Am. J. Pathol.* 185, 2232–2245. doi: 10.1016/j.ajpath.2015.04.016
- Perrot, I., Michaud, H. A., Giraudon-Paoli, M., Augier, S., Docquier, A., Gros, L., et al. (2019). Blocking antibodies targeting the CD39/CD73 immunosuppressive pathway unleash immune responses in combination cancer therapies. *Cell Rep.* 27, 2411.e9–2425.e9.
- Philippe, C., Telerman, S. B., Oulès, B., Pisco, A. O., Shaw, T. J., Elgueta, R., et al. (2018). Spatial and single-cell transcriptional profiling identifies functionally distinct human dermal fibroblast subpopulations. *J. Invest. Dermatol.* 138, 811–825. doi: 10.1016/j.jid.2018.01.016
- Pietras, K., Sjöblom, T., Rubin, K., Heldin, C. H., and Ostman, A. (2003). PDGF receptors as cancer drug targets. *Cancer Cell* 3, 439–443. doi: 10.1016/s1535-6108(03)00089-8
- Pontén, A., Li, X., Thorén, P., Aase, K., Sjöblom, T., Ostman, A., et al. (2003). Transgenic overexpression of platelet-derived growth factor-C in the mouse heart induces cardiac fibrosis, hypertrophy, and dilated cardiomyopathy. *Am. J. Pathol.* 163, 673–682. doi: 10.1016/s0002-9440(10)63694-2
- Prakadan, S. M., Shalek, A. K., and Weitz, D. A. (2017). Scaling by shrinking: empowering single-cell 'omics' with microfluidic devices. *Nat. Rev. Genet.* 18, 345–361. doi: 10.1038/nrg.2017.15
- Prey, S., Ezzedine, K., Doussau, A., Grandoulier, A. S., Barcat, D., Chatelus, E., et al. (2012). Imatinib mesylate in scleroderma-associated diffuse skin fibrosis: a phase II multicentre randomized double-blinded controlled trial. *Br. J. Dermatol.* 167, 1138–1144. doi: 10.1111/j.1365-2133.2012.11186.x
- Rabinowitz, J. D., and Mutlu, G. M. (2019). A metabolic strategy to reverse fibrosis? *Nat. Metab.* 1, 12–13. doi: 10.1038/s42255-018-0013-8
- Ramachandran, P., Dobbie, R., Wilson-Kanamori, J. R., Dora, E. F., Henderson, B. E. P., Luu, N. T., et al. (2019). Resolving the fibrotic niche of human liver cirrhosis at single-cell level. *Nature* 575, 512–518. doi: 10.1038/s41586-019-1631-3
- Rege, T. A., and Hagood, J. S. (2006). Thy-1 as a regulator of cell-cell and cell-matrix interactions in axon regeneration, apoptosis, adhesion, migration, cancer, and fibrosis. *FASEB J.* 20, 1045–1054. doi: 10.1096/fj.05-5460rev
- Rinkevich, Y., Walmsley, G. G., Hu, M. S., Maan, Z. N., Newman, A. M., Drukker, M., et al. (2015). Skin fibrosis. Identification and isolation of a dermal lineage with intrinsic fibrogenic potential. *Science* 348:aaa2151. doi: 10.1126/science.aaa2151
- Roberts, V., Campbell, D. J., Lu, B., Chia, J., Cowan, P. J., and Dwyer, K. M. (2017). The differential effect of apyrase treatment and hCD39 overexpression on chronic renal fibrosis after ischemia-reperfusion injury. *Transplantation* 101, e194–e204.
- Roberts, V., Lu, B., Chia, J., Cowan, P. J., and Dwyer, K. M. (2016). CD39 overexpression does not attenuate renal fibrosis in the unilateral ureteric obstructive model of chronic kidney disease. *Purinerg. Signal.* 12, 653–660. doi: 10.1007/s11302-016-9528-1
- Rothweiler, S., Feldbrügge, L., Jiang, Z. G., Csizmadia, E., Longhi, M. S., Vaid, K., et al. (2019). Selective deletion of ENTPD1/CD39 in macrophages exacerbates biliary fibrosis in a mouse model of sclerosing cholangitis. *Purinerg. Signal.* 15, 375–385. doi: 10.1007/s11302-019-09664-3
- Sanders, Y. Y., Pardo, A., Selman, M., Nuovo, G. J., Tollefsbol, T. O., Siegal, G. P., et al. (2008). Thy-1 promoter hypermethylation: a novel epigenetic pathogenic mechanism in pulmonary fibrosis. *Am. J. Respir. Cell Mol. Biol.* 39, 610–618. doi: 10.1165/rcmb.2007-0322oc
- Santini, M. P., Malide, D., Hoffman, G., Pandey, G., D'Escamard, V., Nomura-Kitabayashi, A., et al. (2020). Tissue-resident PDGFR α (+) progenitor cells contribute to fibrosis versus healing in a context- and spatiotemporally dependent manner. *Cell Rep.* 30, 555.e7–570.e7.
- Seo, J. B., Choi, Y. K., Woo, H. I., Jung, Y. A., Lee, S., Lee, S., et al. (2019). Gemigliptin attenuates renal fibrosis through down-regulation of the NLRP3 inflammasome. *Diabetes Metab. J.* 43, 830–839. doi: 10.4093/dmj.2018.0181
- Shaikh, M. V., Kala, M., and Nivsarkar, M. (2016). CD90 a potential cancer stem cell marker and a therapeutic target. *Cancer Biomark.* 16, 301–307. doi: 10.3233/cbm-160590
- Shaker, M. E., Salem, H. A., Shiha, G. E., and Ibrahim, T. M. (2011). Nilotinib counteracts thioacetamide-induced hepatic oxidative stress and attenuates liver fibrosis progression. *Fund. Clin. Pharmacol.* 25, 248–257. doi: 10.1111/j.1472-8206.2010.00824.x
- Shaw, T. J., and Rognoni, E. (2020). Dissecting fibroblast heterogeneity in health and fibrotic disease. *Curr. Rheumatol. Rep.* 22:33.
- Sinha, M., Sen, C. K., Singh, K., Das, A., Ghatak, S., Rhea, B., et al. (2018). Direct conversion of injury-site myeloid cells to fibroblast-like cells of granulation tissue. *Nat. Commun.* 9:936.
- Soare, A., Györfi, H. A., Matei, A. E., Dees, C., Rauber, S., Wohlfahrt, T., et al. (2020). Dipeptidylpeptidase 4 as a marker of activated fibroblasts and a potential target for the treatment of fibrosis in systemic sclerosis. *Arthritis Rheumatol.* 72, 137–149. doi: 10.1002/art.41058
- Soria, A., Cario-André, M., Lepreux, S., Rezvani, H. R., Pasquet, J. M., Pain, C., et al. (2008). The effect of imatinib (Gleevec) on scleroderma and normal dermal fibroblasts: a preclinical study. *Dermatology* 216, 109–117. doi: 10.1159/000111507
- Souza, A. C., Bocharov, A. V., Baranova, I. N., Vishnyakova, T. G., Huang, Y. G., Wilkins, K. J., et al. (2016). Antagonism of scavenger receptor CD36 by 5A peptide prevents chronic kidney disease progression in mice independent of blood pressure regulation. *Kidney Int.* 89, 809–822. doi: 10.1016/j.kint.2015.12.043
- Spiera, R. F., Gordon, J. K., Mersten, J. N., Magro, C. M., Mehta, M., Wildman, H. F., et al. (2011). Imatinib mesylate (Gleevec) in the treatment of diffuse cutaneous systemic sclerosis: results of a 1-year, phase IIa, single-arm, open-label clinical trial. *Ann. Rheum. Dis.* 70, 1003–1009. doi: 10.1136/ard.2010.143974
- Suwanai, H., Watanabe, R., Sato, M., Odawara, M., and Matsumura, H. (2020). Dipeptidyl peptidase-4 inhibitor reduces the risk of developing hypertrophic scars and keloids following median sternotomy in diabetic patients: a nationwide retrospective cohort study using the national database of health insurance claims of Japan. *Plast. Reconstruct. Surg.* 146, 83–89. doi: 10.1097/prs.00000000000006904

- Suzuki, T., Tada, Y., Gladson, S., Nishimura, R., Shimomura, I., Karasawa, S., et al. (2017). Vildagliptin ameliorates pulmonary fibrosis in lipopolysaccharide-induced lung injury by inhibiting endothelial-to-mesenchymal transition. *Respir. Res.* 18:177.
- Sweetwyne, M. T., and Murphy-Ullrich, J. E. (2012). Thrombospondin1 in tissue repair and fibrosis: TGF- β -dependent and independent mechanisms. *Matrix Biol.* 31, 178–186. doi: 10.1016/j.matbio.2012.01.006
- Tabib, T., Morse, C., Wang, T., Chen, W., and Lafyatis, R. (2018). SFRP2/DPP4 and FMO1/LSP1 define major fibroblast populations in human skin. *J. Invest. Dermatol.* 138, 802–810. doi: 10.1016/j.jid.2017.09.045
- Takagaki, Y., Koya, D., and Kanasaki, K. (2017). Dipeptidyl peptidase-4 inhibition and renoprotection: the role of antifibrotic effects. *Curr. Opin. Nephrol. Hypertens.* 26, 56–66. doi: 10.1097/mnh.0000000000000291
- Tan, C., Jiang, M., Wong, S. S., Espinoza, C. R., Kim, C., Li, X., et al. (2019). Soluble Thy-1 reverses lung fibrosis via its integrin-binding motif. *JCI insight* 4:e131152.
- Thielitz, A., Vetter, R. W., Schultze, B., Wrenger, S., Simeoni, L., Ansoorge, S., et al. (2008). Inhibitors of dipeptidyl peptidase IV-like activity mediate antifibrotic effects in normal and keloid-derived skin fibroblasts. *J. Invest. Dermatol.* 128, 855–866. doi: 10.1038/sj.jid.5701104
- Tillmanns, J., Hoffmann, D., Habbaba, Y., Schmitto, J. D., Sedding, D., Fraccarollo, D., et al. (2015). Fibroblast activation protein alpha expression identifies activated fibroblasts after myocardial infarction. *J. Mol. Cell. Cardiol.* 87, 194–203. doi: 10.1016/j.yjmcc.2015.08.016
- Truffi, M., Sorrentino, L., Monieri, M., Fociani, P., Mazzucchelli, S., Bonzini, M., et al. (2018). Inhibition of fibroblast activation protein restores a balanced extracellular matrix and reduces fibrosis in crohn's disease strictures ex vivo. *Inflamm. Bowel Dis.* 24, 332–345. doi: 10.1093/ibd/izz008
- Uchii, M., Kimoto, N., Sakai, M., Kitayama, T., and Kunori, S. (2016). Glucose-independent renoprotective mechanisms of the tissue dipeptidyl peptidase-4 inhibitor, saxagliptin, in Dahl salt-sensitive hypertensive rats. *Eur. J. Pharmacol.* 783, 56–63. doi: 10.1016/j.ejphar.2016.04.005
- Vickovic, S., Eraslan, G., Salmén, F., Klughammer, J., Stenbeck, L., Schapiro, D., et al. (2019). High-definition spatial transcriptomics for in situ tissue profiling. *Nat. Methods* 16, 987–990. doi: 10.1038/s41592-019-0548-y
- Vorstandlechner, V., Laggner, M., Kalinina, P., Haslik, W., Radtke, C., Shaw, L., et al. (2020). Deciphering the functional heterogeneity of skin fibroblasts using single-cell RNA sequencing. *FASEB J.* 34, 3677–3692. doi: 10.1096/fj.201902001rr
- Vuorinen, K., Gao, F., Oury, T. D., Kinnula, V. L., and Myllärniemi, M. (2007). Imatinib mesylate inhibits fibrogenesis in asbestos-induced interstitial pneumonia. *Exp. Lung Res.* 33, 357–373. doi: 10.1080/01902140701634827
- Wang, X., Chen, Y., Lv, L., and Chen, J. (2009). Silencing CD36 gene expression results in the inhibition of latent-TGF-beta1 activation and suppression of silica-induced lung fibrosis in the rat. *Respir. Res.* 10:36.
- Wang, X. M., Yu, D. M., McCaughan, G. W., and Gorrell, M. D. (2005). Fibroblast activation protein increases apoptosis, cell adhesion, and migration by the LX-2 human stellate cell line. *Hepatology* 42, 935–945. doi: 10.1002/hep.20853
- Wang, Y. M., McRae, J. L., Robson, S. C., Cowan, P. J., Zhang, G. Y., Hu, M., et al. (2012). Cells participate in CD39-mediated protection from renal injury. *Eur. J. Immunol.* 42, 2441–2451. doi: 10.1002/eji.201242434
- Wei, K., Korsunsky, I., Marshall, J. L., Gao, A., Watts, G. F. M., Major, T., et al. (2020). Notch signalling drives synovial fibroblast identity and arthritis pathology. *Nature* 582, 259–264. doi: 10.1038/s41586-020-2222-z
- Worthen, C. A., Cui, Y., Orringer, J. S., Johnson, T. M., Voorhees, J. J., and Fisher, G. J. (2020). CD26 identifies a subpopulation of fibroblasts that produce the majority of collagen during wound healing in human skin. *J. Invest. Dermatol.* 140, 2515.e3–2524.e3.
- Xin, Y., Wang, X., Zhu, M., Qu, M., Bogari, M., Lin, L., et al. (2017). Expansion of CD26 positive fibroblast population promotes keloid progression. *Exp. Cell Res.* 356, 104–113.
- Xu, J., Wang, J., He, M., Han, H., Xie, W., Wang, H., et al. (2018). Dipeptidyl peptidase IV (DPP-4) inhibition alleviates pulmonary arterial remodeling in experimental pulmonary hypertension. *Lab. Invest.* 98, 1333–1346. doi: 10.1038/s41374-018-0080-1
- Yang, R., Elsaadi, S., Misund, K., Abdollahi, P., Vandsemb, E. N., Moen, S. H., et al. (2020). Conversion of ATP to adenosine by CD39 and CD73 in multiple myeloma can be successfully targeted together with adenosine receptor A2A blockade. *J. Immunother. Cancer* 8:e000610. doi: 10.1136/jitc-2020-000610
- Yang, X., Okamura, D. M., Lu, X., Chen, Y., Moorhead, J., Varghese, Z., et al. (2017). CD36 in chronic kidney disease: novel insights and therapeutic opportunities. *Nat. Rev. Nephrol.* 13, 769–781. doi: 10.1038/nrneph.2017.126
- Yang, Y. L., Lin, S. H., Chuang, L. Y., Guh, J. Y., Liao, T. N., Lee, T. C., et al. (2007). CD36 is a novel and potential anti-fibrogenic target in albumin-induced renal proximal tubule fibrosis. *J. Cell. Biochem.* 101, 735–744. doi: 10.1002/jcb.21236
- Yehualaesht, T., O'Connor, R., Begleiter, A., Murphy-Ullrich, J. E., Silverstein, R., and Khalil, N. (2000). A CD36 synthetic peptide inhibits bleomycin-induced pulmonary inflammation and connective tissue synthesis in the rat. *Am. J. Respir. Cell Mol. Biol.* 23, 204–212. doi: 10.1165/ajrcmb.23.2.4089
- Ying, H. Z., Chen, Q., Zhang, W. Y., Zhang, H. H., Ma, Y., Zhang, S. Z., et al. (2017). PDGF signaling pathway in hepatic fibrosis pathogenesis and therapeutics (Review). *Mol. Med.* 16, 7879–7889. doi: 10.3892/mmr.2017.7641
- Yoshida, S., Ikenaga, N., Liu, S. B., Peng, Z. W., Chung, J., Sverdlow, D. Y., et al. (2014). Extrahepatic platelet-derived growth factor- β , delivered by platelets, promotes activation of hepatic stellate cells and biliary fibrosis in mice. *Gastroenterology* 147, 1378–1392. doi: 10.1053/j.gastro.2014.08.038
- Zhang, H., Sun, D., Wang, G., Cui, S., Field, R. A., Li, J., et al. (2019). Alogliptin alleviates liver fibrosis via suppression of activated hepatic stellate cell. *Biochem. Biophys. Res. Commun.* 511, 387–393. doi: 10.1016/j.bbrc.2019.02.065
- Zhao, X., Psarianos, P., Ghorraie, L. S., Yip, K., Goldstein, D., Gilbert, R., et al. (2019). Metabolic regulation of dermal fibroblasts contributes to skin extracellular matrix homeostasis and fibrosis. *Nat. Metab.* 1, 147–157. doi: 10.1038/s42255-018-0008-5

Conflict of Interest: The authors declare that the research was conducted in the absence of any commercial or financial relationships that could be construed as a potential conflict of interest.

Copyright © 2021 Huang, Khoong, Han, Su, Ma, Gu, Li and Zan. This is an open-access article distributed under the terms of the Creative Commons Attribution License (CC BY). The use, distribution or reproduction in other forums is permitted, provided the original author(s) and the copyright owner(s) are credited and that the original publication in this journal is cited, in accordance with accepted academic practice. No use, distribution or reproduction is permitted which does not comply with these terms.



Expression and Pathogenic Analysis of Integrin Family Genes in Systemic Sclerosis

Dan Xu^{1†}, Ting Li^{1†}, Ruikang Wang² and Rong Mu^{1*}

¹ Department of Rheumatology and Immunology, Peking University Third Hospital, Beijing, China, ² Department of Rheumatology and Immunology, Peking University People's Hospital, Beijing, China

Objectives: Emerging evidence shows that integrin members are involved in inflammation and fibrosis in systemic sclerosis (SSc). This study aimed at evaluating the expression of integrin family genes in the skin tissue from SSc patients and exploring the potential pathogenic mechanism.

Methods: We utilized the public datasets of SSc skin tissue from the Gene Expression Omnibus (GEO) database to analyze the expression and clinical significance of integrin family genes in SSc. The expression of integrin members in skin tissue was also assessed by immunohistochemistry. In addition, functional enrichment and pathway analysis were conducted.

Results: Compared with healthy controls, the mRNA and protein levels of *ITGA5*, *ITGB2*, and *ITGB5* were upregulated in the skin of SSc patients. Further analysis indicated that the mRNA expression levels of *ITGA5*, *ITGB2*, and *ITGB5* were positively correlated with modified Rodnan skin thickness score (mRSS). Functional enrichment and pathway analysis showed that integrin members may play multiple roles in the pathogenesis of SSc. Among them, *ITGA5*, *ITGB2*, and *ITGB5* might synergistically promote SSc through affecting extracellular matrix (ECM) turnover, ECM–receptor interaction, focal adhesion, and leukocyte trans-endothelial migration, while *ITGA5* and *ITGB5* also might affect angiogenesis and endothelial cell function. In addition, *ITGA5*, *ITGB2*, and *ITGA5* were associated with different pathways, respectively. *ITGA5* was uniquely enriched for actin organization, while *ITGB5* was for TGF- β signaling and *ITGB2* for immune cell activation.

Conclusion: Our results implied that the abnormal expression of integrin family genes including *ITGA5*, *ITGB2*, and *ITGB5* may participate in multiple pathological processes in SSc. Further investigations are required for confirming this speculation.

Keywords: integrin, systemic sclerosis, skin, bioinformatics analysis, gene

INTRODUCTION

Systemic sclerosis (SSc) is an immune-mediated autoimmune disease, which is characterized by activation of the immune system, dysfunction of endothelial cells, and organ fibrosis (1, 2). The aberrant accumulation of extracellular matrix (ECM) components often disrupts the physiological architecture and leads to angiogenesis and organ fibrosis (3). It has been implied that the interaction between the surrounding ECM, fibroblasts, and endothelial cells is mediated by the expression of specific integrins on the cell surface, which strongly affects cell function (4).

OPEN ACCESS

Edited by:

Isotta Chimenti,
Sapienza University of Rome, Italy

Reviewed by:

Roberto Giacomelli,
University of L'Aquila, Italy
Heiko Golpon,
Hannover Medical School, Germany

*Correspondence:

Rong Mu
murongster@gmail.com

[†]These authors have contributed
equally to this work

Specialty section:

This article was submitted to
Pathology,
a section of the journal
Frontiers in Medicine

Received: 01 March 2021

Accepted: 17 June 2021

Published: 20 July 2021

Citation:

Xu D, Li T, Wang R and Mu R (2021)
Expression and Pathogenic Analysis
of Integrin Family Genes in Systemic
Sclerosis. *Front. Med.* 8:674523.
doi: 10.3389/fmed.2021.674523

Integrins are a large family of heterodimeric transmembrane receptors, comprising α and β subunits. There are 18 α subunit genes (*ITGA1*, *ITGA2*, *ITGA3*, *ITGA4*, *ITGA5*, *ITGA6*, *ITGA7*, *ITGA8*, *ITGA9*, *ITGA10*, *ITGA11*, *ITGA2B*, *ITGAD*, *ITGAE*, *ITGAL*, *ITGAM*, *ITGAV*, *ITGAX*) and 8 β subunit genes (*ITGB1*, *ITGB2*, *ITGB3*, *ITGB4*, *ITGB5*, *ITGB6*, *ITGB7*, *ITGB8*), forming 24 different transmembrane surface receptors in vertebrates (5). Integrins are widely distributed on cell surfaces of normal fibroblast, endothelial cells, epithelial cells, and immune cells. Integrin changes conformation and activates subsequent intracellular signals by recognizing specific extracellular ligands, so as to mediate cell–cell adhesion and cell–matrix adhesion, respond to microenvironment signals, and regulate cell migration and proliferation (6). Emerging evidence shows that integrins also play important roles in autoimmunity (7), angiogenesis (8), and tissue fibrosis (9) by controlling local activation of latent transforming growth factor (TGF)- β , cross-talking with growth factor receptors (10), mediating mechanotransduction (11), and promoting cell adhesion and proliferation (12).

ITGA5, *ITGB1*, *ITGB3*, and *ITGB5* are well-studied integrin members in SSc, which can form $\alpha5\beta1$, $\alpha\nu\beta3$, and $\alpha\nu\beta5$ heterodimeric receptors. Among them, integrin $\alpha\nu\beta3$ and integrin $\alpha\nu\beta5$ were found overexpressed in SSc patients and animal models, which were related to lymphocyte infiltration, TGF- β activation, and collagen accumulation (13). On the other hand, studies on other integrin members still remain sparse. Gene analysis revealed that inflammation mediated by the integrin signaling pathway was a common shared pathway related to SSc (14). All these discoveries made integrin an attractive therapeutic target for SSc. Neutralizing antibody and small molecule inhibitors of integrin $\alpha\nu$ and $\beta1$ were protective in animal models of SSc (13, 15, 16). However, integrin-targeted therapy has not shown significant efficacy in patients yet. Phase II clinical trials of an $\alpha\nu\beta6$ antibody (BG00011) in the treatment of idiopathic pulmonary fibrosis (IPF) and an integrin $\alpha\nu$ monoclonal antibody (abitudumab) in the treatment of SSc-ILD were terminated due to safety and efficacy problems or difficulties in patient inclusion, respectively (clinicaltrials.gov identifier NCT03573505 and NCT02745145). The failure of the above clinical trials may be partly due to the complexity of the integrins in the progression of SSc. This study aimed to explore the key members and roles of integrins in the pathogenesis of SSc, therefore providing insight into its potential value as a therapeutic target for SSc.

METHODS

Microarray Data Acquisition and Processing

To explore the changes of expression profiling and reveal biological processes in the skin of patients with SSc, eligible microarray datasets were downloaded from the Gene Expression Omnibus (GEO, <http://www.ncbi.nlm.nih.gov/geo>) database. The inclusion criteria of microarray datasets were as follows: (1) datasets should be the expression profile of genome-wide mRNA

transcriptome data, (2) datasets consisted of expression profiles in the skin of patients with SSc and normal controls, and (3) datasets were standardized or raw datasets. All gene expression data have previously been published on the GEO database.

Identification of Differentially Expressed Integrin Family Genes

Normalization and log₂ transformation were performed for the raw data to minimize heterogeneity. Probes without gene symbols or genes with more than one probe were removed or averaged, respectively. The merged data were preprocessed by *sav* package to remove batch effects with R software (version 3.5.1). After performing batch normalization, *limma* package was utilized to screen differentially expressed integrin family member genes between SSc patients and healthy controls. Adjusted $p < 0.05$ was considered statistically significant. The correlations between mRNA expression of integrin members and clinical characteristics were analyzed.

Immunohistochemistry (IHC)

Immunohistochemical analysis was performed on 3-mm sections of formalin-fixed, paraffin-embedded tissue. Antigen retrieval was performed by a microwave oven with buffer of citric acid (pH 6.0). Then, endogenous peroxidase activity and non-specific binding were blocked with peroxidase block buffer and 1% bovine serum albumin, respectively. After blocking, sections were incubated with primary antibodies (anti-integrin $\alpha5$ antibody, 1:400, ab150361, Abcam, Cambridge, MA, USA; anti-integrin $\alpha7$ antibody, 1:800, ab203254, Abcam, Cambridge, MA, USA; anti-integrin $\beta2$ antibody, 1:2,000, ab131044, Abcam, Cambridge, MA, USA; anti-integrin $\beta5$ antibody, 1:400, 3629S, CST, Danvers, MA, USA) at 4°C overnight. Subsequently, sections were incubated with HRP conjugate before chromogenic detection using DAB. For the semiquantitative analysis, the H-score method assigned a score of 0–300 to each patient, based on the percentage of cells stained at different intensities (17).

GO and KEGG Enrichment Analyses

Database for Annotation, Visualization, and Integrated Discovery (DAVID) was applied to perform the Gene Ontology (GO) analysis and Kyoto Encyclopedia of Genes and Genomes (KEGG) pathway enrichment analysis. The integrin family genes showed correlation coefficient (r) > 0.5 were analyzed for GO and KEGG enrichment by DAVID. GO analysis included biological processes (BP), cellular components (CC), and molecular functions (MF). The top 10 significant enrichments of BP, CC, and MF ($p < 0.05$ and rank by p -value) and KEGG enrichments ($p < 0.05$) were visualized.

Estimating the Population Abundance of Tissue-Infiltrating Immune and Stromal Cell Populations

The absolute abundance of eight immune and two stromal cell populations were analyzed by Microenvironment Cell Populations-counter (MCP-counter) method (18). In addition, we analyzed the association of integrin members and the

TABLE 1 | Studies included in the analysis^a.

| Dataset | GEO accession no. | Excluded, no. | Included, no. | No. of samples |
|---------------------|-------------------|---------------|---------------|----------------|
| Assassi et al. (19) | GSE58095 | 5 | 97 | 61 SSc, 36 HC |
| Guo et al. (20) | GSE65336 | 68 | 10 | 10 SSc |
| Mantero et al.* | GSE95065 | 0 | 33 | 18 SSc, 15 HC |

Eighty-nine SSc patients and 61 HC were included.

SSc, systemic sclerosis; HC, healthy control.

^aArrays were excluded if the samples were not skin biopsies or if the samples were collected at a second time point.

*Array profiling data can be obtained from the Gene Expression Omnibus (GEO-NCBI) (GSE95065), which is shared by Mantero JCP. et al. The website is <https://www.ncbi.nlm.nih.gov/geo/query/acc.cgi?acc=GSE95065>.

population abundance of tissue-infiltrating immune and stromal cell by Spearman's correlation.

RESULTS

Gene Expression Datasets of SSc

Three expression datasets were obtained with accession numbers of GSE58095, GSE65336, and GSE95065 from the GEO database (19, 20). Totally, skin gene expression profiles of 89 SSc patients and 61 normal controls were enrolled in this study. The detailed information of the four datasets is displayed in **Table 1**.

The Aberrant mRNA Expression of Integrin Genes in SSc Patients

To understand the roles of integrin genes in SSc, we compared the mRNA levels of integrin genes between SSc and normal controls. The results indicated that mRNA levels of *ITGA5*, *ITGA7*, *ITGA8*, *ITGB2*, and *ITGB5* were significantly higher in skin samples of SSc than those of normal controls, while the mRNA levels of *ITGAE* and *ITGB3BP* were significantly lower and other integrins showed no remarkable differences (**Figure 1**).

The Protein Levels of Abnormal Integrins in the Skin Tissues of SSc Patients

We next performed an immunohistochemical analysis to evaluate the expression of integrin $\alpha 5$, integrin $\alpha 7$, integrin $\beta 2$, and integrin $\beta 5$ in the skin tissue from 10 SSc patients and 6 normal controls. Consistent with the results of gene expression profiles from microarray, the protein levels of integrin $\alpha 5$, integrin $\beta 2$, and integrin $\beta 5$ in the skin tissues of SSc patients were significantly increased compared with those in the normal control, respectively. However, the level of integrin $\alpha 7$ was found to have no significant differences between the skin tissues of normal and SSc patients (**Figure 2**).

Association Between Aberrant Expressed Integrin Family Genes and Clinical Features of SSc

To verify the potential roles of aberrant expressed integrin family genes in SSc, correlation analysis and subgroup analysis

between the mRNA levels of *ITGA5*, *ITGB2*, and *ITGB5* and clinical features were performed in GSE58095. The clinical characteristics of SSc subjects from GSE58095 are concluded in **Table 2**. We found that the increased *ITGA5*, *ITGB2*, and *ITGB5* expressions were significantly associated with modified Rodnan skin thickness score (mRSS) (**Figure 3A**). Concerning the SSc subgroups, the mRNA expression levels of *ITGA5* and *ITGB5* were higher in dcSSc skin tissue than in lcSSc (**Figure 3B**). We compared integrin family gene expression in the skin sample according to the type of autoantibody in SSc patients, while we observed that *ITGB2* was downregulated in patients seropositive for anti-centromere antibody (ACA) compared with those lacking specific antibodies. We also found that the gene expression of *ITGB5* was higher in patients seropositive for ACA than in those lacking specific antibodies or those seropositive for either anti-U1 RNP antibody (RNP) or anti-topoisomerase antibody (ATA) (**Figure 3C**).

Correlation Between Aberrant Expressed Integrin Family Genes and the Infiltration of Immune and Stromal Cells in the Skin of SSc

The composition of immune cells, fibroblast, and endothelial cell in the skin of SSc patients and healthy control was analyzed, and the fraction of eight kinds of immune cells was shown in the violin plot (**Figures 4A–J**). As shown, the abundance of monocytic lineage, endothelial cell, and fibroblast was higher in SSc patients than in healthy controls, while the abundance of CD8⁺ T cell was relatively lower in SSc patients.

The mRNA expression of *ITGA5*, *ITGB2*, and *ITGB5* showed significant correlation with the abundance of tissue-infiltrating immune cells or stromal cells in the SSc skin sample. Among them, the mRNA expression level of *ITGA5* was positively correlated with the abundance of fibroblasts ($r = 0.47$, $p < 0.0001$), endothelial cells ($r = 0.44$, $p < 0.0001$), and monocytes ($r = 0.35$, $p < 0.0001$), suggesting that *ITGA5* may participate in the pathogenesis of scleroderma through these cells. The mRNA expression level of *ITGB2* was significantly correlated with the abundance of fibroblasts ($r = 0.64$, $p < 0.0001$), endothelial cells ($r = 0.52$, $p < 0.0001$), T cells ($r = 0.36$, $p < 0.0001$), and myeloid dendritic cells ($r = 0.39$, $p < 0.0001$). The mRNA expression level of *ITGB5* was positively correlated with the abundance of fibroblasts ($r = 0.63$, $p < 0.0001$), endothelial cells ($r = 0.43$, $p < 0.0001$), and monocytes ($r = 0.26$, $p = 0.0021$). The detailed correlation between the abundance of immune and stromal cell types and mRNA expression levels of integrin member genes is shown in **Figure 4K**.

Possible Mechanisms of *ITGA5*, *ITGB2*, and *ITGB5* Involved in SSc

To explore the potential function of *ITGA5*, *ITGB2*, and *ITGB5* in SSc, their co-expressed genes ($r > 0.5$) were analyzed by GO and KEGG in the DAVID database. There were the same GO terms and KEGG pathway that appeared in *ITGA5*, *ITGB2*, and *ITGB5* top enrichment lists, including GO:0005201 (extracellular matrix structural constituent), GO:0005178 (integrin binding), GO:0019838 (growth factor binding), GO:0030020 (extracellular

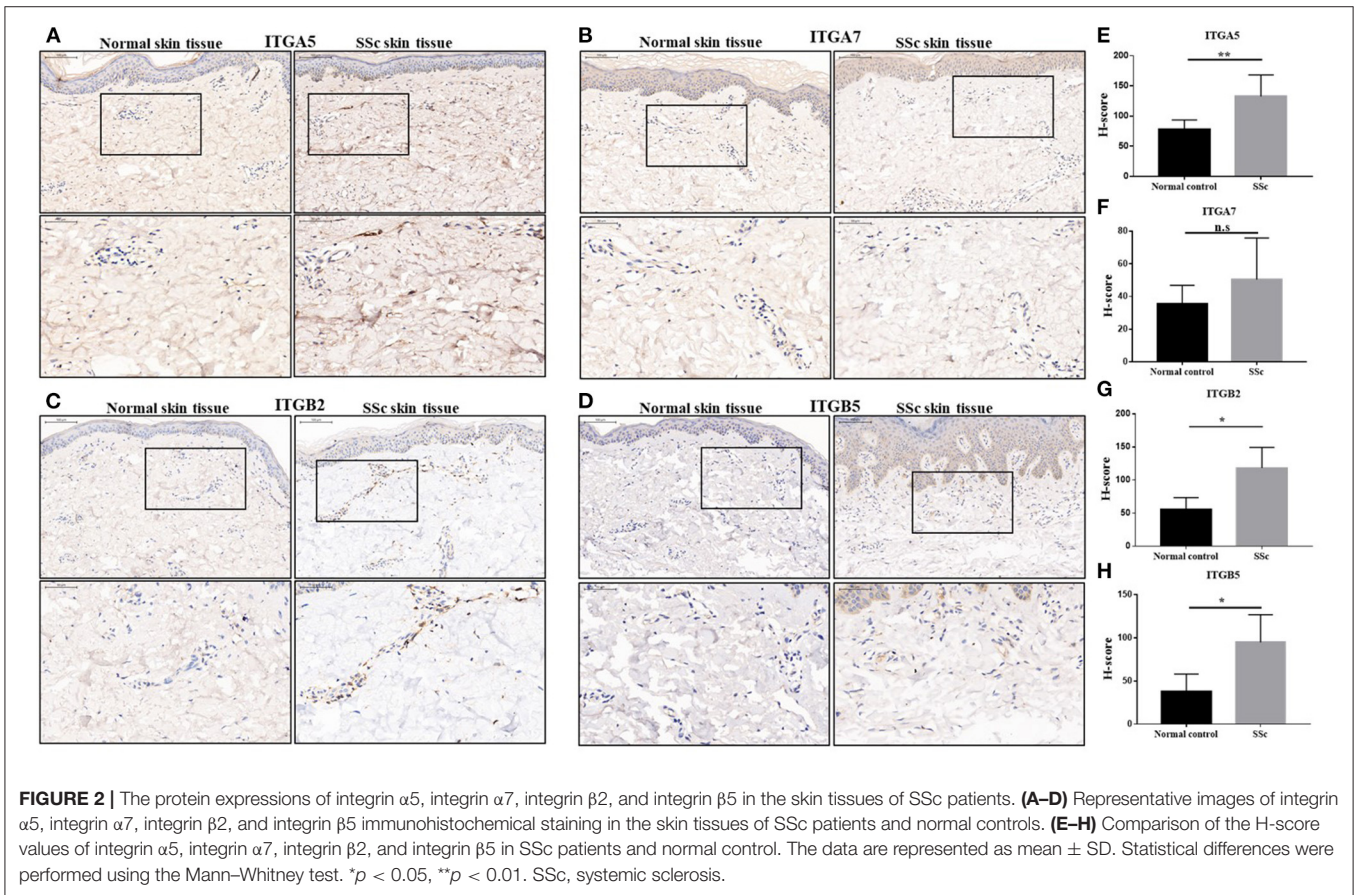
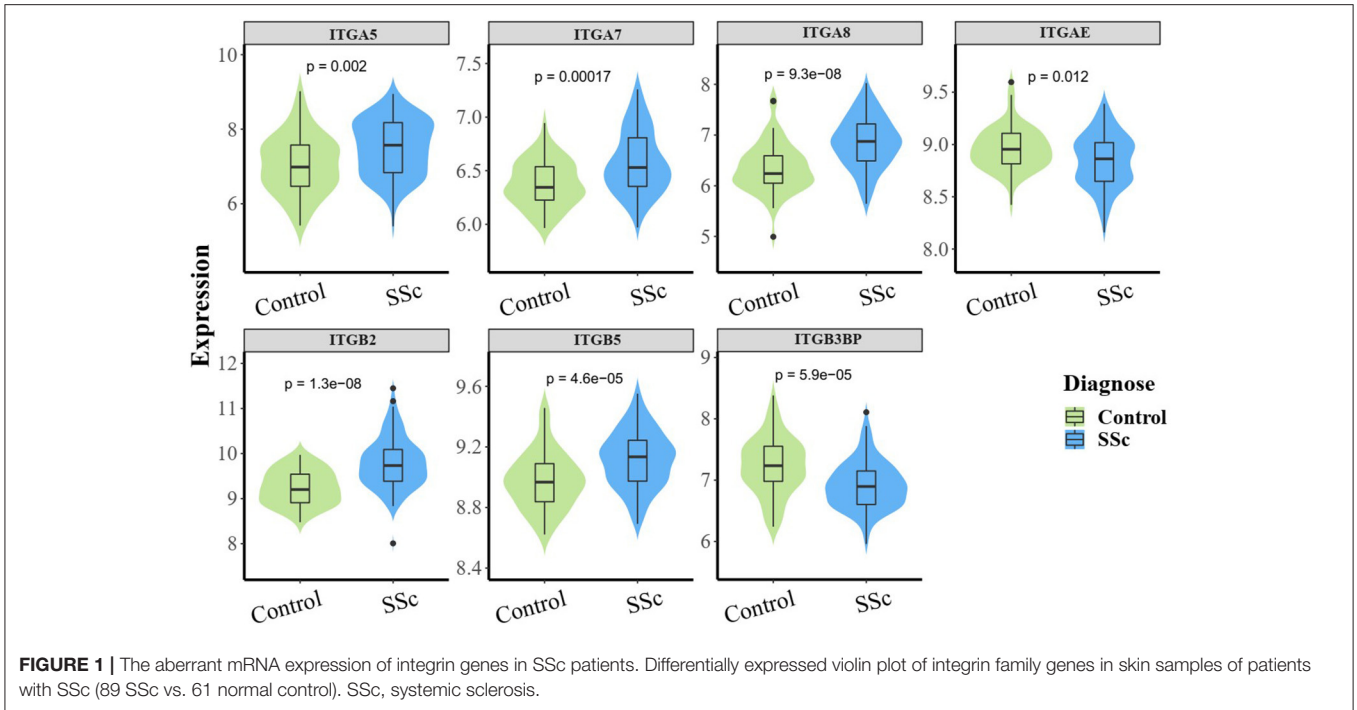


TABLE 2 | Demographic and clinical characteristics of subjects at skin biopsy.

| Characteristics | SSc patients (n = 61) | Controls (n = 36) | p-value |
|-------------------------------------|--------------------------|----------------------|---------|
| Age median (range), years | 54 (22–82) | 50 (23–67) | 0.025 |
| Gender, female/male, n (%) | 45/16 (73.77) | 29/7 (80.56) | 0.448 |
| Type of SSc, n (%) | | | |
| dcSSc | 43 (70.49) | | |
| lcSSc | 18 (29.51) | | |
| Total mRSS, median (range) | 14 (2–39) | | |
| Interstitial lung disease, n (%) | 23 (37.70) | | |
| FVC of predicted %, median (range) | 76 (35–121) | | |
| DLCO of predicted %, median (range) | 61 (23–120) | | |
| Antibody | | | |
| Negative, n (%) | 17 (27.87) | | |
| RNP, n (%) | 3 (4.92) | | |
| ACA, n (%) | 7 (11.48) | | |
| ATA, n (%) | 17 (27.87) | | |
| RNAP, n (%) | 17 (27.87) | | |
| Immunosuppressive agents, n (%) | 17 (27.87) | | |

SSc, systemic sclerosis; dcSSc, *diffused cutaneous systemic sclerosis*; lcSSc, *limited cutaneous systemic sclerosis*; mRSS, *modified Rodnan skin thickness score*; FVC, *forced vital capacity*; DLCO, *carbon monoxide breath diffusion capacity*; RNP, *anti-U1 RNP antibody*; ACA, *anti-centromere antibody*; ATA, *anti-topoisomerase antibody*; RNAP, *anti-RNA polymerase III antibody*.

matrix structural constituent conferring tensile strength), and GO:0048407 (platelet-derived growth factor binding) in molecular function enrichment; GO:0062023 (collagen-containing extracellular matrix), GO:0031012 (extracellular matrix), GO:0005604 (basement membrane), GO:0005788 (endoplasmic reticulum lumen), GO:0005581 (collagen trimer), GO:0005925 (focal adhesion), and GO:0030055 (cell-substrate junction) in cellular components enrichment; GO:0030198 (ECM organization) and GO:0043062 (extracellular structure organization) in biological processes enrichment (**Figures 5A–I**); and hsa04510 (focal adhesion), hsa04512 (ECM–receptor interaction), hsa05144 (malaria), hsa04670 (leukocyte trans-endothelial migration), and hsa04974 (protein digestion and absorption) in KEGG enrichment (**Figures 6A–C**). In summary, *ITGA5*, *ITGB2*, and *ITGB5* might synergistically promote SSc through the extracellular matrix turnover, ECM–receptor interaction, focal adhesion, and leukocyte trans-endothelial migration. It is worth mentioning that *ITGA5*- and *ITGB5*-associated genes were enriched for GO:0001525 (angiogenesis) in the biological processes enrichment.

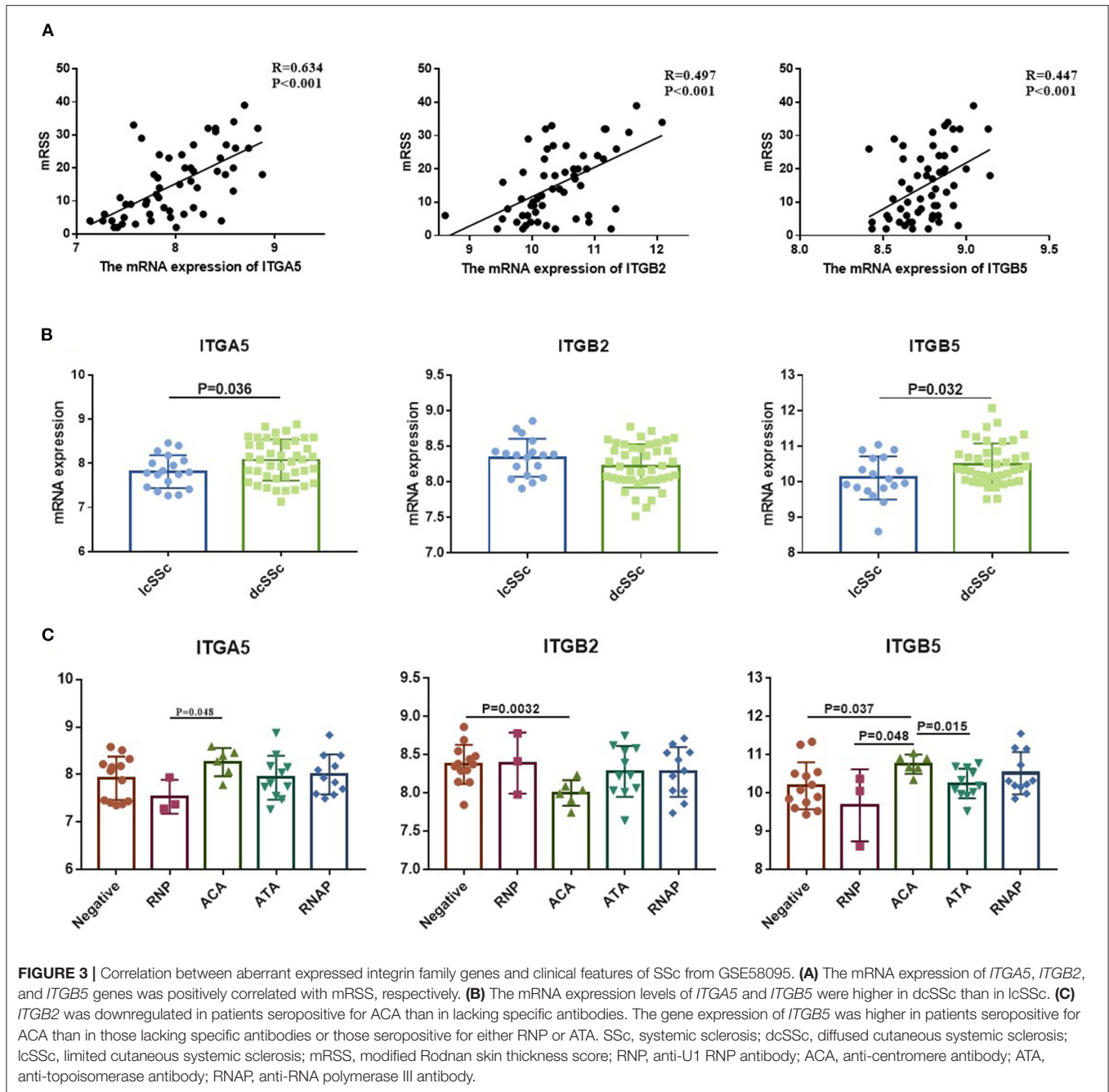
In addition, *ITGA5*-associated genes were uniquely enriched for GO:0007015 (actin filament organization), GO:0051493 (regulation of cytoskeleton organization), GO:0032956 (regulation of actin cytoskeleton organization), GO:0031589 (cell-substrate adhesion), GO:1902903 (regulation of supramolecular fiber organization), GO:0030335 (positive regulation of cell migration), and GO:0032970 (regulation of actin filament-based process). The results indicated that *ITGA5*

might be more involved in the organization and regulation of actin cytoskeleton, cell adhesion, and migration in SSc. *ITGB2*-associated genes were uniquely enriched for GO:0043299 (leukocyte degranulation), GO:0050900 (leukocyte migration), GO:0006909 (phagocytosis), GO:0002275 (myeloid cell activation involved in immune response), GO:0002444 (myeloid leukocyte mediated immunity), GO:0042110 (T-cell activation), GO:0042119 (neutrophil activation), and GO:0002250 (adaptive immune response). These results implied that *ITGB2* might be important for inflammation by cytokine binding and activation of T cells, monocytes, and granulocytes in SSc. *ITGB5* associated genes uniquely enriched for GO:0032963 (collagen metabolic process), GO:0030199 (collagen fibril organization), GO:0071559 (response to transforming growth factor beta), GO:0071560 (cellular response to transforming growth factor beta stimulus), GO:0007179 (transforming growth factor beta receptor signaling pathway), GO:0007178 (transmembrane receptor protein serine/threonine kinase signaling pathway), and GO:0032964 (collagen biosynthetic process). These results indicated that *ITGB5* might be involved in the transforming growth factor beta signaling pathway.

DISCUSSION

Integrin plays important and complex roles in SSc, but integrin-targeted therapy has not shown significant efficacy in SSc patients, which may be due to that the precise role of integrin is currently ambiguous and unsuitable option for treatment target. In this study, we used the GEO database to explore the expression and potential roles of integrin family genes in SSc skin, hoping to find a feasible target. We found that the mRNA and protein levels of *ITGA5*, *ITGB2*, and *ITGB5* were abnormally overexpressed in the skin of SSc. Further analysis indicated that the mRNA levels of *ITGA5*, *ITGB2*, and *ITGB5* were positively correlated with mRSS score. Besides, we also found that the mRNA levels of *ITGB2* and *ITGB5* were associated with positive autoantibodies. *ITGA5*, *ITGB2*, and *ITGB5* showed strong correlations with various stromal cells including endothelial cell and fibroblast, respectively.

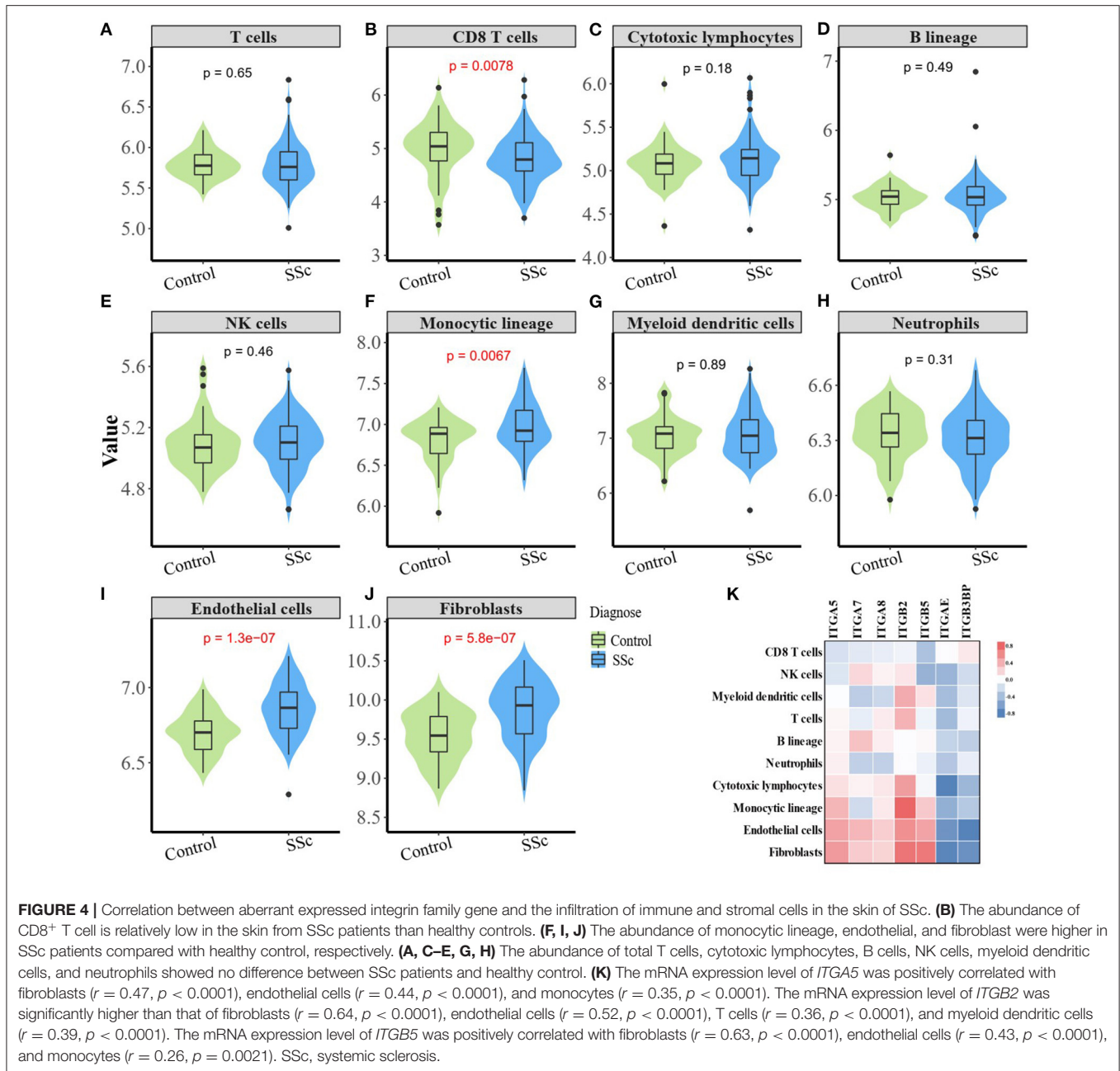
Mechanically, our results showed *ITGA5*, *ITGB2*, and *ITGB5* were mainly enriched for ECM and cell–matrix interaction, indicating that they might promote SSc by affecting ECM turnover, ECM–receptor interaction, focal adhesion, and leukocyte trans-endothelial migration. Growth factor, chemokines, ADP, and thrombin can interact with talin and kindlin, called “inside-out” signaling, and promote the activity of integrins (6, 21). On the other hand, integrins, like integrin $\alpha2\beta1$ (coded by *ITGA2* and *ITGB1*), can directly bind to GFOGER-like motifs of collagen I to enhance collagen synthesis without the help of inside-out signaling (22). On the other hand, integrins bind to ECM ligands and subsequently trigger the accumulation of complex adaptors and signaling proteins, activating integrin downstream signaling pathways, such as the activation of focal adhesion kinase (FAK), SRC, AKT, and ERK pathways, which is known as the “outside-in” signaling, and consequently regulating cell behavior, such as the inhibition of cell death, the regulation



of cytoskeletal dynamics and cellular structure, and intracellular transport or migration (23). In summary, these results indicated that as receptors of ECM components, *ITGA5*, *ITGB2*, and *ITGB5* participate in the fibrosis process through connecting ECM components with FAK, which led to FAK activation, further promoting the proliferation, activation, and migration of fibroblasts and endothelial cells.

Our study also showed that *ITGA5*, *ITGB2*, and *ITGB5* may mediate the migration of leukocytes from blood vessels to skin tissue by interacting with chemokines (CXCL12, CCL2) and vascular endothelial cell adhesion molecules

(JAM3/CDH5/ICAM 1/PECM1) and participate in the immune inflammatory process of SSc. Overexpression of *ITGB2* can recognize ligands such as intercellular adhesion molecule 1 (ICAM-1) and vascular cell adhesion molecule 1 (VCAM-1) on the surface of endothelial cells, and then provide the direct cellular binding to vascular endothelial cells and fibroblasts, which facilitates the infiltration of inflammatory cells to the endothelium and subsequent transmigration (24). A recent study also showed that interleukin 1 β (IL-1 β) not only induced inflammatory but also increased the expression of integrin $\alpha 5\beta 1$ to promote trans-endothelial migration of peripheral blood



mononuclear cells (PBMC) in human brain microvascular endothelial cells (25). Generally speaking, the interaction between inflammatory cells, endothelial cells, and fibroblasts regulated by integrin family members including *ITGA5*, *ITGB2*, and *ITGB5* may lead to the activation of vascular endothelial cells and fibroblasts in SSc. Our results indicated that *ITGA5* and *ITGB5* also synergistically affected angiogenesis and endothelial cell function. Wang et al. found that higher matrix stiffness increased VEGFR2 expression in human umbilical vein endothelial cells and that the integrin $\alpha V\beta 5/Akt/Sp1$ pathway participated in stiffness-mediated effects on VEGFR2 upregulation (26). Integrin $\alpha 5\beta 1$ levels in endothelial cells were

induced in response to several angiogenic factor stimuli, such as IL-8, bFGF, or TNF α . Upregulated integrin $\alpha 5\beta 1$ participated in regulating angiogenesis by interacting with diverse partners such as VEGFR-1, CD97, and uPAR (27–29). In addition, blocking integrin $\alpha 5$ subunits by specific monoclonal antibodies or small peptides has become a potential strategy for anti-angiogenesis therapy (30).

Overall, integrin members have a compensatory and synergistic effect, which may explain why the current therapies targeting integrin have not achieved good efficacy in fibrosis or SSc. Combined therapy targeting multiple integrin members in SSc should be considered.

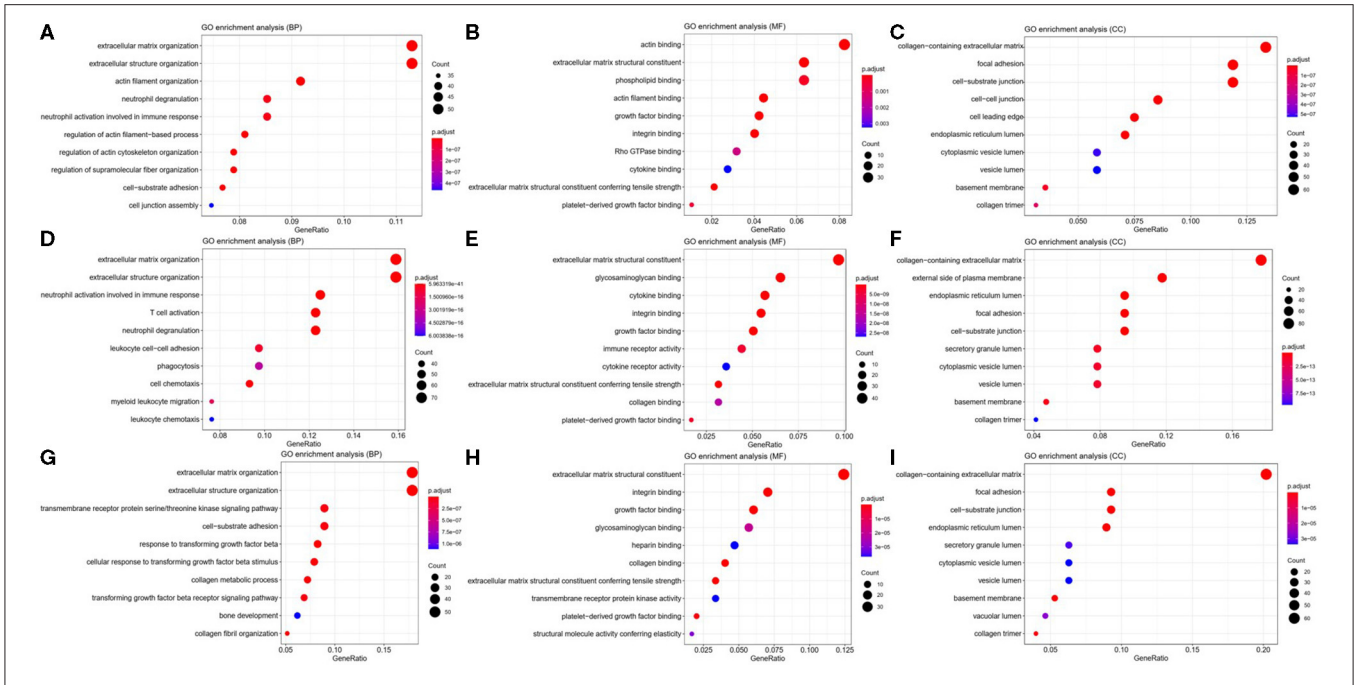


FIGURE 5 | Possible mechanisms of *ITGA5*, *ITGB2*, and *ITGB5* involved in SSc. Top 10 significantly enriched GO terms for *ITGA5* (A–C), *ITGB2* (D–F), and *ITGB5* (G–I). The size of the circle represents gene count. Different colors of circles represent different adjusted *p*-value. Gene ratio means the number of genes in *ITGA5* and *ITGB2/5* co-expressed genes ($r > 0.5$); genes that belong to this pathway divided by the number of genes in the background gene cluster that belong to this pathway. GO, Gene Ontology; SSc, systemic sclerosis.

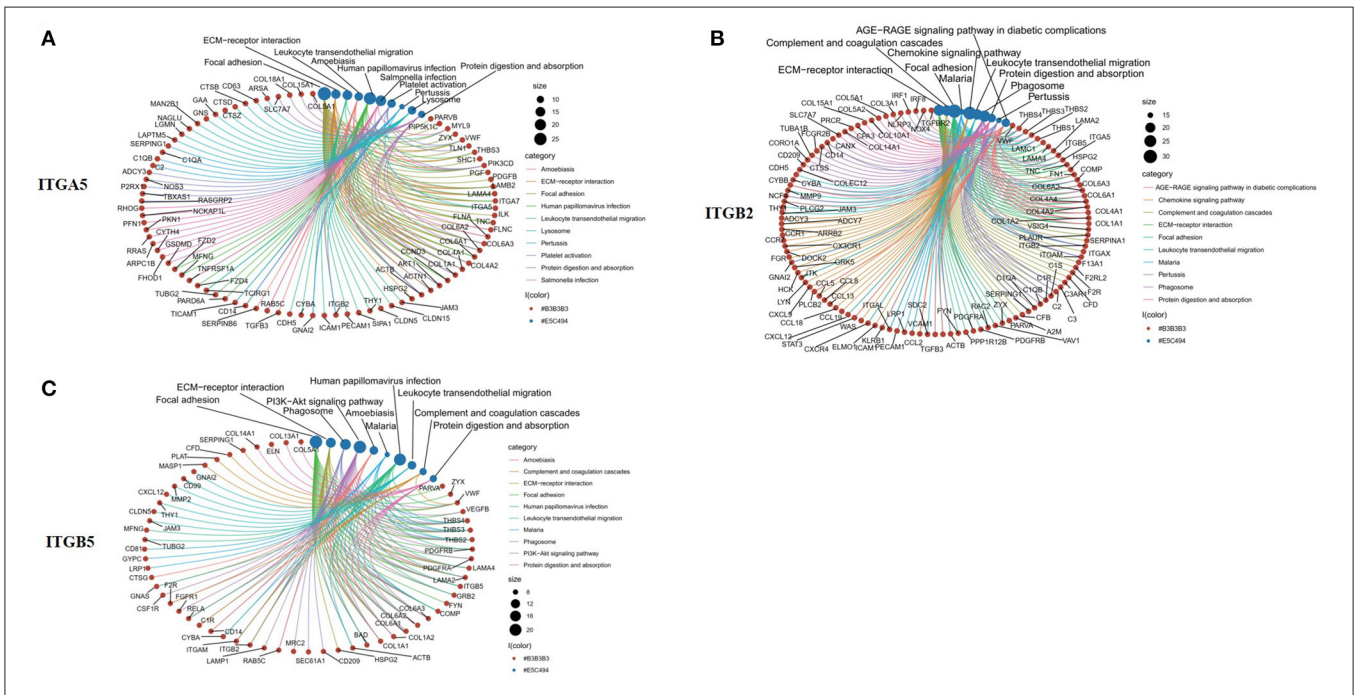


FIGURE 6 | Top 10 significantly enriched KEGG pathway for *ITGA5*, *ITGB2*, and *ITGB5* involved in SSc. (A) *ITGA5*; (B) *ITGB2*; (C) *ITGB5*. The red circle represents genes, and the blue circle represents related signaling pathways enriched by genes. KEGG, Kyoto Encyclopedia of Genes and Genomes; SSc, systemic sclerosis.

Our study also suggested that *ITGA5*, *IGTB5*, and *IGTB2* participated in SSc pathogenesis in unique ways. RNA interference high-throughput assay showed that *ITGA5* is one of the genes that affect the myofibroblast phenotype of SSc skin fibroblasts (31). A higher expression level of *ITGA5* was found in the serum-derived fibroblasts of IPF patients than in the normal cells (32), which facilitated a more aggressive proliferative phenotype of fibroblasts (33). This was consistent with our findings that *ITGA5* mRNA expression was positively correlated with fibroblasts, suggesting that *ITGA5* may mainly affect the phenotype of fibroblasts and affect the process of fibrosis. We also found that *ITGA5* was related with cytoskeleton and actin. Supportively, a previous study showed that *ITGA5* can modulate peripheral actin organization (34). Presumably, *ITGA5* participated in cell stiffness and contraction phenotype, while *ITGB5* participated in TGF- β signaling in SSc patients. *ITGB5* combined with αV can bind to arginine-glycine-aspartic acid (RGD) leading to the activation of TGF- β 1 and the enhancement of TGF- β signaling by physical association with TGF- β RRII (35, 36). Yoshihide et al. found that $\alpha V\beta 5$ was upregulated in scleroderma fibroblasts and that the transient overexpression of $\alpha V\beta 5$ increased the human alpha2 (I) collagen gene expression in normal fibroblasts (37). *ITGB2* correlated with activation of T cell, neutrophil, and monocyte, indicating that *ITGB2* may be involved in the inflammation of SSc. Physiologically, *ITGB2* was important for host defense, which was exclusively expressed in leukocytes promoting leukocyte adhesion and ensuing extravasation (38). In summary, each integrin has its specific role and function in SSc, which involves many aspects such as immunity, inflammation, and fibrosis, indicating that the integrin family members play a wide and important role. In addition, it also reminds us of the importance of further searching for molecules that can simultaneously regulate the activation of several integrin members such as talin and kindlins (6).

This study has some limitations. The protein levels of integrin $\alpha 8$, integrin αE , and integrin $\beta 3$ binding protein remain to be detected in the skin tissues of SSc patients. Second, our study only focused on the integrin mRNA expression in skin samples, leaving the expression and function of integrin in PBMC, lung, and other involved tissues unconsidered. Therefore, further

studies are necessary to validate our findings and conjectures *in vitro* and *in vivo*.

In conclusion, this study revealed that the mRNA and protein levels of *ITGA5*, *IGTB5*, and *IGTB2* were upregulated in the skin tissue of SSc patients. *ITGA5*, *IGTB5*, and *IGTB2* may participate in multiple pathological processes, and preliminary evidence of existing overlapping mechanisms has been noticed. Further studies are warranted.

DATA AVAILABILITY STATEMENT

Publicly available datasets were analyzed in this study. This data can be found here: <https://www.ncbi.nlm.nih.gov/geo/query/acc.cgi?acc=GSE58095> <https://www.ncbi.nlm.nih.gov/geo/query/acc.cgi?acc=GSE65336> <https://www.ncbi.nlm.nih.gov/geo/query/acc.cgi?acc=GSE95065>.

ETHICS STATEMENT

The studies involving human participants were reviewed and approved by the Ethical Committee of the Peking university people's hospital. The patients/participants provided their written informed consent to participate in this study.

AUTHOR CONTRIBUTIONS

RM designed this study. DX, TL, and RW contributed to the data interpretation and analysis. All authors contributed to the drafting and revising of the manuscript and have critically reviewed and approved the final submitted version to be published.

FUNDING

This work was supported by grants from the National Natural Science Foundation of China (No. 81771706).

ACKNOWLEDGMENTS

The gene expression datasets were obtained from the GEO database. We thank all of the investigators for sharing the data.

REFERENCES

- Thannickal VJ, Zhou Y, Gaggar A, Duncan SR. Fibrosis: ultimate and proximate causes. *J Clin Invest.* (2014) 124:4673–7. doi: 10.1172/JCI74368
- Cipriani P, Marrelli A, Liakouli V, Di Benedetto P, Giacomelli R. Cellular players in angiogenesis during the course of systemic sclerosis. *Autoimmun Rev.* (2011) 10:641–6. doi: 10.1016/j.autrev.2011.04.016
- Liakouli V, Cipriani P, Di Benedetto P, Ruscitti P, Carubbi F, Berardicurti O, et al. The role of extracellular matrix components in angiogenesis and fibrosis: possible implication for Systemic Sclerosis. *Mod Rheumatol.* (2018) 28:922–32. doi: 10.1080/14397595.2018.1431004
- Moreno-Layseca P, Icha J, Hamidi H, Ivaska J. Integrin trafficking in cells and tissues. *Nat Cell Biol.* (2019) 21:122–32. doi: 10.1038/s41556-018-0223-z
- Campbell ID, Humphries MJ. Integrin structure, activation, and interactions. *Cold Spring Harb Perspect Biol.* (2011) 3:a004994. doi: 10.1101/cshperspect.a004994
- Sun Z, Costell M, Fassler R. Integrin activation by talin, kindlin and mechanical forces. *Nat Cell Biol.* (2019) 21:25–31. doi: 10.1038/s41556-018-0234-9
- Nolte M, Margadant C. Controlling immunity and inflammation through integrin-dependent regulation of TGF-beta. *Trends Cell Biol.* (2020) 30:49–59. doi: 10.1016/j.tcb.2019.10.002
- Plow EF, Meller J, Byzova TV. Integrin function in vascular biology: a view from 2013. *Curr Opin Hematol.* (2014) 21:241–7. doi: 10.1097/MOH.0000000000000042
- Chen C, Li R, Ross RS, Manso AM. Integrins and integrin-related proteins in cardiac fibrosis. *J Mol Cell Cardiol.* (2016) 93:162–74. doi: 10.1016/j.yjmcc.2015.11.010

10. Eliceiri BP. Integrin and growth factor receptor crosstalk. *Circ Res.* (2001) 89:1104–10. doi: 10.1161/hh2401.101084
11. Sun Z, Guo SS, Fassler R. Integrin-mediated mechanotransduction. *J Cell Biol.* (2016) 215:445–56. doi: 10.1083/jcb.201609037
12. Bachmann M, Kukkurainen S, Hytonen VP, Wehrle-Haller B. Cell Adhesion by Integrins. *Physiol Rev.* (2019) 99:1655–99. doi: 10.1152/physrev.00036.2018
13. Luzina IG, Todd NW, Nacu N, Lockatell V, Choi J, Hummers LK, et al. Regulation of pulmonary inflammation and fibrosis through expression of integrins alphaVbeta3 and alphaVbeta5 on pulmonary T lymphocytes. *Arthritis Rheum.* (2009) 60:1530–9. doi: 10.1002/art.24435
14. Chairta P, Nicolaou P, Christodoulou K. Genomic and genetic studies of systemic sclerosis: a systematic review. *Hum Immunol.* (2017) 78:153–65. doi: 10.1016/j.humimm.2016.10.017
15. Gerber EE, Gallo EM, Fontana SC, Davis EC, Wigley FM, Huso DL, et al. Integrin-modulating therapy prevents fibrosis and autoimmunity in mouse models of scleroderma. *Nature.* (2013) 503:126–30. doi: 10.1038/nature12614
16. Henderson NC, Arnold TD, Katamura Y, Giacomini MM, Rodriguez JD, McCarty JH, et al. Targeting of alphav integrin identifies a core molecular pathway that regulates fibrosis in several organs. *Nat Med.* (2013) 19(12):1617–24. doi: 10.1038/nm.3282
17. Jensen K, Krusenstjerna-Hafstrom R, Lohse J, Petersen KH, Derand H. A novel quantitative immunohistochemistry method for precise protein measurements directly in formalin-fixed, paraffin-embedded specimens: analytical performance measuring HER2. *Mod Pathol.* (2017) 30:180–93. doi: 10.1038/modpathol.2016.176
18. Becht E, Giraldo NA, Lacroix L, Buttard B, Elarouci N, Petitprez F, et al. Estimating the population abundance of tissue-infiltrating immune and stromal cell populations using gene expression. *Genome Biol.* (2016) 17:218. doi: 10.1186/s13059-016-1113-y
19. Assassi S, Swindell WR, Wu M, Tan FD, Khanna D, Furst DE, et al. Dissecting the heterogeneity of skin gene expression patterns in systemic sclerosis. *Arthritis Rheumatol.* (2015) 67:3016–26. doi: 10.1002/art.39289
20. Guo X, Higgs BW, Bay-Jensen AC, Karsdal MA, Yao Y, Roskos LK, et al. Suppression of T cell activation and collagen accumulation by an anti-IFNAR1 mAb, anifrolumab, in adult patients with systemic sclerosis. *J Invest Dermatol.* (2015) 135:2402–9. doi: 10.1038/jid.2015.188
21. Munger JS, Sheppard D. Cross talk among TGF-beta signaling pathways, integrins, and the extracellular matrix. *Cold Spring Harb Perspect Biol.* (2011) 3:a005017. doi: 10.1101/cshperspect.a005017
22. Zeltz C, Gullberg D. The integrin-collagen connection—a glue for tissue repair? *J Cell Sci.* (2016) 129:653–64. doi: 10.1242/jcs.180992
23. Kechagia JZ, Ivaska J, Roca-Cusachs P. Integrins as biomechanical sensors of the microenvironment. *Nat Rev Mol Cell Biol.* (2019) 20:457–73. doi: 10.1038/s41580-019-0134-2
24. Dashti N, Mahmoudi M, Gharibdoost F, Kavosi H, Rezaei R, Imeni V, et al. Evaluation of ITGB2 (CD18) and SELL (CD62L) genes expression and methylation of ITGB2 promoter region in patients with systemic sclerosis. *Rheumatol Int.* (2018) 38:489–98. doi: 10.1007/s00296-017-3915-y
25. Labus J, Woltje K, Stolte KN, Hackel S, Kim KS, Hildmann A, et al. IL-1beta promotes transendothelial migration of PBMCs by upregulation of the FN/alpha5beta1 signalling pathway in immortalised human brain microvascular endothelial cells. *Exp Cell Res.* (2018) 373:99–111. doi: 10.1016/j.yexcr.2018.10.002
26. Wang Y, Zhang X, Wang W, Xing X, Wu S, Dong Y, et al. Integrin alphaVbeta5/Akt/Sp1 pathway participates in matrix stiffness-mediated effects on VEGFR2 upregulation in vascular endothelial cells. *Am J Cancer Res.* (2020) 10:2635–48.
27. Orecchia A, Lacial PM, Schietroma C, Morea V, Zambruno G, Failla CM. Vascular endothelial growth factor receptor-1 is deposited in the extracellular matrix by endothelial cells and is a ligand for the alpha 5 beta 1 integrin. *J Cell Sci.* (2003) 116:3479–89. doi: 10.1242/jcs.00673
28. Tjong WY, Lin HH. The role of the RGD motif in CD97/ADGRE5- and EMR2/ADGRE2-modulated tumor angiogenesis. *Biochem Biophys Res Commun.* (2019) 520:243–9. doi: 10.1016/j.bbrc.2019.09.113
29. Tarui T, Andronicos N, Czekay RP, Mazar AP, Bdeir K, Parry GC, et al. Critical role of integrin alpha 5 beta 1 in urokinase (uPA)/urokinase receptor (uPAR, CD87) signaling. *J Biol Chem.* (2003) 278:29863–72. doi: 10.1074/jbc.M304694200
30. Ramakrishnan V, Bhaskar V, Law DA, Wong MH, DuBridge RB, Breinberg D, et al. Preclinical evaluation of an anti-alpha5beta1 integrin antibody as a novel anti-angiogenic agent. *J Exp Ther Oncol.* (2006) 5:273–86.
31. Chadli L, Sotthwes B, Li K, Andersen SN, Cahir-McFarland E, Cheung M, et al. Identification of regulators of the myofibroblast phenotype of primary dermal fibroblasts from early diffuse systemic sclerosis patients. *Sci Rep.* (2019) 9:4521. doi: 10.1038/s41598-019-41153-w
32. Epstein Shochet G, Brook E, Israeli-Shani L, Edelstein E, Shitrit D. Fibroblast paracrine TNF-alpha signaling elevates integrin A5 expression in idiopathic pulmonary fibrosis (IPF). *Respir Res.* (2017) 18:122. doi: 10.1186/s12931-017-0606-x
33. Shochet GE, Brook E, Bardenstein-Wald B, Grobe H, Edelstein E, Israeli-Shani L, et al. Integrin alpha-5 silencing leads to myofibroblastic differentiation in IPF-derived human lung fibroblasts. *Ther Adv Chronic Dis.* (2020) 11:2040622320936023. doi: 10.1177/2040622320936023
34. Oh MA, Kang ES, Lee SA, Lee EO, Kim YB, Kim SH, et al. PKCdelta and cofilin activation affects peripheral actin reorganization and cell-cell contact in cells expressing integrin alpha5 but not its tailless mutant. *J Cell Sci.* (2007) 120:2717–30. doi: 10.1242/jcs.003566
35. Kim KK, Sheppard D, Chapman HA. TGF-beta1 Signaling and Tissue Fibrosis. *Cold Spring Harb Perspect Biol.* (2018) 10:a022293. doi: 10.1101/cshperspect.a022293
36. Margadant C, Sonnenberg A. Integrin-TGF-beta crosstalk in fibrosis, cancer and wound healing. *EMBO Rep.* (2010) 11:97–105. doi: 10.1038/embor.2009.276
37. Asano Y, Ihn H, Yamane K, Jinnin M, Tamaki K. Increased expression of integrin alphavbeta5 induces the myofibroblastic differentiation of dermal fibroblasts. *Am J Pathol.* (2006) 168:499–510. doi: 10.2353/ajpath.2006.041306
38. Tan SM. The leucocyte beta2 (CD18) integrins: the structure, functional regulation and signalling properties. *Biosci Rep.* (2012) 32:241–69. doi: 10.1042/BSR20110101

Conflict of Interest: The authors declare that the research was conducted in the absence of any commercial or financial relationships that could be construed as a potential conflict of interest.

Copyright © 2021 Xu, Li, Wang and Mu. This is an open-access article distributed under the terms of the Creative Commons Attribution License (CC BY). The use, distribution or reproduction in other forums is permitted, provided the original author(s) and the copyright owner(s) are credited and that the original publication in this journal is cited, in accordance with accepted academic practice. No use, distribution or reproduction is permitted which does not comply with these terms.



Role of PDGF-A/B Ligands in Cardiac Repair After Myocardial Infarction

Kunal Kalra¹, Joerg Eberhard¹, Nona Farbehi², James J. Chong¹ and Munira Xaymardan^{1*}

¹ Faculty of Medicine and Health, The University of Sydney, Sydney, NSW, Australia, ² Garvan Weizmann Centre for Cellular Genomics, Garvan Institute of Medical Research, Sydney, NSW, Australia

Platelet-derived growth factors (PDGFs) are powerful inducers of cellular mitosis, migration, angiogenesis, and matrix modulation that play pivotal roles in the development, homeostasis, and healing of cardiac tissues. PDGFs are key signaling molecules and important drug targets in the treatment of cardiovascular disease as multiple researchers have shown that delivery of recombinant PDGF ligands during or after myocardial infarction can reduce mortality and improve cardiac function in both rodents and porcine models. The mechanism involved cannot be easily elucidated due to the complexity of PDGF regulatory activities, crosstalk with other protein tyrosine kinase activators, and diversity of the pathological milieu. This review outlines the possible roles of PDGF ligands A and B in the healing of cardiac tissues including reduced cell death, improved vascularization, and improved extracellular matrix remodeling to improve cardiac architecture and function after acute myocardial injury. This review may highlight the use of recombinant PDGF-A and PDGF-B as a potential therapeutic modality in the treatment of cardiac injury.

OPEN ACCESS

Edited by:

Elvira Forte,
The Jackson Laboratory,
United States

Reviewed by:

Peter Boor,
RWTH Aachen University, Germany
Malina Ivey,
University of Cincinnati, United States

*Correspondence:

Munira Xaymardan
munira.xaymardan@sydney.edu.au

Specialty section:

This article was submitted to
Molecular and Cellular Pathology,
a section of the journal
Frontiers in Cell and Developmental
Biology

Received: 18 February 2021

Accepted: 20 July 2021

Published: 25 August 2021

Citation:

Kalra K, Eberhard J, Farbehi N,
Chong JJ and Xaymardan M (2021)
Role of PDGF-A/B Ligands in Cardiac
Repair After Myocardial Infarction.
Front. Cell Dev. Biol. 9:669188.
doi: 10.3389/fcell.2021.669188

Keywords: platelet-derived growth factors (PDGF), myocardial infarction, cardiac function, matrix remodeling, angiogenesis

OVERVIEW OF THE MYOCARDIAL INFARCTION PATHOLOGY

Cardiovascular disease (CVD) is the leading cause of human death globally. Development of CVD depends on pathological changes in the vascular wall, including endothelium damage, intimal inflammation, vascular wall thickening by smooth muscle cell (SMC), and fibroblast activation, as well as deposition of calcium and adipose tissue in the vascular wall (Libby and Theroux, 2005). Cellular changes are mediated by humoral factors secreted by the inflammatory and activated or damaged cells, generating a milieu that supports the development of atherosclerosis and vascular pathologies. Myocardial infarction (MI) is one of the major CVD events with substantial morbidity and mortality. Following an MI, cardiomyocytes die in large numbers in the area of “ischemic attack,” and the area is repaired by fibrotic scar tissue as the postnatal cardiomyocytes in mammals possess extremely limited regenerative capacity (Mahmoud et al., 2014).

The level of scar tissue formation and subsequent cardiac function recovery are dependent on a number of factors: (1) The size of the initial ischemic area dictated by the location of the blockage, collateral circulation, health of the microcirculation, and timing of the revascularization treatments (Bax et al., 2003). A larger area of infarct in patients with poorer collateral circulation and microvascular health (in diabetes, for example) leads to greater loss of tissue architecture (Bax et al., 2003; Adel and Nammias, 2010). (2) Infarct expansion dictated by the immune response to the injury. Overreactive immune response after MI may lead to extensive infarct expansion and

worsened cardiac function outcomes (Weisman and Healy, 1987). (3) Remodeling of the scar area in accordance with extracellular matrix reconstitution and to a minor extent, if at all, cardiomyocyte regeneration (Ramos et al., 2018).

OVERVIEW OF THE EFFECT OF PDGF ON CARDIAC TISSUE

By far, the most effective treatment for acute MI has been surgical revascularization, such as stent and bypass surgeries to restore blood supply and use of anticoagulants that prevent total occlusion of the vasculature. Stem cell treatments, especially those involving mesenchymal stem cells (MSCs), have been attempted with the intent to regenerate myocardium and improve cardiac tissue structure. Numerous animal and clinical trials have been conducted with minimally positive results in cardiomyocyte regeneration. However, improvement of cardiac function is seen in most of the trials that is thought to be attributable to the trophic benefit of the injected MSCs. The trophic effect of the MSCs alludes to the fact that cytokines or growth factors may provide similar benefits for MI without the complexity of cell delivery associated with cell culture inconsistencies and donor disparities. Indeed, many cytokines have shown their positive functions in animal models (White and Chong, 2020), but only a few were trialed in humans with the most recognized ones being the VEGF treatments (Taimeh et al., 2013; Mohl et al., 2015; Yla-Herttuala et al., 2017; White and Chong, 2020).

The authors of this review have been involved in animal research of platelet-derived growth factor (PDGF)-AB treatments in MI for many years. Overall experiences have been positive with promising outcomes seen in both rodent and porcine experiments. In a recent study by the Chong Laboratory, recombinant human (rh) PDGF-AB promoted cardiac wound repair by altering the mechanisms of scar formation of the infarcted area in a porcine model of myocardial ischemia-reperfusion. The randomized trial used 36 pigs subjected to a sham procedure or balloon occlusion of the coronary artery with a 7-day intravenous infusion of rhPDGF-AB. One-month post-MI, the survival rate of the pigs improved by 40% compared with the vehicle-treated group due to decreased ventricular arrhythmias as shown by the Holter monitor. Overall cardiac function was improved, presumably by the improved matrix configuration in the infarct area. This study provides insights into the potential clinical application of rhPDGF-AB as an adjunct to current MI treatments (Thavapalachandran et al., 2020).

This observation is supported by recent studies in rodents by our group using systemic delivery of PDGF-AB via jugular catheter connected to a minipump to the myocardial infarcted mice, which has shown improvements in cardiac anatomy and function similar to the porcine study. In addition, echocardiograms have shown a reduction in end-systolic and diastolic dimensions and scar size (Asli et al., 2017). PDGF deliveries using methods of direct intramyocardial injection, slow deliveries using nanofiber or fibrin gel implantation have also produced improved cardiac repair with differences in

ligand isotypes and their delivery approaches producing diverse outcomes (Xaymardan et al., 2004; Zheng et al., 2004; Hsieh et al., 2006a; Awada et al., 2015; **Table 1**).

In addition to cardiac treatments, PDGF ligands have been investigated for their potential role in bone fracture healing in osteoporotic or diabetic animals (Al-Zube et al., 2009; Graham et al., 2009). Exogenous PDGF-BB has been used to treat non-healing ulcers in humans (Mustoe et al., 1994; Pierce et al., 1995). Topical application of PDGF-BB was reported to accelerate the rate of wound healing in both normal and ischemic full-thickness skin wounds, as well as burn wounds (Travis et al., 2014; Gowda et al., 2015), shortening the duration of wound healing with reduced wound contraction (Ehrlich and Freedman, 2002). Improved alveolar bone and periodontal ligament regeneration was possible when used on the patients with periodontitis as reviewed (Khoshkam et al., 2015). The applications also include worrying aspects that the PDGF and other growth factors are increasingly being used in the unregulated areas of cosmetics as wrinkle reduction measure without safety assessments (no peer data available).

PDGF ligands and receptors are essential for revascularization and stromal cell activation required for wound healing. Conversely, as mitogens, potent stimulators of mesenchymal cell angiogenesis, the PDGF/Rs are implicated in many pathological processes such as atherosclerosis, fibrosis, and tumorigenesis (Hoch and Soriano, 2003; Ostman, 2004; Olson and Soriano, 2009; Kong et al., 2014; He et al., 2015; Appiah-Kubi et al., 2016; Wang et al., 2016; Klinkhammer et al., 2018; Bottrell et al., 2019; Roehlen et al., 2020; **Table 2**). Search involving PDGF receptors and cardiac diseases rendered 68 types of cardiac diseases associated with PDGFR α and 106 types with associated PDGFR β ¹. The dichotomy calls for controlled studies on the pharmacodynamic, long-term effect of the ligands before clinical application is implemented.

In this review, we attempt to elucidate the roles of PDGF signaling in the prevention of cell death, improvement of vascularity, and a potential role in myocardial regeneration as well as matrix remodeling. The focus is on the PDGF-A and B ligands and their receptors α and β in cardiac repair. Aberrant signaling of PDGF in pathological conditions is also covered although to a lesser extent due the scope of this review.

ROLE OF PLATELET-DERIVED GROWTH FACTOR IN CARDIAC INJURY MODELS

Platelet-Derived Growth Factor and Platelet-Derived Growth Factor Receptors

PDGFs are a group of multifunctional proteins that play key roles in the processes of embryonic development, organogenesis, and formation of blood vessels (Betsholtz, 1995; Hoch and Soriano, 2003). PDGF consists of four polypeptide chains, namely, the PDGF-A, PDGF-B, PDGF-C, and PDGF-D, which form four

¹https://platform.opentargets.org/target/ENSG00000134853?view=sec:known_drug

TABLE 1 | Publications reporting exogenous platelet-derived growth factor (PDGF)/platelet-derived growth factor receptor (PDGFR) recombinant protein or antibody treatment in cardiac injury.

| Treatment types | Model and species | Outcome |
|--|---|--|
| PDGF-AB combined with VEGF and angiopoietin-2 (Xaymardan et al., 2004) | Rat acute myocardial infarction (MI); intramyocardial injection | Improved cardiac function; increased survival of ear-heart transplant |
| PDGF-AB combined with BMC (Xaymardan et al., 2004) | Rat acute MI; intramyocardial injection | Improved cardiac function; increased survival of transplanted bone marrow cells |
| PDGF-AB (Thavapalachandran et al., 2020) | Porcine infarct reperfusion; intravenous continuous delivery via minipump for 7 days | Improved mortality and cardiac function; vascularity and matrix architecture |
| PDGF-AB (Asli et al., 2019) | Mice cute infarct intravenous continuous delivery via minipump for 5 days | Improved angiogenesis, reduced scar size, and cardiac function |
| PDGF-BB (Hsieh et al., 2006a) | Rat MI; self-assembling peptide nanofibers bearing ligand, sustained release for 14 days | Improved mortality and cardiac function |
| PDGF-A and PDGF-D (Zhao et al., 2011) | Rat with left ventricular anterior transmural MI via ligation of left coronary artery | Enhanced PDGF-A and D during angiogenesis, inflammatory and fibrogenesis response |
| VEGF and PDGF (Awada et al., 2015) | Myocardial injection of factors in fibrin gel | Improvement in cardiac function, ventricular wall thickness, angiogenesis, cardiac muscle survival |
| Neutralizing antibodies to PDGFR α and PDGFR β (Zymek et al., 2006) | Mouse model of ischemic reperfusion; daily injection of anti-PDGFR α and anti-PDGFR β antibodies | Anti-PDGFR α caused reduction in collagen deposition; anti-PDGFR β caused reduction of angiogenesis |

TABLE 2 | Examples of publications reporting effects of endogenous/transgenic PDGF/PDGFR overexpression.

| Treatment types | Model and species | Outcome |
|--|---|--|
| <i>Pdgfa</i> and <i>Pdgfb</i> overexpression (Gallini et al., 2016a) | Transgenic insertion of PDGFs under α -myosin heavy chain (α -MHC) promoter in embryos | <i>Pdgfa</i> resulted in severe fibrosis, increase in cardiac size leading to lethal cardiac failure soon after birth. <i>Pdgfb</i> led to focal fibrosis and moderate cardiac hypertrophy |
| <i>Pdgfa</i> , <i>Pdgfb</i> , <i>Pdgfc</i> and <i>Pdgfd</i> overexpression (Gallini et al., 2016a) | Intramyocardial delivery of <i>Pdgf</i> isoforms using adenoviral vector in adult mice | Varied reactions observed: <i>Pdgfa</i> and <i>c</i> resulting in small scars, while <i>Pdgfb</i> results in extensive scarring |
| PDGF-C overexpression (Ponten et al., 2003) | Transgenic insertion of PDGF-C under α -MHC promoter in embryonic and adult mice | Cardiac fibroblast proliferation, deposition of collagen, hypertrophy, vascular defects, and the presence of Anitschkow cells in the adult myocardium |
| PDGF-D overexpression (Ponten et al., 2005) | Transgenic insertion under α -MHC promoter | Dilated cardiomyopathy and subsequent cardiac failure |

homodimers including PDGF-AA, PDGF-BB, PDGF-CC, and PDGF-DD and one heterodimer, PDGF-AB (Li et al., 2000; Bergsten et al., 2001; Kazlauskas, 2017; Yue et al., 2019).

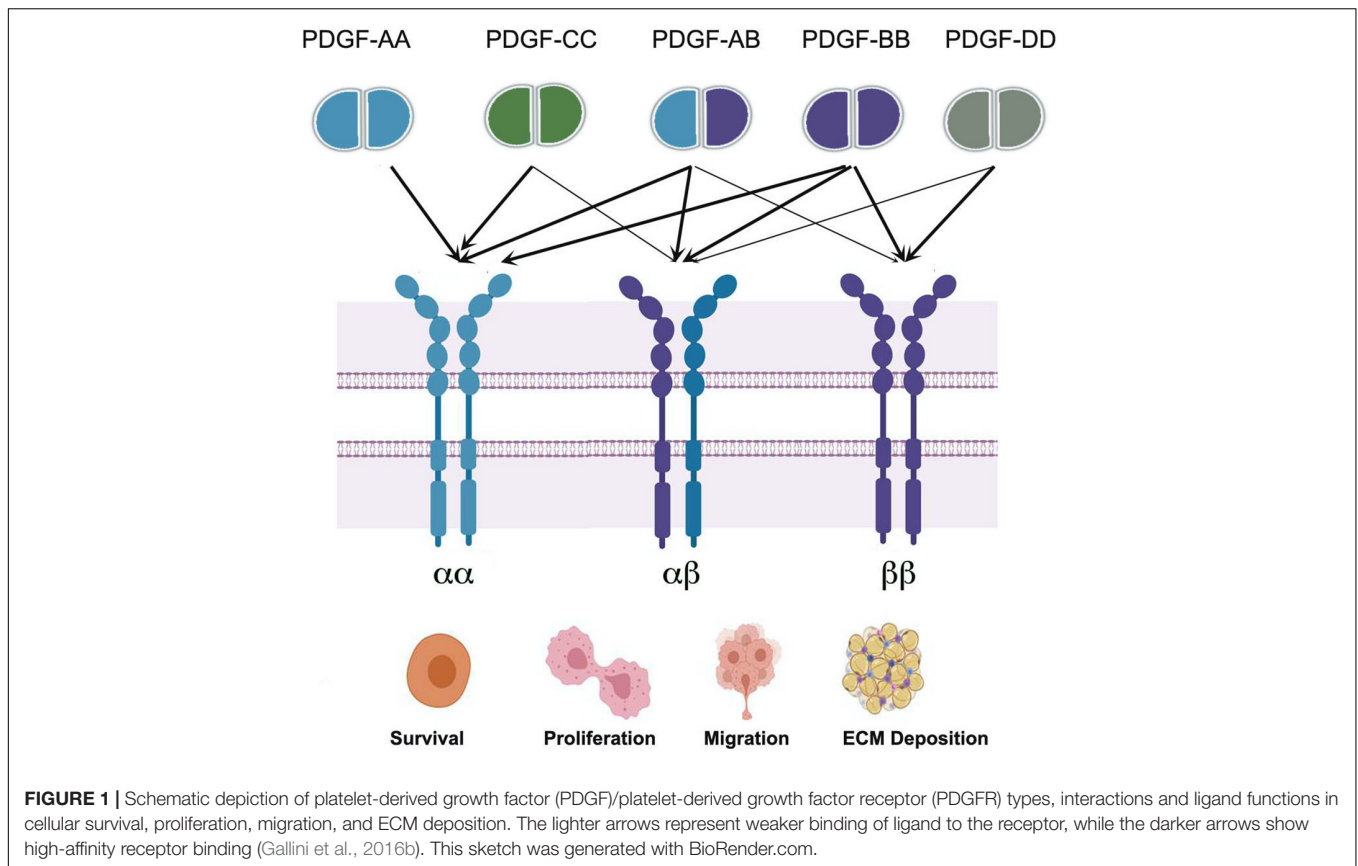
These PDGF ligands exert their functions by binding to two types of receptors (**Figure 1**) that are usually localized to connective tissue cells. PDGF α and β belong to class III receptor tyrosine kinase (RTK) and have different expression patterns and physiological roles. The extracellular region of the receptor consists of five immunoglobulin-like domains that bind to ligands, while the intracellular part is a tyrosine kinase domain for downstream transduction. Downstream signal transduction pathways include phosphatidylinositol 2 kinase, MAPK, PI3K, Src family kinases, and phospholipase C γ (Valius and Kazlauskas, 1993; Chiariello et al., 2001).

The PDGF ligands help maintain homeostasis and remain relatively dormant and tightly controlled in adult tissues with transient enhancement of expression occurring during wound healing. Dysregulation of these processes leads to pathologies such as fibrosis and cancer (Ostman, 2004; Olson and Soriano, 2009).

PDGF ligands are extremely stable molecules even in 100°C heat and varied pH conditions (Antoniades et al., 1979) and, thus, presumably suitable for sustained delivery.

PDGFR α

PDGFR α is expressed by widely distributed non-vascular interstitial fibroblasts (Ivey and Tallquist, 2016; Sebastiao et al., 2018) including a subpopulation of cells marking enriched MSC populations in all organs/tissues (Farahani and Xaymardan, 2015; Ivey and Tallquist, 2016). Detailed single-cell RNA (scRNA) analysis has shown that while the PDGFR α cells in the mouse hearts are mostly fibroblastic in nature, a small population co-expresses endothelial marker CD31, and a further minor population co-expresses macrophage markers. Both CD31 and macrophage marker expressions in PDGFR α cells are upregulated in post-MI hearts at day 3 and day 7 (Farbehi et al., 2019), although it is unclear whether this is due to transdifferentiation or an influx of cells from elsewhere (Souders et al., 2009). It is accepted that cardiac PDGFR α cells are derived either from the mesoderm via the proepicardial organ



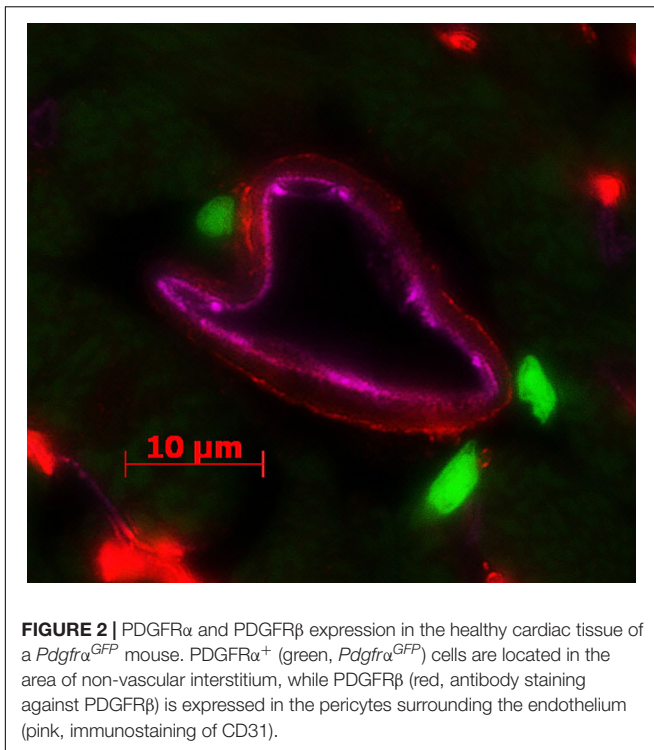
(Soriano, 1997; Chong et al., 2011; Smith et al., 2011) or the neural crest (Tallquist and Soriano, 2003). During homeostasis, they play a supportive role to the parenchymal cells of the tissues and stay relatively dormant. In pathology, PDGFR α signaling including reactivation of epicardium promotes angiogenesis and extracellular remodeling to restore tissue integrity and tensile strength (Horikawa et al., 2015; Quijada et al., 2020).

In mouse hearts, over 70% of the PDGFR α cells are positive for SCA1 (Houlihan et al., 2012), which contains a rare population of cardiac CFU-F-forming cells or so-called MSCs, while the SCA1 negative population does not give rise to CFU-F (Chong et al., 2011). These cells migrate from the epicardial organ at E9.5 in mouse embryos and reside in the type VI collagen matrix outside of the vascular structure (Munoz-Chapuli et al., 2002; Chong et al., 2011). They are negative for, or low in, PDGFR β and other pericyte markers (Santini et al., 2020; **Figure 2**). *Pdgfra* is also expressed in the cardiomyogenic progenitors in the lateral plate mesoderm in embryos prior to heart tube formation (Bloomekatz et al., 2017; Yoon et al., 2018), later diminishing with only a small population of NKX2.5-positive myocytes co-expressing PDGFR α in the right atrial area in embryonic day 8.5 in mice (Prall et al., 2007). PDGFR α -positive cardiomyocyte progenitors may exist in small numbers in adult human hearts, and whether or not this can contribute to the repair of myocardium following injury is unknown (Chong et al., 2013). In embryos, *patch* deletion of *Pdgfra* leads to cardiac defects, including enlarged hearts and septum defects, as well as epicardial malformation,

resulting in early embryonic lethality in mice (Orr-Urtreger et al., 1992; Soriano, 1997; Bax et al., 2010). In adult injury models, PDGFR α cells are thought to mainly give rise to myofibroblasts and lipofibroblasts as reported in models of pulmonary injury (Li et al., 2018) and myofibroblast in cardiac injury model (Asli et al., 2019). The differentiated myofibroblasts express a lower level of PDGFR α tested by scRNA or flow cytometer, respectively.

PDGFR β

PDGFR β is expressed in the cardiac pericytes, which are predominantly found at vascular locations (**Figure 2**). The expression and phosphorylation of *Pdgfr β* in cardiomyocytes increase dramatically in response to pressure overload stress (Chintalgattu et al., 2010; Yue et al., 2019). *Pdgfr β* knockout produces embryonic lethality due to hemorrhage from vascular malformation due to impaired pericytes and/or defects in hemopoiesis. Inactivation of PDGFR β signaling leads to cardiac abnormalities, including ventricular septal defects, late embryonic ventricular dilation, lack of coronary vascular SMCs, myocardial hypertrabeculation, and hemorrhage (Hellstrom et al., 1999; Bjarnegard et al., 2004; Mellgren et al., 2008). Cardiomyocyte-specific inducible deletion of *Pdgfr β* (*Pdgfr β ^{Nkx2.5}*) in embryos, however, do not exhibit remarkable malformation, but when deleted in adults, the mice develop severe ventricular dilation and heart failure in response to pressure overload with a possible mechanism of impaired activation of Akt and MAPK pathways (Chintalgattu et al., 2010).



In recent scRNA studies in adult injuries, PDGFR β is found in circulating fibrocytes and myofibroblasts in kidney fibrosis and myofibroblasts in lung injury models (Kramann et al., 2018; Li et al., 2018).

PDGF-A

Protein is encoded by the PDGF-A gene, which encodes for PDGF-A and VEGF. PDGF-A is proteolytically cleaved to form a subunit and either homodimerize or heterodimerize with the B subunit. PDGF-AA is widely expressed in the embryonic and postnatal tissues including the heart with knockout producing embryonic lethality (Andrae et al., 2014). PDGF-AA acts mostly in a paracrine signaling manner post-gastrulation, interacting with PDGFR α in embryos where the ligand is expressed in endoderm or ectoderm and the receptor predominantly in mesoderm (Bloomekatz et al., 2017). In adults, the ligand is frequently found in the epithelium or endothelium. In the normal adult heart, PDGF-A is shown to be expressed in the interstitial cells where the receptor-positive cells reside, and the level of PDGF-A is significantly increased following MI (Zhao et al., 2011).

PDGF-B

Protein is encoded and proteolytically cleaved similar to the A subunit. This ligand is the only PDGF that binds to all three receptor combinations with high affinity and is required for normal proliferation and recruitment of pericytes and vascular SMCs. Knockout embryos develop septum defects, underdeveloped valvular structure, abnormal cardiac innervation, and hypoplastic compact myocardium largely similar to cases of *Pdgfr β* deletion; *Pdgfr β* knockout embryos also

die from hemorrhage due to the lack of pericyte lining of the blood vessels (Leveen et al., 1994; Van den Akker et al., 2008).

Pdgfa/r α and *Pdgfb/r β* Signaling May Have Distinct Functions in Development and Adult Homeostasis and Pathology

It is believed that *Pdgfa/r α* and *Pdgfb/r β* can cross-activate each other and may have overlapping functions. However, the “overlap” is perhaps partial at best, as mutation of one fails to be compensated by the other during development. Deletion of *Pdgfa/r α* and *Pdgfb/r β* present non-identical developmental malformations. This evidence indicates a lineage independence of *Pdgfa/Pdgfr α* and *Pdgfb/Pdgfr β* signaling. The lack of compensatory offset also indicates that both autocrine and paracrine signaling processes are important in this ligand/receptor interaction. For example, autocrine signaling activation is necessary in early embryos or in pathological states where more homogenous tissue expansion is prioritized, and paracrine signaling may come into play for the organized interactions between diverse cell types to aid in migration and differentiation (Palmieri et al., 1992).

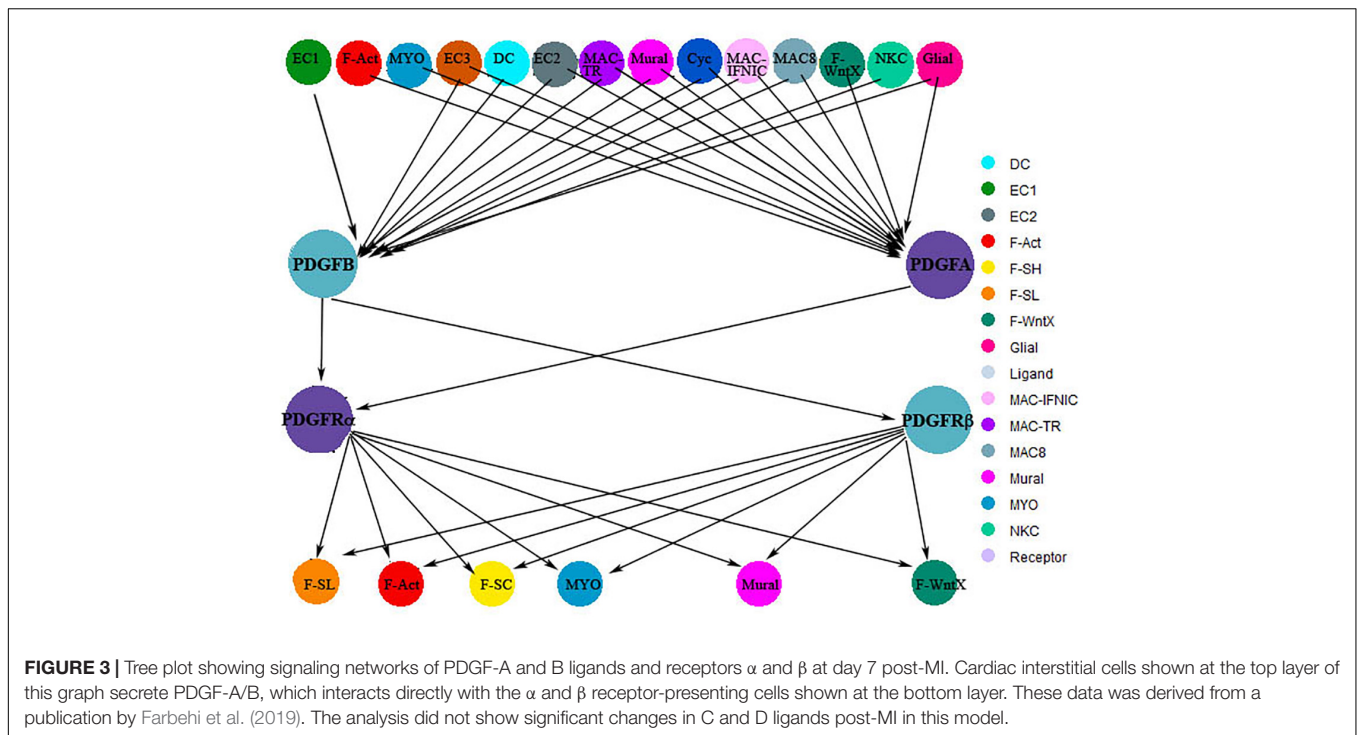
Upregulation of both receptors and PDGF-B is noted at day 7 in a mouse ischemic reperfusion model, with blockage of the PDGFR β causing leaky blood vessels, while blocking the PDGFR α significantly decreases collagen deposition in the infarct, both impairing healing (Zymek et al., 2006). Single-cell analysis at day-7 post-MI has shown involvement of the interstitial cells in PDGF ligand secretion, the cell types including endothelial, fibroblast, immune, and mural cells. The interaction of the ligands with their own receptors and receptors that mediate various cellular activities is illustrated in **Figure 3**, demonstrating the targeting of interstitial cell types that contribute to angiogenesis, collagen deposition, cell proliferation, and mural cell regulations (Farbehi et al., 2019; **Figure 3**).

PDGF-C and D

PDGF-C and D are synthesized and secreted as latent growth factors, which require proteolytic removal of the N-terminal CUB domain for receptor binding. The C and D ligands only form homodimers. C and D ligands work through the dimerized receptors α and β similar to ligands A and B. However, they differ from A and B ligands in their molecular structures with longer pro-sequences that include a large N-terminal CUB domain, and the relative hydrophilicity of these ligands may make them less flexible and have shorter binding duration for receptors compared with A and B ligands, which in turn produce a differed effect of the PDGF signaling cascade, as reviewed (Fredriksson et al., 2004; Chen et al., 2013). *Pdgfc*^{-/-} mice display cleft palate and craniofacial malformation (Ding et al., 2000), while *Pdgfa*^{-/-} mice present mild vascular abnormality and disorganized NG2⁺ pericytes, their offspring are born generally healthy and enjoy a normal lifespan (Gladh et al., 2016).

ROLES IN ANTI-APOPTOSIS

Reducing myocardial cell death following an ischemic insult is desirable and is currently the most effective treatment



available in developed countries where most patients receive percutaneous angioplasties to reduce the duration of ischemia and prevent further cell death (Castellani et al., 2010) but not without complications (Hausenloy and Yellon, 2013; Davidson et al., 2019).

PDGF is a principal survival factor that inhibits apoptosis and promotes proliferation (Harrington et al., 1994). As the mechanisms of cell proliferation and differentiation are intrinsically linked to the process of apoptosis, the default of proliferating cells is to die unless specific survival signals are provided (Harrington et al., 1994). PDGF roles in anti-apoptosis have been linked to activation of cMyc and Ras/PIK13 pathways (Romashkova and Makarov, 1999) in cancer cells and indeed cardiomyocytes (Hsieh et al., 2006a).

In rodents, delivery of PDGF-AB via direct myocardial injection 24 h prior to MI or co-injection with VEGF and angiopoietin-2 at the time of coronary occlusion was able to suppress acute myocardial cell death by >50%, thereby reducing the extent of MI by providing a cardioprotective benefit (Xaymardan et al., 2004).

PDGF-BB was tested on the resistance of apoptotic induction in engineered tissue from neonatal rat cardiomyocytes. The treated hearts were at least partially protected from caspase-3-induced apoptosis (Vantler et al., 2010). Peptide nanofibers (NF) with PDGF-BB injected into the myocardium ensured a sustained release of the PDGF-BB after coronary occlusion in the rats, which dramatically decreased caspase-3 activation after 1 day, reducing apoptosis in a dose-dependent manner. It was demonstrated that the activation of Akt in the myocardium is induced by injection of NF/PDGF-BB, showing that this

strategy induces survival signaling in the myocardium *in vivo* (Hsieh et al., 2006a).

Impaired PDGFR α pathways lead to apoptosis in relevant tissues. *Pdgfra* deletion in embryos resulted in apoptosis in the receptor-expressing tissue, contributing to malformation of the embryos (Qian et al., 2017). Similarly, conditional deletion of *Pdgfra* caused mesenchyme apoptosis and urorectal developmental anomalies in mice (Qian et al., 2019).

PDGFR β signaling is important for cardioprotection as shown in the aortic constriction model where PDGFR β was upregulated and phosphorylated in response to stress. Conditional knockout of *Pdgfr β* (*Pdgfr β ^{Nkx2.5cre}*) leads to ventricular dilation with age and severe heart failure upon induction of pressure overload. AKT/ERB signaling pathways were also indicted in these experiments (Chintalgattu et al., 2010). The protective effect of the PDGF may be dose dependent as shown in cultured vascular MSCs; the increased dose of PDGF-BB induced apoptosis via *bcl2* upregulation or inactivation of BAD (Okura et al., 1998; Zhou et al., 2000).

Overall, the anti-apoptotic properties of the PDGFR α and PDGFR β are reasonably clear. While the ligands and receptors play a certain role in earlier embryonic cardiac development, the mechanism may largely be dependent on epi/endocardial induction. The cardiomyocyte expression of these factors cannot be entirely ruled out and may be minimal. PDGF-B and PDGFR β signaling, on the other hand, seems to be more profoundly involved in the anti-apoptotic function of these factors, achieving cardioprotection through a specific downstream signaling pathway dictated by AKT/ERB.

ROLE IN TARGETING ANGIOGENESIS

The majority of cardiac disorders stem from vascular dysfunction and poor perfusion. The problem further deteriorates after MI, where cardiac hypertrophy and fibrosis cause a further decrease in vascularity to cellularity ratio, worsening perfusion deficit of the cardiac tissue. Encouraging angiogenesis pre- or post-MI will help protect cardiomyocytes from further apoptosis and improve the microenvironment for cellular functions of the heart.

PDGF/R are well-accepted vasculogenic and angiogenic promoters by either direct participation in vascular assembly by α/β receptor-presenting cells or by providing migratory cytokines and extracellular matrix support for vessel formation. *Pdgfra*-positive cells contribute early embryonic endothelial cells in the lateral plate mesoderm (Ding et al., 2013). In adults, *Cre*-induced *Pdgfra* knockout suppressed neovascularized areas in implanted sponge presumably through suppression of the wound matrix assembly (Horikawa et al., 2015). PDGFR β is involved in an assembly of principle vascular cell types, the endothelium, SMA, and pericytes to form blood vessels in many organs of embryos (Hellstrom et al., 1999). PDGF-BB is a major mitogen for vascular endothelial cells and are involved in pericyte recruitment, which also can directly stimulate endothelial cell proliferation *in vitro* as well as in embryonic chorioallantoic (Battegay et al., 1994; De Marchis et al., 2002) and vascular growth in hind limb ischemia model in adult mice (Brown et al., 1995). Injection of PDGF-BB into rabbit myocardium was shown to indirectly stimulate angiogenesis by increasing VEGF protein production (Affleck et al., 2002). Conversely, *Pdgfb*-deficient mice endothelium unable to recruit pericytes, thus, form microaneurysm (Lindahl et al., 1997).

Both PDGFR α and β are expressed in the culture endothelial cells (Lee et al., 2013) and newly formed blood vessels in mouse cornea (Cao et al., 2002). Minor populations of cardiac endothelial cells express PDGFR α with an increase in CD31⁺PDGFR α ⁺ cells seen post-MI, indicating that the PDGFR α is conducive to post-MI angiogenic regulation during cardiac wound healing (Zhao et al., 2011; Awada et al., 2015; Farbehi et al., 2019). PDGF ligands can directly activate both endothelial cells and pericytes. It is also possible that family cross-family PDGF to VEGFR2 interactions exist, for example, VEGF-A is proposed to bind directly to PDGFR α and β ; Conversely, PDGFs crosstalk to VEGF receptors to enact angiogenic function (Mamer et al., 2020).

In MI models, promoting vascularity through both AB and BB ligand delivery has been shown to improve the post-MI milieu and cardiac function, although questions on long-term benefits and effectiveness in humans are still unclear. PDGF-AB (Xaymardan et al., 2004) and BB (Hsieh et al., 2006a) delivery directly into the myocardium in mouse and rat models and systemic delivery in mouse and pig models have all shown improvements in angiogenesis in post-MI cardiac tissue, which is presumably, in part, responsible for improved cardiac function and myocardial anatomy. In these studies, the roles of PDGF-A and B are not dissected. PDGF-AB seems to generate stable vessels and arterioles (Zhang et al., 2009). PDGF-C, as a newer ligand in the PDGF family, has been increasingly shown to induce

angiogenesis via PDGFR α (Cao et al., 2002; Lee and Li, 2018), however, its role has not been investigated from the perspective of cardioprotection.

No pharmacodynamic studies have been performed; however, sustained delivery methods such as intravenous infusions (Chong et al., 2011) and sustained release using nanoparticles (Hsieh et al., 2006a) or fibrin gel (Su et al., 2020) may be superior to one-off direct injections into the myocardium. In the case of one-off injection, concomitant delivery of other factors (e.g., VEGF) may be necessary. The newer PDGF ligand C has been increasingly associated with angiogenesis.

TARGETING CARDIOMYOCYTE PROLIFERATION

The ideal scenario after a cardiac injury would be the regeneration of cardiomyocytes to restore contractile function of the heart, ensuring normal cardiac output. However, rebuilding the myocardium through regeneration of the cardiomyocytes in the adult mammalian seems to be a formidable task. The difficulty is highlighted by the collapse of the “house of cards” built by Anversa et al. around the notion of using bone marrow or cardiac cKit cells to regenerate cardiomyocytes (Davis, 2019).

In reality, carbon-14 dating results indicate that adult cardiomyocytes may have a low-rate cell cycling ability (Bergmann et al., 2009) that is far from sufficient for the heart to recover from a catastrophic insult such as MI. Zebrafish and some amphibians, even neonatal mice, display regrowth of cardiomyocytes predominantly via cell cycle reentry mechanisms (Wills et al., 2008; Porrello et al., 2011), but adult mammalian hearts do not seem to possess this advantage.

Whether or not PDGF can stimulate regeneration of cardiomyocytes is elusive. However, it is clear that PDGFs and their receptors play important roles in the early development during the heart tube formation stage when primordial cardiac crescent myocytes fuse along the midline. PDGF is secreted by the adjacent endoderm to guide the migration and fusion of the heart tube with the mutation of *Pdgfra* disrupting the heart tube assembly in both zebrafish and mice (Bloomekatz et al., 2017). Initial embryonic heart tissue is founded by non-dividing cardiomyocyte progenitors; the proliferation resumes following cardiac looping, especially in the compact myocardium. Cardiomyocyte proliferation is induced by epicardial-derived signals following the establishment of cardiac fibroblasts marked by PDGFR α and predominantly derived from the epicardium (Chong et al., 2011); this indicates the mitotic function of PDGFR α signaling.

As determined by measurements of the atrioventricular length and left ventricular length and width, exposure of rat embryos to PDGF-AA resulted in a 42% increase in total protein levels in the heart but did not result in a significant increase in heart growth. Exposure of embryos to PDGF-BB resulted in a 77% increase in total protein levels and a significant increase in the measured heart parameters. Although a comparison of control and PDGF-AA-treated embryos showed no increase in the overall size of the heart, confocal microscopy showed an increase in

the size and number of myofibrillar bundles in the developing myocardium (Price et al., 2003). No cardiomyocyte proliferation assay was performed; thus, the observation of increased heart size stimulated by PDGF was likely due to hypertrophic response of the cardiomyocytes and interstitial cell proliferation.

Intravenous infusion of PDGF-AB in mice with surgical MI has been shown to increase EDU-positive myocyte numbers in the remote area of the sub-endocardium. However, it is unclear whether the DNA activities are due to cytokinesis or karyokinesis (Asli et al., 2017). The mechanism behind this observation is not clear but mostly likely to be attributed to the paracrine effect of the interstitial cell activation rather than a direct effect.

PDGFR α may demark cardiomyocyte progenitors in mouse and human embryonic stem cells (Uosaki et al., 2012). A rare population of cardiomyocytes express PDGFR α in human fetal and adult hearts, and a small fraction of PDGFR α cells are able to differentiate into cardiomyocytes *in vitro* (Chong et al., 2013) notwithstanding that the *in vivo* effect of these cells in injury repair is unknown. Recently, Yue et al. (2019) reported that with age, levels of phospho-PDGFR β decreased, and this correlated to the loss of cardiomyocyte proliferative capacity after apical resection. For example, high expression of phospho-PDGFR β was seen in mice up to 7-day postnatal age, and only trace amounts were retained in the adult mice hearts. Cardiac-specific and sustained activation of the PDGFR β restore cardiomyocyte regenerative capacity in adult mice. This proliferation was driven by an upregulation of the enhancer of ZESTE homolog2 EHZ2, which promotes the proliferation of cardiomyocytes with the conditional knockout of Ezh2 blocking CM proliferation (Yue et al., 2019), although genetic upregulation of the PDGF pathways may risk extensive fibrosis after injury as discussed below.

PLATELET-DERIVED GROWTH FACTOR IN MATRIX REMODELING/WOUND STRENGTH/ANTI-ARRHYTHMIA: TARGETING FIBROBLASTS

Perhaps the most authentic and prominent roles of the PDGFs are in the areas of improving matrix remodeling and tissue architecture configuration. There is clear evidence that the *Pdgfra* is expressed in most of the mesenchymal cell population, including the post-gastrulation mesoderm/neural crest stem cells, progenitors of bone, teeth, and fibroblasts. These are all matrix producers that provide structural and humoral support to parenchymal cells (not excluding the potential of their own differentiation to parenchymal cell types such as osteocytes and odontoblasts) (Farahani and Xaymardan, 2015). Similarly, *Pdgfrb* is a prominent pericyte marker, participating in the maintenance of vascular bed and extracellular matrix remodeling.

In adults, PDGF-AA or PDGF-AB induce fibroblast proliferation (Lepisto et al., 1995), and PDGF-BB is a potent recruiter of the pericytes and SMA. PDGF-BB has also been shown to alter matrix integrin expressions, which may alter the chemotaxis of the fibroblasts in ECM, therefore, changing the

ECM properties (Xu and Clark, 1996). PDGF-D has been shown to increase fibroblast activity in rat hearts (Zhao et al., 2013).

The mechanistic pathway by which the PDGFs stimulate ECM deposition may be in collaboration with TGF- β through both non-*Smad* and *Smad*-dependent manners (Fischer et al., 2007). Activation of MAPK and PI3K have been shown to modulate the extracellular matrix composition and stiffness via Wnt/ β -catenin (Astudillo, 2020). PDGFR α is required for TGF β signaling of cultured human hepatic satellite cell transdifferentiation to myofibroblasts, and PDGFR α knockdown inhibits *Smad*-dependent TGF β signaling (Liu et al., 2014). Activities of PDGF efficiently are suppressed by TGF β neutralization or interference with the SMAD/T β R1 or PI3K/Akt pathway (Charbonneau et al., 2016). The complexity is not easily dissected but indicative of mutual regulatory effect between these potent ECM modulators.

In the myocardium, interstitial non-cardiomyocyte cells entangled within a network of extracellular matrix proteins providing structural support, network communication, and humoral signaling to the organ, acting as the primary “caretakers” of the health of the extracellular matrix. In acute diseases such as MI, the cardiac fibroblasts rapidly proliferate and change in phenotype and function (e.g., from negligible expression of SMA to SMA-rich myofibroblasts), and deposit extracellular matrix to prevent cardiac rupture in mammals. The types of extracellular matrix deposition may have importance in cardiac tissue elasticity and, therefore, cardiac function recovery. Stiffness and elasticity may also impact the stem/progenitor functions and have further impact on the regeneration of cardiomyocytes and endothelium alike. Studies show that increased stiffness has detrimental effects on cardiac recovery, as it suppresses early cardiac marker expression (Ranganath et al., 2012; Sullivan et al., 2014). Crosstalk of the fibroblasts with cardiomyocytes may also modulate cardiomyocyte proliferation or hypertrophy depending on the fibroblast phenotype (Musa et al., 2013). Utilizing the natural reparative processes of fibroblasts to modify properties of the forming cardiac scar is quietly emerging as an exciting therapeutic avenue.

General consensus regarding the role of PDGF ligands and receptors is that they are profibrotic, and gain of function studies largely support this notion.

Overexpression, or persistent expression of PDGFs or their receptors have serious adverse effect specifically on the heart. For example, the transgenic expression of the natural isoforms of *Pdgfa* and *b* under the α -myosin heavy chain (α -MHC) promoter has shown severe fibrotic reactions, increase in cardiac size, and cardiac failure a week after birth, whereas overexpression of *Pdgfb* showed focal fibrosis and cardiac hypertrophy (Gallini et al., 2016b).

Cardiac-specific overexpression of PDGF-C conditional to α -MHC increased cardiac fibroblast proliferation, collagen deposition, hypertrophy, and vascular defects and, additionally, sex-dependent changes, such as male mice exhibiting hypertrophy and female mice experiencing dilated cardiomyopathy and heart failure (Ponten et al., 2003). Transgenic overexpression of PDGF-D stimulated the proliferation of cardiac interstitial fibroblasts and arterial

vascular SMCs, resulting in cardiac fibrosis followed by dilated cardiomyopathy and subsequent cardiac failure (Ponten et al., 2005). Expression induced by intramyocardial adenoviral-mediated delivery; however, produced slightly mixed results showing that *Pdgfc* and *c* decreased the amount of scar tissue and increased the numbers of PDGFR α -positive fibroblasts, while *Pdgfb* induced large scars with extensive inflammation, and *Pdgfd* produced a small and dense scar (Gallini et al., 2016a).

A recent study on cardiomyocytes differentiated from induced pluripotent stem cells (iPSCs) was derived from an LMNA mutant patient showing single-cell base arrhythmia. The authors found an increase in PDGFR β in these mutant cardiomyocytes. Interestingly, they found that inhibition of the PDGF signaling pathway ameliorated the arrhythmic *in vitro* (Lee et al., 2019).

The recent preclinical porcine study exploring the role of PDGF-AB in the attenuation of myocardial fiber heterogeneity within a scar and organized collagen fiber alignment have shown significant improvements in cardiac function and a reduction in cardiac arrhythmia. Musa et al. (2013) showed that the atrial myocytes demonstrated significant disturbance in calcium channel density to potentially provoke arrhythmia, which can be neutralized when myofibroblasts are pretreated with PDGF-AB.

The role of exogenously delivered ligands in fibrosis is less clear. Types of ligands, dosage, and duration of ligand presence, as well as activated cell types may switch the processes from a protective wound healing and tissue regeneration to adverse effect of fibrosis or tumor formation.

Santini et al. (2020) demonstrated the diversity in the *Pdgfra* cell cultured from injured and uninjured mice skeletal muscle tissues. The study showed that the activated and terminally differentiated *Pdgfra* cells lose their regenerative capacity and display fibrotic activities. A subpopulation of Gli-1-positive PDGFR β cells was more likely to differentiate into myofibroblasts (Kramann et al., 2015) indicating that inhibition or promotion of a specific subpopulation may avoid widespread adverse effect when using the PDGF pathway as a treatment modality.

CONCLUSION AND FUTURE PERSPECTIVE

Preclinical trials in porcine model have shown promising evidence that PDGF-AB exerts a cardioprotective effect following MI with rodent studies reporting similar results (Xaymardan et al., 2004; Zheng et al., 2004; Hsieh et al., 2006a,b; Awada et al., 2015; Asli et al., 2017; Thavapalachandran et al., 2020). Although no human trials have been performed thus far, the results from animal studies suggest a possible clinical application of PDGF ligands in improving therapeutic outcomes in MI patients. Short-term treatments used in swine and rodent studies showed no adverse effects of PDGF-AB when delivered intravenously for 7 days. In addition, the matrix remodeling seen in the porcine model points to a favorable tensile strength augmentation that contributes to improved cardiac function and reduced arrhythmia, which was thought to contribute to the reduced mortality in the subjects. No

extensive scarring was observed in either the pig or mice studies (Asli et al., 2019; Thavapalachandran et al., 2020). Intravenous infusion of PDGF-AB in mice also failed to demonstrate increased myofibroblast activity post-MI using scRNA analysis (Asli et al., 2019). Indeed, there is a clear link between PDGF signaling pathways and fibrosis. The most convincing supporting evidence is derived from genetically upregulated murine models where increased PDGFR α is shown to cause lung fibrosis and conditional knockout of PDGFR α shown to attenuate liver fibrosis (Andrae et al., 2008). However, there is no clear evidence that exogenous ligand delivery would produce similar effects. In fact, improved matrix remodeling seems to be beneficial for the healing of cardiac tissue after injury. Studies of PDGF-AB delivery in pigs resulted in directional synchrony in collagen fibers, which may have contributed to better preserved architecture of the infarcted area and to the vascularity of scar tissue (Thavapalachandran et al., 2020).

Matrix remodeling is one of the mechanisms that facilitates improved functional outcomes after infarction. PDGF pathway regulation also contributes to improved cell survival, increasing angiogenesis and, perhaps to a lesser degree, activation of the cardiomyocyte cell cycling machinery, although this pathway may not be potent enough to induce cellular proliferation and contribute to the regeneration of the myocardium. The exogenous delivery of PDGF to aged mice also compensates for age-related downregulation in the PDGF pathway (Xaymardan et al., 2004).

Inhibition of PDGF pathways, on the other hand, leads to worsened cardiac outcomes in mice after MI. For example, administering PDGF receptor inhibitor imatinib to mice experiencing MI caused a reduction in vascularity and ejection fraction when compared with non-treated mice (Fazel et al., 2006). It can be argued that the imatinib is not specific to PDGFRs as it also impacts c-Kit. However, specific neutralizing antibodies against PDGFR α and β have led to reductions in vascularity and collagen deposition in post-infarction hearts and demonstrated the importance of PDGF receptors in cardiac wound healing (Zymek et al., 2006). Interestingly, neutralizing antibodies also had effects on inflammatory cells, anti-PDGFR α resulted in increased macrophage infiltration, while the inhibition of PDGFR β prolonged the duration of leukocyte infiltration post-MI (Zymek et al., 2006). This indicates that PDGF signaling pathways may have additional roles in immune regulation that impacts repair post-MI. This is further supported by our studies showing M1/M2 conversion in the PDGF-AB-treated mice (Asli et al., 2019). Excessive inflammation is related to fibrosis and worsened infarct expansion, which can be attenuated by anti-inflammatory treatments that produce beneficial effects both in animal models and human trials of MSC treatments, as most of the benefits seem to be attributable to the anti-inflammatory effect of the MSC trophic activities. In some cases, more potent anti-inflammatory drugs are used to treat acute MI patients with improved mortality and cardiac function (Giugliano et al., 2003), although high-dose steroid can produce opposite effects by reducing collagen deposition (Giugliano et al., 2003).

To date, the primary pharmaceutical applications of PDGFs have been the inhibition of PDGF pathways in the treatment of

cancer and the prevention of fibrosis with clinically approved drugs including small inhibitory molecules, such as imatinib, and protein antagonists (Bruggemann et al., 1989; Wollin et al., 2014; Ying et al., 2017; Papadopoulos and Lennartsson, 2018; Olsen et al., 2019). Pharmacological augmentation studies regarding therapeutic roles of PDGFs in cardiac repair and overall wound healing aspects are limited. Studies on direct comparison of all five dimers of PDGFs would be valuable for identifying the most useful isoforms or the combinations of PDGFs that improve mortality and morbidity and cardiac function. Pharmacodynamics on dose, duration, and benefit versus toxicity including longer-term adverse effect will be informative for establishing applicational modalities. These studies will be formidable due to the laboriousness of the cardiac injury models and the cost of the recombinant proteins. Future studies including animal models with risk

factors of hypertension and diabetes would be presentative of the human population with MI risk. The mechanism of the beneficial roles of the PDGF in cardiac healing or regeneration is not elucidated. The complexity of the pathway suggests that the PDGFs provide a multitude of benefits to improve many aspects of cardiac wound healing and may be a promising therapeutic target for the treatment of post-MI cardiac pathologies.

AUTHOR CONTRIBUTIONS

KK drafted the manuscript. NF drafted the figures and data analysis. JE and JC contributed to writing. MX constructed the structure and contributed to writing and proofing. All authors contributed to the article and approved the submitted version.

REFERENCES

- Adel, W., and Nammias, W. (2010). Predictors of contractile recovery after revascularization in patients with anterior myocardial infarction who received thrombolysis. *Int. J. Angiol.* 19, e78–e82.
- Affleck, D. G., Bull, D. A., Bailey, S. H., Albanil, A., Connors, R., Stringham, J. C., et al. (2002). PDGF(BB) increases myocardial production of VEGF: shift in VEGF mRNA splice variants after direct injection of bFGF, PDGF(BB), and PDGF(AB). *J. Surg. Res.* 107, 203–209. doi: 10.1006/jsre.2002.6510
- Al-Zube, L., Breitbart, E. A., O'Connor, J. P., Parsons, J. R., Bradica, G., Hart, C. E., et al. (2009). Recombinant human platelet-derived growth factor BB (rhPDGF-BB) and beta-tricalcium phosphate/collagen matrix enhance fracture healing in a diabetic rat model. *J. Orthop. Res.* 27, 1074–1081. doi: 10.1002/jor.20842
- Andrae, J., Gallini, R., and Betsholtz, C. (2008). Role of platelet-derived growth factors in physiology and medicine. *Genes Dev.* 22, 1276–1312. doi: 10.1101/gad.1653708
- Andrae, J., Gouveia, L., He, L., and Betsholtz, C. (2014). Characterization of platelet-derived growth factor-A expression in mouse tissues using a lacZ knock-in approach. *PLoS One* 9:e105477. doi: 10.1371/journal.pone.0105477
- Antoniades, H. N., Scher, C. D., and Stiles, C. D. (1979). Purification of human platelet-derived growth factor. *Proc. Natl. Acad. Sci. U.S.A.* 76, 1809–1813.
- Appiah-Kubi, K., Wang, Y., Qian, H., Wu, M., Yao, X., Wu, Y., et al. (2016). Platelet-derived growth factor receptor/platelet-derived growth factor (PDGFR/PDGF) system is a prognostic and treatment response biomarker with multifarious therapeutic targets in cancers. *Tumour Biol.* 37, 10053–10066. doi: 10.1007/s13277-016-5069-z
- Asli, N. R., Xaymardan, M., Cornwell, J., Forte, E., Waardenberg, A. J., Janbandhu, V., et al. (2017). PDGFR α signaling in cardiac fibroblasts modulates quiescence, metabolism and self-renewal, and promotes anatomical and functional repair. *bioRxiv* [Preprint] 2017/227979.
- Asli, N. S., Xaymardan, M., Patrick, M., Farbehi, N., Cornwell, J., Forte, E., et al. (2019). PDGFR α signaling in cardiac fibroblasts modulates quiescence, metabolism and self-renewal, and promotes anatomical and functional repair. *bioRxiv* [Preprint] doi: 10.1101/225979
- Astudillo, P. (2020). Extracellular matrix stiffness and Wnt/beta-catenin signaling in physiology and disease. *Biochem. Soc. Trans.* 48, 1187–1198. doi: 10.1042/bst20200026
- Awada, H. K., Johnson, N. R., and Wang, Y. (2015). Sequential delivery of angiogenic growth factors improves revascularization and heart function after myocardial infarction. *J. Control. Release* 207, 7–17. doi: 10.1016/j.jconrel.2015.03.034
- Battegay, E. J., Rupp, J., Iruela-Arispe, L., Sage, E. H., and Pech, M. (1994). PDGF-BB modulates endothelial proliferation and angiogenesis in vitro via PDGF beta-receptors. *J. Cell Biol.* 125, 917–928. doi: 10.1083/jcb.125.4.917
- Bax, J. J., Schinkel, A. F., Boersma, E., Rizzello, V., Elhendy, A., Maat, A., et al. (2003). Early versus delayed revascularization in patients with ischemic cardiomyopathy and substantial viability: impact on outcome. *Circulation* 108(Suppl. 1), II39–II42.
- Bax, N. A., Bleyl, S. B., Gallini, R., Wisse, L. J., Hunter, J., Van Oorschot, A. A., et al. (2010). Cardiac malformations in Pdgfralpha mutant embryos are associated with increased expression of WT1 and Nkx2.5 in the second heart field. *Dev. Dyn.* 239, 2307–2317. doi: 10.1002/dvdy.22363
- Bergmann, O., Bhardwaj, R. D., Bernard, S., Zdunek, S., Barnabe-Heider, F., Walsh, S., et al. (2009). Evidence for cardiomyocyte renewal in humans. *Science* 324, 98–102. doi: 10.1126/science.1164680
- Bergsten, E., Uutela, M., Li, X., Pietras, K., Ostman, A., Heldin, C. H., et al. (2001). PDGF-D is a specific, protease-activated ligand for the PDGF beta-receptor. *Nat. Cell Biol.* 3, 512–516. doi: 10.1038/35074588
- Betsholtz, C. (1995). Role of platelet-derived growth factors in mouse development. *Int. J. Dev. Biol.* 39, 817–825.
- Bjarnegard, M., Enge, M., Norlin, J., Gustafsdottir, S., Fredriksson, S., Abramsson, A., et al. (2004). Endothelium-specific ablation of PDGFB leads to pericyte loss and glomerular, cardiac and placental abnormalities. *Development* 131, 1847–1857. doi: 10.1242/dev.01080
- Bloomekatz, J., Singh, R., Prall, O. W., Dunn, A. C., Vaughan, M., Loo, C. S., et al. (2017). Platelet-derived growth factor (PDGF) signaling directs cardiomyocyte movement toward the midline during heart tube assembly. *Elife* 6:e21172.
- Bottrell, A., Meng, Y. H., Najy, A. J., Hurst, N. Jr., Kim, S., Kim, C. J., et al. (2019). An oncogenic activity of PDGF-C and its splice variant in human breast cancer. *Growth Factors* 37, 131–145. doi: 10.1080/08977194.2019.1662415
- Brown, D. M., Hong, S. P., Farrell, C. L., Pierce, G. F., and Khouri, R. K. (1995). Platelet-derived growth factor BB induces functional vascular anastomoses in vivo. *Proc. Natl. Acad. Sci. U.S.A.* 92, 5920–5924. doi: 10.1073/pnas.92.13.5920
- Bruggemann, T., Andresen, D., and Schroder, R. (1989). [ST-segment analysis in long-term ECG: amplitude and phase response of various systems in comparison with standard ECG and their effect on true original reproduction of ST segment depression]. *Z. Kardiol.* 78, 14–22.
- Cao, R., Brakenhielm, E., Li, X., Pietras, K., Widenfalk, J., Ostman, A., et al. (2002). Angiogenesis stimulated by PDGF-CC, a novel member in the PDGF family, involves activation of PDGFR-alpha and -beta receptors. *FASEB J.* 16, 1575–1583. doi: 10.1096/fj.02-0319com
- Castellani, C., Padalino, M., China, P., Fedrigo, M., Frescura, C., Milanese, O., et al. (2010). Bone-marrow-derived CXCR4-positive tissue-committed stem cell recruitment in human right ventricular remodeling. *Hum. Pathol.* 41, 1566–1576. doi: 10.1016/j.humpath.2009.12.017
- Charbonneau, M., Lavoie, R. R., Lauzier, A., Harper, K., McDonald, P. P., and Dubois, C. M. (2016). Platelet-derived growth factor receptor activation promotes the prodestructive invadosome-forming phenotype of synovial cells

- from patients with rheumatoid arthritis. *J. Immunol.* 196, 3264–3275. doi: 10.4049/jimmunol.1500502
- Chen, P. H., Chen, X., and He, X. (2013). Platelet-derived growth factors and their receptors: structural and functional perspectives. *Biochim. Biophys. Acta* 1834, 2176–2186. doi: 10.1016/j.bbapap.2012.10.015
- Chiariello, M., Marinissen, M. J., and Gutkind, J. S. (2001). Regulation of c-myc expression by PDGF through Rho GTPases. *Nat. Cell Biol.* 3, 580–586. doi: 10.1038/35078555
- Chintalgattu, V., Ai, D., Langley, R. R., Zhang, J., Bankson, J. A., Shih, T. L., et al. (2010). Cardiomyocyte PDGFR-beta signaling is an essential component of the mouse cardiac response to load-induced stress. *J. Clin. Invest.* 120, 472–484. doi: 10.1172/jci39434
- Chong, J. J., Chandrakanthan, V., Xaymardan, M., Asli, N. S., Li, J., Ahmed, I., et al. (2011). Adult cardiac-resident MSC-like stem cells with a proepicardial origin. *Cell Stem Cell* 9, 527–540. doi: 10.1016/j.stem.2011.10.002
- Chong, J. J., Reinecke, H., Iwata, M., Torok-Storb, B., Stempien-Otero, A., and Murry, C. E. (2013). Progenitor cells identified by PDGFR-alpha expression in the developing and diseased human heart. *Stem Cells Dev.* 22, 1932–1943. doi: 10.1089/scd.2012.0542
- Davidson, S. M., Ferdinandy, P., Andreadou, I., Botker, H. E., Heusch, G., Ibanez, B., et al. (2019). Multitarget strategies to reduce myocardial ischemia/reperfusion injury: JACC review topic of the week. *J. Am. Coll. Cardiol.* 73, 89–99. doi: 10.1016/j.jacc.2018.09.086
- Davis, D. R. (2019). Cardiac stem cells in the post-Anversa era. *Eur. Heart J.* 40, 1039–1041. doi: 10.1093/eurheartj/ehz098
- De Marchis, F., Ribatti, D., Giampietri, C., Lentini, A., Faraone, D., Scoccianti, M., et al. (2002). Platelet-derived growth factor inhibits basic fibroblast growth factor angiogenic properties in vitro and in vivo through its alpha receptor. *Blood* 99, 2045–2053. doi: 10.1182/blood.v99.6.2045
- Ding, G., Tanaka, Y., Hayashi, M., Nishikawa, S., and Kataoka, H. (2013). PDGF receptor alpha+ mesoderm contributes to endothelial and hematopoietic cells in mice. *Dev. Dyn.* 242, 254–268. doi: 10.1002/dvdy.23923
- Ding, H., Wu, X., Kim, I., Tam, P. P., Koh, G. Y., and Nagy, A. (2000). The mouse Pdgfr gene: dynamic expression in embryonic tissues during organogenesis. *Mech. Dev.* 96, 209–213. doi: 10.1016/s0925-4773(00)00425-1
- Ehrlich, H. P., and Freedman, B. M. (2002). Topical platelet-derived growth factor in patients enhances wound closure in the absence of wound contraction. *Cytokines Cell Mol. Ther.* 7, 85–90. doi: 10.1080/13684730310001643
- Farahani, R. M., and Xaymardan, M. (2015). Platelet-derived growth factor receptor alpha as a marker of mesenchymal stem cells in development and stem cell biology. *Stem Cells Int.* 2015:362753.
- Farbehi, N., Patrick, R., Dorison, A., Xaymardan, M., Janbandhu, V., Wystub-Lis, K., et al. (2019). Single-cell expression profiling reveals dynamic flux of cardiac stromal, vascular and immune cells in health and injury. *Elife* 8:e43882.
- Fazel, S., Cimini, M., Chen, L., Li, S., Angoulvant, D., Fedak, P., et al. (2006). Cardioprotective c-kit+ cells are from the bone marrow and regulate the myocardial balance of angiogenic cytokines. *J. Clin. Invest.* 116, 1865–1877. doi: 10.1172/jci27019
- Fischer, A. N., Fuchs, E., Mikula, M., Huber, H., Beug, H., and Mikulits, W. (2007). PDGF essentially links TGF-beta signaling to nuclear beta-catenin accumulation in hepatocellular carcinoma progression. *Oncogene* 26, 3395–3405. doi: 10.1038/sj.onc.1210121
- Fredriksson, L., Li, H., and Eriksson, U. (2004). The PDGF family: four gene products form five dimeric isoforms. *Cytokine Growth Factor Rev.* 15, 197–204. doi: 10.1016/j.cytogfr.2004.03.007
- Gallini, R., Huusko, J., Yla-Herttuala, S., Betsholtz, C., and Andrae, J. (2016a). Isoform-specific modulation of inflammation induced by adenoviral mediated delivery of platelet-derived growth factors in the adult mouse heart. *PLoS One* 11:e0160930. doi: 10.1371/journal.pone.0160930
- Gallini, R., Lindblom, P., Bondjers, C., Betsholtz, C., and Andrae, J. (2016b). PDGF-A and PDGF-B induces cardiac fibrosis in transgenic mice. *Exp. Cell Res.* 349, 282–290. doi: 10.1016/j.yexcr.2016.10.022
- Giugliano, G. R., Giugliano, R. P., Gibson, C. M., and Kuntz, R. E. (2003). Meta-analysis of corticosteroid treatment in acute myocardial infarction. *Am. J. Cardiol.* 91, 1055–1059. doi: 10.1016/s0002-9149(03)00148-6
- Gladh, H., Folestad, E. B., Muhl, L., Ehnman, M., Tannenber, P., Lawrence, A. L., et al. (2016). Mice lacking platelet-derived growth factor D display a mild vascular phenotype. *PLoS One* 11:e0152276. doi: 10.1371/journal.pone.0152276
- Gowda, S., Weinstein, D. A., Blalock, T. D., Gandhi, K., Mast, B. A., Chin, G., et al. (2015). Topical application of recombinant platelet-derived growth factor increases the rate of healing and the level of proteins that regulate this response. *Int. Wound J.* 12, 564–571. doi: 10.1111/iwj.12165
- Graham, S., Leonidou, A., Lester, M., Heliotis, M., Mantalaris, A., and Tsidiris, E. (2009). Investigating the role of PDGF as a potential drug therapy in bone formation and fracture healing. *Expert Opin. Investig. Drugs* 18, 1633–1654. doi: 10.1517/13543780903241607
- Harrington, E. A., Bennett, M. R., Fanidi, A., and Evan, G. I. (1994). c-Myc-induced apoptosis in fibroblasts is inhibited by specific cytokines. *EMBO J.* 13, 3286–3295. doi: 10.1002/j.1460-2075.1994.tb06630.x
- Hausenloy, D. J., and Yellon, D. M. (2013). Myocardial ischemia-reperfusion injury: a neglected therapeutic target. *J. Clin. Invest.* 123, 92–100. doi: 10.1172/jci62874
- He, C., Medley, S. C., Hu, T., Hinsdale, M. E., Lupu, F., Virmani, R., et al. (2015). PDGFRbeta signalling regulates local inflammation and synergizes with hypercholesterolaemia to promote atherosclerosis. *Nat. Commun.* 6:7770.
- Hellstrom, M., Kalen, M., Lindahl, P., Abramsson, A., and Betsholtz, C. (1999). Role of PDGF-B and PDGFR-beta in recruitment of vascular smooth muscle cells and pericytes during embryonic blood vessel formation in the mouse. *Development* 126, 3047–3055. doi: 10.1242/dev.126.14.3047
- Hoch, R. V., and Soriano, P. (2003). Roles of PDGF in animal development. *Development* 130, 4769–4784. doi: 10.1242/dev.00721
- Horikawa, S., Ishii, Y., Hamashima, T., Yamamoto, S., Mori, H., Fujimori, T., et al. (2015). PDGFRalpha plays a crucial role in connective tissue remodeling. *Sci. Rep.* 5:17948.
- Houlihan, D. D., Mabuchi, Y., Morikawa, S., Niibe, K., Araki, D., Suzuki, S., et al. (2012). Isolation of mouse mesenchymal stem cells on the basis of expression of Sca-1 and PDGFR- α . *Nat. Protoc.* 7, 2103–2111. doi: 10.1038/nprot.2012.125
- Hsieh, P. C., Davis, M. E., Gannon, J., MacGillivray, C., and Lee, R. T. (2006a). Controlled delivery of PDGF-BB for myocardial protection using injectable self-assembling peptide nanofibers. *J. Clin. Invest.* 116, 237–248. doi: 10.1172/jci25878
- Hsieh, P. C., MacGillivray, C., Gannon, J., Cruz, F. U., and Lee, R. T. (2006b). Local controlled intramyocardial delivery of platelet-derived growth factor improves postinfarction ventricular function without pulmonary toxicity. *Circulation* 114, 637–644. doi: 10.1161/circulationaha.106.639831
- Ivey, M. J., and Tallquist, M. D. (2016). Defining the cardiac fibroblast. *Circ. J.* 80, 2269–2276. doi: 10.1253/circj.16-1003
- Kazlauskas, A. (2017). PDGFs and their receptors. *Gene* 614, 1–7. doi: 10.1016/j.gene.2017.03.003
- Khoshkam, V., Chan, H. L., Lin, G. H., Mailoa, J., Giannobile, W. V., Wang, H. L., et al. (2015). Outcomes of regenerative treatment with rhPDGF-BB and rhFGF-2 for periodontal intra-bony defects: a systematic review and meta-analysis. *J. Clin. Periodontol.* 42, 272–280. doi: 10.1111/jcpe.12354
- Klinkhammer, B. M., Floege, J., and Boor, P. (2018). PDGF in organ fibrosis. *Mol. Aspects Med.* 62, 44–62. doi: 10.1016/j.mam.2017.11.008
- Kong, P., Christia, P., and Frangogiannis, N. G. (2014). The pathogenesis of cardiac fibrosis. *Cell Mol. Life Sci.* 71, 549–574.
- Kramann, R., Machado, F., Wu, H., Kusaba, T., Hoefl, K., Schneider, R. K., et al. (2018). Parabiosis and single-cell RNA sequencing reveal a limited contribution of monocytes to myofibroblasts in kidney fibrosis. *JCI Insight* 3:e99561.
- Kramann, R., Schneider, R. K., DiRocco, D. P., Machado, F., Fleig, S., Bondzie, P. A., et al. (2015). Perivascular Gli1+ progenitors are key contributors to injury-induced organ fibrosis. *Cell Stem Cell* 16, 51–66. doi: 10.1016/j.stem.2014.11.004
- Lee, C., and Li, X. (2018). Platelet-derived growth factor-C and -D in the cardiovascular system and diseases. *Mol. Aspects Med.* 62, 12–21. doi: 10.1016/j.mam.2017.09.005
- Lee, C., Zhang, F., Tang, Z., Liu, Y., and Li, X. (2013). PDGF-C: a new performer in the neurovascular interplay. *Trends Mol. Med.* 19, 474–486. doi: 10.1016/j.molmed.2013.04.006

- Lee, J., Termglinchan, V., Diecke, S., Itzhaki, I., Lam, C. K., Garg, P., et al. (2019). Activation of PDGF pathway links LMNA mutation to dilated cardiomyopathy. *Nature* 572, 335–340. doi: 10.1038/s41586-019-1406-x
- Lepistö, J., Peltonen, J., Vaha-Kreula, M., Niinikoski, J., and Laato, M. (1995). Platelet-derived growth factor isoforms PDGF-AA, -AB and -BB exert specific effects on collagen gene expression and mitotic activity of cultured human wound fibroblasts. *Biochem. Biophys. Res. Commun.* 209, 393–399. doi: 10.1006/bbrc.1995.1516
- Leveen, P., Pekny, M., Gebre-Medhin, S., Swolin, B., Larsson, E., and Betsholtz, C. (1994). Mice deficient for PDGF B show renal, cardiovascular, and hematological abnormalities. *Genes Dev.* 8, 1875–1887. doi: 10.1101/gad.8.16.1875
- Li, R., Bernau, K., Sandbo, N., Gu, J., Preissl, S., and Sun, X. (2018). Pdgfra marks a cellular lineage with distinct contributions to myofibroblasts in lung maturation and injury response. *Elife* 7:e36865.
- Li, X., Ponten, A., Aase, K., Karlsson, L., Abramsson, A., Uutela, M., et al. (2000). PDGF-C is a new protease-activated ligand for the PDGF alpha-receptor. *Nat. Cell Biol.* 2, 302–309. doi: 10.1038/35010579
- Libby, P., and Theroux, P. (2005). Pathophysiology of coronary artery disease. *Circulation* 111, 3481–3488.
- Lindahl, P., Johansson, B. R., Leveen, P., and Betsholtz, C. (1997). Pericyte loss and microaneurysm formation in PDGF-B-deficient mice. *Science* 277, 242–245. doi: 10.1126/science.277.5323.242
- Liu, C., Li, J., Xiang, X., Guo, L., Tu, K., Liu, Q., et al. (2014). PDGF receptor-alpha promotes TGF-beta signaling in hepatic stellate cells via transcriptional and posttranscriptional regulation of TGF-beta receptors. *Am. J. Physiol. Gastrointest. Liver Physiol.* 307, G749–G759.
- Mahmoud, A. I., Porrello, E. R., Kimura, W., Olson, E. N., and Sadek, H. A. (2014). Surgical models for cardiac regeneration in neonatal mice. *Nat. Protoc.* 9, 305–311. doi: 10.1038/nprot.2014.021
- Mamer, S. B., Chen, S., Weddell, J. C., Palasz, A., Wittenkeller, A., Kumar, M., et al. (2020). Author correction: discovery of high-affinity PDGF-VEGFR interactions: redefining RTK dynamics. *Sci. Rep.* 10:11001.
- Mellgren, A. M., Smith, C. L., Olsen, G. S., Eskioçak, B., Zhou, B., Kazi, M. N., et al. (2008). Platelet-derived growth factor receptor beta signaling is required for efficient epicardial cell migration and development of two distinct coronary vascular smooth muscle cell populations. *Circ. Res.* 103, 1393–1401. doi: 10.1161/circresaha.108.176768
- Mohl, W., Gangl, C., Jusic, A., Aschacher, T., De Jonge, M., and Rattay, F. (2015). PICSO: from myocardial salvage to tissue regeneration. *Cardiovasc. Res.* 16, 36–46. doi: 10.1016/j.carrev.2014.12.004
- Munoz-Chapuli, R., Macias, D., Gonzalez-Iriarte, M., Carmona, R., Atencia, G., and Perez-Pomares, J. M. (2002). [The epicardium and epicardial-derived cells: multiple functions in cardiac development]. *Rev. Esp. Cardiol.* 55, 1070–1082.
- Musa, H., Kaur, K., O'Connell, R., Klos, M., Guerrero-Serna, G., Avula, U. M., et al. (2013). Inhibition of platelet-derived growth factor-AB signaling prevents electromechanical remodeling of adult atrial myocytes that contact myofibroblasts. *Heart Rhythm* 10, 1044–1051. doi: 10.1016/j.hrthm.2013.03.014
- Mustoe, T. A., Cutler, N. R., Allman, R. M., Goode, P. S., Deuel, T. F., Prause, J. A., et al. (1994). A phase II study to evaluate recombinant platelet-derived growth factor-BB in the treatment of stage 3 and 4 pressure ulcers. *Arch. Surg.* 129, 213–219. doi: 10.1001/archsurg.1994.01420260109015
- Okura, T., Igase, M., Kitami, Y., Fukuoka, T., Maguchi, M., Kohara, K., et al. (1998). Platelet-derived growth factor induces apoptosis in vascular smooth muscle cells: roles of the Bcl-2 family. *Biochim. Biophys. Acta* 1403, 245–253. doi: 10.1016/s0167-4889(98)00065-2
- Olsen, R. S., Dimberg, J., Geffers, R., and Wagsater, D. (2019). Possible role and therapeutic target of PDGF-D signalling in colorectal cancer. *Cancer Invest.* 37, 99–112. doi: 10.1080/07357907.2019.1576191
- Olson, L. E., and Soriano, P. (2009). Increased PDGFRalpha activation disrupts connective tissue development and drives systemic fibrosis. *Dev. Cell* 16, 303–313. doi: 10.1016/j.devcel.2008.12.003
- Orr-Urtreger, A., Bedford, M. T., Do, M. S., Eisenbach, L., and Lonai, P. (1992). Developmental expression of the alpha receptor for platelet-derived growth factor, which is deleted in the embryonic lethal Patch mutation. *Development* 115, 289–303. doi: 10.1242/dev.115.1.289
- Ostman, A. (2004). PDGF receptors-mediators of autocrine tumor growth and regulators of tumor vasculature and stroma. *Cytokine Growth Factor Rev.* 15, 275–286. doi: 10.1016/j.cytogfr.2004.03.002
- Palmieri, S. L., Payne, J., Stiles, C. D., Biggers, J. D., and Mercola, M. (1992). Expression of mouse PDGF-A and PDGF alpha-receptor genes during pre- and post-implantation development: evidence for a developmental shift from an autocrine to a paracrine mode of action. *Mech. Dev.* 39, 181–191. doi: 10.1016/0925-4773(92)90045-1
- Papadopoulos, N., and Lennartsson, J. (2018). The PDGF/PDGFR pathway as a drug target. *Mol. Aspects Med.* 62, 75–88. doi: 10.1016/j.mam.2017.11.007
- Pierce, G. F., Tarpley, J. E., Tseng, J., Bready, J., Chang, D., Kenney, W. C., et al. (1995). Detection of platelet-derived growth factor (PDGF)-AA in actively healing human wounds treated with recombinant PDGF-BB and absence of PDGF in chronic nonhealing wounds. *J. Clin. Invest.* 96, 1336–1350. doi: 10.1172/jci118169
- Ponten, A., Folestad, E. B., Pietras, K., and Eriksson, U. (2005). Platelet-derived growth factor D induces cardiac fibrosis and proliferation of vascular smooth muscle cells in heart-specific transgenic mice. *Circ. Res.* 97, 1036–1045. doi: 10.1161/01.res.0000190590.31545.d4
- Ponten, A., Li, X., Thoren, P., Aase, K., Sjoblom, T., Ostman, A., et al. (2003). Transgenic overexpression of platelet-derived growth factor-C in the mouse heart induces cardiac fibrosis, hypertrophy, and dilated cardiomyopathy. *Am. J. Pathol.* 163, 673–682. doi: 10.1016/s0002-9440(10)63694-2
- Porrello, E. R., Mahmoud, A. I., Simpson, E., Hill, J. A., Richardson, J. A., Olson, E. N., et al. (2011). Transient regenerative potential of the neonatal mouse heart. *Science* 331, 1078–1080. doi: 10.1126/science.1200708
- Prall, O. W., Menon, M. K., Solloway, M. J., Watanabe, Y., Zaffran, S., Bajolle, F., et al. (2007). An Nkx2-5/Bmp2/Smad1 negative feedback loop controls heart progenitor specification and proliferation. *Cell* 128, 947–959. doi: 10.1016/j.cell.2007.01.042
- Price, R. L., Haley, S. T., Bullard, T. A., Goldsmith, E. C., Simpson, D. G., Thielen, T. E., et al. (2003). Effects of platelet-derived growth factor-AA and -BB on embryonic cardiac development. *Anat. Rec. A Discov. Mol. Cell. Evol. Biol.* 272, 424–433. doi: 10.1002/ar.a.10054
- Qian, C., Wong, C. W. Y., Wu, Z., He, Q., Xia, H., Tam, P. K. H., et al. (2017). Stage specific requirement of platelet-derived growth factor receptor-alpha in embryonic development. *PLoS One* 12:e0184473. doi: 10.1371/journal.pone.0184473
- Qian, C., Wu, Z., Ng, R. C., Garcia-Barcelo, M. M., Yuan, Z. W., Wong, K. K. Y., et al. (2019). Conditional deletion of platelet derived growth factor receptor alpha (Pdgfra) in urorectal mesenchyme causes mesenchyme apoptosis and urorectal developmental anomalies in mice. *Cell Death Differ.* 26, 1396–1410. doi: 10.1038/s41418-018-0216-2
- Quijada, P., Trembley, M. A., and Small, E. M. (2020). The Role of the epicardium during heart development and repair. *Circ. Res.* 126, 377–394. doi: 10.1161/circresaha.119.315857
- Ramos, I. T., Henningson, M., Nezafat, M., Lavin, B., Lorrio, S., Gebhardt, P., et al. (2018). Simultaneous assessment of cardiac inflammation and extracellular matrix remodeling after myocardial infarction. *Circ. Cardiovasc. Imaging* 11:e007453.
- Ranganath, S. H., Levy, O., Inamdar, M. S., and Karp, J. M. (2012). Harnessing the mesenchymal stem cell secretome for the treatment of cardiovascular disease. *Cell Stem Cell* 10, 244–258. doi: 10.1016/j.stem.2012.02.005
- Roehlen, N., Crouchet, E., and Baumert, T. F. (2020). Liver fibrosis: mechanistic concepts and therapeutic perspectives. *Cells* 9:875. doi: 10.3390/cells9040875
- Romashkova, J. A., and Makarov, S. S. (1999). NF-kappaB is a target of AKT in anti-apoptotic PDGF signalling. *Nature* 401, 86–90. doi: 10.1038/43474
- Santini, M. P., Malide, D., Hoffman, G., Pandey, G., D'Escamard, V., Nomura-Kitabayashi, A., et al. (2020). Tissue-resident PDGFRalpha(+) progenitor cells contribute to fibrosis versus healing in a context- and spatiotemporally dependent manner. *Cell Rep.* 30, 555–570.e7.
- Sebastiao, M. J., Pereira, R., Serra, M., Gomes-Alves, P., and Alves, P. M. (2018). Unveiling human cardiac fibroblast membrane proteome. *Proteomics* 18:e1700446.
- Smith, C. L., Baek, S. T., Sung, C. Y., and Tallquist, M. D. (2011). Epicardial-derived cell epithelial-to-mesenchymal transition and fate specification require PDGF receptor signaling. *Circ. Res.* 108, e15–e26.

- Soriano, P. (1997). The PDGF alpha receptor is required for neural crest cell development and for normal patterning of the somites. *Development* 124, 2691–2700. doi: 10.1242/dev.124.14.2691
- Souders, C. A., Bowers, S. L., and Baudino, T. A. (2009). Cardiac fibroblast: the renaissance cell. *Circ. Res.* 105, 1164–1176. doi: 10.1161/circresaha.109.209809
- Su, W., Liu, G., Liu, X., Zhou, Y., Sun, Q., Zhen, G., et al. (2020). Angiogenesis stimulated by elevated PDGF-BB in subchondral bone contributes to osteoarthritis development. *JCI Insight* 5:e135446.
- Sullivan, K. E., Quinn, K. P., Tang, K. M., Georgakoudi, I., and Black, L. D. III (2014). Extracellular matrix remodeling following myocardial infarction influences the therapeutic potential of mesenchymal stem cells. *Stem Cell Res. Ther.* 5:14.
- Taimeh, Z., Loughran, J., Birks, E. J., and Bolli, R. (2013). Vascular endothelial growth factor in heart failure. *Nat. Rev. Cardiol.* 10, 519–530.
- Tallquist, M. D., and Soriano, P. (2003). Cell autonomous requirement for PDGFRalpha in populations of cranial and cardiac neural crest cells. *Development* 130, 507–518. doi: 10.1242/dev.00241
- Thavapalachandran, S., Grieve, S. M., Hume, R. D., Le, T. Y. L., Raguram, K., Hudson, J. E., et al. (2020). Platelet-derived growth factor-AB improves scar mechanics and vascularity after myocardial infarction. *Sci. Transl. Med.* 12:eaay2140. doi: 10.1126/scitranslmed.aay2140
- Travis, T. E., Mauskar, N. A., Mino, M. J., Prindeze, N., Moffatt, L. T., Fidler, P. E., et al. (2014). Commercially available topical platelet-derived growth factor as a novel agent to accelerate burn-related wound healing. *J. Burn Care Res.* 35, e321–e329.
- Uosaki, H., Andersen, P., Shenje, L. T., Fernandez, L., Christiansen, S. L., and Kwon, C. (2012). Direct contact with endoderm-like cells efficiently induces cardiac progenitors from mouse and human pluripotent stem cells. *PLoS One* 7:e46413. doi: 10.1371/journal.pone.0046413
- Valius, M., and Kazlauskas, A. (1993). Phospholipase C-gamma 1 and phosphatidylinositol 3 kinase are the downstream mediators of the PDGF receptor's mitogenic signal. *Cell* 73, 321–334. doi: 10.1016/0092-8674(93)90232-f
- Van den Akker, N. M., Winkel, L. C., Nisancioglu, M. H., Maas, S., Wisse, L. J., Armulik, A., et al. (2008). PDGF-B signaling is important for murine cardiac development: its role in developing atrioventricular valves, coronaries, and cardiac innervation. *Dev. Dyn.* 237, 494–503. doi: 10.1002/dvdy.21436
- Vantler, M., Karikkineth, B. C., Naito, H., Tiburcy, M., Didie, M., Nose, M., et al. (2010). PDGF-BB protects cardiomyocytes from apoptosis and improves contractile function of engineered heart tissue. *J. Mol. Cell. Cardiol.* 48, 1316–1323. doi: 10.1016/j.jmcc.2010.03.008
- Wang, Y., Appiah-Kubi, K., Wu, M., Yao, X., Qian, H., Wu, Y., et al. (2016). The platelet-derived growth factors (PDGFs) and their receptors (PDGFRs) are major players in oncogenesis, drug resistance, and attractive oncologic targets in cancer. *Growth Factors* 34, 64–71. doi: 10.1080/08977194.2016.1180293
- Weisman, H. F., and Healy, B. (1987). Myocardial infarct expansion, infarct extension, and reinfarction: pathophysiologic concepts. *Prog. Cardiovasc. Dis.* 30, 73–110. doi: 10.1016/0033-0620(87)90004-1
- White, S. J., and Chong, J. J. H. (2020). Growth factor therapy for cardiac repair: an overview of recent advances and future directions. *Biophys. Rev.* 12, 805–815. doi: 10.1007/s12551-020-00734-0
- Wills, A. A., Holdway, J. E., Major, R. J., and Poss, K. D. (2008). Regulated addition of new myocardial and epicardial cells fosters homeostatic cardiac growth and maintenance in adult zebrafish. *Development* 135, 183–192. doi: 10.1242/dev.010363
- Wollin, L., Maillet, I., Quesniaux, V., Holweg, A., and Ryffel, B. (2014). Antifibrotic and anti-inflammatory activity of the tyrosine kinase inhibitor nintedanib in experimental models of lung fibrosis. *J. Pharmacol. Exp. Ther.* 349, 209–220. doi: 10.1124/jpet.113.208223
- Xaymardan, M., Zheng, J., Duignan, I., Chin, A., Holm, J. M., Ballard, V. L., et al. (2004). Senescent impairment in synergistic cytokine pathways that provide rapid cardioprotection in the rat heart. *J. Exp. Med.* 199, 797–804. doi: 10.1084/jem.20031639
- Xu, J., and Clark, R. A. (1996). Extracellular matrix alters PDGF regulation of fibroblast integrins. *J. Cell Biol.* 132, 239–249. doi: 10.1083/jcb.132.1.239
- Ying, H. Z., Chen, Q., Zhang, W. Y., Zhang, H. H., Ma, Y., Zhang, S. Z., et al. (2017). PDGF signaling pathway in hepatic fibrosis pathogenesis and therapeutics (Review). *Mol. Med. Rep.* 16, 7879–7889. doi: 10.3892/mmr.2017.7641
- Yla-Herttuala, S., Bridges, C., Katz, M. G., and Korpisalo, P. (2017). Angiogenic gene therapy in cardiovascular diseases: dream or vision? *Eur. Heart J.* 38, 1365–1371.
- Yoon, C., Song, H., Yin, T., Bausch-Fluck, D., Frei, A. P., Kattman, S., et al. (2018). FZD4 marks lateral plate mesoderm and signals with NORRIN to increase cardiomyocyte induction from pluripotent stem cell-derived cardiac progenitors. *Stem Cell Rep.* 10, 87–100. doi: 10.1016/j.stemcr.2017.11.008
- Yue, Z., Chen, J., Lian, H., Pei, J., Li, Y., Chen, X., et al. (2019). PDGFR-beta signaling regulates cardiomyocyte proliferation and myocardial regeneration. *Cell Rep.* 28, 966–978.e4.
- Zhang, J., Cao, R., Zhang, Y., Jia, T., Cao, Y., and Wahlberg, E. (2009). Differential roles of PDGFR-alpha and PDGFR-beta in angiogenesis and vessel stability. *FASEB J.* 23, 153–163. doi: 10.1096/fj.08-113860
- Zhao, T., Zhao, W., Chen, Y., Li, V. S., Meng, W., and Sun, Y. (2013). Platelet-derived growth factor-D promotes fibrogenesis of cardiac fibroblasts. *Am. J. Physiol. Heart Circ. Physiol.* 304, H1719–H1726.
- Zhao, W., Zhao, T., Huang, V., Chen, Y., Ahokas, R. A., and Sun, Y. (2011). Platelet-derived growth factor involvement in myocardial remodeling following infarction. *J. Mol. Cell. Cardiol.* 51, 830–838. doi: 10.1016/j.jmcc.2011.06.023
- Zheng, J., Shin, J. H., Xaymardan, M., Chin, A., Duignan, I., Hong, M. K., et al. (2004). Platelet-derived growth factor improves cardiac function in a rodent myocardial infarction model. *Coron. Artery Dis.* 15, 59–64. doi: 10.1097/00019501-200402000-00009
- Zhou, X. M., Liu, Y., Payne, G., Lutz, R. J., and Chittenden, T. (2000). Growth factors inactivate the cell death promoter BAD by phosphorylation of its BH3 domain on Ser155. *J. Biol. Chem.* 275, 25046–25051. doi: 10.1074/jbc.m002526200
- Zymek, P., Bujak, M., Chatila, K., Cieslak, A., Thakker, G., Entman, M. L., et al. (2006). The role of platelet-derived growth factor signaling in healing myocardial infarcts. *J. Am. Coll. Cardiol.* 48, 2315–2323. doi: 10.1016/j.jacc.2006.07.060

Conflict of Interest: The authors declare that the research was conducted in the absence of any commercial or financial relationships that could be construed as a potential conflict of interest.

Publisher's Note: All claims expressed in this article are solely those of the authors and do not necessarily represent those of their affiliated organizations, or those of the publisher, the editors and the reviewers. Any product that may be evaluated in this article, or claim that may be made by its manufacturer, is not guaranteed or endorsed by the publisher.

Copyright © 2021 Kalra, Eberhard, Farbehi, Chong and Xaymardan. This is an open-access article distributed under the terms of the Creative Commons Attribution License (CC BY). The use, distribution or reproduction in other forums is permitted, provided the original author(s) and the copyright owner(s) are credited and that the original publication in this journal is cited, in accordance with accepted academic practice. No use, distribution or reproduction is permitted which does not comply with these terms.



High-Mobility Group A1 Promotes Cardiac Fibrosis by Upregulating FOXO1 in Fibroblasts

Qingwen Xie^{1,2,3†}, Qi Yao^{1,2,3†}, Tongtong Hu^{1,2,3}, Zhulan Cai^{1,2,3}, Jinhua Zhao^{1,2,3}, Yuan Yuan^{1,2,3}, Qing Qing Wu^{1,2,3*} and Qi-zhu Tang^{1,2,3*}

¹ Department of Cardiology, Renmin Hospital of Wuhan University, Wuhan, China, ² Cardiovascular Research Institute, Wuhan University, Wuhan, China, ³ Hubei Key Laboratory of Cardiology, Wuhan, China

OPEN ACCESS

Edited by:

Isotta Chimenti,
Sapienza University of Rome, Italy

Reviewed by:

Raúl Vivar,
University of Chile, Chile
Guillermo Diaz-Araya,
University of Chile, Chile

*Correspondence:

Qing Qing Wu
qingwu20130@whu.edu.cn
Qi-zhu Tang
qztang@whu.edu.cn

† These authors have contributed
equally to this work

Specialty section:

This article was submitted to
Molecular and Cellular Pathology,
a section of the journal
Frontiers in Cell and Developmental
Biology

Received: 10 February 2021

Accepted: 02 August 2021

Published: 26 August 2021

Citation:

Xie Q, Yao Q, Hu T, Cai Z, Zhao J,
Yuan Y, Wu QQ and Tang Q-z (2021)
High-Mobility Group A1 Promotes
Cardiac Fibrosis by Upregulating
FOXO1 in Fibroblasts.
Front. Cell Dev. Biol. 9:666422.
doi: 10.3389/fcell.2021.666422

High-mobility group A1 (HMGA1) acts as a transcription factor in several cardiovascular diseases. However, the implications of HMGA1 in cardiac fibrosis remain unknown. Here, we investigated the impact of HMGA1 on cardiac fibrosis. A mouse cardiac fibrosis model was constructed *via* subcutaneous injection of isoproterenol (ISO) or angiotensin II (Ang II) infusion. Adult mouse cardiac fibroblasts (CFs) were isolated and cultured. CFs were stimulated with transforming growth factor- β 1 (TGF- β 1) for 24 h. As a result, HMGA1 was upregulated in fibrotic hearts, as well as TGF- β -stimulated CFs. Overexpression of HMGA1 in CFs aggravated TGF- β 1-induced cell activation, proliferation, and collagen synthesis. Overexpression of HMGA1 in fibroblasts, by an adeno-associated virus 9 dilution system with a periostin promoter, accelerated cardiac fibrosis and cardiac dysfunction. Moreover, HMGA1 knockdown in CFs inhibited TGF- β 1-induced cell activation, proliferation, and collagen synthesis. Mechanistically, we found that HMGA1 increased the transcription of FOXO1. The FOXO1 inhibitor AS1842856 counteracted the adverse effects of HMGA1 overexpression *in vitro*. HMGA1 silencing in mouse hearts alleviated Ang II-induced cardiac fibrosis and dysfunction. However, FOXO1 knockdown in mouse hearts abolished the deteriorating effects of HMGA1 overexpression in mice. Collectively, our data demonstrated that HMGA1 plays a critical role in the development of cardiac fibrosis by regulating FOXO1 transcription.

Keywords: cardiac fibrosis, fibroblasts, high-mobility group A1, FOXO1, cardiac dysfunction

INTRODUCTION

Cardiac fibrosis caused by various cardiac injuries is characterized by the production of excessive extracellular matrix (ECM) in the cardiac interstitium, leading to increased ventricular stiffness and diastolic dysfunction, and ultimately giving rise to heart failure (Gyongyosi et al., 2017). It is also caused by various cardiac pathophysiologic insults involving acute myocardial infarction, hypertension, and diabetes mellitus (Asbun and Villarreal, 2006). Neurohormonal activation is the main pathological feature of cardiac fibrosis during cardiac injury (Sekaran et al., 2017). Isoproterenol (ISO), a β -adrenergic agonist, could increase cardiac fibroblasts (CF) proliferation, and collagen synthesis through excessive stimulation of β -adrenergic receptors in the heart (Benjamin et al., 1989). Other neurohumoral factors, such as angiotensin II (Ang II) and transforming growth factor β 1 (TGF- β 1), are also increased during cardiac injury and act as key

contributors to cardiac fibrosis (Cucoranu et al., 2005; Flevaris et al., 2017). Cardiac myofibroblasts come from several different sources, such as resident endothelial cells or circulating immune cells. However, research has shown that resident CFs account for the majority of activated fibroblasts during injury. Currently, the mechanism that regulates the process of cardiac fibrosis is not fully understood.

High-mobility group A1 (HMGA1), a non-histone chromatin-binding protein, is a nuclear architectural factor (Johnson et al., 1989). HMGA1 is a key regulator of a variety of fundamental biological processes, such as embryologic development, cell cycle progression, differentiation, apoptosis, inflammation, and DNA repair. Recent studies have suggested that HMGA1 is closely involved in the regulation of cardiac pathologies. HMGA1 participates in the inflammatory process of atherosclerosis, causing coronary heart disease (Schlueter et al., 2005). Inhibition of HMGA1/NF- κ B signaling attenuates myocardial damage caused by coronary microembolization and improves cardiac function (Su et al., 2018). Moreover, we previously demonstrated that HMGA1 aggravated myocardial inflammation and apoptosis in a sepsis-induced cardiac injury mouse model by regulating both COX-2 and STAT3 signaling (Cai et al., 2020). In diabetic cardiomyopathy, HMGA1 inhibits autophagy by regulating the activity of the miR-222 promoter, thereby aggravating cardiac dysfunction (Wu et al., 2020). Altogether, HMGA1 could be a promising molecule in cardiac fibrosis. In the present study, we aimed to explore the role and mechanism of HMGA1 in cardiac fibrosis induced by ISO or Ang II in mice, as well as in CFs stimulated by TGF- β 1. Periostin, an epithelial ligand and matricellular protein commonly expressed by fibroblasts, has been dissected by many studies as a promoter responsible for controlling gene expression in fibroblasts (Piras et al., 2016; Bao et al., 2020). Thus, in this study, we used an adeno-associated virus 9 delivery system with a periostin promoter to specifically target HMGA1 gene expression in CFs.

MATERIALS AND METHODS

Materials

Isoproterenol (ISO) and TGF- β were purchased from Sigma-Aldrich (St. Louis, MO, United States). Antibodies against HMGA1, α -SMA, MMP9, and PCNA were acquired from Abcam. Antibodies against GAPDH, total FOXO1, and phosphorylated (P)-FOXO1 (9461P) were acquired from Cell Signaling Technology. Antibodies against collagen III were acquired from Santa Cruz Biotechnology. The GT VisionTM + Detection System/Mo&Rb reagent for immunohistochemistry was purchased from Gene Technology (Shanghai, China). An Alexa Fluor 488-conjugated goat anti-rabbit secondary antibody for immunofluorescence was obtained from LI-COR Biosciences.

Animals and Models

C57/BL6J male mice (8 weeks, 25.2 ± 2 g) were purchased from the Chinese Academy of Medical Sciences (Beijing).

All of the animal care and experimental procedures were in compliance with the regulations of the National Institutes of Health Guide for the Care and Use of Laboratory Animals and were approved by the Institutional Animal Use and Care Committee at Wuhan University, China. Mice were divided into four groups in the overexpression experiment ($n = 12$ per group). The mice were given injections of either adeno-associated virus (AAV9)-HMGA1 or AAV9-NC to overexpress or knock down HMGA1. After 1 week, ISO was injected subcutaneously for 14 days (10 mg/kg for 3 days and 5 mg/kg for 11 days) to establish a mouse model of cardiac fibrosis (Jiang et al., 2017). The Ang II-induced cardiac mouse model was established as follows: The mice were injected subcutaneously with Ang II (1,000 ng/kg/min) *via* an osmotic minipump for 28 days (Zhai et al., 2018). They were then divided into four groups in the knockdown experiment ($n = 12$ per group). The mice were subjected to AAV9-shHMGA1 or AAV9-ScRNA to knock down HMGA1 1 week before Ang II infusion. The mice were divided into three groups in the reverse experiment. They were also subjected to AAV9-HMGA1 and AAV9-ShFOXO1, or AAV9-ScRNA to knock down FOXO1 1 week before Ang II infusion. At the end of the ISO or Ang II treatment period, the mice were anesthetized with sodium pentobarbital and sacrificed after echocardiography.

Adeno-Associated Virus Vector

Recombinant AAV9-expressing mouse HMGA1 (AAV9-HMGA1), AAV9-shHMGA1, and AAV9-shFOXO were constructed by Vigene Bioscience Company (Jinan, China) as described in our previous study (Wu et al., 2020). A short, small 1,395-bp periostin promoter was used to induce fibroblast-specific gene delivery (Piras et al., 2016). A total of 60–80 μ l of AAV9-HMGA1/AAV9-shHMGA1/AAV9-shFOXO or AAV9-NC/AAV9-shRNA ($5.0\text{--}6.5 \times 10^{13}$ VG/ml) was injected into the retro-orbital venous plexus of the mice 1 week before ISO or Ang II injection, as described in a previous study (Wu et al., 2020).

Echocardiography

A Mylab 30CV ultrasound system (Esaote S.P.A., Genoa, Italy) and a 10-MHz linear array ultrasound transducer were used to assess the cardiac function of the mice, which were anesthetized with continuous 1.5–2% isoflurane inhalation. Cardiac parameters were assessed by M-mode and two-dimensional echocardiography. The following parameters were collected: left ventricular (LV) ejection fraction (EF), fractional shortening (FS), LV end-systolic diameter (LVESd), and LV end-diastolic diameter (LVEDd).

Cell Culture and Treatments

Cardiac fibroblasts (CFs) were isolated from adult mice (6–8 weeks) as described in our previous study (Liu et al., 2020). After isolation, CFs were cultured in DMEM/F12 with 10% fetal bovine serum (FBS). Two- to four-interval passaging CFs were used. CFs were transfected with adenovirus (Ad)-HMGA1 (MOI = 30) for 8 h to overexpress HMGA1. In the gene silencing experiments, cells were transfected with 100 pmol anti-HMGA1 siRNA for 8 h. TGF- β (10 ng/ml, 24 h) was used to induce CF

activation. To inhibit FOXO1, CFs were treated with AS1842856 (10 μ M, MedChemExpress) for 2 h and then stimulated with TGF- β (10 ng/ml) for another 24 h.

Western Blotting

Heart tissue and CF samples were lysed in radioimmunoprecipitation (RIPA) lysis buffer. Then, 30 μ g of protein from each sample were separated by 10% SDS-PAGE. Protein was then transferred to PVDF membranes, followed by blocking with 5% milk for 1 h. Specific primary antibodies were incubated with PVDF membranes overnight. Then, the corresponding secondary antibodies were incubated with the membranes for 1 h. ECL Western blot detection kits (GE) were used to detect chemiluminescence with a LI-COR Odyssey image system. Protein expression levels were normalized to the matched GAPDH. Image Lab software from Bio-Rad (Hercules, CA, United States) was used for quantification.

Quantitative Real-Time PCR

Heart tissue and CF samples were lysed in TRIzol reagent (Gibco, United States). Total RNA was extracted (Gibco, United States). SYBR green master mix (Bio-Rad, Hercules, CA, United States) reactions were used for PCR. Threshold cycles and melting curve measurements were used to quantify the PCR results. mRNA levels were normalized to the matched GAPDH. The sequences of the primers are shown in **Table 1**.

Histological Examination

Myocardial tissue was fixed with 10% formalin and then dehydrated and embedded in paraffin. After transverse sectioning into 5- μ m sections, the hearts were stained with picosirius red (PSR) to evaluate cardiac fibrosis. Image-Pro Plus software

was used to measure cardiac fibrosis. The mean ratio of the collagen content to the total tissue area of each group was calculated as the collagen volume fraction. The expression of HMGA1 in the myocardium was immunolocalized using an anti-HMGA1 antibody (1:200) and visualized with a DAB-based colorimetric method.

Immunofluorescence Staining

After treatment, CFs were washed with PBS and then fixed with 4% methanol and permeabilized in 0.2% Triton X-100. After washing with PBS, the cells were blocked with 10% goat serum for 1 h. The specific primary antibodies were incubated at 4°C overnight. A fluorescence-labeled secondary antibody was then used to incubate the cells at room temperature for 1 h. CF nuclei were stained with DAPI. An Olympus DX51 fluorescence microscope was used for observation (Tokyo, Japan).

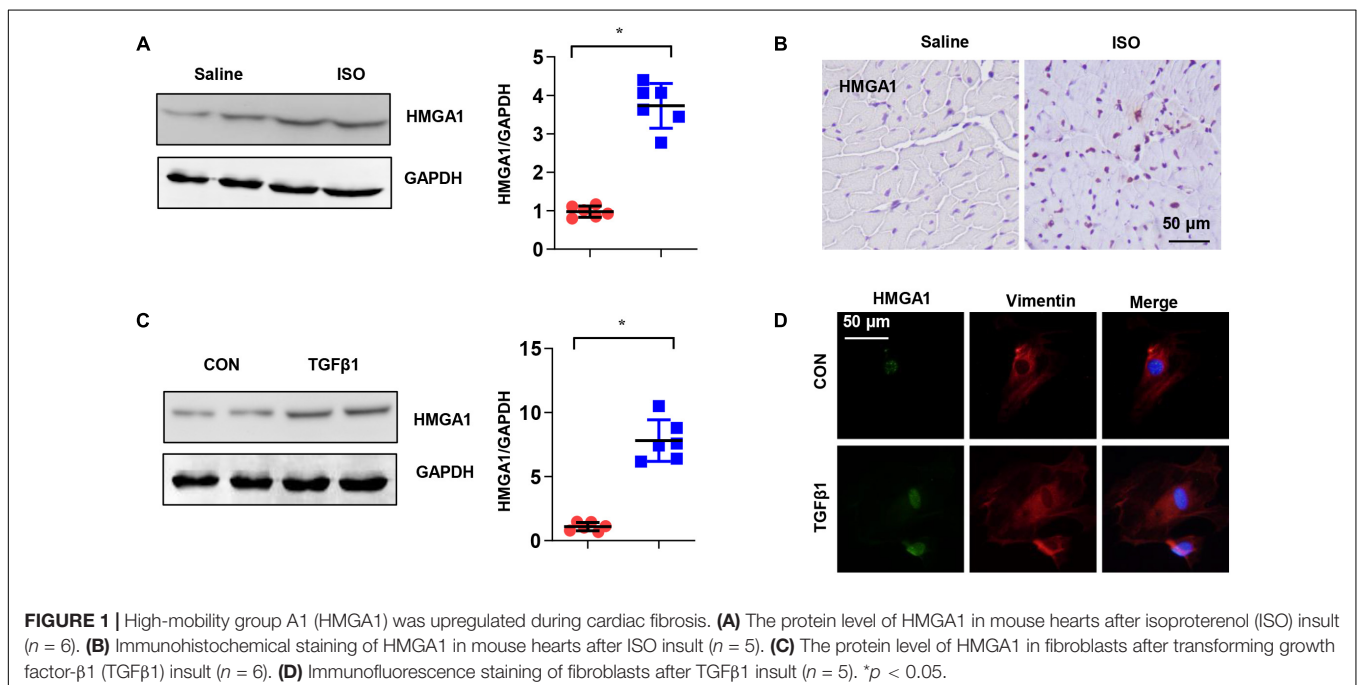
Cell Counting Kit-8

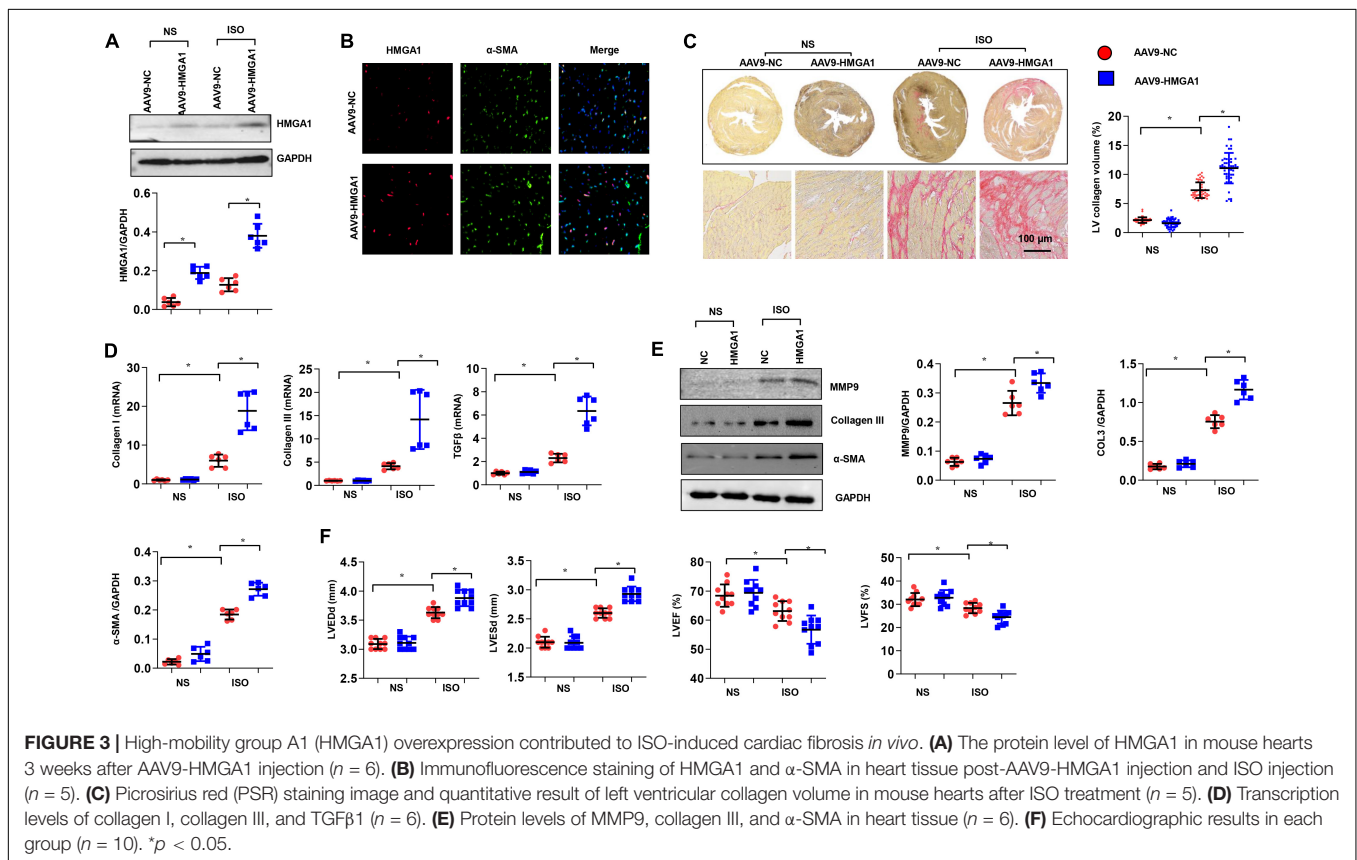
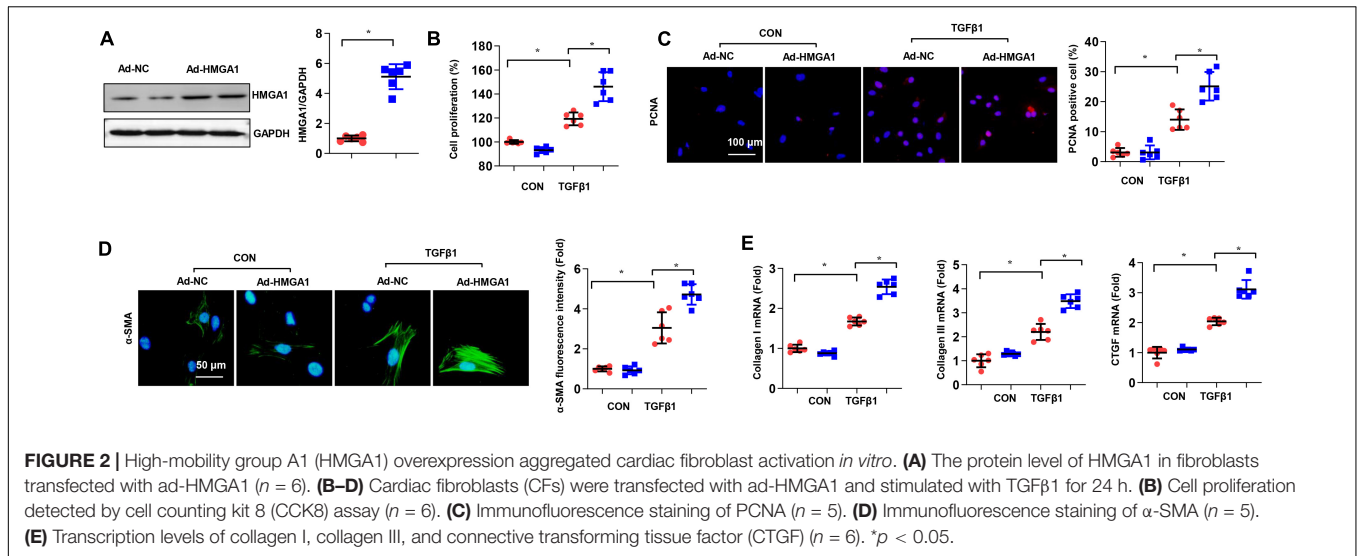
A CCK-8 assay kit was used to detect the proliferation of treated cells. A 100- μ l cell suspension was placed in a 96-well plate, and the cells were treated according to the experimental design.

TABLE 1 | Primer sequences used for RT-PCR.

| mRNA | Forward | Reverse |
|--------------|------------------------|-------------------------|
| Collagen I | AGGCTTCAGTGGTTTGGATG | CACCAACAGCACCATCGTTA |
| Collagen III | AAGGCTGCAAGATGGATGCT | GTGCTTACGTGGACAGTCA |
| CTGF | AGGGCTCTTCTGCGATTTC | CITTTGGAAGGACTCACCGCT |
| TGF- β | ATCCTGTCCAAACTAAGGCTCG | ACCTCTTTAGCATAGTAGTCCCG |
| GAPDH | ACTCCACTCACGGCAAATTC | TCTCCATGGTGGTGAAGACA |

Sequences listed are 5'–3'.



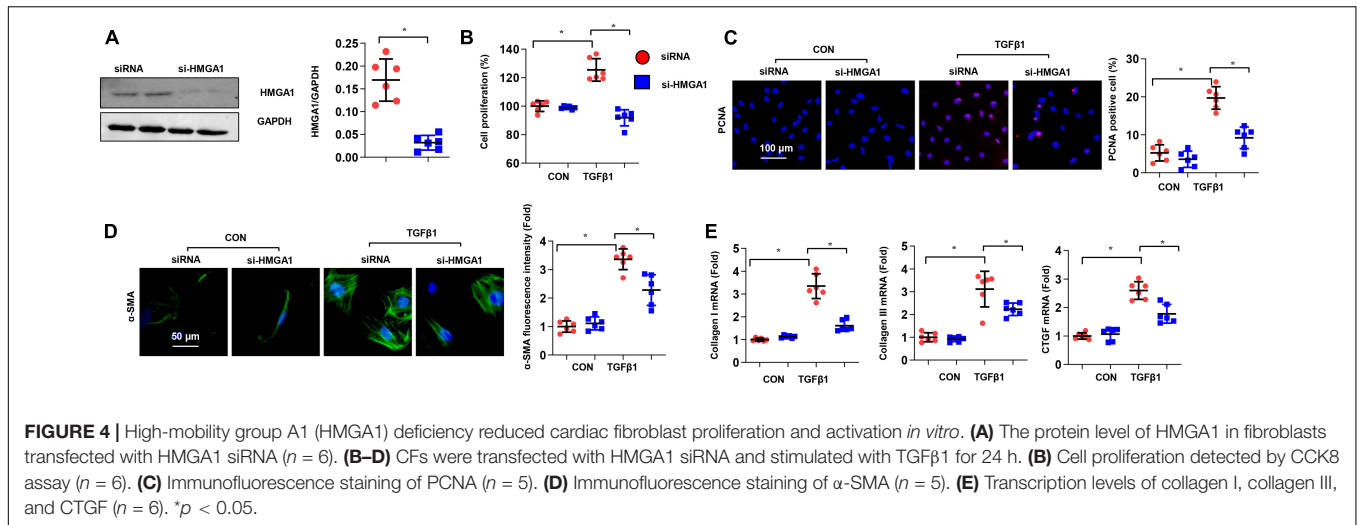


Ten microliters of CCK-8 solution was added to each well and cultured in an incubator for 4 h. The absorbance at 450 nm was measured by an enzyme plate analyzer to determine the cell proliferation activity.

Luciferase Reporter Assay

The amplified fragment of the FOXO1 3'-UTR was subcloned into the luciferase reporter vector (Promega, United States). The

PGL3 basic vector was used as a negative control. Luciferase reporter constructs were packed with an adenoviral system and then cotransfected into CFs with a control plasmid, followed by the indicated stimulation: Ad-HMGA1 transfection or HMGA1 siRNA for 48 h. Then, the cells were harvested and lysed, and the Dual-Luciferase Reporter Assay Kit (Promega, United States) was used to detect the luciferase activity according to the instructions of the manufacturer.



Statistical Analysis

SPSS software, version 21.0, was used to analyze the data. Two-way ANOVA was used to compare data between groups followed by Tukey's *post hoc* test. Student's unpaired *t*-test was used to compare data between two groups. Statistically significant findings were confirmed with a *p*-value < 0.05 .

RESULTS

High-Mobility Group A1 Was Upregulated During Cardiac Fibrosis

To explore the expression of HMGA1, we detected HMGA1 expression in ISO-induced fibrotic mouse hearts and TGF- β -stimulated CFs. HMGA1 protein and mRNA levels were increased in both fibrotic hearts and TGF- β -stimulated CFs (Figures 1A,C). Immunofluorescence staining confirmed that HMGA1, mainly located in the nuclei, was increased in fibrotic heart tissues (Figure 1B) and TGF- β -stimulated CFs (Figure 1D). These alterations indicate that an elevation in HMGA1 could be associated with cardiac fibrosis.

High-Mobility Group A1 Overexpression Aggregated Cardiac Fibroblast Activation *in vitro*

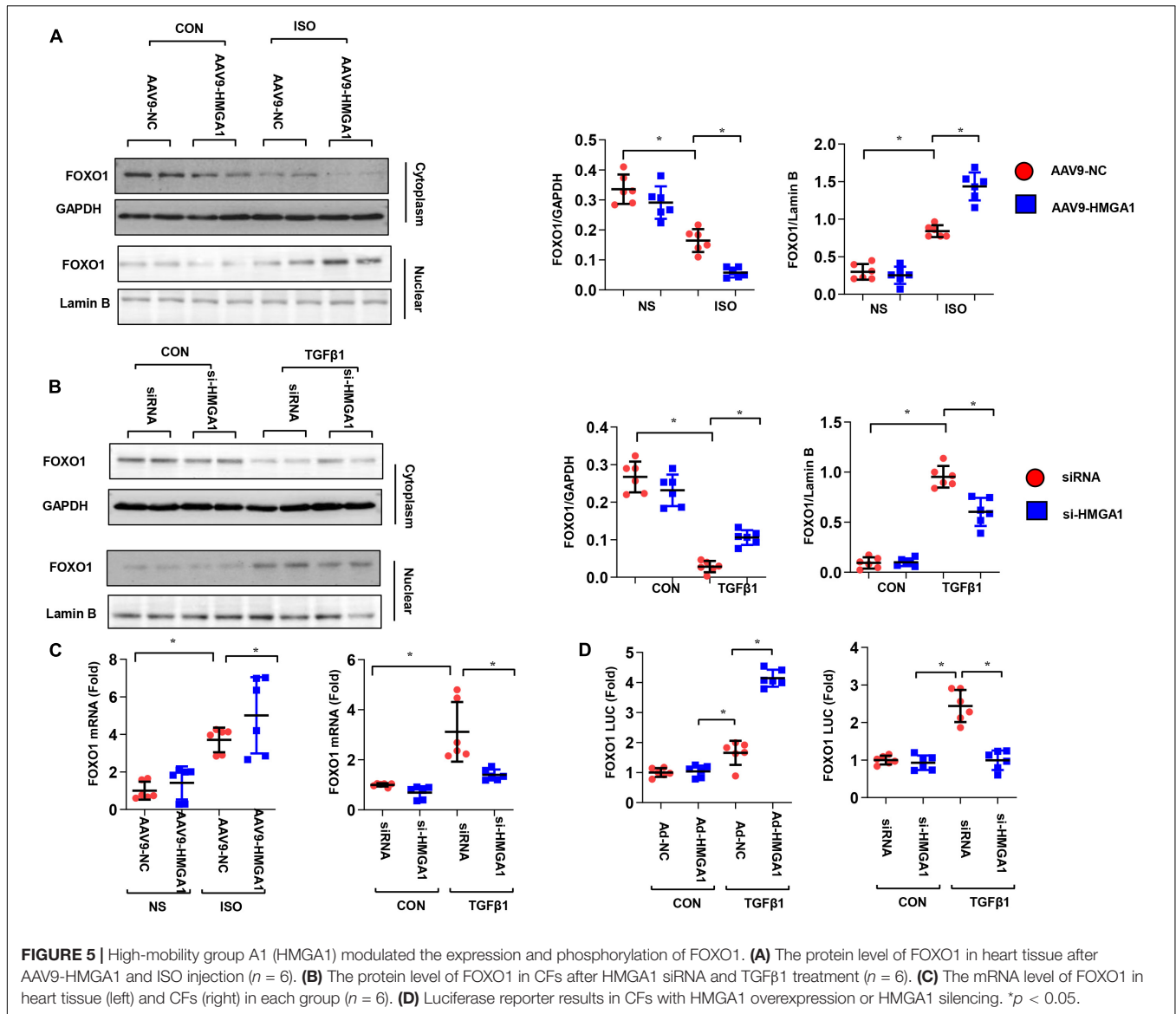
After cardiac injury, stationary CFs in heart tissue are activated in myofibroblasts with active proliferation ability and collagen secretion. Therefore, we further explored the effects of HMGA1 on CFs stimulated by TGF- β *in vitro*. CFs were infected with Ad-HMGA1 to overexpress HMGA1 (Figure 2A). TGF- β stimulation increased cell proliferation, as evidenced by increased PCNA-positive cell numbers and cell proliferation (Figures 2B,C). As expected, TGF- β significantly increased the α -SMA density in CFs (Figure 2D), accompanied by increases in collagen I, collagen III, and CTGF expression at the mRNA level (Figure 2E). HMGA1 overexpression induced TGF- β -induced cell proliferation and activation (Figures 2B–D).

High-Mobility Group A1 Overexpression Contributed to Isoproterenol-Induced Cardiac Fibrosis *in vivo*

To further confirm the role of HMGA1 in cardiac fibrosis, we induced HMGA1 overexpression in fibroblasts *in vivo*. HMGA1 increased at 4 weeks after AAV9-HMGA1 injection (Figure 3A). HMGA1 expression was mainly in CFs, as we used the fibroblast promoter periostin (Figure 3B). Heart tissues from mice subjected to ISO showed intense interstitial fibrosis. ISO injection induced significant cardiac fibrosis, as assessed by increased collagen deposition and increased mRNA levels of the fibrosis markers TGF- β 1, collagen I, and collagen III compared with the NS group. However, HMGA1-overexpressing mice showed aggressive cardiac fibrosis with greater LV collagen deposition in the interstitial area and more upregulated mRNA levels of fibrosis markers than the NC-ISO group (Figures 3C,D). The protein expression of the fibrosis-associated molecules MMP9, collagen III, and α -SMA was also evaluated. ISO was found to induce dramatic increases in these proteins, and HMGA1 overexpression aggregated ISO-induced changes (Figure 3E). Echocardiogram results also revealed that ISO injection induced mouse cardiac dysfunction with reduced LVEF and FS and increased LVEDd and LVESd. Cardiac dysfunction was aggravated by HMGA1 overexpression (Figure 3F). Collectively, these findings suggest that HMGA1 promotes ISO-induced cardiac fibrosis and cardiac dysfunction.

High-Mobility Group A1 Deficiency Reduced Cardiac Fibroblast Proliferation and Activation *in vitro*

Next, we wondered whether HMGA1 deficiency would alleviate cardiac fibrosis pathogenesis. To address this issue, we used siRNA to knock down HMGA1 in CFs. The protein expression levels of HMGA1 decreased in CFs transfected with HMGA1 siRNA (Figure 4A). TGF- β -induced proliferation and activation of fibroblasts were also inhibited after HMGA1 knockdown (Figures 4B–D). In addition, HMGA1 silencing inhibited the

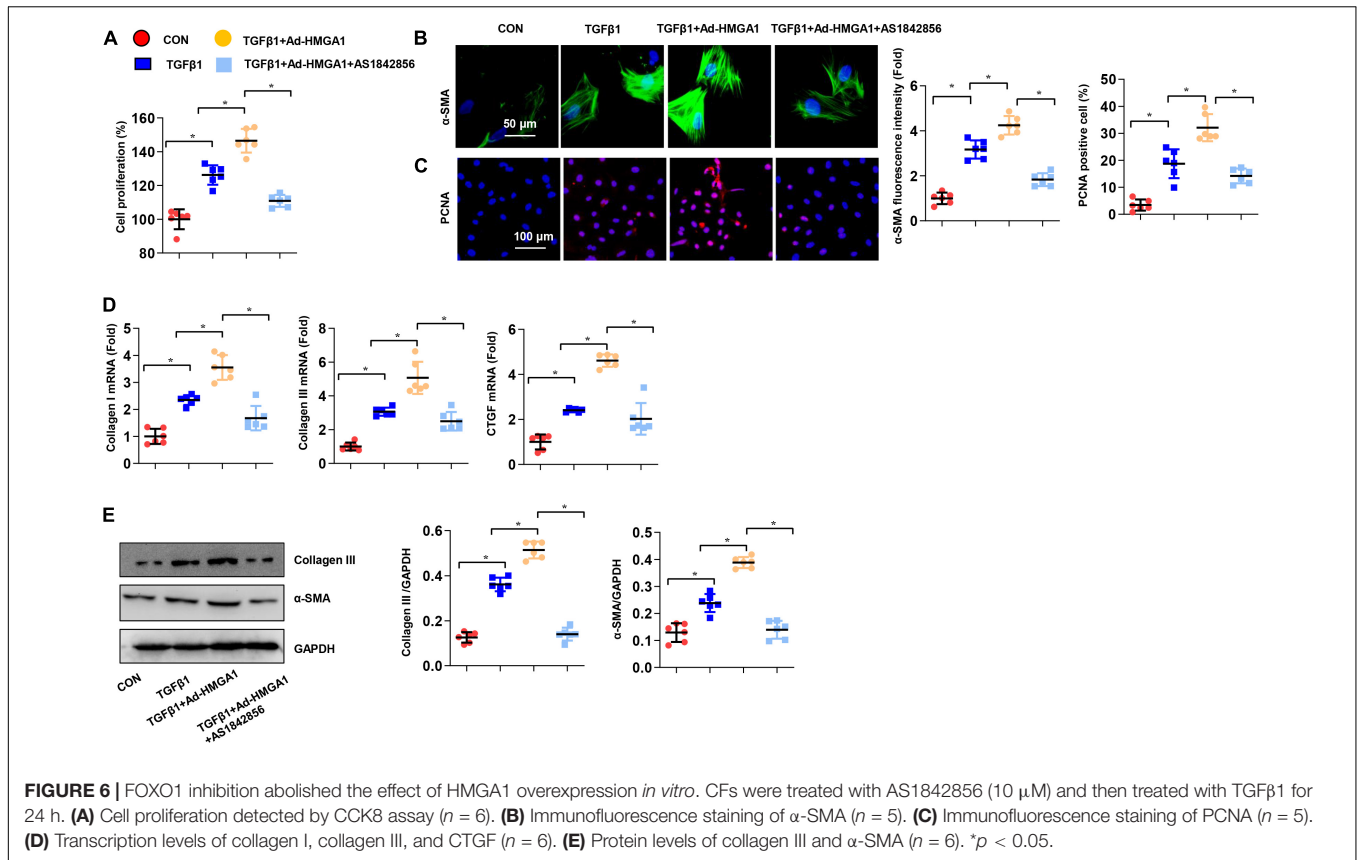


transcription of collagens and CTGF (Figure 4E). Thus, targeting of HMGA1 could be a potential treatment approach for fibrosis disease.

High-Mobility Group A1 Modulated the Expression and Phosphorylation of FOXO1

Evidence has shown that HMGA1 affects FOXO1 (Arcidiacono et al., 2018), a crucial transcription factor in the development of cardiac fibrosis (Arcidiacono et al., 2018; Xin et al., 2018). To explore the mechanisms of HMGA1 in fibrosis, we subsequently measured the total and phosphorylated levels of the FOXO1 protein. Our results showed that ISO stimulation markedly reduced FOXO1 cytoplasm levels and increased FOXO1 protein levels in nuclear mouse heart tissue (Figure 5A). HMGA1 overexpression obviously increased the nuclear level of FOXO1.

Conversely, in TGF- β 1-stimulated fibroblasts, and HMGA1, silencing enhanced the cytoplasmic level of FOXO1 while reducing the nuclear level of FOXO1 (Figure 5B). To test the hypothesis that HMGA1 could play a role in the transcriptional regulation of the FOXO1 gene, we detected the mRNA expression of FOXO1. As shown in Figure 5C, HMGA1 overexpression in heart tissue increased the transcription of FOXO1. HMGA1 silencing in fibroblasts downregulated FOXO1 transcription levels. We further performed reporter gene analysis in CFs. After transfecting the cells with the FOXO1-Luc reporter plasmid bearing the FOXO1 promoter sequence upstream of the luciferase reporter gene, FOXO1-Luc activity was increased in cells with HMGA1 overexpression and decreased in cells with HMGA1 silencing only under TGF β 1 stimulation (Figure 5D). This finding indicates that, during the fibrosis process, HMGA1 promotes the expression of FOXO1 by binding to the FOXO1 promoter and increases FOXO1 nuclear levels.



FOXO1 Inhibition Abolished the Effect of High-Mobility Group A1 Overexpression *in vitro*

To further investigate whether the effects of HMGA1 depend on FOXO1, we used AS1842856 to inhibit FOXO1 in CFs. The CCK-8 assay showed that HMGA1 overexpression promoted fibroblast proliferation, but the inhibition of FOXO1 significantly reduced the proliferative effect (Figure 6A). The inhibitory effect of FOXO1 inhibitors on fibroblast proliferation was further verified by PCNA staining (Figure 6B). In cellular immunofluorescence staining, the expression of α -SMA in fibroblasts was enhanced by TGF- β and HMGA1, while the expression of α -SMA was inhibited by the FOXO1 inhibitor (Figure 6C). Correspondingly, the expression of fibrosis-related genes and proteins decreased with the inhibition of FOXO1 (Figures 6D,E). In summary, HMGA1 affects CF activation and function *via* FOXO1.

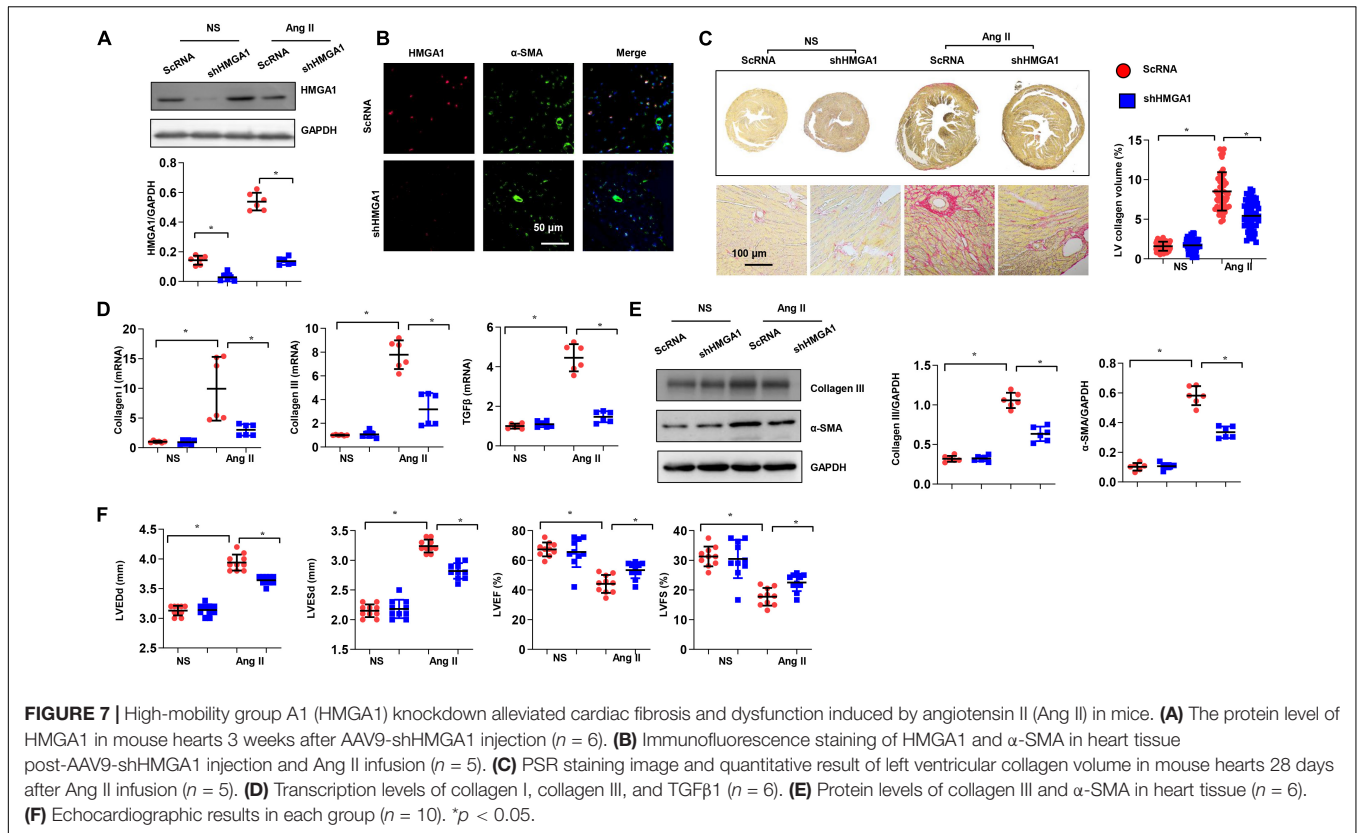
High-Mobility Group A1 Knockdown Alleviated Cardiac Fibrosis and Dysfunction Induced by Angiotensin II in Mice

To further confirm the role of HMGA1 in cardiac fibrosis, we silenced HMGA1 in an Ang II-induced cardiac fibrosis mouse model. AAV9-shHMGA1 injection induced a sharp reduction in HMGA1 expression after 28 days of Ang II

infusion (Figure 7A). The expression of HMGA1 was coincident with the expression of α -SMA, indicating that HMGA1 was downregulated in CFs in heart tissue after Ang II infusion (Figure 7B). Chronic Ang II infusion for 28 days induced significant fibrosis in male C57BL/6 mice, as demonstrated by a significant increase in collagen volume and higher expression of fibrotic markers compared with controls (Figures 7C–E). HMGA1 knockdown dramatically inhibited Ang II-induced cardiac fibrosis, as demonstrated by significant decreases in collagen volume and expression of fibrotic markers (Figures 7C–E). Echocardiography results revealed that mice in the HMGA1 knockdown group exhibited improved cardiac function with higher LVEF and FS and reduced LVEDd and LVESd in response to Ang II infusion (Figure 7F). Considered together, these data suggest that HMGA1 knockdown leads to alleviated cardiac dysfunction in mice challenged with Ang II.

FOXO1 Inhibition Counteracted High-Mobility Group A1-Induced Cardiac Dysfunction

Next, we investigated whether FOXO1 was essential for the effects of HMGA1 *in vivo*. Mice were subjected to both AAV9-shFOXO1 and AAV9-HMGA1 injections and then infused with Ang II for 28 days. AAV9-shFOXO1 induced a significant decrease in FOXO1 expression 28 days after Ang II infusion (Figure 8A), and the fibrotic effect of HMGA1 in the heart induced by Ang



II was counteracted by FOXO1 knockdown, as evidenced by the decreased LV percentage fibrosis and the downregulated mRNA expression of collagen I, collagen III, and TGF- β 1 (Figures 8B,C). The protein expression of collagen III and α -SMA was also reduced in mice subjected to both AAV9-shFOXO1 and AAV9-HMGA1 injections (Figure 8D). Additionally, cardiac function in mice injected with both AAV9-shFOXO1 and AAV9-HMGA1 was also improved compared with mice injected with only AAV9-HMGA1 (Figure 8E). These results further suggested that FOXO1 is the target of HMGA1 involved in cardiac fibrosis.

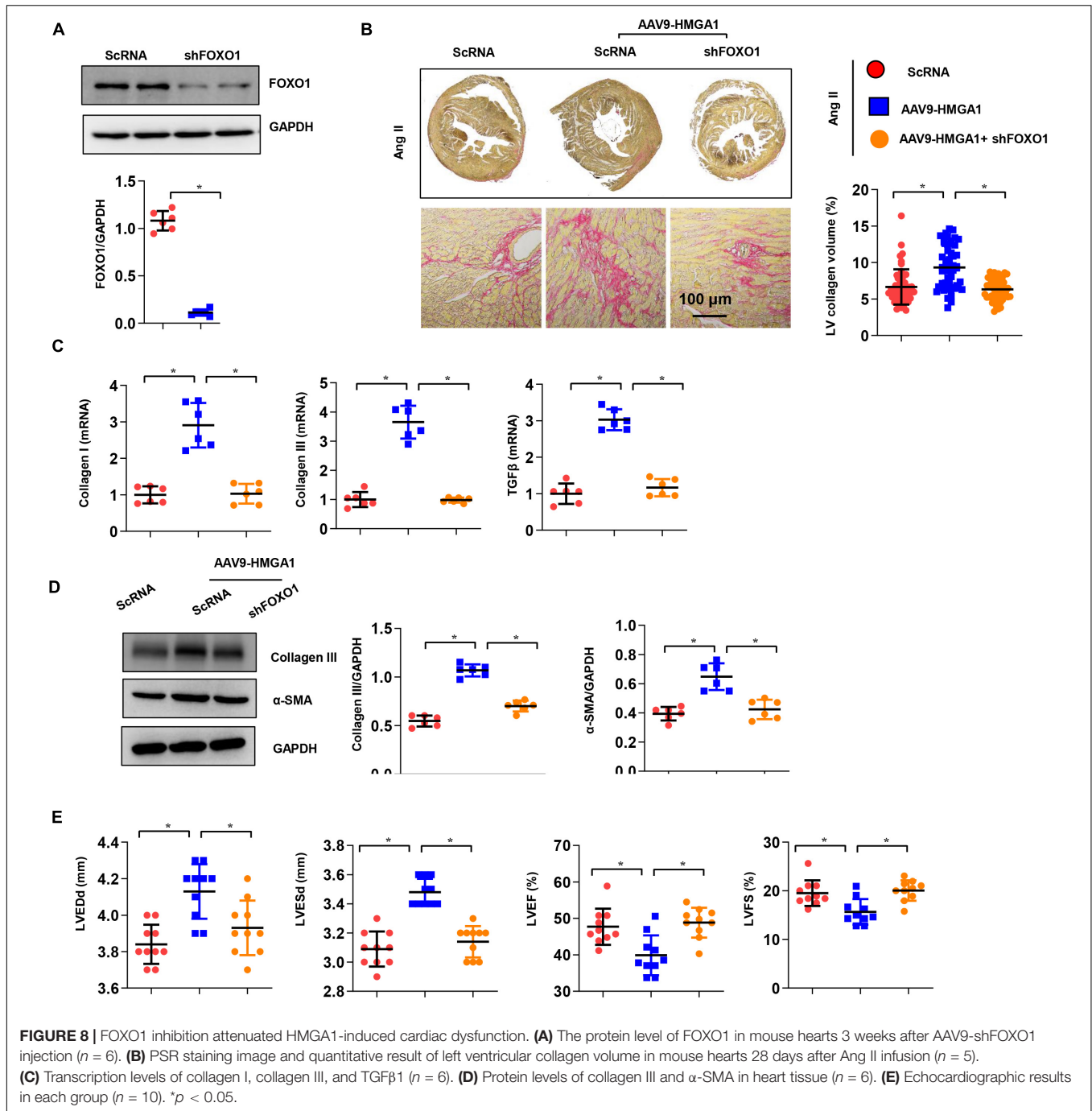
DISCUSSION

We previously provided data indicating that HMGA1 could play an important role in sepsis-induced cardiomyopathy and diabetic cardiomyopathy (Wu et al., 2020). In the present study, we showed that HMGA1 promoted ISO- or Ang II-induced cardiac fibrosis and dysfunction *in vivo*. HMGA1 knockdown blocked the activation and function of CFs. Furthermore, HMGA1 regulated fibroblast activation and function by promoting the transcription of FOXO1.

In the progression of all types of cardiac injury, such as hypertension, myocardial infarction, or diabetes, activated neurohumoral factor trigger CFs to differentiate into active cardiac myofibroblasts (Burke et al., 2019; Gorski et al., 2019; Huang et al., 2019). Myofibroblasts are widely considered to be the cause of cardiac fibrosis, and their excessive ECM secretion

directly leads to the formation of scar tissue (Leask, 2015). They also express the highly contracted protein α -SMA, collagens, and connective transforming tissue factor (CTGF), which reshape the surrounding ECM. HMGA1 expression is very high during embryogenesis, while it is negligible in normal adult tissues (Reeves, 2001). In our study, we showed that the expression level of HMGA1 was upregulated in CFs after stimulation. The high expression of HMGA1 in the heart seems harmful. We previously revealed that HMGA1 increased cardiomyocyte inflammation in a sepsis-induced cardiomyopathy model (Cai et al., 2020); HMGA1 promotes cardiac dysfunction in diabetic cardiomyopathy (Wu et al., 2020). Consistently, we found that HMGA1 increased fibroblast activation and collagen synthesis, leading to aggregated fibrosis and cardiac dysfunction.

FOXO1 is involved in a broad range of cellular processes, including cell cycle arrest, DNA repair, apoptosis, oxidative stress, and glucose metabolism, as well as fibrosis. During the fibrosis process, FOXO1 is upregulated. TGF- β 1 can promote FOXO1 transcription by activating p300 (Bugyei-Twum et al., 2014). Ang II also promotes the transcriptional activity of FOXO1 and increases FOXO1 activation (Li et al., 2019). During cardiac injury, overloaded neurohumoral factors increase FOXO1 activity, which acts as a pathological factor. FOXO1 directly binds to MMPs and the CTGF gene promoter and increases their transcription (Musikant et al., 2019). Moreover, FOXO1 increases fibroblast activation and proliferation *via* the p21-cell cycling pathway (Xin et al., 2018). The main way to regulate FOXO1 activity is the phosphorylation of Akt at



three different sites (T24, S256, and S319), which inhibits their interaction with DNA and promotes their nuclear export and subsequent degradation by the proteasome (Eijkelenboom and Burgering, 2013). In our study, we found that HMGA1 increased the transcription of FOXO1. Moreover, HMGA1 also increased the nuclear level of FOXO1, further enhancing the transcriptional regulation of FOXO1-targeted genes. Previous studies have reported the relationship of HMGA1 and FOXO1 in many other cell types (Chiefari et al., 2018). HMGA1 increases FOXO1 mRNA and protein expression in cultured HepG2 cells

and hepatocytes by combining with the FOXO1 gene promoter (Arcidiacono et al., 2018). HMGA1 is essential for FOXO1-induced IGFBP1 gene expression and, thus, participates in the insulin-mediated pathway (Chiefari et al., 2018). HMGA1 seems to affect cardiac fibrosis by relying on FOXO1. When we inhibited FOXO1 in both *in vitro* and *in vivo* experiments, the deteriorating effects of HMGA1 were counteracted.

It is worth noting that HMGA1 did not affect the promoter activity of FOXO1 only under physical status (Figure 5D). CFs secrete endogenous TGF- β 1, which induces basal fibroblast

activation. In our study, HMGA1 overexpression or knockdown also did not affect the CF phenotype. We previously reported that HMGA1 could regulate the activity of different transcription factors under different conditions (Cai et al., 2020). Thus, further study about how HMGA1 detaches the promoter region of FOXO1 under physical conditions or under basal levels of TGF β 1 should be explored.

To the best of our knowledge, our study is the first to prove that HMGA1 is dramatically increased in cardiac fibrosis. In cardiac fibrosis, HMGA1 levels are elevated in heart tissues and CFs, related to cardiac fibrosis pathogenesis and cardiac dysfunction. HMGA1 silencing ameliorated aberrant cardiac fibrosis. The regulatory role of HMGA1 in FOXO1 is attributed to its deteriorating effect on cardiac fibrosis. Our studies therefore delineate a novel HMGA1-mediated cardiac fibrosis mechanism and provide new insights into HMGA1-associated therapy in fibrosis disease.

DATA AVAILABILITY STATEMENT

The original contributions presented in the study are included in the article/supplementary material, further inquiries can be directed to the corresponding author/s.

REFERENCES

- Arcidiacono, B., Chiefari, E., Messineo, S., Bilotta, F. L., Pastore, I., Corigliano, D. M., et al. (2018). HMGA1 is a novel transcriptional regulator of the FoxO1 gene. *Endocrine* 60, 56–64. doi: 10.1007/s12020-017-1445-8
- Asbun, J., and Villarreal, F. J. (2006). The pathogenesis of myocardial fibrosis in the setting of diabetic cardiomyopathy. *J. Am. Coll. Cardiol.* 47, 693–700. doi: 10.1016/j.jacc.2005.09.050
- Bao, Q., Zhang, B., Suo, Y., Liu, C., Yang, Q., Zhang, K., et al. (2020). Intermittent hypoxia mediated by TSP1 dependent on STAT3 induces cardiac fibroblast activation and cardiac fibrosis. *eLife* 9:e49923.
- Benjamin, I. J., Jalil, J. E., Tan, L. B., Cho, K., Weber, K. T., and Clark, W. A. (1989). Isoproterenol-induced myocardial fibrosis in relation to myocyte necrosis. *Circ. Res.* 65, 657–670. doi: 10.1161/01.res.65.3.657
- Bugyei-Twum, A., Advani, A., Advani, A., Advani, S. L., Zhang, Y., Thai, K., Kelly, D. J., et al. (2014). High glucose induces Smad activation via the transcriptional coregulator p300 and contributes to cardiac fibrosis and hypertrophy. *Cardiovasc. Diabetol.* 13:89. doi: 10.1186/1475-2840-13-89
- Burke, R. M., Lighthouse, J. K., Mickelsen, D. M., and Small, E. M. (2019). Sacubitril/Valsartan decreases cardiac fibrosis in left ventricle pressure overload by restoring PKG signaling in cardiac fibroblasts. *Circ. Heart Fail.* 12:e005565.
- Cai, Z. L., Shen, B., Yuan, Y., Liu, C., Xie, Q. W., Hu, T. T., et al. (2020). The effect of HMGA1 in LPS-induced myocardial inflammation. *Int. J. Biol. Sci.* 16, 1798–1810. doi: 10.7150/ijbs.39947
- Chiefari, E., Arcidiacono, B., Palmieri, C., Corigliano, D. M., Morittu, V. M., Britti, D., et al. (2018). Cross-talk among HMGA1 and FoxO1 in control of nuclear insulin signaling. *Sci. Rep.* 8:8540.
- Cucoranu, I., Clempus, R., Dikalova, A., Phelan, P. J., Ariyan, S., Dikalov, S., et al. (2005). NAD(P)H oxidase 4 mediates transforming growth factor-beta1-induced differentiation of cardiac fibroblasts into myofibroblasts. *Circ. Res.* 97, 900–907. doi: 10.1161/01.res.0000187457.24338.3d
- Eijkelenboom, A., and Burgering, B. M. (2013). FOXOs: signalling integrators for homeostasis maintenance. *Nat. Rev. Mol. Cell Biol.* 14, 83–97. doi: 10.1038/nrm3507
- Flevaris, P., Khan, S. S., Eren, M., Schuldt, A. J. T., Shah, S. J., Lee, D. C., et al. (2017). Plasminogen activator inhibitor Type I controls cardiomyocyte transforming

ETHICS STATEMENT

The animal study was reviewed and approved by the Institutional Animal Use and Care Committee at the Wuhan University, China.

AUTHOR CONTRIBUTIONS

QW and Q-zT conceived and designed the experiments. YY, ZC, QY, and TH performed the experiments. QX and JZ analyzed the data. QW and QX wrote and revised the manuscript. All authors contributed to the article and approved the submitted version.

FUNDING

This work was supported by grants from the National Natural Science Foundation of China (Nos. 81530012 and 81700353), the Hubei Province's Outstanding Medical Academic Leader Program, and the Fundamental Research Funds of the Central Universities (No. 2042017kf0060).

- growth factor-beta and cardiac fibrosis. *Circulation* 136, 664–679. doi: 10.1161/circulationaha.117.028145
- Gorski, D. J., Petz, A., Reichert, C., Twarock, S., Grandoch, M., and Fischer, J. W. (2019). Cardiac fibroblast activation and hyaluronan synthesis in response to hyperglycemia and diet-induced insulin resistance. *Sci. Rep.* 9:1827.
- Gyongyosi, M., Winkler, J., Ramos, I., Do, Q. T., Firat, H., McDonald, K., et al. (2017). Myocardial fibrosis: biomedical research from bench to bedside. *Eur. J. Heart Fail.* 19, 177–191. doi: 10.1002/ehf.696
- Huang, S., Chen, B., Su, Y., Alex, L., Humeres, C., Shinde, A. V., et al. (2019). Distinct roles of myofibroblast-specific Smad2 and Smad3 signaling in repair and remodeling of the infarcted heart. *J. Mol. Cell Cardiol.* 132, 84–97. doi: 10.1016/j.yjmcc.2019.05.006
- Jiang, X. H., Wu, Q. Q., Xiao, Y., Yuan, Y., Yang, Z., Bian, Z. Y., et al. (2017). Evodiamine prevents Isoproterenol-induced cardiac fibrosis by regulating endothelial-to-Mesenchymal transition. *Planta Med.* 83, 761–769. doi: 10.1055/s-0042-124044
- Johnson, K. R., Lehn, D. A., and Reeves, R. (1989). Alternative processing of mRNAs encoding mammalian chromosomal high-mobility-group proteins HMG-I and HMG-Y. *Mol. Cell Biol.* 9, 2114–2123. doi: 10.1128/mcb.9.5.2114-2123.1989
- Leask, A. (2015). Getting to the heart of the matter: new insights into cardiac fibrosis. *Circ. Res.* 116, 1269–1276. doi: 10.1161/circresaha.116.305381
- Li, S., Zhu, Z., Xue, M., Yi, X., Liang, J., Niu, C., et al. (2019). Fibroblast growth factor 21 protects the heart from angiotensin II-induced cardiac hypertrophy and dysfunction via SIRT1. *Biochim. Biophys. Acta Mol. Basis Dis.* 1865, 1241–1252. doi: 10.1016/j.bbdis.2019.01.019
- Liu, C., Hu, T., Cai, Z., Xie, Q., Yuan, Y., Li, N., et al. (2020). Nucleotide-binding oligomerization domain-like receptor 3 deficiency attenuated Isoproterenol-induced cardiac fibrosis via reactive oxygen species/high mobility group box 1 protein axis. *Front. Cell Dev. Biol.* 8:713. doi: 10.3389/fcell.2020.00713
- Musikant, D., Sato, H., Capobianco, E., White, V., Jawerbaum, A., and Higa, R. (2019). Altered FOXO1 activation in the programming of cardiovascular alterations by maternal diabetes. *Mol. Cell. Endocrinol.* 479, 78–86. doi: 10.1016/j.mce.2018.09.003
- Piras, B. A., Tian, Y., Xu, Y., Thomas, N. A., O'Connor, D. M., and French, B. A. (2016). Systemic injection of AAV9 carrying a periostin promoter targets gene expression to a myofibroblast-like lineage in mouse hearts after reperfused myocardial infarction. *Gene Ther.* 23, 469–478. doi: 10.1038/gt.2016.20

- Reeves, R. (2001). Molecular biology of HMGA proteins: hubs of nuclear function. *Gene* 277, 63–81. doi: 10.1016/s0378-1119(01)00689-8
- Schlueter, C., Hauke, S., Loeschke, S., Wenk, H. H., and Bullerdiek, J. (2005). HMGA1 proteins in human atherosclerotic plaques. *Pathol. Res. Pract.* 201, 101–107. doi: 10.1016/j.prp.2004.11.010
- Sekaran, N. K., Crowley, A. L., de Souza, F. R., Resende, E. S., and Rao, S. V. (2017). The role for cardiovascular remodeling in cardiovascular outcomes. *Curr. Atheroscler. Rep.* 19:23.
- Su, Q., Lv, X., Sun, Y., Yang, H., Ye, Z., and Li, L. (2018). Role of high mobility group A1/nuclear factor-kappa B signaling in coronary microembolization-induced myocardial injury. *Biomed. Pharmacother.* 105, 1164–1171. doi: 10.1016/j.biopha.2018.06.098
- Wu, Q. Q., Liu, C., Cai, Z., Xie, Q., Hu, T., Duan, M., et al. (2020). High-mobility group AT-hook 1 promotes cardiac dysfunction in diabetic cardiomyopathy via autophagy inhibition. *Cell Death Dis.* 11:160.
- Xin, Z., Ma, Z., Hu, W., Jiang, S., Yang, Z., Li, T., et al. (2018). FOXO1/3: Potential suppressors of fibrosis. *Age. Res. Rev.* 41, 42–52. doi: 10.1016/j.arr.2017.11.002
- Zhai, C. G., Xu, Y. Y., Tie, Y. Y., Zhang, Y., Chen, W. Q., Ji, X. P., et al. (2018). DKK3 overexpression attenuates cardiac hypertrophy and fibrosis in an angiotensin-perfused animal model by regulating the ADAM17/ACE2 and GSK-3beta/beta-catenin pathways. *J. Mol. Cell. Cardiol.* 114, 243–252. doi: 10.1016/j.yjmcc.2017.11.018
- Conflict of Interest:** The authors declare that the research was conducted in the absence of any commercial or financial relationships that could be construed as a potential conflict of interest.
- Publisher's Note:** All claims expressed in this article are solely those of the authors and do not necessarily represent those of their affiliated organizations, or those of the publisher, the editors and the reviewers. Any product that may be evaluated in this article, or claim that may be made by its manufacturer, is not guaranteed or endorsed by the publisher.
- Copyright © 2021 Xie, Yao, Hu, Cai, Zhao, Yuan, Wu and Tang. This is an open-access article distributed under the terms of the Creative Commons Attribution License (CC BY). The use, distribution or reproduction in other forums is permitted, provided the original author(s) and the copyright owner(s) are credited and that the original publication in this journal is cited, in accordance with accepted academic practice. No use, distribution or reproduction is permitted which does not comply with these terms.



Distinct Metalloproteinase Expression and Functions in Systemic Sclerosis and Fibrosis: What We Know and the Potential for Intervention

Edwin Leong^{1*}, Michael Bezuhy^{2,3} and Jean S. Marshall^{1,2}

¹ Department of Pathology, Dalhousie University, Halifax, NS, Canada, ² Department of Microbiology and Immunology, Dalhousie University, Halifax, NS, Canada, ³ Department of Surgery, Dalhousie University, Halifax, NS, Canada

OPEN ACCESS

Edited by:

Elvira Forte,
Jackson Laboratory, United States

Reviewed by:

Debora Lo Furno,
Università di Catania, Italy
Stefano Ministrini,
University of Zurich, Switzerland

*Correspondence:

Edwin Leong
edwinleong@dal.ca

Specialty section:

This article was submitted to
Integrative Physiology,
a section of the journal
Frontiers in Physiology

Received: 18 June 2021

Accepted: 09 August 2021

Published: 27 August 2021

Citation:

Leong E, Bezuhy M and
Marshall JS (2021) Distinct
Metalloproteinase Expression
and Functions in Systemic Sclerosis
and Fibrosis: What We Know
and the Potential for Intervention.
Front. Physiol. 12:727451.
doi: 10.3389/fphys.2021.727451

Systemic sclerosis (SSc) is a chronic debilitating idiopathic disorder, characterized by deposition of excessive extracellular matrix (ECM) proteins such as collagen which leads to fibrosis of the skin and other internal organs. During normal tissue repair and remodeling, the accumulation and turnover of ECM proteins are tightly regulated by the interaction of matrix metalloproteinases (MMPs) and endogenous tissue inhibitors of metalloproteinases (TIMPs). SSc is associated with dysregulation of the activity of these proteolytic and inhibitory proteins within the tissue microenvironment, tipping the balance toward fibrosis. The resultant ECM accumulation further perpetuates tissue stiffness and decreased function, contributing to poor clinical outcomes. Understanding the expression and function of these endogenous enzymes and inhibitors within specific tissues is therefore critical to the development of therapies for SSc. This brief review describes recent advances in our understanding of the functions and mechanisms of ECM remodeling by metalloproteinases and their inhibitors in the skin and lungs affected in SSc. It highlights recent progress on potential candidates for intervention and therapeutic approaches for treating SSc fibrosis.

Keywords: fibrosis, systemic sclerosis, metalloproteinase, skin, lung, tissue inhibitors of metalloproteinase, inflammation

INTRODUCTION

Systemic sclerosis (SSc) is a complex chronic disease of unknown etiology, with external environmental factors, genetic predisposition, and epigenetic changes implicated in its development (Mora, 2009; Ramos et al., 2015; Angiolilli et al., 2018). SSc is characterized by persistent immune system activation, changes in vascularization, and excessive extracellular matrix (ECM) accumulation leading to fibrosis. There is considerable heterogeneity of clinical presentations in SSc patients, ranging from Raynaud's phenomenon to severe fibrosis affecting critical organ function in severe cases (Sunderkötter and Riemekasten, 2006; Allanore et al., 2015; Varga et al., 2017). SSc can be classified as "limited" or "diffuse," depending on the extent and progression of disease in the skin, with the latter involving more proximal skin locations and having increased impact on internal organ systems (Sobolewski et al., 2019). Uncontrolled fibrosis can

impair organ function to the point of failure and even death (Varga and Abraham, 2007). Current treatments for SSc are limited with variable clinical response (Allanore et al., 2016; Kowal-Bielecka et al., 2017; Varga et al., 2017), and emerging therapeutics target fundamental fibrotic processes associated with SSc (Daoussis and Lioussis, 2019). Metalloproteinases and their regulators play pivotal roles in mediating fibrosis, making them attractive therapeutic targets in SSc. Given their function in homeostasis, a thorough understanding of their roles in healthy and fibrotic tissues is required to develop safe and effective therapies targeting these pathways.

EXTRACELLULAR MATRIX AND ROLES IN FIBROSIS

Early changes in ECM may provide means for better diagnostic accuracy in fibrotic disease (Abignano and Del Galdo, 2014; Burgstaller et al., 2017). However, clinical disease is often well established prior to diagnosis, reducing opportunities for early intervention. Increased ECM accumulation and matrix stiffness decreases tissue function, promoting further damage and perpetuating fibrosis (Lampi and Reinhart-King, 2018; Santos and Lagares, 2018). ECM accumulation and stiffness relay mechanical cues, initiate mechanosensory responses (Herrera et al., 2018; Tschumperlin et al., 2018), and provide major reservoirs for latent TGF- β (Annes et al., 2003; Xu et al., 2018) that is activated by conformational changes to further promote pro-fibrotic processes (Annes et al., 2004; Wipff et al., 2007). Myofibroblasts, a major source of ECM proteins, receive sustained survival and differentiation signals from matrix stiffness (Lagares et al., 2017; Van Caam et al., 2018). Further consequences include reduced nutrient diffusion, hypoxia, and epigenetic modifications of local cell populations (Beyer et al., 2009; Liu et al., 2010; Parker et al., 2014). These can change myofibroblast phenotypes by inducing transcription factor activity (Dupont et al., 2011; Dupont, 2019), specific microRNAs, and DNA methylation processes causing sustained cellular activation independent of the initial insult (Orphanides et al., 1997; Corpechot, 2002; Wang et al., 2006; Altork et al., 2015). Together, these interactions drive multiple amplifying loops, further promoting cellular activation and enhanced ECM deposition (**Figure 1**). Thus, matrix stiffness caused by ECM accumulation needs to be tightly regulated to allow normal tissue remodeling and prevent pathologic fibrosis.

MATRIX METALLOPROTEINASES AND THEIR INHIBITORS

Matrix stiffness is determined by a balance between ECM breakdown and accumulation, with the latter more significant in SSc (Varga and Bashey, 1995). Two main classes of mediators involved in this balance are matrix metalloproteinases (MMPs) and tissue inhibitors of metalloproteinases (TIMPs) (Nagase et al., 2006). Currently, there are 24 known MMPs in humans which are categorized based on their preferred

substrates such as collagenases (MMP1, 8, 13) and gelatinases (MMP2, MMP9) (Loffek et al., 2011). TIMPs are the natural inhibitors of MMPs and classically inhibit ECM degradation (Brew and Nagase, 2010).

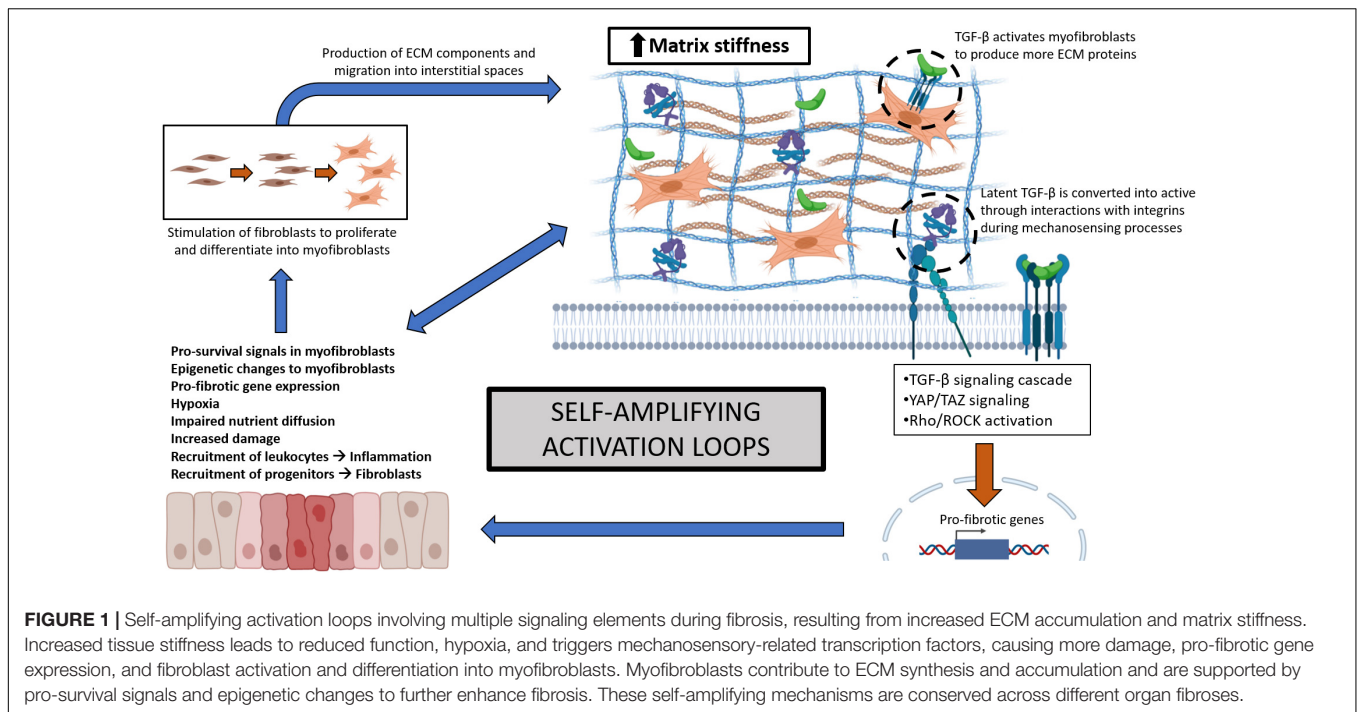
Current disease models suggest that increasing active MMPs and downregulating TIMPs would be beneficial to facilitate proper tissue remodeling and restoration of tissue homeostasis; however, MMPs and TIMPs have physiological implications beyond tissue remodeling (Giannandrea and Parks, 2014) including facilitating inflammation through cellular trafficking, immune cell activation, regulation of cytokines, chemokines, and activity of other MMPs (Nagase et al., 2006; Gaffney et al., 2015). The expression of MMPs is also cell- and tissue-specific and temporally regulated by immune and stromal cells, further adding to the complexity of this system (Pardo and Selman, 2006; Chuang et al., 2019). Finally, MMP functions depend on tissue and disease context (Loffek et al., 2011), and have both pro- and anti-fibrotic effects. To this end, global upregulation of MMPs and downregulation of TIMPs is ineffective in overcoming excessive ECM accumulation. Manipulation of this system requires an understanding of interactions between expressed MMPs and TIMPs within specific organs at specific stages of disease progression to be effective.

METALLOPROTEINASES IN SSC SERUM

Analysis of specific MMPs and TIMPs in the serum of SSc patients suggests possible influences on outcomes in different tissues. MMP7 was increased in SSc patients with considerably higher levels of observable lung fibrosis compared to healthy individuals (Moinzadeh et al., 2011). In contrast, MMP13 was reduced in serum from local and diffuse SSc patients compared to normal controls, with reductions reflecting greater tissue involvement and lung fibrosis (Asano et al., 2006a,b). Adding to the complexity, MMP9 was found increased in serum and tears of SSc patients along with increased TIMP-2, supporting a negative role for these mediators (Waszczykowska et al., 2020). Autoantibodies against MMP3 have been detected in SSc patients, and MMP3 considered beneficial as inhibition is suggested to reduce ECM degradation (Nishijima et al., 2004). It is evident that distinct MMPs may have multifaceted roles in ECM turnover and while MMP-TIMP expression in serum samples serve as potential biomarkers of SSc prognosis, involvement in organ fibrosis is likely far more complex than data on general upregulation or downregulation might suggest.

METALLOPROTEINASES IN SKIN FIBROSIS

The MMP profile in skin tissue is limited and while well-studied in skin pathologies such as wound healing (Kähäri and Saarialho-Kere, 1997; Caley et al., 2015; Nguyen et al., 2016), less is known about their roles in fibrotic cutaneous disorders such as SSc. Skin involvement is present in both milder and severe forms of SSc and there is increased ECM deposition in the skin during fibrosis



progression. A positive correlation is observed between presence of abnormal subtypes of collagen with disease stage and dermal thickness scores (Martin et al., 2012).

Significantly reduced levels of interstitial collagenase MMP1 expression have been found in biopsies of involved skin in a cohort of SSc patients (Frost et al., 2012). This was corroborated by other studies showing markedly reduced MMP1 gene expression and protein levels in dermal fibroblasts isolated from SSc patient skin. Several microRNAs increased in serum and skin of SSc patients were observed to downregulate MMP1 expression (Sing et al., 2012; Zhou et al., 2017). Peripheral blood mononuclear cells from SSc patients produced cytokines and growth factors in response to soluble type 1 collagen *in vitro* that elicited reduced MMP1 production by SSc dermal fibroblasts (Brown et al., 2012), pointing to additional forms of MMP1 regulation. CXCL17, a chemokine implicated in several tissue remodeling and antimicrobial processes, was found reduced in SSc skin and can regulate type 1 collagen expression by MMP1-associated mechanisms (Shimada et al., 2020). Local CXCL17 injections ameliorated fibrotic outcomes in a murine model of bleomycin (BLM)-induced skin fibrosis and CXCL17 treatment reduced type 1 collagen protein while increasing gene and protein expression of MMP1 in healthy human dermal fibroblasts.

MMP3, crucial for inhibition of pro-fibrotic $\alpha 2$ -antiplasmin and ECM deposition, was decreased in SSc fibroblasts (Niwa et al., 2020). MMP3-stimulated SSc fibroblasts decreased α -SMA expression and type 1 collagen production. Given that collagenases function to breakdown ECM materials, in theory increasing skin-specific MMPs and reducing TIMPs should ameliorate fibrosis. However, this is not always the case. Increased MMP9 production was found in SSc patient dermal fibroblasts, positively correlating with the extent of SSc skin pathology

(Kim et al., 2005) and likely due to MMP9 activities independent of ECM degradation, including regulation of inflammatory cytokines and growth factors (Van Den Steen et al., 2002). MMP9 degrades ECM but also other important non-cellular components that maintain effective barriers within the SSc skin microenvironment. A combination of barrier dysfunction and enhanced inflammatory and pro-fibrotic growth factors can enable an influx of immune cells, perpetuating inflammation and established fibrosis (Yu and Stamenkovic, 2000; Kim et al., 2005).

Along with dysregulation of MMPs, TIMPs are reported to be elevated in SSc skin. Fibroblasts derived from SSc biopsies demonstrated increased TIMP-1 compared to those from control skin (Kikuchi et al., 1997). Thus, reducing production of this inhibitor may be beneficial in SSc. The production of TIMP-1 by SSc dermal fibroblasts was reduced when treated with microRNA-29a, associated with increased MMP1 production (Ciechomska et al., 2014). Taken together, modulating the MMP-TIMP balance could potentially reverse the SSc fibroblast phenotype and offer therapeutic opportunities for treatment of skin fibrosis. However, considering the complex expression patterns of metalloproteinases and inhibitors in SSc patient skin, anti-fibrotic strategies involving ECM degradation by MMPs require further clinical study.

In non-SSc fibrotic conditions such as hypertrophic scarring, MMP3 and MMP8 are increased with TIMP members while other classical MMPs decreased. Several MMP-deficient strains of mice have been reported to have little change in phenotype, pointing toward functional redundancy between members of this family (Loffek et al., 2011). However, skin wound healing studies have shown MMP13 promotes rapid collagen remodeling and fibroblast survival, resulting in effective and scarless healing (Toriseva et al., 2007). MMP14-deficient mice demonstrate

insufficient collagen turnover leading to connective tissue pathologies (Holmbeck et al., 1999), indicating that functions of MMP14 may not be readily compensated for by others. Using the BLM-induced skin fibrosis model (Yamamoto et al., 1999), MMP14-deficient mice exhibited significant accumulation of type 1 collagen in the skin but without changes to collagen synthesis (Zigrino et al., 2016), and fibroblasts from their skin showed impaired MMP2 activation. Therefore, MMP14 may be particularly important in degrading dermal ECM components and regulation of other MMPs. Taken together, these studies support studying these MMPs as targets for therapy in SSc skin.

METALLOPROTEINASES IN LUNG FIBROSIS

The lungs are a major affected organ, where SSc manifests as interstitial lung disease (ILD) characterized by extensive fibrosis, leading to decreased functional capacity and even death (Cottin and Brown, 2019). Aberrant expression of MMPs have been reported, but with functions seemingly contrary to their classical ECM proteolytic activities. In multiple studies, elevated MMP7 serum levels have shown a negative correlation with lung function parameters such as forced vital capacity and associated with advanced stages of SSc. These observations suggest that MMP7 may, directly or indirectly, contribute to lung fibrosis, and may serve as a biomarker for SSc progression (Moinzadeh et al., 2011; Stock et al., 2019; Abo Gabal et al., 2020). In bronchoalveolar lavage fluid (BALF) of SSc patients with ILD, MMP9 levels were elevated compared to healthy controls, suggesting involvement in the persistence of inflammatory processes (Andersen et al., 2007). MMP12 is increased in serum and lung tissues of SSc patients with ILD and positively correlates with lung fibrosis severity. MMP12 expression was abundant in regions of thickened alveolar septa and expressed by alveolar macrophages and fibroblasts residing in fibrotic lung compartments (Manetti et al., 2012). A specific MMP12 polymorphism was also found to increase susceptibility to SSc and ILD in a cohort of SSc patients compared to healthy individuals (Manetti et al., 2010; Assassi et al., 2013). While MMP12 functions in SSc-ILD have not been defined, MMP12 downregulated expression of collagenase MMP13 in a *Schistosoma mansoni* Th2-driven model of lung fibrosis (Madala et al., 2010), providing a crucial example of MMP-dependent regulation of other metalloproteinases. Notably, serum MMP13 levels were lower in a subset of SSc patients compared to healthy controls, and reductions associated with significantly greater frequency of reduced vital capacity (Asano et al., 2006b). This suggests that MMP13 is associated with ECM remodeling and deficiency enhances lung fibrosis.

Matrix metalloproteinases have also been examined in idiopathic lung fibrosis (IPF)—another debilitating form of lung pathology arising from aberrant ECM deposition and remodeling. While there are differences between SSc-ILD and IPF, there are notable similarities particularly during the end-stages of the diseases (Herzog et al., 2014). These include signaling arising from injurious stimuli leading to pro-fibrotic events, and a pro-fibrotic phenotypic shift of pulmonary

fibroblasts in response to ECM composition containing collagen, tenascin-C, and mechanical cues resulting from increased tissue stiffness (Brissett et al., 2012; Herzog et al., 2014).

Idiopathic lung fibrosis patient BALF show increased expression of MMPs, with MMP7, MMP8, and MMP9 predominating (Dancer et al., 2011). MMP7 is highly upregulated and activated in IPF patient lungs (Zuo et al., 2002; Fujishima et al., 2010), and is the most upregulated gene encoding for proteins involved in ECM remodeling. MMP7 can promote fibrosis in the early phases by inducing epithelial cell damage but have immunosuppressive and anti-fibrotic potential in persistent fibrotic lung environments in longer-term studies in MMP7-deficient animals (Li et al., 2002; Zuo et al., 2002; Manicone et al., 2009), highlighting disease stage influence on MMP7 involvement. MMP8 can act indirectly to enhance lung fibrosis by cleaving anti-inflammatory IL-10, an inhibitor of TGF- β , maintaining a pro-fibrotic environment (García-Prieto et al., 2010). Increased MMP8 expression was found in IPF patient BALF (Henry et al., 2002; Stijn et al., 2013; Craig et al., 2014) and others have shown MMP8 associated with significant reductions in CXCL10, reported to be anti-fibrotic in lungs (Marie Burdick et al., 1999; Tager et al., 2004; Jiang et al., 2010) by inhibiting lung fibroblast migration and differentiation into myofibroblasts (Craig et al., 2013). MMP3 is upregulated in IPF patients compared to healthy control lungs (Yamashita et al., 2011). MMP3-deficient mice exhibited reduced fibrosis in response to BLM and exogenous recombinant MMP3 promoted pro-fibrotic phenotypes. Further assessments found correlations between increased MMP3 and a collagenolytic by-product endostatin (Heljasvaara et al., 2005), which induces lung epithelial cell apoptosis (Richter et al., 2009) and thus promotes fibrosis.

Despite having pro-fibrotic roles in lungs as described above, specific MMPs show anti-fibrotic functions. Contrary to SSc-ILD, active MMP13 is increased in whole lung samples of IPF patients (Nkyimbeng et al., 2013). In IPF rodent models, MMP13-deficiency demonstrated exacerbated inflammatory responses to lung injury (Sen et al., 2010) and BLM-induced lung fibrosis, associated with increased leukocytic infiltration such as neutrophils (Nkyimbeng et al., 2013) and macrophages (Cabrera et al., 2019). Additionally, MMP13-deficient lung tissues had higher collagen staining and hydroxyproline content. Others showed MMP13-deficient mice having delayed resolution of lung fibrosis through decreased collagenolytic activity (Cabrera et al., 2019). Similarly, MMP19 is increased in IPF patients, and considered indicative of a tissue repair response (Yu et al., 2012). MMP19-deficient mice showed increased α -SMA staining and collagen deposition, possibly exerting its anti-fibrotic effects by mediating expression of cyclo-oxygenase 2 to suppress fibrosis by regulation of fibroblast proliferation and collagen synthesis (Wilborn et al., 1995; Pomianowska et al., 2014; Zhao et al., 2016). Thus, MMP19 may be an important anti-fibrotic metalloproteinase in the lungs through regulation of ECM deposition. MMP9 is classically pro-fibrotic (Kobayashi et al., 2014) and is increased in IPF patient BALF (Henry et al., 2002). However, significant anti-fibrotic activity was shown in a mouse model overexpressing human MMP9 in alveolar macrophages (Cabrera et al., 2007), potentially linked to inhibition of fibroblast

growth (Valentinis et al., 1995). Appropriate regulation of cell growth, repair, and apoptosis were proposed to ameliorate the lung fibrosis in this model.

MMPs IN OTHER SSc-ASSOCIATED ORGAN SYSTEMS

While cardiac, gastrointestinal (GI), and renal organ systems are involved in SSc, MMPs have not been directly studied in such clinical tissues. SSc cardiac complications range from ventricular dysfunction to infarction (Lambova, 2014), resulting in tissue damage and ensuing fibrosis (Tzelepis et al., 2007). In murine models, MMP-1 attenuated cardiac fibrosis development (Foronjy et al., 2008), but MMP-2 promoted ventricular remodeling, leading to failure-associated phenotypes (Bergman et al., 2007). MMP-12 induced production of TGF- β and platelet-derived growth factor, promoting accumulation of macrophage populations involved in fibrotic mechanisms (Stawski et al., 2014). GI manifestations are common in SSc patients, which can lead to fibrosis and ensuing motility and functional aberrations (Sallam et al., 2006; McFarlane et al., 2018). GI MMPs have not been directly studied in SSc, but have important functions in several intestinal inflammatory disorders (Medina and Radomski, 2006; O'Sullivan et al., 2015). While many point

toward detrimental MMP functions during inflammation, one study has shown inhibited MMP synthesis can lead to excessive collagen deposition in fibrotic intestinal muscles (Bailey et al., 2012). Kidney involvement is also prevalent in SSc patients, leading to scleroderma renal crisis (SRC), promoted by interstitial fibrosis amongst other risk factors (Steen, 2014; Chrabaszcz et al., 2020). Direct MMP involvement in SSc-associated renal fibrosis has not been identified, but numerous studies imply a detrimental role of MMPs in early stages of kidney diseases with ECM-degradative features in later stages during scarring and fibrosis (Ke et al., 2017; Zakiyanov et al., 2019). Upregulated peptides in renal pathologies such as angiotensin-II promote renal fibrosis and regulate MMP expression, further affecting remodeling processes (Solini et al., 2011; Pushpakumar et al., 2013).

MMPs AS THERAPEUTIC TARGETS FOR FIBROSIS AND SSc: WHERE ARE WE CURRENTLY?

As outlined above, MMPs demonstrate tissue-dependent and disease-specific expression and functions (summarized in **Table 1**). Clinical translation of broad-spectrum MMP inhibitors

TABLE 1 | Summary table of selected MMPs with therapeutic potential for targeting in SSc skin and lungs to improve fibrosis and ECM accumulation.

| MMP | Skin | Possible function / mechanism in the skin |
|-------|---|---|
| Mmp1 | SSc | Decreased; Collagen breakdown Frost et al. (2012); Sing et al. (2012); Zhou et al. (2017) |
| Mmp3 | SSc | Decreased; Decreased α -SMA and type 1 collagen production Niwa et al. (2020) |
| Mmp9 | SSc | Increased; Regulation of inflammatory cytokines and growth factors; Degrades non-cellular components of the skin barrier, leading to increased infiltration of inflammatory cell Kim et al. (2005) |
| Mmp13 | Wound healing | Rapid collagen remodeling Toriseva et al. (2007) |
| Mmp14 | BLM-induced skin fibrosis | Knockouts show significant type 1 collagen accumulation in skin, and impaired Mmp2 activation Holmbeck et al. (1999); Zigrino et al. (2016) |
| MMP | Lung | Possible function / mechanism in the lungs |
| Mmp3 | IPF | Increased and produces endostatin, a by-product that increases lung epithelial cell death; Knockout mice have less lung fibrosis Heljasvaara et al. (2005); Richter et al. (2009); Yamashita et al. (2011) |
| Mmp7 | SSc-ILD IPF | Increased; Not defined Moinszadeh et al. (2011); Stock et al. (2019); Abo Gabal et al. (2020) Increased in BALF; Associated with epithelial cell damage and neutrophil recruitment in early stages, but associated with immunosuppressive dendritic cell recruitment in late stages Li et al. (2002); Zuo et al. (2002); Manicone et al. (2009); Fujishima et al. (2010) |
| Mmp8 | IPF | Increased in BALF; Cleaves IL-10, a suppressor of TGF- β synthesis; decreased CXCL10 Wilborn et al. (1995); Henry et al. (2002); Tager et al. (2004); Garcia-Prieto et al. (2010); Jiang et al. (2010); Dancer et al. (2011); Craig et al. (2013, 2014); Stijn et al. (2013) |
| Mmp9 | SSc-ILD IPF | Increased; Involved in persistence of inflammatory processes Andersen et al. (2007); Dancer et al. (2011) Increased in BALF; Overexpression in alveolar macrophages in mice showed anti-fibrotic activity via regulation of fibroblast growth Valentinis et al. (1995); Henry et al. (2002); Cabrera et al. (2007); Kobayashi et al. (2014) |
| Mmp12 | SSc-ILD <i>Schistosoma mansoni</i> lung fibrosis | Increased; Not defined Manetti et al. (2010, 2012); Assassi et al. (2013) Knockouts show increased fibrosis and decreased Mmp13 collagenase Madala et al. (2010) |
| Mmp13 | IPF | Increased in whole lung; Knockouts have decreased collagenolytic activity and higher collagen levels Asano et al. (2006a); Sen et al. (2010); Nkyimbeng et al. (2013); Cabrera et al. (2019) |
| Mmp19 | IPF | Increased in IPF patients, but indicative of tissue repair; Knockouts show increased collagen deposition, and may act through regulation of cyclo-oxygenase 2 expression Wilborn et al. (1995); Yu et al. (2012); Pomianowska et al. (2014); Zhao et al. (2016) |

Described roles in other similar types of pathology and disease are also given, with mechanisms that may be translatable to SSc pathology in the skin and lungs.

(MMPs) have been largely unsuccessful despite success in some experimental models (de Meijer et al., 2010), likely due to beneficial MMP functions in homeostasis and immunity (Vandenbroucke and Libert, 2014). This is evidenced by discontinuation of poorly selective MMPs in anti-cancer clinical trials due to adverse responses (Fields, 2019) and lack of MMP-based trials in SSc-ILD (Khanna et al., 2019). Cross-regulation of MMP members further add to the unpredictable impact of MMPs. Novel methods for targeting metalloproteinases are necessary, with increased specificity and localized delivery to fibrotic sites. Developing selective synthetic peptides to block catalytic functions, targeting unique MMP domains to alter function, or manipulating endogenous MMP regulators like microRNAs represent some potential avenues of investigation (Li and Li, 2013; Mohan et al., 2016), serving as basis for novel proposed clinical trials in SSc skin (ClinicalTrials.gov identifier #NCT03740724). New treatment modalities should consider temporal regulation of MMPs and stages of disease in which they are active. Together, new classes of MMPs with improved disease models will help our understanding of MMP profiles observed in fibrotic conditions such as in SSc.

From what is currently known regarding MMPs in skin and lungs of SSc patients, there are likely two main functions of MMPs, first as mediators of inflammation and tissue damage, and second as contributors to ECM remodeling. As previously mentioned, collagenases like MMP1 and MMP3 are reduced in settings of greater SSc skin fibrosis, and experimental models suggest that increasing their levels or activity may have beneficial effects. Conversely, inhibiting others like MMP9 could be beneficial to ameliorate pro-inflammatory triggers of SSc progression. The functions of MMP13 and MMP14 in promoting wound healing may also warrant further investigation in the context of SSc. In SSc-ILD, MMP7, 8, 9, and 12 seem to primarily exacerbate the disease rather than degrade ECM and may justify targeting them for local inhibition. Temporally regulating MMP expression or activity during different disease stages has merit, as demonstrated in the delayed resolution of IPF in MMP13-deficient. Future research should involve detailed human studies which consider disease stage and tissue site when examining the

activities of specific MMPs. Without such information, there is a considerable risk of off-target effects of targeting MMPs.

CONCLUDING REMARKS

Currently, therapeutics targeting regulation of MMP-TIMP balance in SSc have not successfully translated into clinical settings despite considerable effectiveness in pre-clinical models, with a lack of ongoing clinical trials. From previous and current studies, it is evident that MMPs and TIMPs have multiple roles which may either promote or inhibit fibrosis. Moreover, the complex cross-regulation of these molecules necessitates looking at the MMP-TIMP axis as a network rather than individually in the context of disease. The expression of MMPs and TIMPs are highly dependent on inciting stimulus, tissue site, and disease stage, amongst others. To this end, any therapeutic targeting metalloproteinases should be tailored to take these factors into account. Despite the challenges, there remains considerable potential in targeting specific MMP functions as part of a combinatorial treatment regime to target the inflammatory and/or tissue remodeling phases in fibrotic disease, improving the lives of thousands of patients each year.

AUTHOR CONTRIBUTIONS

EL drafted and wrote the manuscript and figures. MB and JM provided guidance, editing, and support with the manuscript. All authors provided conceptual input and reviewed the final manuscript.

FUNDING

EL is the recipient of a DMRF-I3V graduate studentship funded by Dalhousie Medical Research Foundation. This work is supported by the Canadian Institutes of Health Research Grant #THC135230.

REFERENCES

- Abignano, G., and Del Galdo, F. (2014). Quantitating skin fibrosis: innovative strategies and their clinical implications topical collection on scleroderma. *Curr. Rheumatol. Rep.* 16:404.
- Abo Gabal, M. M., Shedid, N. H., Mohamed, E. S., Abdelfattah, W., and Mohamed, S. (2020). The relationship between serum level of matrix metalloproteinase-7 and interstitial lung disease in patients with systemic sclerosis. *Egypt. J. Intern. Med.* 314, 720–725.
- Allanore, Y., Matucci-Cerinic, M., and Distler, O. (2016). Treatment of systemic sclerosis: is there any hope for the future? *RMD Open* 2:e000260. doi: 10.1136/rmdopen-2016-000260
- Allanore, Y., Simms, R., Distler, O., Trojanowska, M., Pope, J., Denton, C. P., et al. (2015). Systemic sclerosis. *Nat. Rev. Dis. Primers* 1:15002.
- Altork, N., Tsou, P. S., Coit, P., Khanna, D., and Sawalha, A. H. (2015). Genome-wide DNA methylation analysis in dermal fibroblasts from patients with diffuse and limited systemic sclerosis reveals common and subset-specific DNA methylation aberrancies. *Ann. Rheum. Dis.* 74, 1612–1620. doi: 10.1136/annrheumdis-2014-205303
- Andersen, G. N., Nilsson, K., Pourazar, J., Hackett, T. L., Kazzam, E., Blomberg, A., et al. (2007). Bronchoalveolar matrix metalloproteinase 9 relates to restrictive lung function impairment in systemic sclerosis. *Respir. Med.* 101, 2199–2206. doi: 10.1016/j.rmed.2007.04.019
- Angiolilli, C., Marut, W., van der Kroef, M., Chouri, E., Reedquist, K. A., and Radstake, T. R. D. J. (2018). New insights into the genetics and epigenetics of systemic sclerosis. *Nat. Rev. Rheumatol.* 14, 657–673.
- Annes, J. P., Chen, Y., Munger, J. S., and Rifkin, D. B. (2004). Integrin $\alpha\beta6$ -mediated activation of latent TGF- β requires the latent TGF- β binding protein-1. *J. Cell Biol.* 165, 723–734. doi: 10.1083/jcb.200312172
- Annes, J. P., Munger, J. S., and Rifkin, D. B. (2003). Making sense of latent TGF β activation. *J. Cell Sci.* 116, 217–224. doi: 10.1242/jcs.00229
- Asano, Y., Ihn, H., Kubo, M., Jinnin, M., Mimura, Y., Ashida, R., et al. (2006a). Clinical significance of serum levels of matrix metalloproteinase-13 in patients with systemic sclerosis. *Rheumatology* 45, 303–307. doi: 10.1093/rheumatology/kei143
- Asano, Y., Ihn, H., Kubo, M., Jinnin, M., Mimura, Y., Ashida, R., et al. (2006b). Clinical significance of serum matrix metalloproteinase-13 levels in patients with localized scleroderma. *Clin. Exp. Rheumatol.* 24, 394–399.

- Assassi, S., Radstake, T. R. D. J., Mayes, M. D., and Martin, J. (2013). Genetics of scleroderma: implications for personalized medicine? *BMC Med.* 11:9. doi: 10.1186/1741-7015-11-9
- Bailey, J. R., Bland, P. W., Tarlton, J. F., Peters, I., Moorghen, M., Sylvester, P. A., et al. (2012). IL-13 promotes collagen accumulation in Crohn's disease fibrosis by down-regulation of fibroblast MMP synthesis: a role for innate lymphoid cells? *PLoS One* 7:e52332. doi: 10.1371/journal.pone.0052332
- Bergman, M. R., Teerlink, J. R., Mahimkar, R., Li, L., Zhu, B.-Q., Nguyen, A., et al. (2007). Cardiac matrix metalloproteinase-2 expression independently induces marked ventricular remodeling and systolic dysfunction. *Am. J. Physiol. Hear. Circ. Physiol.* 292, 1847–1860.
- Beyer, C., Schett, G., Gay, S., Distler, O., and Distler, J. H. W. (2009). Hypoxia. Hypoxia in the pathogenesis of systemic sclerosis. *Arthritis Res. Ther.* 11:220. doi: 10.1186/ar2598
- Brew, K., and Nagase, H. (2010). The tissue inhibitors of metalloproteinases (TIMPs): an ancient family with structural and functional diversity. *Biochim. Biophys. Acta Mol. Cell Res.* 1803, 55–71. doi: 10.1016/j.bbamcr.2010.01.003
- Brissett, M., Veraldi, K. L., Pilewski, J. M., Medsger, T. A., and Feghali-Bostwick, C. A. (2012). Localized expression of tenascin in systemic sclerosis-associated pulmonary fibrosis and its regulation by insulin-like growth factor binding protein 3. *Arthritis Rheum.* 64, 272–280. doi: 10.1002/art.30647
- Brown, M., Postlethwaite, A. E., Myers, L. K., and Hasty, K. A. (2012). Supernatants from culture of type I collagen-stimulated PBMC from patients with cutaneous systemic sclerosis versus localized scleroderma demonstrate suppression of MMP-1 by fibroblasts. *Clin. Rheumatol.* 31, 973–981. doi: 10.1007/s10067-012-1962-z
- Burgstaller, G., Oehrlé, B., Gerckens, M., White, E. S., Schiller, H. B., and Eickelberg, O. (2017). The instructive extracellular matrix of the lung: basic composition and alterations in chronic lung disease. *Eur. Respir. J.* 50:1601805. doi: 10.1183/13993003.01805-2016
- Cabrera, S., Gaxiola, M., Arreola, J. L., Ramírez, R., Jara, P., D'Armiento, J., et al. (2007). Overexpression of MMP9 in macrophages attenuates pulmonary fibrosis induced by bleomycin. *Int. J. Biochem. Cell Biol.* 39, 2324–2338. doi: 10.1016/j.biocel.2007.06.022
- Cabrera, S., Maciel, M., Hernández-Barrionto, D., Calyca, J., Gaxiola, M., Selman, M., et al. (2019). Delayed resolution of bleomycin-induced pulmonary fibrosis in absence of MMP13 (collagenase 3). *J. Physiol. Lung Cell. Mol. Physiol.* 316, 961–976.
- Caley, M. P., Martins, V. L. C., and O'Toole, E. A. (2015). Metalloproteinases and wound healing. *Adv. Wound Care* 4, 225–234. doi: 10.1089/wound.2014.0581
- Chrabaszcz, M., Małyszko, J., Sikora, M., Alda-Malicka, R., Stochmal, A., Matuszkiewicz-Rowska, J., et al. (2020). Renal involvement in systemic sclerosis: an update. *Kidney Blood Press. Res.* 45, 532–548.
- Chuang, H. M., Chen, Y. S., and Harn, H. J. (2019). The versatile role of matrix metalloproteinase for the diverse results of fibrosis treatment. *Molecules* 24:4188. doi: 10.3390/molecules24224188
- Ciechomska, M., O'Reilly, S., Suwara, M., Bogunia-Kubik, K., and Van Laar, J. M. (2014). MiR-29a reduces TIMP-1 production by dermal fibroblasts via targeting TGF- β activated kinase 1 binding protein 1, implications for systemic sclerosis. *PLoS One* 9:e115596. doi: 10.1371/journal.pone.0115596
- Corpechot, C. (2002). Hypoxia-induced VEGF and collagen I expressions are associated with angiogenesis and fibrogenesis in experimental cirrhosis. *Hepatology* 35, 1010–1021. doi: 10.1053/jhep.2002.32524
- Cottin, V., and Brown, K. K. (2019). Interstitial lung disease associated with systemic sclerosis (SSc-ILD). *Respir. Res.* 20:13.
- Craig, V. J., Polverino, F., Lauchó-Contreras, M. E., Shi, Y., Liu, Y., Osorio, J. C., et al. (2014). Mononuclear phagocytes and airway epithelial cells: novel sources of matrix metalloproteinase-8 (MMP-8) in patients with idiopathic pulmonary fibrosis. *PLoS One* 9:e97485. doi: 10.1371/journal.pone.0097485
- Craig, V. J., Quintero, P. A., Fyfe, S. E., Patel, A. S., Knolle, M. D., Kobzik, L., et al. (2013). Profibrotic activities for matrix metalloproteinase-8 during bleomycin-mediated lung injury. *J. Immunol.* 190, 4283–4296. doi: 10.4049/jimmunol.1201043
- Dancer, R. C. A., Wood, A. M., and Thickett, D. R. (2011). Metalloproteinases in idiopathic pulmonary fibrosis. *Eur. Respir. J.* 38, 1461–1467.
- Daoussis, D., and Lioussis, S.-N. (2019). Treatment of systemic sclerosis associated fibrotic manifestations: current options and future directions. *Mediterr. J. Rheumatol.* 30, 33–37. doi: 10.31138/mjr.30.1.33
- de Meijer, V. E., Sverdlow, D. Y., Popov, Y., Le, H. D., Meisel, J. A., Nosé, V., et al. (2010). Broad-spectrum matrix metalloproteinase inhibition curbs inflammation and liver injury but aggravates experimental liver fibrosis in mice. *PLoS One* 5:e11256. doi: 10.1371/journal.pone.0011256
- Dupont, S. (2019). Regulation of YAP/TAZ activity by mechanical cues: an experimental overview. *Methods Mol. Biol.* 1893, 183–202. doi: 10.1007/978-1-4939-8910-2_15
- Dupont, S., Morsut, L., Aragona, M., Enzo, E., Giullitti, S., Cordenonsi, M., et al. (2011). Role of YAP/TAZ in mechanotransduction. *Nature* 474, 179–184.
- Fields, G. B. (2019). The rebirth of matrix metalloproteinase inhibitors: moving beyond the dogma. *Cells* 8:984. doi: 10.3390/cells8090984
- Foronjy, R. F., Sun, J., Lemaitre, V., and d'Armiento, J. M. (2008). Transgenic expression of matrix metalloproteinase-1 inhibits myocardial fibrosis and prevents the transition to heart failure in a pressure overload mouse model. *Hypertens. Res.* 31, 725–735. doi: 10.1291/hyres.31.725
- Frost, J., Ramsay, M., Mia, R., Moosa, L., Musenge, E., and Tikly, M. (2012). Differential gene expression of MMP-1, TIMP-1 and HGF in clinically involved and uninvolved skin in South Africans with SSc. *Rheumatology* 51, 1049–1052. doi: 10.1093/rheumatology/ker367
- Fujishima, S., Shiomi, T., Yamashita, S., Yogo, Y., Nakano, Y., Inoue, T., et al. (2010). Production and activation of matrix metalloproteinase 7 (matrilysin 1) in the lungs of patients with idiopathic pulmonary fibrosis. *Arch. Pathol. Lab. Med.* 134, 1136–1142. doi: 10.5858/2009-0144-0a.1
- Gaffney, J., Solomonov, I., Zehorai, E., and Sagi, I. (2015). Multilevel regulation of matrix metalloproteinases in tissue homeostasis indicates their molecular specificity in vivo. *Matrix Biol.* 44–46, 191–199. doi: 10.1016/j.matbio.2015.01.012
- García-Prieto, E., González-López, A., Cabrera, S., Astudillo, A., Gutiérrez-Fernández, A., and Fanjul-Fernández, M. (2010). Resistance to bleomycin-induced lung fibrosis in MMP-8 deficient mice is mediated by interleukin-10. *PLoS One* 5:e13242. doi: 10.1371/journal.pone.0013242
- Giannandrea, M., and Parks, W. C. (2014). Diverse functions of matrix metalloproteinases during fibrosis. *DMM Dis. Model. Mech.* 7, 193–203. doi: 10.1242/dmm.012062
- Heljasvaara, R., Nyberg, P., Luostarinen, J., Parikka, M., Heikkilä, P., Rehn, M., et al. (2005). Generation of biologically active endostatin fragments from human collagen XVIII by distinct matrix metalloproteinases. *Exp. Cell Res.* 307, 292–304. doi: 10.1016/j.yexcr.2005.03.021
- Henry, M. T., McMahon, K., Mackarel, A. J., Prikk, K., Sorsa, T., Maisi, P., et al. (2002). Matrix metalloproteinases and tissue inhibitor of metalloproteinase-1 in sarcoidosis and IPF. *Eur. Respir. J.* 20, 1220–1227. doi: 10.1183/09031936.02.00022302
- Herrera, J., Henke, C. A., and Bitterman, P. B. (2018). Extracellular matrix as a driver of progressive fibrosis. *J. Clin. Invest.* 128, 45–53. doi: 10.1172/jci93557
- Herzog, E. L., Mathur, A., Tager, A. M., Feghali-Bostwick, C., Schneider, F., and Varga, J. (2014). Interstitial lung disease associated with systemic sclerosis and idiopathic pulmonary fibrosis: how similar and distinct? *Arthritis Rheumatol.* 66, 1967–1978. doi: 10.1002/art.38702
- Holmbeck, K., Bianco, P., Caterina, J., Yamada, S., Kromer, M., Kuznetsov, S. A., et al. (1999). MT1-MMP-deficient mice develop dwarfism, osteopenia, arthritis, and connective tissue disease due to inadequate collagen turnover. *Cell* 99, 81–92. doi: 10.1016/s0092-8674(00)80064-1
- Jiang, D., Liang, J., Campanella, G. S., Guo, R., Yu, S., Xie, T., et al. (2010). Inhibition of pulmonary fibrosis in mice by CXCL10 requires glycosaminoglycan binding and syndecan-4. *J. Clin. Invest.* 120, 2049–2057. doi: 10.1172/jci38644
- Kähäri, V. M., and Saarialho-Kere, U. (1997). Matrix metalloproteinases in skin. *Exp. Dermatol.* 6, 199–213. doi: 10.1016/b978-012545090-4/50009-4
- Ke, B., Fan, C., Yang, L., and Fang, X. (2017). Matrix metalloproteinases-7 and kidney fibrosis. *Front. Physiol.* 8:21. doi: 10.3389/fphys.2017.00021
- Khanna, D., Tashkin, D. P., Denton, C. P., Lubell, M. W., Vazquez-Mateo, C., and Wax, S. (2019). Ongoing clinical trials and treatment options for patients with systemic sclerosis-associated interstitial lung disease. *Rheumatology (U. K.)* 58, 567–579. doi: 10.1093/rheumatology/key151
- Kikuchi, K., Kadono, T., Furue, M., and Tamaki, K. (1997). Tissue inhibitor of metalloproteinase 1 (TIMP-1) may be an autocrine growth factor in scleroderma fibroblasts. *J. Invest. Dermatol.* 108, 281–284. doi: 10.1111/1523-1747.ep12286457

- Kim, W. U., Min, S. Y., Cho, M. L., Hong, K. H., Shin, Y. J., Park, S. H., et al. (2005). Elevated matrix metalloproteinase-9 in patients with systemic sclerosis. *Arthritis Res. Ther.* 7:R71.
- Kobayashi, T., Kim, H. J., Liu, X., Sugiura, H., Kohyama, T., Fang, Q., et al. (2014). Matrix metalloproteinase-9 activates TGF- β and stimulates fibroblast contraction of collagen gels. *Am. J. Physiol. Lung Cell. Mol. Physiol.* 306:L1006.
- Kowal-Bielecka, O., Fransen, J., Avouac, J., Becker, M., Kulak, A., Allnore, Y., et al. (2017). Update of EULAR recommendations for the treatment of systemic sclerosis. *Ann. Rheum. Dis.* 76, 1327–1339.
- Lagares, D., Santos, A., Grasberger, P. E., Liu, F., Probst, C. K., Rahimi, R. A., et al. (2017). Targeted apoptosis of myofibroblasts with the BH3 mimetic ABT-263 reverses established fibrosis. *Sci. Transl. Med.* 9:eal3765. doi: 10.1126/scitranslmed.aal3765
- Lambova, S. (2014). Cardiac manifestations in systemic sclerosis. *World J. Cardiol.* 6:993. doi: 10.4330/wjcv.16.9.993
- Lampi, M. C., and Reinhart-King, C. A. (2018). Targeting extracellular matrix stiffness to attenuate disease: from molecular mechanisms to clinical trials. *Sci. Transl. Med.* 10:eaa0475. doi: 10.1126/scitranslmed.aao0475
- Li, L., and Li, H. (2013). Role of microRNA-mediated MMP regulation in the treatment and diagnosis of malignant tumors. *Cancer Biol. Ther.* 14:796. doi: 10.4161/cbt.25936
- Li, Q., Park, P. W., Wilson, C. L., and Parks, W. C. (2002). Matrilysin shedding of syndecan-1 regulates chemokine mobilization and transepithelial efflux of neutrophils in acute lung injury. *Cell* 111, 635–646. doi: 10.1016/s0092-8674(02)01079-6
- Liu, F., Mih, J. D., Shea, B. S., Kho, A. T., Sharif, A. S., Tager, A. M., et al. (2010). Feedback amplification of fibrosis through matrix stiffening and COX-2 suppression. *J. Cell Biol.* 190, 693–706. doi: 10.1083/jcb.201004082
- Loffek, S., Schilling, O., and Franzke, C.-W. (2011). Biological role of matrix metalloproteinases: a critical balance. *Eur. Respir. J.* 38, 191–208. doi: 10.1183/09031936.00146510
- Madala, S. K., Pesce, J. T., Ramalingam, T. R., Wilson, M. S., Minniccozi, S., Cheever, A. W., et al. (2010). Matrix metalloproteinase 12-deficiency augments extracellular matrix degrading metalloproteinases and attenuates IL-13-dependent fibrosis. *J. Immunol.* 184, 3955–3963. doi: 10.4049/jimmunol.0903008
- Manetti, M., Guiducci, S., Romano, E., Bellando-Randone, S., Conforti, M. L., Ibba-Manneschi, L., et al. (2012). Increased serum levels and tissue expression of matrix metalloproteinase-12 in patients with systemic sclerosis: correlation with severity of skin and pulmonary fibrosis and vascular damage. *Ann. Rheum. Dis.* 71, 1064–1072. doi: 10.1136/annrheumdis-2011-200837
- Manetti, M., Ibba-Manneschi, L., Fatini, C., Guiducci, S., Cuomo, G., Bonino, C., et al. (2010). Association of a functional polymorphism in the matrix metalloproteinase-12 promoter region with systemic sclerosis in an Italian population. *J. Rheumatol.* 37, 1852–1857. doi: 10.3899/jrheum.100237
- Manicone, A. M., Huizar, I., and McGuire, J. K. (2009). Matrilysin (matrix metalloproteinase-7) regulates anti-inflammatory and antifibrotic pulmonary dendritic cells that express CD103 (α E β 7-integrin). *Am. J. Pathol.* 175, 2319–2331. doi: 10.2353/ajpath.2009.090101
- Marie Burdick, S. D., Xu, Z. J., Xue, Y. Y., Keane, M. P., Strieter, R. M., Belperio, J. A., et al. (1999). IFN- γ -inducible protein-10 attenuates bleomycin-induced pulmonary fibrosis via inhibition of angiogenesis. *J. Immunol.* 163, 5686–5692.
- Martin, P., Teodoro, W. R., Velosa, A. P. P., de Moraes, J., Carrasco, S., Christmann, R. B., et al. (2012). Abnormal collagen V deposition in dermis correlates with skin thickening and disease activity in systemic sclerosis. *Autoimmun. Rev.* 11, 827–835. doi: 10.1016/j.autrev.2012.02.017
- McFarlane, I. M., Bhamra, M. S., Kreps, A., Iqbal, S., Al-Ani, F., Saladini-Aponte, C., et al. (2018). Gastrointestinal manifestations of systemic sclerosis. *Rheumatology (Sunnyvale)* 8:235.
- Medina, C., and Radomski, M. W. (2006). Role of matrix metalloproteinases in intestinal inflammation. *J. Pharmacol. Exp. Ther.* 318, 933–938. doi: 10.1124/jpet.106.103465
- Mohan, V., Talmi-Frank, D., Arkadash, V., Papo, N., and Sagi, I. (2016). Matrix metalloproteinase protein inhibitors: highlighting a new beginning for metalloproteinases in medicine. *Metalloproteinases Med.* 3, 31–47. doi: 10.2147/mnm.s65143
- Moynadeh, P., Krieg, T., Hellmich, M., Brinckmann, J., Neumann, E., Müller-Ladner, U., et al. (2011). Elevated MMP-7 levels in patients with systemic sclerosis: correlation with pulmonary involvement. *Exp. Dermatol.* 20, 770–773. doi: 10.1111/j.1600-0625.2011.01321.x
- Mora, G. F. (2009). Systemic sclerosis: environmental factors. *J. Rheumatol.* 36, 2383–2396. doi: 10.3899/jrheum.090207
- Nagase, H., Visse, R., and Murphy, G. (2006). Structure and function of matrix metalloproteinases and TIMPs. *Cardiovasc. Res.* 69, 562–573. doi: 10.1016/j.cardiores.2005.12.002
- Nguyen, T. T., Mobashery, S., and Chang, M. (2016). “Roles of matrix metalloproteinases in cutaneous wound healing,” in *Wound Healing—New insights into Ancient Challenges*, ed. V. A. Alexandrescu (London: IntechOpen).
- Nishijima, C., Hayakawa, I., Matsushita, T., Komura, K., Hasegawa, M., Takehara, K., et al. (2004). Autoantibody against matrix metalloproteinase-3 in patients with systemic sclerosis. *Clin. Exp. Immunol.* 138, 357–363. doi: 10.1111/j.1365-2249.2004.02615.x
- Niwa, H., Kanno, Y., Shu, E., and Seishima, M. (2020). Decrease in matrix metalloproteinase-3 activity in systemic sclerosis fibroblasts causes α 2-antiplasmin and extracellular matrix deposition, and contributes to fibrosis development. *Mol. Med. Rep.* 22, 3001–3007.
- Nkyimbeng, T., Ruppert, C., Shiomi, T., Dahal, B., Lang, G., Seeger, W., et al. (2013). Pivotal role of matrix metalloproteinase 13 in extracellular matrix turnover in idiopathic pulmonary fibrosis. *PLoS One* 8:e73279. doi: 10.1371/journal.pone.0073279
- Orphanides, C., Fine, L. G., and Norman, J. T. (1997). Hypoxia stimulates proximal tubular cell matrix production via a TGF- β 1-independent mechanism. *Kidney Int.* 52, 637–647. doi: 10.1038/ki.1997.377
- O’Sullivan, S., Gilmer, J. F., and Medina, C. (2015). Matrix metalloproteinases in inflammatory bowel disease: an update. *Mediators Inflamm.* 2015:964131.
- Pardo, A., and Selman, M. (2006). Matrix metalloproteinases in aberrant fibrotic tissue remodeling. *Proc. Am. Thorac. Soc.* 3, 383–388. doi: 10.1513/pats.200601-012tk
- Parker, M. W., Rossi, D., Peterson, M., Smith, K., Sikstroř, K., White, E. S., et al. (2014). Fibrotic extracellular matrix activates a profibrotic positive feedback loop. *J. Clin. Invest.* 124, 1622–1635. doi: 10.1172/jci71386
- Pomianowska, E., Sandnes, D., Grzyb, K., Schjølberg, A. R., Aasrum, M., Tveteraas, I. H., et al. (2014). Inhibitory effects of prostaglandin E2 on collagen synthesis and cell proliferation in human stellate cells from pancreatic head adenocarcinoma. *BMC Cancer* 14:413. doi: 10.1186/1471-2407-14-413
- Pushpakumar, S., Kundu, S., Pryor, T., Givvimani, S., Lederer, E., Tyagi, S. C., et al. (2013). Angiotensin-II induced hypertension and renovascular remodeling in tissue inhibitor of metalloproteinase 2 knockout mice. *J. Hypertens.* 31, 2270–2281. doi: 10.1097/hjh.0b013e3283649b33
- Ramos, P. S., Silver, R. M., and Feghali-Bostwick, C. A. (2015). Genetics of systemic sclerosis. *Curr. Opin. Rheumatol.* 27, 521–529.
- Richter, A. G., McKeown, S., Rathinam, S., Harper, L., Rajesh, P., McAuley, D. F., et al. (2009). Soluble endostatin is a novel inhibitor of epithelial repair in idiopathic pulmonary fibrosis. *Thorax* 64, 156–161. doi: 10.1136/thx.2008.102814
- Sallam, H., McNearney, T. A., and Chen, J. D. Z. (2006). Systematic review: pathophysiology and management of gastrointestinal dysmotility in systemic sclerosis (scleroderma). *Aliment. Pharmacol. Ther.* 23, 691–712. doi: 10.1111/j.1365-2036.2006.02804.x
- Santos, A., and Lagares, D. (2018). Matrix stiffness: the conductor of organ fibrosis. *Curr. Rheumatol. Rep.* 20:2.
- Sen, A. I., Shiomi, T., Okada, Y., and D’Armiento, J. M. (2010). Deficiency of matrix metalloproteinase-13 increases inflammation after acute lung injury. *Exp. Lung Res.* 36, 615–624. doi: 10.3109/01902148.2010.497201
- Shimada, S., Makino, K., Jinnin, M., Sawamura, S., Kawano, Y., Ide, M., et al. (2020). CXCL17-mediated downregulation of type I collagen via MMP1 and miR-29 in skin fibroblasts possibly contributes to the fibrosis in systemic sclerosis. *J. Dermatol. Sci.* 100, 183–191. doi: 10.1016/j.jdermsci.2020.09.010
- Sing, T., Jinnin, M., Yamane, K., Honda, N., Makino, K., Kajihara, I., et al. (2012). MicroRNA-92a expression in the sera and dermal fibroblasts increases in patients with scleroderma. *Rheumatology (U. K.)* 51, 1550–1556. doi: 10.1093/rheumatology/kes120
- Sobolewski, P., Mařlińska, M., Wiczorek, M., Łagun, Z., Malewska, A., Roszkiewicz, M., et al. (2019). Systemic sclerosis—multidisciplinary disease: clinical features and treatment. *Reumatologia* 57, 221–233. doi: 10.5114/reum.2019.87619

- Solini, A., Rossi, C., Santini, E., Madec, S., Salvati, A., and Ferrannini, E. (2011). Angiotensin-II and rosuvastatin influence matrix remodeling in human mesangial cells via metalloproteinase modulation. *J. Hypertens.* 29, 1930–1939. doi: 10.1097/hjh.0b013e32834abceb
- Stawski, L., Haines, P., Fine, A., Rudnicka, L., and Trojanowska, M. (2014). MMP-12 deficiency attenuates angiotensin II-induced vascular injury, M2 macrophage accumulation, and skin and heart fibrosis. *PLoS One* 9:e109763. doi: 10.1371/journal.pone.0109763
- Steen, V. D. (2014). Kidney involvement in systemic sclerosis. *Press. Med.* 43, e305–e314.
- Stijn, W., Verleden Stijn, E., Vanaudenaerde Bart, M., Marijke, W., Christophe, D., Jonas, Y., et al. (2013). Multiplex protein profiling of bronchoalveolar lavage in idiopathic pulmonary fibrosis and hypersensitivity pneumonitis. *Ann. Thorac. Med.* 8, 38–45. doi: 10.4103/1817-1737.105718
- Stock, C., De Lauretis, A., Visca, D., Daccord, C., Kokosi, M., Alfieri, V., et al. (2019). Serum biomarkers in SSc-ILD: association with presence, severity and prognosis. *Eur. Respir. J.* 54:A5198.
- Sunderkötter, C., and Riemekasten, G. (2006). Pathophysiology and clinical consequences of Raynaud's phenomenon related to systemic sclerosis. *Rheumatology* 45 (Suppl. 3), iii33–iii35.
- Tager, A. M., Kradin, R. L., Lacamera, P., Bercury, S. D., Campanella, G. S. V., Leary, C. P., et al. (2004). Inhibition of pulmonary fibrosis by the chemokine IP-10/CXCL10. *Am. J. Respir. Cell Mol. Biol.* 31, 395–404. doi: 10.1165/rcmb.1004-0175oc
- Toriseva, M. J., Ala-Aho, R., Karvinen, J., Baker, A. H., Marjomäki, V. S., Heino, J., et al. (2007). Collagenase-3 (MMP-13) enhances remodeling of three-dimensional collagen and promotes survival of human skin fibroblasts. *J. Invest. Dermatol.* 127, 49–59. doi: 10.1038/sj.jid.5700500
- Tschumperlin, D. J., Ligresti, G., Hilscher, M. B., and Shah, V. H. (2018). Mechanosensing and fibrosis. *J. Clin. Invest.* 128, 74–84. doi: 10.1172/jci93561
- Tzelepis, G. E., Kelekis, N. L., Plastiras, S. C., Mitseas, P., Economopoulos, N., Kampolis, C., et al. (2007). Pattern and distribution of myocardial fibrosis in systemic sclerosis: a delayed enhanced magnetic resonance imaging study. *Arthritis Rheum.* 56, 3827–3836. doi: 10.1002/art.22971
- Valentinis, B., Bhala, A., DeAngelis, T., Baserga, R., and Cohen, P. (1995). The human insulin-like growth factor (IGF) binding protein-3 inhibits the growth of fibroblasts with a targeted disruption of the IGF-I receptor gene. *Mol. Endocrinol.* 9, 361–367. doi: 10.1210/me.9.3.361
- Van Caam, A., Vonk, M., Van Den Hoogen, F., Van Lent, P., and Van Der Kraan, P. (2018). Unraveling SSc pathophysiology: the myofibroblast. *Front. Immunol.* 9:2452. doi: 10.3389/fimmu.2018.02452
- Van Den Steen, P. E., Dubois, B., Nelissen, I., Rudd, P. M., Dwek, R. A., and Opdenakker, G. (2002). Biochemistry and molecular biology of gelatinase B or matrix metalloproteinase-9 (MMP-9). *Crit. Rev. Biochem. Mol. Biol.* 37, 375–536. doi: 10.1080/10409230290771546
- Vandenbroucke, R. E., and Libert, C. (2014). Is there new hope for therapeutic matrix metalloproteinase inhibition? *Nat. Rev. Drug Discov.* 13, 904–927. doi: 10.1038/nrd4390
- Varga, J., and Abraham, D. (2007). Systemic sclerosis: a prototypic multisystem fibrotic disorder. *J. Clin. Invest.* 117, 557–567. doi: 10.1172/jci31139
- Varga, J., and Bashey, R. I. (1995). Regulation of connective tissue synthesis in systemic sclerosis. *Int. Rev. Immunol.* 12, 187–199. doi: 10.3109/08830189509056712
- Varga, J., Trojanowska, M., and Kuwana, M. (2017). Pathogenesis of systemic sclerosis: recent insights of molecular and cellular mechanisms and therapeutic opportunities. *J. Scleroderma Relat. Disord.* 2, 137–152. doi: 10.5301/jrsd.5000249
- Wang, Y., Fan, P.-S., and Kahaleh, B. (2006). Association between enhanced type I collagen expression and epigenetic repression of the FLI1 gene in scleroderma fibroblasts. *Arthritis Rheum.* 54, 2271–2279. doi: 10.1002/art.21948
- Waszczykowska, A., Podgórski, M., Waszczykowski, M., Gerlicz-Kowalczyk, Z., and Jurowski, P. (2020). Matrix metalloproteinases MMP-2 and MMP-9, their inhibitors TIMP-1 and TIMP-2, vascular endothelial growth factor and sVEGFR-2 as predictive markers of ischemic retinopathy in patients with systemic sclerosis—case series report. *Int. J. Mol. Sci.* 21:8703. doi: 10.3390/ijms21228703
- Wilborn, J., Crofford, L. J., Burdick, M. D., Kunkel, S. L., Strieter, R. M., and Peters-Golden, M. (1995). Cultured lung fibroblasts isolated from patients with idiopathic pulmonary fibrosis have a diminished capacity to synthesize prostaglandin E2 and to express cyclooxygenase-2. *J. Clin. Invest.* 95, 1861–1868. doi: 10.1172/jci117866
- Wipff, P. J., Rifkin, D. B., Meister, J. J., and Hinz, B. (2007). Myofibroblast contraction activates latent TGF- β 1 from the extracellular matrix. *J. Cell Biol.* 179, 1311–1323. doi: 10.1083/jcb.200704042
- Xu, X., Zheng, L., Yuan, Q., Zhen, G., Crane, J. L., Zhou, X., et al. (2018). Transforming growth factor- β in stem cells and tissue homeostasis. *Bone Res.* 6:2.
- Yamamoto, T., Takagawa, S., Katayama, I., Yamazaki, K., Hamazaki, Y., Shinkai, H., et al. (1999). Animal model of sclerotic skin. I: local injections of bleomycin induce sclerotic skin mimicking scleroderma. *J. Invest. Dermatol.* 112, 456–462. doi: 10.1046/j.1523-1747.1999.00528.x
- Yamashita, C. M., Dolgonos, L., Zemans, R. L., Young, S. K., Robertson, J., Briones, N., et al. (2011). Matrix metalloproteinase 3 is a mediator of pulmonary fibrosis. *Am. J. Pathol.* 179, 1733–1745.
- Yu, G., Kovkharova-Naumovski, E., Jara, P., Parwani, A., Kass, D., Ruiz, V., et al. (2012). Matrix metalloproteinase-19 is a key regulator of lung fibrosis in mice and humans. *Am. J. Respir. Crit. Care Med.* 186, 752–762. doi: 10.1164/rccm.201202-0302oc
- Yu, Q., and Stamenkovic, I. (2000). Cell surface-localized matrix metalloproteinase-9 proteolytically activates TGF- β and promotes tumor invasion and angiogenesis. *Genes Dev.* 14, 163–176.
- Zakiyanov, O., Kalousova, M., Zima, T., and Tesaf, V. (2019). Matrix metalloproteinases in renal diseases: a critical appraisal. *Kidney Blood Press. Res.* 44, 298–330. doi: 10.1159/000499876
- Zhao, J., Shu, B., Chen, L., Tang, J., Zhang, L., Xie, J., et al. (2016). Prostaglandin E2 inhibits collagen synthesis in dermal fibroblasts and prevents hypertrophic scar formation in vivo. *Exp. Dermatol.* 25, 604–610. doi: 10.1111/exd.13014
- Zhou, B., Zhu, H., Luo, H., Gao, S., Dai, X., Li, Y., et al. (2017). MicroRNA-202-3p regulates scleroderma fibrosis by targeting matrix metalloproteinase 1. *Biomed. Pharmacother.* 87, 412–418. doi: 10.1016/j.biopha.2016.12.080
- Zigrino, P., Brinckmann, J., Niehoff, A., Lu, Y., Giebeler, N., Eckes, B., et al. (2016). Fibroblast-derived MMP-14 regulates collagen homeostasis in adult skin. *J. Invest. Dermatol.* 136, 1575–1583. doi: 10.1016/j.jid.2016.03.036
- Zuo, F., Kaminski, N., Eugui, E., Allard, J., Yakhini, Z., Ben-Dor, A., et al. (2002). Gene expression analysis reveals matrix metalloproteinase as a key regulator of pulmonary fibrosis in mice and humans. *Proc. Natl. Acad. Sci. U.S.A.* 99, 6292–6297. doi: 10.1073/pnas.092134099

Conflict of Interest: The authors declare that the research was conducted in the absence of any commercial or financial relationships that could be construed as a potential conflict of interest.

Publisher's Note: All claims expressed in this article are solely those of the authors and do not necessarily represent those of their affiliated organizations, or those of the publisher, the editors and the reviewers. Any product that may be evaluated in this article, or claim that may be made by its manufacturer, is not guaranteed or endorsed by the publisher.

Copyright © 2021 Leong, Bezuhy and Marshall. This is an open-access article distributed under the terms of the Creative Commons Attribution License (CC BY). The use, distribution or reproduction in other forums is permitted, provided the original author(s) and the copyright owner(s) are credited and that the original publication in this journal is cited, in accordance with accepted academic practice. No use, distribution or reproduction is permitted which does not comply with these terms.



Lymphocytes: Versatile Participants in Acute Kidney Injury and Progression to Chronic Kidney Disease

Chujin Cao, Ying Yao* and Rui Zeng*

Division of Nephrology, Tongji Hospital, Tongji Medical College, Huazhong University of Science and Technology, Wuhan, China

Background: Acute kidney injury (AKI) remains a major global public health concern due to its high morbidity and mortality. The progression from AKI to chronic kidney disease (CKD) makes it a scientific problem to be solved. However, it is with lack of effective treatments.

Summary: Both innate and adaptive immune systems participate in the inflammatory process during AKI, and excessive or dysregulated immune responses play a pathogenic role in renal fibrosis, which is an important hallmark of CKD. Studies on the pathogenesis of AKI and CKD have clarified that renal injury induces the production of various chemokines by renal parenchyma cells or resident immune cells, which recruits multiple-subtype lymphocytes in circulation. Some infiltrated lymphocytes exacerbate injury by proinflammatory cytokine production, cytotoxicity, and interaction with renal resident cells, which constructs the inflammatory environment and induces further injury, even death of renal parenchyma cells. Others promote tissue repair by producing protective cytokines. In this review, we outline the diversity of these lymphocytes and their mechanisms to regulate the whole pathogenic stages of AKI and CKD; discuss the chronological responses and the plasticity of lymphocytes related to AKI and CKD progression; and introduce the potential therapies targeting lymphocytes of AKI and CKD, including the interventions of chemokines, cytokines, and lymphocyte frequency regulation *in vivo*, adaptive transfer of ex-expanded lymphocytes, and the treatments of gut microbiota or metabolite regulations based on gut-kidney axis.

Key Message: In the process of AKI and CKD, T helper (Th) cells, innate, and innate-like lymphocytes exert mainly pathogenic roles, while double-negative T (DNT) cells and regulatory T cells (Tregs) are confirmed to be protective. Understanding the mechanisms by which lymphocytes mediate renal injury and renal fibrosis is necessary to promote the development of specific therapeutic strategies to protect from AKI and prevent the progression of CKD.

Keywords: lymphocytes, acute kidney injury, tubular cell damage, renal fibrosis, chronic kidney disease, gut microbiota

OPEN ACCESS

Edited by:

Gonzalo del Monte-Nieto,
Monash University, Australia

Reviewed by:

Yanlin Wang,
University of Connecticut,
United States
Lin-Li Lv,
Southeast University, China

*Correspondence:

Ying Yao
yaoyingkk@126.com
Rui Zeng
zengr126@126.com

Specialty section:

This article was submitted to
Renal and Epithelial Physiology,
a section of the journal
Frontiers in Physiology

Received: 22 June 2021

Accepted: 19 August 2021

Published: 20 September 2021

Citation:

Cao C, Yao Y and Zeng R (2021)
Lymphocytes: Versatile Participants in
Acute Kidney Injury and Progression
to Chronic Kidney Disease.
Front. Physiol. 12:729084.
doi: 10.3389/fphys.2021.729084

INTRODUCTION

Despite the identification of clinical diagnosis and application of dialysis, acute kidney injury (AKI) remains a major global public health concern due to high morbidity and mortality with few systematic efforts to manage it including prevention, diagnosis, and treatments (Mehta et al., 2015). Rodent models of AKI have provided novel insights into the potential pathophysiologic mechanisms, which include hypoxia, oxidative stress, endoplasmic reticulum stress, mitochondrial dysfunction, and inflammation. Hypoxia and oxidative stress induce microvascular endothelium injury and endothelial cell activation with expression change of new markers, which promote the recruitment of inflammatory cells. Resident dendritic cells and macrophages initiate inflammation in response to renal injury. Subsequently, neutrophils and monocytes, which are recruited by chemotactic signals, amplify the inflammation after acute injury. Whereas, lymphocytes, especially T cells, are involved in the whole evolution of injury (Zuk and Bonventre, 2016).

With acute injury, adaptive responses restore cell, and renal tissue homeostasis. However, dysregulated or insufficient repairs impair the regeneration and contribute to chronic kidney disease (CKD) (Zuk and Bonventre, 2016; D'Alessio et al., 2019). Immune cells with high plasticity and diversity participate in almost all the events involved from renal injury to repair and the subsequent fibrosis. For example, the phenotypes of macrophages exert distinct functions in different phases of injury, including M1 proinflammatory cells in the phase of injury and M2 anti-inflammatory cells in the phase of recovery (Huen and Cantley, 2017; Tang et al., 2019). Similarly, lymphocytes possess polytropic subtypes ensure to provide precise and comprehensive regulation of immune response maintenance in injured kidney.

Generally, lymphocytes contain two major categories that are T cells and B cells. T cells, which originate from bone marrow (BM) progenitors, migrate to the thymus for maturation and subsequently export into the periphery, are divided into alpha beta T ($\alpha\beta$ T) cells and gamma delta T ($\gamma\delta$ T) cells according to respective T-cell receptors (TCRs) on their surfaces. $\alpha\beta$ T cells are further classified into cluster of differentiation (CD) 4^+ T cells, CD 8^+ T cells, and double-negative T (DNT) cells, of which naive CD 4^+ T cells differentiate into various helper subsets in immune responses such as T helper (Th)1, Th2, and Th17. In addition, one unique type of T cells, called regulatory T cells (Tregs), plays an important role in immune tolerance and homeostasis (Kumar et al., 2018; Zhu, 2018).

Another type of lymphocytes, named innate lymphoid cells (ILCs), have recently seen a great upsurge in studies related to kidney diseases. Unlike T cells and B cells, ILCs lack diversified and adaptive antigen receptors, which determine their innate-immune properties. ILC1, ILC2, and ILC3 are the innate counterparts of Th1, Th2, and Th17, respectively (Vivier et al., 2018). Besides ILCs, several types of T cells function like innate cells and exist extensively in normal kidneys with tissue-resident characteristics, including invariant natural killer T (iNKT) cells, mucosa-associated invariant T (MAIT) cells, and $\gamma\delta$ T cells. These innate or innate-like lymphoid cells respond earlier to renal damage than adaptive lymphocytes (Turner et al., 2018).

Recent studies have challenged the view that CD 4^+ T helper cell subsets are a cluster of terminally differentiated homogeneous cells, demonstrating that T cells have more powerful plasticity than previously thought. Ulf Panzer et al. summarized the current perceptions of Th17 cell plasticity and heterogeneity in autoimmune kidney diseases and debated the single-side and harmful effect of Th17 cells on renal inflammation (Krebs and Panzer, 2018). In addition, the stability and anti-inflammatory effect of Tregs are also in doubt. Researchers found that with the acquisition of hybrid fates, Tregs became unstable under certain inflammatory conditions and exerted promotion rather than suppression of inflammation (Sakaguchi et al., 2013). Furthermore, ILCs and $\gamma\delta$ T cells are also flexible in the inflammatory milieu with diverse activating signals (Corpuz et al., 2017; Colonna, 2018). Understanding the molecular basis of lymphocyte heterogeneity and plasticity in AKI and CKD may allow the development of therapies to target lymphocytes in a specific manner.

In this review, we summarized the mechanisms by which various types of lymphocytes participate in AKI, subsequent repair and progression to CKD with a focus on T cells and ILCs. Then, we illuminated the diversity and plasticity of these cells with time-course to progression and inflammatory status changes. Finally, we discussed the potential effective therapeutic interventions associated with lymphocytes for AKI and CKD under current studies.

LYMPHOCYTES MEDIATE AKI AND CKD: DIVERSITY AND MECHANISMS

During the past decades, many studies have uncovered that lymphocytes, particularly diverse T cells and ILCs, play a crucial role in postschemic, nephrotoxic, septic, and postrenal AKI as well as subsequent repair and CKD, which are nonautoimmune diseases (shown in **Figure 1**). Ischemia and reperfusion induce sterile inflammation, in which hypoxia-induced sterile cell death or injury causes the release of some ligands, leading to immune responses. Such ligands, called damage-associated molecular patterns (DAMPs), are normally detained intracellularly. However, upon tissue damage, they are released into the extracellular environment where immune responses are activated (Eltzschig and Eckle, 2011). The mechanisms of nephrotoxic AKI have a difference. Due to high blood flow and local metabolism of drugs, the kidneys are extremely sensitive to drug hypersensitivity. Drugs acting as prohapten or haptens turn native renal proteins into neoantigens, activating innate immune responses. And in the effector phase, nephrotoxic AKI is characterized by the infiltration of lymphocytes in the kidney (Perazella, 2019). In addition, sepsis triggers a systemic and activated immune response followed by immune suppression that may make septic AKI more severe than non-septic AKI (Alobaidi et al., 2015). Due to the multiple characteristics and functions of lymphocytes, mechanisms are intricate, by which these cells give full play to their own expertise and interact with infiltrated or intrinsic cells in kidneys. The systematic findings in animal experiments and human studies of AKI are shown in **Tables 1, 2**, respectively.

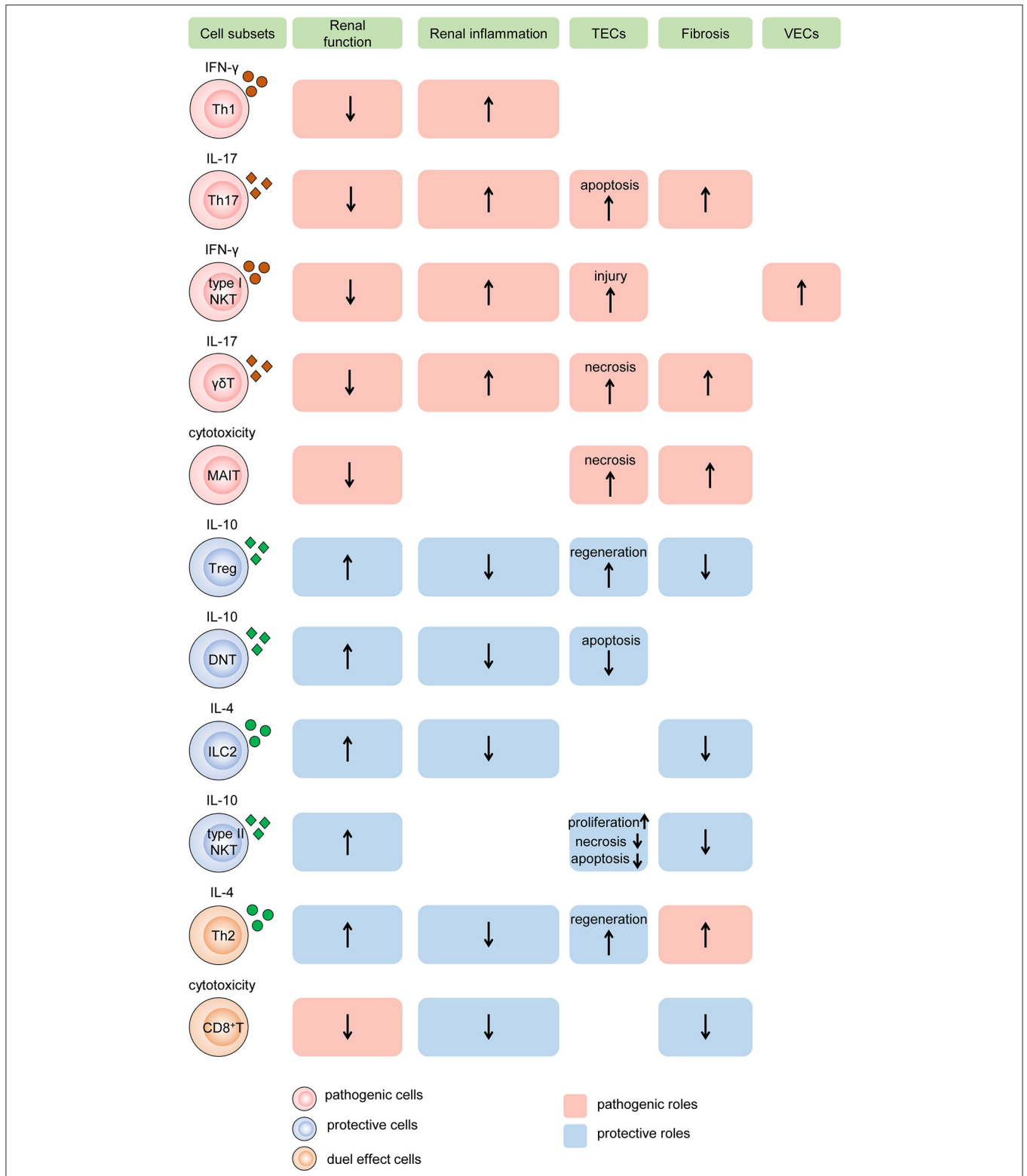


Fig. 1 The roles of diverse lymphocyte subsets on AKI and renal fibrosis.

FIGURE 1 | The roles of diverse lymphocyte subsets on AKI and renal fibrosis. Different subsets of T cells, innate-like lymphocytes, and innate lymphoid cells mediate renal injury and fibrosis by regulating intrinsic cell death, proliferation, and fibroblast formation. In the process, cytokine secretion and cytotoxicity are two major mechanisms. Some subsets of lymphocytes, such as Th1, Th17, type I NKT cells, and γδT cells, produce pathogenic cytokines like IFN-γ, induce renal inflammatory, (Continued)

FIGURE 1 | and impair TECs and VECs, resulting in the decline of renal function and exacerbation of renal fibrosis. While MAIT cells play the pathogenic role by cytotoxicity. Other subtypes, such as Tregs, DNT cells, ILC2, and type II NKT cells, produce protective cytokines like IL-10, reduce renal inflammation, promote TEC repair, leading to preserve renal function and alleviate renal fibrosis. In addition, Th2 and CD8⁺ T cells have dual roles in AKI and CKD. Cells colored red represent that they are pathogenic. Cells colored blue represent that they are protective. Cells colored orange represent that they have dual roles. The rectangle with red background represents the pathogenic role and that colored blue means the protective role. The up arrows mean increased roles, and the down arrows mean decreased roles. Th, T helper cell; NKT, natural killer cell; $\gamma\delta$ T, $\gamma\delta^+$ T cell; MAIT, mucosa-associated invariant T cell; Treg, regulatory T cell; DNT, double-negative T cell; ILC2, type 2 innate lymphoid cell; MAIT, mucosa-associated invariant T cell; IFN- γ , interferon γ ; IL, interleukin; TEC, tubular epithelial cell; VEC, vascular endothelial cell.

TABLE 1 | The systematically findings of lymphocytes in animal experiments of AKI.

| Year | Models | Findings | References |
|------|------------------------------|---|--------------------------------|
| 2001 | IR | 1. Mice with deficiency in CD4 ⁺ T cells, rather than those with deficiency in CD8 ⁺ T cells, were remarkably protected from AKI that was called acute kidney failure (ARF). 2. Adaptive transfer of wild-type CD4 ⁺ T cells for the reconstitution of CD4-deficient mice was found to restore post-ischemic kidney injury. | Burne et al., 2001 |
| 2000 | Cisplatin-induced AKI | Harmful role of CD4 ⁺ T cells was confirmed in murine acute cisplatin nephrotoxicity by adaptive transfer experiments. | Rabb et al., 2000 |
| 2003 | IR | STAT4 deficient in mice mildly improved renal function, whereas STAT6 deficient markedly aggravated function and tubular injury. | Yokota et al., 2003 |
| 2015 | IR | Activated T cells, mostly positive for IL-17, were increased in the kidney after AKI and elevated salt dietary intervention. | Mehrotra et al., 2015 |
| 2006 | IR | Isolation and transfer of T lymphocytes infiltrated in kidney into T cell-deficient mice with renal IRI, reduced the functional and histological injury, thus, suggesting the possible existence of reno-protective T cell populations, Tregs. | Ascon et al., 2006 |
| 2009 | IR | 1. There was a significant recruitment of Tregs into kidneys 3- and 10-days post ischemia. 2. These infiltrated Tregs promoted tubular proliferation and reduced pro-inflammatory cytokine generation. 3. Depletion of Tregs worsen renal function and mortality. | Gandolfo et al., 2009 |
| 2018 | FA-induced AKI | The strong upregulation of CCL20 was confirmed at day 2 of renal injury and persisted for 7 days. | Gonzalez-Guerrero et al., 2018 |
| 2009 | IR | Transfer of wild-type Tregs into immunodeficient mice prevented renal IRI, but transfer of IL-10-deficient Tregs did not. | Kinsey et al., 2009 |
| 2016 | IR | DNT cells expand significantly and become the dominant subsets of the early responders. | Martina et al., 2016 |
| 2020 | Cisplatin-induced AKI | DNT cells alleviate cisplatin-induced dysfunction and structure damage from AKI by reducing apoptosis in kidney proximal tubular epithelial cells (PTECs). | Gong et al., 2020 |
| 2015 | IR | Given the protective role of Th2 and type 2 immunity on AKI, researchers intent to whether ILC2s are also beneficial to kidney injury. | Huang et al., 2015 |
| 2019 | IR | A loss of ILC2s does not alter the severity of IR-induced renal injury suggesting the redundancy of ILC2s for IRI protection. | Cameron et al., 2019b |
| 2018 | α -GalCer-induced AKI | NKT cells injured kidney vascular endothelial cells by perforin-mediated pathway and tubular epithelial cells by TNF- α /FasL pathway, leading to AKI with hematuria in mice. | Uchida et al., 2018 |
| 2014 | Cisplatin-induced AKI | Depletion of $\gamma\delta$ T cells did not ameliorate cisplatin-induced renal injury indicating $\gamma\delta$ T cells were unnecessary to injury. | Chan et al., 2014 |

T Helper Cells

An article published in 2001 provided direct evidence of the pathogenic role of CD4⁺ T cells in AKI induced by ischemia reperfusion (IR). Researchers found that mice with deficiency in CD4⁺ T cells, rather than those with deficiency in CD8⁺ T cells, were remarkably protected from AKI that was called acute kidney failure (ARF) at that time. The following adaptive transfer of wild-type CD4⁺ T cells for the reconstitution of CD4-deficient mice was found to restore

postischemic kidney injury. In addition, the reconstitutions with CD4⁺ T cells lacking the ability of interferon gamma (IFN- γ) production were insufficient to restore kidney injury, which implied IFN- γ -producing CD4⁺ T cell might be a pathogenic factor in AKI (Burne et al., 2001). A similar harmful role of CD4⁺ T cells was confirmed in murine acute cisplatin nephrotoxicity by adaptive transfer experiments (Rabb et al., 2000). In addition, a clinical research showed that CD4⁺ lymphocyte ATP might be a new marker in sepsis-associated

TABLE 2 | The systematically findings of lymphocytes in human studies of AKI.

| Year | Patients | Findings | References |
|------|--|---|--------------------------------|
| 2014 | 23 patients with sepsis | CD4+ lymphocyte adenosine triphosphate (ATP) might be a new marker in sepsis-associated AKI. | Patschan et al., 2014 |
| 2019 | AKI after cardiac surgery | Th1-induced IFN- γ , Th2-induced IL-4, and IL-13 increased after surgery associated with postoperative AKI. | Moledina et al., 2019 |
| 2018 | AKI secondary to glomerular injury (IgA nephropathy) diagnosed based on renal biopsy | CCL20 was increased in human kidneys and urine with AKI and urinary CCL20 was associated with severity. | Gonzalez-Guerrero et al., 2018 |
| 2015 | Sepsis-associated AKI | The ratios of Tregs in peripheral blood might provide a potential biomarker to accurately evaluate prognosis of sepsis. | Chen et al., 2015 |
| 2018 | 20 consecutive patients undergoing multibranch endovascular thoracoabdominal aortic repair | The changes of infiltrated $\gamma\delta$ T cells were correlated with the elevated biomarkers of tubular stress or injury. | Gocze et al., 2018 |

AKI because of its correlation with survival in sepsis (Patschan et al., 2014). In summary, CD4⁺ T cells are generally pathogenic agents in AKI induced by IR, nephrotoxic drugs, and sepsis.

Furthermore, depletion of CD4⁺ T cells was proved to retard UUU-induced renal fibrosis (Liu et al., 2012), and reconstitution of lymphopenic recombination activating gene (RAG)^{-/-} mice with CD4⁺ T cells but not CD8⁺ T cells prior to unilateral ureteric obstruction (UUO) led to more severe renal fibrosis manifesting a significant increase in interstitial expansion and collagen deposition, which revealed the pivotal role of CD4⁺ T cells in renal fibrosis (Tapmeier et al., 2010). Naïve CD4⁺ T cells activated by renal damage signals differentiate into distinct Th cells producing lineage-specific cytokines. How various subtypes of Th cells regulate the process of AKI and renal fibrosis is noteworthy.

T Helper 1 and T Helper 2

T helper (Th) 1 and T helper 2 were initially Th cell subsets reported to preferentially produce IFN- γ and IL-4, respectively. These Th cell differentiations and cytokine productions are regulated by their lineage-specific master transcription factors, including T-bet/signal transducer and activator of transcription (STAT)4 for Th1 and GATA binding protein 3 (GATA3)/STAT6 for Th2 (Zhu, 2018). In experimental animal models, STAT4 deficiency in mice mildly improved renal function, whereas STAT6 deficiency markedly aggravated tubular injury following renal ischemia-reperfusion injury (IRI). T cells from STAT6 knockout mice expressed increased IFN- γ , but reduced IL-4 (Yokota et al., 2003). In addition, IL-4-deficient mice, representing defective Th2 immune responses, were also showed to suffer from a significantly aggravated functional and histological damage after IRI, especially the impairment of tubular regeneration. While IL-12- or IFN- γ -deficient mice with defective Th1 responses were completely protected from IRI by upregulating the expression of HO-1

encoding cytoprotective proteins (Yokota et al., 2003; Marques et al., 2006; de Paiva et al., 2009). A clinical study on biomarkers of AKI after cardiac surgery showed that Th1-induced IFN- γ and Th2-induced IL-4 and IL-13 increased after surgery associated with postoperative AKI (Moledina et al., 2019). The chemokines attracting leukocytes are generated from all types of intrinsic renal cells, such as endothelial, mesangial, tubular epithelial, interstitial cells, and podocyte, and regulate all the steps of leukocyte recruitments, including activation, adhesion, chemoattraction, and transmigration. In normal kidneys, the production of chemokines for proinflammatory T cells is very low but sharply increased under pathophysiological circumstances (Segerer et al., 2000; Chung and Lan, 2011). C-XC motif chemokine ligand (CXCL) 9 and CXCL10 are the two ligands of C motif chemokine receptor (CXCR) 3, which are mainly expressed on activated Th1 cells. The levels of CXCL9 and CXCL10 expression were elevated over time after IR to 72 h consistent with the loss of renal function (Fiorina et al., 2006). These data demonstrate Th1 cells are pathogenic for AKI, while Th2 cells are anti-inflammatory and protective.

Despite the protective role of Th2 in AKI, the benefit does not extend to the subsequent CKD. In 2012, the first direct evidence was provided that Th2 cells depraved renal fibrosis in the UUU mouse model. Thus, researchers put forward inhibition of Th2 differentiation from CD4⁺ T cells as a potential therapeutic intervention for renal fibrosis (Liu et al., 2012). Braga et al. demonstrated the absence of IL-4 was associated with alleviated UUU-induced renal fibrosis with better renal function that was contrary to its role in AKI. In the past, Th2 immunity was considered only as a simple regulator suppressing Th1 immunity to exert the anti-inflammatory function. Currently, the dual effects of Th2 become clear that these cell populations not only engage in protective events in reducing tissue inflammation and activating tissue repair, but also contribute to the development of tissue fibrosis when Th2 cytokine-mediated recovery processes become long-term, excessive, or dysregulated

(Gieseck and Wynn, 2018). Furthermore, the study indicated that Th cell mediated renal injury by regulating macrophage differentiation into anti-inflammatory M2 and fibroblast collagen deposition rather than directly regulate the fibrotic response, and modulation of Th1:Th2 balance may be a potential strategy against renal fibrosis (Braga et al., 2012). These studies suggest that Th2-related immune responses exacerbate renal fibrosis contrary to the effect on AKI.

T Helper 17

The third major Th cell population, Th17 cell, was discovered just several decades ago, which is controlled by the master transcription factors retinoic acid receptor-related orphan receptor (ROR) γ T and STAT3 (Zhu, 2018). Th17 cells are generally perceived as detrimental factors for the pathogenesis of renal autoimmune diseases (Krebs et al., 2017; Dolff et al., 2019). Moreover, recent studies confirmed that Th17 cells also made a vicious influence on non-autoimmune AKI and CKD. Exposure to high-salt diets accelerated the transition from AKI to CKD for mice mediated by lymphocyte activities. Activated T cells, mostly positive for interleukin-17 (IL-17), were increased in the kidney after AKI and elevated with salt dietary intervention. The enhanced Th17 response hastened CKD and interstitial fibrosis and was inhibited by angiotensin II type-1 receptor (AT1R) antagonist, Losartan (Mehrotra et al., 2015). These studies demonstrate that Th17 cells play a pathogenic role in AKI and CKD mainly by IL-17 production.

The proinflammatory function of Th17 cells was achieved partly through IL-17 family of cytokines, which induced the mobilization and activation of neutrophils or participated in macrophage-mediated tissue injury (Kitching and Holdsworth, 2011; Mi et al., 2011; Cortvrindt et al., 2017). The effect of IL-17 on neutrophil recruitment was conducted in the acute phase of injury. IL-17 also contributed to chronic inflammation in lung (Wilson et al., 2010; Mehrotra et al., 2018) and liver (Tan et al., 2013) injuries in spite of low-frequency IL-17-producing cells in the later stage of inflammation, which was a dynamic multistep process (Miossec and Kolls, 2012; Tan et al., 2013). In renal obstruction models, IL-17A, a major member of the IL-17 cytokine family, facilitated renal fibrosis by RANTES-mediated leukocyte infiltration (Peng et al., 2015). However, the effects of therapy targeting IL-17 are contradictory. Several studies showed that systemic inhibition of IL-17 by antagonists significantly reduced renal fibrosis and neutrophil infiltration as well as pulmonary fibrosis and inflammation (Wilson et al., 2010; Miossec and Kolls, 2012; Mehrotra et al., 2017; Orejudo et al., 2019). Nevertheless, some other studies raised doubts due to blockade or deficiency of IL-17A having no beneficial effect on preventing renal fibrosis progression following severe IRI. The different severity of IRI might account for the contradictory conclusions (Thorenz et al., 2017; Rosendahl et al., 2019). Thus, whether the inhibitors of IL-17 cytokine family can be clinically applied remains to be explored. And researchers need to focus on the confirmation of the specific subtype of cytokines in IL-17 family such as IL-17A and IL-17F associated with the pathogenic process of AKI and CKD. In addition, the severity and stages of renal injury are also worthy of consideration.

REGULATORY T CELLS

Isolation and transfer of T lymphocytes infiltrated in kidney into T cell-deficient mice with renal IRI reduced functional and histological injury, thus, suggesting there may be a kind of renoprotective T-cell populations, which was confirmed as Tregs (Ascon et al., 2006). Foxp3 is currently the best marker to identify Tregs, which constitute 5–10% of the total CD4⁺ T-cell populations. Despite the relative low frequency, Tregs are regarded as crucial orchestrators of the regulation of inflammation, the maintenance of immune tolerance, and homeostasis (D'Alessio et al., 2019). In animal experiments, there was significant recruitment of Tregs into kidneys 3- and 10-days postischemia. These infiltrated Tregs promoted tubular proliferation and reduced proinflammatory cytokine generation, and depletion of Tregs worsened renal function and mortality (Gandolfo et al., 2009). C-C motif chemokine ligand (CCL20), expressed by tubular, endothelial, and interstitial cells, is a key attractor for the influx of Tregs as well as Th17 into injured kidneys. CCL20 was upregulated in three models of renal injury induced by over-dose folic acid (FA), cisplatin, and UUO. In FA-induced AKI, the strong upregulation of CCL20 was confirmed at day 2 of renal injury and persisted for 7 days. CCL20 was increased in human kidneys and urine with AKI and urinary CCL20 was associated with severity (Gonzalez-Guerrero et al., 2018). In one clinical study of sepsis-associated AKI, the ratio of Tregs in peripheral blood might provide a potential biomarker to accurately evaluate the prognosis of sepsis (Chen et al., 2015). Another research on patients with AKI demonstrated the positive effect of T-cell immunoglobulin and mucin domain 3 (TIM-3) on Treg protective function (Dong et al., 2019). The mechanisms of Treg protective role in kidney injury refer to the secretions of immunosuppressive cytokines and pro-repair mediators. IL-10 is the major anti-inflammatory molecule produced by Tregs (D'Alessio et al., 2019). IRI induced a significant increase in IL-10⁺ Tregs in the repair phase (Kinsey et al., 2010). Treg reduction caused the increase of neutrophil and macrophage infusion and innate cytokine transcription. Furthermore, transfer of wild-type Tregs into immunodeficient mice prevented renal IRI, but transfer of IL-10-deficient Tregs did not. These data indicate that Tregs regulate renal IRI in early injury stage by suppression of the innate immune responses in an IL-10-mediated manner (Kinsey et al., 2009). In addition, Treg-derived adenosine activates adenosine 2A receptor (A_{2A}R) is expressed on immune cells suppressing inflammation and improving renal function decline after IRI through a programmed cell death (PD-1)-dependent mechanism, which is regulated by CD73, the final enzyme participating in the extracellular adenosine production (Kinsey et al., 2012). Endogenous Toll-like receptor 9 (TLR9) is also an important regulator of AKI by promoting Treg recruitment (Alikhan et al., 2016). These studies imply that expansion of Tregs might be a potential strategy for preventing AKI.

In vitro, Tregs modulated macrophages by inhibiting their activation and downregulating the effector phenotype of macrophages, leading to alleviate chronic kidney injury. The Treg-macrophage inhibitory interaction was transforming growth factor- β (TGF- β)-dependent (Mahajan et al., 2006). Besides that, CD226 deficiency on Tregs exacerbated renal

fibrosis in the UO model by upregulating Th2-related cytokines like IL-4 (Mu et al., 2020). Recently, a single-cell RNA sequencing study showed that tissue-resident IL-33R⁺ and IL-2Ra⁺ Tregs markedly increased following injury in the two mouse models of either kidney repair or fibrosis. Mice with expansion of this population before injury were protected from renal injury and fibrosis. However, despite Tregs showing an upregulation of regenerative and proangiogenic pathways in the repair phase, they expressed markers related to hyperactivation and fibrosis in the fibrotic environment, suggesting the plasticity in Treg function (do Valle Duraes et al., 2020). Many interventions targeting Treg expansion were confirmed to attenuate kidney injury, including the CCL20 blocking agent (Zuk and Bonventre, 2016), the IL-2/anti-IL-2 complex (IL-2C) (Kim et al., 2013), IL-233 (Stremska et al., 2017), resolvin D1 (Luan et al., 2020), mesenchymal stem cell-derived extracellular vesicles (Song et al., 2020), and oxidized ATP (oATP) (Koo et al., 2017). These data suggest that it is necessary to understand the plasticity and heterogeneity of Tregs and figure out the precise function of each Treg subset.

CD8⁺ T Cells

After IRI, renal IFN- γ -producing CD8⁺ T cells were increased (Ascon et al., 2008). Germ-free mice encountered more severe IRI, which was associated with the enhancement of CD8⁺ T cell trafficking to the kidney (Jang et al., 2009). However, unlike CD4⁺ T cells, CD8⁺ T cell deficiency did not alter the renal outcomes of IRI (Burne et al., 2001). In spite of this, the detailed roles of CD8⁺ T cells on AKI are yet to be completely determined.

In the UO mouse model of renal fibrosis, genetic ablation of CD8⁺ T cells increased renal interstitial fibrosis by promoting BM-derived monocyte-to-fibroblast transition, whereas, adoptive transfer of CD8⁺ T cells to CD8 knockout mice decreased fibrosis, which indicated that CD8⁺ T cells might have an anti-fibrotic effect on kidneys. A further study discovered that depletion of CD8⁺ T cells resulted in the higher expression of IL-4 and GATA3 and lower expression of IFN- γ and T-bet on CD4⁺ T cells, suggesting that CD8 knockout primed the immune response of Th1 skewing to that of Th2 (Dong et al., 2016). The infiltrated CD8⁺ T cells from obstructed kidneys expressed perforin, granzyme, and Fas ligand (FasL) that were related to cytotoxicity. The activation of CD8⁺ T cells required the inflammatory milieu, in which chemokines like CCL2, CCL3, CCL4, and CCL5 existed obviously. In addition, CD8⁺ T cells were distributed around fibroblasts to mediate the apoptosis of these profibrotic cells. Moreover, CD11c expression made CD8⁺ T cells express higher levels of the cytotoxicity-associated genes, and *in vitro*, CD11c⁺ CD8⁺ T cells induced fibroblast death (Wang et al., 2016). Thus, promoting CD8⁺ T cell recruitments may be an effective mechanism, by which clusterin (Guo et al., 2016) and astaxanthin (Diao et al., 2019) protect against renal fibrosis.

Double-Negative T Cells

Double-negative T cells identified by CD4⁻ and CD8⁻ are an unconventional component of $\alpha\beta$ T cells, which constitute 20–38% of the $\alpha\beta$ T cell pool in normal kidneys of mice. In

contrast, the frequency levels in the lymph nodes and spleen are lower in only 5–10%. In a steady state, DNT cells in the kidney display an activated phenotype expressing less CD62L with higher expressions of CD44 and CD69 compared to CD4⁺ and CD8⁺ counterparts. Besides that, kidney-resident DNT cells proliferate actively under the steady state and suppress CD4⁺ T cell proliferation *in vitro* (Martina et al., 2016). Many previous studies showed that DNT cells producing IL-17 and IFN- γ expanded in patients with systemic lupus erythematosus (SLE) (Crispin et al., 2008) and were a potential biomarker for SLE (Alexander et al., 2020). They also contributed to other autoimmune diseases such as type-1 diabetes (Ford et al., 2007), Sjögren's syndrome, and psoriasis (Brandt and Hedrich, 2018). In response to IR-induced AKI, DNT cells expanded significantly and become the dominant subsets of the early responders. IL-10 and IL-27 cytokines were markedly expressed in DNT cells in a steady state but altered in IRI with significantly increased IL-10 and slight decreased IL-27 that suggested that DNT cells might be beneficial to prevent AKI depending on IL-10 as conventional cytokine from Tregs. Further study confirmed this hypothesis by adoptive transfer experiments (Martina et al., 2016). DNT cells alleviated cisplatin-induced dysfunction and structure damage in AKI by reducing apoptosis in proximal tubular epithelial cells (PTECs) of the kidney (Gong et al., 2020). Another mechanism of DNT cells in the suppression of immune responses was directly killing effector T cells by antigen-specific recognition and Fas/FasL or perforin/granzyme pathway (Chen et al., 2004; Voelkl et al., 2011). In human kidneys, DNT cells also accounted for a high proportion of T cells, which suggested the prospect of DNT cells for clinical translation (Martina et al., 2016). These studies demonstrate that DNT cells protect mice from AKI in the early stage by regulating cytokine production and the cytotoxic effect, and their roles on CKD remain to be understood.

Innate Lymphoid Cells

Innate lymphoid cells originate from common progenitors with T and B lymphocytes but lack adaptive antigen receptors, which are a heterogeneous population and the innate counterparts of T cells. Based on the major cytokines ILCs produce and the master transcription factors driving their differentiation, ILCs are distinguished from three groups: IFN- γ -producing T-bet⁺ ILC1s, GATA3⁺ ILC2s secreting IL-5, IL-9, IL-13, and amphiregulin, and ROR γ t⁺ ILC3s producing IL-22 and IL-17. ILC1s, ILC2s, and ILC3s correspond to Th1, Th2, and Th17, respectively (Vivier et al., 2018). ILCs are found predominantly resident in barrier organs like the gut, the lung, and the skin, where they maintain tissue homeostasis, regulate against infection and contribute to immune-mediated diseases in mice and humans (Gasteiger et al., 2015). Recently, a novel regulatory subpopulation of ILCs existing in the gut has been identified called ILCregs, which harbor a unique gene identity distinct from that of ILCs or Tregs. ILCregs secrete IL-10 to activate ILC1s and ILC3s, causing protection against innate gut inflammation (Wang S. et al., 2017), but whether they can function as conventional Tregs for reno-protection remains unclear. These data suggest ILCs have a large family and the members exert different functions.

In healthy murine and human kidneys, ILC2s are the major ILC population and play a similar role in AKI and CKD to Th2 due to their co-participating type 2 immunity (Wang Y. M. et al., 2017; Gieseck and Wynn, 2018). Given the protective role of Th2 and type 2 immunity on AKI, the intent of the researchers is to find whether ILC2s are also beneficial to kidney injury. Expanding ILC2s by IL-25 or IL-33 released from damaged epithelial cells significantly improved renal function and alleviated injury after IR with greater amounts of Th2 cytokines such as IL-4, IL-5, and IL-13, which induced M2 macrophage subtype and suppressed M1 *in vitro*. Furthermore, adoptive transfer of ILC2s identically reduced renal functional and histological damage as well as enhancing M2 induction and amphiregulin production in the kidney (Huang et al., 2015; Cao et al., 2018; Gieseck and Wynn, 2018). But the concrete effects of IL-33 treatment depended on the dosage, the duration, and the injury type, which might reverse the advantageous role to a deleterious one (Cameron et al., 2019a). IL-233, a novel hybrid cytokine bearing the activities of IL-2 and IL-33, increased the frequency of ST2-bearing ILC2s in both blood and kidneys to protect mice from IRI (Stremeska et al., 2017). In a doxorubicin-induced nephrotoxic renal injury model, IL-233 treatment not only augmented anti-inflammatory cytokines and attenuated proinflammatory cytokine thus reducing renal inflammation, injury, and fibrosis, but also promoted regeneration with increased expression of genes related to renal progenitor cells and nephron segments (Sabapathy et al., 2019). However, a loss of ILC2s does not alter the severity of IR-induced renal injury suggesting the redundancy of ILC2s for IRI protection, which may be due to the compensation of another type 2 immune cell activation (Cameron et al., 2019b).

Expanded ILC2s by IL-33 were also confirmed to ameliorate glomerulosclerosis in mice with Adriamycin-induced CKD (Wang et al., 2015). Nevertheless, the anti-fibrotic role of ILC2s needs to be well-argued since type 2 immunity is commonly considered as a profibrotic factor such as Th2 response mentioned above (Gieseck and Wynn, 2018). In summary, ILCs alleviate AKI by mechanisms similar to Th2, and their effects on CKD remain to be explored.

Innate-Like T Lymphocytes

Innate-like T lymphocytes, including NKT cells, $\gamma\delta$ T cells, and MAIT cells, are a significant component of innate immunity and they along with ILCs hold a unique capacity for innate responses to maintain homeostasis of the gut (Constantinides, 2018), and the lung (Borger et al., 2019). Their early responses to renal injury also deserve special attention.

Natural Killer T Cells

Natural killer T cells are an unusual T lymphocyte subpopulation that co-expresses the natural killer receptors and TCRs, serving as a bridge between innate and adaptive immunity. These cells are lipid-sensing innate-like T cells, which express semi-invariant $\alpha\beta$ TCR only recognizing glycolipid antigens presented by CD1d, a major histocompatibility complex (MHC)-I-like molecular (Sun et al., 2019). According to the V α 14-J α 18 in TCRs, NKT cells are categorized into type I and type II NKT cells. The

former type, also named iNKT cells, is sensitive to glycolipid α -galactosyl ceramide (α GalCer) and the latter is activated by the self-glycolipid 3-sulfated β -galactosyl ceramide (sulfatide) (Jahng et al., 2004).

Natural killer T cells are not sensitive to non-protein DAMP molecules, but alarms like IL-33 cytokines that are tissue-derived nuclear proteins released after damage, activate NKT cells to recruit neutrophils by IFN- γ and IL-17A release (Ferhat et al., 2018). By this means, NKT cells regulate the initial process of sterile inflammation in the kidney (Li et al., 2007). IFN- γ cytokines are the important downstream effector molecular of NKT cells. Spontaneous, local, and probably extravascular activation events of NKT cells in the liver and kidney result in the local secretion of IFN- γ (Zeng and Howard, 2010; Aguiar et al., 2015). NKT cells injured kidney vascular endothelial cells by perforin-mediated pathway and tubular epithelial cells by tumor necrosis factor (TNF)- α /FasL pathway, leading to AKI with hematuria in mice. The human CD56⁺ T cells, a counterpart of mouse NKT cells, exerted their similar functions (Uchida et al., 2018). Natural Immunoglobulin M (IgM) anti-leukocyte autoantibodies (IgM-ALAs) (Lobo et al., 2017) and A2AR agonists (Li et al., 2012) attenuated AKI by suppressing NKT cells. However, studies on type II NKT cells found that they abrogated kidney IRI. *In vitro*, type II NKT cells attenuated tubular apoptosis after transient hypoxia through hypoxia-inducible factor (HIF)-1 α and IL-10 pathways (Yang et al., 2011).

In adenine-induced renal injury, administration of α GalCer to activate iNKT cells reduced renal fibrosis. CD1d-dependent NKT cells improved non-alcoholic fatty liver disease (NAFLD)-associated CKD *via* reducing renal inflammation, mesangial cell proliferation, and tubular cell apoptosis (Alhasson et al., 2016). Besides that, IL-22 cytokines produced by NKT cells have been proved to play a protective or pathogenic role in chronic inflammation depending on the nature of the influenced tissues and the cytokine microenvironment (Witte et al., 2010; Dudakov et al., 2015). These data imply that NKT cells in the kidney have dual effects depending on the polytropic inflammatory milieu.

Gamma Delta T Cells

Gamma delta T cells are another type of T cells, distinguishing from $\alpha\beta$ T cells based on the distinct TCR types. They are triggered by stress-induced ligands from aberrant cells without antigen processing and presentation, thus acting in the initial phase of injury and playing a major role in bridging innate and adaptive immune responses (Patil et al., 2015).

Gamma delta T cells are one of the sources of IL-17A that is increased in cisplatin-induced AKI and UO-induced renal fibrosis (Huen and Cantley, 2017; D'Alessio et al., 2019). However, depletion of $\gamma\delta$ T cells did not ameliorate cisplatin-induced renal injury, indicating $\gamma\delta$ T cells were unnecessary to injury (Chan et al., 2014). Even so, $\gamma\delta$ T cells responded very quickly to human AKI. The decrease in circulating $\gamma\delta$ T cells and increase in kidney $\gamma\delta$ T cells demonstrated the possibility of their migration from circulation to kidney tissues. The changes of infiltrated $\gamma\delta$ T cells were correlated with the elevated biomarkers of tubular stress or injury (Gocze et al., 2018). Analysis of kidney

biopsy tissues from patients with renal fibrosis showed that larger numbers of $\gamma\delta$ T cells were infiltrated in kidneys with lower estimated glomerular filtration rate (eGFR), which suggested the negative correlation between $\gamma\delta$ T cell number and loss of renal function. In addition, fibrotic tissues contained significantly more $V\delta 1^+$ $\gamma\delta$ T cells, and $CD161^+$ $\gamma\delta$ T cells displayed an innate-like cytotoxic phenotype. Furthermore, the localization and the expression of IL-17A of $\gamma\delta$ T cells implied that they might mediate the survival of PTECs (Law et al., 2019a). These data from animal experiments and clinical studies showed that $\gamma\delta$ T cells are pathogenic factors for renal injury and fibrosis by promoting IL-17A production.

Mucosa-Associated Invariant T Cells

Mucosa-associated invariant T cells are one of the innate-like T cell subtypes recognizing riboflavin metabolites depending on the MHC-related molecule 1. When activated, they rapidly produce various proinflammatory cytokines suggesting their detrimental roles in chronic inflammatory diseases (Howson et al., 2015). MAIT cells are enriched in the gut, liver, and lung to defend against pathogen attack (Le Bourhis et al., 2010). In recent years, only one article published in Journal of the American Society of Nephrology (JASN) addressed that tissue-resident MAIT cells in human kidneys might contribute to the fibrotic process of CKD by complex interactions with PTECs. In this study, researchers found that MAIT cells were increased in the tissue samples from fibrotic kidneys compared with those from non-fibrotic kidneys. And the numbers of MAIT cells were correlated with loss of kidney function. Furthermore, these MAIT cells accumulated adjacent to PTECs, and highly expressed activation marker CD69 cytotoxic molecules perforin and granzyme B, which led to PTEC necrosis (Law et al., 2019b). Despite that, further studies of MAIT cells are necessary to unequivocally determine the non-redundant role in CKD pathogenesis.

Recently, the application of high-dimensional cellular analyses, such as single-cell RNA sequencing (scRNA-seq), has helped researchers to figure out detailed characterization of immune cell population in kidney disease. The research on patients with kidney transplant rejection showed that recipient-origin T-cells expressed proinflammatory genes, whereas donor-origin T-cells expressed oxidative phosphorylation genes, which indicated that T cells from two sources had distinct transcriptional profiles (Malone et al., 2020). In addition, the technique of scRNA-seq has been used to identify $CD4^+$ tissue-resident memory T cells with a Th17 signature in the kidney of patients with antineutrophil cytoplasmic antibody-associated glomerulonephritis and dysfunction of $CD8^+$ T cells in patients with SLE and IgA nephropathy (Krebs et al., 2020; Maria and Davidson, 2020). However, this advanced technique is rarely used in studies on AKI, which may be due to the lack of samples from patients of AKI. Our team has recently identified four subcluster macrophages at different time points in the I/R model and analyzed the transition of $Arg1^+$ macrophages (Cluster 1) into $Ccr2^+$ macrophages (inflammatory Cluster 0) (Zhu et al., 2021). In a further study, we will focus on the identification of

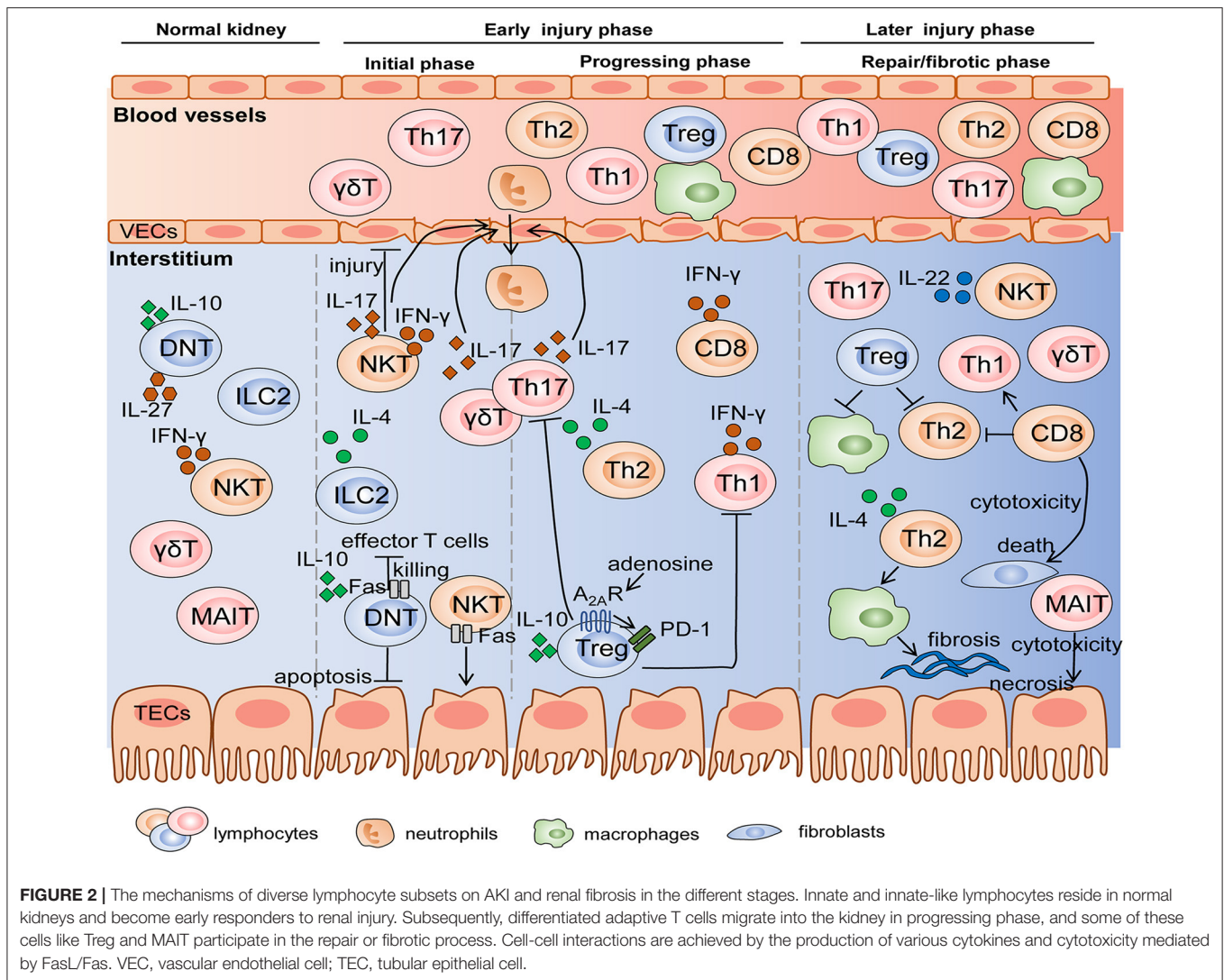
lymphocyte characteristics and analyze different functions of subtypes in AKI and CKD.

VERSATILE LYMPHOCYTES IN AKI AND CKD: CHRONOLOGICAL RESPONSES AND PLASTICITY

The pathogenesis of AKI and CKD is a complicated process with the involvement of multicellular and multifactor in the above elaboration. These pleiotropic immune cells respond to injury in a chronological order according to their immunological characteristics and mechanisms of damage responses (shown in Figure 2). It is indispensable to determine the “time window” of distinct lymphocytes, which will guide precise therapies targeting corresponding effector cells at different stages of injury.

In general, innate and innate-like lymphocytes respond rapidly to organ injury. For instance, NKT cells and $\gamma\delta$ T cells were immediate participants in the hyperacute immune responses following the first 6 h of trauma and hemorrhagic shock (Manson et al., 2019). In the kidney, Hochegger et al. confirmed that $\alpha\beta$ T cells were the major effector cells, whereas $\gamma\delta$ T cells acted as mediator cells in the first 72 h of renal IR-induced injury, bridging immediate innate and subsequent adaptive immunity. Deficiency of $\alpha\beta$ T cells reduced renal functional and histological damage 72 h after IR, but had no influence on renal function 24 h after IR. Moreover, infiltration of $\gamma\delta$ T cells into kidney was equal in $\alpha\beta$ T cell-deficient mice and wild-type mice, whereas, lack of $\gamma\delta$ T cells led to the significant decrease in $\alpha\beta$ T cells until 120 h after IR, suggesting an interaction between $\alpha\beta$ T cells and $\gamma\delta$ T cells. These data indicated that $\gamma\delta$ T cells functioning in the early injury stage might be a driver of $CD4^+$ and $CD8^+$ T responses in the later stage (Hochegger et al., 2007). DNT cells are also early responders, which significantly expanded, and rapidly became the major subpopulation 3 h after IRI and remained dominant until 24 h. However, they decreased to the level below steady state by 72 h after IRI. DNT cells are a dominant kidney-resident subset and largely produce cytokines at the steady state, which may be one explanation why they respond so quickly to AKI in an innate-like manner (Martina et al., 2016). Besides that, NKT cells and ILC2s are also considered as initial responders to kidney injury due to their innate-immune and tissue-resident properties. They are activated and expanded by molecules released from damaged cells without the involvement of antigen-presenting cells, while adaptive T cells need to go through the process of differentiation, thus determining their delayed responses to kidney injury (Cao et al., 2018; Ferhat et al., 2018). Therefore, we cannot ignore the crucial effects of innate and innate-like lymphocytes, a pioneer of AKI, whether they are beneficial or detrimental.

After innate immunity activation, adaptive T lymphocytes come on stage and they persist activated from acute to chronic phase. Th1/Th2 balance regulated renal injury 24 and 48 h after IR (Marques et al., 2006). Th17 cells produced IL-17 cytokines to recruit neutrophils, thus influencing early kidney injury events with dramatical enhancement at day 1 and day 3 post IR and recovery to the baseline at day 7. The second expansion of Th17



cells existed with the high-salt diet hit (Mehrotra et al., 2015, 2019). Tregs trafficked into the kidney to suppress the function of Th1, Th2, and Th17 at day 3 post IR and involved in repair at day 10 (Gandolfo et al., 2009). In addition, Th2 also mediated tubular reparation and promoted fibrosis with excessive repair (Marques et al., 2006). In summary, early responses of innate and resident lymphocytes along with later responses of adaptive T cells participate in the pathogenesis of AKI and T cells related to tissue repair or fibrosis engage in the subsequent CKD progression.

In renal IRI, a clear M1-to-M2 phenotypic switch occurs, which provides the possibility that the same cell possesses plasticity under the changes of microenvironment (Tang et al., 2019). Like macrophages, the plasticity of CD4⁺ T cells is also reflected in immune-mediated kidney disease (Krebs and Panzer, 2018). The expressions of their lineage-specific master transcription factors are dynamic and cross-regulation. The co-expressions of these transcription factors result in CD4⁺ T cell plasticity (Zhu, 2018). Researchers found the conversion of Tregs to IL-17⁺ phenotypic cells enhanced renal fibrosis

in UUO mice, which was prevented by inhibition of histone deacetylase (HDAC) activity suggesting the importance of epigenetic modifications (Wu et al., 2017). Besides CD4⁺ T cells, ILC2s can also switch into ILC1s or ILC3s due to yet unknown triggers (Krabbendam et al., 2018). Differentiated T cells have the potential to dedifferentiate and undergo the shift to another subtype, which is driven by a complex network of signals under the microenvironment of AKI and CKD. Nevertheless, whether this plasticity occurs, which form it presents with and which signals trigger it remains to be further studied, aiming to provide enough evidence of the possibility of modulating cell-cell plasticity to alleviate inflammatory kidney diseases (Rajendran et al., 2019).

POTENTIAL THERAPIES TARGETING LYMPHOCYTES OF AKI AND CKD

Based on the versatile lymphocytes engaging in the process of AKI and CKD, what targeting these players may be potential

TABLE 3 | The treatments targeting of lymphocytes *in vivo*.

| Agents | Descriptions | Species | Models | <i>In vivo</i> effects | References |
|-------------------------------|--|---------|---|---|--------------------------|
| IL-18 Bp | A IL-18 inhibitor | Mouse | IR | T cell infiltration ↓ Renal fibrosis ↓ | Wu et al., 2017 |
| soluble ST2 (sST2) | A decoy receptor Neutralizing IL-33 activity | Mouse | IR | T cell infiltration ↓ Renal function ↓ Renal injury score ↓ Renal fibrosis ↓ | Krabbendam et al., 2018 |
| BX471 | A CCR1 blocker | Mouse | UUO | T cell infiltration ↓ Renal fibrosis ↓ Histopathological injury ↓ | Hochegger et al., 2007 |
| Margatoxin | A Kv1.3-channel inhibitor | Rat | UUO | T cell infiltration, proliferation and cytokine production ↓ Renal fibrosis ↓ | Rajendran et al., 2019 |
| ICG-001 | A Wnt/ β -catenin pathway inhibitor | Rat | 5/6 nephrectomy | T cell infiltration ↓ Renal function ↓ Renal fibrosis ↓ | Anders et al., 2002 |
| YM58343/BTP2 | A calcium-channel inhibitor | Rat | IR | Th17 activation ↓ Renal function ↓ Acute renal injury ↓ Renal fibrosis ↓ | Mehrotra et al., 2019 |
| IL-17Rc | The IL-17Rc soluble receptor | Mouse | IR | Th17 activation ↓ Renal fibrosis ↓ | Mehrotra et al., 2017 |
| Losartan | An angiotensin receptor 1 (AT1) antagonist | Mouse | UUO | Treg accumulation ↑ | Mehrotra et al., 2015 |
| | | Rat | IR | Th17 number ↓ Renal function ↓ Renal fibrosis ↓ | |
| IL-36Rn | IL-36R Antagonist | Mouse | UUO | Th17 differentiation ↓ Renal fibrosis ↓ | Chi et al., 2017 |
| MSCs and paricalcitol | Co-administration of MSCs and a vitamin D receptor agonist | Mouse | UUO | CD4+ and CD8+ T cell accumulation ↓ Th17 differentiation ↓ Renal fibrosis ↓ | Duffy et al., 2014 |
| Trichostatin A (TSA) | A histone deacetylase (HDAC) inhibitor | Mouse | UUO | CD4+IL-17+ T cell percentage ↓ Renal fibrosis ↓ | Maria and Davidson, 2020 |
| Periodate-oxidized ATP (oATP) | A P2X7 receptor (P2X7R) antagonist | Mouse | IR | Treg infiltration ↑ Tubular injury ↓ Renal fibrosis ↓ | Koo et al., 2017 |
| IL-2/ | – | Mouse | IR | Treg number ↑ Renal function ↑ Tubular injury ↓ Renal fibrosis ↓ | Kim et al., 2013 |
| Anti-IL-2 complex (IL-2C) | | | | | |
| Rapamycin | A mTOR inhibitor | Mouse | IR | Treg number ↑ Acute kidney injury ↓ Renal fibrosis ↓ | Liang et al., 2018 |
| Resolvin D1 | An endogenous lipid mediator | Mouse | IR | Treg percentage ↑ Tubular injury ↓ | Luan et al., 2020 |
| IL-233 | A hybrid cytokine bearing IL-2 and IL-33 | Mouse | Cisplatin- and doxorubicin-induced nephrotoxic renal injury | Treg and ILC2 number and proportion ↑ Renal function ↑ Tubular injury ↓ Renal fibrosis ↓ | Sabapathy et al., 2019 |
| | | | | Treg number ↑ Renal function ↑ Tubular injury ↓ | |
| Astaxanthin | A natural and nontoxic xanthophyll carotenoid | Mouse | UUO | CD8+ T cell recruitment ↑ Renal fibrosis ↓ | Diao et al., 2019 |

(Continued)

TABLE 3 | Continued

| Agents | Descriptions | Species | Models | <i>In vivo</i> effects | References |
|--------|--------------|---------|--------|--|--------------------|
| IL-25 | – | Mouse | IR | ILC2 frequency ↑ Tubular injury ↓ | Huang et al., 2015 |
| IL-33 | – | Mouse | IR | ILC2 and Treg number ↑ Renal function ↑ Tubular injury ↓ | Cao et al., 2018 |

strategies for ameliorating the inflammation-mediated diseases, including the interventions of lymphocyte activities *in vivo*, the adaptive transfers of ex-expanded beneficial lymphocytes like Tregs, and the treatments based on the gut-kidney axis.

Targeting of Lymphocytes *in vivo*

BX471, a CCR1 blocker, reduced renal fibrosis in mice of UUO by decreasing the T cell infiltration, which represented that blocking chemokines and respective receptors might be a potential therapeutic strategy for alleviating renal fibrosis (Anders et al., 2002). However, CCL20 blockade increased the severity of FA-induced AKI, which might be related to a lower infiltration of Tregs in spite of a decrease in proinflammatory Th17 influx (Gonzalez-Guerrero et al., 2018). Therefore, the treatments targeting chemokines and their receptors should be considered for their non-specificity for recruiting lymphocytes.

Inhibiting IL-18 by IL-18 binding protein (Bp) also impaired T cell infiltration and reduced IR-induced renal fibrosis (Liang et al., 2018). In addition, IL-25 treatment protected mice against IRI by elevating ILC2 frequency (Huang et al., 2015). Interestingly, the administration of IL-33 is a double-edged sword. On the one hand, IL-33 ameliorated IR-induced AKI by expanding ILC2 and Tregs (Cameron et al., 2019a). On the other hand, soluble ST2 (sST2), a decoy receptor that neutralizes IL-33 activity, also reduced renal IRI by lowering CD3⁺ cell level (Liang et al., 2017). The dosage of IL-33, the duration of administration, and the severity and the stage of renal injury may remarkably alter the responses performed to be beneficial or deleterious. IL-233 is a hybrid cytokine bearing IL-2 and IL-33. IL-233 increased the number of Tregs and ILC2s in doxorubicin-induced nephrotoxic renal injury and enhanced Treg influx in IRI, thus playing a protective role in AKI of the two models (Stremaska et al., 2017; Sabapathy et al., 2019). Moreover, IL-17Rc inhibited Th17 activation leading to significantly mitigate renal fibrosis (Mehrotra et al., 2017). The administration of an IL-36R antagonist after UUO attenuated tubulointerstitial lesions (TILs) that might be associated with the reduction of Th17 differentiation (Chi et al., 2017). IL-2/anti-IL-2 complex (IL-2C) protected against mouse IRI by inducing Treg expansion (Kim et al., 2013). Thus, various cytokines as the main effector molecules are the valuable target of T cells to treat AKI and CKD.

Besides that, as one of the inhibitors of delayed rectifier K⁺-channel, Kv1.3 like margatoxin (Abe et al., 2019) and YM58343/BTP2 (Mehrotra et al., 2019) were expressed on T lymphocytes, and also found to acute injury and chronic fibrosis in rat kidney. T cell infiltration was decreased by a wingless-type

(Wnt)/β-catenin pathway inhibitor, ICG-001, which therefore prevented CKD in a 5/6 nephrectomy model (Xiao et al., 2019). Many other agents, including losartan (Mehrotra et al., 2015), periodate-oATP (Koo et al., 2017), rapamycin (Chen et al., 2016), and resolvin D1 (Luan et al., 2020) augmented Treg accumulation to reduce renal damage and promote recovery. Mesenchymal stem cells (MSCs) supplemented with a vitamin D receptor agonist inhibited Th17 differentiation (Duffy et al., 2014). Astaxanthin promoted CD8⁺ T cell recruitment (Diao et al., 2019), and a HDAC inhibitor, trichostatin A (TSA), lowered CD4⁺ IL-17⁺ T cell percentage (Wu et al., 2017). All of these treatments prevented renal fibrosis. Besides that, Kynorenin as an important immune modulator was found highly predictive for “major adverse kidney events” of contrast induced AKI (Reichetzedder et al., 2017). These data suggest how to expand beneficial T cells and reduce pathogenic ones *in vivo* is the focus issue. In summary, the treatments targeting lymphocytes *in vivo* were listed in Table 3.

Adaptive Transfer of Ex-expanded Lymphocytes

In animal experiments, adaptive transfer of beneficial lymphocytes such as Tregs, DNT cells, and ILC2s can effectively reduce renal injury caused by IR and nephrotoxins. Treg-based cellular therapy has been extensively studied in recent years. Studies have shown that Tregs protect allografts in kidney transplant models of mice due to their immunosuppressive function. However, clinical translation is challenging. Treg preparations, dose, and frequency are worthy of consideration. In addition, the instability and variability of Tregs arise safety concerns, thus Tregs should be identified and quantified prior to transplant trials (Chandran et al., 2017; Tang and Vincenti, 2017; Zwang and Leventhal, 2017; Savage et al., 2018). Nevertheless, Treg therapy has not been applied to treat patients with AKI and CKD. The efficacy and safety need to be further explored. The modifications of beneficial lymphocytes *in vitro* regulate their protective effects. CD73-deficient or A_{2A}R-deficient Tregs failed to protect mice from IRI suggesting that the response to adenosine was required to Treg to suppress inflammation, and the induction of A_{2A}R on Tregs augmenting the protective functions verified this hypothesis (Kinsey et al., 2012). TLR9 expression regulated the migration of transferred Tregs into the kidney (Alikhan et al., 2016). IL-233-treated mice were preferred donors, of which Tregs exerted a beneficial effect on alleviating renal IRI, and this protection depended on the cell dosages (Stremaska et al., 2017). Ex-expanded Tregs also promoted renal

TABLE 4 | Adaptive transfer of ex-expanded lymphocytes.

| Subsets | Dosages | Species of recipients | Methods | Effects | References |
|-----------|---|-----------------------|--------------------------------------|---|-------------------------|
| Tregs | 1.0 × 10 ⁵ cells | Mouse | Before IR | Wild-type Tregs protected mice from IRI. CD73-deficient or A _{2A} R-deficient Tregs failed to protect mice from IRI. Pharmacologic stimulation of A _{2A} R on Tregs augmented the protective functions. | Dong et al., 2019 |
| Tregs | 2.0 × 10 ⁶ cells | Mouse | 24 h before cisplatin administration | Adaptive transfer of wild-type Tregs resulted in less severe cisplatin-induced AKI than that of TLR9-deficient Tregs. TLR9 promoted Treg recruitment. | Kinsey et al., 2010 |
| Tregs | 50 × 10 ³ cells 100 × 10 ³ cells | Mouse | 24 h before IR | Tregs from IL-233-treated mice played better protective roles in IRI at lower doses (50 × 10 ³). Tregs at higher doses (100 × 10 ³) had no protective roles. | Mu et al., 2020 |
| Tregs | 2.0 × 10 ⁶ cells | Mouse | 24 h after IR | Rapamycin-treated Tregs enhanced beneficial effects on reducing IRI on the early (3 d) and later (14 d) repair stages. | Krabbendam et al., 2018 |
| Tregs | 1.2 × 10 ⁶ cells | Mouse | 24 h after IR | Tregs promoted kidney repair after IRI. | Liu et al., 2018 |
| DNT cells | 1.0–1.5 × 10 ⁶ cells | Mouse | 24 h before cisplatin administration | DNT cells attenuated cisplatin-induced AKI. | Alexander et al., 2020 |
| DNT cells | 2.5 × 10 ⁶ cells | Mouse | 24 h before IR | DNT cells protected mice from AKI in a IL-10-dependent manner. | Diao et al., 2019 |
| ILC2s | 1.0 × 10 ⁶ cells | Mouse | 24 h before IR | IL-33-treated ILC2s prevented renal injury in an Areg-dependent manner. Human-derived ILC2s ameliorated renal IRI in mice. | Wang Y. M. et al., 2017 |
| ILC2s | 5.0 × 10 ⁵ cells | Mouse | 24 h before IR | IL-233-treated ILC2s protected mice from IRI | Mu et al., 2020 |

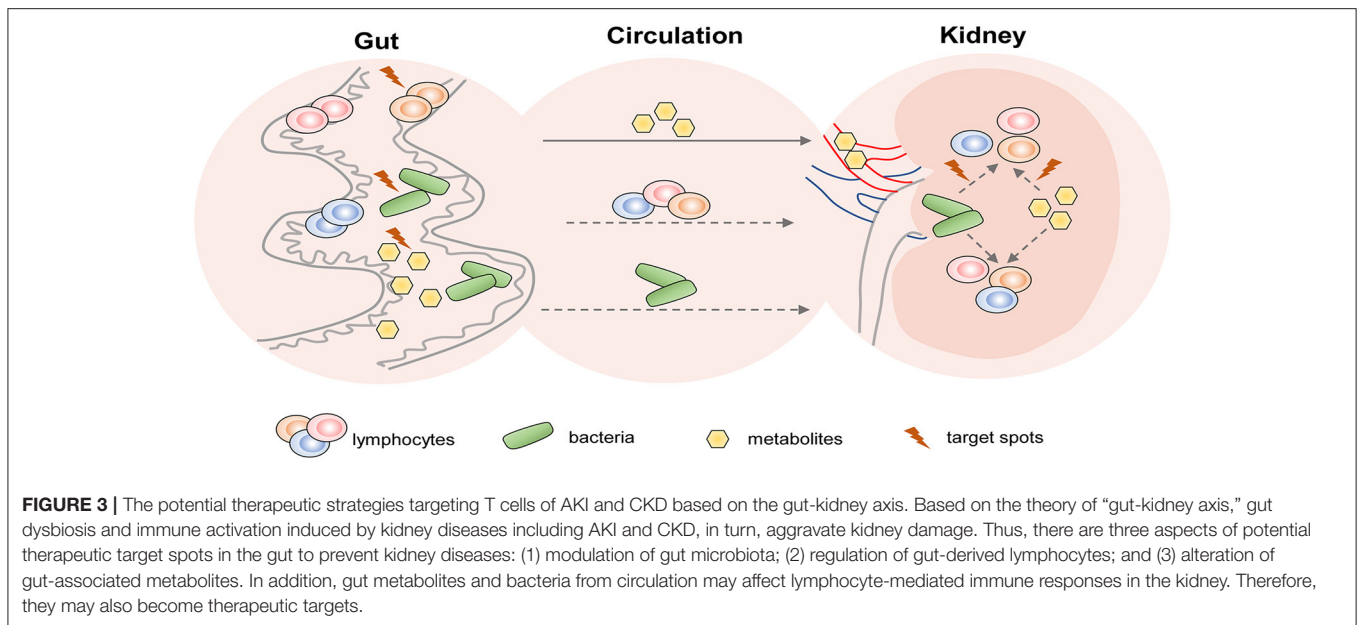
repair and rapamycin, an inhibitor of mammalian target of rapamycin (mTOR), enhanced their pro-repair effects (Gandolfo et al., 2009; Chen et al., 2016). Besides that, DNT cells protected mice against both cisplatin- and IR-induced renal injury, and the process of the latter was in an IL-10-dependent manner (Martina et al., 2016; Gong et al., 2020). For ILC2s, IL-33 and IL-233 treatment promoted their protection of the kidney against IRI. Furthermore, human-derived ILC2s ameliorated renal damage in mice (Stremaska et al., 2017; Sabapathy et al., 2019). In conclusion, the administration of ex-expanded beneficial lymphocytes might prevent renal injury, which is listed in **Table 4**.

Potential Therapeutic Strategies Targeting T Cells Based on the Regulation of the Gut-Kidney Axis

Recently, the crosstalk of gut and kidney has been a hot spot. Gut-derived metabolites, short-chain fatty acids (SCFAs), were confirmed to prevent AKI. *In vitro*, SCFAs regulated the inflammatory process, in which dendritic cells were inhibited in the capacity of induced CD4⁺ and CD8⁺ T cell proliferation (Andrade-Oliveira et al., 2015). Acetate, one of the SCFAs, ameliorated AKI by redressing oxidant-antioxidant imbalance of T cells dependent on nicotinamide adenine dinucleotide phosphate (NADPH) oxidase (NOX2)/reactive oxygen species

(ROS) signaling (Al-Harbi et al., 2018). The intestine microbiota has a potential immunoregulatory role in CKD. The pathogen overgrowth in the gut under the metabolic alterations of uremia, and an increase of bacteria or their component translocation may activate systemic inflammation concerned with lymphocyte-participated immunity (Anders et al., 2013). The development and application of multi-omics analysis technique have helped us to screen out specific-altered gut microbiota and metabolites that may be associated with T cell immunity modulation in kidneys.

Gut microbiota depletion by oral antibiotics was proved to protect against IR-induced AKI in mice and the protective role was related to Th1 and Th17 decrease accompanied by Treg expansion in kidneys (Yang et al., 2020). The reduction of *Lactobacilli* was one of the hallmarks of IRI-induced gut microbial dysbiosis (Yang et al., 2020), and a similar decrease was discovered in CKD (Yang et al., 2019). Oral administration of *Lactobacilli* led to improvements in SCFAs (Vemuri et al., 2019). Therefore, supplementation of probiotics like *Lactobacilli* may be a promising strategy for AKI and CKD therapies. However, the following three questions remained to be solved: (1) Whether the reno-protective role of probiotics is achieved through the modulations of lymphocytes? (2) How do they act on lymphocytes? (3) What is the connection



of lymphocyte alterations between the gut and kidneys? The potential therapeutic strategies of AKI and CKD based on the gut-kidney axis deserve further studies (shown in **Figure 3**).

CONCLUSIONS

Lymphocytes mediate non-autoimmune AKI and subsequent CKD in a full-course manner. The diversity and plasticity of lymphocytes result in their multifunction for renal injury and fibrosis. Innate and adaptive lymphocytes cooperate in the process and present a phenomenon of chronological responses, which suggests the importance of the distinct “time windows” of therapies targeting different lymphocyte subsets. Interventions of lymphocytes *in vivo* and adaptive transfer of these cells have provided the prospect of lymphocyte-related therapeutic strategies. The modulations of gut microbiota and metabolites to regulate AKI- or CKD-associated lymphocyte immune responses show therapeutic potential for future drug development for kidney diseases. Despite many efforts made to explore the mechanisms of lymphocyte regulations to prevent AKI and subsequent renal fibrosis or promote renal repair, some problems

remain to be addressed in the future: (1) What are the sources of the renal infiltrated lymphocytes, and what are the relationships between these lymphocytes and those of extrarenal organs? (2) How to achieve precise intervention on pathogenic lymphocytes without affecting systemic immunity? With the development of the technique of single-cell RNA sequencing, we are looking forward to a deeper understanding of lymphocyte subtypes and functions, which guide more precise and specific interventions to treat AKI and CKD.

AUTHOR CONTRIBUTIONS

CC: writing—original draft. YY: conceptualization and supervision. RZ: writing—reviewing and editing. All authors contributed to the article and approved the submitted version.

FUNDING

This study was financially supported by the National Natural Science Foundation of China (Grant Nos: 81770681, 81974086, 81770684, and 81974087).

REFERENCES

- Abe, N., Toyama, H., Saito, K., Ejima, Y., Yamauchi, M., Mushiaki, H., et al. (2019). Delayed rectifier K(+)-channel is a novel therapeutic target for interstitial renal fibrosis in rats with unilateral ureteral obstruction. *Biomed. Res. Int.* 2019:7567638. doi: 10.1155/2019/7567638
- Aguiar, C. F., Naffah-de-Souza, C., Castoldi, A., Correa-Costa, M., Braga, T. T., Naka, E. L., et al. (2015). Administration of alpha-Galactosylceramide improves adenine-induced renal injury. *Mol. Med.* 21, 553–562. doi: 10.2119/molmed.2014.00090
- Alexander, J. J., Jacob, A., Chang, A., Quigg, R. J., and Jarvis, J. N. (2020). Double negative T cells, a potential biomarker for systemic lupus erythematosus. *Precis. Clin. Med.* 3, 34–43. doi: 10.1093/pccmedi/pbaa001
- Al-Harbi, N. O., Nadeem, A., Ahmad, S. F., Alotaibi, M. R., AlAsmari, A. F., Alanazi, W. A., et al. (2018). Short chain fatty acid, acetate ameliorates sepsis-induced acute kidney injury by inhibition of NADPH oxidase signaling in T cells. *Int. Immunopharmacol.* 58, 24–31. doi: 10.1016/j.intimp.2018.02.023
- Alhasson, F., Dattaroy, D., Das, S., Chandrashekar, V., Seth, R. K., Schnellmann, R. G., et al. (2016). NKT cell modulates NAFLD potentiation of metabolic oxidative stress-induced mesangial cell activation and proximal tubular toxicity. *Am. J. Physiol. Renal Physiol.* 310, F85–F101. doi: 10.1152/ajprenal.00243.2015
- Alikhan, M. A., Summers, S. A., Gan, P. Y., Chan, A. J., Khouri, M. B., Ooi, J. D., et al. (2016). Endogenous toll-like receptor 9 regulates AKI by promoting regulatory T Cell recruitment. *J. Am. Soc. Nephrol.* 27, 706–714. doi: 10.1681/ASN.2014090927

- Alobaidi, R., Basu, R. K., Goldstein, S. L., and Bagshaw, S. M. (2015). Sepsis-associated acute kidney injury. *Semin. Nephrol.* 35, 2–11. doi: 10.1016/j.semnephrol.2015.01.002
- Anders, H.-J., Vielhauer, V., Frink, M., Linde, Y., Cohen, C. D., Blattner, S. M., et al. (2002). A chemokine receptor CCR-1 antagonist reduces renal fibrosis after unilateral ureter ligation. *J. Clin. Invest.* 109, 251–259. doi: 10.1172/JCI0214040
- Anders, H. J., Andersen, K., and Stecher, B. (2013). The intestinal microbiota, a leaky gut, and abnormal immunity in kidney disease. *Kidney Int.* 83, 1010–1016. doi: 10.1038/ki.2012.440
- Andrade-Oliveira, V., Amano, M. T., Correa-Costa, M., Castoldi, A., Felizardo, R. J., de Almeida, D. C., et al. (2015). Gut bacteria products prevent AKI induced by ischemia-reperfusion. *J. Am. Soc. Nephrol.* 26, 1877–1888. doi: 10.1681/ASN.2014030288
- Ascon, D. B., Ascon, M., Satpute, S., Lopez-Briones, S., Racusen, L., Colvin, R. B., et al. (2008). Normal mouse kidneys contain activated and CD3+CD4- CD8-double-negative T lymphocytes with a distinct TCR repertoire. *J. Leukoc. Biol.* 84, 1400–1409. doi: 10.1189/jlb.0907651
- Ascon, D. B., Lopez-Briones, S., Liu, M., Ascon, M., Savransky, V., Colvin, R. B., et al. (2006). Phenotypic and functional characterization of kidney-infiltrating lymphocytes in renal ischemia reperfusion injury. *J. Immunol.* 177, 3380–3387. doi: 10.4049/jimmunol.177.5.3380
- Borger, J. G., Lau, M., and Hibbs, M. L. (2019). The influence of innate lymphoid cells and unconventional T cells in chronic inflammatory lung disease. *Front. Immunol.* 10:1597. doi: 10.3389/fimmu.2019.01597
- Braga, T. T., Correa-Costa, M., Guise, Y. F., Castoldi, A., de Oliveira, C. D., Hyane, M. I., et al. (2012). MyD88 signaling pathway is involved in renal fibrosis by favoring a TH2 immune response and activating alternative M2 macrophages. *Mol. Med.* 18, 1231–1239. doi: 10.2119/molmed.2012.00131
- Brandt, D., and Hedrich, C. M. (2018). TCRalpha(+)CD3(+)CD4(-)CD8(-) (double negative) T cells in autoimmunity. *Autoimmun. Rev.* 17, 422–430. doi: 10.1016/j.autrev.2018.02.001
- Burne, M. J., Daniels, F., El Ghandour, A., Mauyyedi, S., Colvin, R. B., O'Donnell, M. P., et al. (2001). Identification of the CD4+ T cell as a major pathogenic factor in ischemic acute renal failure. *J. Clin. Invest.* 108, 1283–1290. doi: 10.1172/JCI200112080
- Cameron, G. J. M., Cautivo, K. M., Loering, S., Jiang, S. H., Deshpande, A. V., Foster, P. S., et al. (2019b). Group 2 innate lymphoid cells are redundant in experimental renal ischemia-reperfusion injury. *Front. Immunol.* 10:826. doi: 10.3389/fimmu.2019.00826
- Cameron, G. J. M., Jiang, S. H., Loering, S., Deshpande, A. V., Hansbro, P. M., and Starkey, M. R. (2019a). Emerging therapeutic potential of group 2 innate lymphoid cells in acute kidney injury. *J. Pathol.* 248, 9–15. doi: 10.1002/path.5242
- Cao, Q., Wang, Y., Niu, Z., Wang, C., Wang, R., Zhang, Z., et al. (2018). Potentiating tissue-resident Type 2 innate lymphoid cells by IL-33 to prevent renal ischemia-reperfusion injury. *J. Am. Soc. Nephrol.* 29, 961–976. doi: 10.1681/ASN.2017070774
- Chan, A. J., Alikhan, M. A., Odobasic, D., Gan, P. Y., Khouri, M. B., Steinmetz, O. M., et al. (2014). Innate IL-17A-producing leukocytes promote acute kidney injury via inflammasome and Toll-like receptor activation. *Am. J. Pathol.* 184, 1411–1418. doi: 10.1016/j.ajpath.2014.01.023
- Chandran, S., Tang, Q., Sarwal, M., Laszik, Z. G., Putnam, A. L., Lee, K., et al. (2017). Polyclonal regulatory T cell therapy for control of inflammation in kidney transplants. *Am. J. Transplant.* 17, 2945–2954. doi: 10.1111/ajt.14415
- Chen, G., Dong, Z., Liu, H., Liu, Y., Duan, S., Liu, Y., et al. (2016). mTOR signaling regulates protective activity of transferred CD4+Foxp3+ T cells in repair of acute kidney injury. *J. Immunol.* 197, 3917–3926. doi: 10.4049/jimmunol.1601251
- Chen, K., Zhou, Q. X., Shan, H. W., Li, W. F., and Lin, Z. F. (2015). Prognostic value of CD4(+)CD25(+) Tregs as a valuable biomarker for patients with sepsis in ICU. *World J. Emerg. Med.* 6, 40–43. doi: 10.5847/wjem.j.1920-8642.2015.01.007
- Chen, W., Ford, M. S., Young, K. J., and Zhang, L. (2004). The role and mechanisms of double negative regulatory T cells in the suppression of immune responses. *Cell. Mol. Immunol.* 1, 328–335. Available online at: <http://www.cmi.ustc.edu.cn/1/5/328.pdf>
- Chi, H. H., Hua, K. F., Lin, Y. C., Chu, C. L., Hsieh, C. Y., Hsu, Y. J., et al. (2017). IL-36 signaling facilitates activation of the NLRP3 inflammasome and IL-23/IL-17 axis in renal inflammation and fibrosis. *J. Am. Soc. Nephrol.* 28, 2022–2037. doi: 10.1681/ASN.2016080840
- Chung, A. C., and Lan, H. Y. (2011). Chemokines in renal injury. *J. Am. Soc. Nephrol.* 22, 802–809. doi: 10.1681/ASN.2010050510
- Colonna, M. (2018). Innate lymphoid cells: diversity, plasticity, and unique functions in immunity. *Immunity* 48, 1104–1117. doi: 10.1016/j.immuni.2018.05.013
- Constantinides, M. G. (2018). Interactions between the microbiota and innate and innate-like lymphocytes. *J. Leukoc. Biol.* 103, 409–419. doi: 10.1002/JLB.3RI0917-378R
- Corpuz, T. M., Vazquez-Lombardi, R., Luong, J. K., Warren, J., Stolp, J., Christ, D., et al. (2017). IL-2 shapes the survival and plasticity of IL-17-Producing gammadelta T Cells. *J. Immunol.* 199, 2366–2376. doi: 10.4049/jimmunol.1700335
- Cortvrindt, C., Speckaert, R., Moerman, A., Delanghe, J. R., and Speckaert, M. M. (2017). The role of interleukin-17A in the pathogenesis of kidney diseases. *Pathology* 49, 247–258. doi: 10.1016/j.pathol.2017.01.003
- Crispin, J. C., Oukka, M., Bayliss, G., Cohen, R. A., Van Beek, C. A., Stillman, I. E., et al. (2008). Expanded double negative T cells in patients with systemic lupus erythematosus produce IL-17 and infiltrate the kidneys. *J. Immunol.* 181, 8761–8766. doi: 10.4049/jimmunol.181.12.8761
- D'Alessio, F. R., Kurzhagen, J. T., and Rabb, H. (2019). Reparative T lymphocytes in organ injury. *J. Clin. Invest.* 129, 2608–2618. doi: 10.1172/JCI124614
- de Paiva, V. N., Monteiro, R. M., Marques Vde, P., Cenedeze, M. A., Teixeira Vde, P., dos Reis, M. A., et al. (2009). Critical involvement of Th1-related cytokines in renal injuries induced by ischemia and reperfusion. *Int. Immunopharmacol.* 9, 668–672. doi: 10.1016/j.intimp.2008.11.012
- Diao, W., Chen, W., Cao, W., Yuan, H., Ji, H., Wang, T., et al. (2019). Astaxanthin protects against renal fibrosis through inhibiting myofibroblast activation and promoting CD8(+) T cell recruitment. *Biochim. Biophys. Acta Gen. Subj.* 1863, 1360–1370. doi: 10.1016/j.bbagen.2019.05.020
- do Valle Duraes, F., Lafont, A., Beibel, M., Martin, K., Darribat, K., Cuttat, R., et al. (2020). Immune cell landscaping reveals a protective role for regulatory T cells during kidney injury and fibrosis. *JCI Insight.* 5:e130651. doi: 10.1172/jci.insight.130651
- Dolf, S., Witzke, O., and Wilde, B. (2019). Th17 cells in renal inflammation and autoimmunity. *Autoimmun. Rev.* 18, 129–136. doi: 10.1016/j.autrev.2018.08.006
- Dong, Q., Cai, C., Gao, F., Chen, P., Gong, W., and Shen, M. (2019). Defective Treg response in acute kidney injury was caused by a reduction in TIM-3(+) Treg cells. *Immunol. Invest.* 48, 27–38. doi: 10.1080/08820139.2018.1493497
- Dong, Y., Yang, M., Zhang, J., Peng, X., Cheng, J., Cui, T., et al. (2016). Depletion of CD8+ T cells exacerbates CD4+ T cell-induced monocyte-to-fibroblast transition in renal fibrosis. *J. Immunol.* 196, 1874–1881. doi: 10.4049/jimmunol.1501232
- Dudakov, J. A., Hanash, A. M., and van den Brink, M. R. (2015). Interleukin-22: immunobiology and pathology. *Annu. Rev. Immunol.* 33, 747–785. doi: 10.1146/annurev-immunol-032414-112123
- Duffy, M. M., McNicholas, B. A., Monaghan, D. A., Hanley, S. A., McMahon, J. M., Pindjakova, J., et al. (2014). Mesenchymal stem cells and a vitamin D receptor agonist additively suppress T helper 17 cells and the related inflammatory response in the kidney. *Am. J. Physiol. Renal Physiol.* 307, F1412–F1426. doi: 10.1152/ajprenal.00024.2014
- Eltzschig, H. K., and Eckle, T. (2011). Ischemia and reperfusion—from mechanism to translation. *Nat. Med.* 17, 1391–1401. doi: 10.1038/nm.2507
- Ferhat, M., Robin, A., Giraud, S., Sena, S., Goujon, J. M., Touchard, G., et al. (2018). Endogenous IL-33 Contributes To Kidney Ischemia-Reperfusion Injury As An Alarmin. *J. Am. Soc. Nephrol.* 29, 1272–1288. doi: 10.1681/ASN.2017060650
- Fiorina, P., Ansari, M. J., Jurewicz, M., Barry, M., Ricchiuti, V., Smith, R. N., et al. (2006). Role of CXC chemokine receptor 3 pathway in renal ischemic injury. *J. Am. Soc. Nephrol.* 17, 716–723. doi: 10.1681/ASN.2005090954
- Ford, M. S., Chen, W., Wong, S., Li, C., Vanama, R., Elford, A. R., et al. (2007). Peptide-activated double-negative T cells can prevent

- autoimmune type-1 diabetes development. *Eur. J. Immunol.* 37, 2234–2241. doi: 10.1002/eji.200636991
- Gandolfo, M. T., Jang, H. R., Bagnasco, S. M., Ko, G. J., Agreda, P., Satpute, S. R., et al. (2009). Foxp3+ regulatory T cells participate in repair of ischemic acute kidney injury. *Kidney Int.* 76, 717–729. doi: 10.1038/ki.2009.259
- Gasteiger, G., Fan, X., Dikiy, S., Lee, S. Y., and Rudensky, A. Y. (2015). Tissue residency of innate lymphoid cells in lymphoid and nonlymphoid organs. *Science* 350, 981–985. doi: 10.1126/science.aac9593
- Gieseck, R. L. 3rd, Wilson, M. S., and Wynn, T. A. (2018). Type 2 immunity in tissue repair and fibrosis. *Nat. Rev. Immunol.* 18, 62–76. doi: 10.1038/nri.2017.90
- Gocze, I., Ehehalt, K., Zeman, F., Riquelme, P., Pfister, K., Graf, B. M., et al. (2018). Postoperative cellular stress in the kidney is associated with an early systemic gammadelta T-cell immune cell response. *Crit. Care* 22:168. doi: 10.1186/s13054-018-2094-x
- Gong, J., Noel, S., Hsu, J., Bush, E. L., Arend, L. J., Sadasivam, M., et al. (2020). TCR(+)CD4(-)CD8(-) (double negative) T cells protect from cisplatin-induced renal epithelial cell apoptosis and acute kidney injury. *Am. J. Physiol. Renal Physiol.* 318, F1500–F152. doi: 10.1152/ajprenal.00033.2020
- Gonzalez-Guerrero, C., Morgado-Pascual, J. L., Cannata-Ortiz, P., Ramos-Barron, M. A., Gomez-Alamillo, C., Arias, M., et al. (2018). CCL20 blockade increases the severity of nephrotoxic folic acid-induced acute kidney injury. *J. Pathol.* 246, 191–204. doi: 10.1002/path.5132
- Guo, J., Guan, Q., Liu, X., Wang, H., Gleave, M. E., Nguan, C. Y., et al. (2016). Relationship of clusterin with renal inflammation and fibrosis after the recovery phase of ischemia-reperfusion injury. *BMC Nephrol.* 17:133. doi: 10.1186/s12882-016-0348-x
- Hochegger, K., Schatz, T., Eller, P., Tagwerker, A., Heining, D., Mayer, G., et al. (2007). Role of alpha/beta and gamma/delta T cells in renal ischemia-reperfusion injury. *Am. J. Physiol. Renal Physiol.* 293, F741–F747. doi: 10.1152/ajprenal.00486.2006
- Howson, L. J., Salio, M., and Cerundolo, V. (2015). MRI-restricted mucosal-associated invariant T cells and their activation during infectious diseases. *Front. Immunol.* 6:303. doi: 10.3389/fimmu.2015.00303
- Huang, Q., Niu, Z., Tan, J., Yang, J., Liu, Y., Ma, H., et al. (2015). IL-25 elicits innate lymphoid cells and multipotent progenitor Type 2 cells that reduce renal ischemic/reperfusion injury. *J. Am. Soc. Nephrol.* 26, 2199–2211. doi: 10.1681/ASN.2014050479
- Huen, S. C., and Cantley, L. G. (2017). Macrophages in renal injury and repair. *Annu. Rev. Physiol.* 79, 449–469. doi: 10.1146/annurev-physiol-022516-034219
- Jahng, A., Maricic, I., Aguilera, C., Cardell, S., Halder, R. C., and Kumar, V. (2004). Prevention of autoimmunity by targeting a distinct, noninvariant CD1d-reactive T cell population reactive to sulfatide. *J. Exp. Med.* 199, 947–957. doi: 10.1084/jem.20031389
- Jang, H. R., Gandolfo, M. T., Ko, G. J., Satpute, S., Racusen, L., and Rabb, H. (2009). Early exposure to germs modifies kidney damage and inflammation after experimental ischemia-reperfusion injury. *Am. J. Physiol. Renal Physiol.* 297, F1457–F1465. doi: 10.1152/ajprenal.90769.2008
- Kim, M. G., Koo, T. Y., Yan, J. J., Lee, E., Han, K. H., Jeong, J. C., et al. (2013). IL-2/anti-IL-2 complex attenuates renal ischemia-reperfusion injury through expansion of regulatory T cells. *J. Am. Soc. Nephrol.* 24, 1529–1536. doi: 10.1681/ASN.2012080784
- Kinsey, G. R., Huang, L., Jaworska, K., Khutsishvili, K., Becker, D. A., Ye, H., et al. (2012). Autocrine adenosine signaling promotes regulatory T cell-mediated renal protection. *J. Am. Soc. Nephrol.* 23, 1528–1537. doi: 10.1681/ASN.2012010070
- Kinsey, G. R., Huang, L., Vergis, A. L., Li, L., and Okusa, M. D. (2010). Regulatory T cells contribute to the protective effect of ischemic preconditioning in the kidney. *Kidney Int.* 77, 771–780. doi: 10.1038/ki.2010.12
- Kinsey, G. R., Sharma, R., Huang, L., Li, L., Vergis, A. L., Ye, H., et al. (2009). Regulatory T cells suppress innate immunity in kidney ischemia-reperfusion injury. *J. Am. Soc. Nephrol.* 20, 1744–1753. doi: 10.1681/ASN.2008111160
- Kitching, A. R., and Holdsworth, S. R. (2011). The emergence of TH17 cells as effectors of renal injury. *J. Am. Soc. Nephrol.* 22, 235–238. doi: 10.1681/ASN.2010050536
- Koo, T. Y., Lee, J. G., Yan, J. J., Jang, J. Y., Ju, K. D., Han, M., et al. (2017). The P2X7 receptor antagonist, oxidized adenosine triphosphate, ameliorates renal ischemia-reperfusion injury by expansion of regulatory T cells. *Kidney Int.* 92, 415–431. doi: 10.1016/j.kint.2017.01.031
- Krabbandam, L., Bal, S. M., Spits, H., and Golebski, K. (2018). New insights into the function, development, and plasticity of type 2 innate lymphoid cells. *Immunol. Rev.* 286, 74–85. doi: 10.1111/imr.12708
- Krebs, C. F., and Panzer, U. (2018). Plasticity and heterogeneity of Th17 in immune-mediated kidney diseases. *J. Autoimmun.* 87, 61–68. doi: 10.1016/j.jaut.2017.12.005
- Krebs, C. F., Reimers, D., Zhao, Y., Paust, H. J., Bartsch, P., Nuñez, S., et al. (2020). Pathogen-induced tissue-resident memory Th17 (T_{RM}17) cells amplify autoimmune kidney disease. *Sci. Immunol.* 5:eaba4163. doi: 10.1126/sciimmunol.aba4163
- Krebs, C. F., Schmidt, T., Riedel, J. H., and Panzer, U. (2017). T helper type 17 cells in immune-mediated glomerular disease. *Nat. Rev. Nephrol.* 13, 647–659. doi: 10.1038/nrneph.2017.112
- Kumar, B. V., Connors, T. J., and Farber, D. L. (2018). Human T cell development, localization, and function throughout life. *Immunity* 48, 202–213. doi: 10.1016/j.immuni.2018.01.007
- Law, B. M., Wilkinson, R., Wang, X., Kilday, K., Lindner, M., Beagley, K., et al. (2019a). Effector gammadelta T cells in human renal fibrosis and chronic kidney disease. *Nephrol. Dial. Transplant.* 34, 40–48. doi: 10.1093/ndt/gfy098
- Law, B. M. P., Wilkinson, R., Wang, X., Kilday, K., Giuliani, K., Beagley, K. W., et al. (2019b). Human tissue-resident Mucosal-Associated Invariant T (MAIT) cells in renal fibrosis and CKD. *J. Am. Soc. Nephrol.* 30, 1322–1335. doi: 10.1681/ASN.2018101064
- Le Bourhis, L., Martin, E., Peguillet, I., Guihot, A., Froux, N., Core, M., et al. (2010). Antimicrobial activity of mucosal-associated invariant T cells. *Nat. Immunol.* 11, 701–708. doi: 10.1038/ni.1890
- Li, L., Huang, L., Sung, S. S., Lobo, P. I., Brown, M. G., Gregg, R. K., et al. (2007). NKT cell activation mediates neutrophil IFN-gamma production and renal ischemia-reperfusion injury. *J. Immunol.* 178, 5899–5911. doi: 10.4049/jimmunol.178.9.5899
- Li, L., Huang, L., Ye, H., Song, S. P., Bajwa, A., Lee, S. J., et al. (2012). Dendritic cells tolerized with adenosine A(2)AR agonist attenuate acute kidney injury. *J. Clin. Invest.* 122, 3931–3942. doi: 10.1172/JCI63170
- Liang, H., Xu, F., Wen, X. J., Liu, H. Z., Wang, H. B., Zhong, J. Y., et al. (2017). Interleukin-33 signaling contributes to renal fibrosis following ischemia reperfusion. *Eur. J. Pharmacol.* 812, 18–27. doi: 10.1016/j.ejphar.2017.06.031
- Liang, H., Xu, F., Zhang, T., Huang, J., Guan, Q., Wang, H., et al. (2018). Inhibition of IL-18 reduces renal fibrosis after ischemia-reperfusion. *Biomed. Pharmacother.* 106, 879–889. doi: 10.1016/j.biopha.2018.07.031
- Liu, L., Kou, P., Zeng, Q., Pei, G., Li, Y., Liang, H., et al. (2012). CD4+ T Lymphocytes, especially Th2 cells, contribute to the progress of renal fibrosis. *Am. J. Nephrol.* 36, 386–396. doi: 10.1159/000343283
- Liu, Y., Wang, K., Liang, X., Li, Y., Zhang, Y., Zhang, C., et al. (2018). Complement C3 produced by macrophages promotes renal fibrosis via IL-17A secretion. *Front Immunol.* 9:2385. doi: 10.3389/fimmu.2018.02385
- Lobo, P. I., Schlegel, K. H., Bajwa, A., Huang, L., and Okusa, M. D. (2017). Natural IgM and TLR agonists switch murine splenic Pan-B to “Regulatory” cells that suppress ischemia-induced innate inflammation via regulating NKT-1 cells. *Front. Immunol.* 8:974. doi: 10.3389/fimmu.2017.00974
- Luan, H., Wang, C., Sun, J., Zhao, L., Li, L., Zhou, B., et al. (2020). Resolvin D1 protects against ischemia/reperfusion-induced acute kidney injury by increasing treg percentages via the ALX/FP2R pathway. *Front. Physiol.* 11:285. doi: 10.3389/fphys.2020.00285
- Mahajan, D., Wang, Y., Qin, X., Wang, Y., Zheng, G., Wang, Y. M., et al. (2006). CD4+CD25+ regulatory T cells protect against injury in an innate murine model of chronic kidney disease. *J. Am. Soc. Nephrol.* 17, 2731–2741. doi: 10.1681/ASN.2005080842
- Malone, A. F., Wu, H., Fronick, C., Fulton, R., Gaut, J. P., and Humphreys, B. D. (2020). Harnessing expressed single nucleotide variation and single cell RNA sequencing to define immune cell chimerism in the rejecting kidney transplant. *J. Am. Soc. Nephrol.* 31, 1977–1986. doi: 10.1681/ASN.2020030326
- Manson, J., Hoffman, R., Chen, S., Ramadan, M. H., and Billiar, T. R. (2019). Innate-like lymphocytes are immediate participants in the hyper-acute immune response to trauma and hemorrhagic shock. *Front. Immunol.* 10:1501. doi: 10.3389/fimmu.2019.01501

- Maria, N. I., and Davidson, A. (2020). Protecting the kidney in systemic lupus erythematosus: from diagnosis to therapy. *Nat. Rev. Rheumatol.* 16, 255–267. doi: 10.1038/s41584-020-0401-9
- Marques, V. P., Goncalves, G. M., Feitoza, C. Q., Cenedeze, M. A., Fernandes Bertocchi, A. P., Damiao, M. J., et al. (2006). Influence of TH1/TH2 switched immune response on renal ischemia-reperfusion injury. *Nephron Exp. Nephrol.* 104, e48–56. doi: 10.1159/000093676
- Martina, M. N., Noel, S., Saxena, A., Bandapalle, S., Majithia, R., Jie, C., et al. (2016). Double-negative alpha-beta T cells are early responders to AKI and are found in human kidney. *J. Am. Soc. Nephrol.* 27, 1113–1123. doi: 10.1681/ASN.2014121214
- Mehrotra, P., Collett, J. A., Gunst, S. J., and Basile, D. P. (2018). Th17 cells contribute to pulmonary fibrosis and inflammation during chronic kidney disease progression after acute ischemia. *Am. J. Physiol. Regul. Integr. Comp. Physiol.* 314, R265–R273. doi: 10.1152/ajpregu.00147.2017
- Mehrotra, P., Collett, J. A., McKinney, S. D., Stevens, J., Ivancic, C. M., and Basile, D. P. (2017). IL-17 mediates neutrophil infiltration and renal fibrosis following recovery from ischemia reperfusion: compensatory role of natural killer cells in athymic rats. *Am. J. Physiol. Renal Physiol.* 312, F385–F397. doi: 10.1152/ajprenal.00462.2016
- Mehrotra, P., Patel, J. B., Ivancic, C. M., Collett, J. A., and Basile, D. P. (2015). Th-17 cell activation in response to high salt following acute kidney injury is associated with progressive fibrosis and attenuated by AT-1R antagonism. *Kidney Int.* 88, 776–784. doi: 10.1038/ki.2015.200
- Mehrotra, P., Sturek, M., Neyra, J. A., and Basile, D. P. (2019). Calcium channel Orai1 promotes lymphocyte IL-17 expression and progressive kidney injury. *J. Clin. Invest.* 129, 4951–4961. doi: 10.1172/JCI126108
- Mehta, R. L., Cerdá J., Burdman, E. A., Tonelli, M., Garcia-García, G., Jha, V., et al. (2015). International Society of Nephrology's Oby25 initiative for acute kidney injury (zero preventable deaths by 2025): a human rights case for nephrology. *Lancet* 385, 2616–2643. doi: 10.1016/S0140-6736(15)60126-X
- Mi, S., Li, Z., Yang, H. Z., Liu, H., Wang, J. P., Ma, Y. G., et al. (2011). Blocking IL-17A promotes the resolution of pulmonary inflammation and fibrosis via TGF-beta1-dependent and -independent mechanisms. *J. Immunol.* 187, 3003–3014. doi: 10.4049/jimmunol.1004081
- Miossec, P., and Kolls, J. K. (2012). Targeting IL-17 and TH17 cells in chronic inflammation. *Nat. Rev. Drug Discov.* 11, 763–776. doi: 10.1038/nrd3794
- Moledina, D. G., Mansour, S. G., Jia, Y., Obeid, W., Thiessen-Philbrook, H., Koyner, J. L., et al. (2019). Association of T cell-derived inflammatory cytokines with acute kidney injury and mortality after cardiac surgery. *Kidney Int. Rep.* 4, 1689–1697. doi: 10.1016/j.ekir.2019.09.003
- Mu, Y., Zhang, J., Liu, Y., Ma, J., Jiang, D., Zhang, X., et al. (2020). CD226 deficiency on regulatory T cells aggravates renal fibrosis via up-regulation of Th2 cytokines through miR-340. *J. Leukoc. Biol.* 107, 573–587. doi: 10.1002/JLB.2MA1119-174RR
- Orejudo, M., Rodrigues-Diez, R. R., Rodrigues-Diez, R., Garcia-Redondo, A., Santos-Sanchez, L., Randeiz-Garbayo, J., et al. (2019). Interleukin 17A participates in renal inflammation associated to experimental and human hypertension. *Front. Pharmacol.* 10:1015. doi: 10.3389/fphar.2019.01015
- Patil, R. S., Bhat, S. A., Dar, A. A., and Chiplunkar, S. V. (2015). The Jekyll and Hyde story of IL17-Producing gamma-delta T Cells. *Front. Immunol.* 6:37. doi: 10.3389/fimmu.2015.00037
- Patschan, D., Heeg, M., Brier, M., Brandhorst, G., Schneider, S., Muller, G. A., et al. (2014). CD4+ lymphocyte adenosine triphosphate—a new marker in sepsis with acute kidney injury? *BMC Nephrol.* 15:203. doi: 10.1186/1471-2369-15-203
- Peng, X., Xiao, Z., Zhang, J., Li, Y., Dong, Y., and Du, J. (2015). IL-17A produced by both gamma-delta T and Th17 cells promotes renal fibrosis via RANTES-mediated leukocyte infiltration after renal obstruction. *J. Pathol.* 235, 79–89. doi: 10.1002/path.4430
- Perazella, M. A. (2019). Drug-induced acute kidney injury: diverse mechanisms of tubular injury. *Curr. Opin. Crit. Care* 25, 550–557. doi: 10.1097/MCC.0000000000000653
- Rabb, H., Daniels, F., O'Donnell, M., Haq, M., Saba, S. R., Keane, W., et al. (2000). Pathophysiological role of T lymphocytes in renal ischemia-reperfusion injury in mice. *Am. J. Physiol. Renal Physiol.* 279, F525–F531. doi: 10.1152/ajprenal.2000.279.3.F525
- Rajendran, M., Looney, S., Singh, N., Elashiry, M., Meghil, M. M., El-Awady, A. R., et al. (2019). Systemic antibiotic therapy reduces circulating inflammatory dendritic cells and Treg-Th17 plasticity in periodontitis. *J. Immunol.* 202, 2690–2699. doi: 10.4049/jimmunol.1900046
- Reichetzeder, C., Heunisch, F., Einem, G. V., Tsuprykov, O., Kellner, K. H., Dschietzig, T., et al. (2017). Pre-interventional kynurenine predicts medium-term outcome after contrast media exposure due to coronary angiography. *Kidney Blood Press Res.* 42, 244–256. doi: 10.1159/000477222
- Rosendahl, A., Kabiri, R., Bode, M., Cai, A., Klinge, S., Ehmke, H., et al. (2019). Adaptive immunity and IL-17A are not involved in the progression of chronic kidney disease after 5/6 nephrectomy in mice. *Br. J. Pharmacol.* 176, 2002–2014. doi: 10.1111/bph.14509
- Sabapathy, V., Cheru, N. T., Corey, R., Mohammad, S., and Sharma, R. (2019). A novel hybrid cytokine IL233 mediates regeneration following doxorubicin-induced nephrotoxic injury. *Sci. Rep.* 9:3215. doi: 10.1038/s41598-019-39886-9
- Sakaguchi, S., Vignali, D. A., Rudensky, A. Y., Niec, R. E., and Waldmann, H. (2013). The plasticity and stability of regulatory T cells. *Nat. Rev. Immunol.* 13, 461–467. doi: 10.1038/nri3464
- Savage, T. M., Shonts, B. A., Obradovic, A., Dewolf, S., Lau, S., Zuber, J., et al. (2018). Early expansion of donor-specific Tregs in tolerant kidney transplant recipients. *JCI Insight.* 3:e124086. doi: 10.1172/jci.insight.124086
- Seeger, S., Nelson, P. J., and Schlondorff, D. (2000). Chemokines, chemokine receptors, and renal disease: from basic science to pathophysiological and therapeutic studies. *J. Am. Soc. Nephrol.* 11, 152–176. doi: 10.1681/ASN.V111152
- Song, T., Eirin, A., Zhu, X., Zhao, Y., Krier, J. D., Tang, H., et al. (2020). Mesenchymal stem cell-derived extracellular vesicles induce regulatory T cells to ameliorate chronic kidney injury. *Hypertension* 75, 1223–1232. doi: 10.1161/HYPERTENSIONAHA.119.14546
- Stremaska, M. E., Jose, S., Sabapathy, V., Huang, L., Bajwa, A., Kinsey, G. R., et al. (2017). IL233, a novel IL-2 and IL-33 hybrid cytokine, ameliorates renal injury. *J. Am. Soc. Nephrol.* 28, 2681–2693. doi: 10.1681/ASN.2016121272
- Sun, H., Sun, C., Xiao, W., and Sun, R. (2019). Tissue-resident lymphocytes: from adaptive to innate immunity. *Cell. Mol. Immunol.* 16, 205–215. doi: 10.1038/s41423-018-0192-y
- Tan, Z., Qian, X., Jiang, R., Liu, Q., Wang, Y., Chen, C., et al. (2013). IL-17A plays a critical role in the pathogenesis of liver fibrosis through hepatic stellate cell activation. *J. Immunol.* 191, 1835–1844. doi: 10.4049/jimmunol.1203013
- Tang, P. M., Nikolic-Paterson, D. J., and Lan, H. Y. (2019). Macrophages: versatile players in renal inflammation and fibrosis. *Nat. Rev. Nephrol.* 15, 144–158. doi: 10.1038/s41581-019-0110-2
- Tang, Q. Z., and Vincenti, F. (2017). Transplant trials with tregs: perils and promises. *J. Clin. Invest.* 127, 2505–2512. doi: 10.1172/JCI90598
- Tappeier, T. T., Fearn, A., Brown, K., Chowdhury, P., Sacks, S. H., Sheerin, N. S., et al. (2010). Pivotal role of CD4+ T cells in renal fibrosis following ureteric obstruction. *Kidney Int.* 78, 351–362. doi: 10.1038/ki.2010.177
- Thorenz, A., Volker, N., Brasen, J. H., Chen, R., Jang, M. S., Rong, S., et al. (2017). IL-17A blockade or deficiency does not affect progressive renal fibrosis following renal ischaemia reperfusion injury in mice. *J. Pharm. Pharmacol.* 69, 1125–1135. doi: 10.1111/jph.12747
- Turner, J. E., Becker, M., Mittrucker, H. W., and Panzer, U. (2018). Tissue-resident lymphocytes in the kidney. *J. Am. Soc. Nephrol.* 29, 389–399. doi: 10.1681/ASN.2017060599
- Uchida, T., Nakashima, H., Ito, S., Ishikiriyama, T., Nakashima, M., Seki, S., et al. (2018). Activated natural killer T cells in mice induce acute kidney injury with hematuria through possibly common mechanisms shared by human CD56(+) T cells. *Am. J. Physiol. Renal Physiol.* 315, F618–F627. doi: 10.1152/ajprenal.00160.2018
- Vemuri, R., Gundamaraju, R., Shinde, T., Perera, A. P., Basheer, W., Southam, B., et al. (2019). Lactobacillus acidophilus DDS-1 modulates intestinal-specific microbiota, short-chain fatty acid and immunological profiles in aging mice. *Nutrients* 11:1297. doi: 10.3390/nu11061297
- Vivier, E., Artis, D., Colonna, M., Diefenbach, A., Di Santo, J. P., Eberl, G., et al. (2018). Innate lymphoid cells: 10 years on. *Cell* 174, 1054–1066. doi: 10.1016/j.cell.2018.07.017
- Voelkl, S., Gary, R., and Mackensen, A. (2011). Characterization of the immunoregulatory function of human TCR-alpha-beta+ CD4+ CD8- double-negative T cells. *Eur. J. Immunol.* 41, 739–748. doi: 10.1002/eji.201040982

- Wang, H., Wang, J., Bai, Y., Li, J., Li, L., and Dong, Y. (2016). CD11c(+) CD8(+) T cells reduce renal fibrosis following ureteric obstruction by inducing fibroblast apoptosis. *Int. J. Mol. Sci.* 18:1. doi: 10.3390/ijms18010001
- Wang, S., Xia, P., Chen, Y., Qu, Y., Xiong, Z., Ye, B., et al. (2017). Regulatory innate lymphoid cells control innate intestinal inflammation. *Cell* 171, 201–216 e18. doi: 10.1016/j.cell.2017.07.027
- Wang, Y. M., Bakhtiar, M., and Alexander, S. I. (2017). ILC2: There's a new cell in town. *J. Am. Soc. Nephrol.* 28, 1953–1955. doi: 10.1681/ASN.2017040398
- Wang, Y. M., Wang, Y., Harris, D. C. H., Alexander, S. I., and Lee, V. W. S. (2015). Adriamycin nephropathy in BALB/c mice. *Curr. Protoc. Immunol.* 108, 15 28 1–15 28 6. doi: 10.1002/0471142735.im1528s108
- Wilson, M. S., Madala, S. K., Ramalingam, T. R., Gochuico, B. R., Rosas, I. O., Cheever, A. W., et al. (2010). Bleomycin and IL-1beta-mediated pulmonary fibrosis is IL-17A dependent. *J. Exp. Med.* 207, 535–552. doi: 10.1084/jem.20092121
- Witte, E., Witte, K., Warsawska, K., Sabat, R., and Wolk, K. (2010). Interleukin-22: a cytokine produced by T, NK and NKT cell subsets, with importance in the innate immune defense and tissue protection. *Cytokine Growth Factor Rev.* 21, 365–379. doi: 10.1016/j.cytogfr.2010.08.002
- Wu, W. P., Tsai, Y. G., Lin, T. Y., Wu, M. J., and Lin, C. Y. (2017). The attenuation of renal fibrosis by histone deacetylase inhibitors is associated with the plasticity of FOXP3(+)-IL-17(+) T cells. *BMC Nephrol.* 18:225. doi: 10.1186/s12882-017-0630-6
- Xiao, L., Xu, B., Zhou, L., Tan, R. J., Zhou, D., Fu, H., et al. (2019). Wnt/beta-catenin regulates blood pressure and kidney injury in rats. *Biochim. Biophys. Acta Mol. Basis Dis.* 1865, 1313–1322. doi: 10.1016/j.bbdis.2019.01.027
- Yang, J., Kim, C. J., Go, Y. S., Lee, H. Y., Kim, M. G., Oh, S. W., et al. (2020). Intestinal microbiota controls acute kidney injury severity by immune modulation. *Kidney Int.* 26. doi: 10.1016/j.kint.2020.04.048
- Yang, J., Lim, S. Y., Ko, Y. S., Lee, H. Y., Oh, S. W., Kim, M. G., et al. (2019). Intestinal barrier disruption and dysregulated mucosal immunity contribute to kidney fibrosis in chronic kidney disease. *Nephrol. Dial. Transplant.* 34, 419–428. doi: 10.1093/ndt/gfy172
- Yang, S. H., Lee, J. P., Jang, H. R., Cha, R. H., Han, S. S., Jeon, U. S., et al. (2011). Sulfatide-reactive natural killer T cells abrogate ischemia-reperfusion injury. *J. Am. Soc. Nephrol.* 22, 1305–1314. doi: 10.1681/ASN.2010080815
- Yokota, N., Burne-Taney, M., Racusen, L., and Rabb, H. (2003). Contrasting roles for STAT4 and STAT6 signal transduction pathways in murine renal ischemia-reperfusion injury. *Am. J. Physiol. Renal Physiol.* 285, F319–F325. doi: 10.1152/ajprenal.00432.2002
- Zeng, J., and Howard, J. C. (2010). Spontaneous focal activation of invariant natural killer T (iNKT) cells in mouse liver and kidney. *BMC Biol.* 8:142. doi: 10.1186/1741-7007-8-142
- Zhu, H., Cao, C. J., Wu, Z. C., Zhang, H. P., Sun, Z. H., Wang, M., et al. (2021). The probiotic *L. casei* Zhang slows the progression of acute and chronic kidney disease. *Cell Metab.* doi: 10.1016/j.cmet.2021.06.014. [Epub ahead of print].
- Zhu, J. T. (2018). Helper cell differentiation, heterogeneity, and plasticity. *Cold Spring Harb. Perspect. Biol.* 10:a030338. doi: 10.1101/cshperspect.a030338
- Zuk, A., and Bonventre, J. V. (2016). Acute kidney injury. *Annu. Rev. Med.* 67, 293–307. doi: 10.1146/annurev-med-050214-013407
- Zwang, N. A., and Leventhal, J. R. (2017). Cell therapy in kidney transplantation: focus on regulatory T cells. *J. Am. Soc. Nephrol.* 28, 1960–1972. doi: 10.1681/ASN.2016111206

Conflict of Interest: The authors declare that the research was conducted in the absence of any commercial or financial relationships that could be construed as a potential conflict of interest.

Publisher's Note: All claims expressed in this article are solely those of the authors and do not necessarily represent those of their affiliated organizations, or those of the publisher, the editors and the reviewers. Any product that may be evaluated in this article, or claim that may be made by its manufacturer, is not guaranteed or endorsed by the publisher.

Copyright © 2021 Cao, Yao and Zeng. This is an open-access article distributed under the terms of the Creative Commons Attribution License (CC BY). The use, distribution or reproduction in other forums is permitted, provided the original author(s) and the copyright owner(s) are credited and that the original publication in this journal is cited, in accordance with accepted academic practice. No use, distribution or reproduction is permitted which does not comply with these terms.



Amlexanox and Forskolin Prevents Isoproterenol-Induced Cardiomyopathy by Subduing Cardiomyocyte Hypertrophy and Maladaptive Inflammatory Responses

Gabriel Komla Adzika¹, Hongjian Hou^{1,2}, Adebayo Oluwafemi Adekunle¹, Ruqayya Rizvi³, Seyram Yao Adzraku⁴, Kexue Li¹, Qi-Ming Deng⁵, Richard Mprah¹, Marie Louise Ndzie Noah¹, Joseph Adu-Amankwaah¹, Jeremiah Ong'achwa Machuki¹, Wenkang Shang⁶, Tongtong Ma¹, Stephane Koda⁷, Xianluo Ma⁸ and Hong Sun^{1,3*}

OPEN ACCESS

Edited by:

Susanne Sattler,
Imperial College London,
United Kingdom

Reviewed by:

Gobinath Shanmugam,
University of Alabama at Birmingham,
United States
Mohamed Fizur Nagoor Meeran,
United Arab Emirates University,
United Arab Emirates

*Correspondence:

Hong Sun
sunh@xzhmu.edu.cn

Specialty section:

This article was submitted to
Molecular and Cellular Pathology,
a section of the journal
Frontiers in Cell and Developmental
Biology

Received: 02 June 2021

Accepted: 30 August 2021

Published: 24 September 2021

Citation:

Adzika GK, Hou H, Adekunle AO,
Rizvi R, Adzraku SY, Li K, Deng Q-M,
Mprah R, Ndzie Noah ML,
Adu-Amankwaah J, Machuki JO,
Shang W, Ma T, Koda S, Ma X and
Sun H (2021) Amlexanox
and Forskolin Prevents
Isoproterenol-Induced
Cardiomyopathy by Subduing
Cardiomyocyte Hypertrophy
and Maladaptive Inflammatory
Responses.
Front. Cell Dev. Biol. 9:719351.
doi: 10.3389/fcell.2021.719351

¹ Department of Physiology, Xuzhou Medical University, Xuzhou, China, ² The College of Biology and Food, Shangqiu Normal University, Shangqiu, China, ³ Xuzhou Medical University, Xuzhou, China, ⁴ Key Laboratory of Bone Marrow Stem Cell, Department of Hematology, The Affiliated Hospital of Xuzhou Medical University, Xuzhou, China, ⁵ The Key Laboratory of Cardiovascular Remodeling and Function Research, The State and Shandong Province Joint Key Laboratory of Translational Cardiovascular Medicine, Chinese Ministry of Education, Department of Cardiology, Chinese National Health Commission and Chinese Academy of Medical Sciences, Qilu Hospital of Shandong University, Jinan, China, ⁶ Faculty of Biology, Institute of Biochemistry and Molecular Biology, ZBMZ, Albert-Ludwigs University of Freiburg, Freiburg, Germany, ⁷ Laboratory of Infection and Immunity, Department of Pathogenic Biology and Immunology, Xuzhou Medical University, Xuzhou, China, ⁸ Internal Medicine—Cardiovascular Department, People's Hospital of Jiawang District, Xuzhou, China

Chronic catecholamine stress (CCS) induces the occurrence of cardiomyopathy—pathological cardiac hypertrophy (PCH), which is characterized by left ventricular systolic dysfunction (LVSD). Recently, mounting evidence has implicated myocardial inflammation in the exacerbation of pathological cardiac remodeling. However, there are currently no well-defined treatment interventions or regimes targeted at both the attenuation of maladaptive myocardial hypertrophy and inflammation during CCS to prevent PCH. G protein-coupled receptor kinase 5 (GRK5) and adenylyl cyclases (ACs)-cAMP mediates both cardiac and inflammatory responses. Also, GRK5 and ACs are implicated in stress-induced LVSD. Herein, we aimed at preventing PCH during CCS via modulating adaptive cardiac and inflammatory responses by inhibiting GRK5 and/or stimulating ACs. Isoproterenol-induced cardiomyopathy (ICM) was modeled using 0.5 mg/100 g/day isoproterenol injections for 40 days. Alterations in cardiac and inflammatory responses were assessed from the myocardia. Similarities in the immunogenicity of cardiac troponin I (cTnI) and lipopolysaccharide under CCS were assessed, and Amlexanox (35 μ M/ml) and/or Forskolin (10 μ M/ml) were then employed *in vitro* to modulate adaptive inflammatory responses by inhibiting GRK5 or activating ACs-cAMP, respectively. Subsequently, Amlexanox (2.5 mg/100 g/day) and/or Forskolin (0.5 mg/100 g/day) were then translated into *in vivo* during CCS to modulate adaptive cardiac and inflammatory responses. The effects of Amlexanox and Forskolin on regulating myocardial systolic functions and inflammatory responses during CCS were ascertained afterward. PCH mice had excessive myocardial hypertrophy, fibrosis,

and aggravated LVSD, which were accompanied by massive CD68⁺ inflammatory cell infiltrations. *In vitro*, Forskolin-AC/cAMP was effective than Amlexanox-GRK5 at downregulating proinflammatory responses during stress; nonetheless, Amlexanox and Forskolin combination demonstrated the most efficacy in modulating adaptive inflammatory responses. Individually, the translated Amlexanox and Forskolin treatment interventions were ineffective at subduing the pathological remodeling and sustaining cardiac function during CCS. However, their combination was potent at preventing LVSD during CCS by attenuating maladaptive myocardial hypertrophy, fibrosis, and inflammatory responses. The treatment intervention attained its potency mainly *via* Forskolin-ACs/cAMP-mediated modulation of cardiac and inflammatory responses, coupled with Amlexanox inhibition of GRK5 mediated maladaptive cascades. Taken together, our findings highlight the Amlexanox and Forskolin combination as a potential therapeutic intervention for preventing the occurrence of pathological cardiac hypertrophy during chronic stress.

Keywords: chronic catecholamine stress, amlexanox, forskolin, GRK5, adenylyl cyclase, cAMP, inflammation, isoproterenol-induced cardiomyopathy

BACKGROUND

The elevated level of circulating catecholamines during chronic stress is a hallmark for the initiation of adverse remodeling of the left ventricular (LV) (Frey et al., 2004; Liu et al., 2015; Zhang et al., 2019). The progression in LV remodeling has been demonstrated to result in irreversible pathological cardiac hypertrophy (PCH) if there are no timely preventive measures to subdue the excessive firing of neurohormonal stimuli during chronic stress (Schaeuble et al., 2019; Zhang et al., 2019). In recent studies, irreversible hypertrophic cardiomyopathy has been associated with LV systolic dysfunction (LVSD) (Marstrand et al., 2020). Also, the resulting LVSD has been attributed to the distortion of the typical myocardial architecture due to increased LV wall thickness and fibrosis (Galati et al., 2016; Marstrand et al., 2020), thereby making the heart incapable of rapidly replenishing blood for the subsequent ejections (Xie et al., 2013). Although the mechanisms underlying the cardiomyopathy are still being elucidated, the most recent findings have implicated hyperactive myocardial proinflammation responses as a factor hastening the pathological remodeling (Zhao et al., 2017; Weisheit et al., 2021).

In steady state, cardiac resident macrophages have been shown to play crucial roles in reparative functions after cardiac injuries (Heidt et al., 2014). However, an enormous amount of cardiomyocyte deaths (*via* both apoptosis and necrosis) occur during chronic catecholamine stress (CCS) (Whelan et al., 2010; Liu et al., 2015). The apoptotic myocyte directly induces fibrosis (Liu et al., 2015), while troponins released from the necrotic cardiomyocytes serve as a damage-associated

molecular pattern that invokes proinflammatory responses from macrophages in an attempt to curb further deaths (Haider and Stimson, 1993; Kaya et al., 2008; Heidt et al., 2014). However, under CCS conditions, prolonged secretion of proinflammatory cytokines; interleukin (IL) 1 β , IL-2, IL-6, tumor necrosis factor-alpha (TNF α), and interferon-gamma (IFN- γ) results, while the anti-inflammatory cytokines; IL-10, and transforming growth factor-beta (TGF- β) secretions are downregulated (Kaya et al., 2010). The upregulated secretions of IL-6 and TNF α prolong myofibroblast activations and increases interstitial fibrosis markedly, which stiffens the myocardia and causes LVSD (Kaya et al., 2010; Hartupee and Mann, 2016; Hulsmans et al., 2016).

Elucidation of the pathomechanisms underlying the occurrence of PCH has shown the involvements of β -adrenergic receptors (β ARs) and G protein-coupled receptor kinases 5 (GRK5) activities in both cardiomyocytes and immune cells (Hullmann et al., 2014; Adzika et al., 2019). Stimulation of β ARs by physiological levels of catecholamines inducing signaling *via* the stimulatory G protein (G α_s)—adenylyl cyclases (ACs)—cyclic adenosine monophosphate (cAMP) pathway (Adzika et al., 2019). In cardiomyocytes, AC5/AC6-cAMP—L-type calcium channel (LTCC) facilitates inotropic and chronotropic, while in immune cells, AC7-cAMP exerts adaptive immunoregulation on transcriptional factors (TFs) as such; nuclear factor of activated T-cells (NFATs), and NF- κ B (Paur et al., 2012; Raker et al., 2016; Murphy et al., 2019). As such, ACs-cAMP activities are essential for sustaining the myocardial function under physiological states. However, during CCS, signaling *via* the G α_s /ACs/cAMP pathway is impeded, affecting its modulation of cardiac and immune functions.

GRKs modulate the expression and activities of β ARs. While GRK2 engages in β ARs desensitizes, GRK5 phosphorylates the receptors to initiate G protein-coupled receptors (GPCR)-independent signaling, which induces PCH (Gold et al., 2012; Hullmann et al., 2014; Traynham et al., 2016). Also, GRK5

Abbreviations: AC, adenylyl cyclase; ALX, Amlexanox; cAMP, cyclic adenosine monophosphate; CCS, chronic catecholamine stress; cTnI, cardiac troponin I; FSK, Forskolin; GRK, G protein-coupled receptor kinases; ISO, isoproterenol; LPS, lipopolysaccharide; LVSD, left ventricular systolic dysfunction; PCH, pathological cardiac hypertrophy; PM ϕ , peritoneal macrophage; TBK1, TANK-binding kinase 1; TFs, transcriptional factors; TNF α , tumor necrosis factor-alpha; β AR, beta-adrenergic receptors.

translocations into nuclei to maladaptively phosphorylate cardiac hypertrophy and inflammatory TFs; NFATs, myocyte enhancer factor 2 (MEF2), GATA4, and NF- κ B hastens the pathological remodeling (Hullmann et al., 2014).

Currently, there are no stipulated treatment regimens that aim at attenuating PCH during CCS through the simultaneous prevention of maladaptive myocardial hypertrophy, fibrosis, and inflammation. Herein, we demonstrate that during chronic isoproterenol-induced cardiomyopathy (referred to as PCH hereafter), the expression of β ARs, ACs, GRKs, cardiac hypertrophy, and inflammatory TFs are altered. Also, we showed that inflammatory responses elicited by troponin in the PCH hearts were similar to those induced when its activity was mimicked *in vitro* with lipopolysaccharides (LPS) during stress.

GRK5 and ACs were targeted with amlexanox (ALX) and forskolin (FSK), respectively, to explore PCH treatment interventions. ALX has been shown to inhibit GRK5-mediated hypertrophy in PCH models; however, there is no evidence that cardiac functions were preserved (Homan et al., 2014). Also, ALX is demonstrated to inhibit inflammatory responses activated *via* GRK5 (Patil et al., 2011; Quan et al., 2019). The stimulation of ACs by FSK facilitates the bioavailability of cAMP (Huang and Wong, 1989; Chiadak et al., 2016), which might ensure the modulation of cardiac and inflammatory functions during CCS. Therefore, by inhibiting GRK5 and stimulating ACs, we attenuated the hyperactive proinflammatory responses observed *in vitro*. Furthermore, these treatment interventions were translated *in vivo* to assess their therapeutic potential in attenuating PCH through modulation inflammatory and hypertrophy responses.

MATERIALS AND METHODS

Experimental Animals and Models

Male FVB mice aged between 8 and 12 weeks were randomized into groups ($n = 4$ –16 mice per group depending on the experimental setting) and used for both *in vitro* and *in vivo* experiments. Isoproterenol-induced cardiomyopathy models were made by subcutaneous injections of isoproterenol (160504; Sigma) 0.5 mg/100 g/day as previously demonstrated (Lin et al., 2016; Zhou et al., 2017), for 40 days. The equivalents of the placebo (5% v/v dimethyl sulfoxide) were injected to the vehicle (Vhl) group. Also, because it has been shown that laboratory animal handling induces background stress (Gouveia and Hurst, 2019), littermates without any handling were included in the study and designated as the control (Ctrl) group to rule out handling as a contributor to any observed pathological alterations.

PCH preventive models were made by intraperitoneal injection of ALX (ab142825; Abcam) 2.5 mg/100 g/day and/or FSK (1099; Tocris Bioscience, United Kingdom) 0.5 mg/100 g/day. These treatments were administered during the isoproterenol-induced cardiomyopathy modeling (**Supplementary Figure 1**).

The mice were euthanized by cervical dislocation, and macrophages or the hearts were isolated for further analysis.

Electrocardiography and Echocardiography

Mice, 10–11 per treatment group, were mildly sedated with 0.5% isoflurane. The mice were fixed with echo gel, and their body temperatures were monitored and maintained at 37°C for electrocardiography (ECG) data acquisition with Vevo 2100 Ultrasound system (VisualSonics, Toronto, Canada). Simultaneously, global cardiac function was assessed in M-mode with a Vevo 2100 Ultrasound system (VisualSonics, Toronto, Canada). At end-systole and end-diastole, the interventricular septal wall and posterior wall thicknesses, as well as left ventricle internal diameters, were evaluated from the left parasternal longitudinal axis view. Ejection fraction (EF) and fractional shorten (FS) were calculated as described (Jia et al., 2019).

Immune Cell Isolation and Culture

Peritoneal macrophages (PM_{ϕ}) ($n \geq 2 \times 10^6$ cells per treatment group) were isolated from mice as previously described (Ray and Dittel, 2010) but with some modifications. Eight to ten milliliters of 37°C PBS containing 3% fetal bovine serum (FBS) was carefully injected into the peritoneal cavity. The cell suspensions were then collected from the peritoneum after 5 min and centrifuged at 1,500 rpm for 10 min. The pellets of cells were resuspended in 10% FBS and cultured for 48 h. The cells were initially identified using F4/80 (123116; BioLegend) and CD11b (101206; BioLegend). Subsequently, cultured PM_{ϕ} were pre-treated for 1 h with 35 μ M/ml of ALX, and challenged with 10 μ M/ml of ISO and/or 1 μ g/ml LPS along with the same dose of ALX treatment for 24 h. Also, PM_{ϕ} challenged with ISO and LPS was treated with 10 μ M/ml FSK. The combination of ALX and FSK treatment was employed as well. The supernatants were used for ELISA assays, while the PM_{ϕ} were used to assess GRK5 activities *in vitro*.

Enzyme-Linked Immunosorbent Assay

Sera and lysate from *in vivo* models ($n = 7$ –9 mice per treatment group) and cell culture media supernatants from treated PM_{ϕ} were used to assess the concentrations of proinflammatory cytokines (IL-1 β , IL-6, and TNF α), anti-inflammatory cytokines (IL-10 and TGF- β), troponin I and cAMP. IL-1 β (ab197742; Abcam), IL-6 (ab222503; Abcam), TNF α (ab208348; Abcam), IL-10 (ab255729; Abcam), TGF- β (KE10005; Proteintech), cAMP (JL13362; Jianglai Bio, China), and troponin I (JL31923; Jianglai Bio, China) ELISA were performed in triplicates as per the instructions of the manufacturer.

RNA Extraction and Real-Time qPCR

Total RNA was extracted from ventricular apical myocardium ($n = 6$ hearts per treatment group) using TRIzol (15596026; Life technologies). cDNA was synthesized from 1 μ g of RNA using a reverse transcription kit according to the instruction of the manufacturer (FSQ107; Toyobo). The obtained cDNAs were amplified by semiquantitative RT-PCR using SYBR Green Master Mix (Q111-02; Vazyme). The primer sequences used are listed here (**Supplementary Table 1**). The relative gene expressions were normalized to the expressions of GAPDH and were compared as described (Gold et al., 2012).

Immunofluorescence Staining

Cultured and pre-treated PM_φ ($n \geq 2 * 10^6$ cells per treatment group) were fixed and permeabilized with pre-chilled methanol-acetone (ratio 1:1). Non-specific antibody binds were blocked with 1% BSA in PBS for 1 h. PM_φ were then incubated with GRK5 primary antibody (ab64943; Abcam) at 4°C overnight, washed with PBS, and probed with R-PE-conjugated secondary antibody (SA00008-2; Proteintech) at room temperature for 1 h. Next, cells were washed with PBS, conditioned with 0.5% BSA in Hanks' balanced salt solution, and the cytoplasmic membranes were stained with cholera toxin B (CTxB) (C34775, Thermo Fisher Scientific) for 30 min at 4°C. DAPI nuclei staining were done and followed by imaging and assessment of the ratios of nucleic and cytoplasmic GRK5 expressions with ImageJ ($n = 12-15$ cells per four mice).

Histological Analysis of Hypertrophy, Interstitial Fibrosis, and Immune Cells Infiltration

Hearts were excised ($n = 6-10$ mice per treatment group), rinsed, and fixed in 10% formaldehyde overnight. The hearts were then embedded in paraffin and sectioned at 4 μm. Subsequently, H&E (G1120; Solarbio), Masson's trichrome (G1340; Solarbio), wheat germ agglutinin (WGA) (W11261; Thermo Fisher Scientific), and CD68 (ab955; Abcam) immunohistochemical staining were then performed as previously described (Qi et al., 2019). Imaging of tissue slides was done at × 400 magnification and analyzed with ImageJ (1.52a version; National Institute of Health, United States).

Western Blot

Apical myocardia harvested from four to six hearts per treatment group were homogenized in a lysis buffer containing phosphatase and proteinase cocktail inhibitor, in a ratio of 100:1:1, respectively. Lysates of normalized concentrations treated with reducing agents were denatured at 100°C for 10 min and separated on SDS-PAGE gels. The transferred protein bands were blocked and immunoblotted overnight in the following primary antibodies: β₁AR (ab3442; Abcam), β₂AR (ab182136; Abcam), MEF2 (ab64644; Abcam), GRK5 (ab64943; Abcam) GATA4 (ab84593; Abcam), NFAT (ab25916; Abcam), AC5 (PAC-501AP; FabGennix), AC6 (PAC-601AP; FabGennix), AC7 (PAC-701AP; FabGennix), ANP (sc-515701; Santa Cruz Biotechnology), BNP (sc-271185; Santa Cruz Biotechnology), GRK2 (sc-13143; Santa Cruz Biotechnology), pNF-κB (3033T; Cell Signaling Technology), NF-κB (8242T; Cell Signaling Technology), Cleaved Caspase-3 (9661T; Cell Signaling Technology), Collagen Type I (14695-1-AP, Proteintech), Collagen Type III (13548-1-AP, Proteintech), and GAPDH (10494-1-AP; Proteintech). Immunoblots were performed in triplicates and normalized with their respective loading controls.

Statistical Analysis

One-way ANOVA was used for comparing data of multiple groups, and *post hoc* analyses were done using Tukey's multiple comparisons test. Values of $p < 0.05$ were deemed significant.

Using GraphPad Prism (Prism Version 8.0.2), all data were expressed as mean ± SEM.

RESULTS

Chronic Catecholamine Stress Alters Cardiac and Inflammatory Functional Proteins in Mice

Analysis of mRNAs and protein expressions demonstrated that crucial cardiac and inflammatory proteins were altered in the myocardia during CCS compared with under physiological states. βARs, AC5, and AC7 were found depleting, while AC6, β-ARR-1, β-ARR-2, GRK2, and GRK5 were upregulated in the PCH mice hearts (**Supplementary Figures 2A–K**). Also, the TFs: GATA4, NFAT, MEF2, and NF-κB were overexpressed in PCH hearts compared with Ctrl and Vhl hearts (**Supplementary Figures 3A–E**). Cardiac hypertrophy was evident in PCH mice as atrial natriuretic peptide (ANP) and brain natriuretic peptide (BNP) were significantly upregulated in their myocardia than Ctrl and Vhl mice (**Supplementary Figures 2A,J,K**). To ascertain the impact of AC5, AC6, and AC7 alterations in PCH models, cAMP bioavailability was assessed and found to be significantly decreased in myocardial lysates obtained from PCH mice (**Supplementary Figure 2L**).

Troponin and Lipopolysaccharide Elicit Similar Immunogenic Response During Chronic Catecholamine Stress

Immediate assays for cardiac troponin I (cTnI) from sera showed its overt upregulation in PCH mice compared with concentrations in Ctrl and Vhl mice (**Figure 1A**). Assessment of mRNAs of IL-1β, IL-6, TNFα, IFNγ, NF-κB, and IL-10 from the myocardia showed that besides the latter, the proinflammatory cytokines and TF were significant overexpression in PCH hearts (**Figure 1B**).

By using LPS to mimic the immunogenicity of troponin *in vitro*, inflammatory responses elicited under stress were ascertained and compared with the *in vivo* models. The result demonstrated similarities in their immunogenicity. The PM_φ culture with ISO and LPS for 24 h secreted enormous amounts of IL-1β, IL-6, and TNFα just as observed in PCH mice, while IL-10 and TGF-β were also dampened similarly, both *in vitro* and *in vivo* (**Figures 1C–G**).

Amlexanox and Forskolin Combination Inhibits Proinflammatory Responses During Chronic Catecholamine Stress Primarily *via* Cyclic Adenosine Monophosphate-Mediated Immunoregulation

ALX (35 μM/ml) and/or FSK (10 μM/ml) treatments were employed to attenuate the hyperactive proinflammatory cytokine secretions elicited from the PM_φ *in vitro*. Analysis of the concentrations of inflammatory cytokines from these

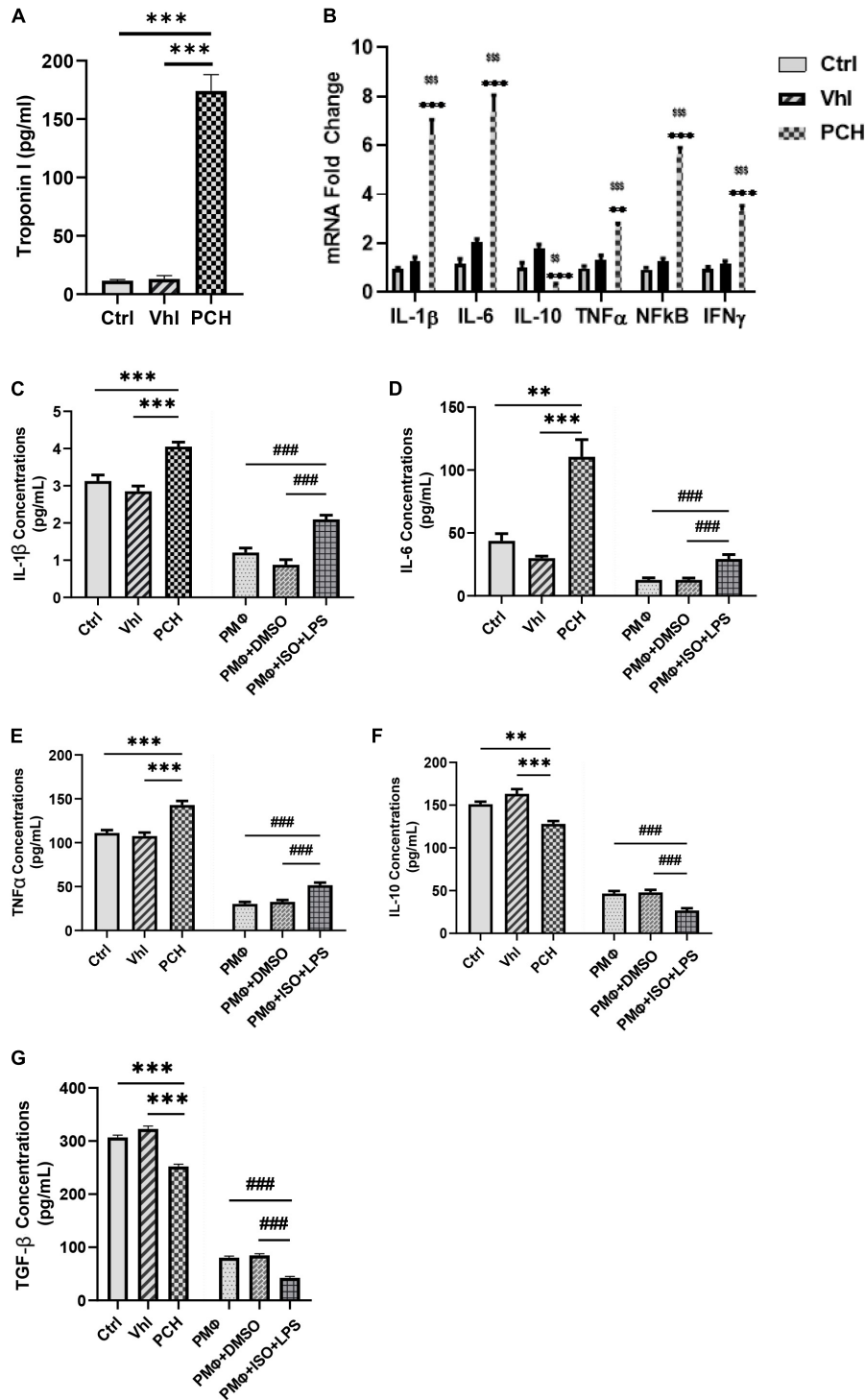


FIGURE 1 | Troponin from necrotic cardiomyocytes and lipopolysaccharides (LPS) elicits similar inflammatory responses during chronic catecholamine stress (CCS). **(A)** Sera concentrations of troponin I were evaluated by ELISA from Control (Ctrl), Vehicle (Vhl), and Pathological cardiac hypertrophy (PCH) groups. **(B)** mRNA expressions of inflammatory markers (IL-1 β , IL-6, TNF α , IFN γ , and NF- κ B) assessed from the myocardial by qRT-PCR ($n = 6$ hearts per treatment group). **(C–G)** Comparison with inflammatory cytokines secretion (IL-1 β , IL-6, TNF α , IL-10, and TGF- β) between PCH mice (*in vivo*) and LPS-challenged peritoneal macrophages (PM ϕ) (*in vitro*) during CCS. All ELISA evaluations were performed in triplicates ($n = 8$ mice per treatment group). Data are expressed as mean \pm SEM. Data were analyzed using one-way ANOVA, followed by Tukey's *post hoc* analysis. Abbreviations: IL, interleukin; TNF α , tumor necrosis factor-alpha; TGF- β , transforming growth factor-beta; IFN γ , interferon-gamma.

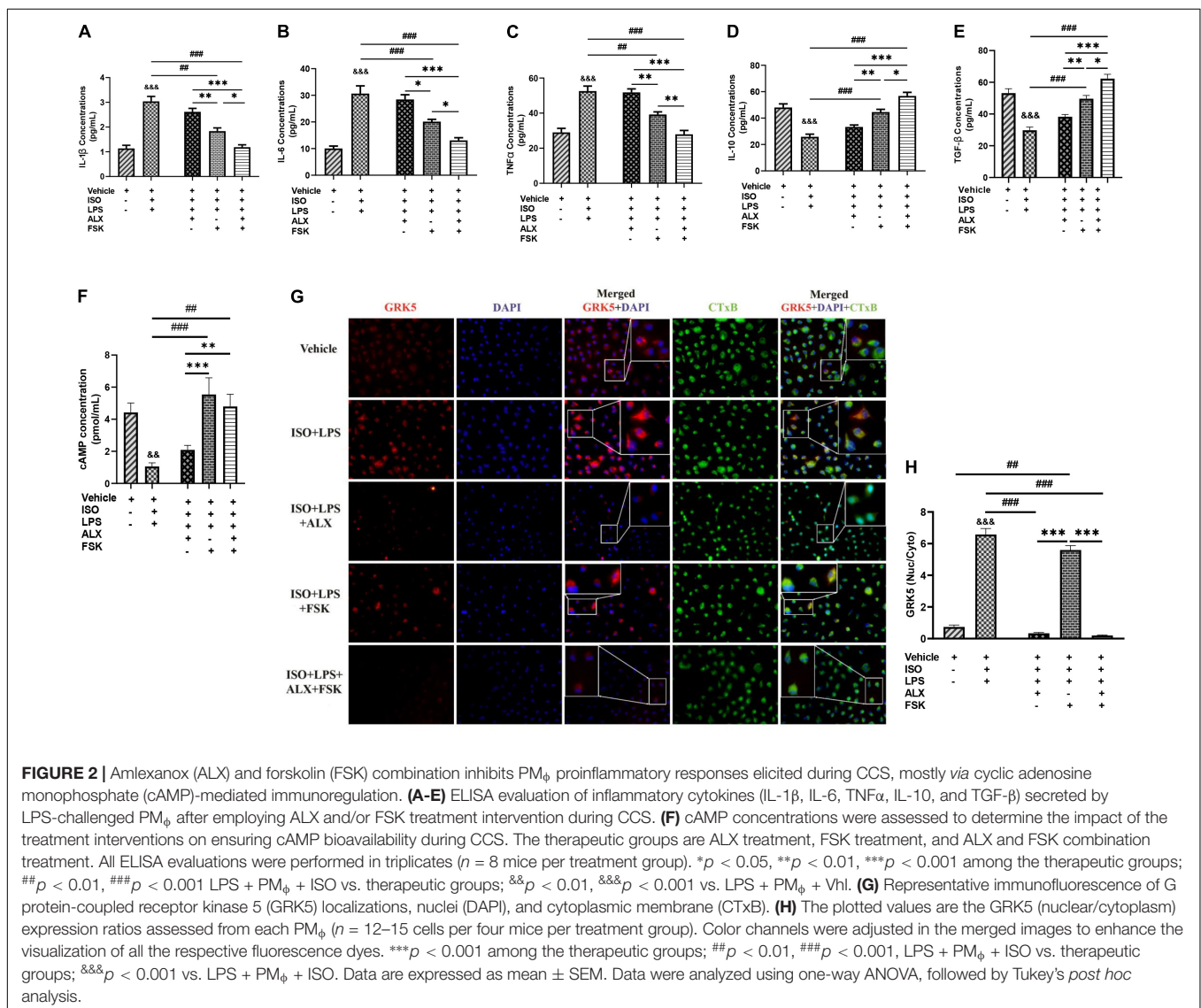
experiments using ELISA demonstrated that ALX treatment could not effectively subdue the hypersecretions of IL-1 β , IL-6, and TNF α ; neither did it upregulate IL-10 and TGF- β secretions during stress. Comparatively, FSK treatment was effective than ALX treatment at decreasing the proinflammatory responses while upregulating IL-10 and TGF- β secretions (Figures 2A–E). Regardless, ALX and FSK combination treatment was the most potent in subduing the hyperactive proinflammatory response.

Assessment of the effect of FSK on ensuring cAMP bioavailability showed that its presence in both the single and combination treatments upregulated cAMP markedly compared with the ISO + LPS and ISO + LPS + ALX groups (Figure 2F). Hence, it is inferred that the potency attained by the combination treatment may have been mainly *via* cAMP-mediated immunoregulation. The validation of this was done by assessing the effect of the therapies on GRK5 expressions. GRK5 cytosolic and nuclear expressions were inhibited by ALX in both the single and combination treatments, while FSK

treatment had increased GRK5 nucleic–cytosolic expression ratio just as ISO + LPS, which had no treatment interventions (Figures 2G,H). However, proinflammatory responses were minimized in the ISO + LPS + FSK (Figures 2A–C), despite the increase in GRK5 nuclear expression.

Amlexanox and Forskolin Combination Attenuates Left Ventricular Systolic Dysfunction in Mice During Chronic Catecholamine Stress

Echocardiography and ECG assessments at the end of *in vivo* model showed that PCH mice had LVSD. The treatments of ALX, FSK, and their combination were employed during CCS in attempts to prevent the LVSD. Cardiac functions assessed after using these treatment interventions showed that ALX failed to prevent the LVSD during CCS, as ejection fraction (EF) and fractional shortening (FS) were still decreased significantly



compared with the control groups. Similarly, FSK treatment did not attenuate the LVSD during CCS but instead caused tachycardia and arrhythmias (Figures 3A–D and Supplementary Figure 3F and Supplementary Table 2). Intriguingly, ALX and FSK combination was found to preserve cardiac function by maintaining EF and FS during CCS.

Amlexanox and Forskolin Combination Normalizes Cardiac and Inflammatory Functional Protein Expression in Mice During Chronic Catecholamine Stress

To ascertain the potential mechanism of action employed by the ALX and FSK combination to prevent the LVSD, the expression of functional proteins and TFs were reassessed. β ARs, AC5, AC6, AC7, GRK2, GRK5, ANP, BNP, GATA4, NFAT, MEF2, and NF- κ B expressions were found to have been altered in PCH mice myocardia (Supplementary Figures 2, 3). However, the ALX and FSK combination prevented significant alteration in the expressions of these proteins, while their individual treatment showed several limitations. β_1 AR and β_2 AR expressions were sustained by all treatment intervention groups.

FSK in both single and combination treatment normalized AC5 and AC7 to physiological levels, while AC6 was upregulated; thus, cAMP concentrations were primarily increased in these groups. Meanwhile, ALX showed a negligible inhibitory effect on GRK2 but prevented GRK5, ANP, and BNP upregulations in both its single and combined treatments with FSK (Figures 3E–O). Nonetheless, GATA4, NFAT, MEF2, and NF- κ B expressions were still upregulated predominantly in the ALX treatment group and followed by the FSK treatment group. Intriguingly, ALX and FSK combination minimized the expressions of these functional proteins and TFs close to physiological levels during CCS (Supplementary Figures 4A–E).

Amlexanox and Forskolin Combination Preserves Mice Myocardial Architecture During Chronic Catecholamine Stress

LV posterior wall thickness (LVPW), LV mass (LVM), and heart weight/body weight (HW/BW) ratio assessments showed their significant increases in PCH mice compared with the Vhl and Ctrl groups (Figure 4A and Supplementary Table 2). However, during CCS, ALX in both single and combination treatment

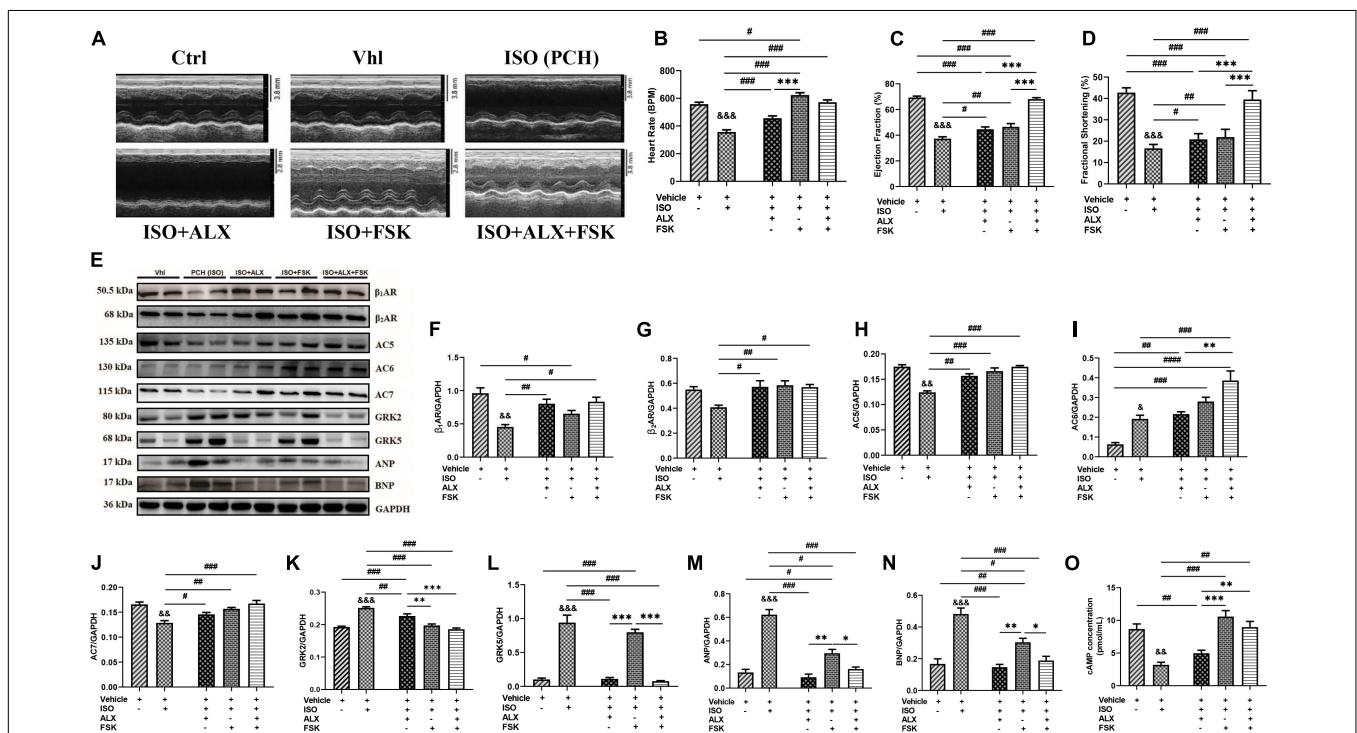
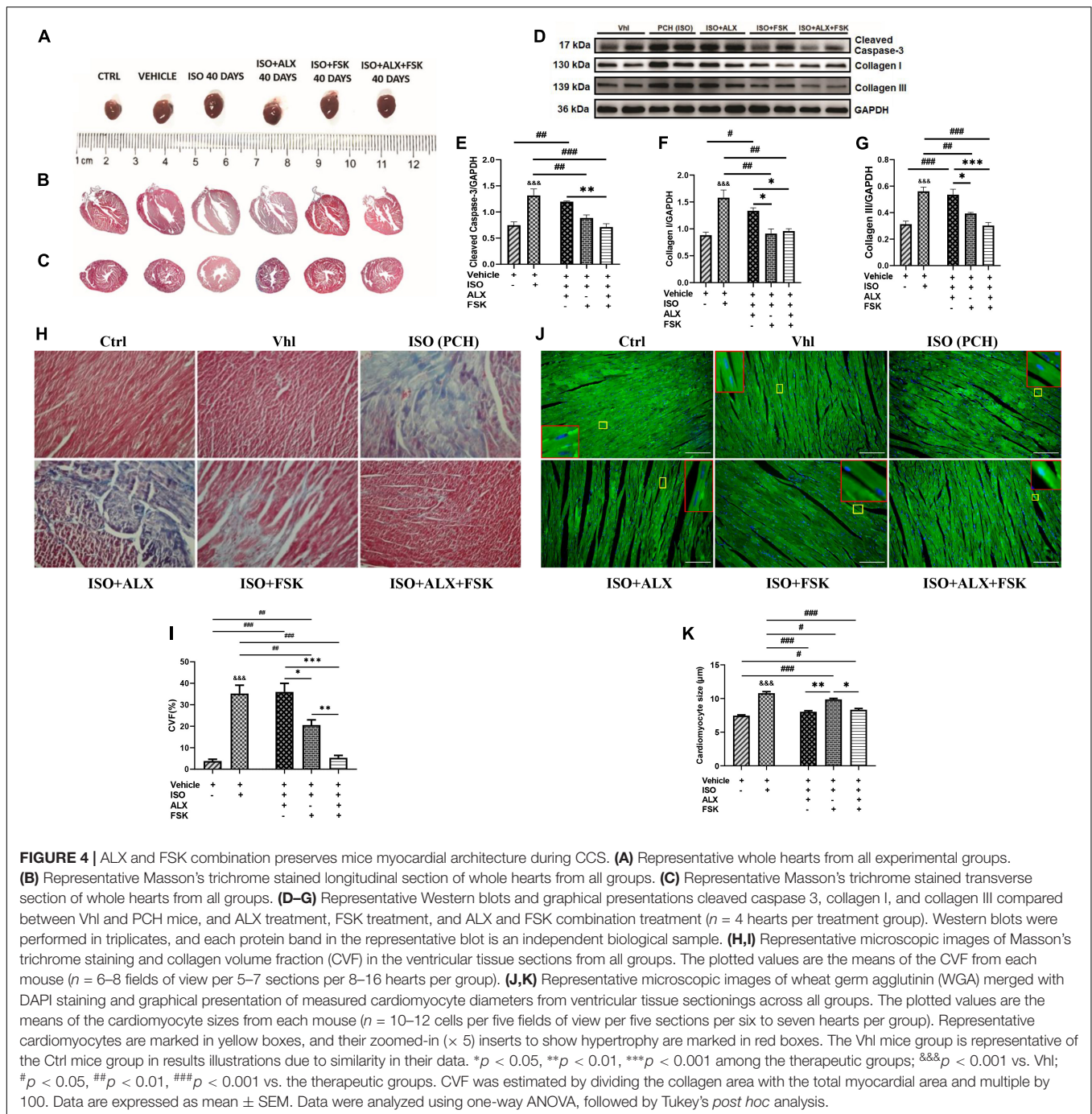


FIGURE 3 | ALX and FSK combination attenuates left ventricular systolic dysfunction (LVSD) in mice during CCS by normalizing protein expressions. **(A)** Representative short-axis view M-mode echocardiogram imaging from Ctrl, Vhl, isoproterenol (ISO), ISO + ALX, ISO + FSK, and ISO + ALX + FSK. **(B–D)** Graphical presentations of heart rates, ejection fraction, and fractional shortening assessments from all models. The Vhl mice group is representative of the Ctrl mice group in the graphical presentations due to similarity in their data. The therapeutic groups are ALX treatment, FSK treatment, and ALX and FSK combination treatment ($n = 10–11$ hearts per treatment group). **(E–N)** Representative Western blots and graphical presentation of β ARs, ACs, GRKs, ANP, and BNP, were assessed from all groups ($n = 4$ hearts per treatment group). Western blots were performed in triplicates, and each protein band in the representative blot is an independent biological sample. **(O)** Graphical represents of cAMP concentrations evaluated by ELISA ($n = 9$ mice per treatment group). * $p < 0.05$, ** $p < 0.01$, *** $p < 0.001$ among the therapeutic groups; && $p < 0.01$, &&& $p < 0.001$ vs. Vhl; # $p < 0.05$, ## $p < 0.01$, ### $p < 0.001$ vs. the therapeutic groups. Data are expressed as mean \pm SEM. Data were analyzed using one-way ANOVA, followed by Tukey's *post hoc* analysis. Abbreviations: β ARs, β -adrenergic receptors; ACs, adenylyl cyclases; GRKs, G-protein-coupled receptor kinases; ANP, atrial natriuretic peptide; BNP, brain natriuretic peptide.



prevented significant increases in LVPW, LVM, and HW/BW; meanwhile, FSK treatment failed to achieve these. Masson's trichrome staining of longitudinal and transverse myocardial sections showed apparent distortions of the gross cardiac morphology of PCH mice. Nonetheless, rather than either ALX or FSK treatments, their combination seemed to have preserved the myocardial architecture during CCS (**Figures 4B,C**). The impacts of the treatment interventions on cardiomyocyte apoptosis and collagen depositions were ascertained to validate this observation. Cleaved caspase-3 (biomarker for apoptosis)

was upregulated in PCH hearts along with significant increases in collagen I and III. In conformity with the histological findings, only the ALX and FSK combination treatment was potent at preventing cardiomyocyte apoptosis and collagen depositions in the heart of the mice during CCS (**Figures 4D–G**). Also, the myocardial collagen volume fraction (CVF) assessed further confirmed that PCH mice had marked interstitial deposits, which was only prevented effectively by the ALX and FSK combination treatment (**Figures 4H,I**). Besides, cardiomyocyte diameters measured from WGA and H&E staining showed

excessive myocyte hypertrophy in PCH hearts. Consistent with attenuating the increases in ANP, BNP, LVPW, HW/BW, and LVM, ALX in both single and combination treatment prevented cardiomyocyte hypertrophy during CCS, while FSK treatment could not (Figures 4J,K and Supplementary Figures 4E,G).

Amlexanox and Forskolin Combination Prevents Proinflammatory Response Aggravation in Mice Myocardia During Chronic Catecholamine Stress

The effects of the treatment interventions in modulating myocardial inflammation were initially ascertained by evaluating their impact on cardiomyocyte necrosis through the immediate sera analysis of the cTnI. Inference from the cTnI concentrations indicated that the ALX treatment was ineffective at preventing necrosis, while FSK treatment did better comparatively. Regardless, ALX and FSK combination was the most potent in preventing necrosis during CCS (Figure 5A). Furthermore, CD68⁺ IHC staining was done to evaluate the efficacies of the treatments in attenuating the aggravated inflammatory cell infiltration observation in PCH hearts (Figures 5B,C) and demonstrated that, while FSK significantly decreased the CD68⁺ cells infiltration than the ALX during CCS, their combination was the most potent at preventing exacerbation

of the inflammatory responses. In conformity, the followed-up cytokine analysis showed that the ALX and FSK combination was the most effective in downregulating IL-1 β , IL-6, and TNF α secretions while enhancing IL-10 and TGF- β . Comparatively, FSK treatment was able to do these better than ALX treatment did during CCS (Figures 5D-H).

DISCUSSION

This study aimed to prevent isoproterenol-induced cardiomyopathy through the attenuation of maladaptive myocardial hypertrophy and inflammatory responses. The preliminary assessment of cardiac and inflammatory functional proteins demonstrated their alteration during CCS compared with physiological states. Typically, β_1 AR expressions were significantly downregulated, while β_2 AR expressions were rarely depleted during CCS. Consistent with previous studies, β_2 AR is implicated in mediating stress-induced cardiovascular diseases (Paur et al., 2012; Spadari et al., 2018). Also, while AC5 expression was decreased during CCS, AC6 was found upregulated. In conformity with these findings, it has been previously shown that AC5 facilitates PKA pathway signaling under physiological conditions, while AC6 mediates stress response for calcium channel modulation via PKA/STAT3

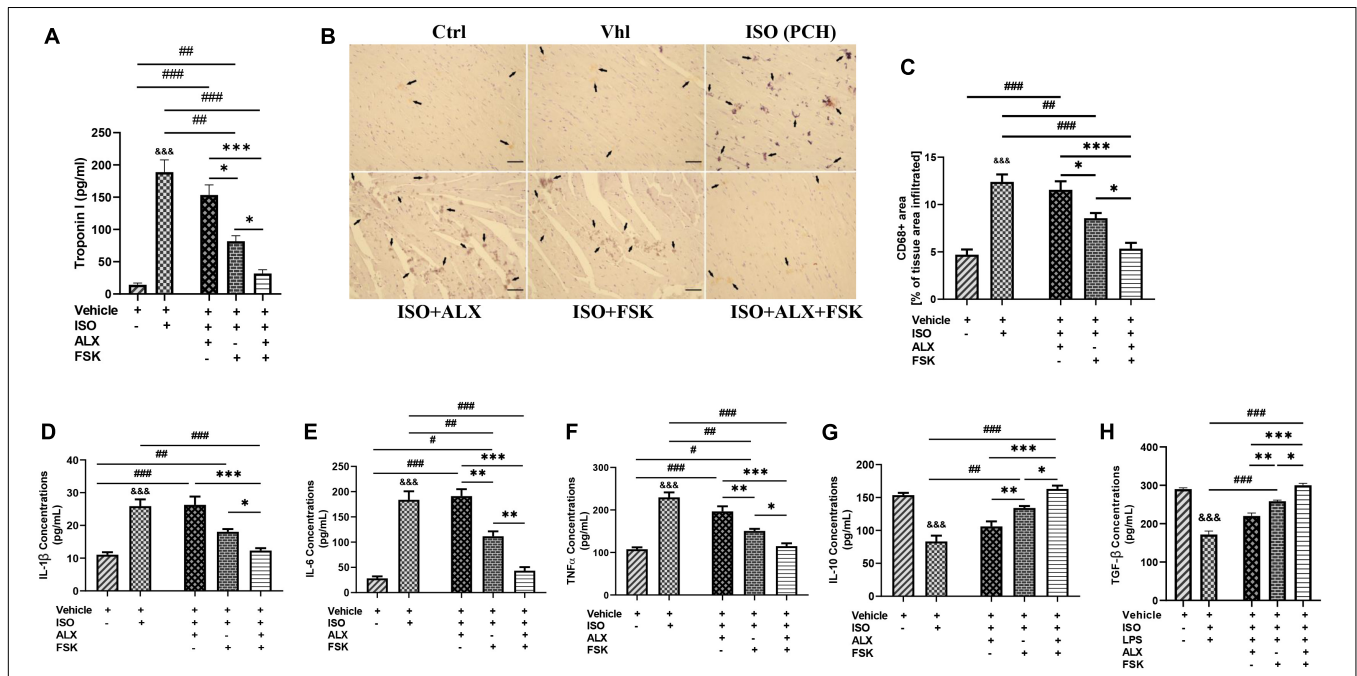


FIGURE 5 | ALX and FSK combination prevents proinflammatory responses aggravation in myocardia during CCS by preventing necrosis. (A) Graphical presentations of evaluated sera concentrations of troponin I from groups. The sera troponin I analysis was performed in triplicates ($n = 8$ mice per treatment group). $*p < 0.05$, $***p < 0.001$, among the therapeutic groups; $\&\&\&p < 0.001$ vs. ISO (PCH); $\#\#p < 0.01$, $\#\#\#p < 0.001$, vs. the therapeutic groups. (B,C) Representative CD68 IHC staining and graphical presentation of the extent of inflammatory cells infiltration into the myocardial of all groups. The Vhl mice group is representative of the Ctrl mice group in results illustrations due to similarity in their data ($n = 6-8$ field of view per six to eight sections per six to seven hearts per group). (D-H) Graphical presentations of inflammatory cytokines (IL-1 β , IL-6, TNF α , IL-10, and TGF- β) were evaluated by ELISA from all groups. The cytokines analysis was performed in triplicates ($n = 7-8$ mice per treatment group). $*p < 0.05$, $**p < 0.01$, $***p < 0.001$, among the therapeutic groups; $\&\&\&p < 0.001$ vs. Vhl; $\#p < 0.05$, $\#\#p < 0.01$, $\#\#\#p < 0.001$ vs. the therapeutic groups. Data are expressed as mean \pm SEM. Data were analyzed using one-way ANOVA, followed by Tukey's *post hoc* analysis.

(Wu et al., 2017). Like AC5, AC7 was downregulated in PCH mice myocardia compared with the Ctrl and Vhl groups. The ELISA, performed to ascertain the impact of the ACs alteration on cAMP bioavailability, showed decreased concentrations in PCH mice as reported in other chronic stress models (Plattner et al., 2015). cAMP mediates crucial cardiac and immunoregulatory functions *via* the modulation of the LTCC, NFAT, MEF2, and NF- κ B in both inflammatory and cardiac cells (Pereira et al., 2015; Raker et al., 2016). Hence, the observed downregulation of cAMP in PCH mice might permit cardiac and inflammatory dysfunctions. We also found that β -ARR-1, β -ARR-2, GRK2, and GRK5 were overexpressed in PCH hearts, which were consistent with the findings of others (Hullmann et al., 2014; Adzika et al., 2019; Sun et al., 2021). GRK2 upregulation increases the internalization of β_1 AR *via* the recruitment of β -ARR-1 in the homologous desensitization process (Adzika et al., 2019; Sun et al., 2021); therefore, this explains the downregulated expression of β_1 AR in PCH myocardia. Conversely, by recruiting β -ARR-2, GRK5 enhances β_2 AR signal progression in a GPCR-independent manner to induce maladaptive hypertrophy and proinflammatory responses *via* phosphorylating NFAT, MEF2, GATA4, and NF- κ B (Patial et al., 2011; Islam et al., 2013; Hullmann et al., 2014; **Figure 6**). Intriguingly, these cardiac and inflammatory TFs were shown overexpressed, along with ANP and BNP upregulated in the PCH myocardia compared with their expressions in the control groups (**Supplementary Figures 3, 4**). These are indicative of the likelihood of GRK5 activities in inflammatory and cardiac cells.

The exacerbation of cardiovascular remodeling by cTnI-induced inflammatory responses has also been widely reported. In these instances, elevated proinflammatory and downregulated anti-inflammatory responses were observed (Kaya et al., 2008; Heidt et al., 2014). The upregulated sera levels of cTnI in PCH mice (**Figure 1A**) indicate the occurrence of excessive cardiomyocyte necrosis. In line with the increased release of cTnI by necrotic cardiomyocytes, proinflammatory responses (IL-1 β , IL-6, TNF α , IFN γ , and NF- κ B) were hyperactive in PCH mice, while anti-inflammatory responses (IL-10 and TGF- β) were dampened, just as demonstrated previously (Kaya et al., 2008).

Furthermore, LPS has been extensively used to induce cardiac inflammation and has been observed to share similarities in the immunogenic responses elicited by troponin (Cai et al., 2020). To validate this, we mimicked cTnI immunogenicity in PCH models with LPS under stress conditions *in vitro*. Comparing cytokine analysis between *in vivo* and *in vitro* experiments confirmed the similarities between cTnI and LPS immunogenicity during stress. Also, although it could be argued that LPS would still elicit proinflammatory responses from PM ϕ under physiological state, a previous study and performed cytokine analysis (data not included) have demonstrated the exacerbation of these responses during CCS (Laukova et al., 2018).

In further *in vitro* investigations, we explored the inhibitory effects of ALX on GRK5 and/or the stimulatory effects of FSK on AC/cAMP synthesis for attenuating the LPS-induced inflammatory responses during stress. The followed-up cytokine analysis demonstrated that only the inhibition of GRK5 during stress could not effectively attenuate the

proinflammatory response elicited from the PM ϕ , although the ALX dosage used was within the range reported previously to halt proinflammatory response in a different pathological model (Quan et al., 2019). Comparatively, FSK-AC/cAMP exerted more anti-inflammatory effects than ALX did; regardless, their combination showed the most potency at exhibiting adaptive immunoregulation. FSK enhanced cAMP bioavailability in single and combined treatments. Consistent with these findings, FSK-AC/cAMP had been reported earlier to exert anti-inflammatory effects *via* NF- κ B inhibition (Chiadak et al., 2016). To validate the mechanism utilized by the ALX and FSK combination to attenuate the proinflammatory responses, immunofluorescence was used to ascertain the expressions of GRK5 among the *in vitro* treatment groups (**Figures 2G,H**). As suggested (Homan et al., 2014), ALX in both single and combination treatment inhibited GRK5 expression and nuclear translocation, while FSK failed to do either, just like the group without treatment interventions (LPS + ISO). However, although GRK5 translocated into the nuclei of LPS + ISO as much as it did in LPS + ISO + FSK, proinflammatory responses were not aggravated in the latter. As such, these were concluded from **Figure 2** and the findings of others: (1) Although ALX inhibited GRK5-mediated proinflammatory response activation, other inflammatory mediators such as kinases, peptides, and amines are still capable of inducing the immune responses (Abdulhaleq et al., 2018), as observed in the LPS + ISO + ALX group. (2) Also, the abolishment of cAMP-dependent adaptive immunoregulation by stress in the LPS + ISO + ALX group may have enabled the observed proinflammatory responses, as demonstrated previously (Bopp et al., 2009; Wehbi and Taskén, 2016). (3) Besides, unlike ALX, which attenuates GRK5-mediated inflammatory responses, FSK-ACs/cAMP adaptively regulates multiple anti-inflammatory cascades (Raker et al., 2016; Wehbi and Taskén, 2016). Hence, in line with previous studies (Bopp et al., 2009; Patial et al., 2011; Chiadak et al., 2016; Raker et al., 2016; Wehbi and Taskén, 2016), we confirmed that ALX and FSK combination attained their potency primarily *via* FSK/ACs/cAMP-mediated adaptive immunoregulation, coupled with ALX inhibiting the activation of maladaptive inflammatory responses *via* GRK5. Based on these findings, it was hypothesized that rather than either FSK or ALX treatment, their combination might attenuate myocardial inflammation, which drives the adverse remodeling of hearts during CCS.

These hypotheses were tested by translating ALX and/or FSK treatments *in vivo* during CCS. At the end of all models, echocardiogram results revealed that the ALX and FSK combination prevent LVSD during CCS, by maintaining typical heart rates, ejection fractions above 65%, and fraction shortenings above 35%. However, ALX treatment failed to maintain proper cardiac function during CCS, while FSK treatment resulted in arrhythmias. Contrary to our findings, Mo et al. (2020) reported that ALX improved cardiac function, but this was in acute myocardial infarction animal models and not during CCS or in an isoproterenol-induced cardiomyopathy model. Also, the ALX dosage they employed was 10 times more than what we used in this study. Nonetheless, our findings regarding FSK-induced arrhythmias were in conformity with the reports from previous

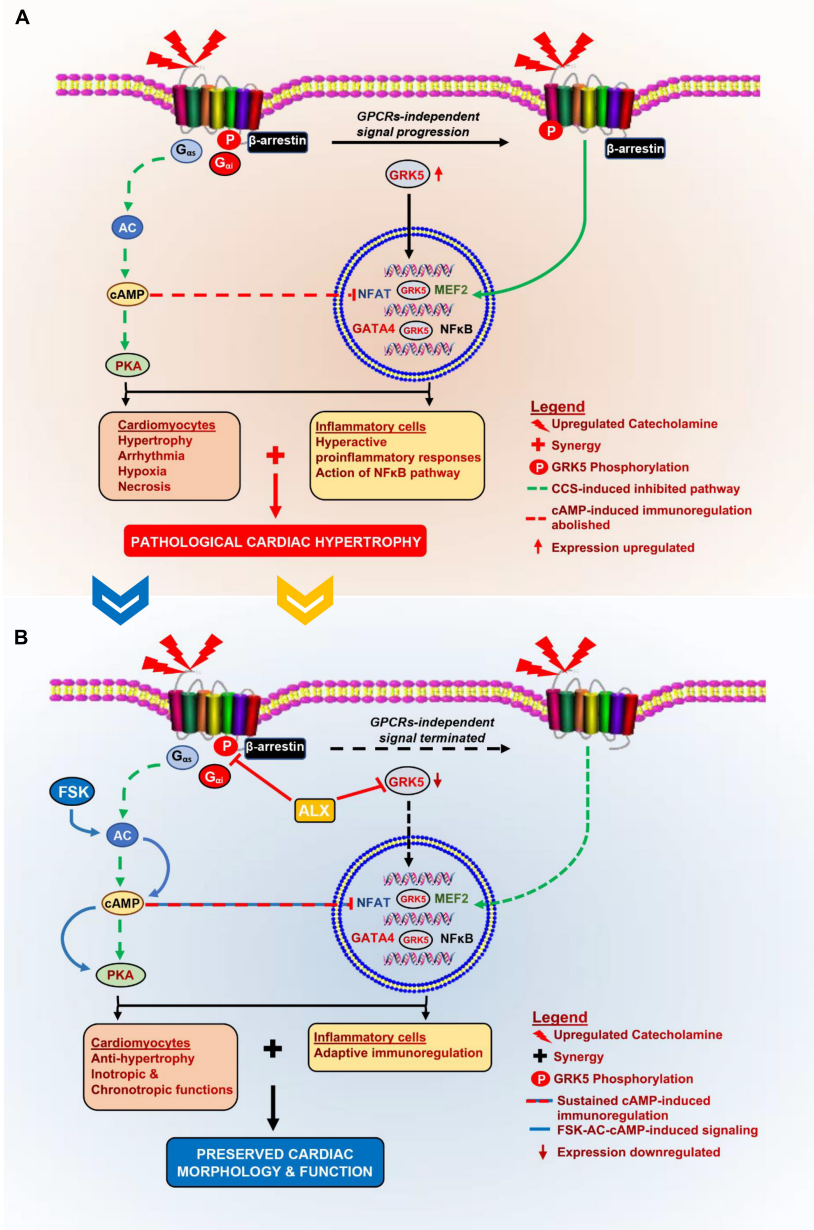


FIGURE 6 | Schematics of the pathomechanism of isoproterenol-induced cardiomyopathy and the mechanisms of ALX and FSK combination treatment. **(A)** During CCS, $G_{\alpha s}$ -AC is decoupled from β ARs, thereby inhibiting cAMP synthesis, which affects cardiac function and immunoregulation in the myocardia adversely. Also, GRK5 upregulates and phosphorylates β ARs as well as translocates into the nuclei to induce GPCRs-independent stimuli signaling. The nuclear activity of GRK5 induces the activation of cardiomyocyte hypertrophy transcriptional factors. These result in excessive cardiomyocyte hypertrophy and hyperactive proinflammatory responses. At the same time, cAMP-mediated adaptive immunoregulation is abolished. The synergy of these cascades results in the exacerbation of collagen deposits which pathologically remodels the heart. **(B)** The administration of ALX and FSK combination facilitates ALX-GRK5 inhibition (expressions and nuclear translocation), which prevents cardiomyocyte hypertrophy; while, FSK-ACs-cAMP modulates adaptive immunoregulation and cardiac inotropic functions. Combining these mechanisms preserves cardiac morphology and prevents left ventricular systolic dysfunction (LVSD) during CCS.

studies (Christ et al., 2014). Intriguingly, tachyarrhythmia did not occur in the combined treatment group despite the presence of FSK, and we speculated that this might be due to an effect exerted by ALX.

Initially, in this study, the occurrence of LVSD was associated with alterations in cardiac and inflammatory proteins in

the myocardia during CCS. As such, to confirm that the treatment interventions influenced their expression to preserve cardiac function, these proteins were reevaluated. In summary, the immunoblotting results showed that the ALX and FSK combination had normalized the expression of all the assessed cardiac and inflammatory proteins besides AC6, which is

specifically responsible for cardiomyocyte protection during stress (Wu et al., 2017).

Although ALX treatment inhibited GRK5, the TFs, GATA4, NFAT, MEF2, and NF- κ B were still overexpressed during CCS (**Supplementary Figure 4**). Consistent with these findings, Hullmann et al. (2014) had earlier suggested that the inhibition of GRK5 might not halt the activation of NFAT, which might have applied to GATA4, MEF2, and NF- κ B as well. Contrarily, FSK single treatment decreased the expression of these TFs, just as Zoccarato et al. (2015) and Chiadak et al. (2016) had demonstrated.

Also, the myocardial morphometric data indicated that the hearts of PCH mice were hypertrophied and had marked fibrosis, which were determined with measured cardiomyocyte diameters, upregulated ANP and BNP upregulation, and Masson's-stained tissues. Further investigations with cleaved caspase-3 and collagen I and III immunoblotting confirmed a significant increase in cardiomyocyte apoptosis and collagen depositions in PCH myocardial. Intriguingly, ALX and FSK combination attenuated excessive cardiomyocyte hypertrophy, apoptosis, and myocardial fibrosis during CCS. Meanwhile, neither ALX nor FSK treatments were able to achieve all the aforementioned individually. ALX treatment downregulated ANP and BNP and attenuated GRK5-induced hypertrophy as suggested (Homan et al., 2014), but it failed to prevent apoptosis, hence, the occurrence of fibrosis. Consistent with these findings, apoptosis has been well demonstrated to aggravate collagen deposition and fibrosis (Hinze and Lagares, 2020). In contrast to ALX treatment, FSK-AC-cAMP significantly inhibited cardiomyocyte apoptosis and fibrosis, just as demonstrated previously (Kwon et al., 2004; Lee et al., 2010; Younce et al., 2013). However, myocardial hypertrophy remained incompletely resolved by FSK treatment. Wolf et al. (2005) had previously reported that myocardial hypertrophy increases tachyarrhythmia susceptibility. Hence, this may have accounted for the observed tachyarrhythmia in the FSK treatment group but not in the ALX and FSK combination group since ALX had attenuated hypertrophy.

Lastly, assessing the effects of the treatment intervention on modulating myocardial inflammation during CCS showed that ALX and FSK combination prevents cardiomyocyte necrosis as sera concentrations of cTnI in mice from this group were significantly downregulated. Hence, cTnI-induced inflammation was attenuated in the ALX and FSK combination treatment group. Individually, in contrast with ALX, FSK-AC-cAMP significantly decreased cTnI (cardiomyocyte necrosis) during CCS, as demonstrated in other studies (Wang et al., 2016). Furthermore, in correlation with the extent of necrosis shown in PCH hearts, enormous amounts of CD68⁺ inflammatory cells were found to have infiltrated their myocardia. This provides supporting evidence that myocardial inflammation is exacerbated by stress, as demonstrated previously (Scally et al., 2019).

Nonetheless, we found that the ALX and FSK combination treatment was the most potent in minimizing CD68⁺ inflammatory cell infiltration into the myocardial during CCS, although FSK treatment also attained this significantly. Similarly, FSK-AC/cAMP has been shown to adaptively modulate myocardial inflammatory responses

(Lee et al., 2010; Shim et al., 2014). However, regarding ALX treatment, we found that it was not effective at decreasing myocardial inflammation, as Mo et al. (2020) had reported. The discrepancies in these findings may be due to the differences in the cardiovascular disease model being investigated and the variation in ALX dosage employed. To complement our findings, the evaluated cytokine concentrates depicted ALX and FSK combination treatment during CCS as the most effective intervention at keeping the gap between proinflammatory (IL-1 β , IL-6, and TNF α) and anti-inflammatory (IL-10 and TGF- β) responses close to a homeostatic immune state. This certainly contributed to the prevention of biased prolonged proinflammatory responses, which could have exacerbated myocyte necrosis, apoptosis, and aggravated interstitial collagen depositions, as shown in other studies (Xiao et al., 2018; Sandstedt et al., 2019).

CONCLUSION

Here, we demonstrated the implication of maladaptive inflammatory response in the pathogenesis of isoproterenol-induced cardiomyopathy. Our findings showed that besides ALX preventing the occurrence of cardiomyocyte hypertrophy, it complemented the efforts of FSK-ACs/cAMP-mediated immunoregulation by abolishing GRK5-mediated induction of inflammatory responses. These combined efforts helped ALX and FSK maintain the myocardial homeostasis, thereby preserving the cardiac morphology and function during CCS (**Figure 6**). Owing to the clinical significance of this study, it is appropriate to acknowledge its limitations. It could be argued that ALX can inhibit I κ B kinases and TANK-binding kinase 1 (TBK1) besides GRK5. Nonetheless, the inhibition of I κ B kinases and TBK1 along with GRK5 by ALX, as demonstrated (Mo et al., 2020), still did not prevent the LVSD in PCH mice models. Also, further studies into determining the toxicity of ALX and FSK combined treatment and its impact on diastolic function and lung congestion during CCS will be required to fully ascertain their therapeutic and translational potentials.

DATA AVAILABILITY STATEMENT

The original contributions presented in the study are included in the article/**Supplementary Material**, further inquiries can be directed to the corresponding author/s.

ETHICS STATEMENT

The animal study was reviewed and approved by the Experimental Animal Centre of Xuzhou Medical University and the Animal Ethics Committee of the Medical University.

AUTHOR CONTRIBUTIONS

GKA conceived the experiments ideas. HS and GKA designed the experiments. GKA and HH isolated and cultured PM ϕ . AA

provided the experimental animals. RR assisted in making the animal models. SA and SK performed PM_φ identification. KL, Q-MD, and XM performed the cardiac function assessments. GKA, TM, and JA-A performed the sera cytokine analysis. GKA, SA, Q-MD, RM, and WS analyzed and interpreted the data. GKA, RM, MN, JA-A, JM, and WS drafted and wrote the manuscript with contributions from all authors. All authors discussed, proofread, and approved the manuscript.

FUNDING

The following grants funded this study; National Natural Science Foundation of China (Nos. 81461138036 and 81370329), Postgraduate Research and Practice Innovation Program of Jiangsu Province, China (KYCX17-1712), and Priority

REFERENCES

- Abdulkhaleq, L. A., Assi, M. A., Abdullah, R., Zamri-Saad, M., Taufiq-Yap, Y. H., and Hezmee, M. N. M. (2018). The crucial roles of inflammatory mediators in inflammation: a review. *Vet. World* 11, 627–635. doi: 10.14202/vetworld.2018.627-635
- Adzika, G. K., Machuki, J. O., Shang, W., Hou, H., Ma, T., Wu, L., et al. (2019). Pathological cardiac hypertrophy: the synergy of adenylyl cyclases inhibition in cardiac and immune cells during chronic catecholamine stress. *J. Mol. Med.* 97, 897–907. doi: 10.1007/s00109-019-01790-0
- Bopp, T., Dehzad, N., Reuter, S., Klein, M., Ullrich, N., Stassen, M., et al. (2009). Inhibition of cAMP degradation improves regulatory T cell-mediated suppression. *J. Immunol.* 182, 4017–4024. doi: 10.4049/jimmunol.0803310
- Cai, Z. L., Shen, B., Yuan, Y., Liu, C., Xie, Q. W., Hu, T. T., et al. (2020). The effect of HMGAI in LPS-induced Myocardial Inflammation. *Int. J. Biol. Sci.* 16, 1798–1810. doi: 10.7150/ijbs.39947
- Chiadak, J. D., Arsenijevic, T., Verstrepen, K., Gregoire, F., Bolaky, N., Delforge, V., et al. (2016). Forskolin Inhibits Lipopolysaccharide-Induced Modulation of MCP-1 and GPR120 in 3T3-L1 Adipocytes through an Inhibition of NFκB. *Mediators Inflamm.* 2016:1431789.
- Christ, T., Rozmaritsa, N., Engel, A., Berk, E., Knaut, M., Metzner, K., et al. (2014). Arrhythmias, elicited by catecholamines and serotonin, vanish in human chronic atrial fibrillation. *Proc. Natl. Acad. Sci. U.S.A.* 111, 11193–11198. doi: 10.1073/pnas.1324132111
- Frey, N., Katus, H. A., Olson, E. N., and Hill, J. A. (2004). Hypertrophy of the heart: A new therapeutic target? *Circulation* 109, 1580–1589. doi: 10.1161/01.cir.0000120390.68287.bb
- Galati, G., Leone, O., Pasquale, F., Olivotto, I., Biagini, E., Grigioni, F., et al. (2016). Histological and histometric characterization of myocardial fibrosis in end-stage hypertrophic cardiomyopathy: a clinical-pathological study of 30 Explanted Hearts. *Circ. Heart Fail.* 9:e003090. doi: 10.1161/cirheartfailure.116.003090
- Gold, J. I., Gao, E., Shang, X., Premont, R. T., and Koch, W. J. (2012). Determining the absolute requirement of G protein-coupled receptor kinase 5 for pathological cardiac hypertrophy: short communication. *Circ. Res.* 111, 1048–1053. doi: 10.1161/circresaha.112.273367
- Gouveia, K., and Hurst, J. L. (2019). Improving the practicality of using non-aversive handling methods to reduce background stress and anxiety in laboratory mice. *Sci. Rep.* 9:20305. doi: 10.1038/s41598-019-56860-7
- Haider, K. H., and Stimson, W. H. (1993). Cardiac troponin-I: a biochemical marker for cardiac cell necrosis. *Dis. Markers* 11, 205–215. doi: 10.1155/1993/901687
- Hartupee, J., and Mann, D. L. (2016). Role of inflammatory cells in fibroblast activation. *J. Mol. Cell. Cardiol.* 93, 143–148. doi: 10.1016/j.yjmcc.2015.11.016
- Heidt, T., Courties, G., Dutta, P., Sager, H. B., Sebas, M., Iwamoto, Y., et al. (2014). Differential contribution of monocytes to heart macrophages in steady-state and after myocardial infarction. *Circ. Res.* 115, 284–295. doi: 10.1161/circresaha.115.303567
- Hinz, B., and Lagares, D. (2020). Evasion of apoptosis by myofibroblasts: a hallmark of fibrotic diseases. *Nat. Rev. Rheumatol.* 16, 11–31. doi: 10.1038/s41584-019-0324-5
- Homan, K. T., Wu, E., Cannavo, A., Koch, W. J., and Tesmer, J. J. (2014). Identification and characterization of amlexanox as a G protein-coupled receptor kinase 5 inhibitor. *Molecules* 19, 16937–16949. doi: 10.3390/molecules191016937
- Huang, X. D., and Wong, T. M. (1989). Arrhythmogenic effect of forskolin in the isolated perfused rat heart: influence of nifedipine or reduction of external calcium [corrected]. *Clin. Exp. Pharmacol. Physiol.* 16, 751–757. doi: 10.1111/j.1440-1681.1989.tb01513.x
- Hullmann, J. E., Grisanti, L. A., Makarewich, C. A., Gao, E., Gold, J. I., Chuprun, J. K., et al. (2014). GRK5-mediated exacerbation of pathological cardiac hypertrophy involves facilitation of nuclear NFAT activity. *Circ. Res.* 115, 976–985. doi: 10.1161/circresaha.116.304475
- Hulsmans, M., Sam, F., and Nahrendorf, M. (2016). Monocyte and macrophage contributions to cardiac remodeling. *J. Mol. Cell. Cardiol.* 93, 149–155. doi: 10.1016/j.yjmcc.2015.11.015
- Islam, K. N., Bae, J. W., Gao, E., and Koch, W. J. (2013). Regulation of nuclear factor κB (NF-κB) in the nucleus of cardiomyocytes by G protein-coupled receptor kinase 5 (GRK5). *J. Biol. Chem.* 288, 35683–35689. doi: 10.1074/jbc.M113.529347
- Jia, D., Jiang, H., Weng, X., Wu, J., Bai, P., Yang, W., et al. (2019). Interleukin-35 promotes macrophage survival and improves wound healing after myocardial infarction in mice. *Circ. Res.* 124, 1323–1336. doi: 10.1161/circresaha.118.314569
- Kaya, Z., Göser, S., Buss, S. J., Leuschner, F., Ottl, R., Li, J., et al. (2008). Identification of cardiac troponin I sequence motifs leading to heart failure by induction of myocardial inflammation and fibrosis. *Circulation* 118, 2063–2072. doi: 10.1161/circulationaha.108.788711
- Kaya, Z., Katus, H. A., and Rose, N. R. (2010). Cardiac troponins and autoimmunity: their role in the pathogenesis of myocarditis and of heart failure. *Clin. Immunol.* 134, 80–88. doi: 10.1016/j.clim.2009.04.008
- Kwon, G., Pappan, K. L., Marshall, C. A., Schaffer, J. E., and McDaniel, M. L. (2004). cAMP Dose-dependently prevents palmitate-induced apoptosis by both protein kinase A- and cAMP-guanine nucleotide exchange factor-dependent pathways in beta-cells. *J. Biol. Chem.* 279, 8938–8945. doi: 10.1074/jbc.M310330200
- Laukova, M., Vargovic, P., Rokytova, I., Manz, G., and Kvetnansky, R. (2018). Repeated stress exaggerates lipopolysaccharide-induced inflammatory response in the rat spleen. *Cell. Mol. Neurobiol.* 38, 195–208. doi: 10.1007/s10571-017-0546-5
- Lee, J. Y., Kim, J. H., Chae, G., Lee, B. K., Ha, K. S., Kwon, Y. G., et al. (2010). Cyclic AMP prolongs graft survival by suppressing apoptosis and inflammatory gene expression in acute cardiac allograft rejection. *Exp. Mol. Med.* 42, 69–79. doi: 10.3858/emmm.2010.42.1.008
- Lin, Y., Zhang, X., Xiao, W., Li, B., Wang, J., Jin, L., et al. (2016). Endoplasmic reticulum stress is involved in DFMO attenuating isoproterenol-induced

Academic Program Development of Jiangsu Higher Education Institutions (PAPD).

ACKNOWLEDGMENTS

We appreciate the inputs of Lu Fu during the assessment of cardiac functions.

SUPPLEMENTARY MATERIAL

The Supplementary Material for this article can be found online at: <https://www.frontiersin.org/articles/10.3389/fcell.2021.719351/full#supplementary-material>

- cardiac hypertrophy in rats. *Cell. Physiol. Biochem.* 38, 1553–1562. doi: 10.1159/000443096
- Liu, W., Wang, X., Mei, Z., Gong, J., Gao, X., Zhao, Y., et al. (2015). Chronic stress promotes the progression of pressure overload-induced cardiac dysfunction through inducing more apoptosis and fibrosis. *Physiol. Res.* 64, 325–334. doi: 10.33549/physiolres.932778
- Marstrand, P., Han, L., Day Sharlene, M., Olivotto, I., Ashley Euan, A., Michels, M., et al. (2020). Hypertrophic cardiomyopathy with left ventricular systolic dysfunction. *Circulation* 141, 1371–1383. doi: 10.1161/CIRCULATIONAHA.119.044366
- Mo, C., Ha, H., Tang, X., Lu, X., Wei, Y., Luo, D., et al. (2020). Protein kinase TBK1/IKK ϵ inhibitor Amlexanox improves cardiac function after acute myocardial infarction in rats. *Panminerva Med.* doi: 10.23736/s0031-0808.20.03937-3 [Epub ahead of print].
- Murphy, J. G., Crosby, K. C., Dittmer, P. J., Sather, W. A., and Dell'Acqua, M. L. (2019). AKAP79/150 recruits the transcription factor NFAT to regulate signaling to the nucleus by neuronal L-type Ca(2+) channels. *Mol. Biol. Cell* 30, 1743–1756. doi: 10.1091/mbc.E19-01-0060
- Patil, S., Shahi, S., Saini, Y., Lee, T., Packiriswamy, N., Appledorn, D. M., et al. (2011). G-protein coupled receptor kinase 5 mediates lipopolysaccharide-induced NF κ B activation in primary macrophages and modulates inflammation in vivo in mice. *J. Cell. Physiol.* 226, 1323–1333. doi: 10.1002/jcp.22460
- Paur, H., Wright, P. T., Sikkil, M. B., Tranter, M. H., Mansfield, C., O'Gara, P., et al. (2012). High levels of circulating epinephrine trigger apical cardiodepression in a β 2-adrenergic receptor/Gi-dependent manner: a new model of Takotsubo cardiomyopathy. *Circulation* 126, 697–706. doi: 10.1161/circulationaha.112.111591
- Pereira, L., Rehmann, H., Lao, D. H., Erickson, J. R., Bossuyt, J., Chen, J., et al. (2015). Novel Epac fluorescent ligand reveals distinct Epac1 vs. Epac2 distribution and function in cardiomyocytes. *Proc. Natl. Acad. Sci. U.S.A.* 112, 3991–3996. doi: 10.1073/pnas.1416163112
- Plattner, F., Hayashi, K., Hernández, A., Benavides, D. R., Tassin, T. C., Tan, C., et al. (2015). The role of ventral striatal cAMP signaling in stress-induced behaviors. *Nat. Neurosci.* 18, 1094–1100. doi: 10.1038/nn.4066
- Qi, L., Chi, X., Zhang, X., Feng, X., Chu, W., Zhang, S., et al. (2019). Kindlin-2 suppresses transcription factor GATA4 through interaction with SUV39H1 to attenuate hypertrophy. *Cell Death Dis.* 10:890. doi: 10.1038/s41419-019-21210
- Quan, M. Y., Song, X. J., Liu, H. J., Deng, X. H., Hou, H. Q., Chen, L. P., et al. (2019). Amlexanox attenuates experimental autoimmune encephalomyelitis by inhibiting dendritic cell maturation and reprogramming effector and regulatory T cell responses. *J. Neuroinflammation* 16:52. doi: 10.1186/s12974-019-1438-z
- Raker, V. K., Becker, C., and Steinbrink, K. (2016). The cAMP pathway as therapeutic target in autoimmune and inflammatory diseases. *Front. Immunol.* 7:123. doi: 10.3389/fimmu.2016.00123
- Ray, A., and Dittel, B. N. (2010). Isolation of mouse peritoneal cavity cells. *J. Vis. Exp.* 35:1488. doi: 10.3791/1488
- Sandstedt, J., Sandstedt, M., Lundqvist, A., Jansson, M., Sopasakis, V. R., Jeppsson, A., et al. (2019). Human cardiac fibroblasts isolated from patients with severe heart failure are immune-competent cells mediating an inflammatory response. *Cytokine* 113, 319–325. doi: 10.1016/j.cyt.2018.09.021
- Scally, C., Abbas, H., Ahearn, T., Srinivasan, J., Mezincescu, A., Rudd, A., et al. (2019). Myocardial and systemic inflammation in acute stress-induced (Takotsubo) Cardiomyopathy. *Circulation* 139, 1581–1592. doi: 10.1161/circulationaha.118.037975
- Schaeuble, D., Packard, A. E. B., McKlveen, J. M., Morano, R., Fourman, S., Smith, B. L., et al. (2019). Prefrontal cortex regulates chronic stress-induced cardiovascular susceptibility. *J. Am. Heart Assoc.* 8:e014451. doi: 10.1161/jaha.119.014451
- Shim, S. H., Kim, D. S., Cho, W., and Nam, J. H. (2014). Coxsackievirus B3 regulates T-cell infiltration into the heart by lymphocyte function-associated antigen-1 activation via the cAMP/Rap1 axis. *J. Gen. Virol.* 95(Pt 9), 2010–2018. doi: 10.1099/vir.0.065755-0
- Spadari, R. C., Cavadas, C., de Carvalho, A., Ortolani, D., de Moura, A. L., and Vassalo, P. F. (2018). Role of Beta-adrenergic receptors and Sirtuin signaling in the heart during aging, heart failure, and adaptation to stress. *Cell. Mol. Neurobiol.* 38, 109–120. doi: 10.1007/s10571-017-0557-2
- Sun, X., Zhou, M., Wen, G., Huang, Y., Wu, J., Peng, L., et al. (2021). Paroxetine attenuates cardiac hypertrophy via blocking GRK2 and ADRB1 Interaction in Hypertension. *J. Am. Heart Assoc.* 10:e016364. doi: 10.1161/jaha.120.016364
- Traynham, C. J., Hullmann, J., and Koch, W. J. (2016). Canonical and non-canonical actions of GRK5 in the heart. *J. Mol. Cell. Cardiol.* 92, 196–202. doi: 10.1016/j.yjmcc.2016.01.027
- Wang, Z., Liu, D., Varin, A., Nicolas, V., Courilleau, D., Mateo, P., et al. (2016). A cardiac mitochondrial cAMP signaling pathway regulates calcium accumulation, permeability transition and cell death. *Cell Death Dis.* 7:e2198. doi: 10.1038/cddis.2016.106
- Wehbi, V. L., and Taskén, K. (2016). Molecular mechanisms for cAMP-mediated immunoregulation in T cells - role of anchored protein kinase A signaling units. *Front. Immunol.* 7:222. doi: 10.3389/fimmu.2016.00222
- Weisheit, C. K., Kleiner, J. L., Rodrigo, M. B., Niepmann, S. T., Zimmer, S., Duerr, G. D., et al. (2021). CX3CR1 is a prerequisite for the development of cardiac hypertrophy and left ventricular dysfunction in mice upon transverse aortic constriction. *PLoS One* 16:e0243788. doi: 10.1371/journal.pone.0243788
- Whelan, R. S., Kaplinskiy, V., and Kitsis, R. N. (2010). Cell death in the pathogenesis of heart disease: mechanisms and significance. *Annu. Rev. Physiol.* 72, 19–44. doi: 10.1146/annurev.physiol.010908.163111
- Wolf, C. M., Moskowitz, I. P., Arno, S., Branco, D. M., Semsarian, C., Bernstein, S. A., et al. (2005). Somatic events modify hypertrophic cardiomyopathy pathology and link hypertrophy to arrhythmia. *Proc. Natl. Acad. Sci. U.S.A.* 102, 18123–18128. doi: 10.1073/pnas.0509145102
- Wu, Y. S., Chen, C. C., Chien, C. L., Lai, H. L., Jiang, S. T., Chen, Y. C., et al. (2017). The type VI adenylyl cyclase protects cardiomyocytes from β -adrenergic stress by a PKA/STAT3-dependent pathway. *J. Biomed. Sci.* 24:68. doi: 10.1186/s12929-017-0367-3
- Xiao, H., Li, H., Wang, J. J., Zhang, J. S., Shen, J., An, X. B., et al. (2018). IL-18 cleavage triggers cardiac inflammation and fibrosis upon β -adrenergic insult. *Eur. Heart J.* 39, 60–69. doi: 10.1093/eurheartj/ehx261
- Xie, M., Burchfield, J. S., and Hill, J. A. (2013). Pathological ventricular remodeling: therapies: part 2 of 2. *Circulation* 128, 1021–1030. doi: 10.1161/circulationaha.113.001879
- Younce, C. W., Burmeister, M. A., and Ayala, J. E. (2013). Exendin-4 attenuates high glucose-induced cardiomyocyte apoptosis via inhibition of endoplasmic reticulum stress and activation of SERCA2a. *Am. J. Physiol. Cell Physiol.* 304, C508–C518. doi: 10.1152/ajpcell.00248.2012
- Zhang, P., Li, T., Liu, Y. Q., Zhang, H., Xue, S. M., Li, G., et al. (2019). Contribution of DNA methylation in chronic stress-induced cardiac remodeling and arrhythmias in mice. *FASEB J.* 33, 12240–12252. doi: 10.1096/fj.201900100R
- Zhao, C. H., Ma, X., Guo, H. Y., Li, P., and Liu, H. Y. (2017). RIP2 deficiency attenuates cardiac hypertrophy, inflammation and fibrosis in pressure overload induced mice. *Biochem. Biophys. Res. Commun.* 493, 1151–1158. doi: 10.1016/j.bbrc.2017.07.035
- Zhou, R., Ma, P., Xiong, A., Xu, Y., Wang, Y., and Xu, Q. (2017). Protective effects of low-dose rosuvastatin on isoproterenol-induced chronic heart failure in rats by regulation of DDAH-ADMA-NO pathway. *Cardiovasc. Ther.* 35:e12241. doi: 10.1111/1755-5922.12241
- Zoccarato, A., Surdo, N. C., Aronsen, J. M., Fields, L. A., Mancuso, L., Dodoni, G., et al. (2015). Cardiac Hypertrophy Is Inhibited by a Local Pool of cAMP Regulated by Phosphodiesterase 2. *Circ. Res.* 117, 707–719. doi: 10.1161/circresaha.114.305892

Conflict of Interest: The authors declare that the research was conducted in the absence of any commercial or financial relationships that could be construed as a potential conflict of interest.

Publisher's Note: All claims expressed in this article are solely those of the authors and do not necessarily represent those of their affiliated organizations, or those of the publisher, the editors and the reviewers. Any product that may be evaluated in this article, or claim that may be made by its manufacturer, is not guaranteed or endorsed by the publisher.

Copyright © 2021 Adzika, Hou, Adekunle, Rizvi, Adzraku, Li, Deng, Mprah, Ndzie Noah, Adu-Amankwaah, Machuki, Shang, Ma, Koda, Ma and Sun. This is an open-access article distributed under the terms of the Creative Commons Attribution License (CC BY). The use, distribution or reproduction in other forums is permitted, provided the original author(s) and the copyright owner(s) are credited and that the original publication in this journal is cited, in accordance with accepted academic practice. No use, distribution or reproduction is permitted which does not comply with these terms.



Estrogen Attenuates Chronic Stress-Induced Cardiomyopathy by Adaptively Regulating Macrophage Polarizations via β_2 -Adrenergic Receptor Modulation

OPEN ACCESS

Hongjian Hou^{1,2†}, Gabriel Komla Adzika^{1†}, Qi Wu¹, Tongtong Ma¹, Yanhong Ma¹, Juan Geng¹, Mingjin Shi¹, Lu Fu¹, Ruqayya Rizvi³, Zheng Gong⁴ and Hong Sun^{1,3*}

Edited by:

Susanne Sattler,
Imperial College London,
United Kingdom

Reviewed by:

Mahmoud El-Mas,
Alexandria University, Egypt
Jose Luis Sanchez-Alonso,
Imperial College London,
United Kingdom
Jun Ren,
University of Washington,
United States

*Correspondence:

Hong Sun
sunh@xzhmu.edu.cn

[†] These authors have contributed
equally to this work and share first
authorship

Specialty section:

This article was submitted to
Molecular and Cellular Pathology,
a section of the journal
Frontiers in Cell and Developmental
Biology

Received: 06 July 2021

Accepted: 31 August 2021

Published: 28 September 2021

Citation:

Hou H, Adzika GK, Wu Q, Ma T,
Ma Y, Geng J, Shi M, Fu L, Rizvi R,
Gong Z and Sun H (2021) Estrogen
Attenuates Chronic Stress-Induced
Cardiomyopathy by Adaptively
Regulating Macrophage Polarizations
via β_2 -Adrenergic Receptor
Modulation.
Front. Cell Dev. Biol. 9:737003.
doi: 10.3389/fcell.2021.737003

¹ Department of Physiology, Xuzhou Medical University, Xuzhou, China, ² The College of Biology and Food, Shangqiu Normal University, Shangqiu, China, ³ Xuzhou Medical University, Xuzhou, China, ⁴ The School of Public Affairs and Governance, Silliman University, Dumaguete, Philippines

Clinical demographics have demonstrated that postmenopausal women are predisposed to chronic stress-induced cardiomyopathy (CSC) and this has been associated with the decrease of estrogen. Meanwhile, recent studies have implicated unsolved myocardial proinflammatory responses, which are characterized by enormous CD86+ macrophage infiltrations as an underlying disease mechanism expediting the pathological remodeling of the heart during chronic stress. However, we had previously demonstrated that estrogen confers cardioprotection *via* the modulation of cardiomyocytes β_2 -adrenoceptors (β_2 AR)-Gs/Gi pathways during stress to lessen the incidence of stress-induced cardiovascular diseases in premenopausal women. Intriguingly, macrophages express β_2 AR profoundly as well; as such, we sought to elucidate the possibilities of estrogen modulating β_2 AR-Gs/Gi pathway to confer cardioprotection during stress *via* immunomodulation. To do this, ovariectomy (OVX) and sham operations (Sham) were performed on female Sprague-Dawley (SD) rats. Two weeks after OVX, the rats were injected with 40 μ g/kg/day of estradiol (E_2). Next, on day 36 after OVX, chronic stress was induced by a daily subcutaneous injection of 5 mg/kg/day of isoproterenol (ISO). The effect of E_2 on relevant clinical cardiac function indexes (LVSP, LVEDP, + dp/dt and -dp/dt), myocardial architecture (cardiomyocyte diameter and fibrosis), β_2 AR alterations, and macrophage (CD86+ and CD206+) infiltrations were assessed. *In vitro*, peritoneal macrophages (PM Φ) were isolated from wild-type and β_2 AR-knockout female mice. The PM Φ were treated with ISO, E_2 , and β_2 AR blocker ICI 118,551 for 24 h, and flow cytometric evaluations were done to assess their phenotypic expression. E_2 deficiency permitted the induction of CSC, which was characterized by cardiac dysfunctions, maladaptive myocardial hypertrophy, unresolved proinflammatory responses, and fibrosis. Nonetheless, E_2 presence/supplementation during stress averted all the aforementioned adverse effects of chronic stress while preventing excessive depletion of β_2 AR. Also, we demonstrated

that E_2 facilitates timely resolution of myocardial proinflammation to permit reparative functions by enhancing the polarization of CD86+ to CD206+ macrophages. However, this adaptive immunomodulation is hampered when β_2 AR is inhibited. Taken together, the outcomes of this study show that E_2 confers cardioprotection to prevent CSC *via* adaptive immunomodulation of macrophage phenotypes, and β_2 AR-mediated signaling is crucial for the polarizations of CD86+ to CD206+ macrophages.

Keywords: chronic stress-induced cardiomyopathy, myocardial inflammation, estrogen, β_2 -adrenoceptors, macrophage polarization

INTRODUCTION

Similar to other cardiovascular diseases (CVDs), chronic stress-induced cardiomyopathy (CSC) has been clinically shown to be predominant in males of all age cohorts, while females are mostly predisposed to its occurrence during their menopausal period (Boese et al., 2017; Ndzie Noah et al., 2021). Recent attempts to elucidate the underlying disease mechanisms have revealed crucial roles played by estrogen during stress to sustain good cardiac health in premenopausal women, besides its reproductive functions (Mori et al., 2011; Boese et al., 2017).

Typically, the clinical manifestations of CSC patients are severe left ventricular (LV) diastolic dysfunction (LVDD) and systolic dysfunctions (LVSD) (Medeiros et al., 2014). The adverse structural remodeling includes excessive LV hypertrophy and massive interstitial fibrosis, which results in the stiffening of the myocardia and causes these cardiac dysfunctions. Also, recent studies have demonstrated that unresolved myocardial inflammatory responses characterized by the enormous influx of proinflammatory macrophages exacerbates CSC and aggravates adverse cardiac remodeling (Wilson et al., 2018; Scally et al., 2019).

Under physiological state, inotropic and chronotropic functions of the heart are mediated by β -adrenergic receptors (β ARs) *via* G stimulatory protein (G_s), mainly β_1 AR and β_2 AR. However, hyperstimulation of the receptors during chronic stress results in the downregulation of β_1 AR mostly, while β_2 AR traffics the stimulatory signal *via* G inhibitory protein (G_i) to prevent cardiac insults (Paur et al., 2012). The homologous desensitization of β ARs which results in the downregulation is induced by G protein-coupled receptor kinases 2 (GRK2) phosphorylation and β -arrestin-1 recruitment (Adzika et al., 2019). Nonetheless, it was demonstrated in previous studies that estrogen ameliorates stress-induced cardiac insults by preventing excessive depletion of β_2 ARs and also facilitating a balance in the G_i/G_s signaling pathways (Cao et al., 2015; Hou et al., 2018). The estrogenic effects of sustaining β_2 AR activities during stress might be likely due to its inhibitory effects on GRK2 (Abraham et al., 2018). Intriguingly, β_2 AR are profoundly expressed on macrophages; hence, estrogen may indirectly modulate their activities and possibly their polarizations into proinflammatory (CD86+ macrophages) or anti-inflammatory (CD206+ macrophages) phenotypes in the myocardia. It is hypothesized that the possible exertion of the aforementioned estrogenic immunoregulation might prevent extensive pathological cardiac remodeling during chronic stress

by subduing maladaptive myocardial hypertrophy, fibrosis, and proinflammatory responses.

Herein, we sought to explore the cardioprotective mechanisms employed by estrogen *via* immunomodulation to decrease the incidence of CSC in female rat models, as understanding these mechanisms will provide the basis for further translational research into preventing CSC in postmenopausal women.

MATERIALS AND METHODS

Experimental Animals and Models

The wild-type and β_2 AR knockout FVB female mice (donated by Professor Daniel Bernstein, Stanford University—United States) and adult female Sprague-Dawley (SD) rats (180–200 g) were used for the experiments ($n = 4$ –8 rats/group). All standard animal house boundary protocols were observed. After ensuring the SD rats were in the same menstrual phase through vaginal mucus examination, bilateral ovariectomy (OVX) and sham surgeries were done as we previously described (Zhang et al., 2021).

As illustrated (Figure 1A), 2 weeks after ovariectomy, the rats were intraperitoneally injected with 40 μ g/kg/day of estradiol (E_2) (E2758; Sigma, St. Louis, MO, United States) for 31 days, as done previously (Zhang et al., 2021). Olive oils of equivalent amounts were administered as a placebo to the control groups. On day 36 after ovariectomy, chronic stress was induced in rats that were being treated with either E_2 or the placebo by subcutaneous injections of isoproterenol (ISO) (160504; Sigma) at 5 mg/kg/day for 10 days, as previously done (Lin et al., 2016; Zhou et al., 2017). Also, the Sham surgery rats had similar ISO and placebo treatments. In total, *in vivo* experiments included the following six groups; (i) Sham group, (ii) OVX group, (iii) OVX + E_2 group, (iv) Sham + ISO group, (v) OVX + ISO group, and (vi) OVX + ISO + E_2 group.

The dosage of E_2 employed was to mimic its physiological levels in rats, as we had demonstrated previously (Liu et al., 2012; Zhang et al., 2021). Also, rather than the high dosage of ISO used in acute stress models, as done previously (Youssef et al., 2021), a relatively milder dosage was used due to the prolonged duration (10 days) of the catecholamine treatment (Zhang et al., 2021).

Hemodynamic Experiment

After properly sedating rats ($n = 7$ rats/group), they were fixed in the supine position, and longitudinal incisions (about 2 cm in

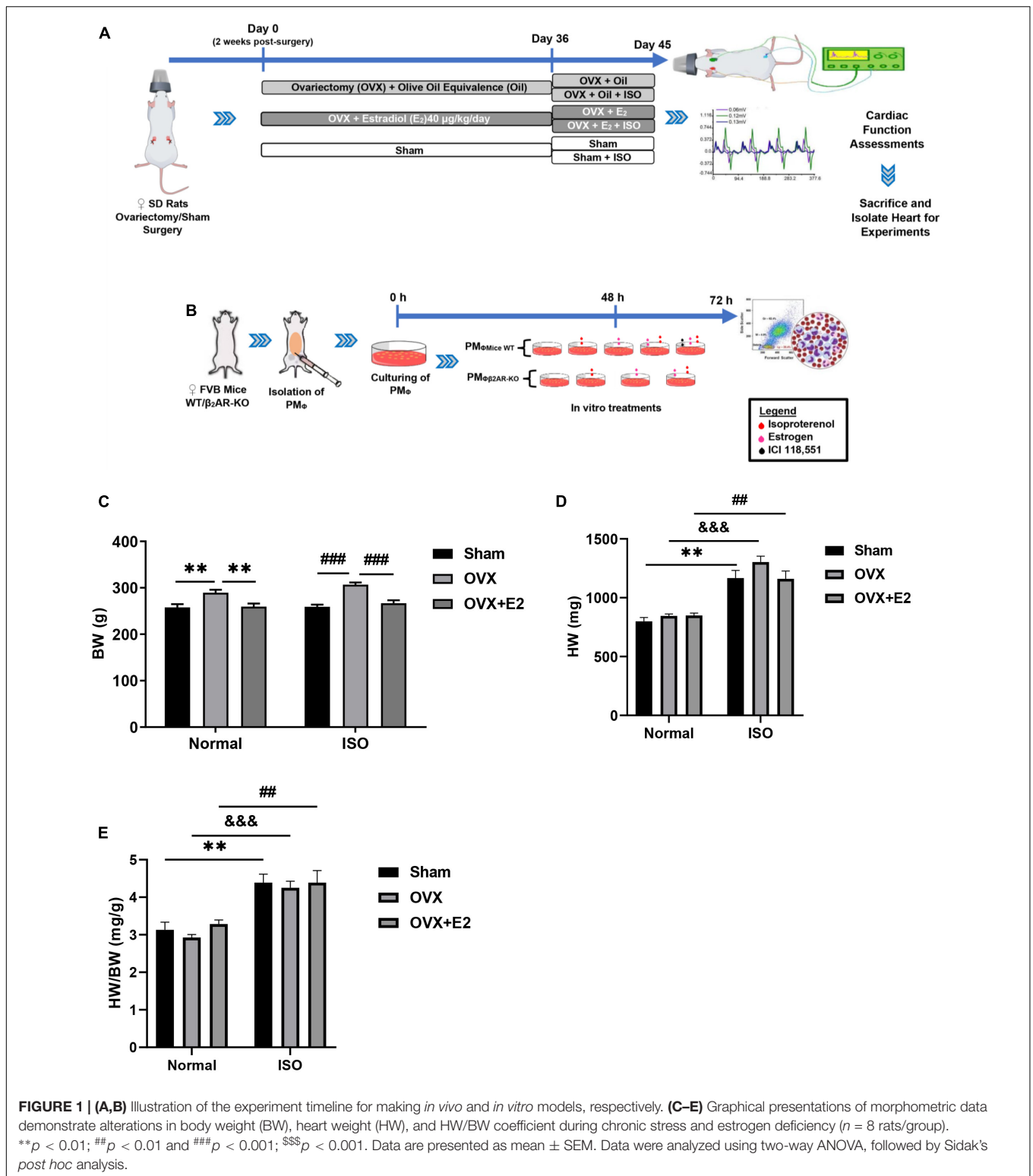


FIGURE 1 | (A,B) Illustration of the experiment timeline for making *in vivo* and *in vitro* models, respectively. **(C–E)** Graphical presentations of morphometric data demonstrate alterations in body weight (BW), heart weight (HW), and HW/BW coefficient during chronic stress and estrogen deficiency ($n = 8$ rats/group). ** $p < 0.01$; ## $p < 0.01$ and ### $p < 0.001$; \$\$\$ $p < 0.001$. Data are presented as mean \pm SEM. Data were analyzed using two-way ANOVA, followed by Sidak's *post hoc* analysis.

length) were made in the mid-neck. By using blunt hemostatic forceps, the fascia and aponeurosis were separated to reveal 1–1.5 cm of the right common carotid artery. The distal end of the right common carotid artery was ligated, and the proximal

end of the right common carotid artery was clamped with an arterial clamp. Next, an ophthalmic scissor was used to nick the artery (in a V-shaped), a heparin-filled catheter attached to a pressure transducer was carefully inserted into the left ventricle.

The left ventricular systolic and end-diastolic pressures and electrocardiography (ECG) were recorded with PowerLab data acquisition system (ADInstruments, North America, Colorado Springs, CO, United States).

Histological Assessment of Myocardia

Excised hearts ($n = 6$ hearts/group) were properly washed with prechilled PBS, blotted with filter paper, and fixed in 4% paraformaldehyde for more than 48 h. Next, the heart specimens were embedded in paraffin, sectioned at 4 μ m thickness, and preserved for histological assessments.

The myocardial sectionings were deparaffinized before performing Masson's trichrome (Maxim Biotechnologies, Fuzhou, China), hematoxylin and eosin (H&E), and immunohistochemical (IHC) staining as previously described (Zhang et al., 2021). The trichrome staining were done to ascertain the collagen volume fraction (CVF) while H&E staining were done to assess cardiomyocyte diameters and help depict the extent of myocardial hypertrophy. Also, IHC staining with CD68 (Abcam, Cambridge, United Kingdom; ab955), CD86 (Bioss, Woburn, MA, United States; BS-1035R), and CD206 (Abcam; ab8918) was done to assess the extent of myocardial infiltrations of inflammatory cells.

Imaging of all stained sections were done at $\times 400$ magnification (IX 71, Olympus, Tokyo, Japan) and analyzed using ImageJ (1.53a version; National Institute of Health, Bethesda, MD, United States).

Quantitative Real-Time PCR

Trizol (Invitrogen Co., Carlsbad, CA, United States) was used to extract RNAs from homogenized myocardia ($n = 4$ hearts/group). After the normalization of RNA concentrations, cDNAs were synthesized using Revertra ace[®] qPCR rt kit (Toyobo, Osaka, Japan). By using SYBR Green Master Mix (Vazyme Biotech, Nanjing, China), the following gene primers (Sangon Biotech, Shanghai, China) were used to evaluate mRNA expressions; (1) Tumor necrosis factor- α (TNF- α), Forward: GAAAGCATGATCCGAGATGTG; Reverse: CACGAGCAGGAATGAGAAGAG, (2) transforming growth factor-beta (TGF- β 1), Forward: ATGGTGGACCGCAACAACGC; Reverse: CTGGCACTGCTTCCCGAATGTC, (3) inducible nitric oxide synthase (iNOS), Forward: TCTTGGAGCGAGTTGTGGATTGT; Reverse: TAGGTGAGG GCTTGCCTGAGTG, (4) arginase 1 (Arg-1), Forward: CGTTG ACCTTGTCTTGT TTTGG; Reverse: CTGGTTCTGTTTCGGT TTGCTG, (5) glyceraldehyde 3-phosphate dehydrogenase (GAPDH), Forward: TCCTGCACCACCAACTGCTTAG; Reverse: AGTGGCAGTGATGGCATGGACT.

The $2^{-\Delta\Delta Ct}$ analysis method was used to evaluate the relative mRNA levels as described (Gold et al., 2012) and have been graphically presented as fold changes compared with the Sham group.

Western Blotting

Proteins were extracted from myocardial apexes ($n = 4$ hearts/group), treated with reducing agents, denatured at 100°C, and separated by gel electrophoresis as previously described

(Hou et al., 2018). Next, the proteins were transferred onto polyvinylidene fluoride (PVDF) membranes, blocked with 1% bovine serum albumin, and incubated in the following primary antibodies at 4°C overnight; ANP (1:1,000, Santa Cruz Biotechnology, Dallas, TX, United States; sc-515701), BNP (1:1,000, Santa Cruz Biotechnology; sc-271185), β_2 AR (1:1,000, Abcam; ab182136), GAPDH (1:4,000, Proteintech, Manchester, United Kingdom; 10494-1-AP). Visualizations of immunoblots were done with enhanced chemiluminescence (Tanon, Shanghai, China). The protein bands were quantified and evaluated by the relative expressions with their GAPDH.

Isolation and Characterization of Peritoneal Macrophages for *in vitro* Experiments

Peritoneal macrophages (PM ϕ) ($n \leq 2 * 10^6$ cells) were harvested from wild-type (WT) and β_2 AR knockout (β_2 AR-KO) FVB female mice by using methods previously demonstrated (Ray and Dittel, 2010). In brief, the mice peritoneum were exposed under aseptic conditions. Five to 10 ml of prewarmed (37°C) 3% fetal bovine serum (FBS) were injected into the peritoneal cavity. Cell suspensions were collected after softly massaging for 5 min and centrifuged at 1,500 rpm for 10 min, and the obtained cell pellets were resuspended and cultured with 10% FBS at 37°C and 5% CO₂ for 48 h. Next, 24 h *in vitro* treatments of cultured PM ϕ included; ISO (10 μ M), E2 (1 nM), and β_2 AR blocker ICI 118,551 (55 nM) (Figure 1B). These treatments were preceded by E2 pretreatments for 1 h, in groups where the estrogenic effects were to be ascertained.

The identification and subtyping of isolated PM ϕ after culturing or treatments were done by flow cytometry BD LSR II (BD Biosciences, San Jose, CA, United States). APC anti-F4/80 (123116; BioLegend, San Diego, CA, United States) and FITC anti-CD11b (101206; BioLegend) antibodies were used to identify the macrophages while PerCP anti-CD86 (105028; BioLegend) and PE anti-CD206 (141706; BioLegend) antibodies were used to differentially identify M1 macrophages and M2 macrophages, respectively. Preparations of cultured or treated PM ϕ for flow cytometry were done as previously described (Zhu et al., 2017). Acquired data were analyzed with FlowJo software (v10; FlowJo LLC, Oregon, OR, United States).

Statistical Analysis

Statistical analysis was performed with GraphPad Prism 5.0 (GraphPad Software, San Diego, CA, United States). All data were presented as mean \pm SEM and compared by two-way ANOVA. p -values < 0.05 were deemed statistically significant.

RESULTS

Estrogen Deficiency Facilitates Weight Gains During Chronic Stress

Analysis of the morphometrics of rats demonstrated that E₂-deficient (OVX) rats gained significant body weights

(BW). This phenomenon is shown to have been further aggravated by chronic stress (ISO) and is accompanied by increases in heart weights (HW) (Figures 1C,D). However, the supplementation with exogenous E_2 (E_{2Exo}) in the OVX + E_2 group and endogenous E_2 (E_{2Endo}) in the Sham group helped to significantly prevent BW gains and slight decrease HW (without statistical significance on comparing among the stress groups). Furthermore, it is shown that the HW/BW coefficient variation between physiological and stress states is more significant in OVX rats (Figure 1E).

Estrogen Deficiency Aggravates Isoproterenol-Induced Cardiac Dysfunction

E_2 deficiency during chronic stress resulted in decreased heart rates (HR) in OVX rats. The supplementation of E_{2Exo} in OVX rats and the presence of E_{2Endo} in Sham rats prevented a significant decrease in HR during chronic stress (Figure 2A). Furthermore, the cardiac function index; LVSP, LVEDP, the rate of pressure development (+dp/dt), and the rate of pressure development decay (-dp/dt) were assessed to ascertain for any occurring dysfunctionalities. It was demonstrated that E_2 deficiency during chronic stress resulted in depressions in LVSP, LVEDP, +dp/dt, and -dp/dt. However, E_{2Endo} and E_{2Exo} prevented significant alterations in these cardiac function indexes during stress (Figures 2B-E).

Estrogen Deficiency Promotes Myocardial Hypertrophy and Fibrosis During Chronic Stress

To ascertain the impact of chronic stress on the myocardial architecture, H&E and trichrome staining were done to evaluate the extent of cardiomyocyte hypertrophy and interstitial collagen deposition, respectively. The measurements of cardiomyocyte diameters from H&E-stained myocardia across all groups demonstrated that, under physiological state, the deficiency of E_2 does not affect the cell sizes. However, E_2 deficiency (in OVX rats) during chronic stress permits excessive cardiomyocyte hypertrophy. Also, the obtained results showed that, while E_2 in general inhibited excessive cardiomyocyte hypertrophy during stress in both Sham and OVX + E_2 groups, E_{2Endo} (in Sham) exhibited much more potent antihypertrophic effects than E_{2Exo} (in OVX + E_2) did (Figures 3A,B). Next, immunoblotting of atrial natriuretic peptide (ANP) and brain natriuretic peptide (BNP) depicted the maladaptive nature of the resulting cardiomyocyte hypertrophy when E_2 is deficient during stress. E_{2Endo} relatively decreased the expressions of both natriuretic peptides; whereas, E_{2Exo} only affected ANP upregulations (Figures 3C-F).

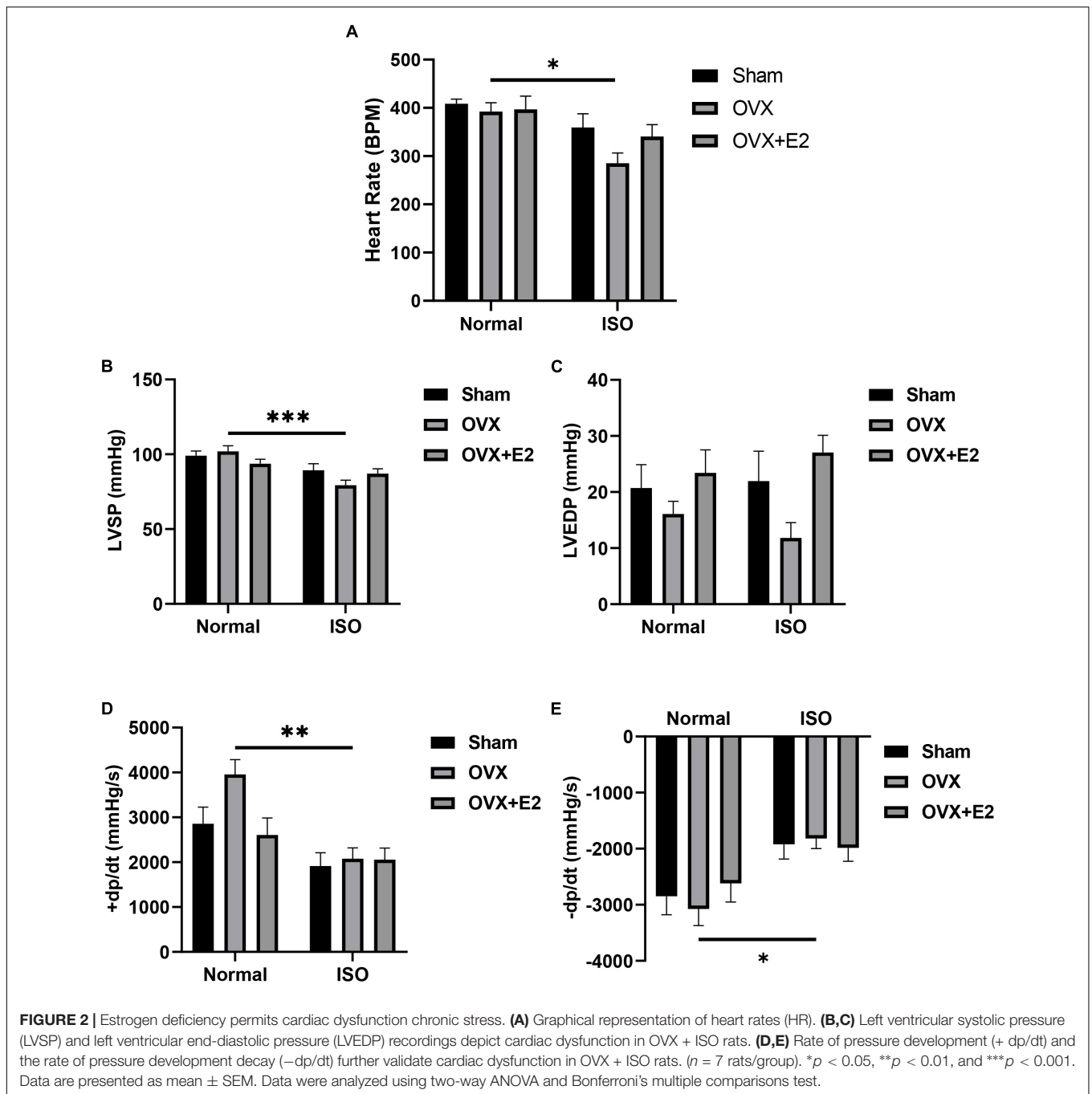
Assessed CVF demonstrated that myocardial interstitial fibrosis increases during chronic stress in OVX rats; however, the results trend showed that the presence of E_2 does ameliorate its severity but without statistical significance on comparing with OVX + E_2 + ISO and Sham + ISO groups (Figures 3G,H).

Estrogen Attenuates Maladaptive Myocardial Inflammatory Responses During Chronic Stress

Myocardial inflammation during chronic stress contributes to aggravated cardiac remodeling (Hulsmans et al., 2018). Hence, we assessed the potentials of E_2 in exerting adaptive immunoregulation in the myocardia during stress. CD68-positive IHC staining demonstrated that, under physiological state, the amount of macrophages infiltrating the myocardia are slightly elevated when E_2 is deficient (in OVX rats). Also, although CD68-positive cell infiltrations were generally increased during chronic stress, significant upregulations only resulted in OVX + ISO rats. The presence of E_{2Endo} and E_{2Exo} in Sham + ISO and OVX + E_2 + ISO, respectively, prevented enormous CD68-positive cell infiltration into the myocardia during stress (Figures 4A,B). Furthermore, by using CD86 and CD206 IHC staining, it is shown that majority of the inflammatory cells infiltrating the myocardia during stress when E_2 is deficient are CD86-positive (proinflammatory) cells, while CD206-positive (anti-inflammatory) cell infiltrations are significantly hampered. However, the contrast of this phenomenon is demonstrated by E_{2Endo} and E_{2Exo} presence in Sham + ISO and OVX + E_2 + ISO, respectively, during stress. The anti-inflammatory cell infiltrations are significantly increased while proinflammatory cell infiltrations were dampened in these groups. Also, it is observed that E_{2Endo} was potent than E_{2Exo} in the adaptive modulation of myocardial inflammatory cell infiltrations (Figures 4C-F). To validate the adaptive immunoregulation exerted by E_2 , mRNAs of proinflammatory (TNF- α and iNOS) and anti-inflammatory (TGF- β 1 and Arg-1) biomarkers were assessed from the myocardia. During chronic stress, E_2 deficiency (in OVX rats) permitted upregulations of TNF- α and iNOS while TGF- β 1 and Arg-1 expressions were downregulated. Conversely, E_2 enhanced the expressions of TGF- β 1 and Arg-1 and decreased TNF- α and iNOS levels (Figures 4G-J).

Estrogenic Adaptive Immunoregulation of Macrophage Polarization Involves Modulation of β_2 AR Signaling Activities

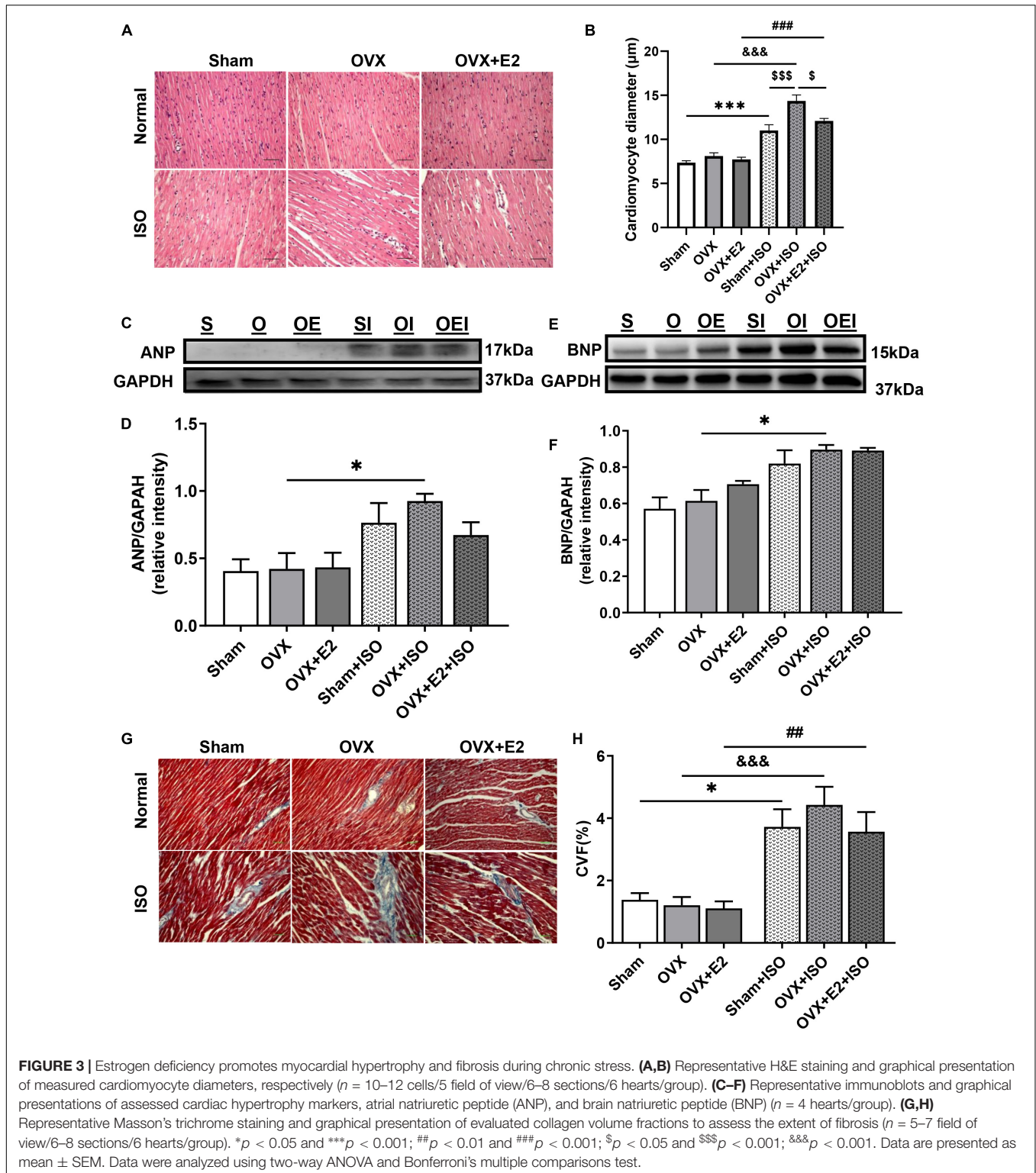
In our previous studies (Hou et al., 2018), it was demonstrated that E_2 conferred cardioprotective effects *via* the modulation of β_2 AR- $G_{\alpha_s}/G_{\alpha_i}$ -mediated signaling cascades during stress. Hence, to elucidate the underlying mechanism employed by E_2 to facilitate timely resolutions of myocardial proinflammatory responses, we again investigated the likely involvement of β_2 AR since they are well expressed in both cardiomyocytes and macrophages. Immunoblotting results showed a significant decrease in β_2 AR expression in OVX + ISO rats (Figures 5A,B). However, the extent of β_2 AR downregulations in Sham + ISO and OVX + E_2 + ISO was relatively lower than OVX + ISO, which showed statistical significance when compared with OVX. Flowcytometry evaluations of PM Φ isolated from WT and β_2 AR-KO and treated with ISO (10 μ M) and/or E_2 (1 nM) along with or without β_2 AR blocker ICI 118,551



(55 nM), demonstrated that the inhibition or obliteration of β_2 AR abolished the adaptive immunoregulatory effects exerted by E_2 during chronic stress. Typically, it is shown that during stress, E_2 enhanced PM_{Φ} polarizations into more CD206+ macrophages (anti-inflammatory phenotype) than CD86+ macrophages (proinflammatory phenotype) when β_2 ARs are not inhibited. However, obliteration of β_2 AR activities (by its KO or blocker ICI 118,551) obstructs the initially observed estrogenic phenomenon and consequently causes an increase in M1 macrophage phenotype (Figures 5C,D).

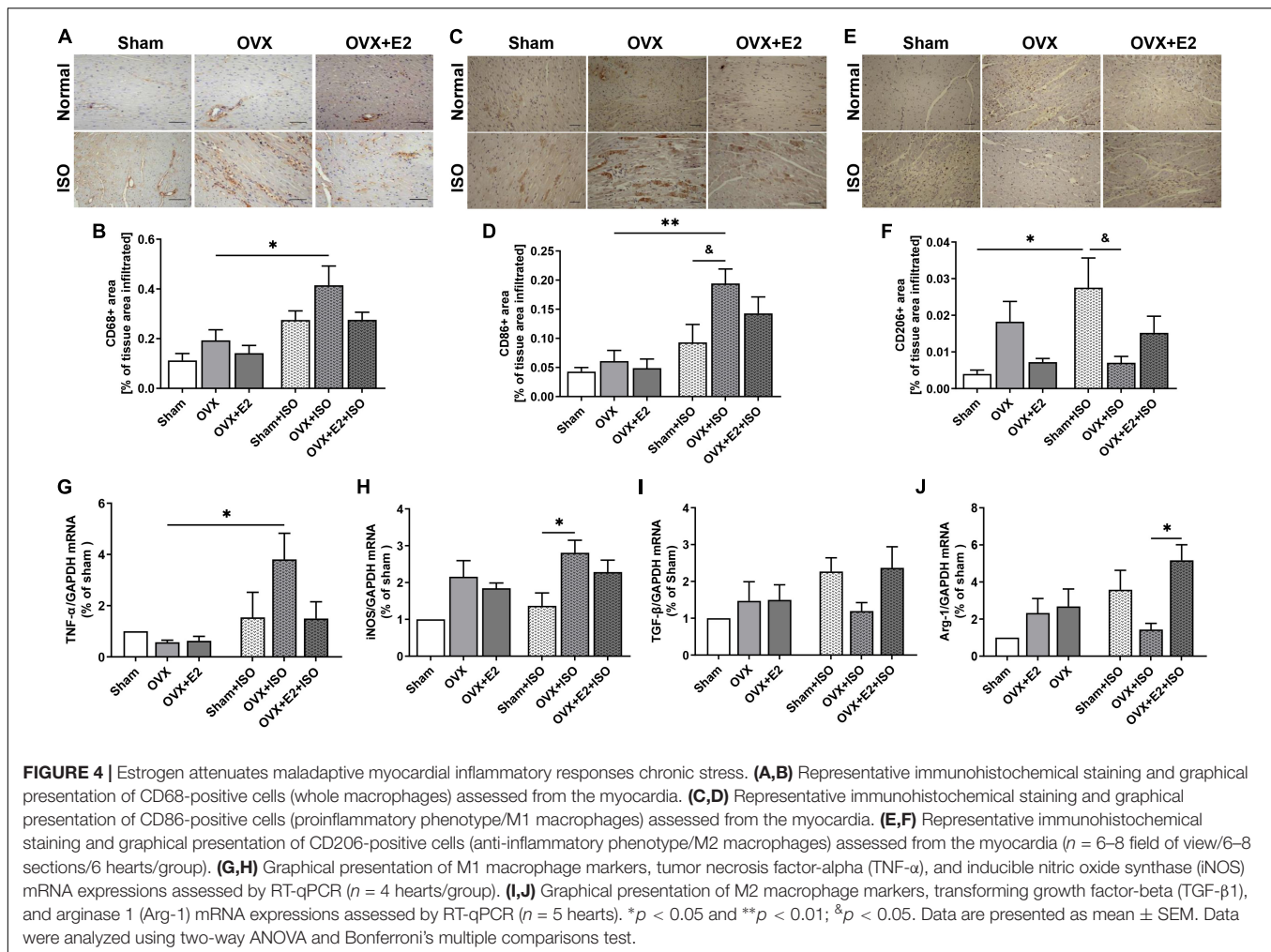
DISCUSSION

Unresolved myocardial inflammatory responses have been clinically demonstrated as an underlying factor expediting the pathological remodeling of the heart during stress (Mori et al., 2011; Wilson et al., 2018; Scally et al., 2019). The homeostatic balance between cardiac proinflammatory and anti-inflammatory macrophage phenotypes is crucial for resolving myocardial inflammation and proper heart functioning (Mouton et al., 2018). However, clinical studies have shown that the



myocardia of CSC patients have massive bias infiltrations of proinflammatory macrophages, which prolongs inflammation without timely resolutions to permit reparative functions of anti-inflammatory macrophages. Hence, in post-stress-induced

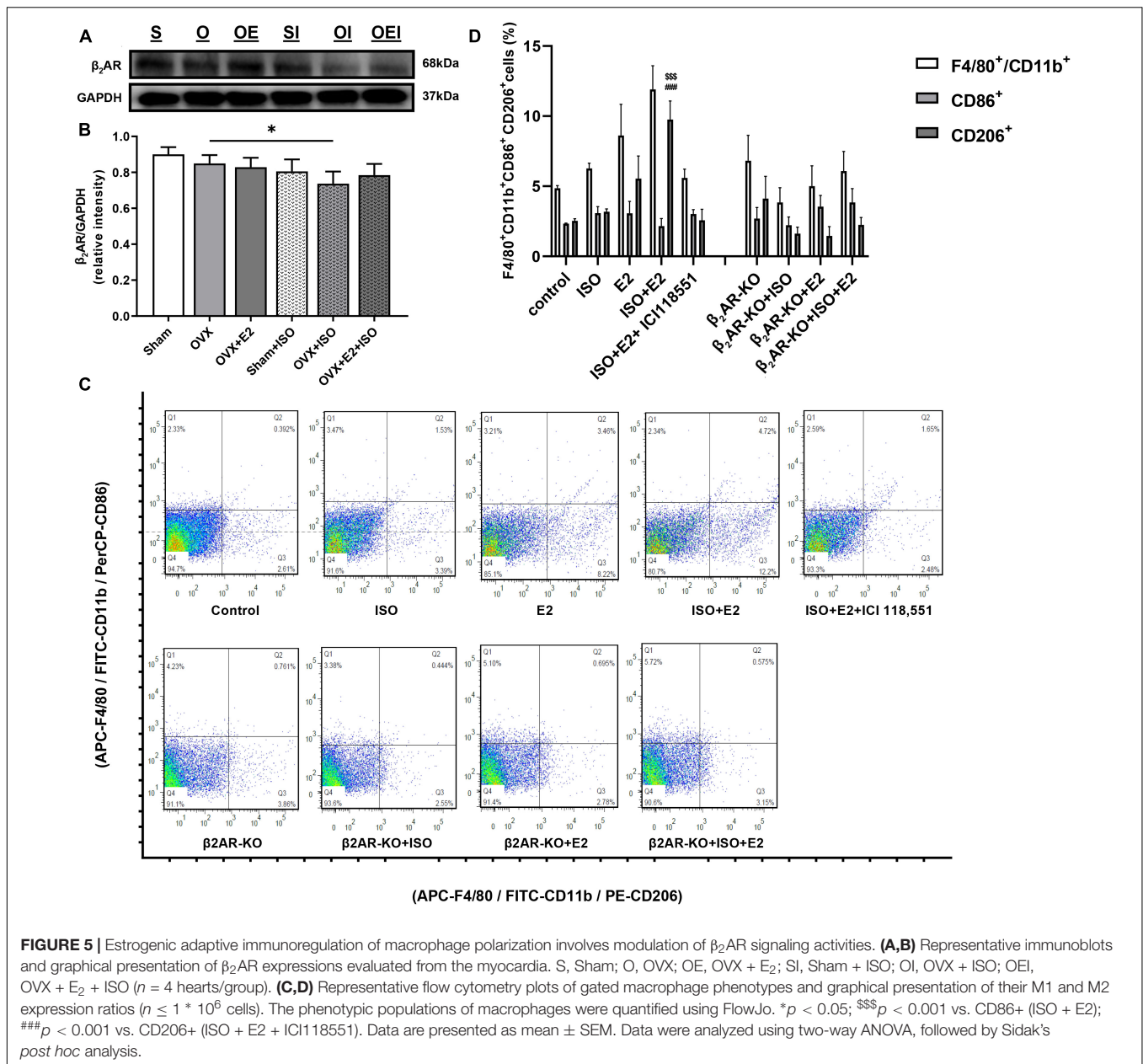
cardiac injuries, the maladaptive proinflammatory responses in the myocardia drives the pathological remodeling of the heart, which is evident by marked fibrosis (Mori et al., 2011; Mouton et al., 2018).



Herein, we demonstrate the mechanistic roles employed by E_2 to protect the heart during chronic stress from an immunoregulatory perspective. Morphometric evaluations revealed significant gains in BW resulting from the deficiency of estrogen in the OVX rats under physiological and chronic stress states. This finding provides supporting evidence that E_2 is crucial for efficient lipid metabolism. In fact, previous studies have demonstrated that E_2 maintains a healthy lipid profile by upregulating bloodstream levels of high-density lipoprotein (HDL) and lowering low-density lipoprotein receptors (LDL) (Lee et al., 2015; Fu et al., 2019; Ndzie Noah et al., 2021). As such, the deficiency of E_2 scaffolded disorders in lipid metabolism that caused weight gain as it permitted increased circulation LDL (bad cholesterol) level which deposited as adipose all over the body as well as in and around vascular tissues and circulatory organs (Lee et al., 2015; Kozakowski et al., 2017). Similar to the previous work of Ren et al. (2003), BW was increased in OVX rats. Also, it was observed that the combination of E_2 deficiency and stress increased HW and HW/BW coefficient more in OVX rats. The HW and HW/BW coefficient increases may be due to increased epicardial adipose and cardiomyocyte hypertrophy. Intriguingly, epicardial adipose has

been shown to be a reservoir for macrophages which infiltrates the myocardia to hasten maladaptive inflammatory responses (Mori et al., 2011). Therefore, the increased accumulation of epicardial adipose resulting from E_2 deficiency predisposes the heart to sustained myocardial inflammation should there be any cardiac insult during stress. Overall, consistent with early findings (Ren et al., 2003; Mori et al., 2011; Michalson et al., 2018), it was demonstrated that E_{2Endo} and its supplementation (E_{2Exo}) prevents excessive weight gains, which ultimately impacts positively on cardiac health.

Clinically, demographics clearly show that normally, females have higher heart rates (HR) and cardiac outputs than males of the same age cohort (Wheatley et al., 2014). In menopause, there is a further increase in HR, which results in short-term arrhythmias (heart palpitations) and are attributed to the loss of E_2 and possibly β_2 AR signaling dysregulation (Carpenter et al., 2021). Interestingly, the contrary was found in this study. The obliteration of E_2 via ovariectomy resulted in a slight decrease in HR under normal state; however, chronic stress in these OVX rats caused a significant reduction in HR. The possible explanation for this outcome is that inotropy and chronotropic functions of the heart are mediated by β_1 AR and β_2 AR; meanwhile, E_2 prevents



their dysregulations and substantial depletion during stress (Hou et al., 2018; Ndzie Noah et al., 2021). Therefore, E₂ deficiency might have permitted dysfunctionalities and downregulation of the β_2 ARs during stress, hence the significant decrease in HR. Also, consistent with previous reports, it was found that the cardiac function index; LVSP, LVEDP, +dp/dt, and -dp/dt were unaffected by E₂ deficiency under physiological state (Mori et al., 2011; Ribeiro et al., 2013). Even so, chronic stimulation of β ARs by ISO during E₂ deficiency demonstrated overt cardiac dysfunctionalities. In contrast, it was demonstrated that E_{2Endo} and E_{2Exo} in the Sham + ISO and OVX + E₂ + ISO rats, respectively, ameliorated these heart dysfunctions to sustain cardiac output during stress.

Further investigations sought to characterize the impact of chronic stress on the myocardial structure during E₂ deficiency. It was observed that cardiomyocyte diameters generally increased during stress; however, the E₂ deficiency permitted maladaptive hypertrophy, which distorted the typical myocardial architecture. This was further proven by the significant upregulations of ANP and BNP in the hearts of OVX rats during chronic stress. Nevertheless, E_{2Endo} (in the Sham rats) showed much potency at minimizing the upregulations of both ANP and BNP during stress, while E_{2Exo} (in the OVX + E₂ rats) was unable to downregulate the latter substantially. In conformity with our findings, Goncalves et al. (2018) and others had early demonstrated that E₂ exerts antihypertrophic effects *via*

GPB (Goldstein et al., 2004). Also, the discrepancies observed between the antihypertrophic effect of E_{2Endo} and E_{2Exo} might have occurred because other ovarian secretions such as vascular endothelial growth factor (VEGF) may complement the efforts of E_2 in preventing maladaptive cardiomyocyte hypertrophy (Cai et al., 2015). Besides, as suggested by Zhang et al. (2021), unlike the E_{2Exo} treatment dose, which remained constant during CSC modeling, the levels of E_{2Endo} are altered due to the estrous cycle in the Sham and could have also contributed to the observed differences in the antihypertrophic effect of E_2 . In addition, it was found that obliteration of E_2 in OVX rats permitted induction of massive interstitial fibrosis; nevertheless, its presence/restoration ameliorated this adverse outcome. We showed that comparatively, E_{2Endo} in the Sham and its supplementation (E_{2Exo}) lessened the extent of fibrosis, just as demonstrated earlier (Mori et al., 2011; Michalson et al., 2018).

The homeostatic balance between proinflammatory and anti-inflammatory macrophages in the myocardia during steady state is crucial for cardiac function, as is the timely trafficking of either of them during injury/cell clearance or reparative process, respectively, essential for preventing adverse heart remodeling (Lavine et al., 2014; Mouton et al., 2018). However, as demonstrated from the postmortem examination of the hearts from CSC patients, proinflammatory macrophages were abundant in the myocardia and were shown to have exacerbated myocardial proinflammatory responses, which may have resulted from stress-induced cardiac insults. The observed biased infiltration of CD86+ macrophages (proinflammatory) hastened the pathological cardiac remodeling as autopsied hearts had marked fibrosis (Wilson et al., 2018; Scally et al., 2019). Similar to these clinical findings, it has been shown in rats that stress causes augmentation of myocardial CD86+ macrophage infiltrations, and the phenomena are worsened by E_2 deficiency (Mori et al., 2011). Following up on these previous studies, consistent findings were made. CD68-positive cell infiltration into the myocardia were increased only under stress conditions; however, E_2 deficiency augmented their infiltration significantly. Nonetheless, E_{2Endo} and its supplementation (E_{2Exo}) to the rats during stress minimized CD68-positive cell infiltration. Assessing the phenotypic ratios with CD86 and CD206 immunostaining revealed the majority of the CD68-positive cells infiltrating the myocardia when E_2 is deficient during stress are CD86-positive cells, while CD206-positive cells are less present. Nevertheless, E_{2Endo} and E_{2Exo} reversed these phenomena by enhancing anti-inflammatory responses in the hearts during stress *via* increasing CD206+ macrophage presence, as similarly reported previously (Xing et al., 2009; Bolego et al., 2013). Validations of the aforementioned findings were done by assessing the mRNA expressions of proinflammatory (TNF- α and iNOS) and anti-inflammatory macrophage (TGF- β and Arg-1) markers from the myocardia of all experimental groups. Similar to the observations of the histological evaluations, TNF- α and iNOS were upregulated during stress and were further elevated significantly when E_2 is deficient. Also, TGF- β and Arg-1 mRNA expressions were downregulated in the myocardia due to E_2 deficiency. Conversely, E_{2Endo} exerted anti-inflammatory effects by enhancing TGF- β and Arg-1 while

decreasing TNF- α and iNOS mRNA expressions during stress. Although E_{2Exo} upregulated TGF- β and Arg-1 and inhibited TNF- α similarly to E_{2Endo} , it was not as potent as E_{2Endo} in downregulating iNOS. The possible explanation of the phenomenon is that ovarian secretions of progesterone might have complimented the inhibitory effects of E_{2Endo} , as it has been reported that besides E_2 , progesterone decreases iNOS levels in non-cardiac tissue (Menziez et al., 2011). However, progesterone is obliterated in OVX + E_2 + ISO rats; hence, it might account for iNOS being significantly downregulated in Sham + ISO than OVX + E_2 + ISO. Nonetheless, the estrogenic anti-inflammatory effects demonstrated here have been similarly reported by Villa et al. (2015) and others (Chen et al., 2021).

Similar to cardiomyocytes, macrophages have profound expressions of β_2 AR and estrogen receptors (ERs), and the cardioprotective effects conferred by E_2 have been demonstrated to mostly involved the synergy of ERs and β_2 AR signaling cascades (Kang et al., 2012; Hou et al., 2018; Machuki et al., 2019; Ndzie Noah et al., 2021). Hence, to elucidate the immunoregulatory mechanisms employed by E_2 to facilitate more CD206+ macrophage polarizations to accelerate the resolution of myocardial inflammation during stress, we investigated the possible involvement of β_2 AR signaling modulation by E_2 -induced cascades. In conformity with our initial speculations, β_2 AR expressions from apical myocardia (constituting cardiomyocytes and infiltrated macrophages) were found to be significantly depleted during chronic stress due to E_2 deficiency, as the presence of E_{2Endo} in the Sham and the supplementation of E_{2Exo} in OVX rats showed a minimal reduction in the expression of the receptor under the same stress condition. Further investigations of β_2 AR involvement deployed the isolations of PM Φ from female WT and β_2 AR-KO mice as well as the use of β_2 AR blocker ICI 118,551 to ascertain if E_2 induced any variations in the phenotypic ratios of the macrophages during stress was affected by impeding β_2 AR signaling. We report that the estrogenic signaling facilitates adaptive immunoregulation by ensuring CD206+ macrophage polarizations to timely resolve inflammation as reported by others (Keselman et al., 2017). However, for the first time, we show the underlying mechanism involves interplays of E_2 , ERs and β_2 AR signaling during stress. Flow cytometric evaluations show that E_2 treatments during stress increased CD206+ macrophage polarizations against CD86+ macrophages; however, the deletion/inhibition of β_2 AR impaired this phenomenon. These observations are possibly because the bioavailability of nitric oxide (NO), which is produced *via* β_2 AR-G α_i -PI3K-Akt-mediated signaling cascade, is crucial for the polarization of macrophages from proinflammatory to the anti-inflammatory phenotype (De Nigris and Prattichizzo, 2021). As such, blockade of β_2 AR signaling disrupts NO bioavailability and abolishes this adaptive immunoregulatory mechanism. Also, E_2 had been shown previously to exert these anti-inflammatory effects primarily *via* estrogen receptor alpha (ER α) (Bolego et al., 2013; Campbell et al., 2014), and although we have demonstrated here the essential involvement of β_2 AR to facilitate the polarizations of CD206+ macrophages, there are

apparent interplays among E_2 , ERs, and β_2 AR to ensure this immunomodulation during stress. Intriguingly, E_2 and ER activities downregulate GRK2, which otherwise would have induced the homologous desensitization and downregulation of β_2 AR during stress (Abraham et al., 2018; Arcones et al., 2021). Therefore, E_2 and ERs indirectly sustain the bioavailability of NO via β_2 AR- $G_{\alpha i}$ -PI3K-Akt signaling by preventing dysregulation of the receptor during stress and enhancing the β_2 AR-mediated CD206+ macrophage polarization.

Taken together, the findings from this study demonstrate the immunoregulatory mechanisms employed by E_2 to confer cardioprotection and lower the incidence of CSC in premenopausal women as compared with postmenopausal women and males of all age cohorts. E_2 exerts this immunoregulatory myocardia protection to prevent pathological cardiac remodeling during stress by ensuring the timely resolution of myocardial proinflammatory responses and enhancing reparative functions of CD206+ macrophage. More importantly, we demonstrate here that the adaptive modulation of macrophage phenotypes by E_2 during stress requires the mediation of β_2 AR signaling. The classical interplays among E_2 , ERs, and β_2 AR discussed by Ndzie Noah et al. (2021) are also shown here, as E_2 and ER activities are in turn required to prevent β_2 AR dysregulations and dysfunctionalities during stress. From a therapeutic standpoint, the findings from this study reechoes the essence of E_2 replacement therapy (E_2 RT) in postmenopausal women, as it reduces the incidence of CSC. However, it is recommended that E_2 RT is initiated within 5–6 years after menopause so as to explore its therapeutic benefits fully while circumventing the adverse outcomes reported by the Women's Health Initiative from their randomized controlled trial (Rossouw et al., 2002; Michalson et al., 2018; Ndzie Noah et al., 2021). Finally, it is deemed necessary to point out the limitations of this study due to its clinical significance. β_1 ARs are essential for myocardial functions and might play other immunologic roles facilitated by E_2 , but they have not been elucidated previously nor in this study. Also, in some instances (Figures 3E,F), (Figures 4C–J), it is shown that E_{2Exo} did not confer anti-inflammatory effects as E_{2Endo} did. However, the fact that other ovarian secretions such as progesterone can complement the anti-inflammatory effects of E_{2Endo} but are obliterated by ovariectomy in the E_{2Exo} treatment group might explain the observed differences. The estrous cycle in the Shams causing alterations in E_{2Endo} levels while E_{2Exo} treatment dosage used remained constant might also account for the shown slight variations in E_{2Endo} and E_{2Exo} effects. Therefore, we stand with

Zhang et al. (2021) in suggesting that E_2 RT should be given at dosages that mimic the concentrations of the estrous cycle to eliminate the observed variations in its cardioprotection efficacy. This will enhance the exploitation of the therapeutic potentials of E_2 RT in attenuation/prevention of CSC via immunomodulation in postmenopausal women.

DATA AVAILABILITY STATEMENT

The original contributions presented in the study are included in the article/supplementary material, further inquiries can be directed to the corresponding author/s.

ETHICS STATEMENT

The animal study was reviewed and approved by the Experimental Animal Centre of Xuzhou Medical University and the Animal Ethics Committee of Xuzhou Medical University (permit no: xz11-12540).

AUTHOR CONTRIBUTIONS

HH conceived the experiment idea. HS, HH, GKA, and QW designed the experiments. HH and GKA isolated and cultured PM ϕ . HH, TM, and YM made animal models. HH, JG, MS, and LF performed cardiac function and histological assessments. HH, GKA, QW, and HS analyzed and interpreted the results. Based on the contributions of all authors, HH drafted the initial manuscript and GKA revised it entirely. HH, GKA, QW, TM, YM, JG, MS, LF, RR, and ZG proofread and approved the manuscript in its current form.

FUNDING

This study was funded by the National Natural Science Foundation of China (grant nos. 81370329 and 81461138036), the Postgraduate Research and Practice Innovation Program of Jiangsu Province (grant no. KYCX18-2167), the Scientific Research Start-up Project of Shangqiu normal University (grant no. 7001/700216), and the Natural Science Foundation of The Jiangsu Higher Education Institutes of China (grant no. 17KJB180016).

REFERENCES

- Abraham, A. D., Schattauer, S. S., and Reichard, K. L. (2018). Estrogen regulation of GRK2 inactivates kappa opioid receptor signaling mediating analgesia, but not aversion. *J. Neurosci.* 38, 8031–8043. doi: 10.1523/JNEUROSCI.0653-18.2018
- Adzika, G. K., Machuki, J. O., Shang, W., Hou, H., Ma, T., Wu, L., et al. (2019). Pathological cardiac hypertrophy: the synergy of adenylyl cyclases inhibition in cardiac and immune cells during chronic catecholamine stress. *J. Mol. Med.* 97, 897–907. doi: 10.1007/s00109-019-01790-0
- Arcones, A. C., Martínez-Cignoni, M. R., Vila-Bedmar, R., Yáñez, C., and Lladó, I. (2021). Cardiac GRK2 protein levels show sexual dimorphism during aging and are regulated by ovarian hormones. *Cells* 10:673. doi: 10.3390/cells10030673
- Boese, A. C., Kim, S. C., Yin, K. J., Lee, J. P., and Hamblin, M. H. (2017). Sex differences in vascular physiology and pathophysiology: estrogen and androgen signaling in health and disease. *Am. J. Physiol. Heart Circ. Physiol.* 313, H524–H545. doi: 10.1152/ajpheart.00217.2016
- Bolego, C., Cignarella, A., Stals, B., and Chinetti-Gbaguidi, G. (2013). Macrophage function and polarization in cardiovascular disease: a role of estrogen signaling?

- Arterioscler. Thromb. Vasc. Biol.* 33, 1127–1134. doi: 10.1161/ATVBAHA.113.301328
- Cai, B., Tan, X., Zhang, Y., Li, X., Wang, X., Zhu, J., et al. (2015). Mesenchymal stem cells and cardiomyocytes interplay to prevent myocardial hypertrophy. *Stem Cells Transl. Med.* 4, 1425–1435. doi: 10.5966/sctm.2015-0032
- Campbell, L., Emmerson, E., Williams, H., Saville, C. R., Krust, A., Chambon, P., et al. (2014). Estrogen receptor- α promotes alternative macrophage activation during cutaneous repair. *J. Invest. Dermatol.* 134, 2447–2457. doi: 10.1038/jid.2014.175
- Cao, X., Zhou, C., Chong, J., Fu, L., Zhang, L., Sun, D., et al. (2015). Estrogen resisted stress-induced cardiomyopathy through increasing the activity of β_2 AR-G α s signal pathway in female rats. *Int. J. Cardiol.* 187, 377–386. doi: 10.1016/j.ijcard.2015.02.113
- Carpenter, J. S., Sheng, Y., Elomba, C. D., Alwine, J. S., Yue, M., Pike, C. A., et al. (2021). A systematic review of palpitations prevalence by menopausal status. *Curr. Obstet. Gynecol. Rep.* 10, 7–13. doi: 10.1007/s13669-020-00302-z
- Chen, Q., Qi, X., Zhang, W., Zhang, Y., Bi, Y., Meng, Q., et al. (2021). Catalpol inhibits macrophage polarization and prevents postmenopausal atherosclerosis through regulating estrogen receptor α . *Front. Pharmacol.* 12:655081. doi: 10.3389/fphar.2021.655081
- De Nigris, V., and Prattichizzo, F. (2021). DPP-4 inhibitors have different effects on endothelial low-grade inflammation and on the M1-M2 macrophage polarization under hyperglycemic conditions. *Diabetes Metab. Syndr. Obes.* 14, 1519–1531. doi: 10.2147/DMSO.S302621
- Fu, W., Gao, X. P., Zhang, S., Dai, Y. P., Zou, W. J., and Yue, L. M. (2019). 17β -estradiol inhibits PCSK9-mediated LDLR degradation through GPER/PLC activation in HepG2 Cells. *Front. Endocrinol.* 10:930. doi: 10.3389/fendo.2019.00930
- Gold, J. I., Gao, E., Shang, X., Premont, R. T., and Koch, W. J. (2012). Determining the absolute requirement of G protein-coupled receptor kinase 5 for pathological cardiac hypertrophy: short communication. *Circ. Res.* 111, 1048–1053. doi: 10.1161/CIRCRESAHA.112.273367
- Goldstein, J., Sites, C. K., and Toth, M. J. (2004). Progesterone stimulates cardiac muscle protein synthesis via receptor-dependent pathway. *Fertil. Steril.* 82, 430–436. doi: 10.1016/j.fertnstert.2004.03.018
- Goncalves, G. K., Scalzo, S., Alves, A. P., Agero, U., Guatimosim, S., and Reis, A. M. (2018). Neonatal cardiomyocyte hypertrophy induced by endothelin-1 is blocked by estradiol acting on GPER. *Am. J. Physiol. Cell Physiol.* 314, C310–C322. doi: 10.1152/ajpcell.00060.2017
- Hou, H., Zhao, Z., Machuki, J. O., Zhang, L., Zhang, Y., Fu, L., et al. (2018). Estrogen deficiency compromised the β_2 (AR)-G α s/Gi coupling: implications for arrhythmia and cardiac injury. *Pflugers Arch.* 470, 559–570. doi: 10.1007/s00424-017-2098-4
- Hulsmans, M., Sager, H. B., Roh, J. D., and Valero-Muñoz, M. (2018). Cardiac macrophages promote diastolic dysfunction. *J. Exp. Med.* 215, 423–440. doi: 10.1084/jem.20171274
- Kang, S., Liu, Y., Sun, D., Zhou, C., Liu, A., Xu, C., et al. (2012). Chronic activation of the G protein-coupled receptor 30 with agonist G-1 attenuates heart failure. *PLoS One* 7:e48185. doi: 10.1371/journal.pone.0048185
- Keselman, A., Fang, X., and White, P. B. (2017). Estrogen signaling contributes to sex differences in macrophage polarization during asthma. *J. Immunol.* 199, 1573–1583. doi: 10.4049/jimmunol.1601975
- Kozakowski, J., Gietka-Czernel, M., Leszczyńska, D., and Majos, A. (2017). Obesity in menopause – our negligence or an unfortunate inevitability? *Prz. Menopauzalny* 16, 61–65. doi: 10.5114/pm.2017.68594
- Lavine, K. J., Epelman, S., Uchida, K., Weber, K. J., Nichols, C. G., Schilling, J. D., et al. (2014). Distinct macrophage lineages contribute to disparate patterns of cardiac recovery and remodeling in the neonatal and adult heart. *Proc. Natl. Acad. Sci. U.S.A.* 111, 16029–16034. doi: 10.1073/pnas.1406508111
- Lee, J. Y., Hyun, H. S., Park, H. G., Seo, J. H., Lee, E. Y., Lee, J. S., et al. (2015). Effects of hormone therapy on serum lipid levels in postmenopausal Korean women. *J. Menopausal Med.* 21, 104–111. doi: 10.6118/jmm.2015.21.2.104
- Lin, Y., Zhang, X., Xiao, W., Li, B., Wang, J., Jin, L., et al. (2016). Endoplasmic reticulum stress is involved in DFMO attenuating isoproterenol-induced cardiac hypertrophy in rats. *Cell. Physiol. Biochem.* 38, 1553–1562. doi: 10.1159/000443096
- Liu, A., Gao, L., Kang, S., Liu, Y., Xu, C., Sun, H., et al. (2012). Testosterone enhances estradiol's cardioprotection in ovariectomized rats. *J. Endocrinol.* 212, 61–69. doi: 10.1530/JOE-11-0181
- Machuki, J. O., Zhang, H. Y., Geng, J., Fu, L., Adzika, G. K., Wu, L., et al. (2019). Estrogen regulation of cardiac cAMP-L-type Ca(2+) channel pathway modulates sex differences in basal contraction and responses to β_2 (AR)-mediated stress in left ventricular apical myocytes. *Cell Commun. Signal.* 17:34. doi: 10.1186/s12964-019-0346-2
- Medeiros, K., O'Connor, M. J., Baicu, C. F., Fitzgibbons, T. P., Shaw, P., Tighe, D. A., et al. (2014). Systolic and diastolic mechanics in stress cardiomyopathy. *Circulation* 129, 1659–1667. doi: 10.1161/CIRCULATIONAHA.113.002781
- Menzies, F. M., Henriquez, F. L., Alexander, J., and Roberts, C. W. (2011). Selective inhibition and augmentation of alternative macrophage activation by progesterone. *Immunology* 134, 281–291. doi: 10.1111/j.1365-2567.2011.03488.x
- Michalson, K. T., Groban, L., Howard, T. D., Shively, C. A., Sophonsritsuk, A., Appt, S. E., et al. (2018). Estradiol treatment initiated early after ovariectomy regulates myocardial gene expression and inhibits diastolic dysfunction in female cynomolgus monkeys: potential roles for calcium homeostasis and extracellular matrix remodeling. *J. Am. Heart Assoc.* 7:e009769. doi: 10.1161/JAHA.118.009769
- Mori, T., Kai, H., Kajimoto, H., Koga, M., Kudo, H., Takayama, N., et al. (2011). Enhanced cardiac inflammation and fibrosis in ovariectomized hypertensive rats: a possible mechanism of diastolic dysfunction in postmenopausal women. *Hypertens. Res.* 34, 496–502. doi: 10.1038/hr.2010.261
- Mouton, A. J., DeLeon-Pennell, K. Y., Rivera Gonzalez, O. J., Flynn, E. R., Freeman, T. C., Saucerman, J. J., et al. (2018). Mapping macrophage polarization over the myocardial infarction time continuum. *Basic Res. Cardiol.* 113:26. doi: 10.1007/s00395-018-0686-x
- Ndzie Noah, M. L., Adzika, G. K., Mprah, R., Adekunle, A. O., Adu-Amankwaah, J., and Sun, H. (2021). Sex-gender disparities in cardiovascular diseases: the effects of estrogen on eNOS, lipid profile, and NFATs during catecholamine stress. *Front. Cardiovasc. Med.* 8:639946. doi: 10.3389/fcvm.2021.639946
- Paur, H., Wright, P. T., Sikkil, M. B., Tranter, M. H., Mansfield, C., O'Gara, P., et al. (2012). High levels of circulating epinephrine trigger apical cardiodepression in a β_2 -adrenergic receptor/Gi-dependent manner: a new model of Takotsubo cardiomyopathy. *Circulation* 126, 697–706. doi: 10.1161/CIRCULATIONAHA.112.111591
- Ray, A., and Dittel, B. N. (2010). Isolation of mouse peritoneal cavity cells. *J. Vis. Exp.* 35:1488. doi: 10.3791/1488
- Ren, J., Hintz, K. K., Roughead, Z. K., Duan, J., Colligan, P. B., Ren, B. H., et al. (2003). Impact of estrogen replacement on ventricular myocyte contractile function and protein kinase B/Akt activation. *Am. J. Physiol. Heart Circ. Physiol.* 284, H1800–H1807. doi: 10.1152/ajpheart.00866.2002
- Ribeiro, R. F. Jr., Potratz, F. F., Pavan, B. M., Forechi, L., Lima, F. L., Fiorim, J., et al. (2013). Carvedilol prevents ovariectomy-induced myocardial contractile dysfunction in female rat. *PLoS One* 8:e53226. doi: 10.1371/journal.pone.0053226
- Rossouw, J. E., Anderson, G. L., Prentice, R. L., LaCroix, A. Z., Kooperberg, C., Stefanick, M. L., et al. (2002). Risks and benefits of estrogen plus progestin in healthy postmenopausal women: principal results from the Women's health initiative randomized controlled trial. *JAMA* 288, 321–333. doi: 10.1001/jama.288.3.321
- Scally, C., Abbas, H., Ahearn, T., Srinivasan, J., Mezincescu, A., Rudd, A., et al. (2019). Myocardial and systemic inflammation in acute stress-induced (Takotsubo) cardiomyopathy. *Circulation* 139, 1581–1592. doi: 10.1161/CIRCULATIONAHA.118.037975
- Villa, A., Rizzi, N., Vegeto, E., Ciana, P., and Maggi, A. (2015). Estrogen accelerates the resolution of inflammation in macrophagic cells. *Sci. Rep.* 5:15224. doi: 10.1038/srep15224
- Wheatley, C. M., Snyder, E. M., Johnson, B. D., and Olson, T. P. (2014). Sex differences in cardiovascular function during submaximal exercise in humans. *Springerplus* 3:445. doi: 10.1186/2193-1801-3-445
- Wilson, H. M., Cheyne, L., Brown, P. A. J., Kerr, K., Hannah, A., Srinivasan, J., et al. (2018). Characterization of the myocardial inflammatory response in acute stress-induced (Takotsubo) cardiomyopathy. *JACC Basic Transl. Sci.* 3, 766–778. doi: 10.1016/j.jacbs.2018.08.006

- Xing, D., Nozell, S., Chen, Y. F., Hage, F., and Oparil, S. (2009). Estrogen and mechanisms of vascular protection. *Arterioscler. Thromb. Vasc. Biol.* 29, 289–295. doi: 10.1161/ATVBAHA.108.182279
- Youssef, M. E., El-Mas, M. M., Abdelrazek, H. M., and El-Azab, M. F. (2021). α_7 -nAChRs-mediated therapeutic angiogenesis accounts for the advantageous effect of low nicotine doses against myocardial infarction in rats. *Eur. J. Pharmacol.* 898:173996. doi: 10.1016/j.ejphar.2021.173996
- Zhang, L., Li, C., Yang, L., Adzika, G. K., Machuki, J. O. A., Shi, M., et al. (2021). Estrogen protects vasomotor functions in rats during catecholamine stress. *Front. Cardiovasc. Med.* 8:679240. doi: 10.3389/fcvm.2021.679240
- Zhou, R., Ma, P., Xiong, A., Xu, Y., Wang, Y., and Xu, Q. (2017). Protective effects of low-dose rosuvastatin on isoproterenol-induced chronic heart failure in rats by regulation of DDAH-ADMA-NO pathway. *Cardiovasc. Ther.* 35:e12241. doi: 10.1111/1755-5922.12241
- Zhu, Y., Zhang, L., Lu, Q., Gao, Y., Cai, Y., Sui, A., et al. (2017). Identification of different macrophage subpopulations with distinct activities in a mouse model of oxygen-induced retinopathy. *Int. J. Mol. Med.* 40, 281–292. doi: 10.3892/ijmm.2017.3022

Conflict of Interest: The authors declare that the research was conducted in the absence of any commercial or financial relationships that could be construed as a potential conflict of interest.

Publisher's Note: All claims expressed in this article are solely those of the authors and do not necessarily represent those of their affiliated organizations, or those of the publisher, the editors and the reviewers. Any product that may be evaluated in this article, or claim that may be made by its manufacturer, is not guaranteed or endorsed by the publisher.

Copyright © 2021 Hou, Adzika, Wu, Ma, Ma, Geng, Shi, Fu, Rizvi, Gong and Sun. This is an open-access article distributed under the terms of the Creative Commons Attribution License (CC BY). The use, distribution or reproduction in other forums is permitted, provided the original author(s) and the copyright owner(s) are credited and that the original publication in this journal is cited, in accordance with accepted academic practice. No use, distribution or reproduction is permitted which does not comply with these terms.



The Potential Use of Cannabis in Tissue Fibrosis

Nazar Pryimak, Mariia Zaiachuk, Olga Kovalchuk* and Igor Kovalchuk*

Department of Biological Sciences, University of Lethbridge, Lethbridge, AB, Canada

OPEN ACCESS

Edited by:

Susanne Sattler,
Imperial College London,
United Kingdom

Reviewed by:

Selvi Enrico,
Siena University Hospital, Italy
Elaine Cristina Dalazen Gonçalves,
Federal University of Santa Catarina,
Brazil

*Correspondence:

Olga Kovalchuk
olga.kovalchuk@uleth.ca
Igor Kovalchuk
igor.kovalchuk@uleth.ca

Specialty section:

This article was submitted to
Molecular and Cellular Pathology,
a section of the journal
Frontiers in Cell and Developmental
Biology

Received: 26 May 2021

Accepted: 06 September 2021

Published: 11 October 2021

Citation:

Pryimak N, Zaiachuk M,
Kovalchuk O and Kovalchuk I (2021)
The Potential Use of Cannabis
in Tissue Fibrosis.
Front. Cell Dev. Biol. 9:715380.
doi: 10.3389/fcell.2021.715380

Fibrosis is a condition characterized by thickening or/and scarring of various tissues. Fibrosis may develop in almost all tissues and organs, and it may be one of the leading causes of morbidity and mortality. It provokes excessive scarring that exceeds the usual wound healing response to trauma in numerous organs. Currently, very little can be done to prevent tissue fibrosis, and it is almost impossible to reverse it. Anti-inflammatory and immunosuppressive drugs are among the few treatments that may be efficient in preventing fibrosis. Numerous publications suggest that cannabinoids and extracts of *Cannabis sativa* have potent anti-inflammatory and anti-fibrogenic properties. In this review, we describe the types and mechanisms of fibrosis in various tissues and discuss various strategies for prevention and dealing with tissue fibrosis. We further introduce cannabinoids and their potential for the prevention and treatment of fibrosis, and therefore for extending healthy lifespan.

Keywords: fibrosis, anti-fibrotic, *Cannabis sativa*, cannabinoids, inflammation

INTRODUCTION

Fibrosis is a pathology associated with the replacement of parenchyma with connective tissue during the healing process. Fibrosis is defined as an excessive growth, stiffness, and sometimes scarring of different tissues or organs along with an imputed overaccumulation of extracellular matrix (ECM) components and collagen (Liu, 2011). Fibrotic illness is not well understood, it has a poor outcome and is mainly untreatable, all of which is compared to the terminal stage of cancer (Wernig et al., 2017). This condition is a lifelong pathological anomaly that may occur in various organs (Table 1), with a higher frequency in the skin, liver, heart, kidneys, and lungs.

Different types of fibrosis have been recognized based on anatomical location such as pulmonary [idiopathic pulmonary fibrosis (IPF), cystic fibrosis, emphysema], liver (cirrhosis, portal hypertension, hepatocellular carcinoma) or skin (keloids, systemic sclerosis). The most well-known and studied example of fibrosis is IPF. This condition is a lifelong, incurable illness targeting lungs. This disease usually affects middle-aged people and older adults and is characterized by a long-lasting cough along with difficulties in breathing of an unknown origin; besides IPF is very difficult to diagnose. Many IPF patients struggle with an acute worsening of breathing that is correlated with high mortality. The progression rate of this condition is very unpredictable. Some patients can deteriorate very quickly, while others may remain asymptomatic for many years. There is no generally approved treatment for this disease. The development of treatments is focused on fibroproliferation and fibrogenesis (Liu, 2011; Fujimoto et al., 2015; Hoyer et al., 2019). Because of insensitivity to pharmacological treatments, an average survival time is 3 years.

Epidemiological data on fibrosis in different organs is well documented in the literature. For example, an incidence of IPF varies between 0.6 and 17.4 per 100,000 population per year

TABLE 1 | Main types of fibrosis.

| Organ/tissue | Type of fibrosis | References |
|--------------------------|-------------------------------|-------------------------------------|
| Skin | Hypertrophic scar | Rabello et al. (2014) |
| | Systemic sclerosis | Allanore et al. (2015) |
| Heart | Cardiac fibrosis | Hinderer and Schenke-Layland (2019) |
| | Hypertrophic cardiomyopathy | Ho et al. (2010) |
| | Cardiac dysfunction | Khan and Sheppard (2006) |
| | Valvular disease | |
| | Arrhythmia | |
| Bone marrow | Myelofibrosis | Zahr et al. (2016) |
| | Myelodysplastic syndrome | Hinderer and Schenke-Layland (2019) |
| | Chronic myelogenous leukemia | |
| Liver | Cirrhosis | Šmíd (2020) |
| | Portal hypertension | |
| | Hepatocellular carcinoma | |
| Retroperitoneum | Retroperitoneal fibrosis | Vaglio and Maritati (2016) |
| Gut | Intestinal fibrosis | Hinderer and Schenke-Layland (2019) |
| | Enteropathies | |
| | Inflammatory bowel disease | |
| Joint | Arthrofibrosis | Usher et al. (2019) |
| Brain and nervous system | Glial scar | Hinderer and Schenke-Layland (2019) |
| | Alzheimer | |
| Eye | Subretinal fibrosis | Friedlander (2007) |
| | Epiretinal fibrosis | Khaw et al. (2020) |
| | Vision loss | |
| Lung | Idiopathic pulmonary fibrosis | Barratt et al. (2018) |
| | Cystic fibrosis | Friedlander (2007) |
| | Pulmonary hypertension | Smith et al. (2013) |
| | Thromboembolic disease | Farghaly and El-Abdin (2015) |
| Mediastinum | Mediastinal fibrosis | Rajput et al. (2000) |
| Pancreas | Pancreatic fibrosis | Klöppel et al. (2004) |
| | Cystic fibrosis | Madácsy et al. (2018) |
| | Chronic pancreatitis | Klöppel (2007) |
| | Duct obstruction | Apte et al. (2011) |
| Kidney | Renal fibrosis | Liu (2011) |
| | Cystic fibrosis | Yahiaoui et al. (2009) |
| | Nephrogenic systemic fibrosis | Waikhom and Taraphder (2011) |
| | Chronic kidney disease | Panizo et al. (2021) |
| | Renal anemia | Xiao and Liu (2013) |

(Ley and Collard, 2013), two third of all patients were 60 years and above, and the highest prevalence was reported among patients of 80 years and above – 165.9 per 100,000 population (Raimundo et al., 2016). In Caucasians, cystic fibrosis occurs roughly in 1 in 3,000–4,000 births; and among other races, cystic fibrosis is less frequent, 1 in 4,000–10,000 in Latin Americans and 1 in 15,000–20,000 in African Americans, and even less in Asian Americans (Sanders and Fink, 2016). As to liver cirrhosis, according to 2017 data, 112 million compensated cases were reported worldwide (Sepanlou, 2020), and in patient who were more than 65 years old, a risk of severe liver fibrosis was 3.78 times higher (Kim et al., 2015). Also, more than 100 million cases of keloid are reported annually worldwide (Gauglitz et al., 2011; Li et al., 2017).

There is generally no good treatment of fibrosis and complete recovery is nearly impossible. Treatment includes various anti-inflammatory and anti-fibrotic agents with various degree of success. In this respect, cannabinoids and *Cannabis sativa* extracts, known for their strong anti-inflammatory potential,

may be serve as useful additives to treatment of fibrosis. In this review, we will cover the pathology of fibrosis and current therapy of fibrosis as well as introduce basic components of endocannabinoid system (ECS) and propose potential use of cannabinoids for treatment of fibrosis.

PHASES OF NORMAL WOUND HEALING AND FIBROSIS

In most cases, fibrosis occurs after acute or more often chronic damage to tissues, followed by abnormal repair. There are two ways of repair of the injured tissues. The first one is the regeneration by the propagation of undamaged cells of parenchyma and the maturation of stem cells – normal wound healing process. The second one is scar tissue formation through the accumulation of connective tissues – tissue fibrosis. The regeneration is a possibility of damaged tissues to be repaired and their defective elements to be restored. Cells that remain

undamaged are able to proliferate and maintain the structure of the tissue. In some cases, fibrosis may occur due to a critical tissue injury or as a result of the inability of injured tissue to accomplish the repair. Fibrosis occurs due to either a large amount of collagen deposition associated with the long-lasting inflammation or ischemic necrosis. Cell proliferation is handled by growth factors, although the central role is played by ECM and maturation of stem cells (Ocleston et al., 2010).

Different types of cells, such as fibroblasts, vascular endothelial cells, and some fragments of injured tissues proliferate along with the repair of damaged tissues. In fibrosis and scarring, tissue repair is characterized by the proliferation of connective tissues rather than parenchymal tissues that happens upon normal regeneration (Galliot et al., 2017).

Phases of Wound Healing

Wound healing consists of four main phases, including hemostasis, inflammation, proliferation or granulation and remodeling or maturation, each phase lasting from days to months (Figure 1).

Abnormal wound healing resulting in scar formation also includes similar phases/steps, such as inflammation, cell proliferation, and remodeling, but is characterized by more extensive deposition of collagen, fibrin, fibronectin, etc. (Profyris et al., 2012).

The First Phase – Hemostasis

The most crucial step is not to restore a tissue but to stop bleeding from the injured place. Coagulation starts exactly after trauma and finishes within hours. Collagen assists this process in the damaged area. Hemostasis consists of two subphases, *primary* and *secondary* hemostasis. Primary hemostasis is the formation of a plug at the injured place where endothelial cells become exposed. In the secondary hemostasis, there are two main pathways of blood clotting: the *extrinsic* and the *intrinsic* pathways, and they come together in the common pathway. The extrinsic pathway is a primary stage in plasma mediated secondary hemostasis. Due to tissue damage, tissue factor (TF also known as platelet tissue factor or factor III) is released in the plasma, which results in binding of factor VIIa and calcium to boost the activation of factor X to Xa (Figure 2). The intrinsic pathway includes factors I (fibrinogen), II (prothrombin), IX (Christmas factor), X (Stuart–Prower factor), XI (Plasma thromboplastin), and XII (Hageman factor) (Robertson and Miller, 2018). The common pathway includes steps from the activation of factor X to the formation of active thrombin which brakes fibrin into a cross-linked complex.

The Second Phase – Inflammation

Inflammation plays a central role in normal wound healing and fibrosis. Tissue repair and regeneration also depend on the extent of injury and inflammation. When the injury is extensive in the presence of chronic inflammation, repair may predominate even when the damaged cells can regenerate.

In normal circumstances, the inflammatory microenvironment quickly handles the damaged particles or pathogens. The essential factors of inflammation and

fibrogenesis are summarized below (Table 2; Newton and Dixit, 2012; Kendall and Feghali-Bostwick, 2014).

The Third Phase – Proliferation and Granulation

Cell proliferation is an essential component of tissue repair, wound healing and fibrogenesis. There are several types of cells, such as epithelial cells, endothelial cells, and fibroblasts that participate in fibrogenesis and normal process of healing of the wound.

Mesothelial cells originate from the embryonic mesoderm and play an essential role during trauma or infection. For instance, in pleural injuries, they assist in transporting white cells. Also, as a result of mesothelial-to-mesenchymal transition (MMT), these cells, might be genetically reprogrammed after the influence of specific stimuli. In a recent mouse model, the lineage analysis of stem cells demonstrated that MMT increased the proliferation of myofibroblasts and hepatic satellite cells during liver fibrogenesis (Tirado and Koss, 2018).

Fibrocytes are of a mesenchymal origin and are phenotypically inactive due to a low amount of rough endoplasmic reticulum. These cells produce fibroblastic components such as collagen, fibronectin, and vimentin. When influenced by TGF- β , they can produce alpha-smooth muscle actin (α -SMA) which plays a role in angiogenesis and immunity. Fibrocytes can also migrate to the damaged area with blood flow (de Oliveira and Wilson, 2020).

Fibroblasts originate from the embryonic mesoderm tissues. Due to the chemotaxis feature, fibroblasts are able to migrate within tissue in response to chemical stimuli. In case of injury, they can cause contraction of the matrix that leads to the sealing of the open wound. Fibroblasts play an important role in fibrogenesis, for example, TGF- β 1 dependent differentiation into myofibroblasts (Weiskirchen et al., 2019).

Epithelial cells are located in different areas of the body, such as skin, urinary tract, blood vessels, and internal organs. One of the critical features is their ability to differentiate into different types of cells. During epithelial-to-mesenchymal transition (EMT), epithelial cells become transited cells that become sensitive to the fibroblast's specific protein (FSP1). The plasticity of epithelial cells allows them to become a source of myofibroblasts in the damaged cells (Macara et al., 2014).

Endothelial cells are mainly responsible for the formation of a barrier in the endothelium of capillaries, venules, vein, arterioles, and arteries. Being stimulated by TGF- β , endothelial cells can release α -SMA and become able to convert into mesenchymal cells (endothelial-to-mesenchymal-transition, EndMT). It was demonstrated that EndMT could lead to fibrosis in the organs such as heart, kidney, and lungs (Sakai and Tager, 2013).

Pericytes are fibroblast-like cells that surround endothelial cells in blood vessels. Pericytes are able to contract and consequently control blood flow. In the case study, it was suggested that this type of cells produce α -SMA, neural/glial antigen (NG2) and platelet-derived growth factor receptor- β (PDGFR- β). Moreover, they are a source of myofibroblasts in pulmonary tissues. Another study reported that Foxd1 progenitor-derived pericytes prominently lead to the lung fibrosis (Sakai and Tager, 2013).

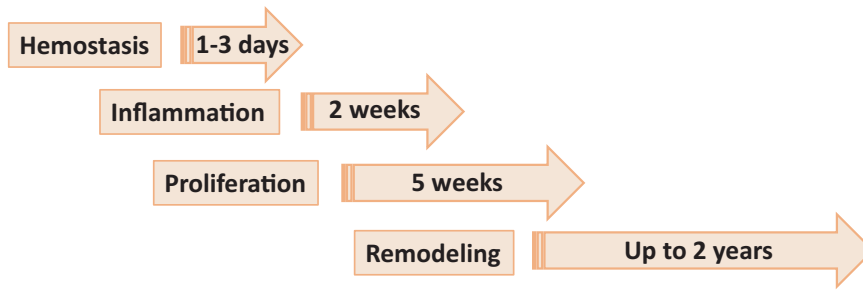


FIGURE 1 | Phases of wound healing. Phase 1, hemostasis is the process of clot formation to stop bleeding, and includes steps such as vasoconstriction, aggregation of platelets and migration of leukocytes. Phase 2, inflammation is the process of cleaning the wound and preparing for the formation of new blood vessels. It includes processes such as release of antibacterial molecules by neutrophils, engulfing of pathogens and debris by macrophages, and release of angiogenic substances to stimulate angiogenesis and granulation. Phase 3, proliferation (or granulation) – the process allowing to bring the wound edges together and seal it. It includes proliferation of the wound by fibroblasts, with secretion of glycoproteins and collagen, followed by migration of epithelial cells from the wound edges and formulation of granulation tissues. Phase 4, remodeling (or maturation) phase is mostly a continuation of proliferation phase resulting in formation of proper tissue.

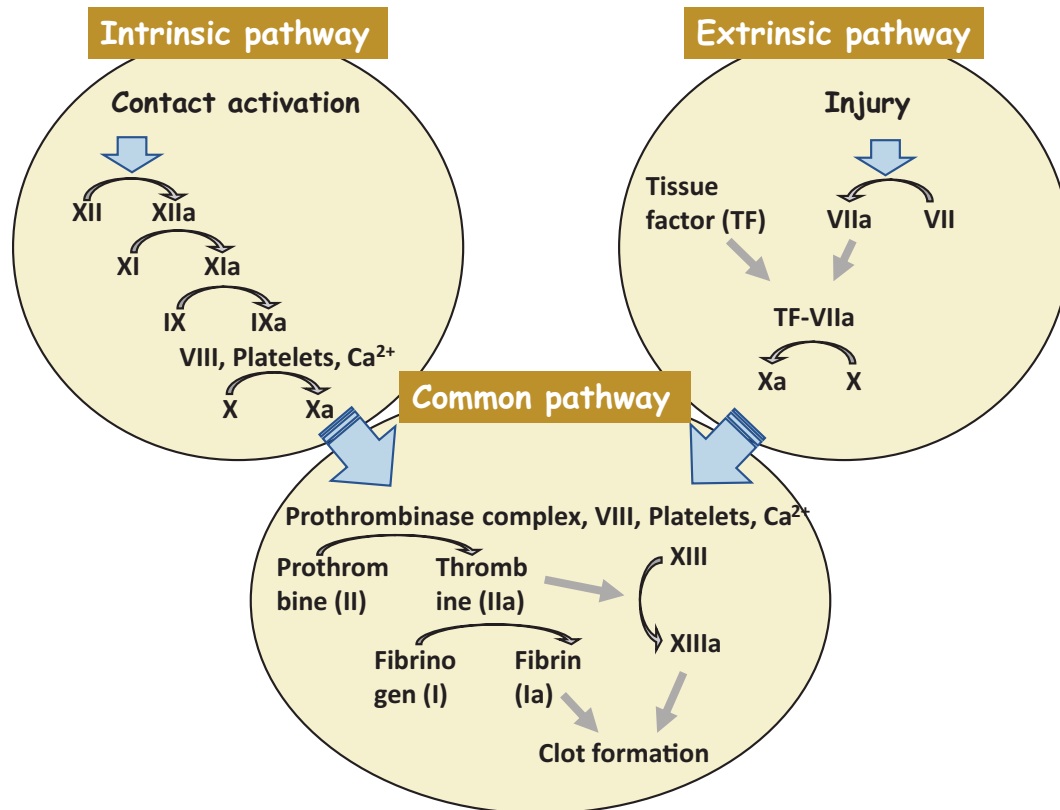


FIGURE 2 | A clot formation cascade. There are three steps of the clotting (coagulation) cascade: the intrinsic pathway (factors XII, XI, IX, and VIII), the extrinsic pathway (factor VII), and the common pathway. During clotting, cascade factor X may be activated by the extrinsic and intrinsic pathways. The common pathway consists of steps from the activation of factor X to the clot formation. Factors that are activated are shown with a lowercase “a”.

Vascular smooth muscle cells are responsible for the relaxation and contraction of blood vessels. As a result of the injury, they produce α -SMA, vimentin, desmin, and other compounds. It has also been shown that collagen type I is induced by bradykinin secretion in vascular smooth muscle cells through the TGF- β 1 activation (Liu et al., 2017).

There are two main processes involved in proliferation phase of repair: *formation of granulation tissues* and *wound contraction*. Wound contraction usually starts on day 2–3 and is finished within 2 weeks. The primary cells that are responsible for this process are myofibroblasts, the unique cells that have features of fibroblasts and smooth muscle. The main role of these cells is

TABLE 2 | Key mediators of inflammation and fibrogenesis.

| | Substance | Production site | Effects | References | |
|--|---|---|---|--|---------------------------|
| Profibrotic factors acting on fibroblasts | TGF β | White blood cells | Transformation of resident (subcutaneous, pulmonary, etc.) fibroblasts to myfibroblasts. Stimulation of collagen and fibronectin transcription. Stimulation of resting monocytes and inhibition of activated macrophages. | Frangogiannis (2020) | |
| | IL-1 β | Fibroblasts, macrophages | Inflammation promotion and fibrotic responses (in part, through activation of TNF α). | Lopez-Castejon and Brough (2011) | |
| | IL-6 | T cells, skeletal muscle cells, macrophages | Regulation of inflammation (pro- and anti-inflammatory). Stimulation of cellular differentiation and fibrosis. | Tanaka et al. (2014) | |
| | IL-13 | Mast cells, T lymphocytes, eosinophils and basophils | Stimulation of TGF β production, proliferation of fibroblasts, collagen and MMP production. | Marone et al. (2019) | |
| | IL-33 | Smooth muscle cells, epithelial and endothelial cells | Signals through ST2 to initiate and enhances profibrogenic cytokine production in a macrophage-dependent manner. | Li et al. (2014) | |
| | TNF α | Macrophages, T lymphocytes, NK cells, mast cells, eosinophils | Stimulation of inflammation and fibrosis, in part through TGF- β signaling pathway, activation of myfibroblasts and increased secretion of MMPs. | Yoshimatsu et al. (2020) | |
| | FGFs | Various parenchymal cells | Fibrosis enhancement through binding and activation of fibroblast growth factor receptor (FGFR). | Xie et al. (2020) | |
| | PDGF | Platelets, smooth muscle cells, endothelial cells and macrophages | Stimulation differentiation, proliferation, and ECM production via interaction with PDGF α and PDGF β receptors on myfibroblasts. | Klinkhammer et al. (2018) | |
| | Leukotrienes (LTB4, LTC4, LTD4, LTE4) | White blood cells | Stimulation of fibroblasts proliferation and production of the matrix via modulation of the production of cyclic AMP by interaction with G-protein adenylate cyclase. | Kowal-Bielecka et al. (2007) | |
| | Profibrotic factors released from fibroblasts | VEGF | Macrophages, fibroblasts, platelets | Angiogenesis promotion. Facilitates monocyte recruitment and infiltration of fibrotic tissues mediated through a VEGF-dependent sinusoidal permeability, leading either to resolution or promotion of fibrosis. | Yang et al. (2014) |
| IL-1 | | Fibroblasts | Facilitates inflammation and fibrosis through autocrine stimulation of IL-1 receptor. | Kelly et al. (2019) | |
| IL-6 | | Fibroblasts | Facilitation of inflammation and fibrosis through binding of IL-6 to IL-6R α receptor, which then associates with the signal-transducing gp130 protein to facilitate phosphorylation of the transcription factor STAT-3. Phosphorylated STAT-3 regulates expression of pro-fibrotic genes. | Kobayashi et al. (2015) | |
| IL-33 | | Dermal and cardiac fibroblasts | Promotion of inflammation and fibrosis by signaling through ST2 and activating TGF β production. | Kotsiou et al. (2018) | |
| Angiotensin II | | Macrophages and myfibroblasts | Promotion of TGF β mediated heart remodeling. Fibrosis enhancement via the angiotensin type 1 receptor (AT1). | Rosenkranz (2004) | |
| IGFII | | Fibroblasts | Stimulation of fibrosis through mannose-6-phosphate/insulin-like growth factor receptor (M6P/IGFII receptor) in turn activating latent transforming growth factor β (L-TGF- β). | Ghahary et al. (2000) | |
| IGFBP-3 | | | Fibrosis initiation and enhancement by binding IGF-I and ECM components, inducing the production of extracellular matrix components such as collagen type I and fibronectin. Inhibit IGF mediated proliferation (via MEK/ERK and PI3K/AKT). | Pilewski et al. (2005) | |
| IGFBP-5 | | | | Yasuoka et al. (2009) | |
| Antifibrotic factors acting on fibroblasts | | PGE ₂ | Almost all nucleated cells | Inhibition of fibroblast proliferation and suppression of collagen production. Promotion of normal fibroblast apoptosis through EP2/EP4 signaling and a reduction in the Akt activity. | Huang et al. (2009) |
| | | HGF | Fibroblast | Prevents fibrosis and induces tissue repair acting through Met receptor and supporting the growth in epithelial and endothelial cells, but not in myfibroblasts. | Panganiban and Day (2011) |
| | PPAR ligands | Expressed in almost all tissues | Potent antifibrotic effects, reduction of β -catenin levels. Regulate the fate determination of mesenchymal cell lineage. | Jeon et al. (2017) Vallée et al. (2017) | |

the contraction of the wound by up to 80%. Granulation tissue is soft in touch and has a pink color. Granulation is a sign of tissue repair; it is formed by three steps: the inflammatory

phase, the clearance phase, and the ingrowth of granulation tissue (**Figure 3**). During the *inflammation phase*, cells that are predominantly involved in the process are monocytes and

neutrophils. The *clearance phase* is characterized by the release of autolytic enzymes from dying cells as well as enzymes from neutrophils; macrophages also clear necrotic debris. The final phase is the *ingrowth of granulation tissue* during which granulation tissue is formed. This phase can be divided into two processes: angiogenesis and fibrogenesis (Baum and Duffy, 2011; Bochaton-Piallat et al., 2016; Alhaji et al., 2020).

Angiogenesis (neovascularization) is the development of blood vessels. Angiogenesis could be the result of sprouting either from pre-existing blood vessels or from stem cells. There are a few steps in the angiogenesis from pre-existing blood vessels. The first one involves *vessel dilation* that is mediated by NO, and the second step includes an *increased vascular permeability* that is mediated by the vascular endothelial growth factor (VEGF). The next step is a *breakdown of the basement membrane* and the formation of a vessel sprout. The other step is the *migration of endothelial cells* toward chemotactic and *angiogenic stimuli* that cause a proliferation of endothelial cells and their maturation leading to capillary tube remodeling. The final phase of angiogenesis is the *accumulation of periendothelial cells* (pericyte) (Papetti and Herman, 2002).

Angiogenesis from stem cells develops from endothelial precursor cells (EPC) stored in the bone marrow, and if needed, they migrate to the place of injury (Aldair and Montani, 2010).

The Fourth Phase – Healthy Remodeling or Remodeling With Fibrogenesis

Remodeling (maturation phase) after injury usually takes place from several weeks to months or years and depends on what type of tissue is damaged, injury location, and the associated comorbidities (infections, arteriosclerosis, vein thrombosis, nutritional status, diabetes, and some drugs). During remodeling phase, rate of synthesis of collagen by fibroblasts exceeds the rate at which it is degraded, resulting in continuous increase in the amount of collagen. Remodeling includes three steps: *functional recovery*, *wound contraction* and an *increased tensile strength* of the wound (Cañedo-Dorantes and Cañedo-Ayala, 2019). The maturation phase is characterized by the formation of scar tissue as well as by the absence of inflammatory cells (neutrophils, macrophages) and the termination of blood vessel proliferation. Granulation tissue in the scar is replaced by dense collagen. The scar initially consists of a provisional matrix that contains fibrin, fibronectin, and collagen type III, but later on, collagen type III is replaced by collagen type I (Reinke and Sorg, 2012). The next step is wound contraction, with the main goal being a reduction of a gap between two cut margins. Myofibroblasts play a key role during this phase. **Figure 4** shows all major processes of differentiation, activation or transition of various cells into myofibroblasts. Collagen type I is responsible for the last step – an increase in the strength of the wound. The recovery of ~80% of the original tissue strength will usually take up to 3 months.

Skin wound healing can be subdivided into *primary* and *secondary unions* (Alhaji et al., 2020). By primary union (first intention), regeneration occurs with a minimum scarring tissue, for example, a clean surgical wound. By secondary union (secondary intention), the wound has the larger tissue defects with a wide distance between edges; wound healing by secondary

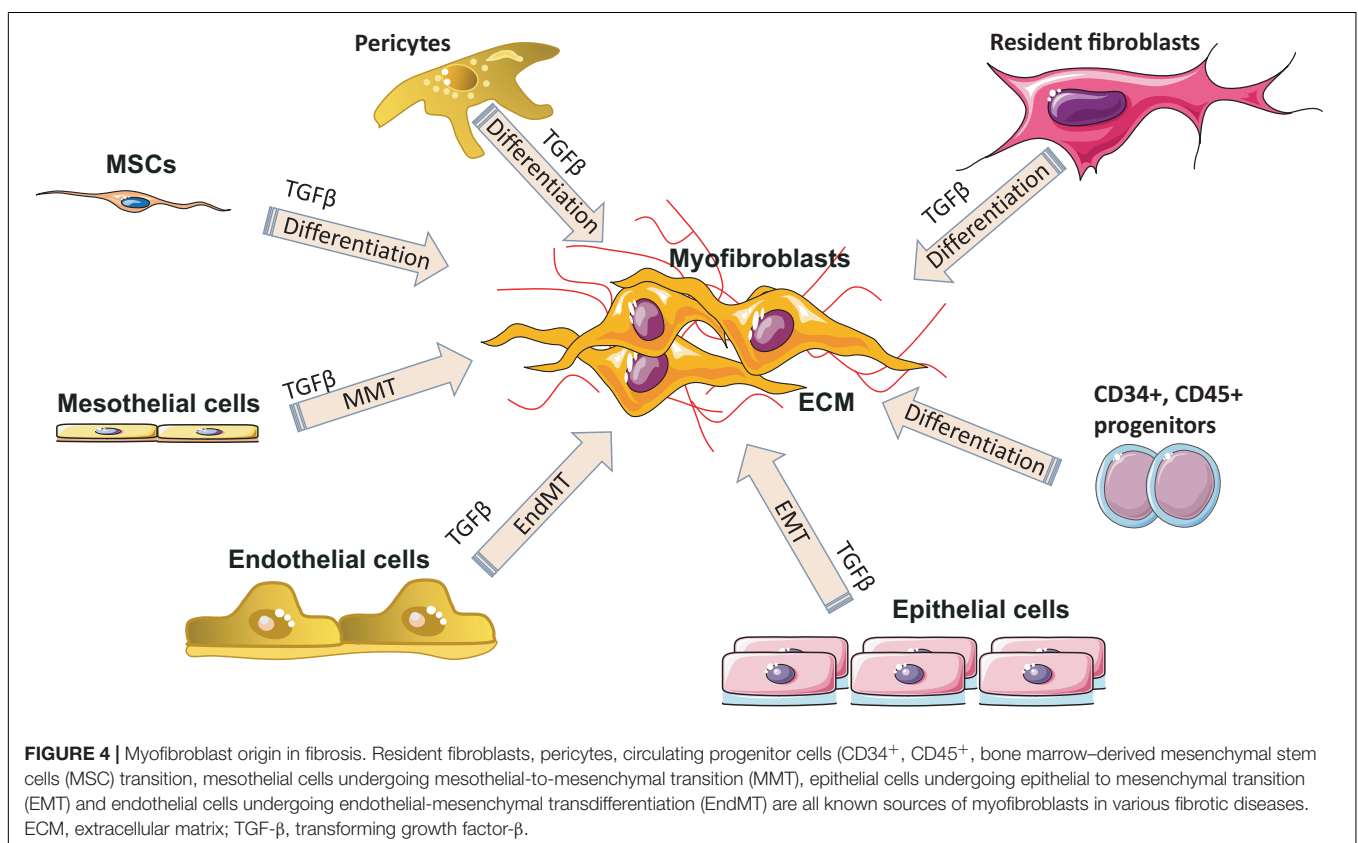
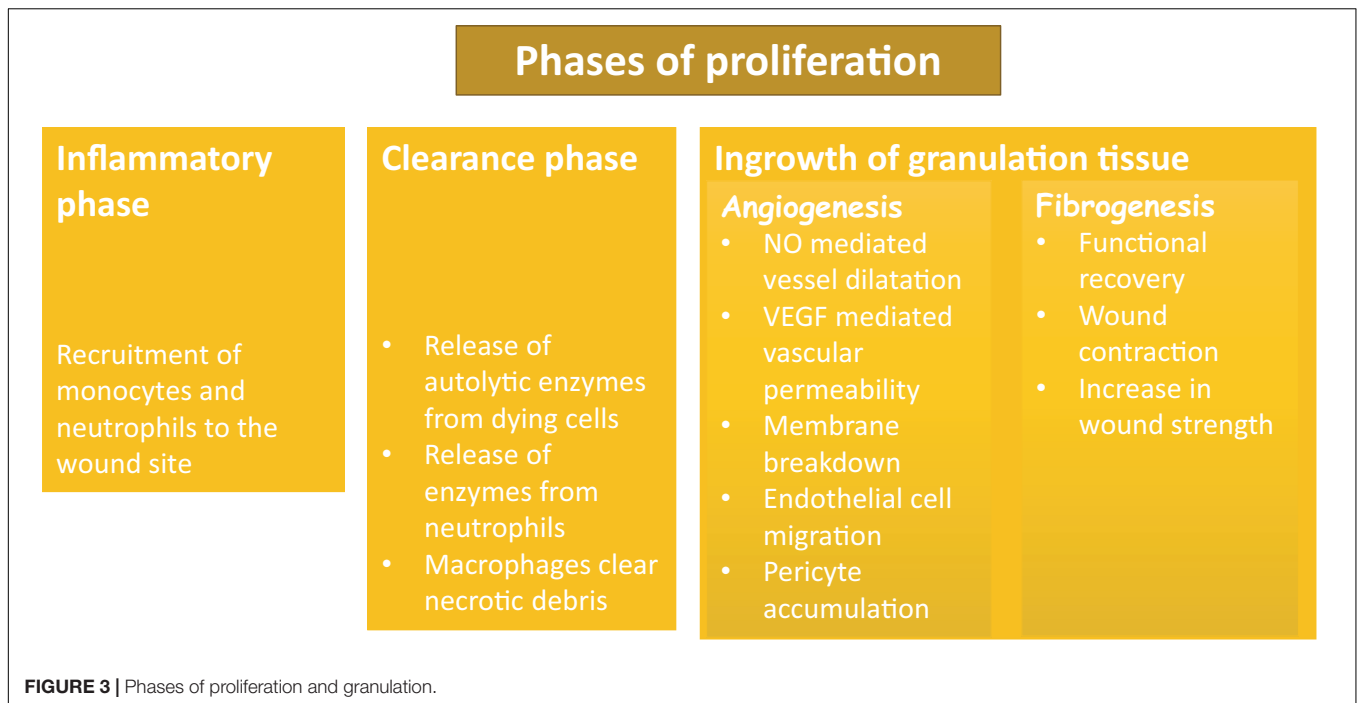
intention occurs by regeneration and scarring. In some cases, due to abnormal wound healing, keloids or hypertrophic scars might occur. In a hypertrophic scar, there is a build-up of extra collagen fibers, which results in the elevation of the scar. Fibrillar collagen fibers are located parallel to the epidermis with a lumpy red scar, and they do not extend beyond the original scarring area. Usually, hypertrophic scars affect younger individuals with the delayed healing of wounds caused by underlying conditions such as infections, and usually, there is an improvement with the treatment. Morphologically keloids are characterized as eosinophilic, focally fragmented complexes of haphazardly arranged collagen. Also, in comparison with hypertrophic scars, one-third of keloids have α -SMA-expressing myofibroblasts. The scar tissue in keloids grows beyond the inflammation area, and it is difficult to treat (Moshref et al., 2010).

Physiological Injury Healing vs. Pathological Fibrosis

Fibrosis of the organ tissues is caused by parenchymal cell destruction (*alteration* or *injury* phase); as a result of tissue trauma, macrophages become active and enter the damaged area. Also, local immune cells create chemokines and cytokines which activate mesenchymal cells located close to the injury area. The next step is the initiation of the production of ECM and the elevated manufacturing of pro-inflammatory cytokines and angiogenic factors (Weiskirchen et al., 2019). After trauma, cells produce inflammatory mediators that provoke the anti-fibrinolytic coagulation cascade, the first step of which is the coagulation. During this stage, known as *inflammation* stage, platelets are activated and form fibrin clots. Next, platelets liberate inflammatory chemokines. Then the infiltration of leukocytes happens into the injured site, and they excrete profibrotic cytokines (TGF- β and IL-13). Neutrophils are typically engaged in the infiltration process earlier than lymphocytes and macrophages (Rosales, 2018).

The *proliferation* stage follows the inflammation stage; during this stage, fibroblasts become active, and myofibroblasts induce and deposit ECM that will be a framework through the tissue regeneration action. The last step is *remodeling* (Gonzalez et al., 2016). In physiological recovery, the extra volume of ECM is degraded, myofibroblasts and fibroblasts go through apoptosis, and inflammatory cells leave the recovered tissues. On the other hand, the fibrosis process extends inflammation, and myofibroblasts stimulate the elevated accumulation of ECM which leads to the creation of a perpetual fibrotic scar. The contrasting features that distinguish fibrosis from normal wound healing are chronic inflammation, the persistence of myofibroblast activity, MMP-TIMP imbalance, and the excessive ECM deposition. These differences are very important to be understood from the therapeutic point of view because drugs can be prescribed to target these particular molecular disturbances.

Fibroblasts control synthesis and catabolism of collagen as well as an increase in collagen amount by MMPs and their inhibitors (tissue inhibitors of TIMPs). Changing the balance between these mechanisms will cause the elevation or dropping of collagen amount inside the injured area. In addition, an



increasing number of mesenchymal cells will aggravate response. During the remodeling phase, fibroblasts synthesize collagen at a higher rate than they degrade it, leading to the continuous

accumulation of collagen. Generally, inflammation stimulates fibrosis. According to some reports, however, fibrosis is not always driven by inflammation. This fact clarifies the shortage

of efficacy of anti-inflammatory mediators in the management of the fibrotic disease (Wynn, 2007; Kryczka and Boncela, 2015).

Fibrosis Prevention and Treatment Options

Prevention strategies for the development of fibrosis are very important in the modern world because life expectancy and the patients' quality of life are expected to rise gradually. When patients are aware of avoidable risk factors for this condition, they, for example, should quit smoking to prevent the development of pulmonary fibrosis and should treat all acute diseases in time to prevent the development of chronic conditions. There are unavoidable factors such as genetics, the existing comorbidities (diabetes mellitus, herpes virus infection), the environmental exposures, air pollution as well as chronic use of some medications that also have to be considered (Zaman and Lee, 2018).

Anti-inflammatory drugs are widely used to manage fibrosis due to a strong connection between inflammation and fibrosis (Suthahar et al., 2017; Lands and Stanojevic, 2019; Simon et al., 2019). As a result of better understanding of the pathology of fibrosis, molecular targets of this condition and modern drugs affecting it have been recently discovered. A single-component medication is characterized by the presence of a single component that can target either extracellular or intracellular factors. The main extracellular targets are MMPs, growth factors, TNF. Most of the drugs targeting intracellular factors are small molecules; they can easily translocate inside the cytoplasm compared to other large molecules, like monoclonal antibodies.

There are four categories of intracellular factors that can be targeted by anti-fibrotic medicine: nuclear receptors, enzymes, other proteins, and epigenetic factors (Li et al., 2017). The antifibrotic medications suppress kinases located in the cytoplasm, and moreover, they inhibit the translocation of transcription factors responsible for the expression of profibrotic genes.

Epigenetic regulators represent a very specific category of anti-fibrotic treatment. The main targets of epigenetic-based management of fibrosis are microRNAs (miRNAs). Anti-miRs – are miRNA oligonucleotides that are able to complementary bind to miRNAs involved in fibrosis and neutralize them when deposited inside the cell. miRNAs like let-7, miR-21, miR-29, miR-155 play an important role in fibrosis, particularly in TGF- β control. Let-7 and miR-29 are antifibrotic; in contrast, miR-21 and miR-155 are profibrotic, and their expression will rise during the fibrosis. On the other hand, the decreased expression of miR-29 in systemic sclerosis (SSc) fibroblasts leads to the increased levels of type I and III collagen. The reduction of miR-29 was noted in the fibrotic reaction in the lungs, heart, and kidneys. IL-4, TGF- β , and PDGF-B reduced the level of miR-29 in SSc fibroblasts as well as in the bleomycin-induced model of skin fibrosis (Maurer et al., 2010; Harmanci et al., 2017). According to another study, miR-21 was highly elevated in animal and human models of transplant kidney nephropathy. MiR-21^{-/-} mice experienced less interstitial fibrosis in response to kidney injury; this was pheno-copied in wild-type mice that were treated

with anti-miR-21 oligonucleotides. The peroxisome proliferator-activated receptors (Ppar α) and Mpv17l are two main metabolic pathways that are key targets for miR-21. Also, miR-21 down-regulated inhibitors of angiogenesis and migration, especially the RECK (the reversion-inducing cysteine-rich protein with Kazal motifs) and the atypical matrix metalloproteinase (MMP) inhibitor that led to the enhanced MMP activity in kidney injury (Chau et al., 2012). As a result of the administration of oligonucleotides that silenced miR-21, a reversal of the deleterious action of miR-21 in kidney injury was noted. Some studies demonstrated a significant effect of miR-21 on pulmonary and cardiac fibrosis (Thum et al., 2008).

In multi-component therapy, several approaches are combined, with numerous ingredients acting on numerous targets. In fibrosis, there are multiple pathological pathways and multi-component drugs that are able to modulate these pathways and create synergistic effects. In the **Table 3**, single and multi-component medications used nowadays in the treatment of fibrosis are summarized (Li et al., 2017).

Only nintedanib and pirfenidone have been approved by FDA for the treatment of fibrosis, particularly of IPF, and ruxolitinib has been approved by FDA for the treatment of myelofibrosis; other medications are still experimental, and some of them are undergoing clinical trials the results of which might help improve the understanding of the fibrosis pathway.

Nintedanib medication is a small molecule kinase inhibitor that reduces the proliferation and migration of lung fibroblasts. Nintedanib inhibits receptor tyrosine kinases (RTKs), for instance, FGFR1-3, VEGFR1-3, Fns-like tyrosine kinase-3 (FLT3), PDGFR α and β . Also, this drug inhibits kinase signaling pathways. Its main side effects are nausea, diarrhea, and liver dysfunction (Wind et al., 2019; Valenzuela et al., 2020). In clinical practice, a long-term use of nintedanib is still discussed. Research in this area will help improve patient outcomes (Valenzuela et al., 2020). Pirfenidone treatment mainly reduces fibroblast proliferation and causes the inhibition of collagen synthesis and down-regulation of profibrotic cytokines. As a result of inhibition, it causes the suppression of TGF- β 2 mRNA levels and TGF- β 2 protein and the suppressed expression of the TGF- β pro-protein convertase furin. Also, this drug decreases the MMP-11 protein levels. It should be noted that pirfenidone has some severe side effects such as photosensitivity, nausea, stomach pain and many others that may lead to medication intolerance and discontinuation (Hughes et al., 2016; Margaritopoulos et al., 2016; Moran-Mendoza et al., 2019). Ruxolitinib is widely used in myelofibrosis treatment. This drug is a kinase inhibitor that is selective for JAK1 and 2. The main role of these kinases is the regulation of growth factor signaling and cytokine release. The known side effects of this medicine are anemia, thrombocytopenia, increased liver enzymes, and diarrhea (Elli et al., 2019).

The Role of Cannabinoids and Cannabis in Inflammation and Fibrosis

Recently, the ECS has received a significant attention from mainstream medical professionals, being viewed as an important

TABLE 3 | Single- and multi-component medications targeting fibrosis factors.

| Group | Target or mechanism type | Mechanism of action | Drug name | Disease | Reference/trial identifier |
|---|-----------------------------|--------------------------------|--------------------------------------|---|---|
| Single-component medications targeting extracellular factors | | | | | |
| Growth factor | Extracellular | TGF- β , inhibitor | Pirfenidone | IPF | Margaritopoulos et al. (2016) |
| | TGF- β signaling | | | | |
| Cytokines | PDGF/VEGF | PDGFR, antagonist | Imatinib | SSc, nephrogenic systemic fibrosis, IPF | NCT00677092 NCT00613171 NCT00131274 |
| | | VEGFR/PDGFR, antagonist | Nintedanib | Scleroderma, IPF | NCT02597933 NCT01335464 |
| | TNF | TNF, inhibitor | Talidomide | IPF | NCT00162760 |
| | | TNF, inhibitor | Etanercept | IPF | NCT00063869 |
| | | TNF, inhibitor | Belimumab | SSc | NCT01670565 |
| | Interleukin | IL-1R1, antagonist | Anakinra | Cystic fibrosis | Iannitti et al. (2016) |
| IL-1 β R, antagonist | | Rilonacept | SSc | NCT01538719 | |
| Interferon | IFN- γ R, stimulant | Actimmune | IPF, cystic fibrosis, liver fibrosis | NCT00047658 NCT00043303 NCT00043316 | |
| MMP/TIMP | MMP/TIMP | MMP/TIMP, inhibitor | Marimastat | Liver fibrosis | de Meijer et al. (2010) |
| Other proteins and peptides | Endothelin | ET-1 receptor, antagonist | Macitentan | IPF | NCT00903331 |
| | | | Bosentan | IPF | NCT00070590 NCT00319696 NCT01395732 |
| | Angiotensin II | AT1 receptor, antagonist | Ambrisentan | IPF, SSc | NCT00879229 NCT01051960 |
| | | | Losartan | Cystic fibrosis, Liver fibrosis | NCT00298714 NCT03206788 |
| | GPCR | Prostacyclin receptor, agonist | Iloprost | SSc | NCT00109681 |
| | | | Treprostinil | IPF, SSc | NCT00703339 NCT00775463 |
| Single-component medications targeting intracellular factors | | | | | |
| Enzymes | mTOR | mTORC1/2, inhibitor | Rapamycin (Sirolimus) | Renal intestinal fibrosis | NCT01079143 |
| | JAK-STAT | JAK1/JAK2, inhibitor | Ruxolitinib | Myelofibrosis | NCT00952289 |
| | PI3K-Akt | Akt, inhibitor | Omipalisib | IPF | NCT01725139 |
| | MAPK | MAPK, inhibitor | MMI-0100 | IPF, cardiac fibrosis | Xu et al. (2014) |
| | NF- κ B | IKK, inhibitor | IMD-1041 | Cardiac fibrosis | Tanaka et al. (2012) |
| Nuclear receptors | PPAR | PPAR- γ , agonist | Rosiglitazone | Liver fibrosis | NCT00492700 |
| Other proteins | Intracellular | SMAD2/3, inhibitor | Pirfenidone | IPF, SSc | NCT00287729 NCT01933334 |
| | | | Pentoxifylline | Skin fibrosis | NCT00001437 |
| | TGF- β signaling | SMAD3, inhibitor | SiS-3 Glycyrrhizin | Renal fibrosis, liver fibrosis | NCT00686881 Meng et al. (2015) |
| Epigenetics | miRNA | miR-21, inhibitor | Anti-miR-21 | IPF, renal fibrosis | Liu et al. (2010) Chau et al. (2012) |
| Multi-component drugs | | | | | |
| | TGF- β /MMP-2c | | Fuzhenghuayu capsule (FZHY) | Liver fibrosis | NCT00854087 NCT02241616 |
| | TNF- α /TGF- β | | Danggui-Buxue-Tang (DBTG) | IPF | Lv et al. (2012) |

TGF- β , transforming growth factor- β ; PDGF, platelet-derived growth factor; PDGFR, platelet-derived growth factor receptor; VEGF, vascular endothelial growth factor; VEGFR, vascular endothelial growth factor receptor; TNF, tumor necrosis factor; IFN- γ R, interferon- γ receptor; MMP, matrix metalloproteinase; TIMP, tissue inhibitor of metalloproteinase; ET-1 receptor, endothelin-1 receptor; AT1 receptor, angiotensin II receptor type 1; GPCR, G protein-coupled receptor; mTOR, mechanistic target of rapamycin; mTORC1, mechanistic target of rapamycin complex 1; JAK-STAT, janus kinase/signal transducers and activators of transcription; PI3K-Akt, phosphoinositide 3-kinase/protein kinase B; MAPK, mitogen-activated protein kinase; NF- κ B, nuclear factor kappa-light γ -chain- enhancer of activated B cells; IKK, I-kappa B kinase; SMAD3, mothers against decapentaplegic homolog 3.

therapeutic target for many pathological conditions. Human physiology significantly depends on a proper function of this system. The ECS has been established as an important homeostatic regulator. It affects almost all functions of the body. It consists of endocannabinoids (2-AG, AEA), their metabolic enzymes and receptors, including cannabinoid receptors 1 (CB1), cannabinoid 2 (CB2), transient receptor potential channels of the vanilloid subtype 1 and 2 (TRPV1, TRPV2), G protein-coupled receptors 18, 55, 119 (GPR18, GPR55, GPR119) (Laezza et al., 2020). Cannabinoid receptors are highly expressed in cells involved in two subtypes of immunity, adaptive and innate. For example, CB1 and CB2 receptors are expressed in the natural killer cells, macrophages, T and B cells (Chiurchiù, 2016). In general, activation of the CB2 receptor leads to anti-inflammatory effects. Since the expression of CB1 receptors is lower in the immune cells than the expression of CB2 receptors, their function in the immune system still remains controversial (Turcotte et al., 2016). CB2^{-/-} mice exhibit abnormalities in the development of T and B cells (Ziring et al., 2006). Cannabinoids, mainly by modulating the expression of ECS receptors induce apoptosis of immune cells, and inhibit their proliferation; suppress pro-inflammatory cytokines production, and induce T-regulatory cells (Nagarkatti et al., 2009). The imbalance in the ECS can significantly impact the proper functioning of the whole organism, including fibrosis and inflammation processes. For example, the activation of the CB1 receptor leads to fibrogenesis, while the enhancement of the CB2 receptor inhibits fibrosis progression (Mallat et al., 2011). In animal models, it was demonstrated that the deletion of CB1 caused an improvement of liver fibrosis, whereas CB2 deletion resulted in an elevated amount of collagen accumulation and an increased inflammation (Patsenker and Stickel, 2016). Concerning inflammation, the use of CB2 receptor agonists was documented to inhibit the infiltration of inflammatory cells into liver tissue. In addition, CB2 receptor knockout mice had the more profound inflammation and damage to the liver than wild-type mice (Batkai et al., 2007).

Cannabis is widely known as a plant with psychoactive properties. It includes over 500 compounds such as different cannabinoids, terpenes, terpenoids, fatty acids, and flavonoids. Cannabinoids (known as phytocannabinoids in contrast to endocannabinoids) act via the ECS. The most abundant are cannabidiol (CBD) and Δ^9 -tetrahydrocannabinol (Δ^9 -THC); they are the most studied cannabinoids with numerous documented medicinal properties (Zurier and Burstein, 2016; Lafaye et al., 2017). The uniqueness of the effect of cannabis extracts is in entourage effect. Often, but not always, cannabis extracts have more profound effects on various disease and conditions than isolated cannabinoids (Kovalchuk and Kovalchuk, 2020). This is due to modifying effects of minor cannabinoids, terpenes and other molecules that frequently act as amplifiers, acting on the same receptors. Looking at the enormous varieties of cannabis cultivars nowadays, it is clear that research in this field should continue to discover new possibilities of fibrosis treatment (Russo, 2019).

Cannabinoids as Anti-inflammatory Agents

According to previous reports, some of the cannabinoids can be used as anti-inflammatory agents (Zurier and Burstein, 2016; Wang et al., 2020). Currently in medical practice, these substances have little documented negative effect on patients in comparison with other drugs. Cannabinoids have other mechanisms of action on inflammation in comparison with nonsteroidal anti-inflammatory drugs (NSAIDs). NSAIDs inhibit the activity of cyclooxygenase enzymes, prostaglandins (Zurier and Burstein, 2016). Recently, it has been discovered that cannabinoid receptor signaling regulates the proliferation and function of fibroblasts which are crucial cells in scar formation (Nagarkatti et al., 2009). By suppressing inflammation, they may stop the progression of repair by scarring. It has been shown that cannabinoids and cannabis extracts suppress the pro-inflammatory cytokines IL-2, IL-1 β , TNF- α , IFN- γ , IL-12, IL-8, IL-6 in different cell lines and animal models. Due to this, the inflammatory process will be prominently inhibited (Nagarkatti et al., 2009).

One of the anti-inflammatory mechanisms of cannabinoids is through the regulation of mitochondrial homeostasis. CBD has been shown to alleviate cerebral ischemia in rats by reducing brain oedema, blood-brain barrier permeability, infarction size, and neurological deficit. This effect was due to the increased expression of Na⁺/Ca²⁺ exchanger proteins (Khaksar and Bigdeli, 2017). When blood flow is restored in the ischemic area, it causes inflammation and oxidative-stress-related injury in the affected area. CBD has demonstrated a neuroprotective effect in oxygen-glucose-deprivation/reperfusion *in vitro* model by reducing the oxidative stress, improving mitochondrial bioenergetics and modulating the glucose metabolism (Sun et al., 2017). In contrast, THC treatment of the trophoblast cell line, HTR8/SVneo, showed a reduction in mitochondrial respiratory function and membrane potential. This data suggested that THC can cause dysfunction of mitochondria (Walker et al., 2021). When THC effect was evaluated on mitochondria, extracted from the rat brain, similar results were obtained: it enhanced oxidative stress and induced mitochondrial dysfunction in the brain (Wolff et al., 2015).

Cannabis extracts were even proposed to be used for prevention and treatment of COVID-19. Significant inhibitory effects on the key receptor protein Ace2 required for SARS-Cov2 virus entry in the gateway entry tissues was found in response to several cannabis extracts (Wang et al., 2020). Similarly, several other extracts were found to be potent inhibitors of major pro-inflammatory molecules responsible for severe COVID-19 progression (Wang et al., 2020).

It was also shown that cannabis users living with HIV have lower neuroinflammation. This was confirmed by demonstrating that marijuana users had lower levels of CD16⁺ monocytes and inducible protein 10 (IP-10) compared to HIV-infected patients non-cannabis users (Rizzo et al., 2018).

Cannabinoids as Anti-fibrotic Agents

A lot of research has already been done, and currently many studies are undergoing on the use of endo-, synthetic, and phytocannabinoids in the fibrosis field. In one *in vivo* study

where a mouse model of type I cardiomyopathy was used, it was demonstrated that CBD treatment diminished the diabetes-associated cardiac fibrosis. A significant decrease of collagen deposition and the expression of profibrotic genes like MMP-2, MMP-9, TGF- β , connective tissue growth factor, fibronectin and collagen-1 were noted (Montecucco and Di Marzo, 2012).

Liver fibrosis is a usual complication of many long-lasting liver illnesses such as viral hepatitis B and C, non-alcoholic steatohepatitis, drug-induced liver injury, alcohol abuse, and autoimmune conditions. In long-lasting liver damage, the activated hepatic stellate cells (HSCs) and myofibroblasts are the main contributors to the development of liver cirrhosis and hepatocellular cancer (Fu et al., 2011). An *in vitro* study performed on HSCs documented that CBD induced the programmed cell death of these cells (Lim et al., 2011). This effect was independent of cannabinoid receptors and was the result of endoplasmic reticulum stress induction. In addition, CBD enhanced the pro-apoptotic pathway IRE1/ASK1/c-Jun N-terminal kinase, which resulted in HSCs death. This CBD-induced programmed cell death of activated HSCs was confirmed *in vitro* in human, mouse and rat cell lines, but not in the quiescent cell lines. The well-known fact that the activated HSCs play a crucial role in the development and continuation of liver fibrosis supports the fact that cannabis extracts might be turned into promising antifibrotic drugs as they lead to the selective apoptosis of activated HSCs. The results of this study are very encouraging for further investigation of CBD *in vivo* (Lim et al., 2011). In addition, a meta-analysis of nine studies performed on 5,976,026 patients concluded that marijuana did not elevate the prevalence or progression of liver fibrosis in patients with hepatitis C or hepatitis C HIV co-infection (Hosein Mohimani et al., 2017). Also, it was noted that marijuana users had a reduced prevalence of non-alcoholic fatty liver disease (NAFLD). Furthermore, these patients consumed more sodas and alcohol, therefore the healthy lifestyle was not a cause of the reduced prevalence of NAFLD. This effect might be induced by reducing fat depositions via omega-3 fatty acids and the impact of CBD on insulin sensitivity (Hosein Mohimani et al., 2017).

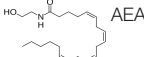
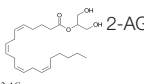
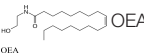
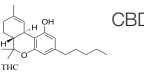
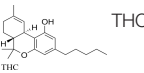
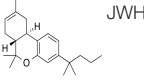
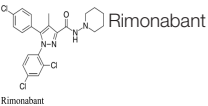
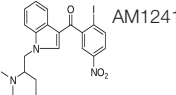
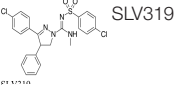
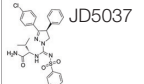
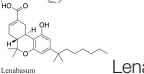
Concerning the effect of THC, it has been shown that it also inhibits the proliferation of liver myofibroblasts and stellate cells via CB2 receptors and leads to their programmed cell death. Due to this, THC may also possess antifibrotic properties (Tam et al., 2011).

The endocannabinoid AEA also demonstrated the anti-fibrogenic features by suppressing the proliferation of HSC and induction of necrosis. The elevated AEA levels were documented in cirrhotic patients, which might be a response to fibrosis. This endogenous cannabinoid can trigger the topical inflammatory response and systemic dilatation of vessels, therefore the opportunity for fibrosis treatment was restricted (Parfieniuk and Flisiak, 2008). Another endocannabinoid, 2-AG, was considered as a fibrogenic agent. When used in higher doses *in vitro* on HSC, it activated fibrosis via the membrane cholesterol-dependent mechanism (Tam et al., 2011). Another endogenous cannabinoid, oleoylethanolamide (OEA), was used in a mouse model of hepatic fibrosis and showed the inhibition of collagen deposition and suppression of collagen type I and III gene expression, α -SMA,

MMP2, MMP9, and TIMP1. These effects were mediated through the PPAR α mechanisms (McVicker and Bennett, 2017).

Synthetic cannabinoids were also shown to be beneficial for fibrosis treatment. An *in vitro* study performed on pulmonary fibroblasts demonstrated that JWH133, a CB2 receptor agonist, suppressed the collagen type I and α -SMA and inhibited the proliferation and migration of fibroblasts. These effects were reversed by the use of a CB2 receptor antagonist, SR144528. *In vivo* studies on bleomycin-induced lung fibrosis in mice, showed that JWH133 decreased the lung density, and the fibrotic score and histological results illustrated the suppression of the collagen accumulation and inflammatory response. In both models, this particular synthetic cannabinoid inhibited the crucial pathway of fibrogenesis, TGF- β 1/Smad2 (Fu et al., 2017). WIN-55,212, a nonselective CB1 and CB2 receptor agonist as well as JWH133 were assessed on the mouse model of systemic sclerosis. They prevented the development of dermal and pulmonary fibrosis and inhibited the proliferation of fibroblasts. CB2^{-/-} mice developed a significantly enhanced skin and lung fibrosis compared with CB2^{+/+} mice, indicating significant influence of the CB2 receptor on fibrosis development (Servettaz et al., 2010). Rimonabant, a CB1 receptor antagonist, was assessed on rat models of liver cirrhosis induced by carbon tetrachloride. Fibrosis was prominently suppressed by the use of this synthetic cannabinoid in rats compared with rats in the vehicle group. Rimonabant downregulated the fibrogenic (TIMP-1, TGF- β , MMP13, MMP2, MMP9, MMP1, MMP8) and inflammatory mediator (TNF- α , MCP-1) genes. In addition, Rimonabant treatment induced a prominent increase in the expression of the CB2 receptor (Giannone et al., 2012). Another study demonstrated that chronic stimulation of CB2 receptor with selective CB2 receptor agonist, JWH-133, leads to regression of fibrosis in cirrhotic rats. This selective agonist suppressed the inflammatory infiltrate, decreased fibrosis, lowered the number of activated hepatic stellate cells, and improved arterial pressure in comparison to the vehicle group. In addition, JWH-133 reduced levels of α -SMA and collagen and elevated levels of MMP-2 in the liver tissue of rats with cirrhosis in comparison with untreated rats with cirrhosis. This data provided promising results for the possibility to use selective CB2 receptor agonists as a treatment modality of hepatic fibrosis in humans (Muñoz-Luque et al., 2008). Another study tested the effect of a selective CB2 receptor agonist, AM1241, on myocardial fibrosis post-myocardial infarction in mice. The echocardiography results demonstrated that AM1241 significantly enhanced cardiac function; downregulated expression of collagen I, collagen III, TIMP-1, and plasminogen activator inhibitor (PAI)-1. When primary cardiac fibroblasts were exposed to hypoxia and serum deprivation to simulate ischemia, AM1241 was able to reduce α -SMA, collagen I and collagen III; this effect was partially abrogated by the Nrf2 siRNA transfection. Moreover, the CB2 receptor agonist, AM1241, activated and enhanced the translocation of Nrf2 to the nucleus and inhibited the TGF- β 1/SMAD3 pathway. These data suggest that activation of the CB2 receptor might be one of the key targets to combat heart fibrosis after myocardial infarction (Li et al., 2016). The chronic peripheral pharmaceutical

TABLE 4 | Anti-fibrotic effect of cannabinoids.

| Compound | The mechanism of action | References |
|---|---|---|
| Endocannabinoids | | |
|  <p>AEA</p> | Suppressing the proliferation of HSCs and induces their necrosis | Parfieniuk and Flisiak (2008) |
|  <p>2-AG</p> | Generally considered as a fibrogenic agent, however, it is able to suppress fibrosis via the membrane cholesterol-dependent mechanism. | Tam et al. (2011) |
|  <p>OEA</p> | The inhibition of collagen deposition and suppression of collagen type I and III gene expression, α -SMA, MMP2, MMP9, and TIMP1. These effects were mediated through the PPAR α mechanisms. | McVicker and Bennett (2017) |
| Phytocannabinoids | | |
|  <p>CBD</p> | The apoptosis induction of HSCs as result of the induction of endoplasmic reticulum stress and the enhancement of the pro-apoptotic pathway IRE1/ASK1/c-Jun N-terminal kinase. | Lim et al. (2011) |
|  <p>THC</p> | The inhibition of miofibroblast proliferation and stellate cells, the induction of their apoptosis via CB2 receptors. | Tam et al. (2011) |
| Synthetic cannabinoids | | |
|  <p>JWH-133</p> | The suppression of collagen type I and α -SMA, inhibition of fibroblast proliferation and migration. The down-regulation of the TGF- β 1/Smad2 pathway. | Fu et al. (2017) Muñoz-Luque et al. (2008) |
|  <p>Rimonabant</p> | The suppression of expression of fibrogenic mediators (TIMP-1, TGF- β , MMP13, MMP2, MMP9, MMP1, MMP8, TNF- α , MCP-1) | Giannone et al. (2012) |
|  <p>AM1241</p> | The downregulation of expression of collagen I, collagen III, TIMP-1, and plasminogen activator inhibitor. The inhibition of the TGF- β 1/SMA α 3 pathway. | Li et al. (2016) |
|  <p>SLV319</p> | The suppression of glucose transporter 2; reduction in glucose reabsorption. | Hinden et al. (2018) |
|  <p>JD5037</p> | The suppression of glucose transporter 2; reduction in glucose reabsorption. | Hinden et al. (2018) |
|  <p>Lenabasum</p> | Stimulating PPAR- γ signaling | Gonzalez et al. (2012) |

blockage of CB1 receptor (by SLV319 or JD5037 selective CB1 receptor antagonists) or genetic inactivation of CB1 receptors in the renal proximal tubule cells reduced kidney inflammation, suppressed tubulointerstitial fibrosis, and diminished diabetic-induced changes in the kidneys in mice. Also, the downregulation of the CB1 receptor suppressed glucose transporter 2, which resulted in reduced glucose reabsorption. These data supported the fact that peripheral CB1 receptor antagonists might be useful in treating patients with diabetic nephropathy (Hinden et al., 2018). A synthetic analog of THC, ajulemic acid (lenabasum), being a CB2 agonist, significantly prevented the development

of bleomycin-induced skin fibrosis in mice and suppressed its progression. In addition, it inhibited collagen synthesis by skin fibroblasts obtained from patients with scleroderma. These effects were achieved by stimulating PPAR- γ signaling (Gonzalez et al., 2012). Lenabasum has been shown to have an anti-inflammatory capacity by directly affecting both arachidonic acid pathways (Burstein, 2021). Lenabasum was the only synthetic cannabinoid studied in human fibrotic diseases. A Phase II, randomized, placebo-controlled trial in adults suffering from systemic sclerosis showed promising results (NCT03398837); a high improvement rate on the immunosuppressant therapy background, and high

improvement on mycophenolate that has an anti-fibrotic activity and prevents pulmonary deterioration in pulmonary fibrosis was observed. Unfortunately, the primary endpoint was not met during this trial (Spiera et al., 2021). **Table 3** summarizes type of cannabinoids and their mechanism of action (**Table 4**).

Into Potential Mechanisms of Anti-fibrotic Effects of Cannabinoids – Role of MicroRNAs

The mechanisms of anti-fibrotic effects of cannabinoids are likely very diverse. Cannabinoids may target all steps of normal and abnormal wound healing, as shown on **Figure 5**.

Recent reports demonstrate the role of miRNAs in regulation of cannabinoid receptors and anti-fibrotic effect of cannabinoids. miRNAs like miR-30b-5p, miR-21, miR-155, miR-146a, miR-141, and miR-222 appear to be pro-inflammatory, while miRNAs like miR-187, miR-149, miR-145, and miR-99b are anti-inflammatory.

miR-30b-5p was found to be involved in CB1-mediated NLRP3 inflammasome activation. The study performed on mice with liver injury induced by carbon tetrachloride (CCl₄) or methionine-choline-deficient, and high fat (MCDHF) diet showed that there is a relationship between CB1 receptor and Nod-like receptor family pyrin domain containing 3 (NLRP3) inflammasome in liver inflammation. The expression of the CB1 receptor was increased in hepatic tissue of mice with liver injury. CB1 receptor agonist, arachidonyl-2'-chloroethylamide, enhanced expression of NLRP3 inflammasome and its activation in macrophages. AM281, a CB1 receptor antagonist, inhibited NLRP3 expression and activation of the inflammasome and reduced hepatic inflammation in CCl₄- and MCDHF-treated mice. When miR-30b-5p agomir was administered, it targeted NLRP3 and mitigated liver inflammation. These results suggested that CB1/miR-30b-5p axis is able to modulate the activation of NLRP3 inflammasome and expression of NLRP3 in macrophages in liver inflammatory disease (Yang et al., 2020).

Cannabinoids can alter the expression of miR-155, a master regulator of inflammation (Mahesh and Biswas, 2019). Administration of selective CB2 receptor agonist AM1241 significantly reduced expression of TLR4, α -SMA, TGF- β 1, miR-155, p65 NFkB, TNF- α , IL-6, IL-1 β and vimentin genes caused by thioacetamide. Moreover, it significantly upregulated E-cadherin, glutathione content, and superoxide dismutase. This study showed that AM1241 reduces fibrosis, by activating the CB2 receptor, and inhibiting TLR4/miR-155/NFkB p65 pathway (Ali et al., 2021).

Chronic administration of THC significantly increased the expression of anti-inflammatory miRNAs including miR-187, miR-149, miR-145, miR-99b, miR-24, and miR-10a dysregulated by acute infection with Simian Immunodeficiency Virus (SIV). THC administration also reduced viral load, gastrointestinal inflammation, and the overall disease progression (Chandra et al., 2015). Another study, performed on rhesus macaques with chronic SIV infection with an intention to cause fibrosis, showed that THC prevented fibrosis and upregulated ten

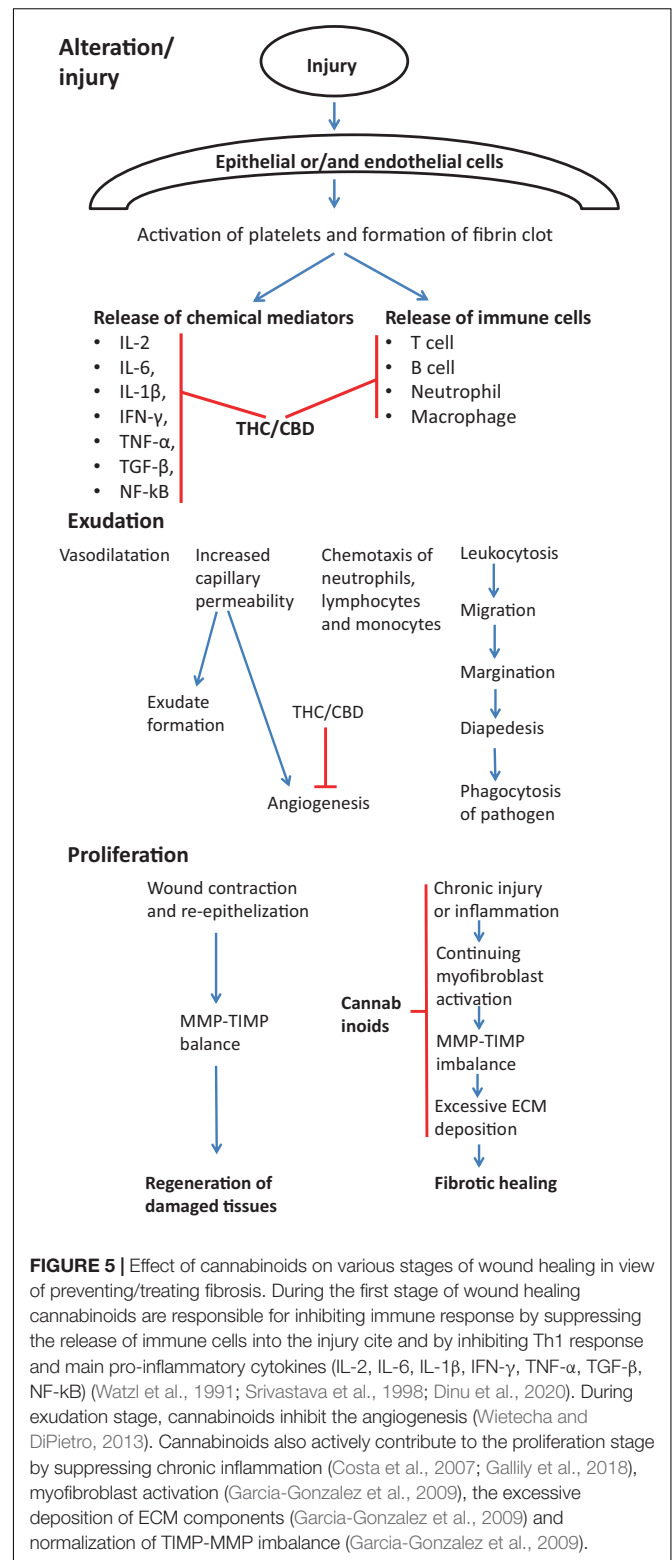


FIGURE 5 | Effect of cannabinoids on various stages of wound healing in view of preventing/treating fibrosis. During the first stage of wound healing cannabinoids are responsible for inhibiting immune response by suppressing the release of immune cells into the injury site and by inhibiting Th1 response and main pro-inflammatory cytokines (IL-2, IL-6, IL-1 β , IFN- γ , TNF- α , TGF- β , NF-kB) (Watzl et al., 1991; Srivastava et al., 1998; Dinu et al., 2020). During exudation stage, cannabinoids inhibit the angiogenesis (Wietecha and DiPietro, 2013). Cannabinoids also actively contribute to the proliferation stage by suppressing chronic inflammation (Costa et al., 2007; Gallily et al., 2018), myofibroblast activation (Garcia-Gonzalez et al., 2009), the excessive deposition of ECM components (Garcia-Gonzalez et al., 2009) and normalization of TIMP-MMP imbalance (Garcia-Gonzalez et al., 2009).

miRNAs, including pro-inflammatory miRNAs miR-21, miR-141 and miR-222 and miR-204, that directly targets matrix metalloproteinase 8 (MMP-8), an enzyme that degrades collagen (Kumar et al., 2019). In addition, THC inhibited proliferation

TABLE 5 | A comparison of target molecules in treatment of fibrosis using modern therapy vs. cannabis treatment.

| A single-component medication: | Cannabis |
|---|---|
| The mechanism of action of a single-component medication vs. cannabis | |
| <ul style="list-style-type: none"> • TGF-β inhibitor (Pirfenidone) • PDGFR antagonist (Imatinib) • TNF inhibitor (Talidomide, Etanercept, Belimumab) • IL-1 antagonist (Anakinra, Rilonacept) • IFN-γ stimulant (Actimmune) • MMP/TIMP inhibitor (Marimastat) • mTOR inhibitor (Rapamycin) • JAK-STAT inhibitor (Ruxolitinib) • PI3K-Akt inhibitor (Ompalisib) • MAPK inhibitor (MMI-0100) • NF-κB inhibitor (IMD-1041) • miR-21 inhibitor (Anti-miR-21) | <ul style="list-style-type: none"> • TGF-β inhibitor • TNF inhibitor • MMP/TIMP inhibitor |
| The mechanism of action of a multi-component medication vs. cannabis | |
| A multi-component medication: | Cannabis |
| <ul style="list-style-type: none"> • TGF-β/MMP-2c inhibitor (Fuzhenghuayu) • TNF-α/TGF-β inhibitor (Danggui-Buxue-Tang) | <ul style="list-style-type: none"> • TGF-β1/Smad2 inhibitor |

and activation of T cells, suppressed PD-1 expression, and elevated the percentage of anti-inflammatory macrophages in intestinal tissue. These results suggest that THC is an important modulator of miRNA expression and can suppress intestinal inflammation and may prevent lymph node fibrosis (Kumar et al., 2019).

In another study, lipopolysaccharide (LPS) was used to stimulate the BV-2 microglial cells, and CBD had a much more significant effect than THC on the expression of cluster miRNAs (Juknat et al., 2019). While LPS increased the expression of many pro-inflammatory miRNAs, including miR-155, miR-146a, and miR-21, associated with Toll-like receptor (TLR) and NF- κ B signaling, the CBD suppressed the expression of miR-155 and miR-146a. Moreover, it was demonstrated that LPS modulates the Notch signaling pathway by increasing the mRNA expression of Notch ligand Dll1. CBD and THC were able to reduce the expression of this ligand. Since the CBD+LPS group increased the expression of miR-34a and downregulated the expression of its target gene Dll1, it was suggested that miR-34a could be involved in the Notch signaling pathway modulation and, as a result, in reducing inflammation (Juknat et al., 2019).

Cannabidiol was demonstrated to trigger apoptosis in human neuroblastoma cell lines by downregulation of let-7a expression and, as a consequence, upregulation of caspase-3 and several growth arrest genes. In addition, CBD upregulated the expression of has-mir-1972 and caused decreased expression of BCL2L1 and SIRT2 genes (Alharris et al., 2019).

Yet another study showed that THC treatment can suppress the activation of Th1/Th17 lineage commitment via regulation of miRNA expression (Sido et al., 2016). When C57BL/6 mice with delayed-type hypersensitivity were treated with THC, oedema and immune cells infiltration subsided at the place of antigen rechallenge. Delayed-type hypersensitivity caused an increased expression of miR-21 and inhibition of miR-29b; miR-21 elevates the Th17 differentiation via inhibiting SMAD7, while miR-29b is

IFN- γ inhibitor. THC was able to reverse this miRNA imbalance. Moreover, when primary cells from these mice were transfected with miR-21 inhibitor or miR-29b mimic, the expression of SMAD7 increased, and the expression of IFN- γ decreased (Sido et al., 2016).

In another study, when C3H/HeJ mice were administered staphylococcal enterotoxin B (SEB), it caused an acute mortality; in contrast, mice that received THC had a 100% survival rate and did not show any respiratory distress signs, hunched posture, or fur ruffling. In addition, the THC administration significantly reduced the vascular leak in comparison to the staphylococcal enterotoxin B exposure group. The staphylococcal infection caused the induction of miRNA-17-92 cluster, including miR-18a, which targeted the inhibitor of PI3K/Akt pathway, leading to suppression of T regulatory cells (Rao et al., 2015).

Another study showed that THC administered in post-staphylococcal enterotoxin B exposure protected mice from acute respiratory distress syndrome and toxicity. THC significantly downregulated let7a-5p and miR-34-5p, which target SOCS1, FoxP3, NOS1, and CSF1R as well as inhibited the pro-inflammatory cytokines, such as TNF- α and IFN- γ . This study suggested that THC can alter miRNA expression in the lungs, suppress the cytokine storm, and as a consequence, might cause mitigation of SEB-mediated pulmonary injury (Mohammed et al., 2020).

A combination of THC plus CBD suppressed neuroinflammation in murine experimental autoimmune encephalomyelitis (EAE) model and suppressed Th1 and Th17 cells via modulating miRNA expression. In addition, this combinational treatment reduced levels of CD4+ T cells and pro-inflammatory molecules such as TNF- α , IL-1 β , IL-6, IFN- γ , IL-17, and TBX21) while elevating anti-inflammatory molecules (IL-4, IL-10, TGF- β , STAT5b, and FoxP3). Microarray analysis of miRNA of CD4+ T cells showed that THC+CBD administration significantly inhibited miR-122-5p, miR-27b-5p, miR-155-5p,

miR-150-5p, miR-146a-5p, miR-31-5p, miR-21a-5p and upregulated miR-7116 and miR-706-5p (Al-Ghezi et al., 2019).

miR-29a appears to be one of the regulators of response to cannabinoids. miR-29a diminishes diabetic nephropathy via modulation of CB1 signaling. Upregulated expression of the CB1 receptor, TNF- α , IL-6, IL-1 β , collagen IV, and downregulated expression of PPAR- γ was noted in streptozotocin-induced diabetic mice. In contrast, overexpression of miR-29a in mice negatively regulated CB1 receptor, blocking upregulation of pro-inflammatory and fibrogenic compounds, and substantially decreasing kidney hypertrophy. The overexpression of miR-29a also renewed PPAR- γ signaling. These data demonstrated that interaction among miR-29a, CB1 receptor, and PPAR- γ signaling plays a significant role in protecting renal tissue from developing fibrosis (Tung et al., 2019).

Cannabis and Cannabinoids May Replace the Known Therapies for Fibrosis

Due to the lack of effective therapies for fibrosis, new more effective and modern therapies with less side effects need to be developed. The currently used drugs suppress the fibrogenetic pathways and reduce the progression of fibrosis. Similarly, cannabis extracts can also affect key profibrotic factors and pathways. Cannabinoid signaling regulates the proliferation and function of fibroblasts which are crucial cells in scar formation. The active suppression of fibroblast proliferation leads to the inhibition of collagen formation and deposition. As previously explained, cannabinoids can actively suppress inflammation by downregulating the pro-inflammatory cytokines such as IL-2, IL-1 β , TNF- α , IFN- γ , IL-12, IL-8, IL-6, IL-15 (Wang et al., 2020). Due to this effect of cannabis, the fibrosis progression may stop. In comparison with drugs currently applied for treating pulmonary fibrosis, cannabinoids can also suppress the MMP/TIMP, PPAR and other pathways involved in fibrogenesis (Table 5). We can conclude that cannabis affects the same pathways as other drugs currently used medicine in fibrosis treatment, but it has a little- documented negative effects on patients as compared to other drugs used.

CONCLUSION

Fibrosis is a pathological process that may affect many organs. Significant improvement in understanding the tissue fibrosis

REFERENCES

- Aldair, T., and Montani, J. (2010). "Chapter 1. Overview of Angiogenesis," in *Angiogenesis*, eds N. Granger and J. Granger (San Rafael: Morgan & Claypool Life Sciences), 1–10.
- Al-Ghezi, Z. Z., Miranda, K., Nagarkatti, M., and Nagarkatti, P. S. (2019). Combination of cannabinoids, Δ^9 -tetrahydrocannabinol and cannabidiol, ameliorates experimental multiple sclerosis by suppressing neuroinflammation through regulation of miRNA-mediated signaling pathways. *Front. Immunol.* 10:1921. doi: 10.3389/fimmu.2019.01921
- Alhaji, M., Bansal, P., and Goyal, A. (2020). *Physiology, Granulation Tissue*. Florida: StatPearls, 4–7.
- Alharris, E., Singh, N. P., Nagarkatti, P. S., and Nagarkatti, M. (2019). Role of miRNA in the regulation of cannabidiol-mediated apoptosis in neuroblastoma cells. *Oncotarget* 10, 45–59. doi: 10.18632/oncotarget.26534
- Ali, A. M., El-Tawil, O. S., Al-Mokaddem, A. K., and Abd El-Rahman, S. S. (2021). Promoted inhibition of TLR4/miR-155/ NF κ B p65 signaling by cannabinoid receptor 2 agonist (AM1241), aborts inflammation and progress of hepatic fibrosis induced by thioacetamide. *Chem. Biol. Interact.* 336, 109398. doi: 10.1016/j.cbi.2021.109398
- Allanore, Y., Simms, R., Distler, O., Trojanowska, M., Pope, J., and Denton, C. (2015). Systemic sclerosis. *Nat. Rev. Dis. Prim.* 1:15002. doi: 10.1038/nrdp.2015.2

pathways may give us a chance in the future to discover an effective antifibrotic treatment. Many studies have been performed to understand the molecular mechanisms, the cellular basis, and the most prominent characteristics of fibrosis in human organs. Molecules like TNF α play a key role in the establishment of inflammation and pathogenesis of fibrosis. At the same time, TNF α may be used a therapeutic agent that can resolve the established pulmonary fibrosis (Redente et al., 2014), further confirming that we do not have a clear picture of mechanisms and pathways of fibrosis.

In most tissues and organs, the fibrosis mechanisms are similar, but the regeneration and regression processes are different across organs and tissues. Mainly this diversity is due to the difference in the regenerative capacity of each tissue or organ (Friedman, 2015).

Based on reports presented in this review, we propose that single cannabinoids and components of cannabis extracts can positively interact with the key profibrotic factors and pathways. In comparison with modern antifibrotic medications, cannabinoids have fewer negative effects on patient's health.

We conclude that modulation of ECS should be a modern approach for the treatment of different fibrotic conditions. This aspect of treatment has not been sufficiently studied. More detailed research should be done to find a patient-oriented treatment and improve patients' quality of life. It would be very encouraging to find the curative option for this devastating condition that will help millions of patients worldwide.

AUTHOR CONTRIBUTIONS

NP, OK, and IK contributed to the conceptualization and design. NP and MZ contribute to the draft preparation. OK and IK contributed to the analysis, editing, and supervision. All authors were involved in a review preparation and editing.

ACKNOWLEDGMENTS

The authors acknowledge the financial support of NSERC and MITACS. The content of the manuscript has been included in NP's Master's thesis.

- Apte, M., Pirola, R., and Wilson, J. (2011). The fibrosis of chronic pancreatitis: new insights into the role of pancreatic stellate cells. *Antioxid. Redox Signal.* 15, 2711–2722. doi: 10.1089/ars.2011.4079
- Barratt, S., Creamer, A., Hayton, C., and Chaudhuri, N. (2018). Idiopathic Pulmonary Fibrosis (IPF): an Overview. *J. Clin. Med.* 7:201. doi: 10.3390/jcm7080201
- Batkai, S., Osei-Hyiaman, D., Pan, H., El-Assal, O., Rajesh, M., and Mukhopadhyay, P. (2007). “Cannabinoid-2 receptor mediates protection against hepatic ischemia/reperfusion injury. *FASEB J.* 21, 1788–1800. doi: 10.1096/fj.06-7451com
- Baum, J., and Duffy, H. S. (2011). CityPaws Animal Hospital 1823. *J. Cardiovasc. Pharmacol.* 57, 376–379. doi: 10.1097/FJC.0b013e3182116e39
- Bochaton-Piallat, M. L., Gabbiani, G., and Hinz, B. (2016). The myofibroblast in wound healing and fibrosis: answered and unanswered questions. *F1000Res.* 5:F1000. doi: 10.12688/f1000research.8190.1
- Burstein, S. (2021). Molecular Mechanisms for the Inflammation-Resolving Actions of Lenabasum. *Mol. Pharmacol.* 99, 125–132. doi: 10.1124/molpharm.120.00083
- Cañedo-Dorantes, L., and Cañedo-Ayala, M. (2019). Skin acute wound healing: a comprehensive review. *Int. J. Inflamm.* 2019:15. doi: 10.1155/2019/3706315
- Chandra, L. C., Kumar, V., and Torben, W. (2015). Chronic Administration of Δ 9 -Tetrahydrocannabinol Induces Intestinal Anti-Inflammatory MicroRNA Expression during Acute Simian Immunodeficiency Virus Infection of Rhesus Macaques. *J. Virol.* 89, 1168–1181. doi: 10.1128/JVI.01754-14
- Chau, B. N., Xin, C., Hartner, J., Ren, S., Castano, A. P., Linn, G., et al. (2012). MicroRNA 21 promotes fibrosis of the kidney by silencing metabolic pathways. *Sci. Transl. Med.* 4, 121–139. doi: 10.1126/scitranslmed.3003205
- Chiurchiù, V. (2016). Endocannabinoids and Immunity. *Cannabis Cannabinoid Res.* 1, 59–66. doi: 10.1089/can.2016.0002
- Costa, B., Trovato, A. E., Comelli, F., Giagnoni, G., and Colleoni, M. (2007). The non-psychoactive cannabis constituent cannabidiol is an orally effective therapeutic agent in rat chronic inflammatory and neuropathic pain. *Eur. J. Pharmacol.* 556, 75–83. doi: 10.1016/j.ejphar.2006.11.006
- de Meijer, V. E., Sverdlow, D. Y., Popov, Y., Le, H. D., Meisel, J. A., and Nose, V. (2010). Broad-spectrum matrix metalloproteinase inhibition curbs inflammation and liver injury but aggravates experimental liver fibrosis in mice. *PLoS One* 5:e11256. doi: 10.1371/journal.pone.0011256
- de Oliveira, R. C., and Wilson, S. E. (2020). Fibrocytes, wound healing, and corneal fibrosis. *Invest. Ophthalmol. Vis. Sci.* 61:28. doi: 10.1167/iovs.61.2.28
- Dinu, A. R., Florin Rogobete, A., Bratu, T., Popovici, S. E., Bedreag, O. H., and Papurica, M. (2020). “Cannabis Sativa Revisited-Crosstalk between microRNA Expression, Inflammation, Oxidative Stress, and Endocannabinoid Response System in Critically Ill Patients with Sepsis. *Cells* 9, 1–23. doi: 10.3390/cells9020307
- Elli, E. M., Baratè, C., Mendicino, F., Palandri, F., and Palumbo, G. A. (2019). Mechanisms Underlying the Anti-inflammatory and Immunosuppressive Activity of Ruxolitinib. *Front. Oncol.* 9:1186. doi: 10.3389/fonc.2019.01186
- Farghaly, S., and El-Abdin, A. Z. (2015). Pulmonary fibrosis as a risk factor for thromboembolic disease. *Egypt. J. Bronchol.* 9, 160–164. doi: 10.4103/1687-8426.158056
- Frangogiannis, N. G. (2020). Transforming growth factor- β in tissue fibrosis. *J. Exp. Med.* 217:e20190103. doi: 10.1084/jem.20190103
- Friedlander, M. (2007). Fibrosis and diseases of the eye. *J. Clin. Invest.* 117, 576–586. doi: 10.1172/JCI31030
- Friedman, S. L. (2015). *Clarity and Challenges in Tissue Fibrosis. in Innovative Medicine.* Japan: Springer, 187–194. doi: 10.1007/978-4-431-55651-0_16
- Fu, Q., Zheng, Y., Dong, X., Wang, L., and Jiang, C. G. (2017). Activation of cannabinoid receptor type 2 by JWH133 alleviates bleomycin-induced pulmonary fibrosis in mice. *Oncotarget* 8, 103486–103498. doi: 10.18632/oncotarget.21975
- Fu, R., Wu, J., Ding, J., Sheng, J., Hong, L., and Sun, Q. (2011). “Targeting transforming growth factor β RII expression inhibits the activation of hepatic stellate cells and reduces collagen synthesis. *Exp. Biol. Med.* 236, 291–297. doi: 10.1258/ebm.2010.010231
- Fujimoto, H., Kobayashi, T., and Azuma, A. (2015). Idiopathic Pulmonary Fibrosis Treatment – OFEV[®](nintedanib) Capsules. *Clin. Med. Insights Circ. Respir. Pulm. Med.* 9, 179–185. doi: 10.4137/CCRPM.S23321
- Gallily, R., Yekhtin, Z., and Hanuš, L. O. (2018). The Anti-Inflammatory Properties of Terpenoids from Cannabis. *Cannabis Cannabinoid Res.* 3, 282–290. doi: 10.1089/can.2018.0014
- Galliot, B., Crescenzi, M., Jacinto, A., and Tajbakhsh, S. (2017). Trends in tissue repair and regeneration. *Development* 144, 357–364. doi: 10.1242/dev.144279
- Garcia-Gonzalez, E., Selvi, E., Balistreri, E., Lorenzini, S., and Maggio, R. (2009). Maria-Rita Natale “Cannabinoids inhibit fibrogenesis in diffuse systemic sclerosis fibroblasts. *Rheumatology* 48, 1050–1056. doi: 10.1093/rheumatology/kep189
- Gauglitz, G. G., Korting, H. C., Pavicic, T., Ruzicka, T., and Jeschke, M. G. (2011). Hypertrophic scarring and keloids: pathomechanisms and current and emerging treatment strategies. *Mol. Med.* 17, 113–125. doi: 10.2119/molmed.2009.00153
- Ghahary, A., Tredget, E. E., Shen, Q., Kilani, R. T., Scott, P. G., and Houle, Y. (2000). Mannose-6-phosphate/IGF-II receptors mediate the effects of IGF-1-induced latent transforming growth factor β 1 on expression of type I collagen and collagenase in dermal fibroblasts. *Growth Factors* 17, 167–176. doi: 10.3109/08977190009001066
- Giannone, F. A., Baldassarre, M., Domenicali, M., Zaccherini, G., Trevisani, F., and Bernardi, M. (2012). Reversal of liver fibrosis by the antagonism of endocannabinoid CB1 receptor in a rat model of CCl 4-induced advanced cirrhosis. *Lab. Invest.* 92, 384–395. doi: 10.1038/labinvest.2011.191
- Gonzalez, A. C. D. O., Andrade, Z. D. A., Costa, T. F., and Medrado, A. R. A. P. (2016). Wound healing - A literature review. *An. Bras. Dermatol.* 91, 614–620. doi: 10.1590/abd1806-4841.20164741
- Gonzalez, E. G., Selvi, E., Balistreri, E., Akhmetshina, A., Palumbo, K., and Lorenzini, S. (2012). Synthetic cannabinoid ajulemic acid exerts potent antifibrotic effects in experimental models of systemic sclerosis. *Ann. Rheum. Dis.* 71, 1545–1551. doi: 10.1136/annrheumdis-2011-200314
- Harmanci, D., Erkan, E. P., Kocak, A., and Akdogan, G. G. (2017). Role of the microRNA-29 family in fibrotic skin diseases. *Biomed. Rep.* 6, 599–604. doi: 10.3892/br.2017.900
- Hinden, L., Udi, S., Drori, A., Gammal, A., Nemirovski, A., and Hadar, R. (2018). Modulation of Renal GLUT2 by the Cannabinoid-1 Receptor: implications for the Treatment of Diabetic Nephropathy. *J. Am. Soc. Nephrol.* 29, 434–448. doi: 10.1681/ASN.2017040371
- Hinderer, S., and Schenke-Layland, K. (2019). Cardiac fibrosis – A short review of causes and therapeutic strategies. *Adv. Drug Deliv. Rev.* 146, 77–82. doi: 10.1016/j.addr.2019.05.011
- Ho, C. Y., López, B., Coelho-Filho, O. R., Lakdawala, N. K., Cirino, A. L., and Jarolim, M. S. P. (2010). Myocardial Fibrosis as an Early Manifestation of Hypertrophic Cardiomyopathy. *N. Engl. J. Med.* 363, 552–563. doi: 10.1056/NEJMoa1002659
- Hoseini Mohimani, P. A. P., Gurevich, A., Mikheenko, A., Garg, N., Nothias, L. F., Ninomiya, A., et al. (2017). HHS Public Access. *Physiol. Behav.* 176, 139–148.
- Hoyer, N., Prior, T. S., Bendstrup, E., Wilcke, T., and Shaker, S. B. (2019). Risk factors for diagnostic delay in idiopathic pulmonary fibrosis. *Respir. Res.* 20:103. doi: 10.1186/s12931-019-1076-0
- Huang, S. K., White, E. S., Wettlaufer, S. H., Grifka, H., Hogaboam, C. M., and Thannickal, V. J. (2009). Prostaglandin E2 induces fibroblast apoptosis by modulating multiple survival pathways. *FASEB J.* 23:4317. doi: 10.1096/fj.08-128801
- Hughes, G., Toellner, H., Morris, H., Leonard, C., and Chaudhuri, N. (2016). Real World Experiences: pirfenidone and Nintedanib are Effective and Well Tolerated Treatments for Idiopathic Pulmonary Fibrosis. *J. Clin. Med.* 5:78. doi: 10.3390/jcm5090078
- Iannitti, R. G., Napolioni, V., Oikonomou, V., De Luca, A., Galosi, C., and Pariano, M. (2016). ARTICLE IL-1 receptor antagonist ameliorates inflammasome-dependent inflammation in murine and human cystic fibrosis. *Nat. Commun.* 7:10791. doi: 10.1038/ncomms10791
- Jeon, K. I., Phipps, R. P., Sime, P. J., and Huxlin, K. R. (2017). Antifibrotic Actions of Peroxisome Proliferator-Activated Receptor γ Ligands in Corneal Fibroblasts Are Mediated by β -Catenin-Regulated Pathways. *Am. J. Pathol.* 187, 1660–1669. doi: 10.1016/j.ajpath.2017.04.002
- Juknat, A., Gao, F., Coppola, G., Vogel, Z., and Kozela, E. (2019). miRNA expression profiles and molecular networks in resting and LPS-activated BV-2 microglia—Effect of cannabinoids. *PLoS One* 14:e0212039. doi: 10.1371/journal.pone.0212039

- Kelly, P., Meade, K. G., and O'Farrelly, C. (2019). Non-canonical inflammasome-mediated IL-1 β production by primary endometrial epithelial and stromal fibroblast cells is NLRP3 and caspase-4 dependent. *Front. Immunol.* 10:102. doi: 10.3389/fimmu.2019.00102
- Kendall, R. T., and Feghali-Bostwick, C. A. (2014). Fibroblasts in fibrosis: novel roles and mediators. *Front. Pharmacol.* 5:123. doi: 10.3389/fphar.2014.00123
- Khaksar, S., and Bigdeli, M. R. (2017). Anti-excitotoxic effects of cannabidiol are partly mediated by enhancement of NCX2 and NCX3 expression in animal model of cerebral ischemia. *Eur. J. Pharmacol.* 794, 270–279. doi: 10.1016/j.ejphar.2016.11.011
- Khan, R., and Sheppard, R. (2006). Fibrosis in heart disease: understanding the role of transforming growth factor- β 1 in cardiomyopathy, valvular disease and arrhythmia. *Immunology* 118, 10–24. doi: 10.1111/j.1365-2567.2006.02336.x
- Khaw, P. T., Bouremel, Y., Brocchini, S., and Henein, C. (2020). The control of conjunctival fibrosis as a paradigm for the prevention of ocular fibrosis-related blindness. 'Fibrosis has many friends,'. *Eye* 34, 2163–2174. doi: 10.1038/s41433-020-1031-9
- Kim, I. H., Kisseleva, T., and Brenner, D. A. (2015). Aging and liver disease. *Curr. Opin. Gastroenterol.* 31, 184–191. doi: 10.1097/MOG.0000000000000176
- Klinkhammer, B. M., Floege, J., and Boor, P. (2018). PDGF in organ fibrosis. *Mol. Aspects Med.* 62, 44–62. doi: 10.1016/j.mam.2017.11.008
- Klöpffel, G. (2007). Chronic pancreatitis, pseudotumors and other tumor-like lesions. *Mod. Pathol.* 20, 113–131. doi: 10.1038/modpathol.3800690
- Klöpffel, G., Detlefsen, S., and Feyerabend, B. (2004). Fibrosis of the pancreas: the initial tissue damage and the resulting pattern. *Virchows Arch.* 445, 1–8. doi: 10.1007/s00428-003-0958-0
- Kobayashi, T., Tanaka, K., Fujita, T., Umezawa, H., Amano, H., and Yoshioka, K. (2015). Bidirectional role of IL-6 signal in pathogenesis of lung fibrosis. *Respir. Res.* 16, 1–14. doi: 10.1186/s12931-015-0261-z
- Kotsiou, O. S., Gourgoulis, K. I., and Zarogiannis, S. G. (2018). IL-33/ST2 axis in organ fibrosis. *Front. Immunol.* 9:2432. doi: 10.3389/fimmu.2018.02432
- Kovalchuk, O., and Kovalchuk, I. (2020). Cannabinoids as anticancer therapeutic agents. *Cell Cycle* 19, 961–989. doi: 10.1080/15384101.2020.1742952
- Kowal-Bielecka, O., Kowal, K., Distler, O., and Gay, S. (2007). Mechanisms of Disease: leukotrienes and lipoxins in scleroderma lung disease—insights and potential therapeutic implications. *Nat. Clin. Pract. Rheumatol.* 3, 43–51. doi: 10.1038/ncprheum0375
- Kryczka, J., and Boncela, J. (2015). Leukocytes: the Double-Edged Sword in Fibrosis. *Mediators Inflamm.* 2015, 1–10. doi: 10.1155/2015/652035
- Kumar, V., Torben, W., Mansfield, J., Alvarez, X., Vande Stouwe, C., and Li, J. (2019). Cannabinoid Attenuation of Intestinal Inflammation in Chronic SIV-Infected Rhesus Macaques Involves T Cell Modulation and Differential Expression of Micro-RNAs and Pro-inflammatory Genes. *Front. Immunol.* 10:914. doi: 10.3389/fimmu.2019.00914
- Laezza, C., Pagano, C., Navarra, G., Pastorino, O., Chiara Proto, M., and Fiore, D. (2020). The endocannabinoid system: a target for cancer treatment. *Int. J. Mol. Sci.* 21:747. doi: 10.3390/ijms21030747
- Lafaye, G., Karila, L., Blecha, L., and Benyamina, A. (2017). Cannabis, cannabinoids, and health. *Dialogues Clin. Neurosci.* 19, 309–316. doi: 10.31887/DCNS.2017.19.3/glafaye
- Lands, L. C., and Stanojevic, S. (2019). Oral non-steroidal anti-inflammatory drug therapy for lung disease in cystic fibrosis. *Cochrane Database Syst. Rev.* 4:CD001505. doi: 10.1002/14651858.CD001505.pub5
- Ley, B., and Collard, H. R. (2013). Epidemiology of idiopathic pulmonary fibrosis. *Clin. Epidemiol.* 5, 483–492. doi: 10.2147/CLEP.S54815
- Li, D., Guabiraba, R., Besnard, A., Komai-Koma, M., Jabir, M. S., and Zhang, L. (2014). IL-33 promotes ST2-dependent lung fibrosis by the induction of alternatively activated macrophages and innate lymphoid cells in mice. *J. Allergy Clin. Immunol.* 134, 1422–1432.e11. doi: 10.1016/j.jaci.2014.05.011
- Li, X., Hana, D., Tian, Z., Gao, B., Fana, M., and Lia, C. (2016). Activation of Cannabinoid Receptor Type II by AM1241 Ameliorates Myocardial Fibrosis via Nrf2-Mediated Inhibition of TGF- β 1/Smad3 Pathway in Myocardial Infarction Mice. *Cell. Physiol. Biochem.* 39, 1521–1536. doi: 10.1159/000447855
- Li, X., Zhu, L., Wang, B., Yuan, M., and Zhu, R. (2017). Drugs and targets in fibrosis. *Front. Pharmacol.* 8:855. doi: 10.3389/fphar.2017.00855
- Lim, M. P., Devi, L. A., and Rozenfeld, R. (2011). Cannabidiol causes activated hepatic stellate cell death through a mechanism of endoplasmic reticulum stress-induced apoptosis. *Cell Death Dis.* 2:e170. doi: 10.1038/cddis.2011.52
- Liu, G., Friggeri, A., Yang, Y., Milosevic, J., Ding, Q., and Thannickal, V. J. (2010). miR-21 mediates fibrogenic activation of pulmonary fibroblasts and lung fibrosis. *J. Exp. Med.* 207, 1589–1597. doi: 10.1084/jem.20100035
- Liu, Y. (2011). Cellular and molecular mechanisms of renal fibrosis. *Nat. Rev. Nephrol.* 7, 684–696. doi: 10.1038/nrneph.2011.149
- Liu, Z., Changa, A. N., Grinnell, F., Trybus, K. M., Milewicz, D. M., and Stull, J. T. (2017). Vascular disease-causing mutation, smooth muscle α -actin R258C, dominantly suppresses functions of α -actin in human patient fibroblasts. *Proc. Natl. Acad. Sci. U. S. A.* 114, E5569–E5578. doi: 10.1073/pnas.1703506114
- Lopez-Castejon, G., and Brough, D. (2011). Understanding the mechanism of IL-1 β secretion. *Cytokine Growth Factor Rev.* 22, 189–195. doi: 10.1016/j.cytogfr.2011.10.001
- Lv, J., Zhao, Z., Chen, Y., Wang, Q., Tao, Y., and Yang, L. (2012). The Chinese herbal decoction Danggui Buxue Tang inhibits angiogenesis in a rat model of liver fibrosis. *Evid. Based Complement Alternat. Med.* 2012:284963. doi: 10.1155/2012/284963
- Macara, I. G., Guyer, R., Richardson, G., Huo, Y., and Ahmed, S. M. (2014). Epithelial homeostasis. *Curr. Biol.* 24, R815–R825. doi: 10.1016/j.cub.2014.06.068
- Madácsy, T., Pallagi, P., and Maleth, J. (2018). Cystic Fibrosis of the Pancreas: the Role of CFTR Channel in the Regulation of Intracellular Ca²⁺ Signaling and Mitochondrial Function in the Exocrine Pancreas. *Front. Physiol.* 9:1585. doi: 10.3389/fphys.2018.01585
- Mahesh, G., and Biswas, R. (2019). *MicroRNA-155: A Master Regulator of Inflammation. Journal of Interferon and Cytokine Research.* Available online at: <https://pubmed.ncbi.nlm.nih.gov/30998423/>. ([Accessed: April 11, -Apr-2021]). doi: 10.1089/jir.2018.0155
- Mallat, A., Teixeira-Clerc, F., Deveaux, V., Manin, S., and Lotersztajn, S. (2011). The endocannabinoid system as a key mediator during liver diseases: new insights and therapeutic openings. *Br. J. Pharmacol.* 163, 1432–1440. doi: 10.1111/j.1476-5381.2011.01397.x
- Margaritopoulos, G. A., Vasarmidi, E., and Antoniou, K. M. (2016). Pirfenidone in the treatment of idiopathic pulmonary fibrosis: an evidence-based review of its place in therapy. *Core Evid.* 11, 11–22. doi: 10.2147/CE.S76549
- Marone, G., Granata, F., Pucino, V., Pecoraro, A., Heffler, E., and Loffredo, S. (2019). The intriguing role of interleukin 13 in the pathophysiology of asthma. *Front. Pharmacol.* 10:1387. doi: 10.3389/fphar.2019.01387
- Maurer, B., Stanczyk, J., Jungel, A., Akhmetshina, A., Trenkmann, M., and Brock, M. (2010). MicroRNA-29, a key regulator of collagen expression in systemic sclerosis. *Arthritis Rheum.* 62, 1733–1743. doi: 10.1002/art.27443
- McVicker, B. L., and Bennett, R. G. (2017). Novel anti-fibrotic therapies. *Front. Pharmacol.* 8:318. doi: 10.3389/fphar.2017.00318
- Meng, X. M., Tang, P. M. K., Li, J., and Lan, H. Y. (2015). TGF- β /Smad signaling in renal fibrosis. *Front. Physiol.* 6:82. doi: 10.3389/fphys.2015.00082
- Mohammed, A., Alghetaa, H., Sultan, M., Singh, N. P., Nagarkatti, P., and Nagarkatti, M. (2020). Administration of Δ 9-Tetrahydrocannabinol (THC) Post-Staphylococcal Enterotoxin B Exposure Protects Mice From Acute Respiratory Distress Syndrome and Toxicity. *Front. Pharmacol.* 11:893. doi: 10.3389/fphar.2020.00893
- Montecucco, F., and Di Marzo, V. (2012). At the heart of the matter: the endocannabinoid system in cardiovascular function and dysfunction. *Trends Pharmacol. Sci.* 33, 331–340. doi: 10.1016/j.tips.2012.03.002
- Moran-Mendoza, O., Colman, R., Kalluri, M., Cabaltea, C., and Harle, I. (2019). A comprehensive and practical approach to the management of idiopathic pulmonary fibrosis. *Expert Rev. Respir. Med.* 13, 601–614. doi: 10.1080/17476348.2019.1627204
- Moshref, S. S., Mufti, S. T., Moshref, S. S., and Mufti, S. T. (2010). Keloid and Hypertrophic Scars: comparative Histopathological and Immunohistochemical Study. *JKAU Med. Sci* 17, 3–22. doi: 10.4197/Med.17-3-1
- Muñoz-Luque, J., Ros, J., Fernández-Varo, G., Tugues, S., Morales-Ruiz, M., and Alvarez, C. E. (2008). 'Regression of fibrosis after chronic stimulation of cannabinoid CB2 receptor in cirrhotic rats. *J. Pharmacol. Exp. Ther.* 324, 475–483. doi: 10.1124/jpet.107.131896
- Nagarkatti, P., Pandey, R., Rieder, S. A., Hegde, V. L., and Nagarkatti, M. (2009). Cannabinoids as novel anti-inflammatory drugs. *Future Med. Chem.* 1, 1333–1349. doi: 10.4155/fmc.09.93

- Newton, K., and Dixit, V. M. (2012). Signaling in innate immunity and inflammation. *Cold Spring Harb. Perspect. Biol.* 4:a006049. doi: 10.1101/cshperspect.a006049
- Occleston, N. L., Metcalfe, A. D., Boanas, A., Burgoyne, N. J., Nield, K., and O'Kane, S. (2010). Therapeutic improvement of scarring: mechanisms of scarless and scar-forming healing and approaches to the discovery of new treatments. *Dermatol. Res. Pract.* 2010:405262. doi: 10.1155/2010/405262
- Panganiban, R. A. M., and Day, R. M. (2011). Hepatocyte growth factor in lung repair and pulmonary fibrosis. *Acta Pharmacol. Sin.* 32, 12–20. doi: 10.1038/aps.2010.90
- Panizo, S., Martínez-Arias, L., Alonso-Montes, C., Cannata, P., Martín-Carro, B., and Fernández-Martín, J. L. (2021). Fibrosis in chronic kidney disease: pathogenesis and consequences. *Int. J. Mol. Sci.* 22, 1–19. doi: 10.3390/ijms22010408
- Papetti, M., and Herman, I. M. (2002). Mechanisms of normal and tumor-derived angiogenesis. *Am. J. Physiol. Cell Physiol.* 282, C947–70. doi: 10.1152/ajpcell.00389.2001
- Parfieniuk, A., and Flisiak, R. (2008). Role of cannabinoids in chronic liver diseases. *World J. Gastroenterol.* 14, 6109–6114. doi: 10.3748/wjg.14.6109
- Patsenker, E., and Stickel, F. (2016). Cannabinoids in liver diseases. *Clin. Liver Dis.* 7, 21–25. doi: 10.1002/cld.527
- Pilewski, J. M., Liu, L., Henry, A. C., Knauer, A. V., and Feghali-Bostwick, C. A. (2005). Insulin-like growth factor binding proteins 3 and 5 are overexpressed in idiopathic pulmonary fibrosis and contribute to extracellular matrix deposition. *Am. J. Pathol.* 166, 399–407. doi: 10.1016/S0002-9440(10)62263-8
- Profyris, C., Tziotzios, C., and Do Vale, I. (2012). Cutaneous scarring: pathophysiology, molecular mechanisms, and scar reduction therapeutics: part I: the molecular basis of scar formation. *J. Am. Acad. Dermatol.* 66, 1–10. doi: 10.1016/j.jaad.2011.05.055
- Rabello, F. B., Souza, C. D., and Farina, J. A. (2014). Update on hypertrophic scar treatment. *Clinics* 69, 565–573. doi: 10.6061/clinics/2014(08)11
- Raimundo, K., Chang, E., Broder, M. S., Alexander, K., Zazzali, J., and Swigris, J. J. (2016). Clinical and economic burden of idiopathic pulmonary fibrosis: a retrospective cohort study. *BMC Pulm. Med.* 16:2. doi: 10.1186/s12890-015-0165-1
- Rajput, A., Rajan, K., Vardhan, V., Tewari, S., and Borcar, J. (2000). Mediastinal Fibrosis. *Med. J. Armed Forces India* 56, 82–84. doi: 10.1016/S0377-1237(17)30106-5
- Rao, R., Nagarkatti, P. S., and Nagarkatti, M. (2015). Δ^9 Tetrahydrocannabinol attenuates Staphylococcal enterotoxin B-induced inflammatory lung injury and prevents mortality in mice by modulation of miR-17-92 cluster and induction of T-regulatory cells. *Br. J. Pharmacol.* 172, 1792–1806. doi: 10.1111/bph.13026
- Redente, E. F., Keith, R. C., Janssen, W., Henson, P. M., Ortiz, L. A., and Downey, G. P. (2014). “Tumor necrosis factor- α accelerates the resolution of established pulmonary fibrosis in mice by targeting profibrotic lung macrophages. *Am. J. Respir. Cell Mol. Biol.* 50, 825–837. doi: 10.1165/rcmb.2013-0386OC
- Reinke, J. M., and Sorg, H. (2012). Wound repair and regeneration. *Eur. Surg. Res.* 49, 35–43. doi: 10.1159/000339613
- Rizzo, M. D., Crawford, R. B., Henriquez, J. E., Aldhamen, Y. A., Gulick, P., and Amalfitano, A. (2018). HIV-infected cannabis users have lower circulating CD16+ monocytes and IFN- γ -inducible protein 10 levels compared with nonusing HIV patients. *AIDS* 32, 419–429. doi: 10.1097/QAD.0000000000001704
- Robertson, S., and Miller, M. R. (2018). Ambient air pollution and thrombosis. *Part. Fibre Toxicol.* 15, 1–16. doi: 10.1186/s12989-017-0237-x
- Rosales, C. (2018). Neutrophil: a cell with many roles in inflammation or several cell types? *Front. Physiol.* 9:113. doi: 10.3389/fphys.2018.00113
- Rosenkranz, S. (2004). TGF- β 1 and angiotensin networking in cardiac remodeling. *Cardiovasc. Res.* 63, 423–432. doi: 10.1016/j.cardiores.2004.04.030
- Russo, E. B. (2019). The case for the entourage effect and conventional breeding of clinical cannabis: no ‘Strain,’ no gain. *Front. Plant Sci.* 9:1969. doi: 10.3389/fpls.2018.01969
- Sakai, N., and Tager, A. M. (2013). Fibrosis of two: epithelial cell-fibroblast interactions in pulmonary fibrosis. *Biochim. Biophys. Acta* 1832, 911–21. doi: 10.1016/j.bbdis.2013.03.001
- Sanders, D. B., and Fink, A. K. (2016). Background and Epidemiology. *Pediatr. Clin. North Am.* 63, 567–584. doi: 10.1016/j.pcl.2016.04.001
- Sepanlou, S. G. (2020). The global, regional, and national burden of cirrhosis by cause in 195 countries and territories, 1990–2017: a systematic analysis for the Global Burden of Disease Study 2017. *Lancet Gastroenterol. Hepatol.* 5, 245–266. doi: 10.1016/S2468-1253(19)30349-8
- Servettaz, A., Kavian, N., Nicco, C., Deveaux, V., Chereau, C., and Wang, A. (2010). “Targeting the cannabinoid pathway limits the development of fibrosis and autoimmunity in a mouse model of systemic sclerosis. *Am. J. Pathol.* 177, 187–196. doi: 10.2353/ajpath.2010.090763
- Sido, J. M., Jackson, A. R., Nagarkatti, P. S., and Nagarkatti, M. (2016). Marijuana-derived Δ -9-tetrahydrocannabinol suppresses Th1/Th17 cell-mediated delayed-type hypersensitivity through microRNA regulation. *J. Mol. Med.* 94, 1039–1051. doi: 10.1007/s00109-016-1404-5
- Simon, T. G., Henson, J., Osganian, S., Masia, R., Chan, A. T., and Chung, R. T. (2019). Daily Aspirin Use Associated With Reduced Risk For Fibrosis Progression In Patients With Nonalcoholic Fatty Liver Disease. *Clin. Gastroenterol. Hepatol.* 17, 2776–2784.e4. doi: 10.1016/j.cgh.2019.04.061
- Šmid, V. (2020). Liver fibrosis. *Vnitr. Lek.* 66, e36–e41. doi: 10.36290/vnl.2020.078
- Smith, J. S., Gorbett, D., Mueller, J., Perez, R., and Daniels, C. J. (2013). Pulmonary hypertension and idiopathic pulmonary fibrosis: a dastardly duo. *Am. J. Med. Sci.* 346, 221–225. doi: 10.1097/MAJ.0b013e31827871dc
- Spiera, R., Kuwana, M., Khanna, D., Hummers, L., Frech, T., and Stevens, W. (2021). OP0171 Phase 3 trial of Lenabasum, a CB2 agonist, for the treatment of diffuse cutaneous systemic sclerosis (DCSSC). *Ann. Rheum. Dis.* 80, 102–103. doi: 10.1136/annrheumdis-2021-eular.1795
- Srivastava, M. D., Srivastava, B. I. S., and Brouhard, B. (1998). Δ^9 Tetrahydrocannabinol and cannabidiol alter cytokine production by human immune cells. *Immunopharmacology* 40, 179–185. doi: 10.1016/S0162-3109(98)00041-1
- Sun, S., Hu, F., Wu, J., and Zhang, S. (2017). Cannabidiol attenuates OGD/R-induced damage by enhancing mitochondrial bioenergetics and modulating glucose metabolism via pentose-phosphate pathway in hippocampal neurons. *Redox Biol.* 11, 577–585. doi: 10.1016/j.redox.2016.12.029
- Suthahar, N., Meijers, W. C., Silljé, H. H. W., and de Boer, R. A. (2017). From Inflammation to Fibrosis—Molecular and Cellular Mechanisms of Myocardial Tissue Remodelling and Perspectives on Differential Treatment Opportunities. *Curr. Heart Fail. Rep.* 14, 235–250. doi: 10.1007/s11897-017-0343-y
- Tam, J., Liu, J., Mukhopadhyay, B., Cinar, R., Godlewski, G., and Kunos, G. (2011). Endocannabinoids in liver disease. *Hepatology* 53, 346–355. doi: 10.1002/hep.24077
- Tanaka, T., Narazaki, M., and Kishimoto, T. (2014). IL-6 in inflammation, Immunity, And disease. *Cold Spring Harb. Perspect. Biol.* 6, 16295–16296. doi: 10.1101/cshperspect.a016295
- Tanaka, T., Ogawa, M., Suzuki, J., Sekinishi, A., Itai, A., and Hirata, Y. (2012). Inhibition of I κ B phosphorylation prevents load-induced cardiac dysfunction in mice. *Am. J. Physiol. Circ. Physiol.* 303, H1435–H1445. doi: 10.1152/ajpheart.00290.2012
- Thum, T., Gross, C., Fiedler, J., Fischer, T., Kissler, S., and Bussen, M. (2008). MicroRNA-21 contributes to myocardial disease by stimulating MAP kinase signalling in fibroblasts. *Nature* 456, 980–984. doi: 10.1038/nature07511
- Tirado, M., and Koss, W. (2018). Differentiation of mesothelial cells into macrophage phagocytic cells in a patient with clinical sepsis. *Blood* 132:1460. doi: 10.1182/blood-2018-07-859991
- Tung, C. W., Ho, C., Hsu, Y. C., Huang, S. C., Shih, Y. H., and Lin, C. L. (2019). MicroRNA-29a attenuates diabetic glomerular injury through modulating cannabinoid receptor 1 signaling. *Molecules* 24:264. doi: 10.3390/molecules24020264
- Turcotte, C., Blanchet, M. R., Laviolette, M., and Flamand, N. (2016). The CB2 receptor and its role as a regulator of inflammation. *Cell Mol. Life Sci.* 73, 4449–4470. doi: 10.1007/s00018-016-2300-4
- Usher, K. M., Zhu, S., Mavropalias, G., Carrino, J. A., Zhao, J., and Xu, J. (2019). Pathological mechanisms and therapeutic outlooks for arthrofibrosis. *Bone Res.* 7, 9. doi: 10.1038/s41413-019-0047-x
- Vaglio, A., and Maritati, F. (2016). Idiopathic retroperitoneal fibrosis. *J. Am. Soc. Nephrol.* 27, 1880–1889. doi: 10.1681/ASN.2015101110
- Valenzuela, C., Torrisi, S. E., Kahn, N., Quaresma, M., Stowasser, S., and Kreuter, M. (2020). Ongoing challenges in pulmonary fibrosis and insights from the nintedanib clinical programme. *Respir. Res.* 21, 1–15. doi: 10.1186/s12931-019-1269-6

- Vallée, A., Lecarpentier, Y., Guillevin, R., and Vallée, J. N. (2017). Interactions between TGF- β 1, canonical WNT/ β -catenin pathway and PPAR β ; in radiation-induced fibrosis. *Oncotarget* 8, 90579–90604. doi: 10.18632/oncotarget.21234
- Waikhom, R., and Taraphder, A. (2011). Nephrogenic systemic fibrosis: a brief review. *Indian J. Dermatol.* 56, 54. doi: 10.4103/0019-5154.77554
- Walker, O. L. S., Gurm, H., Sharma, R., Verma, N., May, L. L., and Raha, S. (2021). Delta-9-tetrahydrocannabinol inhibits invasion of HTR8/SVneo human extravillous trophoblast cells and negatively impacts mitochondrial function. *Sci. Rep.* 11:4029. doi: 10.1038/s41598-021-83563-9
- Wang, B., Kovalchuk, A., Li, D., Rodriguez-Juarez, R., Ilnytskyi, Y., Kovalchuk, I., et al. (2020). In search of preventive strategies: novel high-CBD Cannabis sativa extracts modulate ACE2 expression in COVID-19 gateway tissues. *Aging* 12, 22425–22440. doi: 10.20944/preprints202004.0315.v1
- Watzl, B., Scuderì, P., and Watson, R. R. (1991). Marijuana components stimulate human peripheral blood mononuclear cell secretion of interferon-gamma and suppress interleukin-1 alpha in vitro. *Int. J. Immunopharmacol.* 13, 1091–1097. doi: 10.1016/0192-0561(91)90160-9
- Weiskirchen, R., Weiskirchen, S., and Tacke, F. (2019). Organ and tissue fibrosis: molecular signals, cellular mechanisms and translational implications. *Mol. Aspects Med.* 65, 2–15. doi: 10.1016/j.mam.2018.06.003
- Wernig, G., Chenc, S., Cuib, L., Van Nesteb, C., Tsaia, J. M., and Kambham, N. (2017). Unifying mechanism for different fibrotic diseases. *Proc. Natl. Acad. Sci. U. S. A.* 114, 4757–4762. doi: 10.1073/pnas.1621375114
- Wietecha, M. S., and DiPietro, L. A. (2013). Therapeutic Approaches to the Regulation of Wound Angiogenesis. *Adv. Wound Care* 2, 81–86. doi: 10.1089/wound.2011.0348
- Wind, S., Schmid, U., Freiwald, M., Marzin, K., Lotz, R., and Ebner, T. (2019). Clinical Pharmacokinetics and Pharmacodynamics of Nintedanib. *Clin. Pharmacokinet.* 58, 1131–1147. doi: 10.1007/s40262-019-00766-0
- Wolff, V., Schlagowski, A. I., Rouyer, O., Charles, A. L., Singh, F., Auger, C., et al. (2015). Tetrahydrocannabinol induces brain mitochondrial respiratory Chain dysfunction and increases oxidative stress: a potential mechanism involved in cannabis-related stroke. *Biomed Res. Int.* 2015:323706. doi: 10.1155/2015/323706
- Wynn, T. A. (2007). Common and unique mechanisms regulate fibrosis in various fibroproliferative diseases. *J. Clin. Invest.* 117, 524–529. doi: 10.1172/JCI31487
- Xiao, L., and Liu, Y. (2013). Fibrosis and anaemia in CKD—two beasts, one ancestor. *Nat. Rev. Nephrol.* 9, 563–565. doi: 10.1038/nrneph.2013.179
- Xie, Y., Sul, N., Yang, J., Tan, Q., Huang, S., and Jin, M. (2020). FGF/FGFR signaling in health and disease. *Signal Transduct. Target. Ther.* 5:181. doi: 10.1038/s41392-020-00222-7
- Xu, L., Yates, C. C., Lockyer, P., Xie, L., Bevilacqua, A., and He, J. (2014). MMI-0100 inhibits cardiac fibrosis in myocardial infarction by direct actions on cardiomyocytes and fibroblasts via MK2 inhibition. *J. Mol. Cell Cardiol.* 77, 86–101. doi: 10.1016/j.yjmcc.2014.09.011
- Yahiaoui, Y., Jablonski, M., Hubert, D., Mosnier-Pudar, H., Noël, LHI, and Stern, M. (2009). Renal Involvement in Cystic Fibrosis: diseases spectrum and clinical relevance. *Clin. J. Am. Soc. Nephrol.* 4, 921–928. doi: 10.2215/CJN.00750209
- Yang, L., Kwon, J., Popov, Y., Gajdos, G. B., Ordog, T., and Brekken, R. A. (2014). Vascular endothelial growth factor promotes fibrosis resolution and repair in mice. *Gastroenterology* 146, 1339–1350.e1. doi: 10.1053/j.gastro.2014.01.061
- Yang, L., Tian, L., Zhang, Z., Zhou, X., Ji, X., and Liu, F. (2020). “Cannabinoid Receptor 1/miR-30b-5p Axis Governs Macrophage NLRP3 Expression and Inflammasome Activation in Liver Inflammatory Disease. *Mol. Ther. Nucleic Acids* 20, 725–738. doi: 10.1016/j.omtn.2020.04.010
- Yasuoka, H., Hsu, E., Ruiz, X. D., Steinman, R. A., Choi, A. M. K., and Feghali-Bostwick, C. A. (2009). The fibrotic phenotype induced by IGFBP-5 is regulated by MAPK activation and Egr-1-dependent and -independent mechanisms. *Am. J. Pathol.* 175, 605–615. doi: 10.2353/ajpath.2009.080991
- Yoshimatsu, Y., Wakabayashi, I., Kimuro, S., Takahashi, N., Takahashi, K., and Kobayashi, M. (2020). TNF- α enhances TGF- β -induced endothelial-to-mesenchymal transition via TGF- β signal augmentation. *Cancer Sci.* 111, 2385–2399. doi: 10.1111/cas.14455
- Zahr, A. A., Salama, M. E., Carreau, N., Tremblay, D., Verstovsek, S., and Mesa, R. (2016). Bone marrow fibrosis in myelofibrosis: pathogenesis, prognosis and targeted strategies. *Haematologica* 101, 660–671. doi: 10.3324/haematol.2015.141283
- Zaman, T., and Lee, J. S. (2018). Risk Factors for the Development of Idiopathic Pulmonary Fibrosis: a Review. *Curr. Pulmonol. Rep.* 7, 118–125. doi: 10.1007/s13665-018-0210-7
- Ziring, D., Wei, B., Velazquez, P., Schrage, M., Buckley, N. E., and Braun, J. (2006). Formation of B and T cell subsets require the cannabinoid receptor CB2. *Immunogenetics* 58, 714–725. doi: 10.1007/s00251-006-0138-x
- Zurier, R. B., and Burstein, S. H. (2016). Cannabinoids, inflammation, and fibrosis. *FASEB J.* 30, 3682–3689. doi: 10.1096/fj.201600646R

Conflict of Interest: The authors declare that the research was conducted in the absence of any commercial or financial relationships that could be construed as a potential conflict of interest.

Publisher’s Note: All claims expressed in this article are solely those of the authors and do not necessarily represent those of their affiliated organizations, or those of the publisher, the editors and the reviewers. Any product that may be evaluated in this article, or claim that may be made by its manufacturer, is not guaranteed or endorsed by the publisher.

Copyright © 2021 Pryimak, Zaiachuk, Kovalchuk and Kovalchuk. This is an open-access article distributed under the terms of the Creative Commons Attribution License (CC BY). The use, distribution or reproduction in other forums is permitted, provided the original author(s) and the copyright owner(s) are credited and that the original publication in this journal is cited, in accordance with accepted academic practice. No use, distribution or reproduction is permitted which does not comply with these terms.



Cardiomyocyte-Specific RIP2 Overexpression Exacerbated Pathologic Remodeling and Contributed to Spontaneous Cardiac Hypertrophy

Jing-jing Yang^{1,2†}, Nan Zhang^{1,2†}, Zi-ying Zhou^{1,2}, Jian Ni^{1,2}, Hong Feng³, Wen-jing Li^{1,2}, Shan-qi Mou^{1,2}, Hai-ming Wu², Wei Deng^{1,2}, Hai-han Liao^{1,2*} and Qi-zhu Tang^{1,2*}

OPEN ACCESS

Edited by:

Isotta Chimenti,
Sapienza University of Rome, Italy

Reviewed by:

Kelly Crowe,
Mount St. Joseph University,
United States
Robert Morris Blanton,
Tufts Medical Center, United States

*Correspondence:

Qi-zhu Tang
qztang@whu.edu.cn
Hai-han Liao
liaohaihan@whu.edu.cn

†These authors have contributed
equally to this work

Specialty section:

This article was submitted to
Molecular and Cellular Pathology,
a section of the journal
Frontiers in Cell and Developmental
Biology

Received: 30 March 2021

Accepted: 08 September 2021

Published: 18 October 2021

Citation:

Yang J-j, Zhang N, Zhou Z-y, Ni J,
Feng H, Li W-j, Mou S-q, Wu H-m,
Deng W, Liao H-h and Tang Q-z
(2021) Cardiomyocyte-Specific RIP2
Overexpression Exacerbated
Pathologic Remodeling
and Contributed to Spontaneous
Cardiac Hypertrophy.
Front. Cell Dev. Biol. 9:688238.
doi: 10.3389/fcell.2021.688238

¹ Department of Cardiology, Renmin Hospital of Wuhan University, Wuhan, China, ² Hubei Key Laboratory of Metabolic and Chronic Diseases, Wuhan, China, ³ Department of Geriatrics, Renmin Hospital of Wuhan University, Wuhan, China

This study aimed to investigate the role and mechanisms of Receptor interacting protein kinase 2 (RIP2) in pressure overload-induced cardiac remodeling. Human failing or healthy donor hearts were collected for detecting RIP2 expression. RIP2 cardiomyocyte-specific overexpression, RIP2 global knockout, or wild-type mice were subjected to sham or aortic banding (AB) surgery to establish pressure overload-induced cardiac remodeling *in vivo*. Phenylephrine (PE)-treated neonatal rat cardiomyocytes (NRCMs) were used for further investigation *in vitro*. The expression of RIP2 was significantly upregulated in failing human heart, mouse remodeling heart, and Ang II-treated NRCMs. RIP2 overexpression obviously aggravated pressure overload-induced cardiac remodeling. Mechanistically, RIP2 overexpression significantly increased the phosphorylation of TAK1, P38, and JNK1/2 and enhanced I κ B α /p65 signaling pathway. Inhibiting TAK1 activity by specific inhibitor completely prevented cardiac remodeling induced by RIP2 overexpression. This study further confirmed that RIP2 overexpression in NRCM could exacerbate PE-induced NRCM hypertrophy and TAK1 silence by specific siRNA could completely rescue RIP2 overexpression-mediated cardiomyocyte hypertrophy. Moreover, this study showed that RIP2 could bind to TAK1 in HEK293 cells, and PE could promote their interaction in NRCM. Surprisingly, we found that RIP2 overexpression caused spontaneous cardiac remodeling at the age of 12 and 18 months, which confirmed the powerful deterioration of RIP2 overexpression. Finally, we indicated that RIP2 global knockout attenuated pressure overload-induced cardiac remodeling *via* reducing TAK1/JNK1/2/P38 and I κ B α /p65 signaling pathways. Taken together, RIP2-mediated activation of TAK1/P38/JNK1/2 and I κ B α /p65 signaling pathways played a pivotal role in pressure overload-induced cardiac remodeling and spontaneous cardiac remodeling induced by RIP2 overexpression, and RIP2 inhibition might be a potential strategy for preventing cardiac remodeling.

Keywords: cardiac remodeling, spontaneous cardiac remodeling, RIP2, TAK1, MAPK

INTRODUCTION

Pathological cardiac remodeling is a common pathological process for all cardiovascular diseases to develop and progress into heart failure (Wu et al., 2017; Morita and Komuro, 2018). Despite advances in medical technology and medicine discovery, heart failure remains to be a severe condition with high morbidity and mortality worldwide and a satisfactory treatment strategy is still to be expected (Yancy et al., 2017). Studies have suggested that targeting cardiac remodeling at an early stage might be a prospective strategy for preventing the development and progress of heart failure (Wu et al., 2017; Gibb and Hill, 2018; Gonzalez et al., 2018). Although cardiac remodeling has drawn much attention, the underlying mechanisms remain to be largely unknown. More studies are needed for clarifying underlying mechanisms in cardiac remodeling.

Receptor interacting protein kinase 2 (RIP2) belongs to Tyrosine kinase-like family (Humphries et al., 2015). RIP2 contains a homologous kinase domain in its N-terminal, a caspase activation and recruitment domain in its C-terminal and a bridging intermediate domain between N- and C-terminal (Humphries et al., 2015). RIP2 could receive signal transduction from nucleotide-binding oligomerization domain-containing protein 2 (NOD2) (Humphries et al., 2015). Muramyl dipeptide (MDP) combined to the leucine-rich repeat regions of NOD2 and mediated NOD oligomerization (Humphries et al., 2015). Oligomerized NOD proteins bound to the CARD domains of RIP2 kinase, which resulted in RIP2 polyubiquitination and led to recruitment of TAK1 and IKK complexes to activate IKK/NF- κ B and MAPKs/AP1 signaling pathways (Humphries et al., 2015). Both IKK/NF- κ B and MAPKs/AP1 are key signaling pathways involved in pathological remodeling (Rose et al., 2010; Wu et al., 2017); however, it remains to be defined whether RIP2 overexpression could exacerbate pathological cardiac remodeling *via* these signaling pathways.

Several studies have explored the role and mechanisms of RIP2 in different cardiovascular diseases. Jacquet et al. (2008) demonstrated that RIP2 deficiency showed no obvious effects on ischemia-associated cardiac function and infarction size, because RIP2 was not the mediator of downstream signaling in ischemia-treated cardiomyocyte (Jacquet et al., 2008). In another study on heart ischemia, investigators presented that RIP2 deficiency enhanced myocardial damage area and markedly decreased cardiac function *via* promoting vascular endothelial growth factor (VEGF) expression for activating ERK1/2 and resulting in endothelial permeability and inflammation (Andersson et al., 2015). However, Li et al. (2015) demonstrated that RIP2 deficiency significantly attenuated ventricular remodeling after ischemia *via* inhibiting the NF- κ B and p38 MAPK signaling pathways. Recently, Zhao et al. (2017) demonstrated that global knockout of RIP2 attenuated pressure overload-induced cardiac remodeling *via* reducing toll-like receptor4/myeloid differentiation factor 88/nuclear factor kappa B (TLR4/MyD88/NF- κ B) and MAPKs activity.

According to these descriptions, RIP2 was considered to play important roles in cardiovascular disease; however, the exact role and mechanisms of RIP2 in cardiomyocytes remained to be

controversial. In this study, we presented that pro-hypertrophy stimuli promoted RIP2 overexpression *in vivo* and *in vitro*. With the pathological cardiac hypertrophy mouse model, we firstly demonstrated that cardiomyocyte-specific expression of RIP2 could exacerbate pressure overload-induced pathological cardiac hypertrophy. Moreover, RIP2 overexpression caused spontaneous cardiac hypertrophy and RIP2 knockout *in vivo* and silence *in vitro* could attenuate pathological cardiac remodeling and NRCM hypertrophy, respectively.

MATERIALS AND METHODS

Animals

All experimental procedures in this study were approved by the Animal Care and Use Committee of Renmin Hospital of Wuhan University and were performed in accordance with the National Institutes of Health (NIH) Guide for the Care and Use of Laboratory Animals.

To generate cardiomyocyte-specific RIP2 transgenic mice, full-length RIP2 cDNA was cloned into plasmid under control of cardiac α -MHC promoter (**Supplementary Figure 1A**). Then, the plasmid was linearized and was microinjected into fertilized mouse embryos for giving birth to cardiomyocyte-specific RIP2 overexpression mice. These transgene mice were identified by PCR analysis of tail genomic DNA. Primers used for transgene mice identification in this manuscript were listed as follows: forward: ATCTCCCCATAAGAGTTTGAGTC, and reverse: ATGTCCCTCCTTCTGGTGAC. According to the results of Western blots, the mice of RIP2 transgene (TG) line 2 were chosen for the following experiments (**Supplementary Figure 1B**). Non-transgenic mice (NTG) born in the same nest were used as control group. Global RIP2-knockout mice (007017) were purchased from the Jackson Laboratory and were mated with C57B/6L for nine generations. Male mice (age 8–10 weeks, weight 24.5–25.5 g) were used for subsequent experiments. All animals were raised in specific-pathogen-free (SPF) conditions in the Cardiovascular Research Institute of Wuhan University. Mice were allowed access to food and water freely with a 12-h light/dark cycle.

Established Cardiac Hypertrophy Mouse Model

A cardiac hypertrophy mouse model was established by aortic banding (AB) surgery according to our previous publications (Liao et al., 2015; Yuan et al., 2016). Briefly, mice were anesthetized by intraperitoneal injection of pentobarbital sodium (50 mg/kg, Sigma). After adequate anesthesia without a toe pinch reflex, the left chest was opened at the second intercostal space *via* blunt dissection to find out the thoracic aorta. A 27-gauge needle was tied to the aorta with a 7-0 silk suture. After ligation of the aorta and needle, the needle was quickly removed and the aortic constriction was confirmed by Doppler analysis. Animals in the sham group were subjected to the same procedure without ligation. Surgery operation and analyses were carried out in a blinded manner. Angiotensin II (Ang II, 1.1 mg/kg/day)

was infused with Alzet Osmotic Pumps 2002 to induce the Ang II-induced cardiac hypertrophy mouse model.

Specific Inhibitor Administration

To clarify the signaling pathways located downstream of RIP2, a specific inhibitor for TAK1 (Takinib, 253863-19-3, Med ChemExpress, United States) was dissolved in DMSO and then was administered to NTG and TG mice (5 mg/kg/day) for 4 weeks to inhibit TAK1 activity. The mice in the control group (VEH group) were treated with an identical dose of DMSO to the TAK1 group (the mice treated with inhibitor of TAK1). The treatment was started after 3 days of AB surgery.

Mouse Heart Harvest

Four weeks after surgery, mouse cardiac function was examined by echocardiography and pressure-volume loop under inhalation anesthesia with 1.5% isoflurane. Then, the mice were sacrificed by cervical dislocation. The body weight (BW), heart weight (HW), lung weight (LW), and tibia length (Tib) were recorded for the following analysis. Mouse hearts were randomly assigned into a pathological staining group or a molecular analysis group.

Echocardiography for Cardiac Function Analysis

Echocardiography was carried out by a MyLab 30CV ultrasound (Biosound Esaote Inc.) equipped with a 10-MHz linear array ultrasound transducer. Echocardiography was performed under continuous anesthesia with 1.5% isoflurane. M-mode tracings were recorded at the mid-papillary muscle level at the short axis of the left ventricle (LV). The LV end-systolic diameter (LVEDs) and LV end-diastolic diameter (LVEDd) were measured by M-mode tracing with a sweep speed of 50 mm/s. LV ejection fraction (EF) and fractional shortening (FS) were calculated according to LVEDs and LVEDd.

Pressure-Volume Loop for Hemodynamic Analysis

Hemodynamic changes were assessed in mice anesthetized by inhaling 1.5% isoflurane. A microtip catheter transducer (SPR-839, Millar Instruments, Houston, TX, United States) was inserted into the carotid artery until it arrived at the left ventricle. Heart rates and pressure signals were recorded *via* an ARIA pressure-volume conductance system coupled to a Powerlab/4SP A/D converter. The data collected from hemodynamics measurement were analysis by PVAN data analysis software.

Histological Staining Analysis

Mouse hearts were harvested and were immersed into 10% KCl solution for arresting in its diastole phase. Then, the mouse hearts were fixed in 10% formalin for 12 h and were dehydrated according to standard histological protocols. Dehydrated hearts were embedded in paraffin for preparing 4- to 5- μ m tissue slices. Hematoxylin-eosin (HE) staining was performed to observed heart cross-sectional area and calculate cardiomyocyte sizes. Picrosirius red (PSR) staining was performed to assess the fibrosis

in mouse heart. HE and PSR staining images were obtained using the light microscopy (Nikon). The histological analysis was performed using a quantitative digital image analysis system (Image-Pro Plus, version 6.0).

Cell Culture and Treatment

The neonatal rat cardiomyocytes (NRCMs) were isolated from 1- to 3-day-old Sprague-Dawley (SD) rats using the methods as described in previous studies (Liao et al., 2015; Yuan et al., 2016). Briefly, neonatal rat hearts were minced into 1- to 2-mm³ pieces and were digested with PBS containing 0.1% trypsin and 0.05% collagenase type II. Differential attachment culture was performed to separate cardiac fibroblasts from cardiomyocytes. NRCMs were counted and seeded at a density of 1×10^6 cells per well in six-well plates or 2×10^5 cells per well in 12-well plates. After 36 h culture in medium with BrdU, NRCMs were transfected with adenoviruses carrying a target gene sequence for another 24 h.

In this study, adenoviruses were constructed containing sequences encoding human RIP2 and short-hairpin RNA-targeting at RIP2 (Ad-shRNA RIP2). The sequences used for RIP2 knockdown were listed as follows: ShRNA1 (Top Strand: 5'-CACCGCTCGACAGTGAAAGAAATGACGAATCATTCTTTCCTGTCGAGC-3', Bottom Strand: 5'-AAAAGCTCGACAGTGAAAGAAATGATTTCGTCATTCTTTCCTGTCGAGC-3'), ShRNA2 (Top Strand: 5'-CACCGCATAGTTACTGAA TACATGCCGAAGCATGTATTCAGTAACTATGC-3', Bottom Strand: 5'-AAAAGCATAGTTACTGAATACATGCTTCGGCAT GTATTCAGTAACTATGC-3'), shRNA 3 (Top Strand: 5'-CACCGCATGATATATACAGCTATGCCGAAGCATAGCTGTA TATATCATGC-3', Bottom Strand: 5'-AAAAGCATGATA TATACAGCTATGCTTCGGCATAGCTGTATATATCATGC-3'). Similar adenoviruses carrying sequences of green fluorescent protein and short hairpin RNA was used for control. NRCMs were transfected with adenoviruses with a multiplicity of infection (MOI) of 50 per cell for 4 h and then the culture medium containing adenoviruses was removed and fresh complete culture medium was added for another 24 h of culturing. Then, NRCMs were treated with angiotensin II (Ang II, 1 μ M) or phenylephrine (PE, 50 μ M) for succeeding experiments.

Immunofluorescence Staining

Immunofluorescence staining was performed to examine the specific overexpression of RIP2 in cardiomyocytes of mouse hearts. Briefly, frozen heart sections were fixed for 15 min at room temperature after covering sections with 4% formaldehyde. After rinsing three times for 5 min for these fixed sections, blocking buffer was added for 60 min. Then, these sections were incubated with primary antibodies (anti-RIP2, 1:200 and anti- α -actin, 1:200) overnight at 4°C. The incubated sections were rinsed three times for 5 min the next day and then were incubated with fluorochrome-conjugated secondary antibody (1:1,000) for 1 h at room temperature in the dark. After rinsing three times for 5 min in PBS, these sections were covered with coverslip slides with Prolong Gold Antifade Reagent for taking pictures with fluorescence microscope in the dark.

Immunofluorescence staining was also performed to assess cardiomyocyte hypertrophy *in vitro*. Briefly, NRCMs were transfected with adenoviruses or siRNA for 24 h and then were treated with PE for another 48 h. The cells were washed with PBS, fixed with 4% paraformaldehyde for 15 min, and then permeabilized with 0.2% Triton X-100 (Amresco, 0649) for 5 min. Cells were blocked in 10% goat serum and then stained with α -actinin (Millipore, 05-384, 1:100) for overnight at 4°C. After discarding the primary antibody the next day, cells were incubated with secondary antibody conjugated with Alexa fluor 488 (1:200) for 1 h. After discarding the secondary antibody, cells were covered by glass slides with DAPI (Invitrogen, S36939) for fluorescent photography in dark. The surface area of cardiomyocytes was assessed using a quantitative digital image analysis system (Image Pro-Plus, version 6.0).

Co-immunoprecipitation

To test the interaction between TAK1 and RIP2 in HEK 293 cells, human TAK1 and RIP2 gene was cloned into pcDNA5-HA-C1 and pcDNA5-Flag-C1, respectively. pcDNA5-TAK1-HA (2 μ g) and pcDNA5-RIP2-Flag (2 μ g) was co-transfected into HEK293 cells. After 24 h of expression, cells were harvested and lysed in lysis buffer containing protease inhibitor.

To test PE promoting the interaction of RIP2 and TAK1, NRCMs were transfected with AdRIP2 with 50 MOI for 4 h and then the culture medium containing adenoviruses was removed and fresh complete culture medium was added for another 24 h of culturing. Then, NRCMs were treated with PE (50 μ M) for 24 h. Cells were harvested and lysed in lysis buffer containing protease inhibitor.

To clear non-specific protein binding, about 1 mg of protein of each sample was incubated with normal rabbit immunoglobulin G (1 μ g) and protein A/G-agarose beads (20 μ l) (Thermo Fisher Scientific, United States) for 1 h at 4°C, and then supernatants were collected after 14,000 g centrifugation for 5 min. Collected supernatants were incubated with the indicated primary antibody (1 μ g) overnight at 4°C. The next day, 40 μ l of protein A/G-agarose beads was added for another 3 h with gentle shaking. After 1000 g centrifugation for 5 min, protein A/G-agarose beads were collected and boiled in loading buffer for the next Western blots analysis.

Western Blot Analysis

Tissue or cell proteins were prepared according to published protocols (Liao et al., 2015; Yuan et al., 2016). Briefly, mouse heart tissue or NRCMs were lysed in RIPA lysis buffer for total protein extraction. BCA Protein Assay Kit was used for quantifying protein concentration. Proteins (50 μ g/sample) from different samples were used for SDS-PAGE electrophoresis and subsequently transferred to PVDF membrane (Millipore). After blocking with 5% BSA for 1 h, blots were then incubated with primary antibodies overnight at 4°C. The next day, these blots were incubated with secondary antibody conjugated with peroxidase (1:10,000, the Jackson Laboratory) for 1 h at room temperature. All blots were visualized using ChemiDoc™ XRS+ (Bio-Rad). The bands were quantified and analyzed using Image-Pro Plus 6.0. The expression of specific proteins was normalized to

corresponding GAPDH before relative quantitative analysis. The primary antibodies used in this study were purchased from Cell Signaling Technology (CST): GAPDH (#2118, 1:1,000), p-ERK1/2^{Thr202/Tyr204} (#4370, 1:1,000), T-ERK1/2 (#4695, 1:1,000), p-p38^{Thr180/Tyr182} (#4511, 1:1,000), T-p38 (#9212, 1:1,000), p-JNK^{Thr183/Tyr185} (#4668, 1:500), T-JNK (#9258, 1:1,000), RIP2 (#4142, 1:1,000), p-TAK1^{Thr184/187} (#4508, 1:500), T-TAK1 (#5206, 1:500), TGF- β , p-smad3^{ser423/425} (#8769, 1:500), and T-smad3 (#9513, 1:1,000).

Real Time Quantitative Polymerase Chain Reaction

Total RNA was extracted from the left mouse ventricular cells using TRIzol reagent (Invitrogen, United States) and was converted into cDNA using the Transcriptor First Strand cDNA Synthesis Kit (Roche, 04896866001) according to the manufacturer's protocol. SYBR Green (Roche, 04707516001) was used to detect the amplification of target genes. *Gapdh* gene expression was used as internal reference gene. The sequences of primers for real time quantitative polymerase chain reaction (RT-PCR) were provided in our previously published article (Liao et al., 2015).

Human Heart Samples

Human failing hearts were obtained from the left ventricular wall of dilated cardiomyopathy patients accepting heart transplants. Normal heart samples were collected from the left ventricular wall of healthy donor hearts without a successful matched patient on time. All procedures associated with use of human heart samples were approved by Renmin Hospital of Wuhan University, Wuhan, China. Procedures complied strictly with the principles outlined in the Declaration of Helsinki. Informed consent was signed by patients or families of prospective heart donors.

Statistical Analysis

Data are presented as mean \pm SEM. Statistical comparisons among different groups were performed by one-way analysis of variance (ANOVA) followed by a Tukey's *post hoc* test. The differences between two groups are determined by ANOVA followed by a two-tailed unpaired Student's *t*-test. All data were analyzed using SPSS 22.0 software (SPSS Inc, Chicago). $p < 0.05$ was considered significant.

RESULTS

Receptor Interacting Protein Kinase 2 Expression Was Upregulated in Hypertrophic Cardiomyocytes or Hearts

Angiotensin II (Ang II, 1 μ M) or PE (50 μ M) treatment could remarkably enhance RIP2 expression in isolated NRCMs at 1, 3, and 6 h, respectively (Figures 1A,B). RIP2 expression was significantly upregulated after 1, 2, 4, and 8 weeks of pressure overload, respectively, compared to sham surgery group (Figure 1C). In addition, RIP2 expression was also significantly upregulated in Ang II-treated mouse hearts at 1, 3, 7, and

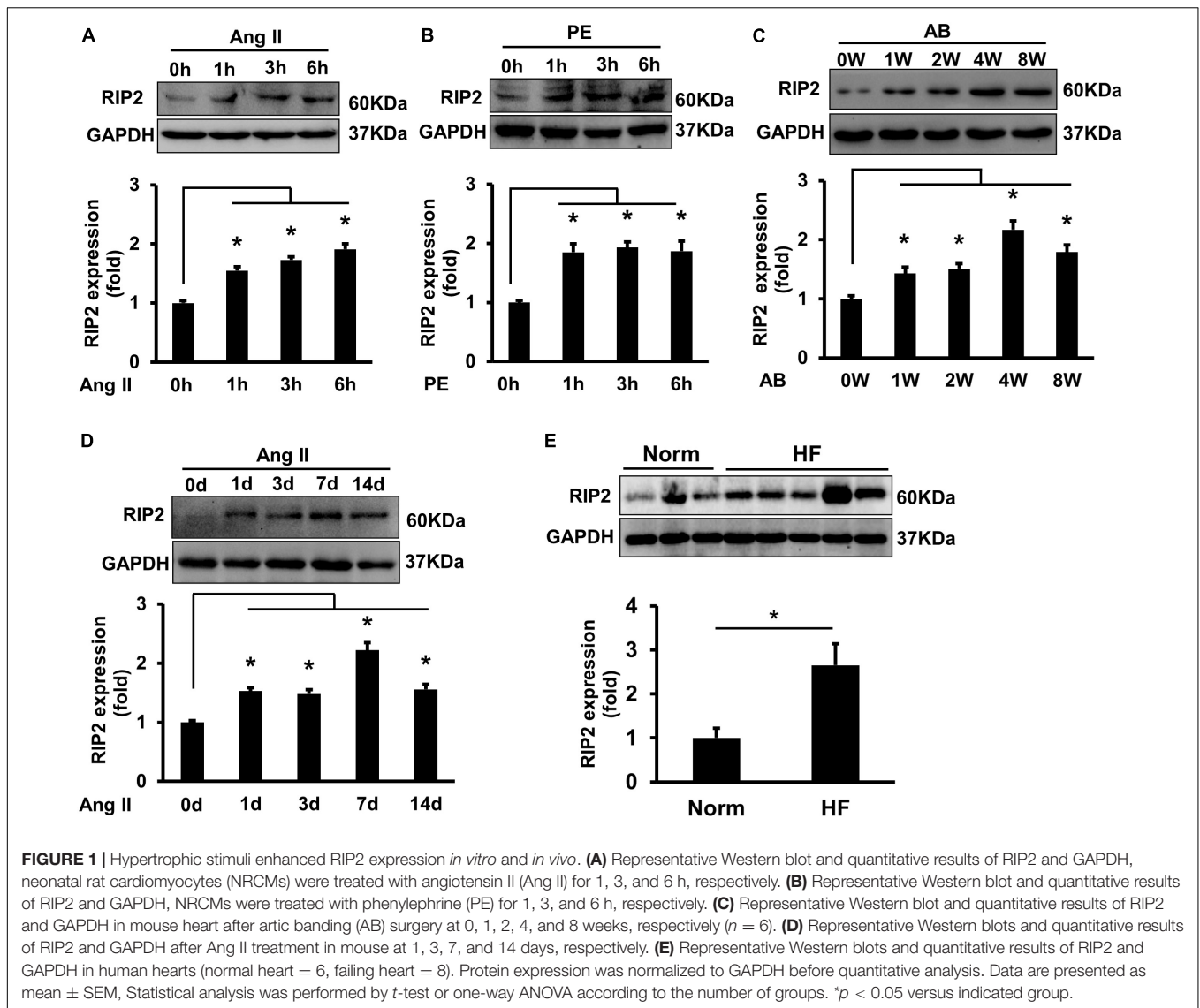


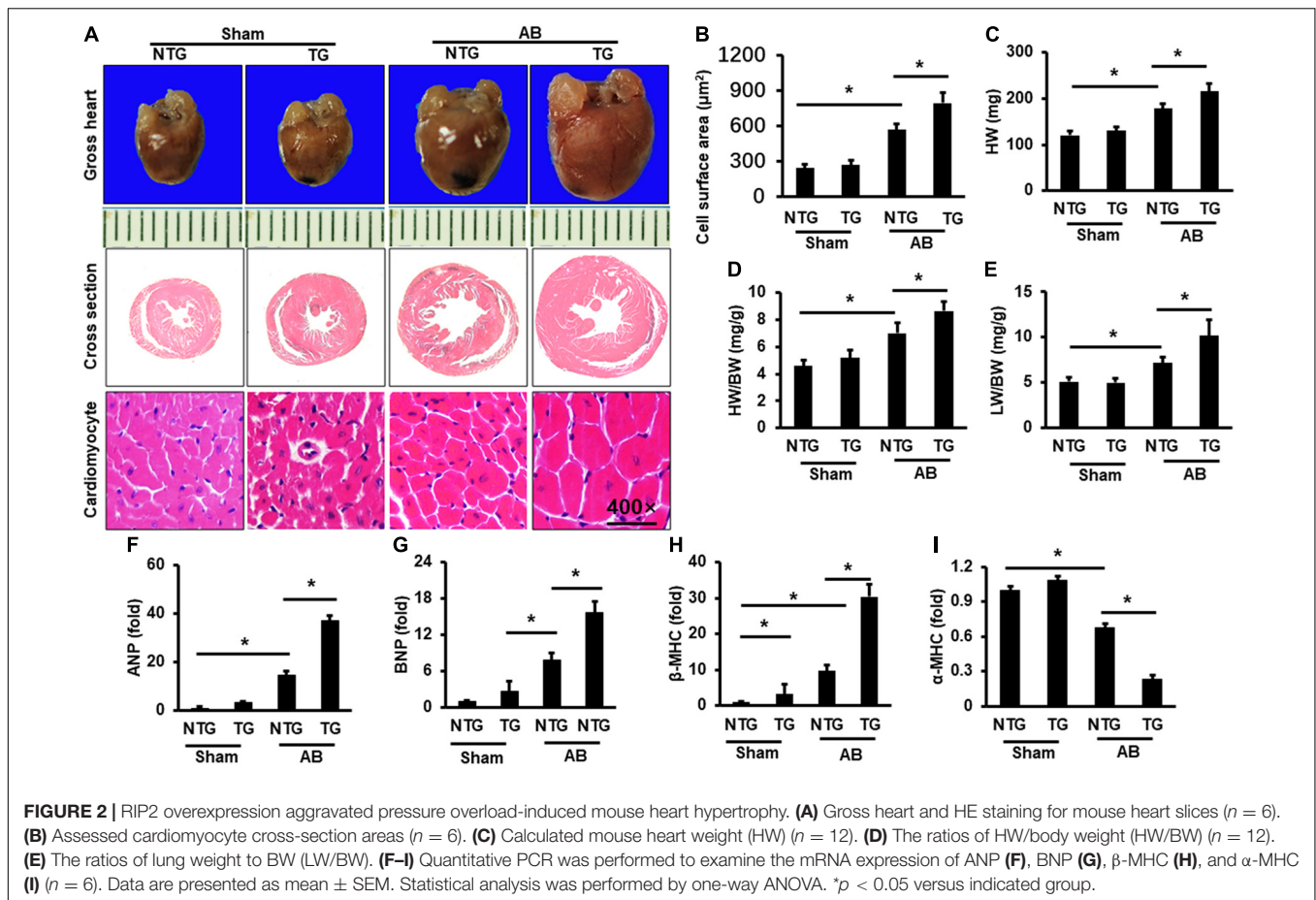
FIGURE 1 | Hypertrophic stimuli enhanced RIP2 expression *in vitro* and *in vivo*. **(A)** Representative Western blot and quantitative results of RIP2 and GAPDH, neonatal rat cardiomyocytes (NRCMs) were treated with angiotensin II (Ang II) for 1, 3, and 6 h, respectively. **(B)** Representative Western blot and quantitative results of RIP2 and GAPDH, NRCMs were treated with phenylephrine (PE) for 1, 3, and 6 h, respectively. **(C)** Representative Western blot and quantitative results of RIP2 and GAPDH in mouse heart after aortic banding (AB) surgery at 0, 1, 2, 4, and 8 weeks, respectively ($n = 6$). **(D)** Representative Western blots and quantitative results of RIP2 and GAPDH after Ang II treatment in mouse at 1, 3, 7, and 14 days, respectively. **(E)** Representative Western blots and quantitative results of RIP2 and GAPDH in human hearts (normal heart = 6, failing heart = 8). Protein expression was normalized to GAPDH before quantitative analysis. Data are presented as mean \pm SEM. Statistical analysis was performed by *t*-test or one-way ANOVA according to the number of groups. * $p < 0.05$ versus indicated group.

14 days, respectively (Figure 1D). We also presented that RIP2 was significantly upregulated in human failure hearts with dilated cardiomyopathy compared to normal donor hearts (Figure 1E). These results strongly indicated that RIP2 was involved in regulating the process of pathological cardiac remodeling and heart failure.

Receptor Interacting Protein Kinase 2 Overexpression Aggravated Pressure Overload-Induced Mouse Heart Hypertrophy

RIP2 transgene mice (TG) was constructed as described in Supplementary Figure 1. Western blots were used to test the overexpression of RIP2 in mouse heart (Supplementary Figure 1B). Mice with intermediate expression of RIP2 were selected for the following experiments (Supplementary Figure 1B). Immunofluorescence staining was used to indicate

that RIP2 has specific overexpression in cardiomyocytes of TG mice (Supplementary Figure 2). TG mice and their littermate mice (also named non-transgenic mice, NTG) were subjected to AB surgery for 4 weeks to establish mouse model of pressure overload-induced cardiac hypertrophy. As shown in Figure 2, pressure overload markedly induced cardiac hypertrophy evidenced by enlarged cardiomyocyte surface area (CSA) and increased heart weight (HW), heart weight/body weight (HW/BW), and lung weight/body weight (LW/BW) compared to the Sham group (Figures 2A–E); however, RIP2 overexpression further exacerbated cardiac hypertrophy compared with the NTG + AB group evidenced by further increased CSA, HW, HW/BW, and LW/BW (Figures 2A–E). No significant difference in CSA, HW, HW/BW, and LW/BW was detected between the NTG and TG group without AB surgery (Figures 2A–E). Consistently, pressure overload significantly increased the mRNA expression of hypertrophy-associated markers including atrial natriuretic peptide (ANP),



brain natriuretic peptide (BNP), and β -myosin heavy chain (β -MHC, a marker of the fetal gene reversion program) but decreased α -myosin heavy chain (α -MHC) expression in the NTG + AB group compared to the Sham group (Figures 2F–I). However, RIP2 overexpression further significantly increased expression of ANP, BNP, and β -MHC but decreased α -MHC expression (Figures 2F–I). Moreover, we also noted that RIP2 expression could increase β -MHC expression in the TG group compared to the NTG group without AB surgery (Figure 2H), but there was no difference in mortality between the NTG and TG group after AB operation for 4 weeks (data not shown).

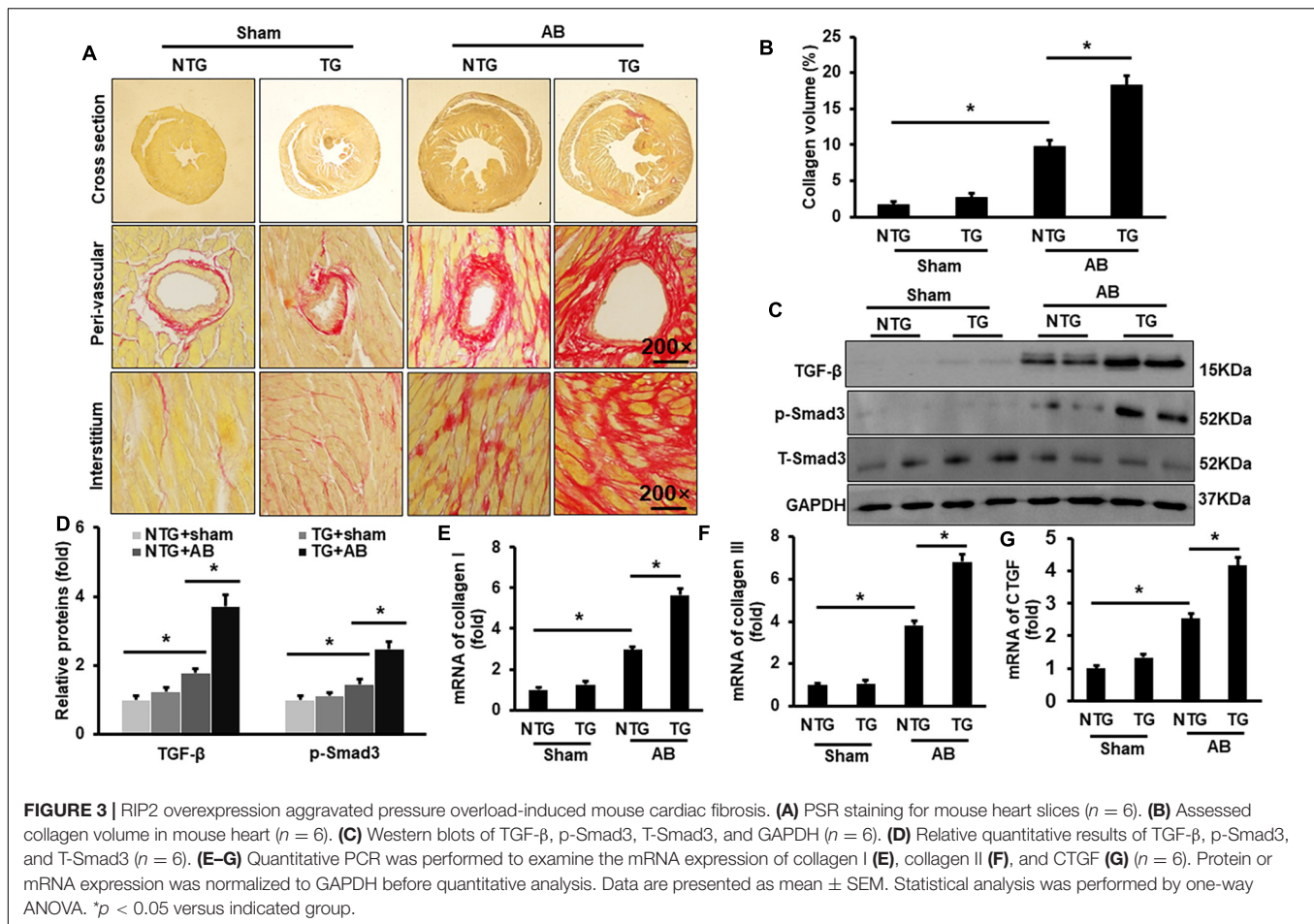
Receptor Interacting Protein Kinase 2 Overexpression Exacerbated Aortic Banding-Induced Cardiac Fibrosis

Picosirius red (PSR) was performed to evaluate cardiac fibrosis. Pressure overload induced significant fibrosis in the AB group compared to the Sham groups (Figures 3A,B). RIP2 overexpression further exacerbated pressure overload-induced cardiac fibrosis (Figures 3A,B). Pressure overload significantly activated the TGF- β /Smad3 signaling pathway in the NTG+AB group compared to the NTG + Sham group (Figures 3C,D), which could be further strengthened in the TG + AB group compared to the NTG + AB group (Figures 3C,D). Consistently,

the mRNA expression of fibrosis-associated markers, including collagen I, collagen III, and connective tissue growth factor (CTGF), was significantly upregulated in the NTG + AB group compared to the NTG + Sham group (Figures 3E–G). RIP2 overexpression further significantly boosted expression of these fibrosis-associated markers (Figures 3E–G).

Receptor Interacting Protein Kinase 2 Overexpression Aggravated Pressure Overload-Induced Cardiac Dysfunction

Echocardiography was performed to evaluate mouse cardiac function. No significant difference was examined between the NTG and TG group without AB surgery (Figures 4A–E). Pressure overload markedly increased left ventricle end-diastolic diameter (LVEDd) and LV- end-systolic diameter (LVEDs) but decreased ejection fraction (EF) and fractional shortening (FS) in the NTG + AB group compared to the NTG + Sham group (Figures 4B–E); RIP2 overexpression further significantly increased LVEDd and LVEDs and decreased EF and FS in the TG + AB group compared to the NTG + AB group (Figures 4B–E). However, there were no differences in heart rate (HR) among the four groups (Figure 4F). In addition, pressure-volume loop analysis showed that pressure overload significantly induced decline of maximal rate of pressure development (dp/dt



max), minimum rate of pressure development (dp/dt min), and stroke volume (Figures 4G–I), which could be further exacerbated after RIP2 overexpression (Figures 4G–I). Thus, RIP2 overexpression remarkably exaggerated pressure overload-induced mouse heart dysfunction.

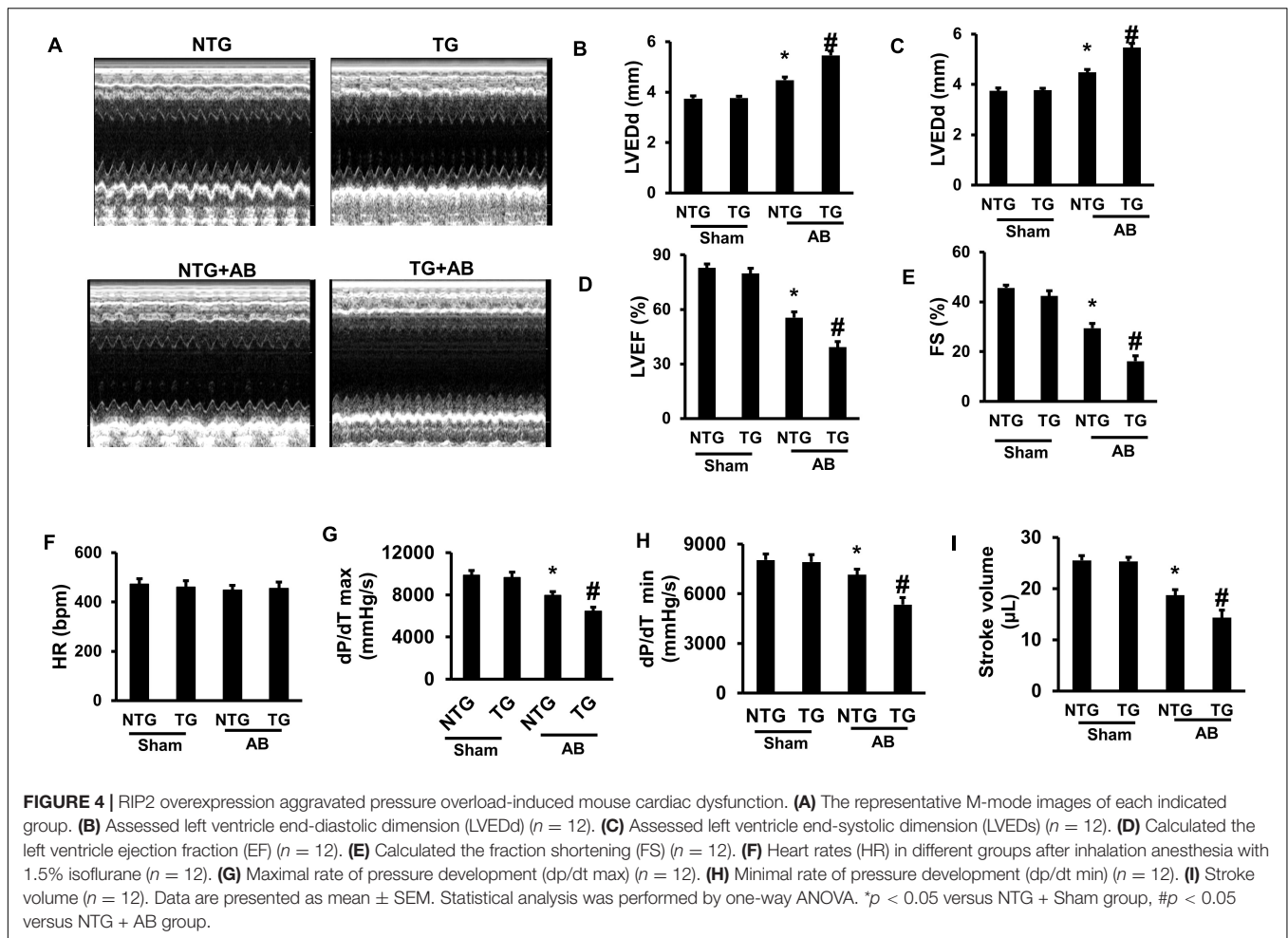
Receptor Interacting Protein Kinase 2 Overexpression Activated the TAK1/JNK1/2/P38 Signaling Pathway

RIP2 was suggested to regulate MAPK signaling in previous studies (Humphries et al., 2015), and MAPK signaling participated in regulation of pathological cardiac hypertrophy (Wu et al., 2017). This study firstly evaluated the phosphorylation status in the TAK1/MAPK pathway. Pressure overload induced hyperphosphorylation of ERK1/2, JNK1/2, p38, and TAK1 in the NTG + AB compared to the NTG + Sham group (Figures 5A–F). RIP2 overexpression further activated phosphorylation of JNK1/2 and p38 in the TG + AB group compared to the NTG + AB group but did not further activate ERK1/2 phosphorylation (Figures 5A–F). Moreover, we could also observe that RIP2 overexpression significantly activated JNK1/2 and TAK1 phosphorylation at baseline (Figures 5A,C,F).

Previous studies have demonstrated that RIP2 could mediate activation of the I κ B α /NF- κ B/p65 signaling pathway (Humphries et al., 2015; Zhao et al., 2017). In this study, we also demonstrated that pressure overload could cause significant hyperphosphorylation of I κ B α and p65 in the NTG + AB group compared to the NTG + Sham group (Figures 5G–I). RIP2 overexpression could further activate the phosphorylation of I κ B α and p65 in the TG + AB group compared to the NTG+AB group (Figures 5G–I).

Treatment of TAK1-Specific Inhibitor Completely Counteracted Receptor Interacting Protein Kinase 2 Overexpression-Mediated Cardiac Remodeling

Receptor interacting protein kinase 2 overexpression significantly increased HW, HW/BW, and LW/BW in the TG + VEH group (the RIP2 transgene mice treated with DMSO) compared to the NTG + VEH group (the non-transgene littermates treated with DMSO) after AB operation for 4 weeks (Figures 6A–C); however, no significant difference in HW, HW/BW, and LW/BW could be observed between the TG + TAKI (the RIP2 transgene mice treated with inhibitor of TAK1) and the NTG + TAKI group



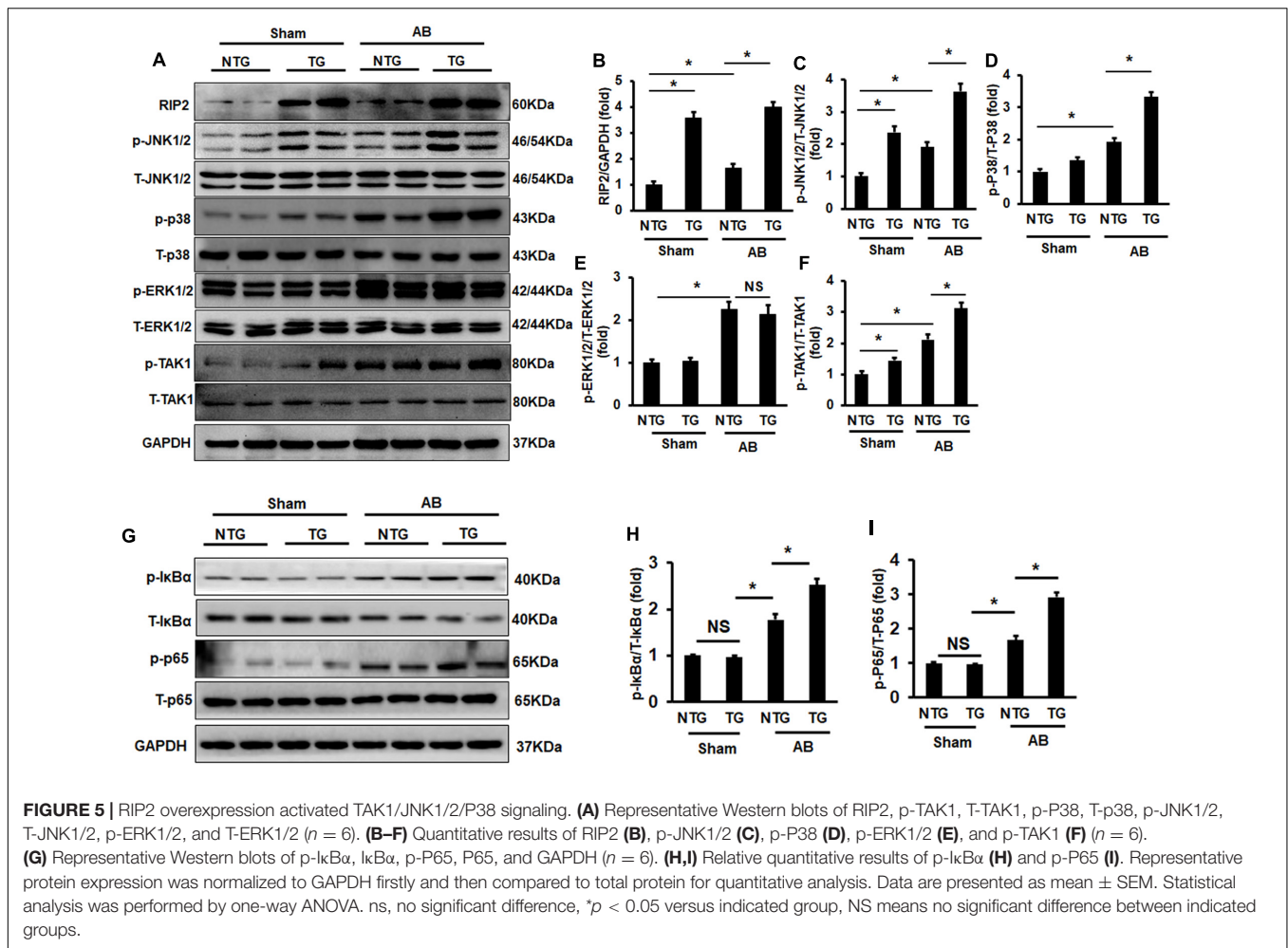
(the non-transgene littermates treated with inhibitor of TAK1) (Figures 6A–C). RIP2 overexpression remarkably exaggerated pressure overload-induced cardiomyocyte hypertrophy and interstitial fibrosis, which also exhibited no significant difference between the TG + TAKI and NTG + TAKI group (Figures 6D–F). Mechanistically, TAKI-specific inhibitor completely inhibited RIP2-mediated hyperphosphorylation of TAK, JNK1/2, and P38 (Figures 6G–L); moreover, TAKI could offset the activation the I κ B α and P65 attributed to RIP2 overexpression after AB for 4 weeks (Figures 6M–O).

Receptor Interacting Protein Kinase 2 Overexpression Exacerbated Cardiomyocyte Hypertrophy and Binding to TAK1 *in vitro*

To further clarify whether the hyperphosphorylation of TAK1/JNK1/2/P38 signaling was essential for RIP2-mediated cardiomyocyte hypertrophy, NRCMs was isolated and transfected with adenovirus for RIP2 overexpression (Ad-RIP2) or specific small interfering RNA for TAK1 silence (siTAK1), as shown in Figure 7. Ad-RIP2-mediated RIP2 overexpression significantly activated phosphorylation of

TAK1, JNK1/2, and P38 compared to the PE + GFP group (Figures 7A–E); however, siTAK1-mediated TAK1 silence completely blunted RIP2 overexpression-induced JNK1/2 and P38 phosphorylation compared to the PE + Ad-RIP2 group (Figures 7A,D,E). We also observed that RIP2 overexpression further enlarged PE-mediated NRCMs hypertrophy in the PE + Ad-RIP2 group compared to PE treatment group, which could be prevented by TAK1 silence *via* co-transfecting with siTAK1 (Figure 7F). Consistently, RIP2 overexpression notably exaggerated PE-induced expression of fetal genes, including ANP, BNP, and β -MHC in the PE + Ad-RIP2 group compared to the PE group (Figures 7H,I,K), and further exaggerated α -MHC downregulation in the PE + Ad-RIP2 group compared to the PE + GFP group (Figure 7J). Co-transfection of siTAK1 completely inhibited RIP2-mediated upregulation of ANP, BNP, and β -MHC, and downregulation of α -MHC (Figures 7H–K).

By transfecting HEK293T cells with HA-tagged TAK1 and Flag-tagged RIP2, we found that RIP2 could combine with TAK1 (Figures 7L,M). Through immunoprecipitation experiments in NRCM, we also demonstrated that PE or Ang II treatment could promote interaction between TAK1 and RIP2 as well as activate TAK1 phosphorylation (Figures 7N,O). These investigations confirmed that RIP2 overexpression contributed



to cardiomyocyte hypertrophy by mediated phosphorylation of JNK1/2 and p38 *via* directly recruited and activated TAK1.

Receptor Interacting Protein Kinase 2 Silence Could Inhibit Phenylephrine-Induced Neonatal Rat Cardiomyocytes Hypertrophy *in vitro*

Because this study has presented that pro-hypertrophic stimuli could enhance RIP2 overexpression, we next investigate whether RIP2 knockdown could inhibit PE-induced NRCM hypertrophy. Adenovirus-mediated shRNA expression was used to knock down RIP2 expression *in vitro* (Figures 8A,B). PE treatment could promote NRCM hypertrophy significantly; however, RIP2 knockdown could remarkably prevent PE-induced NRCM hypertrophy (Figures 8C,D). Consistently, the hypertrophy-associated markers including ANP, BNP, and β -MHC were significantly upregulated in the PE group compared to the VEH group (Figure 8E). These upregulated markers were markedly inhibited in the PE + shRNA group compared to the PE + Scram group (Figure 8E). Mechanistically, PE treatment significantly induced upregulation of RIP2 and hyperphosphorylation of TAK1, JNK1/2, and P38 (Figures 8F–J);

however, RIP2 knockdown significantly inhibited PE-induced hyperphosphorylation of TAK1, JNK1/2, and P38 (Figures 8F–J).

Receptor Interacting Protein Kinase 2 Overexpression Resulted in Spontaneous Cardiac Hypertrophy and Fibrosis

There were no significant differences in EF and FS between the NTG group and TG group at the age of 3 and 6 months. However, the TG mice showed a significant reduction of EF and FS compared with NTG mice at the age of 12 months, which were further decreased significantly in the 18-month-old TG group compared to the 12-month-old group (Figures 9A,B). Consistently, mice in the 12-month-old TG group had a significant higher HW/BW and LW/BW compared to the 12-month-old NTG group, which was further increased in the 18-month-old TG group compared to the 12-month-old TG group (Figures 9C,D). HE and PSR staining exhibited that RIP2 overexpression caused a significant cardiomyocyte hypertrophy and myocardial fibrosis spontaneously in the 12- and 18-month-old TG groups compared to the NTG mice of the same age group (Figures 9E–H). The deterioration of RIP2

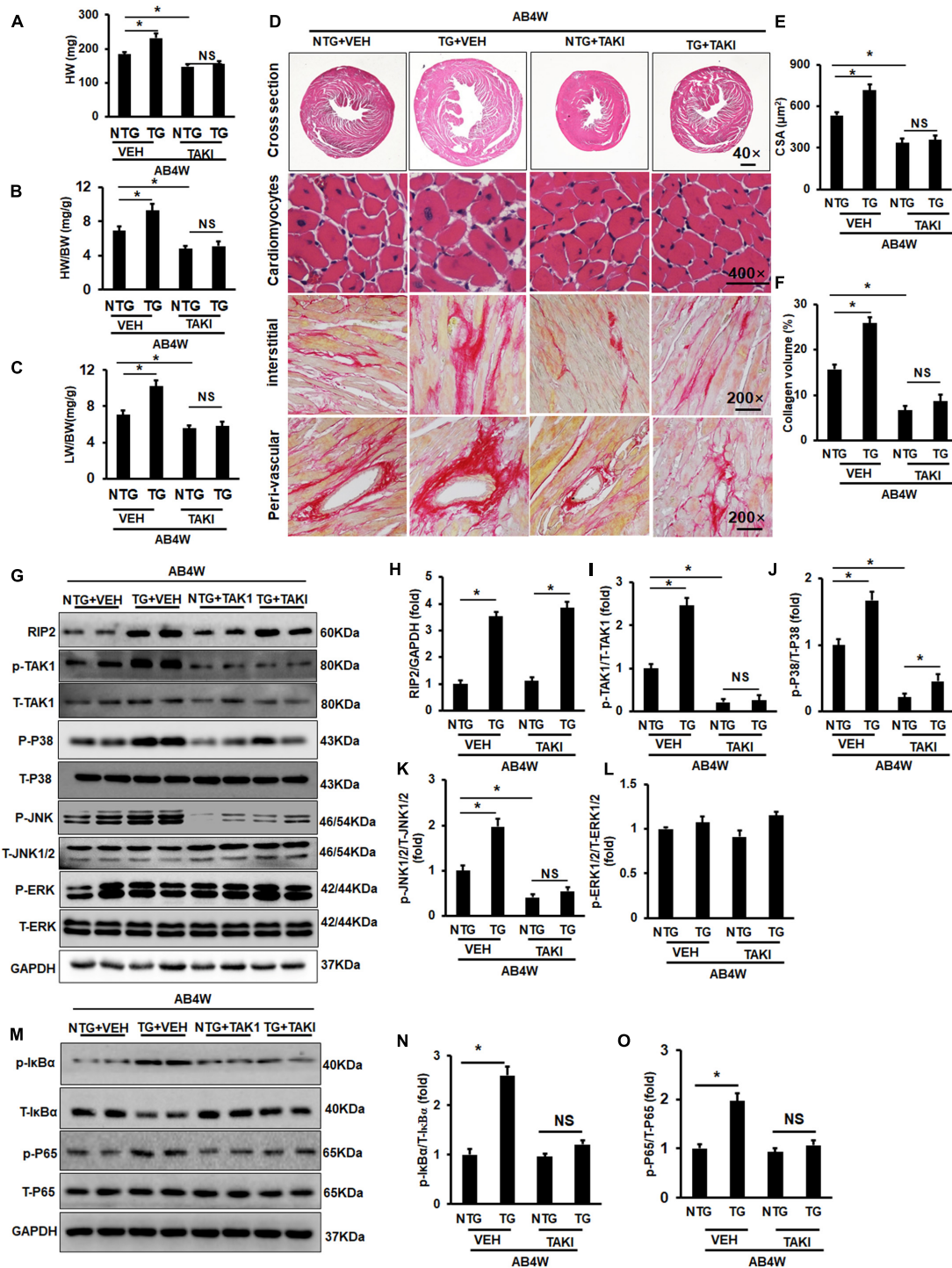


FIGURE 6 | Inhibition of TAK1 thoroughly blocked the pro-hypertrophic effect of RIP2 overexpression. **(A)** Calculated mouse heart weight (HW) ($n = 12$), the “VEH” meant the mice in indicated groups treated with DMSO (the solvent for inhibitor of TAK1), the “TAKI” meant the mice in indicated groups treated with inhibitor of TAK1, and the “AB4W” represented aortic banding operation for 4 weeks. **(B)** Calculated the ratios of HW/body weight (HW/BW) ($n = 12$). **(C)** Calculated the ratios of lung weight/BW (LW/BW) ($n = 12$). **(D)** HE and PSR staining for mouse heart slices ($n = 6$). **(E)** Assessed cardiomyocyte cross-section areas (CSA) ($n = 6$). **(F)** Assessed collagen volume in mouse heart sections ($n = 6$). **(G)** Representative Western blots of indicated proteins ($n = 6$). **(H–L)** Quantitative results of RIP2, p-TAK1, p-P38, p-JNK1/2, and p-ERK1/2, respectively ($n = 6$). **(M)** Representative Western blots of indicated proteins ($n = 6$). **(N,O)** Representative Western blot of relative proteins and the corresponding quantitative results of p-IkBα/T-IkBα and p-P65/T-P65. Protein expression was normalized to GAPDH firstly and then compared to total protein for quantitative analysis. Data are presented as mean \pm SEM. Statistical analysis was performed by one-way ANOVA. * $p < 0.05$ versus indicated group. NS means no significant difference between indicated groups.

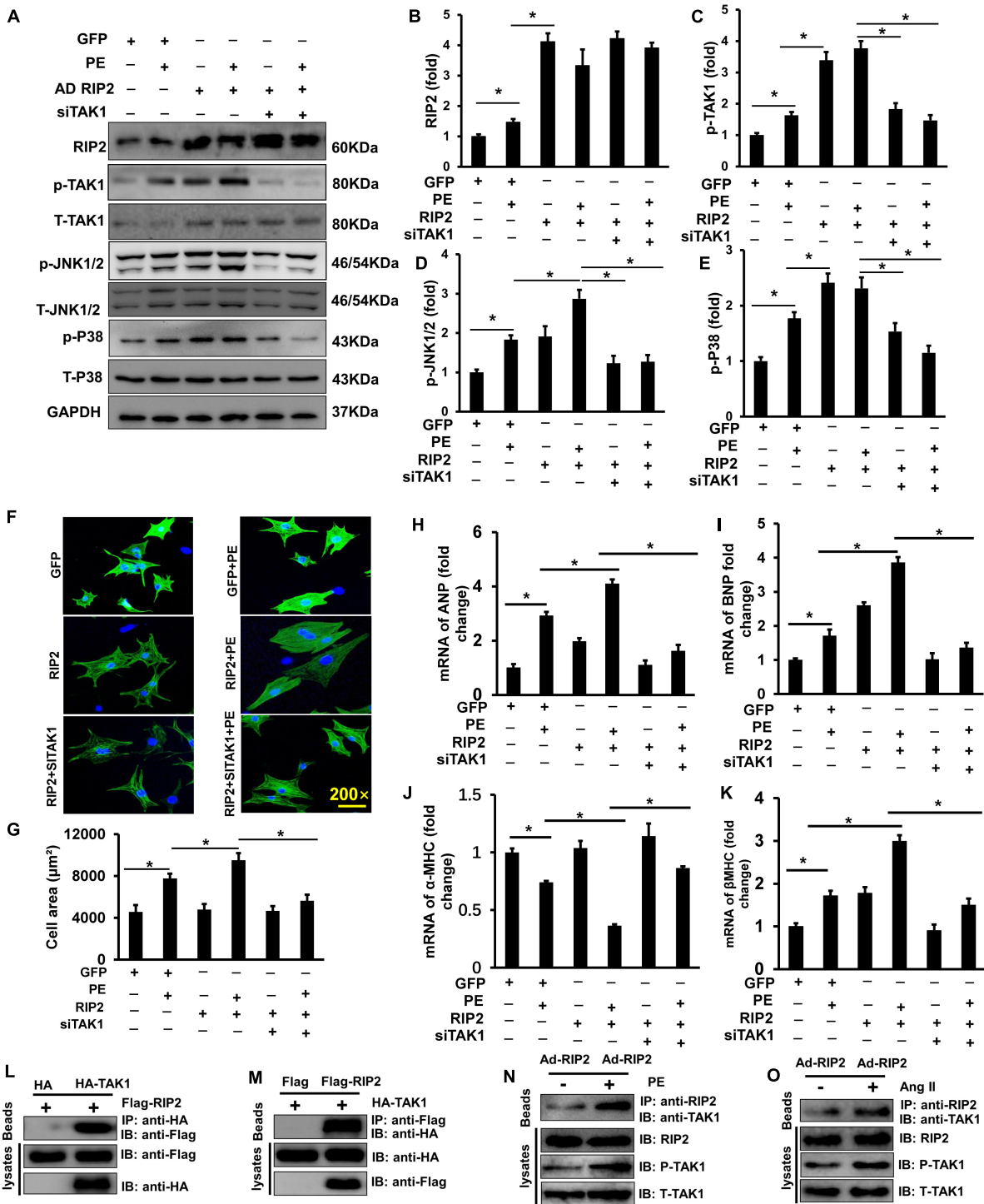
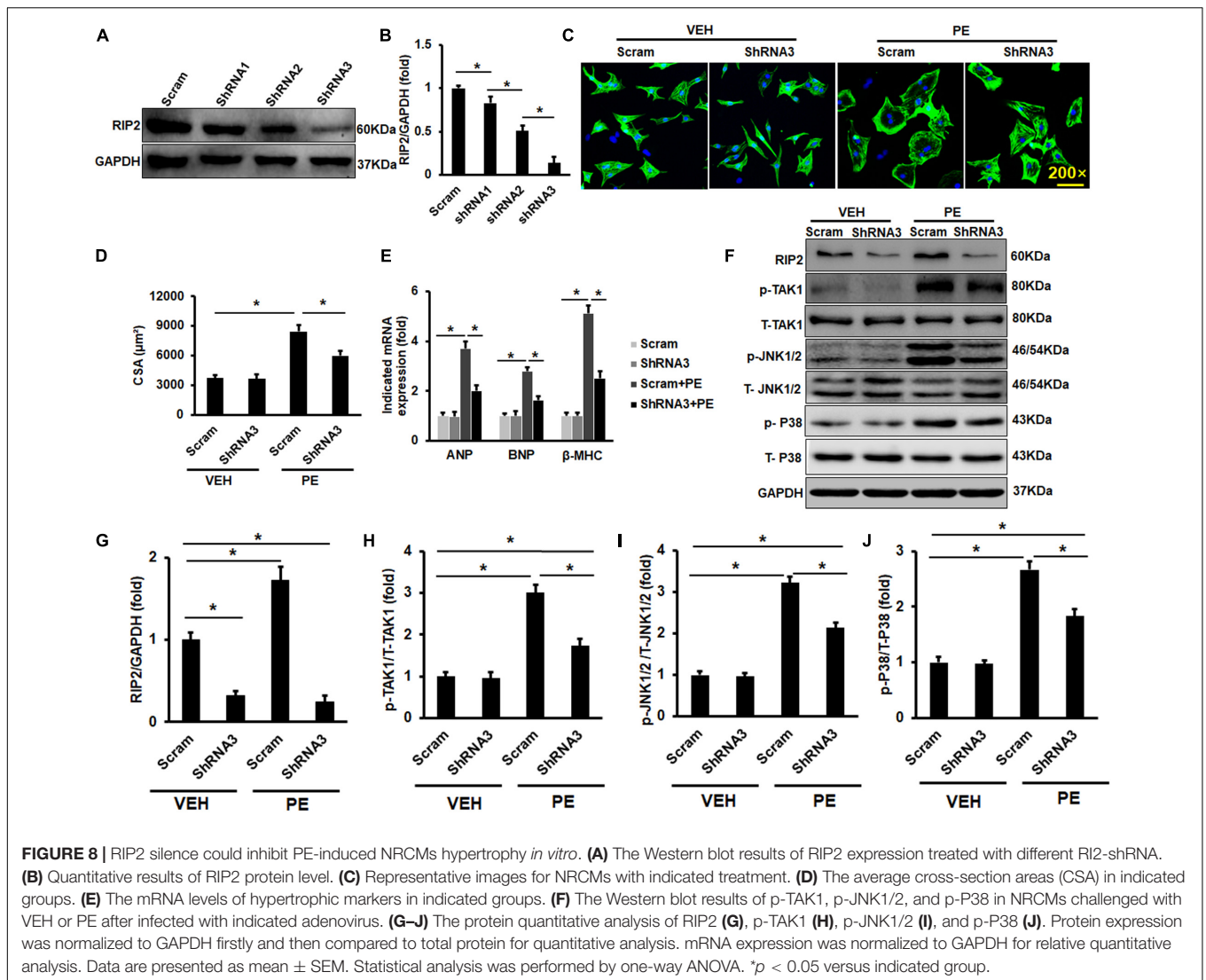


FIGURE 7 | RIP2 overexpression exacerbated cardiomyocyte hypertrophy and binding to TAK1. **(A)** Representative Western blots of RIP2, p-TAK1, T-TAK1, p-JNK1/2, T-JNK1/2, p-P38, and T-P38 after co-transfecting with AdRIP2 or siRNA for TAK1 (siTAK1) in PE-induced hypertrophic cellular model. **(B–E)** Quantitative results of RIP2 **(B)**, p-TAK1 **(C)**, p-JNK1/2 **(D)**, and p-P38 **(E)**. **(F)** Immunofluorescence staining of NRCMs with the anti- α -actinin antibody after PE treatment for 48 h. **(G)** Assessed surface area of NRCMs after PE treatment for 48 h. **(H–K)** Quantitative PCR was performed to examine the mRNA expression levels of ANP, BNP, α -MHC, and β -MHC after PE treatment for 48 h. **(L,M)** HEK293T cell was co-transfected with pcDNA-HA-TAK1 or pcDNA-Flag-RIP2. After incubating for 48 h, HEK293T cell was harvested and was lysed. Cellular lysates were used for immunoprecipitation (IP) with antibodies against HA **(L)** or Flag **(M)**. **(N,O)** The PE **(N)** and Ang II **(O)** exacerbate the interaction of RIP2 and TAK1, and activate TAK1. Protein expression was normalized to GAPDH firstly and then compared to total protein for quantitative analysis. mRNA expression was normalized to GAPDH for relative quantitative analysis. Data are presented as mean \pm SEM. Statistical analysis was performed by one-way ANOVA. * $p < 0.05$ versus indicated group.



overexpression was more significant in the TG group at age of 18 months compared to 12 months (Figures 9E–H). Taken together, RIP2 overexpression further aggravated spontaneous cardiac hypertrophy and fibrosis as aging.

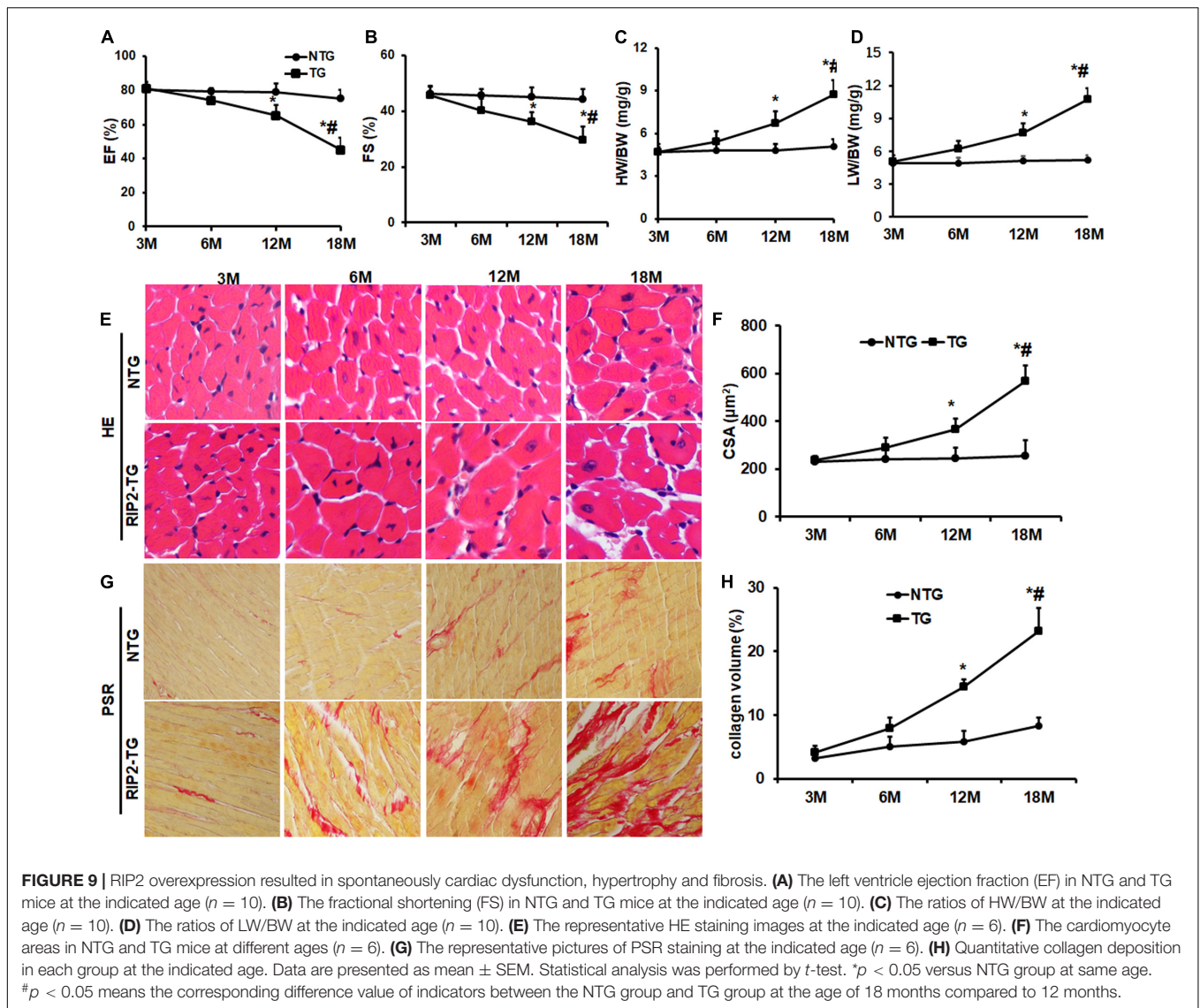
Receptor Interacting Protein Kinase 2 Knockout Attenuated Pressure Overload-Induced Cardiac Remodeling *in vivo*

Pressure overload significantly induced cardiac hypertrophy evidenced by increased HW, HW/BW, LW/BW, CSA, and collagen deposition, all of which could be significantly attenuated by RIP2 knockout (Figures 10A–F). Consistently, pressure overload promoted overexpression of pro-hypertrophy and fibrosis-associated genes including ANP, BNP, collagen I, and collagen III, all of which could be significantly downregulated after RIP2 knockout (Figures 10G–J). Mechanistically, RIP2

knockout significantly inhibited hyperphosphorylation of TAK1, JNK1/2, P38, P65, and IκBα (Figures 10K–R).

DISCUSSION

This study revealed that RIP2 was upregulated in failing human hearts with dilated cardiomyopathy and mouse hearts or NRCMs challenged with pro-hypertrophy stimuli. RIP2 overexpression exacerbated pathological cardiac hypertrophy and caused spontaneous cardiac hypertrophy, which had not been reported previously. RIP2 knockout *in vivo* or knockdown *in vitro* could remarkably attenuate pathological-associated remodeling. According to our *in vivo* and *in vitro* remodeling models, we clearly demonstrated that RIP2 overexpression activated TAK1/JNK1/2/P38 and IκBα/P65 signaling. Moreover, immunoprecipitation indicated that the RIP2–TAK1 interaction might be essential for RIP2-mediated malignant activation of TAK1/JNK1/2/P38 and IκBα/P65 signaling.



This study demonstrated that RIP2 overexpression could significantly promote p38 and JNK1/2 phosphorylation activation. Many studies have exhibited that the activation of MAPK (p38, JNK1/2, and ERK1/2) signaling during pathological stress accelerated the process and development of cardiac hypertrophy and transformation to heart failure (Rose et al., 2010; Yokota and Wang, 2016; Gallo et al., 2019). MAPKs are key signaling transduction nodes that receive many upstream signaling and transmit tens of signal pathways to downstream (Rose et al., 2010). MAPK signaling regulated many biological events including proliferation, differentiation, metabolism, survival, and apoptosis (Rose et al., 2010). Direction inhibition of MAPKs might disrupt some normal physiological functions; thus, investigators have been trying their best to seek upstream regulating mechanisms of MAPK activation with the hope of finding out new therapeutic ways to treat malignant cardiac remodeling or heart failure without disrupting physiological functions.

This study clearly demonstrated that RIP2 was an upstream regulating kinase of MAPK, and inhibiting RIP2 upregulation might be a potential strategy for preventing malignant cardiomyocyte hypertrophy.

Li et al. (2015) showed that RIP2 overexpression could aggravate myocardial infarction-associated cardiac remodeling by boosting p38 hyperphosphorylation. RIP2 could also cause myocardial p38 dual phosphorylation in endotoxin component MDP-treated mouse heart (Jacquet et al., 2008). However, in another article of exposure to MDP before ischemia-reperfusion injury, RIP2-dependent activation of TAK1/JNK1/2 MAPK signaling markedly reduced infarction mouse heart size (Sicard et al., 2009). In triple-negative breast cancer cell, RIP2 overexpression promoted cell migration and invasion *via* activating JNK1/2 and NF- κ B signaling pathways (Singel et al., 2014). These studies showed that RIP2 seemed to regulate p38/MAPK or JNK1/2 MAPK depending on different cell or disease circumstances, respectively. We firstly demonstrated that

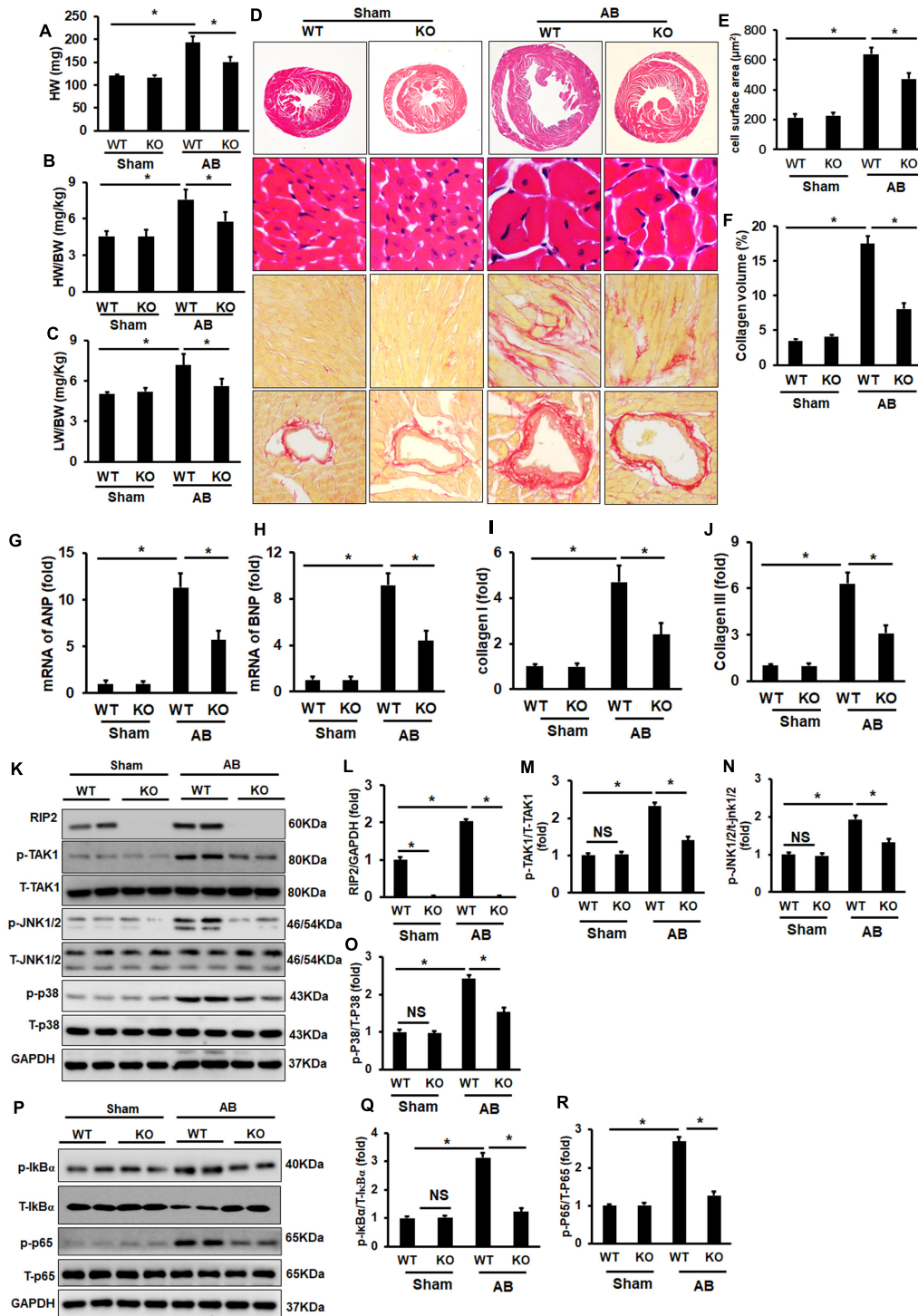


FIGURE 10 | RIP2 knockout attenuated pressure overload-induced cardiac remodeling. **(A–C)** The heart weight (HW) of wild-type mice (WT) and RIP2 global knockout (KO) mice subjected with AB or sham operation **(A)**; calculated the ratios of HW/body weight (HW/BW) **(B)**; calculated the ratios of lung weight/ BW (LW/BW) **(C)**. **(D)** HE and PSR staining for mouse heart slices (n = 6). **(E)** Assessed cardiomyocyte cross-section areas (CSA) (n = 6). **(F)** Assessed collagen volume in mouse heart sections (n = 6). **(G–J)** Relative mRNA levels of ANP **(G)**, BNP **(H)**, Collagen I **(I)**, and Collagen III **(J)**. **(K)** Representative Western blots of RIP2, p-TAK1, T-TAK1, p-P38, T-p38, p-JNK1/2, T-JNK1/2, and GAPD (n = 6). **(L–O)** Quantitative results of RIP2 **(L)**, p-TAK1 **(M)**, p-JNK1/2 **(N)**, and p-P38 **(O)** (n = 6). **(P)** Representative Western blots of p-IkBα, p-P65, T-P65, and GAPDH. **(Q)** The fold change of p-IkBα in four groups. **(R)** The fold change of p-P65 in the indicated groups. Protein expression was normalized to GAPDH firstly and then compared to total protein for quantitative analysis. The mRNA level was normalized to GAPDH and then for quantitative analysis. Data are presented as mean ± SEM. Statistical analysis was performed by one-way ANOVA. *p < 0.05 versus the indicated group.

TAK1 inhibition could completely prevent RIP2 overexpression-induced malignant mouse heart hypertrophy.

TAK1 is a key molecular node and locates at upstream of MAPK signaling (Ji et al., 2016; Li et al., 2016). TAK1 overactivation under different disease conditions could significantly exacerbate malignant cardiac hypertrophy (Ji et al., 2016; Li et al., 2016); however, TAK1-specific ablation in mouse heart caused spontaneous cardiac remodeling and heart failure (Li et al., 2014). Because TAK1 plays important roles in regulating many physiological activities, including cell apoptosis (Li et al., 2014), innate and adaptive immune (Sato et al., 2005), development (Jadrich et al., 2006), and cardiomyocyte differentiation (Monzen et al., 2001), it is necessary to find out a way to maintain TAK1 phosphorylation at its physiological level neither over-activation nor excessive inhibition in treating cardiac remodeling. This study indicated that RIP2 located at the upstream of TAK1, inhibiting RIP2 upregulation, might avoid disturbance of normal physiological activities of TAK1.

In this manuscript, we firstly exhibited that RIP2 overexpression in cardiomyocytes aggravated pressure overload-induced cardiac remodeling and led to spontaneous cardiac remodeling. In addition, our research also exhibited that global deletion of RIP2 could prevent pressure overload-induced cardiac hypertrophy. Consistently, Zhao et al. (2017) reported that RIP2 knockout could mitigate AB-induced cardiac hypertrophy, fibrosis, and inflammation *via* reducing TLR4/MyD88/NF- κ B, MAPKs, and TGF- β /Smad signaling. We further clarified in this study that RIP2 mediated MAPK (JNK1/2 and p38) and I κ B α /p65 activation *via* binding and phosphorylating TAK1. Recently, Lin et al. (2020) demonstrated that RIP2 upregulation could promote mitochondrial antiviral signaling protein (MAVS) expression, exaggerating pressure overload-induced pathological remodeling. Our data in this study and these published findings suggested that RIP2 inhibition might be a potential strategy for treating malignant cardiac remodeling.

Another problem was how RIP2 was upregulated and activated in cardiomyocytes challenged with pro-hypertrophic stimuli. MDP-mediated NOD2 oligomerization contributes to the classical activation of RIP2 activity resulting in activating I κ B α /NF- κ B/p65 and MAPKs/AP1 signaling (Humphries et al., 2015). Obviously, RIP2 activation in this manuscript was not from MDP-mediated NOD2 oligomerization. Except for NOD2-mediated RIP2 activity regulation, several E3 ubiquitin ligases, such as Pellino3, ITCH, TRAF6, cIAP, and XIAP, have been suggested to catalyze RIP2 ubiquitination. ITCH-mediated RIP2 ubiquitination has been demonstrated to inhibit NF- κ B signaling. From these investigations, we know that the upstream regulation pathway of RIP2 is complex, and some other investigations are necessary to clarify the upstream regulating mechanism of RIP2 in the process and development of malignant cardiac hypertrophy in succeeding studies.

CONCLUSION

This study clearly presented that RIP2 was upregulated and was a key molecular switch for the development and progress

of pathological cardiac hypertrophy. RIP2 overexpression could lead to spontaneous cardiac dysfunction and remodeling even without challenging pressure overload, which meant that RIP2 was a key regulator for cardiac remodeling and was a powerful target for treating cardiac remodeling. Mechanically, upregulated RIP2 after pathological stimuli could contribute to RIP2-TAK1 interactions, resulting in TAK1 phosphorylation and activation, which further induced phosphorylation and activation of MAPKs (JNK1/2 and p38) and I κ B α /P65, resulting in malignant cardiac hypertrophy. Thus, inhibition of RIP2 upregulation or its interaction with TAK1 might be a potential strategy for preventing pathological cardiac hypertrophy.

DATA AVAILABILITY STATEMENT

The original contributions presented in the study are included in the article/**Supplementary Material**, further inquiries can be directed to the corresponding author/s.

ETHICS STATEMENT

The studies involving human participants were reviewed and approved by the Ethics Committee of Renmin Hospital of Wuhan University. The patients/participants provided their written informed consent to participate in this study. The animal study was reviewed and approved by Animal Care and Use Committee of Renmin Hospital of Wuhan University.

AUTHOR CONTRIBUTIONS

J-JY and NZ finished most of the work in this study (including WB, qPCR, HE, and PSR staining). JN and HF were responsible for data collection and analysis. W-JL, Z-YZ, and S-QM completed the extraction of neonatal rat cardiomyocytes. H-MW was responsible for animal operation. H-HL and Q-ZT designed and conducted this study. All authors contributed to the article and approved the submitted version.

FUNDING

This work was supported by grants from the National Natural Science Foundation of China (81530012 and 81800217), the National Key R&D Program of China (2018YFC1311300), the Development Center for Medical Science and Technology National Health and Family Planning Commission of the People's Republic of China (The prevention and control project of cardiovascular disease, 2016ZX-008-01), and the Fundamental Research Funds for the Central Universities (2042018kf1032).

SUPPLEMENTARY MATERIAL

The Supplementary Material for this article can be found online at: <https://www.frontiersin.org/articles/10.3389/fcell.2021.688238/full#supplementary-material>

Supplementary Figure 1 | (A) The schematic diagram of construction of specifically overexpressing RIP2 in cardiomyocytes. **(B)** The western-blot result of RIP2 protein and fold changes of RIP2 in different transgenic lines. * $P < 0.05$ versus indicated group.

Supplementary Figure 2 | Immunofluorescence staining detected RIP2 expression in mouse heart, red represented α -actin, green represented rip2, blue represent nucleus. Negative: without addition of RIP2 and α -actin antibody in the staining process, WT, wild type; KO, knockout; TG, Transgene.

REFERENCES

- Andersson, L., Scharin Tang, M., Lundqvist, A., Lindbom, M., Mardani, I., Fogelstrand, P., et al. (2015). Rip2 modifies VEGF-induced signalling and vascular permeability in myocardial ischaemia. *Cardiovasc. Res.* 107, 478–486. doi: 10.1093/cvr/cvv186
- Gallo, S., Vitacolonna, A., Bonzano, A., Comoglio, P., and Crepaldi, T. (2019). ERK: a key player in the pathophysiology of cardiac hypertrophy. *Int. J. Mol. Sci.* 20:2164. doi: 10.3390/ijms20092164
- Gibb, A. A., and Hill, B. G. (2018). Metabolic coordination of physiological and pathological cardiac remodeling. *Circ. Res.* 123, 107–128. doi: 10.1161/CIRCRESAHA.118.312017
- Gonzalez, A., Ravassa, S., Lopez, B., Moreno, M. U., Beaumont, J., San Jose, G., et al. (2018). Myocardial remodeling in hypertension. *Hypertension* 72, 549–558. doi: 10.1161/HYPERTENSIONAHA.118.11125
- Humphries, F., Yang, S., Wang, B., and Moynagh, P. N. (2015). RIP kinases: key decision makers in cell death and innate immunity. *Cell Death Differ.* 22, 225–236. doi: 10.1038/cdd.2014.126
- Jacquet, S., Nishino, Y., Kumphune, S., Sicard, P., Clark, J. E., Kobayashi, K. S., et al. (2008). The role of RIP2 in p38 MAPK activation in the stressed heart. *J. Biol. Chem.* 283, 11964–11971. doi: 10.1074/jbc.M707750200
- Jadrich, J. L., O'Connor, M. B., and Coucouvanis, E. (2006). The TGF beta activated kinase TAK1 regulates vascular development in vivo. *Development* 133, 1529–1541. doi: 10.1242/dev.02333
- Ji, Y. X., Zhang, P., Zhang, X. J., Zhao, Y. C., Deng, K. Q., Jiang, X., et al. (2016). The ubiquitin E3 ligase TRAF6 exacerbates pathological cardiac hypertrophy via TAK1-dependent signalling. *Nat. Commun.* 7:11267. doi: 10.1038/ncomms11267
- Li, C. Y., Zhou, Q., Yang, L. C., Chen, Y. H., Hou, J. W., Guo, K., et al. (2016). Dual-specificity phosphatase 14 protects the heart from aortic banding-induced cardiac hypertrophy and dysfunction through inactivation of TAK1-P38MAPK/JNK1/2 signaling pathway. *Basic Res. Cardiol.* 111:19. doi: 10.1007/s00395-016-0536-7
- Li, L., Chen, Y., Doan, J., Murray, J., Molkenin, J. D., and Liu, Q. (2014). Transforming growth factor beta-activated kinase 1 signaling pathway critically regulates myocardial survival and remodeling. *Circulation* 130, 2162–2172. doi: 10.1161/CIRCULATIONAHA.114.011195
- Li, L., Wang, X., Chen, W., Qi, H., Jiang, D. S., Huang, L., et al. (2015). Regulatory role of CARD3 in left ventricular remodelling and dysfunction after myocardial infarction. *Basic Res. Cardiol.* 110:56. doi: 10.1007/s00395-015-0515-4
- Liao, H. H., Zhang, N., Feng, H., Zhang, N., Ma, Z. G., Yang, Z., et al. (2015). Oleoalcohol alleviated pressure overload-induced cardiac remodeling. *Mol. Cell Biochem.* 409, 145–154. doi: 10.1007/s11010-015-2520-1
- Lin, H. B., Naito, K., Oh, Y., Farber, G., Kanaan, G., Valaperti, A., et al. (2020). Innate immune Nod1/RIP2 signaling is essential for cardiac hypertrophy but requires mitochondrial antiviral signaling protein for signal transductions and energy balance. *Circulation* 142, 2240–2258. doi: 10.1161/CIRCULATIONAHA.119.041213
- Monzen, K., Hiroi, Y., Kudoh, S., Akazawa, H., Oka, T., Takimoto, E., et al. (2001). Smads, TAK1, and their common target ATF-2 play a critical role in cardiomyocyte differentiation. *J. Cell Biol.* 153, 687–698. doi: 10.1083/jcb.153.4.687
- Morita, H., and Komuro, I. (2018). Heart failure as an aging-related phenotype. *Int. Heart J.* 59, 6–13. doi: 10.1536/ihj.17-519
- Rose, B. A., Force, T., and Wang, Y. (2010). Mitogen-activated protein kinase signaling in the heart: angels versus demons in a heart-breaking tale. *Physiol. Rev.* 90, 1507–1546. doi: 10.1152/physrev.00054.2009
- Sato, S., Sanjo, H., Takeda, K., Ninomiya-Tsuji, J., Yamamoto, M., Kawai, T., et al. (2005). Essential function for the kinase TAK1 in innate and adaptive immune responses. *Nat. Immunol.* 6, 1087–1095. doi: 10.1038/ni1255
- Sicard, P., Jacquet, S., Kobayashi, K. S., Flavell, R. A., and Marber, M. S. (2009). Pharmacological postconditioning effect of muramyl dipeptide is mediated through RIP2 and TAK1. *Cardiovasc. Res.* 83, 277–284. doi: 10.1093/cvr/cvp055
- Singel, S. M., Batten, K., Cornelius, C., Jia, G., Fasciani, G., Barron, S. L., et al. (2014). Receptor-interacting protein kinase 2 promotes triple-negative breast cancer cell migration and invasion via activation of nuclear factor-kappaB and c-Jun N-terminal kinase pathways. *Breast Cancer Res.* 16:R28. doi: 10.1186/bcr3629
- Wu, Q. Q., Xiao, Y., Yuan, Y., Ma, Z. G., Liao, H. H., Liu, C., et al. (2017). Mechanisms contributing to cardiac remodeling. *Clin. Sci.* 131, 2319–2345. doi: 10.1042/CS20171167
- Yancy, C. W., Jessup, M., Bozkurt, B., Butler, J., Casey, D. E. Jr., Colvin, M. M., et al. (2017). 2017 ACC/AHA/HFSA focused update of the 2013 ACCF/AHA guideline for the management of heart failure: a report of the american college of cardiology/american heart association task force on clinical practice guidelines and the heart failure society of america. *Circulation* 136, e137–e161.
- Yokota, T., and Wang, Y. (2016). p38 MAP kinases in the heart. *Gene* 575, 369–376.
- Yuan, Y., Yan, L., Wu, Q. Q., Zhou, H., Jin, Y. G., Bian, Z. Y., et al. (2016). Mnk1 (mitogen-activated protein kinase-interacting kinase 1) deficiency aggravates cardiac remodeling in mice. *Hypertension* 68, 1393–1399.
- Zhao, C. H., Ma, X., Guo, H. Y., Li, P., and Liu, H. Y. (2017). RIP2 deficiency attenuates cardiac hypertrophy, inflammation and fibrosis in pressure overload induced mice. *Biochem. Biophys. Res. Commun.* 493, 1151–1158.

Conflict of Interest: The authors declare that the research was conducted in the absence of any commercial or financial relationships that could be construed as a potential conflict of interest.

Publisher's Note: All claims expressed in this article are solely those of the authors and do not necessarily represent those of their affiliated organizations, or those of the publisher, the editors and the reviewers. Any product that may be evaluated in this article, or claim that may be made by its manufacturer, is not guaranteed or endorsed by the publisher.

Copyright © 2021 Yang, Zhang, Zhou, Ni, Feng, Li, Mou, Wu, Deng, Liao and Tang. This is an open-access article distributed under the terms of the Creative Commons Attribution License (CC BY). The use, distribution or reproduction in other forums is permitted, provided the original author(s) and the copyright owner(s) are credited and that the original publication in this journal is cited, in accordance with accepted academic practice. No use, distribution or reproduction is permitted which does not comply with these terms.



Augmented Liver Uptake of the Membrane Voltage Sensor Tetraphenylphosphonium Distinguishes Early Fibrosis in a Mouse Model

Himanshi Pandita¹, Esteban Mezey² and Shanmugasundaram Ganapathy-Kanniappan^{1*}

¹ Division of Interventional Radiology, Russell H. Morgan Department of Radiology and Radiological Science, The Johns Hopkins University School of Medicine, Baltimore, MD, United States, ² Division of Gastroenterology and Hepatology, Department of Medicine, The Johns Hopkins University School of Medicine, Baltimore, MD, United States

OPEN ACCESS

Edited by:

Gonzalo del Monte-Nieto,
Monash University, Australia

Reviewed by:

Chuantao Tu,
Shanghai Fourth People's
Hospital, China
John J. Lemasters,
Medical University of South Carolina,
United States

*Correspondence:

Shanmugasundaram
Ganapathy-Kanniappan
gshanmu1@jhmi.edu

Specialty section:

This article was submitted to
Integrative Physiology,
a section of the journal
Frontiers in Physiology

Received: 05 March 2021

Accepted: 21 September 2021

Published: 25 October 2021

Citation:

Pandita H, Mezey E and
Ganapathy-Kanniappan S (2021),
Augmented Liver Uptake of the
Membrane Voltage Sensor
Tetraphenylphosphonium
Distinguishes Early Fibrosis in a Mouse
Model. *Front. Physiol.* 12:676722.
doi: 10.3389/fphys.2021.676722

Mitochondrial (mito-) oxidative phosphorylation (OxPhos) is a critical determinant of cellular membrane potential/voltage. Dysregulation of OxPhos is a biochemical signature of advanced liver fibrosis. However, less is known about the net voltage of the liver in fibrosis. In this study, using the radiolabeled [³H] voltage sensor, tetraphenylphosphonium (TPP), which depends on membrane potential for cellular uptake/accumulation, we determined the net voltage of the liver in a mouse model of carbon tetrachloride (CCl₄)-induced hepatic fibrosis. We demonstrated that the liver uptake of ³H-TPP significantly increased at 4 weeks of CCl₄-administration (6.07 ± 0.69% ID/g, *p* < 0.05) compared with 6 weeks (4.85 ± 1.47% ID/g) and the control (3.50 ± 0.22% ID/g). Analysis of the fibrosis, collagen synthesis, and deposition showed that the increased ³H-TPP uptake at 4 weeks corresponds to early fibrosis (F1), according to the METAVIR scoring system. Biodistribution data revealed that the ³H-TPP accumulation is significant in the fibrogenic liver but not in other tissues. Mechanistically, the augmentation of the liver uptake of ³H-TPP in early fibrosis concurred with the upregulation of mito-electron transport chain enzymes, a concomitant increase in mito-oxygen consumption, and the activation of the AMPK-signaling pathway. Collectively, our results indicate that mito-metabolic response to hepatic insult may underlie the net increase in the voltage of the liver in early fibrosis.

Keywords: liver fibrosis, membrane-voltage sensor, tetraphenylphosphonium (TPP), mitochondrial respiration, electron transport chain, carbon tetrachloride, liver voltage

INTRODUCTION

Liver fibrosis/cirrhosis represents a worldwide health problem, and epidemiological data indicate that 70–80% of cirrhotic patients develop primary liver cancer, hepatocellular carcinoma (Hernandez-Gea and Friedman, 2011). Liver fibrosis results from chronic inflammation and/or injury to the liver parenchyma. Irrespective of the cause, liver fibrosis may lead to cirrhosis and remains a major cause of liver failure (Farazi and DePinho, 2006; Amann et al., 2009).

Emerging reports underscore the role of mitochondrial (mito-) dynamics and alterations in mito-metabolism in liver diseases (Han et al., 2012; McCommis and Finck, 2019).

Mito-dysfunction and structural abnormalities are the hallmarks of advanced liver fibrosis/cirrhosis (Krahenbuhl et al., 2000; Rodrigues and Steer, 2000; Grattagliano et al., 2011; Kang et al., 2016; Mansouri et al., 2018). Particularly, mito-oxidative phosphorylation (OxPhos) is impaired in the hepatocytes of advanced fibrosis and cirrhosis implying a switch in energy metabolism (Ganapathy-Kanniappan et al., 2014; Nishikawa et al., 2014). In contrast, in hepatic stellate cells (HSCs), the fibrogenic phenotype exhibits enhanced mito-bioenergetics, resulting in elevated mito-membrane potential (MMP, $\Delta\psi_m$) (Gajendiran et al., 2018). However, there is paucity in the documentation of net MMP of the liver in fibrogenesis. Noteworthy, OxPhos and the related electron transport chain (ETC) impact the mito-electrochemical gradient, a critical determinant of the net MMP. In this study, we investigated whether the mito-response/sensitivity to hepatic insult in early phases of fibrogenesis affects the net liver-MMP. Using the radiolabeled [^3H] voltage sensor, tetraphenylphosphonium (TPP), which depends on membrane potential for cellular uptake/accumulation (Moreno et al., 2015), we determined the liver uptake of ^3H -TPP in a mouse model of carbon tetrachloride (CCl_4)-induced hepatic fibrosis.

Tetraphenylphosphonium and its analogs are extensively employed molecular probes in the analysis of MMP and the related bioenergetics (Kamo et al., 1979; Wan et al., 1993). In fact, one of the earliest reports, in the late 1960s, demonstrated the application of TPP as a chemical indicator of MMP (Lieberman et al., 1969). The specificity and selectivity of the cellular TPP uptake and its correlation with MMP have been widely documented. Experimentally, in human skin fibroblasts, the cellular uptake of TPP correlates with the MMP, and a decrease in MMP reduces its cellular uptake (Rugolo and Lenaz, 1987). Besides, several TPP-conjugated therapeutic agents have also been shown to target cells with elevated mito-activity (Han et al., 2014; Pathak et al., 2014; Gajendiran et al., 2018). Thus, the mito-specificity of the TPP uptake has been well-established (Chen, 1988). Due to the relevance of mito-alterations in human pathophysiology, labeling TPP for application in positron emission tomography (PET) imaging is explored and successfully demonstrated in cardiac disease (Shoup et al., 2011; Gurm et al., 2012). Chemically, ^{18}F -fluorophenyl-triphenylphosphonium is an analog of TPP with the substitution of fluorophenyl for one of the phenyl groups. Functionally, both TPP and ^{18}F -triphenylphosphonium exhibit the lipophilic cationic property, and the affinity to accumulate within mitochondria depending on the MMP. Thus, radiolabeled [^3H]-TPP and the ^{18}F -triphenylphosphonium differ only in their imaging potential by PET (^{18}F). Nevertheless, in hepatic fibrosis, there is a paucity in the experimental documentation of liver voltage, particularly in the early and advanced stages of progression.

Many factors including hepatotoxins are known to trigger progressive fibrotic disease of the liver (Wynn, 2008; Wynn and Ramalingam, 2012). Clinically, although less frequent, the intake of some therapeutics is known to cause hepatotoxicity and in some cases fibrogenesis (Zachariae et al., 1987; McDonnell and Braverman, 2006; Navarro and Senior, 2006; Han et al., 2013). Therefore, in this study, we intended to investigate the

MMP ($\Delta\psi_m$) of global liver in hepatotoxin-induced fibrosis. The CCl_4 -induced liver-injury model is a well-established and widely used model of hepatotoxicity-induced fibrosis (Mehendale et al., 1994; Wang et al., 2007; Jin et al., 2011; Karthikeyan et al., 2016). As the objective of the model is to induce CCl_4 -based hepatotoxicity, we used olive oil (vehicle), a non-toxic, emulsifying agent that facilitates complete and homogenous mixing of CCl_4 . The control group animals received just the vehicle (olive oil). Thus, our objective was to determine if CCl_4 -induced hepatic fibrogenesis alters the MMP, net voltage of the liver. Furthermore, we evaluated its correlation with fibrogenesis and mito-respiration.

MATERIALS AND METHODS

Radiolabeled [^3H]-TPP

Tetraphenylphosphonium bromide, [phenyl- ^3H], i.e., ^3H -TPP at a concentration of 37 MBq/ml was synthesized and supplied by the American Radiolabeled Chemicals Inc. (St Louis, MO, USA).

Chemicals and Reagents

Unless otherwise mentioned, all chemicals were purchased from Sigma-Aldrich Co., (St. Louis, MO, USA). Primary antibodies such as AMPK $\beta 1$ (#4150), phospho (p)-AMPK $\beta 1$ (#4181), eIF2 α (#9722), p-eIF2 α (#3597), β -actin (#4970), mitoSTAT3 (#9139), and cytochrome C oxidase IV (COX IV; #4844) were from Cell Signaling Technologies Inc. (Danvers, MA, USA). Antibodies such as $\text{F}_1\text{-F}_0$ ATPase (5E) (#SC-81874) and mitochondrial-encoded cytochrome C oxidase subunit 1 (MT-CO1; #PA5-26688) were from Santa Cruz Biotechnology Inc. (CA, USA) and Thermo-Fisher Scientific Inc. (Grand Island, NY, USA), respectively. Secondary antibodies were purchased from Cell Signaling Technologies Inc. (#7076; #7174), Santa Cruz Biotechnology (#SC-2004), or Bio-Rad Laboratories (#170-6516) (Hercules, CA, USA). The alanine aminotransferase (ALT) assay kit to determine the liver function was procured from Bio Vision Inc. (San Francisco, CA, USA).

Fibrogenesis by CCl_4

Animal experiments were performed as approved by the Institutional Animal Care and Use Committee. To establish the liver fibrosis model, 3–4 week old male C57BL/6 mice (15–20 g body weight) were procured from the Charles River Laboratories Inc. (Wilmington, MA, USA) and maintained in a temperature-controlled room with an alternating 12-h dark and light cycle. To determine the fibrotic stage, mice were randomly divided into control (vehicle, $n = 7$) and experimental groups ($n = 7$) representing 2, 4, and 6 weeks of CCl_4 administration. Fibrogenesis was induced by intraperitoneal administration of 20% solution of CCl_4 (Sigma Chemical Co., St. Louis, MO, USA) in olive oil (vehicle) (Mehendale et al., 1994; Wang et al., 2007; Jin et al., 2011; Karthikeyan et al., 2016), at a dose of 0.5 $\mu\text{l/g}$ bodyweight every week thrice for up to 6 weeks. Histopathology and analysis of fibrosis markers were used to determine the early fibrotic stage.

Histopathology and Staging Fibrosis

Liver fixed in 10% of phosphate-buffered formalin (Polysciences, Warrington, PA, USA) was dehydrated with graded ethanol, embedded in wax (Paraplast Plus; McCormick Scientific, Richmond, IL, USA), sliced at 5 μ m, mounted on slides, and oven-dried, and deparaffinized and subjected to H and E staining as previously described (Ganapathy-Kanniappan et al., 2012). To detect collagen deposition, the liver sections were stained using Sirius Red stain (PolySciences Inc. Warrington, PA, USA) or Masson's trichrome stain (Sigma Aldrich, St. Louis, MO) as per the instructions of suppliers. Quantification of collagen staining was performed using ImageJ software (National Institutes of Health, Bethesda, US) (Schneider et al., 2012). Staging of the fibrosis was performed according to the METAVIR scoring system in which on a 5-point scale, F0 denotes no fibrosis (normal) and F4 refers to advanced cirrhosis (Poynard et al., 1997). Further experiments were performed using the control (F0) and early phase (F1) fibrogenic liver.

TaqMan Real-Time Polymerase Chain Reaction

Quantification of the fibrosis marker gene, collagen1 α 1 (*Col1 α 1*) was performed using TaqMan Universal Master Mix II with UNG (Applied Biosystems, MA, USA) in a Quant Studio 12K Flex Real-Time PCR System (Applied Biosystems) as described (Gajendiran et al., 2018). In brief, total RNA was extracted using the Trizol reagent (Thermo Fisher Scientific), followed by RNA clean-up (RNeasy kit, Qiagen Inc. Valencia, CA, USA) and subjected to reverse transcription using the High Capacity cDNA Reverse Transcription Kit (Applied Biosystems). Thus, the cDNAs synthesized were subjected to the real-time polymerase chain reaction (qPCR) using gene-specific Taqman probes, i.e., *Col1 α 1* (Probe ID: Mm00801666_g1) and β 2-microglobulin (internal control, Probe ID: Mm00437762_m1) obtained from ThermoFisher Scientific Inc.

3 H-TPP Liver Uptake and Biodistribution Studies

Liver uptake and tissue distribution of 3 H-TPP in the respective groups (i.e., control and early phase, F1) were determined by tail vein injection of 370 kBq (10 μ Ci) of 3 H-TPP (Min et al., 2004). Animals were euthanized 1 h post-injection, the blood was collected by cardiac puncture, and other organs were harvested for further analysis. All solid and liquid wastes of radioactive material were disposed of as per the institutional guidelines of the Radiation Safety Office. Quantification of the tissue uptake of 3 H-TPP was performed as follows: a known quantity of tissue (e.g., 50 mg) was solubilized in the SolvableTM (Perkin Elmer Co., Waltham, MA, USA) as per the instructions of the supplier, followed by the addition of UltimaGoldTM scintillation cocktail reagent (Perkin Elmer Co.), and the 3 H was counted using a Beckman LS-6,500 liquid scintillation counter. Radioactivity determinations were normalized by the weight of the tissue and the amount of radioactivity injected, obtaining the percentage of injected dose/gram tissue (% ID/g) (Sands et al., 1994).

Isolation of Mouse Liver Mitochondria

Mouse liver mitochondria were isolated as described (Rogers et al., 2011). The method of isolation is relevant for functional analysis such as the rate of respiration (oxygen consumption) using the Seahorse XF⁹⁶ extracellular flux analyzer (Seahorse Bioscience, Billerica, MA, USA). Furthermore, the isolation procedure has been validated by several laboratories as well (Rogers et al., 2011; Iuso et al., 2017). In brief, mouse liver was extracted, rinsed with ice-cold phosphate-buffered saline to remove blood, and the liver was minced in \sim 10 volumes of ice-cold mito-isolation buffer (MIB), pH 7.2 [70 mM sucrose, 210 mM mannitol, 5 mM HEPES, 1 mM EGTA, and 0.5% (w/v) fatty acid-free BSA]. All subsequent steps of the preparation were performed on ice. The minced tissue was homogenized using a Glass/Teflon Potter Elvehjem homogenizer with not more than 10 strokes. Homogenate was centrifuged at 800 \times g for 10 min at 4°C. Following centrifugation and careful removal of the lipid layer, the remaining supernatant was filtered through a double-layer cheesecloth into a separate tube and centrifuged at 8,000 \times g for 10 min at 4°C. The supernatant was removed, the pellet containing the bulk of the mitochondria was resuspended in MIB, and the centrifugation was repeated. The final pellet was resuspended in a minimal volume of MIB. For functional assays, such as metabolic flux analysis, the mitochondria were used fresh and as quickly as possible. The rest of the mito-samples was stored at -80°C until further use. The protein concentration was determined using a 2D-Quant Kit (GE Healthcare, Piscataway, NJ, USA) (Ganapathy-Kanniappan et al., 2009).

Immunoblotting

Immunoblotting was performed as described (Kunjithapatham et al., 2015). Control, F1 and F3 liver lysates, as well as the mitochondria isolated from the corresponding livers were subjected to relevant immune detection. In brief, a known quantity of the liver tissue was washed in PBS and homogenized in ice-cold RIPA lysis buffer containing protease and phosphatase inhibitor cocktails at 4°C using a Dounce homogenizer. The homogenates were centrifuged at 12,000 \times g for 15 min at 4°C, the clear supernatants were collected, and the protein concentration was determined using a 2D-Quant Kit (GE Healthcare, Piscataway, NJ, USA). The samples were then resolved on a 4–12% Bis-Tris gel by electrophoresis with MOPS running buffer and blotted onto PVDF membranes (BioRad, Hercules, CA, USA) followed by immunoblotting with specific antibodies. Immune complexes were visualized by using the ECL-detection kit (GE Healthcare).

Metabolic Flux Analysis

The mitochondria isolated from the mouse liver as mentioned above were used to determine the oxygen consumption rate (OCR) (Rogers et al., 2011; Iuso et al., 2017) using the Seahorse XF⁹⁶ extracellular flux analyzer (Seahorse Bioscience, Billerica, MA, USA). In brief, an equal amount (\sim 5 μ g) of control and F1-mitochondria were plated into the Seahorse XF⁹⁶ assay plate, and all subsequent steps including the addition of substrate, reagents, and ADP and the duration of

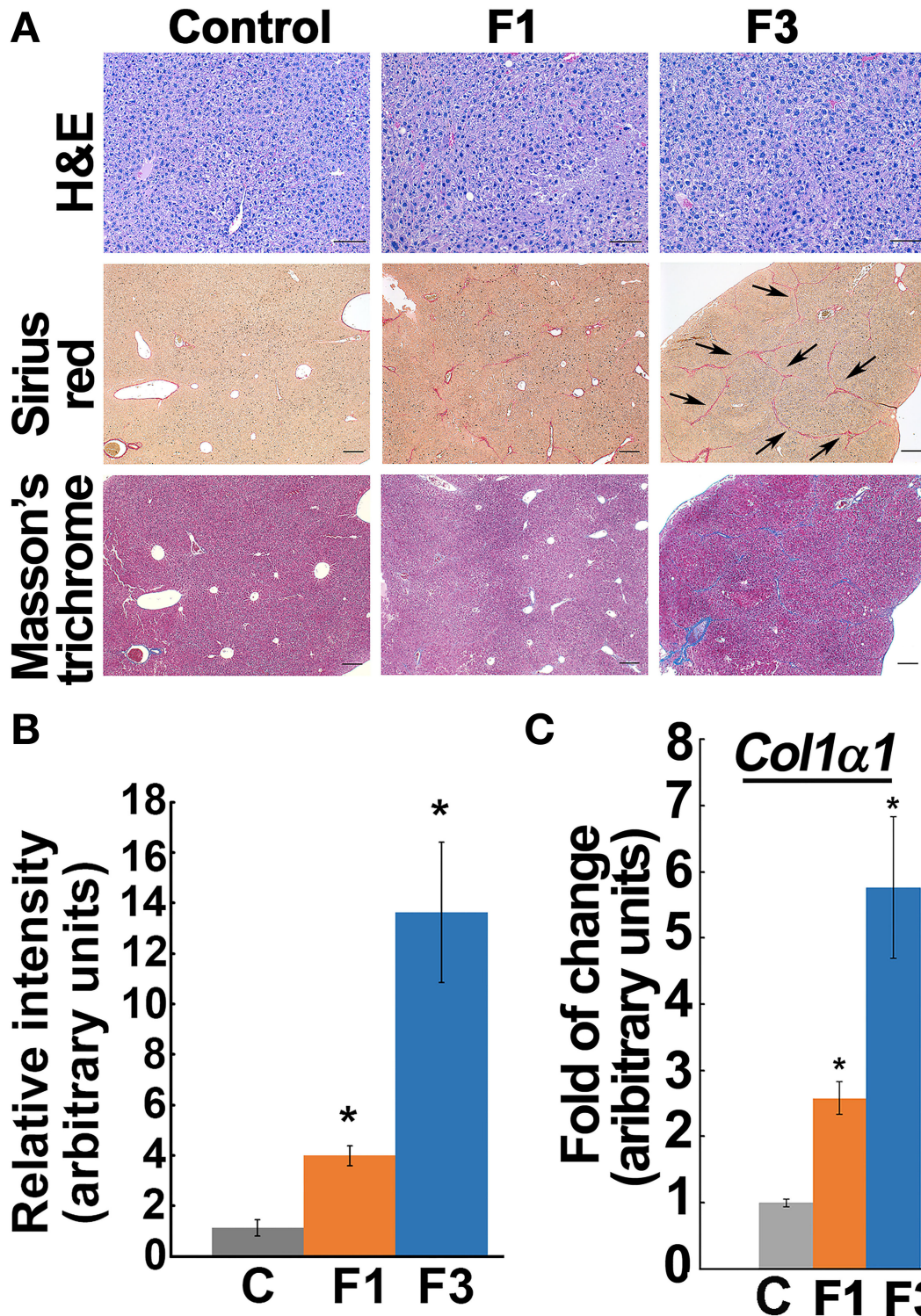


FIGURE 1 | Staging early and advanced fibrosis in carbon tetrachloride (CCl₄) model. **(A)** Histochemical staining of liver from control and experimental groups showed minimal collagen deposit, i.e., early fibrosis (F1), at 4 weeks of CCl₄-administration. At 6 weeks, the bridging phenotype (indicated by arrows) and increased collagen deposition as verified by Sirius Red and Masson's trichrome indicate advanced fibrosis (F3). Based on the METAVIR scoring system, the 4 and 6 weeks of CCl₄ administration correspond to F1 and F3 stages, respectively. Scale bar represents 100 μm in the Hand E staining and 200 μm in the Sirius Red and Masson's trichrome staining. **(B)** Bar graph shows quantification of collagen Sirius stain using ImageJ software. **(C)** *Col1α1* expression increased in the corresponding early (F1) and advanced (F3) fibrotic liver. Data represent mean ± SE (n = 5), t-test, *p < 0.05.

the assay were followed as described (Rogers et al., 2011). Unlike the cell-based assay, in this study, we used the organelle, mitochondria isolated from the respective livers. Thus, the absence of any cellular source renders the extracellular acidification rate (ECAR) inapplicable. Then, the MMP was determined based on the mito-uptake of Tetramethylrhodamine, methyl ester (TMRM) (Scaduto and Grotyohann, 1999). In brief, mitochondria (0.5 mg/ml) that were isolated from control and F1 and F3 livers were incubated with 5 mM glutamate, 5 mM malate, and 0.5 μ M TMRM. Fluorescence at 546 and 573 nm excitation was monitored using an emission wavelength of 590 nm.

Transmission Electron Microscopy

Control and fibrotic liver tissues were harvested and thoroughly rinsed in PBS buffer prior to the fixation. For mito-studies, the mitochondria were isolated from the respective mouse liver as described above. The liver and the corresponding mitochondria were fixed in 2.5% glutaraldehyde, 3 mM MgCl₂, and 0.1 M cacodylate buffer, pH 7.2 overnight at 4°C. After buffer rinse, samples were post-fixed in 0.8% potassium ferrocyanide reduced 1% osmium tetroxide in buffer (1 h) on ice in the dark followed by 0.1 M sodium cacodylate buffer rinse. Samples were left at 4°C overnight in buffer, rinsed with 0.1 M maleate buffer, *En bloc* stained with 2% uranyl acetate (0.22 μ m filtered, 1 h, dark) in 0.1 M maleate, dehydrated in a graded series of ethanol, and embedded in Eponate 12 (Ted Pella) resin. Samples were polymerized at 60°C overnight. Thin sections, 60–90 nm, were cut with a diamond knife on the Reichert-Jung Ultracut E ultramicrotome and picked up with Formvar coated copper slot grids. Grids were stained with 2% uranyl acetate in 50% methanol, followed by lead citrate, and observed using a Philips CM120 at 80 kV. Images were captured with an AMT XR80 high-resolution (16-bit) 8 Mpixel camera.

Statistical Analysis

All data were analyzed using VassarStats (Lowry, 2004), and the difference between the two means was assessed by using either Mann–Whitney–Wilcoxon (MWW) test (unpaired) or the paired *t*-test as appropriate. The probabilities of $p < 0.05$ or as indicated were considered as significant.

RESULTS

Staging Early and Advanced Liver Fibrosis in CCl₄ Model

Histochemical staining by Sirius Red and Masson's trichrome for the fibrosis marker, "collagen deposition" demonstrated that 4 weeks of CCl₄-exposure induced minimal fibrosis, i.e., collagen deposits without bridging, and corresponded to the F1-stage according to the METAVIR fibrosis score (Figures 1A,B, Supplementary Figure 1), whereas, liver from 6 weeks of CCl₄-exposure led to increased collagen deposition and showed the characteristic "bridging fibrosis" corresponding to stage F3 (Figures 1A,B). Quantification of the *Colla1* mRNA reflected the progression of fibrosis from early (F1) to advanced (F3) at 4 and 6 weeks of CCl₄-administration (Figure 1C). ALT activity, one of the markers of liver function also showed a significant increase in F1 and F3 and corroborated the hepatic insult in CCl₄-induced fibrogenesis (Supplementary Figure 2).

³H-TPP Liver Uptake and Biodistribution in CCl₄ Model

The liver uptake of ³H-TPP in mice indicated a significant increase in F1-liver (6.08 \pm 0.69% ID) compared with the vehicle control (3.51 \pm 0.23% ID/g) and F3-liver (4.85 \pm 1.48% ID) (Figure 2A, Supplementary Figure 3A). Then, quantification of ³H-TPP-uptake by various organs between the control and F1 and F3 livers showed that only liver but not blood, heart,

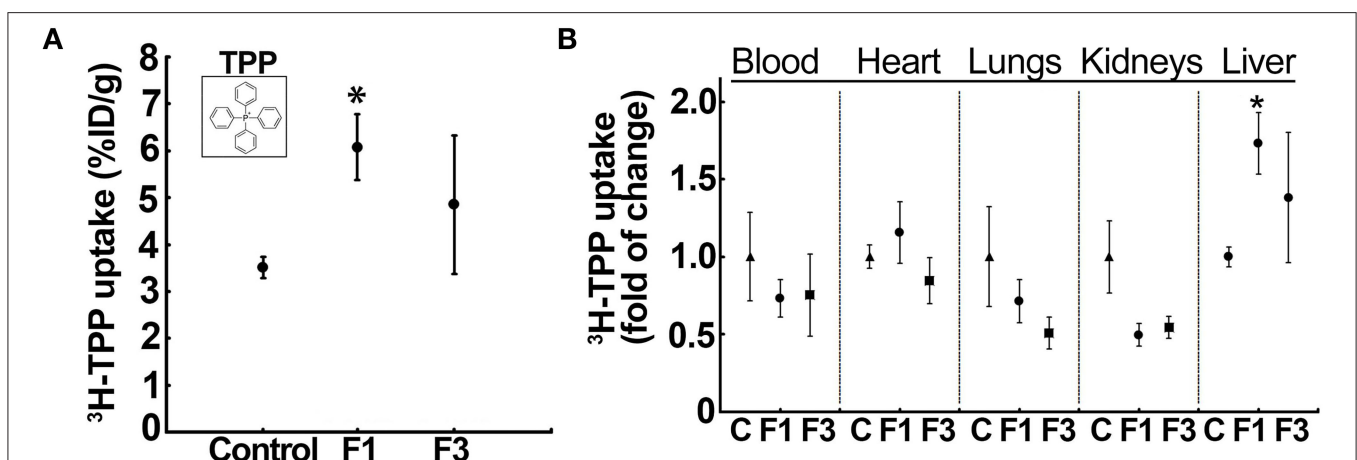


FIGURE 2 | Liver uptake of the voltage-sensor, ³H-tetraphenylphosphonium (TPP), increases in early fibrosis. **(A)** ³H-TPP uptake (percentage of the injected dose, % ID) significantly increased in the F1 liver compared with the vehicle control and F3. Insert: chemical structure of TPP used as radiolabeled (³H)-TPP. Data represent mean \pm SE ($n = 5$) MWW test ($*p < 0.05$). **(B)** Tissue distribution of ³H-TPP at F1 showed a significant increase in the liver uptake but not in other tissues, indicating hepatic fibrosis-related elevation in the net membrane potential of the liver. Data represent mean \pm SE ($n = 5$). MWW test ($*p < 0.05$). Control, F1, early-stage fibrosis, F3, and advanced stage fibrosis. The vehicle (olive oil) controls of each batch (different weeks) were aggregated in a single group for analysis.

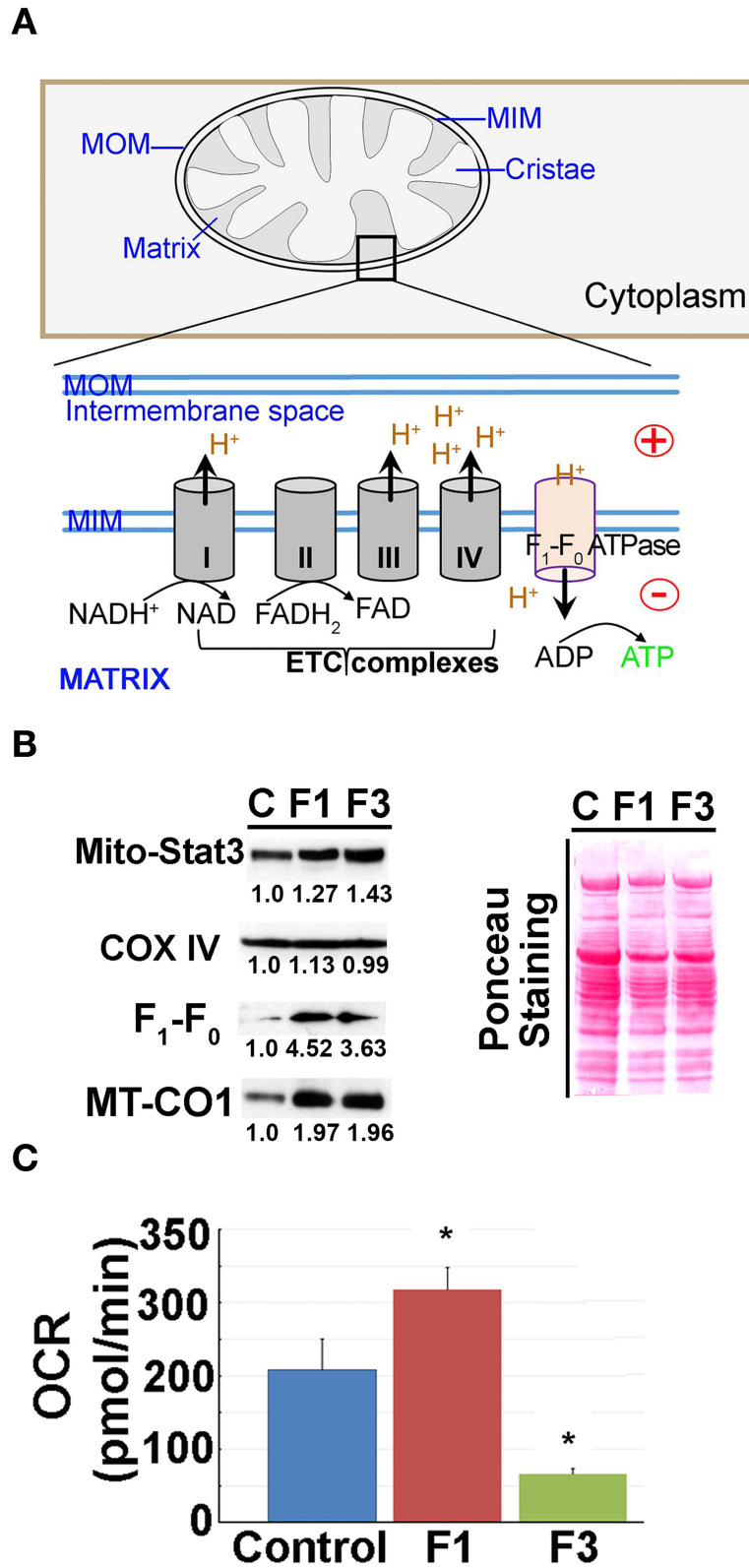


FIGURE 3 | Mitochondrial (mito-) oxidative phosphorylation (OxPhos) upregulated in early fibrosis. **(A)** Schematic diagram showing the overview of the regulation of mito-membrane potential. In OxPhos, ETC complexes release protons (H^+) into the space between the inner (MIM) and outer membranes (MOM) of mitochondria. H^+ (Continued)

FIGURE 3 | accumulation establishes an electrochemical gradient leading to a negative potential (–) in the matrix. Thus, a higher rate of OxPhos (e.g., ATP synthesis) results in increased negative potential in the mito-matrix. **(B)** Immunoblot of mito-proteins shows an increase in mito-translocation of STAT3, F₁-F₀ ATP synthase, and MT-CO1. COX IV remained unaltered. Immunoblot was re-probed for different targets to maintain the loading control. Numerical values at the bottom of the immunoblots represent the densitometry quantification of respective signals. Ponceau staining of the membrane shown for overall protein profile. **(C)** Metabolic flux analysis showing the oxygen consumption rate (OCR) of mitochondria isolated from the control, and F1 and F3 livers. Mitochondria showing a net increase in the OCR in the F1 liver. Unlike the typical cell-based assay, in this study, we used the mitochondria isolated from the respective livers as referred in the “Materials and methods” section. Hence, the extracellular acidification rate (ECAR) which is pertinent in the cellular assay is inapplicable. Data represent mean ± SE (*n* = 3), *t*-test (**p* < 0.05).

lungs, and kidneys demonstrate a statistically significant fold of increase in the accumulation of the voltage sensor, i.e., ³H-TPP (**Figure 2B**, **Supplementary Figure 3B**). The results show that the liver accumulation of ³H-TPP is significant in early fibrogenesis.

Noteworthy, ³H-TPP liver uptake significantly correlated with the serum ALT activity that showed a marked elevation in F1 (**Supplementary Figure 4A**). Then, the liver morphology as observed by transmission electron microscopy (TEM) corroborated the fibrotic phenotype of the F1 liver. Control liver showed normal morphology (e.g., subcellular organelles and glycogen granules) with no indicators of fibrogenesis (**Supplementary Figure 4B**). Conversely, CCl₄-administered mice (F1) showed characteristic features of fibrosis such as the occurrence of multiple vesicles, fat droplets, presence of active Kupffer cells at the sinusoid with endothelial cell lining, and presence of collagen fibers (**Supplementary Figure 4B**).

Liver Mito-OxPhos Capacity in CCl₄ Model

As critical determinants of membrane voltage, we then investigated the OxPhos/ETC enzymes (**Figure 3A**). Immunoblot analysis of mitochondria isolated from the control and F1 and F3 livers showed upregulation of ETC/OxPhos enzymes, F₁-F₀ ATP synthase, and MT-CO1 (**Figure 3B**). A concurrent increase in mito-translocation of STAT3 (regulator of OxPhos) implied fibrogenesis-related augmentation of OxPhos activity. Then, metabolic flux analysis of mitochondria isolated from the control and fibrotic livers showed distinctively elevated respiration (i.e., OCR) in F1 compared with the control (**Figure 3C**, **Supplementary Figure 5**). Intriguingly, OCR of F3 mitochondria diminished significantly (**Figure 3C**, **Supplementary Figure 5**). Further investigation of mito-uptake of TMRM, an indicator of MMP, also revealed an increase in TMRM uptake at F1 compared with control implying elevated mito-activity in the early stages of fibrosis (**Supplementary Table 1**). Mito-investigation by TEM *ex vivo* showed that the mito-morphology in early fibrosis remained intact and unaffected (F1) similar to the control, whereas, F3 liver showed more mitochondria with variations in appearance (**Figure 4A**). Corroborating the impaired mito-capacity in F3 and the level of *p*-AMPK and *p*-eIF2 α , indicators of metabolic stress showed a marked elevation in the F3 liver (**Figure 4B**). Collectively, mito-metabolic response to hepatic insult augments the net voltage of the liver in early fibrosis (**Figure 4C**).

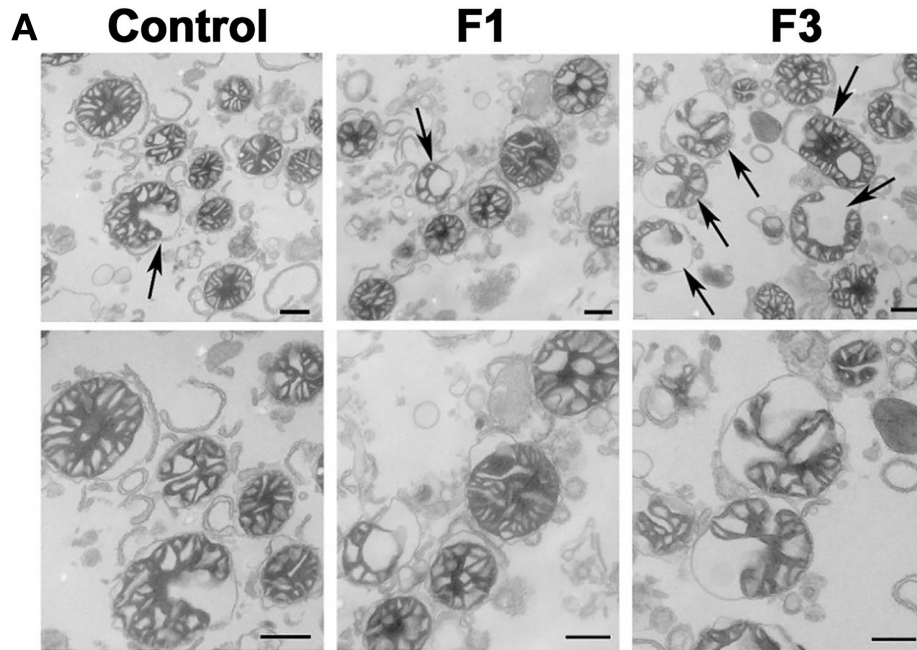
DISCUSSION

This study shows that the liver uptake of the membrane voltage sensor, ³H-TPP significantly increases in early fibrosis

as confirmed by the onset of collagen deposition. Then, the upregulation of the OxPhos enzymes with a concomitant increase in mito-respiration in early fibrosis (F1) concurred with the augmented liver uptake of ³H-TPP. TPP has been implicated in the assessment pathophysiology of cancer (Min et al., 2004; Madar et al., 2007), cardiac disease (Higuchi et al., 2011; Gurm et al., 2012), and others, through the functional imaging modalities such as PET. However, its relevance in liver fibrosis/cirrhosis remains unknown, primarily due to the lack of any experimental study on the overall membrane voltage of the liver. Our findings provide the primary evidence that liver voltage may enable the detection of the fibrogenic liver at an early stage.

Mechanistically, the cellular uptake and the intramitochondrial accumulation of TPP depend on the electrochemical gradient across respective membranes, i.e., at cellular and mito-levels. The net positive/negative charge of the electrochemical gradient determines the membrane potential or the voltage. In principle, as cationic lipophilic agents, the intracellular entry of TPP is facilitated by the cellular/plasma membrane voltage which is generally –30 to –60 mV. Then, in metabolically active mitochondria, consequential to the functions such as the OxPhos/ETC, and/or increase in the total mito-matrix volume, the MMP remains increased (–150 to –180mV). Such an elevated MMP enables 100× to 500× more mito-accumulation of the lipophilic cations (e.g., TPP and TMRM fluorescent dye) (Murphy, 2008; Zielonka et al., 2017). Conversely, the TPP or TMRM uptake is reduced or decreased in cells with diminished MMP, i.e., membrane-depolarization, underscoring the role of MMP in TPP uptake. Accordingly, the propensity of TPP to accumulate in cells with higher MMP is exploited for the therapeutic targeting of mitochondria in preclinical investigations (Han et al., 2014; Pathak et al., 2014; Marrache and Dhar, 2015). Collectively, the plasma membrane voltage, mito-matrix volume, and membrane potential impact the rate of TPP uptake. Nevertheless, our findings from the CCl₄ (hepatotoxicity)-induced model of fibrogenesis indicate that unlike the advanced fibrosis (Krahenbuhl et al., 2000; Rodrigues and Steer, 2000; Sun and Kisseleva, 2015), liver-mitochondria of the early phase of hepatic insult exhibit augmented respiration/ETC activity indicating the involvement of MMP in the increased liver accumulation of TPP.

In addition, multiple lines of evidence indicate that hepatotoxicity-induced apoptosis may promote cell proliferation and the associated mito-functions, as a compensatory mechanism, at least in the initial stages (Mehendale et al., 1994; Trost and Lemasters, 1997; Lemasters and Holmuhamedov, 2006; Jones et al., 2010; Bajt et al., 2011; Rehman et al., 2016;



B
Liver Lysate

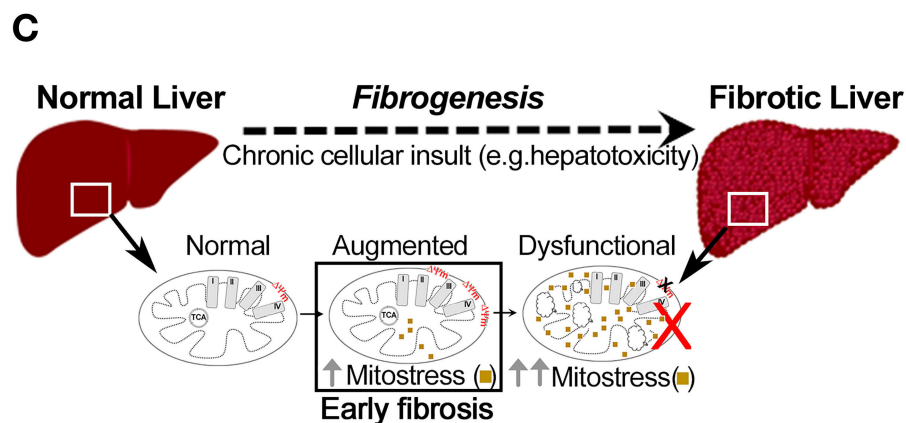
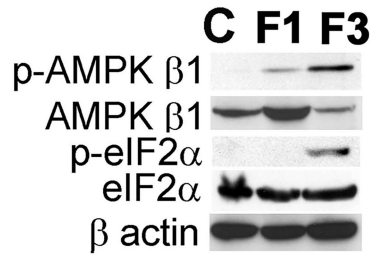


FIGURE 4 | Mitochondria in fibrosis. (A) Transmission electron microscopy (TEM) observation of liver mitochondria in fibrosis. Mito-morphology in F1 remains similar to the control liver, whereas, in F3, mitochondria with altered morphology were prominent. Upper panel: arrows indicate variation in the appearance of mitochondria. Lower panel: magnification of the respective upper panel. Scale: 500 nm. (C) Control, F1, early, and F3, and advanced stages of fibrosis. (B) Immunoblot of the total liver protein shows CCl₄-dependent induction of metabolic stress as indicated by the upregulation of p-AMPK β1 and p-eIF2α. β-actin is shown as the loading control. (C) Mito-response to hepatic insult in early fibrosis augments net voltage of the liver.

Wimborne et al., 2020). Since mito-function is an integral part of cell growth and proliferation, it is plausible that the overall increase in MMP is perhaps a result of increased mito-biogenesis, mito-activity, and/or the cell number. However, our data on the mito-respiration, a functional assay (which used an equal quantity of mitochondria), revealed an enhanced rate of oxygen consumption (under normalized mito-content) compared with the control, indicative of augmented mito-activity.

Then, several elegant reviews have underscored the role of STATs, particularly STAT3 in liver pathophysiology (Kong et al., 2012; Yang and Rincon, 2016). Transcriptionally, STAT3 promotes aerobic glycolysis and downregulates OxPhos. Conversely, its translocation to mitochondria preserves mito-function, upregulates OxPhos, and promotes survival (Poli and Camporeale, 2015). In fact, STAT3 regulates the functional efficiency of ETC complexes suggesting its critical role in cellular respiration (Wegrzyn et al., 2009). Intriguingly, in liver pathology, STAT3 plays two distinctive roles depending on the hepatic cell type; in hepatocytes, it is cytoprotective, whereas, in the HSCs, it is profibrogenic (Kong et al., 2012). Thus, an increase in mito-translocation of STAT3 as a mito-stress indicator and concurrent upregulation of F₁-F₀ ATP synthase and MT-CO1 in F1 implies a mito-metabolic stress response in early fibrogenesis. It remains to be known whether the enhanced uptake of TPP in fibrogenesis is relevant in other fibrogenic conditions (e.g., viral infection, biliary fibrosis) or limited to chemically (CCl₄)-induced fibrosis.

Liver fibrosis and cirrhosis are pathological sequelae for several chronic liver diseases that may eventually lead to death, hence early diagnosis is critical for the management of the disease (Farazi and DePinho, 2006; Hernandez-Gea and Friedman, 2011). Despite significant progress in other imaging modalities (Tapper and Loomba, 2018), such as MR elastography (MRE) and transient elastography (TE), that rely on the elasticity/stiffness of the fibrotic/cirrhotic liver, the potential of PET diagnostic-imaging of liver fibrosis remains obscure. In this study, we reported an experimental study for a new PET-relevant functional marker that may have implications in the early diagnosis of liver fibrosis.

The diagnostic/therapeutic potential of membrane voltage has been recognized in human diseases (e.g., cancer and cardiac disease) (Min et al., 2004; Madar et al., 2007; Higuchi et al., 2011; Gurm et al., 2012; Rehman et al., 2016), hence understanding the net liver-voltage during the initial phases of fibrogenesis may have clinical implications. Mito-membrane voltage-dependent PET imaging relies on the difference in membrane voltage between normal and abnormal cells/tissues. However, in liver fibrosis/cirrhosis, until now, there is no known functional marker or a molecular mechanism that is applicable or relevant for voltage-dependent PET-imaging. In this study, we reported

a potential PET-relevant functional marker that on further validation may have implications in the early diagnosis of liver fibrosis. Nevertheless, it remains to be determined whether the ~2-fold increase in the fibrotic-liver uptake of ³H-TPP in our mouse model could still be exploited in the functional imaging to distinguish fibrosis. Future studies using clinically relevant probes are underway to delineate the significance and translational potential of mito-membrane voltage-dependent PET imaging in the early detection of liver fibrosis.

DATA AVAILABILITY STATEMENT

The original contributions presented in the study are included in the article/**Supplementary Material**, further inquiries can be directed to the corresponding authors.

ETHICS STATEMENT

The animal study was reviewed and approved by Institutional Animal Care and Use Committee (IACUC), Johns Hopkins University School of Medicine.

AUTHOR CONTRIBUTIONS

EM and SG-K conceived this study and wrote the manuscript. SG-K designed the experiments, performed mito-isolation, functional experiments, and data analysis. HP and SG-K performed *in vivo* investigation, histochemical staining, and TEM studies. All authors contributed to the article and approved the submitted version.

ACKNOWLEDGMENTS

We thank Edmond Jacobs for the help in the tail-vein injection of ³H-TPP. We also thank Michelle-Acoba and Dr. Steven Claypool for the help in Seahorse metabolic flux analyzer. We sincerely acknowledge the help provided by Barbara Smith of Electron Microscope Facility, School of Medicine in TEM image acquisition, and Prof. Norman Barker of the Department of Pathology for the help in photomicrography of histopathology slides. We acknowledge the support from the Willis C. Maddrey endowment for liver research at Johns Hopkins and the Bright Star award (SG-K) from the Radiology department.

SUPPLEMENTARY MATERIAL

The Supplementary Material for this article can be found online at: <https://www.frontiersin.org/articles/10.3389/fphys.2021.676722/full#supplementary-material>

REFERENCES

- Amann, T., Bataille, F., Spruss, T., Muhlbauer, M., Gabele, E., Scholmerich, J., et al. (2009). Activated hepatic stellate cells promote tumorigenicity of hepatocellular carcinoma. *Cancer Sci.* 100, 646–653. doi: 10.1111/j.1349-7006.2009.01087.x
- Bajt, M. L., Ramachandran, A., Yan, H. M., Lebofsky, M., Farhood, A., Lemasters, J. J., et al. (2011). Apoptosis-inducing factor modulates mitochondrial

- oxidant stress in acetaminophen hepatotoxicity. *Toxicol. Sci.* 122, 598–605. doi: 10.1093/toxsci/kfr116
- Chen, L. B. (1988). Mitochondrial membrane potential in living cells. *Annu. Rev. Cell Biol.* 4, 155–181. doi: 10.1146/annurev.cb.04.110188.001103
- Farazi, P. A., and DePinho, R. A. (2006). Hepatocellular carcinoma pathogenesis: from genes to environment. *Nat. Rev. Cancer.* 6, 674–687. doi: 10.1038/nrc1934
- Gajendiran, P., Vega, L. I., Itoh, K., Sesaki, H., Vakili, M. R., Lavasanifar, A., et al. (2018). Elevated mitochondrial activity distinguishes fibrogenic hepatic stellate cells and sensitizes for selective inhibition by mitotrophic doxorubicin. *J. Cell. Mol. Med.* 22, 2210–2219. doi: 10.1111/jcmm.13501
- Ganapathy-Kanniappan, S., Geschwind, J. F., Kunjithapatham, R., Buijs, M., Vossen, J. A., Tchernyshyov, I., et al. (2009). Glyceraldehyde-3-phosphate dehydrogenase (GAPDH) is pyruvylated during 3-bromopyruvate mediated cancer cell death. *Anticancer Res.* 29, 4909–4918.
- Ganapathy-Kanniappan, S., Karthikeyan, S., Geschwind, J. F., and Mezey, E. (2014). Is the pathway of energy metabolism modified in advanced cirrhosis? *J. Hepatol.* 61, 452. doi: 10.1016/j.jhep.2014.04.017
- Ganapathy-Kanniappan, S., Kunjithapatham, R., Torbenson, M. S., Rao, P. P., Carson, K. A., Buijs, M., et al. (2012). Human hepatocellular carcinoma in a mouse model: assessment of tumor response to percutaneous ablation by using glyceraldehyde-3-phosphate dehydrogenase antagonists. *Radiology* 262, 834–845. doi: 10.1148/radiol.11111569
- Grattagliano, I., Russmann, S., Diogo, C., Bonfrate, L., Oliveira, P. J., Wang, D. Q., et al. (2011). Mitochondria in chronic liver disease. *Curr. Drug Targets* 12, 879–893. doi: 10.2174/138945011795528877
- Gurm, G. S., Danik, S. B., Shoup, T. M., Weise, S., Takahashi, K., Laferrier, S., et al. (2012). 4-[18F]-tetraphenylphosphonium as a PET tracer for myocardial mitochondrial membrane potential. *JACC Cardiovasc. Imaging* 5, 285–292. doi: 10.1016/j.jcmg.2011.11.017
- Han, D., Dara, L., Win, S., Than, T. A., Yuan, L., Abbasi, S. Q., et al. (2013). Regulation of drug-induced liver injury by signal transduction pathways: critical role of mitochondria. *Trends Pharmacol. Sci.* 34, 243–253. doi: 10.1016/j.tips.2013.01.009
- Han, D., Ybanez, M. D., Johnson, H. S., McDonald, J. N., Mesrobian, L., Sancheti, H., et al. (2012). Dynamic adaptation of liver mitochondria to chronic alcohol feeding in mice: biogenesis, remodeling, and functional alterations. *J. Biol. Chem.* 287, 42165–42179. doi: 10.1074/jbc.M112.377374
- Han, M., Vakili, M. R., Soleymani Abyaneh, H., Molavi, O., Lai, R., and Lavasanifar, A. (2014). Mitochondrial delivery of doxorubicin via triphenylphosphine modification for overcoming drug resistance in MDA-MB-435/DOX cells. *Mol. Pharm.* 11, 2640–2649. doi: 10.1021/mp500038g
- Hernandez-Gea, V., and Friedman, S. L. (2011). Pathogenesis of liver fibrosis. *Annu. Rev. Pathol.* 6, 425–456. doi: 10.1146/annurev-pathol-011110-130246
- Higuchi, T., Fukushima, K., Rischpler, C., Isoda, T., Javadi, M. S., Ravert, H., et al. (2011). Stable delineation of the ischemic area by the PET perfusion tracer 18F-fluorobenzyl triphenyl phosphonium after transient coronary occlusion. *J. Nucl. Med.* 52, 965–969. doi: 10.2967/jnumed.110.085993
- Iuso, A., Repp, B., Biagosch, C., Terrile, C., and Prokisch, H. (2017). “Assessing mitochondrial bioenergetics in isolated mitochondria from various mouse tissues using Seahorse XF96 analyzer,” in *Mitochondria: Practical Protocols*, eds D. Mokranjac, and F. Perocchi (Berlin: Springer Science + Business Media LLC), 217–230. doi: 10.1007/978-1-4939-6824-4_13
- Jin, Z., Sun, R., Wei, H., Gao, X., Chen, Y., and Tian, Z. (2011). Accelerated liver fibrosis in hepatitis B virus transgenic mice: involvement of natural killer T cells. *Hepatology* 53, 219–229. doi: 10.1002/hep.23983
- Jones, D. P., Lemasters, J. J., Han, D., Boelsterli, U. A., and Kaplowitz, N. (2010). Mechanisms of pathogenesis in drug hepatotoxicity putting the stress on mitochondria. *Mol. Interv.* 10, 98–111. doi: 10.1124/mi.10.2.7
- Kamo, N., Muratsugu, M., Hongoh, R., and Kobatake, Y. (1979). Membrane potential of mitochondria measured with an electrode sensitive to tetraphenyl phosphonium and relationship between proton electrochemical potential and phosphorylation potential in steady state. *J. Membr. Biol.* 49, 105–121. doi: 10.1007/BF01868720
- Kang, J. W., Hong, J. M., and Lee, S. M. (2016). Melatonin enhances mitophagy and mitochondrial biogenesis in rats with carbon tetrachloride-induced liver fibrosis. *J. Pineal Res.* 60, 383–393. doi: 10.1111/jpi.12319
- Karthikeyan, S., Potter, J. J., Geschwind, J. F., Sur, S., Hamilton, J. P., Vogelstein, B., et al. (2016). Deregulation of energy metabolism promotes antifibrotic effects in human hepatic stellate cells and prevents liver fibrosis in a mouse model. *Biochem. Biophys. Res. Commun.* 469, 463–469. doi: 10.1016/j.bbrc.2015.10.101
- Kong, X., Horiguchi, N., Mori, M., and Gao, B. (2012). Cytokines and STATs in liver fibrosis. *Front. Physiol.* 3:69. doi: 10.3389/fphys.2012.00069
- Krahenbuhl, L., Ledermann, M., Lang, C., and Krahenbuhl, S. (2000). Relationship between hepatic mitochondrial functions *in vivo* and *in vitro* in rats with carbon tetrachloride-induced liver cirrhosis. *J. Hepatol.* 33, 216–223. doi: 10.1016/S0168-8278(00)80362-1
- Kunjithapatham, R., Geschwind, J. F., Devine, L., Boronina, T. N., O’Meally, R. N., Cole, R. N., et al. (2015). Occurrence of a multimeric high-molecular-weight glyceraldehyde-3-phosphate dehydrogenase in human serum. *J. Proteome Res.* 14, 1645–1656. doi: 10.1021/acs.jproteome.5b00089
- Lemasters, J. J., and Holmuhamedov, E. (2006). Voltage-dependent anion channel (VDAC) as mitochondrial governor—thinking outside the box. *Biochim. Biophys. Acta* 1762, 181–190. doi: 10.1016/j.bbadis.2005.10.006
- Liberman, E. A., Topaly, V. P., Tsofina, L. M., Jasaitis, A. A., and Skulachev, V. P. (1969). Mechanism of coupling of oxidative phosphorylation and the membrane potential of mitochondria. *Nature* 222, 1076–1078. doi: 10.1038/2221076a0
- Lowry, R. (2004). *VassarStats: Website For Statistical Computation*. Poughkeepsie, NY.
- Madar, I., Ravert, H., Nelkin, B., Abro, M., Pomper, M., Dannals, R., et al. (2007). Characterization of membrane potential-dependent uptake of the novel PET tracer 18F-fluorobenzyl triphenylphosphonium cation. *Eur. J. Nucl. Med. Mol. Imaging* 34, 2057–2065. doi: 10.1007/s00259-007-0500-8
- Mansouri, A., Gattolliat, C. H., and Asselah, T. (2018). Mitochondrial dysfunction and signaling in chronic liver diseases. *Gastroenterology* 155, 629–647. doi: 10.1053/j.gastro.2018.06.083
- Marrache, S., and Dhar, S. (2015). The energy blocker inside the power house: mitochondria targeted delivery of 3-bromopyruvate. *Chem. Sci.* 6, 1832–1845. doi: 10.1039/C4SC01963F
- McCommis, K. S., and Finck, B. N. (2019). Treating hepatic steatosis and fibrosis by modulating mitochondrial pyruvate metabolism. *Cell. Mol. Gastroenterol. Hepatol.* 7, 275–284. doi: 10.1016/j.jcmgh.2018.09.017
- McDonnell, M. E., and Braverman, L. E. (2006). Drug-related hepatotoxicity. *N. Engl. J. Med.* 354, 2191–2193. doi: 10.1056/NEJMc060733
- Mehendale, H. M., Roth, R. A., Gandolfi, A. J., Klauunig, J. E., Lemasters, J. J., and Curtis, L. R. (1994). Novel mechanisms in chemically induced hepatotoxicity. *FASEB J.* 8, 1285–1295. doi: 10.1096/fasebj.8.15.8001741
- Min, J. J., Biswal, S., Deroose, C., and Gambhir, S. S. (2004). Tetraphenylphosphonium as a novel molecular probe for imaging tumors. *J. Nucl. Med.* 45, 636–643.
- Moreno, A. J., Santos, D. L., Magalhaes-Novais, S., and Oliveira, P. J. (2015). Measuring mitochondrial membrane potential with a tetraphenylphosphonium-selective electrode. *Curr. Protoc. Toxicol.* 65, 1–16. doi: 10.1002/0471140856.tx2505s65
- Murphy, M. P. (2008). Targeting lipophilic cations to mitochondria. *Biochim. Biophys. Acta* 1777, 1028–1031. doi: 10.1016/j.bbabi.2008.03.029
- Navarro, V. J., and Senior, J. R. (2006). Drug-related hepatotoxicity. *N. Engl. J. Med.* 354, 731–739. doi: 10.1056/NEJMra052270
- Nishikawa, T., Bellance, N., Damm, A., Bing, H., Zhu, Z., Handa, K., et al. (2014). A switch in the source of ATP production and a loss in capacity to perform glycolysis are hallmarks of hepatocyte failure in advance liver disease. *J. Hepatol.* 60, 1203–1211. doi: 10.1016/j.jhep.2014.02.014
- Pathak, R. K., Marrache, S., Harn, D. A., and Dhar, S. (2014). Mitochondria targeted molecular scaffold for efficacious delivery of metabolic modulator dichloroacetate. *ACS Chem. Biol.* 9, 1178–1187. doi: 10.1021/cb400944y
- Poli, V., and Camporeale, A. (2015). STAT3-mediated metabolic reprogramming in cellular transformation and implications for drug resistance. *Front. Oncol.* 5:121. doi: 10.3389/fonc.2015.00121
- Poynard, T., Bedossa, P., and Opolon, P. (1997). Natural history of liver fibrosis progression in patients with chronic hepatitis C. The OBSVIRC, METAVIR, CLINIVIR, and DOSVIRC groups. *Lancet* 349, 825–832. doi: 10.1016/S0140-6736(96)07642-8

- Rehman, H., Liu, Q., Krishnasamy, Y., Shi, Z., Ramshesh, V. K., Haque, K., et al. (2016). The mitochondria-targeted antioxidant MitoQ attenuates liver fibrosis in mice. *Int. J. Physiol. Pathophysiol. Pharmacol.* 8, 14–27.
- Rodrigues, C. M., and Steer, C. J. (2000). Mitochondrial membrane perturbations in cholestasis. *J. Hepatol.* 32, 135–141. doi: 10.1016/S0168-8278(00)80200-7
- Rogers, G. W., Brand, M. D., Petrosyan, S., Ashok, D., Elorza, A. A., Ferrick, D. A., et al. (2011). High throughput microplate respiratory measurements using minimal quantities of isolated mitochondria. *PLoS ONE* 6:e21746. doi: 10.1371/journal.pone.0021746
- Rugolo, M., and Lenaz, G. (1987). Monitoring of the mitochondrial and plasma membrane potentials in human fibroblasts by tetraphenylphosphonium ion distribution. *J. Bioenerg. Biomembr.* 19, 705–718. doi: 10.1007/BF00762304
- Sands, H., Gorey-Feret, L. J., Cocuzza, A. J., Hobbs, F. W., Chidester, D., and Trainor, G. L. (1994). Biodistribution and metabolism of internally 3H-labeled oligonucleotides. I. Comparison of a phosphodiester and a phosphorothioate. *Mol. Pharmacol.* 45, 932–943.
- Scaduto, R. C. Jr, and Grotyohann, L. W. (1999). Measurement of mitochondrial membrane potential using fluorescent rhodamine derivatives. *Biophys. J.* 76, 469–477. doi: 10.1016/S0006-3495(99)77214-0
- Schneider, C. A., Rasband, W. S., and Eliceiri, K. W. (2012). NIH Image to ImageJ: 25 years of image analysis. *Nat. Methods* 9, 671–675. doi: 10.1038/nmeth.2089
- Shoup, T. M., Elmaleh, D. R., Brownell, A. L., Zhu, A., Guerrero, J. L., and Fischman, A. J. (2011). Evaluation of (4-[18F]Fluorophenyl)triphenylphosphonium ion. A potential myocardial blood flow agent for PET. *Mol. Imaging Biol.* 13, 511–517. doi: 10.1007/s11307-010-0349-2
- Sun, M., and Kisseleva, T. (2015). Reversibility of liver fibrosis. *Clin. Res. Hepatol. Gastroenterol.* 39(Suppl. 1):60. doi: 10.1016/j.clinre.2015.06.015
- Tapper, E. B., and Loomba, R. (2018). Non-invasive imaging biomarker assessment of liver fibrosis by elastography in NAFLD. *Nat. Rev. Gastroenterol. Hepatol.* 15, 274–282. doi: 10.1038/nrgastro.2018.10
- Trost, L. C., and Lemasters, J. J. (1997). Role of the mitochondrial permeability transition in salicylate toxicity to cultured rat hepatocytes: implications for the pathogenesis of Reye's syndrome. *Toxicol. Appl. Pharmacol.* 147, 431–441. doi: 10.1006/taap.1997.8313
- Wan, B., Doumen, C., Duszynski, J., Salama, G., and LaNoue, K. F. (1993). A method of determining electrical potential gradient across mitochondrial membrane in perfused rat hearts. *Am. J. Physiol.* 265:445. doi: 10.1152/ajpheart.1993.265.2.H445
- Wang, L., Potter, J. J., Rennie-Tankersley, L., Novitskiy, G., Sipes, J., and Mezey, E. (2007). Effects of retinoic acid on the development of liver fibrosis produced by carbon tetrachloride in mice. *Biochim. Biophys. Acta* 1772, 66–71. doi: 10.1016/j.bbadis.2006.08.009
- Wegrzyn, J., Potla, R., Chwae, Y. J., Sepuri, N. B., Zhang, Q., Koeck, T., et al. (2009). Function of mitochondrial Stat3 in cellular respiration. *Science* 323, 793–797. doi: 10.1126/science.1164551
- Wimborne, H. J., Hu, J., Takemoto, K., Nguyen, N. T., Jaeschke, H., Lemasters, J. J., et al. (2020). Aldehyde dehydrogenase-2 activation decreases acetaminophen hepatotoxicity by prevention of mitochondrial depolarization. *Toxicol. Appl. Pharmacol.* 396:114982. doi: 10.1016/j.taap.2020.114982
- Wynn, T. A. (2008). Cellular and molecular mechanisms of fibrosis. *J. Pathol.* 214, 199–210. doi: 10.1002/path.2277
- Wynn, T. A., and Ramalingam, T. R. (2012). Mechanisms of fibrosis: therapeutic translation for fibrotic disease. *Nat. Med.* 18, 1028–1040. doi: 10.1038/nm.2807
- Yang, R., and Rincon, M. (2016). Mitochondrial Stat3, the need for design thinking. *Int. J. Biol. Sci.* 12, 532–544. doi: 10.7150/ijbs.15153
- Zachariae, H., Schroder, H., Foged, E., and Sogaard, H. (1987). Methotrexate hepatotoxicity and concentrations of methotrexate and folate in erythrocytes—relation to liver fibrosis and cirrhosis. *Acta Derm. Venereol.* 67, 336–340.
- Zielonka, J., Joseph, J., Sikora, A., Hardy, M., Ouari, O., Vasquez-Vivar, J., et al. (2017). Mitochondria-targeted triphenylphosphonium-based compounds: syntheses, mechanisms of action, and therapeutic and diagnostic applications. *Chem. Rev.* 117, 10043–10120. doi: 10.1021/acs.chemrev.7b00042

Conflict of Interest: The authors declare that the research was conducted in the absence of any commercial or financial relationships that could be construed as a potential conflict of interest.

Publisher's Note: All claims expressed in this article are solely those of the authors and do not necessarily represent those of their affiliated organizations, or those of the publisher, the editors and the reviewers. Any product that may be evaluated in this article, or claim that may be made by its manufacturer, is not guaranteed or endorsed by the publisher.

Copyright © 2021 Pandita, Mezey and Ganapathy-Kanniappan. This is an open-access article distributed under the terms of the Creative Commons Attribution License (CC BY). The use, distribution or reproduction in other forums is permitted, provided the original author(s) and the copyright owner(s) are credited and that the original publication in this journal is cited, in accordance with accepted academic practice. No use, distribution or reproduction is permitted which does not comply with these terms.



Erratum: Augmented Liver Uptake of the Membrane Voltage Sensor Tetraphenylphosphonium Distinguishes Early Fibrosis in a Mouse Model

Frontiers Production Office*

Frontiers Media SA, Lausanne, Switzerland

Keywords: liver fibrosis, membrane-voltage sensor, tetraphenylphosphonium (TPP), mitochondrial respiration, electron transport chain, carbon tetrachloride, liver voltage

An erratum on

Augmented Liver Uptake of the Membrane Voltage Sensor Tetraphenylphosphonium Distinguishes Early Fibrosis in a Mouse Model

by Pandita, H., Mezey, E., and Ganapathy-Kanniappan, S. (2021). *Front. Physiol.* 12:676722. doi: 10.3389/fphys.2021.676722

Due to a production error, the following words were misspelled: “Fibro genic liver” in the Materials and Methods and Discussion sections should be “fibrogenic liver”; and “Fibro genesis” in the Materials and Methods section should be “fibrogenesis.”

A correction has been made to the **MATERIALS AND METHODS** section, subsection **Histopathology and Staging Fibrosis:**

“Liver fixed in 10% of phosphate-buffered formalin (Polysciences, Warrington, PA, USA) was dehydrated with graded ethanol, embedded in wax (Paraplast Plus; McCormick Scientific, Richmond, IL, USA), sliced at 5 μ m, mounted on slides, and oven-dried, and deparaffinized and subjected to H and E staining as previously described (Ganapathy-Kanniappan et al., 2012). To detect collagen deposition, the liver sections were stained using Sirius Red stain (PolySciences Inc. Warrington, PA, USA) or Masson’s trichrome stain (Sigma Aldrich, St. Louis, MO) as per the instructions of suppliers. Quantification of collagen staining was performed using ImageJ software (National Institutes of Health, Bethesda, US) (Schneider et al., 2012). Staging of the fibrosis was performed according to the METAVIR scoring system in which on a 5-point scale, F0 denotes no fibrosis (normal) and F4 refers to advanced cirrhosis (Poynard et al., 1997). Further experiments were performed using the control (F0) and early phase (F1) fibrogenic liver.”

A correction has been made to the **DISCUSSION** section, first paragraph:

“This study shows that the liver uptake of the membrane voltage sensor, 3 H-TPP significantly increases in early fibrosis as confirmed by the onset of collagen deposition. Then, the upregulation of the OxPhos enzymes with a concomitant increase in mito-respiration in early fibrosis (F1) concurred with the augmented liver uptake of 3 H-TPP. TPP has been implicated in the assessment pathophysiology of cancer (Min et al., 2004; Madar et al., 2007), cardiac disease (Higuchi et al., 2011; Gurm et al., 2012), and others, through the functional imaging modalities such as PET. However, its relevance in liver fibrosis/cirrhosis remains unknown, primarily due to the lack of any experimental study on the overall membrane voltage of the liver. Our findings provide the primary evidence that liver voltage may enable the detection of the fibrogenic liver at an early stage.”

OPEN ACCESS

Approved by:

Frontiers Editorial Office,
Frontiers Media SA, Switzerland

*Correspondence:

Frontiers Production Office
production.office@frontiersin.org

Specialty section:

This article was submitted to
Integrative Physiology,
a section of the journal
Frontiers in Physiology

Received: 06 December 2021

Accepted: 06 December 2021

Published: 22 December 2021

Citation:

Frontiers Production Office (2021)
Erratum: Augmented Liver Uptake of
the Membrane Voltage Sensor
Tetraphenylphosphonium
Distinguishes Early Fibrosis in a Mouse
Model. *Front. Physiol.* 12:830151.
doi: 10.3389/fphys.2021.830151

A correction has been made to the **MATERIALS AND METHODS** section, subsection Fibrogenesis by CCl₄:

“Animal experiments were performed as approved by the Institutional Animal Care and Use Committee. To establish the liver fibrosis model, 3–4 week old male C57BL/6 mice (15–20 g body weight) were procured from the Charles River Laboratories Inc. (Wilmington, MA, USA) and maintained in a temperature-controlled room with an alternating 12-h dark and light cycle. To determine the fibrotic stage, mice were randomly divided into control (vehicle, $n = 7$) and experimental groups

($n = 7$) representing 2, 4, and 6 weeks of CCl₄ administration. Fibrogenesis was induced by intraperitoneal administration of 20% solution of CCl₄ (Sigma Chemical Co., St. Louis, MO, USA) in olive oil (vehicle) (Mehendale et al., 1994; Wang et al., 2007; Jin et al., 2011; Karthikeyan et al., 2016), at a dose of 0.5 μl/g bodyweight every week thrice for up to 6 weeks. Histopathology and analysis of fibrosis markers were used to determine the early fibrotic stage.”

The publisher apologizes for this mistake. The original version of this article has been updated.

REFERENCES

- Ganapathy-Kanniappan, S., Kunjithapatham, R., Torbenson, M. S., Rao, P. P., Carson, K. A., Buijs, M., et al. (2012). Human hepatocellular carcinoma in a mouse model: assessment of tumor response to percutaneous ablation by using glyceraldehyde-3-phosphate dehydrogenase antagonists. *Radiology* 262, 834–845. doi: 10.1148/radiol.11111569
- Gurm, G. S., Danik, S. B., Shoup, T. M., Weise, S., Takahashi, K., Laferrier, S., et al. (2012). 4-[18F]-tetraphenylphosphonium as a PET tracer for myocardial mitochondrial membrane potential. *JACC Cardiovasc. Imaging* 5, 285–292. doi: 10.1016/j.jcmg.2011.11.017
- Higuchi, T., Fukushima, K., Rischpler, C., Isoda, T., Javadi, M. S., Ravert, H., et al. (2011). Stable delineation of the ischemic area by the PET perfusion tracer 18F-fluorobenzyl triphenyl phosphonium after transient coronary occlusion. *J. Nucl. Med.* 52, 965–969. doi: 10.2967/jnumed.110.085993
- Jin, Z., Sun, R., Wei, H., Gao, X., Chen, Y., and Tian, Z. (2011). Accelerated liver fibrosis in hepatitis B virus transgenic mice: involvement of natural killer T cells. *Hepatology* 53, 219–229. doi: 10.1002/hep.23983
- Karthikeyan, S., Potter, J. J., Geschwind, J. F., Sur, S., Hamilton, J. P., Vogelstein, B., et al. (2016). Deregulation of energy metabolism promotes antifibrotic effects in human hepatic stellate cells and prevents liver fibrosis in a mouse model. *Biochem. Biophys. Res. Commun.* 469, 463–469. doi: 10.1016/j.bbrc.2015.10.101
- Madar, I., Ravert, H., Nelkin, B., Abro, M., Pomper, M., Dannals, R., et al. (2007). Characterization of membrane potential-dependent uptake of the novel PET tracer 18F-fluorobenzyl triphenylphosphonium cation. *Eur. J. Nucl. Med. Mol. Imaging* 34, 2057–2065. doi: 10.1007/s00259-007-0500-8
- Mehendale, H. M., Roth, R. A., Gandolfi, A. J., Klaunig, J. E., Lemasters, J. J., and Curtis, L. R. (1994). Novel mechanisms in chemically induced hepatotoxicity. *FASEB J.* 8, 1285–1295. doi: 10.1096/fasebj.8.15.8001741
- Min, J. J., Biswal, S., Deroose, C., and Gambhir, S. S. (2004). Tetraphenylphosphonium as a novel molecular probe for imaging tumors. *J. Nucl. Med.* 45, 636–643.
- Poynard, T., Bedossa, P., and Opolon, P. (1997). Natural history of liver fibrosis progression in patients with chronic hepatitis C. The OBSVIRC, METAVIR, CLINIVIR, and DOSVIRC groups. *Lancet* 349, 825–832. doi: 10.1016/S0140-6736(96)07642-8
- Schneider, C. A., Rasband, W. S., and Eliceiri, K. W. (2012). NIH Image to ImageJ: 25 years of image analysis. *Nat. Methods* 9, 671–675. doi: 10.1038/nmeth.2089
- Wang, L., Potter, J. J., Rennie-Tankersley, L., Novitskiy, G., Sipes, J., and Mezey, E. (2007). Effects of retinoic acid on the development of liver fibrosis produced by carbon tetrachloride in mice. *Biochim. Biophys. Acta* 1772, 66–71. doi: 10.1016/j.bbadis.2006.08.009

Publisher's Note: All claims expressed in this article are solely those of the authors and do not necessarily represent those of their affiliated organizations, or those of the publisher, the editors and the reviewers. Any product that may be evaluated in this article, or claim that may be made by its manufacturer, is not guaranteed or endorsed by the publisher.

Copyright © 2021 Frontiers Production Office. This is an open-access article distributed under the terms of the Creative Commons Attribution License (CC BY). The use, distribution or reproduction in other forums is permitted, provided the original author(s) and the copyright owner(s) are credited and that the original publication in this journal is cited, in accordance with accepted academic practice. No use, distribution or reproduction is permitted which does not comply with these terms.



Targeting Mechanosensitive Piezo1 Alleviated Renal Fibrosis Through p38MAPK-YAP Pathway

Yuanyuan Fu¹, Pengzhi Wan², Jie Zhang¹, Xue Li³, Jia Xing¹, Yu Zou¹, Kaiyue Wang¹, Hui Peng^{1,3}, Qizhuo Zhu¹, Liu Cao^{5*} and Xiaoyue Zhai^{1,4*}

¹Department of Histology and Embryology, Basic Medical College, China Medical University, Shenyang, China, ²Department of Nephrology, First Affiliated Hospital of China Medical University, Shenyang, China, ³Department of Nephrology, Shengjing Hospital of China Medical University, Shenyang, China, ⁴Institute of Nephropathology, China Medical University, Shenyang, China, ⁵Department of Basic Medical College, China Medical University, Shenyang, China

OPEN ACCESS

Edited by:

Isotta Chimenti,
Sapienza University of Rome, Italy

Reviewed by:

Rachel Katherine Miller,
University of Texas Health Science
Center at Houston, United States
Gloria Garofolo,
Centro Cardiologico Monzino, Italy

*Correspondence:

Liu Cao
lcao@cmu.edu.cn
Xiaoyue Zhai
xyzhai@cmu.edu.cn

Specialty section:

This article was submitted to
Molecular and Cellular Pathology,
a section of the journal
Frontiers in Cell and Developmental
Biology

Received: 14 July 2021

Accepted: 21 October 2021

Published: 05 November 2021

Citation:

Fu Y, Wan P, Zhang J, Li X, Xing J,
Zou Y, Wang K, Peng H, Zhu Q, Cao L
and Zhai X (2021) Targeting
Mechanosensitive Piezo1 Alleviated
Renal Fibrosis Through p38MAPK-
YAP Pathway.
Front. Cell Dev. Biol. 9:741060.
doi: 10.3389/fcell.2021.741060

Renal fibrosis is the most common pathological manifestation of a wide variety of chronic kidney disease. Increased extracellular matrix (ECM) secretion and enhanced microenvironment stiffening aggravate the progression of renal fibrosis. However, the related mechanisms remain unclear. Here, we evaluated the mechanism by which ECM stiffness aggravates renal fibrosis. In the present study, renal mesangial cells (MCs) were cultured on polyacrylamide hydrogels with different stiffness accurately detected by atomic force microscope (AFM), simulating the *in vivo* growth microenvironment of MCs in normal kidney and renal fibrosis. A series of *in vitro* knockdown and activation experiments were performed to establish the signaling pathway responsible for mechanics-induced MCs activation. In addition, an animal model of renal fibrosis was established in mice induced by unilateral ureteral obstruction (UUO). Lentiviral particles containing short hairpin RNA (sh RNA) targeting Piezo1 were used to explore the effect of Piezo1 knockdown on matrix stiffness-induced MCs activation and UUO-induced renal fibrosis. An *in vitro* experiment demonstrated that elevated ECM stiffness triggered the activation of Piezo1, which increased YAP nuclear translocation through the p38MAPK, and consequently led to increased ECM secretion. Furthermore, these consequences have been verified in the animal model of renal fibrosis induced by UUO and Piezo1 knockdown could alleviate UUO-induced fibrosis and improve renal function *in vivo*. Collectively, our results for the first time demonstrate enhanced matrix stiffness aggravates the progression of renal fibrosis through the Piezo1-p38MAPK-YAP pathway. Targeting mechanosensitive Piezo1 might be a potential therapeutic strategy for delaying the progression of renal fibrosis.

Keywords: renal fibrosis, matrix stiffness, extracellular matrix secretion, Piezo1, YAP

INTRODUCTION

Chronic kidney disease (CKD) has become a serious public health problem endangering human health, which affects ~10% of global population (Qiu et al., 2018). Renal fibrosis is the most common pathological manifestation of a wide variety of CKD, which characterized by excessive deposition of extracellular matrix (ECM) including collagen fibers and fibronectin (Imamura et al., 2018). Currently, there are very limited therapeutics to treat renal fibrosis effectively. So, the need to explore its unknown mechanisms and prevent the progression of this disease is urgent.

Mechanical information is increasingly recognized as comprehensive regulator of cell biological behavior. Abnormal mechanotransduction is correlated with the progression and severity of diseases including fibrosis (Li et al., 2019), cancer (Lee et al., 2019), and cardiovascular defects (Yamashiro et al., 2020). Increased ECM stiffness through collagen deposition or crosslinking accelerates ECM secretion and subsequently aggravates the progression of renal fibrosis, which forms a vicious positive feedback loop (Chen et al., 2014). Thus, targeting the mechanotransduction signaling pathway induced by enhanced ECM stiffness may provide a therapeutic strategy for renal fibrosis. As one of the inherent cells of the kidney, mesangial cells (MCs) have the function of maintaining the metabolic balance of ECM under normal physiological conditions (Huang et al., 2017). MCs can be activated and produce large amounts of ECM in renal fibrosis. However, the effect of extracellular matrix mechanical microenvironment on MCs is not clear.

The transcription factor Yes-associated protein (YAP) in the Hippo signaling pathway can be activated to translocate to nucleus by mechanical force stimulation (Dupont et al., 2011; Cobbaut et al., 2020). Furthermore, YAP binds to transcriptional enhanced associate domain (TEAD) in the nucleus, which affects target gene such as CTGF and then cell proliferation and differentiation, tissue regeneration and organ size determination (Zhang et al., 2014; Brusatin et al., 2018). It has been reported that increased ECM stiffness activates YAP, which leads to ECM deposition and then contributes to increased ECM stiffness (Cai et al., 2021). Despite these important findings, the molecular mechanisms by which MCs sense and transduce the mechanical signals to activate YAP needs to be further explored.

Piezo1, an emerging mechanical force receptor on the cell membrane, has been shown to respond to a wide range of mechanical forces, such as substrate stiffness, shear flow extrusion and tissue compression (Chen et al., 2018). Piezo1 can directly respond to mechanical force stimulation without the activation of other proteins or second messenger signals (Syeda et al., 2016). Reports have shown that Piezo1 is widely expressed in the kidney, bladder and endothelial cells (Dalghi et al., 2019). Piezo1-mediated sensing of mechanical force regulates physiological functions such as vasculogenesis (Li J. et al., 2014), bone homeostasis and innate immunity (Solis et al., 2019). However, it is not clear whether Piezo1 acts as an upstream mechanical response to YAP in renal fibrosis.

In our study, MCs were cultured on hydrogels with different stiffness *in vitro* to simulate the growth microenvironment of MCs in normal kidney and renal fibrosis. A series of *in vitro* knockdown and reverse experiments were performed to establish the signaling pathway responsible for matrix stiffness-induced MC activation. The results demonstrated that Piezo1 function as a sensor of matrix stiffness and play a crucial role in YAP-mediated ECM accumulation, and the signaling transduction was relied on p38 MAPK phosphorylation. Furthermore, an animal model of renal fibrosis induced by unilateral ureteral obstruction (UUO) was used to observe the Piezo1-p38MAPK-YAP signaling pathway also plays a role *in vivo* and the intervention of Piezo1 can alleviate the progression of renal fibrosis. This study explores

the mechanism of renal fibrosis in terms of mechanical force, to provide a better perspective for preventing the process of renal fibrosis.

MATERIALS AND METHODS

Animals

Six-to eight-week-old male C57Bl/6 mice weighing 20–25 g were obtained from the Liaoning Changshen to the Ethics code of the World Medical Association for the animal care and were approved by the Medical Ethics Committee of China Medical University.

Unilateral Ureteral Occlusion Model and *in vivo* shRNA Treatment

The UUO model was established as described in previous study (Hoel et al., 2021). Briefly, the flank was exposed via a midline incision in the under aseptic conditions, the left ureter was exposed and ligated. Piezo1 shRNA and its negative controls were injected once with a dose of 2×10^7 TU in 0.1 ml saline solution via the tail vein at 3 days after UUO, and the kidney specimens and blood samples were collected on 14 days after UUO operation. The shRNA sequences were as follows: Piezo1 shRNA, 5'-GCATCTTCTCAGCCACTACT-3'.

Histopathologic Examination of Renal Tissue

Paraffin-embedded kidney tissues were cut into 4 μ m thick sections and mounted on slides. After deparaffinization and rehydration, the paraffin sections were stained with Masson's trichrome (Jiancheng) to assess the histopathologic changes in the kidneys according to the manufacturer's instructions. Three different fields were selected from per section, and three sections per animal were evaluated to obtain a mean value. Three mice from each group were used to obtain an overall value for subsequent statistical analysis.

For immunohistochemistry, after deparaffinization and rehydration, the paraffin sections were boiled with EDTA (pH = 8.0) for 2 min and 40 s at high pressure. The sections were then washed with PBS and incubated with goat serum for approximately 30 min. The sections were then incubated with anti-Fibronectin (ab2413, Abcam, 1:1,000), anti- α -SMA (130,621, Absin, Shanghai, China, 1:100) at 4°C overnight. Next the tissue sections were washed and incubated with biotinylated goat anti-rabbit IgG at room temperature for 1 h. The results were visualized with diaminobenzidine (DAB) (1809270031, MXB-BIO, Fuzhou, China). Hematoxylin was used as a counterstain. Images were taken with a camera mounted on a Nikon microscope (Eclipse 90i, Nikon, Tokyo, Japan).

Preparation of Hydrogels

First, a 0.25% LAP initiator solution (EFL, Suzhou, China) was prepared in a brown bottle to protect it from light, and then incubated in a 60°C water bath for 30 min to dissolve. The

solution was shaken every 10 min. The dissolved LAP standard solution was filtered with a 0.22 μm sterile filter for further use. Second, 0.5 g of the GelMA hydrogel (EFL, Suzhou, China) was put into a centrifuge tube, and the standard LAP initiator solution was added at different doses. The hydrogel was dissolved in a water bath at 60°C away from light for 30 min and filtered with a sterile filter. The hydrogel solution was then immediately injected into a Petri dish, and irradiated with an ultraviolet light source at 405 nm for approximately 1 min to solidify it.

Substrate Stiffness Measurements

Atomic force microscope (AFM) was used to determine the stiffness and surface topography of the hydrogels. AFM experiments were conducted using a Bioscope Catalyst AFM (Dimension icon, Bruker Corporation, United States) set on an inverted fluorescence microscope (Nikon, Tokyo, Japan). The probe was an MLCT-type, and the cantilever had a nominal spring constant of 0.01 N/m. First, the AFM tip was instructed to contact the base of the Petri dish to obtain the force curves and then calibrate the deflection sensitivity of the cantilever. Second the spring constants of the cantilever beam were calibrated by the thermal tuning method. Subsequently, the AFM tip was controlled and made to contact the surface of the hydrogel on the Petri dish. AFM senses the deformation of a cantilever, the tip of which interacts with the sample surface, to measure the force between the tip and sample surface (**Supplementary Figure S1A**). The morphology of the samples was measured by keeping the interaction between the tip and the surface constant (Li et al., 2014c). By pressing the tip onto the surface and measuring deformation of the cantilever, the stiffness of the samples was calculated using physical models (Liu et al., 2015). Fifty positions of the hydrogel were randomly selected from each group and used to obtain the force curves. Finally, the hydrogel young's modulus was computed using the Hertz model (Li et al., 2014b). The roughness of hydrogel surface was flat relative to the cells (**Supplementary Figure S1B**). The stiffness of the hydrogels was 2 ± 0.32 kPa and 50 ± 1.57 kPa, which are consistent with the elasticities of the normal kidney and sclerotic kidney, respectively (**Supplementary Figure 1C**).

Cellular Culture and Treatment

Immortalized mouse renal MCs (SV40-MES-13) were purchased from the Procell Life Science&Technology Co.,Ltd. (Wuhan, China) and cultured in DMEM/F12 containing 5% fetal bovine serum (FBS), 0.5% penicillin and streptomycin in an atmosphere of 5% CO₂ at 37 °C. Following overnight serum deprivation, the SV40-MES-13 cells were seeded on cover slips coated with either 2 kPa (soft) or 50 kPa (stiff) hydrogels, and then treated with the YAP inhibitor Super-TDU (Selleckchem, Houston, TX, United States, s8554), Piezo1 activator Yoda-1 (Selleckchem, s6678), MEK1/2 inhibitor PD0325901 (MedChemExpress, Shanghai, China, HY-131295), JNK inhibitor SP600125 (MedChemExpress, HY-12041), or the p38 kinase inhibitor SB203580 (MedChemExpress, HY-10256) for 48 h.

Lentiviral Short Hairpin RNA Transfection

Lentiviral particles containing short hairpin RNA (sh RNA) targeting Piezo1 and non-silencing shRNA were purchased from SyngenTech Co., Ltd. (Beijing, China). SV40-MES-13 cells were transfected with lentivirus containing Piezo1 shRNA to knockdown Piezo1, while the scrambled non-silencing shRNA sequence was used as a negative control (NC). The shRNA sequences were as follows: NC shRNA, 5'-CCTAAGGTTAAGTCGCCCTCGC-3', Piezo1 shRNA, 5'-GCATCTTTCAGCCACTACT-3'. The transfection efficiency was determined by immunoblotting. Western blot analysis was used to verify the transfection efficiency (**Supplementary Figure S2**).

Cell Viability Assay

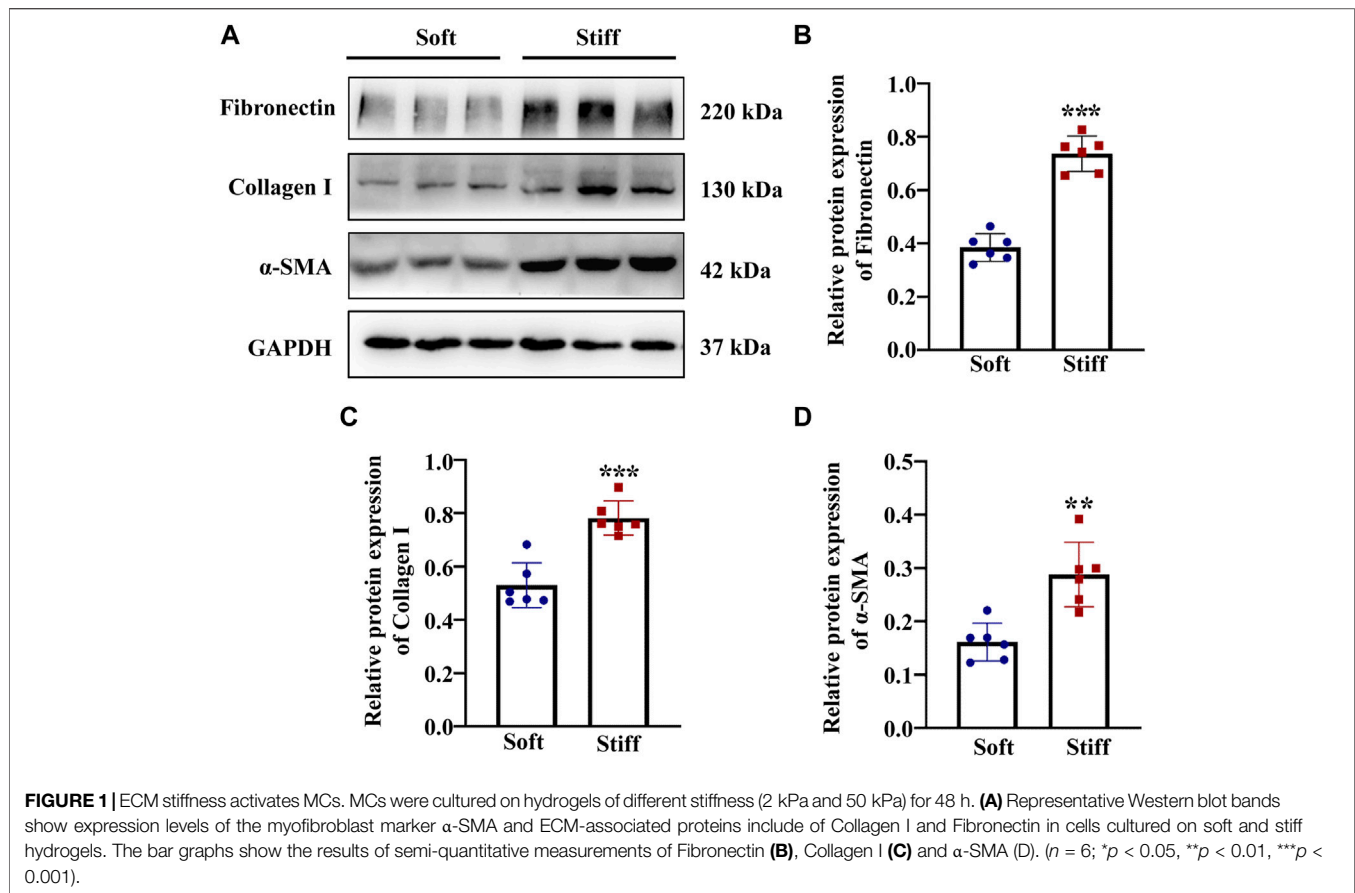
Cell viability assay was performed with a Cell Counting Kit-8 (CCK-8) (MedChemExpress, Shanghai, China, HY-K0301) according to the manufacturer's instructions. Briefly, cells were seeded in 96-well plates and treated with different concentrations of Super-TDU, the CCK-8 solutions were added and incubated for 4 h. Absorption at 450 nm was subsequently measured on the Varioskan Flash (Thermo Fisher, United States). Each experiment was repeated three times individually. The results were expressed as a percentage of the control that was set as 1.

Real-Time PCR

Total RNA was isolated using TRIzol reagent (Invitrogen, Carlsbad, CA, United States) according to the manufacturer's protocol. Briefly, 1 μg of RNA was reverse transcribed into cDNA using the Primer Script RT reagent kit (DRR047A, Takara, Japan). Quantitative PCR was carried out using an ABI 7500 real-time PCR system (Applied Biosystems, Darmstadt, Germany). The mRNA levels were normalized to GAPDH. The relative expression was calculated by the 2^(- $\Delta\Delta\text{Ct}$) method. The primer sequences are as follows: Piezo1 forward: 5'-TACGCCGAGGTGTGCTGGAC-3' and reverse: 5'-GCTGGTGTCTGTGCATGCTAC-3'.

Western Blot Analysis

Renal tissues and SV40-MES-13 cells were lysed with RIPA lysis buffer containing protease and phosphatase inhibitors. The concentration of protein was estimated with a BCA protein assay kit (Beyotime Biotechnology, Shanghai, China), and the lysates were diluted until their protein concentration was to 2 $\mu\text{g}/\mu\text{l}$. After normalization, equal amounts proteins were separated on SDS-polyacrylamid gels. The samples were separated by applying a constant voltage of 100 V for 1.5 h and then transferred onto PVDF membranes. After nonspecific sites were blocked with Tris-buffered saline (TBS) containing 0.1% Tween 20 and 5% defatted dried milk, the membranes were incubated with anti-Piezo1 (78,446, Novas Biological, Littleton, Colorado, United States, 1:1,000), anti-p-p38MAPK (4,511, Cell Signaling Technology, 1:1,000), anti-p38MAPK (8,690, Cell Signaling Technology, 1:1,000), anti-p-ERK (4,370, Cell Signaling Technology, 1:1,000), anti-ERK (4,695, 1:1,000, Cell Signaling Technology), anti-p-JNK (sc6254, Santa Cruz Biotechnology, Dallas, TX, United States, 1:500), anti-JNK(sc7345, Santa Cruz Biotechnology, 1:500), anti-YAP



(ab205270, Abcam, 1:1,000), anti-Collagen I (0,088, Wanleibio, Shenyang, China, 1:500), anti-Fibronectin (ab2413, Abcam, 1:1,000), anti-p-YAP (13,008, Cell Signaling Technology, 1:1,000), anti-MST1 (AF2367, Affinity Biosciences, 1:1,000), MST1 (22245-1-AP, Proteintech, 1:1,000), p-LATS1 (AF7170, Affinity Biosciences, 1:1,000), LATS1 (17049-1-AP, Proteintech, 1:1,000) and rabbit anti-GAPDH (7,021, Affinity, Shanghai, China, 1:1,000) at 4°C overnight. The blots were incubated with a horseradish peroxidase-conjugated goat anti-rabbit or anti-mouse secondary antibody (P448, DAKO, Glostrup, Denmark, 1:200) at room temperature for 1 h. Finally, the blots were visualized using a bioanalytical imaging system (Azure Biosystems, Dublin, CA, United States).

Immunofluorescence Detection

Treated cells were fixed with 4% paraformaldehyde, washed with immunofluorescence detergent solution and blocked with 3% BSA for 30 min at room temperature. To visualize microfilaments, the cells were incubated with FITC-conjugated phalloidin (Beyotime Biotechnology, Shanghai, China) for 1 h at room temperature. To visualize YAP and α -SMA, the cells were incubated with anti-YAP (14,074, Cell Signaling Technology, 1:100), anti- α -SMA (130,621, Absin, Shanghai, China, 1:100) overnight at 4°C. Next day, the cells were washed and incubated with secondary antibody conjugated to the fluorescent markers FITC or TRITC at room temperature for 1 h in the dark, and then stained with 4',6'-diamidino-2-phenylindole

(Beyotime, Shanghai, China) for 10 min to visualize nuclei. The results were observed under a confocal microscope (Eclipse C1, Nikon, Tokyo, Japan). YAP nuclearstaining was quantified by counting the YAP staining-positive cells and then normalizing to the total cell number in each image. Three different fields were selected from a cell-cultured coverslip, and three parallel experiments for each treatment were performed.

Statistics

All analyses were performed using SPSS software, version 21.0 (SPSS Inc, Chicago, IL, United States), and all experiments were performed at least in triplicate. Data on the net optical density of the bands are presented as the means \pm standard deviations (SDs), and one-way analysis of variance followed by the Bonferroni test was used to compare the two different treatment groups. The unpaired two-sided Student's *t* test was used to analyze difference between two groups. Differences with a *p* value of < 0.05 were considered statistically significant.

RESULTS

Extracellular Matrix Stiffness Activates MCs via YAP

The mechanical properties of the cellular microenvironment play an essential role in determining cellular function and fate (Vining

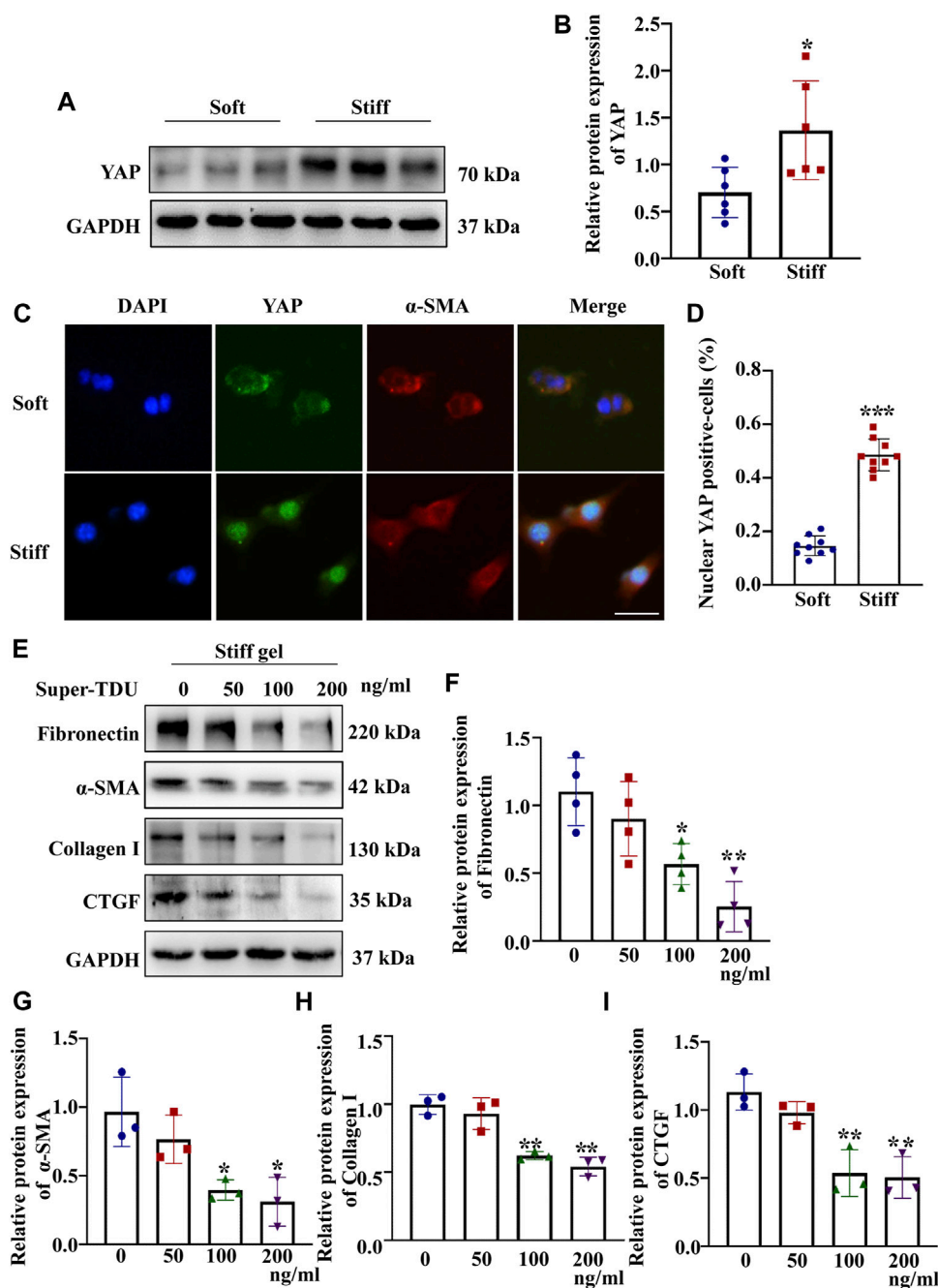


FIGURE 2 | ECM stiffness activates MCs through YAP. MCs were cultured on hydrogels of different stiffness (2 and 50 kPa) for 48 h. **(A)** Representative Western blot bands show the protein expression level of YAP. **(B)** The bar graph shows the result of semi-quantitative measurement of YAP ($n = 6$; * $p < 0.05$, ** $p < 0.01$, *** $p < 0.001$). **(C)** Representative photomicrographs show fluorescence staining with anti- α -SMA (red) and anti-YAP (green) antibodies in cells cultured on the soft and stiff hydrogels. Scale bar = 25 μ m. **(D)** The percentage of cells with predominantly nuclear YAP staining. ($p < 0.001$). **(E)** Western blot bands show expression levels of Fibronectin, Collagen 1, α -SMA and CTGF after which MCs were incubated with Super-TDU at various concentrations on the stiff gel (50 kPa) for 24 h. The bar graph shows the results of semi-quantitative of Fibronectin **(F)**, α -SMA **(G)** Collagen 1 **(H)** and CTGF **(I)** measurements ($n = 3$; * $p < 0.05$, ** $p < 0.01$, *** $p < 0.001$).

and Mooney, 2017). To test the effect of ECM stiffness on MCs, the protein expression of myofibroblast markers (α -SMA) and ECM-associated proteins (Collagen I and Fibronectin) was measured after the MCs had been cultured on matrices of different stiffness for 48 h. The results showed that the

α -SMA, Collagen I and Fibronectin protein expression levels were higher in MCs cultured on the stiff (50 kPa) hydrogel than in those cultured on the soft hydrogel (2 kPa) (**Figures 1B–D**). Moreover, to test whether ECM stiffness affects YAP in MCs, the expression and location of YAP were measured in cells

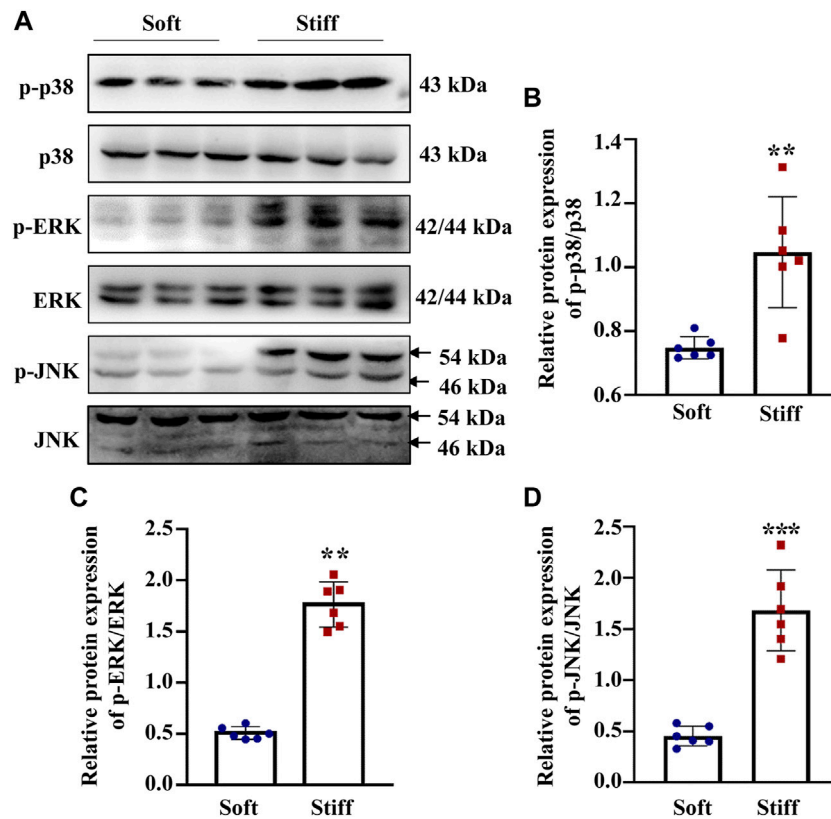


FIGURE 3 | ECM stiffness promotes MAPK signaling pathway activation. **(A)** Representative western blot bands show the protein expression levels of p-p38, p38, p-ERK, ERK, p-JNK and JNK. **(B)** The bar graph shows the result of semi-quantitative measurement of p-p38/p38. **(C)** The bar graph shows the result of semi-quantitative measurement of p-ERK/ERK. **(D)** The bar graph shows the result of semi-quantitative measurement of p-JNK/JNK ($n = 6$; * $p < 0.05$, ** $p < 0.01$, *** $p < 0.001$).

cultured on the soft and stiff hydrogels. As shown in **Figure 2B**, YAP protein expression was significantly increased in cells cultured on the stiff hydrogel. In addition, YAP translocation into the nucleus from the cytoplasm increased as the stiffness of the hydrogel increased. Notably, cells cultured in hydrogel with greater stiffness showed localization of YAP to the nucleus in conjunction with the increased expression of the myofibroblast marker α -SMA (**Figure 2C**). In addition, pretreatment of cells with Super-TDU, a YAP inhibitor, specifically inhibited the expression of CTGF, Fibronectin, α -SMA and Collagen I in cells cultured on the stiffer hydrogel (**Figures 2F–I**). The dose of Super-TDU was selected on the basis of CCK-8 assay (**Supplementary Figure S6**). Based on these results, we selected 0, 50, 100, and 200 ng/ml as Super-TDU administration concentrations for subsequent experiments to eliminate the interference of Super-TDU-induced cell death. These results demonstrate that ECM stiffness activates YAP to promote MCs activation.

p38MAPK Regulates Extracellular Matrix Stiffness-Induced YAP Activation

Having established that YAP plays a key role in mediating ECM stiffness-induced MC activation, we wanted to explore which

signaling pathway regulates ECM stiffness-induced YAP nuclear localization. Studies have shown that the MAPK signaling pathway mediates the regulation of YAP activation. In our experiment, we found that cells cultured on the stiff hydrogel expressed more p-p38, p-JNK and p-ERK proteins (**Figures 3B–D**) than cells cultured on the soft hydrogel. To further evaluate the role of the MAPK signaling pathway in ECM stiffness-induced YAP activation, cells cultured on the stiffer hydrogel were treated with an MEK1/2 inhibitor (PD0325901), a JNK inhibitor (SP600125), or a p38 kinase inhibitor (SB203580). Interestingly, only SB203580, the p38 kinase inhibitor, inhibited YAP expression (**Figure 4B**) and blocked YAP nuclear localization (**Figure 4D**) induced by the enhanced stiffness. SP600125 and PD0325901 treatment did not alter the expression of YAP (**Supplementary Figure S3**). In addition, SB203580 decreased the expression of α -SMA, Collagen I and Fibronectin (**Figures 4F–H**). These results indicate that ECM stiffness induced YAP activation through p38MAPK.

Piezo1 Mediates the Activation of YAP Through p38MAPK

Piezo1 can sense microenvironmental stiffness and transduce the external mechanical stimuli into the intracellular signaling

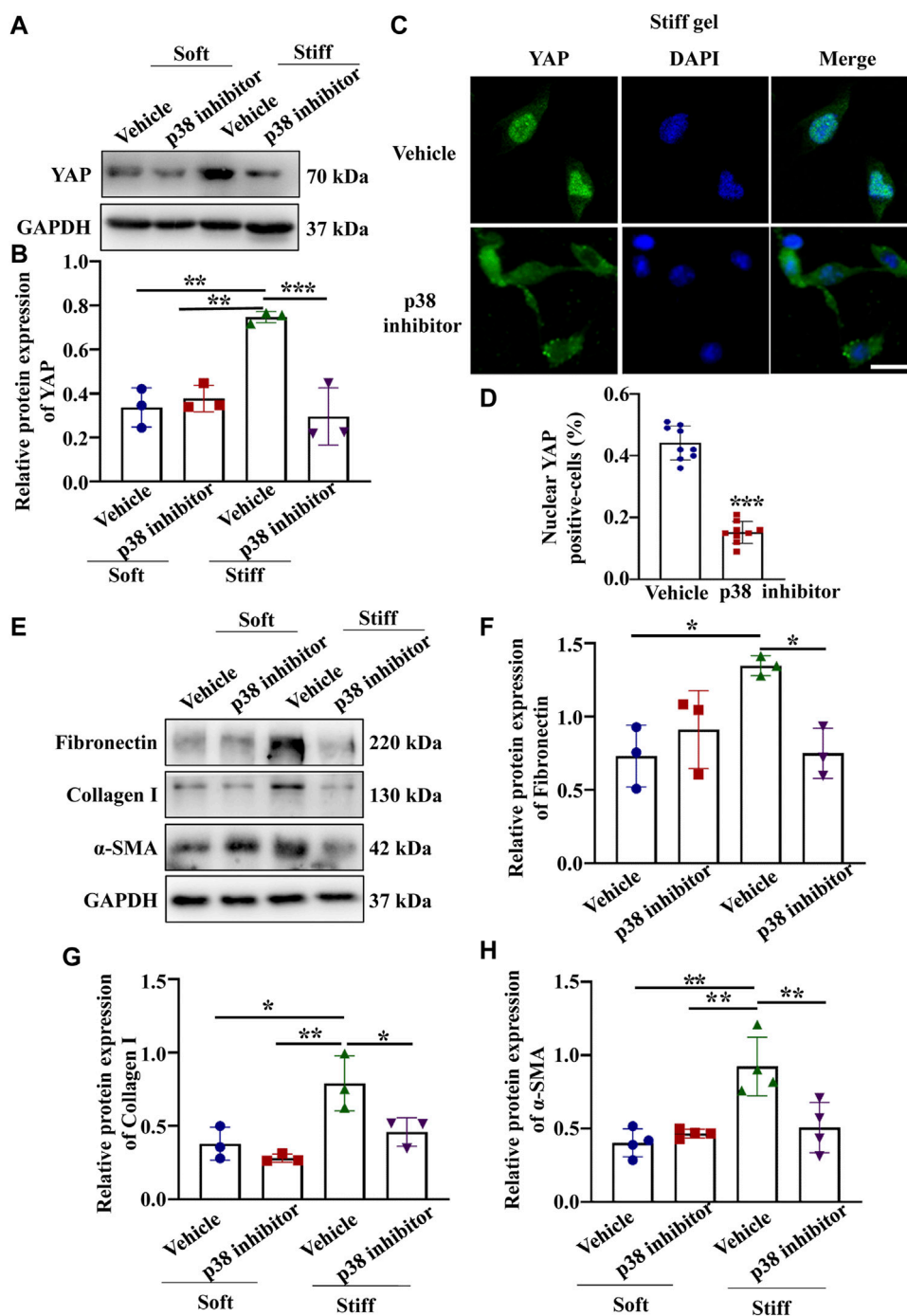


FIGURE 4 | p38 inhibitor blocked YAP activation and ECM protein expression induced by enhanced hydrogel stiffness. MCs were treated with vehicle or a p38 inhibitor and cultured on hydrogels with different stiffness. **(A)** Representative Western blot bands showing YAP expression in each group. **(B)** Semi-quantitative measurement of YAP ($n = 3$; * $p < 0.05$, ** $p < 0.01$, *** $p < 0.001$). **(C)** Representative photomicrograph showing fluorescence staining of YAP in cells treated with vehicle and a p38 inhibitor grown on the stiff hydrogels. Scale bar = 25 μm. **(D)** The percentage of cells with predominantly nuclear YAP staining. (***, $p < 0.001$). **(E)** Representative western blot bands show the protein expression levels of Fibronectin, Collagen 1 and α-SMA after MCs were treated with vehicle or a p38 inhibitor and cultured on the soft and stiff hydrogels. The bar graph shows the result of semi-quantitative measurement of Fibronectin **(F)**, Collagen I **(G)** and α-SMA **(H)** ($n = 3$; * $p < 0.05$, ** $p < 0.01$, *** $p < 0.001$).

pathway (Dasgupta and McCollum, 2019). In our experiments, we found that the Piezo1 protein expression level was increased in cells cultured on the stiff hydrogel compared to those cultured on

the soft hydrogel (Figure 5B). To explore how Piezo1 mediates cellular responses to ECM stiffness, we silenced Piezo1 in MCs by transfection with lentiviral shRNA targeting Piezo1 and cultured

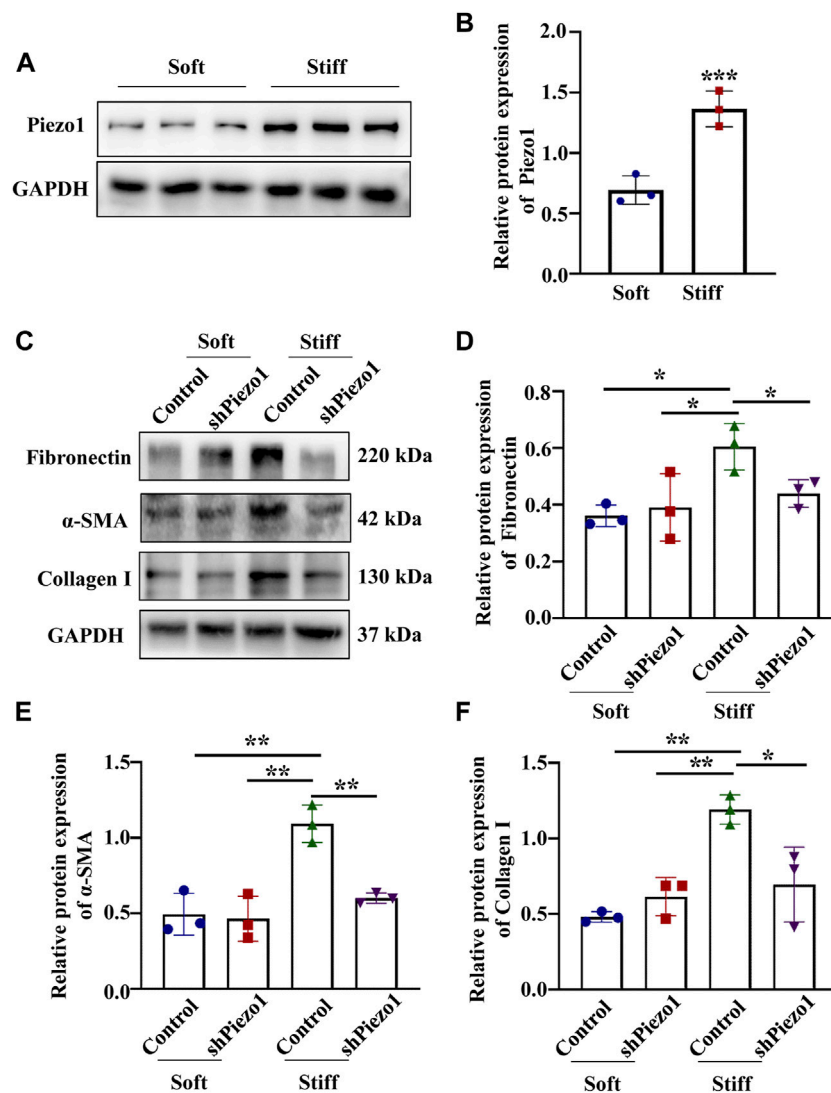


FIGURE 5 | Piezo1 knockdown reduced ECM protein levels. **(A)** Representative western blot bands of Piezo1 in MCs cultured on hydrogels with a stiffness of 2 kPa or 50 kPa for 48 h. **(B)** The bar graphs show the results of semi-quantitative measurement of Piezo1 ($n = 6$; * $p < 0.05$, ** $p < 0.01$, *** $p < 0.001$). **(C)** MCs were transfected with shNC or sh Piezo1 and grown on soft and stiff gels. Representative western blot bands of Fibronectin, α -SMA and Collagen I. The bar graph shows the result of semi-quantitative measurement of Fibronectin **(D)**, α -SMA **(E)** and Collagen I **(F)**. ($n = 3$; * $p < 0.05$, ** $p < 0.01$, *** $p < 0.001$).

the cells on stiff or soft hydrogel. Western blot analysis showed that Piezo1 knockdown reduced the protein levels of Fibronectin, α -SMA and Collagen I (**Figures 5D–F**). The Western blot results also showed that Piezo1 knockdown decreased p-p38 and YAP protein expression (**Figures 6B,C**). We also found that more cells transfected with Piezo1 shRNA displayed YAP nuclear exclusion than cells transfected with nontargeting shRNA (**Figure 6E**).

We then treated cells grown on the soft hydrogel with a p38 kinase inhibitor (SB203580) and a specific Piezo1 agonist (Yoda-1). we found that cells treated with Yoda-1 displayed higher YAP, Fibronectin Collagen I and α -SMA expression (**Figures 7B–E**) than the control cells. Moreover, the expression of YAP, Fibronectin Collagen I and α -SMA expression reduced in cells

treated with Yoda-1 and SB203580 when compared with cells applied for Yoda-1 alone. These results suggested that Piezo1 induced nuclear YAP translocation through p38 MAPK as ECM stiffness increased.

Piezo1 Knockdown Alleviated Renal Fibrosis Induced by UUO through p38MAPK-YAP Pathway.

To explore whether Piezo1-p38MAPK-YAP signaling pathway play a role in renal fibrosis and block the pathway could provide a potential therapeutic target for postponing the development of renal fibrosis, an animal model of renal fibrosis induced by UUO was established and a loss-of-function experiment was carried out by using shRNA of Piezo1 in UUO mice. Firstly, we found that the UUO group showed increased serum levels of BUN and creatinine as compared to

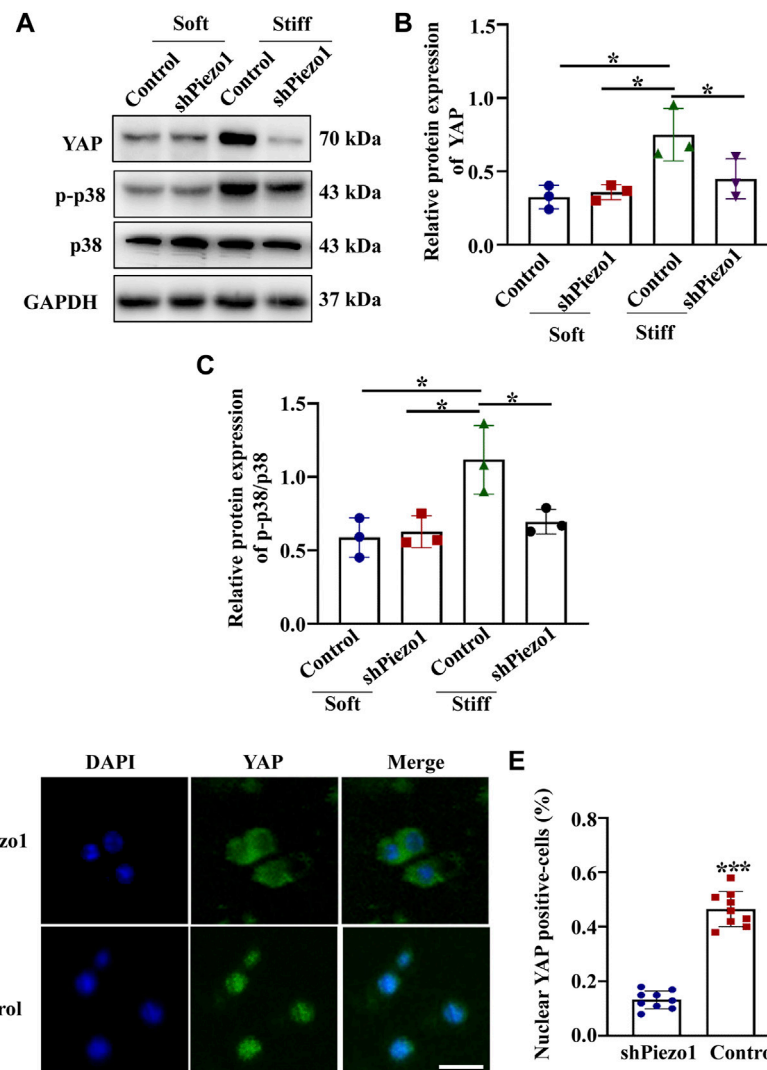


FIGURE 6 | Piezo1 knockdown reduced YAP and p-p38 expression. MCs were transfected with shNC or sh Piezo1 and grown on soft and stiff gels. **(A)** Representative western blot bands of YAP, p-p38 and p38. Semi-quantitative measurement of YAP **(B)** and p-p38/p38 ($n = 3$ * $p < 0.05$, ** $p < 0.01$, *** $p < 0.001$). **(D)** Representative photomicrographs show fluorescence staining with anti-YAP after MCs were transfected with shNC or sh Piezo1 and grown on stiff gels. Scale bar = 25 μm . **(E)** The percentage of cells with predominantly nuclear YAP staining. ($p < 0.001$).

the control group, whereas in Piezo1 knockdown UUO mice, this apparent upregulation was alleviated. The serum levels of BUN and creatinine did not differ between the UUO group and UUO + sh NC group (shNC refers to empty vector without Piezo1 shRNA) (Figures 8A,B). Masson staining further demonstrated that renal fibrosis was alleviated in Piezo1 knockdown UUO mice. The results showed that comparison with control group, the deposition of blue stained collagen fibers significantly up-regulated in the peritubular interstitial region in UUO and UUO + sh NC treated groups, however, the collagen fibers deposited were significantly reduced when Piezo1 was knocked down in UUO group (Figure 8D). In addition, compared to the UUO group, Piezo1 knockdown UUO mice showed decreased levels of the renal fibrosis markers α -SMA, Collagen I and Fibronectin (Figures 9B–D). Consistent with the

results, immunostaining staining shown that α -SMA was widely expressed in the perivascular interstitial region and in smooth muscle cells in UUO and UUO + sh NC groups, and the α -SMA expression significantly reduced after Piezo1 shRNA administration, and was mainly expressed in smooth muscle cells. The fibronectin protein was widely expressed in the interstitial region in UUO and sh-NC treated UUO groups, whereas the distribution was significantly decreased in UUO treated with Piezo1 shRNA group (Figure 9E).

To verify that Piezo1 knockdown alleviate renal fibrosis through the p38MAPK-YAP pathway, we examined the expression of p-p38, p38 and YAP expression in four groups. As shown in Figures 10B,E, Piezo1 mRNA and protein level up-regulated significantly in comparison with the control, and they were downregulated after Piezo1 knockdown in UUO treated

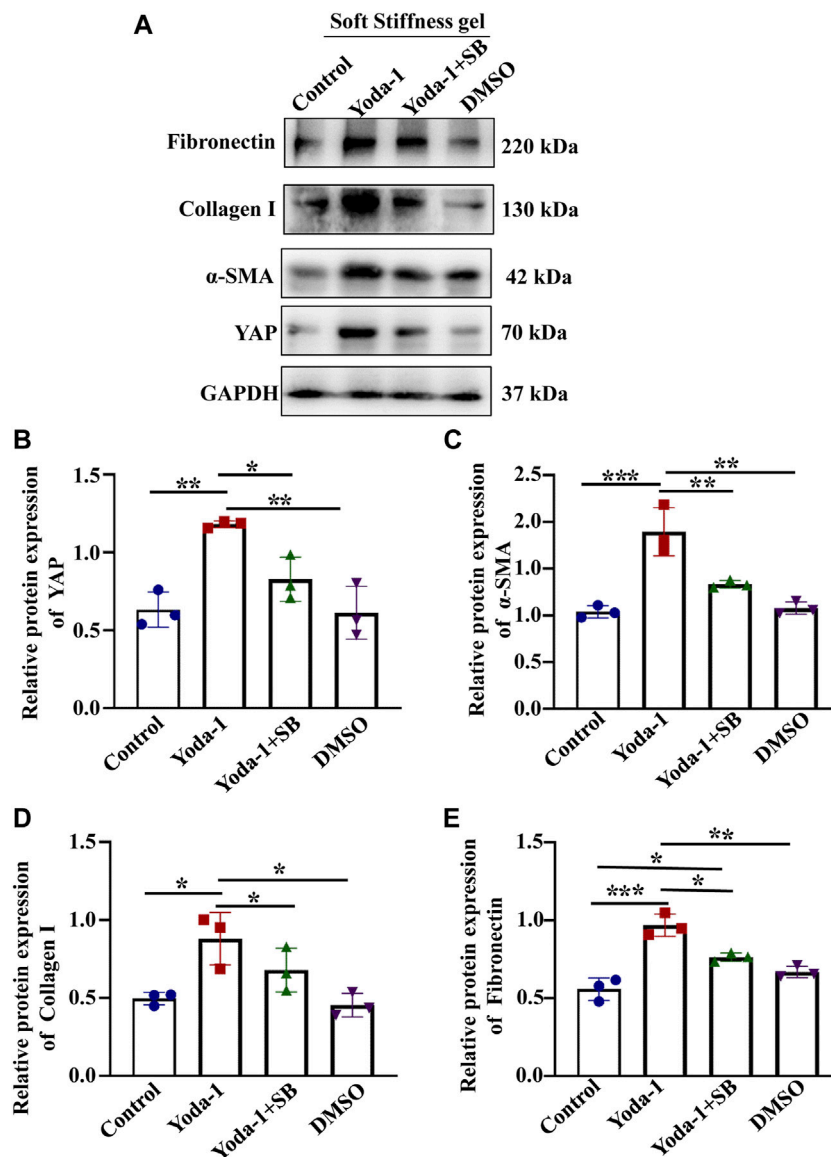


FIGURE 7 | p38 MAPK inhibitor reduced the increased YAP expression and ECM secretion induced by Piezo1 activator. **(A)** MCs were incubated with Yoda-1 and SB for 48 h on the soft gel. **(A)** Representative western blot bands represent the protein expression levels of Fibronectin, Collagen 1, α-SMA and YAP. The bar graph shows the result of semi-quantitative measurement of Fibronectin **(B)**, α-SMA **(C)**, Collagen I **(D)** and YAP **(E)**. ($n = 3$; * $p < 0.05$, ** $p < 0.01$, *** $p < 0.001$).

mice. Western blot results demonstrated that compared with the control, YAP protein level and p-p38/p38 ratio were increased significantly in UUO group, but they were reduced significantly after Piezo1 sh RNA administration in comparison with the UUO group (**Figures 10C,D**). Altogether, these results indicated that Piezo1 knockdown alleviated renal fibrosis induced by UUO through p38MAPK-YAP pathway.

DISCUSSION

It is generally accepted that changes in cellular mechanical microenvironment play an essential role in cell behavior and

progression of disease (D'Urso and Kurniawan, 2020; Silver et al., 2021). In the present study, we investigated the mechanism of renal fibrosis from the perspective of mechanical force. Our results showed that ECM stiffness could promote excessive secretion of ECM by MCs through the Piezo1-p38MAPK-YAP signaling pathway, in addition, the Piezo1-p38MAPK-YAP signaling pathway has been verified to play a role in the animal model of renal fibrosis induced by UUO and targeting mechanosensitive Piezo1 attenuates the progression of renal fibrosis.

YAP is the prime mediator of the Hippo pathway, and its expression and cellular distribution were reported to be mechanically regulated by ECM stiffness (Ghasemi et al., 2020; Zhang et al., 2020). In the present study, we found that the

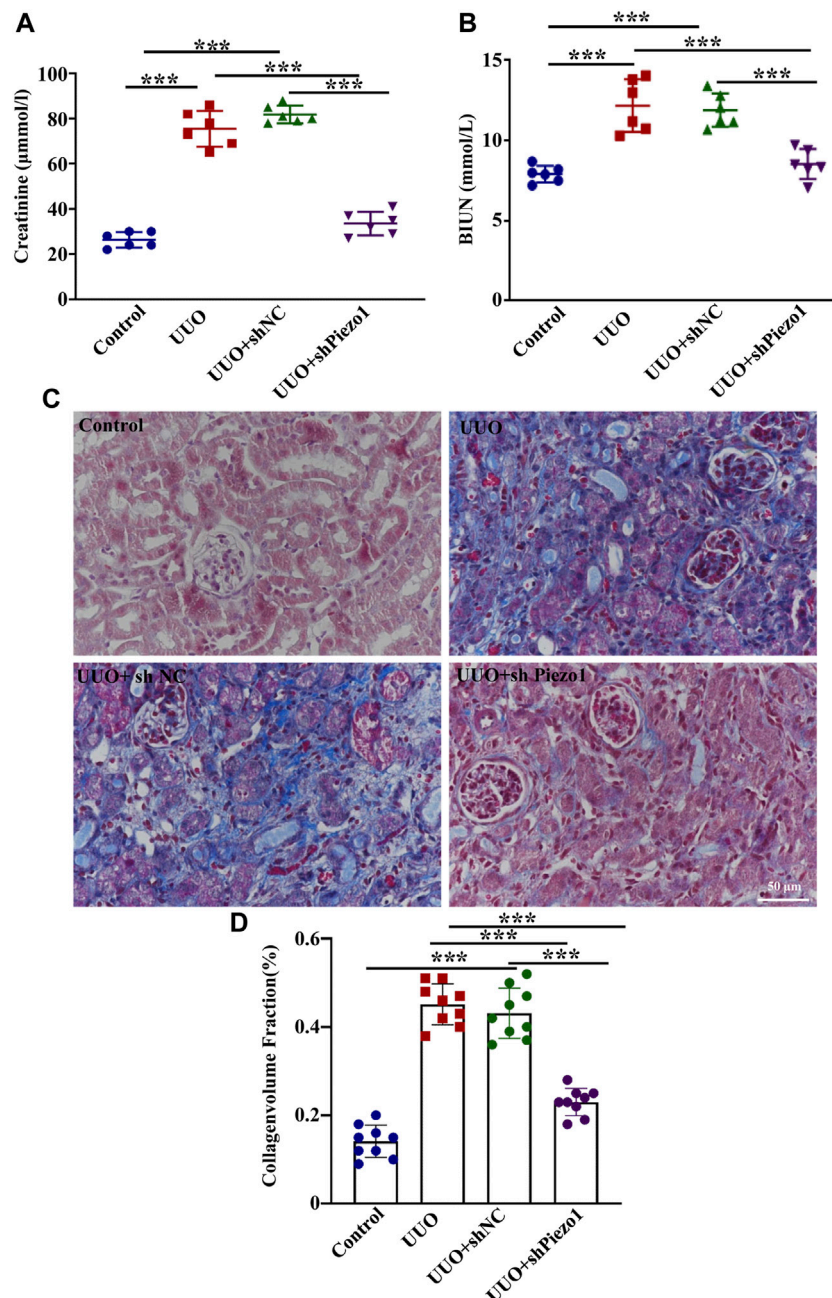
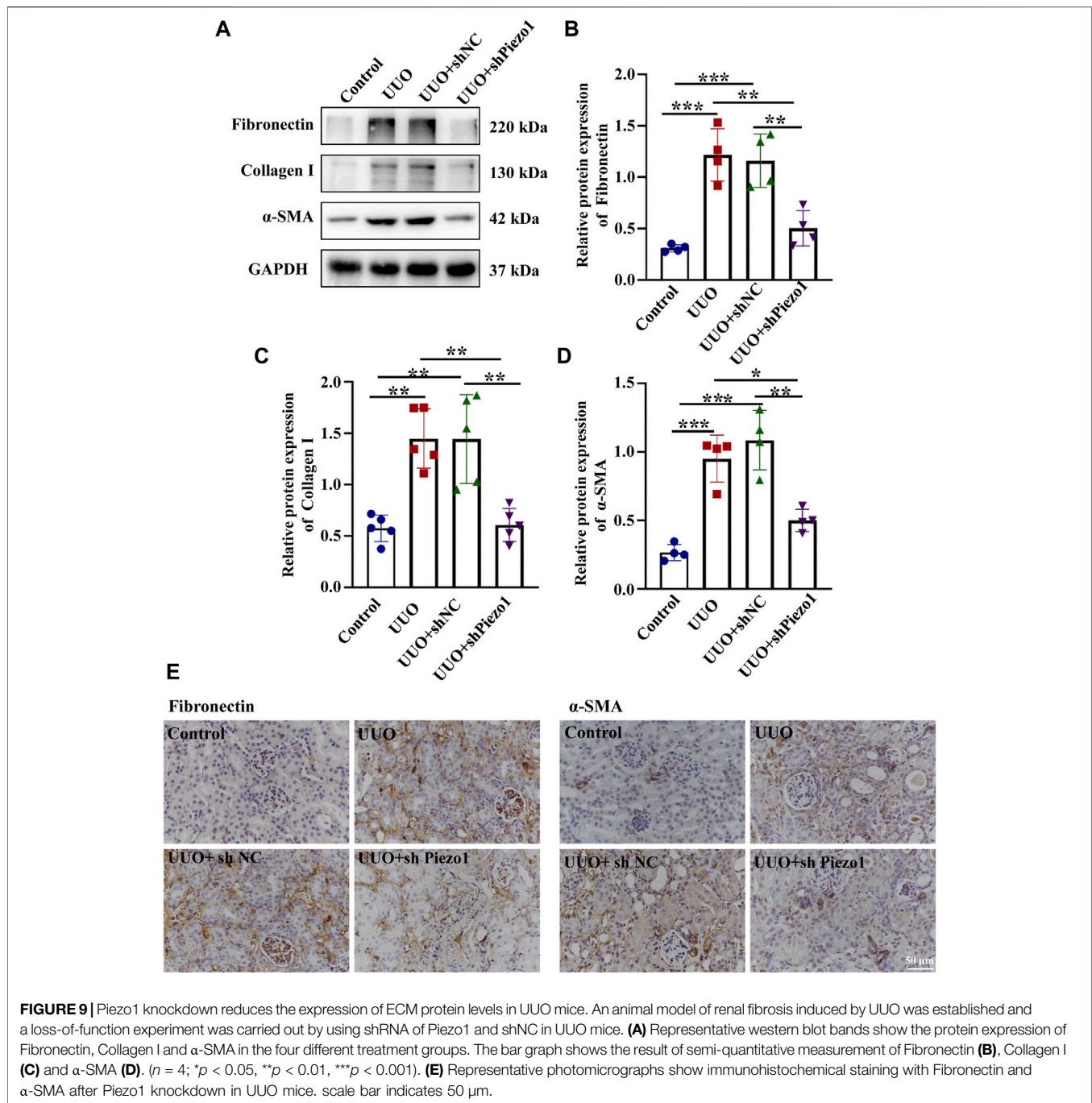


FIGURE 8 | Piezo1 knockdown improved renal function in UUO mice. An animal model of renal fibrosis induced by UUO was established and a loss-of-function experiment was carried out by using shRNA of Piezo1 and shNC in UUO mice. shNC refers to empty vector without Piezo1 shRNA. Renal function is assessed by **(A)** plasma creatinine and **(B)** BUN levels. ($n = 6$; * $p < 0.05$, ** $p < 0.01$, *** $p < 0.001$). **(C)** Masson staining reveals the excessive deposition of ECM (blue) in four different treatment groups. **(D)** The collagenvolume fraction in four different treatment groups (* $p < 0.05$, ** $p < 0.01$, *** $p < 0.001$).

expression of YAP in kidney was elevated in response to UUO. In addition, the results demonstrated that YAP could be activated by enhanced ECM stiffness and translocate to the nucleus, moreover, the inhibition of YAP impeded CTGF expression and ECM secretion. Consistent with our results, Cheng *et al.* reported that matrix stiffness can activate fibroblasts in a YAP-dependent manner (Liang *et al.*, 2017). It was also reported that in fibroblasts, ECM stiffness mechanoactivates YAP, which

promotes the production of profibrotic mediators and ECM proteins (Noguchi *et al.*, 2018). Altogether, these results demonstrated that increased YAP-induced ECM production in MCs is mediated by enhanced ECM stiffness in renal fibrosis. However, how ECM stiffness regulates YAP expression and localization remains unknown.

Existing studies have shown that the entry of YAP into the nucleus is regulated by a variety of signaling pathway. However,



as a key protein of Hippo signaling pathway, YAP has been reported participated in the Hippo signaling pathway in many studies and its mechanism is relatively clear (Yu et al., 2015). That is, the upstream regulatory element NF2 of Hippo signaling pathway can activate the core kinase chains Mst1/2 and LATS1/2 of Hippo pathway, and then regulate the activity and localization of YAP (Pancieria et al., 2017). Bioinformatic analysis of protein-protein interactions in STRING v.10 provided a protein network associated with MAPK and YAP (**Supplementary Figure S5**). Moreover, cancer studies have

demonstrated that enhanced matrix stiffness accelerates the migration of hepatocellular carcinoma cells via MAPK-YAP signaling (Qiu et al., 2020). However, it is not clear whether YAP is regulated by MAPK in renal fibrosis. Here, we established that p38 serves as an important link between ECM stiffness and YAP activation. p38, a member of the MAPK family, is a key regulator of proliferation, apoptosis and autophagy (Wang et al., 2017; Lee et al., 2020). Our results showed that p-p38, p-JNK, and p-ERK protein expression was significantly elevated in cells cultured on the stiff hydrogel compared with cells grown on

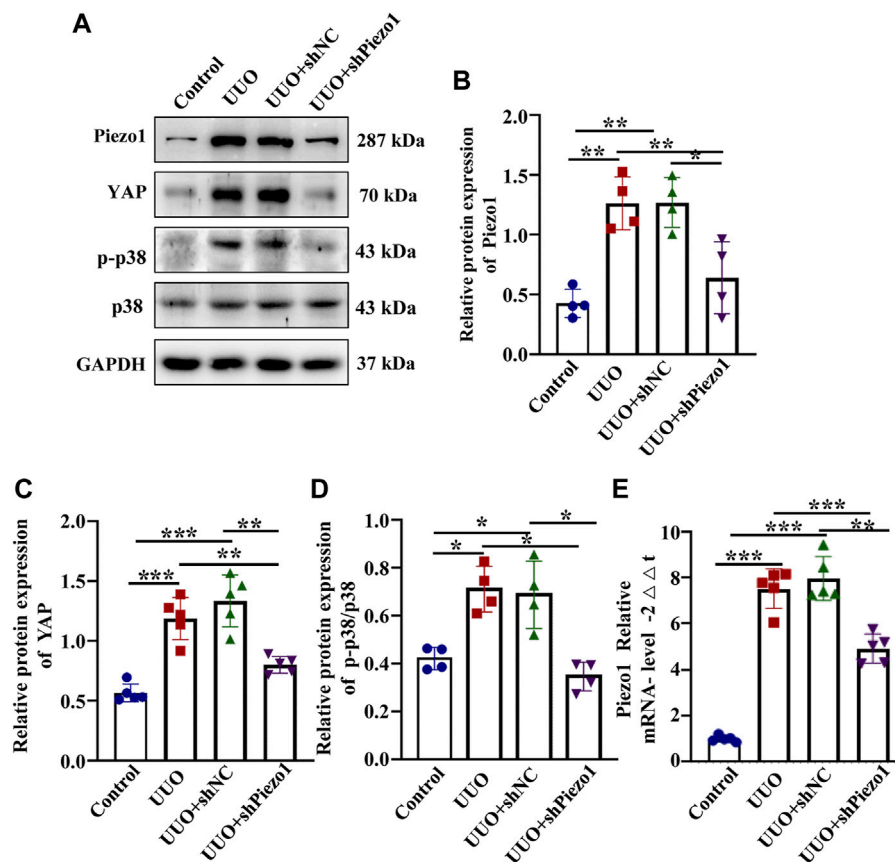


FIGURE 10 | Piezo1 knockdown alleviates renal fibrosis through p38MAPK-YAP pathway. An animal model of renal fibrosis induced by UUO was established and a loss-of-function experiment was carried out by using shRNA of Piezo1 and shNC in UUO mice. **(A)** Representative western blot bands show the protein expression of Piezo1, p-p38, p38 and YAP in four different treatment groups. The bar graph shows the result of semi-quantitative measurement of Piezo1 **(B)**, p-p38/p38 **(C)** and YAP **(D)** ($n = 4$; $*p < 0.05$, $**p < 0.01$, $***p < 0.001$). **(E)** Relative mRNA expression of Piezo1 in four different treatment groups. ($n = 5$, $*p < 0.05$, $**p < 0.01$, $***p < 0.001$).

the soft gel. However, only the p38 kinase inhibitor could prevent YAP activation induced by enhanced hydrogel stiffness. Guan *et al.* reported that the TEA domain (TEAD) family of DNA-binding transcription factors to which YAP binds to regulate gene expression, directly interact with p38 without scaffold proteins (Lin *et al.*, 2018). Another report has demonstrated that p38, YAP, and TEAD are complexed together in cardiac fibroblasts (Bugg *et al.*, 2020). The *in vivo* results also demonstrated that the p-p38 level was higher in the UUO model than in control mice. Previous studies have shown that the p-p38/p38 ratio is increased in renal fibrosis induced by UUO (Gu *et al.*, 2019). In addition, mechanical force can stimulate the activation of p38MAPK to regulate cellular behavior (Bugg *et al.*, 2020). It also has been demonstrated that p38 induces YAP nuclear translocation by inhibiting the components of Hippo pathway (Hsu *et al.*, 2020). To investigate the effects of p38 inhibitor on Hippo components expression and the level of YAP phosphorylation. The results demonstrated that the p-MST1/MST1 and p-LATS/LATS increased significantly in cells treated with p38 inhibitor when compared to the control, and the expression of p-YAP also enhanced when added to p38 inhibitor (**Supplementary**

Figure S6). Therefore, it is speculated that P38 may regulate YAP in two ways, the first one is that p38 can activate YAP by inhibiting Hippo pathway and the second is that p38 can directly regulate YAP without relying on other proteins. These results indicate that ECM stiffness serves upstream of the MAPK signaling axis and activates the phosphorylation of p38 MAPK, triggering YAP activation and a downstream cascade.

As p38MAPK is an intracellular molecule, it cannot directly sense surrounding mechanical signals. The membrane protein that senses mechanical signals and transduces these signals to p38MAPK to regulate renal fibrosis remains to be fully defined. Piezo1 has been reported to be an important sensor of various aspects of mechanotransduction (Wang *et al.*, 2019). It is widely expressed in various tissues, including the kidney, and can be directly activated by mechanical forces acting on the cell membrane (Yoneda *et al.*, 2019). Our results demonstrated that stiff substrate facilitates Piezo1 activation. Moreover, we also found that a significant increase in Piezo1 expression in renal fibrosis induced by UUO. *In vitro* results showed that Piezo1 silencing reduced ECM expression and YAP nucleation. In addition, YAP

expression and ECM secretion dramatically increased after administrated the Yoda-1, whereas they were reduced significantly in cells treated with Yoda-1 and SB203580 when compared with cells applied for Yoda-1 alone. These results further demonstrate that p38MAPK involved in the regulation of YAP and ECM levels by Piezo1. Moreover, *in vivo* experiment showed that Piezo1 knockdown could alleviate renal fibrosis and renal function, and which the process mediated by the p38MAPK-YAP pathway. Piezo proteins are subunits of calcium ion-permeable nonselective cation channels that respond to mechanical force (Liu et al., 2020). When Piezo1 activated by mechanical force, it causes a massive influx of calcium ions into the cell. It has been reported that the increase of calcium in cells is related with p38 MAPK activation (Zhou et al., 2021). Turner *et al.* reported that p38 is activated downstream of Piezo1-mediated Ca²⁺ entry, increasing IL-6 secretion (Blythe et al., 2019). Also, in bone homeostasis, Piezo1 has been reported that induce YAP-dependent expression of several ECM such as type II and IX collagens (Wang et al., 2020). However, it has been reported that Piezo1 could act upstream of YAP in oral squamous cell carcinoma (Hasegawa et al., 2021). We speculate that the hierarchical relationship between PIEZO1 and YAP may be dependent on this cell context, or that there is a positive feedback regulation between PIEZO1 and YAP.

In conclusion, elevated ECM stiffness could activate Piezo1, which increased YAP activity through the p38MAPK. This increased YAP protein promotes ECM secretion, thereby contributing to the progression of renal fibrosis. Moreover, the progression of renal fibrosis can be alleviated by intervening Piezo1. These results highlight the importance of Piezo1 and the potential utility of Piezo1 as a biomarker and therapeutic target of renal fibrosis.

DATA AVAILABILITY STATEMENT

The original contributions presented in the study are included in the article/**Supplementary Material**, further inquiries can be directed to the corresponding author.

REFERENCES

- Blythe, N. M., Muraki, K., Ludlow, M. J., Stylianidis, V., Gilbert, H. T. J., Evans, E. L., et al. (2019). Mechanically Activated Piezo1 Channels of Cardiac Fibroblasts Stimulate P38 Mitogen-Activated Protein Kinase Activity and Interleukin-6 Secretion. *J. Biol. Chem.* 294 (46), 17395–17408. doi:10.1074/jbc.RA119.009167
- Brusatin, G., Panciera, T., Gandin, A., Citron, A., and Piccolo, S. (2018). Biomaterials and Engineered Microenvironments to Control YAP/TAZ-dependent Cell Behaviour. *Nat. Mater* 17 (12), 1063–1075. doi:10.1038/s41563-018-0180-8
- Bugg, D., Bretherton, R., Kim, P., Olszewski, E., Nagle, A., Schumacher, A. E., et al. (2020). Infarct Collagen Topography Regulates Fibroblast Fate via P38-Yes-Associated Protein Transcriptional Enhanced Associate Domain Signals. *Circ. Res.* 127 (10), 1306–1322. doi:10.1161/circresaha.119.316162
- Cai, X., Wang, K.-C., and Meng, Z. (2021). Mechanoregulation of YAP and TAZ in Cellular Homeostasis and Disease Progression. *Front. Cel Dev. Biol.* 9, 673599. doi:10.3389/fcell.2021.673599

ETHICS STATEMENT

The animal study was reviewed and approved by the animal study was reviewed and approved by Medical Ethics Committee of China Medical University.

AUTHOR CONTRIBUTIONS

YF designed the experiments, performed most experiments, analyzed data, and wrote the manuscript. PW was involved in improving experimental design. JZ analyzed the data and editing the manuscript. XL helped revise the manuscript, and YZ helped in animal experiments. JX and KW helped analyzed the histology and histopathology, and HP and QZ helped interpret data. LC provided a lot of constructive suggestions and polished up the article. XZ designed and supervised all experiments, and edited the manuscript. All authors read and approved the final manuscript.

FUNDING

The work was financially supported by the National Natural Science Foundation of China (contract Nos. 31371219 and 31971115) and Nature Foundation of Liaoning Province of China under Grant 2021-KF-12-03.

ACKNOWLEDGMENTS

We gratitude the Shenyang Institute of Automation, Chinese Academy of Sciences for the support in microenvironmental stiffness testing.

SUPPLEMENTARY MATERIAL

The Supplementary Material for this article can be found online at: <https://www.frontiersin.org/articles/10.3389/fcell.2021.741060/full#supplementary-material>

- Chen, W.-C., Lin, H.-H., and Tang, M.-J. (2014). Regulation of Proximal Tubular Cell Differentiation and Proliferation in Primary Culture by Matrix Stiffness and ECM Components. *Am. J. Physiology-Renal Physiol.* 307 (6), F695–F707. doi:10.1152/ajprenal.00684.2013
- Chen, X., Wanggou, S., Bodalia, A., Zhu, M., Dong, W., Fan, J. J., et al. (2018). A Feedforward Mechanism Mediated by Mechanosensitive Ion Channel PIEZO1 and Tissue Mechanics Promotes Glioma Aggression. *Neuron* 100 (4), 799–815. doi:10.1016/j.neuron.2018.09.046
- Cobbaut, M., Karagil, S., Bruno, L., Diaz de la Loza, M. D. C., Mackenzie, F. E., Stolinski, M., et al. (2020). Dysfunctional Mechanotransduction through the YAP/TAZ/Hippo Pathway as a Feature of Chronic Disease. *Cells* 9 (1), 151. doi:10.3390/cells9010151
- D'Urso, M., and Kurniawan, N. A. (2020). Mechanical and Physical Regulation of Fibroblast-Myofibroblast Transition: From Cellular Mechanoreponse to Tissue Pathology. *Front. Bioeng. Biotechnol.* 8, 609653. doi:10.3389/fbioe.2020.609653
- Dalghi, M. G., Clayton, D. R., Ruiz, W. G., Al-Bataineh, M. M., Satlin, L. M., Kleyman, T. R., et al. (2019). Expression and Distribution of PIEZO1 in the Mouse Urinary Tract. *Am. J. Physiology-Renal Physiol.* 317 (2), F303–f321. doi:10.1152/ajprenal.00214.2019

- Dasgupta, I., and McCollum, D. (2019). Control of Cellular Responses to Mechanical Cues through YAP/TAZ Regulation. *J. Biol. Chem.* 294 (46), 17693–17706. doi:10.1074/jbc.REV119.007963
- Dupont, S., Morsut, L., Aragona, M., Enzo, E., Giulitti, S., Cordenonsi, M., et al. (2011). Role of YAP/TAZ in Mechanotransduction. *Nature* 474 (7350), 179–183. doi:10.1038/nature10137
- Ghasemi, H., Mousavibahar, S. H., Hashemnia, M., Karimi, J., Khodadadi, I., Mirzaei, F., et al. (2020). Tissue Stiffness Contributes to YAP Activation in Bladder Cancer Patients Undergoing Transurethral Resection. *Ann. N.Y. Acad. Sci.* 1473 (1), 48–61. doi:10.1111/nyas.14358
- Gu, L., Wang, Y., Yang, G., Tilyek, A., Zhang, C., Li, S., et al. (2019). Ribes Diacanthum Pall (RDP) Ameliorates UUO-Induced Renal Fibrosis via Both Canonical and Non-canonical TGF- β Signaling Pathways in Mice. *J. Ethnopharmacology* 231, 302–310. doi:10.1016/j.jep.2018.10.023
- Hasegawa, K., Fujii, S., Matsumoto, S., Tajiri, Y., Kikuchi, A., and Kiyoshima, T. (2021). YAP Signaling Induces PIEZO1 to Promote Oral Squamous Cell Carcinoma Cell Proliferation. *J. Pathol.* 253 (1), 80–93. doi:10.1002/path.5553
- Hoel, A., Osman, T., Hoel, F., Elsaid, H., Chen, T., Landolt, L., et al. (2021). Axl-inhibitor Bemcentinib Alleviates Mitochondrial Dysfunction in the Unilateral Ureter Obstruction Murine Model. *J. Cel Mol Med* 25, 7407–7417. doi:10.1111/jcmm.16769
- Hsu, P. C., Yang, C. T., Jablons, D. M., and You, L. (2020). The Crosstalk between Src and Hippo/YAP Signaling Pathways in Non-small Cell Lung Cancer (NSCLC). *Cancers (Basel)* 12 (6). doi:10.3390/cancers12061361
- Huang, B. Y., Hu, P., Zhang, D. D., Jiang, G. M., Liu, S. Y., Xu, Y., et al. (2017). C-type Natriuretic Peptide Suppresses Mesangial Proliferation and Matrix Expression via a MMPs/TIMPs-independent Pathway *In Vitro*. *J. Receptors Signal Transduction* 37 (4), 355–364. doi:10.1080/10799893.2017.1286674
- Imamura, M., Moon, J.-S., Chung, K.-P., Nakahira, K., Muthukumar, T., Shingarev, R., et al. (2018). RIPK3 Promotes Kidney Fibrosis via AKT-dependent ATP Citrate Lyase. *JCI Insight* 3 (3). doi:10.1172/jci.insight.94979
- Lee, J. Y., Chang, J. K., Dominguez, A. A., Lee, H.-p., Nam, S., Chang, J., et al. (2019). YAP-independent Mechanotransduction Drives Breast Cancer Progression. *Nat. Commun.* 10 (1), 1848. doi:10.1038/s41467-019-09755-0
- Lee, S., Rauch, J., and Kolch, W. (2020). Targeting MAPK Signaling in Cancer: Mechanisms of Drug Resistance and Sensitivity. *Ijms* 21 (3), 1102. doi:10.3390/ijms21031102
- Li, J., Hou, B., Tumova, S., Muraki, K., Bruns, A., Ludlow, M. J., et al. (2014a). Piezo1 Integration of Vascular Architecture with Physiological Force. *Nature* 515 (7526), 279–282. doi:10.1038/nature13701
- Li, M., Liu, L., Xi, N., Wang, Y., Xiao, X., and Zhang, W. (2014b). Nanoscale Imaging and Mechanical Analysis of Fc Receptor-Mediated Macrophage Phagocytosis against Cancer Cells. *Langmuir* 30 (6), 1609–1621. doi:10.1021/la4042524
- Li, M., Xiao, X., Zhang, W., Liu, L., Xi, N., and Wang, Y. (2014c). Nanoscale Distribution of CD20 on B-Cell Lymphoma Tumour Cells and its Potential Role in the Clinical Efficacy of Rituximab. *J. Microsc.* 254 (1), 19–30. doi:10.1111/jmi.12112
- Li, S., Li, C., Zhang, Y., He, X., Chen, X., Zeng, X., et al. (2019). Targeting Mechanics-Induced Fibroblast Activation through CD44-RhoA-YAP Pathway Ameliorates Crystalline Silica-Induced Silicosis. *Theranostics* 9 (17), 4993–5008. doi:10.7150/tno.35665
- Liang, M., Yu, M., Xia, R., Song, K., Wang, J., Luo, J., et al. (2017). Yap/Taz Deletion in Gli+ Cell-Derived Myofibroblasts Attenuates Fibrosis. *Jasn* 28 (11), 3278–3290. doi:10.1681/asn.2015121354
- Lin, K. C., Moroishi, T., Meng, Z., Jeong, H.-S., Plouffe, S. W., Sekido, Y., et al. (2018). Author Correction: Regulation of Hippo Pathway Transcription Factor TEAD by P38 MAPK-Induced Cytoplasmic Translocation. *Nat. Cel Biol* 20 (9), 1098. doi:10.1038/s41556-018-0101-8
- Liu, M., Zheng, M., Xu, H., Liu, L., Li, Y., Xiao, W., et al. (2015). Anti-pulmonary Fibrotic Activity of Salvianolic Acid B Was Screened by a Novel Method Based on the Cyto-Biophysical Properties. *Biochem. Biophysical Res. Commun.* 468 (1–2), 214–220. doi:10.1016/j.bbrc.2015.10.127
- Liu, T.-t., Du, X.-f., Zhang, B.-b., Zi, H.-x., Yan, Y., Yin, J.-a., et al. (2020). Piezo1-Mediated Ca²⁺ Activities Regulate Brain Vascular Pathfinding during Development. *Neuron* 108 (1), 180–192. e185. doi:10.1016/j.neuron.2020.07.025
- Noguchi, S., Saito, A., and Nagase, T. (2018). YAP/TAZ Signaling as a Molecular Link between Fibrosis and Cancer. *Ijms* 19 (11), 3674. doi:10.3390/ijms19113674
- Panciera, T., Azzolin, L., Cordenonsi, M., and Piccolo, S. (2017). Mechanobiology of YAP and TAZ in Physiology and Disease. *Nat. Rev. Mol. Cel Biol* 18 (12), 758–770. doi:10.1038/nrm.2017.87
- Qiu, C., Huang, S., Park, J., Park, Y., Ko, Y.-A., Seasock, M. J., et al. (2018). Renal Compartment-specific Genetic Variation Analyses Identify New Pathways in Chronic Kidney Disease. *Nat. Med.* 24 (11), 1721–1731. doi:10.1038/s41591-018-0194-4
- Qiu, D., Zhu, Y., and Cong, Z. (2020). YAP Triggers Bladder Cancer Proliferation by Affecting the MAPK Pathway. *Cmar Vol. 12*, 12205–12214. doi:10.2147/cmar.s273442
- Silver, B. B., Zhang, S. X., Rabie, E. M., and Nelson, C. M. (2021). Substratum Stiffness Tunes Membrane Voltage in Mammary Epithelial Cells. *J. Cel Sci* 134. doi:10.1242/jcs.256313
- Solis, A. G., Bielecki, P., Steach, H. R., Sharma, L., Harman, C. C. D., Yun, S., et al. (2019). Author Correction: Mechanosensation of Cyclical Force by PIEZO1 Is Essential for Innate Immunity. *Nature* 575 (7784), E7. doi:10.1038/s41586-019-1755-5
- Syeda, R., Florendo, M. N., Cox, C. D., Kefauver, J. M., Santos, J. S., Martinac, B., et al. (2016). Piezo1 Channels Are Inherently Mechanosensitive. *Cel Rep.* 17 (7), 1739–1746. doi:10.1016/j.celrep.2016.10.033
- Vining, K. H., and Mooney, D. J. (2017). Mechanical Forces Direct Stem Cell Behaviour in Development and Regeneration. *Nat. Rev. Mol. Cel Biol* 18 (12), 728–742. doi:10.1038/nrm.2017.108
- Wang, L., You, X., Lotinun, S., Zhang, L., Wu, N., and Zou, W. (2020). Mechanical Sensing Protein PIEZO1 Regulates Bone Homeostasis via Osteoblast-Osteoclast Crosstalk. *Nat. Commun.* 11 (1), 282. doi:10.1038/s41467-019-14146-6
- Wang, Y.-Y., Zhang, H., Ma, T., Lu, Y., Xie, H.-Y., Wang, W., et al. (2019). Piezo1 Mediates Neuron Oxygen-Glucose Deprivation/reoxygenation Injury via Ca²⁺/calpain Signaling. *Biochem. Biophysical Res. Commun.* 513 (1), 147–153. doi:10.1016/j.bbrc.2019.03.163
- Wang, Y., Xia, C., Lv, Y., Li, C., Mei, Q., Li, H., et al. (2017). Crosstalk Influence between P38MAPK and Autophagy on Mitochondria-Mediated Apoptosis Induced by Anti-fas Antibody/Actinomycin D in Human Hepatoma Bel-7402 Cells. *Molecules* 22 (10), 1705. doi:10.3390/molecules22101705
- Yamashiro, Y., Thang, B. Q., Ramirez, K., Shin, S. J., Kohata, T., Ohata, S., et al. (2020). Matrix Mechanotransduction Mediated by Thrombospondin-1/integrin/YAP in the Vascular Remodeling. *Proc. Natl. Acad. Sci. USA* 117 (18), 9896–9905. doi:10.1073/pnas.1919702117
- Yoneda, M., Suzuki, H., Hatano, N., Nakano, S., Muraki, Y., Miyazawa, K., et al. (2019). PIEZO1 and TRPV4, Which Are Distinct Mechano-Sensors in the Osteoblastic MC3T3-E1 Cells, Modify Cell-Proliferation. *Ijms* 20 (19), 4960. doi:10.3390/ijms20194960
- Zhang, W., Gao, Y., Li, P., Shi, Z., Guo, T., Li, F., et al. (2014). VGLL4 Functions as a New Tumor Suppressor in Lung Cancer by Negatively Regulating the YAP-TEAD Transcriptional Complex. *Cell Res* 24 (3), 331–343. doi:10.1038/cr.2014.10
- Zhang, X., Cai, D., Zhou, F., Yu, J., Wu, X., Yu, D., et al. (2020). Targeting Downstream Subcellular YAP Activity as a Function of Matrix Stiffness with Verteporfin-Encapsulated Chitosan Microsphere Attenuates Osteoarthritis. *Biomaterials* 232, 119724. doi:10.1016/j.biomaterials.2019.119724
- Zhou, Z., Zhou, B., Chen, H., Lu, K., and Wang, Y. (2021). Oxidative Stress Activates the Nrf2-Mediated Antioxidant Response and P38 MAPK Pathway: A Possible Apoptotic Mechanism Induced by BDE-47 in Rainbow trout (*Oncorhynchus mykiss*) Gonadal RTG-2 Cells. *Environ. Pollut.* 287, 117341. doi:10.1016/j.envpol.2021.117341

Conflict of Interest: The authors declare that the research was conducted in the absence of any commercial or financial relationships that could be construed as a potential conflict of interest.

Publisher's Note: All claims expressed in this article are solely those of the authors and do not necessarily represent those of their affiliated organizations, or those of the publisher, the editors, and the reviewers. Any product that may be evaluated in this article, or claim that may be made by its manufacturer, is not guaranteed or endorsed by the publisher.

Copyright © 2021 Fu, Wan, Zhang, Li, Xing, Zou, Wang, Peng, Zhu, Cao and Zhai. This is an open-access article distributed under the terms of the Creative Commons Attribution License (CC BY). The use, distribution or reproduction in other forums is permitted, provided the original author(s) and the copyright owner(s) are credited and that the original publication in this journal is cited, in accordance with accepted academic practice. No use, distribution or reproduction is permitted which does not comply with these terms.



ADAM17, A Key Player of Cardiac Inflammation and Fibrosis in Heart Failure Development During Chronic Catecholamine Stress

Joseph Adu-Amankwaah¹, Gabriel Komla Adzika¹, Adebayo Oluwafemi Adekunle¹, Marie Louise Ndzie Noah¹, Richard Mprah¹, Aisha Bushi², Nazma Akhter¹, Fei Huang¹, Yaxin Xu¹, Seyram Yao Adzraku³, Iqra Nadeem⁴ and Hong Sun^{1*}

¹Department of Physiology, Xuzhou Medical University, Xuzhou, China, ²Xuzhou Medical University, Xuzhou, China, ³Key Laboratory of Bone Marrow Stem Cell, Department of Hematology, The Affiliated Hospital of Xuzhou Medical University, Xuzhou, China, ⁴Department of Neurobiology and Anatomy, Xuzhou Medical University, Xuzhou, China

OPEN ACCESS

Edited by:

Isotta Chimenti,
Sapienza University of Rome, Italy

Reviewed by:

Julie Pires Da Silva,
University of Colorado Anschutz
Medical Campus, United States
Laurel A. Grisanti,
University of Missouri, United States

*Correspondence:

Hong Sun
sunh@xzhmu.edu.cn

Specialty section:

This article was submitted to
Molecular and Cellular Pathology,
a section of the journal
Frontiers in Cell and Developmental
Biology

Received: 29 June 2021

Accepted: 16 November 2021

Published: 13 December 2021

Citation:

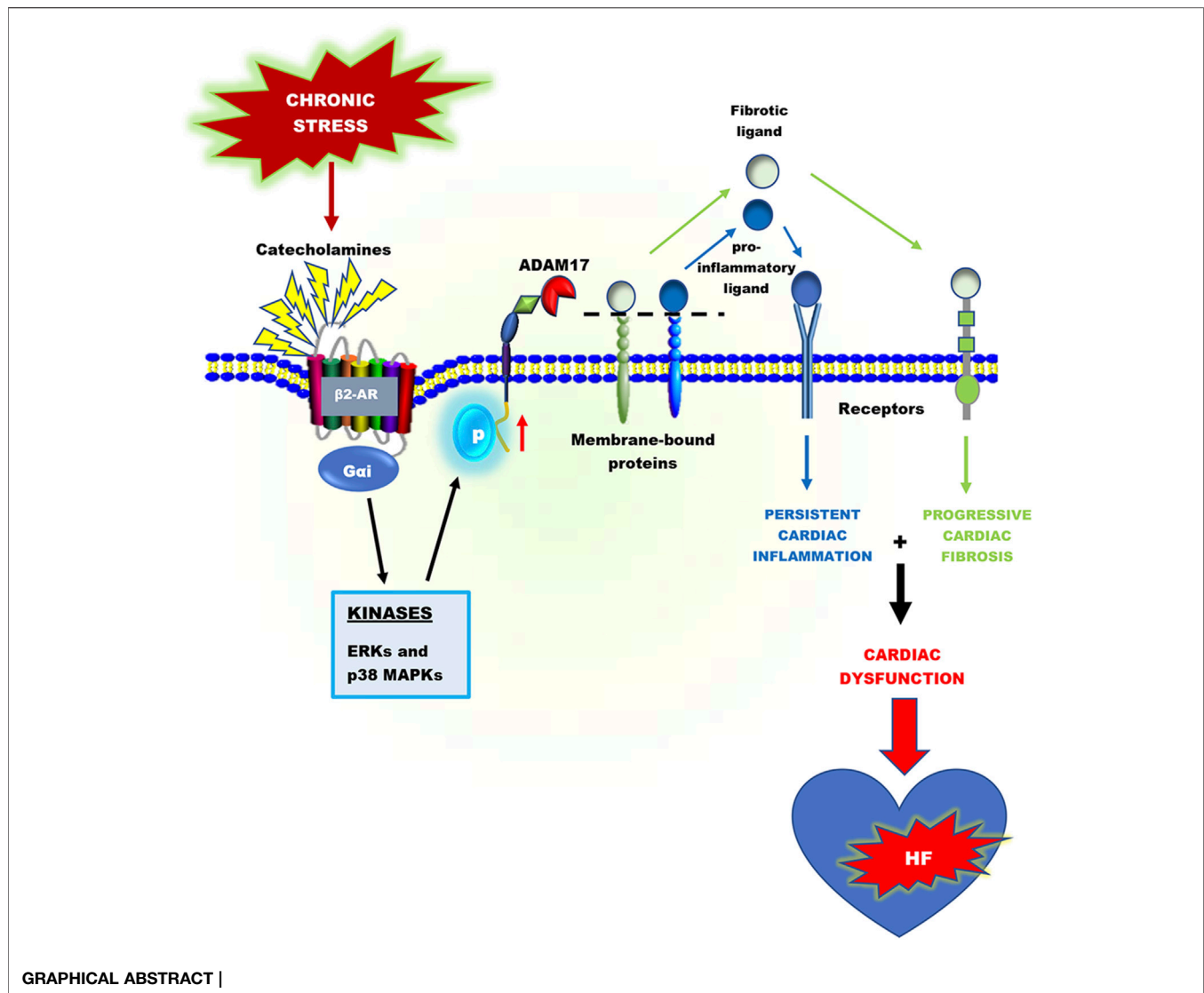
Adu-Amankwaah J, Adzika GK, Adekunle AO, Ndzie Noah ML, Mprah R, Bushi A, Akhter N, Huang F, Xu Y, Adzraku SY, Nadeem I and Sun H (2021) ADAM17, A Key Player of Cardiac Inflammation and Fibrosis in Heart Failure Development During Chronic Catecholamine Stress. *Front. Cell Dev. Biol.* 9:732952. doi: 10.3389/fcell.2021.732952

Heart failure development is characterized by persistent inflammation and progressive fibrosis owing to chronic catecholamine stress. In a chronic stress state, elevated catecholamines result in the overstimulation of beta-adrenergic receptors (β ARs), specifically β 2-AR coupling with Gai protein. Gai signaling increases the activation of receptor-stimulated p38 mitogen-activated-protein-kinases (p38 MAPKs) and extracellular signal-regulated kinases (ERKs). Phosphorylation by these kinases is a common way to positively regulate the catalytic activity of A Disintegrin and Metalloprotease 17 (ADAM17), a metalloprotease that has grown much attention in recent years and has emerged as a chief regulatory hub in inflammation, fibrosis, and immunity due to its vital proteolytic activity. ADAM17 cleaves and activates proinflammatory cytokines and fibrotic factors that enhance cardiac dysfunction via inflammation and fibrosis. However, there is limited information on the cardiovascular aspect of ADAM17, especially in heart failure. Hence, this concise review provides a comprehensive insight into the structure of ADAM17, how it is activated and regulated during chronic catecholamine stress in heart failure development. This review highlights the inflammatory and fibrotic roles of ADAM17's substrates; Tumor Necrosis Factor α (TNF α), soluble interleukin-6 receptor (sIL-6R), and amphiregulin (AREG). Finally, how ADAM17-induced chronic inflammation and progressive fibrosis aggravate cardiac dysfunction is discussed.

Keywords: heart failure, cardiac inflammation, cardiac fibrosis, ADAM17, metalloenzymes, pro-inflammatory cytokines, fibrotic factors

INTRODUCTION

Heart failure (HF) is a serious clinical and public health issue that affects over 23 million people globally, resulting in significant mortality, morbidity, and healthcare expenditures (Ayoub et al., 2017; Orso et al., 2017; Frantz et al., 2018). Despite advances in understanding its pathophysiology and treatment, the prognosis of patients with HF remains poor. Approximately 2–17% of patients die during their first hospital stay, with over 50% of patients dying within 5 years (Ayoub et al., 2017).



Chronic stress-induced adverse cardiac remodeling and HF are generally associated with prolonged activation of proinflammatory responses (Adzika et al., 2021; Huo S. et al., 2021). In an inflammatory driven HF, the inflammatory responses are orchestrated by myosin and troponin (damage-associated molecular patterns (DAMPs)) released from necrotic cardiomyocytes. These cardiac antigens activate and induce the infiltration of neutrophils, macrophages, dendritic cells, as well as T and B cells into the myocardia (Lafuse et al., 2020; Adzika et al., 2021). Following cardiac injury, neutrophils and CD86⁺ macrophages are rapidly recruited to the injured area, where they initiate inflammatory responses with the goal of cleaning up dead cell debris. However, excessive accumulation and/or delayed switch from these proinflammatory cells infiltration to reparative inflammatory cells (such as CD206⁺ macrophages) has detrimental effects. By releasing reactive oxygen species, granular components, and proinflammatory mediators such as tumor necrosis factor-alpha (TNF α), soluble interleukin-6

receptor (sIL-6R), and CXC chemokine receptor 2 (CXCR2), neutrophils and macrophages contribute to adverse myocardial injury and remodeling (Adu-Amankwaah et al., 2021a; Ma, 2021). Additionally, the activation of T and B lymphocytes by dendritic cells has been shown to play crucial roles in myocardial inflammation (Santos-Zas et al., 2018; Santos-Zas et al., 2021). Ultimately, without timely resolution of these proinflammatory responses and initiates of reparative functions, genes encoding proinflammatory mediators and fibrotic factors are upregulated excessively (Epelman et al., 2014; Heidt et al., 2014; Adamo et al., 2020).

Proteolytic cleavage of transmembrane proteins is a vital post-translational modification that controls several transmembrane proteins' biological function, including proinflammatory mediators and growth factors (Lichtenthaler et al., 2018; Düsterhöft et al., 2019). Amid the 560 proteases encoded in the human genome, A Disintegrin and Metalloprotease 17 (ADAM17) has grown much attention in recent years and has

emerged as a chief regulatory hub in inflammation, fibrosis, and immunity due to its vital proteolytic activity (Düsterhöft et al., 2019). In immune and non-immune cells, ADAM17 cleaves a number of substrates, including ligands of the epidermal growth factor receptor (EGFR), adhesion molecules, proinflammatory cytokines, and chemokines and their receptors. Some of these substrates include amphiregulin (AREG), epigen, epi-regulin, neuregulin, tomoegulin-2, transforming growth factor- α (TGF- α), heparin-binding epidermal growth factor (HB-EGF), TNF α , tumor necrosis factor β (TNF β), the TNF receptors 1 and 2 (TNFR 1 and 2), and interleukin-6 receptor (IL-6R), CXCR2, collagen XVII, desmoglein-2 and nectin-4 (Black et al., 1997; Moss et al., 1997; Tellier et al., 2006; Reddy et al., 2009; Riethmueller et al., 2017; Kawai et al., 2021). According to Cabron et al. ADAM17 is a key regulator of soluble TNF α surface levels in proinflammatory macrophages and dendritic cells (Cabron et al., 2018). Additionally, sIL-6R and CXCR2 on human and mouse neutrophils surfaces are regulated by ADAM17 (Wright et al., 2014; Mishra et al., 2015).

In a physiological state, the expressions of ADAM17 in immune and non-immune cells are regulated by transcriptional and post-transcriptional factors, including nuclear factor kappa B (NF- κ B) and Brahma-related gene 1 (BRG1). Furthermore, subcellular localization in the perinuclear region of cells has been shown to regulate ADAM17's activity (Chemaly et al., 2017; Adu-Amankwaah et al., 2021a). Overexpression and chronic activation of ADAM17 can trigger excessive release of TNF α , sIL-6R, and CXCR2 on the surface of proinflammatory cells, which play crucial roles in the pathogenesis of several inflammatory diseases, including heart failure. Increased levels of TNF α , sIL-6R and CXCR2 have been implicated in immune cells (CD86⁺ macrophages, neutrophils, and dendritic cells) trafficking, migration, and activation as well as inducing excessive fibrosis, myocardial stiffness, and left ventricular diastolic dysfunction (Cumberbatch and Kimber, 1992; Bozkurt et al., 1998; Satoh et al., 2000; Russo et al., 2009; Jones et al., 2010; Anderson et al., 2013; Arokiasamy et al., 2017).

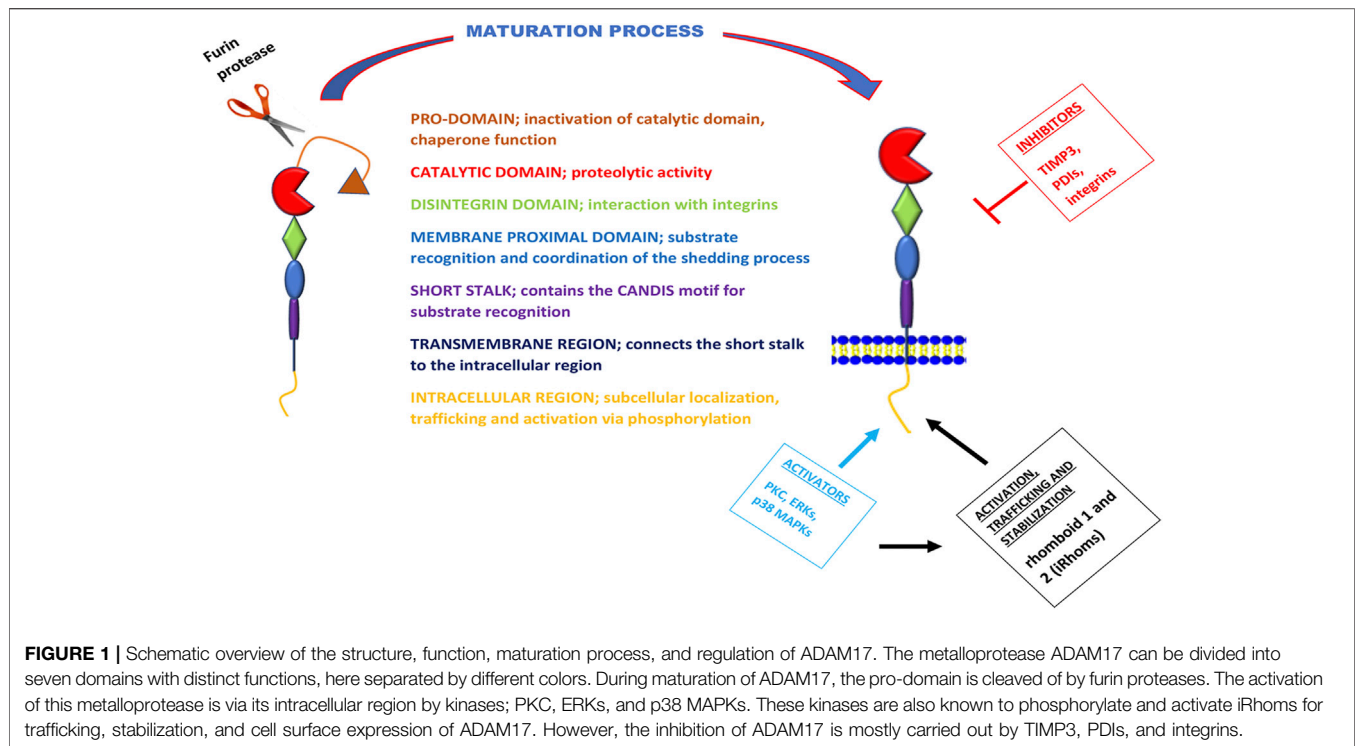
Several studies have shown that myocardial ADAM17, TNF α , and sIL-6R expressions in both mRNA and protein levels are higher in patients with cardiovascular diseases and complications, although ADAM17's expression is downregulated in a normal state (Satoh et al., 1999; Damás et al., 2000; Satoh et al., 2000; Satoh et al., 2004; Anderson et al., 2013). Thus, establishing a positive correlation between ADAM17 and heart failure development. The increased expression of ADAM17, TNF α , and sIL-6R has a vital implication in aggravating cardiac dysfunction during heart failure development (Satoh et al., 1999; Satoh et al., 2000; Satoh et al., 2004; Adu-Amankwaah et al., 2021a). Additionally, pro-AREG, a bi-functional growth factor converted to its active form by ADAM17, is crucially involved in enhancing cardiac fibrosis and aggravating cardiac dysfunction (Liu et al., 2018). Besides inducing HF *via* facilitating hyperactive proinflammatory responses, ADAM17 has been implicated along with HB-EGF and betacellulin (BTC), and angiotensin-converting enzyme 2 (ACE2) in causing congenital heart diseases and hypertensive-induced HF, respectively

(Jackson et al., 2003; de Queiroz et al., 2015; Xu et al., 2017; Mukerjee et al., 2019). This comprehensive review provides an insight into the structure of ADAM17, how it is activated and regulated during chronic catecholamine stress in heart failure development. This review highlights the inflammatory and fibrotic roles of ADAM17's substrates; TNF α , sIL-6R, and sAREG. Finally, how ADAM17-induced chronic inflammation and progressive fibrosis aggravate cardiac dysfunction is also discussed.

A DISINTEGRIN AND METALLOPROTEASE 17 AND OTHER RELATED METALLOPROTEINASES

Overview

A disintegrin and metalloproteinases (ADAMs) consist of membrane-bound proteins that belong to a Zn²⁺-dependent protease superfamily. They are similar to other metalloenzymes, including matrix metalloproteinases (MMPs), meprins, and snake venom metalloproteinases (SVMP) (Calvete et al., 2007; Gooz, 2010). Physiologically, ADAMs and their related metalloenzymes are widely expressed in various body tissues and regulate diverse cellular activities, including cell migration, adhesion, proteolysis, and cellular signaling (Black et al., 1997; Jones et al., 2016). Hence, it is not astonishing that alterations in the expression or function of these proteases are implicated in several pathologies, including cancer, rheumatoid arthritis, kidney fibrosis, diabetes, Alzheimer's disease, and cardiovascular diseases (Sandgren et al., 1990; Black et al., 1997; Satoh et al., 2000; Umemura et al., 2014; Kefaloyianni et al., 2016; Zhang et al., 2016; Kim et al., 2020; Shalaby et al., 2020; Adu-Amankwaah et al., 2021a). Increasing evidence suggests that various ADAMs and other related metalloenzymes play crucial roles in cardiovascular pathophysiology *via* the modulation of inflammation, angiogenesis, metabolism, cell proliferation, and cell migration (Adu-Amankwaah et al., 2021a; Kawai et al., 2021). Among the ADAMs identified so far (22 in humans, 34 in mice), ADAM8, 9, 10, 12, 17, 19 and closely related metalloenzymes including MMP2, MMP9, and meprin β are associated with cardiovascular conditions such as hypertension, atherosclerosis, aortic aneurysms, restenosis, acute coronary syndrome, cardiomyopathies and HF (Papazafropoulou and Tentolouris, 2009; Broder and Becker-Pauly, 2013; Zhang et al., 2016; Adu-Amankwaah et al., 2021a; Kawai et al., 2021). According to Wichert et al., active meprin β is capable of inducing the proteolytic activities of ADAM9, 10, and 17 *via* specific prodomain cleavage (Wichert et al., 2019). The activation of MMP2 and MMP9 is part of the downstream signaling of ADAM10 and 17, which are closely related in structure and function (Xiao et al., 2012; Jones et al., 2013). While ADAM10's expression may be important in cancer and neurological disorders, ADAM17 is primarily responsible for coordinating proinflammatory responses during stress. The various substrates of ADAMs have been extensively reviewed elsewhere (Kawai et al., 2021). Remarkably, several members of the ADAM family share the same substrates, and this nonspecific relationship between ADAMs and their substrates complicates and intrigues the physiology of ADAMs. However, the main focus of this



review is to elucidate the mechanistic signaling pathways of ADAM17 in HF development during chronic stress.

ADAM17 was discovered in 1997 and named TACE (TNF α converting enzyme), as it was initially known as the protease that converts membrane-bound pro-TNF α (mTNF α) to a soluble form through its cleavage activity (Black et al., 1997; Moss et al., 1997). However, recent studies show that this protease is not only responsible for the liberation of soluble TNF α (sTNF α) but has a relatively broad spectrum of over 90 substrates (Black et al., 1997; Moss et al., 1997; Lammich et al., 1999; Garton et al., 2003; Reddy et al., 2009; Riethmueller et al., 2017). ADAM17 can be activated by intracellular kinases, which include phosphate kinase c (PKC), receptor-stimulated p38 mitogen-activated-protein-kinases (p38 MAPKs), and extracellular signal-regulated kinases (ERKs) (Bell and Gööz, 2010; Xu et al., 2012; Adu-Amankwaah et al., 2021a). These kinases can also phosphorylate and activate rhomboid 1 and 2 (also known as iRhoms or pseudoproteases) (Grieve et al., 2017), which are responsible for trafficking, stabilization as well as activation of ADAM17 (Adrain and Freeman, 2012; McIlwain et al., 2012; Maretzky et al., 2013; Li et al., 2015). Its inhibition is mostly done *via* tissue inhibitor of metalloproteinase 3 (TIMP3), integrins and protein disulfide isomerases (PDIs) (Düsterhöft et al., 2013; Düsterhöft et al., 2019; Park et al., 2019; **Figure 1**).

A Disintegrin and Metalloprotease 17's Structure

ADAM17 is a type-I transmembrane protein (Bode et al., 1993; Düsterhöft et al., 2019) with a similar class III snake venom

metalloenzymes structure (Bode et al., 1993; Gooz, 2010). It comprises a prodomain, a catalytic domain, a disintegrin-like domain, a membrane-proximal domain (MPD), and a short stalk region, which together forms the extracellular part of the protease and are linked to an intracellular region (ICR) by a transmembrane part (Grötzinger et al., 2017). The catalytic domain possesses this metalloprotease's proteolytic activity (Bode et al., 1993; Stöcker et al., 1995; Black et al., 1997); however, the preceding prodomain has chaperone-like functions that inhibit this catalytic activity, and it is cleaved off by furin proteases during the maturation of the protease (Schlöndorff et al., 2000). Though this cleavage step was primarily considered a prerequisite for the proteolytic activity of ADAM17, a study by Schwarz et al., revealed that ADAM17 was also active when cleavage by furin proteases was prevented by mutagenesis of the cleavage site (Schwarz et al., 2013). The disintegrin-like domain is needed for the interaction with integrins, a feature that ADAM17 shares with other ADAM family members (Bode et al., 1993; Düsterhöft et al., 2019). However, the membrane-proximal domain is only found in ADAM10 and ADAM17, but not the other family members (Stöcker et al., 1995; Grötzinger et al., 2017), and it is crucially involved in substrate recognition and coordination of the shedding process (Düsterhöft et al., 2013). The membrane-proximal domain is regulated by two disulfide bonds that are vulnerable to isomerization by PDI activity (Düsterhöft et al., 2013). The stalk region of ADAM17 contains the CANDIS motif (Conserved ADAM 17 Dynamic Interaction Sequence), which is located closer to the membrane-proximal domain near the plasma membrane and is vital for substrate recognition (Düsterhöft et al., 2014; Düsterhöft et al., 2019; **Figure 1**).

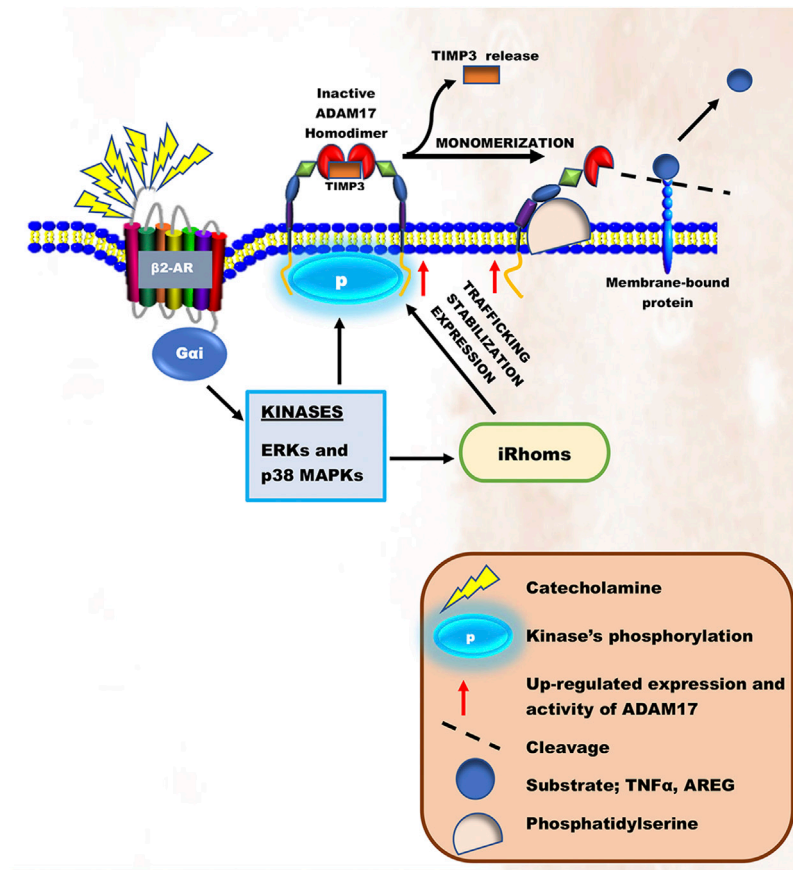


FIGURE 2 | Schematic illustration of ADAM17's activation during chronic catecholamine stress. Elevated catecholamines owing to chronic stress results in overstimulation of β -2-ARs coupling with Gai. Gai signaling induces the activation of intracellular kinases, ERKs and p38 MAPKs. These kinases are known to either directly phosphorylate and activate ADAM17 or activate iRhoms responsible for trafficking, stabilization, and cell surface expression of ADAM17, thereby initiating its cleaving process.

ACTIVATION OF A DISINTEGRIN AND METALLOPROTEASE 17 DURING CHRONIC STRESS

Chronic stress is a renowned risk factor for several cardiovascular diseases (Kivimäki and Steptoe, 2018). One of the central neural pathways activated by stress is the autonomic nervous system. During chronic stress, the sympathetic nervous system can be continuously activated, which results in elevated levels of catecholamines (epinephrine and norepinephrine) (Won and Kim, 2016). Epinephrine and norepinephrine function as hormones and neurotransmitters that maintain homeostasis *via* adrenergic receptors (ARs), including alpha-adrenergic receptors (α -ARs) and beta-adrenergic receptors (β -ARs). Studies have demonstrated the involvement of ADAM17 with α 1-AR (Chen et al., 2006) and β -AR signaling (Zhu and Steinberg, 2021). β -ARs account for the majority of the total ARs in the heart (O'Connell et al., 2014), particularly in apical myocytes (Paur et al., 2012; Machuki et al., 2019) and cardiac non-myocytes such as endothelial and immune cells (Myagmar et al., 2017; Adzika et al., 2021). Hence, a continuous increase in the levels of

epinephrine and norepinephrine can result in overstimulation of β -ARs (Machuki et al., 2019). Epinephrine is a more potent ligand for β -ARs compared to norepinephrine (Scanzano and Cosentino, 2015). β -ARs are 7-transmembrane, G-protein coupled receptors which are divided into four subtypes, namely; β 1-AR, β 2-AR, β 3-AR, and β 4-AR (Ahlquist, 1948; Bylund et al., 1994; Granneman, 2001). In the heart, the β 1-AR, β 2-AR, and β 3-AR are all broadly expressed, with the β 1-AR having the highest expression and the β 3-AR having the lowest (Ahlquist, 1948; Madamanchi, 2007). The β 4-AR is a low-affinity state of the β 1-AR that is yet to be genetically and pharmacologically characterized (Granneman, 2001). The β 2-AR and β 3-AR can couple with Gas or Gai while β 1-AR primarily couples with Gas when activated (Machuki et al., 2019; Schena and Caplan, 2019). In physiological state, the activation of β 2-AR and β 3-AR couple with Gas (Adzika et al., 2019; Machuki et al., 2019) and Gai (Tchivileva et al., 2009; Schena and Caplan, 2019), respectively. Among these β ARs, β 2-AR is rarely depleted during stress, and it is also the most implicated in mediating signaling cascades in ventricular apical myocytes, cardiac endothelial and immune cells resulting in the

initiation and progression of cardiovascular diseases (Paur et al., 2012; Adzika et al., 2019; Adu-Amankwaah et al., 2021a).

In the heart, the overstimulation of β -ARs on ventricular apical myocytes, cardiac endothelial and immune cells due to elevated levels of circulating catecholamine desensitize β 1-ARs (Bristow et al., 1990; Paur et al., 2012; Machuki et al., 2019). According to Zhu and Steinberg, the inactivation of β 1-ARs and its irresponsiveness to catecholamines in cardiomyocytes during stressful events is *via* a mechanism involving N-terminal truncation at R³¹JL³² by ADAM17 (Zhu and Steinberg, 2021). As such, β 2-ARs coupling to Gai is induced (Bristow et al., 1990; Paur et al., 2012; Machuki et al., 2019; Adzika et al., 2021). In short-terms, Gai signaling increases via Akt/PI3K/p38 MAPKs/ERKs to prevent cardiac insult (Magocsi et al., 2007; Lajevic et al., 2011; Hou et al., 2018). Recent findings have suggested that the prolonged hyperstimulation of β 2-ARs on ventricular apical myocytes and cardiac immune cells induces the bindings of β -arrestin-2 and G protein-coupled receptor kinases (GRKs) to scaffold non-canonical signaling that activates ERKs and p38 MAPKs activities maladaptively, ultimately resulting in HF (Shenoy et al., 2006; Paur et al., 2012; Adzika et al., 2019; Adzika et al., 2021). Intriguingly, ADAM17 initiates its adverse remodeling cascade upon being phosphorylated by these kinases directly and indirectly. For instance, during the maturation of ADAM17, ERK-dependent threonine 735 (Thr735) phosphorylation is vital for it to reach the secretory pathway (Díaz-Rodríguez et al., 2002; Chemaly et al., 2017). Also, indirect ERKs or p38 MAPKs phosphorylation at 14-3-3 binding sites on the N-terminal of iRhoms turns to induce ADAM17's trafficking, stabilization, and cell surface expressions (Bell and Gööz, 2010; Adrain and Freeman, 2012; McIlwain et al., 2012; Xu et al., 2012; Li et al., 2015; Grieve et al., 2017). On the cell surface, mature ADAM17 proteins exist as inactive homodimers coupled to their inhibitor, TIMP3. However, activation of the ERK or p38 MAPK pathway directly phosphorylates Thr735 on the intracellular domain of ADAM17 and transforms it from a dimer structure into an active monomer structure liberating it from TIMP3 (Xu et al., 2012; Chemaly et al., 2017). Following monomerization, ADAM17 then binds to the phosphatidylserine exposure at the outer leaflet of the cell membrane via its MPD and CANDIS, thereby initiating its cleaving process (Gooz, 2010; **Figure 2**).

A DISINTEGRIN AND METALLOPROTEASE 17 IN CARDIAC INFLAMMATION

ADAM17 plays a key role in cardiac inflammation, as it can cleave and activate several proinflammatory cytokines and their receptors. The most prominent examples include the cytokine TNF α , the TNFR 1 and 2, and the IL-6R (Black et al., 1997; Moss et al., 1997; Tellier et al., 2006; Reddy et al., 2009; Riethmueller et al., 2017).

Tumor Necrosis Factor α and its Receptors

The cytokine TNF α is a typical type-II transmembrane protein that belongs to the TNF superfamily (Düsterhöft et al., 2019). It is expressed as a membrane-bound protein, activated by the

cleavage process of ADAM17 to release sTNF α (Black et al., 1997; Moss et al., 1997). The majority of the proinflammatory activities of TNF α are attributed to its soluble form. This cytokine activation can signal via two different receptors, TNFR1 and TNFR2 (Defer et al., 2007; Salmeri et al., 2015), expressed on cardiac myocytes (Defer et al., 2007). Interestingly, TNFR1 and 2 can also be cleaved from the surface of cells by ADAM17, and the resulting soluble TNFR (sTNFR) ectodomains retain their ability to bind mTNF α and therefore act as antagonistic decoy receptors (Rego et al., 2013; **Figure 3**). Besides their function as decoy receptors, sTNFR1 and 2 can also perform a very different biological function by binding to mTNF α on the cell surface and inducing signals within TNF α -expressing cells. This concept is known as "reverse signaling," which is common among other TNF family members (Juhász et al., 2013). Although both TNFR1/2 can bind to the ligand sTNF α , the intracellular signaling cascades triggered, and the biological responses are markedly different (Düsterhöft et al., 2019). Most importantly, the intracellular region of TNFR1 contains a death domain capable of inducing direct programmed cell death when activated, which is absent in the intracellular region of TNFR2 (Düsterhöft et al., 2019). The binding of sTNF α to TNFR2 can result in the activation of nuclear factor kappa B (NF- κ B) (Albensi, 2019; Adu-Amankwaah et al., 2021a), which is also expressed in myocytes, cardiac endothelial, and immune cells (Li et al., 2020). The NF- κ B complex exists in an inactive state in the cytoplasm (Ghosh et al., 1998; Albensi, 2019). However, activation of TNFR2 can interact with the I κ B kinase (IKK) complex resulting in the phosphorylation of I κ B, subsequently causing I κ B ubiquitination and degradation, leading to the activation of NF- κ B dimer (Li and Karin, 2000; Israél, 2010). When activated, it then migrates into the nucleus (Sen and Smale, 2010) or mitochondria (Bottero et al., 2001; Cogswell et al., 2003). In the nucleus, it encodes genes of proinflammatory cytokines (pro-IL-18 and pro-IL-1 β) and NLR family pyrin domain containing 3 (NLRP3) (Sen and Smale, 2010; Albensi, 2019). NLRP3 is an intracellular sensor that identifies a wide range of environmental irritants, microbial motifs, and endogenous danger signals, resulting in the formation and activation of the NLRP3 inflammasome. Activation of the inflammasome triggers caspase 1, which in turn, cleaves pro-IL-1 β and pro-IL-18 to release their soluble forms (Bauernfeind et al., 2009; Xing et al., 2017; Swanson et al., 2019), thereby inducing necrosis and inflammation in cardiac cells (Li et al., 2018). Studies show that activated NF- κ B can stimulate the intrinsic apoptotic pathway in the mitochondria *via* releasing cytochrome c, which triggers caspase cascades resulting in programmed cell death (Liu et al., 2004; Albensi, 2019; Adu-Amankwaah et al., 2021a; **Figure 3**). Irrefutably, increased levels of TNF α in the stress state has been linked to the pathophysiology of heart failure development in various clinical investigations (Ferrari et al., 1995; De Biase et al., 2003; Dunlay et al., 2008) and animal models (Bozkurt et al., 1998; Bryant et al., 1998; Moe et al., 2004; Guggilam et al., 2007; Adzika et al., 2021; Hou H. et al., 2021). For instance, a study carried out by Bryant et al. reveals that cardiac myocytes' overproduction of TNF α is sufficient to cause heart failure, implying that this cytokine plays a causative role in

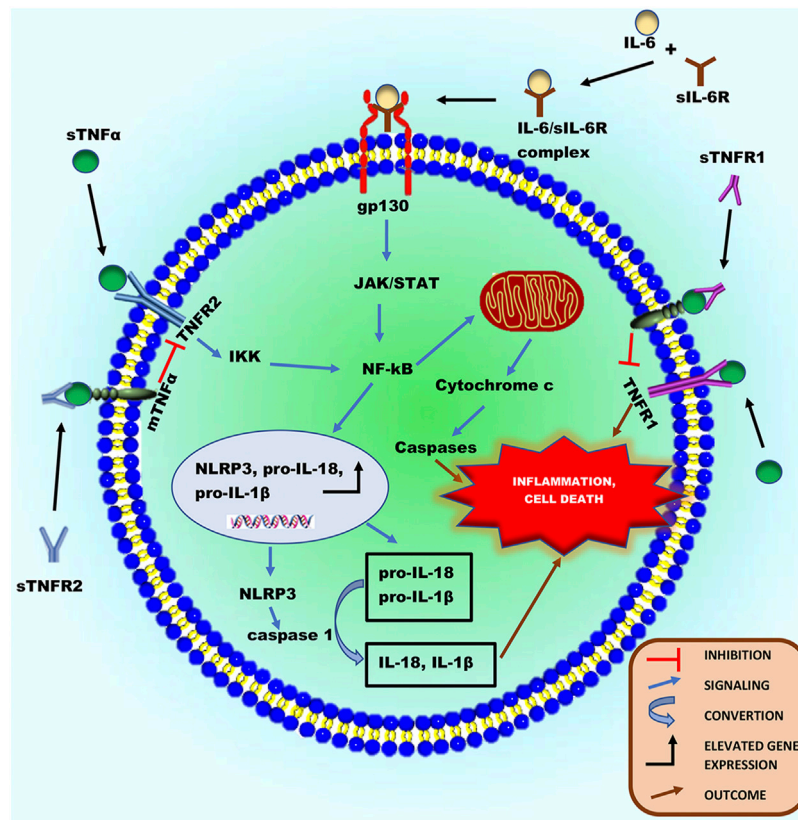


FIGURE 3 | Schematic illustration of the inflammatory roles of ADAM17's substrates, sTNF α and sIL-6R in a cardiac cell during chronic catecholamine stress. Following the proteolytic processing of ADAM17, sTNF α and IL-6 can bind to TNFR1/2 and sIL-6R, respectively activating downstream signaling cascades. Activated TNFR1 can directly induce inflammation and programmed cell death. The activation of TNFR2 can cause it to interact with the I κ B kinase (IKK) complex resulting in the phosphorylation of I κ B, thereby activating NF- κ B. Also, the IL-6/sIL-6R complex formed from IL-6 binding to sIL-6R can directly activate the ubiquitously expressed glycoprotein-130 (gp130), thereby activating NF- κ B. Activated NF- κ B can either migrate into the nucleus or mitochondria. In the nucleus, it encodes genes of proinflammatory cytokines (pro-IL-18 and pro-IL-1 β) and NLRP3, increasing their protein expression. NLRP3 inflammasome can activate caspase 1, which in turn cleaves pro-IL-1 β and pro-IL-18 to release their soluble forms, to induce necrosis and inflammation in cardiac cells. Additionally, in the mitochondria, activated NF- κ B can stimulate intrinsic apoptotic pathways via releasing cytochrome c, which triggers caspase cascades resulting in programmed cell death and inflammation.

the development of heart failure (Bryant et al., 1998). In an experimental heart failure model, *in vivo* TNF α inhibition reduced cardiac mitochondrial dysfunction, oxidative stress, and apoptosis (Moe et al., 2004). Additionally, in heart failure rats, TNF- α inhibition reduced chronic catecholamine-induced stress in the paraventricular nucleus and ameliorated cardiac function (Guggilam et al., 2007).

IL-6 and its Receptor

IL-6 is a pleiotropic cytokine released in response to perturbations in homeostasis (Fontes et al., 2015). This cytokine has well-defined pro- and anti-inflammatory properties when activated. Interestingly, its receptor, IL-6R, can be cleaved by ADAM17 (Riethmueller et al., 2017; Garbers et al., 2018). The properties of IL-6 are determined by its stimulation and signaling processes. Thus, acute stimulation of IL-6 is mostly protective, while its chronic response causes long-term signaling leading to inflammation and autoimmunity (Fontes et al., 2015). Signaling

via the membrane-bound IL-6 receptor (IL-6R) termed "classic signaling," can only occur on cell types that express surface IL-6R, including hepatocytes and certain leukocytes' subpopulations such as neutrophils (Wolf et al., 2014). However, signaling via soluble forms of the IL-6R, called IL-6 trans-signaling, can occur on all body cells since the IL-6/sIL-6R complex can directly bind to and activate the ubiquitously expressed glycoprotein-130 (gp130) without the need of a membrane-bound IL-6R (Wolf et al., 2014; Düsterhöft et al., 2019). IL-6 trans-signaling accounts mainly for the cytokine's proinflammatory properties (Fontes et al., 2015; Düsterhöft et al., 2019). The glycoprotein-130 (gp130) receptor is widely expressed in mammals, including the developing and adult hearts (Podewski et al., 2003). In physiological state, activation of gp130 in the heart by IL-6 type cytokines induces signaling through three main pathways: 1) the Janus kinase/signal transducer and activator of transcription (JAK/STAT) pathway, 2) the phosphatidylinositol-3-kinase-dependent (PI3K)/Akt pathway and 3) the Ras/mitogen-activated protein

kinase (MAPK) and extracellular signal-regulated kinase (ERK) signaling pathway (Podewski et al., 2003; Fischer and Hilfiker-Kleiner, 2008). These pathways have been demonstrated to play vital roles in cardiac development and protection (Yajima et al., 2006; Fischer and Hilfiker-Kleiner, 2008). However, in a chronic stress state characterized by elevated IL-6 and sIL-6R, continuous activation of gp130 in the heart can induce cardiac inflammation via gp130/JAK/STAT pathway (Podewski et al., 2003). This pathway can promote NF- κ B activation, resulting in the release of proinflammatory cytokines, formation, and activation of inflammasomes, which mediate cell death and cardiac inflammation (Fischer and Hilfiker-Kleiner, 2008; **Figure 4**). Undeniably, it has been revealed that increased levels of gp130 proteins and IL-6 cytokines are strong predictive markers for morbidity and mortality in patients with HF (Fischer and Hilfiker-Kleiner, 2008). According to Ritschel et al., elevated levels of circulating sIL-6R and IL-6 were linked to future cardiovascular events and mortality in patients, implying that the IL-6 signaling pathway plays an essential role in the development of HF (Ritschel et al., 2016). Studies have also reported that the local gp130 receptor system in myocytes is altered in failing human hearts (Podewski et al., 2003; Fischer and Hilfiker-Kleiner, 2008). Furthermore, many animal studies have demonstrated that in a stress state, upregulated levels of IL-6 in myocardia enhance the development of heart failure while its inhibition improves cardiac function. (Lai et al., 2012; Zhao et al., 2016; Adzika et al., 2021; Hou H. et al., 2021; Huo S. et al., 2021).

Currently, ADAM17 has not been directly associated with the regulation of T and B cells functions in the myocardia; however, these immune cells secrete TNF α , which is keenly regulated by ADAM17 (Opata et al., 2013; Yang et al., 2013; Adu-Amankwaah et al., 2021a). Also, ADAM17's targets on T and B cells have been implicated in their migration, differentiation, and effector functions (Link et al., 2017). Typically, Marczyńska et al. demonstrated that the costimulatory ligand, ICOS ligand (ICOSL), is preferentially downregulated on the surface of B cells in an ADAM17-dependent way, despite the fact that recombinant ADAM17 does not proteolyze it *in vitro* (Marczyńska et al., 2014). Therefore, it can be speculated that ADAM17 might directly regulate T and B cells' functions in the myocardia during inflammation.

A DISINTEGRIN AND METALLOPROTEASE 17 IN CARDIAC FIBROSIS

ADAM17 is known to activate amphiregulin (AREG) via its proteolytic cleavage activity (Liu et al., 2018). AREG is synthesized as a type-I transmembrane protein (pro-AREG) that can engage in juxtacrine signaling on adjacent cells (Berasain and Avila, 2014). Alternatively, after proteolytic processing, the release of soluble AREG (sAREG) can act as an autocrine or paracrine factor (Berasain and Avila, 2014). sAREG is a ligand of the EGFR (Berasain and Avila, 2014; Liu et al., 2018), widely expressed on cardiac myocytes and fibroblasts (Berasain and Avila, 2014; Liu et al., 2018). In a physiological

state, activation of EGFR in the heart induces major intracellular signaling cascades governing fibroblasts proliferation, migration, and collagen synthesis. However, prolonged activation of EGFR in a chronic stress state characterized by continuous elevation of sAREG can enhance cardiac fibroblast activation, proliferation, differentiation to myofibroblast, migration, and collagen synthesis (Liu et al., 2018). The binding of sAREG to EGFR, causes the receptor to undergo a conformational change inducing homo- or heterodimers formation (Dawson et al., 2005; Rayego-Mateos et al., 2018). This precedes an intracellular domain activation in its tyrosine residues by phosphorylation, promoting these same residues' autophosphorylation in their homolog. Autophosphorylation of EGFR can activate it to induce the JAK/STAT pathway (Dawson et al., 2005; Rayego-Mateos et al., 2018). This signaling pathway plays a vital role in transducing stress and growth signals in the heart during cardiac fibrosis (Wagner and Siddiqui, 2012). The activation of the JAK/STAT pathway can increase the gene expression of fibroblasts and pro-fibrotic factors such as transforming growth factor-beta (TGF- β) (Wang et al., 2002). Physiologically, cardiac fibroblasts are responsible for the homeostasis of the extracellular matrix (ECM), which provides a structural scaffold for cardiomyocytes, distributes mechanical forces through the cardiac tissue, and mediates electrical conduction (Travers et al., 2016). However, elevated fibroblasts can result in fibroblast activation, both mechanically by altered activation patterns and chemically by inflammatory mediators (Wang et al., 2002). Notably, elevated TNF α and IL-6 secretions from macrophages, T and B lymphocytes during chronic inflammation also contributes to the aggravation of cardiac fibrosis as these cytokines stimulate fibroblast proliferation, differentiation to myofibroblast, and their migration (Wang et al., 2002; Adekunle et al., 2021). Also, TGF- β plays a vital role in ECM remodeling, cell mobility, and modulation of immune function. Increased levels of it are crucial in cell differentiation and proliferation of activated fibroblasts to myofibroblasts (Baum and Duffy, 2011). Myofibroblasts are not present in normal cardiac tissue unless during cardiac injury (Manabe et al., 2002). Myofibroblasts can induce pathological ECM remodeling (Manabe et al., 2002) via the expression of smooth muscle alpha-actin (α -SMA) (Sousa et al., 2007), collagen synthesis, and secretion of MMPs (Manabe et al., 2002). MMPs are responsible for the breakdown of the extracellular matrix in many diseases (Liu et al., 2006). Chronic secretion of MMPs in the heart leads to the degradation of collagen and elastin into peptide fragments resulting in elevated collagen deposition in the ECM, leading to scar formation. Although the formation of fibrotic scar tissue is an adaptive way of maintaining the structural integrity and pressure-generating capacity of the heart, myofibroblast persistence due to chronic stress can eventually result in the development of adverse changes in ventricular structure and compliance, which characterizes cardiac fibrosis (Liu et al., 2006; **Figure 4**). Intriguingly, ADAM17 upregulation does enhance the secretions of the aforementioned cytokine from both innate and adaptive immune cells either via direct or indirect cascade to cause maladaptive interstitial fibrosis.

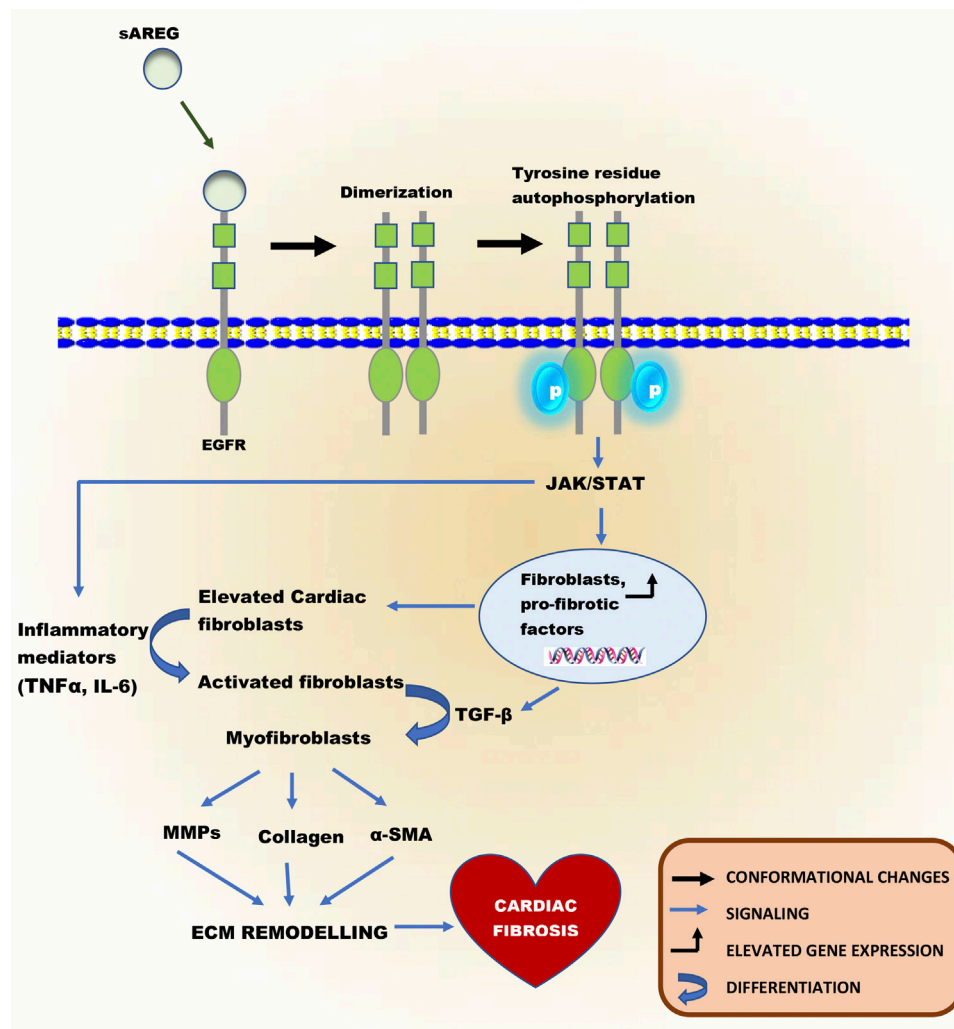


FIGURE 4 | Schematic illustration of the fibrotic role of sAREG, a substrate of ADAM17. After the proteolytic process of ADAM17, sAREG can activate EGFR, which is widely expressed on cardiac cells. The binding of sAREG to EGFR causes the receptor to undergo a conformational change known as “Dimerization,” resulting in homo- or heterodimers formation. This precedes an intracellular domain activation in its tyrosine residues by phosphorylation, promoting these same residues’ autophosphorylation in their homolog. Autophosphorylation of EGFR can activate it to induce the JAK/STAT pathway, leading to an increase in gene and protein expression of fibroblasts and pro-fibrotic factors such as TGF-β. Elevated fibroblasts can result in fibroblast activation, both mechanically by altered activation patterns and chemically by inflammatory mediators. Activated fibroblasts are transformed into myofibroblasts by TGF-β. Myofibroblasts are not present in normal cardiac tissue unless during cardiac injury and can induce pathological ECM remodeling, which characterizes cardiac fibrosis via the expression of α-SMA, collagen synthesis, and secretion of MMPs.

SYNERGY OF A DISINTEGRIN AND METALLOPROTEASE 17-INDUCED INFLAMMATION AND FIBROSIS IN HEART FAILURE DEVELOPMENT

HF development is characterized by a progressive condition associated with left ventricular (LV) systolic or diastolic dysfunction resulting in insufficient oxygen and nutrient supply to peripheral organs. It can exist in two main forms, namely, HF with preserved ejection fraction (HFpEF) and HF with reduced ejection fraction (HFrEF) (Van Linthout and Tschöpe, 2017; Adu-Amankwaah et al., 2021b). HFpEF is accompanied by diastolic

dysfunction characterized by impaired ventricle relaxation and filling, increased ventricle stiffness, and elevated filling pressure to respond to pressure overload (Adekunle et al., 2021). On the flip side, HFrEF is associated with systolic dysfunction characterized by impaired left ventricular contractility, resulting in a reduced ejection fraction (Tanai and Frantz, 2015). Cardiac inflammation and fibrosis play a central role in HF development (Liu et al., 2018). Both can trigger HF development under several conditions, ranging from acute stress to chronic catecholamine stress.

The outcome of inflammation and fibrosis can contribute to the pathogenesis of the two main forms of HF. Although elevated serum concentrations of proinflammatory cytokines and fibrotic factors are common in both forms of HF, the pathomechanisms

involved in each are different. For HFpEF, studies reveal that the outcome of chronic inflammation leads to progressive fibrosis, which eventually results in LV hypertrophy (Manabe et al., 2002; Salles et al., 2007; Wynn, 2008). Excessive increase in ECM components and cross-linking during LV hypertrophy can induce myocardial stiffness, thereby triggering HFpEF-specific, characterized by concentric cardiac remodeling and LV diastolic dysfunction (Paulus and Tschöpe, 2013). For example, collagen I which stiffens the myocardia, accounts for about 80% of the total collagen in the myocardia and increases most during LV hypertrophy (Barison et al., 2015). In addition, excessive cross-linking during LV hypertrophy stiffens the collagen matrix, making it more difficult to be broken down by proteinases (Travers et al., 2016). According to Hieda et al., increased myocardial stiffness is frequently observed in patients with HFpEF (Hieda et al., 2020). Regarding HFrEF, excessive cardiomyocyte death preceding necrosis or apoptosis due to persistent cardiac inflammation can result in cardiac atrophy. Continued loss of cardiac tissue can induce systolic dysfunction leading to HFrEF-specific, characterized by eccentric cardiac remodeling and dysfunction (Van Linthout and Tschöpe, 2017). Undeniably, several large studies have reported that patients with HFrEF characterized by systolic dysfunction have elevated serum levels of proinflammatory cytokines such as TNF α , IL-6, and IL-1 β (Torre-Amione et al., 1996; Rauchhaus et al., 2000; Deswal et al., 2001).

CONCLUSION AND FUTURE PERSPECTIVES

ADAM17 is widely expressed by several mammalian cells. Evidence suggests that the number of identified substrates of this metalloprotease keeps increasing, implying that ADAM17 may play a central role in regulating several physiological and pathophysiological processes. Hence, its implicated in several human diseases as such heart failure is expected. Although, current drug treatments and the subsequent use of recognized medications have reduced mortality and hospitalization rate, particularly in HF patients with reduced ejection fraction (Berliner and Bauersachs, 2017), HF remain a major clinical and public health concern since it affects more than 23 million worldwide (Ayoub et al., 2017; Orso et al., 2017; Frantz et al., 2018); hence there is still a lot to discover about this condition which will serve as a key in establishing specific treatment and management guidelines to significantly reduced the rate of HF. This comprehensive review has provided extensive insight into the mechanisms underlying catecholamine-induced HF. Therefore, therapeutic prospects for the treatment and management of catecholamine-induced HF should also target the inhibition of ADAM17 and/or antagonize its activation and activities.

For decades, ADAM17 has been the subject of intense research. Since its identification as the tumor necrosis factor convertase, it has been an important therapeutic target, particularly in the setting of inflammatory diseases. Nonetheless, developing medications that target ADAM17 has proven more difficult than anticipated. This is owing to ADAM17's multifunctionality, which includes the release

of approximately 90 other substrates aside from tumor necrosis factor (TNF), as well as its structural similarities to other metalloproteinases (Calligaris et al., 2021). The most promising targets of ADAM17 (without any significant physiological consequences) appear to be inhibiting its phosphorylation by ERKs, p38 MAPKs, iRhom1, and iRhom2. These regulators are vital for trafficking, stabilization, and activation of ADAM17 (Bell and Gööz, 2010; Adrain and Freeman, 2012; McIlwain et al., 2012; Xu et al., 2012; Li et al., 2015; Grieve et al., 2017). Usage of pharmacologic agents capable of impeding ADAM17 phosphorylation by ERKs and p38 MAPKs may be an attractive potential target for downregulating ADAM17's proteolytic activity. Also, it is well-known that iRhom2 is mainly expressed in proinflammatory immune cells, such as macrophages and neutrophils (Adrain and Freeman, 2012), whereas iRhom1 is predominantly expressed in non-immune cells (Issuree et al., 2013; Chemaly et al., 2017). Hence, it is tempting to hypothesize that inhibition of iRhom2 would aid in the downregulation of ADAM17 with no effects on non-immune cells. iRhom1 activities may then compensate for the iRhom2 blockade. Also, the inhibition of ADAM17 could be achieved by injecting its natural inhibitors (TIMP3, PDIs, and integrins). Notably, injection of TIMP3 has been shown to prevent heart failure post-myocardial infarction (Martz, 2014; Takawale et al., 2017; Chintalgattu et al., 2018). PDIs can also interact directly with ADAM17's MPD, which catalyzes the isomerization of two disulfide bridges, lowering ADAM17's activity (Willems et al., 2010). Furthermore, the binding of integrin $\alpha 5 \beta 1$ to ADAM17 *via* its disintegrin domain, according to Bax et al., inhibited its activity by altering its mediated cell adhesion and migration (Bax et al., 2004). Besides its natural inhibitors, miRNAs such as miR-124 (Sun et al., 2013), miR-145 (Doberstein et al., 2013), miR-152 (Su et al., 2014), and miR-326 (Cai et al., 2015) have been shown to suppress ADAM17 expression and limit substrate release by binding directly to the ADAM17 3'-UTR.

The modulation of ADAM17 is key in ameliorating cardiac function *via* attenuation of myocardial inflammation during chronic catecholamine stress. Thus, minimizing the levels of TNF α and other proinflammatory cytokines is necessary for the heart's normal function; hence, inhibiting ADAM17 which facilitates the activities of these cytokines, might enhance cardiac health or delay the progression of its pathological remodeling into HF.

AUTHOR CONTRIBUTIONS

The review idea was conceived by JA-A. JA-A drafted and wrote the manuscript. With the supervision of HS; JA-A, GA, AA, MN, RM, AB, NA, FH, YX, SA, and IN revised and proofread the manuscript. All authors read and approved the submitted version.

FUNDING

This work was supported by the National Natural Science Foundation of China (grant No. 81461138036, No. 81370329),

The Natural Science Foundation of the Jiangsu Higher Education Institutes of China (grant No. 17KJB180016), and the Priority Academic Program Development of Jiangsu Higher Education Institutions (PAPD).

REFERENCES

- Adamo, L., Rocha-Resende, C., Prabhu, S. D., and Mann, D. L. (2020). Reappraising the Role of Inflammation in Heart Failure. *Nat. Rev. Cardiol.* 17, 269–285. doi:10.1038/s41569-019-0315-x
- Adekunle, A. O., Adzika, G. K., Mprah, R., Ndzie Noah, M. L., Adu-Amankwaah, J., Rizvi, R., et al. (2021). Predominance of Heart Failure with Preserved Ejection Fraction in Postmenopausal Women: Intra- and Extra-cardiomyocyte Maladaptive Alterations Scaffolded by Estrogen Deficiency. *Front. Cell Dev. Biol.* 9, 685996. doi:10.3389/fcell.2021.685996
- Adrain, C., and Freeman, M. (2012). New Lives for Old: Evolution of Pseudoenzyme Function Illustrated by iRhoms. *Nat. Rev. Mol. Cell Biol.* 13, 489–498. doi:10.1038/nrm3392
- Adu-Amankwaah, J., Adzika, G. K., Adekunle, A. O., Ndzie Noah, M. L., Mprah, R., Bushi, A., et al. (2021a). The Synergy of ADAM17-Induced Myocardial Inflammation and Metabolic Lipids Dysregulation during Acute Stress: New Pathophysiologic Insights into Takotsubo Cardiomyopathy. *Front. Cardiovasc. Med.* 8, 696413. doi:10.3389/fcvm.2021.696413
- Adu-Amankwaah, J., Mprah, R., Adekunle, A. O., Ndzie Noah, M. L., Adzika, G. K., Machuki, J. O. A., et al. (2021b). The Cardiovascular Aspect of COVID-19. *Ann. Med.* 53, 227–236. doi:10.1080/07853890.2020.1861644
- Adzika, G. K., Hou, H., Adekunle, A. O., Rizvi, R., Adzraku, S. Y., Li, K., et al. (2021). Amlexanox and Forskolin Prevents Isoproterenol-Induced Cardiomyopathy by Subduing Cardiomyocyte Hypertrophy and Maladaptive Inflammatory Responses. *Front. Cell Dev. Biol.* 9, 719351. doi:10.3389/fcell.2021.719351
- Adzika, G. K., Machuki, J. O. A., Shang, W., Hou, H., Ma, T., Wu, L., et al. (2019). Pathological Cardiac Hypertrophy: The Synergy of Adenylyl Cyclases Inhibition in Cardiac and Immune Cells during Chronic Catecholamine Stress. *J. Mol. Med.* 97, 897–907. doi:10.1007/s00109-019-01790-0
- Ahlquist, R. P. (1948). A Study of the Adrenotropic Receptors. *Am. J. Physiol. Legacy Content* 153, 586–600. doi:10.1152/ajplegacy.1948.153.3.586
- Albensi, B. C. (2019). What Is Nuclear Factor Kappa B (NF- κ B) Doing in and to the Mitochondrion? *Front. Cell Dev. Biol.* 7, 154. doi:10.3389/fcell.2019.00154
- Anderson, D. R., Poterucha, J. T., Mikuls, T. R., Duryee, M. J., Garvin, R. P., Klassen, L. W., et al. (2013). IL-6 and its Receptors in Coronary Artery Disease and Acute Myocardial Infarction. *Cytokine* 62, 395–400. doi:10.1016/j.cyt.2013.03.020
- Arokiasamy, S., Zakian, C., Dillaway, J., Wang, W., Nourshargh, S., and Voisin, M.-B. (2017). Endogenous TNF α Orchestrates the Trafficking of Neutrophils Into and Within Lymphatic Vessels During Acute Inflammation. *Sci. Rep.* 7, 44189. doi:10.1038/srep44189
- Ayoub, K. F., Pothineni, N. V. K., Rutland, J., Ding, Z., and Mehta, J. L. (2017). Immunity, Inflammation, and Oxidative Stress in Heart Failure: Emerging Molecular Targets. *Cardiovasc. Drugs Ther.* 31, 593–608. doi:10.1007/s10557-017-6752-z
- Barison, A., Grigoratos, C., Todiere, G., and Aquaro, G. D. (2015). Myocardial Interstitial Remodelling in Non-Ischaemic Dilated Cardiomyopathy: Insights from Cardiovascular Magnetic Resonance. *Heart Fail. Rev.* 20, 731–749. doi:10.1007/s10741-015-9509-4
- Bauernfeind, F. G., Horvath, G., Stutz, A., Alnemri, E. S., Macdonald, K., Speert, D., et al. (2009). Cutting Edge: NF- κ B Activating Pattern Recognition and Cytokine Receptors License NLRP3 Inflammasome Activation by Regulating NLRP3 Expression. *J. Immunol.* 183, 787–791. doi:10.4049/jimmunol.0901363
- Baum, J., and Duffy, H. S. (2011). Fibroblasts and Myofibroblasts: What are we Talking About? *J. Cardiovasc. Pharmacol.* 57, 376–379. doi:10.1097/fjc.0b013e3182116e39
- Bax, D. V., Messent, A. J., Tart, J., Van Hoang, M., Kott, J., Maciewicz, R. A., et al. (2004). Integrin α 5 β 1 and ADAM-17 Interact *In Vitro* and Co-localize in

ACKNOWLEDGMENTS

We acknowledge the help of Prof. Festus Adzaku, Dr. Innocent Afeke, and Miss Mary Nyarko for proofreading the entire manuscript.

- Migrating HeLa Cells. *J. Biol. Chem.* 279, 22377–22386. doi:10.1074/jbc.m400180200
- Bell, H. L., and Gööz, M. (2010). ADAM-17 Is Activated by the Mitogenic Protein Kinase ERK in a Model of Kidney Fibrosis. *Am. J. Med. Sci.* 339, 105–107. doi:10.1097/MAJ.0b013e3181cb4487
- Berasain, C., and Avila, M. A. (2014). Amphiregulin. *Semin. Cell Developmental Biol.* 28, 31–41. doi:10.1016/j.semcdb.2014.01.005
- Berliner, D., and Bauersachs, J. (2017). Current Drug Therapy in Chronic Heart Failure: the New Guidelines of the European Society of Cardiology (ESC). *Korean Circ. J.* 47, 543–554. doi:10.4070/kcj.2017.0030
- Biase, L., Pignatelli, P., Lenti, L., Tocci, G., Piccioni, F., Riandino, S., et al. (2003). Enhanced TNF α and Oxidative Stress in Patients with Heart Failure: Effect of TNF α on Platelet O₂ - Production. *Thromb. Haemost.* 90, 317–325. doi:10.1160/th03-02-0105
- Black, R. A., Rauch, C. T., Kozlosky, C. J., Peschon, J. J., Slack, J. L., Wolfson, M. F., et al. (1997). A Metalloproteinase Disintegrin that Releases Tumour-Necrosis Factor- α from Cells. *Nature* 385, 729–733. doi:10.1038/385729a0
- Bode, W., Gomis-Rüth, F.-X., and Stöckler, W. (1993). Astacins, Serralyins, Snake Venom and Matrix Metalloproteinases Exhibit Identical Zinc-Binding Environments (HEXXHXXGXXH and Met-Turn) and Topologies and Should Be Grouped into a Common Family, the 'metzincins'. *FEBS Lett.* 331, 134–140. doi:10.1016/0014-5793(93)80312-i
- Bottero, V., Busuttill, V., Loubat, A., Magné, N., Fischel, J. L., Milano, G., et al. (2001). Activation of Nuclear Factor kappaB Through the IKK Complex by the Topoisomerase Poisons SN38 and Doxorubicin: A Brake to Apoptosis in HeLa Human Carcinoma Cells. *Cancer Res.* 61, 7785–7791.
- Bozkurt, B., Kribbs, S. B., Clubb, F. J., Jr., Michael, L. H., Didenko, V. V., Hornsby, P. J., et al. (1998). Pathophysiologically Relevant Concentrations of Tumor Necrosis Factor- α Promote Progressive Left Ventricular Dysfunction and Remodeling in Rats. *Circulation* 97, 1382–1391. doi:10.1161/01.cir.97.14.1382
- Bristow, M. R., Hershberger, R. E., Port, J. D., Gilbert, E. M., Sandoval, A., Rasmussen, R., et al. (1990). Beta-adrenergic Pathways in Nonfailing and Failing Human Ventricular Myocardium. *Circulation* 82, I12–I25.
- Broder, C., and Becker-Paul, C. (2013). The Metalloproteases Meprin α and Meprin β : Unique Enzymes in Inflammation, Neurodegeneration, Cancer and Fibrosis. *Biochem. J.* 450, 253–264. doi:10.1042/bj20121751
- Bryant, D., Becker, L., Richardson, J., Shelton, J., Franco, F., Peshock, R., et al. (1998). Cardiac Failure in Transgenic Mice with Myocardial Expression of Tumor Necrosis Factor- α . *Circulation* 97, 1375–1381. doi:10.1161/01.cir.97.14.1375
- Bylund, D. B., Eikenberg, D. C., Hieble, J. P., Langer, S. Z., Lefkowitz, R. J., Minneman, K. P., et al. (1994). International Union of Pharmacology Nomenclature of Adrenoceptors. *Pharmacol. Rev.* 46, 121–136.
- Cabron, A.-S., El Azzouzi, K., Boss, M., Arnold, P., Schwarz, J., Rosas, M., et al. (2018). Structural and Functional Analyses of the Shedding Protease ADAM17 in HoxB8-Immortalized Macrophages and Dendritic-Like Cells. *J. Immunol.* 201, 3106–3118. doi:10.4049/jimmunol.1701556
- Cai, M., Wang, Z., Zhang, J., Zhou, H., Jin, L., Bai, R., et al. (2015). Adam17, a Target of Mir-326, Promotes Emt-Induced Cells Invasion in Lung Adenocarcinoma. *Cell Physiol. Biochem.* 36, 1175–1185. doi:10.1159/000430288
- Calligaris, M., Cuffaro, D., Bonelli, S., Spanò, D. P., Rossello, A., Nuti, E., et al. (2021). Strategies to Target ADAM17 in Disease: From its Discovery to the iRhom Revolution. *Molecules* 26. doi:10.3390/molecules26040944
- Calvete, J., Marcinkiewicz, C., and Sanz, L. (2007). KTS and RTS-Disintegrins: Anti-angiogenic Viper Venom Peptides Specifically Targeting the α 1 β 1 Integrin. *Curr. Pharm. Des.* 13, 2853–2859. doi:10.2174/138161207782023766
- Chemaly, M., Mcgilligan, V., Gibson, M., Clauss, M., Watterson, S., Alexander, H. D., et al. (2017). Role of Tumour Necrosis Factor Alpha Converting Enzyme (TACE/ADAM17) and Associated Proteins in Coronary Artery Disease and

- Cardiac Events. *Arch. Cardiovasc. Dis.* 110, 700–711. doi:10.1016/j.acvd.2017.08.002
- Chen, L., Hodges, R. R., Funaki, C., Zoukhr, D., Gaivin, R. J., Perez, D. M., et al. (2006). Effects of α 1D-adrenergic Receptors on Shedding of Biologically Active EGF in Freshly Isolated Lacrimal Gland Epithelial Cells. *Am. J. Physiol. Cell Physiol.* 291, C946–C956. doi:10.1152/ajpcell.00014.2006
- Chintalgattu, V., Greenberg, J., Singh, S., Chiueh, V., Gilbert, A., O'Neill, J. W., et al. (2018). Utility of Glycosylated TIMP3 Molecules: Inhibition of MMPs and TACE to Improve Cardiac Function in Rat Myocardial Infarct Model. *Pharmacol. Res. Perspect.* 6, e00442. doi:10.1002/prp2.442
- Cogswell, P. C., Kashatus, D. F., Keifer, J. A., Guttridge, D. C., Reuther, J. Y., Bristow, C., et al. (2003). NF- κ B and I κ B α Are Found in the Mitochondria. *J. Biol. Chem.* 278, 2963–2968. doi:10.1074/jbc.m209995200
- Cumberbatch, M., and Kimber, I. (1992). Dermal Tumour Necrosis Factor-Alpha Induces Dendritic Cell Migration to Draining Lymph Nodes, and Possibly Provides One Stimulus for Langerhans' Cell Migration. *Immunology* 75, 257–263.
- Damås, J. K., Eiken, H. G., Oie, E., Bjerkeli, V., Yndestad, A., Ueland, T., et al. (2000). Myocardial Expression of CC- and CXC-Chemokines and Their Receptors in Human End-Stage Heart Failure. *Cardiovasc. Res.* 47, 778–787. doi:10.1016/s0008-6363(00)00142-5
- Dawson, J. P., Berger, M. B., Lin, C.-C., Schlessinger, J., Lemmon, M. A., and Ferguson, K. M. (2005). Epidermal Growth Factor Receptor Dimerization and Activation Require Ligand-Induced Conformational Changes in the Dimer Interface. *Mol. Cell Biol.* 25, 7734–7742. doi:10.1128/mcb.25.17.7734-7742.2005
- De Queiroz, T. M., Xia, H., Filipeanu, C. M., Braga, V. A., and Lazartigues, E. (2015). α -Lipoic Acid Reduces Neurogenic Hypertension by Blunting Oxidative Stress-Mediated Increase in ADAM17. *Am. J. Physiol. Heart Circ. Physiol.* 309, H926–H934. doi:10.1152/ajpheart.00259.2015
- Defer, N., Azroyan, A., Pecker, F., and Pavoine, C. (2007). TNFR1 and TNFR2 Signaling Interplay in Cardiac Myocytes. *J. Biol. Chem.* 282, 35564–35573. doi:10.1074/jbc.m704003200
- Deswal, A., Petersen, N. J., Feldman, A. M., Young, J. B., White, B. G., and Mann, D. L. (2001). Cytokines and Cytokine Receptors in Advanced Heart Failure. *Circulation* 103, 2055–2059. doi:10.1161/01.cir.103.16.2055
- Díaz-Rodríguez, E., Montero, J. C., Esparis-Ogando, A., Yuste, L., and Pandiella, A. (2002). Extracellular Signal-Regulated Kinase Phosphorylates Tumor Necrosis Factor Alpha-Converting Enzyme at Threonine 735: A Potential Role in Regulated Shedding. *Mol. Biol. Cell* 13, 2031–2044.
- Doberstein, K., Steinmeyer, N., Hartmetz, A.-K., Eberhardt, W., Mittelbronn, M., Harter, P. N., et al. (2013). MicroRNA-145 Targets the Metalloprotease ADAM17 and Is Suppressed in Renal Cell Carcinoma Patients. *Neoplasia* 15, 218–IN31. doi:10.1593/neo.121222
- Dunlay, S. M., Weston, S. A., Redfield, M. M., Killian, J. M., and Roger, V. L. (2008). Tumor Necrosis Factor- α and Mortality in Heart Failure. *Circulation* 118, 625–631. doi:10.1161/circulationaha.107.759191
- Düsterhöft, S., Jung, S., Hung, C. W., Tholey, A., Sönnichsen, F. D., Grötzing, J., et al. (2013). Membrane-Proximal Domain of a Disintegrin and Metalloprotease-17 Represents the Putative Molecular Switch of its Shedding Activity Operated by Protein-Disulfide Isomerase. *J. Am. Chem. Soc.* 135, 5776–5781. doi:10.1021/ja400340u
- Düsterhöft, S., Höbel, K., Oldefest, M., Lokau, J., Waetzig, G. H., Chalaris, A., et al. (2014). A Disintegrin and Metalloprotease 17 Dynamic Interaction Sequence, the Sweet Tooth for the Human Interleukin 6 Receptor. *J. Biol. Chem.* 289, 16336–16348.
- Düsterhöft, S., Lokau, J., and Garbers, C. (2019). The Metalloprotease ADAM17 in Inflammation and Cancer. *Pathol. Res. Pract.* 215, 152410.
- Epelman, S., Lavine, K. J., Beaudin, A. E., Sojka, D. K., Carrero, J. A., Calderon, B., et al. (2014). Embryonic and Adult-Derived Resident Cardiac Macrophages Are Maintained through Distinct Mechanisms at Steady State and during Inflammation. *Immunity* 40, 91–104. doi:10.1016/j.immuni.2013.11.019
- Ferrari, R., Bachetti, T., Confortini, R., Opasich, C., Febo, O., Corti, A., et al. (1995). Tumor Necrosis Factor Soluble Receptors in Patients with Various Degrees of Congestive Heart Failure. *Circulation* 92, 1479–1486. doi:10.1161/01.cir.92.6.1479
- Fischer, P., and Hilfiker-Kleiner, D. (2008). Role of Gp130-Mediated Signalling Pathways in the Heart and its Impact on Potential Therapeutic Aspects. *Br. J. Pharmacol.* 153 (Suppl. 1), S414–S427. doi:10.1038/bjp.2008.1
- Fontes, J. A., Rose, N. R., and Čiháková, D. (2015). The Varying Faces of IL-6: From Cardiac protection to Cardiac Failure. *Cytokine* 74, 62–68. doi:10.1016/j.cyto.2014.12.024
- Frantz, S., Falcao-Pires, I., Balligand, J.-L., Bauersachs, J., Brutsaert, D., Ciccarelli, M., et al. (2018). The Innate Immune System in Chronic Cardiomyopathy: a European Society of Cardiology (ESC) Scientific Statement from the Working Group on Myocardial Function of the ESC. *Eur. J. Heart Fail.* 20, 445–459. doi:10.1002/ejhf.1138
- Garbers, C., Heink, S., Korn, T., and Rose-John, S. (2018). Interleukin-6: Designing Specific Therapeutics for a Complex Cytokine. *Nat. Rev. Drug Discov.* 17, 395–412. doi:10.1038/nrd.2018.45
- Garton, K. J., Gough, P. J., Philalay, J., Wille, P. T., Blobel, C. P., Whitehead, R. H., et al. (2003). Stimulated Shedding of Vascular Cell Adhesion Molecule 1 (VCAM-1) is Mediated by Tumor Necrosis Factor- α -Converting Enzyme (ADAM 17). *J. Biol. Chem.* 278, 37459–37464. doi:10.1074/jbc.m305877200
- Ghosh, S., May, M. J., and Kopp, E. B. (1998). NF- κ B and REL PROTEINS: Evolutionarily Conserved Mediators of Immune Responses. *Annu. Rev. Immunol.* 16, 225–260. doi:10.1146/annurev.immunol.16.1.225
- Gooz, M. (2010). ADAM-17: The Enzyme that Does it All. *Crit. Rev. Biochem. Mol. Biol.* 45, 146–169. doi:10.3109/10409231003628015
- Granneman, J. G. (2001). The Putative β 4-adrenergic Receptor is a Novel State of the β 1-adrenergic Receptor. *Am. J. Physiol. Endocrinol. Metab.* 280, E199–E202. doi:10.1152/ajpendo.2001.280.2.e199
- Grieve, A. G., Xu, H., Künzel, U., Bambrough, P., Sieber, B., and Freeman, M. (2017). Phosphorylation of iRhom2 at the Plasma Membrane Controls Mammalian TACE-dependent Inflammatory and Growth Factor Signalling. *Elife* 6, e23968. doi:10.7554/eLife.23968
- Grötzing, J., Lorenzen, I., and Düsterhöft, S. (2017). Molecular Insights into the Multilayered Regulation of ADAM17: The Role of the Extracellular Region. *Biochim. Biophys. Acta Mol. Cell Res.* 1864, 2088–2095.
- Guggilam, A., Haque, M., Kerut, E. K., Mcilwain, E., Lucchesi, P., Seghal, I., et al. (2007). TNF- α Blockade Decreases Oxidative Stress in the Paraventricular Nucleus and Attenuates Sympathoexcitation in Heart Failure Rats. *Am. J. Physiol. Heart Circ. Physiol.* 293, H599–H609. doi:10.1152/ajpheart.00286.2007
- Heidt, T., Courties, G., Dutta, P., Sager, H. B., Sebas, M., Iwamoto, Y., et al. (2014). Differential Contribution of Monocytes to Heart Macrophages in Steady-State and After Myocardial Infarction. *Circ. Res.* 115, 284–295. doi:10.1161/circresaha.115.303567
- Hieda, M., Sarma, S., Hearon, C. M., Jr., Dias, K. A., Martinez, J., Samels, M., et al. (2020). Increased Myocardial Stiffness in Patients with High-Risk Left Ventricular Hypertrophy. *Circulation* 141, 115–123. doi:10.1161/circulationaha.119.040332
- Hou, H., Adzika, G. K., Wu, Q., Ma, T., Ma, Y., Geng, J., et al. (2021). Estrogen Attenuates Chronic Stress-Induced Cardiomyopathy by Adaptively Regulating Macrophage Polarizations via β 2-Adrenergic Receptor Modulation. *Front. Cell Dev. Biol.* 9, 737003. doi:10.3389/fcell.2021.737003
- Hou, H., Zhao, Z., Machuki, J. O. a., Zhang, L., Zhang, Y., Fu, L., et al. (2018). Estrogen Deficiency Compromised the β 2AR-Gs/Gi Coupling: Implications for Arrhythmia and Cardiac Injury. *Pflugers Arch. Eur. J. Physiol.* 470, 559–570. doi:10.1007/s00424-017-2098-4
- Huo, S., Shi, W., Ma, H., Yan, D., Luo, P., Guo, J., et al. (2021). Alleviation of Inflammation and Oxidative Stress in Pressure Overload-Induced Cardiac Remodeling and Heart Failure via IL-6/STAT3 Inhibition by Raloxifene. *Oxid. Med. Cell Longev.* 2021, 6699054. doi:10.1155/2021/6699054
- Israël, A. (2010). The IKK Complex, a Central Regulator of NF- κ B Activation. *Cold Spring Harb Perspect. Biol.* 2, a000158. doi:10.1101/cshperspect.a000158
- Issuree, P. D., Maretzky, T., Mcilwain, D. R., Monette, S., Qing, X., Lang, P. A., et al. (2013). iRHOM2 is a Critical Pathogenic Mediator of Inflammatory Arthritis. *J. Clin. Invest.* 123, 928–932. doi:10.1172/JCI66168
- Jackson, L. F., Qiu, T. H., Sunnarborg, S. W., Chang, A., Zhang, C., Patterson, C., et al. (2003). Defective Valvulogenesis in HB-EGF and TACE-Null Mice Is Associated with Aberrant BMP Signaling. *EMBO J.* 22, 2704–2716. doi:10.1093/emboj/cdg264
- Jones, A. V., Lambert, D. W., Speight, P. M., and Whawell, S. A. (2013). ADAM 10 is Over Expressed in Oral Squamous Cell Carcinoma and Contributes to Invasive Behaviour through a Functional Association with α v β 6 Integrin. *FEBS Lett.* 587, 3529–3534. doi:10.1016/j.febslet.2013.09.010

- Jones, G. W., Mcloughlin, R. M., Hammond, V. J., Parker, C. R., Williams, J. D., Malhotra, R., et al. (2010). Loss of CD4+ T Cell IL-6R Expression during Inflammation Underlines a Role for IL-6 Trans Signaling in the Local Maintenance of Th17 Cells. *J. Immunol.* 184, 2130–2139. doi:10.4049/jimmunol.0901528
- Jones, J. C., Rustagi, S., and Dempsey, P. J. (2016). ADAM Proteases and Gastrointestinal Function. *Annu. Rev. Physiol.* 78, 243–276. doi:10.1146/annurev-physiol-021014-071720
- Juhász, K., Buzás, K., and Duda, E. (2013). Importance of Reverse Signaling of the TNF Superfamily in Immune Regulation. *Expert Rev. Clin. Immunol.* 9, 335–348.
- Kawai, T., Elliott, K. J., Scalia, R., and Eguchi, S. (2021). Contribution of ADAM17 and Related ADAMs in Cardiovascular Diseases. *Cell Mol. Life Sci.* 78, 4161–4187. doi:10.1007/s00018-021-03779-w
- Kefaloyianni, E., Muthu, M. L., Kaeppler, J., Sun, X., Sabbiseti, V., Chalaris, A., et al. (2016). ADAM17 Substrate Release in Proximal Tubule Drives Kidney Fibrosis. *JCI Insight* 1. doi:10.1172/jci.insight.87023
- Kim, H. J., Trinh, N. T., Choi, Y., Kim, W., Min, K. H., Kang, S. O., et al. (2020). ADAM17 Genetic Variants and the Response of TNF- α Inhibitor in Rheumatoid Arthritis Patients. *Pgpm* 13, 81–88. doi:10.2147/pgpm.s235035
- Kivimäki, M., and Steptoe, A. (2018). Effects of Stress on the Development and Progression of Cardiovascular Disease. *Nat. Rev. Cardiol.* 15, 215–229.
- Lafuse, W. P., Wozniak, D. J., and Rajaram, M. V. S. (2020). Role of Cardiac Macrophages on Cardiac Inflammation, Fibrosis and Tissue Repair. *Cells* 10. doi:10.3390/cells10010051
- Lai, N. C., Gao, M. H., Tang, E., Tang, R., Guo, T., Dalton, N. D., et al. (2012). Pressure Overload-Induced Cardiac Remodeling and Dysfunction in the Absence of Interleukin 6 in Mice. *Lab. Invest.* 92, 1518–1526. doi:10.1038/labinvest.2012.97
- Lajevic, M. D., Suleiman, S., Cohen, R. L., and Chambers, D. A. (2011). Activation of P38 Mitogen-Activated Protein Kinase by Norepinephrine in T-Lineage Cells. *Immunology* 132, 197–208. doi:10.1111/j.1365-2567.2010.03354.x
- Lammich, S., Kojro, E., Postina, R., Gilbert, S., Pfeiffer, R., Jasionowski, M., et al. (1999). Constitutive and Regulated -Secretase Cleavage of Alzheimer's Amyloid Precursor Protein by a Disintegrin Metalloprotease. *Proc. Natl. Acad. Sci.* 96, 3922–3927. doi:10.1073/pnas.96.7.3922
- Li, H., Xia, Z., Chen, Y., Qi, D., and Zheng, H. (2018). Mechanism and Therapies of Oxidative Stress-Mediated Cell Death in Ischemia Reperfusion Injury. *Oxid Med. Cell Longev.* 2018, 2910643. doi:10.1155/2018/2910643
- Li, N., and Karin, M. (2000). Signaling Pathways Leading to Nuclear Factor-Kb Activation. *Methods Enzymol.* 319, 273–279. doi:10.1016/s0076-6879(00)19027-5
- Li, X., Bian, Y., Pang, P., Yu, S., Wang, X., Gao, Y., et al. (2020). Inhibition of Dectin-1 in Mice Ameliorates Cardiac Remodeling by Suppressing NF-Kb/nlrp3 Signaling after Myocardial Infarction. *Int. Immunopharmacol.* 80, 106116. doi:10.1016/j.intimp.2019.106116
- Li, X., Maretzky, T., Weskamp, G., Monette, S., Qing, X., Issuree, P. D. A., et al. (2015). iRhoms 1 and 2 are Essential Upstream Regulators of ADAM17-Dependent EGFR Signaling. *Proc. Natl. Acad. Sci. U.S.A.* 112, 6080–6085. doi:10.1073/pnas.1505649112
- Lichtenthaler, S. F., Lemberg, M. K., and Flührer, R. (2018). Proteolytic Ectodomain Shedding of Membrane Proteins in Mammals—Hardware, Concepts, and Recent Developments. *EMBO J.* 37, e99456. doi:10.15252/emboj.201899456
- Link, M. A., Lücke, K., Schmid, J., Schumacher, V., Eden, T., Rose-John, S., et al. (2017). The Role of ADAM17 in the T-Cell Response against Bacterial Pathogens. *PLoS One* 12, e0184320. doi:10.1371/journal.pone.0184320
- Liu, H., Ma, Y., Pagliari, L. J., Perlman, H., Yu, C., Lin, A., et al. (2004). TNF- α -Induced Apoptosis of Macrophages Following Inhibition of NF-Kb: A Central Role for Disruption of Mitochondria. *J. Immunol.* 172, 1907–1915. doi:10.4049/jimmunol.172.3.1907
- Liu, L., Jin, X., Hu, C.-F., Zhang, Y.-P., Zhou, Z. e., Li, R., et al. (2018). Amphiregulin Enhances Cardiac Fibrosis and Aggravates Cardiac Dysfunction in Mice with Experimental Myocardial Infarction Partly through Activating EGFR-dependent Pathway. *Basic Res. Cardiol.* 113, 12. doi:10.1007/s00395-018-0669-y
- Liu, P., Sun, M., and Sader, S. (2006). Matrix Metalloproteinases in Cardiovascular Disease. *Can. J. Cardiol.* 22 (Suppl. B), 25b–30b. doi:10.1016/s0828-282x(06)70983-7
- Ma, Y. (2021). Role of Neutrophils in Cardiac Injury and Repair Following Myocardial Infarction. *Cells* 10, 1676. doi:10.3390/cells10071676
- Machuki, J. O. a., Zhang, H.-Y., Geng, J., Fu, L., Adzika, G. K., Wu, L., et al. (2019). Estrogen Regulation of Cardiac cAMP-L-type Ca²⁺ Channel Pathway Modulates Sex Differences in Basal Contraction and Responses to β 2AR-mediated Stress in Left Ventricular Apical Myocytes. *Cell Commun Signal* 17, 34. doi:10.1186/s12964-019-0346-2
- Madamanchi, A. (2007). Beta-Adrenergic Receptor Signaling in Cardiac Function and Heart Failure. *Mcgill J. Med.* 10, 99–104.
- Magosci, M., Vizi, E. S., Selmecezy, Z., Brózik, A., and Szelenyi, J. (2007). Multiple G-Protein-Coupling Specificity of β -adrenoceptor in Macrophages. *Immunology* 122, 503–513. doi:10.1111/j.1365-2567.2007.02658.x
- Manabe, I., Shindo, T., and Nagai, R. (2002). Gene Expression in Fibroblasts and Fibrosis. *Circ. Res.* 91, 1103–1113. doi:10.1161/01.res.0000046452.67724.b8
- Marczynska, J., Ozga, A., Włodarczyk, A., Majchrzak-Gorecka, M., Kulig, P., Banas, M., et al. (2014). The Role of Metalloproteinase ADAM17 in Regulating ICOS Ligand-Mediated Humoral Immune Responses. *J. Immunol.* 193, 2753–2763. doi:10.4049/jimmunol.1302893
- Maretzky, T., Mcilwain, D. R., Issuree, P. D. A., Li, X., Malapeira, J., Amin, S., et al. (2013). iRhom2 Controls the Substrate Selectivity of Stimulated ADAM17-Dependent Ectodomain Shedding. *Proc. Natl. Acad. Sci.* 110, 11433–11438. doi:10.1073/pnas.1302553110
- Martz, L. (2014). Taking TIMP3 to Heart. *Science-Business eXchange* 7, 246. doi:10.1038/scibx.2014.246
- Mcilwain, D. R., Lang, P. A., Maretzky, T., Hamada, K., Ohishi, K., Maney, S. K., et al. (2012). iRhom2 Regulation of TACE Controls TNF-Mediated Protection Against Listeria and Responses to LPS. *Science* 335, 229–232. doi:10.1126/science.1214448
- Mishra, H. K., Long, C., Bahaie, N. S., and Walcheck, B. (2015). Regulation of CXCR2 Expression and Function by a Disintegrin and Metalloprotease-17 (ADAM17). *J. Leukoc. Biol.* 97, 447–454. doi:10.1189/jlb.3hi0714-340r
- Moe, G. W., Marin-Garcia, J., Konig, A., Goldenthal, M., Lu, X., and Feng, Q. (2004). *In Vivo* TNF- α Inhibition Ameliorates Cardiac Mitochondrial Dysfunction, Oxidative Stress, and Apoptosis in Experimental Heart Failure. *Am. J. Physiol. Heart Circ. Physiol.* 287, H1813–H1820. doi:10.1152/ajpheart.00036.2004
- Moss, M. L., Jin, S.-L. C., Milla, M. E., Burkhart, W., Carter, H. L., Chen, W.-J., et al. (1997). Cloning of a Disintegrin Metalloproteinase that Processes Precursor Tumour-Necrosis Factor-Alpha. *Nature* 385, 733–736. doi:10.1038/385733a0
- Mukerjee, S., Gao, H., Xu, J., Sato, R., Zsombok, A., and Lazartigues, E. (2019). ACE2 and ADAM17 Interaction Regulates the Activity of Presympathetic Neurons. *Hypertension* 74, 1181–1191. doi:10.1161/hypertensionaha.119.13133
- Myagmar, B. E., Flynn, J. M., Cowley, P. M., Swigart, P. M., Montgomery, M. D., Thai, K., et al. (2017). Adrenergic Receptors in Individual Ventricular Myocytes: The Beta-1 and Alpha-1B are in All Cells, the Alpha-1A is in a Subpopulation, and the Beta-2 and Beta-3 Are Mostly Absent. *Circ. Res.* 120, 1103–1115. doi:10.1161/circresaha.117.310520
- O'connell, T. D., Jensen, B. C., Baker, A. J., and Simpson, P. C. (2014). Cardiac Alpha-1-Adrenergic Receptors: Novel Aspects of Expression, Signaling Mechanisms, Physiologic Function, and Clinical Importance. *Pharmacol. Rev.* 66, 308–333. doi:10.1124/pr.112.007203
- Opat, M. M., Ye, Z., Hollifield, M., and Garvy, B. A. (2013). B Cell Production of Tumor Necrosis Factor in Response to Pneumocystis Murina Infection in Mice. *Infect. Immun.* 81, 4252–4260. doi:10.1128/iai.00744-13
- Orso, F., Fabbri, G., and Maggioni, A. P. (2017). Epidemiology of Heart Failure. *Handb Exp. Pharmacol.* 243, 15–33. doi:10.1007/164_2016_74
- Papazafropoulou, A., and Tentolouris, N. (2009). Matrix Metalloproteinases and Cardiovascular Diseases. *Hippokratia* 13, 76–82.
- Park, S., Lee, E. S., Park, N. H., Hwang, K., and Cho, E. G. (2019). Circadian Expression of TIMP3 Is Disrupted by UVB Irradiation and Recovered by Green Tea Extracts. *Int. J. Mol. Sci.* 20. doi:10.3390/ijms20040862
- Paulus, W. J., and Tschöpe, C. (2013). A Novel Paradigm for Heart Failure with Preserved Ejection Fraction: Comorbidities Drive Myocardial Dysfunction and

- Remodeling through Coronary Microvascular Endothelial Inflammation. *J. Am. Coll. Cardiol.* 62, 263–271. doi:10.1016/j.jacc.2013.02.092
- Paur, H., Wright, P. T., Sikkil, M. B., Tranter, M. H., Mansfield, C., O'gara, P., et al. (2012). High Levels of Circulating Epinephrine Trigger Apical Cardiodepression in a β 2-adrenergic receptor/Gi-dependent Manner: A New Model of Takotsubo Cardiomyopathy. *Circulation* 126, 697–706. doi:10.1161/circulationaha.112.111591
- Podewski, E. K., Hilfiker-Kleiner, D., Hilfiker, A., Morawietz, H., Lichtenberg, A., Wollert, K. C., et al. (2003). Alterations in Janus Kinase (JAK)-signal Transducers and Activators of Transcription (STAT) Signaling in Patients with End-Stage Dilated Cardiomyopathy. *Circulation* 107, 798–802. doi:10.1161/01.cir.0000057545.82749.ff
- Rauchhaus, M., Doehner, W., Francis, D. P., Davos, C., Kemp, M., Liebenthal, C., et al. (2000). Plasma Cytokine Parameters and Mortality in Patients with Chronic Heart Failure. *Circulation* 102, 3060–3067. doi:10.1161/01.cir.102.25.3060
- Rayego-Mateos, S., Rodrigues-Diez, R., Morgado-Pascual, J. L., Valentijn, F., Valdivielso, J. M., Goldschmeding, R., et al. (2018). Role of Epidermal Growth Factor Receptor (EGFR) and its Ligands in Kidney Inflammation and Damage. *Mediators Inflamm.* 2018, 8739473. doi:10.1155/2018/8739473
- Reddy, A. B., Ramana, K. V., Srivastava, S., Bhatnagar, A., and Srivastava, S. K. (2009). Aldose Reductase Regulates High Glucose-Induced Ectodomain Shedding of Tumor Necrosis Factor (TNF)-alpha via Protein Kinase C-delta and TNF-Alpha Converting Enzyme in Vascular Smooth Muscle Cells. *Endocrinology* 150, 63–74. doi:10.1210/en.2008-0677
- Rego, S. L., Swamydas, M., Kidiyoor, A., Helms, R., De Pianta, A., Lance, A. L., et al. (2013). Soluble Tumor Necrosis Factor Receptors Shed by Breast Tumor Cells Inhibit Macrophage Chemotaxis. *J. Interferon Cytokine Res.* 33, 672–681. doi:10.1089/jir.2013.0009
- Riethmueller, S., Somasundaram, P., Ehlers, J. C., Hung, C. W., Flynn, C. M., Lokau, J., et al. (2017). Proteolytic Origin of the Soluble Human IL-6R *In Vivo* and a Decisive Role of N-Glycosylation. *PLoS Biol.* 15, e2000080. doi:10.1371/journal.pbio.2000080
- Ritschel, V. N., Seljeflot, I., Arnesen, H., Halvorsen, S., Eritsland, J., Fagerland, M. W., et al. (2016). Circulating Levels of IL-6 Receptor and Gp130 and Long-Term Clinical Outcomes in ST-Elevation Myocardial Infarction. *J. Am. Heart Assoc.* 5. doi:10.1161/JAHA.115.003014
- Russo, R. C., Guabiraba, R., Garcia, C. C., Barcelos, L. S., Roffé, E., Souza, A. L., et al. (2009). Role of the Chemokine Receptor CXCR2 in Bleomycin-Induced Pulmonary Inflammation and Fibrosis. *Am. J. Respir. Cell Mol. Biol.* 40, 410–421. doi:10.1165/rcmb.2007-0364oc
- Salles, G. F., Fiszman, R., Cardoso, C. R., and Muxfeldt, E. S. (2007). Relation of Left Ventricular Hypertrophy with Systemic Inflammation and Endothelial Damage in Resistant Hypertension. *Hypertension* 50, 723–728. doi:10.1161/hypertensionaha.107.093120
- Salmeri, F. M., Laganà, A. S., Sofò, V., Triolo, O., Sturlese, E., Retto, G., et al. (2015). Behavior of Tumor Necrosis Factor- α and Tumor Necrosis Factor Receptor 1/ tumor Necrosis Factor Receptor 2 System in Mononuclear Cells Recovered from Peritoneal Fluid of Women with Endometriosis at Different Stages. *Reprod. Sci.* 22, 165–172. doi:10.1177/1933719114536472
- Sandgren, E. P., Luetke, N. C., Palmiter, R. D., Brinster, R. L., and Lee, D. C. (1990). Overexpression of TGF Alpha in Transgenic Mice: Induction of Epithelial Hyperplasia, Pancreatic Metaplasia, and Carcinoma of the Breast. *Cell* 61, 1121–1135. doi:10.1016/0092-8674(90)90075-p
- Santos-Zas, I., Lemarié, J., Tedgui, A., and Ait-Oufella, H. (2018). Adaptive Immune Responses Contribute to Post-ischemic Cardiac Remodeling. *Front. Cardiovasc. Med.* 5, 198. doi:10.3389/fcvm.2018.00198
- Santos-Zas, I., Lemarié, J., Zlatanova, I., Cachanado, M., Seghezzi, J. C., Benamer, H., et al. (2021). Cytotoxic CD8(+) T Cells Promote Granzyme B-dependent Adverse post-ischemic Cardiac Remodeling. *Nat. Commun.* 12, 1483. doi:10.1038/s41467-021-21737-9
- Satoh, M., Iwasaka, J., Nakamura, M., Akatsu, T., Shimoda, Y., and Hiramori, K. (2004). Increased Expression of Tumor Necrosis Factor-Alpha Converting Enzyme and Tumor Necrosis Factor-Alpha in Peripheral Blood Mononuclear Cells in Patients with Advanced Congestive Heart Failure. *Eur. J. Heart Fail.* 6, 869–875. doi:10.1016/j.ejheart.2004.02.007
- Satoh, M., Nakamura, M., Saitoh, H., Satoh, H., Maesawa, C., Segawa, I., et al. (1999). Tumor Necrosis Factor-Alpha-Converting Enzyme and Tumor Necrosis Factor-Alpha in Human Dilated Cardiomyopathy. *Circulation* 99, 3260–3265. doi:10.1161/01.cir.99.25.3260
- Satoh, M., Nakamura, M., Satoh, H., Saitoh, H., Segawa, I., and Hiramori, K. (2000). Expression of Tumor Necrosis Factor-Alpha-Converting Enzyme and Tumor Necrosis Factor-Alpha in Human Myocarditis. *J. Am. Coll. Cardiol.* 36, 1288–1294. doi:10.1016/s0735-1097(00)00827-5
- Scanzano, A., and Cosentino, M. (2015). Adrenergic Regulation of Innate Immunity: a Review. *Front. Pharmacol.* 6, 171. doi:10.3389/fphar.2015.00171
- Schena, G., and Caplan, M. J. (2019). Everything You Always Wanted to Know about β (3)-AR * (* but Were Afraid to Ask). *Cells* 8, 357. doi:10.3390/cells8040357
- Schlöndorff, J., Becherer, J. D., and Blobel, C. P. (2000). Intracellular Maturation and Localization of the Tumour Necrosis Factor Alpha Convertase (TACE). *Biochem. J.* 347 (Pt 1), 131–138.
- Schwarz, J., Broder, C., Helmstetter, A., Schmidt, S., Yan, I., Müller, M., et al. (2013). Short-term TNF α Shedding Is Independent of Cytoplasmic Phosphorylation or Furin Cleavage of ADAM17. *Biochim. Biophys. Acta* 1833, 3355–3367. doi:10.1016/j.bbamcr.2013.10.005
- Sen, R., and Smale, S. T. (2010). Selectivity of the NF- κ B Response. *Cold Spring Harb Perspect. Biol.* 2, a000257. doi:10.1101/cshperspect.a000257
- Shalaby, L., Thounaojam, M., Tawfik, A., Li, J., Hussein, K., Jahng, W. J., et al. (2020). Role of Endothelial ADAM17 in Early Vascular Changes Associated with Diabetic Retinopathy. *J. Clin. Med.* 9. doi:10.3390/jcm9020400
- Shenoy, S. K., Drake, M. T., Nelson, C. D., Houtz, D. A., Xiao, K., Madabushi, S., et al. (2006). Beta-Arrestin-Dependent, G Protein-independent ERK1/2 Activation by the Beta2 Adrenergic Receptor. *J. Biol. Chem.* 281, 1261–1273. doi:10.1074/jbc.m506576200
- Sousa, A. M., Liu, T., Guevara, O., Stevens, J., Fanburg, B. L., Gaestel, M., et al. (2007). Smooth Muscle Alpha-Actin Expression and Myofibroblast Differentiation by TGFbeta Are Dependent upon MK2. *J. Cell Biochem.* 100, 1581–1592. doi:10.1002/jcb.21154
- Stöcker, W., Grams, F., Baumann, U., Reinemer, P., Gomis-Rüth, F. X., Mckay, D. B., et al. (1995). The Metzincins-Topological and Sequential Relations between the Astacins, Adamalysins, Serralysins, and Matrixins (Collagenases) Define a Superfamily of Zinc-Peptidases. *Protein Sci.* 4, 823–840. doi:10.1002/pro.5560040502
- Su, Y., Wang, Y., Zhou, H., Lei, L., and Xu, L. (2014). MicroRNA-152 Targets ADAM17 to Suppress NSCLC Progression. *FEBS Lett.* 588, 1983–1988. doi:10.1016/j.febslet.2014.04.022
- Sun, Y., Li, Q., Gui, H., Xu, D. P., Yang, Y. L., Su, D. F., et al. (2013). MicroRNA-124 Mediates the Cholinergic Anti-Inflammatory Action through Inhibiting the Production of Pro-inflammatory Cytokines. *Cell Res.* 23, 1270–1283. doi:10.1038/cr.2013.116
- Swanson, K. V., Deng, M., and Ting, J. P. (2019). The NLRP3 Inflammasome: Molecular Activation and Regulation to Therapeutics. *Nat. Rev. Immunol.* 19, 477–489. doi:10.1038/s41577-019-0165-0
- Takawale, A., Zhang, P., Azad, A., Wang, W., Wang, X., Murray, A. G., et al. (2017). Myocardial Overexpression of TIMP3 after Myocardial Infarction Exerts Beneficial Effects by Promoting Angiogenesis and Suppressing Early Proteolysis. *Am. J. Physiol. Heart Circ. Physiol.* 313, H224–h236. doi:10.1152/ajpheart.00108.2017
- Tanai, E., and Frantz, S. (2015). Pathophysiology of Heart Failure. *Compr. Physiol.* 6, 187–214. doi:10.1002/cphy.c140055
- Tchivileva, I. E., Tan, K. S., Gambarian, M., Nackley, A. G., Medvedev, A. V., Romanov, S., et al. (2009). Signaling Pathways Mediating Beta3-Adrenergic Receptor-Induced Production of Interleukin-6 in Adipocytes. *Mol. Immunol.* 46, 2256–2266. doi:10.1016/j.molimm.2009.04.008
- Tellier, E., Canault, M., Rebsomen, L., Bonardo, B., Juhan-Vague, I., Nalbone, G., et al. (2006). The Shedding Activity of ADAM17 is Sequestered in Lipid Rafts. *Exp. Cell Res* 312, 3969–3980. doi:10.1016/j.yexcr.2006.08.027
- Torre-Amione, G., Kapadia, S., Benedict, C., Oral, H., Young, J. B., and Mann, D. L. (1996). Proinflammatory Cytokine Levels in Patients with Depressed Left Ventricular Ejection Fraction: a Report from the Studies of Left Ventricular Dysfunction (SOLVD). *J. Am. Coll. Cardiol.* 27, 1201–1206. doi:10.1016/0735-1097(95)00589-7

- Travers, J. G., Kamal, F. A., Robbins, J., Yutzey, K. E., and Blaxall, B. C. (2016). Cardiac Fibrosis: The Fibroblast Awakens. *Circ. Res.* 118, 1021–1040. doi:10.1161/circresaha.115.306565
- Umemura, M., Isozaki, T., Ishii, S., Seki, S., Oguro, N., Miura, Y., et al. (2014). Reduction of Serum ADAM17 Level Accompanied with Decreased Cytokines after Abatacept Therapy in Patients with Rheumatoid Arthritis. *Int. J. Biomed. Sci.* 10, 229–235.
- Van Linthout, S., and Tschöpe, C. (2017). Inflammation - Cause or Consequence of Heart Failure or Both? *Curr. Heart Fail. Rep.* 14, 251–265. doi:10.1007/s11897-017-0337-9
- Wagner, M. A., and Siddiqui, M. A. (2012). The JAK-STAT Pathway in Hypertrophic Stress Signaling and Genomic Stress Response. *JAKSTAT* 1, 131–141. doi:10.4161/jkst.20702
- Wang, X., Shaw, S., Amiri, F., Eaton, D. C., and Marrero, M. B. (2002). Inhibition of the Jak/STAT Signaling Pathway Prevents the High Glucose-Induced Increase in Tgf-Beta and Fibronectin Synthesis in Mesangial Cells. *Diabetes* 51, 3505–3509. doi:10.2337/diabetes.51.12.3505
- Wichert, R., Scharfenberg, F., Colmorgen, C., Koudelka, T., Schwarz, J., Wetzel, S., et al. (2019). Meprin β Induces Activities of A Disintegrin and Metalloproteinases 9, 10, and 17 by Specific Prodomain Cleavage. *FASEB J.* 33, 11925–11940. doi:10.1096/fj.201801371r
- Willems, S. H., Tape, C. J., Stanley, P. L., Taylor, N. A., Mills, I. G., Neal, D. E., et al. (2010). Thiol Isomerases Negatively Regulate the Cellular Shedding Activity of ADAM17. *Biochem. J.* 428, 439–450. doi:10.1042/bj20100179
- Wolf, J., Rose-John, S., and Garbers, C. (2014). Interleukin-6 and its Receptors: A Highly Regulated and Dynamic System. *Cytokine* 70, 11–20. doi:10.1016/j.cyto.2014.05.024
- Won, E., and Kim, Y. K. (2016). Stress, the Autonomic Nervous System, and the Immune-Kynurenine Pathway in the Etiology of Depression. *Curr. Neuropharmacol.* 14, 665–673. doi:10.2174/1570159x14666151208113006
- Wright, H. L., Cross, A. L., Edwards, S. W., and Moots, R. J. (2014). Effects of IL-6 and IL-6 Blockade on Neutrophil Function *In Vitro* and *In Vivo*. *Rheumatology* 53, 1321–1331. doi:10.1093/rheumatology/keu035
- Wynn, T. A. (2008). Cellular and Molecular Mechanisms of Fibrosis. *J. Pathol.* 214, 199–210. doi:10.1002/path.2277
- Xiao, L. J., Lin, P., Lin, F., Liu, X., Qin, W., Zou, H. F., et al. (2012). ADAM17 Targets MMP-2 and MMP-9 via EGFR-MEK-ERK Pathway Activation to Promote Prostate Cancer Cell Invasion. *Int. J. Oncol.* 40, 1714–1724. doi:10.3892/ijo.2011.1320
- Xing, Y., Yao, X., Li, H., Xue, G., Guo, Q., Yang, G., et al. (2017). Cutting Edge: TRAF6 Mediates TLR/IL-1R Signaling-Induced Nontranscriptional Priming of the NLRP3 Inflammasome. *J. Immunol.* 199, 1561–1566. doi:10.4049/jimmunol.1700175
- Xu, J., Sriramula, S., Xia, H., Moreno-Walton, L., Culicchia, F., Domenig, O., et al. (2017). Clinical Relevance and Role of Neuronal AT(1) Receptors in ADAM17-Mediated ACE2 Shedding in Neurogenic Hypertension. *Circ. Res.* 121, 43–55. doi:10.1161/circresaha.116.310509
- Xu, P., Liu, J., Sakaki-Yumoto, M., and Derynck, R. (2012). TACE Activation by MAPK-Mediated Regulation of Cell Surface Dimerization and TIMP3 Association. *Sci. Signal.* 5, ra34. doi:10.1126/scisignal.2002689
- Yajima, T., Yasukawa, H., Jeon, E. S., Xiong, D., Dorner, A., Iwatate, M., et al. (2006). Innate Defense Mechanism against Virus Infection within the Cardiac Myocyte Requiring Gp130-STAT3 Signaling. *Circulation* 114, 2364–2373. doi:10.1161/circulationaha.106.642454
- Yang, H., Li, T., Wei, J., Zhang, H., and He, S. (2013). Induction of Tumor Necrosis Factor (TNF) Release from Subtypes of T Cells by Agonists of Proteinase Activated Receptors. *Mediators Inflamm.* 2013, 165453. doi:10.1155/2013/165453
- Zhang, P., Shen, M., Fernandez-Patron, C., and Kassiri, Z. (2016). ADAMs Family and Relatives in Cardiovascular Physiology and Pathology. *J. Mol. Cell Cardiol.* 93, 186–199. doi:10.1016/j.yjmcc.2015.10.031
- Zhao, L., Cheng, G., Jin, R., Afzal, M. R., Samanta, A., Xuan, Y. T., et al. (2016). Deletion of Interleukin-6 Attenuates Pressure Overload-Induced Left Ventricular Hypertrophy and Dysfunction. *Circ. Res.* 118, 1918–1929. doi:10.1161/circresaha.116.308688
- Zhu, J., and Steinberg, S. F. (2021). $\beta(1)$ -Adrenergic Receptor N-Terminal Cleavage by ADAM17; the Mechanism for Redox-Dependent Downregulation of Cardiomyocyte $\beta(1)$ -Adrenergic Receptors. *J. Mol. Cell Cardiol.* 154, 70–79. doi:10.1016/j.yjmcc.2021.01.012

Conflict of Interest: The authors declare that the research was conducted in the absence of any commercial or financial relationships that could be construed as a potential conflict of interest.

Publisher's Note: All claims expressed in this article are solely those of the authors and do not necessarily represent those of their affiliated organizations, or those of the publisher, the editors and the reviewers. Any product that may be evaluated in this article, or claim that may be made by its manufacturer, is not guaranteed or endorsed by the publisher.

Copyright © 2021 Adu-Amankwaah, Adzika, Adekunle, Ndzie Noah, Mprah, Bushi, Akhter, Huang, Xu, Adzraku, Nadeem and Sun. This is an open-access article distributed under the terms of the Creative Commons Attribution License (CC BY). The use, distribution or reproduction in other forums is permitted, provided the original author(s) and the copyright owner(s) are credited and that the original publication in this journal is cited, in accordance with accepted academic practice. No use, distribution or reproduction is permitted which does not comply with these terms.



circHIPK3 Exacerbates Folic Acid-Induced Renal Tubulointerstitial Fibrosis by Sponging miR-30a

Yan Wu¹, Junjun Luan¹, Congcong Jiao¹, Shiwen Zhang², Cong Ma¹, Yixiao Zhang³, Jingqi Fu⁴, En Yin Lai⁵, Jeffrey B. Kopp⁶, Jingbo Pi^{4*} and Hua Zhou^{1*}

¹ Department of Nephrology, Shengjing Hospital of China Medical University, Shenyang, China, ² Department of Critical Care Medicine, Fushun Central Hospital, Fushun, China, ³ Department of Urology, Shengjing Hospital of China Medical University, Shenyang, China, ⁴ Program of Environmental Toxicology, School of Public Health, China Medical University, Shenyang, China, ⁵ Department of Physiology, School of Basic Medical Sciences, Zhejiang University School of Medicine, Hangzhou, China, ⁶ Kidney Disease Section, NIDDK, NIH, Bethesda, MD, United States

OPEN ACCESS

Edited by:

Gonzalo del Monte-Nieto,
Monash University, Australia

Reviewed by:

Isha Sharma,
Northwestern University,
United States
Bi-Cheng Liu,
Southeast University, China

*Correspondence:

Hua Zhou
huazhou_cmu@163.com
Jingbo Pi
jbpi@cmu.edu.cn

Specialty section:

This article was submitted to
Renal and Epithelial Physiology,
a section of the journal
Frontiers in Physiology

Received: 27 May 2021

Accepted: 24 November 2021

Published: 04 January 2022

Citation:

Wu Y, Luan J, Jiao C, Zhang S,
Ma C, Zhang Y, Fu J, Lai EY, Kopp JB,
Pi J and Zhou H (2022) circHIPK3
Exacerbates Folic Acid-Induced Renal
Tubulointerstitial Fibrosis by Sponging
miR-30a. *Front. Physiol.* 12:715567.
doi: 10.3389/fphys.2021.715567

Renal tubulointerstitial fibrosis is a common pathological feature of progressive chronic kidney disease (CKD), and current treatment has limited efficacy. The circular RNA circHIPK3 is reported to participate in the pathogenesis of various human diseases. However, the role of circHIPK3 in renal fibrosis has not been examined. In this study, we aimed to determine whether and how circHIPK3 might participate in the pathogenesis of renal fibrosis. Mice received a peritoneal injection of folic acid (250 mg/kg). Of note, 30 days later, renal fibrosis was present on periodic acid–Schiff (PAS) and Masson staining, and mRNA and protein of profibrotic genes encoding fibronectin (FN) and collagen 1 (COL1) were increased. Renal circHIPK3 was upregulated, while miR-30a was downregulated, assessed by quantitative PCR (qPCR) and fluorescence *in situ* hybridization (FISH). The expression of transforming growth factor beta-1 (TGF- β 1) was increased by qPCR analysis, immunoblotting, and immunofluorescence. Renal circHIPK3 negatively correlated with miR-30a, and kidney miR-30a negatively correlated with TGF- β 1. Target Scan and miRanda algorithms predicted three perfect binding sites between circHIPK3 and miR-30a. We found that circHIPK3, miR-30a, and TGF- β 1 colocalized in the cytoplasm of human tubular epithelial cells (HK-2 cells) on FISH and immunofluorescence staining. We transfected circHIPK3 and a scrambled RNA into HK-2 cells; miR-30a was downregulated, and the profibrotic genes such as TGF- β 1, FN, and COL1 were upregulated and assessed by qPCR, immunoblotting, and immunofluorescence staining. Third, the upregulation of circHIPK3, downregulation of miR-30a, and overproduction of profibrotic FN and COL1 were also observed in HK-2 cells exposed to TGF- β 1. Finally, renal biopsies from patients with chronic tubulointerstitial nephritis manifested similar expression patterns of circHIPK3, miR-30a, and profibrotic proteins, such as TGF- β 1, FN, and COL1 as observed in the experimental model. A feed-forward cycle was observed among circHIPK3, miR-30a, and TGF- β 1. Our results suggest that circHIPK3 may contribute to progressive renal fibrosis by sponging miR-30a. circHIPK3 may be a novel therapeutic target for slowing CKD progression.

Keywords: renal fibrosis, circHIPK3, miR-30a, TGF- β 1, renal biopsy

INTRODUCTION

Renal tubulointerstitial fibrosis is a common pathologic feature of all chronic kidney diseases (CKDs), which affects 8–16% of the population worldwide and is a leading cause of death (Chen T. et al., 2019). At present, there are few effective therapies to prevent or retard the progression of tubulointerstitial fibrosis. Reducing the prevalence of CKD requires an in-depth understanding of the pathogenesis of tubulointerstitial fibrosis and the discovery of novel therapeutic agents targeting key mediators of tubulointerstitial fibrosis.

Circular RNA (circRNA) is a class of non-coding RNA molecules, produced with 3' to 5' back splicing, in which an upstream 3' splicing site is joined with a downstream 5' splicing site (Li et al., 2015). circRNAs participate in the pathogenesis of various human diseases by sponging microRNAs (miRNAs), consequently regulating gene expression at the transcriptional level (Dong et al., 2017; Li et al., 2017; Tan et al., 2017; Zhao et al., 2017). However, a possible interaction between circRNA and miRNA in renal tubulointerstitial fibrosis has not been explored.

Recently, circHIPK3 has been identified in several human and animal tissues (Zheng et al., 2016). circHIPK3 regulates cell growth, and migration by sponging multiple miRNAs, such as miR-124, miR-7, miR-30a, miR-193a, miR-338-3p, miR-107, miR-124, and miR-524 in cancers and non-kidney diseases (Shan et al., 2017; Chen et al., 2018; Liu et al., 2018; Zeng et al., 2018; Hong et al., 2020; Liu Z. et al., 2020; Shu et al., 2020; Yin and Cui, 2020). circHIPK3 promotes metastasis in gastric cancer *via* miR-653-5p/miR-338-3p (Jin et al., 2020) and by sponging miR-508-3p in clear cell renal cell carcinoma (Han et al., 2020).

The circHIPK3 is also involved in fibrosis in non-neoplastic tissues. circHIPK3 regulates cardiac fibroblast proliferation, migration, and phenotypic switching *via* the miR-152-3p/TGF- β 2 axis under hypoxic conditions (Liu W. et al., 2020). The inhibition of circHIPK3 prevents angiotensin II-induced cardiac fibrosis by sponging miR-29b-3p (Ni et al., 2019). circHIPK3 regulates lung fibroblast-to-myofibroblast transition by competing with miR-338 (Zhang et al., 2019). Recently, circHIPK3 has been reported to exacerbate diabetic nephropathy and promote proliferation through sponging miR-185 (Liu et al., 2021). However, the role of circHIPK3 in the progression of renal tubulointerstitial fibrosis remains to be fully characterized.

This study aimed to determine whether circHIPK3 contributes to renal tubulointerstitial fibrosis and to identify the underlying mechanisms. In an experimental mouse model and in human tissues, we found that renal circHIPK3 was upregulated, while miR-30a was downregulated. Consequently, transforming growth factor beta-1 (TGF- β 1) was overproduced. In a feed-forward loop, TGF- β 1 induced an increase in circHIPK3.

MATERIALS AND METHODS

Mouse Folic Acid-Induced Renal Tubulointerstitial Fibrosis Model

Male C57BL/6 mice (age = 16 weeks old, weight = 25–30 g, $n = 12$) were purchased from the Beijing Vital River Laboratory

Animal Technology (Beijing, China). Mice were housed under standard conditions. The mice were randomly divided into two groups, namely, normal control (NC) group and FA group. FA was injected into the abdominal cavity of mice with a dosage of 250 mg/kg. Equal volumes of 0.3 mmol/L NaHCO₃ were injected into the NC group. Of note, 30 days later, mice were weighed and euthanized with carbon dioxide. Kidneys were collected and placed at 80°C for further analysis. Animal studies were approved in advance by the Animal Care and Use Committee of China Medical University (15052111) and were performed following the NIH Animal Care and Use Guidelines.

HK-2 Cell Culture and Transfection of circHIPK3 or Stimulation of Transforming Growth Factor Beta-1

Immortalized human renal proximal tubular epithelial cells (HK-2 cells) were purchased from ATCC (Manassas, VA, United States) and cultured in DMEM/F12 medium supplemented with 10% FBS at a culture density of 2×10^5 cells in a six-well plate (Costar, Corning, NY, United States) at 37°C and 5% CO₂. Cultured HK-2 cells were transfected with the circular sequence of circHIPK3 [pCDH-CMV-5' circular Frame (1)-has_circHIPK3-3' circular Frame(1)-EF1-copGFP-T2A-puro]/scrambled sequence [pCDH-CMV-5' circular Frame (1)-MCS-3' circular Frame(1)-EF1-copGFP-T2A-puro] as negative control (SynGenTech, Beijing, China) using Lipofectamine 3000 (Invitrogen, CA, United States) for 48 h according to the instructions of the manufacturer. Cultured HK-2 cells were stimulated with hTGF- β (250 pg/ml) for 48 h. Cells were collected for RNA and protein extraction after the transfection of circHIPK3 or the stimulation of TGF- β 1 for the analysis by quantitative PCR (qPCR) and Western blotting.

Patients With Chronic Tubulointerstitial Nephritis

Patients with chronic tubulointerstitial nephritis on biopsy were from the Department of Nephrology at Shengjing Hospital of China Medical University between January 2019 and March 2020. Diagnoses were made by a nephropathologist following established criteria. Normal human kidney tissues were obtained at the time of renal cancer surgery. These tissues are located at least 5 cm away from the tumors as we previously described (Luan et al., 2018). All subjects provided written consent, and the research protocol was approved in advance by the Institutional Review Board of the China Medical University.

Kidney Histology

Tissue sections (3 μ m) were cut from paraffin-embedded human or mouse kidney blocks, deparaffinized, and rehydrated. Tissues were stained with periodic acid–Schiff (PAS) and Masson stains. The tubular injury was scored on PAS staining described previously, and the renal tubulointerstitial fibrosis area was presented as the percentage of the whole kidney cross-section on Masson staining using ImageJ software (NIH, Bethesda, MD, United States) on 15 randomly selected fields

(200× magnification) as previously described (Liu et al., 2009; Luan et al., 2020).

Quantitative PCR

Total RNA was extracted from frozen kidney tissue and HK-2 cells using TRIzol reagent (Life Technologies, Carlsbad, CA, United States), and the RNA concentration was determined using a NanoDrop 2000 spectrophotometer (ThermoFisher, Waltham, MA, United States). Total RNA (250 ng per sample) was subjected to reverse transcription using Prime Script RT Reagent Kit for circHIPK3, fibronectin (FN), collagen 1 (COL1), and TGF- β 1 and to reverse transcription using TransScript miRNA First-Strand cDNA Synthesis SuperMix (TransGen Biotech, Beijing, China) for miR-30a and followed by PCR with SYBR Premix Ex Taq (Takara, Dalian, China). Real-time fluorescence was detected with QuantStudio 6 Flex quantitative PCR system (Applied Biosystems, Carlsbad, CA, United States). The relative expression level of each gene was expressed as $2^{-\Delta\Delta Ct}$ of each measurement. Glyceraldehyde-3-phosphate dehydrogenase (GAPDH), b-actin, or α -tubulin was used as an endogenous control for mRNAs and circHIPK3. Sno202 or U6 was used as an endogenous control for miR-30a. Primers were designed using Primer Express (Applied Biosystems, Carlsbad, CA, United States) and synthesized by Life Technologies (Shanghai, China) (Table 2).

Immunoblotting

Kidney samples and HK-2 cells were sonicated and resuspended in radioimmunoprecipitation assay buffer with protease inhibitors. Protein concentration was measured using a bicinchoninic acid assay kit. Equal amounts of protein were separated by SDS-PAGE and transferred into polyvinylidene difluoride (PVDF) membranes (Millipore Immobilon-P, Darmstadt, Germany). After blocking with 5% skimmed milk, membranes were incubated with primary antibodies against FN, COL1, and TGF- β 1 at 4°C overnight. Following repeated washing, the membranes were incubated with horseradish peroxidase-conjugated secondary antibody for 1 h at room temperature. The antibody-antigen reactions were determined using a high-sig ECL Western blotting substrate and visualized by the Tanon 5500 imaging system. Protein loading variation was normalized by α -tubulin, β -actin, or GAPDH. For quantitative analysis, blot density was analyzed with NIH ImageJ software. The protein level is expressed as the ratio of blot density from individual protein to its housekeeping antibody. Antibody information is presented in Supplementary Table 1.

Immunofluorescence Staining

Paraffin-embedded human and mouse kidney tissues were cut at 2- μ m thickness, deparaffinized, and rehydrated. Antigens were retrieved, and non-specific binding was blocked. Kidney sections were incubated with antibodies directed against FN, COL1, and TGF- β 1. Slides with HK-2 cells were incubated with these three antibodies at 4°C overnight, followed by incubation with Alexa-594/Alexa-488 donkey anti-rabbit/anti-mouse IgG (Supplementary Table 1) at room temperature for 1 h in the dark. After three washes with phosphate-buffered saline (PBS), slides were mounted with diamidino-phenyl indole (DAPI) for 10 min.

Images were captured by immunofluorescence microscopy (Nikon, Tokyo, Japan). Specific staining for each target protein was quantified as integrated optical density expressed per unit area by Image-Pro Plus 6.0 (Media Cybernetics, MD, United States), as described previously (Luan et al., 2020; Qi et al., 2020).

Fluorescence *in situ* Hybridization

Fluorescence *in situ* hybridization (FISH) was performed on kidney tissue and HK-2 cells following the protocol of the manufacturer. Paraffin-embedded human kidney tissue sections were cut at 4- μ m thickness. Sections were deparaffinized, rehydrated, and digested with trypsin at 37°C for 30 min. Slides with kidney sections or cultured HK-2 cells were hybridized with a digoxigenin-horseradish peroxidase (DIG-HRP)-labeled oligonucleotide probe complementary to circHIPK3 or miR-30a at 37°C overnight, followed by incubation with anti-DIG-HRP (Servicebio, Wuhan, China) for 50 min, fluorescein isothiocyanate-tyramide signal amplification for 5 min, and DAPI to stain DNA for 5 min. Images were captured by immunofluorescence microscopy (Nikon, Tokyo, Japan) as described previously (Luan et al., 2020).

Statistical Analyses

GraphPad Prism 8.0 software (GraphPad, San Diego, CA, United States) was used to perform statistical analyses. The quantitative data were expressed as mean \pm SD. Differences between the two groups were analyzed by the *t*-test. Correlations between two variables were analyzed by Pearson's linear correlation analysis. *p*-Value < 0.05 was accepted as statistically significant.

RESULTS

Folic Acid-Induced Renal Tubulointerstitial Fibrosis in Mice

Mice with 250 mg/kg of FA administration developed renal tubulointerstitial fibrosis on day 30 after the injection. Collagen hyperplasia and inflammatory cell infiltration were shown in the tubulointerstitial area on PAS and Masson staining in FA mice. The tubular injury score and the area of renal fibrosis were elevated in the FA group compared to the NC group (Figure 1A). In the FA group, the mRNA levels of FN and COL1 were increased on qPCR (Figures 1B,C). The protein expression of FN and COL1 was increased by both Western blotting analysis (Figure 1D) and immunofluorescence staining (Figure 1E).

Expression of Renal circHIPK3/miR-30a/Transforming Growth Factor Beta-1 in Folic Acid-Induced Renal Tubulointerstitial Fibrosis in Mice

Since circHIPK3 has been reported to participate in the fibrosis of the heart and lung in animal models, we investigated the expression of circHIPK3/miR-30a/TGF- β 1 in mouse kidney tissue. We found that circHIPK3 was upregulated, while

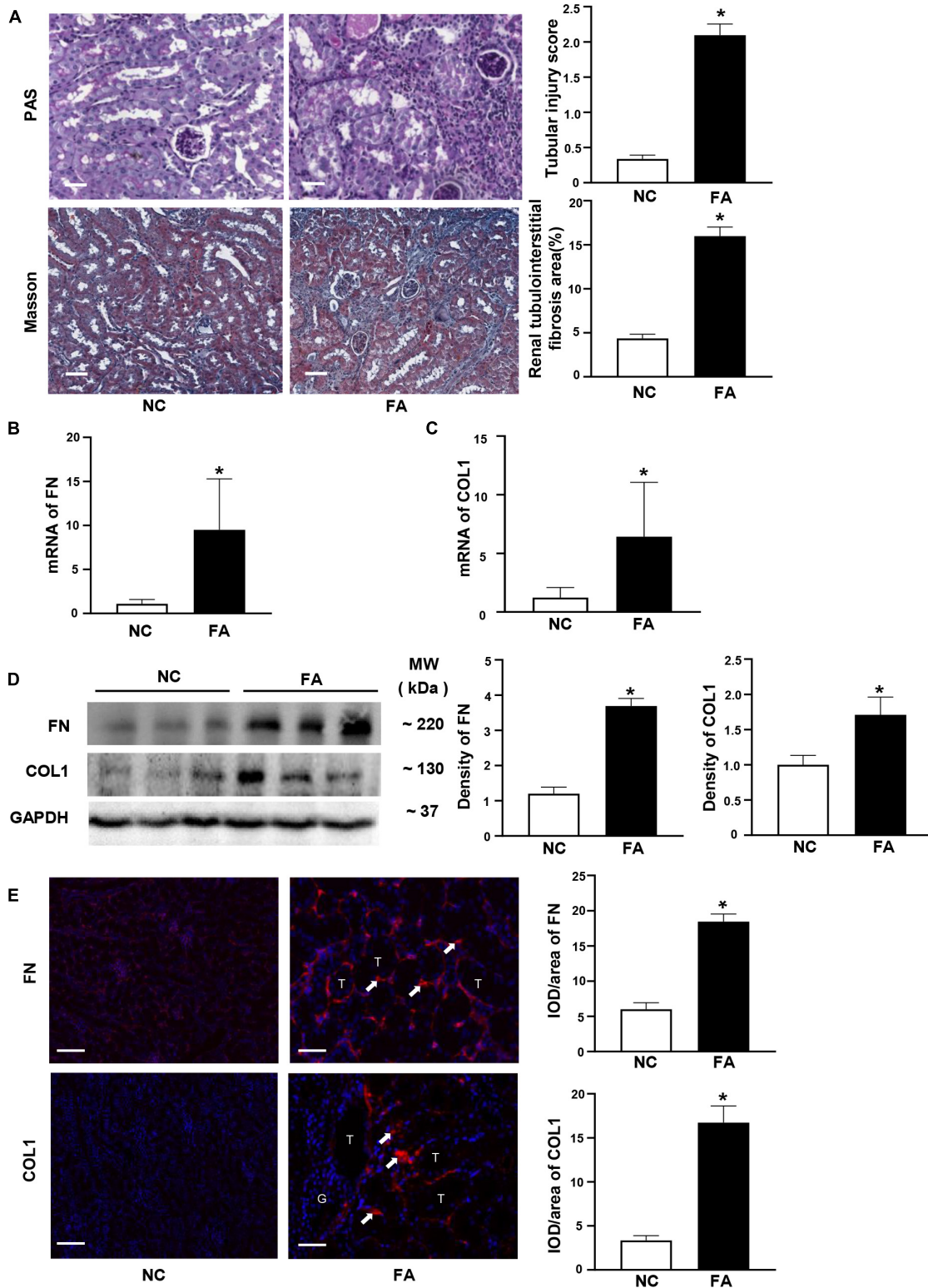
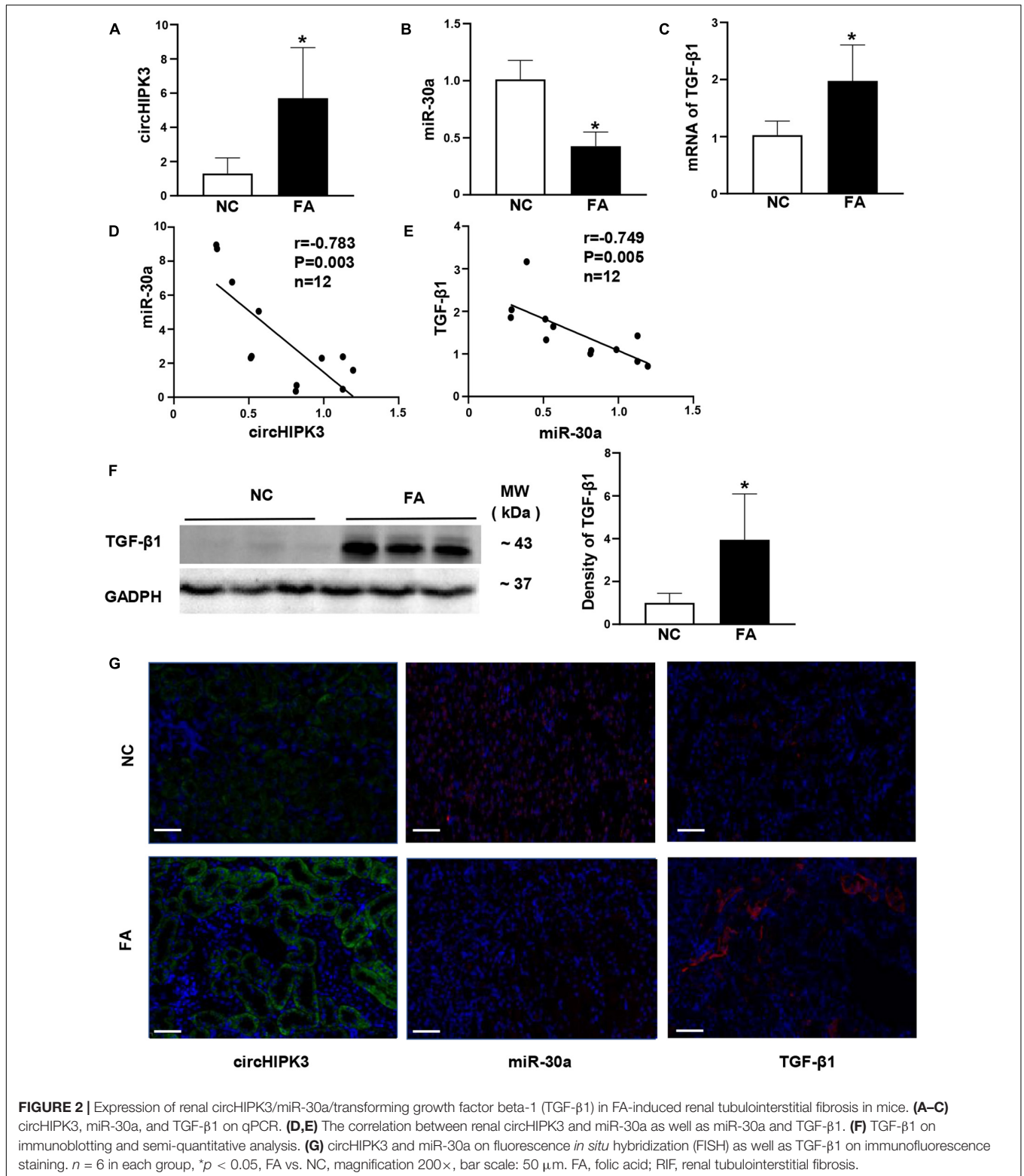


FIGURE 1 | Typical renal fibrosis and the expression of fibronectin (FN)/collagen 1 (COL1) in folic acid (FA)-induced renal tubulointerstitial fibrosis in mice. **(A)** Periodic acid-Schiff (PAS) and Masson staining and semi-quantitative analysis. **(B,C)** mRNA levels of FN and COL1 on quantitative PCR (qPCR). **(D)** Proteins levels of FN and COL1 on immunoblotting and semi-quantitative analysis. **(E)** Expression of FN and COL1 (arrow) on immunofluorescent staining and semi-quantitative analysis. $n = 6$ in each group, * $p < 0.05$, FA vs. NC, magnification 200 \times , bar scale: 50 μ m. FA, folic acid; RIF, renal tubulointerstitial fibrosis.



miR-30a expression was decreased, and TGF- β 1 was increased (Figures 2A–C) in FA-induced renal tubulointerstitial fibrosis in mice compared to control mice. Importantly, circHIPK3 was negatively correlated with miR-30a, and miR-30a was

also negatively correlated with TGF- β 1 mRNA by the qPCR analysis (Figures 2D,E). TGF- β 1 protein production was also increased in FA-induced renal tubulointerstitial fibrosis mice by immunoblotting (Figure 2F).

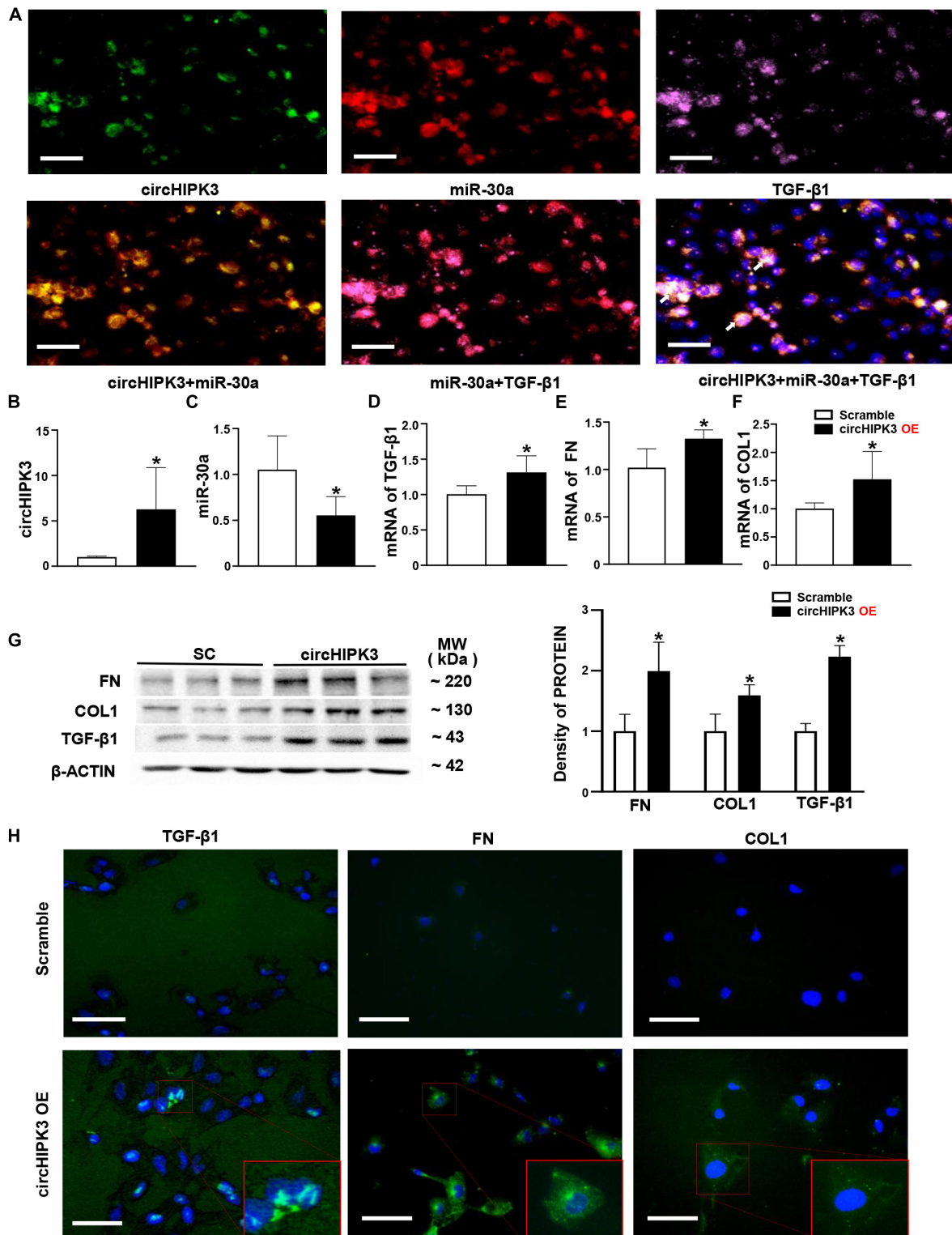
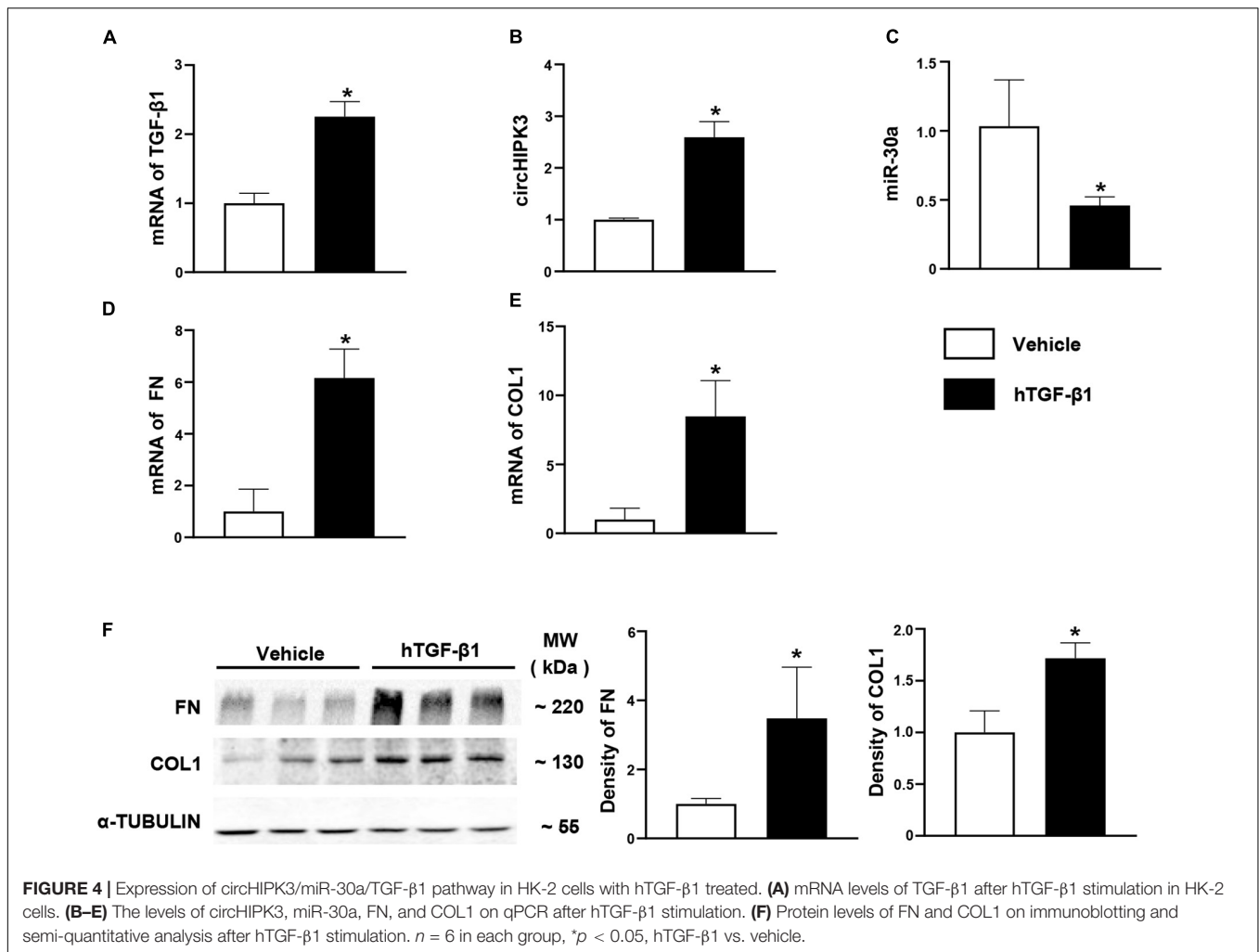


FIGURE 3 | Overexpression of circHIPK3 in HK-2 cells. **(A)** The colocalization in the cytoplasm of circHIPK3, miR-30a, and TGF-β1 is shown. **(B)** The levels of circHIPK3 on qPCR after circHIPK3 overexpression. **(C–F)** The levels of miR-30a, TGF-β1, fibronectin (FN), and collagen 1 (COL1) using qPCR after overexpression of circHIPK3. **(G)** Protein levels of FN, COL1, and TGF-β1 on immunoblotting and semi-quantitative analysis after the overexpression of circHIPK3. **(H)** The expression of TGF-β1, FN, and COL1 assessed by immunofluorescence with circHIPK3 overexpression. Magnification 400×, bar scale: 100 μm. *n* = 6 in each group, **p* < 0.05, circHIPK3 vs. scrambled RNA.



We used additional methods to evaluate the renal expression of circHIPK3/miR-30a/TGF-β1 in kidney tissue. FISH staining demonstrated that circHIPK3 and miR-30a are mainly located in tubules. Positive TGF-β1 staining located in tubules and tubulointerstitial area on immunostaining. The direction of renal circHIPK3/miR-30a/TGF-β1 was the same as qPCR or Western blotting in FA-treated mice compared to control mice (Figure 2G).

Overexpression of circHIPK3 in HK-2 Cells

Based on the location of circHIPK3/miR-30a in FA-treated mice, we further utilized renal tubular cell line HK-2 cells to explore the roles of circHIPK3 in mice manifesting renal tubulointerstitial fibrosis. First, we found that circHIPK3, miR-30a, and TGF-β1 were mainly colocalized in the cytoplasm of normal HK-2 cells by triple staining, involving two FISH studies and one immunostaining (Figure 3A).

Then, we transfected the plasmid of circHIPK3 to upregulate circHIPK3 in HK-2 cells for 48 h. We found that the circHIPK3 level was nearly fivefold higher than that in the scrambled group

(Figure 3B). Consequently, miR-30a was downregulated, and mRNA of TGF-β1 was upregulated on the qPCR analysis in HK-2 cells with the transfection of circHIPK3 compared to scrambled RNA sequence (Figures 3C,D). The expression changes of circHIPK3/miR-30a/TGF-β1 were similar to the changes of these genes in mouse kidney tissue. In addition, we examined two more profibrotic genes such as FN and COL1. We found that mRNAs of FN and COL1 were also upregulated in HK-2 cells with the overexpression of circHIPK3 (Figures 3E,F), similar to the TGF-β1 RNA expression change on qPCR. The protein levels of TGF-β1, FN, and COL1 were regulated similar to the RNA levels, which was confirmed by both Western blotting (Figure 3G) and immunofluorescence staining (Figure 3H) in HK-2 cells with the transfection of circHIPK3 compared to the scrambled RNA.

Expression of circHIPK3/miR-30a/Profibrotic Genes in HK-2 Cells With Transforming Growth Factor Beta-1 Stimulation

The TGF-β1 is an important regulator of renal fibrosis and has been used to induce the overproduction of profibrotic proteins

in human primary renal tubular epithelial cells *in vitro* studies from our group (Zhou H. et al., 2013) and others. In this study, we investigated the changes of circHIPK3/miR-30a/profibrotic genes such as FN and COL1 in HK-2 cells 48 h after exposure to human TGF- β 1. In HK-2 cells, circHIPK3 level was increased 2.5-fold, and miR-30a expression was decreased by >50% with TGF- β 1 stimulation compared to vehicle stimulant (Figures 4A–C). FN mRNA was also increased nearly sixfold, and COL1 mRNA was elevated by eightfold (Figures 4D,E). Consistent with mRNA expression changes of FN and COL1, protein expression was also increased in HK-2 cells following human TGF- β 1 exposure compared to the vehicle, on the Western blot analysis (Figure 4F).

Renal circHIPK3/miR-30a/Profibrotic Proteins in Human Subjects

Finally, circHIPK3/miR-30a/profibrotic proteins were examined in kidney tissue from human subjects with chronic tubulointerstitial nephritis (cTIN) as relevant renal tubulointerstitial fibrosis tissue and normal tissue adjacent to kidney tumor as NC. The clinical characteristics of human subjects enrolled in the study are displayed in Table 1. Typical tubulointerstitial fibrosis was observed on Masson staining

TABLE 1 | Clinical characteristics of human subjects.

| No. | Age | Gender | eGFR (ml/min/1.73 m ²) |
|-----|-----|--------|------------------------------------|
| 1 | 50 | F | 139 |
| 2 | 58 | M | 127 |
| 3 | 70 | M | 94 |
| 4 | 67 | F | 46 |
| 5 | 46 | M | 66 |
| 6 | 37 | M | 50 |

eGFR, estimated glomerular filtration rate based on the CKD-EPI formula. Cases 1–3, normal control kidney tissue from patients with a kidney tumor. Cases 4–6, renal biopsies from patients with chronic tubulointerstitial nephritis.

TABLE 2 | Sequences of primers used in real-time quantitative PCR (qPCR).

| Gene | Forward (5'-3') | Reverse (5'-3') |
|----------------------|---------------------------|-------------------------|
| FN (has) | CGGTGGCTGTCAAGTCAAAG | AAACCTCGGCTTCTCCATAA |
| FN (mus) | ATGTGGACCCCTCCTGATAGT | GCCAGTGATTTGAGCAAAGG |
| COL1 (has) | GAGGGCCAAAGACGAAGACATC | CAGATCACGTCATCGCACAAAC |
| COL1 (mus) | GACATGTTCAAGCTTTGTGGACCTC | GGGACCCCTTAGGCCATTGTGTA |
| TGF- β 1 (has) | CAATTCCTGGCGATACCTCAG | GCACAACCTCCGGTGACATCAA |
| TGF- β 1 (mus) | CCCGAAGCGGACTACTATGC | CATAGATGGCGTTGTTGCGG |
| circHIPK3 (has) | CCAGTGACAGTTGTGACAGCTACC | GCCAAACGTGCCTCGACCAAG |
| circHIPK3 (mus) | GGATCGGCCAGTCATGTATC | ACCGCTTGGCTATACTTTGA |
| GAPDH (has) | GGAGCGAGATCCCTCCAAAAT | GGCTGTTGTCATACTTCTCATGG |
| Actin (mus) | TTCTTCTTGGGTATGGAAT | GAGCAATGATCTTGATCTTC |
| miR-30a (has/mus) | TGTAACATCCTCGACTGGAAAG | |
| U6 (has) | GCTTCGGCAGCACATATACTAAAAT | |
| Sno202 (mus) | GCTGTACTGACTTGATGAAAGTACT | |

FN, fibronectin; COL1, collagen 1; TGF- β 1, transforming growth factor beta-1; GAPDH, glyceraldehyde-3-phosphate dehydrogenase.

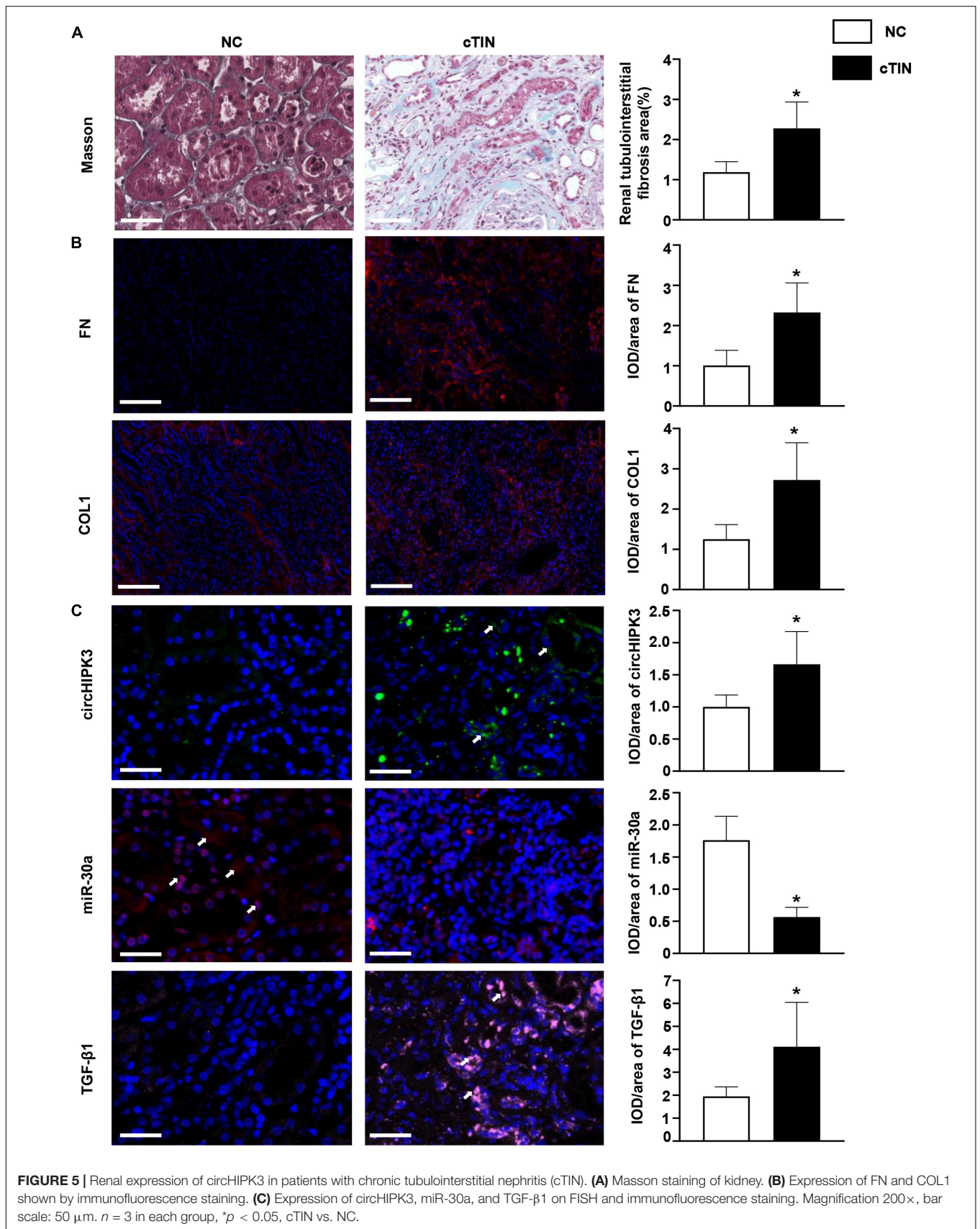
in renal biopsies from cTIN patients compared to normal human kidney tissues (Figure 5A). Fibrotic proteins FN and COL1 were increased in cTIN patients compared to NC on immunofluorescence staining (Figure 5B). The expression of circHIPK3 was upregulated, and miR-30a was downregulated, and excess TGF- β 1 protein was present in renal biopsies from cTIN patients compared to NC kidney tissue on FISH or immunofluorescence staining (Figure 5C). It was consistent with the expression of circHIPK3/miR-30a/TGF- β 1 in FA-induced renal tubulointerstitial fibrosis mice and HK-2 cells with circHIPK3 transfection.

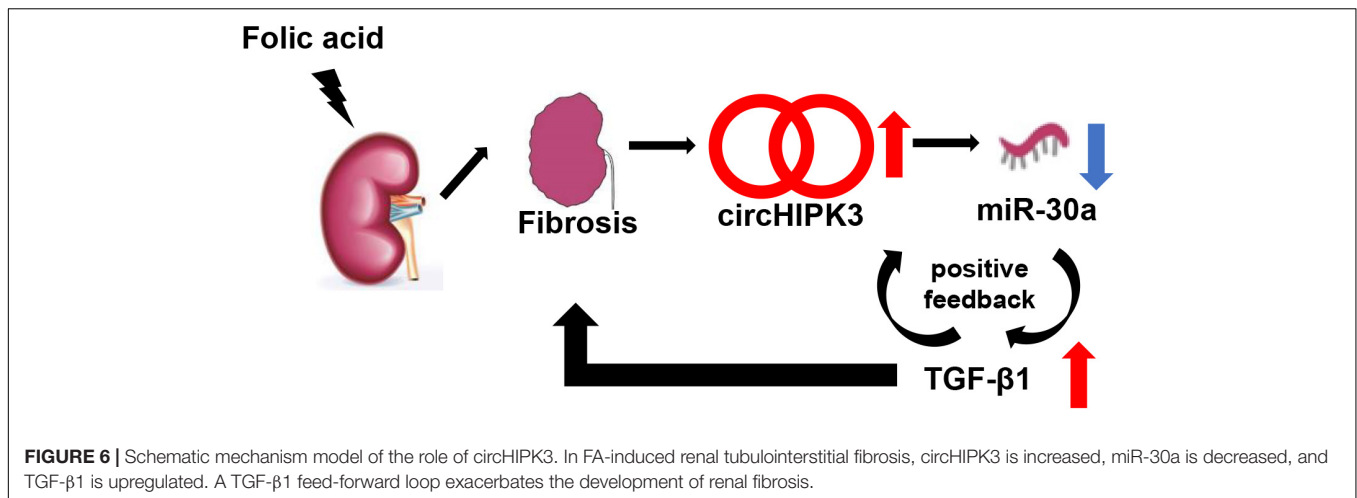
DISCUSSION

The major findings of this study are as follows. First, renal circHIPK3 was upregulated, miR-30a was downregulated, and there was increased RNA expression of profibrotic genes, such as those encoding TGF- β 1, FN, and COL1, in mice with FA-induced renal tubulointerstitial fibrosis and in renal biopsies from patients with cTIN. Second, the transfection of circHIPK3 to HK-2 resulted in the downregulation of miR-30a and the upregulation of TGF- β 1, FN, and COL1. Third, circHIPK3, miR-30a, and TGF- β 1 showed colocalization in normal HK-2 cells. Fourth, a feed-forward cycle was found among circHIPK3, miR-30a, and TGF- β 1.

It has been established that circRNAs contribute to the initiation and progression of CKD. We have reported that circHLA-C plays an important role in lupus nephritis patients by regulating miR-150 (Luan et al., 2018). Exosomal circ_DLGAP4 promotes diabetic kidney disease progression by sponging miR-143 (Bai et al., 2020). circRNA_010383 acts as a sponge for miR-135a and contributes to renal fibrosis in experimental diabetic nephropathy (Peng et al., 2020).

The circHIPK3, derived from exon2 of the HIPK3 gene, is highly conserved in the genomes of mice, rats, and humans. circHIPK3 plays an important role in heart and lung fibrosis. circHIPK3 regulates cardiac fibrosis through sponging





miR-152-3p and miR-29b-3p, respectively (Ni et al., 2019; Liu W. et al., 2020). circHIPK3 also regulates lung fibroblast-to-myofibroblast transition by miR-338 (Zhang et al., 2019). Most recently, circHIPK3 has been reported to be upregulated in early-phase diabetic nephropathy and to promote mesangial proliferation through sponging miR-185 (Liu et al., 2021). However, the role of circHIPK3 in renal fibrosis has not been reported.

In this study, we found that circHIPK3 was overexpressed in the late phase of experimental renal tubulointerstitial fibrosis induced by FA, which initiates renal tubular injury. Meanwhile, miR-30a was downregulated, and the profibrotic genes such as those encoding TGF-β1, FN, and COL1 were upregulated (**Figure 1** and **Supplementary Figure 1**). These data demonstrate that circHIPK3 contributes to the development and progression of FA-induced renal fibrosis.

What mechanisms are involved in circHIPK3-mediated FA-induced renal fibrosis? Several studies have shown that circHIPK3 exerts various biological functions by acting as a sponge with multiple RNAs (Zheng et al., 2016). As a competitive endogenous RNA, circHIPK3 regulates cell growth and migration by sponging miR-30a in retinal vascular (Shan et al., 2017). circHIPK3 and miR-30a have three perfect match seeds (Chen B. et al., 2019), and miR-30a binds the 3'UTR of TGF-β1 (Bogusławska et al., 2018).

We asked whether circHIPK3 participates in the pathogenesis of FA-induced renal fibrosis by sponging miR-30a. We performed the triple localization of circHIPK3, miR-30a, and TGF-β1 and showed the coexpression of three molecules in the cytoplasm of normal HK-2 cells; this suggested that three molecules interact. This hypothesis is supported by the reports of these three genes being coexpressed in various cell types (Bogusławska et al., 2018; Chen B. et al., 2019).

To experimentally verify whether the circHIPK3/miR-30a/TGF-β1 axis contributes to renal fibrosis, we transfected circHIPK3 into HK-2 cells. We found that the overexpression of circHIPK3 downregulated miR-30a and stimulated overproduced TGF-β1, FN, and COL1 on either mRNA or protein levels (**Figure 3**). The expression of the circHIPK3/miR-30a/TGF-β1

pathway was also observed in renal biopsies from patients with cTIN, i.e., a renal tubular injury initiated clinical renal fibrosis disease (**Figure 5**). These results provided that more evidence of circHIPK3/miR-30a/TGF-β1 initiates tubular injury and thereby contributes to FA-induced renal tubulointerstitial fibrosis.

The TGF-β1 is a major driver of tissue fibrosis, and its protein expression is regulated by miR-30a in various cell types (Bogusławska et al., 2018). In the rat peritoneal fibrosis model, miR-30a expression is negatively correlated with TGF-β1 expression. The overexpression of miR-30a blocks TGF-β1-induced peritoneal fibrosis *via* inhibiting EMT and collagen production (Zhou Q. et al., 2013). In carbon tetrachloride-induced rat liver fibrosis, miR-30a serves as a crucial suppressor of TGF-β1 signaling in hepatic stellate cells activation (Zheng et al., 2018). Similarly, we found that the downregulation of miR-30a by circHIPK3 sponging resulted in the overexpression of TGF-β1 and profibrotic proteins, such as FN and COL1. Taken together, these results from diverse models provide compelling evidence that the circHIPK3/miR-30a/TGF-β1 axis contributes to the pathogenesis of renal fibrosis.

In vitro, we studied TGF-β1-stimulated HK-2 cells and found that TGF-β1 stimulation increases circHIPK3, decreases miR-30a, and promotes the production of profibrotic proteins, such as FN and COL1. This suggested that a positive feedback loop may exist among circHIPK3, miR-30a, and TGF-β1 in renal fibrosis (**Figure 6**). Similar positive feedback has also been noted in miR-150 and TGF-β1 in human primary proximal tubular cells in our previous study (Zhou H. et al., 2013). Renal fibrosis is the characteristic of progressive CKD, and many pathways may contribute among them being circHIPK3/miR-30a/TGF-β1. Future studies might extend this study by using circHIPK3 knockout mice or using circHIPK3 RNAi delivery.

CONCLUSION

The data presented in this study suggest that circHIPK3 contributes to the pathogenesis of renal fibrosis by sponging miR-30a and thereby increasing the production of profibrotic

TGF- β 1 protein. circHIPK3 may be a novel therapeutic target for renal fibrosis.

DATA AVAILABILITY STATEMENT

The original contributions presented in the study are included in the article/**Supplementary Material**, further inquiries can be directed to the corresponding authors.

ETHICS STATEMENT

The studies involving human participants were reviewed and approved by the Institutional Review Board of Shengjing Hospital of China Medical University. The patients/participants provided their written informed consent to participate in this study. The animal study was reviewed and approved by Animal Care and Use Committee of China Medical University.

AUTHOR CONTRIBUTIONS

YW conceived and supervised the study. YW and JL designed the experiments and wrote the manuscript. YW, JL, CJ, SZ, and CM

performed the experiments. JF, JP, and HZ cosupervised the work process. YW and YZ provided renal tissues and the clinical data of patients. YW, JL, and CJ analyzed the data. EL, JK, and HZ revised the manuscript. All authors contributed to the article and approved the submitted version.

FUNDING

This study was supported by the National Natural Science Foundation of China (81770698 and 82170740 to HZ), the National Key R&D Program of China (2017YFC0907400 to YZ), the Key R&D guidance plan of Liaoning Province (2019JH8/10300009 to HZ), the LiaoNing Revitalization Talents Program (XLYC2002081 to HZ), and the Pandeng Scholar of Education Department of Liaoning Province (2013222 to HZ). JK was supported by the Intramural Research Program, NIDDK, NIH.

SUPPLEMENTARY MATERIAL

The Supplementary Material for this article can be found online at: <https://www.frontiersin.org/articles/10.3389/fphys.2021.715567/full#supplementary-material>

REFERENCES

- Bai, S., Xiong, X., Tang, B., Ji, T., Li, X., Qu, X., et al. (2020). Exosomal circ_DLGAP4 promotes diabetic kidney disease progression by sponging miR-143 and targeting ERBB3/NF- κ B/MMP-2 axis. *Cell Death Dis.* 11:1008. doi: 10.1038/s41419-020-03169-3
- Boguslawska, J., Rodzik, K., Popławski, P., Kędzierska, H., Rybicka, B., Sokół, E., et al. (2018). TGF- β 1 targets a microRNA network that regulates cellular adhesion and migration in renal cancer. *Cancer Lett.* 412, 155–169. doi: 10.1016/j.canlet.2017.10.019
- Chen, B., Yu, J., Guo, L., Byers, M., Wang, Z., Chen, X., et al. (2019). Circular RNA circHIPK3 promotes the proliferation and differentiation of chicken myoblast cells by sponging miR-30a-3p. *Cells* 8:177. doi: 10.3390/cells8020177
- Chen, G., Shi, Y., Liu, M., and Sun, J. (2018). circHIPK3 regulates cell proliferation and migration by sponging miR-124 and regulating AQP3 expression in hepatocellular carcinoma. *Cell Death Dis.* 9:175. doi: 10.1038/s41419-017-0204-3
- Chen, T., Knicely, D., and Grams, M. (2019). Chronic Kidney disease diagnosis and management: a review. *JAMA* 322, 1294–1304. doi: 10.1001/jama.2019.14745
- Dong, Y., He, D., Peng, Z., Peng, W., Shi, W., Wang, J., et al. (2017). Circular RNAs in cancer: an emerging key player. *J. Hematol. Oncol.* 10:2. doi: 10.1186/s13045-016-0370-2
- Han, B., Shaolong, E., Luan, L., Li, N., and Liu, X. (2020). CircHIPK3 promotes clear cell renal cell carcinoma (ccRCC) cells proliferation and metastasis via altering of miR-508-3p/CXCL13 signal. *Oncotargets Ther.* 13, 6051–6062. doi: 10.2147/ott.s251436
- Hong, W., Zhang, Y., Ding, J., Yang, Q., Xie, H., and Gao, X. (2020). circHIPK3 acts as competing endogenous RNA and promotes non-small-cell lung cancer progression through the miR-107/BDNF signaling pathway. *Biomed. Res. Int.* 2020:6075902. doi: 10.1155/2020/6075902
- Jin, Y., Che, X., Qu, X., Li, X., Lu, W., Wu, J., et al. (2020). CircHIPK3 promotes metastasis of gastric cancer via miR-653-5p/miR-338-3p-NRP1 axis under a long-term hypoxic microenvironment. *Front. Oncol.* 10:1612. doi: 10.3389/fonc.2020.01612
- Li, T., Jia, Y., Wang, Q., Shao, X., and Lv, R. (2017). Circular RNA: a new star in neurological diseases. *Int. J. Neurosci.* 127, 726–734. doi: 10.1080/00207454.2016.1236382
- Li, Y., Zheng, Q., Bao, C., Li, S., Guo, W., Zhao, J., et al. (2015). Circular RNA is enriched and stable in exosomes: a promising biomarker for cancer diagnosis. *Cell Res.* 25, 981–984. doi: 10.1038/cr.2015.82
- Liu, F., Wei, C., Wu, S., Chenier, I., Zhang, S., Filep, J., et al. (2009). Apocynin attenuates tubular apoptosis and tubulointerstitial fibrosis in transgenic mice independent of hypertension. *Kidney Int.* 75, 156–166. doi: 10.1038/ki.2008.509
- Liu, R., Zhang, M., and Ge, Y. (2021). Circular RNA HIPK3 exacerbates diabetic nephropathy and promotes proliferation by sponging miR-185. *Gene* 765:145065. doi: 10.1016/j.gene.2020.145065
- Liu, W., Wang, Y., Qiu, Z., Zhao, R., Liu, Z., Chen, W., et al. (2020). CircHIPK3 regulates cardiac fibroblast proliferation, migration and phenotypic switching through the miR-152-3p/TGF- β 2 axis under hypoxia. *PeerJ* 8:e9796. doi: 10.7717/peerj.9796
- Liu, X., Liu, B., Zhou, M., Fan, F., Yu, M., Gao, C., et al. (2018). Circular RNA HIPK3 regulates human lens epithelial cells proliferation and apoptosis by targeting the miR-193a/CRYAA axis. *Biochem. Biophys. Res. Commun.* 503, 2277–2285. doi: 10.1016/j.bbrc.2018.06.149
- Liu, Z., Guo, S., Sun, H., Bai, Y., Song, Z., and Liu, X. (2020). Circular RNA CircHIPK3 elevates CCND2 expression and promotes cell proliferation and invasion through miR-124 in Glioma. *Front. Genet.* 11:1013. doi: 10.3389/fgene.2020.01013
- Luan, J., Fu, J., Wang, D., Jiao, C., Cui, X., Chen, C., et al. (2020). miR-150-based RNA interference attenuates tubulointerstitial fibrosis through the SOCS1/JAK/STAT pathway in vivo and in vitro. *Mol. Ther. Nucleic Acids* 22, 871–884. doi: 10.1016/j.omtn.2020.10.008
- Luan, J., Jiao, C., Kong, W., Fu, J., Qu, W., Chen, Y., et al. (2018). circHLA-C plays an important role in lupus nephritis by sponging miR-150. *Mol. Ther. Nucleic Acids* 10, 245–253. doi: 10.1016/j.omtn.2017.12.006
- Ni, H., Li, W., Zhuge, Y., Xu, S., Wang, Y., Chen, Y., et al. (2019). Inhibition of circHIPK3 prevents angiotensin II-induced cardiac fibrosis by sponging miR-29b-3p. *Int. J. Cardiol.* 292, 188–196. doi: 10.1016/j.ijcard.2019.04.006
- Peng, F., Gong, W., Li, S., Yin, B., Zhao, C., Liu, W., et al. (2020). circRNA_010383 acts as a sponge for miR-135a and its downregulated expression contributes to renal fibrosis in diabetic nephropathy. *Diabetes* doi: 10.2337/DB200203
- Qi, H., Fu, J., Luan, J., Jiao, C., Cui, X., Cao, X., et al. (2020). miR-150 inhibitor ameliorates adriamycin-induced focal segmental glomerulosclerosis. *Biochem. Biophys. Res. Commun.* 522, 618–625. doi: 10.1016/j.bbrc.2019.11.096

- Shan, K., Liu, C., Liu, B., Chen, X., Dong, R., Liu, X., et al. (2017). Circular noncoding RNA HIPK3 mediates retinal vascular dysfunction in diabetes mellitus. *Circulation* 136, 1629–1642. doi: 10.1161/circulationaha.117.029004
- Shu, T., Yang, L., Sun, L., Lu, J., and Zhan, X. (2020). CircHIPK3 promotes thyroid cancer tumorigenesis and invasion through the Mirna-338-3p/RAB23 axis. *Med. Princ. Pract.* doi: 10.1159/000512548
- Tan, W., Lim, B., Anene-Nzelu, C., Ackers-Johnson, M., Dashi, A., See, K., et al. (2017). A landscape of circular RNA expression in the human heart. *Cardiovas. Res.* 113, 298–309. doi: 10.1093/cvr/cvw250
- Yin, H., and Cui, X. (2020). Knockdown of circHIPK3 facilitates temozolomide sensitivity in glioma by regulating cellular behaviors through miR-524-5p/KIF2A-mediated PI3K/AKT pathway. *Cancer Biother. Radiopharm.* 36, 556–567. doi: 10.1089/cbr.2020.3575
- Zeng, K., Chen, X., Xu, M., Liu, X., Hu, X., Xu, T., et al. (2018). CircHIPK3 promotes colorectal cancer growth and metastasis by sponging miR-7. *Cell Death Dis.* 9:417. doi: 10.1038/s41419-018-0454-8
- Zhang, J., Lu, J., Xie, H., Wang, D., Ni, H., Zhu, Y., et al. (2019). circHIPK3 regulates lung fibroblast-to-myofibroblast transition by functioning as a competing endogenous RNA. *Cell Death Dis.* 10:182. doi: 10.1038/s41419-019-1430-7
- Zhao, Z., Li, X., Jian, D., Hao, P., Rao, L., and Li, M. (2017). Hsa_circ_0054633 in peripheral blood can be used as a diagnostic biomarker of pre-diabetes and type 2 diabetes mellitus. *Acta Diabetol.* 54, 237–245. doi: 10.1007/s00592-016-0943-0
- Zheng, J., Wang, W., Yu, F., Dong, P., Chen, B., and Zhou, M. (2018). MicroRNA-30a suppresses the activation of hepatic stellate cells by inhibiting epithelial-to-mesenchymal transition. *Cell Physiol. Biochem.* 46, 82–92. doi: 10.1159/000488411
- Zheng, Q., Bao, C., Guo, W., Li, S., Chen, J., Chen, B., et al. (2016). Circular RNA profiling reveals an abundant circHIPK3 that regulates cell growth by sponging multiple miRNAs. *Nat. Commun.* 7:11215. doi: 10.1038/ncomms11215
- Zhou, H., Hasni, S., Perez, P., Tandon, M., Jang, S., Zheng, C., et al. (2013). miR-150 promotes renal fibrosis in lupus nephritis by downregulating SOCS1. *J. Am. Soc. Nephrol.* 24, 1073–1087. doi: 10.1681/asn.2012080849
- Zhou, Q., Yang, M., Lan, H., and Yu, X. (2013). miR-30a negatively regulates TGF- β 1-induced epithelial-mesenchymal transition and peritoneal fibrosis by targeting Snai1. *Am. J. Pathol.* 183, 808–819. doi: 10.1016/j.ajpath.2013.05.019

Conflict of Interest: The authors declare that the research was conducted in the absence of any commercial or financial relationships that could be construed as a potential conflict of interest.

Publisher's Note: All claims expressed in this article are solely those of the authors and do not necessarily represent those of their affiliated organizations, or those of the publisher, the editors and the reviewers. Any product that may be evaluated in this article, or claim that may be made by its manufacturer, is not guaranteed or endorsed by the publisher.

Copyright © 2022 Wu, Luan, Jiao, Zhang, Ma, Zhang, Fu, Lai, Kopp, Pi and Zhou. This is an open-access article distributed under the terms of the Creative Commons Attribution License (CC BY). The use, distribution or reproduction in other forums is permitted, provided the original author(s) and the copyright owner(s) are credited and that the original publication in this journal is cited, in accordance with accepted academic practice. No use, distribution or reproduction is permitted which does not comply with these terms.

Advantages of publishing in Frontiers



OPEN ACCESS

Articles are free to read for greatest visibility and readership



FAST PUBLICATION

Around 90 days from submission to decision



HIGH QUALITY PEER-REVIEW

Rigorous, collaborative, and constructive peer-review



TRANSPARENT PEER-REVIEW

Editors and reviewers acknowledged by name on published articles

Frontiers

Avenue du Tribunal-Fédéral 34
1005 Lausanne | Switzerland

Visit us: www.frontiersin.org

Contact us: frontiersin.org/about/contact



REPRODUCIBILITY OF RESEARCH

Support open data and methods to enhance research reproducibility



DIGITAL PUBLISHING

Articles designed for optimal readership across devices



FOLLOW US

@frontiersin



IMPACT METRICS

Advanced article metrics track visibility across digital media



EXTENSIVE PROMOTION

Marketing and promotion of impactful research



LOOP RESEARCH NETWORK

Our network increases your article's readership